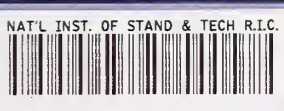

NBS Special Publication 705

Precision Measurement and Calibration: Electricity

A.O. McCoubrey - Editor

1985

U.S. DEPARTMENT OF COMMERCE
National Bureau of Standards

The National Bureau of Standards[1] was established by an act of Congress on March 3, 1901. The Bureau's overall goal is to strengthen and advance the nation's science and technology and facilitate their effective application for public benefit. To this end, the Bureau conducts research and provides: (1) a basis for the nation's physical measurement system, (2) scientific and technological services for industry and government, (3) a technical basis for equity in trade, and (4) technical services to promote public safety. The Bureau's technical work is performed by the National Measurement Laboratory, the National Engineering Laboratory, the Institute for Computer Sciences and Technology, and the Institute for Materials Science and Engineering.

The National Measurement Laboratory

Provides the national system of physical and chemical measurement; coordinates the system with measurement systems of other nations and furnishes essential services leading to accurate and uniform physical and chemical measurement throughout the Nation's scientific community, industry, and commerce; provides advisory and research services to other Government agencies; conducts physical and chemical research; develops, produces, and distributes Standard Reference Materials; and provides calibration services. The Laboratory consists of the following centers:

- Basic Standards[2]
- Radiation Research
- Chemical Physics
- Analytical Chemistry

The National Engineering Laboratory

Provides technology and technical services to the public and private sectors to address national needs and to solve national problems; conducts research in engineering and applied science in support of these efforts; builds and maintains competence in the necessary disciplines required to carry out this research and technical service; develops engineering data and measurement capabilities; provides engineering measurement traceability services; develops test methods and proposes engineering standards and code changes; develops and proposes new engineering practices; and develops and improves mechanisms to transfer results of its research to the ultimate user. The Laboratory consists of the following centers:

- Applied Mathematics
- Electronics and Electrical Engineering[2]
- Manufacturing Engineering
- Building Technology
- Fire Research
- Chemical Engineering[2]

The Institute for Computer Sciences and Technology

Conducts research and provides scientific and technical services to aid Federal agencies in the selection, acquisition, application, and use of computer technology to improve effectiveness and economy in Government operations in accordance with Public Law 89-306 (40 U.S.C. 759), relevant Executive Orders, and other directives; carries out this mission by managing the Federal Information Processing Standards Program, developing Federal ADP standards guidelines, and managing Federal participation in ADP voluntary standardization activities; provides scientific and technological advisory services and assistance to Federal agencies; and provides the technical foundation for computer-related policies of the Federal Government. The Institute consists of the following centers:

- Programming Science and Technology
- Computer Systems Engineering

The Institute for Materials Science and Engineering

Conducts research and provides measurements, data, standards, reference materials, quantitative understanding and other technical information fundamental to the processing, structure, properties and performance of materials; addresses the scientific basis for new advanced materials technologies; plans research around cross-country scientific themes such as nondestructive evaluation and phase diagram development; oversees Bureau-wide technical programs in nuclear reactor radiation research and nondestructive evaluation; and broadly disseminates generic technical information resulting from its programs. The Institute consists of the following Divisions:

- Inorganic Materials
- Fracture and Deformation[3]
- Polymers
- Metallurgy
- Reactor Radiation

[1]Headquarters and Laboratories at Gaithersburg, MD, unless otherwise noted; mailing address Gaithersburg, MD 20899.
[2]Some divisions within the center are located at Boulder, CO 80303.
[3]Located at Boulder, CO, with some elements at Gaithersburg, MD.

Precision Measurement and Calibration: Electricity

Selected Papers on the Realization and Maintenance of the Fundamental Electrical Units and Related Topics

A.O. McCoubrey, Editor

Center for Basic Standards
National Measurement Laboratory
National Bureau of Standards
Gaithersburg, MD 20899

A compilation of previously published papers by the National Bureau of Standards including selected abstracts by non-NBS authors. This publication is a supplement to NBS Special Publication 300, Volume 3 (1968) and NBS Handbook 77, Volume II (1961)

Issued October 1985

U.S. DEPARTMENT OF COMMERCE, Malcolm Baldrige, Secretary
NATIONAL BUREAU OF STANDARDS, Ernest Ambler, Director

Library of Congress Catalog Card Number: 85-600580

National Bureau of Standards Special Publication 705
Natl. Bur. Stand. (U.S.), Spec. Publ. 705, 850 pages (Oct. 1985)
CODEN: XNBSAV

U.S. GOVERNMENT PRINTING OFFICE
WASHINGTON: 1985

For sale by the Superintendent of Documents, U.S. Government Printing Office, Washington, DC 20402

FOREWORD

The requirements of industry and commerce for accurate measurements have been the central focus of the National Bureau of Standards since the turn of the century. The Bureau's research and development programs help incorporate the advances of science and technology into the national measurement standards of the United States. They also improve the methods for making measurements, and permit NBS to refine its services -- services that are essential to the use of measurement throughout the economy. Today, when the country is spending an estimated $163 billion on measurement, the mission of NBS takes on special significance. The Bureau's work is critical to the nation as we respond to challenges of international trade in high technology products and the demands of national defense.

That is why it is especially important that the results of NBS measurement-related programs be made available in a format that is both effective and efficient for industry. Based upon past demand, the Precision Measurement and Calibration series of NBS publications has proven to be a valuable tool for industrial metrologists. These are compilations of previously published papers of NBS technical staff members, bringing together information that is widely scattered in the technical literature. Recent advances now require new compilations to serve those who depend upon NBS technology. The latest volume is an important addition to this series.

Ernest Ambler
Director

Editor's Note

The Precision Measurement and Calibration Series of publications was initiated early in 1961 by the compilation, in three volumes, of approximately 150 previously published papers of the technical staff of the National Bureau of Standards. The series was extended and brought up to date in the years from 1968 through 1972 by the compilation, in ten volumes, of more than 500 additional previously published papers of the NBS staff. The demand for these past editions of the Precision Measurement and Calibration Series and the related sales provide convincing evidence for the usefulness of the compilations. They serve to collect the results of NBS programs that are otherwise scattered very widely throughout the technical literature. In the collected form they are readily accessible to practical specialists in the measurement standards laboratories of government and industry.

The present extension of the Precision Measurement and Calibration Series in the field of Electricity has been undertaken in view of the past success of the series and continuing requests from industry for more publication of NBS work in a form that meets the needs of practicing metrologists. The new volume is mainly a compilation of papers published during the most recent twelve years by the Electricity Division staff in the NBS Center for Basic Standards. This collection of papers is, therefore, focused upon the realization of the SI unit of electricity (the ampere) in the United States, the practical maintenance of this unit in terms of the volt and the ohm and topics concerned with the NBS calibration of related industrial electrical measurement standards. While the compilation includes papers on the transfer of d.c. units to a.c. measuring devices, it is by no means complete in terms of NBS publications in the field of power frequencies, audio frequencies or radio frequencies. Many of the programs of the Electrosystems Division (Gaithersburg), the Electromagnetic Fields Division (Boulder) and the Electromagnetics Technology Division (Boulder) are concerned with topics that, as in the past, fall within a d.c. and low frequency classification; however, it is no longer possible to include all the NBS publications from these programs within the scope of a single volume. While it has been necessary to limit the scope of this new volume primarily to papers published by the staff of the NBS Electricity Division, an effort has been made to address a wider range of interests by including, in appendices, the most recent publications of bibliographies by the Electrosystems Division, the Electromagnetic Fields Division and the Electromagnetic Technology Division.

An additional effort to extend the usefulness of this volume has been made by including, as in the past, abstracts of closely related papers by authors in other organizations. These abstracts reflect only a small fraction of such possibilities and no special NBS endorsement of the related publications is implied. Likewise, there is no implication that other equally important publications do not exist.

The present compilation has been reviewed by a number of colleagues within NBS and their comments have been incorporated. In this connection, the Editor is particularly indebted to: Frank Hermach (Co-editor, with Ron Dziuba, of Precision Measurement and Calibration; Electricity-Low Frequency, issued December 1968), John Hastings, Robert Cutkosky, Barry Taylor and Oscars Petersons. Their comments and suggestions all contributed substantially to the usefulness of the collection.

Draft copies of this compilation were also reviewed by a number of members of the National Conference of Standard Laboratories (NCSL). All of the comments and suggestions received from this group were very positive and adoption of all the recommendations was only limited by the scope and size of the compilation. It quickly became clear that papers on measurement assurance programs, as well as papers involving different regions of the frequency spectrum and other areas of electrical technology must be considered as possible candidates for future volumes in the series.

Reviews by members of NCSL included recommendations for a number of additions and deletions that contributed substantially to the practical value of the work. In this connection it is a pleasure to acknowledge the contributions of Laurel Auxier and Arno Ehman of Beckman Instruments, Carl Quinn of Simco Electronics, Fred Hume of Fluke, David Workman of Martin Marietta Aerospace (Denver), Robert Weber and Klaus Jaeger of Lockheed Missiles and Space, Graham Cameron of the Department of Defence (Canada), William Simmons of Barrios Technology, Hartwell Keith and Gary Davidson of TRW, and Timothy Driver of Sprague Electric.

Arthur McCoubrey, Editor

Table of Contents

SURVEY PAPERS ON ELECTRICITY

Metrologia 21, 37–39 (1985)

metrologia

Letter to the Editor

Impact of Quantized Hall Resistance on SI Electrical Units and Fundamental Constants*

B. N. Taylor

Electricity Division, National Bureau of Standards, Gaithersburg, MD 20899, USA

Received: November 7, 1984

Abstract

With the discovery of the quantum Hall effect the SI units ampere, volt, and ohm may be realized with high accuracy by performing four fundamental-constant determinations requiring only a consistent set of laboratory electrical units. Accurate values in SI units for most other constants, including the Avogadro and fine-structure constants, may also be obtained from the same measurements.

In two previous publications in this journal [1, 2] the author emphasized the important role that the fundamental constants can play in realizing the *Système International d'Unités* (SI) unit of current, the ampere, and how a direct measurement of the ampere can provide an accurate, indirect value for the Avogadro constant. With the discovery of the quantum Hall effect [3] the possibilities for realizing SI electrical units via fundamental-constant determinations has significantly increased and it is the purpose of this note to briefly summarize these possibilities. In particular, it will be shown how the determination of four electric unit-dependent constants measured only in terms of a consistent set of laboratory electrical units can be used to realize with high accuracy the SI units ampere, volt, and ohm, and at the same time provide accurate values in SI units for most other fundamental constants including the Avogadro constant N_A and the fine-structure constant α.

The four constants are the quantized Hall resistance $R_H \equiv h/e^2$ (h is the Planck constant and e the elementary charge), the Josephson frequency-voltage ratio $2e/h$, the proton gyromagnetic ratio obtained by the low-field method γ'_p(low) (the prime means that the protons are in a spherical sample of pure H_2O at 25 °C), and the Faraday constant F. (It is assumed throughout this note that the quantized Hall resistance is a true measure of h/e^2, i.e., that any corrections are negligibly small.)

A number of other constants are needed in addition to these four but they are either defined numbers or electric-unit-independent constants which are well known. They are the permeability of vacuum $\mu_0 \equiv 4\pi \times 10^{-7}$ H/m, the speed of light in vacuum $c \equiv 299\,792\,458$ m/s, the molar mass of the proton M_p, the Rydberg constant for infinite mass R_∞, the magnetic moment of protons in H_2O in units of the Bohr magneton μ'_p/μ_B, and the ratio of the proton mass to the electron mass m_p/m_e.

For simplicity we assume that R_H, $2e/h$, γ'_p(low), and F are measured in the same laboratory and thus in terms of the same laboratory electrical units. The latter are taken to be V_{LAB} defined in terms of the mean emf of a group of chemical cells, Ω_{LAB} defined in terms of the mean resistance of a group of resistors, and $A_{LAB} = V_{LAB}/\Omega_{LAB}$. It is further assumed that all four quantities are measured at the same time so that drifts in the laboratory units are of no consequence. We may then define the following three quantities at a given time:

$$K_A \equiv A_{LAB}/A \qquad K_V \equiv V_{LAB}/V \qquad K_\Omega \equiv \Omega_{LAB}/\Omega\,,$$

where A, V, and Ω are, of course, the SI units ampere, volt, and ohm. In practice, determining the ratios K_A, K_V, and K_Ω is what is meant by realizing the SI definitions of the ampere, volt, and ohm, respectively.

From these definitions and the known relationships among the fundamental constants [4] one may derive the following equations[1]:

* Official contribution of the National Bureau of Standards, not subject to copyright in the United States

[1] Since $\gamma'_p(\text{high})_{LAB} = F_{LAB}(\mu'_p/\mu_B)\,(m_p/m_e)/M_p$, where γ'_p(high) is the proton gyromagnetic ratio determined by the high-field method, $\gamma'_p(\text{high})_{LAB}$ can be used in place of F_{LAB} without altering the principal conclusions of this note. However, a γ'_p(high) experiment is more akin to the direct realization of the SI ampere via a force balance than is a Faraday-constant experiment

$$K_A = \left[\frac{M_p}{(\mu_p'/\mu_B)\,(m_p/m_e)}\;\frac{\gamma_p'(\mathrm{low})_{LAB}}{F_{LAB}}\right]^{1/2} \tag{1}$$

$$K_V = \left[\frac{\mu_0^4 c^6 M_p^3}{16\,{}^2R_\infty^2(\mu_p'/\mu_B)\,(m_p/m_e)^3}\times \frac{\gamma_p'(\mathrm{low})_{LAB}\,(2\,e/h)_{LAB}^2}{(R_H)_{LAB}^4\,F_{LAB}^3}\right]^{1/6} \tag{2}$$

$$K_\Omega = \left[\frac{\mu_0^2 c^3(\mu_p'/\mu_B)}{16\,R_\infty}\;\frac{(2\,e/h)_{LAB}}{(R_H)_{LAB}^2\,\gamma_p'(\mathrm{low})_{LAB}}\right]^{1/3} \tag{3}$$

$$N_A = [(R_H)_{LAB}\,(2\,e/h)_{LAB}\,F_{LAB}]/2 \tag{4}$$

$$\alpha^{-1} = \left[\frac{(\mu_p'/\mu_B)}{2\,\mu_0 R_\infty}\;\frac{(R_H)_{LAB}\,(2\,e/h)_{LAB}}{\gamma_p'(\mathrm{low})_{LAB}}\right]^{1/3}, \tag{5}$$

where the subscript LAB indicates that these quantities are to be measured in terms of the appropriate laboratory units. The latter are Ω_{LAB}, V_{LAB}^{-1}, A_{LAB}^{-1} and A_{LAB} for R_H, $2e/h$, $\gamma_p'(\mathrm{low})$ and F, respectively. It should be emphasized that *none of Eqs. (1)–(5) contains an electric-unit-dependent constant which must be measured in SI electrical units.* In principle, all that is required to define V_{LAB} and Ω_{LAB} and thus to determine $(R_H)_{LAB}$, $(2e/h)_{LAB}$, $\gamma_p'(\mathrm{low})_{LAB}$ and F_{LAB} is a battery and a resistor!

It is also possible to derive equations involving these same quantities from which one may obtain indirect values in SI units for most other fundamental constants of interest (except those involving the gas constant). For example, we note the following relations:

$$2\,e/h = (2\,e/h)_{LAB}\,K_V^{-1} \tag{6}$$

$$R_H = (R_H)_{LAB}\,K_\Omega = \mu_0 c\,\alpha^{-1}/2 \tag{7}$$

$$e = 2\,K_A/[(R_H)_{LAB}\,(2\,e/h)_{LAB}] \tag{8}$$

$$h = (\mu_0 c/2)\alpha^{-1}e^2 \tag{9}$$

$$m_e = (M_p/N_A)/(m_p/m_e)\,, \tag{10}$$

where all quantities are in SI units except those with the subscript LAB and K_V, K_Ω, K_A, α^{-1} and N_A are to be taken from Eqs (1)–(5) as appropriate.

It is of interest to evaluate Eqs (1)–(10) using existing measurements in order to see what levels of uncertainty can be achieved with present-day measurement techniques. The National Bureau of Standards (NBS) is the only laboratory to date which has completed determinations of the four required electric-unit-dependent constants [5–8]. However, the experiments were not carried out at the same time but over the 9-year period 1975–1984. Although V_{NBS} has been maintained constant in time via the Josephson effect with an estimated uncertainty of a few parts in 10^8 since 1972 July 1 [6], Ω_{NBS} and thus also A_{NBS} may not be assumed to be time invariant because Ω_{NBS} is defined in terms of the mean resistance of five Thomas-type one-ohm resistors. Indeed, there is strong evidence that since the early 1970's Ω_{NBS} has been decreasing at the rate of about 0.06 ppm/year [9]. Nevertheless, for illustrative purposes we assume that all four constants were determined at the same time and in terms of the same laboratory units.

Table 1. Uncertainties of constants used to evaluate Eqs. (1)–(10)

Quantity	Uncertainty[a] (ppm)	Refs.
$(R_H)_{NBS}$	0.047	[5]
$(2e/h)_{NBS}$	0.031	[6]
$\gamma_p'(\mathrm{low})_{NBS}$	0.21	[7]
F_{NBS}	1.33	[8, 10]
μ_0	defined	
c	defined	
M_p	0.012	[11, 10]
R_∞	0.0010	[12, 13, 10]
(μ_p'/μ_B)	0.012	[14, 10]
m_p/m_e	0.043	[15]

[a] All uncertainties are one-standard-deviation estimates. The uncertainties of F_{NBS}, M_p, R_∞, and μ_p'/μ_B are based in part on analyses carried out by the author in connection with the 1983 least-squares adjustment of the fundamental constants [10]

The one-standard-deviation uncertainties of the four NBS measurements as well as those of the other required constants are given in Table 1. These uncertainties, Eqs. (1)–(10), and a straightforward application of the law of error propagation then lead to the results given in Table 2. The latter clearly show the power of the fundamental-constant or indirect route to the realization of SI electrical units; the uncertainties of these indirect values of K_A, K_V, and K_Ω are comparable with or significantly less than the uncertainties which can be achieved by direct measurement. This statement applies as well to the indirect values of the other constants listed in Table 2 in those cases where direct measurements actually exist.

In conclusion we point out that the four electric-unit-dependent constants $(R_H)_{LAB}$, $(2e/h)_{LAB}$, $\gamma_p'(\mathrm{low})_{LAB}$ and F_{LAB} need not be measured in the same laboratory if they can be reexpressed in terms of the units of one particular laboratory as they existed at a specific time. If, in fact, a number of laboratories use the Josephson and quantum Hall effects to define their units of voltage and resistance and to maintain them constant in time, then a measurement of $\gamma_p'(\mathrm{low})_{LAB}$ by any one of them at any time and of

Table 2. Uncertainties of quantities obtained from Eqs. (1)–(10) evaluated with constants having the uncertainties given in Table 1

Quantity	Uncertainty[a] (ppm)
K_A	0.67
K_V	0.67
K_Ω	0.077
N_A	1.33
α^{-1}	0.073
$2e/h$	0.67
R_H	0.073
e	0.68
h	1.34
m_e	1.33

[a] All uncertainties are one-standard-deviation estimates assuming that the four constants $(R_H)_{NBS}$, $(2e/h)_{NBS}$, $\gamma'_p(\text{low})_{NBS}$, and F_{NBS} of Table 1 were measured at the same time and in terms of the same laboratory units

F_{LAB} by any one of them at any time will enable all of them to determine their respective values of K_A, K_V and K_Ω. With this in mind we emphasize the potential importance of an improved determination of F_{LAB}. A measurement of the latter with an uncertainty of 0.5 ppm, which seems feasible, would yield a value of $2e/h$ with about half this uncertainty and a value of N_A of about the same uncertainty. It will be most difficult for direct measurements of either of these constants to achieve such accuracies.

Acknowledgements. Helpful discussions with B. F. Field and E. R. Williams are gratefully acknowledged. The data analyses carried out in connection with the 1983 least-squares adjustment of the fundamental constants were done in collaboration with E. R. Cohen.

References

1. B. N. Taylor: Metrologia **9**, 21–23 (1973)
2. B. N. Taylor: Metrologia **12**, 81–83 (1976)
3. K. v. Klitzing, G. Dorda, M. Pepper: Phys. Rev. Lett. **45**, 494–497 (1980)
4. See for example Refs. [1–3] and also: B. N. Taylor, W. H. Parker, D. N. Langenberg: Rev. Mod. Phys. **41**, 375–496 (1969); E. R. Cohen, B. N. Taylor: J. Phys. Chem. Ref. Data **2**, 663–734 (1973)
5. M. E. Cage, R. F. Dziuba, B. F. Field: IEEE Trans. Instrum. Meas. IM-**34**, July 1985 (to be published)
6. B. F. Field, T. F. Finnegan, J. Toots: Metrologia **9**, 155–166 (1973)
7. E. R. Williams, P. T. Olsen: Phys. Rev. Lett. **42**, 1575–1579 (1979)
8. V. E. Bower, R. S. Davis. J. Res. Natl. Bur. Stand. **85**, 175–191 (1980); L. J. Powell, T. J. Murphy, J. W. Gramlich: J. Res. Natl. Bur. Stand. **87**, 9–19 (1982); V. E. Bower, R. S. Davis, T. J. Murphy, P. J. Paulsen, J. W. Gramlich, L. J. Powell: J. Res. Natl. Bur. Stand. **87**, 21–22 (1982)
9. B. N. Taylor: J. Res. Natl. Bur. Stand. (to be published)
10. E. R. Cohen, B. N. Taylor: J. Phys. Chem. Ref. Data (to be published)
11. A. H. Wapstra, G. Audi: Nucl. Phys. A (to be published)
12. S. R. Amin, C. D. Caldwell, W. Lichten: Phys. Rev. Lett. **47**, 1234–1238 (1981)
13. J. E. M. Goldsmith, E. W. Weber, T. W. Hänsch: Phys. Rev. Lett. **41**, 1525–1528 (1978)
14. W. D. Phillips, W. E. Cooke, D. Kleppner: Metrologia **13**, 179–195 (1977)
15. R. S. Van Dyck, Jr., F. L. Moore, P. B. Schwinberg: Bull. Am. Phys. Soc. **28**, 791 (1983); and private communication, 1983

Report on the New NBS Determination of the Proton Gyromagnetic Ratio

EDWIN R. WILLIAMS, GEORGE R. JONES, MEMBER, IEEE, JUN-SHOU SONG, WILLIAM D. PHILLIPS, AND PAUL T. OLSEN, MEMBER, IEEE

Abstract—We describe a new measurement of the proton gyromagnetic ratio in H_2O, γ'_p, now in progress at NBS, including the construction of a single layer precision solenoid, the measurement of its dimensions by an inductive technique, and our latest dimensional measurement results. We also discuss other improvements made since our last γ'_p determination.

I. Introduction

THE measurement of the proton gyromagnetic ratio in H_2O by the weak field method involves measuring two quantities. First, one measures the dimensions of a precision solenoid and calculates the magnetic field produced when a known current is passed through the solenoid windings. Second, one measures the precession frequency of protons in a sample of H_2O placed in this calculable field using standard nuclear magnetic resonance (NMR) techniques. The ratio of the NMR angular frequency to the calculated flux density is $\gamma'_p(\text{low})$. The dimensional measurements have always been the more difficult part of the determination.

In this paper we describe our present experiment which employs a newly constructed precision solenoid. We also discuss the major changes we have made in our previous experiment [1] and why we expect these changes to improve our accuracy from 0.2 ppm to better than 0.05 ppm.

The major motivation for a new $\gamma'_p(\text{low})$ experiment is to help test basic physical theories via the fundamental constants. In particular, the fine structure constant, α, can be obtained from the Josephson effect measurement of $2e/h$ and $\gamma'_p(\text{low})$ via the following equation:

$$\alpha^{-2} = \frac{c}{4R_\infty} \frac{1}{(\Omega_{NBS}/\Omega)} \frac{\mu'_p}{\mu_B} \frac{(2e/h)_{NBS}}{\gamma'_p(\text{low})_{NBS}} . \tag{1}$$

Here c is the speed of light in vacuum; R_∞ is the Rydberg constant for infinite mass; Ω_{NBS}/Ω is the ratio of the National Bureau of Standards (NBS) as-maintained ohm to the absolute or SI (International System) ohm; μ'_p/μ_B is the magnetic moment of the proton in units of the Bohr magneton (throughout, the prime indicates protons in a spherical sample of pure H_2O at 25 °C); $(2e/h)_{NBS}$ is the ratio of twice the elementary charge to the Planck constant measured in terms of the NBS as-maintained volt using the ac Josephson effect; and $\gamma'_p(\text{low})_{NBS}$ is the proton gyromagnetic ratio measured in terms of the NBS as-maintained ampere.

The accurate determination of $\gamma'_p(\text{low})$ has become even more important with the discovery of the quantum Hall effect. The pertinent equation to obtain α from the quantized Hall resistance R_H is

$$\alpha^{-1} = \frac{2}{\mu_0 c} \frac{\Omega_{NBS}}{\Omega} (R_H)_{NBS} \tag{2}$$

where μ_0 is the permeability of free space. Equations (1) and (2) can be combined to eliminate the quantity Ω_{NBS}/Ω, yielding

$$\alpha^{-3} = \frac{1}{2\mu_0 R_\infty} \frac{\mu'_p}{\mu_B} \frac{(2e/h)_{NBS}}{\gamma'_p(\text{low})_{NBS}} (R_H)_{NBS}. \tag{3}$$

Equation (3) is obviously not independent of (2) but represents an alternative path to obtain α from the Hall resistance. However, the cube root dependence of (3) helps reduce the uncertainty in α. Of course, all three results could be combined together to obtain a least squares value for α. It is clear that by measuring γ'_p and Ω_{NBS}/Ω more accurately, we can improve our understanding of the ac Josephson effect and the quantum Hall effect, while testing quantum electrodynamics which requires α for the evaluation of its theoretical expressions (e.g., for the anomalous moment of the electron). Since the completion of our last γ'_p experiment three other experimental results have been published. (These experiments are reviewed in [2]). The National Physical Laboratory in England and the Mendelyeev Institute of Metrology in the USSR have reported values of γ'_p that are in complete disagreement with our 1979 result (10–15 standard deviation discrepancies). In contrast, the Chinese value obtained at the National Institute of Metrology agrees with our value. A new determination of γ'_p should shed light on these discrepancies.

The dominant source of uncertainty in our previous experiment was the measurement of the diameter of the solenoid. We attempted to eliminate the need for a diameter measurement by using a special distribution of currents [1], but this technique does not work well on short solenoids. We have, therefore, constructed a long solenoid that will allow us to eliminate the need to measure the diameter.

Manuscript received August 20, 1984. This work was supported in part by the U.S. Department of Energy and the U.S. Air Force Office of Scientific Research.

E. R. Williams, G. R. Jones, W. D. Phillips, and P. T. Olsen are with the National Bureau of Standards, Washington, DC.

J. S. Song is with the National Bureau of Standards, Washington, DC, as a Guest Scientist from Chongqing University, People's Republic of China.

II. Construction of a Long Single-Layer Solenoid

We fabricated the new 2.2-m long 0.3-m diam, fused silica solenoid by lapping techniques developed specifically for precision solenoid construction at NBS by Curtis, Moon, and Sparks in 1932 [3]. In about 1958, Driscoll perfected the technique while lapping the solenoid used in our previous determination. Because of the critical role of the solenoid in determining γ_p'(low), we feel it is of interest to summarize briefly its fabrication.

We started with a rough cylindrical form of fused silica (actually magnetically purified silica sand fused together) 2.2 m long, with a 25-mm wall thickness, manufactured by U.S. Fused Quartz Company.[1] The form was first ground into a cylinder using a large lathe on which we mounted a grinding wheel. A special lathe was then constructed for the lapping process by cutting an old lathe in the middle and extending it to handle the 2.2-m cylinder. This was necessary because we could not use the large lathe for the time consuming lapping process. We lapped the cylinder with a lap that made contact on two generators of the cylinder ±45° from the top. This lap was constrained so that it would not rotate with the cylinder but was free to sit on the top of the cylinder. With grit applied, the lap was gently guided up and down the cylinder. Frequently the cylinder had to be cleaned and measurements taken of the diameter along its length. The time spent lapping various areas was adjusted so as to obtain a diameter constant to a few micrometers. A slight ellipticity (~3 μm) was detected and corrected by painting selected areas where less lapping was desired.

This cylinder was then mounted in the large lathe, and a helix of 24 threads/inch was ground 0.3-mm deep. It was then returned to the lapping lathe where a special lap was used to smooth the helical thread. To make this lap we machined an inside thread into a 1-cm thick brass ring such that this ring could, in principle, be threaded onto the 0.3-m diam helix ground in the cylinder. The brass ring, which was 10-cm long, was then cut along the axial direction into short pieces 3-cm wide. A total of 46 of the 3 cm × 10 cm lap segments was spaced along four generators of the cylinder. Two generators were located at ±60° from the vertical, and two were at ±30°. The segments were then epoxied to a lap form made of fused silica, while the lap segments were held with their threads seated securely in the grooves of the cylinder while spaced along the four generators.

The final lapping then proceeded as grit was applied to the rotating cylinder, and this 46 segment lap was driven back and forth along the top of the cylinder by the helical groove. The lapping process, of course, averages out the variation in the pitch of the helical groove. However, the diameter must be measured repeatedly and the lapping time adjusted at various positions along the cylinder to keep the diameter constant. A short lap made of 14 segments was used for correcting small variations in the diameter. The final helical groove took on a smooth, nearly sinusoidal shape, and the lapping was stopped when a 0.8-mm wire would fit tightly in this sinusoidal groove.

We then wound the solenoid by drawing wire through dies directly onto the cylindrical form. We started with 1-mm diam oxygen-free pure copper that was plated with 1 μm of gold. The final wire diameter of 0.8 mm was obtained after drawing through two dies.

The newly constructed solenoid was then taken to the nonmagnetic facility where the measurement of its dimensions and NMR frequency will be completed without any further movement of the solenoid. A shower of an insulating liquid, Fluorinert FC-43 manufactured by the 3M Corporation, is used to cool the solenoid and control its temperature to 0.02 °C. The temperature coefficient of expansion of the fused silica is about 0.5 ppm/°C.

III. Measuring the Solenoid

The solenoid has 2100 turns spaced about 1 mm/turn, and it is necessary to measure their position and changes in diameter to about 0.02 μm. We have constructed a new measuring apparatus for this purpose, but the principles upon which it is based are the same as in our earlier effort [4]. The following is a brief summation of the method.

The basic idea is to use a magnetic inductive technique to locate the current in the windings. Coils A and A′ in Fig. 1 form a linear differential transformer which locates the axial position of the current injected into selected (or activated) turns of the solenoid. Coils A and A′ are connected so that their output voltages cancel when centered on these activated turns, and a servo system locks the coil assembly to the null point with a precision of 0.02 μm. A mirror (corner cube M′) located in the center of the coil assembly is part of a laser interferometer system, with the reference mirror (M) located in the center of a second linear differential transformer.

We choose to activate 10 turns at one time, and under computer control move the current injector to any selected 10 turns until information about all 2100 turns of the solenoid is obtained. Coils B, B′, and C form a radius-to-voltage transducer which measures the variations in the radius of the injected current loop. The voltage induced in coil C is inversely proportional to the radius of the activated turns. To detect small changes, we first "buck out" most of the voltage in coil C by using the two coils B and B′. At the same time that we are bucking out the voltage in coil C, we are also increasing the sensitivity of this three-coil system to changes in the radius R of the solenoid because the voltage in coils B and B′ increases when the radius R increases. This three-coil radius-to-voltage transducer is then calibrated by having a few turns of wire on both ends of the solenoid that are 50 μm larger at one end and 60 μm smaller at the other end.

In order to insure the valid measurement of the axial and radial variations, we use 10 other coils on the probe to measure the motion of the probe in the other degrees of freedom. Fig. 2 is a cross section of the probe in the plane of the injected current. The coils labeled V are wired in opposition, as are those labeled H; they are used to measure the vertical and horizontal displacements using the gradient of the magnetic field produced by the activated turns. The coils VA are wired

[1] Mention of a manufacturer does not signify an endorsement by the U.S. National Bureau of Standards, nor does it imply that the item is the only or best item for any purpose.

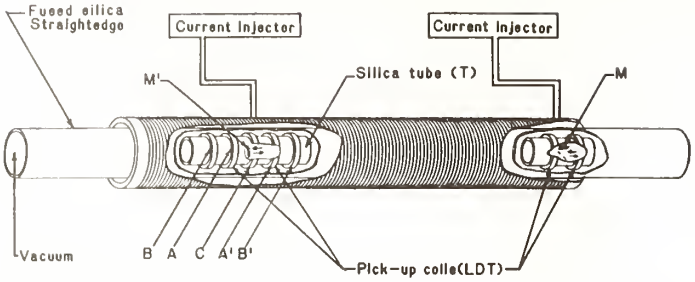

Fig. 1. Solenoid dimensional measurement system used to determine the axial position and radial variations of the wires. The five coils A, A′, B, B′, and C are attached to a silica tube, T, and can be pushed or pulled along the axis of the solenoid. Coils A and A′ locate the axial position of the injected current and coils B, B′, and *C* form a diameter-to-voltage transducer. Mirrors M and M′ are part of a laser interferometer. The fused silica straight edge is used to guide the five-coil probe and forms part of the vacuum chamber.

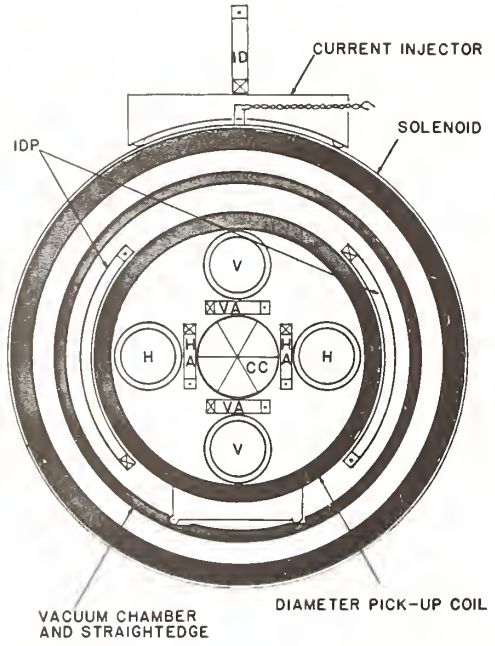

Fig. 2. Cross section of the pick-up probe and solenoid in the plane of the activated loop on the solenoid. A corner cube, CC, is located at the center. The coils marked V measure the vertical displacement, H the horizontal displacement, HA the horizontal angle, and VA the vertical angle. To measure the injector displacement, current is injected into the coil ID instead of the solenoid and the voltage in coil IDP is detected.

as one coil at the center and oriented orthogonally to the field of the activated turns. This pair measures the vertical angle (pitch), while HA measures the horizontal angle (yaw). The coil labeled ID is used in combination with the coil IDP to detect the current injector displacement with respect to the probe. Using these 10 coils, corrections are applied to the axial position and radial variation raw readings, in order to account for the fact that the straight edge that controls the position of the probe is not perfectly straight and that the current injector does not traverse the top of the solenoid perfectly. The radial variations voltage signal depends quadratically on the V, H, VA, and HA signals, and it is imperative that the probe is centered where this dependence is an extremum in order to reduce the effect of straight-edge imperfections.

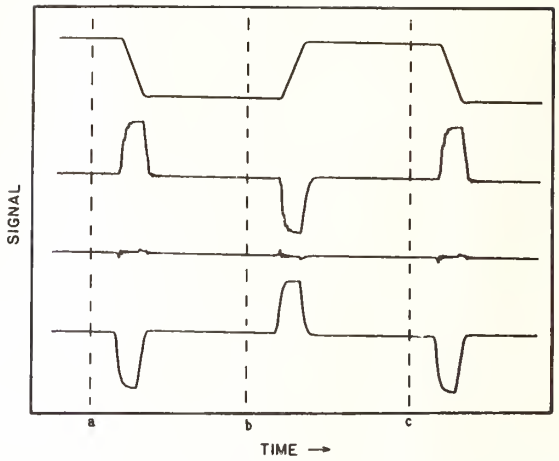

Fig. 3. Injection current and resulting signal. Upper trace: current injected into a portion of the solenoid. Second trace: voltage observed across the pick-up coils when the probe is displaced +250 μm from the center of the activated loop. Third trace: probe is centered. Bottom trace: probe is displaced −250 μm. Letters indicate various times along the oscilloscope trace.

Another source of systematic error is very important and its elimination of interest. If the injected current is a sinewave, then an "end effect" error is introduced. Because this current induces a voltage in the other windings of the solenoid and because there is some capacitance between turns, some current flows in these windings, thereby producing an error signal in the pick-up coils [5]. This effect varies inversely with the square of the frequency and increases as the injection position approaches the end of the solenoid. We eliminate it by employing the special waveform for the injected current shown in the upper trace of Fig. 3. (This waveform is now generated by a digital waveform generator.) The output of the detector coil is just the derivative of the injected current. The second trace of Fig. 3 shows this output and results when the probe is +250 μm off null; the last trace is the output for −250 μm off null. In the next to last trace we are locked to the null. Using a lock-in amplifier with a flat frequency response, we can look at the integral of the output voltage from time a to time b, minus the integral from *b* to *c*. This integral is proportional to the mutual inductance or total flux change in the pick-up coil. The transient signals, however, integrate to zero. The effectiveness of this method is demonstrated by either showing that the null position is independent of frequency or that it is independent of the phase of the lock-in. We find an error of less than 0.04 μm for a phase shift of up to 90°.

The entire system is automated with a PDP-11 computer and CAMAC interface. The laser interferometer is a two-frequency, Zeeman-split laser system manufactured by Hewlett-Packard, and its frequency is measured against an iodine stabilized laser [6]. The entire interferometer is in a vacuum, so there is no correction due to the index of refraction of air. The laser and probe displacement are aligned by using split photo diodes. With these diodes we can keep the alignment error to less than 0.01 ppm.

Fig. 4 shows measurements of the new solenoid in the critical central region (±600 mm). We are now concentrating on this region because the uncertainty in the calculated field due

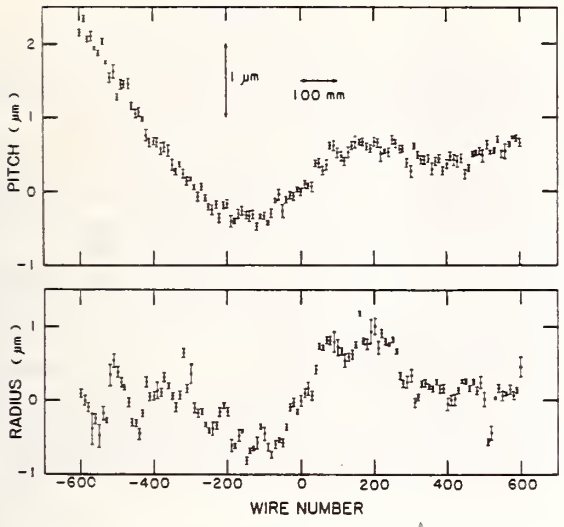

Fig. 4. Radial variations (bottom) in μm and axial position variations (top) in micrometers versus wire number (~1 mm/wire number). The radial variations are with respect to the center wires. For the axial variations a uniform pitch of 1.058588936 mm/turn has been subtracted from the laser interferometer reading at each wire number. The error bars are meant to represent one standard deviation uncertainty estimates.

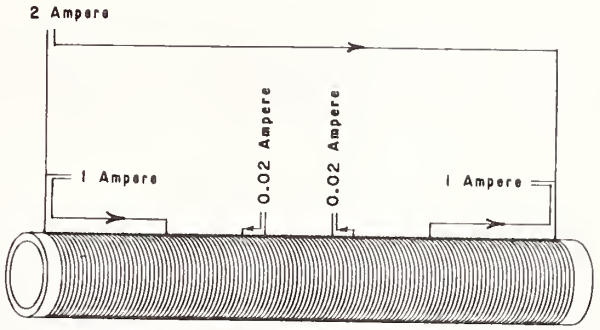

Fig. 5. Compensation scheme for obtaining an "infinite" solenoid for NMR measurements. By using five current sources connected as indicated, a magnetic field is produced that is both uniform to 2 parts in 10^8 over a 6-cm sphere and essentially independent of the average diameter of the solenoid. Leakage between the five current sources must be kept very low.

to the measurement uncertainty of the outer windings is significantly less. Current is injected into 10 turns at a time, so that the data plotted is the average position of the ten turns. The axial variations are a measure of turn position after a uniform pitch of 1.058588936 mm/turn has been subtracted from the laser readings of that position. The radial variations are a plot of the difference in radius of the ten turns at the indicated axial position relative to the center ten turns. These measurements show that the current in the solenoid flows within a few micrometers of where current in a perfect solenoid would flow.

IV. The Diameter Problem

With the high accuracy of the radius variation and pitch measurements, the diameter measurement should be the limiting factor in the experiment. The basic problem in determining the diameter is that even if one makes a perfect measurement of the position of the surface of the copper wire, it is still difficult to know where the current flows in the wire. The technique developed to eliminate the need for a diameter measurement is to find a coil geometry which produces a magnetic field that is nearly independent of the average diameter. With a long solenoid we are able to find a suitable configuration in which extra current can be added to selected turns near the end of the solenoid. If done properly, this, in effect, gives us the same properties of an infinitely long solenoid; namely, that the magnetic field is independent of diameter and is uniform at the center. With the aid of a computer, we found a configuration where the sum of the radius-variation weighting factor for each turn approaches zero, and the second-, fourth-, and sixth-order gradients are compensated. The result (see Fig. 5) is that our solenoid can produce a field that has the same diameter dependence as a 1-km long solenoid (i.e., the uncertainty due to the diameter measurement is essentially eliminated) and a field that is uniform to 2 parts in 10^8 over a 6-cm diam spherical volume at the center of the solenoid. (The water sample for the NMR measurements need only be 4 cm in diameter.)

V. Other Improvements

There is a remote chance that leakage between two adjacent turns will cause an error in the calculated field. For our single helix solenoid a resistance of 30 kΩ across the most critical wires will result in a 0.01 ppm error. The problem is that the low resistance of the winding makes such leakage difficult to detect. The technique we have developed to avoid this problem is very simple: We inject a dc current (5 A) into each turn, one turn at a time. If there is leakage to an adjacent turn, a leakage current will flow in it. However, the finite resistance of that turn produces a small voltage drop that can be detected with a pair of potential leads connected to the neighboring wire. A leakage of 30 kΩ gives a voltage of 3×10^{-8} V; and using a sensitive null detector and an automated system, we can test every wire.

The other major problem that we plan to solve is the correction for the magnetic susceptibility of the fused silica cylinder. We have taken three core samples and from their measured small susceptibilities have calculated that the correction to the magnetic field is very small (<0.01 ppm), but this assumes that the form is homogeneous. To verify that it is in fact homogeneous, we must measure the susceptibility correction directly. To this end, we have constructed a large (0.6 m diam by 2.2 m long) solenoid wound on a fused-silica cylinder. We will measure changes in the field produced by this large solenoid as we lower our precision solenoid in and out of this field. We must detect changes of 0.01 ppm to measure the susceptibility correction to the same accuracy.

VI. Conclusion

We are presently measuring our new solenoid with an accuracy of 0.05 ppm. We have a precision of 0.02 ppm and expect to improve the accuracy of the measurements to this level.

We plan to carry out the NMR part of the experiment within the next four to six months. This should give us a 0.1 ppm preliminary value of γ_p'. We then plan to spend another year

testing for systematic effects before obtaining final results. Ultimately we hope to obtain a value of $\gamma'_p(\text{low})_{\text{NBS}}$ with an uncertainty of 0.05 ppm or less, which should yield a value of α with an uncertainty of about 0.02 ppm.

Acknowledgment

The authors would like to thank E. Muth and D. Trammell for their dedication in helping to construct the solenoid; H. Layer who calibrated the laser; G. Barrett who helped analyze data; K. Maruyama, an NBS Guest Scientist from the Tokyo Institute of Technology, Japan, who designed the injector probe, and F. Fickett, of NBS/Boulder, for measuring the susceptibility of the solenoid form material.

References

[1] E. R. Williams and P. T. Olsen, "New measurement of the proton gyromagnetic ratio and a derived value of the fine-structure constant accurate to a part in 10^7," *Phys. Rev. Lett.*, vol. 42, pp. 1575-1579, June 1979.

[2] E. R. Williams, P. T. Olsen, and W. D. Phillips, "The proton gyromagnetic ratio in H_2O—a problem in dimensional metrology," in *Precision Measurement and Fundamental Constants II*, Natl. Bur. Stand. (U.S.), Spec. Publ. 617 (USGPO, Washington, DC), B. N. Taylor and W. D. Phillips, Eds., 1984, pp. 497-504.

[3] H. L. Curtis, C. Moon, and C. M. Sparks, "A determination of the absolute Ohm, using an improved self inductor," *J. Res. Natl. Bur. Stand.*, vol. 21, pp. 375-423, Oct. 1938, and private communication with R. L. Driscoll.

[4] E. R. Williams and P. T. Olsen, "A noncontacting magnetic pickup probe for measuring the pitch of a precision solenoid," *IEEE Trans. Instrum. Meas.*, vol. IM-21, pp. 376-379, Nov. 1972.

[5] H. P. Layer, "A portable iodine stabilized helium-neon laser," *IEEE Trans. Instrum. Meas.*, vol. IM-29, pp. 358-361, Dec. 1980.

Journal of Research of the National Bureau of Standards
Volume 90, Number 2, March–April 1985

New Results From Previously Reported NBS Fundamental Constant Determinations

B. N. Taylor
National Bureau of Standards, Gaithersburg, MD 20899

Accepted: December 13, 1984

A new treatment of previously reported results of three electric-unit-dependent fundamental constant experiments carried out at NBS over the last decade or so yields accurate, indirect values in SI units for a number of important quantities. These include the fine-structure constant α, the Avogadro constant N_A, the Josephson frequency-voltage ratio $2e/h$, and the quantized Hall resistance $R_H \equiv h/e^2$.

Key words: Avogadro constant; Faraday constant; fine-structure constant; Josephson frequency-voltage ratio; proton gyromagnetic ratio; quantized Hall resistance.

1. Introduction

Over the last decade or so the National Bureau of Standards (NBS) has reported the results of three high accuracy fundamental constant determinations carried out in terms of NBS as-maintained electrical units. The three quantities are the Faraday constant F_{NBS} determined in 1975 using a silver-perchloric acid coulometer [1][1]; the low field gyromagnetic ratio of the proton $(\gamma'_{p,L})_{NBS}$ measured in 1978 using the so-called weak or low field method (the prime means the protons are in a spherical sample of pure H_2O at 25 °C) [2]; and the quantized Hall resistance $(R_H)_{NBS} \equiv (h/e^2)_{NBS}$ (h is the Planck constant and e the elementary charge) determined in 1983–1984 [3][2] using the quantum Hall effect [6] in GaAs-$Al_xGa_{1-x}As$ heterostructures. Here and throughout this paper the subscript NBS indicates NBS electrical units; lack of a subscript indicates *Le Système International d'Unités* (SI) units.

The NBS as-maintained electrical units in terms of which F_{NBS}, $(\gamma'_{p,L})_{NBS}$, and $(R_H)_{NBS}$ have been measured are $(V_{NBS}/\Omega_{NBS}) = A_{NBS}$ and Ω_{NBS}. Here V_{NBS} is the NBS volt maintained constant in time since 1972 July 1 using the ac Josephson effect with an uncertainty of a few parts in 10^8, the value of the Josephson frequency-voltage ratio $2e/h$ adopted for this purpose being [7]

$$(2e/h)_{NBS} = 483593.420 \text{ GHz}/V_{NBS}. \quad (1)$$

This implies that the ratio $K_V \equiv V_{NBS}/V$, where V is the SI volt, is given by

$$K_V \equiv V_{NBS}/V \quad (2a)$$

$$= (2e/h)_{NBS}/(2e/h) \quad (2b)$$

and may be assumed to be time invariant within a few parts in 10^8.

The quantity Ω_{NBS} is the NBS ohm defined in terms of the mean resistance of five wire-wound, one-ohm resistors of the Thomas-type. Because Ω_{NBS} is based on artifact standards, one must assume that it is a time-varying unit. This implies that the ratio

About the Author: B. N. Taylor, a physicist, is chief of the Electricity Division in the NBS Center for Basic Standards.

[1]Numbers in brackets indicate literature references.

[2]The result reported in Ref. [3] supplants entirely that given in Ref. [4] since the temperature dependence of R_H, as described in Ref. [5], was not properly taken into account in the earlier work of Ref. [4]. We assume throughout this paper that the quantized Hall resistance is a legitimate measure of h/e^2, i.e., that any corrections are negligibly small.

$$K_\Omega \equiv \Omega_{NBS}/\Omega \tag{3}$$

also varies with time.

The NBS ampere A_{NBS} is not separately maintained but is defined in terms of the NBS ohm and volt: $A_{NBS} = V_{NBS}/\Omega_{NBS}$. It thus follows that A_{NBS} also varies with time as does the ratio

$$K_A \equiv A_{NBS}/A \tag{4a}$$

$$= K_V/K_\Omega \ . \tag{4b}$$

The actual NBS electrical units in terms of which F_{NBS}, $(\gamma'_{p,L})_{NBS}$, and $(R_H)_{NBS}$ were measured are, respectively, A_{NBS}, A_{NBS}^{-1}, and Ω_{NBS}. Because A_{NBS} and Ω_{NBS} are time varying units as just discussed and the three experiments were carried out over a 10-year period, the three results cannot be readily combined to obtain values for other quantities such as the fine-structure constant α and Avogadro constant N_A. This is unfortunate since, had they been measured at the same time, it would have been a straightforward procedure to derive accurate, indirect values in SI units for these constants as well as for most others of interest. The relevant equations for doing so may be obtained from the known relationships among the constants [8–11]; some of the more important expressions are:

$$\alpha^{-1} = \left[\frac{(\mu'_p/\mu_B)}{2\mu_0 R_\infty} \frac{R_H(t)_{NBS}(2e/h)_{NBS}}{\gamma'_{p,L}(t)_{NBS}}\right]^{1/3} \tag{5}$$

$$N_A = [R_H(t)_{NBS}(2e/h)_{NBS}F(t)_{NBS}]/2 \tag{6}$$

$$2e/h = \left[\frac{16^2 R_\infty^{\,2}(\mu'_p/\mu_B)(m_p/m_e)^3}{\mu_0^{\,4} c^6 M_p^{\,3}}\right.$$

$$\left. \times \frac{R_H(t)_{NBS}^4 (2e/h)_{NBS}^4 F(t)_{NBS}^3}{\gamma'_{p,L}(t)_{NBS}}\right]^{1/6} \tag{7}$$

$$R_H = \mu_0 c \alpha^{-1}/2 = R_H(t)_{NBS} K_\Omega(t)_{NBS} \tag{8a}$$

$$= \left[\frac{\mu_0^2 c^3 (\mu'_p/\mu_B)}{16 R_\infty} \frac{R_H(t)_{NBS}(2e/h)_{NBS}}{\gamma'_{p,L}(t)_{NBS}}\right]^{1/3} \tag{8b}$$

$$F = \left[\frac{M_p}{(\mu'_p/\mu_B)(m_p/m_e)} \gamma'_{p,L}(t)_{NBS} F(t)_{NBS}\right]^{1/2} \tag{9}$$

$$K_\Omega(t) = \left[\frac{\mu_0^2 c^3 (\mu'_p/\mu_B)}{16 R_\infty} \frac{(2e/h)_{NBS}}{R_H(t)_{NBS}^2 \gamma'_{p,L}(t)_{NBS}}\right]^{1/3}, \tag{10}$$

where the time dependencies of $(R_H)_{NBS}$, $(\gamma'_{p,L})_{NBS}$, and F_{NBS} have been explicitly indicated [$(2e/h)_{NBS}$ is time independent since V_{NBS} is defined in terms of it through eq (1)]. In these expressions $\mu_0 \equiv 4\pi \times 10^{-7}$ H/m is the permeability of vacuum; $c \equiv 299792458$ m/s is the speed of light in vacuum; μ'_p/μ_B is the magnetic moment of the proton in units of the Bohr magneton (0.012 parts-per-million or ppm current uncertainty[3]); R_∞ is the Rydberg constant for infinite mass (0.0010 ppm current uncertainty); M_p is the molar mass of the proton (0.012 ppm current uncertainty); and m_p/m_e is the ratio of the proton mass to the electron mass (0.043 ppm current uncertainty).

In the past, these and related expressions have been evaluated by assuming that Ω_{NBS} has been constant in time and by allowing an additional uncertainty of about 0.01 ppm per year for its possible drift [1,2,4]. However, recent comparisons of Ω_{NBS} with the resistance units of other national laboratories show that since about 1970 the NBS ohm has likely been decreasing by approximately 0.06 ppm/yr. In the course of reviewing the implications of such a drift on eqs (5–10), it became apparent that the problem of the time variation of Ω_{NBS} could be neatly solved by making use of one other NBS result, namely, the determination in 1973–1974 via the NBS calculable cross capacitor of the ratio $K_\Omega \equiv \Omega_{NBS}/\Omega$ [12]. With the addition of this single measurement, the drift rate of the NBS ohm may be uniquely determined, the values of $(R_H)_{NBS}$, $(\gamma'_{p,L})_{NBS}$, and F_{NBS} converted to the same measurement date, and eqs (5–10) and their numerous extensions readily evaluated. The only critical assumption required is that the drift of the NBS ohm has been linear since the time of the calculable capacitor determination of K_Ω. However, this is supported by the observed linear time dependencies of the measured differences between each of the five resistors which comprise Ω_{NBS} and their mean [13].

We now briefly summarize how the calculation proceeds. The linear drift rate assumption enables one to write

$$K_\Omega(t) \equiv \Omega(t)_{NBS}/\Omega = K_\Omega(t_\Omega)[1 + b(t - t_\Omega)], \tag{11}$$

where t is the time in years measured from some arbitrary date, t_Ω is the mean date of the NBS calculable capacitor experiment with $K_\Omega(t_\Omega)$ the mean value obtained, and b is the relative drift rate of Ω_{NBS}.[4] It then

[3] Throughout, all uncertainties are one standard deviation estimates.

[4] The time period over which K_Ω was measured was sufficiently short and the random scatter sufficiently large that the effect of the drift of Ω_{NBS} was indiscernible and hence negligible. This is also true of the measurements of F_{NBS}, $(\gamma'_{p,L})_{NBS}$, and $(R_H)_{NBS}$.

follows from this equation and the way Ω_{NBS} enters the determination of F_{NBS}, $(\gamma'_{p,L})_{NBS}$, and $(R_H)_{NBS}$ that

$$F(t)_{NBS}=F(t_F)_{NBS}[1+b(t-t_F)] \quad (12)$$

$$\gamma'_{p,L}(t)_{NBS}=\gamma'_{p,L}(t_\gamma)_{NBS}[1-b(t-t_\gamma)] \quad (13)$$

$$R_H(t)_{NBS}=R_H(t_R)_{NBS}[1-b(t-t_R)], \quad (14)$$

where t_F, t_γ, and t_R are the mean dates of the Faraday constant, proton gyromagnetic ratio, and quantized Hall resistance determinations, respectively, and $F(t_F)_{NBS}$, $\gamma'_{p,L}(t_\gamma)_{NBS}$, and $R_H(t_R)_{NBS}$ are the mean values obtained. The drift rate b may then be calculated by substituting eq (13) for $\gamma'_{p,L}(t)_{NBS}$ into eq (10) and equating the result to eq (11) with $t=t_R$. Once b is in hand, eqs (5–10) may be evaluated with the aid of eqs (12–14). Of course, the law of error propagation must be strictly obeyed in order to obtain correct uncertainties for the calculated quantities.

We have carried out such calculations with the data listed in tables 1 and 2, to which these comments apply:

Table 1. The values quoted for the nonexact constants are based on the results reported in the original references and (with the exception of m_p/m_e) analyses carried out by the author in connection with the 1985 least squares adjustment of the fundamental constants [14]. However, these analyses have generally led to only minor changes in the original results.

Table 2. Only the value of F_{NBS} has been at all changed from that originally reported. The 0.2 ppm net increase arises from a number of positive and negative corrections. New measurements of the Au and Ta impurity content of the silver used in the experiment [20] were specifically undertaken as a result of the author's reanalysis of the experiment for the 1985 adjustment. It should be noted that the 0.031 ppm uncertainty assigned $(2e/h)_{NBS}$ is an estimate of how well the NBS Josephson effect voltage standard apparatus implements the definition of V_{NBS} [see eq (1)]. The uncertainties associated with relating the working voltage standards used in the $(\gamma'_{p,L})_{NBS}$ and F_{NBS} experiments to the voltage standards used to preserve or store V_{NBS} between Josephson effect calibrations are included in the uncertainties assigned F_{NBS} and $(\gamma'_{p,L})_{NBS}$ as given in the table.

The results of the calculations are:

$$\alpha^{-1}=137.035981(12)\ (0.089\ \text{ppm}) \quad (15)$$

$$R_H=25812.8041(23)\ \Omega\ (0.089\ \text{ppm}) \quad (16)$$

$$2e/h=483597.91(32)\ \text{GHz}\cdot\text{V}^{-1}\ (0.67\ \text{ppm}) \quad (17)$$

$$N_A=6.0221438(80)\times10^{23}\ \text{mol}^{-1}\ (1.33\ \text{ppm}) \quad (18)$$

$$F=96485.381(65)\ \text{A}\cdot\text{s}\cdot\text{mol}^{-1}\ (0.67\ \text{ppm}), \quad (19)$$

Table 1. Summary of defined and electric-unit-independent constants used to evaluate eqs (5–10).

Quantity	Numerical value[1]	Uncertainty (ppm)	Refs.
μ_0	$4\pi\times10^{-7}$	defined	
c	299792458	defined	
μ'_p/μ_B	0.001520993127(18)	0.012	[15,14]
R_∞	10973731.529(11)	0.0010	[16,17,14]
M_p	0.001007276470(12)	0.012	[18,14]
m_p/m_e	1836.152470(79)	0.043	[19]

[1]The units for μ_0 are $\text{H}\cdot\text{m}^{-1}$; for c, $\text{m}\cdot\text{s}^{-1}$; for R_∞, m^{-1}; for M_p, $\text{kg}\cdot\text{mol}^{-1}$.

Table 2. Summary of NBS electric-unit-dependent data used to evaluate eqs (5–10).

Quantity	Mean date of measurement	Value[1]	Uncertainty (ppm)	Refs.
$(2e/h)_{NBS}$	Continuous since 1972 July 1	483593.420(15)	0.031	[7]
F_{NBS}	1975 March 15	96486.19(13)	1.33	[1,20,14]
$(\gamma'_{p,L})_{NBS}$	1978 March 22	2.67513229(57)	0.21	[2]
$(R_H)_{NBS}$	1983 November 27	25812.8420(12)	0.047	[3]
$K_\Omega\equiv\Omega_{NBS}/\Omega$	1973 December 2	$1-0.819(27)\times10^{-6}$	0.027	[12]

[1]The units for $(2e/h)_{NBS}$ are $\text{GHz}\cdot\text{V}_{NBS}^{-1}$; for F_{NBS}, $\text{A}_{NBS}\cdot\text{s}\cdot\text{mol}^{-1}$; for $(\gamma'_{p,L})_{NBS}$, $10^8\ \text{s}^{-1}\cdot\text{T}_{NBS}^{-1}$; for $(R_H)_{NBS}$, Ω_{NBS}. Note that in the $(\gamma'_{p,L})_{NBS}$ experiment the NBS tesla $T_{NBS}\propto A_{NBS}$.

with $b = (-0.0650 \pm 0.0102)$ ppm/yr.[5] The value for K_Ω on 1985 January 1 is $1-(1.539\pm0.107)$ ppm. While it is not the purpose of this paper to make detailed comparisons of these results with others obtained by either direct or indirect means, we do note that in most cases where other values exist the agreement is statistically acceptable. We further point out that the value of $2e/h$ derived here is (9.29 ± 0.67) ppm larger than the value used to define V_{NBS}, implying that V_{NBS} is (9.29 ± 0.67) ppm smaller than the SI volt [see eq (2b)]. This value of $2e/h$ is also (8.09 ± 0.67) ppm larger than the value 483594 GHz/V which is in use in many other national laboratories and which was recommended by the Comité Consultatif d'Electricité in 1972 [23].

In closing we emphasize that the values given here for the various constants, in particular the fine-structure constant, *are the best that can be obtained based solely on existing NBS electrical measurements*.[6] If the three quantities $(\gamma'_{p,L})_{NBS}$, $(R_H)_{NBS}$, and K_Ω had been determined at the same time, then any two would have been sufficient to determine α^{-1}. For example, eq (5) yields a value of α^{-1} from $(\gamma'_{p,L})_{NBS}$ and $(R_H)_{NBS}$. The comparable equations for the two other pairs of measurements are[7]

$$\alpha^{-1} = \left[\frac{c(\mu'_p/\mu_B)}{4R_\infty}\frac{(2e/h)_{NBS}}{K_\Omega(\gamma'_{p,L})_{NBS}}\right]^{1/2} \tag{20}$$

$$\alpha^{-1} = 2(R_H)_{NBS}K_\Omega/\mu_0 c. \tag{21}$$

By treating the drift rate of the NBS ohm as a variable we remove the redundancy or overdetermination inherent in the three measurements and obtain a unique value for α^{-1} and all other quantities. Since this approach eliminates the distinction between the so-called Josephson effect value of α^{-1} traditionally derived from eq (20) and the quantum Hall effect value derived from eq (21), perhaps the value given here should simply be referred to as the NBS condensed matter value.

I gratefully acknowledge helpful discussions with B. F. Field and E. R. Williams and the assistance of V. E. Bower, R. S. Davis, E. R. Williams, P. T. Olsen, M. E. Cage, R. F. Dziuba, and B. F. Field in reviewing their experiments. The data analyses carried out in connection with the 1985 least squares adjustment of the fundamental constants were performed in collaboration with E. R. Cohen.

References

[1] Bower, V. E., and R. S. Davis, J. Res. Natl. Bur. Stand. **85**, 175 (1980)/Powell, L. J.; T. J. Murphy and J. W. Gramlich, J. Res. Natl. Bur. Stand. **87**, 9 (1982)/Bower, V. E.; R. S. Davis, T. J. Murphy, P. J. Paulsen, J. W. Gramlich, and L. J. Powell, J. Res. Natl. Bur. Stand. **87**, 21 (1982).

[2] Williams, E. R., and P. T. Olsen, Phys. Rev. Lett. **42**, 1575 (1979).

[3] Cage, M. E.; R. F. Dziuba and B. F. Field, IEEE Trans. Instrum. Meas. **IM-34**, June 1985, to be published.

[4] Tsui, D. C.; A. C. Gossard, B. F. Field, M. E. Cage, and R. F. Dziuba, Phys. Rev. Lett. **48**, 3 (1982).

[5] Cage, M. E.; B. F. Field, R. F. Dziuba, S. M. Girvin, A. C. Gossard, and D. C. Tsui, Phys. Rev. B **30**, 2286 (1984).

[6] Klitzing, K.V.; G. Dorda and M. Pepper, Phys. Rev. Lett. **45**, 494 (1980).

[7] Field, B. F.; T. F. Finnegan and J. Toots, Metrologia **9**, 155 (1973).

[8] Taylor, B. N., IEEE Trans. Instrum. Meas. **IM-34**, June 1985, to be published.

[9] Taylor, B. N., Metrologia **12**, 81 (1976); Metrologia **9**, 21 (1973).

[10] Cohen, E. R., and B. N. Taylor, J. Phys. Chem. Ref. Data **2**, 663 (1973).

[11] Taylor, B. N.; D. N. Langenberg and W. H. Parker, Rev. Mod. Phys. **41**, 375 (1969).

[12] Cutkosky, R. D., IEEE Trans. Instrum. Meas. **IM-23**, 305 (1974).

[13] Dziuba, R. F., private communication (1984).

[14] Cohen, E. R., and B. N. Taylor, J. Phys. Chem. Ref. Data, to be published.

[15] Phillips, W. D.; W. E. Cooke and D. Kleppner, Metrologia **13**, 179 (1977).

[16] Amin, S. R.; C. D. Caldwell and W. Lichten, Phys. Rev. Lett. **47**, 1234 (1981).

[17] Goldsmith, J. E. M.; E. W. Weber and T. W. Hänsch, Phys. Rev. Lett. **41**, 1525 (1978).

[18] Wapstra, A. H., and G. Audi, Nucl. Phys. A, to be published.

[19] Van Dyck, R. S. Jr.; F. L. Moore and P. B. Schwinberg, Bull. Am. Phys. Soc. **28**, 791 (1983) and private communication (1983).

[20] Greenberg, R. R., private communication (1984).

[21] Thompson, A. M., Metrologia **4**, 1 (1968)/Clothier, W. K., Metrologia **1**, 35 (1965).

[22] Leclerc, G., and T. J. Witt, private communication (1984).

[23] Com. Int. Poids Mes., Com. Consult. d'Electricité Trav. 13e Session (1972) p. E-13.

[5] This value is in agreement with $b = -(0.0562\pm0.0048)$ ppm/yr which the author derived from a linear least squares fit to the results of direct and indirect comparisons of Ω_{NBS} with the unit of resistance Ω_{NML} maintained constant in time by Australia's National Measurement Laboratory (NML) with the NML calculable cross capacitor [21]. We also note that the Bureau International des Poids et Mesures unit of resistance Ω_{BIPM} is based on the mean of six resistors, two of which are of the same type used to define Ω_{NBS}. Comparisons of Ω_{BIPM} with Ω_{NML} dating back to 1964 show that Ω_{BIPM} varies quite linearly with time. Since the time dependencies of the measured differences between Ω_{BIPM} and each of the two NBS resistors which partially define Ω_{BIPM} are also observed to be linear [22], it may be concluded that the linear drift rate assumption for Ω_{NBS} is justified. If in fact one assumes the existence of a quadratic component, any reasonable estimate of its magnitude is sufficiently small that its effect is inconsequential.

[6] "Best" or "recommended" values in the traditional sense would, of course, require taking into account the relevant data available from all sources.

[7] Note that eliminating K_Ω from eqs (20) and (21) yields eq (5) while equating the two yields eq (10).

Electrical Units, Fundamental Constants, and the 1983 Least Squares Adjustment

BARRY N. TAYLOR, FELLOW, IEEE

Abstract—This review touches upon four topics: (1) The International System or SI electrical units, specifically, the volt (V), ohm (Ω), ampere (A), and the so-called laboratory or as-maintained units for the same quantities; (2) the relationships between these laboratory units, experiments to realize their SI definitions, and the fundamental constants of nature; (3) the 1983 least squares adjustment of the constants; and (4) future electrical measurements research which can improve our knowledge of the constants.

I. Units

THIS section reviews the International System or SI definitions of the SI *base* electrical unit, the ampere, and the two most often used *derived* electrical units, the volt and ohm; how in practice these three units are represented in the laboratory; and how these practical laboratory representations are maintained.

A. SI Electrical Units

The ampere is related to the three SI *base* mechanical units, the second, meter, and kilogram [1], [2]. The second is defined as the duration of 9 192 631 770 periods of the radiation corresponding to the transition between the two hyperfine levels of the ground state of the cesium 133 atom.

The meter is defined as the length of the path travelled by light in vacuum in 1/299 792 458 of a second. This is equivalent to adopting an exact value for the speed of light in vacuum c, namely,

$$c \equiv 299\ 792\ 458 \text{ m/s}. \tag{1}$$

The kilogram, the only SI unit still based on an artifact, is defined as the mass of the international prototype of the kilogram kept at the International Bureau of Weights and Measures (BIPM) in Sèvres, France (a suburb of Paris).

The SI unit of force, the newton (N), is *derived* from these three base mechanical units using Newton's second law; it is defined as that force which gives to a mass of one kilogram an acceleration of one meter per second, per second. Thus $1\ \text{N} = 1\ \text{kg} \cdot \text{m} \cdot \text{s}^{-2}$. The SI unit of energy, the joule (symbol J), is derived from the newton and meter and is defined as the work done when the point of application of a 1-N force moves a distance of 1 m in the direction of the force. Hence $1\ \text{J} = 1\ \text{N} \cdot \text{m}$. Finally, the SI unit of power, the watt (W), is derived from the joule and the second, and is defined as the power which in one second gives rise to energy of one joule. Thus $1\ \text{W} = 1\ \text{J} \cdot \text{s}^{-1}$.

Manuscript received September 26, 1984.

The author is with the Electricity Division, National Bureau of Standards. Gaithersburg, MD 20899.

The ampere is then defined as that constant current which, if maintained in two straight parallel conductors of infinite length, of negligible cross section, and placed one meter apart in vacuum, would produce between these conductors a force equal to 2×10^{-7} N/m of length. This definition implies via the Biot-Savart law that the magnetic permeability of vacuum μ_0 is an exact constant given by

$$\mu_0 \equiv 4\pi \times 10^{-7}\ \text{N/A}^2. \tag{2}$$

The SI units for potential difference (electromotive force) and electric resistance, the volt (V) and the ohm (Ω), respectively, are then *derived* from the watt (and thus the three base mechanical units) and from the base electrical unit, the ampere, as follows:

The volt is the difference of electric potential between two points of a conducting wire carrying a constant current of 1 A, when the power dissipated between these points is equal to 1 W.

The ohm is the electric resistance between two points of a conductor when a constant potential difference of 1 V, applied to these points, produces in the conductor a current of 1 A, the conductor not being the seat of any electromotive force.

B. Laboratory or As-Maintained Electrical Units

Because the SI definitions of the volt (V), ohm (Ω), and ampere (A) are difficult to realize in practice, national standards laboratories (such as the National Bureau of Standards in the U.S.) have historically used practical representations of them based on artifacts. For example, a group of electrochemical standard cells of the Weston type (each with an EMF of order 1.018 V) may serve to define the laboratory or as-maintained unit of voltage V_{LAB}, and a group of precision wire-wound resistors of the Thomas or similar type (each with a resistance of order 1 Ω) may serve to define the laboratory or as-maintained unit of resistance Ω_{LAB} [3]. The laboratory unit of current A_{LAB} is then defined in terms of V_{LAB} and Ω_{LAB} via

$$A_{\text{LAB}} = V_{\text{LAB}}/\Omega_{\text{LAB}} \tag{3}$$

and does not have its own separate representation.

Such an as-maintained system of electrical units immediately raises two questions: 1) How does one ensure that V_{LAB} and Ω_{LAB} are *contant in time*, based as they are on artifacts? 2) How does one ensure that V_{LAB} and Ω_{LAB} are *consistent with*

their SI definitions? Problem 1 introduces the idea of monitoring or *maintaining* laboratory units while Problem 2 introduces the idea of carrying out *absolute realizations* of the SI electrical units. Ideally, one would like to solve both problems simultaneously, that is, maintain a unit constant in time and consistent with its SI definition by the same means, at the same time, and at a level of accuracy which is in keeping with the inherent stability of the artifacts. However, because this stability is at the level of parts in 10^7 per year (or for some very well-aged cells and resistors at the level of parts in 10^8 per year), it has not yet proved feasible to do so in most laboratories. The two problems are, therefore, considered separately.

C. Maintaining Laboratory Units

Most national laboratories now use the ac Josephson effect in superconductors to maintain their unit of voltage. For our purposes a Josephson device may be viewed as a perfect frequency-to-voltage converter, the constant of proportionality being the invariant fundamental constant ratio $2e/h$ (e is the elementary charge, h is the Planck constant). Because frequencies can be readily measured to very high accuracy (parts in 10^{13} if necessary), the Josephson effect can be used to define and maintain V_{LAB} to an accuracy limited only by the accuracy with which the voltage across the Josephson device can be compared with the EMF of a standard cell. Typically this is in the range 0.01–0.1 parts-per-million (symbol ppm). (Throughout this paper all uncertainties are meant to correspond to one standard deviation estimates.) The defining equation for V_{LAB} is

$$(2e/h)_{LAB} \equiv 483\ 59?\ \text{GHz}/V_{LAB} \tag{4}$$

where $(2e/h)_{LAB}$ is the specific value of $2e/h$ adopted by the laboratory to define V_{LAB}. (The question mark is meant to indicate that several different values are in use at the various national laboratories; 483 594 is the most common numerical value.) The standard cell now serves only as a "flywheel," that is, as a means of preserving or storing V_{LAB} between Josephson effect measurements.

While not yet in as wide a use as the Josephson effect, the quantum Hall effect (QHE) [4] promises to do for resistance-unit maintenance what the Josephson effect has done for voltage-unit maintenance. For our purposes a QHE device can be viewed as a resistor the resistance of which depends only on the fundamental constant ratio h/e^2. Thus the QHE, which manifests itself in certain semiconductor devices when cooled to cryogenic temperatures and in the presence of a large magnetic field, can be used to define and maintain Ω_{LAB} to an accuracy limited only by the accuracy with which the resistance of the device can be compared with the resistance of a 1-Ω resistor. Eventually this is expected to be in the range 0.01 to 0.1 ppm for all laboratories; 0.05 ppm is the smallest uncertainty reported to date. The defining equation for Ω_{LAB} is

$$(h/e^2)_{LAB} \equiv 25\ 812.8?\ \Omega_{LAB} \tag{5}$$

where, by analogy with (4), $(h/e^2)_{LAB}$ is the specific value of h/e^2 adopted by the laboratory to define Ω_{LAB}. (In this case the question mark means that a specific value has yet to be adopted by any laboratory.) The combination of constants h/e^2 has been termed the quantum Hall resistance R_H. It is related to the inverse fine-structure constant α^{-1} (which is ≅137), the dimensionless coupling constant or fundamental parameter of quantum electrodynamic theory (QED), by

$$h/e^2 \equiv R_H = \mu_0 c\alpha^{-1}/2. \tag{6}$$

Since μ_0 and c are exact constants, if α^{-1} is known with a given uncertainty, R_H will be known with the same uncertainty. By analogy with the standard cell, the 1-Ω resistor now serves only to store Ω_{LAB} between QHE measurements.

II. Absolute Realizations and Fundamental Constants

While the Josephson and quantum Hall effects allow V_{LAB} and Ω_{LAB} to be maintained constant in time to between 0.01 and 0.1 ppm, thereby solving Problem 1 of Section I-B, unless $2e/h$ and R_H are known in SI units to the same level of accuracy, the as-maintained and SI systems of electrical units will not be consistent and Problem 2 will remain unsolved. In practice there are two general approaches to determining $2e/h$ and R_H in SI units. The first is to carry out experiments to realize *directly* the SI definitions of V, Ω, and A; the second is to carry out experiments to determine various fundamental constants from which V, Ω, and A may be *indirectly* derived. As will shortly be shown, at the present time the latter approach often yields smaller uncertainties than the former.

A. Absolute Realizations: Direct

Currently, direct absolute realizations of the SI electrical units are based on experiments which use electromagnetic theory in combination with the SI definitions. Experiments to realize the SI electrical units as they are actually defined (see Section I-A) are as yet too imprecise to be of interest. The following is a brief summary of how the SI volt, ohm, and ampere are being realized directly at present.

1) *Volt*: By measuring the force between electrodes to which a voltage known in terms of V_{LAB} has been applied, and the capacitance between the electrodes (determined in SI units via a calculable cross-capacitor), the ratio V_{LAB}/V can be obtained. In practice, determining this ratio is what is meant by the terms "absolute realization of the volt" or "realization of the SI volt." Defining $(K_V)_{LAB} \equiv V_{LAB}/V$ and recognizing that $(2e/h)_{LAB}$ is used to define V_{LAB}, we may write

$$(K_V)_{LAB} \equiv V_{LAB}/V = (2e/h)_{LAB}/(2e/h). \tag{7}$$

A realization of the SI volt is thus equivalent to determining $2e/h$ in SI units (recall that $(2e/h)_{LAB}$ is an adopted number with no uncertainty). The smallest uncertainty reported to date for such an experiment is 2.4 ppm, some two orders of magnitude larger than the uncertainty with which V_{LAB} may be maintained via the Josephson effect.

2) *Ohm*: The SI ohm may be realized using a so-called Thompson-Lampard calculable cross-capacitor which allows the capacitance of a special configuration of electrodes to be calculated (in SI units) to very high accuracy from a single length measurement and the permittivity of vacuum, ϵ_0. (Since $\epsilon_0 = 1/\mu_0 c^2$ and μ_0 and c are exactly known constants, ϵ_0 is also exactly known.) The impedance of the calculable

capacitor is compared with the 1-Ω resistance standards which represent Ω_{LAB} using a complex series of bridges. Defining $(K_\Omega)_{LAB} \equiv \Omega_{LAB}/\Omega$ and recognizing that $(R_H)_{LAB}$ is used to define Ω_{LAB}, we may write

$$(K_\Omega)_{LAB} \equiv \Omega_{LAB}/\Omega = R_H/(R_H)_{LAB}. \quad (8)$$

A realization of the SI ohm is thus equivalent to determining R_H in SI units, which in turn is equivalent to determining the inverse fine-structure constant [see (6)]. The uncertainty in such an experiment is on the order of 0.05–0.1 ppm, comparable to the yearly stability of good resistance standards and the accuracy with which Ω_{LAB} may be currently maintained via R_H. However, because of the complexity of the experiment only one laboratory in the world has yet been able to maintain their laboratory unit of resistance consistently via the calculable capacitor. It would thus appear that the QHE will become the method of choice in most laboratories.

3) *Ampere*: By measuring the force between coils of known dimensions carrying a current known in terms of A_{LAB}, the ratio A_{LAB}/A can be determined. Defining $(K_A)_{LAB} \equiv A_{LAB}$/A, we may write

$$(K_A)_{LAB} \equiv A_{LAB}/A = (K_V)_{LAB}/(K_\Omega)_{LAB}. \quad (9)$$

A realization of the SI ampere measures neither $2e/h$ or R_H but the product $(2e/h)R_H$ [see (7) and (8)], which is equivalent to measuring the elementary charge e in SI units. The smallest uncertainty reported to date for such an experiment is 4 ppm, about two orders of magnitude larger than the uncertainty with which A_{LAB} can be maintained via the Josephson and quantum Hall effects.

B. Absolute Realizations: Indirect

As indicated above, $(K_V)_{LAB}$, $(K_\Omega)_{LAB}$, and $(K_A)_{LAB}$ may also be obtained from appropriate combinations of various fundamental physical constants. The constants required, in addition to the exactly defined quantities μ_0, c, $(2e/h)_{LAB}$, and $(R_H)_{LAB}$ discussed above, are:

1) *Rydberg Constant for Infinite Mass* R_∞:

$$R_\infty = \mu_0^2 c^3 m_e e^4/8h^3$$

where m_e is the mass of the electron. It is determined from high precision laser spectroscopic measurements of the low-lying energy levels of the hydrogen atom and is presently known to an accuracy of 0.0010 ppm (one part in 10^9).

2) *Magnetic Moment of the Proton in* H_2O *in Units of the Bohr Magneton* μ_p'/μ_B: μ_p'/μ_B is determined by comparing the electron spin-flip frequency in the hydrogen atom obtained using a hydrogen maser operating at a magnetic field of several tenths tesla to the proton spin-flip frequency of protons in an H_2O sample in the same magnetic field as measured by nuclear magnetic reasonance (NMR). Its current uncertainty is 0.012 ppm. (The Bohr magneton $\mu_B \equiv eh/2\pi m_e$.)

3) *Molar Mass of the Proton* M_p: M_p, the mass of one mole of protons, is determined via mass spectrometry on the unified atomic mass scale defined such that the molar mass of the ^{12}C atom is exactly 0.012 kg. It has an uncertainty of 0.012 ppm at present.

4) *Ratio of the Proton Mass to the Electron Mass* m_p/m_e: m_p/m_e is obtained from measurements of the cyclotron frequencies of sequentially trapped protons and electrons in a high-magnetic field. Its present uncertainty is 0.043 ppm.

5) *Inverse Fine-Structure Constant* α^{-1}: $\alpha^{-1} = 2h/\mu_0 ce^2$ may be obtained by combining an experimental value for the anomalous magnetic moment of the electron a_e determined from measurements of various resonance frequencies of a single electron trapped in a magnetic field and the theoretical quantum electrodynamic or QED expression for a_e. The uncertainty of $\alpha^{-1}(a_e)$ is currently 0.073 ppm. A value of α^{-1} with a current uncertainty of 0.16 ppm can be obtained by combining measurements of the ground-state hyperfine splitting of muonium ν_{Mhfs} and the ratio of the magnetic moment of the muon to that of the proton μ_μ/μ_p with the theoretical expression for the splitting. (Muonium, Mu, is the μ^+e^- atom where μ^+ is the positive muon.)

6) *Faraday Constant* F: The Faraday constant in laboratory units F_{LAB} is determined electrochemically by measuring via a coulometer the number of moles of a substance such as silver deposited by a known charge. The number of moles is found from the mass of the material deposited and its molar mass, the latter determined in a separate experiment using mass spectrometry. The charge is found from the current measured in terms of A_{LAB} times its duration of flow. The most accurate determination of F_{LAB} to date has an uncertainty of 1.3 ppm.

7) *Gyromagnetic Ratio of the Proton in* H_2O, γ_p': $\gamma_p' = \omega_p'/B$ where ω_p' is the NMR angular frequency of protons in H_2O in an applied magnetic field B. It may be determined by two different methods which in fact yield two different quantities because of the way the laboratory or as-maintained electrical units enter the determination of B. $\gamma_p'(\text{low})_{LAB}$, where the "low" indicates a low magnetic field on the order of 0.001 T, is obtained when B is calculated from the measured dimensions of a precision solenoid carrying a current known in terms of A_{LAB}. $\gamma_p'(\text{high})_{LAB}$, where "high" indicates a high magnetic field on the order of 0.5 T, is obtained when B is determined by measuring the force on a conductor of known dimensions carrying a current known in terms of A_{LAB}. At present the most accurate determinations of $\gamma_p'(\text{low})_{LAB}$ and $\gamma_p'(\text{high})_{LAB}$ have uncertainties of 0.21 and 1.0 ppm, respectively.

8) *Avogadro Constant* N_A: N_A may be obtained from various measurements on a pure, highly perfect, single crystal. The relevant equation for silicon is

$$N_A = \frac{[M(\text{Si})/\rho(\text{Si})]}{\sqrt{8}\, d_{220}^3(\text{Si})}. \quad (10)$$

Here M(Si) is the molar mass of silicon, usually determined via mass spectrometry; ρ(Si) is its density, usually determined via hydrostatic weighing against standards whose densities have been determined from their dimensions and mass; and d_{220} is the (220) lattice plane spacing repeat distance determined via combined X-ray and optical interferometry. The present uncertainty in N_A obtained this way is about 1.3 ppm.

Because the above electric-unit dependent constants (F and γ_p') may not be measured in the same laboratory, they may not be expressed in the same laboratory units. It is possible, however, to re-express all such quantities in terms of a single set of

laboratory units with little loss of accuracy by using the known values of $(2e/h)_{LAB}$ and $(R_H)_{LAB}$ or the results of direct unit comparisons carried out by means of transportable voltage and resistance standards. In what follows it is assumed that all such quantities have been so re-expressed.

Using the above fundamental constants one can derive a number of different equations for the quantities $(K_V)_{LAB}$, $(K_\Omega)_{LAB}$, and $(K_A)_{LAB}$. For example for the volt one has

$$(K_V)_{LAB} = \left[\frac{\mu_0 c^2 M_p (2e/h)^2_{LAB}}{16 R_\infty (m_p/m_e)\alpha^{-1} N_A}\right]^{1/2}. \tag{11}$$

Based on the uncertainties given for the relevant constants entering this relation, it yields an *indirect* value of $(K_V)_{LAB}$ with an uncertainty of about 0.65 ppm, nearly four times less than the uncertainty of the most accurate *direct* volt balance determination. [In this equation and those that follow $(2e/h)_{LAB}$ and $(R_H)_{LAB}$ are taken as exact since they are adopted values used to define V_{LAB} and Ω_{LAB}. The resulting uncertainty for $(K_V)_{LAB}$, $(K_\Omega)_{LAB}$, or $(K_A)_{LAB}$ is then the uncertainty in the relationship between the *defined* laboratory unit and the corresponding SI unit. If one wants the uncertainty in the relationship between the laboratory unit *as-maintained* and the corresponding SI unit then the uncertainty associated with the implementation of the definition of the laboratory unit must also be taken into account by assigning an appropriate uncertainty to $(2e/h)_{LAB}$ and $(R_H)_{LAB}$.]

For the ohm one may write

$$(K_\Omega)_{LAB} = \frac{\mu_0 c \alpha^{-1}}{2(R_H)_{LAB}} \tag{12}$$

as well as

$$(K_\Omega)_{LAB} = \left[\frac{\mu_0^2 c^3 (\mu'_p/\mu_B)(2e/h)_{LAB}}{16 R_\infty (R_H)^2_{LAB} \gamma'_p(\text{low})_{LAB}}\right]^{1/3}. \tag{13}$$

Equations (12) and (13) both yield an indirect value of $(K_\Omega)_{LAB}$ with an uncertainty of about 0.07 ppm, comparable with the uncertainty of direct calculable capacitor determinations.

Finally, for the ampere one has

$$(K_A)_{LAB} = \left[\frac{\gamma'_p(\text{low})_{LAB}}{\gamma'_p(\text{high})_{LAB}}\right]^{1/2} \tag{14}$$

as well as

$$(K_A)_{LAB} = \left[\frac{M_p \gamma'_p(\text{low})_{LAB}}{(m_p/m_e)(\mu'_p/\mu_B) F_{LAB}}\right]^{1/2} \tag{15}$$

where use has been made of the following relation to derive (15) from (14):

$$\gamma'_p(\text{high})_{LAB} = F_{LAB}(\mu'_p/\mu_B)(m_p/m_e)/M_p. \tag{16}$$

(Since the uncertainties of μ'_p/μ_B, m_p/m_e, and M_p are all below 0.05 ppm, (16) implies that with little additional uncertainty a measurement of F_{LAB} may be viewed as a measurement of γ'_p(high) and vice versa.) The uncertainty of the indirect value of $(K_A)_{LAB}$ from (14) is about 0.5 ppm and that from (15) about 0.7 ppm. These uncertainties are significantly less than the uncertainties of direct current balance determinations which are in the range 4–10 ppm.

A number of conclusions may be drawn from the above. First, indirect realizations of the SI definitions of the volt and ampere based on fundamental constant experiments are at present significantly more accurate than direct volt or current balance realizations. For the ohm the two different approaches have comparable uncertainties. Second, the uncertainties associated with these indirect realizations are still rather larger than the uncertainties associated with the implementation of the definitions of V_{LAB} and Ω_{LAB} based on the Josephson and quantum Hall effects (perhaps a factor of 10 for the volt and a factor of 2 for the ohm). Thus it is still not yet possible to achieve the desirable goal of having the as-maintained system of electrical units consistent with the SI to the same level of accuracy with which the as-maintained system can be implemented. Third, it is clear that the fundamental physical constants have a critical role to play in the maintenance and realization of the electrical units and that it is a reciprocal relationship—the accurate determination of fundamental constants requires a reliable system of as-maintained units. Indeed, the critical role the electrical units play in the fundamental constants field is clearly evident in the 1983 least squares adjustment of the fundamental constants as discussed in the following section.

III. The 1983 Least Squares Adjustment

The purpose of a least squares adjustment of the fundamental physical constants is to generate a self consistent set of "best values" of the constants for general use in science and technology based on all the data available at a given epoch. Comprehensive studies of the constants were pioneered in the late 1920's by R. T. Birge and continued by others including J. W. M. DuMond, E. R. Cohen, and Bearden and colleagues. The most recent adjustment was carried out by Cohen and Taylor in 1973 [5] under the auspices of the CODATA (Committee on Data for Science and Technology) Task Group on Fundamental Constants. It served to update the comprehensive review and adjustment published by Taylor, Parker, and Langenberg in 1969 [6], and the set of best values resulting from it was officially adopted for international use by CODATA at its Eighth General Assembly in September 1973. This set is still that currently recommended.

In the last decade or so an extraordinary amount of new experimental and theoretical work relating to the fundamental constants has been reported which now renders the 1973 set of recommended values obsolete. Thus the author, again in collaboration with E. R. Cohen and under the sponsorship and guidance of the CODATA Task Group on Fundamental Constants, is undertaking a new adjustment to replace that of 1973. What follows is a brief summary of this effort (still not quite complete at the time of writing) which will be called the "1983 Least Squares Adjustment of the Fundamental Physical Constants."

A. Some Definitions

A least squares adjustment of the constants is generally carried out by dividing the available data into two groups. One group

is known as the "stochastic input data" and consists of the less precisely measured quantities entering the adjustment and which are subject to adjustment. Examples from the quantities already discussed include $(K_\Omega)_{LAB}$, F_{LAB}, $[\gamma'_p(\text{high})]_{LAB}$, and μ_μ/μ_p.

In the 1983 adjustment the electric-unit dependent stochastic data are expressed in BIPM units as they existed on January 1, 1983, namely, V_{BI83}, Ω_{BI83}, and $A_{BI83} = V_{BI83}/\Omega_{BI83}$. The BIPM has been maintaining its laboratory unit of voltage via the Josephson effect since January 1, 1976, with the adopted value $(2e/h)_{76\text{-BI}} \equiv 483\ 594\ \text{GHz}/V_{76\text{-BI}}$. Defining $K_V \equiv V_{BI83}/V$ it then follows that

$$K_V \equiv V_{BI83}/V \tag{17a}$$

$$= V_{76\text{-BI}}/V = (2e/h)_{76\text{-BI}}/(2e/h) \tag{17b}$$

$$= 483\ 594\ \text{GHz} \cdot V_{76\text{-BI}}^{-1}/(2e/h). \tag{17c}$$

The BIPM laboratory unit of resistance is currently defined in terms of the mean resistance of six 1-Ω resistors so that Ω_{BI83} is based on the mean value of these resistors on January 1, 1983. Thus one simply has

$$K_\Omega \equiv \Omega_{BI83}/\Omega \tag{18}$$

and

$$K_A \equiv A_{BI83}/A \tag{19a}$$

$$= K_V/K_\Omega. \tag{19b}$$

The second group of data is termed the "auxiliary constants" and consists of quantities which are sufficiently accurate in comparison with the stochastic data that if included in the adjustment as stochastic data, their adjusted (or output) values and uncertainties would change negligibly compared with their input values and uncertainties. Thus the auxiliary constants are not subject to adjustment. Examples from the quantities already discussed include R_∞, μ'_p/μ_B, M_p, and m_p/m_e.

The two main selection criteria for considering individual items for inclusion in the 1983 adjustment are (1) availability prior to December 31, 1983 due to publication deadlines and the time required for review and analysis; and (2) the requirement that the item make a nontrivial contribution to the adjustment. For example, if a direct measurement of a quantity contributes only a few percent to the determination of the adjusted value of the quantity, then it should be excluded because it is clearly not a competitive determination. (In a least squares adjustment $w_i = 1/s_i^2$ where w_i is the weight of the ith stochastic input datum and s_i its one standard deviation uncertainty.)

B. The Data and Their Consistency

At the time of writing 12 different types of stochastic input data are being considered for inclusion in the 1983 adjustment with a total of 34 individual items. Some older measurements of comparatively large uncertainty are initially being included in the hope that they might clarify a number of discrepancies which exist among the more accurate data. These 34 items are summarized in Table I. The two values of α^{-1} listed are $\alpha^{-1}(a_e)$ and $\alpha^{-1}(^4\text{He})$ as obtained from the experimental determination of, and theoretical expression for, the anomalous magnetic moment of the electron and a certain fine-structure splitting in atomic helium, respectively.

A detailed discussion of the consistency of these data is beyond the scope of this paper. However, a few highlights will be given in order to further indicate the many inter-relationships which exist among the constants and the critical role of the electrical units and electric-unit dependent quantities. First we comment on the consistency of like data, for example, the six values of $\gamma'_p(\text{low})_{BI83}$, and then on the consistency of unlike data as implied by various expressions involving different constants, such as (11) and (16) and others to be given below.

On the assumption that only a difference between two quantities two or more times their combined standard deviation uncertainty $s_c = [s_1^2 + s_2^2]^{1/2}$ is statistically significant, the main like-data inconsistencies are between the several values of γ'_p (both low and high) and the two values of $d_{220}(\text{Si})$. For example, the most accurate value of $\gamma'_p(\text{low})_{BI83}$ differs from the two next most accurate values by $12s_c$ and $7.6s_c$, respectively, and these two differ from each other by $2.4s_c$; the first and second most accurate values of $\gamma'_p(\text{high})_{BI83}$ differ by $2.4s_c$; and the two values of $d_{220}(\text{Si})$ differ by $7.7s_c$.

The unlike data may be compared in many different ways; the focus here will be on those which tend to clarify the inconsistencies between like data. We first note that the *indirect* value of $\gamma'_p(\text{high})_{BI83}$ obtained from F_{BI83} via (16) is in excellent agreement with the most accurate of the four *direct* measurements; the two differ by only $0.8s_c$. Thus the second most accurate value of $\gamma'_p(\text{high})$ is suspect (see previous paragraph).

Next we compare the two direct values of α^{-1} listed in Table I, namely, $\alpha^{-1}(a_e)$ and $\alpha^{-1}(^4\text{He})$, with 10 indirect values derived from the following expressions using the data of Table I:

$$\alpha^{-1}(R_H) = 2(R_H)_{BI83} K_\Omega/\mu_0 c \tag{20}$$

$$\alpha^{-1}(\gamma'_p) = \left[\frac{c(\mu'_p/\mu_B)(2e/h)_{76\text{-BI}}}{4R_\infty K_\Omega \gamma'_p(\text{low})_{BI83}}\right]^{1/2} \tag{21}$$

$$\alpha^{-1}(\text{Mu}) = [C_{Mhfs}(\mu_\mu/\mu_p)/\nu_{Mhfs}]^{1/2} \tag{22}$$

where C_{Mhfs} is obtained from the theory of the muonium hyperfine splitting and the ratio C_{Mhfs}/ν_{Mhfs} has an uncertainty of 0.14 ppm. To obtain the three quantum Hall resistance and six proton gyromagnetic ratio values of α^{-1} from (20) and (21), respectively, the weighted mean of the five individual, relatively consistent values of K_Ω is used (uncertainty < 0.07 ppm). To obtain the single muonium hyperfine splitting value of α^{-1} from (22), the weighted mean of the two individual and consistent values of μ_μ/μ_p is used (0.3-ppm uncertainty). The result of the comparison is that all 12 values of α^{-1} are reasonably consistent except the two obtained from the two next most accurate values of $\gamma'_p(\text{low})_{BI83}$. Thus these values of $\gamma'_p(\text{low})_{BI83}$ are definitely suspect. It is significant that the uncertainty of a number of these indirect values of α^{-1} is comparable with the 0.073 ppm uncertainty of $\alpha^{-1}(a_e)$ (within a factor of 2-3) and a value with essentially the *same* uncertainty as $\alpha^{-1}(a_e)$

TABLE I
SUMMARY OF TENTATIVE STOCHASTIC INPUT DATA FOR THE 1983 LEAST SQUARES ADJUSTMENT

Quantity	No. of values	Uncertainties (ppm)
K_Ω	5	0.11; 0.12; 0.18; 0.22; 0.36
K_A	6	4.0; 5.8; 6.1; 7.7; 7.9; 9.7
K_V	1	2.4
F_{BI83}	1	1.3
$\gamma_p'(\text{low})_{BI83}$	6	0.24; 0.52; 0.61; 0.82; 2.1; 3.2
$\gamma_p'(\text{high})_{BI83}$	4	1.0; 3.2; 3.6; 7.5
$d_{220}(\text{Si})$	2	0.1; 0.21
$M(\text{Si})/\rho(\text{Si})$	1	1.15
$(R_H)_{BI83}$	3	0.11; 0.14; 0.32
α^{-1}	2	0.073; 0.78
μ_μ/μ_p	2	0.36; 0.53
ν_{Mhfs}	1	0.036

and also consistent with it can be derived from

$$\alpha^{-1}(R_H/\gamma_p') = \left[\frac{(\mu_p'/\mu_B)(R_H)_{BI83}(2e/h)_{76\text{-}BI}}{2\mu_0 R_\infty \gamma_p'(\text{low})_{BI83}}\right]^{1/3} \quad (23)$$

using the most accurate value of $(R_H)_{BI83}$ and $\gamma_p'(\text{low})_{BI83}$.

We next compare the unlike data via the values of N_A they imply. Seven such values may be readily obtained from the data of Table I, two from (10) using the two different values of $d_{220}(\text{Si})$ and the single value of $M(\text{Si})/\rho(\text{Si})$; one from

$$N_A = \frac{\mu_0 c(2e/h)_{76\text{-}BI}\alpha^{-1}F_{BI83}}{K_\Omega} \quad (24)$$

and four from

$$N_A = \frac{\mu_0 c M_p(2e/h)_{76\text{-}BI}\alpha^{-1}\gamma_p'(\text{high})_{BI83}}{(\mu_p'/\mu_B)(m_p/m_e)K_\Omega} \quad (25)$$

where in both these equations the weighted mean value of K_Ω is used and $\alpha^{-1}(a_e)$ is taken for α^{-1}. The result of the comparison is that the three values of N_A obtained from F_{BI83}, the most accurate value of $\gamma_p'(\text{high})_{BI83}$, and one of the two values of $d_{220}(\text{Si})$ are in good agreement (and have uncertainties between 1.0 and 1.4 ppm as well), but disagree with the value of N_A obtained from the other measurement of $d_{220}(\text{Si})$. The latter is thus suspect and the second most accurate value of $\gamma_p'(\text{high})_{BI83}$ is definitely questionable.

Finally, we compare the unlike data via the values of K_V they imply. Fourteen values may be readily derived from the data of Table I which together with the one direct measurement gives a total of 15. Six values follow from the direct measurements of K_A via

$$K_V = K_A K_\Omega. \quad (26)$$

Four values from measurements of $\gamma_p'(\text{low})_{BI83}$ and $\gamma_p'(\text{high})_{BI83}$ carried out in the same laboratory using the relation

$$K_V = \left[\frac{K_\Omega^2 \gamma_p'(\text{low})_{BI83}}{\gamma_p'(\text{high})_{BI83}}\right]^{1/2} \quad (27)$$

[see (14) and (26)]; one value using (27) with $\gamma_p'(\text{high})_{BI83}$ replaced by F_{BI83} via (16) and where both $\gamma_p'(\text{low})_{BI83}$ and F_{BI83} were measured in the same laboratory; two values using (11) with N_A obtained from (10) using the single value of $M(\text{Si})/\rho(\text{Si})$ and the two values of $d_{220}(\text{Si})$; and one value from

$$K_V = \left[\frac{M_p c(2e/h)_{76\text{-}BI}K_\Omega}{4R_\infty(m_p/m_e)(\alpha^{-1})^2 F_{BI83}}\right]^{1/2} \quad (28)$$

where here and in the other equations (as appropriate) the weighted mean is used for K_Ω and $\alpha^{-1}(a_e)$ for α^{-1}. The result of this comparison tends to confirm most of what had been concluded from the earlier comparisons, namely, that the two next most accurate values of $\gamma_p'(\text{low})_{BI83}$ are inconsistent with the most accurate value and that the most accurate value for $\gamma_p'(\text{high})_{BI83}$, the value of F_{BI83}, and one of the values of $d_{220}(\text{Si})$ are highly consistent but that the other value of

d_{220}(Si) is in considerable disagreement with these data. Unfortunately, however, the values of K_V derived from the direct measurements of K_A via (26), as well as the single direct measurement of K_V, have such large uncertainties that most are consistent with the majority of the indirect values. Thus at the present time they are not capable of clarifying (i.e., either supporting or refuting) the $\gamma'_p(\text{low})_{BI83}$, $\gamma'_p(\text{high})_{BI83}$, and d_{220}(Si) inconsistencies.

C. Least Squares Adjustment

To carry out a least squares adjustment of the constants, a subset of constants, known as the adjustable constants or "unknowns," is chosen in terms of which stochastic input datum can be individually expressed, if necessary with the aid of the auxiliary constants. The adjustable constants are selected in such a way that the resulting equations, known as the observational equations, are statistically independent. The total number of observational equations is thus equal to the number of items of stochastic data. Substituting the numerical values for the auxiliary constants and stochastic data and using a computer, the observational equations may be solved for the unknowns and their uncertainties. (The least squares procedure automatically takes into account all possible "routes" to the adjustable constants, both direct and indirect.) In the 1983 adjustment the adjustable constants or unknowns are most likely to be taken as α^{-1}, K_V, K_Ω, d_{220}(Si), and μ_μ/μ_p. The resulting 12 different observational equations (34 total) for the 12 different kinds of stochastic data listed in Table I would then be as given in Table II.

The least squares adjustment using all 34 data items of Table I has χ^2 of about 320 for 29 degrees of freedom. The gross disagreement of some of the data discussed is, of course, responsible for such a large (statistically improbable) χ^2.

In the last several years much work has been done on the problem of how best to handle inconsistent data in a least squares adjustment of the constants [7]. While final decisions have not yet been made regarding the 1983 adjustment data, based on the analyses done to date it may tentatively be concluded that the 1983 recommended values for many constants will differ significantly from their 1973 counterparts. For example, it is likely that e will decrease by approximately 7 ppm and that its uncertainty will decrease from nearly 3 to less than 0.5 ppm; for h the comparable changes will be -15 ppm and from 5.4 to less than 1 ppm; and for N_A +15 ppm and from 5.1 to less than 1 ppm.

These changes come about because e, h, and N_A are related to the adjustable constants α^{-1} and K_V through

$$e = [(\mu_0 c/4)(2e/h)_{76\text{-BI}}]^{-1}(\alpha^{-1})^{-1}K_V \tag{29}$$

$$h = [\mu_0 c/2]\,\alpha^{-1}e^2 \tag{30}$$

$$N_A = [M_p/(m_p/m_e)\mu_0 R_\infty]\,(\alpha^{-1})^{-3}e^{-2}. \tag{31}$$

The values of the quantities in brackets and α^{-1} will probably change little compared with their 1973 values—tenths of ppm at most (with the exception of m_p/m_e, all the quantities in brackets were auxiliary constants in the 1973 adjustment as well as in the 1983 adjustment). However, it is likely that the adjusted value of K_V will decrease by approximately 7.5 ppm and its uncertainty from 2.6 to less than 0.5 ppm due to the new and highly accurate indirect values of K_V implied by (11), (27), and (28). From (29), (30), and (31) it follows that a 7.5 ppm decrease in the value of K_V will lead to a decrease in the value of e of the same amount, twice as large a decrease in h, and twice as large an increase in N_A. Moreover, since the 1983 adjusted value of α^{-1} will probably have an uncertainty of less than 0.1 ppm, the uncertainty in e will be about the same as that in K_V and the uncertainties in h and N_A will be about twice as large.

It is important to realize that the approximate 7.5 ppm change in K_V likely to result from the 1983 adjustment implies that the value of $2e/h$ in general use for volt maintenance purposes using the ac Josephson effect is smaller than the SI value by this amount. As a consequence, the as-maintained units of voltage of the various national laboratories are smaller than the SI volt by about 7.5 ppm. A readjustment of the various laboratory units to bring them into better agreement with the SI system is expected within the next few years [8].

TABLE II
PROBABLE OBSERVATION EQUATIONS FOR THE 1983 LEAST SQUARES ADJUSTMENT[a]

$$K_\Omega = \{K_\Omega\}$$

$$K_V = \{K_V\}$$

$$K_V K_\Omega^{-1} = \{K_A\}$$

$$(\alpha^{-1})^{-2}K_V^{-2}K_\Omega = \frac{4R_\infty(m_p/m_e)}{M_p c(2e/h)_{76\text{-BI}}}\{F_{BI83}\}$$

$$(\alpha^{-1})^{-2}K_\Omega^{-1} = \frac{4R_\infty}{c(\mu'_p/\mu_B)(2e/h)_{76\text{-BI}}}\{\gamma'_p(\text{low})_{BI83}\}$$

$$(\alpha^{-1})^{-2}K_V^{-2}K_\Omega = \frac{4R_\infty}{c(\mu'_p/\mu_B)(2e/h)_{76\text{-BI}}}\{\gamma'_p(\text{high})_{BI83}\}$$

$$d_{220}(\text{Si}) = \{d_{220}(\text{Si})\}$$

$$(\alpha^{-1})^{-1}K_V^{-2}d_{220}^3(\text{Si}) = \frac{16R_\infty(m_p/m_e)}{M_p\mu_0 c^2(2e/h)^2_{76\text{-BI}}}\left\{\frac{M(\text{Si})}{\rho(\text{Si})}\right\}$$

$$\alpha^{-1}K_\Omega^{-1} = \frac{2}{\mu_0 c}\{(R_H)_{BI83}\}$$

$$\alpha^{-1} = \{\alpha^{-1}\}$$

$$\mu_\mu/\mu_p = \{\mu_\mu/\mu_p\}$$

$$(\alpha^{-1})^{-2}(\mu_\mu/\mu_p) = C_{Mhfs}^{-1}\{\nu_{Mhfs}\}$$

[a] The curly brackets indicate numerical value only.

IV. Future Electrical Measurements Research

We conclude with a brief discussion of future electrical measurements research which can improve our knowledge of the fundamental physical constants.

Of highest priority would seem to be the direct measurement,

via a force balance experiment or its equivalent, of either $(K_V)_{LAB}$ or $(K_A)_{LAB}$ to an accuracy of 0.1-0.3 ppm. Such a measurement could unequivocally resolve the present discrepancy between the two available values of d_{220}(Si) [see (10), (11), (26)] as well as clarify the discrepancies associated with the two next most accurate values of γ'_p(low) [see (14), (27)].

A new direct determination of $\gamma'_p(\text{low})_{LAB}$ to an accuracy of 0.1 ppm could also clarify the current γ'_p(low) problem, while if coupled with a new measurement of either $\gamma'_p(\text{high})_{LAB}$ or F_{LAB} with an accuracy of 0.5 ppm, could contribute to the resolution of the d_{220}(Si) problem [see (10), (11), (14), (15), (26)].

Measurements of $(R_H)_{LAB}$ and $(K_\Omega)_{LAB}$ with uncertainties at the few hundredths ppm level could also be of major importance. For example, in combination with the new measurement of $\gamma'_p(\text{low})_{LAB}$ advocated above such a value of $(R_H)_{LAB}$ would provide the means for determining α^{-1} to an accuracy considerably less than 0.05 ppm and one which does not require the absolute realization of an electrical unit [see (23)]. This value could then be compared with that obtained directly from $(R_H)_{LAB}$ and $(K_\Omega)_{LAB}$ [see (20)] as well as $\alpha^{-1}(a_e)$ (0.073 ppm current uncertainty and soon to be reduced by about a factor of 3). Such over-determination or "redundancy" is of critical importance in the fundamental constants field since agreement between values obtained by a variety of methods is the only way one can ensure that there are no unsuspected systematic errors plaguing particular experiments.

Finally, work needs to be done to develop improved transport standards, especially for resistance, so that the results of absolute ohm realizations and quantum Hall resistance measurements carried out in different laboratories can be critically compared. Since it is unlikely that transport standards with the requisite parts in 10^8 stability upon shipment can be developed as readily for voltage as for resistance, new direct comparisons of the Josephson volt standard apparatus of the various national laboratories should be undertaken to ensure that the claimed accuracies of a few parts in 10^8 are justified. Such comparisons of Ω_{LAB} and V_{LAB} could contribute significantly to improving our confidence in the consistency of the laboratory electrical measurement systems of the various countries throughout the world, as well as in the 1983 and subsequent sets of recommended values of the fundamental physical constants.

Note Added in Proof. Since this paper was submitted for publication, it was decided to consider data available through early 1985 for possible inclusion in the new adjustment and to rename it the "1985 Least Squares Adjustment of the Fundamental Physical Constants." However, the paper's basic contents and conclusions are unaltered by this decision.

References

[1] *The International System of Units (SI)*, P. T. Goldman and R. J. Bell, Eds., Natl. Bur. Stand. (US), Spec. Publ. 330. Washington, DC: U.S. Government Printing Office, 1981.

[2] "Documents concerning the new definition of the meter," *Metrologia*, vol. 19, no. 4, pp. 163-177, 1983.

[3] It is not the purpose of this tutorial to provide a comprehensive bibliography. Rather, the reader is referred to [5] and [6], and to various relevant articles in this volume and in the following references:
Atomic Masses and Fundamental Constants 5, J. H. Sanders and A. H. Wapstra, Eds. New York: Plenum, 1976.
Metrology and Fundamental Constants, Proc. of the International School of Physics "Enrico Fermi," Course LXVIII, A. Ferro Milone, P. Giacomo, and S. Leschiutta, Eds. Amsterdam: North Holland, 1980. See especially, the article by B. W. Petley, "Electrical metrology and fundamental constants," pp. 358-463.
Atomic Masses and Fundamental Constants 6, J. A. Nolen, Jr. and W. Benenson, Eds. New York: Plenum, 1980.
Precision Measurement and Fundamental Constants II, B. N. Taylor and W. D. Phillips, Eds., Natl. Bur. Stand. (US), Spec. Publ. 617. Washington, DC: U.S. Government Printing Office, 1984.
Quantum Metrology and Fundamental Physical Constants, P. H. Cutler and A. A. Lucas, Eds., NATO Advanced Study Institute Series, Series B: Physics, vol. 98. New York: Plenum, 1983.
The Fundamental Physical Constants and the Frontier of Measurement, B. W. Petley. Bristol: Adam Hilger, 1984.

[4] K. v. Klitzing, G. Dorda, and M. Pepper, "New method for high accuracy determination of the fine-structure constant based on quantized Hall resistance," *Phys. Rev. Lett.*, vol. 45, no. 6, pp. 494-497, Aug. 11, 1980. See also the several papers on the quantum Hall effect in this volume.

[5] E. R. Cohen and B. N. Taylor, "The 1973 least-squares adjustment of the fundamental constants," *J. Phys. Chem. Ref. Data*, vol. 2, no. 4, pp. 667-734, 1973.

[6] B. N. Taylor, W. H. Parker, and D. N. Langenberg, "Determination of e/h, using macroscopic quantum phase coherence in superconductors: Implications for quantum electrodynamics and the fundamental physical constants," *Rev. Mod. Phys.*, vol. 41, no. 3, pp. 375-496, July 1969. Also published as *The Fundamental Constants and Quantum Electrodynamics*. New York: Academic, 1969.

[7] B. N. Taylor, "Numerical comparisons of several algorithms for treating inconsistent data in a least-squares adjustment of the fundamental constants," Natl. Bur. Stand. (US), Report No. NBSIR 81-2426, Jan. 1982.

[8] P. Giacomo, "News from the BIPM," *Metrologia*, vol. 20, no. 1, pp. 25-30, 1984.

NBSIR 75-935

THE NATIONAL MEASUREMENT SYSTEM FOR ELECTRICITY

Norman B. Belecki
Bernadine L. Dunfee
Oskars Petersons

Electricity Division
Institute for Basic Standards
National Bureau of Standards
Washington, D.C. 20234

Issued September 1978

U.S. DEPARTMENT OF COMMERCE, Juanita M. Kreps, *Secretary*
Dr. Sidney Harman, *Under Secretary*
Jordan J. Baruch, *Assistant Secretary for Science and Technology*
NATIONAL BUREAU OF STANDARDS, Ernest Ambler, *Director*

PREFACE

The National Measurement System for Electricity is that system of people, organizations, standards, apparatus, and software which performs the function of providing quantitative information on materials, manufactured items, and processes through the measurement of their physical properties or parameters. This report is one of a series of similar reports produced by the Institute for Basic Standards (IBS) of the National Bureau of Standards to provide a complete description of that system, of which IBS is the foundation. The format of this report is common to the series and was chosen to provide uniformity and completeness.

The authors would like to express their appreciation to their many colleagues who supplied information and perceptions for inclusion in this study. Special appreciation goes to those who arranged or hosted visits at private and government organizations for the authors and others of the Division staff. We would like to also acknowledge the work of Denise Prather, who assisted in the production of the final draft. Finally we are most indebted for the efforts of Sylvia Ramboz, who was responsible for the production of the manuscripts for two interim reports as well as this document; and for her comments, suggestions, and encouragement.

CONTENTS

LIST OF FIGURES

LIST OF TABLES

THE NATIONAL MEASUREMENT SYSTEM FOR ELECTRICITY

Norman B. Belecki
Bernadine L. Dunfee
Oskars Petersons

Electricity Division
Institute for Basic Standards

June 1976

EXECUTIVE SUMMARY

Electrical measurements are of critical importance due to the universal use of electricity as the primary means for the transmission and control of energy and data. The National Measurement System for Electricity is that set of laboratories, organizations, documents and people which make possible and are responsible for all electrical measurements made in the U.S. at all levels of accuracy. This document summarizes the results of a four-year study of that system.

The structure of the system may be conceived as having a number of components, each serving a particular sector of society and each having distinct characteristics reflecting differing requirements. Two major components exist: the industrial electronics component and the electric power industry component. There are a number of minor parts in each.

Electrical measurements in the system's industrial electronics component are used to ensure quality and reliability of materials and manufactured products, to provide for interchangeability of components and parts, and to control meanufacturing processes.

This component can also be further subdivided into two general areas: the measurement-intensive industry segment and the general industry segment. Measurement-intensive industry and its measurement system are characterized by high technology and the need for a very high degree of product reliability. Included in this portion of the defense, communication, computer, and electronic component industries. Measurement accuracy within this segment is ensured by a hierarchical laboratory system in each organization. Test equipment used for quality and process control is calibrated periodically using precision instruments which are in turn calibrated by comparison with primary standards in the corporate standards are then periodically calibrated at the National Bureau of Standards or intercompared regularly with standards which have been so calibrated. This system, which in large organizations can have a complex hierarchy of laboratories, is primarily the result of the quality control requirements of DoD, GSA, and NASA procurement contracts, the requirements of regulatory agencies such as EPA and OSHA and logistics constraints.

In the general industry segment of the system, quality control requirements are usually less stringent than in the high technology segment; accuracies are generally lower; and the manufacturing processes are less affected by absolute accuracy of measurements. Thus, organizations in this portion of the system are inclined to buy calibration and repair services from instrumentation manufacturers, large corporate laboratories in the aerospace industry, or companies specializing in calibration and repair work. As previously noted, each of these generally maintains a rigid, well-defined measurement support system.

There appears to be a number of problems and shortcomings in the industrial electronics component of the system. Among the most important are a lack of standards (written and artifact) for the support of dynamic, high-speed electrical measuring instruments and automated test systems; the non-availability in certain areas of procedures and test techniques of guaranteed reliability; a potential future shortage of competent measurement personnel; a failure on the part of some people in the system to perceive that calibration is not always a sufficient condition for assurance of measurement quality; and an inherent rigidity in the government contractural requirements which stifles innovative approaches to measurement problems.

The electric power industry segment of the National Measurement System for Electricity can also be divided into two parts: operational and research for improved electric power transmission and distribution. Electrical measurements play an important role in the day-to-day operation of the nation's electric power systems. They are used to control the generation and transmission of electricity, to provide a basis for equitable exchange (energy metering), and for testing machinery and equipment supplied to the power companies.

Measurement support for both of these areas is generally provided by the measurement laboratories of power companies and those of the electrical equipment manufacturers. In the energy metering area, many of the state and local public utility commissions which regulate the power companies require acceptance testing of watthour meters as well as retesting of older meters. NBS calibration of physical standards and electrical apparatus, both at NBS and in the power companies' and manufacturers' laboratories, ensures the overall integrity of the system.

Most of the industry - both utilities and manufacturers - is adequately equipped to measure traditional quantities such as current and voltage at levels up to 15 kilovolts. Fewer companies, especially in the utility sector, have capabilities above 100 kilovolts. At extra-high voltage (EHV) and ultra-high voltage (UHV), the utility companies, with rare exceptions, have little measurement and calibration capability. Such capability, however, does exist with the manufacturers of large electrical equipment. With respect to nontraditional quantities, such as transient high voltages and currents, measurement capability is generally available only with the large equipment manufacturers.

The quality and consistency of electric power system-related measurements, including traceability to NBS-maintained standards, follow the above pattern of measurement capability. Whenever the calibrations are relatively simple and inexpensive, and if there is also regulatory incentive to do adequate work, the system is in excellent condition. A good example is watthour meter calibrations. But for higher voltage, and especially for non-conventional measurements where the calibrations are difficult to perform and reliable methods are not always readily available, the system has deficiences. Included in this category and EHV and UHV steady-state measurements, and transient measurements in general.

Electricity will become the predominant form of energy in use before the end of the century. Consequently, a large research and development effort funded by the Energy Research and Development Administration and the Electric Power Research Institute is being directed at ways to increase the transmission capability and efficiency of the country's electric power systems. New high voltage and electrical-related measurements are required as transmission technology advances. Examples of new technologies include cryogenic transmission systems, UHV overhead lines, compressed-gas insulated substations, and high-voltage direct-current transmission systems. Each is a relatively measurement-intensive, emerging-technology area. While some older types of measurement methodologies can be adapted for these new areas, generally they cannot and some significant deficiencies now exist including measurements for accelerated aging tests of electrical insulation, and traceability to national standards for impulse measurements.

Two important additional components of the National Measurement System for Electricity are associated with the scientific community and consumer electronics. Measurements made in laboratories not under DoD or NASA contract are generally supported by local instrumentation shops. In contrast with the usual practice in the industrial electronics component, periodic recalibration is unusual - calibration is generally performed only before and after a crucial experiment, or as part of a special maintenance effort. Measurements in support of consumer electronics, such as TV, stereo systems, citizen band and amateur radio, auto electronics, and general electrical work are usually of low accuracy. Consequently, manufacturers' claims of test equipment accuracy are accepted until malfunction occurs. This portion of the system has few, if any, serious measurement problems.

In summary, the Electricity Division of NBS provides the basis for that uniform system of electrical measurement in the U.S. which permits equity in trade, interchangeability of components, the transmission and distribution of electric power, a means of maintenance for electronic equipment, the ability to control the quality of production, and the general advance of science and technology. This is achieved by developing improved means for realizing, maintaining, and disseminating the basic electrical units; by calibrating electrical standards, instruments, and systems for industry, government, and the academic community; by developing new instrumentation and measurement methods; by obtaining basic data and determining fundamental constants related to the electrical units; by ensuring that electrical measurements carried out in the U.S. are consistent with those made in other countries; and by providing advisory and consultative services.

1. INTRODUCTION

The National Electrical Measurement System began to assume its present form around the beginning of this century. At that time the uses of electricity were limited to the easy transmission and use of energy in manufacturing and transportation and for lighting and primitive means of communication (telephone and telegraph). The establishment in 1901 of the National Bureau of Standards led to the foundation of a uniform system of electrical measurement where none had existed before; a foundation which permitted and expedited the development of electrotechnology which has made our present way of life possible. Since then the measurement system has continuously grown in magnitude and scope along with the industries it supports [1].

Today the system pervades every aspect of modern life. The electric power industry is the largest in the United States [2]. The electronics industry is one of the larger industries as well, and its products make possible the inexpensive production of goods and services throughout the rest of industry. Our present level of electrotechnology is only possible because a uniform system of electrical measurement exists. This system provides scientists, electrical engineers, and quality control engineers with a common language and thereby minimizes the need for trial-and-error approaches to design by permitting the existance of necessary data bases and allowing the meaningful communication of technical information in quantified detail. It is also true that the level of sophistication and general quality of all electrical-electronic products as well as many others are predicated, among other factors, on the state of the measurement system. The stability with time of the units of measure, the compatibility of measurements throughout the system, and the effectiveness with which new requirements are anticipated and dealt with are key factors which establish bounds on the level and rate of advance of technology. The system permits interchangeability, at affordable cost, of parts with very high levels of precision, a vital part of modern manufacturing technology.

The study of the National Electrical Measurement System, the results of which are summarized in this report, is intended to provide a complete picture of the system at the present time, and to forecast its future posture, needs, and shortcomings, The present intensive study is also to provide a data base for program planning within the National Bureau of Standards, a data base which will be expanded over the years as the result of a continuous surveillance of the system. The study was carried out primarily in two parts. Technical data were gathered as the result of visits to companies, correspondence with colleagues, interviews with visitors to the NBS, and interactions with fellow members of standards committees by Electricity Division personnel. Economic data were gleaned primarily from the literature. Because of the nature of the Electrical Measurement System, separate studies were not conducted on each measurement area. Rather, the system was observed as consisting of two unique sets of users, the electric power industry and the electronics industry. The term "electronics industry" as used here refers not only to the manufacturers of electronic components, modules, instruments, and systems, but to the users of these as well. Each of these will be further subdivided as the report progresses. Since the system is so large and pervasive, no attempt was made to define its size exactly. Recurring structural features make sampling an effective means of viewing the system.

As a result of the study, it was determined that:

(a) the system is adequately equipped and manned to support most measurements of a static nature;

(b) although most new instruments are designed and specified for use under computer control, there is virtually no capability in the system as a whole to support dynamic measurements; i.e., measurements in which time is a factor;

(c) there are expected to be increasing pressures from government regulatory agencies and from industrial firms engaged in international commerce for the establishment of a system for accrediting standards, calibration, and testing laboratories of various types;

(d) future sophisticated instrumentation, if not designed for computer control, will contain small control and logic units called microprocessore, creating a need for methods of verification of measurement implementation software;

(e) there exists a need, whose urgency is being determined, for improved measurements of electrical conductivity for application to non-destructive materials testing;

(f) because of the energy crisis, there is a need for new measurement methodologies for the support of energy-related research, especially in the areas of electric power;

(g) there is a lack of capability within the electric power industry to perform ultra-high voltage measurements;

(h) the exchange of technical information takes place in the system at an unacceptably low level.

It must be noted that consideration in this study was not given to those electrical measurements associated with the processing of semiconductor materials. Such measurements are addressed in depth by the impact study of the Electronic Technology Division of NBS.

2. STRUCTURE OF THE ELECTRICAL MEASUREMENT SYSTEM

2.1 Conceptual System

The system provides the capability for measurement of electrical quantities shown in table 1 below in the frequency range between dc and 1 MHz.

Table 1. Electrical quantities and units

Quantity	Units
Capacitance (C)	Farad
Current (I)	Ampere
Charge (Q)	Coulomb
Potential Difference (E)	Volt
Inductance (L)	Henry
AC-DC difference, voltage	(Unitless)
AC-DC difference, current	(Unitless)
AC-DC difference, resistance	(Unitless)
Power	Watt
Energy	Watthour or Joule
Ratio, resistive	(Unitless)
Ratio, dc voltage	(Unitless)
Ratio, ac voltage	(Unitless)
Ratio, current	(Unitless)

The above are measured in terms of the so-called legal units, those embodied in physical standards maintained by the National Bureau of Standards or defined by them as a function of physical constants. These units are - to the degree practical - compatible with the SI (Système International) units.

The Système International de'Unites provides the internationally accepted theoretical basis for the metric units of measure. In it, seven base units - the metre, the kilogram, the second, the kelvin, the mole, the candela, and the ampere - are regarded as being dimensionally independent and all other units stem from them, either through known physical relationships or defining equations [1]. In practice a set of four independent equations is available to define the six basic electrical quantities given at the top of table 1 with their symbols. They are $E=IR$ (Ohm's Law); $Q=It$ (t is time); $C=Q/E$; and $L=E/\frac{dI}{dt}$. These can serve to define only four of these quantities. The system is completed by requiring the unit of electrical energy to be equal to the unit of mechanical energy and devising electromechanical experiments - absolute experiments - involving force and length (whose product is energy) and corresponding electrical quantities to realize in practice two of the electrical units.

Absolute experiments are very complex and time-consuming, require the most meticulous approach, and involve the design and construction of special apparatus. Moreover, in the case of the ampere and volt, the uncertainties of the results are very large by comparison with those attainable using either artifacts, such as standard resistors or capacitors, or physical phenomena (e.g., the Josephson effect) to carry forth defined units. It is for these reasons our system of legal units exists. Figure 1 shows in detail the derivation of assigned values for the legal electrical units. In the past, absolute experiments have been performed to realize the ampere by comparing the force between current-carrying coils of known geometry to that exerted by the earth's gravitational field on a known mass. This was done most recently at NBS in 1967 using a Pellat-type electrodynomometer. The result was the determination that the ratio of the NBS ampere (derived from the legal units) to the SI ampere equals 1.0000105 with a probable error of 7 parts in a million.

These results as well as those of four other experiments formed the basis for an eleven part per million adjustment in 1969 to the value of the ampere as derived from the units maintained in Sevres by the Bureau International des Poids et Mesures - the International Bureau of Weights and Measures, which by the treaty of the Metre maintains electrical and physical units to promote international measurement uniformity. In consequence of this adjustment and drifts in the U.S. volt measured with respect to the BIPM volt, the U.S. legal volt was changed by 8.4 parts in a million on January 1, 1969. U.S. laboratories were informed of this change and advised to make the appropriate adjustments to the assigned values of their standard cell emfs through correspondence and technical publications in the media.

The ohm has in the past been determined in absolute measure using a specially constructed coil system of known geometry. The mutual inductance of such a system may be determined from its geometry and dimensions using electromagnetic theory. A commutated dc method may then be used to obtain the

value of a resistance as a linear function of the mutual inductance (length) and the rate of commutation (time). The resulting overall uncertainty of the last experiment of this type performed at NBS in 1948-1949 was 10 parts per million [2] - rather large especially when compared to the precision with which resistance standards may be intercompared (∿0.01 ppm) and their drift rates relative to one another (∿0.05 ppm/year). More recently, it has been determined using a calculable cross capacitor. This device is based upon the theorem of Thompson and Lampard which describes geometric conditions for the construction of a device whose capacitance is a known function of the displacement of a moveable electrode and hence can be calculated if the displacement can be measured. A quadrature bridge is then used to effect a calibration of resistance in terms of capacitance. This experiment thus establishes both the farad and the ohm in absolute measure. This is a much more accurate experiment than either the previously-described ohm determination or the ampere determination, having an uncertainty of 0.06 ppm [3].

The volt may also be obtained in absolute measure. Experiments are now underway at NBS and in the national laboratories of several other countries. The NBS experiment involves the measurement of the dc voltage applied to concentric cylindrical capacitors in terms of the electrostatic force generated between them as a function of their relative displacement and the charge in capacitance resulting from the displacement. The target accuracies of these experiments is of the order of 1-3 ppm. When completed, these determinations will not only provide the difference between the maintained and SI units of voltages, but when coupled with the results of the Farad-Ohm determination, will constitute an indirect determination of the SI ampere for comparison with previous directly-obtained values.

The legal units are maintained at NBS in the form of assigned values to groups of artifact standards. The legal farad is embodied in a group of ten, very stable, fused-silica capacitors [4]. The mean capacitance of the group has been assigned from absolute capacitance determinations. The legal ohm is the mean 4-terminal resistance of a group of Thomas-type standard resistors immersed in oil at 25°C under a power dissipation of 0.01 watts. This value is slightly inconsistent with the results of absolute experiments and will be adjusted after further work. It is not anticipated that this adjustment will be as large as one part per million.

The ampere, however, cannot be conveniently maintained using a physical standard. Instead, the absolute measurements of resistance and current are used to derive an absolute volt from which a legal unit of voltage may be assigned. Until 1972, the volt was maintained via a group of saturated standard cells in a temperature-controlled enclosure. Since July 1, 1972, use has been made of the ac Josephson effect to maintain the legal unit. The ac Josephson effect is a superconducting, pair-tunneling phenomenon - the discovery of which has permitted the construction of a linear frequency-to-voltage converter whose proportionality constant is invariant with respect to time and other factors at the part in 10^9 level [5]. Figure 1 depicts the derivation of the basic electrical units. It does not show an experiment for the direct absolute determination of the volt presently underway. Table 2 gives characteristics of the artifacts embodying the legal units. Appendix B contains a description of both the primary electrical standards and the working standards used to provide for the dissemination of the electrical units.

The other quantities listed in Table 1 are derivable at various levels of accuracy over their ranges. Accuracies of calibrations of standards in each of these areas are more than adequate to meet most static measurement requirements except the following:

(a) Capacitance between 30 kHz and 1 MHz, needed to support measurements resulting from increasing carrier frequencies in communications systems.

(b) AC voltage from 0.1 Hz to 100 Hz at millivolt levels and below for the support of vibration measurements aboard helicopters.

(c) DC conductivity measurements in ferrous and nonferrous metals for the support of nondestructive testing of airframes and other structures.

The standards and capabilities mentioned to this point apply only to static measurements, i.e., those measurements for which the time of measurement is not a constraint. The advent of integrated circuits and the resulting enormous increase in complexity of electronics has resulted in requirements for many more measurements in industry to ensure the quality of products and for maintenance purposes. Manual measurement methods are totally inadequate to the demand. Fortunately this same new technology has provided the system with the tools needed to perform measurements at very high speeds - fast settling instrumentation to convert analog electrical parameters to encoded digital signals, high-speed data handling equipment for routing digital and analog signals, and readily available inexpensive digital computers to control experiments, collect data, direct it

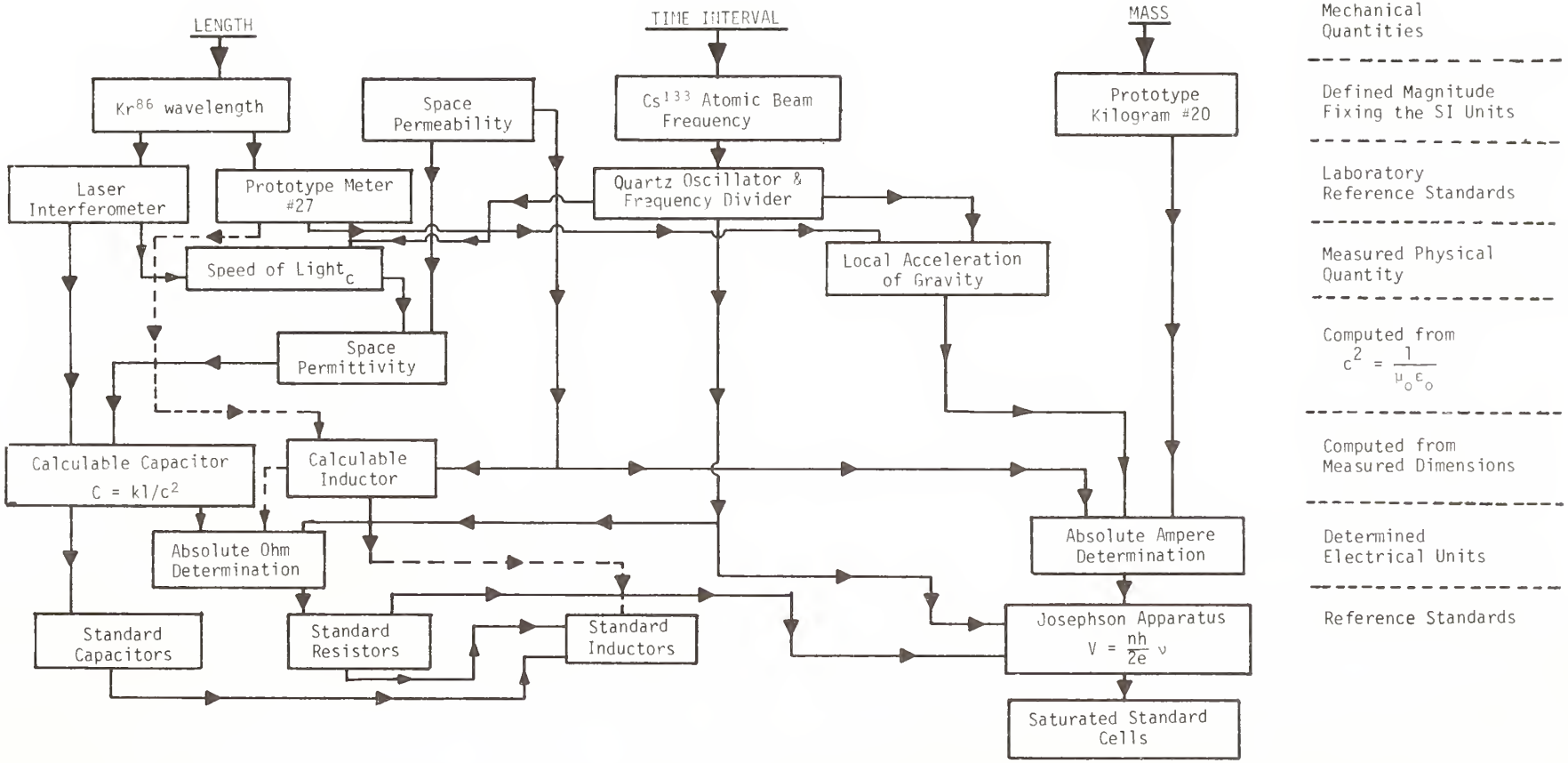

Figure 1. The derivation of the electrical units

Table 2. Characteristics of the basic legal units.

Unit	Artifact	Nominal Value	Maintenance Accuracy	Absolute Accuracy
Ohm	Thomas-type resistor	1 ohm	0.08 ppm	.06 ppm
Volt	Josephson apparatus	10 mV	0.1 ppm	7.8 ppm
Farad	Fused-silica capacitor	10 pF	0.4 ppm	0.034 ppm
Henry	Maxwell-Wein bridge	--	200 ppm	200 ppm

[a]Maintenance accuracy is that with which a perfect standard of equal magnitude could be calibrated.

[b]Absolute accuracy is the accuracy with which the difference between the SI and legal units has been reported.

to storage devices, and perform the mathematical manipulations necessary to put it in useful form.

Unfortunately, standards to provide a basis of accuracy for these high-speed or dynamic measurements simply do not exist. There is no common, well-defined terminology for describing the performance of these modern measurement tools, nor are there accepted test methods or artifact standards for verifying their accuracy under use conditions. There is no reliable way of precisely determining the trade-off between speed of measurement and accuracy. Presently, dynamic measurements are supported through the rapid measurement of static standards, a practice which does nothing to verify the capability to measure the rapidly-varying parameters characteristic of modern electronics. Other time-related properties of the measurement instrumentation such as the rate at which they should sample, the frequency of the measurements made, or delay times after switching are determined on a trial-and-error basis. Such standards as do exist are the intracompany standards of each of the instrumentation and module companies and, while they serve to achieve a degree of uniformity within each company's product line, are not directly relatible on an intercompany basis and certainly not available to the customers of the companies. In fact, such standards are considered proprietary in that they seriously affect product development in one of the most competitive marketplaces in existance.

This lack of standards and measurement verification capability results in undue costliness of measurement equipment, in hardware, testing and design costs, and in unfulfilled measurement capabilities. Undue cost accrues as the result of overspecification of components and modules at design time. In addition, validation procedures must be developed by trial-and-error techniques where adquuate standards do not exist.

A program for the development of standards and test techniques to support the dynamic measurement of electrical parameters has recently been initiated within the NBS. It is visualized that the hardware and written standards developed in this program will be made available to manufacturers and users of electronic measurement equipment in the form of calibration services, measurement assurance programs, and publications. As such they will provide the basis needed for uniform and compatible dynamic measurements throughout the country in the same way that existing standards now do for manually-made measurements.

2.2 Basic Technical Infrastructure

2.2.1 Documentary Specification System

2.2.1.1 Standardization Institutions

There are basically two major international standardizing organizations impacting the Electrical Measurement System. The International Electrotechnical Commission (IEC) is concerned with the production of standards, terminology, and specifications in support of electrotechnology. It has approximately 75 technical committees to perform this function. A list of those technical committees most affecting the system is given in table 3. In this country, a delegate to each committee of interest is appointed by the chairman of the national committee. The delegate, in the case of each proposed standard, attempts to develop a consensus U.S. position by getting technical support from interested parties in industry and government. The work of the IEC is very important to U.S. foreign trade activities. If standards which are essentially incompat-

ible with common American practice are developed, they could be used against the U.S. in restraint of trade. More importantly, standards developed overseas tend to be restrictive in two other ways. In many cases, methodology is stressed rather than performance. This tends to inhibit technological advancement in some product areas. Furthermore, the level of technology reflected in some standards is low by comparison to that in the U.S. These two factors can readily couple to close foreign markets to U.S. manufacturers.

Table 3. IEC committees affecting the Electrical Measurement System

Committee	Title
1	Terminology
3	Graphical Symbols
13	Measuring Instruments
25	Quantities and Units, and their Letter Symbols
38	Instrument Transformers
42	High Voltage Testing Techniques
45	Nuclear Instrumentation
50	Environmental Testing
56	Reliability and Maintainability
62	Electrical Equipment in Medical Practice
66	Electronic Measuring Equipment

The International Organization for Legal Metrology (OIML) is a recently-formed group concerned with legal aspects of metrology, such as weights and measures. Within OIML is a pilot secretariat, Secretariat 13, for the measurement of electric and magnetic quantities which is concerned with the provision of traceability for those kinds of measurements presently legally required. Secretariat 13 is held by the U.S. and has the subcommittees listed in table 4.

Within the U.S., there are a wide variety of legal and regulatory standards which impact the Electrical Measurement System. In the electronics world, traceability requirements for suppliers are made mandatory through contract by the federal government's largest consumers: the Department of Defense, the Department of Transportation, and the National Aeronautics and Space Administration. The Department of Energy requires that all contractors running installations for them have a stylized quality control system, and they provide for the servicing of those systems through their laboratory in Albuquerque, NM, run by the Sandia Corporation.

Table 4. OIML Pilot Secretariat 13

Measurement of Electric and Magnetic Quantities

Subcommittee	Title
13.1	International Compatibility of Primary Etalons
13.2	Power Meters (wattmeters)
13.3	Energy Meters for Direct Connection
13.4	Energy Meters Designed to be Used With Measurement Transformers
13.5	Measurement Transformers
13.6	Indicating Instruments for Voltage, Current and Frequency
13.7	Recording Instruments for Voltage, Current and Frequency

The Department of Defense contractually requires of its suppliers compliance with military specifications MIL-Q-9858A, Quality Program Requirements; MIL-I-45208A, Inspection System Requirements; and MIL-C-45662A, Calibration System Requirements. By doing so, it forces manufacturers to set up calibration and quality control systems which require periodic calibration of all measurement equipment, traceability to national standards in the case of all such calibrations, complete documentation of the calibration system including test procedures and traceability, and any instrument undergoing calibration to be tested using standards at least four times more accurate than it is. NASA has a similar but more rigid set of regulations - NPC 200-1A, Quality Assurance Provisions for Space Contractors. The Department of Transportation requires traceability in its highway safety test programs by specifying compliance with provisions of the Society of Automotive Engineers' Standard J211b.

Of great potential impact are new and forthcoming requirements of the Occupational Safety and Health Administration (OSHA). That organization has proposed that all industrial electronic and electrical equipment comply with certain minimum safety standards. Furthermore, it is proposed that all devices be tested for compliance in certified testing laboratories and that tests must be conducted in a laboratory not belonging to the manufacturer of the item being tested. At present these proposals are being appealed by industrial groups.

The electric power industry subset of the measurement system is also affected by the mandatory safety requirements of the Occupational Safety and Health Administration. Safety testing will be required of apparatus used in work environments. Once again it is likely that all testing will be done by accredited laboratories.

At present, the Food and Drug Administration fosters safety standardization in the manufacture of medical devices and instrumentation by sponsoring and promoting the generation and adoption of standards with the voluntary cooperation of industrial concerns, medical experts, and their own experts. Recently (May 1976) enacted and signed into law is The Medical Device Safety Amendment to the Food, Drug and Cosmetic Act, which will set up control mechanisms for medical instrumentation administered by the Food and Drug Administration. These mechanisms will range from having to obtain approval before marketing to simply having to register products in such a way as to enable an effective recall process in the event defects are found. In addition, manufacturers will be subject to a number of standards called Good Manufacturing Practices. These Good Manufacturing Practices, about to be promulgated, will require the existance of formal quality control procedures (in many cases where none exist now) and, in some areas of critical application, the establishment of formal calibration support systems with measurements required to be accurate in terms of national standards. This will result in the creation of new standards laboratories and perhaps in recognition of new types of measurement applications.

The bulk of the regulations affecting the electric power industry come from state utility regulatory commissions. These commissions have broad powers in regulating the operations of electric utility companies. They approve rates and siting of power plants and major transmission lines; to some extent they have a jurisdiction over the quality of electric power service--occasionally they prescribe tolerances for the supply voltage; they regulate the accuracy of watthour meters and the quality control systems which have been set up to test both newly-acquired and previously-installed meters.

There are a large number of voluntary standards organizations impacting the Electrical Measurement System. The majority are listed in table 5. Those organizations whose titles are starred have the greatest impact since they produce standards which have affect on the higher accuracy measurement processes, instruments, and artifact standards which support the system. NBS personnel participate in the activities of a number of committees sponsored by each of these organizations.

Table 5. Voluntary standards sponsoring organizations

Aerospace Industries Association
American Home Lighting Institute
*American National Standards Institute
American Society for Quality Control
American Society for Testing and Materials
American Welding Society
Association of American Battery Manufacturers
Association of Edison Illuminating Companies
Audio Engineering Society
*Edison Electric Institute
Electric Apparatus Service Association
*Electronic Industries Association
*Institute of Electrical and Electronic Engineers
Institute of High Fidelity
Institute of Printed Circuits
*Instrument Society of America
National Association of Relay Manufacturers
*National Electrical Manufacturers Association
Radio Technical Commission for Aeronautics
Resistance Welder Manufacturers Association
*Scientific Apparatus Manufacturers Association
Society of Automotive Engineers
Underwriters Laboratories
Variable Resistive Components Institute

* Organizations having major impact

2.2.1.2 Survey of Documentary Standards

A survey on documentary standards affecting the electrical measurement system was performed. Consideration of documentary standards in the electrical area shows that the documents may be divided into six categories: safety specifications and testing methods, terminology, dimensional requirements for compatibility, testing methods to determine electrical properties, performance parameter specifications and testing, and reliability assurance procedures. It is apparent that all except dimensional requirements involve or affect electrical measurements in some fashion. Since there was no evident valid means of ranking or quantifying these various effects, and since any document directly concerning etalons (artifact standards), measurement apparatus, and instrumentation would be more likely to have a large impact on the measurement system, those documents were considered separately.

Investigation of documents sanctioned by the International Electrotechnical Commission showed that, of the population of 759 standards and supplements, 45 referred directly to etalons, instrumentation, and precision measuring equipment. Most of these specify moderate accuracy instrumentation. Of the remainder, perhaps ten percent deal with terminology and symbols and another ten percent with dimensional specifications. As has been pointed out, the remainder have a bearing on the segment of the system dealing with the testing of export products for compliance with these standards to assure acceptance abroad. And, although a third or more of the remaining documents refer to radio frequency measurements above 1 MHz and therefore outside the scope of this study, measurements at those frequencies require a degree of low frequency measurement support [6].

A similar investigation of standards issued by the American National Standards Institute and having bearing on electricity and electronics, revealed that, of 944 standards, supplements, and handbooks issued, 20 provided definitions, specifications of performance, and test and verification methodology for standards, instrumentation, and precision measurement apparatus. Terminology is largely concentrated in C42.100, the Institute of Electrical and Electronic Engineers (IEEE) Standard Dictionary of Electrical Terms. About ten percent of the documents in this study specify dimensions for compatibility. The remainder specify or outline tests or measurements of various electrical parameters. The standards sanctioned by this institute are perhaps the most universally accepted in this country. A very high percentage of them have been adopted directly from the work of other groups such as the IEEE, the National Electrical Manufacturers Association, and the American Society for Testing and Materials [6]. mary standards

Generally speaking, IEEE standards dealing directly with measurement apparatus, instrumentation, and etalons have been adopted by the American National Standards Institute and, hence, are covered above. Standards and recommended practices produced by the Instrument Society of America deal primarily with the application of instrumentation to industrial processes and with the use and measurement of transducers. There are 18 such procedures involving electronic instrumentation. Standards produced by the Electronic Industries Association deal primarily with electrical testing of components and with electronics in the manufacturing process.

The Edison Electric Institute, the Association of Edison Illuminating Companies, and the National Electrical Manufacturers Association have contributed to standards for electric power systems, either through sponsorship of, or participation in, ANSI committees. In the measurements field three standards are very prominent: ANSI C12 (watthour meters, electricity metering; committee is chaired and co-sponsored by NBS); ANSI C57.13 (instrument transformers); ANSI C93.2 (coupling capacitor voltage transformers) [7]. The IEEE is a very important contributor to the measurement and test standards for electric power systems through the Power System Instrumentation and Measurements (PSIM) Committee and its subcommittees and working groups. This committee is responsible for about 10 standards, most of which have been adopted by ANSI.

There are two areas in which the standards reviewed have little or no impact. The first is the area of the dynamic measurement of electrical processes in which timing is a significant factor. With the increasing use in this country of computer-driven measurement equipment, standardization of terminology and specification of valid timing test methods are necessary to relieve the chaos which presently exists in the marketplace for that type of equipment [6]. (See also Appendix C.)

Methodology for testing the measurement system is not well documented as such. Although documentation of tests on certain types of instruments is available, techniques for the verification of the measurements are not documented. No mention is made in published standards of the type of system-output sampling that is employed in many of the Measurement Assurance Programs being carried out by the NBS.

The importance of these voluntary standards is reflected by the support given to their generation by industry and the government. Most standards committees meet at least biannually and the meetings are generally well attended even though the participants are from various parts of the country. And, although the use of these standards in this country is on a voluntary basis, their generation gives a solid technical base for U.S. input for international standards work, the results of which may carry the force of law in other countries. Heavy and successful U.S. activity in that area is needed to enhance our export trade posture.

2.2.2 Instrumentation System

2.2.2.1 Measurement Tools and Techniques

Practical (end use) measurements in the Electrical Measurement System are supported by a hierarchical structure resembling an inverted pyramid with the National Bureau of

Standards as its base. At NBS, the legal electrical units, which have been determined in terms of the theoretical (SI) units, are maintained and disseminated to the standards and calibration laboratories of the community. (See Appendix E for a list of NBS primary and working electrical standards.) The units are transferred there from standards to a class of instrumentation commonly known as test equipment. It is this test equipment which provides the means for the calibration and maintenance of virtually all electronic and electrical equipment in the country, regardless of its nature.

A few basic types of standards, used in corporate standards and calibration laboratories and supported by NBS, are used to tie the units embodied in test equipment to the legal units. Table 6 lists these basic standards. Standards are arranged in descending order of performance capabilities where more than one are listed. Approximate accuracy capabilities are expressed in parts per million (0.0001%) in parentheses.

In parallel with the hierarchical organization mentioned above, there are similar technical chains of measurement traceability from NBS standards to the end uses. Examples of these are to be seen in figures 2 and 3 which depict the traceability of applied voltage measurements in the electronics industry and applied energy measurements in the electric power area, respectively.

The dissemination of electrical units is generally accomplished in one of two fashions. In the traditional calibration method, the standard to be calibrated is taken to the laboratory in which the standard used to calibrate it is kept. It is then calibrated, and returned. Although this approach has the merit of being easily managed and is generally adequate in most situations, it has a number of technical flaws. The standard is not calibrated in the environment in which it will be used. Hence possible environmental effects tend to be overlooked. The same holds for the electrical conditions of use. Checks are not made on the veracity of the measurement made in the use of the standard; and no assessment of the stability of the standard during the physical transfer is generally made. Alternatively, the units may be disseminated by using suitably tested transport devices to sample the quality of measurements being made in the measurement chain. This latter

Table 6. Basic units and industrial standards

Unit of	Starting Level	Standards
DC voltage	1.02 V	Saturated standard cell enclosures (0.5)†; solid state reference devices (5), unsaturated standard cells (50)
DC resistance	10^{n*} ohm	Primary standard resistors (0.1-1); Rosa-type and other intermediate standard resistors (1-15); resistance transfer boxes and precision decade resistors (10-250); resistive shunts (50)
DC resistance ratio	1/1	Hamon devices (0.02); precision resistive dividers (0.05); standard volt boxes (5); potentiometers (10)
Capacitance	10 pF	Fused-silica dielectric capacitors (0.4); gas dielectric capacitors - 3-terminal (3-100); gas dielectric capacitors - 2-terminal (50-1,000)
Inductance	100 mH	Air core standard inductors (200-2,000)
AC voltage ratio	N/A	Inductive voltage dividers (0.1); instrument transformers (100-300); high voltage transformers (100-3,000)
AC-DC voltage difference	N/A	Multijunction thermal voltage converters (5-10); Hermach-type thermal voltage converters (5-100)
Power	N/A	Wattmeters (100-10,000)
Energy	N/A	Watthour meters (200-1,000)
AC current ratio	N/A	Current transformers (100-300)

†Numbers in parentheses are approximate uncertainties in ppm.

*n can be any whole number between -4 and 14.

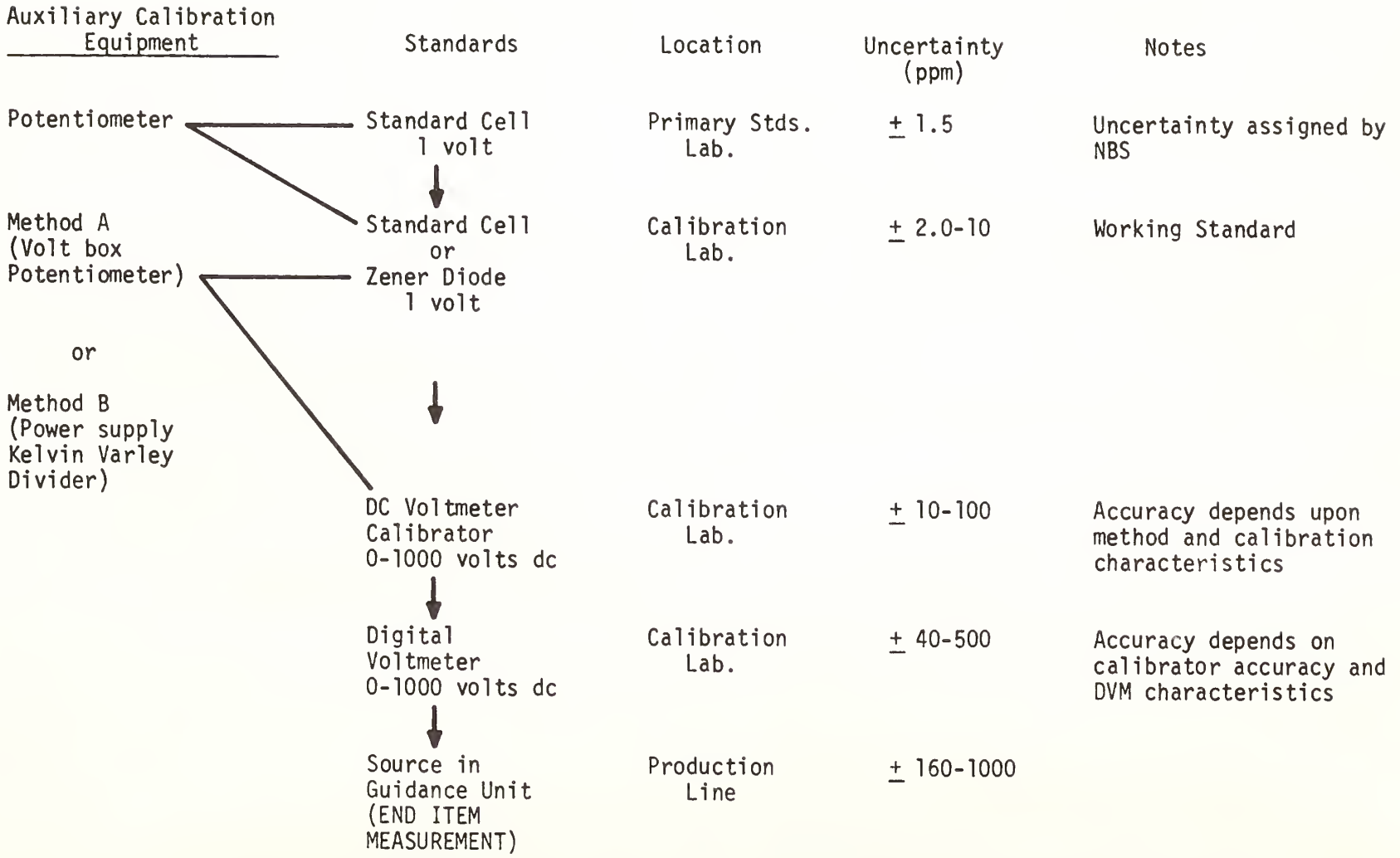

Figure 2. Traceability of voltage measurements

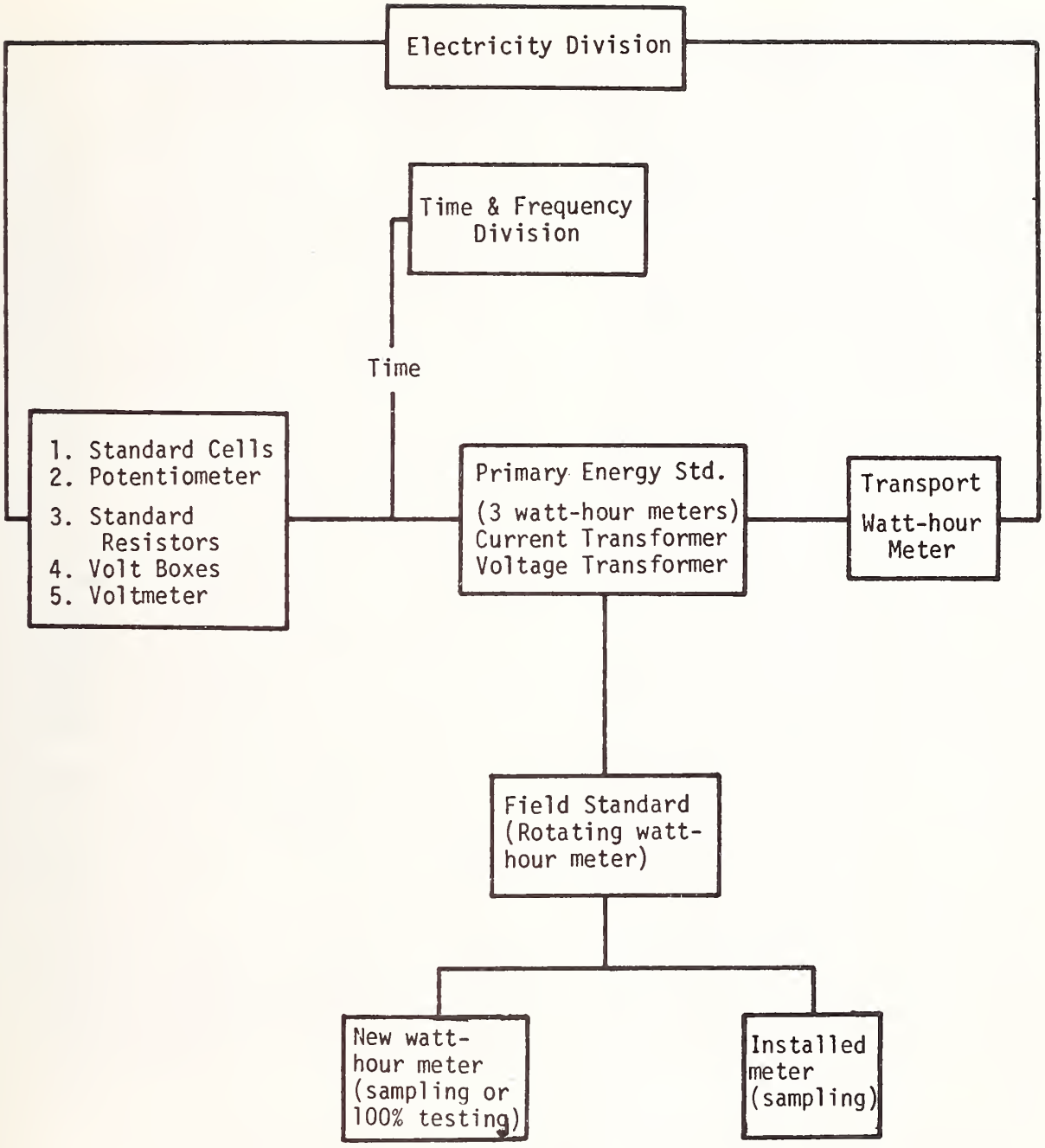

Figure 3. Traceability of energy measurements

method is somewhat more complicated in terms of data analysis and management and more costly in labor, but gives a more realistic picture of system performance. This approach is now being used more and more for dissemination purposes, especially where high accuracy is desired for the dissemination of the basic units between primary laboratories, or in cases where a suspicion exists that a measurement process is in trouble.

Technical information is disseminated throughout the system in the following ways:

(a) written calibration procedures,

(b) manufacturers' instruction manuals and user newsletters,

(c) informal contacts between colleagues,

(d) technical papers published in the open literature, and

(e) voluntary standards (previously discussed).

Most information is probably disseminated through the use of published procedures. Most government quality control contractual requirements demand the establishment of a library of written procedures covering everything from data handling to instrument calibration. Such procedures are exchanged throughout the segment of industry supporting the government through GIDEP, the Government Industry Data Exchange Program. Participation in this data-bank program is now mandatory for Defense Department contractual suppliers. Procedures must be submitted at a given rate by each participant for inclusion in a giant data bank. The bank is accessible to all participants. (GIDEP is not confined to calibration information. Other aspects include reliability data, instrumentation applications, etc.)

Many manufacturers include calibration instructions as well as application instructions in the user manuals supplied with instrumentation. This is probably the second major source of technical information in the system. The others seem to be less significant.

2.2.2.2 The Electronic and Electrical Instrumentation Industry

The instrumentation industry [8,9] is the only source of those measurement tools which provide the foundation for the quality of all manufactured products and, in some cases, provide the enabling means of their manufacture. Instruments are manufactured to measure every electrical parameter with accuracies ranging from those to be found in standards laboratories (parts per million) to five percent for analog panel meters. Their use with transducers enables the measurement of other physical parameters, such as temperature, strain, force, pressure, resistance, etc., as well. Instruments can be as simple as the dwell-tachometer used to tune an automobile or as complicated as a system for the checkout of inertial navigators, employing dozens of separate pieces of test equipment, capable of 0.005% accuracy in some cases and completely under the control of a computer.

Measurement instrumentation and control equipment enable the large volume, high quality, and low cost mass production which has made our high standard of living possible. The ready availability of digital computers as well as of reliable, accurate instrumentation capable of being computer-driven has led to the increasing use of electronic process control systems in areas such as the petrochemical industry to replace existing pneumatic, hydraulic, or manual systems. Electronic systems have the virtue of being able to respond much more rapidly - nearly instantaneously - to process changes than mechanical systems and offer greater flexibility in that process modifications may be readily brought about through software rather than hardware changes. In addition, the use of digital logic makes availabile a capability for decision-making of a complex nature.

Electrical measurements are necessary to the maintenance of this type of electronic equipment as well as all others of a durable nature.

A representative list of electronic instruments used for calibration, maintenance, testing, and analysis is given in table 7. Table 8 is a list of the major manufacturers of basic standards and primary calibration equipment in common use in standards laboratories in the U.S. It is not exhaustive.

Table 7. List of common instruments

Acoustic noise generators
Admittance meters
Ammeters
Amplifiers (over 30 types)
Analog-to-digital converters
Audio frequency analyzers
Audio mixers
Audio test oscillators
Automotive test systems
Bridges (17 types)
Calibrators (current, voltage, oscilloscope)
Current sources
Data recorders
Decade boxes (capacitance, resistance)
Digital comparators
Digital filters
Digital-to-analog converters
Digital voltmeters
Distortion analyzers
Electronic integrators
Electronic micrometers
Electrostatic voltmeters
Fluxmeters
Function generators
Harmonic analyzers
Hysteresis plotters
Interferometers
Instrument transformers
Multitester meters
Operational power supplies
Oscilloscopes
Peak power meters
Potentiometers
Reflectometers
Sampling voltmeters
Tachometers
Telemetry modulators
Vibration meters
Voltage-to-frequency converters
Volt ratio boxes
Watthour meters
Wattmeters

Table 8. List of electrical standards manufacturers

Beckman Instruments, Inc.
James G. Biddle Co.
Electro Scientific Industries
Engelhard Industries
Eppley Laboratories
General Electric Company
GenRad
Guildline Instruments Ltd.
Hewlett-Packard Company
John Fluke Manufacturing Company
Julie Research Laboratories
Keithley Instruments
Knopp Inc.
Leeds and Northrup Company
Penn Airborne Products
Sangamo Electric Company
Tittex
Victoreen
Western Electric Company, Inc.
Yokagawa Electric Works

Test equipment and instrumentation manufacturers constitute a much larger segment of industry (SIC Codes 3811, 3821, 3822, and 3825). Total estimated sales in these categories for 1976, according to the Domestic and International Business Administration, U.S. Department of Commerce, were in excess of $7.7 billion [10]. Domestic customers included every segment of industry using high technology.

Electrical measuring instruments shipments were estimated to value $2.1 billion in 1975 and are expected to increase to $2.4 billion in 1976 [10]. Test instrumentation accounts for 60 percent of the output of this SIC (3825). Low accuracy meters, used in panels and switchboards, and portable meters constitute 28 percent, and watthour and other integrating meters make up the remainder. The test equipment industry is a high technology industry which is noted for rapid exploitation of technological advances. Some manufacturers spend as much as ten percent of their annual sales on research and development [9].

The growing semiconductor market, increases in the complexity of components, and their growing application to consumer products has generated an expanding market for automatic test equipment for production line quality testing and adjustment. Automatic test equipment is increasingly being used by semiconductor device users as well as manufacturers. Digital instruments are rapidly replacing analog equipment due to substantial cost reductions and the minimization of reading error.

The instrumentation market is expected to expand over the next few years as manufacturers are spurred by the need to conserve energy and costs and reduce pollution.

In the category of Engineering and Scientific Instruments (3811), navigational and guidance instruments, and automatic pilots for ships, aircraft, and space vehicles comprised nearly one half of the industrial output. Thirty percent was composed of laboratory instruments and equipment. The remainder was composed of engineering apparatus for meteorological, hydrological, geological, civil, and mechanical engineering purposes. Production of measurement and control instrumentation was expected to reach $2.8 billion in 1976 [10]. The process control portion of this industry is the portion to be considered part of the electrical instrumentation industry. There is a high degree of activity in this area spurred by manufacturers' demands for processes which are more economical or efficient and which have reduced energy consumption and environmental impact.

Exports of all instrumentation are presently at the $60.1 million level [10], having risen sharply over the last two years. Although the U.S. holds a strong lead in the most advanced instrumention, foreign competition is increasing. The recent increase in exports is expected to moderate somewhat in the future and imports are expected to increase slightly [9].

2.2.3 Reference Data

Some reference data, i.e., physical constants and other similar data, are generated in the NBS and the academic portion of the measurement system and used primarily by research scientists seeking to test and improve physical theory. Examples of such data are measured values for γ_p, the gyromagnetic ratio of the proton, and e/h, the ratio of electronic charge to Planck's constant [5, 11], both obtained experimentally at NBS. Recent accurate measurements of the speed of light have made more accurate determinations of the absolute ohm possible [3,11].

Although their use throughout the bulk of the measurement system is limited, their determination has a fundamental impact on the values of the basic maintained electrical units and as a source of improved methodology for monitoring the stability of those units. Furthermore, much work has been done at NBS to supply least-squares adjusted values for the fundamental physical constants [12]. These values, internationally sanctioned by CODATA, the Committee on Data for Science and Technology of the International Council of Scientific Unions, tie together all of the remote branches of physics and are universally used by theoretical and research physicists. Data of this type are disseminated by publication in the scientific literature.

A more widely used type of reference data is that of electrical performance characteristics used by all design engineers. This type of data is disseminated by publication in various engineering and scientific handbooks, prepared by technical institutions and private corporations, such as those given in table 9.

Data in these handbooks range from conductivity of wire, breakdown characteristics ("volt-time curves") for sphere gaps, and Kerr electro-optical coefficients to recommended circuits for various applications. The most universal of them are obtained as the result of experiments done in national laboratories such as NBS, and in universities. Others, such as transistor performance characteristics, are published by semiconductor device manufacturers. All are essential to the efficient functioning of the design engineer and the experimentalist. It is apparent that if these data were not generally available, each new advance in technology and each design of a new circuit would come only after a long period of trial and error, measurement and experimentation.

2.2.4 Reference Materials

The direct role of reference materials in the Electrical Measurement System is limited to two areas: those of eddy-current measurements of the conductivity of non-ferrous metals and measurements of resistivity of silicon used in the semiconductor industry. The eddy-current technique is widely used in the aircraft industry and its metals suppliers as a non-destructive means of determining the heat treat of alloys, notably those of aluminum and titanium. Such measurements are commonly made using eddy-current conductivity meters which actually measure the change of inpedence of a probe, driven at a certain frequency, caused by its coupling with a conducting material. Such meters are calibrated using small standard samples (coupons) of metals manufactured either by Boeing Aircraft Corporation or the manufacturers of the meters. The conductivity of the coupons is generally determined in terms of the legal unit of resistance using dc measurement methods performed on rather large samples of materials which are then cut up.

However, dc measurements thus made are of the average conductivity through the entire metal piece and in one direction only. Eddy-current measurements are localized in a small

Table 9. Sample sources of reference data for engineers

Source	Publisher
Reference Data for Radio Engineers	International Telephone and Telegraph Corporation, New York, NY
Handbook of Chemistry and Physics	Chemical Rubber Publishing Co., Cleveland, OH
The Semiconductor Data Book	Motorola Semiconductor Products, Phoenix, AZ
Formulas for Computing Capacitance and Inductance, NBS Circular 594	National Bureau of Standards, Washington, DC
American Institute of Physics Handbook	American Institute of Physics, New York, NY
Digital Logic Handbook	Digital Equipment Corp., Maynard, MA
The Transistor and Diode Data Book	Texas Instruments, Dallas, TX

volume in contact with the probe and usually limited to a shallow depth. Because of the structure of most metal samples, (grain orientation, impurities, local strain, etc.) the local conductivity can vary widely and intercomparisons of eddy-current meters and conductivity coupons have revealed some rather large discrepancies in measurements being made. Accordingly, NBS has been approached by a number of aircraft companies to establish material standards in order to eliminate these discrepancies and to remove the confusion which exists in this area. In 1977, NBS held a workshop in this area to identify the problems associated with these measurements and identify other areas where standards are needed. Plans have been made and work is underway to establish national standards of conductivity in the range between 1% and 100% of the conductivity of copper. Based upon this work, eddy-current conductivity standards or coupons of various metals will be made available through the Standard Reference Materials Program.

Standard reference samples of silicon are available through the Standard Reference Materials Program to support the measurement of the resistivity of semiconductor materials. This SRM results from work done by the NBS Electronic Technology Division and will be reported in that Division's impact report.

2.2.5 Science and People

Electrical metrology involves the direct application of principles of physics and electrical engineering to the solution of measurement problems. The role of physics is most evident in basic metrology work; the development of instrumentation and the assembly of sophisticated instruments into measurement systems. The major contribution of the measurement system to its undergirding science and technology is to provide a common means of communication, a universal technical language without which the transfer of knowledge and technology within the system would be impossible. Without such data transfer, the advanced technological society we find in the United States would not be possible.

There is heavy involvement of professional societies in the Electrical Measurement System. They provide a means of informal and formal communication of knowledge throughout the system through their meetings and publications. The following is a list of these societies:

1. Institute of Electrical and Electronic Engineers; Group on Instrumentation and Measurement
2. Instrument Society of America; Metrology Division
3. Precision Measurements Association
4. National Conference of Standards Laboratories
5. American Society for Quality Control
6. American Society for Testing and Materials
7. American Physical Society
8. IEEE Groups on
   a. Automatic Control
   b. Biomedical Engineering
   c. Circuits & Systems
   d. Communications
   e. Industrial Electronics and Control Instrumentation
   f. Reliability and Maintainability
9. IEEE Power Engineering Society

The first four of these are groups dealing directly with electrical metrology and its applications. Their members produce document standards, engage in measurement activities, such as round-robins, and, most importantly, communicate and encourage communications by means of meetings, colloquia, conferences, seminars, and producing various

publications. The remaining are more peripherally involved in that their activities are supported by the system and they provide the system with backup technology and information.

The major electrical metrology publications commonly used in the U.S. are:

Metrologia
IEEE Transactions on Instrumentation and Measurement
IEEE Transactions on Power Apparatus and Systems
Measurements and Data
Instrumentation Technology
Review of Scientific Instruments

All feature technical papers on metrology in various application areas or sectors of the measurement system. More specific, detailed information on specific calibration problems is disseminated through documented calibration procedures as discussed previously.

Measurements people generally fall into one of five categories: physicist, electronic engineer, electrical engineer, statistician, or electronic technician. Those in the first four receive their professional training in universities and colleges. Electronics technicians generally receive their education as the result of military service and occasionally through correspondence or technical schools. All can improve or augment their background through the many seminars and short courses in metrology and electronics offered around the country. The field of metrology is fortunate in having a very high degree of dedication on the part of its workers.

2.3 Realized Measurement Capability

The graphs on the following two pages represent measurement accuracies available throughout the measurement system. It must be understood that they represent an oversimplification of an extremely complex interacting set of parameters. For example, the question of a specified time frame in which a measurement is made has been ignored. Environmental and power line effects have been likewise ignored. The fact that a good metrologist can coax performance far in excess of manufacturers' specifications from measurement instrumentation, given appropriate resources or complete freedom of choice regarding methodology, is not represented. In essence, the graphs represent a compilation of manufacturers' specifications and known behavior traits of populations of standards in common usage. In the interest of brevity, ac quantities have been shown at one frequency, 1000 Hz in the case of capacitance and inductance, 60 Hz in the case of energy and current ratio, and 10 kHz in the case of rms ac voltage.

The instrumentation available is adequate for the fulfillment of static measurement needs at the present time in most cases. Recent evidence, however, indicates the possible existance of a hitherto unsuspected loss of measurement accuracy as a result of high accuracy electronic instruments having been physically transported, either to be calibrated or for use elsewhere. The problem is presently being investigated.

Another problem area, whose importance is emphasized in light of present economic conditions, is the cost of maintaining an instrument in calibration. Many new instruments are being designed with self-checking features to permit extension of calibration intervals or the elimination of periodic calibrations. A method of testing the verity of self-test features is desperately needed.

More and more measurements are being made by automatic test systems; assemblies of off-the-shelf commercial instruments, customized apparatus, and interconnecting circuitry, all controlled by computer. Generally such systems have some self-test capability which provides a functional check and perhaps a limited calibration using an internal standard as a reference. The self-test capability must be periodically augmented by calibrations. Usually this is accomplished by removing critical pieces of apparatus to a remote laboratory for individual calibrations which are assumed valid when the system is reassembled. Rarely are systems calibrated as systems, despite the fact that, because of temperature, interface, and electrical grounding and shielding problems, they tend to be somewhat more than the sum of their parts. The major restraining factors of systems calibration seem to be lack of acceptance of the approach by military and other government inspectors and the nonavailability of hardware specifically designed for the purpose. There does at present seem to be a growing awareness of the advantages of this methodology.

There are a few areas in which present measurement technology has fallen behind requirements. There is a problem, previously discussed, regarding the use of samples of nonferrous metals as conductivity standards for nondestructive testing purposes. Another area is that of ac voltage measurements throughout the audio frequency range. Improved measurements in this area are needed to support modern ac voltage measurement equipment. A third area is that of the measurement of impedance (capacitance) in the frequency range between 10 kHZ and 100 kHz.

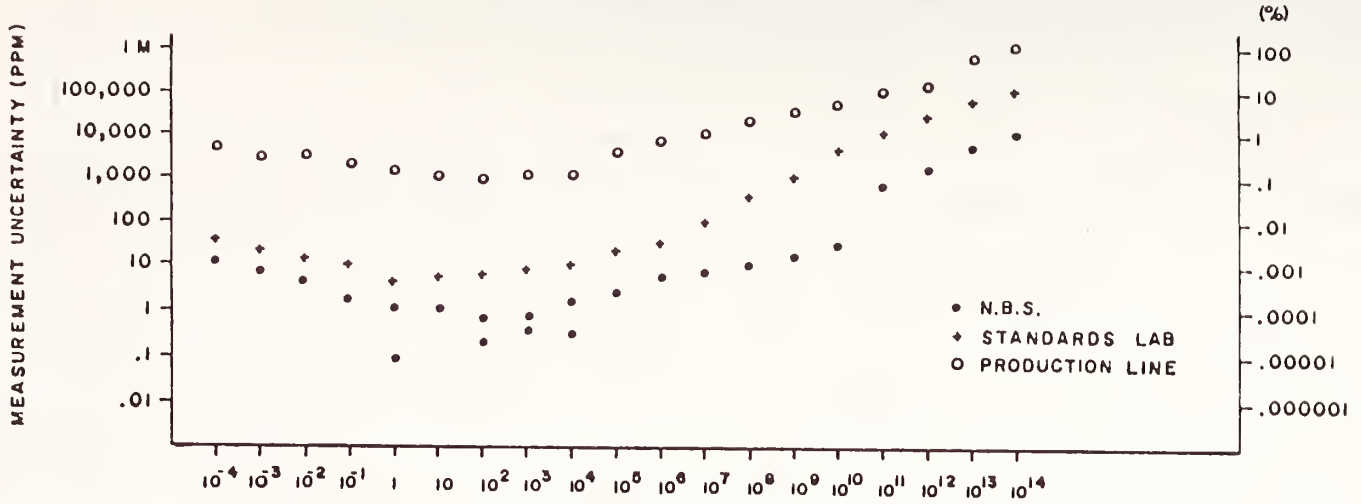

TYPICAL UNCERTAINTIES IN RESISTANCE MEASUREMENTS

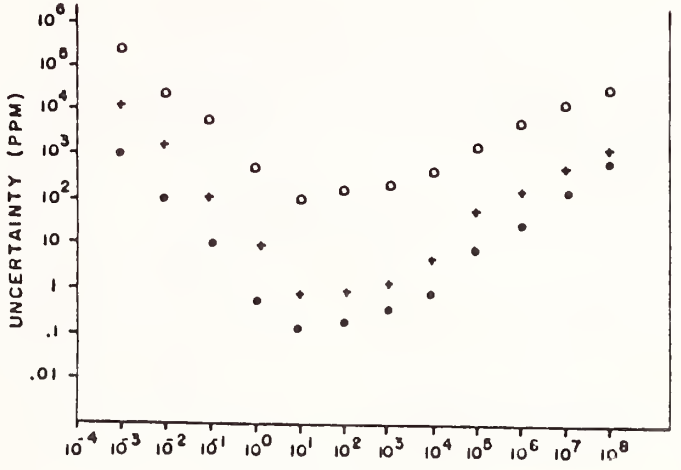

TYPICAL UNCERTAINTY IN CAPACITANCE MEASUREMENTS

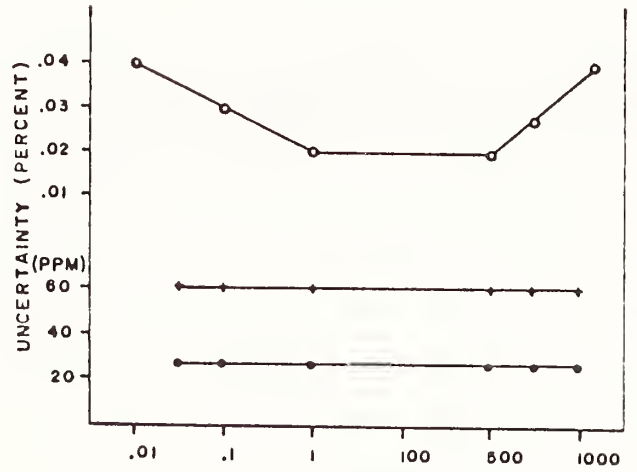

TYPICAL ACCURACY FOR rms VOLTAGE MEASUREMENTS (AT 10 kHz)

FIGURE 4a. UNCERTAINTIES OF MEASUREMENTS

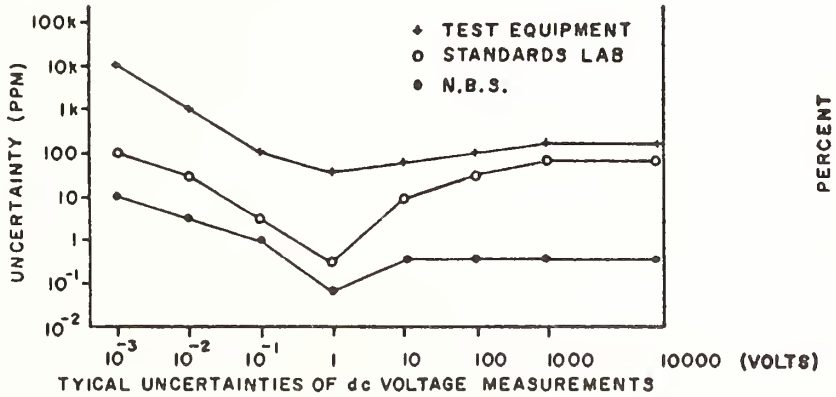

TYICAL UNCERTAINTIES OF dc VOLTAGE MEASUREMENTS

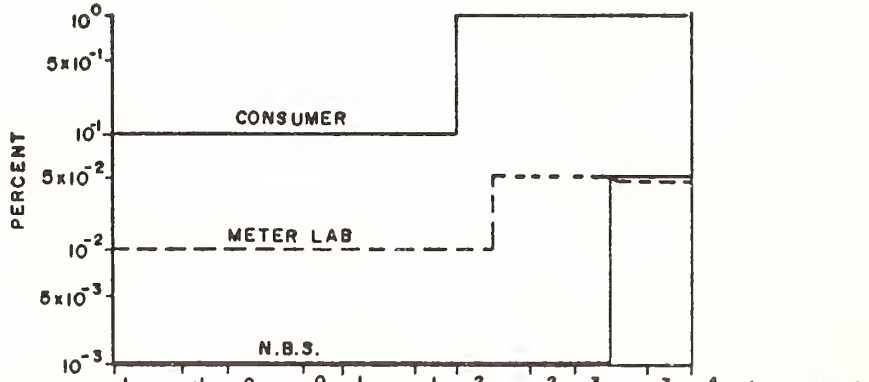

TYPICAL UNCERTAINTIES OF CURRENT RATIO MEASUREMENTS AT 60Hz

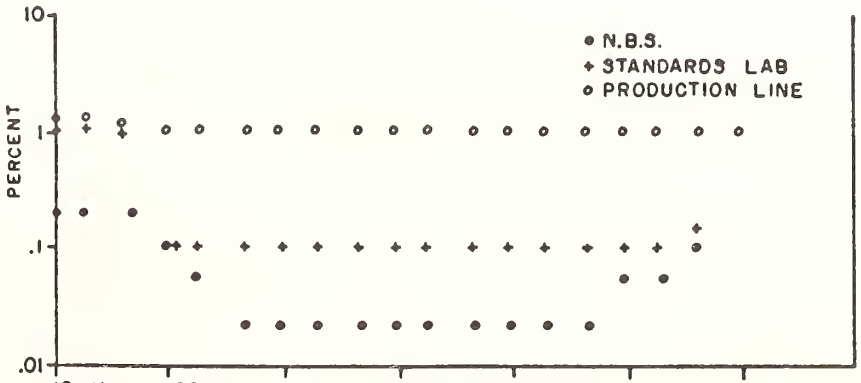

TYPICAL UNCERTAINTIES OF INDUCTANCE MEASUREMENTS

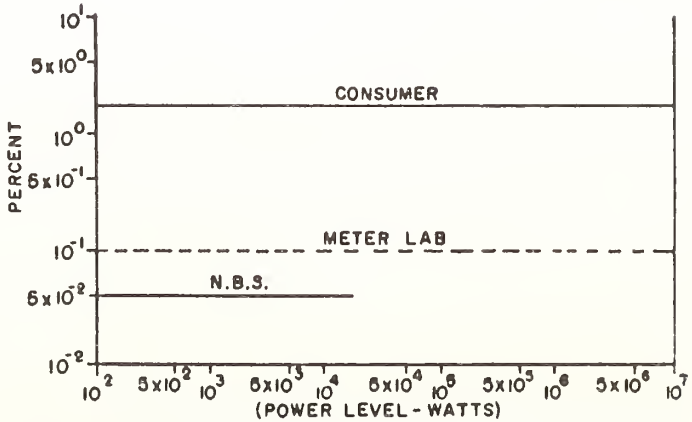

TYPICAL UNCERTAINTIES OF ENERGY MEASUREMENTS AT 60Hz

FIGURE 4b. UNCERTAINTIES OF MEASUREMENTS

The communications industry is in a trend toward increasing carrier frequencies into this range and have requested calibration data there.

The energy crisis has created some high voltage measurement problem areas. Because of the limited supplies of petroleum, electric energy will comprise an increasingly larger share of all energy consumed. Efforts are underway, sponsored by the Department of Energy and the Electric Power Research Institute, to develop more efficient and safer ways to transmit electric power. These efforts require new or improved methods and standards for measurements of impedance, ratio, voltage, and current at voltages as high as 1.2 million volts. They are needed for the evaluation of dielectric losses in insulators at cryogenic temperatures under high voltage conditions, for measurement of electric fields caused by ultra-high voltage transmission lines (to test biological effects), and for the measurement of high voltage transient signals to test their effects on lines, measurement apparatus, switchgear, etc.

As noted, the entire section thus far has concerned only static measurements, measurements in which time is not a critical factor. However, the timing of a measurement is increasingly important for two reasons. Because of the ever-increasing complexity of electronic modules, components, instruments, and systems, more and more testing is required for quality control purposes. As testing is the factor which limits the production rate of electronic goods, increasing emphasis is being placed on "thruput".

Secondly modern electronic circuitry is more usefully characterized in terms of transient responses to changing input conditions. This leads naturally to the need to measure rapidly varying parameters, to be concerned with wave shapes as well as integrated energy content. This can only be done by "sampling" or measurements at high speed.

In order to increase the speed at which measurements are made, a whole new world of automatic testing has evolved. Analog-to-digital converters with microsecond measurement times are computer-controlled and switched in systems which permit thorough testing of complicated circuits in relatively short time.

Along with this evoluation has come a degree of chaos. The conclusions of a recently-held workshop on "Critical Electrical Measurement Needs and Standards for Modern Electronic Instrumentation" [13] are:

(a) There is a need to introduce time as a measurement parameter as a result of requirements of automatic test and control systems.

(b) A host of new parameters have resulted from the application of automated systems to the production line, parameters for the measurement of which there are no standards, techniques, or even a common terminology.

(c) A need for a new or higher accuracy measurement has resulted from recent work at the leading edge of measurement technology in electronics.

From these, a number of critical, specific areas needing immediate attention were indicated. Among them were:

(1) capacitor and resistor characterization under pulsed conditions;

(2) dynamic performance characterization for modern signal conditioning and data conversion devices, such as aperature times of sample-hold amplifiers, resolution-time product for analog comparators, jitter error of digital-to-analog converters, etc.;

(3) characterization of settling times for precision sources and measurement devices, for example digital voltmeters and programmable power supplies;

(4) transport standards for system performance validation to be used as a basis for Measurement Assurance Programs;

(5) effects of dynamic loading on sources;

(6) prediction of long-term performance of components and devices from short-term behavior, for example, relating output noise and device reliability;

(7) improved transportable dc standards based upon solid state technology which would be immune to short-circuit or loading damage, not materially effected by temperature fluctuation, and perhaps at more useful levels of voltage, current, or resistance than are present standards;

(8) measurement of dielectric hysterisis in capacitors and other components; and

(9) generation of nonsinusoidal, high crest factor precision signals for true rms calibrations.

The workshop was attended by 24 participants who represented a variety of industrial and government organizations. The abstract, preface, and list of participants from the final report of the workshop (published as NBS Technical Note 865) are appended [Appendix C].

2.4 Dissemination and Enforcement Network

2.4.1 Central Standards Authorities

The Bureau International des Poids et Mesures (BIPM) is the supranational authority of the electrical measurements world. In its laboratories are housed artifacts embodying international standards of voltage and resistance. At three-year intervals, BIPM undertakes the intercomparison of transportable standards of voltage and resistance from the major national laboratories of the world and its own international standards. The published results of these intercomparisons are generally accepted as quantifying the differences among the units of the participating countries. BIPM also sponsors international exchanges, such as a present round-robin intercomparison of transportable capacitance standards. Such devices are measured at various national laboratories and the results submitted to BIPM. At the conclusion of the experiment the results are published.

The Consultative Committee on Electricity, to which the Chief of the Electricity Division, NBS, is a delegate, advises and recommends courses of action to BIPM in matters dealing with electrocal metrology.

The National Bureau of Standards is the delegated legal authority for electrical measurements in the United States. Public Law 617, 81st Congress (21 July 1950), states in Section 12:

> "It shall be the duty of the Secretary of Commerce to establish the values of the primary electric and photometric units in absolute measure, and the legal values for those units shall be those represented by, or derived from national reference standards maintained by the Department of Commerce."

Most nations with modern technological capabilities have organizations performing the function of maintaining legal electrical units. Aside from minimizing the effects of discrepancies between legal electrical units on export trade, the major interaction between these laboratories and the Electrical Measurement System is to provide an international redundancy in the realization of the absolute electrical units. Parallel experiments, perhaps with differing approaches and performed under different roofs, offer the best opportunity to eliminate the effects of unidentifiable systematic errors from experimental results. Since adjustments to units are made as the result of these experiments, redundancy in them is of great importance.

2.4.2 State and Local Offices of Weights and Measures

The Electrical Measurement System only interacts with the weights and measures field to the extent of providing the basis for design and maintenance of any electronic equipment used in that field.

2.4.3 Standards and Testing Laboratories and Services

Three kinds of laboratories provide measurement services to the Electrical Measurement System. Standards laboratories are those laboratories which can provide for the calibration of electrical standards with accuracies within an order of magnitude of those offered by NBS. They may well be, and usually are, capable of providing calibration services for nearly any type of instrument over any range of parameters and at any accuracy level up to those of the basic standards. A calibration laboratory, on the other hand, calibrates and repairs test equipment and production-line equipment of more moderate accuracy. The third type of laboratory is a testing laboratory. Although it may offer services similar to the other two, it is characterized by facilities for environmental, safety, and performance testing.

The first two types can be either the basic measurement laboratory of a large corporation, the service repair department of an instrument manufacturer, or a small private company dealing only in those services mentioned. Standards laboratories tend to be of the first two varieties, whereas calibration laboratories tend to be of the third.

Within the electric power industry one can make a distinction between the utility and manufacturing sectors. The major utility companies each operate a kind of laboratory which can be characterized as a mixture of the standards and calibrating laboratory with some functions of a testing laboratory. With respect to accuracy, the most demanding requirement is for watthour meter and instrument transformer calibration. For these functions the laboratory maintains high quality standards, with accuracies within an order of magnitude of those of NBS standards. The same laboratory usually also calibrates and repairs test instruments for the company. Finally, the laboratory may have jurisdiction over the acceptance tests of all incoming and in-service watthour meters and instrument transformers. The latter is a function of a testing laboratory.

Within the manufacturing sector, the typical laboratory can be classified as a testing facility employed in quality control and performance testing of a company's products. This laboratory may obtain standards services from a standards laboratory elsewhere within the company, may occasionally ask for NBS help, or may rely on traceability through the supplier of the measuring instruments.

Appendix D contains a list, drawn from the sources indicated, of standards and calibration laboratories whose services are available to extra-company organizations. It is not exhaustive. The 138 laboratories listed, along with others of their kind and the major military and corporate laboratories supplying services only within their own and subcontracting organizations, provide the traceability skeleton supporting the body of electrical measurements in this country.

Of federal laboratories other than NBS, apparently only three offer electrical calibration services on a fee basis. They are:

(a) U.S. Army Electronics Command, Ft. Monmouth, NJ
(b) Naval Air Rework Facility, Norfolk, VA
(c) Navy Eastern Standards Laboratory, Washington, DC

Other military and NASA laboratories will generally provide a contractor with services if they are not elsewhere available, or if it is to the advantage of the government.

All the above-mentioned and those included in the referenced appendix are laboratories having services available to outside organizations on a fee basis. No mention has been made to this point of the remaining group, namely, those laboratories which provide services only internally, to their own organization. Of the 222 standards laboratories listed in *A Directory of Standards Laboratories* [14], 164 have dc and low frequency capability, and only 65 choose to make that service available to outside firms or organizations.

An analysis was made in 1973 of NBS calibration clientele for the purpose of determining, among other things, the general magnitude of the Electrical Measurement System. A representative sample of clients' names was classified by primary SIC code by Dun and Bradstreet. The resulting list of code numbers was filtered to remove obvious measurement-void categories. Dun and Bradstreet's data base, which contains information on over 3 million U.S. companies, was then searched to provide information on all companies in the relevant group with numbers of employees in excess of 25. Information was provided on 12,865 companies. Even though this figure is not an accurate count of measurement-intensive organizations due to the way the individual SIC code numbers are assigned, it is a good protrayal of the extensiveness of the measurement system. In fact, the figure is on the low side because companies engaged in routine measurements without rigid traceability requirements are not included. Efforts to sample this grey area of the system have been minimal due to financial constraints.

For companies not having rigid traceability requirements, the measurement system may flow through the company via the electronic maintenance shop or the outside organization which performs this function for them. Many of the laboratories in Appendix C also perform repair functions.

For organizations which must maintain traceability because of contractual or legal requirements, the flow of electrical units through the system becomes more stylized. The flow of the electrical units through such an organization is depicted in figure 5. The corporate or primary laboratory may receive its units from NBS or from any outside laboratory. It is repsonsible for the most accurate standards in the organization.

The actual organizational relationship of these various components varies from corporation to corporation. An extremely large corporation, such as Boeing Aircraft, may have a corporate standards laboratory which serves as a single tie between NBS and all of its calibration laboratories. Other large companies such as Honeywell and IBM have a standards laboratory at each location and many such laboratories have standards calibrated by NBS. Other corporations such as 3M and General Electric do not make the use of any particular structure mandatory. Each operating division is autonomous and may pursue its quality assurance program quite independently.

In smaller organizations the standards and calibration facilities are usually combined. Occasionally even the maintenance shop is in the same organization, if not in the same room. These basic elements are always present, however, even if not structurally distinct. Take the case, for example, of a small company employing about 800 persons, which is concerned with the manufacture of temperature and air speed transducers and allied instrumentation. They have need of extremely accurate resistance standards because of their temperature work. However, their dc voltage requirements are not as stringent. They have their resistance standards calibrated at NBS, but their corporate voltage standard is a digital voltmeter calibrator which is calibrated for them periodically by another company in the area.

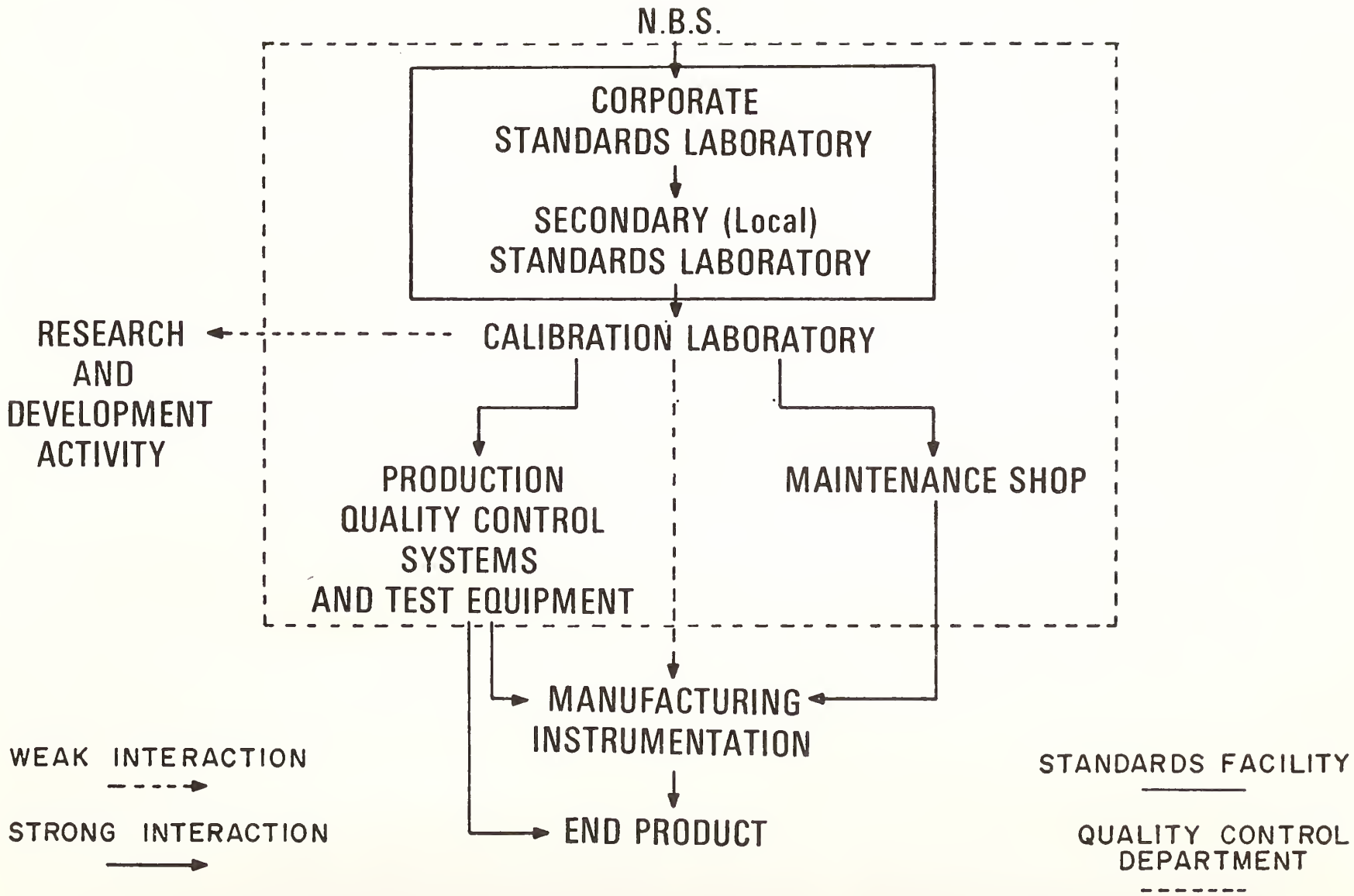

Figure 5. Typical corporate support structure

Representative organizational charts for two large corporations and the U.S. Air Force are to be found in Appendix E.

The specific structure of any given part of the measurement system is a function of the technical requirements of the end product, the legal obligations of the organization, the financial resources available, and the standards, apparatus, and test equipment available to meet the ultimate measurement requirements.

2.4.4 Regulatory Agencies

Table 10 gives the titles of regulatory agencies and agency categories impacting the Electrical Measurement System.

Table 10. Regulatory agencies and agency categories

Federal Government

1. Nuclear Regulatory Commission
2. Environmental Protection Agency
3. Federal Aviation Administration
4. Food and Drug Administration
5. National Highway Traffic Safety Administration
6. Occupational Safety and Health Administration

State Governments

State Public Utility Commission

The Nuclear Regulatory Commission (NRC) has the function of being Federal watchdog over radioactive materials in this country for both security and safety purposes. They have issued regulations which compel the formation of quality assurance programs in nuclear power plants and fuel reprocessing facilities. Regulation 10CFR50, "Licensing of Production and Utilization Facilities" has an Appendix B entitled "Quality Assurance Criteria for Nuclear Power Plants and Fuel Reprocessing Plants." This Appendix and corresponding Regulatory Guides call for periodic calibration of all measuring equipment. The result of such regulations is the establishment of standards and calibration laboratories at all nuclear use and processing sites to ensure the quality of measurements at such sites.

The Commission is presently in the process of revising these regulations to improve their clarity. The National Bureau of Standards is anticipated to be called upon to provide technical assistance in this activity.

The Environmental Protection Agency (EPA) has an indirect effect on the Electrical Measurement System. The instrumentation, which is required by the agency and by industry to monitor pollution, is used mostly for analytical and accoustic measurements. Sales of such instruments are increasing at a rapid rate, sparked by large increases in federal and private research and development in this area [9]. This equipment is basically electronic in nature and, as such, requires maintenance, if not electrical calibration.

The Federal Aviation Administration (FAA) is responsible for all air travel safety in the U.S. It regulates the communications and navigation equipment used in the air travel system. A measurement laboratory facility is maintained in Atlantic City, NJ, which supports a network of navigation aids such as radar systems, landing systems, and beacons at airports throughout the country, in addition to a test facility for avionics on the Atlantic City site. In addition, the FAA is now in the process of implementing a program for the periodic recall and calibration of all test equipment in its system. This new calibration structure may be ultimately supported by the standards laboratory of the FAA maintenance and repair depot in Oklahoma City.

The Food and Drug Administration, as was pointed out previously, is expanding into the regulation of medical devices. Aside from the proposed regulatory program for new products described in Sec. 2.2.1.1, they are involved in a program to ensure safety through the proper level of application of voltage to x-ray tubes. It was found as a result that the voltage dividers used for measurement of cathode voltages were poorly calibrated at best and improper x-ray dosages resulted. Bureau of Radiological Health support resulted in the establishment of a calibration service for such dividers at NBS.

The National Highway Traffic Safety Administration is responsible for enforcement of the application of safety standards to automobiles. The group monitors the whole field of automobile safety testing. Use is made of Society of Autmotive Engineers' specifications to detail methods to be followed in the testing and to prescribe requirements for quality assurance. Periodic test and calibration of measurement instrumentation using standards traceable to NBS are features of SAE Standard J21b. Manufacturers are required to abide by its provisions.

The Occupational Safety and Health Administration generates job-related safety regulations. Its major impact on the Electrical

Measurement System is its requirement that certain devices be safety-tested in accredited laboratories. That requirement is expected to be the forerunner of many future requirements for laboratory accreditation programs. None of the methodologies yet proposed embodies a valid scheme to ensure the proper behavior of standards, instruments, and systems on a continuous basis, either through careful monitoring or any other means. A real need exists for a technically-valid scheme for accreditation.

State Public Utility Commissions, in addition to regulating the rates charged consumers of electric power, regulate the system by which energy transfer is monitored to determine total user costs.

Watthour measurements are used to quantify energy distributed within the power system for metering purposes. The electric power companies are generally required by the Public Utility Regulatory Commisions in individual states to supply users with watthour meters accurate to within 2%. Refunds are required for overcharges if the meter regulation is found to be in error -- faster than nominal -- by more than 2%. While power companies are entitled to recompense from users should the meter err in their favor, they generally do not bill such users because of the bad publicity which could result. Because of this situation, power companies typically calibrate new watthour meters with an uncertainty of 0.1-0.2 %. Measurements at this relatively high level of accuracy also permit new meters to be inspected using sampling techniques, thus avoiding the large amount of work required to inspect 100% of the incoming lot. Because this practice is common in the power industry, meter manufacturers must also use strict measurement tolerances.

Installed meters are generally recalibrated throughout the industry. However, there is no industry-wide established interval between calibrations. This interval ranges generally from five to fifteen years and in most instances is done on a sampling basis with 100% recalibration only being performed on the basis of poor results from an initial group of tests. These measurements are made with the same uncertainty as are those on new meters.

Of all quasi-regulatory activities, procurement regulations governing suppliers of the Department of Defense and the National Aeronautics and Space Administration have the greatest impact on the measurement system. The present hierarchical system of laboratories, accuracy needs at the primary standards level, and the generation of use of detailed calibration procedures all stem from the enforced application of MIL-C-45662a, MIL-Q-9858a, MIL-I-45208a, and the equivalent NASA regulations, all detailed previously.

2.5 Direct Measurement Transactions Matrix

2.5.1 Analysis of Suppliers and Users

The organizational input-output matrix in Figure 6 is a portrayal of the present magnitude and importance of measurement transactions among various segments of the economic system. Each entry in the array gives the magnitude, role of changes, import, adequacy, and type of transaction according to the code in Figure 7. An "X" as a particular entry indicates that the transaction was excluded from the study for some reason. Entries of "0", "X", or "?" require no further information for that transaction. It must be remarked that the matrix is only a qualitative portrayal. The uncertainties in each ranking factor are high (±2) as it is difficult to quantify relationships such as quantity or volume in the context of various sizes and technical contents of industries. The general approach taken was that a measurement capability could not cease to exist, since in that sense, the "Importance" entry would be 4 by any rational consideration for each transaction. In addition, those industries which require measurements, instrumentation, and standards closest to the state-of-the-art" naturally are more familiar to the authors and received more attention during the course of the study as they are the most likely source of measurement problems.

2.5.2 Highlights re Major Users

Although virtually every segment of manufacturing depends to some extent on the ability to make electrical measurements, major users of the measurement system have a very stringent need for an accurate measurement capability. These are the aerospace industry, the calibration and repair industry, civilian agencies of the Federal government, electronic component manufacturers, computer manufacturers, the Department of Defense, the instrumentation industry, the power industry, and research institutes. It should be understood that technical measurement problems to be found in this system are generally not unique to a specific segment of industry in the SIC sense. Rather they are generally associated with a broad class of activity such as instrument maintenance or quality control of electronic products and accordingly are not belabored in this section. Pressing problems which are industry-peculiar are mentioned.

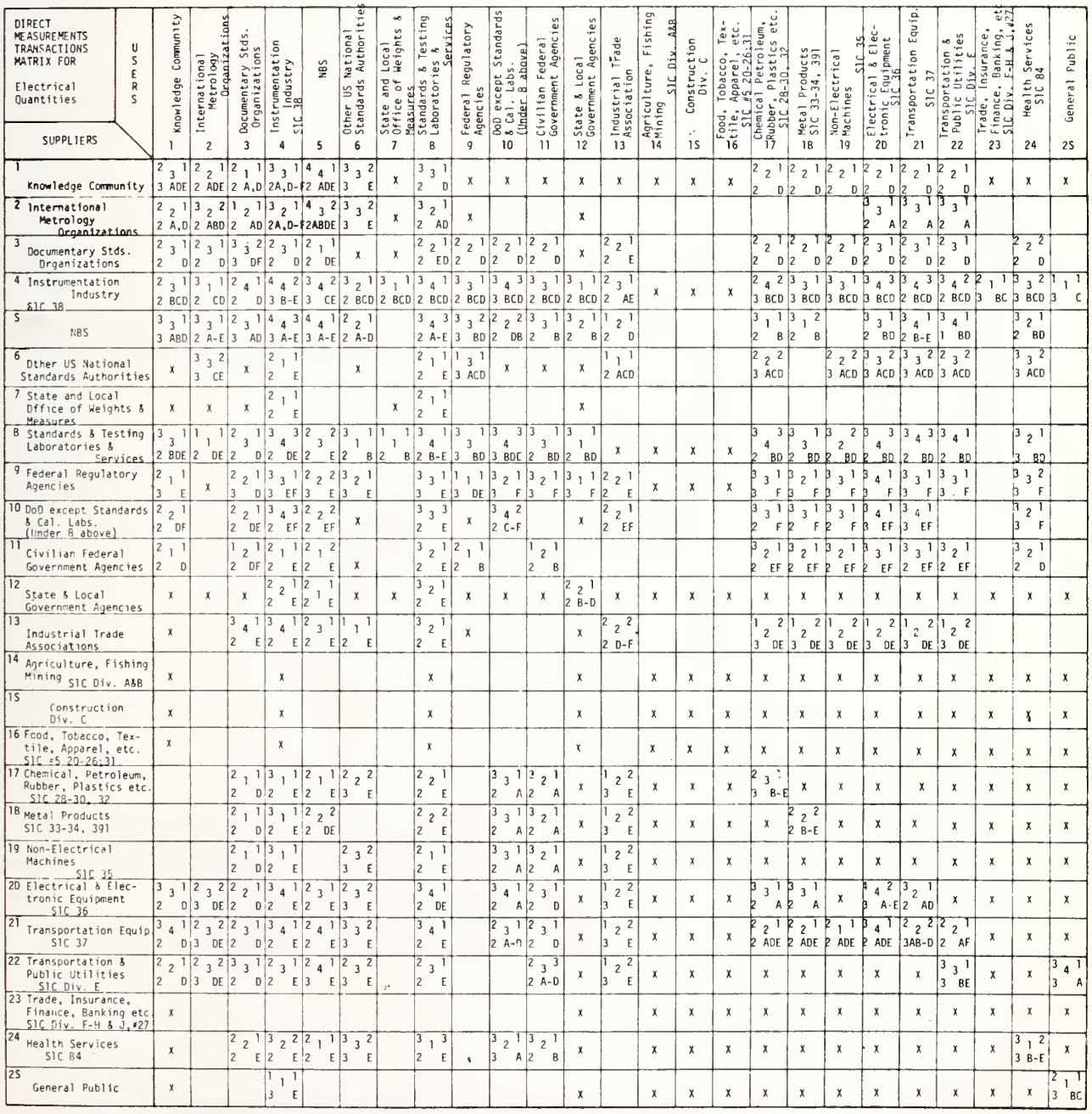

DIRECT MEASUREMENTS TRANSACTIONS MATRIX FOR Electrical Quantities / SUPPLIERS	USMS	1 Knowledge Community	2 International Metrology Organizations	3 Documentary Stds. Organizations	4 Instrumentation Industry SIC 38	5 NBS	6 Other US National Standards Authorities	7 State and Local Office of Weights & Measures	8 Standards & Testing Laboratories & Services	9 Federal Regulatory Agencies	10 DoD except Standards & Cal. Labs. (Under 8 above)	11 Civilian Federal Government Agencies	12 State & Local Government Agencies	13 Industrial Trade Association	14 Agriculture, Fishing Mining SIC Div. A&B	15 Construction Div. C	16 Food, Tobacco, Textile, Apparel, etc. SIC #5 20-26;31	17 Chemical Petroleum, Rubber, Plastics etc. SIC 28-30, 32	18 Metal Products SIC 33-34, 391	19 Non-Electrical Machines SIC 35	20 Electrical & Electronic Equipment SIC 36	21 Transportation Equip. SIC 37	22 Transportation & Public Utilities SIC Div. E	23 Trade, Insurance, Finance, Banking, etc. SIC Div. F-H & J,#27	24 Health Services SIC 84	25 General Public
1 Knowledge Community		2 3 1 3 ADE	2 2 1 2 ADE	2 1 1 2 A,D	3 3 1 2A,D-F	4 4 1 2 ADE	3 3 2 3 E	X	3 3 1 2 D	X	X	X	X	X	X	X	X	2 2 1 2 D	2 2 1 2 D	2 2 1 2 D	2 2 1 2 D	2 2 1 2 D	2 2 1 2 D	X	X	X
2 International Metrology Organizations		2 2 1 2 A,D	3 2 2 2 ABD	1 2 1 2 AD	3 2 1 2A,D-F	4 3 2 2ABDE	3 3 2 3 E	X	3 2 1 2 AD	X			X								3 3 1 2 A	3 3 1 2 A	3 3 1 2 A			
3 Documentary Stds. Organizations		2 3 1 2 D	2 3 1 2 D	3 3 2 3 DF	2 3 1 2 D	2 1 1 2 DE	X	X	2 2 1 2 ED	2 2 1 2 D	2 2 1 2 D	2 2 1 2 D	X	2 2 1 2 E				2 2 1 2 D	2 2 1 2 D	2 2 1 2 D	2 2 1 2 D	2 3 1 2 D	2 3 1 2 D	2 3 1 2 D		2 2 2 2 D	
4 Instrumentation Industry SIC 38		2 3 1 2 BCD	3 1 1 2 CD	2 4 1 2 D	4 4 2 3 B-E	3 4 2 3 CE	3 2 1 2 BCD	3 1 1 2 BCD	3 4 1 2 BCD	3 3 1 2 BCD	3 4 3 3 BCD	3 3 1 2 BCD	3 1 1 2 BCD	2 3 1 2 AE	X	X	X	2 4 2 3 BCD	3 3 1 3 BCD	3 3 1 3 BCD	3 4 3 3 BCD	3 4 3 2 BCD	3 4 2 2 BCD	2 1 1 3 BC	3 3 2 3 BCD	1 1 1 3 C
5 NBS		3 3 1 3 ABD	3 3 1 2 A-E	2 3 1 3 AD	4 4 3 3 A-E	4 4 1 3 A-E	2 2 1 2 A-D		3 4 3 2 A-E	3 3 2 3 BD	2 2 2 2 DB	3 3 1 2 B	3 2 1 2 B	1 2 1 2 D				3 1 1 2 B	3 1 2 2 B		3 3 1 2 BD	3 4 1 2 B-E	3 4 1 1 BD		3 2 1 2 BD	
6 Other US National Standards Authorities		X	3 3 2 3 CE	X	2 1 1 2 E		X		2 1 1 2 E	1 3 1 3 ACD	X	X	X	1 1 1 2 ACD				2 2 2 3 ACD		2 2 2 3 ACD	3 3 2 3 ACD	3 3 2 3 ACD	2 3 2 3 ACD		3 3 2 3 ACD	
7 State and Local Office of Weights & Measures		X	X	X	2 1 1 2 E			X	2 1 1 2 E				X													
8 Standards & Testing Laboratories & Services		3 3 1 2 BDE	1 1 1 2 DE	2 3 1 2 D	3 4 3 2 DE	2 3 2 2 E	3 1 1 2 B	1 1 1 2 B	3 4 1 2 B-E	3 1 1 3 BD	3 4 3 3 BDC	3 3 1 2 BD	3 1 1 2 BD	X	X	X	X	3 4 3 2 BD	3 3 1 2 BD	3 2 2 2 BD	3 4 3 2 BD	3 4 3 2 BD	3 4 1 2 BD		3 2 1 3 BD	
9 Federal Regulatory Agencies		2 1 1 3 E	X	2 2 1 3 D	3 3 1 3 EF	2 2 2 3 E	3 2 1 3 E		3 3 1 3 E	1 1 1 3 DE	3 2 1 3 F	3 2 1 3 F	3 1 1 3 F	2 2 1 2 E	X	X	X	3 3 1 3 F	3 2 1 3 F	3 3 1 3 F	3 4 1 3 F	3 3 1 3 F	3 3 1 3 F		3 3 2 3 F	
10 DoD except Standards & Cal. Labs. (Under 8 above)		2 2 1 2 DF		2 2 1 2 DE	3 4 3 2 EF	2 2 2 2 EF	X		3 3 3 2 E	X	3 4 2 2 C-F		X					3 3 1 2 F	3 3 1 2 F	3 3 1 2 F	3 4 1 3 EF	3 4 1 3 EF		3 2 1 3 F	
11 Civilian Federal Government Agencies		2 1 1 2 D		1 2 1 2 DF	2 1 1 2 E	2 1 2 2 E	X		3 2 1 2 E	2 1 1 2 B		1 2 1 2 B						3 2 1 2 EF	3 2 1 2 EF	3 2 1 2 EF	3 3 1 2 EF	3 3 1 2 EF	3 2 1 2 EF		3 2 1 2 D	
12 State & Local Government Agencies		X	X	X	2 2 1 2 E	2 1 1 2 E	X	X	3 2 1 2 E	X	X	X	2 2 1 2 B-D	X	X	X	X	X	X	X	X	X	X	X	X	X
13 Industrial Trade Associations		X		3 4 1 2 E	3 4 1 2 E	2 3 1 2 E	1 1 1 2 E		3 2 1 2 E	X				2 2 2 2 D-F				1 2 2 3 DE	1 2 2 3 DE	1 2 2 3 DE	1 2 2 3 DE	1 2 2 3 DE	1 2 2 3 DE		1 2 2 3 DE	
14 Agriculture, Fishing Mining SIC Div. A&B		X			X				X				X		X	X	X	X	X	X	X	X	X	X	X	X
15 Construction Div. C		X			X				X				X		X	X	X	X	X	X	X	X	X	X	X	X
16 Food, Tobacco, Textile, Apparel, etc. SIC #5 20-26;31		X			X				X				X		X	X	X	X	X	X	X	X	X	X	X	X
17 Chemical, Petroleum, Rubber, Plastics etc. SIC 28-30, 32				2 1 1 2 D	3 1 1 2 E	2 1 1 2 E	2 2 2 3 E		2 2 1 2 E		3 3 1 2 A	3 2 1 2 A	X	1 2 2 3 E	X	X	X	2 3 1 3 B-E	X	X	X	X	X	X	X	X
18 Metal Products SIC 33-34, 391				2 1 1 2 D	3 1 1 2 E	2 2 2 2 DE			2 2 2 2 E		3 3 1 2 A	3 2 1 2 A	X	1 2 2 3 E	X	X	X	X	2 2 2 2 B-E	X	X	X	X	X	X	X
19 Non-Electrical Machines SIC 35				2 1 1 2 D	3 1 1 2 E		2 3 2 3 E		2 1 1 2 E		3 3 1 2 A	3 2 1 2 A	X	1 2 2 3 E	X	X	X	X	X	X	X	X	X	X	X	X	X
20 Electrical & Electronic Equipment SIC 36		3 3 1 2 D	2 3 2 3 DE	2 2 1 2 D	3 4 1 2 E	2 3 1 2 E	2 3 2 3 E		3 4 1 2 DE		3 4 1 2 A	2 3 1 2 D	X	1 2 2 3 E	X	X	X	3 3 1 2 A	3 3 1 2 A	X	4 4 2 3 A-E	3 2 1 2 AD	X	X	X	X
21 Transportation Equip SIC 37		3 4 1 2 D	2 3 2 3 DE	2 3 1 2 D	3 4 1 2 E	2 4 1 2 E	3 3 2 3 E		3 4 1 2 E		2 3 1 2 A-D	2 3 1 2 D	X	1 2 2 3 E	X	X	X	2 2 1 2 ADE	2 2 1 2 ADE	2 1 1 2 ADE	3 4 1 2 ADE	2 2 2 3AB-D	2 2 1 2 AF	X	X	X
22 Transportation & Public Utilities SIC Div. E		2 2 1 2 D	2 3 2 3 DE	3 3 1 2 D	2 3 1 2 E	2 4 1 3 E	2 3 2 3 E		2 3 1 2 E			2 3 3 2 A-D	X	1 2 2 3 E	X	X	X	X	X	X	X	X	3 3 1 3 BE	X	X	3 4 1 3 A
23 Trade, Insurance, Finance, Banking etc. SIC Div. F-H & J,#27		X											X		X	X	X	X	X	X	X	X	X	X	X	X
24 Health Services SIC 84		X		2 2 1 2 E	3 2 2 2 E	2 1 1 2 E	3 3 2 3 E		3 1 3 2 E		3 2 1 3 A	3 2 1 2 B	X		X	X	X	X	X	X	X	X	X	X	3 1 2 3 B-E	X
25 General Public		X			1 1 1 3 E								X		X	X	X	X	X	X	X	X	X	X	X	2 1 1 3 BC

Figure 6. MATRIX

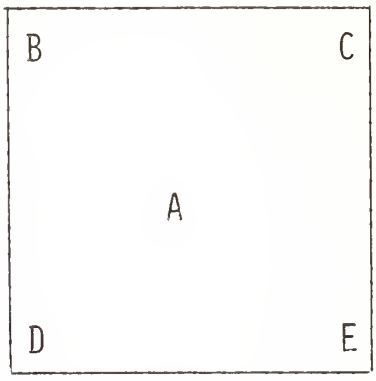

A. Volume or quantity of transaction

0 - Trivial (other entries not needed)
1 - Minor
2 - Moderate
3 - Above average
4 - Major
X - Excluded from study

B. Importance

1. Convenience; not essential
2. Economically important
3. Legally required; no alternative source
4. Absolutely essential

C. Adequacy of Transaction

1. Under control
2. Marginally adequate
3. Deficient, but useful
4. Out of control; totally inadequate

D. Rate of change of transactions

1. Declining volume (negative)
2. Stable (0)
3. Growing (+)
4. Explosive growth (very +)

E. Type of transaction

A. End use measurement data (specifications, etc)
B. Other measurement services (calibrations, etc.)
C. Measurement instrumentation and software
D. Measurement "How to" information
E. Measurement requirements information
F. Legal performance specifications

FIGURE 7. CODE FOR TRANSACTION MATRIX

Aerospace (SIC Codes 3721, 3724, 3728, 3761, 3764, 3769, and 3662). The aerospace industry is that segment of manufacturing which produces space vehicles and aircraft and their supporting electronics systems for both military and civilian applications. It is a high technology industry (engineers and scientists employed, 161,000) which makes extensive use of electronics in the develop ment and manufacture of its products, and especially, for their weapons and guidance systems. The industry is a large one, with estimated sales of products and services in 1974 of $20.9 billion of aircraft and parts, $9.6 billion of electronic systems support equipment, and $5.8 billion of guided missiles and space vehicles [9]. Estimated total sales (1976) are $35.7 billion with an estimated electronics content in excess of $20 billion. The estimated exports value of aerospace equipment for 1976 is $7.6 billion, the third consecutive year that this industry's exports have exceeded $7 billion. This industry embodies 2,107 establishments and employs about 928,000 workers [10].

The primary impact of this industry is upon our national defense. Slightly over ten percent of the aircraft produced were sold to the Department of Defense as were all guided missiles. These products are vital to the national security. Important secondary benefits have come from this source. Consumer electronic products have been revolutionized by such spin-offs from the aerospace industry as monolithic large-scale integrated circuits whose low cost, reliability, and small size per unit function have permitted the production of quartz crystal watches, pocket calculators, and miniature radio sets at exceedingly low cost.

An increasing portion of the output of the electronic systems component (SIC Code 3662) of this industry is being consumed by civilian-oriented commercial and industrial firms. This is due to the need in industry to make more use of digital data transmission, automated process and quality control, and telecommunications to offset rising labor costs and lower profit margins. Such areas as satellite communications systems, data networks, land-mobile radio communications. and interactive, broadband cable communications systems contribute heavily to this increase.

The electronic systems component is an area in which exports are expected to rise sharply, 23%, from 1975 to 1976. This is largely due to increased consumption in the developing nations and, particularly, the oil-producing nations of the Middle East. These countries, particularly Iran, Saudi Arabia, and Indonesia, are attempting to develop their industrial bases in the avionics, industrial, electronics, and communications areas, in addition to increasing their military sophistication [10]. Exports in this area are expected to increase for the next five years.

Electrical measurements in the aerospace industry are used to characterize electronic circuitry of all types, both for the assurance of quality and compatibility in manufacture and for maintenance while in service. Accuracy requirements for so-called end measurements are quite high (as high as 10 ppm, in some cases) due to the sophistication and precision of guidance and weapons systems. Since nearly all companies in this category are contractors or subcontractors to the Department of Defense or to the National Aeronautics and Space Administration, the industry is subject to the provisions of the regulations used by these government agencies to assure quality in the systems and vehicles procured. The concepts there outlined are instrumental in making the accuracies required of an individual corporate calibration support structure quite high.

Measurement problems faced by the aerospace industry are as follows:

(a) to reduce the cost of quality control efforts in the face of a slightly deflated market while adhearing to DoD and NASA requirements and regulations [10,13,15]; and

(b) measurement problems inherent in the use and support of automatic test equipment, such as those resulting from failure to calibrate under use conditions (e.g., making dynamic use of A-D converters which have been calibrated statically) [15,16].

Calibration and repair of test equipment (SIC Code 7393). There is a small industry in the U.S. having to do solely with the calibration and repair of instruments, test equipment, and standards. Most companies involved in this activity are quite small, having annual incomes of less than $500,000 and employing less than 25 people. These companies supply calibration and repair services to a variety of industries, such as small component manufacturers, transducer makers, small electronic job shops, and other companies whose calibration needs are so modest that the establishment of an internal capability would be unduly costly. (Such service is provided also on a fee basis by the corporate standards laboratories of many large corporations. See Appendix D.)

Equipment used by such companies ranges from state-of-the-art standards and calibration equipment to older test equipment of relatively poor accuracy. This results in a wide range of capabilities being available, from the state-of-the-art to meter accuracies, that is, three to five percent. In

most cases the capability is equal to the job performed. Problems related to electrical measurements in this industry seem to be logistical in nature. Lack of facilities for training, poor communications of technical data, increasing costs of publications, and an increasing shortage of experienced technicians are a few examples.

Civilian agencies of the Federal government (SIC Div. 1). Those civilian agencies which have or support (as opposed to require) an electrical measurements capability are as follows: Federal Aviation Administration, Bureau of Reclamation, Energy Research and Development Administration, National Aeronautics and Space Administration, Tennessee Valley Authority, and National Oceanic and Atmospheric Administration. FAA activity was covered in Sec. 2.4.4. The Bureau of Reclamation operates Hoover Dam and leases power generated thereby to five regional power companies. The organization has a standards laboratory that supports all of the maintenance and power monitoring equipment on the site.

The Department of Energy (DOE) has a contracted primary standards laboratory in Albuquerque, NM, run by the Sandia Corporation, which is responsible for supporting and assuring quality of measurements and contractural compliance with calibration requireemnts at each of the DOE field sites. The National Aeronautics and Space Administration (NASA) maintains a large number of standards laboratories, one at each of its major centers and tracking facilities. NASA has an extremely large test equipment inventory which is used to support space electronics, its computer network, communications equipment, tracking systems, and aircraft. Many of these laboratoies are staffed by contractors but the agency owns all of the equipment.

The Tennessee Valley Authority laboratory at Chickamauga Dam, TN, supports the power monitoring equipment and electronic maintenance areas at that facility. The National Oceanic and Atmospheric Administration supports the test and measuring equipment it uses in its investigation of undersea and atmospheric phenomena by maintaining a standards and calibration facility at the Navy Yard Annex in Washington, DC.

The social impacts of these agencies are wide-ranging. The Department of Energy plays an ever more important role in the search for means of alleviating our energy shortage. Since it is a highly technical endeavor, the use of measuring apparatus is heavy, and electrical measurements, especially those at high voltages, are of prime importance. NASA is concerned not only with space ventures but also with air transportation problems. Technical spin-offs of its programs have resulted in the creation of whole new technologies such as integrated circuit technology.

Electronic components (SIC Code 367). The industry employs about 359,000 people in about 2,500 establishments. The industry's gross sales were $10 billion in calendar year 1975, and are projected to exceed $11 billion in 1976 [10]. Exports in this field are at the $1 billion mark and increasing rapidly; up 23% from 1974 to 1975. It produces such components of electronic equipment as resistors, capacitors, inductors, diodes, transistors, integrated circuits, tubes, and rheostats. By doing so, the industry provides versatility and cost effectiveness for every electronics-intensive industry such as those involving the production of automotive electronics, communications equipment, instrumentation and process control equipment, etc.

Measurements are vital to this industry for both product quality control and development of new products. The biggest measurement problems faced here are those concerned with the proper calibration of very high-speed component testers. Such equipment is used to test large numbers of resistors, capacitors, or other components at a high rate of test. Even more importantly, complex integrated circuits must be thoroughly tested in a short time frame. The time taken per measurement is generally much shorter than the time per measurement allowed in the calibration process, and for that reason the calibration data may not be valid when the tester is used on the production line.

There are a few problems having to do with the state-of-the-art in measurements. For example, solid-state device manufacturers are generally convinced that some of the voltage reference devices they produce have stabilities in the sub part-per-million (ppm) range over the short-term and long-term (a few weeks) may be as stable as 1 or 2 ppm. Few, if any, of these same manufacturers, however, have a measurement capability adequate to determine this. Such capability would mean a cost savings to industry as a whole because if these devices are indeed capable of such stabilities, more accurate instruments could be built and instruments being built at present accuracies would require less frequent calibrations and possibly less maintenance. Even if the reference devices were not found to be as stable, an improved measurement capability would result in the ability to determine their stability with fewer measurements taken over a shorter time span. Manufactured devices

could thus be much more easily categorized and sorted. Similar problems exist in the scaling processes for other units such as resistors.

Computer manufacturers (SIC Code 3573). Sales of the computer industry were $10.4 billion for 1975 and are estimated to increase to $12.1 billion in 1976 [10]. This rapidly growing industry (current growth rate is about 14% per year) is estimated to have 179,000 employees. Its output products, computers, large and small, and peripheral equipment, are being used more and more throughout our society. They are used as accounting machines, problem solvers, process controllers, navigation aids, machinery controllers, and in nearly every other situation where decisions must be made and action taken on the basis of numerical data. The advent and continuing improvement of the minicomputer, a small, inexpensive, and reliable computer, and the microprocessor, a computer on a chip, have made the tremendous power and capability of the computer available to virtually every segment of industry. Small scale processes are being automated at a very rapid rate, thus providing some offset to the ever-rising cost of labor in this country.

Since most computers are electronic, electrical measurements play an important role in their manufacture. Each component that is received is checked to its specification at most companies. Testing is done at each stage of the assembly of such a device. The equipment used for all such testing must be maintained and calibrated and most large computer companies have corporate standards and calibration laboratories to perform this function. Electrical measurement problems in the computer industry are related to the use and support of the automatic test sets which perform the quality assurance function. Some problems result from applying static calibration data to dynamic testing situations. A particular problem of great current interest results from the giant number of measurements required to test a digital circuit to an adequate degree. Even if it is solved, however, there will be increasing need, as semiconductor components become faster responding and more complex, to make measurements of both digital signal response and dielectric properties of components at higher speeds and with greater reliability. The state of technology is pushing the few standards which do exist in this area. Another problem area is the measurement of impedances, especially inductors, in the frequency range between 10 kHz and 1 MHz.

The Department of Defense. The Department of Defense is very heavily involved with electronics in communications, weapons, guidance, and navigational systems. The Department will have spent $2.6 billion for research, development, testing, and evaluation of such equipment and $1.61 billion for the procurement of electronics systems for FY 75. Total spending for FY 75 on electronics products as estimated by the Department of Defense is $9.6 billion [9,10]. Assuming a five-year lifetime of electronics equipment in the military, using marketing data for the past five years such as surveys performed annually by Electronics magazine, one can calculate a $6 billion inventory of equipment which must be maintained. This is done with a huge inventory of test equipment supported by a hierarchical laboratory system in each of the four services. To illustrate the magnitude of the problem, the 1972 edition of Air Force Technical Order 33K-1-100 lists by part number over 28,500 individual items in the inventory requiring calibration periodically. In excess of sixty percent of this inventory requires electrical measurements [17] for its support.

The Department of Defense is the largest single consumer in the country and, accordingly, wields a trememdous impact on the marketplace. Technical spin-offs from its programs, much as is the case with NASA - who, for example, are credited for the accelerated development of large-scale integrated circuit technology - have served to advance the technology base of our society.

The Department maintains a system of inspectors in various organizations (Defense Contract Administration Service; Air Force, Navy, Army Plant Representative Offices; etc.) to ensure compliance with the calibration and quality assurance providions of the procurement specifications listed in Sec. 2.2.1.1. In this way, it influences the nature of the measurement system in a large segment of industry.

As mentioned before, the main use of electrical measurements within the Department of Defense is to maintain its extremely large inventory of electronic systems and equipment and the test equipment used to support it. The major current problem areas are:

(a) the support of automatic test and checkout equipment [13,16];
(b) the support of equipment at remote locations; and
(c) in the face of decreased defense spending, to optimize the entire calibration and maintenance structure [13,15].

Problems in each of these areas have two aspects. The first is the need for dynamic standards and methods for their use to support or verify measurements made under time

constraint with automatic test equipment, especially that under computer control. Such standards simply do not exist and their absence both prevents direct verification of the quality of individual measurements made by present equipment and limits the advance of automatic testing by confining its application to the measurement of those parameters for which static standards exist. For example, the so-called third generation ATE system makes measurements using sampling techniques and arrives at final results through harmonic or Fourier analysis software. System capabilities are given, however, only in terms of derated rms or average voltage measurement specifications as lack of knowledge of the information content of a single sample and a lack of arbitrary wave form standards precludes the precise calibration of such a system. (Specifications are derated relative to the potential accuracy of the sampling device.)

The second aspect has to do with the achievement of adequate measurement accuracy at acceptable cost. Accuracy requirements for the support of end items in the military inventory are gradually becoming more stringent as electronic components and systems increase in quality and sophistication and improved reliability is sought for strategic or economic reasons. At the same time budget decreases result in reduced resources for measurement support and quality activities. Support equipment for new systems and test equipment used in development and repair activities include new instruments with performance characteristics rivaling the best measurement capabilities of the typical DoD calibration laboratory.

These factors result in the need for the development of new calibration procedures, better training of technicians and, in some instances, exhancement of calibration and measurement accuracies through new standards or more sophisticated measurement experiments. Automated systems for the calibration of general purpose test equipment, the use of MAP techniques for the support of line calibration laboratories, and in situ tests of both ATE systems and electronics in aircraft, field installations and surface vessels are all being employed to deal with these problems.

Detailed technical problems within the system are dealt with by the professional staffs of the Air Force, Army, and Navy metrology engineering centers. Specific, long-term problems are dealt with by these people. In those instances where the advancement of measurement science or new standards are required, the DoD enlists the help of NBS through the sponsorship of engineering projects. Typical objectives of such projects are the development of an all-cryogenic voltage standard accurate at the part in 10^8 level; the design of a low-frequency, low-voltage measurement instrument to enhance vibration measurement capabilities; and the development of an automated capacitance bridge with which DoD primary laboratories can provide improved service at reduced cost. In addition to providing this measurement science support, the NBS serves as a basis of measurement uniformity for the DoD system by supporting the four primary standards laboratories through calibration services and MAP activities.

The instrumentation industry. This industry was covered in Sec. 2.2.2.2.

Electric power industry (SIC 3825, 3511, 361, 362, and 491. The electric power industry has two components, the generation and distribution of power (SIC 491) and the manufacture of equipment for the generation and monitoring of electric power.

The generation, distribution, and sale of electric energy is the largest single business in the U.S. Approximate sales in 1973 were $31.7 billion and in 1974 were $39.1 billion. In 1975 the industry sold over 1.7 trillion kilowatthours to nearly 82 million customers for an estimated revenue of $47.9 billion [18,19].

The production of turbines and turbine generator sets produced shipments valued at $2.4 billion in 1975. Shipments for 1976 are expected to increase by about eight percent to $2.5 billion. Seventy-three businesses employ 47,000 workers in the production of this equipment [18]. Production of transformers, switch gear, and industrial controls for power distribution (SIC Codes 3612, 3613, 3622) totaled $6.7 billion in 1975 and is expected to reach $7.1 billion in 1976. More than 200 firms are engaged in the production of transformers alone and employ over 50,000 people [9,10]. Electrical measurements are required by this segment of the industry for quality control purposes. The levels of accuracy to be found are generally lower than those at the state-of-the-art and readily achievable with off-the-shelf instrumentation, but they are required to enable quality of these goods. No major metrology problems are evident here.

In addition to being one of the key industries in the U.S., the electric power industry supplies most of the rest of industry with motive energy. This is done through a system of interlocking grids of independent power companies. Electrical measurements are necessary for the monitoring and control of the power flow in the grid as well

as for energy metering by both power companies and their customers. Measurement problems include:

(a) the determination of transformer ratios at high voltages;
(b) the characterization of high voltage capacitors;
(c) the measurement of the dissipation factor of high voltage capacitors;
(d) the accurate calibration of watthour meters;
(e) the development of techniques for measurements in support of research to improve the transmission and distribution of electric power;
(f) the measurement of transient signals at high voltages; and
(g) the development of time-of-day metering techniques to enable the use of a rate scale in which the price of electricity increases during periods of peak demand.

NBS is involved in each of the above areas. The High Voltage Measurements Section is engaged in research and development programs generally supported by the Electric Power Research Institute and the Department of Energy designed to achieve the measurement capabilities at high voltages needed to support both basic research and power system operations. Examples of such projects are those to provide capability for measurement of pulses and transients of up to several million volts, to develop systems for the *in situ* calibration of coupling capacitor voltage transformers at voltages up to megavolt levels, and to improve the standards used for the measurement of current and power at power line frequencies.

In addition, NBS calibration services provide the basis for uniform measurement of electrical parameters necessary to day-to-day power company operations. NBS calibrations of standard cells, resistors, and watthour meters stand behind all measurements made for metering purposes, including those using the watthour meters found on every home in the U.S. Companies rely on NBS calibrations of high voltage capacitors, transformers and shunt reactors to maintain the efficiency of the power distribution system throughout the country. These services could not be provided without a strong, ongoing research effort in high voltage measurement technology such as exists in NBS today.

Research. In this category fall all independent research organizations, universities, and national laboratories. Since much of the research done in every field is experimental, the ability to make accurate electrical measurements is a necessity. An example of how precise measurements are needed is seen in a program at the University of Pennsylvania for the study of the electrical properties of solid-state, cryogenic Josephson junctions. The purpose of this work was to determine an experimental value for the quantity e/h with sufficient accuracy to enable its use in the verification of quantum electrodynamic theory. To do this, a measurement of its voltage output had to be made with the maximum available accuracy, that is 0.1 ppm relative to the legal volt. This necessitated the construction of a special instrumentation and the initiation of a special effort, both at NBS and the University of Pennsylvania, to verify the accuracy of the University's voltage standards.

A second example is to be found at Argonne National Laboratory, where extremely precise calorimetry work requires that voltage and resistance measurements be made with accuracies in the part per million realm. The experimenter is compelled to keep his own set of standards which are calibrated at NBS.

The energy crisis and the resulting perception that electricity will become the dominant means of energy utilization has fostered research, sponsored primarily by the Department of Energy (DOE) and the Electric Power and Research Institute (EPRI), for the increased generation and improved transmission of electric power. This research is being carried out in industry, at universities, and in various national laboratories, such as Brookhaven and Oak Ridge. Typical projects are the investigation of the use of superconducting transmission lines, ultra-high voltage overhead lines, direct current transmission, solar energy, and cryogenic motors and generators. Approximately $14.3 million has been invested in FY 76 for transmission and distribution research by DOE and $20.6 million by EPRI for calendar year 1976 [19].

The success of such research hinges on the ability to make accurate measurements at high voltages and under difficult environmental conditions and in many cases adequate techniques and standards for such measurements do not exist. As mentioned in the previous section, NBS is undertaking a number of research projects to establish the required measurement methodology. Examples of projects specifically bearing on energy-related research are those of applying the Kerr effect to map electric fields, the design and construction of pulsed current and voltage generators and associated measurement apparatus to enable calorimetric determinations of thermal/physical properties of materials used in nuclear reactors, and the development of calibration techniques in support of instrumentation used to determine the

effects of fields associated with voltage transmission lines on plant and animal life.

In other areas, NBS work in the fundamental constants field provides data contributing to the verification of physical theory, such as quantum electrodynamic theory. NBS has ongoing efforts in areas requiring precise electrical measurements. Determinations of the ampere, volt, Faraday, ohm, and the gyromagnetic ratio of the proton are presently underway. NBS has participated in the most recent (1973) least-squares adjustment of fundamental physical constants published by CODATA, the Committee on Data for Science and Technology. Another such adjustment is to be carried out in 1980.

As has been shown, the National Electrical Measurement System pervades most of the major industries and government agencies to a larger extent. As might be expected, measurement problems and requirements stem from two sources, the use of electronics as an implementor of manufacturing quality and process control, computations, and communications and the electric power industry and its needs for efficient power generation, distribution, and metering. Measurement technology in the former instance covers the range from dc to 1 megahertz at modest levels of voltage and power whereas in the second case measurements are generally of electrical parameters at dc and 60 Hz and high power and voltage levels.

Through its calibration and research activities, NBS provides the measurement system with its base, thereby ensuring needed stability and accuracy in terms of SI units. High-technology industries with the most stringent accuracy requirements provide the interface with NBS needed to enable virtually all electrical measurements made in the U.S. to be expressed in terms of the national units. Measurement accuracy in areas of more than modest requirement is ensured by systems in which the instruments used to make the measurements are calibrated periodically using standards or test equipment with accuracy capabilities from four to ten times better in each case. A chain composed of such calibration links reaches from most commercial instrumentation back to standards supported by NBS. The system remains viable due to measurement research performed at NBS and in the instrumentation industry.

3. IMPACT, STATUS, AND TRENDS OF THE MEASUREMENT SYSTEM

3.1.1 Functional, Technological, and Scientific Applications

The use of electrical measurements generally falls into one of four categroies - the production of reference data, setting and testing to specifications, maintenance and reliability activities, or the control of manufacturing processes. Reference data, including physical and engineering data covered in Section 2.2.3, is vital to designers of virtually all high-technology products. The Electrical Measurement System ensures that such data have universal meaning by providing common reference bases in the electrical units, both for those experimentalists who produce the data and for those designers who must use the characteristics of materials, circuits, etc. in an engineering application.

The next major use of electrical measurements is in vendor determination of performance characteristics of manufactured products and customer testing of those same devices to ensure that their specifications or the manufacturers claims are actually being met. Most commercial electronics and electrical merchandise is traded in this fashion. Electronic components, modules, instruments, devices and systems are generally tested, sometimes on a sampling basis, to specifications prior to their acceptance. The measurement system is the foundation for all aspects of this type of activity. The availability of universal units of measure permits interchangeability of electronic components and modules (a must for the mass production and subsequent maintenance of complex electronics) and multiple manufacturers of commonly used circuit elements. These factors, coupled with inexpensive production techniques, enable all electronics products to be produced inexpensively and to function with a high degree of reliability.

Electrical measurements are vital to maintenance and reliability functions throughout the electronics user community. Test equipment is used both to ensure the proper operation of functional electronic equipment, such as radar sets, inertial guidance units, etc. used in critical applications (i.e., space and weapons systems) on a periodic basis and as a means of trouble-shooting and repairing nonfunctional electrical and electronic equipment. This test equipment is generally checked or calibrated periodically using more accurate standards and equipment through the echelon system of standards and calibration laboratories which exists throughout industry and most government agencies involved with technology.

The final major use of electrical measurements is for the control of industrial manufacturing processes. Early automatic control of manufacturing processes was achieved through pneumatics and electro-mechanical servomechanisms. Besides being a prime source of power for the process itself, pneumatics gave the design engineer the ability to implement various control algorithms tending to optimize the process. The advent of electronic amplifiers enabled the implementation of these same functions electrically with many control adjustments difficult or impossible to achieve pneumatically. Also over the years the development of transducers, devices which produce electrical signals of a known relationship to the magnitude of a particular physical quantity, has gradually extended the versatility of electronic control. The advent of the inexpensive digital computer along with electronic instrumentation with digital data outputs has hastened the application of electronics in the control field. Control systems based on digital computers have the advantages of speed of response, economy, and software signal conditioning. Not only does the latter make possible the use of exceedingly complex control algorithims, but it also permits extreme flexibility of modification without extensive hardware changes.

The most stringent measurement requirements come from the instrumentation industry, the aerospace industry, and the Department of Defense. The DoD and the NASA generate stringent requirements for the accuracy and reliability of guidance, weapons, and navigation systems. Accuracy requirements of better then 0.001% for various electrical parameters exist in some of the new operational equipment itself. This level of requirement places a burden on the instrumentation industry which is called upon to provide the test equipment and support standards necessary to the development, production, testing, and maintenance of the operational equipment. Further the test equipment and standards themselves must be verified and maintained in all three of these areas of the economy. NBS plays a vital role in this function by providing calibrations of standards, Measurement Assurance Program services, reference data, and training services.

Less accurate — but in some cases no less stringent — requirements come from the electric power and the semiconductor industries. In addition to the routine measurements of electric power for revenue purposes, the power industry requires many difficult measurements under field conditions for both operational and research purposes. Examples of these are given in the previous section. Large scale integration techniques have per-

mitted a great growth in complexity of circuit elements. Meanwhile, the ever-decreasing cost of these same products has lead to their use in many applications in which reliability is critical, such as electronic control of automobile brakes, medical life support systems and instrumentation, and aircraft navigation systems. Testing of these circuit elements must be done, therefore, accurately and rapidly to achieve utility and low cost. This simple factor has lead to a surge of interest in automated testing and requirements for support of electrical measurements made "on the fly". There is a plethora of dynamic data conversion devices on the market with which such measurements may be made. Lacking are the standards which form the means by which a translation may be made from traditional standards and measurements, which involve no time constraints, to the new requirements for dynamic measurements.

On the other end of the measurement spectrum lie those electrical measurements which are part of the day-to-day experience of the typical man on the street. Examples are those made in the course of tuning an automobile; for repairing television, radio, or high-fidelity audio equipment; to maintain home consumption of electric power; and to provide for the safe navigation of commercial airlines. Instruments used in the former two cases are generally only supported by the measurement system upon their failure. The accuracies required in support of most consumer services are readily obtainable since they lie in the 1 to 5 percent range.

Electrical measurements are used to control the quality of any item manufactured by an automatic process. The use of transducers, which convert other physical parameters into electrical parameters, coupled with electrical instruments with digital outputs enable any physical or chemical production process to be run under computer control. Thermocouples, strain gages, tachometers, and fluid level meters are examples of transducers. Table 11 lists some articles whose production is made possible by electrical measurements.

Table 11. Representative heavily measurement-dependent products

Electronic
Components (resistors, capacitors, etc)
Computers
Digital watches
Electronic calculators
Frequency standards
Guidance systems
Navigation equipment
Stereo receivers
Other
Engine blocks
Oil, gasoline
Plastics
Rayon, nylon fabric
Steel
Synthetic rubber

3.1.2 Economic Impacts - Costs and Benefits

The costs incurred by the economy annually for electrical measurements are very low by comparison with benefits received. A survey of the manpower available in the calibration laboratories listed in the NCSL Directory of Standards Laboratories shows a total of 878 engineers and 3208 technicians for all measurement areas [14]. A conservative estimate was made that there are roughly 1000 measurement engineers and 5000 technicians in that portion of the measurement system which provides standards and calibration support to the remainder of the system. Approximate labor and overhead costs for that number of people are estimated to total no more than $130 million per year. The remainder of the system is many hundred times larger and difficult to quantify. The degree of capital intensiveness of the measurement system is illustrated by the annual expenditure of over $5.6 billion for new measurement instrumentation, of which $1.3 billion is test equipment [9].

The above manpower figures are totally exclusive of test engineers and technicians whose functions are not primarily concerned with calibration measurements. Virtually every electronics engineer (except digital logic designers) must rely on electrical measurements as a tool necessary to the performance of his function.

Over the past ten years, in excess of $94 billion worth of electronic systems and communications equipment were sold in the U.S. [10,20]. All of this equipment requires maintenance support, and much requires periodic calibration to insure its proper operation. During the same period over $11 billion worth of electronic test equipment was sold for that purpose [9,10]. All of this apparatus requires periodic calibration. The scientific apparatus inventory is estimated at $12 billion for that same 10-year period [9].

The electronics market as a whole is supported by this measurement capability. Gross sales for the industry were forecast at $64.9 billion in 1977 [21]. New automated systems developed explicitly for testing integrated

circuits, which are becoming more and more complex, enabled achievement of this sales figure. This represents about a 9% growth, despite materials shortages and a general economic decline.

3.1.3 Social and Human Impacts

The largest social impacts of the electrical measurements system lie in the medical field and the public safety areas. Modern instrumentation has made possible great strides in diagnostic medicine. The bodies of patients in intensive care units are monitored on a twenty-four hour basis by computer-controlled instrumentation systems. These systems not only alert medical staff members to impending crises, but provide a powerful tool in the analysis of the patient's condition. There are under development automated systems which would give physical examinations to individuals without requiring a doctor in attendance. Electronic measurement equipment and computers form the basis for new systems to perform internal scans via ultrasonics or x-rays.

In the safety area, measurements are vital to ensure the reliability of electronic equipment such as braking and ignition systems for automobiles and navigation and landing systems for aircraft. The failure of any of these systems could be calamitous, whether due to component failure or electrical interference. Reliable measurements are necessary to avoid failures from either cause.

3.2 Status and Trends of the System

The electronics sector. At the present time the National Electrical Measurement System is capable of handling nearly all of the traditional measurement needs of our economy. The accuracies available within the system for so-called static electrical measurements, i.e., those in which the measurement is not constrained to take place within a particular time interval, far exceed any technical accuracy requirements. The common practice of insisting upon accuracy ratios in calibrations of between three- and ten-to-one, a practice fostered by the Department of Defense and NASA, generally ensures that specified accuracies are delivered within the calibration traceability chain. However, the system does have a serious fault which is not entirely technical in nature and which is being increasingly recognized and dealt with. This fault is the lack of redundancy or feedback in the rigidly stylized, hierarchical calibration/traceability structure to ensure that the applied measurements supported by the system are in fact appropriate and adequate and their quality has not been adversely affected by such factors as environment, electromagnetic interference, or poor power lines. Commercial and government organizations are slowly recognizing the need for periodic sampling of measurements being made on the production line, in the aircraft, or at the power substation.

There are several areas in which traditional measurements needs are, at present, unfulfilled. The most urgent of these are:

(a) characterization and specification of power line properties. There have been failures and erroneous data from instrumentation caused by spikes or hash in the power line. The medical profession and medical instrumentation industry are most severely affected by this problem due to the seriousness of potential consequences. A committee dealing with the problem has been formed under the auspices of the National Committee for Clinical Laboratory Standards. The establishment of specifications and measurement techniques for interfering signals on power lines will enable the design of better instruments and provide a basis for settling the issue of legal liability for consequences of error. This issue arises from the fact that instrument makers do not specify the limitations of their equipment in that regard and hospitals are not legally bound to ensure a specified purity of content of the power mains.

(b) measurement of ac voltages at low amplitudes (<50 mV) and frequencies (<50 Hz). This measurement capability would be used with transducers to make measurements of low frequency vibrations such as those characteristic of trucks and helicopters. The Department of Defense and the transportation industry require the ability to test the susceptibility of various items of critical nature to damage by truck or air transportation.

(c) impedance measurements in the upper ends of the low radio frequency range (20 kHz to 1 MHz). These impedances measurements are needed to support an increase in carrier frequencies in some communications systems. Increases in carrier frequency will result in proportional increases in message capability.

(d) studies relating to reliability and the predicition of long-term performance of components and assemblies based on short-term, high-precision data needed by the electronics industry for general improvements in their product line.

(e) measurements of phase angle in the frequency range from 1 Hz to 30 kHz. Phase angle measurements are important to the testing of components, solid state circuits, and test equipment used in and to support communications and weapons systems. In the lat-

ter, some of the more precise measurements are required for testing synchro's and resolvers used to position the antenna of search and target acquisition radar.

There are two other perceived problems which affect the system. Technical information is disseminated primarily by word-of-mouth (between colleagues), through sales efforts of instrument companies, and by technical publications in such journals as IEEE Transactions on Instrumentation and Measurement, Instrumentation Technology, Metrologia, and Measurements and Data. Articles in the above tend to be academic in nature. Despite the existence of the Government Industry Data Exchange Program, which has a library of calibration procedures, and the above-mentioned means of communication, useful technical information on a how-to-do-it level does not reach the bench-level metrologists and those outside the precise measurements field (i.e., quality control or automatic test equipment engineers). In many instances there is conflict instead of cooperation fostered by ignorance and no means of communication. NBS is planning a series of publications and seminars to help meet this need.

The second is in the area of manpower. Many of the highly-skilled technicians and engineers in the field are on the verge of retirement. New people in the field tend to remain there only temporarily. Metrology may in the future be caught in a three-way trap between the lack of communications and informal education opportunities, the decline of the armed forces as a source of experienced people, and the increasing sophistication of new instrumentation, which requires a higher level of education and appreciation for its proper support.

Two major factors presently affect the system and will apparently do so for the foreseeable future. These are the revolution taking place in the electronics industry, and the energy crisis. Advances in semiconductor fabrication technology and the application of new semiconductor structures to circuit design are resulting in the availability of very complex digital and analog circuits in small, component-sized packages. As a result an increasing number of standard circuits, such as amplifiers, computer processing units, power supplies, digital multipliers, analog-to-digital converters, etc., are as available to the designer as resistors, transistors, and tubes have been in the past. Because of this ready availability, electronic equipment has increased — and will continue to increase - in functional complexity and sophistication, while its cost has dropped.

The solid state revolution has fostered a parallel phenomenon in the computer field. Minicomputers, which have only readily been available for about the past 10 years, have so improved that new models offer sophistication which could be found only on large systems costing hundreds of thousands of dollars not long ago. Yet a system with a fair-sized memory, reasonable software, and a mass-storage peripheral can be purchased for well under $15,000 at the present time. And, now available are microprocessors, central processing units on a chip, with fairly comprehensive capabilities. These devices are inexpensive enough to permit their inclusion in electronic equipment to replace the hand-wired logic circuitry normally used there for controlling operations and transmitting data.

The above considerations have had and will continue to have a major impact on both measurement requirements and the tools or means by which measurements can be made. The increasing complexity of components, sub-assemblies, equipment items, and electronics systems have resulted in increasingly complex tests necessary to ensure quality in the manufacture of such equipment, proper performance while in use, and affordable maintenance for it in the event of malfunction. Typically, tests may be comprised of hundreds or thousands of measurements.

The only way that such tests can be performed in a reasonable time and with cost puter to control the measurements, acquire and process the data, and analyse the results. Cost effectiveness is increased by running the system at a higher rate of speed. Therefore, the thrusts of the instrumentation industry are in the direction of increased accuracy of measurement at increasing speeds, and of making the instruments as compatible as possible with computers. The impact of this industry on the measurement system is heightened by the fact that the designers of automatic test equipment (ATE) systems for both military and commercial applications design these systems using the specifications for off-the-shelf test instruments as building blocks in the design. This leads to performance problems if the instruments used do not perform as expected because of environmental noise, or ground problems. It may also lead to calibration support problems requiring high-grade portable standards.

The future will bring even more complexity. The Department of Defense now requires testability. Many new prime systems will have the functional capability to test themselves. Most circuits will be designed with testability in mind, that is, with special input and output lines with the sole function of expediting testing. Some digital

devices will actually contain two similar circuits with auxiliary circuits to compare their behavior. Much is being done to lay the foundation for the development of system testers, portable devices which can exercise a test system under use conditions by simulating a typical units under test [13,15,16].

The industrial and commercial sector tends to have less stringent accuracy requirements for electrical measurements than the military/aerospace sector. This results from the lower technology level found in general industry. On the other hand, measurements are required to be made under severe ambient conditions. Because of this factor and the need for a means of coping with a general decline in productivity, the use of automatic test and control systems will increase rapidly in this sector over the foreseeable future. Much effort is being expended in development of computer-aided manufacturing (CAM) technology, the use of robots, and application of computer-aided design (CAD) techniques in various areas of industry, as well as in the use of automatic test equipment and transducers for quality assurance.

Automatic test equipment as used in the commercial sector differs in another way from that developed for the military/aerospace complex. Military and space operations have a critical nature due to the high potential for loss of life, property, and national existence. This fact and the often unique nature of the equipment employed in those programs leads to the procurement of specially-designed or "custom" measurement instruments and automatic test systems suited for testing of a specific prime system. In the commercial sector cost considerations tend to force the use of off-the-shelf commercial instrumentation for automatic testing purposes. This practice is expected to be positively affected by the recent adoption of standards (IEEE 488 and American National Standards Institute CAMAC standards) whose conventions for interfacing instruments and other devices to computers are beginning to be adopted in the instrumentation industry.

The improvements of semiconductor technology have had a significant impact on the instrumentation industry in a variety of ways as shown above. Perhaps the greatest impact is the growing use of microprocessors within instruments. Not only are these small computers used to perform calculations on raw data to enable the display of useful information (such as temperature instead of voltage for thermocouple applications), but in a more basic function, that of controlling the internal operation of the instrument. Contemporary voltmeters and other electronic measurement instruments function using dedicated logic circuits to control timing, range changing, and the conversion of analog signals to digital information. Changes in the mode of operation can only be made by circuit modification. Use of microprocessors will permit modification of the instrument's operation through software, resulting in more flexibility of design and lower production costs. Most instrumentation companies are actively engaged in the application of microprocessors to their product line. At this point in time, announcements have been made of new voltmeters, counters, oscilloscopes, and multi-channel scanning systems, all based on microprocessors.

At the present time, artifact standards, apparatus and standard measurement techniques to support dynamic measurements of electrical quantities simply are non-existent. Details of state-of-the-art dynamic measurement techniques are the proprietary secrets of the manufacturers of instruments and signal-conversion devices. As a result, manufacturers and users of automatic test equipment and systems attempt to ensure the quality of performance of such systems through the manual calibration of system components or the measurement of known static quantities by the system. Neither process gives valid assurance of adequacy of performance. Such assurance is virtually impossible without appropriate standards.

The lack of standards also affects the development of new systems. The designer may now use published equipment specifications (which in many cases are not uniform in meaning) to achieve an approximation of his design goal and then use measurement results to "fine tune" the system because standards are not available as design tools. He may alternatively over-specify in speed and accuracy to ensure good results. Unneeded accuracy and speed are costly and may lull the designer to believe he has no analog measurement problems when in fact one may be created by external considerations, such as the impedance characteristics of the interface between the system and the unit under test.

That the development and establishment of standards for dynamic measurements of electrical quantities are a necessity to ease future growth of technology was one of the conclusions reached during a workshop held at NBS in September 1974. The workshop, which had 24 participants, representative of bpth manufacturers and users, was convened to identify critical measurement needs and discuss standards for modern electronic instrumentation. A whole host of standards and measurement techniques whose need results from the semiconductor and computer revolutions were identified [13]. They are best summarized in the abstract of the workshop report, NBS Technical Note 865, given

in Appendix C of this report.

The need for a static measurement capability will not diminish in the future. This is true as static standards must form the basis for uniformity and stability of performance with time for all dynamic instrumentation. The present electrical standards which provide the basis for accuracy for static measurements are of materials and combinations of materials inherently more stable than are semiconductor devices.

In addition, automated equipment is not yet capable of trouble-shooting and repairing electronics equipment. Although automatic fault diagnosis for both digital and analog circuitry is a rapidly expanding area, the techniques and philosophy are as yet primitive. The construction of present day equipment is such that machine repair would be prohibitively costly. General purpose maintenance instrumentation must be calibrated and repaired itself.

Consumer electronics is another rapidly growing field which will have an effect on the measurement system. At present, the main function of the measurement system in the consumer's market is to enable the maintenance and repair of equipment. However, the use of electronics for both safety and energy conservation purposes is growing rapidly in the automobile industry. The potential for disaster due to failure of electronic ignition or braking systems will lead to more measurements for reliability or quality control either voluntarily, as the result of government regulation, or as the economic consequence of successful litigation by crash victims or their survivors.

Another area of consumer electronics which will increasingly impact the system is that of medical instrumentation, both by increasing the amount of support required and by generating new measurement problems. Not only is this use of instrumentation in hospitals and medical research facilities on the increase, but the summer of 1976 will mark the beginning of regulation in this field by the Food and Drug Administration. Manufacturers of analytical instrumentation are aware of their liabilities resulting both from government action and from malpractice suits. A major problem at the present time is the electrical environment in which instrumentation must function. A means of quantifying the "purity" of the 60-Hz power line is needed, both to optimize the design of instrument power supplies and to enable hospitals to have proper electrical configurations.

The most important needs for the future generated by the electronics portion of the National Electrical Measurement System may thus be summarized as:

(a) the need for standards for the dynamic measurement of electrical quantities such as voltage, impedance, and power;

(b) the measurement methodology which must be used with the above standards;

(c) the education of systems designers in the necessity for and the use of the above, before maintenance and failure costs escalate to render system use impractical;

(d) the establishment of methods and apparatus to test computer-driven systems as systems, under conditions of actual use;

(e) the development of a theory to minimize the number of points requiring testing in a complex system;

(f) a standard and measurement method by which to assess the quality of ac power available from the mains;

(g) the characterization of long-term reliability and stability of electronic components on the basis of short-term measurements (perhaps of parameters such as noise);

(h) standards for phase measurements and for impedance measurements in the frequency range from 20 kHz to 1 MHz;

(i) the development of improved switches and relays;

(j) better mechanisms for the communication of technical and management information throughout the system;

(k) a mechanism to ensure that regulatory and other government agency requirements o n the system are technically, economically, and logistically relaistic; and

(l) standardization in the computer software used for systems implementation of measurements.

The electric power industry. This subset of the National Electrical Measurement System requires a considerable measurement capability, both to carry out its day-to-day operations, and in support of research, the urgency for which has been created by the energy crisis. Support of operations requires a capability to perform measurements of voltage, current, and impedance at voltages as high as 765,000 volts, a means of measuring energy accurately at 60 Hz, measurements of transient (lightning impulse, switching surges) voltages at levels in excess of 2 MV, and the characterization of dielectrics.

Line-to-line voltages for bulk power transmission in use or under consideration by the industry are generally grouped in one of three categories. The high voltage (HV) group extends from 69 kV (69,000 volts) to 230 kV. Overhead lines are used for both short and long distance movement of power while underground cables are restricted to short distances. A considerable amount of

very long distance power transfer (e.g., between power companies) takes place on overhead lines at extra high voltages (EHV), some at 345 kV, but most at 500 kV. EHV lines at 765 kV are operational but under somewhat limited use. One option for power transfer in the future is by UHV (ultra-high voltage) lines. Voltages ranging from 1.1 to 1.5 million volts are being considered. For distribution of electric power, moderately high voltages between 200 and 45,000 volts are employed.

Measurements of voltage and current at these transmission and distribution voltage levels are performed by means of voltage and current transformers which reduce the magnitude of these parameters to a level where they may be handled using conventional low voltage meters. Both at HV and EHV levels, inductively coupled transformers are used, but at EHV there is a trend to use capacitive voltage transformers. Measurement capability for the calibration of transformers for the HV range is generally adequate throughout the industry. For the EHV range the capability of calibrating current and voltage transformers is generally limited to the manufacturers of high voltage equipment. The capability of calibrating capacitive transformers (coupling capacitor voltage transformers -- CCVT's) in the place of installation has recently been developed at NBS with the support of the Electric Power Research Institute. The use of high voltage reactors and capacitors to reduce circulating quadrature currents in transmission systems, and thus, reactive power, leads to a need for the accurate measurement of impedance and phase angle for this type of device. This capability is generally available only with the manufacturers.

Energy measurements are widely made by the electric power industry for billing purposes. This is a very well-established area; it relates ultimately to the accuracy of simple, residential-type watthour meters and to more complicated industrial, commercial, and inter-utility metering systems. There are over 80 million watthour meters in the U.S., practically all of them rotating, induction-type devices. State utility commissions legally require that such meters do not exhibit a certain maximum error, usually 2%. The systems by which these meters are calibrated are detailed in Sec. 4.2.1. That this portion of the Measurement System is under adequate control has been demonstrated by means of a round-robin experiment performed jointly by NBS and the Edison Electric Institute [22].

Testing of the integrity of insulation of equipment is an important part of the quality control process of the electric voltage equipment is subjected to very high steady state and transient overvoltages which must be measured with accuracies in the 3 to 5% range. Such accuracies are difficult to achieve as present instrumentation capable of handling the high voltages required has a poor pulse response characteristic. A commonly used transient is the standard lightning impulse (1.2 microsecond front, 50 microsecond tail) which, for existing transmission voltages, can be in excess of two million volts.

Another specialized test for the quality of insulation is that for the level of partial (corona) discharges. The problems here are the complexity of instrumentation needed and the necessity to isolate the measured phenomenon from interference. The basic accuracy is not a particular problem. Problems do arise, nonetheless, due to the sophistication of the measurement operation and the interpretation of data.

The following is a list of representative measurement problems presently being identified in day-to-day power industry operations:

1. Stability of EHV capacitive transformers is unknown. Hence, their usefulness in monitoring extra-high voltage is limited.
2. Means for calibrating impulse voltage measuring systems are insufficient. Traceability is usually only through the manufacturer of the equipment. Periodic rechecking is not widely practiced.
3. There is a lack of convenient and reliable instrumentation to measure the power of loads with very low power factors.
4. Measurement and test procedures to predict the life of insulation systems are inadequate.
5. Interpretation of data from corona and partial discharge measurements requires additional research.
6. There are problems associated with the very limited market of high voltage instruments. Often they are one of a kind; there is little opportunity to obtain enough experience to optimize the design.
7. There is need for more in-service testing since many equipment types cannot be removed from use for test purposes. In-service measurement methods and instruments are needed.
8. The industry could benefit from more training of personnel in measurement and test techniques.

The above problems must be resolved by the electric power sector in order to identify components of optimum systems for the future. The NBS role in solving these is to ensure that the required measurement capability exists and is available where these problems are addressed.

The energy crisis, the rapid depletion of petrochemical fuel reserves, and the future promise of thermonuclear energy have spurred a diversity of energy-related research efforts [19,23-26]. The effectiveness of many of these efforts depends on the availability of appropriate electrical measurement capabilities. In some areas, the key measurements are those generally associated with the electronics community. For example, the reliability of control and other auxilliary electronic systems is recognized as a problem area. The operation and security of future electric power networks are foreseen to be more heavily computer-based, and contain large amounts of sophisticated instrumentation for monitoring and control of various parameters [26].

Work is going on in energy storage and intermittent generation facilities to enable the main power system generators to handle only the base loads. Batteries are under development for storage of energy generated during off-peak hours for eventual peak-time consumption. Measurements must be made to characterize the discharge of prototype batteries, as well as to determine their behavior under rapidly varying conditions of use. Other areas dependent on electrical measurement are those involving magnetohydrodynamics and fuel cells [26,27].

By observing the current developments in electric energy measuring devices and in metering practices, one may expect early introduction of all-electronic metering systems. This meter may be a more sophisticated device combining the functions of watthour, demand, and power factor meters. It may be coupled to telemetry and computer systems for automatic reading and time-of-the-day metering. The accuracy requirements may be similar to those of conventional instruments, but the calibration procedures may be different.

Requirements for measurements at high voltages come largely from R&D efforts to improve the capacity and efficiency of the nation's system for the transmission of electric power from generating sites to areas of use and the distribution of that power within each area. In discussing these measurement requirements, the development of future electric power systems must be considered.

The principal driving forces appear to be: (1) a continuing increase in the consumption of electric power, requiring expanded transmission facilities; and (2) concern for usable systems. The right-of-way available for overhead transmission will be limited, requiring an increase in voltage to transmit more power. However, there are some doubts whether further increases will be permitted because of potentially adverse environmental effects. There will be pressures to put more transmission lines underground.

Some potential systems, for which research and development is underway or under consideration, are outlined below [23-29]:

- Transmission Systems
  - Overhead
    - UHV 60 Hz up to 1500 kV
    - EHV and UHV dc up to 1200 kV
  - Underground
    - Higher voltage tape cables (765 kV ac)
    - Higher voltage extruded cables (to 138 kV and 230 kV ac)
    - DC cables
    - SF_6-insulated systems
    - Cryogenic systems
  - Substations (SF_6-insulated)
  - Underground cables (improve reliability and efficiency, reduce cost)
  - Transformers (improve efficiency)
  - Metering (time-of-day metering, remote reading, all-electronic meters).

There will be requirements for many new types of measurement techniques at high voltages occasioned by the above. A few of these are the capability of making accurate dielectric loss measurements under cryogenic and other adverse conditions, the measurement of transient voltages at UHV, the performance of needed calibrations (transformers, reactors, capacitors) in an atmosphere of SF_6, and accurate measurements of electric fields in non-uniform regions for environmental safety purposes. In addition, new calibration techniques will probably be needed for such new types of measurement apparatus as electronic wattmeters, capacitive voltage transformers, and the electro-optical devices which may replace conventional current transformers at EHV and UHV levels.

In conclusion, the power industry subset of the NEMS generally functions well, although in several instances the industry could benefit from improved measurements and tests. The difficulty lies not so much in the accuracy which can be achieved under laboratory conditions and in the traceability to basic standards, but in the very hostile environment in which the measurements have to be performed. Many tests are difficult and expensive to stage because of high voltage considerations and the size of the equipment. Often, measurements are made to elucidate physical processes, e.g., those responsible for insulation aging and deterioration. In such a case, the problem is frequently associated with trying to relate the measurement results with the physical processes, a research problem on what to measure, not necessarily one of accuracy. Most of the

above problems are dealt with by the industry itself or appropriate agencies in the Federal and state governments. NBS' responsibility is for the development of measurement techniques and standards needed to solve these problems. NBS has neither the mission or resources to tackle these problems directly itself.

Looking into the future, one sees great activity in the development of new and improved electric transmission and distribution systems. There is and will be a need for new measurements to facilitate the development and to enable the operations of new systems.

4. SURVEY OF NBS SERVICES

4.1 The Past

Calibration services for basic electrical standards have gradually improved in accuracy over the past twenty years. During that period, the concept of measurement assurance became the basis for new services as described later in this section. In the high voltage measurements area some reduction in capability within the NBS facility resulted from the loss of the Van Ness Street facility. In 1967, work was begun on a new method of dissemination, utilizing the measurement transfer approach. Spurred on by problems in the area of dc voltage measurements in standards and calibration laboratories, the effort culminated with the establishment in 1970 of the Volt Transfer Program as an alternative to standard cell calibrations at NBS. In this program, use is made of specially-tested transport standards to monitor the ability of the client laboratory to make measurements of high accuracy and precision, as well as to transfer the unit. The Program has proven to be a powerful tool for the diagnosis of measurement problems as well as a means for disseminating the volt at improved accuracies. Since then similar programs in capacitance, resistance, energy, and voltage ratio have been put into operation.

A new area of *in situ* high voltage measurements stemmed from the loss of NBS in-house measurement capability above 100 kV and the development of portable bridges based on the current comparator principle. NBS equipment and personnel calibrate transformers, shunts, and capacitors at the actual site and under the conditions of use. A similar approach is being taken for the calibration of high current transformers.

Over the years, the Electricity Division has contributed a wealth of new standards and equipment to the measurement industry. A partial list includes the Wenner bridge and magnetometer, the Rosa and Thomas-type standard resistors, the Hermach thermal transfer ac-dc voltage converter, the Cutkosky ac thermometer bridge and the Cutkosky fused silica dielectric capacitor. All of these have been adopted for commercial manufacture, or provided significant contribution to other products.

4.2 The Present - Scope of NBS Services

4.2.1 Description of NBS Services

Structure of the Electricity Division. The Electricity Division's goal is to provide within the U.S. the central basis of a com-

plete and consistent system of electrical measurements, standards, and related data required by industry, commerce, government, and the scientific community in their efforts to advance science, technology, and equity in trade for the public good. To achieve this goal the Division has set the following objectives:

(a) to realize, with continuing improvement, the electrical units and to develop improved means for their maintenance and dissemination;
(b) to maintain and disseminate the electrical units and to test and calibrate electrical standards, instruments, and systems;
(c) to develop methods and instrumentation for the solution of problems requiring electrical measurement;
(d) to determine essential data and constants requiring or related to electrical measurements when not available with sufficient accuracy elsewhere;
(e) to serve actively in organizations which set standards for electrical measurements and devices and to otherwise disseminate the Division's specialized knowledge; and
(f) to evaluate the U.S. system of electrical measurements and to coordinate it with the systems of other countries to achieve international compatibility.

The basic responsibilities of the *Absolute Electrical Measurements Section* are to relate the U.S. legal electrical units, the ampere, farad, ohm, and volt, to the absolute or SI (Systeme International) units; to develop new and improved reference standards for the SI units; to develop means for maintaining surveillance of such referance standards; and to develop improved means for disseminating the electrical units.

Until recent years, the legal electrical units have been maintained by NBS using artifact (physical) standards, the stability of which depended upon materials whose properties are generally affected by environmental changes (temperature, physical shock, etc.) and impurities, either physical or chemical. For example, the value of a standard resistor, in addition to being sensitive to temperature changes, may undergo a long-term drift as the result of changes in the intermolecular structure of the wire of which it is made due to a physical shock and consequent deformation. This structure would in time tend to slowly return to that of an annealed state and the wire resistivity would reflect this slow change by its drift. Although so-called absolute experiments, which relate the electrical units to the mechanical units, are performed from time to time, they cannot because of their very nature be performed often enough nor, for most parameters, accurately enough to be of use in ascertaining the drift rates of the artifact standards in which are embodied the legal units.

It is natural, therefore, that a significant portion of the Section's activity is taken to exploit processes whose propeties depend upon fundamental physical constants for use as primary electrical standards. For example, the U.S. legal volt has been defined since 1972 in terms of e/h, the ratio of the electronic charge to Planck's constant. This is done by the use of Josephson junctions, weakly coupled junctions of superconductors which act as precise, linear, frequency-to-voltage converters for which e/h is a conversion factor. Section work currently includes the development of all cryogenic instruments based on the Josephson effect and dc current transformer techniques to improve the quality of the volt (reduce random error) by an order of magnitude to one part in 10^8 and the exploitation of the Josephson effect for commercially-available laboratory voltage standards at the one part per million level. Because of the nature of the process, such a device would never need calibration.

Work in this area and on related voltage measurements has led to a number of "spin-off" advancements in measurement technology. Examples include the development of high accuracy, sub-millivolt potentiometric methods, new techniques for the dissemination of the volt (MAP's), application of sophisticated statistical techniques to standard cell intercomparisons and other measurements, development of automation techniques, and the design of the world's "cleanest" automated switching systems.

Present activity in the area of absolute measurements includes the determination of the farad and ohm from the unit of length via the calculable capacitor. This device is capable of producing a change in capacitance very precisely related to the displacement of its guard electrodes. After a development period of a decade, a preliminary measurement of the ohm has been made with an accuracy of 0.05 parts in a million [3]. Perhaps equally significant are the developments which were required to achieve the capabilities of maintaining the farad at the commensurate level of stability and of making the translation between the unit of capacitance at 5 picofarads, as measured using ac techniques, and the unit of dc resistance at one ohm. New capacitance standards based on the use of a deposited, fused silica dielectric were developed. Although they are inherently quite stable (less than 0.1 ppm per year drift), their large temperature coef-

ficient required development of temperature control and measurement techniques at the microkelvin level of precision. These were later successfully applied in the construction of a new type of standard cell enclosure. More sensitive amplification and bridge techniques developed for the necessary scaling from 0.5 to 1000 pF (10^5 ohms at 1592 Hz) are now being employed in the development of automated equipment for impedance intercomparisons.

Other measurement activities currently underway in the Absolute Electrical Measurements Section include measurements of the proton gyromagnetic ratio, using the low-field method; the measurement of the Faraday, using the silver coulometer; the planning of new experiments of the ampere and γ_p using the high-field method; and the exploitation of cryogenic techniques for the measurement of resistance standards.

The equipment and facilities available cover the range from cryogenic and microwave apparatus to precision dc potentiometers and ac bridges. The NBS nonmagnetic facility, under the jurisdiction of the Section, is available for research requiring a well-characterized and controllable magnetic environment. A sputtering laboratory is presently being set up as a tool for cryogenic and solid state thin film research.

The Absolute Electrical Measurements Section provides the technical base for all of the measurement activities of the Division. It disseminates the units of capacitance and voltage to the Electrical Reference Standards Section which, in turn, passes needed units to the other two sections. The latter three provide the majority of direct technical services to the National Measurement System.

The Electrical Instruments Section is responsible for the development of standards and measurement methodology to support modern, high-speed, electronic instrumentation. Efforts are underway to provide for the determination of the accuracy of modular analog-to-digital and digital-to-analog converters under both static and dynamic conditions. The characterization of high-speed sampling devices will also be investigated. Time and speed-related properties which require standards for measurement are risetime, dynamic or instantaneous input impedance, settling curve characterization, aperature time (length and start point), etc. It is expected that the techniques discovered will "spill over" into the lower speed, high accuracy instrumentation area. Previous work done in the Section on measurements of rms ac voltage using thermal converter techniques is being applied to the development of improved ac voltage standards, needed for the support of modern instrumentation.

Experience gained from earlier work on the development of a sampling wattmeter will be used to solve two critical problems. The sampling techniques and mathematical theory with which to compute the phase angle difference between two alternating signals are known. Their application to the actual measurement situation is being made. The feasibility of using sampling techniques for the measurement of the power of irregular waveforms is being studied as well.

The *High Voltage Measurements Section* provides measurement support for the electric power industry and its suppliers and users, in addition to conducting research and development in measurement techniques and instrumentation for use at voltage and power levels which exceed those normally encountered in a standards laboratory. Calibration services are provided for current, voltage, and energy measurements at power line frequencies and voltages, as well as for high voltage devices, such as transformers, dc and ac voltage dividers, and impulse dividers. Typically, the Section is concerned with measurements at voltages in the range from several hundred volts to several hundred kilovolts; reactive power levels are frequently of the order of several hundred megavolt-amperes.

The scope of the Section activities is illustrated by the following current research and calibration projects:

(a) alternating voltage measurements - voltage (potential) transformers and other types of high voltage dividers; bridges and comparators for calibrating voltage transformers and dividers;

(b) direct voltage measurements - resistive dividers; generating voltmeters; electrostatic voltmeters;

(c) measurement of transient voltages - electro-optic techniques (utilization of Kerr cell); resistive pulse dividers;

(d) impedance measurements at high voltage - high voltage standard capacitors; standards for power factor correction capacitors; high voltage capacitance bridges; self-balancing bridges for measuring losses in shunt reactors; and

(e) measurement of current in high voltage lines - optical telemetry techniques.

The *Electrical Reference Standards Section* is primarily responsible for the dissemination of the basic U. S. legal electrical units (capacitance, inductance, resistance, and voltage). These units are disseminated through the calibration in NBS laboratories of standard resistors, capac-

itors, inductors, and voltage cells owned by organizations from all segments of industry and government. The units are extended through the calibration of potentiometers, bridges, volt ratio standards, inductive voltage dividers, and other ratio devices.

The units of capacitance, resistance, and voltage are disseminated additionally by means of cooperative Measurement Assurance Program (MAP) services for those laboratories requiring the ultimate in accuracy or desiring to characterize their measurement processes. These programs employ the use of extremely accurate transportable standards and carefully designed experiments to determine the uncertainty with which the client continues the dissemination process.

The Section also engages in applied research work to advance the state-of-the-art of both the maintenance and dissemination processes. One example of such work is the development of the Measurement Assurance Program for capacitance. The measurement assurance concept leads to determination of an all-embracing uncertainty statement, the product of characterizing the capability of a client's laboratory to make a specific measurement. This is done by regarding the total calibration, maintenance, and dissemination process to any point as a system and statistically sampling the output of that system on a basis dictated by the measurement needs of the system. Through the use of NBS transport standards, all random and systematic errors are determined, including effects of time, transportation, operators, equipment, grounding, and ambient conditions. After satisfactory performance has been documented, information from the system is used as feedback to reassign the values of the client's standards to agree with the legal units. The pursuit of a MAP service for capacitance entailed a study of the transport and temperature characteristics of commercial capacitors at the 1000-pF level and, as a result, the design, construction, and testing of a new transport standard.

The Division also serves the National Measurement System through its committee activities, consulting efforts, outside-sponsored research and development work, and by publishing the results of its research and development work, including that done to support NBS measurement services. Table 12 shows the various technical outputs of the Division and the approximate level of effort expended in each. It must be noted that, because of overlap, the percentages add to more than one hundred.

External sources of program guidance direction are the Office of the Director, IBS; Office of Measurement Services, IBS; the U.S. Army; the U.S. Navy; the Department of Defense Calibration Coordination Group (CCG); Department of Energy (DOE); the Electric Power Research Institute; the National Conference of Standards Laboratories; the NAS/NAE/NRC Evaluation Panel; and colleagues in industry. Since we work in close cooperation on a day-to-day basis with counterparts in the primary laboratories of the three DOD services, we are kept keenly aware of measurement needs in those laboratories. The CCG funds projects of joint interest to the Division and the military calibration structure. Recently, relations have been formalized with the National Conference of Standards Laboratories which represents the largest part of the Division's constituency.

Thus, the Electricity Division realizes, maintains, and disseminates the electrical units and related quantities to the Electrical Measurement System. These parameters are disseminated through the Measurement Assurance Programs and through the calibration of electrical standards and instruments. The quantities disseminated by the Division are all derived from three basic maintained units, those of resistance, capacitance, and voltage, and the unitless electrical quantities of resistance ratio, impedance ratio, and ac-dc current difference. The units and related quantities disseminated and the means of their dissemination are shown in table 13, page 48.

The technical infrastructure has two components. One is created as a result of the measurement support requirements of the electronics field and the other is the result of requirements of the electric power industry. The requirements of the electronics industry are of higher accuracy and over a more limited range of voltage and current than those of the power industry. They cover a wider frequency range, however, going up to 1 MHz in some cases. Power companies are generally concerned only with dc, 60 Hz, and pulse measurements, but at voltage and currents as high as 2 million volts and 50,000 amperes, respectively.

Measurements for Electronics.

(a) DC Measurements.

Voltage measurements of signals ranging from a few millivolts (thermocouple outputs) to 100 volts (power supplies for cathode ray and other tubes) are required by the electronics field. The basic unit of dc voltage is disseminated by the Electricity Division in two ways. The more accurate is the Volt Transfer Program in which an NBS transport standard is used to determine the difference between the client's unit of voltage and the legal unit. The uncertainty of this process

Table 12. Electricity Division technical outputs

Results and Reports from Sponsored Research and Development 20%

1. DoD CCG (71.5k$)
2. DOE (262.7k$)
3. Health, Education, and Welfare (FDA/BRH) (5k$)
4. Navy (36k$)
5. Electric Power Research Institute (148k$ - over several years)
6. DoD (20k$)
7. DoD (Army (7.5k$)

Committee Activities 5%

1. IEC (International Electrotechnical Commission)
2. ANSI (American National Standards Institute)
3. IEEE (Institute of Electrical and Electronics Engineers)
4. OIML (International Organization for Legal Metrology)
5. Internal NBS activities

Consulting 78%

1. Army
2. Navy
3. Air Force
4. NBS
5. Aerospace Industry
6. General Industry
7. Electronics Industry
8. Standards Producers

Calibrations and Testing (Estimated 377k$ FY76 Income) 78%

Industry (80%) - Aerospace
Electronics
Instrumentation
General
Power

Other NBS - Heat Division
Physical Chemistry Division
Office of Weights and Measures
Applied Radiation Division
Optical Physics Division
Electronic Technology Division

Government (15%) - Navy
Army
Air Force
NASA
Interior (Bureau of Reclamation)
NOAA
FAA
FDA (HEW)
Bonneville Power Administration
Public Health Service (HEW)
EPA
TVA

Measurement Assurance Programs (Estimated 45k$ FY76 Income) 12%

1. NASA
2. DOE
3. Aerospace Industries
4. Power Industry
5. DoD
6. Instrumentation Industry

Publication of NBS-Supported Research and Development 40%

1. Metrologia
2. IEEE Transactions
3. IEEE Proceedings

Table 13. Dissemination services of the Electricity Division

Quantity Disseminated	Means
DC Volt	Volt Transfer Program Standard Cell Calibrations Solid State Voltage Reference Device Calibrations
Resistance	Resistance Transfer Service Standard Resistor Calibrations Shunt Calibrations
Capacitance	Capacitance Transfer Service Standard Capacitor Calibrations Calibration of Power Factor Capacitors
Inductance	Standard Inductor Calibrations
Ratio	Inductive Voltage Divider Calibrations Current & Voltage Transformer Calibrations HV Transformer Calibrations Pulse Divider Calibrations Volt Ratio MAP Volt Box Calibrations Resistive Apparatus Calibrations Resistive Voltage Divider (HV) Calibrations
AC-DC Difference	Thermal Voltage & Current Converter Calibrations
Power	Wattmeter Calibrations
Energy	Watthour Meter Calibrations

is about 0.42 ppm. The other way is through the calibration of saturated standard cells submitted by the client to the Division for test. The uncertainty of the test is 0.4 ppm, but transportation effects can raise that to 1.0 ppm in any context of use.

Resistance measurements are used for a large variety of purposes in the electronics industry. The most stringent requirements come from the instrumentation industry where precision resistance components are used in ratio applications such as ladders (resistive scaling networks) for analog-to-digital converters and in operational amplifier circuits to provide accurate gain factors. The unit of resistance is disseminated in two ways from the Division. The Resistance Program service in which, like the Volt Transfer Program, a set of transport standards is used to determine the difference between the unit as disseminated by the client and the legal unit. The Division also provides for the calibration of standard resistors of decade values between 10^{-4} and 10^{14} ohms. The uncertainty associated with the Resistance Transfer Service depends upon the nominal value of resistors used and the capability of the client. Transfers at the one- ohm level have been made with a total uncertainty of 0.2 ppm. The uncertainty of a regular calibration is 0.08 ppm at that level, but transportation effects and errors incurred in the client's laboratory are not included.

Resistance ratio measurements are used primarily as tools to scale or subdivide the units of voltage and resistance. They are used in the calibration of test equipment such as digital voltmeter calibrators and digital multimeters and in the calibration of other resistive apparatus such as resistance bridges, potentiometers, volt boxes, and ratio sets.

The types of devices used for such measurements are potentiometers, volt boxes, voltage dividers, universal ratio sets, and Kelvin-Varley dividers. Of these, the last two are the least specialized. They may be used to calibrate any of the others. They can also serve as instruments for two and four-terminal resistance measurements and voltage measurements.

Resistance ratios have the useful quality that they can be established to very high accuracies without the use of standards. Consequently, measurements of ratio quantities are not legally required to be traceable to national standards. However, the Division calibrates ratio measuring devices since the facilities for doing so, with very high accuracies and with a minimum of diffi-

culty, are available. Calibration uncertainties for these devices are generally related to the resolution of the device (except for volt boxes) and range from 0.02 ppm to several hundred ppm.

The Division also offers the Volt Ratio Measurement Assurance Program. It is similar in concept to both the Volt Transfer Program and the Resistance Transfer Service except that, if measurement difficulties are encountered, a transportable measuring instrument can be sent to the client to be used as a trouble-shooting device. The uncertainty, due to transportation and measurement, of such a transfer is 1.5 ppm and it embraces uncertainties due to transportation and measurement errors at the client's laboratory, as well as at NBS.

(b) AC Measurements.

The unit of capacitance is disseminated mainly through the calibration of standard capacitors with values of 10, 100 and 1000 pF at 50, 60, 400 and 1000 Hz. The uncertainties of these measurements are 0.5, 0.6 and 5.0 ppm, respectively. The large increase in uncertainty for the 1000-pF capacitor is due to the different construction of the standards used at that level. A typical standards laboratory should be able to use these standards to make measurements of capacitance in that range of magnitude with no large increase in uncertainty. Such a laboratory would usually have a group of 1000-pF capacitors as a standard and with normal equipment should be able to make measurements with a total uncertainty of less than ten parts per million. This has been borne out experimentally in tests with military laboratories.

Inductance measurements are primarily used industrially for testing of component chokes and for quality checking of magnetic recording heads during production. Accuracies required and available in this area are low. Bridges used to make inductance measurements on the production line are accurate to 1% at best, and the capability of the Electricity Division to report the values of standard inductors with an accuracy of 200 ppm is apparently adequate for current and known future needs.

AC voltage measurements are made primarily with digital voltmeters at the applications level. Accuracies of such meters can be as high as 0.05% over a range of voltages from 0 to 1000 volts. They are calibrated using commercially available calibrators which are accurate to about 0.02%. These devices are calibrated by using an ac-dc thermal voltage converter to permit comparison between their outputs and those of very well-calibrated dc sources, known as calibrators. The dc calibrators are then verified using standard cells and resistive ratio devices. The ac-dc thermal voltage converter is the critical element in this chain since it permits the determination of rms values of ac voltage using dc voltage standards. These devices are calibrated by the Electricity Division with ranging between 5 and 200 ppm accuracies.

AC impedance ratio measurements are primarily used as calibration tools. The most commonly used device in the electronics field is the inductive voltage divider. This device is used to subdivide input voltages with amplitudes as great as 100 volts with a minimum adjustment of 10^{-7} of the input voltage. Such devices are calibrated by the Division with accuracies of 0.5 ppm of input voltage (in phase) and 5 ppm of input voltage (quadrature).

Measurements for the Power Industry. The power industry used electrical measurements in the control and monitoring of power. The main quantities measured are energy, voltage, voltage and current ratio, and capacitance.

Energy measurements are used to meter energy distributed within the power system for billing purposes. As stated previously, the power companies are required by the various state regulatory power commissions to supply users with watthour meters accurate to 2% with a 98% probability. Meter accuracies are checked by sampling. Higher accuracy in such measurements can result in smaller sample sizes, leading to considerable savings. Typically, power companies prefer to make such measurements to 0.5% to minimize the probability of fiscal loss by carrying out tests at higher levels of confidence. A sampling of several utility companies revealed that new meters were well within ±0.5%; old meters, retested in sampling operations, were within 1%. Meter manufacturers must accordingly use strict measurement tolerances.

There are two routes whereby a utility can obtain electric energy standards from NBS. The most direct one is via a client's rotating watthour meter standard which is sent to NBS for calibration. A variation of this route is the Measurement Assurance Program (MAP) whereby an NBS-owned meter is shipped to the client, who calibrates it as an unknown item in his test circuit. This procedure is preferable since it permits testing of the client's entire system.

The second, or the dc calibration route, consists of the client obtaining from NBS the standards of resistance, voltage, (both dc) and frequency. In addition, the ac-dc

difference of the client's special wattmeter is also determined by NBS. The standards of resistance and voltage provide the client with the standard for the dc power. Utilizing the ac-dc difference of his wattmeter, he can produce a known ac power. This is integrated using standard time (obtained from standard frequency signals) to produce the ac energy. See figure 3.

In the past, the dc standards were considered more stable and more easily transferable than the rotating watthour meter. Establishing an ac energy standard in this manner requires more work on the client's part. Until recently, the rotating standard was considered as too fragile a device for transport, unless hand-carried. During the past four years, NBS has successfully shipped rotating standards within the Measurement Assurance Program without adverse effects. It should be added that while most of the largest utilities get their standards directly from NBS, there are utility companies, particularly the small ones which rely on the standards of other utility companies.

High voltage measurements are used for the monitoring of energy flow in high voltage lines. This is done by using transformers to reduce voltages and currents in transmission lines to a level at which they may be measured by low voltage instrumentation such as watthour meters.

The accuracy requirements for transformers in metering service are specified in American National Standards Institute publications. The Standard C12-1975, Code for Electricity Metering, states that corrections for transformer errors do not have to be applied if the transformers are of the 0.3% accuracy class (correction less than 0.3%). Another standard, C57.13-1968, Requirements for Instrument Transformers, requires that the equipment for calibration of metering transformers be accurate to 0.1%. No standards exist for the higher echelon devices - the reference transformers. The NBS-reported accuracy of 0.03% for transformers above 100 kV has not resulted in any complaints; nevertheless, a desirability for 0.01% or even 0.002% accuracy has been mentioned by various individuals in the industry.

High voltage impedance measurements are used to measure the capacitance and loss angle of power factor correction capacitors, and the impedance and phase angle of shunt reactors. These devices are used to reduce the reactive power in a transmission system. Failure to do so would result in power circulating uselessly through the system. Such devices are calibrated by the manufacturer using as a standard a gas dielectric capacitor. The manufacturer's measurement system may be checked out by an on-site calibration of his standard and bridge using an NBS bridge and standard. Calibrations of capacitors rated up to 1000 μF and 100 kVA ratings can be done at NBS.

Appendix B contains a list of primary and working standards used at NBS in support of the measurement system.

4.2.2 Users of NBS Services

The users of the services made available by the Electricity Division fall into the same general categories as do the major components serviced by the Measurement System. The major categories are given below.

Table 14. Users of NBS services

Instrumentation Industry
Department of Defense
Aerospace Industries
Communications Systems Manufacturers
Electric Power Industry
Electrical Component Manufacturers
General Manufacturing Industries
Independent Calibration and Testing Laboratories
Civilian Government Agencies
Universities

User categories are listed roughly in order of their dependence upon the services offered. As has been stated previously, the services provide the basis for accuracy of all measurements which are in turn used to assure the quality, volume, and advancing technology of produced goods.

4.2.3 Alternate Sources

There are no alternate sources for the most important service that the Electricity Division renders the Electrical Measurement System. The Division provides the research and development effort necessary to enable the system to fulfill its needs in a timely fashion. Other organizations are well-equipped, have competent staffs, and are able to supply calibrations of standards at accuracies approaching those available at NBS for certain parameters. But none are motivated to make the magnitude of investment required for, nor have the responsibility for providing for, the research and development in basic metrology needed to support the entire system. No one organization matches the breadth of the NBS capability and none match its capacity for future improvements or for responding to changing needs. For the measurement system

to function in an optimum way, services and research must go hand in hand.

Commerce and industry today, even more than at the turn of the century, require traceability of measurements to a single source as a necessity for accuracy, without which interchangeability of parts, ready repair, compatibility of electronic devices, and ease of design would all be impossible. In addition, because of its role as the premier source of standards for electro-technology and the fact that it is funded publicly and represents no special interest, the Electricity Division is able to act as a neutral third party - an arbiter in areas of technical dispute involving measurements.

Scenarios have been proposed to consider what would be the results of turning the bulk of the metrology dissemination and calibration work over to state or private calibration laboratories. To do so would result in isolation of the Electricity Division from the bulk of its user community and hence render it less, rather than more, responsive to the needs of the system. The difficulty of moving technology out to the system would increase due to this isolation.

4.2.4 Funding Sources for NBS Services

The development of new services and the improvement of existing calibration services are supported by congressionally-appropriated funds (NBS budget), augmented by funding from private and government agencies outside NBS on a contractural basis. Typically, the Division has about 20% of its budget provided in this manner. Most of this comes from the Department of Defense, to augment work in support of its measurement systems; and from EPRI, the Electric Power Research Institute, and the Department of Energy, for energy-related work. In addition, federal law requires the complete recovery of the costs of providing calibration, measurement transfer, and other routine services from the users of such services. Revenue from this source constitutes approximately 14% of the Division's budget.

4.2.5 Mechanisms for Supplying Services

Dissemination services take place through three mechanisms: the calibration of client standards at NBS; Measurement Assurance Program services, which involve the use of NBS transport standards to sample the measurement process output at a given place; and *in situ* calibrations of such devices as high voltage transformers and capacitors by NBS personnel using NBS apparatus and standards.

Dissemination of metrology information is provided for by sponsorship of Division seminars and workshops, publications in the scientific literature, participation in standards committee activities by staff members, publication of tutorial articles such as Technical Notes, and by individual personal interaction with members of the metrology fraternity at large.

4.3 Impact of NBS Services

4.3.1 Economic Impact of Major User Classes

Although no accurate quantitative assessment of leverage is possible, an appreciation of the potential impact of NBS services may be gained by a consideration of the gross annual sales figures of those segments of industry it supports as shown in table 15.

The Defense Department, of course, is vital to the well-being of our nation. It depends on measurements to ensure weapons system reliability, and indirectly through the aerospace and electronics industries,

Table 15. Electricity Division user classes

	SIC Code	Number of People	Value of Shipments (billions of $) CY 75	Number of Companies
Electronic Systems	3662	330,000	9.6	86
Components	367	412,000	10.6	1420
Computers	3573	175,000	9.7	610
Engineering & Scientific Instrumentation	3811	43,000	1.4	721
Measuring & Control Instrumentation	3821	72,000	2.1	817
Test Equipment	3825	70,000	2.2	622
Power Equipment	351	44,000	2.4	74
Transformers	34433	18,000	.9	40
Electric Power	491	317,000	47.9	225
Aerospace	372,376	615,000	26.2	1225

superiority through technical sophistication. All of these industries, with the exception of the electric power industry, produce high technology products and contribute heavily to our high standard of living. The power industry applies research and uses high technology to provide us with the means to utilize energy conveniently and is responsible in large measure for the industrial base of the country.

4.3.2 Technological Impact of Services

Calibration and MAP services of the Electricity Division provide both the electronic and electrical power industry segments of the measurement system with the stable, basic electrical units upon which the accuracy of measurements throughout the system depends. This support is vital to the development of new, sophisticated instrumentation and to the maintenance and continuing effective use of the very large existing national inventory of test equipment and measurement instrumentation. This inventory of electrical measurement apparatus is the only viable means of providing quality control for manufacturing processes throughout industry, ensuring operational readiness of our sophisticated weapons systems, enabling the high degree of reliability of electronics and equipment vital to our manned space operations, making possible the reliable and smooth functioning of the nation's communications and transportation networks, and providing for the efficient and effective distribution of electric power to industrial and domestic consumers throughout the country. The importance of instrumentation and the measurements it makes is borne out by two factors. The expected increase in test and measuring equipment for electrical quantities alone is 11% between 1975 and 1976 and that growth rate is expected to continue through 1985, by which time $6.5 billion in instruments will be produced annually [11]. This growth rate, especially in times of economic hardship, is an indication of the need for measurements. Secondly, to this must be coupled the fact that the measurement capability per unit cost of instrumentation is rising dramatically due to the semiconductor revolution and the inclusion of microprocessors in individual instruments [30]. Standards maintained by the Electricity Division and used to disseminate the electrical units allow measurements made by this instrumentation to be consistent throughout the country and stable over time.

NBS services, such as consultative and committee activities and publication of metrology research and development work, are aimed at promulgating measurement technology so that measurements may be made more efficiently, effectively, and accurately throughout the system. NBS representation is most widespread on those technical committees of the Institute of Electrical and Electronics Engineers, the American National Standards Institute, and the International Electrotechnical Commission which deal with electrical measurements. Literally hundreds of inquiries per year about various electrical measurements problems are handled by staff members.

Publications concerning measurement techniques have a heavy impact on the measurement community. Over 3000 copies of NBS Technical Note 430, Designs for Surveillance of the Volt Maintained by a Small Group of Saturated Standard Cells by Eicke and Cameron have been distributed. The measurement techniques set forth in this document were at the time of publication virtually unknown in the electrical measurements field outside of NBS and have since been adopted by a significant number of metrology laboratories. This has resulted in general improvement in the quality of voltage measurements in standards laboratories as well as permitted the identification of potentially serious measurement problems.

Some of the areas of technology and industry heavily supported in both development and operational phases by the measurement system are semiconductors, discrete electronic components, instrumentation (a user as well as an implementor); communication; navigation; chemistry; metals; and computers. Electrical measuring instruments provide the basic tools for physical, biomedical and chemical research as well.

4.3.3 Pay-off from Changes in NBS Services

Two notable changes have occurred in recent years in services offered by the Electricity Division. The first is the increasing use of Measurement Assurance Program services, starting with the Volt Transfer Program, for the dissemination of the electrical units. In the case of all of these services there have been two immediate technical effects: the units have been transferred with higher accuracy; and invalid measurement techniques at users' locations have been identified and their use curtailed due to NBS analysis of data.

In a number of cases, there has been a third payoff. The techniques used in the process have been successfully applied to the users' individual measurement system.

The most definitive economic benefit has been the extension of the interval between calibrations for the clientele using these services. This is made possible by the

improved accuracy of the transfer and the methodology by which the data are reduced, in comparison with usual methods used to ensure measurement traceability. The greatest measurable economic impact of this type of service will most likely result from the application of these specific techniques to effect a reduction in cost of supplying measurement support to production lines and throughout quality control systems.

For a group of five California companies, the availability of MAP services has meant a completely new method of establishing traceability. In the past, each company sent standards of voltage and resistance annually to NBS for intercomparison. Now, each year only one of the companies becomes involved in an NBS voltage or resistance transfer. During the same period of time, the group undertakes a five-way intercomparison of the appropriate units for each company, using measurement transfer techniques. They have reduced the cost of traceability significantly in this fashion and each now has confidence in the standards of the others should a failure occur in his own [31].

The second major change in the Division's services occurred as a result of closing the old NBS high voltage (HV) laboratory in Washington, DC. In 1970, a decision was made and implemented to move the low and intermediate voltage support facilities and offices of the High Voltage Measurements Section to the Gaithersburg site. The HV laboratory was intended to be retained as a field station and used whenever the need arose for voltage levels above 50 kV.

However, in 1971, the General Services Administration, the owner of the laboratory and site, asked NBS on short notice to vacate the facilities in order to make the land available for the Washington Technical Institute. NBS abandoned the laboratory and transferred the equipment for a nominal sum to another government agency. Thus, NBS gave up, and the Division lost, a facility whose replacement cost today would range from $5 to $10 million.

The basic reasons for this closing were complex: low calibration workload, a lack of funding of high voltage research by other agencies; its vulnerable position as an isolated facility away from the main NBS campus; and NBS program priority decisions.

To retain some capability for calibrations and research in the high voltage measurements area, especially for measurements required in revenue metering, a new mode of operation was begun. Instead of doing all HV work in-house at NBS, measurement services above 100 kV are offered as on-site calibrations. Division staff members go either to customers' high voltage laboratories or to one which belongs to an acceptable third party. The NBS instruments and standards used are designed with portability in mind. For calibrations and research below 100 kV, and intermediate voltage in-house facility has been established at the NBS Gaithersburg (MD) location.

This change in NBS facilities extensively affected the electric power industry. While retaining an acceptable calibration capability, it reduced the Division's capability and flexibility to contribute to the research requirements of electric power transmission systems. The level of power industry support in the sixties, when the future of the NBS high voltage laboratory was debated, may not have indicated the need for it. However, the situation changed significantly in the past few years.

The principal reason is the energy crunch and the associated emphasis on energy-related R&D. Electric power R&D in industry has been focused by the formation of the Electric Power Research Institute (EPRI), which is the R&D arm of the power industry; and the Department of Energy, which controls the public funds related to energy research.

The combined transmission and distribution (T&D) budget for these organizations is about $40 million annually. The size of the measurements component is difficult to assess exactly since it is diffused throughout the entire program, but a safe estimate, based on the problems of which NBS is aware, would be at least 1% of this or $400k annually.

In the past two years, power systems related OA work in the Electricity Division has increased from a negligible amount to about $250k annually. Further increases still could be made if facilities and manpower were available.

In summary, the potential need for measurements R&D related to electric power systems is at least $400k annually. Even if other constraints were removed, we could not undertake such a program fully without having access to our own or a closely located HV laboratory. It also must be added that T&D research (including measurements R&D) relates to a projected capital investment of $150 to $200 billion over the next 15 years.

4.4 Evaluation of NBS Program

The Electricity Division program is generally consistent with the needs of the electrical measurement system but inadequate in several areas, such as the dynamic electrical standards area, due for the most part to limited resources, both of personnel and funding. The most powerful tool for determining the needs of the measurement system for the Division's services and output is the expertise of the technical staff of the Division. By keeping current with trends and advances in instrumentation and electronics, staff members identify potential areas where NBS measurement support will be needed as well as up-to-date tools to help supply that support.

Other agency sponsors constitute a powerful means of identifying needs. In the electrical power area, responsibility for the development of nearly all future technology is in the hands of the Division's two major sponsors, the Department of Energy (government) and the Electric Power Research Institute (private sector). Widespread Division contacts within these two organizations ensure early recognition of needs within the power industry.

State-of-the-art advancements in electronics, systems, and instrumentation generally result from fulfillment of the new weapons requirements of the Department of Defense. The Division has a very close coupling with the Defense Department through its Calibration Coordination Group. This DoD group, which over the years has sponsored a large amount of metrology development work in the Division, apprises NBS staff members of future measurement requirements in the military system.

The National Conference of Standards Laboratories is a management-oriented organization comprised of companies and government agencies with metrology interests. This group is highly representative of the Electricity Division's clientele as there is greater than a 80% overlap of NCSL member companies and the Division's calibration services users. Recently, the Executive Board of that organization approved a plan to constitute an NCSL liaison board to the Electricity Division. This board will serve both to provide inputs for future planning in the Division and as a vehicle for the dissemination of technical and management information from NBS to NCSL member companies.

The National Academy of Sciences/National Academy of Engineering/National Research Council Evaluation Panel for the Electricity Division reviews the programs in the Division, generally on an annual basis, and provides valuable input for the determination of future program directions. The most recent such panel had eight members representing the viewpoints of the power industry, the Federal energy research program, the Department of Defense, the academic community, the electronics industry, the research community, and the instrumentation industry. The Panel's reports contain comments and recommendations on technical, managerial, and administrative matters as well as suggestions for new directions. The annual meetings between the Panel and staff members, although perhaps too brief, are very beneficial for the exchange of technical information and views too detailed to be of use in management reports.

The most recent Panel was in full support of the Division's ongoing programs, and especially highlighted the need for work to be done in the areas of measurements in support of high voltage research and development and high-speed dynamic standards for modern electronic instrumentation. The Panel identified communications between the Division and its constituency as being a major problem and commented on the process of setting long-term development goals in the rapidly developing area of modern instrumentation.

As needs are identified, program priorities must be established. These priorities are the result of careful consideration of the degree to which response to the need falls within the NBS mission, the magnitude of the need, the resources (including expertise) available to deal with the problem, and the likelihood of success in an appropriate time frame.

Major needs of the system for NBS services include those for:

(a) basic standards to maintain stable national electrical units;
(b) means of disseminating the units;
(c) "how-to-to-it" metrology information;
(d) dynamic measurement standards for modern instrumentation;
(e) techniques for the measurement of impedance, voltage, current, and dielectric properties at high voltages; and
(f) the determination of fundamental physical constants, such as the Faraday and 2e/h.

The Electricity Division has on-going programs to respond to each of these areas of need. Because of the widespread need of these services and the need for an impartial, technically competent organization to deliver them, it is clear that they can be performed only by a federal government agency. NBS is the only agency with the expertise and statutory responsibility for providing them.

4.5 The Future

Activities in the Electricity Division are at present undergoing a period of change. Advantage has been taken of the completion of a large number of projects in traditional areas to effect reprogramming to bring effort to bear on the solution of problems in new measurement areas. The Electricity Division's capability to provide support for static measurements in the general instrumentation are generally more than adequate to meet present needs. However, similar support is lacking for the dynamic measurements (i.e., those made under a time constraint) of electrical quantities such as are made under computer control. Hence a considerable effort is being devoted to a program to establish measurement methodology and standards in support of modern, high-speed instrumentation. Investigations are proceeding to establish standards and instrumentation to investigate high-speed analog-to-digital and digital-to-analog conversion modules. A program to establish methodology for the proper support and implementation of electronic test equipment of high accuracy is underway on a modest scale. The Division is midway in the development of a system to provide an accurate measurement base for the semiconductor industry at the 10-volt level.

All of this activity is in response to the needs perceived by Division personnel which led to a workshop in September of 1974 to identify and quantify Critical Electrical Measurement Needs and Standards for Modern Electronic Instrumentation. The Workshop was attended by 24 engineers and scientists representing a variety of industrial viewpoints. Automatic test equipment users, instrument manufacturers, systems users and manufacturers, and the semiconductor module industry were represented, mostly at the engineering manager, or vice-president level. The general conclusion of the Workshop supported the Electricity Division's perception of needs in this area. Other hitherto unidentified needs were made known, most notably in the areas of pulse responses of components, dielectric hysteresis, and the characterization of ac line voltage with respect to transients, dynamic impedance, etc. [see Appendix C].

In the area of dissemination of information, a program has been started to generate a series of tutorial publications covering various aspects of electrical metrology useful to the personnel of a typical standards or calibration laboratory. An effort is being made to establish an Electricity Division newsletter in one technical journal and to publish overview articles in other, more generally based, periodicals, in order to expose Division programs to the scientific and engineering community and thus engender feedback.

In discussing the measurements for electric power systems this report implicitly and explicitly recognizes two areas: (1) the areas related to the "traditional" quantities such as voltage, current, impedance and, especially, power and energy; and (2) that area related to research and development of new apparatus and systems, primarily for transmission and distribution. In the latter area are also included those specialized and difficult measurements employed in the design and quality control of present systems.

The delineation between the two areas is not very rigid and the term "traditional" must be tempered since it does not imply lack of need for research and development activity. As the instrumentation and transmission technologies change, NBS must meet the changing measurement requirements for these basic electrical quantities. As discussed elsewhere in this report, a very important item in this first category is the measurement of electric energy. Although currently this area is well in control, new instrumentation and metering practices will be introduced within the next five years which will place additional requirements on the NBS services. Electronic watthour meters are appearing in interutility and large commercial and industrial metering installations. Load management based on variable rates for electric energy is being considered. A more sophisticated instrument combining the functions of a watthour meter and a demand meter has been suggested. As with the conventional induction-type watthour meters, not only will the accuracy and reliability be of concern, but also the ease of remote reading and control and interfacing with a central computing facility. Although its role is not entirely clear at the moment, NBS will be required to provide rather different kinds of supportive measurement services in the future in addition to the present routine calibrations and MAP services. New developments in this area will be closely watched.

In measuring the traditional steady state quantities, problems exist in calibrations at higher voltages, where relatively few organizations have a capability of calibrating voltage transformers. Traceability to the fundamental NBS-maintained standards is weak. The Electricity Division will try to alleviate this situation by promoting field calibration services and through specific projects such as the development of the system for calibration of coupling capacitor voltage transformers in substations.

With respect to the other area concerned with R&D and specialized measurements, there

are numerous unresolved problems now and certainly more will become evident as the R&D in new transmission systems progresses. The weakest area now is concerned with the measurement of high voltage transients, especially at extra high voltage (EHV) and ultra-high voltage (UHV) levels. NBS will continue to work in impulse measurements with particular emphasis on transferring our capabilities to the power industry. Contingent upon the availability of resources, work should be done on devices for measuring voltage, current and power in high voltage dc transmission systems.

The Division will follow the developments of new transmission systems and provide its expertise for solving measurements-related problems. This area is proper for extra-NBS support. An example is the development of a superconducting ac transmission system. High voltage measurements research related to the insulation of superconducting cables is already being performed. Superconducting systems will have very high current capabilities. New methods will be needed to measure these currents.

Another new transmission system under development uses SF_6-insulated conductors. Nonconventional measuring methods appear to offer cost and accuracy advantages in these systems. This entire area is ripe for exploration.

If overhead transmission enters the UHV region, electro-optical current transformers will become very attractive. The NBS will be in the best position to evaluate their accuracy capabilities by virtue of measurement techniques in the UHV region developed here.

Potentially adverse effects on environment due to high electric fields, audible noise and electromagnetic interference are of great concern in connection with new EHV and UHV overhead systems. The Division will offer measurement assistance to the agencies primarily concerned with this problem.

Reprogramming efforts to respond to all of these needs made evident a serious weakness in the Division. The Division simply lacks the proper resources, people, and funding to mount a comprehensive program in each area without seriously eroding the supporting basic measurement program - there is concern that a proper job cannot be done without ignoring clear responsibilities in the traditional areas.

On the other hand, there would be a large negative impact if the Division were to fail to meet the needs being addressed by these various activities. The state of the electronic marketplace is one of chaos with respect to high-speed electronics. Lack of common terminology and universally accepted test procedures makes procurement by specification a difficult and hazardous procedure. Since the definitions of temporal parameters are nebulous, different interpretations are used by different manufacturers and the buyer has no means of evaluation except in terms of a specific application. The net result is that much money is wasted on useless purchases and the over-specification of components to ensure adequate performance. The presence of an authoritative, technically competent, neutral "third party" such as NBS, is urgently needed in the area to establish commonality.

Why should NBS be involved in any of this? The Federal government is the only organization that can afford to look past tomorrow to the future in the area of measurement science and standards. Industrial concerns must have staying-in-business as a first consideration. That generally means a minimum of long-range (10-20 year) research programs, and a great deal of motivation for keeping potential profit-making results of such research secret.

The National Bureau of Standards is the only government organization with the base, the expertise, and the legislative charter to perform these functions. No other government laboratory has appropriate facilities or staff. Research in measurement methodology would not be the primary concern where other national needs such as national defense are the responsibility of the organization. The country needs one organization in which measurement activities and standards are the primary concern as at NBS.

5. SUMMARY AND CONCLUSIONS

The National Measurement System for Electricity has two major components; those of electronics and the electric power industry. These are separately identified because of the distinctly different nature of the measurements required in each. The former is comprised of the electronics and instrumentation industries and their users, while the power subset of the system is comprised of the electric utilities, manufacturers of generating, transmitting and distributing apparatus and, to some extent, the users of electric energy.

The present measurement capability of the electronics subset is more than adequate to support traditional measurements (those made manually or without time constraint) except in a very few limited cases such as, low frequency, low amplitude ac voltage measurements and upper audio and lower radio frequency impedance measurements. However, due to the impact of advances in semiconductor technology on the instrumentation, computer, and electronics industries, and the resultant increases in complexity of components, devices, and systems, a larger and larger percentage of measurements is being made by electronic instrumentation under computer control and under conditions in which time is a constraining factor. This leap forward in measurement technology has not been matched by the development of appropriate standards of measurements. Designers of automatic test systems and equipment do not have the benefits of either physical or written standards for dynamic electrical measurements as tools. Common terms, such as aperature and settling time, used to describe dynamic properties of measurement equipment, do not have universally accepted definitions. Also, physical standards, analogous to standard resistors, capacitors, and cells, for the quantification of dynamic properties do not exist. Designers and users of modern test equipment and instrumentation must use costly trial and error or "overkill" methods for both the development and maintenance of such equipment. Development of future, more accurate and faster systems will be hampered by lack of such standards.

In the electric power industry subset, which deals basically with energy, voltage, current, and impedance measurements at 60 Hz, some at very high voltage and impulse measurements at high voltages, the present capabilities are generally adequate to support today's operational requirements. However, the electric power industry is beginning an era of great change. The main forces for change are the energy crisis and the appreciation of the small size of the remaining supply of petroleum. Research efforts to improve the capacity and efficiency of electric power generation, transmission, and distribution have been expanded greatly over the past few years. New measurement methods and standards are drastically needed to enable this research to reach fruition and to support and maintain the new power systems expected to result. Measurement methods are needed for such things as calibration of capacitive coupled voltage transformers (CCVT's) for use at 500 kV and above; evaluating various types of prototype distributions systems, such as underground dc and gas insulated, cryogenic, or extruded insulation systems, and overhead systems ranging as high as 1.5 million volts; evaluation of environmental and interference effects of ultra-high voltage overhead lines; and development of tests to ensure that equipment on such lines can withstand transient overvoltage and surge currents caused by lightning and switching. Energy metering, done largely at the present time using rotating electrodynamic meters, will require new measurement support with the advent of electronic meters which will be used for demand and time of day metering purposes and may eventually employ telemetry techniques for instant transmission of consumption information to the utilities.

There are a few common problems with widespread effects on the entire system. Among them are:

(a) a lack of availability of "how-to-do-it" measurement information throughout the system;

(b) a shortage of manpower with specific metrology training and a resulting widespread lack of sophistication in measurement technology as practiced;

(c) heavy emphasis on "traceability", largely fostered by Department of Defense quality requirements, which causes much attention to be focused on equipment specifications and calibrations rather than measurement technology. This tends to slow the development of new and improved methods of providing measurement support where it counts, on the production line or at the weapons system; and

(d) a lack of recognition of the formal metrology structure as an asset rather than a required artifact in a large percentage of industry.

Specific recommendations resulting from this study are:

General

Develop a mechanism to foster and support the use of Measurement Assurance philosophy and techniques within industry to provide subsistence to measurements made for quality control, manufacturing, or maintenance purposes.

Develop more formal contact between the Electricity Division and the instrumentation industry, perhaps through the aegis of the Scientific Apparatus Manufacturers Association.

Establish national standards and improved measurement methodologies for the ac measurement of conductivity in metals in support of non-destructive testing in industry.

In support of electronics

Investigate new technology for providing measurement support for automatic test systems, perhaps in conjunction with Defense Department efforts in this area.

Examine microprocessor technology and the applications of microprocessors to instrumentation to lay the foundation for support for future generations of sophisticated "smart" instruments.

Provide improved methods for the measurement of ac voltages at low amplitudes in the sub-audio frequency range and the measurement of impedance in the upper audio range for the support of vibration and communications instrumentation respectively.

In support of the power industry

Provide for development of measurement methodologies for the characterization of the insulating properties of various materials and systems at high voltages and under various conditions and configurations (such as for superconducting cables).

Contribute to the development of electronic watthour meters to develop the new standards and measurement techniques necessary to their support.

Promote the use of field calibrations and measurement assurance programs in the area of high voltage.

Continue research in high voltage impulse measurements and develop mechanisms to disseminate the resulting technology to industry.

Develop new approaches and devices for the measurement of voltage, current, and power in high voltage dc transmission systems.

Investigate methods for measurement of the extremely high currents which will be carried by superconducting cables.

Develop methods for the precise measurement of electric fields in regions of extreme nonlinearity for environmental protection and safety testing purposes.

APPENDIX A

THE MEASUREMENT SYSTEM STUDY

The starting point in efforts to date has been the group of organizations constituting our calibration clientele. The general plan for this study is outlined below:

a. Identify calibration clients and associated economic data.
b. Classify clients by industry or major product(s).
c. Select sample of clients to visit to determine measurement needs, technical problem areas, and organizational structure.
d. Identify corporations and industries who are not clientele but who are engaged in the same kinds of endeavors.
e. Sample non-client organizations of maximum economic, social, and political importance to determine the methods employed to achieve product quality assurance in those organizations.
f. Garner detailed information about specific needs via interviews, workshops, etc.

Using information supplied by the Office of Measurement Services (NBS), a listing of all users of our calibration services in FY 72 has been compiled. The clients on this list were then classified in one of the categories shown subsequently. Each organization was assigned up to three numbers representing one primary and two secondary activities. These were based on personal knowledge and on descriptions found in *Standard and Poor's Index*. In addition, annual income figures from either the *Standard and Poor's Index* or the *Dun and Bradstreet Million Dollar* and *Middle Market Indicies* were gathered for each customer. This information was added to that supplied on punch cards by the Office of Measurement Services and sorted. There were three sorts made, one by each of the primary and secondary activities of each company. As a result of the first sort, 52 companies are unclassified; 17 are in the aerospace industry; 49 manufacture instrumentation; 21 manufacture components; 43 are power industry-related; 7 are universities; 9 are other Federal government agencies; and 32 are in general manufacturing, for a total of 230 companies. A meeting of the study authors was held on the receipt of these printouts and a number of pertinent decisions were made.

It was decided that a separate substudy should be made of the power industry in view of the percentage of the Division's clientele it represents, the annual income it has, the role it plays in our society, and the energy crisis. The chief of the High Voltage Section undertook this substudy because of the mission of the Section and his personal contacts within the electric power industry.

A minimum sample size for each of several categories was decided upon, based upon the perception of the degree of impact NBS has on each category and knowledge of the uniformity of measurement technology within the category. The table below gives each of these categories and the sampling size chosen.

SAMPLE SIZE FOR CLIENTS

Category	Sample Size
201 Precision Apparatus	100%
212 DC-LF Test Equipment	100%
100 Aerospace Industries	25%
209 Systems	10%
600 Other Agencies	100%
300 Component Manufacturers	2 of each subcategory
800 Calibration Laboratories	As many as possible

The type of information which would be sought of each sample was also discussed. Answers to the following questions would be sought:

a. What are the corporate quality control organizational and technical structures?
b. Do you perform calibrations for other organizations? How Much? For whom?
c. What is the name of the key researcher in your company (Chief Scientist, perhaps)?
d. What is the annual expenditure on electrical measurements in your company? How is it spent?
e. What measurement areas are most critical to your final product?
f. What measurement or measurement-related problems do you have? Can NBS help?
g. What products are most critically affected by measurements?
h. Would you be aided by improved or new NBS services? What areas? Why?
i. What are the desired accuracies of measurements at the end item? Who determines these? Why are they what they are? What are the consequences of not supplying the desired accuracies?
j. Are you a military contractor? Are you subject to any regulatory agency policies?

It also seemed desirable to inform our contact, in advance of a visit by Division personnel, of the capabilities of the NBS and especially of the Division. Accordingly, an effort has been made to inform him by letter or telephone of the specific purpose of the visit so he could be prepared. It would be difficult, otherwise, to get past the corporate standards laboratory into the applied areas of the system.

In gathering information from *Standard and Poor's Index* and from the two publications of Dun and Bradstreet, it became apparent that NBS has direct contact with only a small percentage of the electrical measurement system. It had been originally decided that the Division must sample that part of NEMS it does not normally interact directly with. To do that the services of Dun and Bradstreet were enlisted. The list of clients previously mentioned was expanded to include FY 73 clients and each plant location served. The local office of Dun and Bradstreet determined the primary Standard Industrial Classification (SIC) Code for each company of a large sample. After discarding 17 of the 35 SIC codes thus obtained due to obvious lack of relevance, a contract was issued to Dun and Bradstreet to supply the Division with Dun's Market Identifiers for each of the companies in their file having one of the 16 primary SIC codes and more than 20 employees. Information has been supplied for 12,865 companies in the United States.

We hope to obtain additional samples by interrogating people who visit the Division.

In the past four years over 90 plant locations have been visited by Electricity Division personnel. Before this study was formally initiated, the purpose of most visits was the discussion of measurement problems. The next pages contain a representative list of locations visited.

Technical forecasting is always involved in program planning, whether explicitly or implicitly. In the past, technology forecasting for this Division has been done by two groups of experts, one (unorganized) within the Division and the other outside of the Division, the NAS/NRC/NAE Advisory Panel.

The technology forecasting portion of this study has been accomplished by doing a formal review of trends and forecasts already published for the electrical field by trade and industrial associations, professional societies, and other government agencies.

SAMPLE LIST OF PLACES VISITED

Associated Engineering Company
Matthew, NC 29105

Autonetics
Rockwell International
3370 Miraloma Avenue
Anaheim, CA 92803

Ball Brothers Research Corporation
P. O. Box 1062
Boulder Industrial Park
Boulder, CO 80302

Baltimore Gas and Electric Company
531E Madison Street
Baltimore, MD 21203

Beckman Instruments, Inc.
2500 Harbor Boulevard
Fullerton, CA 92634

Bendix Environmental Science Division
1400 Taylor Avenue
Baltimore, MD 21204

Boeing Company
Aerospace Division
P. O. Box 399
Seattle, WA 98124

Brookhaven National Laboratory
Brookhaven, NY

Dickson Electronics Corporation
P. O. Box 1390
Scottsdale, AZ 85252

Duke Power Company
P.O. Box 2178
Charlotte, NC 28201

Fairchild Semiconductor
4300 Redwood Highway
San Rafael, CA 94902

Ford Motor Company
21500 Oakwood Boulevard
P. O. Box 1704
Dearborn, MI 48121

General Electric Company
Ordnance Systems
100 Plastics Avenue
Pittsfield, MA 02101

Global Associates
Mississippi Test Facility
Bay St. Louis, MS 39520

Hewlett Packard Company
815 SW 14th Street
Loveland, CO 80537

Hewlett Packard Company
Automatic Testing Division
Mountain View, CA

Hewlett Packard Company
Microwave Division
Palo Alto, CA

Honeywell Industries
5558 Port Royal Road
Springfield, VA 22151

Honeywell, Inc.
Government & Aeronautical Products Div.
2600 Ridgway Parkway
Minneapolis, MN 55413

Honeywell, Inc.
Test Instruments Division
4800 East Dry Creek Road
Denver, CO 80217

Honeywell, Inc.
5303 Shilshole Ave., NW
Seattle, WA 98107

Hughes Aircraft Company
Centinela & Teale Streets
Culver City, CA 09230

IBM
Systems Manufacturing Division
Monterey & Cottle Roads
San Jose, CA 95193

Jet Propulsion Lab
California Institute of Technology
4800 Oak Grove Drive
Pasadena, CA 91103

John Fluke Manufacturing Co.
P. O. Box 7428
Seattle, WA 98133

Julie Research Laboratories
211 West 61st Street
New York, NY 10023

Leeds & Northrup Company
Sumneytown Pike
North Wales, PA 19454

Linde Corporation
Tarrytown, NY

Lockheed Missiles & Space Company
P.O. Box 504
Sunnyvale, CA 94088

Martin Marietta Corporation
Denver Division
P. O. Box 179
Denver, CO 80210

Melpar
Division of LTV Electrosystems
7700 Arlington Boulevard
Falls Church, VA 22046

3M Company
3M Center
Bldg. 216-1S
St. Paul, MN 55101

Newark Aerospace Guidance &
Metrology Center
Newark Air Force Station, OH 43055

Optimation Industries
Northridge, CA

Patuxent Naval Air Station
Patuxent River, MD 20670

Oak Ridge National Laboratory
Oak Ridge, TN

Philadelphia Electric Company
2301 Market Street, N4-1
Philadelphia, PA 19103

Rosemount Engineering Company
12001 West 78th Street
Eden Prairie, MN 55343

Shallcross Manufacturing
Preston Street
Selma, NC 27576

Sperry Rand Corporation
UNIVAC Division
Univac Park
P.O. Box 3525
St. Paul, MN 55101

TRW Systems Group
One Space Park
Redondo Beach, CA 90278

United Air Lines
San Francisco International Airport
San Francisco, CA 94128

Westinghouse Electric Corporation
P. O. Box 1637
Baltimore-Washington International
Airport
Baltimore, MD 21303

Westinghouse Electric Corporation
Astronuclear Laboratory
P. O. Box 10864
Pittsburgh, PA 15236

Westinghouse Electric Company
Raleigh, NC

CATEGORIES OF CALIBRATION CLIENTELE

100 Aerospace Industry
- 101 Prime Contractors (Airframe)
- 102 Subcontractors (Miscellaneous)
- 103 Subcontractors (Propulsion)
- 104 Subcontractors (Guidance)
- 105 Consultants

200 Instrumentation
- 201 Precision Apparatus Manufacturers
- 202 DC-LF Test Equipment Manufacturers
- 203 Analog-to-Digital, Digital-to-Analog Conversion Equipment
- 204 Medical Instrumentation
- 205 Process Control Computer and Data Acquisition Products
- 206 Nuclear Instrumentation
- 207 Communications Equipment
- 208 Recording Equipment
- 209 Systems
- 210 Chemical Instruments
- 211 Pollution Monitoring Equipment
- 212 Microwave Test Equipment
- 213 Temperature Measuring Equipment

300 Component Manufacturers
- 301 Resistors
- 302 Capacitors
- 303 Inductors
- 304 Solid State Reference Devices
- 305 Integrated Circuits
- 306 Switchgear
- 307 Electron Tubes
- 308 General
- 309 Batteries

400 Power Industry Related
- 401 Transmission Monitoring Equipment
- 402 Generating Equipment Manufacturing
- 403 Power Measuring Equipment
- 404 Power Generation
- 405 Consultants

500 Universities

600 Other Government Agenices
- 601 Army
- 602 Navy
- 603 Air Force
- 604 NASA
- 605 Bonneville Power Administration
- 606 Public Health Service
- 607 FDA
- 608 NOAA
- 609 FAA
- 610 EPA
- 611 TVA
- 612 Bureau of Mines
- 613 ERDA

700 General Industry
- 701 Automobile Industry
- 702 Waste Management
- 703 Electric Motors
- 704 Electric Generators
- 705 Metals Products
- 706 Nuclear Research
- 707 General Research
- 708 Computer Manufacturing
- 709 General Manufacturing
- 710 Chemicals
- 711 Consumer Products
- 712 Services
- 713 Sales

800 Calibration Laboratories

APPENDIX B

NBS PRIMARY AND WORKING ELECTRICAL STANDARDS

The following identifies the number and type of standards used to maintain the various electrical units and working standards for the dissemination processes. The term "primary" as used below refers not only to those standards used to maintain the basic electrical units, but to those which enable measurements to be made under conditions differing from those under which the basic units are maintained. Examples of the latter are standard resistors especially designed for stable characteristics at very high currents. The list does not contain measurement apparatus (except when such apparatus embodies a unit), or intermediate standards used for scaling, or the check standards used to maintain statistical control over the various measurement processes.

Sec. 1. RESISTANCE

Primary Standards

5 Thomas (NBS) One-ohm Standard Resistors

Working Standards used at Low Currents (0.01 W or less)

10^{-4} ohm	4 Reichsanstalt (commercial) Standard Resistors
10^{-3}	4 Reichsanstalt (commercial) Standard Resistors
10^{-2}	4 Reichsanstalt (commercial) Standard Resistors
10^{-1}	4 Reichsanstalt (commercial) Standard Resistors
10^{0}	5 Thomas (NBS) One-ohm Standard Resistors (The Primary Group)
10^{0}	15 Thomas (commercial and NBS) One-ohm Standard Resistors (MAP)
10^{1}	4 Rosa (commercial) Standard Resistors
10^{2}	2 Special, high-stability (commercial) Standard Resistors
10^{2}	2 Special, high-stability (commercial) Standard Resistors (MAP)
10^{3}	2 Special, high-stability (commercial) Standard Resistors
10^{4}	2 Special, high-stability (commercial) Standard Resistors (MAP)
10^{4}	4 Special, high-stability (commercial) Standard Resistors
10^{5}	4 Special, high-stability (commercial) Standard Resistors
10^{6}	4 Rosa (commercial) Standard Resistors
	4 Rosa (commercial) Standard Resistors
	2 Wirewound (commercial) Standard Resistors
10^{7}	2 Film (commercial) Standard Resistors
	2 Series/parallel (NBS) Resistance Boxes
10^{8}	2 Wirewound (commercial) Standard Resistors
	2 Film (commercial) Standard Resistors
	2 Series/parallel (NBS) Resistance Boxes
10^{9}	2 Film (commercial) Standard Resistors
	1 Series/parallel (NBS) Resistance Boxes
10^{10}	1 Series/parallel (NBS) Resistance Box
10^{11}	1 Series/parallel (NBS) Resistance Box
	Scott (NBS) Capacitive Discharge Apparatus
10^{12}	Scott (NBS) Capacitive Discharge Apparatus
10^{13}	Scott (NBS) Capacitive Discharge Apparatus
10^{14}	Scott (NBS) Capacitive Discharge Apparatus
10^{15}	Scott (NBS) Capacitive Discharge Apparatus

Primary Standards for Resistance at High Currents

10^{-5} ohm	1 Wolfe (commercial) High Current Standard
	1 Reichsanstalt (commercial) High Current Standard
10^{-4}	1 Wolfe (commercial) High Current Standard
	1 Reichsanstalt (commercial) High Current Standard
10^{-3}	1 Wolfe (commercial) High Current Standard
	1 Reichsanstalt (commercial) High Current Standard
10^{-2}	3 Reichsanstalt (commercial) High Current Standards
10^{-1}	3 Reichsanstalt (commercial) High Current Standards
10^{0}	2 Reichsanstalt (commercial) High Current Standards
	1 Thomas (NBS) Standard Resistor

All except Primary Low Current Standards are also Working Standards

Sec. 2. PRECISION APPARATUS

Primary Standards

Primary Low Current Resistance Standards (Sec. 1)
2 NBS-specified (commercial) Universal Ratio Sets
1 Dunfee-Dziuba (NBS) Primary Volt Ratio Standard
Two-stage (NBS) Inductive Voltage Divider
One-stage (commercial) Inductive Voltage Divider

Working Standards

2 NBS-specified (commercial) Universal Ratio Sets (same as above)
1 Dunfee-Dziuba (NBS) Primary Volt Ratio Standard (same as above)
2 Dziuba (NBS) Portable Volt Ratio Standards
1 Wheatstone (commercial) Bridge
1 Direct Reading Ratio Set (commercial)
1 Direct Reading Ratio Set (NBS)
12 Rosa (commercial) 100-k ohm Resistors
1 Two-stage (NBS) Inductive Voltage Divider (same as above)
1 One-stage (commercial) Inductive Voltage Divider (same as above)

Sec. 3. IMPEDANCE MEASUREMENTS

Primary Standards

1 Cutkosky (NBS) Valculable Capacitor
10 Cutkosky Fused-Silica Dielectric Capacitors (10 pF)
Primary Low Current Resistance Standards (See Sec. 1)

Working Standards for Measurements of Capacitance

1 Cutkosky (NBS) Fused-Silica 10-pF Capacitor
1 Type-12 (commercial) Capacitance Bridge
5 Nitrogen Dielectric (commercial) Standard Capacitors

Working Standard for Measurement of Inductance

1 Maxwell-Wein (NBS) Bridge

Sec. 4. VOLTAGE

Primary Standard

Denenstein-Finnegan (NBS) AC Josephson Effect Apparatus

Working Standards

2 Cutkosky (NBS) Standard Cell Enclosures
1 NBS Oil Bath (NBS 11)
8 (commercial) Standard Cell Enclosures (MAP)

Sec. 5. AC-DC TRANSFER STANDARDS

Primary Standards

12 NBS-specified (commercial) Single-junction Evanohm Thermoelements
2 NBS-specified (commercial) Multi-junction Evanohm Thermoelements

Working Standards

2 sets (NBS) Coaxial Voltage Converters
2 sets NBS-specified (commercial) Thermal Current Converters
1 (NBS) Wattmeter
1 Yokagawa (commercial) Wattmeter

Sec. 6. TRANSFORMERS

Voltage

Primary & Working Standards

Petersons (NBS) High Voltage Current Comparator Bridge

Current

Primary Standards

2 Souders (NBS) Two-stage Transformers

Working Standards

3 Compensated (NBS) Current Comparators

Sec. 7. HIGH VOLTAGE & ENERGY

DC Voltage Dividers

Primary Standards

Primary Resistance Standards (Sec. 1)
3 Park (NBS) High Voltage Dividers

Working Standards

3 Park NBS High Voltage Dividers (same as above)
10 Rosa (commercial) Standard Resistors

DC Kilovoltmeters

Primary Standards

Primary Resistance Standards (Sec. 1)
Primary Voltage Standards (Sec. 4)
3 Park (NBS) High Voltage Dividers

Working Standards

3 Park (NBS) High Voltage Dividers (same as above)
1 (commercial) Digital Voltmeter

AC Voltage Dividers

Primary & Working Standards

Petersons (NBS) High Voltage Current Comparator Bridge

AC Kilovoltmeters

Primary Standards

Primary Voltage Standards (Sec. 4)
Petersons (NBS) High Voltage Current Comparator Bridge

Working Standards

Petersons (NBS) High Voltage Current Comparator Bridge (same as above)
1 (commercial) Electrostatic Voltmeter

Sec. 7. HIGH VOLTAGE & ENERGY (Continued)

Capacitors (High Voltage)

Primary Standards

Primary Capacitance Standard (Sec. 3)
Hillhouse (NBS) High Voltage Capacitor

Working Standards

2 Nitrogen Dielectric (commercial) Standard Capacitors

Watthour Meters

Primary Standards

Primary Voltage Standards (Sec. 4)
Primary Resistance Standards (Sec. 1)
Primary Time Interval Standards

Working Standards

Lentner (NBS) Current Comparator Energy System
4 Rotating (commercial) Watthour Meters

Impulse Dividers

Primary Standards

Primary Resistance Standards (Sec. 1)
Primary Voltage Standard Resistive Divider (Sec. 4)

Working Standard

Kerr Cell Apparatus

APPENDIX C

"CRITICAL ELECTRICAL MEASUREMENT NEEDS AND STANDARDS FOR MODERN ELECTRONIC INSTRUMENTATION"

WORKSHOP REPORT ABSTRACT, PREFACE, AND LIST OF ATTENDEES

Abstract

Recognizing the proliferation of sophisticated modern electronic instrumentation in the field of electrical measurements, the Electricity Division of the National Bureau of Standards recently initiated a new program in the general area of dynamic measurements and standards in support of such instrumentation. Recognizing further that the vastness and complexity of the field would require, at the earliest stages of the program, identification of the most critical problem areas, the Electricity Division held a workshop on 23 and 24 September 1974, at the Bureau's Gaithersburg site, to assist it in ascertaining just what these areas in fact were. The basic idea of the Workshop was to bring together a broadly representative group of some 25 leading manufacturers and prime users, working in a free and open atmosphere, in order to have them delineate the present and future critical support needs in the field of dynamic electrical measurements for modern electronic instrumentation, with emphasis on physical standards, standardized measurement methods, new calibration and measurement assurance services, relevant data, and, most important, new measurement methodologies. The overall objectives of the Workshop were generally met, and a number of significant specific programs and projects consistent with the mission of the Electricity Division were identified. Three categories broadly cover the needs as defined at the Workshop:

1. The need to introduce time as a measurement parameter has resulted from the requirements of automatic test and control systems. Specific areas considered critical are:

a. Pulsed component measurements.
b. Dynamic performance characterization for modern signal conditioning and data conversion devices: Digital-to-analog and analog-to-digital converters, sample-and-hold amplifiers, comparators, etc. Required measurements include settling, aperture and acquisition times. Basic new capabilities will be needed, including precision, non-sinusoidal waveform generation and "standard" digital-to-analog converters.
c. Methodologies and techniques for characterizing precision ac and dc sources and measurement devices with respect to settling time.

2. The emergence of measurements into the "real world" or the production line via the automatic system has introduced a host of new parameters. Areas requiring significant effort include:

a. Investigation of transportable standards for validation of static and dynamic system performance: ac and dc voltage, impedance, pulses, settling times.
b. Techniques for characterizing sources and measurement devices with respect to switched or dynamic loading.
c. Prediction of long-term performance, reliability and lifetime from short-term evaluation for a host of passive components, semiconductors, and signal sources.
d. Noise standards and methodologies.
e. Continuing effort to improve transportable dc standards and dissemination at higher voltage levels.
f. Characterization of the ac line voltage-waveforms, under- and over-voltages, transients, dynamic impedance, etc.
g. Inclusion of a capability for environmental control and variation for devices and instruments under calibration, in all work undertaken by the Bureau.
h. Extension of Measurement Assurance Programs (MAP's), especially into the above new areas.

3. Recent work at the leading edge of measurement technology in electronics has resulted in the need for new, or higher accuracy, measurements. For example:

a. Increased dependence on capacitors as storage devices has made dielectric hysteresis a parameter of importance. Significant measurement work should be started in this area.
b. Phase difference measurements to extremely high accuracies are needed to calibrate industrial instrumentation.
c. Higher accuracy power measurements, particularly for non-sinusoidal waveforms, are needed to calibrate instrumentation in the field.

d. Non-sinusoidal, high crest-factor precision signals are needed to calibrate true RMS converters and meters.

e. High accuracy electronic instrumentation requires reduction in ac calibration uncertainties to 10 ppm, at least over the audio range.

Longer-term, "frontier" areas in each of the above groups were also identified. They are not specified in the above listings since they involve work at still more basic levels, on ground that is presently terra incognita. Nevertheless, they furnish insight into the overall technical/philosophic climate, and are useful for that reason. Items in this category include:

1. Measurement problems in systems, including effects of history, measurement interactions, self-calibration, etc.
2. Evaluation and standardization of system software.
3. Calibration of medical equipment.
4. Replacement of standard cells.
5. Replacement of thermal ac/dc converters.
6. Non-swept but broad-response measurements - impulse, noise, other.
7. Basic work on the physics of dielectric absorption; component drift; device noise; failure mechanisms; switches; and relays.
8. Provision of improved measurement accuracy for virtually all dynamic measurements, at the wafer probe level.

In addition to the identification of these specific and general needs, the Workshop provided strong evidence that both the manufacturing and user communities in the electronic instrumentation field look to the Electricity Division to provide the technological leadership in these newer areas that it has previously furnished in the more traditional electrical measurement areas. Indeed, there was a good deal of support for the idea of keeping the electronics community informed of Division work-in-progress, with emphasis on projects targeted by the Workshop.

Keywords: Data conversion; dynamic measurements; electrical measurements; electronic instrumentation; signal conditioning; system; time domain.

Preface

It is apparent that the continued, orderly growth of the electronics industry is increasingly hampered by a lack of standards and methodologies in a number of crucially important electrical measurement areas.

The explosive growth of electronics during the last decade has brought with it a host of unsolved measurement problems. Yet at this critical historical juncture, electronics is a key technology in the prospective solutions to some of society's major outstanding concerns including energy, pollution, and productivity, to name but three. It is, therefore, mandatory that a responsible, capable organization without specific industrial affiliation, assume a leadership role in providing the necessary measurement standards and methodologies, as well as in establishing new electrical measurement programs for which need is both broad and identified, but whose implementation by specific industrial organizations would be impractical.

The Electricity Division of the National Bureau of Standards has traditionally dealt with the measurement and generation of electrical signals in the dc to 30 kHz range, as well as with the properties of electrical components in that range. In effect, with the one possible minor (philosophical) exception of phase, the Division has devoted itself to amplitude or magnitude measurements for the various electrical parameters. Some of these have been generated and/or transmuted by mechanical and electro-mechanical means, others more recently by electronic, and others in future undoubtedly by light, but the electrical (usually amplitude) parameters have had similar properties and required the same disciplines for measurement.

Now, automatic systems for test, process control, medical applications, and so forth are using electrical quantities at higher speeds than heretofore. Ten years ago a precision dc, dialable 6- or 7-digit source did not need a settling time specification; today, "programmable" sources have such specifications, since the system architect must know how long it will take for this stimulus to settle to within a given accuracy. In many instances total system speed, hence all-important throughput, dollar payback and/or justification, will be limited by such settling times.

Thus, to precision electrical measurements has been added the temporal parameter. In a manner analogous to the changeover from frequency to time domain work in filter synthesis in the early sixties, measurement must now turn from exclusive attention in the

frequency domain, to characterization involving time as well, e.g., settling time to x microvolts in y microseconds is an electrical, analog, amplitude measurement with the time factor added.

The Workshop which this report describes and summarizes, is the means chosen by the Electricity Division to establish direct communication with key elements of the electronics industry among both manufacturers and users, for the purpose of ascertaining the industry's electrical measurement needs, both general and specific. The enthusiasm engendered by the Workshop itself attests to the fact that the time has come for leadership and action: In spite of difficult times and severe cost pressures, 24 outstanding organizations were willing to send top personnel to the 2-day Workshop, disrupting busy schedules, and at considerable financial expense.

This report on the Workshop results must inevitably reflect some of the author's technical biases, developed over the course of 25 years of varied design, management and consulting experience in the fields of electronics, measurements and standards. During that interval the technology has made tremendous advances, so that in many areas it is virtually unrecognizable in comparison with its major jumping-off point directly following the Second World War. Indeed, some of those advances are the direct result of work accomplished at or backed up by programs of the Electricity Division of the NBS, notably during what might be termed the measurement "explosion" of the decade of the sixties.

By the same token, it is hoped that the author's general breadth of design and measurement exposure during those same years of experience, plus long-standing and continuing interactions with the Bureau, have provided a balanced view of the Workshop results in this report. If this has been accomplished, the Division programs resulting from the Workshop can form the basis for new and crucially-important electrical measurement technology for electronics in the forthcoming decade.

It is impossible to convey here the excitement felt by virtually all participants during the Workshop which helped to make the author's task as moderator both rewarding and enjoyable. The excitement was undoubtedly due in part to the professional challenge offered by the opportunity for open, free-swinging exchange among the outstanding group of participating engineers and scientists. But it clearly reflected, as well, the participants' recognition of the large and important work that so critically needs to be done, and their enthusiastic reception of the role of the Electricity Division in grasping the initiative to establish relevant new programs on a priority basis. There was, in short, the excitement resulting from the pervasive feeling of being part of an undertaking that was both significant and effective.

I should like to express my thanks to the Electricity Division and to Dr. Barry N. Taylor in particular, for giving me the opportunity to contribute to this important work. I should also like to add my own personal thanks to the participants and their organizations, as it is they who are truly responsible for the Workshop's success.

Peter Richman
Consulting Engineer

WORKSHOP ATTENDEES

Mr. Loyle E. Baltz
Principal Test Engineer
Ford Motor Company
Allen Park, MI

Mr. Eduard F. Boeckmann
Chief Engineer
Angstrohm Precision, Inc.
Hagerstown, MD

Mr. Warren C. Collier
Manager, TM 500 Design, Engineering
Tektronix, Inc.
Beaverton, OR

Mr. Thomas J. Coughlin
Product Engineering Manager
Component Systems
General Radio Company
Concord, MA

Mr. Jack D. Dougherty
Chief, DC & Low Frequency Standards
Laboratory
Newark Air Force Station, OH

Mr. George W. Herron
Senior Engineer
Keithley Instruments, Inc.
Cleveland, OH

Mr. Donald E. Lawrence
Project Manager
Hewlett-Packard Company
Sunnyvale, CA

Mr. David R. Ludwig
Vice President
Advanced Development and Planning
Teledyne Philbrick
Dedham, MA

Mr. Edward P. Mueller
Biomedical Engineer
Food and Drug Administration
Rockville, MD

Mr. William A. Plice
Senior Project Staff Engineer
Honeywell, Inc.
St. Louis Park, MN

Mr. Robert C. Raybold
Head, Institute for Basic Standards
Automation Group
National Bureau of Standards
Washington, DC

Mr. Bruce A. Renz
Head, Systems Measurement Section
American Electric Power Service Corp.
New York, NY

Mr. David B. Schneider
Calibration Product Specialist, ATE
John Fluke Manufacturing Co., Inc.
Seattle, WA

Mr. Frederick B. Seeley
Chief, Electromagnetics Engineering Branch
U. S. Army Metrology and Calibration Center
Redstone Arsenal, AL

Mr. Robert M. Shaw
Fellow Engineer
Westinghouse Electric Corporation
Baltimore, MD

Mr. Lewis R. Smith
Engineering Manager
Analog Devices, Inc.
Norwood, MA

Mr. Douglas C. Strain
President
Electro Scientific Industries, Inc.
Portland, OR

Mr. Robert P. Talambiras
Corporate Director of Advanced Development
Analogic Corporation
Elmwood Park, NJ

Mr. David S. Terrett
General Manager, Research & Development
ADT Security Systems
New York, NY

Mr. James C. Tripp
Engineering Supervisor
Linear Test Development Group
National Semiconductor Corporation
Santa Clara, CA

Mr. Robert H. Verity
Manager, Standards Laboratory
Leeds & Northrup Corporation
North Wales, PA

Mr. William R. Walters
Chief Engineer
Codi Semiconductors
Fairlawn, NJ

Mr. F. Mansfield Young
Director of Engineering
Teradyne, Inc.
Boston, MA

Mr. Ray A. Zuck
Director of Operations
Geometric Data Corporation
Wayne, PA

APPENDIX D

STANDARDS AND CALIBRATION LABORATORIES

CODE: Type of Service
- S - Primary standards
- C - Calibrations
- B - Both
- T - Testing

Type of Organization:
- C - Corporate laboratory
- I - Instrument manufacturing
- P - Calibration & metrology lab solely or mostly

No code indicates exact nature of service not known to authors.

Laboratory	Member NCSL	Type of Service Code	Type of Organization Code
AEL, Colmar, PA			
AEL Communications, Lansdale, PA		B	C
AIL Technological, City of Industry, CA		B	P
AVCO Corporation, Charleston, SC	X	B	C
AVCO Corporation, Lycoming Div., Stratford, CT		C	C
AVCO Corporation, Richmond, IN		S	C
Aerojet Nuclear, Idaho Falls, ID	X	B	C
Ailtech Cutler Hammer Co., Farmingdale, NY		C	C
Airtron Div., Litton Systems, Morris Plains, NY		C	C
All Systems, Morristown, NJ			
Allis Chalmers Mfg. Co., Milwaukee, WI	X	B	C
American Electronic Labs, Lansdale, PA		B	P
American Geophysical & Instrumentation, Gardena, CA		B	P
American Instrument Service, Philadelphia, PA		B	P
Ark Electronics, Willow Grove, PA		C	P
B&K Instruments, Cleveland, OH		C	P
BLH Electronics, Waltham, MA		?	?
Ballantine Laboratories, Boonton, NJ		C	I
Ball Brothers Research, Boulder, CO	X	B	C
Bath Iron Works Corporation, Bath, ME	X	C	C
Beckman Instruments, Fullerton, CA	X	B	C
Beech Aircraft Corporation, Wichita, KS	X	B	C
Bell Aerospace Co., Buffalo, NY	X	B	C
Bendix Corporation, Teterboro, NJ	X	S	C
James G. Biddle Co., Plymouth Meeting, PA	X	B	I
Blake Electronics, Inc., Greendale, WI		C	
Boeing, Wichita, KS		C	C
Boeing Aerospace Group, Seattle, WA	X	B	C
Brunswick Engineering, Inc., Northbrook, IL		C	
Burroughs Corporation, Paoli, PA		B	C
Calibration Central, Alexandria, VA	C	C	
Certified Calibration Labs, Inc., Philadelphia, PA	S	C	P
Collins Radio Co., Cedar Rapids, IA	X	B	C
Communications Satellite Corp., Clarksburg, MD	X	B	C
Computer Diode Co., Fairlawn, NJ	X	B	I

Sources: A Directory of Standards Laboratories, 1974 Edition, National Council of Standards Laboratories, Washington, DC, 1974.
Electronics '75 Buyers' Guide, McGraw-Hill, New York, NY, 1975.
eem 75/76, electronic engineers master catalog, United Technical Publications, Garden City, NY, 1975.
Electronic Design's Gold Book, Hayden Publishing Company, Rochelle Park, NJ, 1975.

Laboratory	Member NCSL	Type of Service Code	Type of Organization Code
Comtel Corporation, Detroit, MI		C	
Cox & Co., New York, NY	X	B	C
DBA Systems, Melbourne, FL		C	
Dalmo Victor, Belmont, CA	X	B	C
Davidson Optronics, West Covina, CA		C	P
Dayton T. Brown, Inc., Bohemia, NY	X	B	P
Detroit Edison Co., Detroit, MI	X	B	C
Dillon, W. C. & Co., Van Nuys, CA			
Douglas Instrument Lab, Boston, MA		B	P
Dow Chemical Co., Rocky Flats, CO	X	C	C
EG&G, Albuquerque, NM		C	C
EG&G, Las Vegas, NV	X	C	C
E. I. DuPont de Nemours, Aiken, SC	X	B	C
EIL Instruments, Timonium, MD	X	B	P
Electrical Instrument Service, Mt. Vernon, NY	X	B	P
Electrical Science Services, Cambridge, MA		C	
Electrical Testing Labs, Inc., New York, NY	X	B,T	P
Electro Scientific Industries, Portland, OR	X	B	I
Electronic Marketing Associates, Kensington, MD		C	
Eppley Laboratories, Newport, RI		B	I
E-Systems, Dallas, TX	X	B	C
Fairchild Space & Electronics, Germantown, MD		C	C
Fischer/Porter Co., Warminister, PA		C	
John Fluke Mfg. Co., Seattle, WA	X	B	I
Foxboro Co., Foxboro, MA	X	B	C
Gage Corp., Philadelphia, PA	X	C	P
General Dynamics, Groton, CT	X	B	C
General Dynamics, Quincy, MA		C	C
General Dynamics, San Diego, CA	X	B	C
General Electric, Bay St. Louis, MS	X	B	C
General Electric, Dallas, TX		C	C
General Electric, Pittsfield, MA	X	B	C
General Electric, Schenectady, NY	X	B	C
General Electric, Seattle, WA		C	C
General Electric, Syracuse, NY	X	B	C
General Electric Instrumentation, Inglewood, CA		S	C
General Environments Corp., Morton Grove, IL	C	P	
GENRAD, West Concord, MA	X	B	I
Greentron, Inc., Greenville, SC		C	P
Guildline Instruments, Inc., Larchmont, NY	X	S	I
H-B Instrument Co., Philadelphia, PA		C	I
Hamilton Technology, Lancaster, PA		C	C
Harris Intertype, Melbourne, FL	X	B	C
Hercules Inc., Magna, UT	X	C	C
Hewlett-Packard Co., Palo Alto, CA		C	I
Hewlett-Packard, Santa Clara, CA		B	I
Hoffman Engineering Corp., Old Greenwich, CT		C	
Honeywell, Inc., Aerospace Div., St. Petersburg, FL	X	C	P
Honeywell, Inc., Annapolis, MD		C	P
Honeywell, Inc., Burlington, MA		C	P
Honeywell, Inc., Chicago, IL		C	P
Honeywell, Inc., Cleveland, OH		C	P
Honeywell, Inc., Denver, CO	X	B	P
Honeywell, Inc., Detroit, MI		C	P
Honeywell, Inc., Downey, CA		C	P
Honeywell, Inc., Hazelwood, MO		C	P
Honeywell, Inc., Fairborn, OH		C	P
Honeywell, Inc., King of Prussia, PA		C	P
Honeywell, Inc., Minneapolis, MI		B	C

Laboratory	Member NCSL	Type of Service Code	Type of Organization Code
Honeywell, Inc., San Diego, CA		C	C
Honeywell, Inc., Springfield, VA		C	P
Honeywell, Inc., Sunnyvale, CA		C	P
Honeywell, Inc., Westfield, NJ		C	P
Hy-Cal Engineering, Sante Fe Springs, CA		S	P
Hughes Aircraft, Culver City, CA		B	C
Hughes Aircraft, Fullerton, CA		C	C
IIT Research Institute, Chicago, IL	X	B	P
Incal Service Corp., Stanford, CT		C	P
Infinite, Inc., Cape Canaveral, FL		C	P
Inland Testing Labs, Inc., Morton Grove, IL	X	S	P
Instrument Labs Corp., Chicago, IL		C	P
Intergalactic Corporation, Salt Lake City, UT		C	
Julie Research Labs, New York, NY		B	I
KC Calibration Lab, Kansas City, KS		C	
Kahl Scientific Instr. Corp., El Cajon, CA		S	P
Keithley Instruments, Cleveland, OH		B	I
Key Instruments, Gardena, CA		C	P
LTI Research Foundation, Lowell, MA	X	B	P
Lab Instrument Service, Campbell, CA		C	
Lear Siegler, Santa Monica, CA		C	C
Leeds & Northrup, North Wales, PA	X	B	I
Lehighton Electronics, Lehighton, PA		C	
Librascope, Div. of Litton, Glendale, CA		C	C
Lockheed Aircraft Service, Ontario, CA		C	C
Lockheed-California, Burbank, CA	X	B	C
Lockheed Electronics, Houston, TX	X	B	C
Lockheed-Georgia, Marietta, GA		B	C
Lockheed Missiles & Space Co., Sunnyvale, CA	X	B	C
3M Corp., St. Paul, MN	X	B	C
Main Electronics, Wichita, KS		C	P
Mancib Co., Burlington, MA		C	P
Martin Marietta, Denver, CO	X	B	C
Martin Marietta, Marietta, GA	X	B	C
McDonnell Aircraft Co., St. Louis, MO	X	B	C
McDonnell Douglas Astronautics, Long Beach, CA	X	B	C
McDonnell Douglas Astronautics, West Huntington Beach, CA	X	B	C
Micro-Radian Instruments, Seal Beach, CA		C	P
JR Miles Corporation, Elk Grove Village, IL		C	
Montedoro-Whitney, San Luis Obispo, CA		B	P
National Astro Labs, Burbank, CA		B	P
National Camera, Inc., Englewood, CO		C	
New Era Products, Cleveland, OH		C	P
Newport News Ship Building & Drydock, Newport News, VA		C	C
New York Testing Labs, Westbury, NY		C	P
North American Rockwell, Anaheim, CA	X	B	C
North American Rockwell, Rocketdyne Div., McGregor, TX		B	C
Nucleus Corp., Madison Heights, MI		C	P
Ogden Technology Labs, Fullerton, CA		B	P
Optronic Labs, Silver Spring, MD		C	
Ormond Inc., Sante Fe Springs, CA		C	P
PTS Electronics, Inc., Bloomington, IN		C	
Penn Airborne Products, Southampton, PA		B	I
Pioneer/Instrumentation, Cleveland, OH		B	P
QVS Inc., East Orange, NJ		C	
RCA, Gov't Services, Moorestown, NJ		B	C
RCA International Service Corp., Camden, NJ		B	C
RCA International Service Corp., Patrick AFB, FL	X	B	C

Laboratory	Member NCSL	Type of Service Code	Type of Organization Code
Ram Meter, Inc., Ferndale, MI		C	P
Ramsey Engineering, Anaheim, CA		C	P
Raytheon Submarine Signal, Portsmouth, RI	X	B	C
Reliance Electric Co., Cleveland, OH		C	P
Robertshaw Controls Co., Richmond, VA		C	
Rockwell Engineering Co., Indianapolis, IN		C	P
Rutherford Research Products, Rutherford, NJ		C	P
SSCO Standards Laboratory, Detroit, MI		B	P
Sanders Associates, Nashua, NH	X	B	C
Scientific Leasing Services, Lake Success, NY		C	
Sensitive Research Instruments, Mt. Vernon, NY		C	P
Simpson Electric Co., Elgin, IL		C	
Singer Co., Kearfott Div., Little Falls, ND	X	B	C
Sperry Electronic Tube Div., Gainesville, FL		B	C
Stabro Labs, Salt Lake City, UT		B	P
States Electronic Corp., Blundworth Marine, Linden, NJ		C	C
Sunshine Scientific Instruments, Inc., Philadelphia, PA		B	P
Sweetman Calibration Services, Pennsauken, NJ	X	B	P
Systron Donner, Concord, CA	X	S	C
TRW Systems, Redondo Beach, CA	X	B	C
Taylor Instrument, Process Control Div., Rochester, NY		B	C
Technicians Unlimited, Lexington, MA		C	
Teledyne Brown Engineering, Huntsville, AL		C	C
Teledyne McCormick Selph, Hollister, CA		C	C
Teledyne Systems Co., Northridge, CA	X	B	C
Texas Instruments, Houston, TX		C	P
Thwing-Albert Instrument, Philadelphia, PA		C	P
Transducers, Whittier, CA		C	
UNIVAC, Utica, NY	X	S	C
Union Carbide, Oak Ridge, TN	X	B	C
Varian, Palo Alto, CA	X	S	I
Viking Labs, Sunnyvale, CA		B	C
Westinghouse Electric Co., Baltimore, MD	X	B	C
Westinghouse Electric Co., Pittsburgh, PA	X	B	C
Weston Instruments, Newark, NJ	X	B	I

This listing of calibration and standards laboratories is not to be taken as an endorsement by the National Bureau of Standards of laboratories included, or as an indication of the quality of calibrations available from either listed or unlisted organizations.

APPENDIX E

TYPICAL MEASUREMENT SUPPORT STRUCTURES

On the following pages are representative functional diagrams of two corporations and their measurement support structures. On the following page is depicted the structure by which the U.S. Air Force, through a network of over 140 calibration facilities, provides world wide measurement support for over $400 million worth of electronic test equipment with which maintenance and operational support for weapons, communications, navigation, guidance and medical systems are supplied.

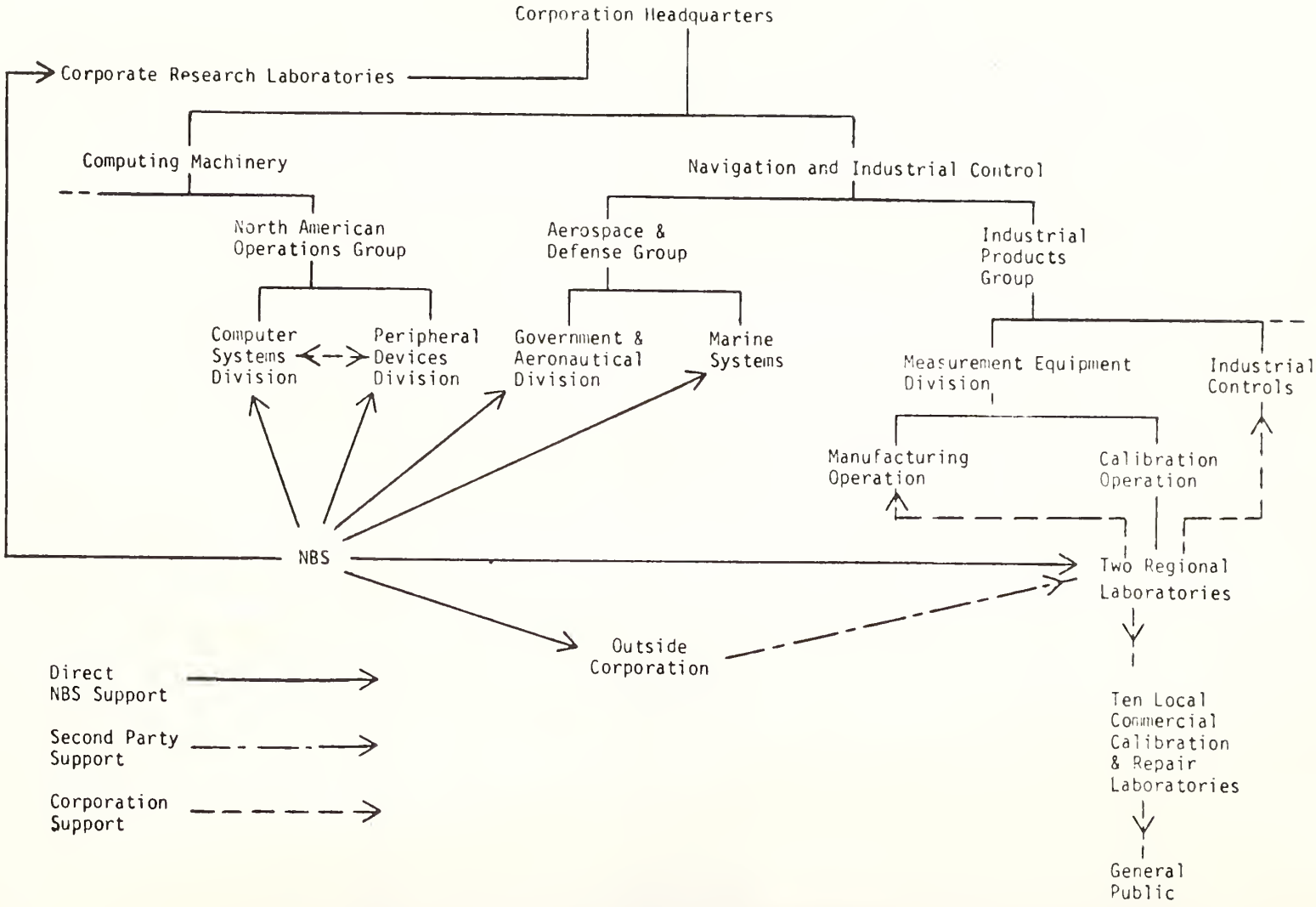

Typical Corporate
Measurement Support Structure

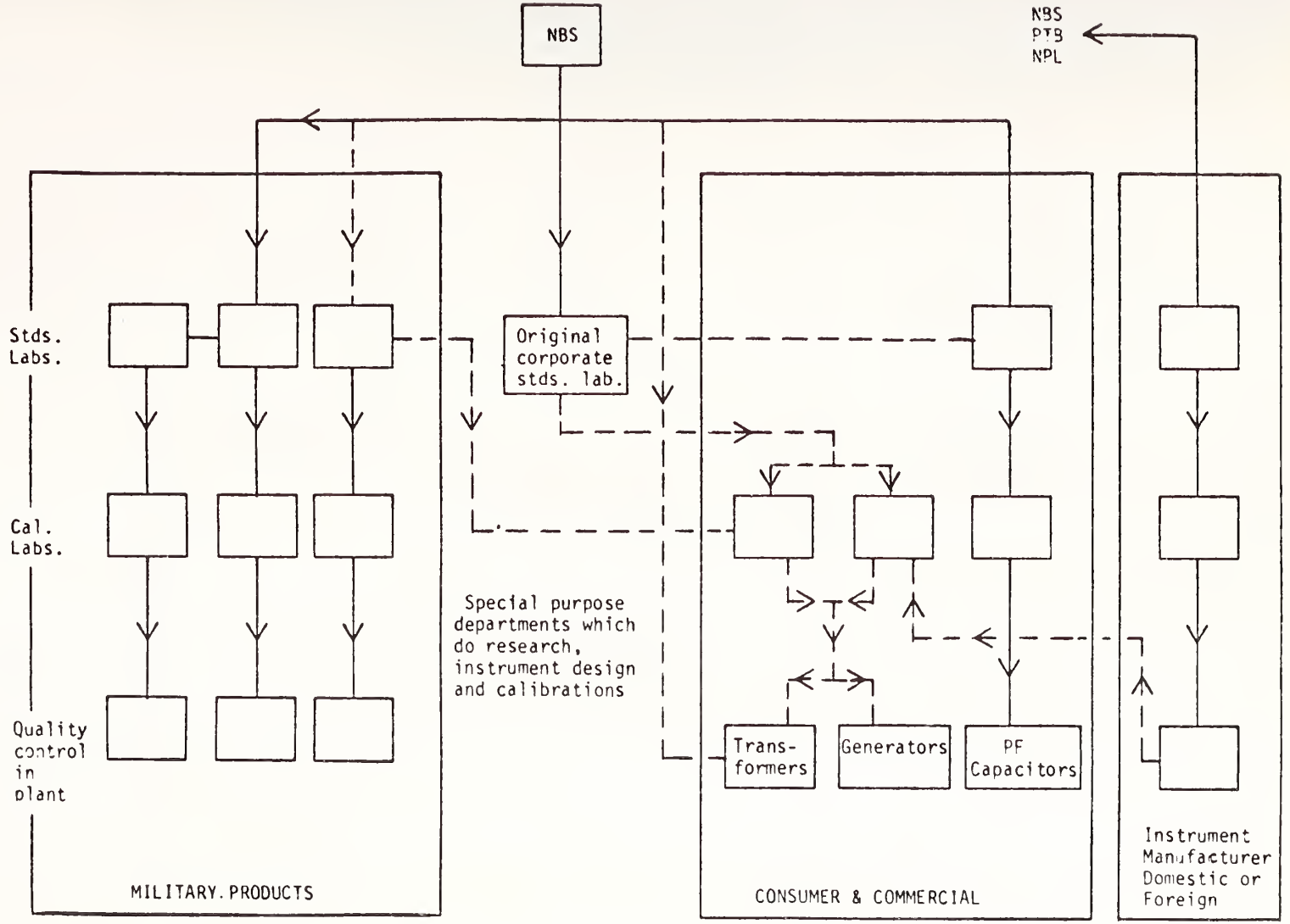

Strong ties _____
Weak ties - - - - - - -

Typical Corporate
Measurement Support Structure

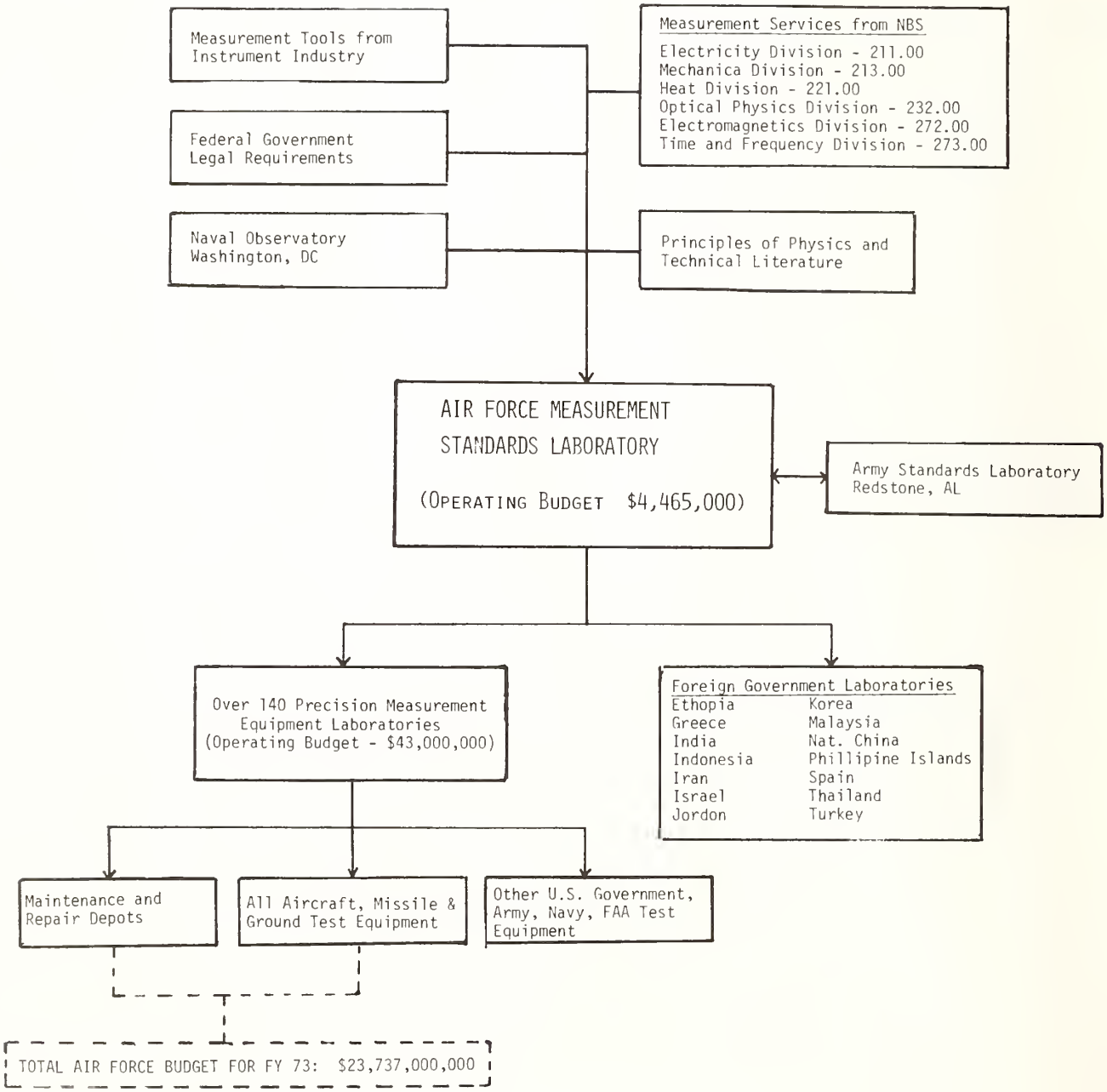

Air Force Metrology Structure - FY 73

REFERENCES

[1] The International System of Units (SI), Nat. Bur. Stand. (U.S.), Spec. Publ. 330, 49 pages (1972).

[2] Thomas, J. A., Peterson, C., Cooter, I. E., and Kotter, F. R., An Absolute Measurement of Resistance by the Wenner Method, J. Res. NBS (U.S.), 43, No. 4 (1949) RP2025.

[3] Cutkosky, R. D., New NMS Measurements of the Absolute Farad and Ohm, IEEE Trans. Instrum. Meas. IM-23, No. 4, 305-309 (Dec. 1974).

[4] Cutkosky, R. D. and Lee, L. H., Improved Ten-picofarad Fused-silica Dielectric Capacitor, J. Res. NBS (U.S.), 69C (Engr. & Instr.), No. 3, 173-179 (July-Sept. 1965).

[5] Field, B. F., Finnegan, T. F., and Toots, J., Volt Maintenance at NBS via 2e/h: A New Definition of the NBS Volt, Metrologia 9, No. 4, 155-156 (1973).

[6] American National Standards Institute 1976 Catalog (Am. Nat. Stand. Inst., NY, 1974).

[7] Harvey, G. F., editor, Standard and Practices for Instrumentation - Fourth Edition (Instr. Soc. Amer., Pittsburgh, PA 1974).

[8] Electronic Engineers Master (United Technical Publications, Garden City, NY, 1974).

[9] U.S. Industrial 1975 Outlook with projections to 1980, Department of Commerce, 432 pages (1975).

[10] U.S. Industrial 1976 Outlook with projections to 1985, Department of Commerce, 465 pages (1976).

[11] Evenson, K. M., Wells, J. S., Peterson, F. R., Danielson, B. L., Day, G. W., Barger, R. L., and Hall, J. L., Speed of Light from Direct Frequency and Wavelength Measurements of the Methane-Stabilized Laser, Phys. Rev. Lett. 29, 1346 (1972).

[12] Cohen, E. R. and Taylor, B. N., The 1973 Least-squares Adjustment of the Fundamental Constants, Journal of Physical and Chemical Reference Data, 2, No. 4, 663 (1973).

[13] Richman, P., editor, Critical Electrical Measurement Needs and Standards for Modern Electronic Instrumentation, Nat. Bur. Stand. (U.S.), Tech. Note 865, 74 pages (May 1975).

[14] A Directory of Standards Laboratories - 1975 Edition (National Conference of Standards Laboratories, Washington, 1975).

[15] Use of off-the-shelf electronic test equipment to reduce costs, shorten leadtimes, assure reliability, and simplify logistics, Report of the Task Force on Science Board, Department of Defense, Washington (Feb. 1976).

[16] Minutes of Automatic Test Equipment Conference and Workshop (April 1976) by Industry Ad Hoc Automatic Test Equipment Project for the Navy, National Project for the Navy, National Security Industrial Assn., Washington, DC, to be published late 1976.

[17] Technical Manual - Calibration Technical Orders, Responsibilities and Calibration Measurement Areas, TO 33K-1-100, U.S. Air Force (March 1972).

[18] 1975 Annual Statistical Report, Electrical World 183, No. 6, 44-75 (March 1975).

[19] A Summary of Program Emphasis for 1976, Electric Power Research Institute, Palo Alto, CA (1976).

[20] U.S. Industrial Outlook 1974 with projections to 1980, Department of Commerce, 385 pages (1974).

[21] U.S. Markets Forecast 1977, Electronics, Vol. 50, No. 1, p. 90 (Jan. 6, 1977).

[22] Houghton, S., Transfer of the Kilowatthour, IEEE Trans. on Power Apparatus and Systems, Vol. P94, No. 4, 1232 (Jul./Aug. 1975).

[23] A National Plan for Energy Research, Development and Demonstration: Creating Energy Choices for the Future, ERDA 48, Vol. 2, Energy Research and Development Agency (June 1975).

[24] IEEE Power Engineering Society Proceedings of Conference on Research for the Power Industry, IEEE, NY (1973).

[25] Underground Power Transmission, Electric Research Council, NY (1971).

[26] Electric Utilities Industry Research and Development Goals through the Year 2000, Electric Research Council, NY (1971).

[27] EPRI Transmission and Distribution Division Report, EPRI Journal, Vol. 3, 28 (April 1976).

[28] EPRI Transmission and Distribution Division Report, EPRI Journal, Vol. 1, 40 (February 1976).

[29] EPRI Transmission and Distribution Division Report, EPRI Journal, Vol. 2, 34 (March 1976).

[30] Allen, R., Instrumentation: smaller and smarter, IEEE Spectrum, Vol. 13, No. 1, 68 (Jan 1976).

[31] Eicke, W.G., Jr., and Auxier, L. M., Regional Maintenance of the Volt Using NBS Volt Transfer Techniques, IEEE Trans. Instrum. Meas., IM-23, No. 4, 290-294 (Dec. 1974).

BIBLIOGRAPHY

1. Cochran, R. D., *Measures for Progress,* Nat. Bur. Stand.(U.S.) Misc. Publ. 275, 703 pages (1966).

2. Coombs, C. F. Jr., Editor, *Basic Electronic Instrument Handbook* (McGraw-Hill, New York, NY, 1972).

3. Department of Commerce, Current Industrial Reports: Selected Instruments and Related Products (U.S. Department of Commerce, Washington, DC, 28 pages, 1973).

4. Driscoll, R. L., Measurement of Current with a Pellat-type Electrodynamometer, J. Res. NBS (U.S.), 60, No. 4, 287-296 (April 1958).

5. Driscoll, R. L. and Cutkosky, R. D., Measurement of Current with the National Bureau of Standards Current Balance, J. Res. NBS (U.S.), 60, No. 4, 297-305 (April 1958).

6. Dun and Bradstreet, *Million Dollar Directory, 1974,* (New York, NY, 1974).

7. Harris, F. K., *Electrical Measurements* (John Wiley & Sons, New York, NY, 784 pages, 1952).

8. Hermach, F. L. and Dziuba, R. F., Editors, *Precision Measurement and Calibration - Electricity - Low Frequency,* NBS (U.S.) Spec. Publ. 300, Vol. 3, 489 pages (Dec. 1968).

9. Lerner, W., *Statistical Abstract of the U.S. - 1975,* (Department of Commerce, Washington, DC, 1028 pages, 1974).

10. Office of Management and Budget (U.S.), *Standard Industrial Classification Manual, 1972* (U.S. Government Printing Office, 150 pages, 1972).

11. Olsen, P. T. and Williams, W. E., A More Accurate Determination of γ'_p Through Improved Techniques, IEEE Trans. Instrum. Meas., IM-23, No. 4, 302-305 (Dec. 1974).

12. Perry, John, *The Story of Standards,* (Funk & Wagnells, New York, NY, 271 pages, 1955).

13. Terman, F. E. and Pettit, J. M., *Electronic Measurements, 2nd Edition* (McGraw-Hill, New York, NY 707 pages, 1952).

INSTRUMENT SOCIETY of AMERICA

22nd Annual ISA Conference and Exhibit • September 11-14, 1967, Chicago, Illinois

Preprint Number MS-1-MESTIND-67

LOW-FREQUENCY ELECTRICAL CALIBRATIONS AT THE NATIONAL BUREAU OF STANDARDS

F. L. Hermach - Senior Member
Chief, Electrical Instruments Section
National Bureau of Standards
Washington, D. C.

ABSTRACT

Charts are presented to show the present range and accuracy of NBS calibrations of standards of resistance, capacitance, inductance, voltage, and current, from direct current through 50 kHz. The chains of measurements by which these and other calibrations are related to the basic NBS standards of voltage and resistance are also shown.

INTRODUCTION

There are many electric and magnetic quantities to be measured, such as resistance, voltage and flux density. Measurements of most of them are made over many decades of both magnitude and frequency, with an amazing variety of standards and instruments. Thus it is certainly impractical to offer a calibration service at NBS to cover all of these variables. NBS concentrates instead on the calibration* of a few types of standards of the highest stability and accuracy. Because of this stability, the scientist or engineer can then verify the accuracy of his measurements with only infrequent periodic calibrations of these standards.

This paper briefly describes these calibration services and the NBS electrical standards on which they are based. It is a revision of an earlier paper[1], with charts which now show the accuracies normally available in calibrations, at established fees, of commercial standards of the highest grade[2]. (This information was not given in the earlier paper.) These charts also show the best accuracies attainable at present in the calibration of "ideal" standards, by special tests with the NBS research equipment. This equipment is generally not available for normal calibration services.

NBS STANDARDS

Figure 1 shows the major electrical standards which are used by NBS in the calibration program. The lines indicate the major relationships between them. For clarity, some minor relationships and the kinds of calibrations performed are now shown.

The internationally-accepted prototype standards of mass, length, and time are given in the top row of the figure. The meter is now defined as a certain number of wave lengths of the orange-red line of Krypton 86 and the meter bar is a reference, rather than a prototype, standard[3]. The atomic second is now defined in terms of a specified transition of Cesium 133, and stable oscillators serve as working standards of frequency (Hz)[4]. The kilogram is still defined as the mass of the prototype Pt-Ir standard.

Two experiments are performed at NBS to determine the basic electrical units in terms of these three standards and two measured constants, the speed of light in vacuo (c) and the acceleration of gravity (g). They are simple in principle but extremely difficult and involved in practice because of the accuracy required. One experiment consists in constructing a capacitor from gage bars and computing its capacitance in electromagnetic units (about 1 pF) from the length of the bars and the speed of light. With suitable bridges the step up is made at 1592 Hz to two 10,000-pF capacitors (X_C = 10,000 Ω), across to two 10,000-Ω resistors of known ac-dc difference, and down to 1-Ω resistors[5]. The final step is taken because 1-Ω Thomas-type resistors are still the most stable impedance standards known. The average resistance of a group of such resistors serves to maintain the ohm at NBS between such absolute determinations.

The other experiment consists in "weighing the ampere" with a current balance, and is thus based directly on the defintion of the ampere in terms of the force between current-carrying conductors[6]. One conductor (coil) is suspended from one arm of a balance, and the change in force when its current is reversed is measured in terms of the acceleration of gravity on a known mass. The voltage drop in a 1-Ω standard resistor carrying this measured direct current is then used to determine the emf of a group of saturated standard cells, which, in turn, maintain the volt at NBS.

Direct-reading ratio-sets were developed at NBS to calibrate resistors by the substitution method, and to step up and down on the resistance scale[7]. No line leads to them in Figure 1 because their accuracy depends on ratios of resistors, not on the unit of resistance. Standard cells are calibrated by connecting the known and unknown cells in opposition and measuring the small voltage difference with a low-range thermofree potentiometer. Potentiometers and volt boxes are calibrated with

*Calibration is used here as the process of making appropriate measurements to determine the correct value of a standard.

Superior numbers refer to similarly-numbered references at the end of this paper.

universal and direct-reading ratio-sets[7,8]. With these the user can then extend the d-c voltage scale very accurately.

AC-DC transfer instruments are comparators for determining the equality of a-c and d-c currents, a-c and d-c voltages, and a-c and d-c powers[9,10]. At NBS they serve chiefly to determine how well other ac-dc comparators do this. Since such comparators are very stable, the user can then make accurate a-c measurements based on his known d-c standards.

A-C bridges extend the scale of capacitance and inductance measurements, but NBS calibrates only the more stable capacitors and inductors, with which bridges can be checked. A-C voltage dividers or a-c potentiometric networks are used to determine the ratios (expressed as complex numbers) of the phasor voltages and currents of the NBS standard transformers and inductive voltage dividers, which, in turn, are used to calibrate other standards. In principle the ratios of these networks are also independent of units, but in practice some of the component impedors are measured with the d-c ratio sets and a-c bridges. Build-up or "boot-strap" techniques are used for the newer current comparators and audio frequency current transformers[11,12].

The standard watthour meters and standards for magnetic measurements depend on the other standards as shown in Figure 1[13,14].

ACCURACY CHARTS

The charts of figures 2 through 6 show the uncertainty (accuracy) in the calibrations of standards at NBS, as a function of the magnitude of the quantity being measured. Because of the wide ranges, logarithmic scales are used. In each figure the uncertainty is considered as the "limit of error" which should be exceeded only very rarely. It includes the calculated imprecision (at least three times the standard deviation of the average) plus the estimated limits of the systematic errors of the NBS working standards and the calibration process. It does not include the differences between the absolute units and the legal units maintained at NBS[5,6].

The solid lines and circles in each figure show the accuracies normally available in the calibration of commercially available standards of the highest grade, by established techniques, and for the fees given in the published NBS fee schedules. These accuracies include allowances for short-time variations in the standards under test under the controlled conditions at NBS, but not for possible larger variations in other environments nor for long-time drifts or other changes. The dotted lines and open circles show the best accuracies that might be attainable by special techniques, and, with repeated tests made with great care and effort in the calibration of "ideal standards" (which are perfectly stable and free from environmental influences).

Figure 2, for resistors, shows the familiar "accuracy triangle," with the peak at the value of the 1-ohm basic standard. Note that only decimal multiples and sub-multiples of 1 ohm are shown; NBS does not usually offer calibrations of other values nor does it maintain an accurate resistance-measuring facility as such. However, stable standards of any nominal value can be calibrated at greater cost and lesser accuracy than standards of neighboring values on the decimal scale. Thomas-type 1-ohm resistors are normally calibrated to 1 ppm in terms of the ohm maintained at NBS (i.e., the uncertainty is 1 ppm as shown by the solid circle indicating available accuracy at this point). High quality direct-reading and universal ratio sets (not shown in Figure 2) can be calibrated with an uncertainty not exceeding 1 ppm of input resistance. Using relatively simple equipment and established calibration procedures many users of these ratio devices could themselves perform these calibrations with comparable uncertainties*.

The chart for capacitance measurements, Figure 3, should be three-dimensional, with frequency as another independent variable. One would expect, in a rough way, an "accuracy cone" with the peak at 1 pF and 1592 Hz, where the best measurements with the computable capacitor have been made.

The dotted line in Figure 3 shows the sensitivity limit at 1592 Hz of a new research bridge which is being developed in conjunction with a new calculable capacitor. The estimated accuracy of the capacitor is also shown. The accuracy of the research bridge for stepping up and down from its value (0.5 pF) will, of course, be somewhat poorer than the sensitivity limit indicated.

Some of the contours for normal calibrations of the best available commercial capacitors are shown as solid lines in the figures. Note the extremely wide ranges in magnitude (10^{-9} to 10^{2} μF) and in frequency (60 to 10000 Hz).

Some sealed three-terminal air capacitors from 10 to 1000 pF have shown unusual stabilities. Projected improvements in the NBS ratio arm bridge should make it possible to measure such capacitors to at least 10 ppm. Even better accuracy may be required to calibrate 10 pF sealed capacitors of fused silica with silvered electrodes, which are apparently stable to better than 1 ppm/year[15].

Standard inductors are calibrated with standard capacitors in a Maxwell Wien bridge. Some of the contours in the accuracy cone are shown in Figure 4.

---

*This is true for many types of range-extending ratio standards (which do not involve the units). In many cases, however, the equipment and techniques are quite involved, and verification of the accuracy of the results by "round-robin tests" of a traveling standard in several laboratories, or by a direct calibration of a few ranges at NBS, may be very desirable.

The available accuracy is generally limited by the environmental conditions affecting the bridge and the standards being calibrated.

The charts of voltage measurements (Figures 5 and 6) are complicated not only because of applied frequency but also because NBS does not offer a voltage calibration service as such. Only the d-c voltage of a standard cell is available directly (and is determined to 1 ppm in terms of the volt maintained at NBS). The scale is extended in voltage and frequency by the calibrations of ratio standards and ac-dc transfer standards. With these and a standard cell the user can then make accurate d-c and a-c measurements. The ratio standards (potentiometers, fixed resistance dividers, and transformers) are generally used with respect to some reference voltage, such as the emf of a cell for d-c ratio standards, and 100 V (approximately line voltage) for a-c standards. They have upper and lower voltage limits. The chart therefore shows the accuracy of the ratio V/V_r, where V is given along the abscissa, and V_r is this reference. Note that this is the accuracy of the indicated ratio, not of a fraction of the applied voltage. (A 1000/1 volt box certified to 0.001 percent of ratio has one-hundredth the uncertainty of a 1-ppm-of-input voltage divider at this same ratio.) Potentiometers of the highest grade are normally calibrated to 3 ppm at 1 V, volt boxes to 10 ppm of ratio, decade transformers to 0.5 ppm of input voltage at 1 kHz, and voltage transformers to 0.03 percent of ratio at 60 Hz. AC-DC transfer instruments for voltage measurements are normally calibrated to 50 ppm from 20 Hz to 20 kHz and 100 ppm at 5 Hz to 50 kHz. The dotted lines show the "attainable" accuracies.

The chart for current measurements, Figure 7, is similar. Here NBS offers only calibrations of d-c shunts (for use with a potentiometer), a-c ratio standards, and ac-dc transfer standards. A chart for power and energy measurements would be based on the NBS standard transfer wattmeter, which is known to better than 50 ppm of the applied volt-amperes at 60 Hz and 0.1 percent at 2 kHz. The NBS group of five standard watthour meters are calibrated periodically in terms of the d-c standards through this wattmeter, and are in turn used to calibrate standard watthour meters to 0.05 percent at 60 Hz.

SUMMARY

These charts show the accuracies normally available at present, as well as the best attainable under the restrictions given. The ranges and accuracies of low-frequency electrical measurements are increasing rapidly, so that this is a far-from-static field. The results of research and development at NBS and elsewhere will be incorporated in improved NBS calibration services as rapidly as resources permit.

The author thanks Chester Peterson for Figures 2, 3, and 4, and for the ideas he has expressed during discussions of this subject.

KEYWORDS

electrical calibrations, electrical standards, low-frequency calibrations, low-frequency standards.

REFERENCES

1. Low Frequency Electrical Calibrations at the National Bureau of Standards, F. L. Hermach, NBS Miscellaneous Publication 248, Paper No. 1.5, 1962.

2. Calibration and Test Services of the National Bureau of Standards, NBS Miscellaneous Publication 250, (consult latest edition).

3. Actions of 11th Conference on Weights and Measures, NBS Technical News Bulletin, 44, 199, Dec. 1960.

4. World Sets Atomic Definition of Time, NBS Technical News Bulletin, 48, 209, Dec. 1964.

5. Evaluation of the NBS Unit of Resistance Based on a Computable Capacitor, R. D. Cutkosky, Journal of Research NBS, 65A, 147, 1961.

6. Measurement of Current with the NBS Current Balance, R. L. Driscoll and R. D. Cutkosky, Journal of Research NBS, 60, 297, 1958.

7. Precision Resistors and Their Measurements, J. L. Thomas, NBS Circular 470, 1948.

8. Method for Calibrating a Standard Volt Box, B. L. Dunfee, Journal of Research NBS, 67C, 1963.

9. Thermal Converters for Audio-Frequency Voltage Measurements of High Accuracy, F. L. Hermach and E. S. Williams, IEEE Trans. on Instrumentation and Measurement, Vol. IM-15, No. 4, Dec. 1966.

10. Standard Electrodynamic Wattmeter and AC-DC Transfer Instrument, J. H. Park and A. B. Lewis, Journal of Research NBS, Vol. 25, p. 545, 1940.

11. The Precise Measurement of Current Ratios, N. L. Kusters, IEEE Trans. on Instrumentation and Measurement, Vol. IM-13, No. 4, Dec. 1964.

12. The Design and Performance of Multirange Current Transformer Standards for Audio Frequencies, B. L. Dunfee, IEEE Trans. on Instrumentation and Measurement, Vol. IM-14, No. 4, Dec. 1965.

13. Precise Comparison Method of Testing AC Watthour Meters, A. W. Spinks and T. L. Zapf, Journal of Research NBS, 53, 95, 1954.

14. Basic Magnetic Quantities and the Measurement of Magnetic Properties of Materials, R. L. Sanford and I. L. Cooter, NBS Monograph 47, 1962.

15. Improved 10-Picofarad Fused Silica Dielectric Capacitor, R. D. Cutkosky and L. H. Lee, Journal of Research NBS, Sect. C., Vol. 69C, No. 3, July-Sept. 1965.

ILLUSTRATIONS

FIGURE 1

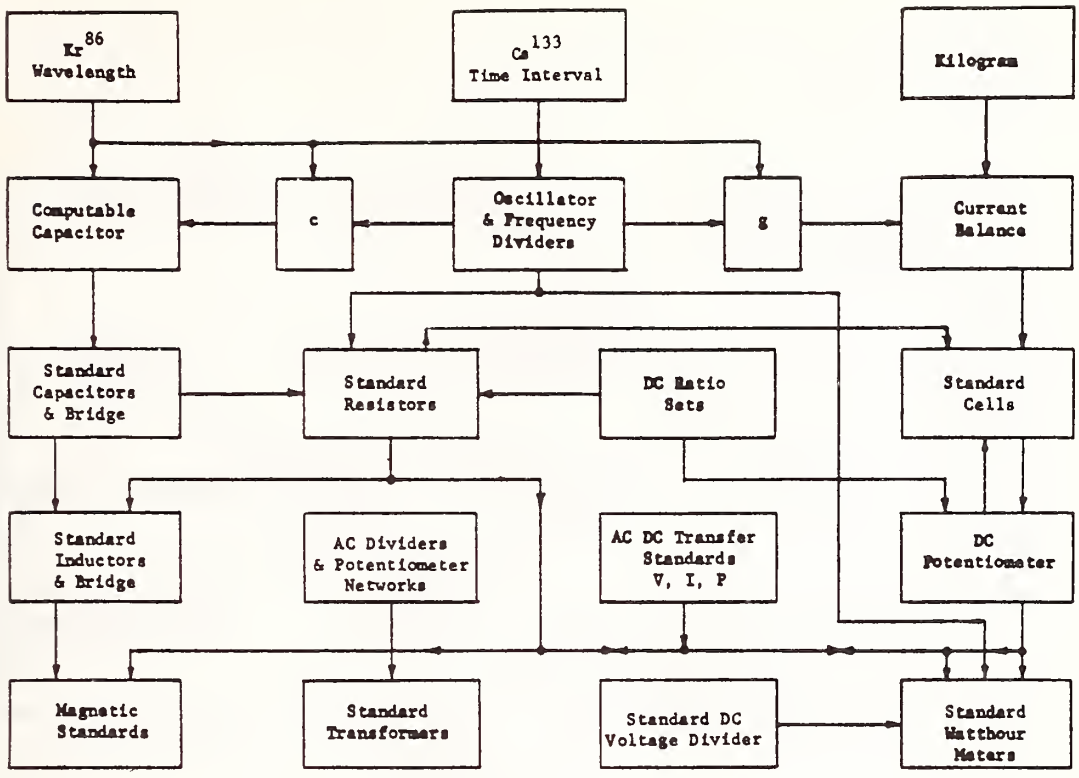

FIGURE 2

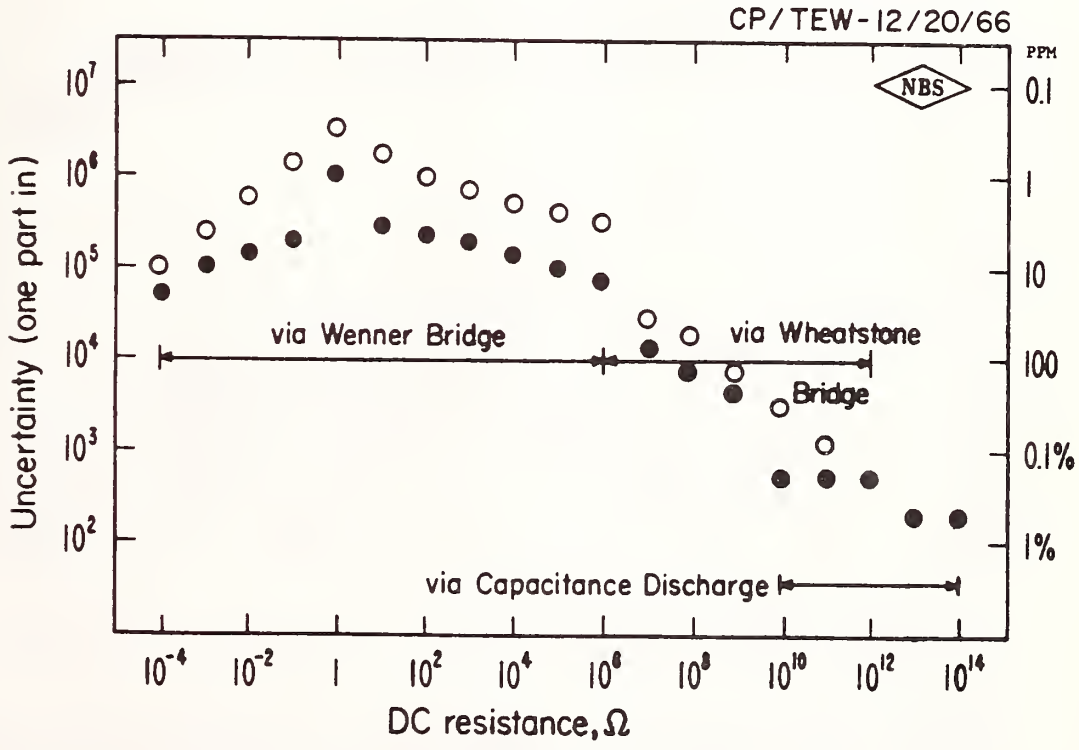

M5-1-MESTIND-67

FIGURE 3

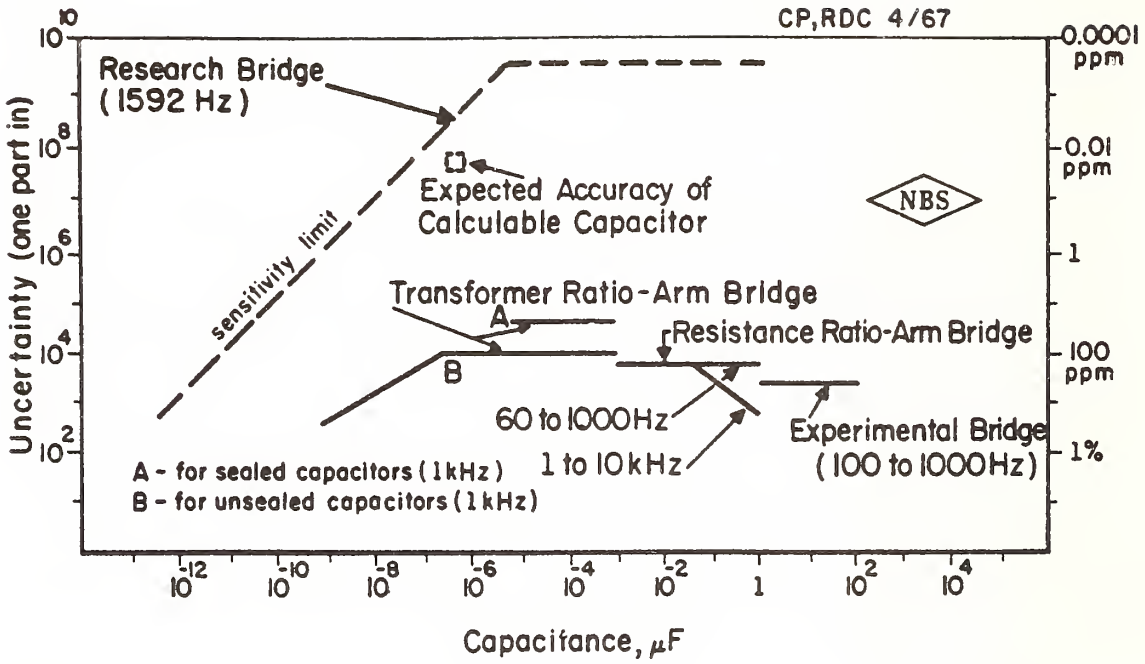

FIGURE 4

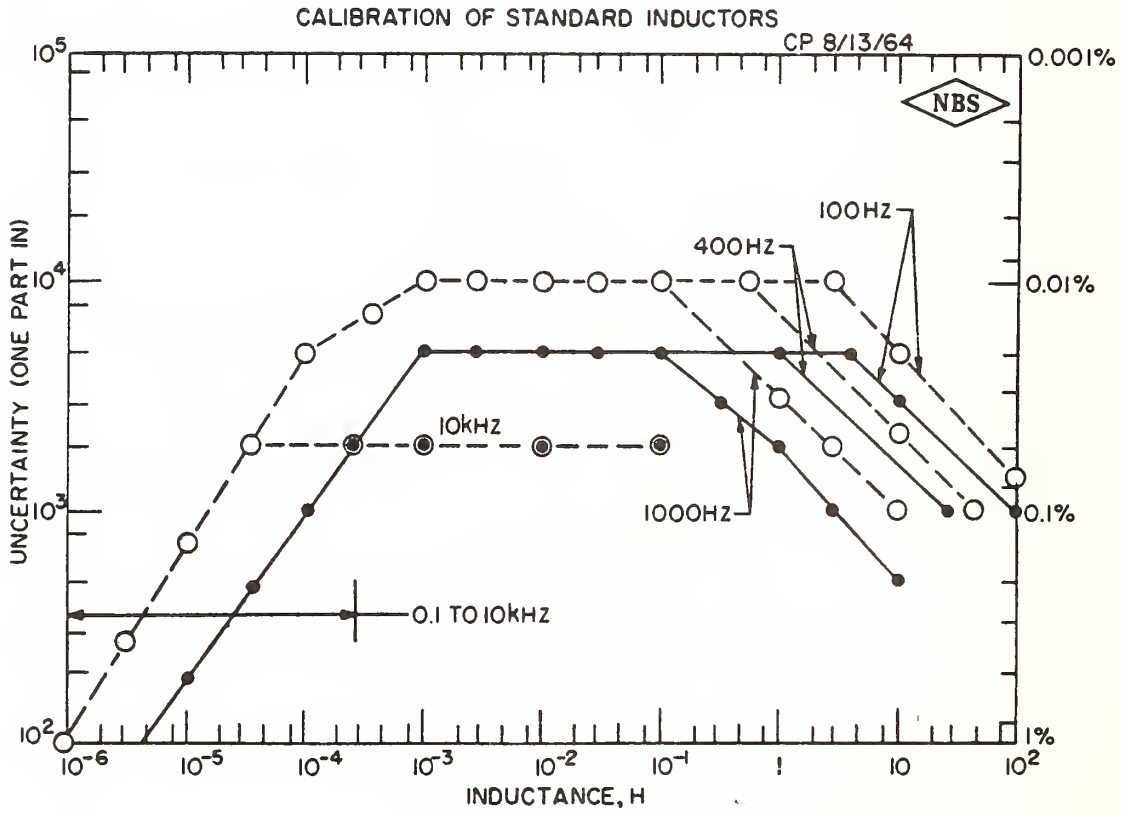

M5-1-MESTIND-67

FIGURE 5

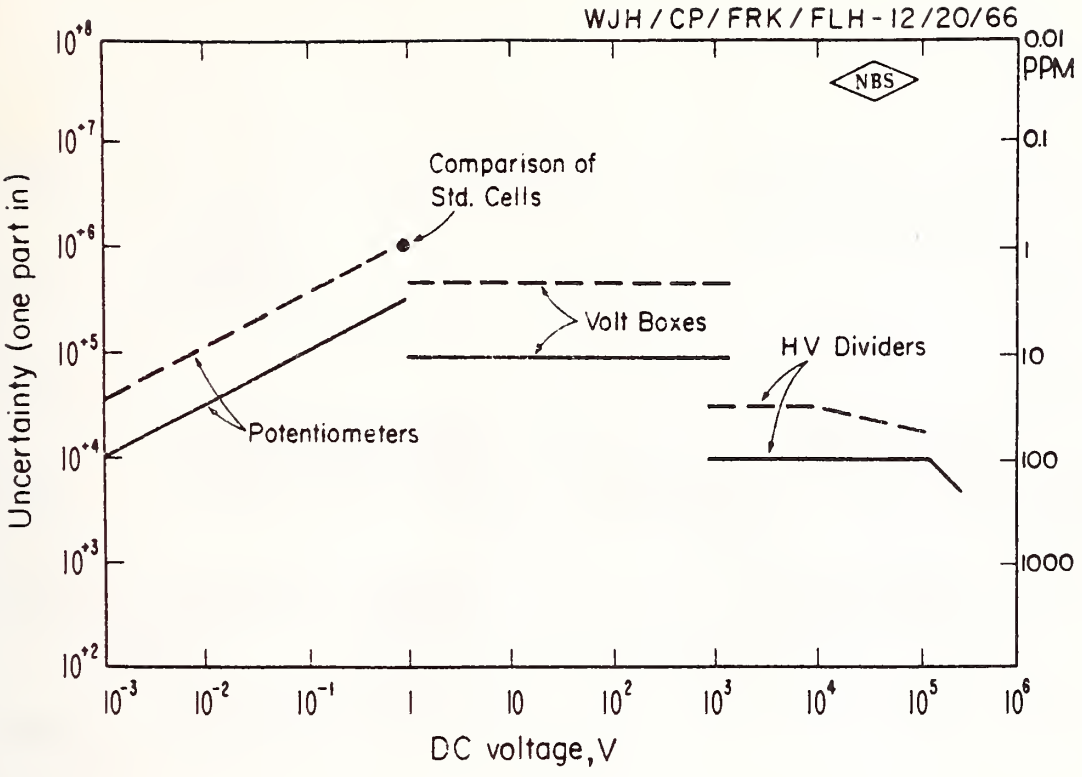

FIGURE 6

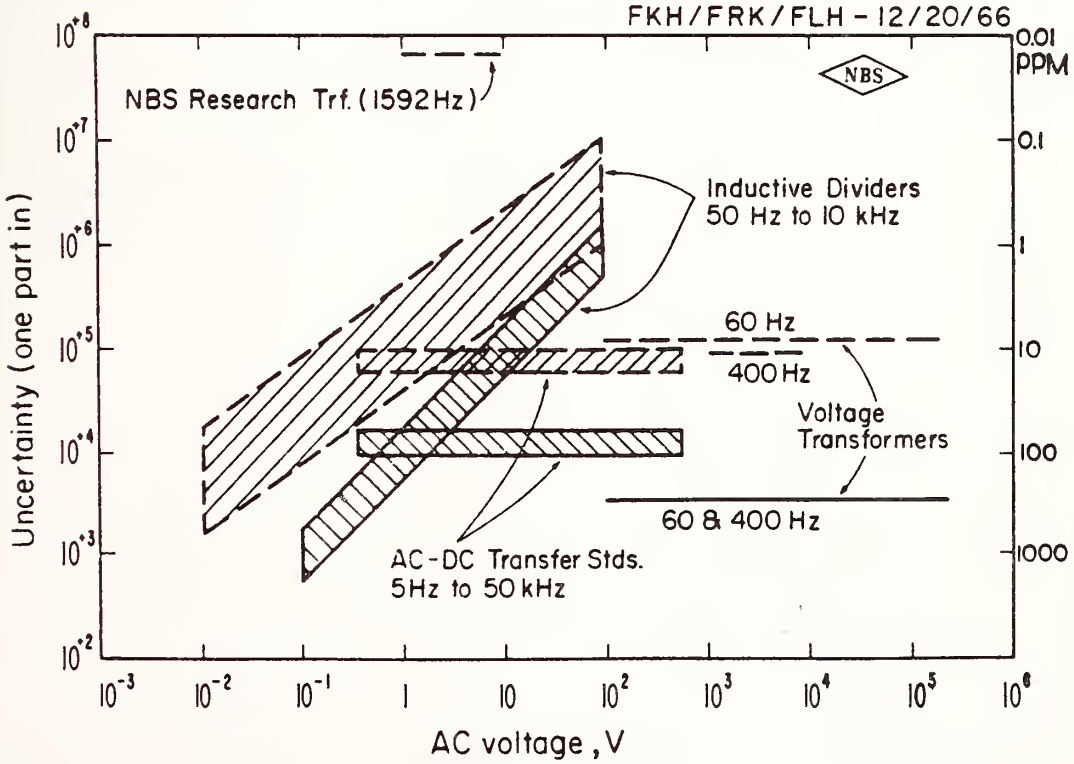

M5-1-MESTIND-67

FIGURE 7

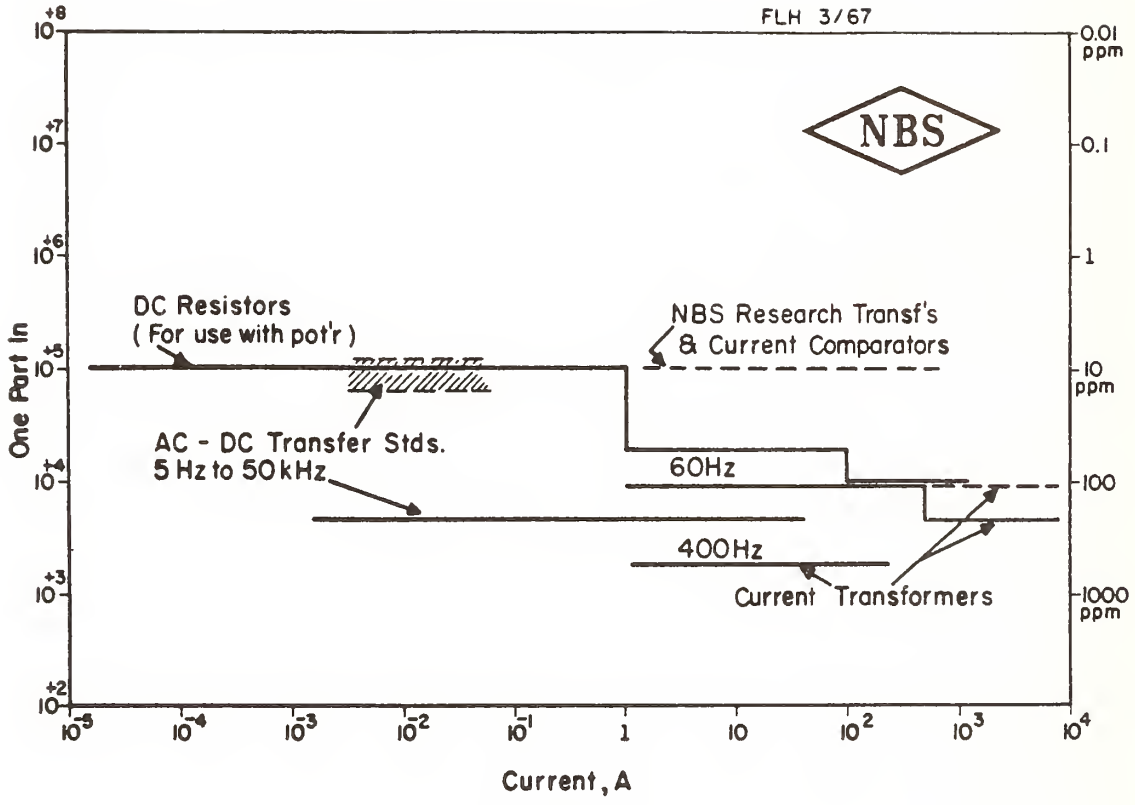

M5-1-MESTIND-67

USCOMM-NBS-DC

ABSOLUTE VALUES OF ELECTRICAL UNITS - I
Realization of Electrical Units: Classical Methods

The NBS Absolute Ampere Experiment

PAUL T. OLSEN, MEMBER, IEEE, VINCENT E. BOWER, WILLIAM D. PHILLIPS, EDWIN R. WILLIAMS, AND GEORGE R. JONES, JR.

Abstract—We have constructed a current balance with superconducting field coils for the realization of the SI ampere by comparing mechanical to electrical work. The estimated ultimate accuracy of the realization is 0.1 ppm. We describe and present preliminary results obtained with a room temperature version of the apparatus.

I. Introduction

THE practical electrical units can be maintained by a national standards laboratory, such as NBS, with remarkable accuracy and precision. The unit of voltage, defined in terms of the ac Josephson effect, is stable in time and routinely maintained to a few parts in 10^8 [1]. In the same way, the unit of resistance could be defined in terms of the quantum Hall effect, with a reproducibility and long-term stability of about four parts in 10^8 [2]. Unfortunately, the relationship between these "as-maintained" units and the more fundamental SI electrical units (defined only in terms of the units of mass, length, and time) is not nearly so well established. The SI definition of resistance can be related to the practical definition by calculable capacitor experiments [3] to a few parts in 10^8, but the SI definition of voltage is related to the practical or laboratory unit to an accuracy of only a few parts in 10^6 or worse [4].

Historically, the relationship between the SI and practical units of voltage has been determined by a realization of the SI definition of the ampere (A): "the ampere is that current which, when passed through two parallel, infinitely long wires of negligible cross section 1-m apart, produces a force between them of 2×10^{-7} N/m of length." The comparison of this SI ampere to the practical ampere, defined by the practical volt and ohm, completes the link between the SI and as-maintained systems of electrical units.

There are also various indirect methods for arriving at the ratio of the SI to as-maintained amperes. Generally, these involve combining a number of measurements of fundamental constants, such as the Faraday, the Avogadro constant, the gyromagnetic ratio of the proton, the Josephson frequency-voltage ratio and others, some of which involve electrical measurements and some of which involve force measurements. A comparison of such indirect measurements of the SI ampere with direct realization of the definition indicates large discrepancies [4]; in fact, the value for the ratio of the SI to laboratory ampere $K_A = A_{LAB}/A$ given in the latest (1973) adjustment of the fundamental constants [5] may be in error by as much as 10 parts per million (ppm).

The traditional method for realizing the SI definition of the ampere has been to construct a set of coils of accurately known dimensions, calculate from the dimensions the force which one coil system will exert on the other for a given current in each, and then to compare the calculated force to the actual force, as measured using a balance, when a current known in as-maintained units is passed through the coils. In this case we have

Manuscript received August 20, 1984.

The authors are with the Electricity Division, National Bureau of Standards, Gaithersburg, MD 20899.

$$K_A = \frac{A_{NBS}}{A} = \left[\frac{I_1 I_2}{F_{12}} C(R)\right]^{1/2} \quad (1)$$

where I_1 and I_2 are the currents, in laboratory units, in each of the coils, F_{12} is the force between them, and $C(R)$ is the calculated geometrical factor based on measurements of the dimensions and separation of the coils.

There are two key problems in performing this traditional realization of the ampere. First, the dimensions of a physical object such as a coil of wire are notoriously difficult to measure to accuracies at the ppm level. The problem arises in large part from difficulties with either mechanical or optical measurements of dimensions: one cannot accurately locate surfaces of objects which are at some level deformable and reflect light with unknown phase shifts. Furthermore, even if the mechanical dimensions of a coil were accurately determined, the electrical dimensions would still be uncertain because of the nonuniform distribution of current caused by strains or impurities in the wire.

Second, since accurate geometric measurements of each wire in the coils are needed, the coils must be wound in a single layer. This limits the magnetic field and thus the force which the coils can produce. Typical ampere balances operate with forces equivalent to only a few grams. Because the balance used to measure this force must carry the large dead weight of the coil as well as operate in the presence of convective air currents driven by the warm coils, weighing uncertainties are a significant limitation to the achievable accuracy.

In order to avoid the uncertainties of dimensional measurement, a new method [6] for realizing the ampere has been proposed. Consider an ampere balance as two coil systems, coil 1 (the field coil) being fixed in space and coil 2 (the suspended coil) being allowed to move in the field of the first coil. The force exerted on coil 2 by coil 1 is

$$F_{12}(z) = I_1 I_2 \cdot dM_{12}(z)/dz \quad (2)$$

where I_1 and I_2 are the currents in the two coils and M_{12} is the mutual inductance between the two coils. Only the z component of the force is considered since only vertical forces can be measured (i.e., compared to gravitational forces on known masses) using a balance. If we now consider that coil 2 carries no current, but moves vertically in the field of coil 1, a voltage will be induced across coil 2 in which

$$V = I_1 \, dM_{12}/dt. \quad (3)$$

Combining (2) and (3), assuming that I_1 is a constant, and that the functional form of $M_{12}(z)$ does not change, we have

$$\frac{F(z)}{V} = \frac{I_2}{dz/dt} \quad (4)$$

where dz/dt is the vertical velocity of the coil under the conditions described for (3). If we integrate (2) and (3) over intervals such that the endpoints Z_1 and Z_2 for the integration of (2) correspond to the positions of the suspended coil at the endpoints t_1 and t_2 for the integration of (3), we have

$$\int_{Z_1}^{Z_2} F(z)\, dz = I_2 \int_{t_1}^{t_2} V(t)\, dt. \quad (5)$$

In both (4) and (5), all electrical quantities are in SI units.

Making the substitutions $I = K_A I_{NBS}$ and $V = K_A K_\Omega V_{NBS}$, where $K_\Omega = \Omega_{NBS}/\Omega$, we have

$$K_A = \left[\frac{\int_{z_1}^{z_2} F(z)\, dz}{I_2 K_\Omega \int_{t_1}^{t_2} V(t)\, dz}\right]^{1/2} \quad (6)$$

which replaces (1) for the realization of the ampere. Note that (5) is simply a statement that mechanical work equals electrical work.

Several features of (6) are particularly attractive: No coil dimensions are required, and only the displacements of the coil with respect to an arbitrary reference plane need be measured. This type of measurement is easy to accomplish interferometrically and is not limited by uncertainties in optical phase shifts or in the nature of current distributions. The only requirement is that the effective geometry for the force measurement be the same as for the voltage measurement. Since no geometric measurements other than the displacement of the suspended coil are needed, both the field coil and the suspended coil can be multilayer coils, or even superconducting as long as the superconducting current paths do not change significantly during a measurement. In this way both large forces and large voltages can be produced making accurate measurements of these quantities easier, and the realization of the ampere by (6) will no longer be limited by the same dimensional uncertainties that restrict realization by (1).

In general, there is no fundamental difficulty in achieving forces and voltages large enough to be measured with an accuracy of 0.1 ppm or better, and displacements of a few centimeters are routinely measured to such accuracy. Thus it is realistic to assume that the new ampere realization can achieve an improvement of about two orders of magnitude over the accuracy achieved with present current balances.

II. Apparatus

We have constructed an apparatus for realizing the ampere according to (6). The mechanical portion of the apparatus is shown in Fig. 1. The field coils B are rigidly connected to the marble platform H which is attached to a massive limestone pier J. Two complete versions of this coil system have been constructed. One, designed for preliminary testing, is made from copper wires wound on an aluminum form. With a current of 8 A it produces a radial field of 2.9×10^{-3} T at the location of the suspended coil C. The second version is made of 20 superconducting coils wound on glass-epoxy forms, and produces a field of 0.20 T with a current of 10 A. The current distribution in the two versions of the field coils is nearly identical, so they have similar properties except for the magnitude of the field. The copper coils are immersed in a temperature controlled oil bath which removes the nearly 3 kW of heat dissipated. The superconducting coils are contained in a liquid He cryostat which consumes 1–2 liters of He per hour. The design of the coil system is described in more detail in [7]. The suspended coil C is made of 4956 turns of copper wire wound on a fiberglass-epoxy form. It has a mean diameter of

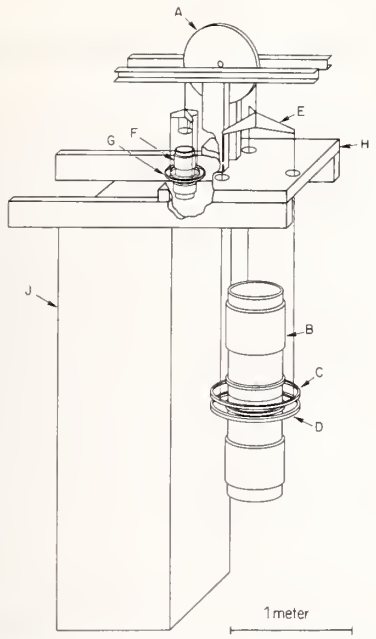

Fig. 1. A simplified scale drawing of the NBS absolute ampere experiment. The separate parts are identified, as follows:
A. The balance is an aluminum disk or wheel approximately 61 cm in diameter by about 2.5 cm in thickness. At the hub is a silicon carbide knife the edge of which rests on a boron carbide plane. A thin brass band strung over the top of the wheel is connected to three pronged "spiders" on each side. The scale pans are in turn attached to the spiders.
B. The magnetic field coil consists of four separate windings. The large upper and lower sections provide the main magnetic field. The axial fields are in opposition so at the mid-plane of the coil the magnetic field is in the radial direction. The smaller inner coils (compensation coils) add some field shaping to the primary radial field such that the radial field varies inversely with the radius.
C. The movable suspended coil or MSC has a mean diameter of 70 cm. It is bifilar-wound in three coplanar sections producing a coil with a square cross section, 1 cm on a side. The change in force on the MSC upon reversal of the current through it is counter-balanced by an appropriate known standard mass placed on the right-hand scale pan. An uncalibrated mass on the left-hand scale pan provides for approximate equilibrium of the balance during the velocity–EMF portion of the measurement. Attached to the MSC coil are the moving arms of the multi-axis laser interferometer which monitors the vertical displacement for both parts of the experiment (i.e., the velocity–EMF measurement and the force–distance measurement).
D. The fixed suspended coil is wound identically to the MSC and is suspended from the marble platform H. This coil is used to monitor the unwanted movement of the fixed field-producing coils and supports the fixed arms of the laser interferometer.
E. The right-hand spider, connected to a thin brass strap, wrapped around the rim of the balance wheel, supports the MSC and the scale pan on which the known standard mass is placed.
F and G. The auxiliary magnet coil, F, is a scaled down, room temperature version of the main magnet coil. This magnet, together with the auxiliary drive coil, G, controls the motion of the balance during the velocity–EMF portion of the measurement.
H. The massive marble slab is cantilevered on heavy wooden beams from the top of a substantial limestone pier J. The platform is quite stable and is as mechanically quiet as any other site at the NBS facility.
The balance and all components above the marble platform are housed in a styrofoam insulated wooden cabinet. The suspended coils are housed in a smaller wooden cabinet suspended from the marble slab by three aluminum tubes. Inside the three tubes are three more tubes of smaller diameter which support the fixed suspended coil. Inside these three tubes are three other tubes which support the movable suspended coil from the spider which in turn is attached to the brass strap around the balance wheel.

70 cm and a resistance of 9 kΩ. When a 3.33-mA current is reversed in the suspended coil the force changes by the equivalent of 15 g when the copper field coils are used, and 1000 g when the superconducting field coils are used. When the suspended coil is moved vertically at 0.667 mm/s, the generated voltage is 20 mV for the copper and 1 V for the superconducting coils. The suspended coil fits around the outside of the oil bath or cryostat containing the field coils.

The field coils B, including the additional trim windings near the midplane of the system, have been computer designed to optimize simultaneously a number of parameters of the magnetic field at the position of the suspended coil. The force (or generated voltage) on the suspended coils varies by only 180 ppm for a 6-cm vertical displacement, and the force has extrema at the center and endpoints of the displacement. The force varies by less than 15 ppm for a 1-percent change in the diameter of the suspended coil, and is also relatively insensitive to small transverse or angular displacements of the suspended coil. Because of this insensitivity to changes in the suspended coil geometry and position, reasonable care will ensure that the geometry during the force measurement implied by (2) will be similar enough to that during the voltage measurement implied by (3) that they may be combined to obtain (6). The force does depend strongly on the geometry of the field coils, so one must rely on the temperature stability of the oil bath or cryostat, and of the mechanical support structure to maintain this constant.

The suspended coil is attached by means of a spider E to the balance A which measures the force and provides the displacement of the coil. The balance is in the form of a wheel whose central pivot is a knife edge. A metal band 2.5-cm wide and 5×10^{-3}-cm thick hangs over the rim of the wheel and supports the spider and suspended coil on one side and an auxiliary spider and coil on the other side. The use of this wheel and band configuration rather than the more usual beam and knife edge suspension allows a vertical displacement of the suspended coil with virtually no horizontal displacement. This is important because the balance can only measure vertical forces (since it compares the magnetic forces to known gravitational ones). Thus while horizontal forces do not contribute to the measured force, horizontal displacements do contribute to the generated voltage, so that combining (2) and (3) is no longer valid. In our experiment the symmetry of the construction ensures that horizontal forces are small, and the use of the wheel and band ensures that horizontal displacements are small. Together, this makes the error from these causes acceptably small.

A miniature version F and G of the coil system B and C hangs from a spider on the opposite side of the balance. These auxiliary coils provide the force needed to drive the balance and translate the suspended coil during the voltage measurement phase of the ampere realization. With a fixed current in the auxiliary field coil F, a varying current in G applies a variable force to the balance. The auxiliary suspended coil G is would in such a way that it links no flux to the suspended coil C. Thus as the current in G changes, there is no voltage induced into C from this extraneous source.

A "fixed suspended coil" D, would identically to the "moving suspended coil" C, is suspended rigidly from the marble slab

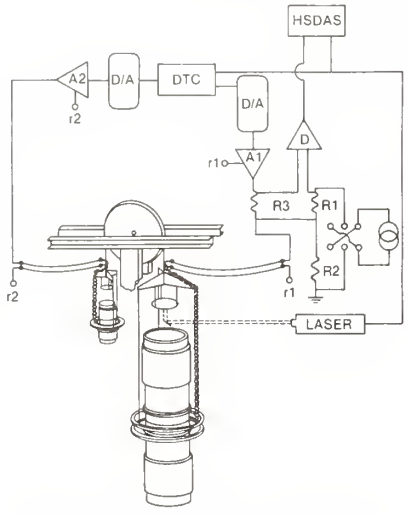

Fig. 2. A block diagram of the weighing servo.

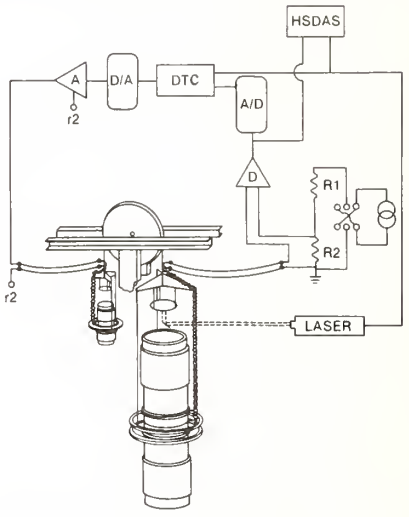

Fig. 3. A block diagram of the voltage-velocity servo.

H. The two coils are connected in opposition so that voltages induced by changes in external magnetic fields or by motion of the field coils B are canceled out. Coil D is also used to define the reference plane for measurement of the displacement of coil C. Ideally the reference should be provided by the coils B, but this is difficult in practice since they are in an oil bath or a cryostat. By measuring both the position and voltage of coil C with respect to coil D we effectively eliminate any effect from motion of B since its position is electrically transferred to coil D.

The entire balance assembly, including the wheel and the suspended coils, is contained in a thermally isolated, double "box within a box" enclosure. The dewar or oil bath containing the field coils is not within the inner enclosure, but its surface temperature is maintained close to that inside the enclosure. The temperature gradient inside the enclosure is arranged to minimize convective air currents. Balance operations such as changing weights are accomplished remotely by hydraulic drives, so that the balance enclosure need never be entered after the balance is assembled. Damping mechanisms inside the enclosure reduce swinging and torsion pendulum motions of the suspended coil.

The force measurement phase of the ampere realization is accomplished by alternately removing and replacing a calibrated mass on a scale pan attached to the spider E, while servoing the position of the moving suspended coil to a constant displacement from the fixed suspended coil. The servo is accomplished by varying the current in the suspended coil. The balance is arranged so that removing or replacing the mass results in a reversal of the current in the suspended coil. For our preliminary measurements we infer the displacement of coil C with respect to D from the displacement of the pan attached to the spider with respect to the marble slab H. Ultimately the displacement of C compared to D will be measured directly.

Fig. 2 shows the force measurement and servo circuit. A desk-top computer (DTC) measures the position of the pan as determined by the laser interferometer system. The DTC computes the difference (error) from the desired position as well as the time derivative and integral of the error. Numbers proportional to the error and its integral are summed and converted to a voltage in the digital-to-analog (D/A) converter. This voltage drives a voltage to current converter ($A1$) which supplies current to the suspended coil through a calibrated 300-Ω resistor $R3$, with the current returned to $r1$. In a similar manner, the derivative of the position error is applied to the auxiliary suspended coil on the other side of the balance.

The current in the main suspended coil is measured by comparing the voltage drop it produces in $R3$ to the voltage drop in $R1$. $R1$ is a standard 1-kΩ resistor supplied by a stable 1-mA current source. The difference between the voltages on $R3$ and $R1$ is measured by the calibrated detector D, which in turn is read by the high speed data acquisition system (HSDAS). The HSDAS also records the position of the suspended coils. When the mass is removed or replaced, the servo system reverses the current in the suspended coil, so as to keep the position of the coil constant. Accordingly, the 1-mA current in $R1$ is reversed to keep the difference voltage seen by the detector small. The 1-mA current source is calibrated by comparing the voltage on $R1$ to the voltage of a standard cell which is ultimately calibrated in terms of the Josephson effect.

The current in the auxiliary suspended coil, which is proportional to the derivative of the position error, is not measured, because it averages to zero. This separation of the derivative feedback signal reduces the noise in the measurement of the current in the suspended coil and has much the same effect as filtering.

Fig. 3 shows the circuit for the voltage measurement phase of the experiment. The voltage induced in the suspended coil as it moves is compared to the voltage drop in the 20-Ω resistor $R2$, which is driven by the same 1 mA current source used for the force measurement. The difference (error) voltage is

amplified by detector D and converted to a digital form by the A/D converter. The DTC reads this error signal, and computes its time derivative, offset, and time integral. Numbers proportional to each of these are summed and converted to a voltage in the D/A converter, and to a current in $A2$. This current is applied to the auxiliary coil which drives the balance in such a way as to keep the error voltage near zero. Thus the induced voltage in the suspended coil is held nearly constant by controlling its velocity via the servo loop. One could, of course, servo the velocity to a constant value and measure the changing voltage, but we prefer to servo the voltage so as to avoid uncertainties from measuring a changing voltage with a detector having a long time-constant.

While the DTC measures the error voltage on the suspended coil, it also monitors the coil position. When the coil approaches the end of its range of motion, the 1-mA current source is instructed to slowly reverse the current in $R2$, which in turn causes the velocity of the coil to reverse under servo control. During the period between reversals, the HSDAS records measurements of the time and of the position and error voltage of the coil. About 5000 such measurements are made during the 60 s required for the coil to cover its range of travel.

For both the force and voltage measurements the reversals (of current in the suspended coil or of direction of velocity) serve to cancel the effects of zero offsets in the detector or data acquisition system, and of thermal EMF's. These drop out when one calculates the change in current or voltage upon reversal.

III. Experimental Procedure

As of this writing we have only taken data using the copper, oil-cooled field coils. The procedures for taking data are partially automated and are still being refined. Because of the expense of the liquid He required to run the superconducting coils, we intend to perfect our procedures using the copper coils before beginning to use the superconducting ones.

At the beginning of a measurement the 1-mA current source is calibrated against a standard cell. The suspended coil is at the bottom of its travel, held down by the calibrated mass. This defines the zero position of the coil. The standard mass is lifted from the pan on the suspended coil side of the balance, and the detection and feedback circuit is configured for voltage data as in Fig. 3. The DTC automatically and repeatedly runs the suspended coil up and down over its travel while the operator instructs the HSDAS to record time, position, and voltage error for a predetermined distance after each velocity reversal occurs.

When a sufficient number of traversals are accumulated, requiring 5-15 min of real time, the system is reconfigured for force measurement as in Fig. 2. The calibrated mass is lowered onto the pan on the suspended coil side and a counterweight, half the mass of the calibrated mass, is placed on the opposite pan. During the changeover the 1-mA current source is recalibrated. Within 3-5 min after the voltage measurement ends, we begin force measurements.

Readings of the position and current of the suspended coil are made for about 60 s, after which the calibrated mass is lifted slightly off the pan. When the position of the suspended coil has stabilized, the current in the suspended coil has reversed under servo control and the reference current has been reversed manually, readings of coil current and position are resumed. About 100 s of real time separates the start of "mass on" and "mass off" measurements. After a total real time similar to that spent on voltage measurement, the system is again configured for voltage measurement, with a recalibration of the 1-mA current source during the changeover.

The alternation of voltage and force measurements continues for several hours, which constitutes the data for one day. In principle, the evaluation of K_A using (6) would require force measurements at a number of different positions z of the suspended coil. In fact, we have taken force measurements at only one position, and used the extensive voltage measurements to infer how the force would vary over the range of motion of the coil. Ultimately the validity of this procedure will be confirmed by actual measurement of the force at different positions.

The data are analyzed so as to cancel the first-order effects of drift in the experimental conditions, as well as to cancel most effects of thermal EMF's and zero offsets. For the voltage measurement data, the time integral $\int V dt$ is computed from the known reference voltage, the measured voltage offset or error voltage, and the times. The range of integration is between two fixed points in space. This is done for each set of data constituting a single traversal of the suspended coil in a given direction. The integrals for two "up" traversals are used to calculate an interpolated value for the up integral at the mean time for the down traversal which occurred between them. The difference between the interpolated up integral and the down integral gives a value for the time integral of the voltage which is free to first-order of thermal and zero offsets and drifts. The interpolation and subtraction procedure is continued for all the data in a given group of voltage measurements. Typically, the standard deviation of a set voltage-time integral differences, taken over 5-15 min, is less than 5 ppm. This is a measure of the minute to minute scatter in the voltage phase of the measurement. The expected effect on the value of K_A is half of this because of the square root in (6).

The force measurements are analyzed in a similar way. The current is calculated from the known reference voltage, the value of the resistance $R3$, and the measured error voltage. All the readings for a set with the suspended coil current in a given direction are averaged and the mean time of measurement is computed. Interpolated differences between the opposite current directions are calculated as in the case of voltage measurements. Differences obtained in this way are free to first order of drift in the balance point of the wheel, and thermal or zero offsets and drifts. A set of current differences obtained over a 5-15-min period typically has a standard deviation of less than 5 ppm, representing the minute to minute variation of the force measurement, which contributes half that uncertainty to K_A.

The averages of the interpolated force and voltage measurements are now combined to yield a value of K_A which is free of drift in the coil characteristics such as current in the field coils, or geometry changes in the coil system. This is done,

for example, by interpolating a value for the voltage integral at the mean time of a force measurement. Following (6), the interpolated voltage integral difference is multiplied by the average suspended coil current difference on reversal, multiplied by Ω_{NBS}/Ω, and divided into the product of the calibrated mass, m, the acceleration of gravity, g, and the distance over which the voltage integrals are calculated. A correction is made for the expected variation with z in the force mg based on the measured variation of the voltage integral over segments of the total path traveled by the coils.

In this way a value for K_A is obtained for every pair of voltage measurements with a force measurement between and every pair of force measurements with a voltage measurement between. These interpolated results are free to first-order of such changes as drifts in the current in the field coils or geometric changes in the coils. The standard deviation of a set of such measurements of K_A taken on a single day is on the order of 2 ppm. This within-a-day scatter is an important measure of the ability to detect systematic errors: errors more than several times smaller than this scatter will be difficult to evaluate experimentally in a short period of time. Day to day scatter of the value of K_A is of similar importance, and is thought to be of the order of 3 ppm, although at this stage there is not sufficient data to adequately evaluate this scatter. Day to day variations include the effects of resistor and voltage reference drift which we have only recently brought under control by using good quality standard resistors and standard cells.

IV. Systematic Errors

Before a value for K_A may be given, a number of possible systematic errors need to be evaluated. Below, we list some of the errors which may affect the ampere experiment and which we intend to evaluate experimentally.

One such error is balance motion. Effects from balance motion may arise in two ways. Horizontal motion of the suspended coil makes the assumption of vertical forces implicit in (2) invalid, as has been discussed previously in this paper. We will need to measure the magnitude of any horizontal motion and the size of any associated horizontal forces. Motion of the suspended coil also exerts mechanical forces on the balance wheel which oscillates with the periods of the swinging and torsion motions of the coil. These motions do exist, and it must be confirmed that their effect averages to zero, or a correction needs to be applied.

There is a relatively large drift in the balance point of the wheel, equivalent to as much as 100 ppm in an hour or so. With such a large drift a first-order drift correction may not be sufficient. The drift is probably caused by an air temperature change between the upper and lower portions of the balance enclosure, which results in a change in the buoyancy of the main suspended coil which hangs lower than the auxiliary suspended coil on the other side of the balance. This effect occurs even when the density of the two coils is matched to avoid drifts when the average air density in the balance enclosure changes.

The effects of leakages and thermal offsets in the calibration of the current source used to provide reference voltages need to be carefully evaluated.

The effect of measuring the displacement of the scale pan rather than of the suspended coil must be evaluated, or the system changed to measure the correct displacement.

The effect of nearby magnetic materials remains to be evaluated. Most magnetic materials are excluded from the laboratory, but some, such as the laser, remain.

Leakage between windings of the suspended coil can cause an error if this leakage depends on the voltage applied, since this would result in a different effective geometry for the force and voltage phases of the measurement.

When the superconducting windings are used, it will be necessary to determine the effect of the susceptibility of the superconducting wire.

Any residual effects due to coupling between the auxiliary drive coils and the main suspended coil must be measured.

V. Expected Results

With the present configuration, using the copper field coils, we have achieved a statistical uncertainty on the order of 3 ppm for about an hour's worth of real time spent accumulating data, with day to day variations expected to be 3 ppm. With this apparatus it should be possible to evaluate systematics at the 2-ppm level or better, yielding a value of K_A accurate to that level. When the superconducting coils are used, the voltage and force will increase by about a factor of 50. This should reduce the statistical error due to fluctuations in these quantities by that same factor. We believe that most of the scatter which we experience falls into this category.

Among the errors which will not be reduced when we use the superconducting system are those related to the distance measurement and those related to short-term fluctuations in current supplies. We do not foresee any difficulty in having the fluctuations in the current supplies below the 0.1 ppm level, and our experience with the interferometric distance measurements indicates that measurements better than 0.1 ppm over 6 cm should not be a problem. Thus we expect that in the superconducting version of our ampere experiment we should achieve a statistical precision better than 0.1 ppm.

Until we have examined all of the sources of systematic error, it will be impossible to predict with confidence the accuracy limit we will ultimately achieve. Nevertheless, we do not see any indication that errors significantly greater than 0.1 ppm will limit the final result. Furthermore, the projected statistical precision gives us confidence that we will be able to evaluate the systematic errors at the sub-0.1-ppm level.

In conclusion, we expect that the present experiment with copper field coils will yield a value of K_A within an uncertainty by one to a few ppm, while we expect to achieve a final accuracy of 0.1 ppm when the superconducting field coils are used. It is even possible that refinements in experimental techniques will allow us to reach uncertainties in the 0.01-ppm range, which opens the interesting possibility of using a current balance and the as-maintained electrical units to monitor the stability of the unit of mass.

Acknowledgment

The authors would like to thank J. A. Hammond and M. Zumberge for measuring the acceleration of gravity, g, at the site of our ampere balance; R. S. Davis for calibrating the mass used; R. F. Dziuba for calibrating the resistors; J. E. Sims for calibrating the standard cells; and G Barrett for assistance in taking the data.

References

[1] B. F. Field, T. F. Finnegan, and J. Toots, "Volt maintenance at NBS via 2e/h: A new definition of the NBS volt," *Metrologia*, vol. 9, p. 155. 1973.

[2] M. E. Cage, R. F. Dziuba, and B. F. Field, "A test of the quantum Hall effect as a resistance standard," *IEEE Trans. Instrum. Meas.*, pp. 301–303, this issue.

[3] R. D. Cutkosky, "New NBS measurements of the absolute farad and ohm," *IEEE Trans. Instrum. Meas.*, vol. IM-23, p. 305, 1974.

[4] B. N. Taylor, "Is the present realization of the absolute ampere in error?" *Metrologia*, vol. 12, p. 81, 1976.

[5] B. N. Taylor, W. H. Parker, and D. N. Langenberg, *Rev. Mod. Phys.*, vol. 41, p. 375, 1969; and E. R. Cohen and B. N. Taylor, *J. Phys. Chem. Ref. Data*, vol. 2, p. 663, 1973.

[6] B. P. Kibble, "A measurement of the gyromagnetic ratio of the proton by the strong field method," *Atomic Masses and Fundamental Constants*, vol. 5, J. H. Sanders and A. H. Wapstra, Eds. New York: Plenum, 1976, p. 545.

[7] W. Y. Chen, J. R. Purcell, P. T. Olsen, W. D. Phillips, and E. R. Williams, "Design and construction of a superconducting magnet system for the absolute ampere experiment," in *Advances in Cryogenic Engineering*, vol. 27, R. W. Fast, Ed. New York: Plenum, 1982, p. 97.

IEEE TRANSACTIONS ON INSTRUMENTATION AND MEASUREMENT, VOL. IM-29, NO. 4, DECEMBER 1980

The Realization of the Ampere at NBS

PAUL T. OLSEN, MEMBER, IEEE, MARVIN E. CAGE, WILLIAM D. PHILLIPS, AND EDWIN R. WILLIAMS

Abstract—**We present a method for the realization of the ampere based on Faraday's induction law and using a modification of the classic Pellat balance. A preliminary apparatus has been constructed and initial measurements have been obtained. This balance is also compared with a balance similar to one proposed earlier.**

Introduction

Throughout the history of the National Bureau of Standards (NBS), the direct measurement of the NBS ampere in terms of the fundamental units of mass, length, and time has been periodically performed. The last such measurement occurred in 1968 [1]. In the past, these measurements have been essential to establish an accurately known national voltage reference. At present, a more accurate ampere determination is essential to help resolve discrepancies that exist among the measured values of some of the fundamental physical constants [2].

The NBS effort to carry out a sub-parts per million (ppm) ampere determination is now in progress: a new coil system has been designed and construction will soon begin; a multi-axis laser interferometer system has been obtained and tested; a data acquisition system designed for remote operation and high-speed data rates has been installed; and a preliminary ampere balance in the form of a Pellat "electrodynamometer" has been assembled and is now in operation [3]. This report describes the preliminary ampere balance and briefly discusses the resolution of this instrument.

Theory of the Measurement

Following a proposal by Kibble [4],[1] the need for measuring the dimensions of a physical object has been replaced by the need to effectively measure the change in mutual inductance between two coils while they move relatively to each other. A Pellat-type balance is an especially good instrument with which to study and develop appropriate measurement techniques. It has a current-carrying coil which is permitted to rotate in an externally applied magnetic field (usually established by means of a current in a solenoid or Helmholtz pair) and which experiences a torque tending to align its axis with that of the magnetic field.

The torque on the rotatable coil is given by

$$T(\theta) = I_1 I_2 (dM_{12}/d\theta) \tag{1}$$

where I_1 and I_2 are the currents in the rotatable and external circuits, respectively, M_{12} is the mutual inductance, and θ is the rotation angle.

The integral of this torque in moving the coil between two angles (initial and final) is then

$$W = \int_{\theta_i}^{\theta_f} T(\theta)d\theta = I_1 I_2 \int_{\theta_i}^{\theta_f} dM = I_1 I_2 [M_{12}(\theta_f) - M_{12}(\theta_i)]. \tag{2}$$

If the coil is now allowed to rotate with its circuit open, the magnitude of the EMF generated is

$$\epsilon(t) = I_2 (dM/dt). \tag{3}$$

Integrating this EMF over time (from time t_1 to time t_2) one obtains

$$\int_{t_1}^{t_2} \epsilon(t)dt = I_2 \int_{t_1}^{t_2} dM = I_2 [M_{12}(t_2) - M_{12}(t_1)]. \tag{4}$$

If t_1 and t_2 are the times when the coil is at angles θ_i and θ_f, respectively, of (2) we may divide (2) by (4) to obtain

$$I_1 = \int_{\theta_i}^{\theta_f} T(\theta)d\theta \Big/ \int_{t_i}^{t_f} \epsilon(d)dt. \tag{5}$$

Since the numerator of (5) is just the work done by the electrical torque in rotating the coil between θ_i and θ_f, it can be replaced by any equivalent expression. In particular, this work is equal to the work done by a vertical external force applied at the end of a balance beam when that external force just balances the magnetic force on the movable coil. This force can be measured experimentally by weighing. Expressed this way, (5) becomes

$$I_1 = \int_{z_i}^{z_f} F_z(z)dz \Big/ \int_{t_i}^{t_f} \epsilon(t)dt \tag{6}$$

where z_i and z_f are the vertical positions of the end of the balance arm at angles θ_i and θ_f, respectively.

Equation (6) can be written explicitly in terms of NBS electrical units so that we finally obtain

$$K_A \equiv (A_{\mathrm{NBS}}/A) = \left[\int_{z_i}^{z_f} F(z)dz \Big/ \left(I_{\mathrm{NBS}}(\Omega_{\mathrm{NBS}}/\Omega) \int_{t_i}^{t_f} \epsilon_{\mathrm{NBS}}(t)dt \right) \right]^{1/2} \tag{7}$$

Manuscript received July 21, 1980. This project was supported by the National Bureau of Standards.

The authors are with Electrical Measurements and Standards Division, Center for Absolute Physical Quantities, National Bureau of Standards, Code 521, Washington, DC 20234.

[1] In addition to Kibble's paper two other ideas are also reflected in the present Pellat experiment. In 1972, D. S. Sullivan suggested measuring the integral of I times ϵ and comparing it to the mechanical work done on a superconducting motor [7]. Also, C. H. Page in 1971 suggested to one of the authors, E. R. Williams, that the derivative of the mutual inductance with respect to the balance pan displacement is a constant for the Pellat balance.

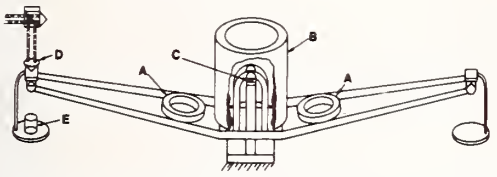

Fig. 1. The general appearance of the Pellat-type ampere balance with the rotating coil B, the central knife edge C, and the standard mass E. Added to the Pellat balance for the present measurement are: the torque coils A and the corner cube for the laser interferometer system D. An additional torque coil (not shown) is placed inside the rotatable coil. The three torque coils are electrically connected in series. The third coil prevents the torque coils from inducing an EMF into the rotatable coil.

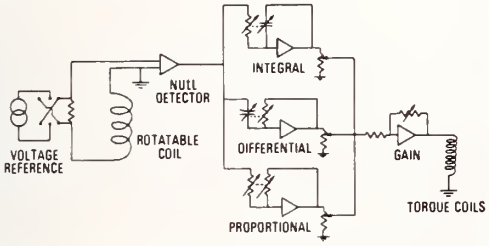

Fig. 2. The voltage of a reference source is compared to the EMF of the rotatable coil. This voltage difference is amplified and drives a current into the torque coils. This current provides the torque required to maintain the angular velocity of the rotatable coil such that the EMF produced in the rotatable coil is constant and equal to the reference voltage.

where $F(z)$ is the product of the acceleration due to gravity and the mass on the pan at the position z. I_{NBS} is the magnitude of the current in the movable coil expressed in terms of the NBS unit of current; Ω_{NBS}/Ω is the ratio of the NBS unit of resistance to the absolute or SI unit of resistance as measured by the calculable capacitor [5]; and ϵ_{NBS} is the magnitude of the induced voltage expressed in terms of the NBS unit of voltage.

The $\int_{z_i}^{z_f} F(z)dz$ term is computed from many static weighings made along the path from z_i to z_f with a current I_{NBS} in the rotating balance coil. The $\int_{t_i}^{t_f} \epsilon_{NBS}(t)dt$ term is measured in a separate experiment when the coil is moved from position z_i to z_f in a time $t_f - t_i$ at a nearly constant velocity and the current I_{NBS} is not flowing in the rotating coil. The geometry and the current of the stationary coil must remain unchanged during all these measurements or an appropriate correction must be made.

Measurement of the Voltage Integral

The evaluation of the integral $\int_{t_1}^{t_2} \epsilon(t)dt$ establishes all of the geometrical specifications of the Pellat balance. The time t_1 begins when the balance beam is tilted to the θ_i position and ends at time t_2 when the balance beam has rotated to θ_f.

In reality, neither θ_i nor θ_f is measured, but rather the vertical displacement of the primary scale pan. The apparatus is shown in Fig. 1.

In actual operation, the induced voltage is held constant via a servosystem, and the time intervals required to travel predetermined distances are recorded over the path length. There is less of a problem in measuring the induced voltage with a detector having a long response time if the measured voltage is held nearly constant.

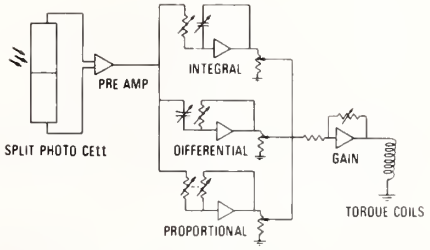

Fig. 3. A mirror mounted on the axis of rotation of the rotating coil reflects a laser beam onto a split photovoltaic cell. An unbalance in the illumination produces a dc voltage across the photo-cell. The amplified signal produces a current in the torque coils which rotates the balance beam until the output voltage of the photo-cell is zero. This servosystem controls the balance point to a few microradians.

Fig. 2 shows a simplified schematic of the servo system which maintains the constant EMF. The balance arm is driven to rotate about the central knife edge so that the EMF generated in the rotatable coil equals that of the reference voltage. When the rotation nears either end, an optical sensor triggers a reversing switch which inverts the polarity of the reference voltage causing the balance to reverse its direction of rotation. The laser interferometer is used to trigger a clock reading when a predetermined number of fringes has been counted. After an initial settling time, the EMF integral can be calculated from the sum of all voltage measurements between any two time measurements taken between reversal points.

Each time a specified number of interferometer fringes is counted, the data acquisition system reads the accumulated time of a 1-MHz clock and the difference between the reference voltage and the EMF generated in the rotating coil. This correction voltage, typically less than 1 μV with noise of a few tenths μV, is also used to drive the servo system. The reference voltage, about 1 mV and stable to a few ppm, is also monitored at frequent intervals. The measured reference and correction voltages are added to give the coil voltage. Data are taken with the balance swinging in both directions to cancel the effects of voltage offsets and thermal EMF's. Integration of the coil voltage over time is done numerically, and the results for numerous pairs of up and down swings are averaged.

Measurement of the Force Integral

Fig. 3 shows the abbreviated schematic of the weighing servosystem. A mirror located on the rotatable coil reflects a laser beam onto a split photovoltaic cell. The analog servosystem fixes the balance beam in such a position that the laser beam equally illuminates each half of the photovoltaic cell. This servo system fixes the angle of the balance beam to within several microradians.

A mass of 1500 mg is added to the scale pan on which the corner cube is mounted. The current in the rotatable coil is adjusted to nearly counterbalance the torque of the standard mass at the end of the balance beam. The servo system provides the additional torque with current in the torque coils. The torque coils are calibrated frequently by noting the change in current in them for a known change in current in the rotatable coil. The vertical position of the scale pan is read from the interferometer.

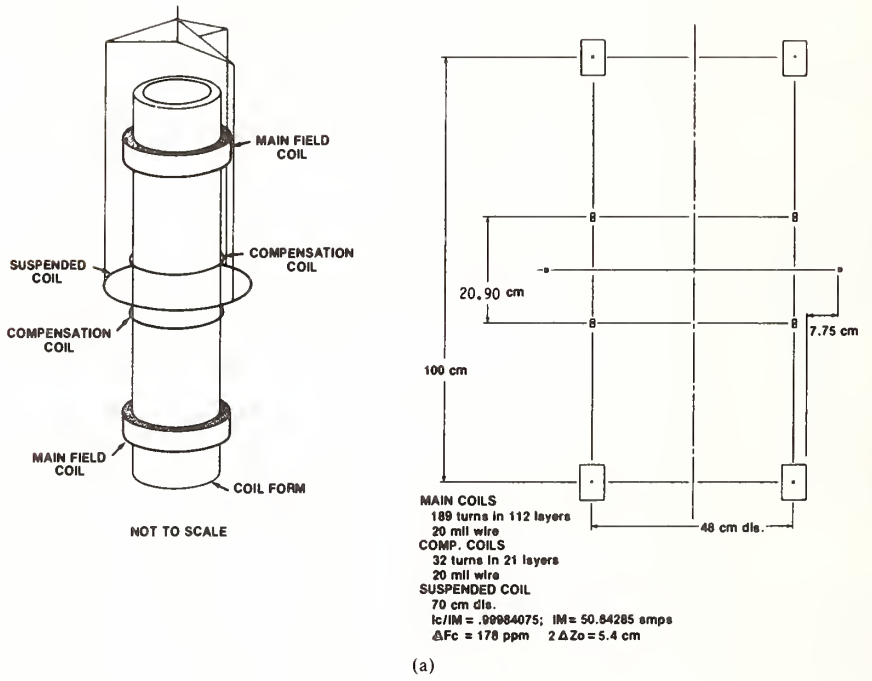

(a)

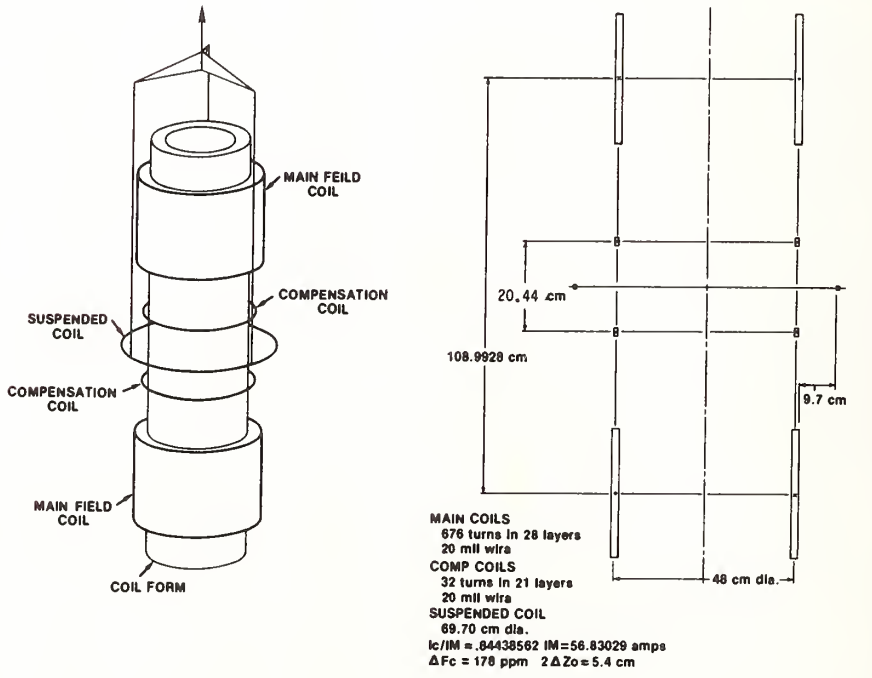

(b)

Fig. 4. (a) and (b) The design criteria are given for two possible current balances. The magnetic field producing coils and compensation coils are superconducting. The suspended coil carrying 10 ampere-turns produces a vertical force of 1 kg. The force on the suspended coil is to first order independent of its diameter and of the vertical displacement about the midplane of the field coils. A change in the diameter of the suspended coil by 1 cm changes the vertical force by less than 20 ppm. Vertical displacements (z_0) of 2.7 cm above or below the midplane produce a change ΔF_c in the vertical force of 178 ppm, with currents I_M in the field coils and I_c in the compensating coils as noted. Both superconducting coil systems shown produce the identically same force on the suspended coil. This permits the manufacturer to select the design which he feels would give the best performance from cryogenic considerations.[2]

[2] The system described here is similar to that of [6] except that it is simpler to construct and requires a standard type of dewar.

A current reversal in the rotatable coil occurs simultaneously with the removal of the standard mass on the scale pan. Each set of weighings at a position z constitutes one value of the integrand of $\int_{z_i}^{z_f} F(z)dz$. Weighings are then repeated over the range z_i to z_f and the results are numerically integrated.

The statistical uncertainty of a single set of weighings at one position which requires 5 min, including calibration of the servo system, is less than 30 ppm. Data taken over 45 min, including reversals of the current, are scattered from similar sets by less than 10 ppm. We expect a substantial improvement when some care is taken in the mounting and mechanical isolation of the balance.

Measurement Results

Measurements with the Pellat balance to date have concentrated on the development of control equipment and measurement techniques. Therefore, we have not evaluated in detail the effect of systematic uncertainties. The scatter between different sets of measurements of voltage and force integrals implies a statistical uncertainty of about 10 ppm in K_A.

Discussion

Previously, it was stated that the Pellat balance is a good instrument to evaluate the recently proposed method [4] of measuring K_A. The most attractive feature is that there is only one degree of freedom: rotation. The rotatable coil of the Pellat balance, in a uniform magnetic field, has a constant voltage induced in it for a constant vertical velocity of the scale pan. Similarly, a constant current in the rotatable coil will support in equilibrium a single mass on the scale pan at any vertical position of the scale pan.

Our Pellat balance is a modification of an existing balance. The balance was supported on wooden piers resting on a cement floor. The 1-mT magnetic field was supplied by Helmholtz coils wound on wooden forms. Thus major improvements are clearly possible. However, a difficulty with the Pellat balance is its sensitivity to changes in the dimensions of the rotatable coil. Our rotatable coil has 43 000 turns of 0.2-mm diameter copper wire. Thermal expansion of the copper changes the coil's area by about 40 ppm/°C, and the torque produced varies as the area. The height of the coil also changes by about 20 ppm/°C, thus affecting the balance sensitivity. Even more critical is the shift of mass on the balance beam as the rotatable coil diameter changes dimensions. The coil is not anchored uniformly on the balance beam so the coil "creeps" along it. Considering that the mass of the rotatable coil is approximately 2 kg and has a diameter of about 10 cm, the balance moment could change by as much as 0.4 gm·cm/°C.

Our experience has convinced us that the Pellat balance, properly supported and with a stronger external magnetic field, could be used to measure K_A to the ppm level. Control of the rotatable coil temperature, by always maintaining constant power in the coil, would greatly reduce the effects described above.

Future Plans

The eventual NBS high accuracy (parts in 10^7) ampere determination will use an instrument which more closely resembles the classical current balance (see Fig. 4 (a) and (b)) [6]. In this system, the magnetic field coils will be superconducting, while the force coil, suspended from the arm of a balance, will be at room temperature. Because of the high current densities in the superconducting field coils, both the EMF generated in the moving coil and the vertical force to be measured will increase by about 3 orders of magnitude over those in the preliminary Pellat balance described above. These will result in a thousandfold improvement in the voltage and force measurements. The velocity measurements will be made in a manner similar to that described for the Pellat balance.

Contrary to all previous ampere balances, however, the vertical force on the suspended coil will be, to first order, independent of its diameter and nearly independent of vertical position for a substantial displacement about the midplane of the field coils, i.e., for 5- to 6-cm total displacement.

The swing of the balance beam will cause lateral motion of the suspended coil as it travels vertically. A balance now under consideration, however, will servo the vertical path of the suspended coil to eliminate lateral motions by providing the flat of the central knife with the ability to move in a horizontal plane.

To eliminate the problem of the motion of the cryogenic field coils, a coil similar to the suspended coil will be prepositioned and fixed around the outside of the dewar. This coil, which defines a reference plane, will have an EMF generated in it should the field coils move. All voltage and displacement measurements of the suspended coil will be made with respect to this voltage and this position reference plane.

Acknowledgment

The authors would like to thank J. A. Hammond for measuring the acceleration due to gravity g at our experimental site. This accurate value will be utilized in our forthcoming experiment.

References

[1] R. L. Driscoll and P. T. Olsen, report to Comité Consultatif d'Electricité, Comité International des Poids et Mesures, 12th Session, 1968.
[2] B. N. Taylor, "Is the present realization of the absolute ampere in error?" *Metrologia*, vol. 12, p. 81, 1976.
[3] R. L. Driscoll, "Measurement of current with a Pellat-type electrodynamometer," *J. Res. Nat. Bur. Std.*, vol. 60, p. 287, 1958.
[4] B. P. Kibble, "A measurement of the gyromagnetic ratio of the proton by the strong field method," *Atomic masses and Fundamental Constants*, vol. 5, J. H. Sanders and A. H. Wapstra Eds. New York: Plenum, 1976, p. 545.
[5] R. D. Cutkosky, "New NBS measurements of the absolute Farad and Ohm," *IEEE Trans. Instrum. Meas.*, vol. IM-23, p. 305, 1974.
[6] P. T. Olsen, W. D. Phillips, and E. R. Williams, "A proposed coil system for the improved realization of the absolute ampere," *J. Res. Nat. Bur. Std.*, vol. 85, p. 4, 1980.
[7] P. B. Sullivan and N. V. Frederick, "Can superconductivity contribute to the determination of the absolute ampere?" *IEEE Trans. Magnetics*, vol. MAG-13, p. 396, 1977.

JOURNAL OF RESEARCH of the National Bureau of Standards
Volume 85, No. 4, July-August 1980

A Proposed Coil System for the Improved Realization of the Absolute Ampere

P. T. Olsen,* W. D. Phillips* and E. R. Williams*

National Bureau of Standards, Washington, D.C. 20234

April 1, 1980

In order to resolve the discrepancies which presently exist between the directly measured values of the absolute or SI ampere and the calculated values obtained indirectly from other fundamental physical constant determinations, one must design an absolute ampere experiment which will produce a result with an uncertainty of one half part per million or less. A new approach recently proposed by Kibble promises such sub-ppm accuracy. Presented here is the design and evaluation of a coil system which will fulfill the requirements of this new approach.

Key words: Absolute ampere; current balance; magnetic force; radial magnetic field; superconducting coils.

1. Introduction

One of the first experiments conducted at the National Bureau of Standards (NBS) was that of determining the as maintained unit of electrical current in terms of the absolute ampere. To date three different methods have been employed: the classical current balance, the ratio-of-radii method, and the electrodynamometer method.

1.1. The classical current balance

A pair of equal diameter coaxial coils with their axes vertical and electrically connected so that their axial magnetic fields are in opposition, produce a purely radial magnetic field at the mid-plane. A third coil (also with its axis vertical) is suspended from the arm of a precision balance in this radial magnetic field. The interaction between the magnetic field produced by the coil pair and the current in the suspended coil produces a vertical force on the suspended coil that is measured with the balance. The expected force is calculated from the measured physical dimensions of the coil system. The difference in the actual force from that calculated is an indication of the difference between the laboratory, or as-maintained unit of current, and the absolute ampere as defined in the Systeme International d'Unites (SI) [1].[1]

1.2. The ratio-of-radii method

The ratio-of-radii technique is in general identical to the classical current balance except that the coils do not have to be measured quite so carefully. Only the ratio of the radii of the coils producing the radial field to that of the suspended coil needs to be measured. This ratio is determined by measuring the ratio of currents in the field and suspended coils needed to produce a null field at the center. The critical dimensional measurement here is of the centrally located probe used as the zero field sensor since the finite size of this object significantly influences the accuracy of the ratio [2].

1.3. The electrodynamometer method

The Pellat balance or electrodynamometer consists of a small coil mounted on a balance beam. The coil axis is positioned orthogonally to a uniform magnetic field at the center of a precision solenoid. In this technique, the torque on the small coil is measured. The torque constant of the balance is calculated from the dimensional measurements of the coils and balance beam [3,4].

Common to all three methods is the small mass used as a restoring force on the scale pan of the balance, typically one to two grams. The mass of the system on the balance beam is approximately one kilogram, so a weighing of 1 part in 10^9 is necessary in order to just achieve an experimental uncertainty of 1 part in 10^6 or 1 ppm (part per million). Since a

*Center for Absolute Physical Quantities National Measurement Laboratory.
[1] Figures in brackets indicate literature references at the end of this paper.

weighing of 1 part in 10^9 is not readily achievable, the previous experiments were already limited to several ppm uncertainty. This restriction, combined with the tedious measurements for determining the actual size of some physical object, limited the accuracy of all previous experiments to a value considerably in excess of 1 ppm.

In addition to making direct current balance measurements of K_A, the ratio of the as-maintained ampere to the absolute or SI ampere, it is possible to compute a value of K_A through the route of other measured fundamental constants. At the present time, these computed values of K_A exhibit much less uncertainty than the several direct measurements of K_A. Yet these derived values of K_A generally disagree among themselves and they in turn disagree with the direct current balance determinations of K_A [5].

In light of the recent advances in technological tools such as the computer, laser interferometry, and cryogenic techniques, it appears that a conventional current balance experiment could be conducted to yield a result for K_A with an uncertainty of better than 1 ppm. Examinations of past experiments indicates that the chances of success would greatly improve if: (a) the electromagnetic force to be measured was increased by two or three orders of magnitude; and (b) the need for super-accurate dimensional measurements of a physical body of inconvenient geometrical shape were lessened or eliminated.

B. P. Kibble of the National Physical Laboratory (NPL), has proposed a new method of conducting an absolute ampere experiment which appears to have the capability of measuring K_A to an uncertainty of significantly less than 1.0 ppm [6,7]. Kibble's approach eliminates the need to measure the physical size of coils and allows a three order of magnitude increase in the electromagnetic force. This paper follows Kibble's general approach and presents a unique coil geometry by which the absolute ampere should be measurable to an accuracy approaching 0.1 ppm.

2. Theory

Although the new method proposed by Kibble has been published, for the sake of clarity the idea is briefly developed here.

A length of wire, ℓ, traversing a uniform magnetic field, **B**, at a constant velocity, v, has a voltage potential difference ε induced at its ends according to

$$\varepsilon = \ell \cdot (\mathbf{B} \times \mathbf{v}) = \mathbf{v} \cdot (\ell \times \mathbf{B}). \tag{1}$$

When the wire is stationary and a steady current, I, flows within it, a force is exerted on the wire given by

$$\mathbf{F} = I\ell \times \mathbf{B}. \tag{2}$$

It is sufficient for our purposes to examine the situation where ℓ, **B**, and v are orthogonal. Both ℓ and **B** are the same in eqs (1) and (2), so eq (2) can be written as

$$F = \varepsilon I/v. \tag{3}$$

Applying the above equations to the classical current balance, one can imagine a coil of N turns and radius a_o in a uniform radial magnetic field, B_r. The coil is positioned in the center of and co-planar with the radial magnetic field. The term ℓ can be identified with the coil circumference times the number of turns on the coil. Imagine now the coil traversing the radial field in an axial direction at a given velocity, v_z. An emf ε is developed across the coil terminals and is measured in terms of a laboratory as-maintained unit of voltage. In analogy with eq. (1), its magnitude is given by

$$\varepsilon = \varepsilon_{NBS}(V_{NBS}/V) = N2\pi a_o B_r v_z \tag{4}$$

Here, V_{NBS} is the NBS as-maintained unit of voltage, V the absolute or SI volt, and ε_{NBS} the induced emf measured in terms of V_{NBS}.

Assuming in eq (4) that the velocity v_z is measured in terms of the meter and the second, then the product of the number of turns N times the circumference $2\pi a_o$ times the magnitude of the magnetic field B_r is "calibrated" and given by

$$N2\pi a_o B_r = \varepsilon_{NBS}(V_{NBS}/V)/v_z. \tag{5}$$

Now imagine the same coil being suspended in the same radial magnetic field from a balance beam and carrying a current I measured in terms of the NBS as maintained unit of current, A_{NBS}. The resulting force is then determined by use of the balance, a calibrated mass m, and knowledge of the local value of the gravitational acceleration, g. In analogy with eq (3) one obtains

$$F = mg = N2\pi a_o B_r I = N2\pi a_o B_r I_{NBS}(A_{NBS}/A). \tag{6}$$

Using eq (5) we obtain

$$mgv_z = \varepsilon_{NBS} I_{NBS}(V_{NBS}/V)(A_{NBS}/A). \tag{7}$$

Noting that $V_{NBS} = A_{NBS}\Omega_{NBS}$, where Ω_{NBS} is the NBS as-maintained unit of resistance, yields finally

$$K_A \equiv (A_{NBS}/A) = \left[\frac{mgv_z}{\varepsilon_{NBS} I_{NBS}(\Omega_{NBS}/\Omega)}\right]^{1/2} \tag{8}$$

The ratio of the NBS ohm to the absolute ohm, Ω_{NBS}/Ω, may be obtained using the calculable cross capacitor to an accuracy of a few parts in 10^8 [8]. The quantity g may be obtained to the same accuracy by using an absolute gravime-

ter. The remaining terms in the square brackets are measured during the course of the experiment. It should also be noted that eq (8) can be shown to hold when the force, velocity, and induced emf are replaced by their average values [See Appendix A] [6,7].

3. Design

The classical current balance configuration is inherently a good design. This configuration contains a high degree of symmetry as well as being a relatively simple geometry to construct. The current balance configuration would lend itself very nicely to the Kibble approach if it were possible to compensate the radial magnetic field component such that: (i) the force on the suspended coil is relatively independent of its axial location ($dF/dz \approx 0$); and (ii) the force on the suspended coil is relatively independent of its own diameter $2a_0(dF/da_0 \approx 0)$.

The reason for condition (i) is that in the first part of the experiment, the suspended coil is made to traverse the radial field axially at a constant velocity. Unless $dF/dz \approx 0$, the generated emf will be difficult to ascertain at any particular instant of time because of the response time of the suspended coil and of the detector system. This situation leads to the desirability of the condition $dF/dz = 0$, particularly at the beginning and end of its travel. Condition (ii) is desirable because when the velocity is measured, the suspended coil will not have a current flowing through it, but there will be a current present when measuring the force. The heat generated by this current could change the diameter of the suspended coil by as much as 25 ppm/°C. While a heat source could be used to keep the power dissipation in the suspended coil constant, it would be desirable to minimize this systematic error by careful design

With these two fundamental conditions in mind the analytical solution can begin.

The analysis of the classical current balance starts with the following equation which gives the force acting on one current loop by another current loop (see fig. 1) [9].

$$F_z = \frac{I_1 I_2 zk}{\sqrt{a_1 a_2}} [(\frac{2-k^2}{1-k^2}) E - 2K]\pi. \qquad (9)$$

Here, K and E are the complete elliptic integrals of the first and second kind, respectively. The modulus k is

$$k = [\frac{4a_1 a_2}{z^2 + (a_1 + a_2)^2}]^{1/2}. \qquad (10)$$

After some consideration, one soon realizes that the primary magnetic field producing coils of the classical current balance cannot simultaneously meet conditions (i) and (ii) stated above. It will thus be necessary to add "compensation coils" in a configuration such as shown in figure 2. Unfortunately, applying the force equation (9) to such a system and attempting to solve for a configuration satisfying conditions (i) and (ii) is quite difficult. Thus it was decided that a computer would be used to examine many of the possible configurations. After some preliminary calculations the following possibilities were examined, assuming a fixed a_2:

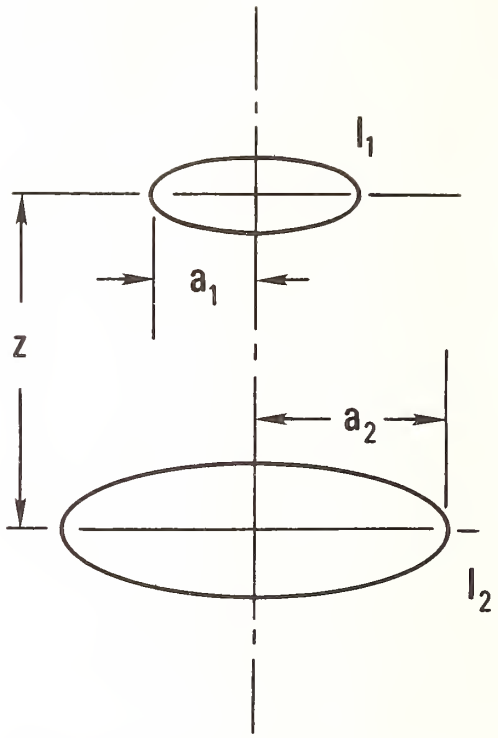

FIGURE 1. *Two coaxial loops are separated by a distance* z.
Current loop 1 has a radius of a_1 and a current of I_1; Current loop 2 has a radius of a_2 and a current of I_2.

$$0 < a_1 \leqslant a_2$$
$$0 < z_1 \text{ to greater than } z_2$$
$$0.2a_2 < z_2 < 2a_2$$
$$-10 < (I_1/I_2) < 10$$

The shaded region of figure 2 was the volume studied to see if solutions consistent with conditions (i) and (ii) existed. The suspended coil of diameter $2a_0$ would be located somewhere in this region.

The immediate results indicated, as would be expected, that there is not a unique solution but that many solutions exist.

What follows is a description of the solution considered to be the most appropriate for the task intended. For ease of discussion, $2a_2$, the diameter of the outer fixed coil, was chosen to be 100 cm but note that once the relative values

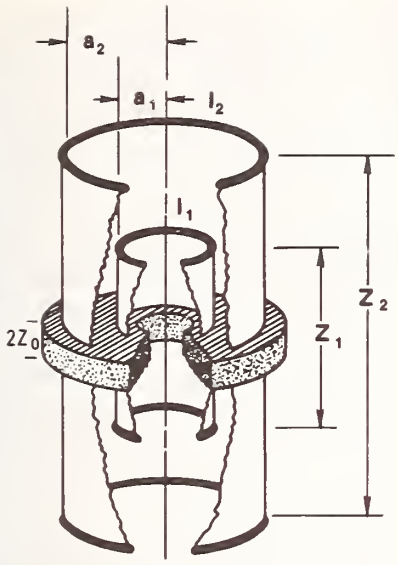

FIGURE 2. *A four coil system consists of two coil pairs.*
The coil pairs are coaxial and concentric. The magnetic fields in the axial direction produced by the upper coils in each pair are opposed by the axial direction magnetic fields produced by the lower coils in each pair. The resultant magnetic field in the shaded region is almost entirely directed in the radial direction. The computer searched the shaded volume for a region where the magnetic field behavior was such that when a current loop, coaxial with the coil pairs, was suspended in the region, the current loop would have a constant vertical force exerted on it regardless of its diameter or vertical position.

for all coil diameters as well as the separation of the fixed coils are determined, the entire apparatus may be scaled up or down without affecting the vertical force exerted on the suspended coil, provided that both the number of windings and the current in the windings remain constant. On the scale chosen, the diameter of the suspended coil at which favorable solutions were found is around 78 cm.

Figure 3 shows the variation in force on the suspended coil as a function of its vertical position for various separations of the coil pairs. All solutions show a similar behavior. The z axis is the vertical displacement of the suspended coil about the mid-plane ($z = 0$) of the fixed coil assembly. The change in force on the suspended coil relative to that at the mid-plane is designated ΔF. The positive position at which $\Delta F/dz = 0$ is defined to be z_0. Thus, the dashed line is the locus of the points z_0. The change in force on the suspended coil at z_0 relative to the force at the mid-plane is designated ΔF_0. The ΔF_0 and z_0 values are determined by separation of the two pairs of fixed coils and can be adjusted by changing z_1 and z_2, the separation of the fixed coil pairs. The curves a through e show the ΔF as a function of z. From one curve to the next (a to e), z_1 and z_2, the separation of the fixed coils, have been increased in the manner indicated. From eq (3), we can see that the change in emf generated for a constant velocity is proportional to ΔF. It is desirable to have ΔF and $\Delta\varepsilon$ as small as possible for accurate measurements of F_{ave} and ε_{ave}. At the same time, it is desirable to have large z_0,

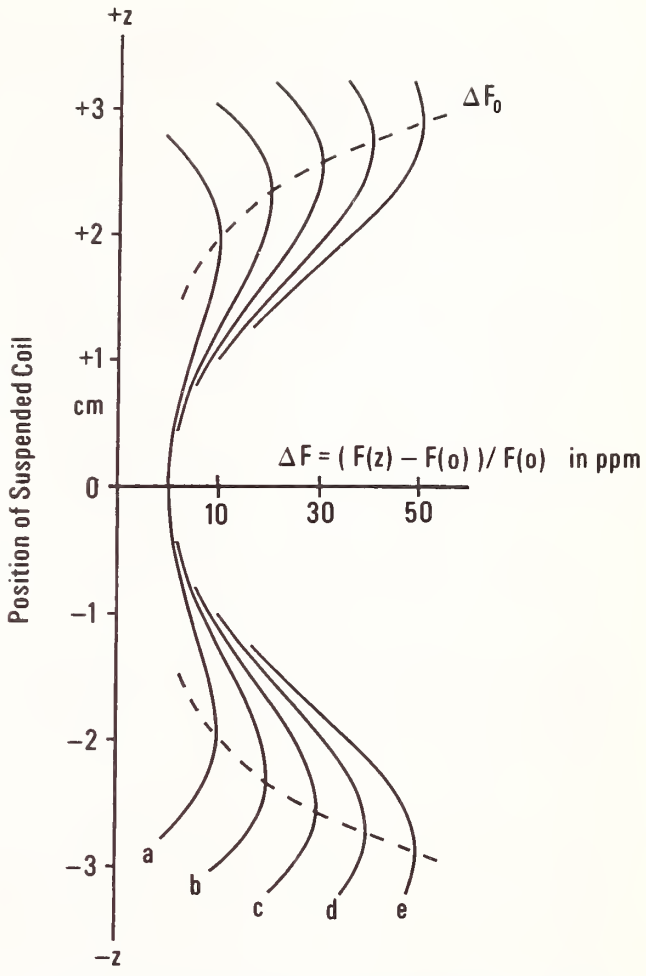

FIGURE 3. *The change in vertical force on the suspended coil is a function of its vertical displacement about the mid-plane of the fixed coil system.*
The object of the fixed coil design is to allow a maximum suspended coil displacement for the least amount of total force change. The dotted line connects the locus of points at which $\Delta F/dz = 0$. While ΔF_0 is the force change in ppm at the point where $\Delta F/dz = 0$ referenced to the mid-plane force.
The ΔF as a function of z was calculated for a coil system where $a_1 = 11$ cm, $a_2 = 50$ cm, $I_1/I_2 = 5.5438$, a_0 (the radius of the suspended coil) = 39 cm.

Curve	ΔF_0 (ppm)	z_2 (cm)	z_1 (cm)
a	10	87.6836	51.5370
b	20	87.8432	51.6166
c	30	87.9702	51.6796
d	40	88.0794	51.7336
e	50	88.1768	51.7816

since the total coil displacement $2z_0$ must be measured accurately. Therefore we must compromise between the desire for a large z_0 and a small ΔF_0.

Figure 4a shows the solutions for the separation of the fixed coils. The abscissa is the diameter of the inner fixed coil $2a_1$. The ordinate on the left side is the separation of the outer coils z_2 and the ordinate on the right side is the separate of the inner fixed coils z_1. For $2a_1$ greater than 24.0 cm, there is a gradual deterioration of the features desirable

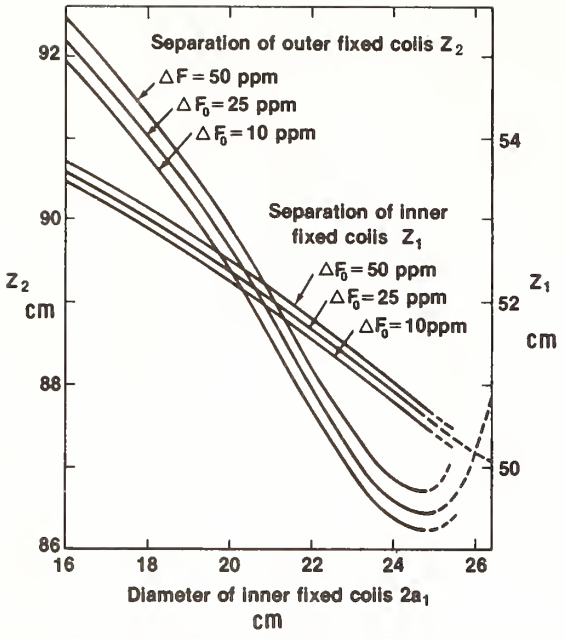

FIGURE 4a. For a fixed $2a_2$, *the diameter of the outer fixed coils, the separation of the fixed inner and outer coils* z_1 *and* z_2 *can be plotted as a function of* $2a_1$, *the diameter of the inner fixed coils.*

For a $2a_1$ greater than about 25 cm, z_2, the separation of the outer fixed coils, increases very rapidly.

for a working current balance. Specifically, the force becomes increasingly sensitive to changes in the diameter of the suspended coil. Three curves are shown for each coil separation corresponding to a ΔF_0 of 10, 25 and 50 ppm (as labeled). The next figure (fig. 4b) shows the working length or total usable distance $2z_0$ that the suspended coil can travel. The abscissa is $2a_1$, the diameter of the inner fixed coils. The total usable length is shown for a $\Delta F_0 = 10$, 25, and 50 ppm. The usable length decreases slightly for an increase in $2a_1$ but the change is really insignificant. For a further increase in ΔF_0, the total usable length of travel of the suspended coil does not increase significantly.

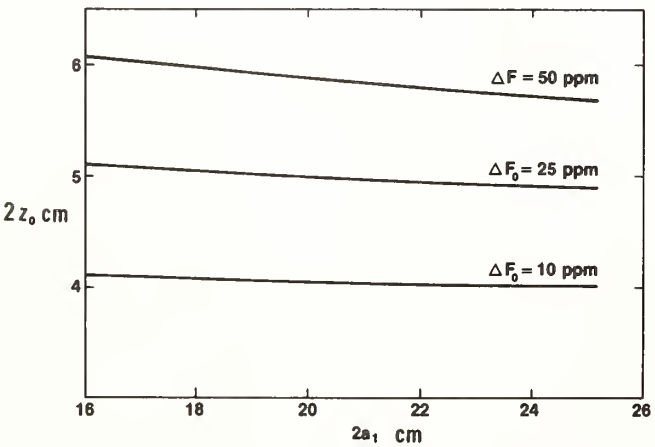

FIGURE 4b. *The total measurable length* $2z_0$ *as a function of* ΔF_0 *is plotted against* $2a_1$, *the diameter of the inner fixed coils.*

While there is a decrease in $2z_0$ for an increase in $2a_1$, the decrease is not significant.

For ease in operation, it would be desirable to have the same current passing through all of the fixed coils. It has been determined, though, that for a specific force to be exerted on the suspended coil for a given current in the fixed coils, that the number of turns of wire on each pair of fixed coils is a function of the diameter ($2a_1$) of the inner fixed coils. Figure 4c gives the required turns ratio (N_1/N_2) of inner fixed coils to outer fixed coils as well as the number of turns required on the outside fixed coils N_2 as a function of $2a_1$. The abscissa is $2a_1$. The left ordinate is the turns ratio while the right ordinate is the number of turns on each outer fixed coil.

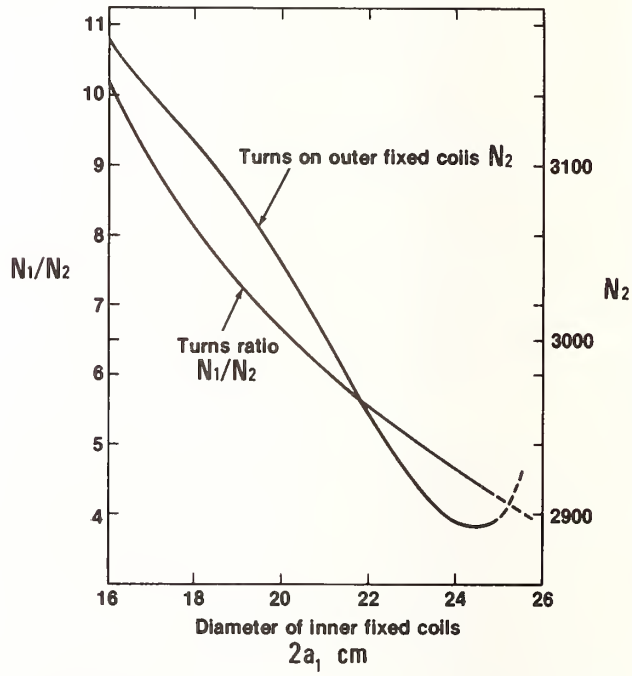

FIGURE 4c. *The number of turns of wire required on each of the fixed coils are plotted with respect to* $2a_1$, *the diameter of the inner fixed coils.*

The current in the wire as well as the vertical force on the suspended coil are constant. Clearly the most advantageous design would call for an inner coil diameter of about 24 cm. For this choice the total wire necessary for both the inner and outer fixed coil is the least.

Figures 4 *a*, *b*, and *c* contain the necessary information required to build the field coils of a current balance. It was previously stated that a deterioration takes place for $2a_1$, inner fixed coil diameter, much greater than 24 cm. For $2a_1$ less than 16 cm, solutions continue but from figure 4c, one can see that the number of turns on the inner fixed coils increases very rapidly without benefit; therefore it is impractical to consider a further decrease in $2a_1$. On the other hand, a larger $2a_1$ decreases the total number of turns on both coils. As an example, for $2a_1 = 20$ cm, each of the outer fixed coils contains 3043 turns and the inner fixed coils contain 20,169 turns. For $2a_1 = 24$ cm, each of the outer fixed coils contains 2895 turns and the inner fixed coils contain 13,518 turns. This corresponds to about 6000 m less wire. As for the current in these windings, 0.6 A pro-

duces a force of 0.049 N on the suspended coil when the suspended coil is energized with 10 Ampere-turns (At). Correspondingly 6 A generates a 0.49 N force and 60 A generates 4.9 N. Upon a current reversal of the 10 At in the suspended coil the counter-balancing mass required is 10, 10^2, and 10^3 g respectively.

4. Coil geometry evaluation

Figures 5a, b, and c show the force gradient over the area of interest where the maximum ΔF_0 on the suspended coil is approximately 10, 25, and 50 ppm respectively. The change in the force is plotted based on the calculated force exerted on a "test" circular filament whose diameter is allowed to expand from $2a_0 - 2$ cm (76 cm) to $2a_0 + 2$ cm (80 cm). The test filament is also displaced vertically about the mid-plane ($z = 0$) to 3 cm above and below the mid-plane ($z = +3$ cm and -3 cm). The radial distance, a_0, on the plane corresponds to the radius of the suspended coil. The dotted line shows the path of the suspended coil as it travels vertically about $z = 0$. Only the negative travel is shown since the force gradients are symmetrical about the mid-plane. The change in the peak ΔF_0 occurs by changing only the spacings z_1 and z_2. The vertical force of course does decrease when the coil spacings are increased, about 0.6 percent from $\Delta F_0 = 10$ ppm to $\Delta F_0 = 50$ ppm. This decrease can be then corrected by increasing the current in the fixed coils.

5. Current balance specifics

From figures 5a, b, and c, it can be seen that the extent of available travel $2z_0$ of the suspended coil varies from about 4 cm for a ΔF_0 of 10 ppm to about 6 cm for a ΔF_0 of 50 ppm. This distance must be accurately measured and pretty well sets the scale of the apparatus to be built. For a total vertical travel of the suspended coil from $z = -3$ cm to $z = +3$ cm, an uncertainty of 0.01 μm in the displacement will yield a corresponding experimental uncertainty of 0.17 ppm for the case where ΔF_0 is a maximum of 50 ppm.

The dimensions of the apparatus used in all of the following evaluation calculations are:

The diameter of the outer fixed coils ($2a_2$) is 1.0 m.
The diameter of the inner fixed coils ($2a_1$) is 0.22 m.
The diameter of the suspended coil ($2a_0$) is 0.78 m.
The separation of the outer fixed coils (z_2) is 0.879 m.
The separation of the inner fixed coils (z_1) is 0.517 m.
The current ratio or turns ratio (N_1 of the inner fixed coil to that of the outer fixed coils is 5.54.

17.75×10^4 Ampere-turns on the outer fixed coils and 98.32×10^4 At on the inner fixed coils will produce a force on the suspended coil that can be counter-balanced by a mass of 1 kg when the suspended coil contains 10 At.

The magnetic field of the fixed coils will generate a one volt d.c. signal across the suspended coil when the suspended coil containing 4081 turns traverses in the axial direction at a constant velocity of 0.5 mm/s. A current of 2.45 mA in such a suspended coil is required to produce a force that will support a mass of 1 kg.

Obviously, the specifications just presented will require that the fixed coils of the current balance be superconducting. A current of 60 A in the fixed coils will require that there be 2960 turns on the outer fixed coils and 16,390 turns on the inner fixed coils. The fixed coils are not very unusual and should not be difficult to produce.

The suspended coil does present a problem if it is also to be at cryogenic temperatures. Since the balance will have to be at room temperature along with the standard mass, some feed-through system would have to be devised which would transfer the force on the suspended coil up to the balance arm. The suspended coil cannot be in the liquid helium but will have to be in a separate vessel and helium gas used to carry away the heat. An alternate method is to have the suspended coil in its own special dewar with that dewar suspended from the balance beam. The first method allows the laser interferometer optical components to be directly mounted onto the coil forms. The index of refraction, however, will have to be continuously monitored. The second method will have the interferometer optical components attached to the outside of the dewar. This will introduce an additional uncertainty in the measurements of length. The index of refraction however can be more easily monitored.

A third method is to have the suspended coil at room temperature. Certainly a room temperature suspended coil greatly reduces the mechanical difficulties and should be seriously considered.

The total length of wire needed on the suspended coil is 10,000 m. With AWG 36 gauge oxygen free high conductivity copper wire, the resistance is 13.6 kΩ. Measuring the generated d.c. emf with a 50 Hz band width limits the accuracy to about 0.1 ppm due to Johnson noise. However integrating the voltage over a 120 *s* period limits the experimental accuracy to about 0.002 ppm. When weighing, the current will produce about 90 mW of heating. This power will increase the temperature of the coil by less than 0.03 °C. Such a room temperature coil will have a mass of about 2.2 kg assuming the copper wire to be wound on a bobbin of low-expansion glass. Such a system is very appealing to start with and exhibits the possibility of reducing the uncertainty in K_A by an order of magnitude immediately. On the other hand, one can imagine the ultimate current balance having the suspended coil at cryogenic temperatures. Such a system would compare the generated emf directly to the output voltage of a Josephson junction at the 5 mV level. Whereas

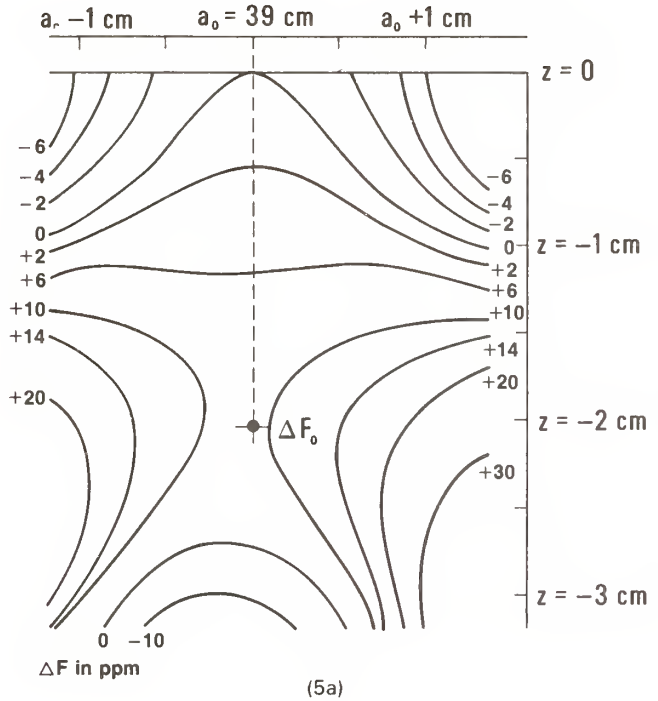

(5a)

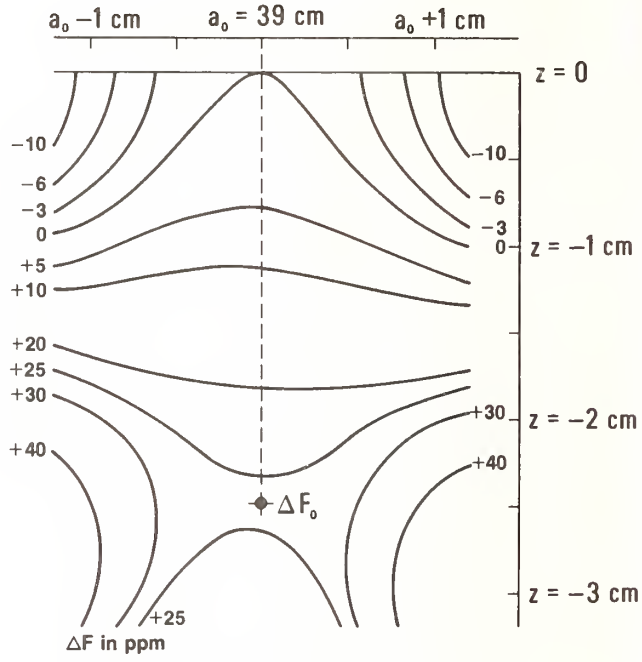

(5b)

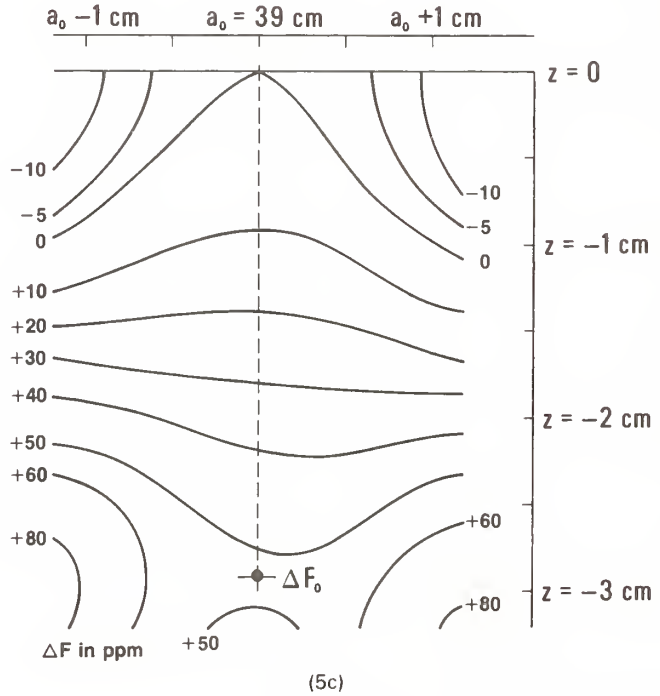

(5c)

FIGURE 5. *Figures a, b, and c show the computed force on a test current filament, coaxial with the fixed coils, whose radius a_0 is permitted to change from 38 to 40 cm.*

This test filament is at the same time displaced vertically from the mid-plane ($z = 0$) to + and − 3 cm. At the mid-plane position the vertical force on the current filament is a maximum at $a_0 = 39$ cm. For off mid-plane positions, with $a_0 = 39$ cm, the force increases to a maximum at z_0 (indicated by ΔF_0). At this point the ΔF is at a minimum for changes in a_0. The figure 5 mappings were made for a $2a_1$ of about 20 cm but the results are very similar for all $2a_1$ which gave a useful solution.

the room temperature coil has an axial velocity of 0.5 mm/s to generate 1 V with a sampling time of 120 s, the all-cryogenic system would have an axial velocity of 0.0025 mm/s and a sampling time of 24×10^3 s, assuming all other factors remained constant.

6. Effect of Possible Coil Misalignments

It is generally easier to compute results for perfect coils ideally aligned than it is to produce such an assembly. The following are the computed results for various misalignments.

(1) The change in the vertical force on the suspended coil for the case where the midplanes of the inner and outer coil pairs are not coincident turns out to be the most critical (see table 1a). Table 1a shows the change in force in ppm on the suspended coil at the midplane $z = 0$ for misalignments in the axial direction of 0, 0.004, 0.008, 0.012, 0.016, and 0.020 cm. For the suspended coil at vertical positions of 1, 2, 3, and 4 cm away from the midplane, the change in force in ppm is given as the change in force from the midplane position for that particular misalignment. This misalignment superimposes a linear force gradient on the ideal force gradient in the left column. The force at the mid-plane changes a very small amount as indicated at the position $z = 0$ for the displacements of 0.004, etc. For the off mid-plane positions of the suspended coil where $z = 1, 2$ etc., the gradients ΔF from the mid-plane force become quite asymmetric rather rapidly. Fortunately, this misalignment is one which can be measured and perhaps corrected for using techniques from the authors' previous experience in the gamma-p experiment. (10, 11).

(2) Table 1b shows the change in the vertical force on the suspended coil for the case where the inner fixed coil assembly is not coaxial with the outer and suspended coils (radial misalignment). The force gradients are symmetrical about $z = 0$. The change in force at the mid-plane ($z = 0$) is with respect to the force for perfect alignment while the change in force for positions off the mid-plane are with respect to the mid-plane force for that particular misalignment.

TABLE 1a. *The variation in the vertical force on the suspended coil for the case where either the inner or outer fixed coil assemblies are misaligned in the axial direction. The quantity given is ΔF in ppm. The ΔF at $z = 0$ is referenced to the force for perfect alignment, while the ΔF at vertical displacements of the suspended coil is referenced to the force at the mid-plane for that particular misalignment*

Displacement Z (cm) of suspended coil	Misalignment (cm) in axial direction					
	0.000	0.004	0.008	0.012	0.016	0.020
+4	−42.7	−56.0	−69.4	−82.7	−96.1	−109.41
+3	+18.68	+8.93	−0.817	−10.57	−20.32	−30.07
+2	+21.99	+15.62	+9.24	+2.86	−3.51	−9.89
+1	+7.56	+4.41	+1.26	−1.89	−5.04	−8.19
0	0	−0.006	−0.025	−0.056	−0.10	−0.157
−1	+7.56	+10.716	+13.87	+17.02	+20.17	+23.32
−2	+21.99	+28.37	+34.74	+41.12	+47.49	+53.86
−3	+18.68	+28.42	+38.17	+47.91	+57.65	+67.39
−4	−42.7	−29.4	−16.0	−2.719	+10.61	+23.93

TABLE 1b. *The variation in the vertical-force on the suspended coil for the case where the inner fixed coil assembly is misaligned in the radial direction. The quantity given is ΔF in ppm. The ΔF at $z = 0$ is referenced to the force for perfect alignment, while the ΔF at vertical displacements of the suspended coil is referenced to the force at the mid-plane for that particular misalignment.*

Displacement Z (cm) of suspended coil	Misalignment (cm) in radial direction					
	0.0	0.4	0.8	1.2	1.6	2.0
+4	−42.7	−36.9	−19.6	+9.33	+49.9	+102.3
+3	+18.68	+21.97	+31.84	+48.33	+71.47	+101.3
+2	+21.99	+23.47	+27.90	+35.29	+45.67	+59.0
+1	+7.56	+7.94	+9.05	+10.91	+13.52	+16.88
0	0	+31.4	+125	+282	+500	+780

Note: ΔF is symmetrical about the midplane of the coil system.

(3) Table 1c shows the change in vertical force on the suspended coil for the case where the outer fixed coil assembly is not coaxial with the inner and suspended coils (radial misalignment). The change in force at the mid-plane ($z = 0$) is with respect to the force for perfect alignment while the change in force for positions off the mid-plane are with respect to the mid-plane force for that particular misalignment.

(4) Table 1d shows the change in vertical force on the suspended coil for the case where the suspended coil is not coaxial with the inner and outer coils (radial misalignment). It should be noted that the amount of misalignment given in tables 1b–1d is 100 times greater than the axial misalignment of table 1a. The change in force on the suspended coil at the mid-plane for the outer fixed coils radially misaligned is opposite the change in force for the case where the inner fixed coils are radially misaligned. The change in force at the mid-plane ($z = 0$) is with respect to the force for perfect alignment while the change in force for positions off the mid-plane are with respect to the mid-plane force for that particular misalignment. Even though the force change is substantial (some 30 ppm for a 4 mm displacement), there is very little change in the force gradient for the suspended coil being off the mid-plane.

(5) Table 1e shows the change in the vertical force on the suspended coil for the case where the suspended coil is tilted about the center of the system. The change in force at the mid-plane ($z = 0$) is with respect to the force for perfect alignment while the change in force for positions off the mid-plane are with respect to the mid-plane force for that particular misalignment.

(6) Table 1f shows the change in the vertical force on the suspended coil for the case where the outer fixed coil assembly is tilted about the center of the system. The change in force at the mid-plane ($z = 0$) is with respect to the force for perfect alignment while the change in force for positions off the mid-plane are with respect to the mid-plane force for that particular misalignment.

(7) Table 1g shows the change in the vertical force on the suspended coil for the case where the inner fixed coil assembly is tilted about the center of the system. The change in force at the mid-plane ($z = 0$) is with respect to the force for perfect alignment while the change in force for positions off the mid-plane are with respect to the mid-plane force for that particular misalignment.

TABLE 1c. *The variation in the vertical force on the suspended coil for the case where the outer fixed coil assembly is misaligned in the radial direction. The quantity given is ΔF in ppm. The ΔF at z = 0 is referenced to the force for perfect alignment, while the ΔF at vertical displacements of the suspended coil is referenced to the force at the mid-plane for that particular misalignment.*

Displacement Z (cm) of suspended coil	Misalignment (cm) in radial direction					
	0.0	0.4	0.8	1.2	1.6	2.0
+4	−42.7	−42.3	−45.2	−48.4	−52.8	−58.5
+3	+18.68	+18.32	+17.26	+15.48	+12.99	+9.78
+2	+21.99	+21.83	+21.36	+20.57	+19.47	+18.04
+1	+7.56	+7.53	+7.41	+7.21	+6.93	+6.58
0	0	−32.04	−128.2	−288.0	−513.0	−801.0

Note: ΔF is symmetrical about the midplane of the coil system.

TABLE 1d. *The variation in the vertical force on the suspended coil for the case where the suspended coil is misaligned in the radial direction. The quantity given is ΔF in ppm. The ΔF at z = 0 is referenced to the force for perfect alignment, while the ΔF at vertical displacements of the suspended coil is referenced to the force at the mid-plane for that particular misalignment.*

Displacement Z (cm) of suspended coil	Misalignment (cm) in radial direction					
	0.0	0.4	0.8	1.2	1.6	2.0
+4	−42.7	−37.6	−22.1	+3.66	+39.9	+86.6
+3	+18.68	+21.6	+30.4	+45.1	+65.8	+92.5
+2	+21.99	+23.3	+27.3	+33.9	+43.2	+55.1
+1	+7.56	+7.90	+8.89	+10.5	+12.9	+15.9
0	0	−0.67	−2.75	−6.48	−12.3	−20.6

Note: ΔF is symmetrical about the midplane of the coil system.

(8) Table 1h shows the change in the vertical force on the suspended coil for the case where both fixed coil assemblies are tilted as a unit about the center of the system. The change in force at the mid-plane ($z = 0$) is with respect to the force for perfect alignment while the change in force for positions off the mid-plane are with respect to the mid-plane force for that particular misalignment.

Of all the misalignments, the most critical is that where the midplanes of the fixed coil pairs do not coincide. The least critical alignment apparent in the vertical force on the suspended coil is where the suspended coil is either radially or angularly misaligned.

TABLE 1e. *The variation in the vertical force on the suspended coil for the case where the suspended coil is tilted about the center of the system. The quantity given is ΔF in ppm. The ΔF at z = 0 is referenced to the force for perfect alignment, while the ΔF at vertical displacements of the suspended coil is referenced to the force at the mid-plane for that particular misalignment.*

Displacement Z (cm) of suspended coil	Tilt in degrees									
	0.0	0.2	0.4	0.6	0.8	1.0	2.0	4.0	6.0	8.0
+4	−42.7	−43.1	−44.9	−47.9	−52.1	−57.5	−102.0	−283.0	.....	.....
+3	+18.68	+18.28	+17.28	+15.56	+13.20	+10.12	−15.45	−118.0	−290.0	.....
+2	+21.99	+21.61	+21.16	+20.41	+19.35	+17.97	+6.51	−39.4	−116.0	−225.0
+1	+7.56	+7.41	+7.30	+7.11	+6.85	+6.50	+3.62	−7.90	−27.2	−54.0
0	0	+0.0076	+0.30	+0.67	+1.18	+1.85	+6.76	+16.4	−3.47	−108.0

Note: ΔF is symmetrical about the midplane of the coil system.

TABLE 1f. *The variation in the vertical force on the suspended coil for the case where the outer fixed coil assembly is tilted about the center of the system. The quantity given is ΔF in ppm. The ΔF at z = 0 is referenced to the force for perfect alignment, while the ΔF at vertical displacements of the suspended coil is referenced to the force at the mid-plane for that particular misalignment.*

Displacement Z (cm) of suspended coil	Tilt in degrees					
	0.0	0.2	0.4	0.6	0.8	1.0
+4	−42.7	−42.6	−42.6	−42.7	−42.8	−42.9
+3	+18.68	+18.56	+18.54	+18.49	+18.51	+18.43
+2	+21.99	+21.71	+21.78	+21.69	+21.76	+21.72
+1	+7.56	+7.40	+7.45	+7.38	+7.45	+7.44
0	0	−1.39	−5.75	−12.94	−23.08	−36.09

Note: ΔF is symmetrical about the midplane of the coil system.

TABLE 1g. *The variation in the vertical force on the suspended coil for the case where the inner fixed coil is tilted about the center of the system. The quantity given is ΔF in ppm. The ΔF at z = 0 is referenced to the force for perfect alignment, while the ΔF at vertical displacements of the suspended coil is referenced to the force at the mid-plane for that particular misalignment.*

Displacement Z (cm) of suspended coil	Tilt in degrees					
	0.0	0.2	0.4	0.6	0.8	1.0
+4	−42.7	−43.1	−44.9	−48.0	−52.0	−57.4
+3	+18.68	+18.28	+16.80	+15.87	+18.08	+10.53
+2	+21.99	+21.93	+21.28	+20.54	+19.65	+18.42
+1	+7.56	+7.34	+7.24	+7.09	+6.88	+6.82
0	0	−4.50	−18.1	−41.1	−73.2	−114.7

Note: ΔF is symmetrical about the midplane of the coil system.

TABLE 1h. *The variation in the vertical force on the suspended coil for the case where the entire fixed coil assembly is tilted about the center of the system. The quantity given is ΔF in ppm. The ΔF at z = 0 is referenced to the force for perfect alignment, while the ΔF at vertical displacements of the suspended coil is referenced to the force at the mid-plane for that particular misalignment.*

Displacement Z (cm) of suspended coil	Tilt in degrees					
	0.0	0.2	0.4	0.6	0.8	1.0
+4	−42.7	−43.2	−44.9	−48.1	−52.3	−57.8
+3	+18.68	+18.20	+16.71	+15.73	+12.96	+10.33
+2	+21.99	+21.87	+21.29	+20.46	+19.64	+18.38
+1	+7.56	+7.30	+7.25	+7.03	+6.88	+6.83
0	0	−5.90	−23.86	−54.08	−96.3	−150.7

Note: ΔF is symmetrical about the midplane of the coil system.

7. Non Vertical Forces

Perhaps even more important than the change in vertical forces for coil misalignment, is the unmeasured horizontal forces acting on the suspended coil. In the calibrating part (the measuring of the generated emf) of the experiment, a horizontal force translates into an error emf if there is any horizontal velocity. This "horizontal" emf adds directly to the vertical emf and becomes an error in the force calibration unless it is properly accounted for.

Table 2a shows the horizontal force on the suspended coil for a misalignment in the radial direction of the suspended coil and for vertical positions of the suspended coil up to $z = 4$ cm from the mid-plane of the system. The horizontal force is an odd function about the mid-plane. The forces given here are in parts per million (ppm) of the vertical force. The sign indicates direction i.e. if negative, the force is away from the central position, positive is a restoring force. Of course if the direction of current is reversed in the suspended coil then the direction of all forces is reversed.

Table 2b is a tabulation of horizontal forces for the case where the suspended coil is tilted. Results are shown for tilts up to 2 degrees. The force is perpendicular to the axis of rotation of the coil. The horizontal force is given in ppm of the vertical force for perfect alignment.

The classical current balance configuration has the characteristic that when there is just angular (tilt) misalignment, there is no torque on the suspended coil at the mid-plane. Table 3a summarizes the torques present on the suspended coil when the only misalignment is a tilt over the coil range of vertical displacement of the suspended coil from $z = +4$ cm to -4 cm. The values given are in units of length (μm). The torque is normalized to the vertical force of the perfectly aligned system.

Table 3b shows the torque for the case where the inner fixed coil pair is tilted. Table 3c shows the torque for the case where the outer fixed coil pair is tilted. These torques are opposite and tend to cancel when it is the entire fixed coil assembly that is tilted.

TABLE 2a. *Ratio of horizontal force to vertical force (in ppm) on the suspended coil for the case where the suspended coil is misaligned in the radial direction.*

Displacement Z (cm) of suspended coil	Misalignment (cm) in the radial direction									
	0.0	0.1	0.2	0.3	0.4	0.5	0.8	1.2	1.6	2.0
+4	0.0	−10.7	−21.2	−31.4	−41.1	−49.9	−70.2	−75.2	−43.7	+37.5
+3	0.0	−2.4	−4.7	−6.7	−8.2	−9.2	−7.2	−12.5	+60.4	+146.5
+2	0.0	+1.1	+2.3	+3.7	+5.4	+7.5	+17.2	+41.6	+85.2	+154.8
+1	0.0	+1.4	+2.8	+4.4	+6.0	+7.9	+15.2	+30.9	+56.2	+94.7
0	0.0	0.0	0.0	0.0	0.0	0.0	0.0	0.0	0.0	0.0
−1	0.0	−1.4	−2.8	−4.4	−6.0	−7.9	−15.2	−30.9	−56.2	−94.7
−2	0.0	−1.1	−2.3	−3.7	−5.4	−7.5	−17.2	−41.6	−85.2	−154.8
−3	0.0	+2.4	+4.7	+6.7	+8.2	+9.2	+7.2	+12.5	−60.4	−146.5
−4	0.0	+10.7	+21.2	+31.4	+41.1	+49.9	+70.2	+75.2	+43.7	−37.5

TABLE 2b. *Ratio of horizontal force to vertical force (in ppm) on the suspended coil for the case where the suspended coil is tilted about the center of the system.*

Displacement Z (cm) of suspended coil	Tilt in degrees					
	0.0	0.4	0.8	1.2	1.6	2.0
+4	0.0	+3.9	+8.1	+12.4	+17.2	+22.7
+3	0.0	+0.90	+1.9	+3.0	+4.4	+6.1
+2	0.0	−0.03	−0.02	+0.06	+0.25	+0.58
+1	0.0	−0.09	−0.17	−0.23	−0.27	−0.27
0	0.0	−0.03	−0.05	−0.08	−0.11	−0.14

Note: The force ratio is symmetrical about the midplane of the coil system.

TABLE 3a. *Ratio of torque to vertical force acting on suspended coil (unit of μm) for the case where the suspended coil is tilted about the center of the system.*

Displacement Z (cm) of suspended coil	Tilt in degrees						
	0.0	0.2	0.4	0.6	0.8	2.0	4.0
+4	0.0	−13.8	−27.6	−41.4	−55.4	−135.8	−264.1
+3	0.0	−10.5	−20.9	−31.4	−41.9	−103.0	−200.5
+2	0.0	−7.04	−14.1	−21.1	−28.1	−69.2	−134.8
+1	0.0	−3.54	−7.07	−10.6	−14.1	−34.8	−67.8
0	0.0	0.0	0.0	0.0	0.0	+0.0	0.0
−1	0.0	+3.54	+7.07	+10.6	+14.1	+34.8	+67.8
−2	0.0	+7.04	+14.1	+21.1	+28.1	+69.2	+134.8
−3	0.0	+10.5	+20.9	+31.4	+41.9	+103.0	+200.5
−4	0.0	+13.8	+27.6	+41.4	+55.4	+135.8	+264.1

TABLE 3b. *Ratio of torque to vertical force acting on suspended coil (unit of μm) for the case where the inner fixed coil is tilted.*

Displacement Z (cm) of suspended coil	Tilt in degrees				
	0.0	2.0	4.0	6.0	8.0
+4	0.0	+34.0	+69.0	+106.4	+147.2
+3	0.0	+24.1	+49.0	+75.6	+104.8
+2	0.0	+15.4	+31.3	+48.4	+67.2
+1	0.0	+7.5	+15.2	+23.6	+32.8
0	0.0	0.0	0.0	0.0	0.0
−1	0.0	−7.5	−15.2	− 23.6	−32.8
−2	0.0	−15.4	−31.3	− 48.4	−67.2
−3	0.0	−24.1	−49.0	−75.6	−104.8
−4	0.0	−34.0	−69.0	−106.4	−147.2

TABLE 3c. *Ratio of torque to vertical force acting on suspended coil (in units of μm) for the case where the outer fixed coil is tilted.*

Displacement Z (cm) of suspended coil	Tilt in degrees				
	0.0	2.0	4.0	6.0	8.0
+4	0.0	−169.8	−333.2	−483.6	−613.6
+3	0.0	−127.1	−249.5	−362.2	−460.1
+2	0.0	−84.6	−166.1	−241.3	−306.6
+1	0.0	−42.3	−83.0	−120.6	−153.3
0	0.0	0.0	0.0	0.0	0.0
−1	0.0	+42.3	+83.0	+120.6	+153.3
−2	0.0	+84.6	+166.1	+241.3	+306.6
−3	0.0	+127.1	+249.5	+362.2	+460.1
−4	0.0	+169.8	+333.2	+483.6	+613.6

Table 3d shows the torque on the suspended coil when there is a misalignment in the radial direction between the fixed coil assembly and the suspended coil. This torque is by far the largest of all the other torques calculated. The torque is relatively constant over the expected vertical positions of the suspended coil and increases fairly linearly with increased misalignment.

Most of the effects of coil misalignment are small, but they will have to be monitored and corrections will have to be applied. For the case of vertical forces, if perfect alignment is not possible, the experimental accuracy will be unaffected, as long as the misalignment does not change during the course of operation. The chance for a change in alignment can develop during the measurement of voltage.

TABLE 3d. Ratio of torque to vertical force acting on suspended coil (in units of μm) for the case where the suspended coil is misaligned in the radial direction.

Displacement Z (cm) of suspended coil	Tilt in degrees					
	0.0	0.2	0.4	0.6	0.8	1.0
+4	0.	849	1696	2546	3396	4248
+3	0	849	1698	2548	3398	4250
+2	0	849	1698	2548	3399	4251
+1	0	849	1698	2548	3399	4250
0	0	849	1698	2548	3398	4250

Note: ΔF is symmetrical about the midplane of the coil system.

In this instance, the suspended coil will be changing its axial position at a uniform velocity with respect to the fixed coils. This action can occur by displacing the fixed coils, by displacing the suspended coil through movement of the entire balance, or by allowing the balance to swing. Either of the three methods will require a positive servo system to either keep the velocity constant or the generated emf constant. Certainly, the swinging of the balance is the most attractive since it requires the least effort. The swinging of the balance however naturally produces a misalignment in the radial direction of the suspended coil when it travels from $+z_0$ to $-z_0$. Depending upon the length of the balance beam, though, this displacement can be kept small. For a balance beam with a half length of 40 cm, the maximum radial displacement is about 0.11 cm. From Table 2a, it can be found that the horizontal force is about 2.6 ppm of the vertical force. This horizontal force results in an additional displacement of less than 1 μm when the vertical distance from the knife edge to the suspended coil is 1 m. The horizontal force produced is a negligible error in the vertical force measurement. However, this horizontal force translates into a generated emf into the suspended coil during the calibration part of the experiment and yet does not add to the vertical force. This is a potential systematic error if not properly taken into account.

The maximum calculated horizontal velocity is 3.75×10^{-3} cm/s as compared to the vertical velocity of 5×10^{-2} cm/s. This will increase or decrease the emf measured at the end points by 0.195 μV in one volt. If the initial velocity is negative at $z = +3$ and the Δemf is positive then the Δemf will also be positive at $z = -3$. Therefore a systematic error will result and a correction must be applied. This correction can be calculated from a measurement of the horizontal force.

8. Conclusion

The first part of the experiment involves calibrating the force balance through the measurement of a d.c. voltage and a velocity. Both of these measurements are difficult but possible at the 0.1 ppm level of uncertainty.

The second part of the experiment, "weighing the force", will be relatively easy. Considering that the mass of the suspended coil will be approximately 2.2 kg and the vertical electromagnetic force will be counter-balanced by mass of 1.0 kg, a weighing to 5×10^{-9} (16 μg) will result in an uncertainty of 0.02 ppm in the force measurement. While a guest worker at NBS, Mr. H. Nakamura of the Electrotechnical Laboratory, Japan developed a very good servo-system for the NBS current balance [10]. Mr. Nakamura's contribution will certainly allow the force to be weighed to 0.02 ppm or better.

We hope that the apparatus outlined above (resembling fig. 6) will resolve the confusion that now exists in present determinations of K_A. The undertaking is a large scale experiment with much apparatus to be constructed. The exact time required for achieving the ultimate accuracy in the experiment is not easily determinable, nor is the ultimate ac-

General Appearance of Compensated Current Balance

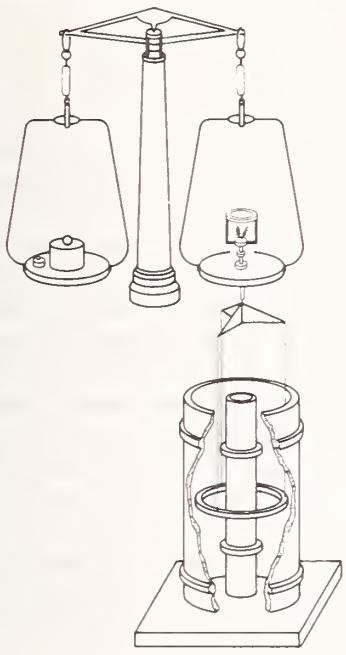

(not to scale)

FIGURE 6. *The general appearance of the compensated current balance is shown.*

The mass on the left scale pan of the halance is sufficient to counterbalance the mass of the suspended coil plus the downward vertical force exerted on the suspended coil. When the current in the suspended coil is reversed, then a mass M is added to the right scale pan to offset the upward vertical force. Thus the mass M is sufficient to counterhalance the upward vertical force plus the negative of the downward vertical force.

curacy itself. However, with reasonable support, it may be expected that a value with an uncertainty in the neighborhood of a few tenths ppm is possible within a few years.

The new ampere measurement will not only help resolve the discrepancies which now exist among several fundamental constant determinations, but will also enable the present value of $2e/h$ used for volt monitoring applications to be brought closer to its absolute value in terms of mass, length, and time. In the future, the sensitivity of the apparatus can be used to monitor the stability of the kilogram with respect to time, by utilizing the stability of the Josephson voltage standard and the calculable capacitor. Since the force developed is sufficient to counterbalance one kilogram with only 2 mA in the suspended coil, the apparatus can be used to calibrate other mass standards in terms of the kilogram by merely determining a current ratio.

Even though the absolute ampere experiment as outlined above is an ambitious project, one must consider that the authors propose to measure the ampere to an accuracy 50 times better than it has ever been measured, and that absolute ampere determinations have a 100 year history of effort. Advances do not come easily.

The authors wish to thank Mr. Robert E. Kleimann and Mrs. Sheila A. Taylor for their assistance in writing the computer programs and in the operation of the computer.

9. Appendix A

The derivations leading to equation 8 can also be described in an integral form. This integral approach is very useful because the quantities that come into the final result are more easily measured in the laboratory.

The force in the z direction between two coils of a mutual inductor is given by

$$F_z = I_1 I_2 (\partial M_{12}/\partial z) \tag{A1}$$

The integral of this force from an initial position z_i to a final position z_f is:

$$\int_{z_i}^{z_f} F_z dz = I_1 I_2 [M_{12}(z_f) - M_{12}(z_i)]. \tag{A2}$$

The emf generated in coil 1 when a current I_2 is in coil 2 is

$$\varepsilon_1(t) = -I_2(dM_{12}/dt) \tag{A3}$$

which can be integrated from time t_1 to t_2:

$$\int_{t_1}^{t_2} \varepsilon(t) dt = -I_2 [M_{12}(t_2) - M_{12}(t_1)]. \tag{A4}$$

Now if t_1 is the time the moving coil passes the position z_i and t_2 the time the coil pass z_f then we can divide eq (A2) by eq (A4)

$$I_1 = \left(\int_{z_i}^{z_f} F_z dz \Big/ \int_{t_1}^{t_2} \varepsilon_1(t) dt\right) \tag{A5}$$

This is the integral form of eq (3) and can be written explicitly in terms of NBS units so that eq (8) becomes

$$K_A \equiv (A_{NBS}/A) = \left[\frac{\int_{z_i}^{z_f} m(z) g dz}{I_{NBS}(\Omega_{NBS}/\Omega)\int_{t_i}^{t_f} \varepsilon_{NBS}(t) dt}\right]^{1/2} \tag{A6}$$

The $\int_{z_i}^{z_f} m(z) g\, dz$ is computed from many static weighings made along the path from z_i to z_f with a current I_{NBS} in the balance coil. The $\int_{t_1}^{t_2} \varepsilon_{NBS}(t) dt$ is measured in a separate experiment when the coil is moved from position z_i to z_f in a time $t_1 - t_2$ at a nearly constant velocity and the current I_{NBS} is not flowing in coil 1. The geometry and the current of coil 2 must remain unchanged during all these measurement or an appropriate correction must be made.

10. Appendix B

An interesting variation on this method for measuring the ampere occurs if one restricts the moveable coil to a single, rotational degree of freedom. Such a rotatable coil placed in the nearly uniform field produced by an external circuit forms the basis of the classic electrodynamometer or Pellat balance [3]

The torque on the rotatable coil is given by

$$T(\theta) = I_1 I_2 (dM_{12}/d\theta) \tag{B1}$$

where I_1 and I_2 are the currents in the external and rotatable circuits respectively, M_{12} is the mutual inductance and θ is the rotation angle. The integral of this torque in moving the coil betwen two angles is then

$$W = \int_{\theta_i}^{\theta_f} T(\theta)d\theta = I_1 I_2 \int_{\theta_i}^{\theta_f} dM_{12} = I_1 I_2 [M_{12}(\theta_f) - M_{12}(\theta_i)] \tag{B2}$$

If the coil is now allowed to rotate with its circuit open, the magnitude of the emf generated is

$$\varepsilon(t) = I_1 (dM_{12}/dt) \tag{B3}$$

Integrating this emf over time one obtains

$$\int_{t_1}^{t_2} \varepsilon(t)dt = I_1 \int_{t_i}^{t_f} dM_{12} = I_1 [M_{12}(t_2) - M_{12}(t_1)] \tag{B4}$$

If t_1 and t_2 are the times when the coil is at angles θ_i and θ_f of eq (B2) we may divide eq (B2) we may divide eq (B2) by eq (B4) to obtain

$$I_1 = \int_{\theta_i}^{\theta_f} T(\theta)d\theta / \int_{t_1}^{t_2} \varepsilon(t)dt \tag{B5}$$

Since the numerator of eq (B5) is just the work done by the electrical torque in rotating the coil between θ_i and θ_f, it can be replaced with any equivalent expression for this work. In particular, this work is equal to the work done by a vertical external force applied at the end of a balance beam attached to the moveable coil when that external force just balances the electrical force. This force is what can be measured experimentally by weighing. Expressed this way eq (B5) becomes

$$I_1 = \int_{z_i}^{z_f} F_z(z)dz / \int_{t_1}^{t_2} \varepsilon(t)dt, \tag{B6}$$

where z_i and z_f are the vertical positions of the end of the balance arm at angles θ_i and θ_f. This is identical to eq (A5) and leads directly to eq (A6) for K_A.

A major disadvantage of the method described in this appendix is that the force and the emf depend directly on the area of the moveable coil, in contrast to the geometry described in the body of the text, where they are essentially independent of the area of the moveable coil. Because of this, temperature control problems are more critical for the rotating coil. On the other hand, the rotary coil has the advantage of being constrained to move with one degree of freedom. As a result problems of non-vertical forces and torques which must be considered in the coil system described in the text do not affect the rotating coil. Since no displacements other than rotation are allowed, no emf's are generated and no work is done other than by the forces explicity considered.

11. Appendix C

The true current balance field coils will have windings of finite cross section. Below, results and specifications have been tabulated for field coils which must provide enough radial magnetic field to exert a vertical force of 4.9 N on a circular filament of 78 cm diameter containing a 10 ampere current.

The outer field coil consists of a bundle of square cross section containing 54 × 54 of 0.0508 cm diameter conductors. The mean diameter of the coil is 100 cm.

The inner field coil consists of a bundle of rectangular cross section containing 115 (radial) × 116 (axial) of 0.0508 cm diameter conductors. The mean diameter of the coil is 24 cm.

Table C1.

z_2 (cm)	z_1 (cm)	I_2A	I_1/I_2	ΔF_0 (ppm)	$2\Delta z_0$ (cm)
86.1186	50.6786	59.1834593	1.0021216	7.1	3.5
86.2328	50.7328	59.2713175	1.0019726	12.3	3.9
86.3470	50.7848	59.3612670	1.0017318	19.2	4.5
86.5090	50.8712	59.4762047	1.0019700	33.2	5.1
86.5710	50.9024	59.5219867	1.0019812	39.2	5.4
86.6292	50.9314	59.5652223	1.0019806	45.4	5.6
86.7336	50.9832	59.6429316	1.0019745	58.0	6.2
86.8282	51.0302	59.7132118	1.0019770	70	6.3

12. Appendix D

The coincidence of the mid-planes of each of the two coil pairs is the most critical alignment. A misalignment, in the axial direction, of the mid planes by as much as 0.004 cm begins to introduce an undesirable linear gradient in the force along the z-direction. This misalignment could be correctable by mechanically adjusting either coil pair along the axis. However figure D-1 shows the positions of correction coils which provides the ability to effectively "reposition" the large field coils by + or − 0.2 cm in the axial or z-direction electrically. Table D-1 gives the ampere-turns, as a percent of the ampere-turns of the main coil, required to effectively reposition one of the large diameter field coils in the axial direction. Each correction coil has the same number of turns. Electrically they are connected in opposition.

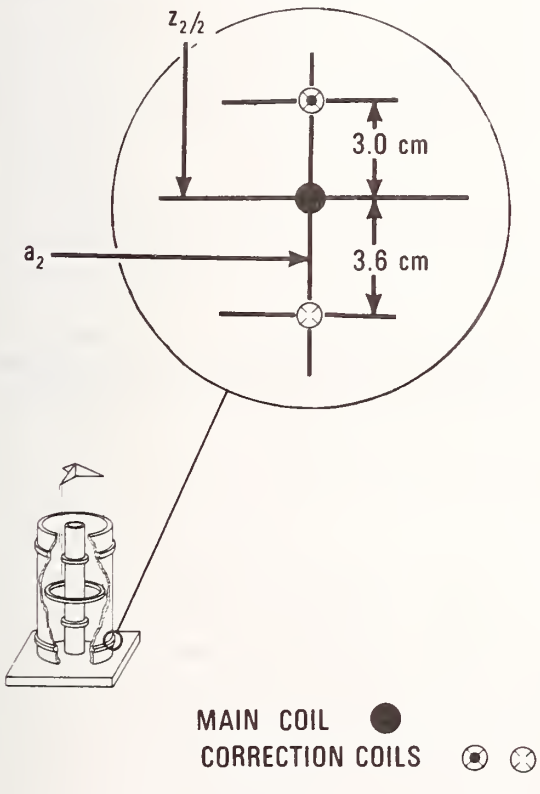

FIGURE D-1.

TABLE D-1

Coil misalignment in cm	correction coil ampere-turns in percent of main ampere-turns
−0.20	−3.04519
−0.15	−2.28639
−0.10	−1.52593
−0.05	−0.76380
+0.05	+0.76547
+0.10	+1.53262
+0.15	+2.30145
+0.20	+3.07197

13. References

[1] Driscoll, R. L., and Cutkosky, R. D. Measurement of Current with the National Bureau of Standards Current Balance, J. Res. Nat. Bur. Stand. (U.S.), Vol. **60**, No. 4, 297-305 (April 1958).

[2] Curtis, H. L., Curtis, R. W., and Critchfield, C. L. An Absolute Determination of the Ampere, Using Improved Coils, J. Res. Nat. Bur. Stand. (U.S.), Vol. **22**, 485-517 (May 1939).

[3] Driscoll, R. L. Measurement of Current with a Pellat-Type Electrodynamometer, J. Res. Nat. Bur. Stand. (U.S.), Vol. **60**, No. 4, 287-296 (April 1958).

[4] Driscoll, R. L., and Olsen, P. T. report to Comite Consultatif d'Electricite, Comite International des Poids at Measures, 12th Session, (1968).

[5] Taylor, B. N. Is the Present Realization of the Absolute Ampere in Error, Metrologia **12**, 81 (1976).

[6] Kibble, B. P., and Robinson, I. Feasibility Study for a Moving Coil Apparatus to Relate the Electrical and Mechanical SI Units, NPL Report DES No. 40, (1977).

[7] Kibble, B. P., A Measurement of the Gyromagnetic Ratio of the Proton by the Strong Field Method, Atomic Masses and Fundamental Constants **5**, ed. by J. H. Sanders and A. H. Wapstra (Plenum Publishing Corp., New York, 1976) p. 545.

[8] Cutkosky, R. D., New NBS Measurements of the Absolute Farad and Ohm, IEEE Trans. Instrum. Meas. **IM-23**, 305, (1974).

[9] Snow, C., Formulas for Computing Capacitance and Inductance, NBS Circular 544 (1954).

[10] Williams, E. R., and Olsen, P. T., A Non-contacting Magentic Pick-up Probe for Measuring the Pitch of a Precision Solenoid, IEEE Trans. Instrum. Meas., **IM-21**, 376 (1972).

[11] Olsen, P. T., and Williams, E. R., A More Accurate Determination of γ_p Through Improved Dimensional Measurement Techniques, IEEE Trans. Instrum. Meas., **IM-23**, 302 (1974).

[12] Nakamura, H., A Serv-Controlled Balance for the Absolute Ampere Determination, Jap. J. Appl. Phys. **17**, 1397, (1978).

Reprinted by permission from IEEE TRANSACTIONS ON INSTRUMENTATION AND MEASUREMENT
Vol. IM-23, No. 4, December 1974, pp. 305-309

New NBS Measurements of the Absolute Farad and Ohm

ROBERT D. CUTKOSKY, FELLOW, IEEE

Abstract—A recently completed calculable cross capacitor in conjunction with a previously described collection of ac and dc bridges has made possible a highly accurate measurement of the farad and the ohm. The cross capacitor and its auxiliary equipment, as well as those components of the measurement system which have not been covered in prior publications, are described in detail. The measurements indicate that the National Bureau of Standards (NBS) unit of capacitance is given by $F_{NBS} = 1\ F + 1.787\ \mu F$, and that the NBS unit of resistance is given by $\Omega_{NBS} = 1\ \Omega - 0.819\ \mu\Omega$.

INTRODUCTION

FOLLOWING the theoretical and experimental development of the calculable cross capacitor by Thompson and Lampard of the National Standards Laboratory of Australia [1], a research effort was initiated at the National Bureau of Standards (NBS) to utilize these principles in an absolute measurement of the farad and the ohm. The initial NBS effort in this field [2] was completed in 1960 and provided an absolute measurement of the ohm with an estimated uncertainty of about 2 parts in 10^6. These measurements provided the basis for the present NBS unit of capacitance, F_{NBS}. The NBS unit of resistance Ω_{NBS} was not adjusted at that time, because the unit in existence since 1948 was found to be substantially correct. The activities of our laboratory since 1960 have been directed toward improving the equipment and techniques which were used in the initial effort with the objective of completing an absolute ohm measurement with an uncertainty on the order of a few parts in 10^8.

Manuscript received July 3, 1974; revised August 20, 1974. This paper is a contribution of the National Bureau of Standards and is not subject to copyright.
The author is with the Electricity Division, National Bureau of Standards, Washington, D. C. 20234.

ORGANIZATION OF MEASUREMENT SYSTEM

The starting point in the NBS absolute ohm measurement is a 0.5-pF calculable cross capacitor, the capacitance

of which can be determined from a measurement of its length. This instrument is used to measure the capacitance of a transportable 10-pF reference capacitor which can be carried from the basement room containing the cross capacitor to a large second floor laboratory containing the other components of the measurement system.

The second floor laboratory contains the bank of 10-pF reference capacitors that maintain the NBS unit of capacitance. An ac bridge with a nominal voltage ratio of 10:1 is used in two stages to measure two 1000-pF capacitors. These capacitors are used in turn as two arms of a special frequency-dependent bridge called a quadrature bridge for measuring the ac resistances of two 10^5-Ω resistors. These resistors are then compared with a transportable 1000-Ω resistor through the use of a 100:1 ac bridge that utilizes the 10:1 voltage ratio bridge just cited and a 10:1 current comparator [3].

The transportable 1000-Ω resistor is then carried to the laboratory in which the NBS bank of 1-Ω reference resistors is maintained. The stepup from the 1-Ω level to the 1000-Ω transportable resistor is performed in this laboratory using dc techniques with the aid of Hamon dividers and a dc comparator.

Essential special auxiliary equipment includes a low noise parametric preamplifier, instruments for measuring the voltage dependence of capacitors and other components, a transformer calibrator, and all of the equipment necessary for determing the frequency dependence of the cross capacitor and of the transportable 1000-Ω resistor. Except for the cross capacitor itself and equipment related to its use, all of the special instruments and techniques used in this work have been described in a series of publications dating back to 1962 [3]–[7]. The attention of this paper is accordingly concentrated on the construction and operation of the cross capacitor and on those aspects of the measurement system which have not already been adequately covered.

CROSS CAPACITOR

The NBS cross capacitor utilizes the now classic geometry which was first exploited by Clothier [8]. Our system contains four vertical cylindrical electrodes with diameters of 6.35 cm which were lapped to an accuracy of ± 0.1 μm and which are located in a square array with clearances of 3.60 mm between adjacent electrodes. A grounded cylindrical shield with an inside diameter of 18.16 cm surrounds the four electrodes. A movable shield rod with a diameter of 2.72 cm is partially inserted between the electrodes from the top and is located horizontally by polytetraflouroethylene rings which are placed around the shield rod and which lightly touch all four electrodes. This shield rod may by translated vertically by means of a pulley and counterweight system to vary the cross capacitance of the instrument in a controlled manner. The lower end of the shield rod is composed of an Invar fitting which is terminated with a vertical tube 22.4 mm long with an outside diameter of 10.0 mm. The geometry of this tube was chosen to eliminate the first-order dependence of capacitance upon electrode taper and angular misalignment which could otherwise seriously affect the measurements.

An optical flat is mounted inside the Invar fitting just above the misalignment compensation tube. A similar Invar fitting with a second optical flat is mounted just above the lower ends of the electrodes. The lower fitting can be adjusted either mechanically or electrically by means of a piezoelectric transducer (PZT) to make the flats precisely parallel. The PZT can also be used to displace the lower flat vertically over a range slightly larger than 1 fringe. Provision has been made to dither the lower flat over a range of a few hundredths of a fringe at a frequency of 10 Hz. The two flats form the plates of a Fabry–Perot interferometer which is illuminated by a Lamb-dip stabilized helium-neon laser. The optical system contains a polarizer and quarter-wave plate to minimize the amount of light returning to the laser, a beam expanding telescope to fill the 7-mm-diameter Fabry–Perot resonator, a 50-cm focal length lens to focus the interference fringes, and an adjustable pinhole at the focal plane of the lens to select the light from the center of the fringe pattern and to allow it to strike a phototransistor. The 10-Hz component of the phototransistor output resulting from dithering the lower flat is amplified and detected with a phase sensitive detector. The detector output is amplified and fed back to the PZT to lock the interferometer on the center of a fringe.

The shield rod contains two cylindrical sections 7 mm long which are electrically insulated from the rest of the shield rod. These sections are of the same diameter as the shield rod and are connected via sliding contacts to separate terminals on the housing of the capacitor. One of these sections is located a few millimeters above the Invar fitting containing the upper flat, and the other is about 10 cm farther up. These sections make it possible to monitor variations in the interelectrode spacing and in the angle between the shield rod and the electrode axis as the shield rod is displaced through its range of travel through measurements of the direct capacitance between each cylindrical section and each capacitor electrode. These sections are shorted to the case of the capacitor when cross-capacitance measurements are being made.

The cross capacitor becomes slightly nonlinear when the shield rod is set to produce a cross capacitance smaller than 0.2 pF, and has a maximum capacitance of 0.7 pF. Within this normal operating range of 0.5 pF, only the expected nonlinearity at the 0.2-pF end of the range has been found. The capacitance nonlinearity at the 0.2-pF end of its range was determined by comparing the rates of change of capacitance with shield rod displacement, with the shield rod set to yield various cross capacitances down to 0.06 pF. The function relating departure from linearity to normal capacitance was found to be exponential and indicated that at the 0.2-pF setting the nonlinearity amounted to 7.0×10^{-9} pF. A correction of 14 parts in in 10^9 was accordly applied to the 0.5-pF capacitance difference.

The uncertainty in cross capacitance caused by imprecise mechanical construction and alignment is estimated

to be smaller than 1 part in 10^8. A correction of 3 parts in 10^9 to account for a slight error in the laser beam direction was applied. The wavelength of our present laser is unfortunately not completely stable, and at present limits our capacitance accuracy. The capacitor is normally evacuated to a sufficiently small pressure so that correction for changes either in the laser wavelenght or in the dielectric constant of the capacitor is unnecessary.

The distributed capacitances and inductances in the leads and electrodes of the calculable capacitor result in a small frequency dependence. The distributions of these parasitic impedances were determined by direct measurements coupled with some estimates of end effects. The total correction for these internal loading effects including the capacitive loading correction for the transformer used to compare the calculable capacitor with the 10-pF transportable reference capacitor was found to be +9 parts in 10^9 at 1592 Hz.

ALTERNATING CURRENT MEASUREMENTS

The capacitance of the calculable capacitor is compared with that of a transportable 10-pF reference capacitor in a bridge containing a special transformer which supplies 200 V at 1592 Hz to the capacitor. When the calculable capacitor is set to yield 0.2 pF, the reference capacitor is connected to a tap supplying 4 V, and when it is set to yield 0.7 pF the reference capacitor is connected to a tap supplying 14 V. The critical ratios of this transformer were measured using larger fixed capacitors which can be accurately calibrated through the use of a previously described 10:1 voltage ratio bridge [3]. The open circuit ratio correction for the special transformer was found to be −71 parts in 10^9. The remaining features of the bridge used for comparing the cross capacitor with the 10-pF reference capacitor and in determining the fringe number are similar to those described by Clothier [8].

The impedance of the transportable 10-pF reference capacitor at 1592 Hz is compared with the impedance of a 1000-Ω transportable resistor using a set of bridges described in an earlier paper [3]. The four-pair 10:1 voltage bridge was calibrated through the use of a set of eleven 10-pF capacitors by means of the permutation method [9], but modifications were made so that better advantage could be taken of the four-pair configuration. The voltage dependencies of all of the capacitors involved in the step-up and in the calibrations were measured on an absolute basis using a new version of the system described by Shields [10]. The only capacitors for which the voltage dependence corrections were larger than 1 part in 10^9 were two 1000-pF capacitors used to calibrate a 10:1 ac current comparator. This comparator was part of a 100:1 bridge used for the ac measurement of the 1000-Ω transportable resistor. Two different pairs of capacitors were used for this calibration. The voltage dependencies of the capacitors over the 20-V to 200-V range varied from 82 parts in 10^9 to 154 parts in 10^9, but after the corrections were applied, all of the measurements of the current comparator ratio agreed within 2 parts in 10^9.

TRANSPORTABLE RESISTOR

The 1000-Ω transportable resistor consists of nine 1000-Ω Evanohm resistors wound on mica cards. The individual cards are connected in series parallel and mounted in a sealed metal can nearly filled with oil. The can is in turn immersed in a temperature-regulated oil bath. This resistor is measured with both ac current and with dc current, and it is necessary to correct for any ac–dc resistance difference which may exist. Two special coaxial resistors, one of 100 Ω and one of 1000 Ω, were constructed to investigate this possibility [11]. Each of these resistors consists of a single length of Evanohm wire about 30 cm long and of suitable diameter mounted along the axis of an oil-filled tubular return conductor with a diameter of 5 cm. Shielded current and potential terminals were provided at each end. Complete calculations of the field distributions and eddy currents were made to allow an assessment of the frequency dependencies of the two resistors. A comparison of the ratios of the two resistors at 1592 Hz and at 15920 Hz showed close consistency with the calculations, both in resistance and in phase angle. On the basis of the calculations, the 1000-Ω coaxial resistor was assigned a resistance difference from dc to 1592 Hz of 8 parts in 10^{10} which is not significant, but which does not include a possible dc error attributable to the Peltier effect [12], which could arise from the use of spot welding to fasten the resistance wire to its terminals. A microscopic examination of the welded junction showed a discolored section of Evanohm wire extending out from the weld for a distance of about 0.2 mm. It was subsequently determined that annealing a piece of Evanohm wire substantially changes its thermoelectric coefficient, so that a thermoelectric junction could exist 0.2 mm from each end of the resistance wire, possibly causing the dc resistance to be abnormally high due to the Peltier effect.

A second special 1000-Ω resistor was built to determine whether or not the Peltier effect in the coaxial 1000-Ω resistor was significant. This resistor consists of a length of resistance wire about 3 m long folded twice to form a four-wire cage 75 cm long. The wires are separated by 1 cm throughout the length of the system and produce a quadrupole field, which is not strongly coupled to the metal supports and shield structure. Current and potential terminals for each end of the resistor consist of pieces of 0.07-mm diameter copper wire 1 cm long soldered to heavier copper lead wires with low thermal solder. The 0.07-mm wires were placed parallel to each other and about 3 mm apart on a beryllium oxide heat sink. The resistance wire was placed over the copper wires and perpendicular to them and clamped in place with a second beryllium oxide heat sink. The contact resistance of this purely mechanical connection was about 0.1 Ω. The resistor was easily trimmed to ± 100 ppm by releasing the clamping pressure and moving the resistance wire as required. The finished resistor was immersed in an oil bath for temperature control.

The quadrupole resistor was not expected to exhibit an

appreciable Peltier effect because of the absence of thermoelectric junctions in the portions of the resistor common to the current and potential circuits. A verification of the absence of Peltier errors was made by connecting a nanovoltmeter between a normally open extension of the Evanohm resistance wire and the adjacent clamped junction. A current was then passed through the 1000-Ω section of the resistor via the innermost of the four clamped junctions. Reversing the sign of the current had no effect on the nanovoltmeter reading. Some eddy current errors could exist, but this would cause an apparent increase of resistance with frequency.

The coaxial 1000-Ω resistor is believed to be substantially free of eddy current errors, but if it were troubled with the Peltier effect, its resistance would appear to decrease with frequency. Measurements of the ratio of the two special 1000 Ω resistors at dc and at 1592 Hz agreed within 5 parts in 10^9, which is interpreted as indicating that neither resistor has a significant frequency dependence.

The ac–dc difference of the transportable resistor was determined by comparison with the coaxial 1000-Ω resistor. The difference has changed from 484×10^{-9} in 1970 to 535×10^{-9} on January 29, 1974. In February or March of 1974 the phase angle of the transportable resistor changed abruptly by about 43 μrad. Subsequently, its ac–dc difference was determined to be 460×10^{-9}. The dc resistance of the transportable resistor was always larger than the ac resistance.

DIRECT CURRENT MEASUREMENTS

All of the dc comparisons relating the 1000-Ω transportable resistor to the NBS legal ohm as maintained with 1-Ω resistors were made directly or under the supervision of T. E. Wells of the Electrical Reference Standards Section, NBS Electricity Division. Two separate buildup processes were used. In the first process, a Hamon divider with ten 10-Ω coils was first compared in the parallel mode with the 1-Ω standard resistors using a current comparator. Then, again using the current comparator, the Hamon divider was compared in the series mode with a second Hamon divider containing ten 100-Ω coils, first to measure the series-parallel combination of nine of the coils, and second to measure the tenth coil individually. Finally, the second Hamon divider was connected in the series mode and compared with the 1000-Ω transportable resistor in a conventional Wheatstone bridge. In the second process, a Hamon divider with thirty-two 32-Ω coils was compared in the parallel mode with the 1-Ω standard resistors using a current comparator. Then it was compared in the series mode with a 1024-Ω resistor consisting of a 1000-Ω resistor in series with a 24-Ω resistor. A separate measurement of the 24-Ω resistor yielded the value of the 1000-Ω section, which was finally compared with the transportable resistor. The two processes were found to agree within the uncertainty limits of the measurements, or about 2 parts in 10^8.

MEASUREMENT RESULTS

The measurement process consisted of performing the ac calibrations relating the 10-pF transportable capacitor to the 1000-Ω transportable resistor twice on a Monday or Tuesday, and twice again on the following Thursday or Friday. On the intervening Wednesday, the 10-pF capicitor was calibrated by reference to the calculable capacitor, and the 1000-Ω resistor was compare with the bank of 1-Ω resistors maintaining the NBS legal ohm. These sequences were repeated every month or two, with the intervals between measurements being devoted to calibrating the bridges and determining the required corrections as outlined earlier.

Table I summarizes the results obtained. The standard deviations associated with the average values of both F_{NBS} and Ω_{NBS} are well below one part in 10^9, which is negligible compared with the possible systematic errors. Estimates of the effects of possible systematic errors are itemized in Table II. The error in the measurement of Ω_{NBS} is almost certainly less than the direct sum of the listed systematic errors, but could easily exceed their root sum square (rss) sum. If a single number must be assigned to the uncertainly of the measurement of Ω_{NBS}, a value of 0.06 ppm (95-percent confidence level) would not be unreasonable.

A comparison between the work reported here and the absolute ohm work of the National Standards Laboratory (NSL) of Australia [13] can be made by making use of the periodic resistance intercomparisons performed at the International Bureau of Weights and Measures (BIPM). The BIPM has reported for the series of intercomparisons made between January and April 1973 that $\Omega_{NBS} = \Omega_{69-BI} + 0.2\ \mu\Omega$, and $\Omega_{NSL} = \Omega_{69-BI} + 0.33\ \mu\Omega$ [14]. Very recent work at the NSL has indicated that the resistance of the shield return lead of their ac–dc transfer resistor has increased by 0.19 ppm of the total resistance since it was last measured in 1967 [15]. This shield resistance was included in their four-pair ac measurements, but its assigned value was added to the results of their dc measurements. It is not known when the change occurred, but it is believed probable that most of the change occurred before their measurement of the transportable resistors which were involved in the BIPM resistance intercomparisons. If the entire 0.19-ppm correction is applied to the 1973 intercomparisons, the BIPM result would become $\Omega_{NSL} = \Omega_{69-BI} + 0.52\ \mu\Omega$, so that $\Omega_{NBS} = \Omega_{NSL} - 0.32\ \mu\Omega$. The NSL unit is maintained to be in accordance with the SI definition, but they had been using $c = 2.997925 \times 10^8$ m/s for the speed of light. We have used $c = 2.9979245S \times 10^8$ m/s, as was recommended for international adoption in 1973 [16]. Since the speed of light enters the capacitance equations as $1/c^2$, the NBS unit of resistance as measured through the BIPM by NSL should be corrected by 0.280 ppm, or Ω_{NBS} (NSL) $= 1\,\Omega - 0.60\ \mu\Omega$. The discrepancy with our result, $\Omega_{NBS} = 1\,\Omega - 0.819\ \mu\Omega$, is 0.22 ppm. This is larger than expected in view of the reported NSL uncer-

TABLE I

SUMMARY OF MEASUREMENTS OF F_{NBS} AND Ω_{NBS} IN SI UNITS, TAKING $c = 2.99792458 \times 10^8$ m/s[a]

Date	10-pF Capacitor	F_{NBS}	1000-Ω Resistor	Ω_{NBS}
9/12/73	+5.522	+1.798	+9.409	−0.819
10/24/73	+5.542	+1.798	+9.553	−0.822
11/28/73	+5.523	+1.775	+9.667	−0.821
1/23/74	+5.533	+1.784	+9.832	−0.708[b]
4/3/74	+5.532	+1.782	+10.073	−0.813
	average:	+1.787	average of four:	−0.819

[a] Corrections in parts per million to indicated quantities or standards are tabulated.

[b] This measurement was discarded because the dc comparison exhibited internal discrepancies as large as 2 parts in 10^7.

TABLE II

ESTIMATES OF THE EFFECTS OF POSSIBLE SYSTEMATIC ERRORS ON THE MEASUREMENT OF Ω_{NBS} (95-PERCENT CONFIDENCE LEVEL)

Possible Systematic Errors	Error Estimates (ppm)
Drift in laser wavelength between calibrations	0.010
Imperfection of calculable capacitor electrode straightness and alignment	0.010
Misalignment of laser beam in capacitor	0.002
Diffraction error due to laser aperture diameter	0.001
Load corrections for calculable capacitor	0.007
Residual gas in calculable capacitor	0.004
Drift between calibrations and measurement uncertainties of transformer ratios	0.007
Uncertainty in capacitance voltage dependence measurement	0.003
Temperature uncertainty of transportable resistor	0.004
Frequency dependence of transportable resistor	0.005
Self-heating effects in transportable resistor	0.004
Uncertainty in dc stepup, 1 to 1000 Ω	0.050
direct sum:	0.107
rss sum:	0.054

tainty of 0.2 ppm and our own estimated uncertainty of 0.06 ppm, and in view of the fact that a direct intercomparison of capacitance standards between NBS and NSL indicates agreement within 0.02 ppm. This implies that very little of the discrepancy can be attributed to the calculable capacitors.

A second intercomparison of the NBS unit of resistance with that of the BIPM was made in May 1973 and indicated that $\Omega_{NBS} = \Omega_{69-BI} - 0.17$ μΩ [17]. This result was not used in the formal assignment of the NBS unit of resistance in terms of the BIPM unit because the first intercomparison seemed to be in closer agreement with the trend through measurements dating back to 1957, and because some comparisons of 10^4-Ω resistors also indicated closer agreement with the first series of intercomparisons. If the second intercomparison is taken to be correct, one would obtain, using the same corrections as above, Ω_{NBS} (NSL) = 1Ω–0.97 μΩ, which differs from the NBS result by 0.15 ppm, but with the opposite sign.

It is clear that further study of the resistance transfer problem must be made. Although the precise cause of the discrepancy is not yet known, it has been noticed that the NBS transportable resistors do not return immediately to their original rates after their return from other laboratories. It has been suggested that the problem may be related to the fact that NBS normally measures its resistors at 25°C and determines their values at 20°C through a fairly quick series of temperature coefficient measurements, whereas the BIPM normally measures the resistors after a rather long stabilization period at 20°C. This difference in technique cannot explain all of the discrepant results, but points to the resistance transfer as the least reliable part of the intercomparison process. A direct interchange of resistance standards between NBS and NSL which is now underway may help resolve the discrepancies.

REFERENCES

[1] A. M. Thompson and D. G. Lampard, "A new theorem in electrostatics and its application to calculable standards of capacitance," *Nature*, vol. 177, p. 888, 1956.

[2] R. D. Cutkosky, "Evaluation of the NBS unit of resistance based on a computable capacitor," *NBS J. Res.*, vol. 65A, pp. 147–158, May–June 1961.

[3] ——, "Techniques for comparing four-terminal-pair admittance standards," *NBS J. Res.*, vol. 74C, pp. 63–78, July and Dec. 1970.

[4] ——, "Four-terminal-pair networks as precision admittance and impedance standards," *Commun. Elec.*, vol. 70, pp. 19–22, Jan. 1964.

[5] R. D. Cutkosky and L. H. Lee, "Improved ten-picofarad fused silica dielectric capacitor," *NBS J. Res.*, vol. 69C, pp. 173–179, July–Sept. 1965.

[6] R. D. Cutkosky, "A varactor null detector for audio frequency capacitance bridges," *IEEE Trans. Instrum. Meas.*, vol. IM-17, pp. 232–238, Dec. 1968.

[7] ——, "An ac resistance thermometer bridge," *NBS J. Res.*, vol. 74C, pp. 15–18, Jan. and June 1970.

[8] W. K. Clothier, "A calculable standard of capacitance," *Metrologia*, vol. 1, pp. 36–55, Apr. 1965.

[9] R. D. Cutkosky and J. Q. Shields, "The precision measurement of transformer ratios," *IRE Trans. Instrum.*, vol. I-9, pp. 243–250, Sept. 1960.

[10] J. Q. Shields, "Voltage dependence of precision air capacitors," *NBS J. Res.*, vol. 69C, pp. 265–274, Oct.–Dec. 1965.

[11] R. J. Haddad, "A resistor calculable from dc to $\omega = 10^5$ rad/s," M.S. thesis, School Eng. Appl. Sci., George Washington Univ., Apr., 1969.

[12] C. G. M. Kirby and M. J. Laubitz, "The error due to the Peltier effect in direct-current measurements of resistance," *Metrologia*, vol. 9, pp. 103–106, Sept. 1973.

[13] A. M. Thompson, "An absolute determination of resistance based on a calculable standard of capacitance," *Metrologia*, vol. 4, pp. 1–7, Jan. 1968.

[14] G. Leclerc, *Rapport sur la 13e comparison des etalons nationaux de resistance electrique*, Bur. Int. Poids Mesures, Sèvres, France, Jan.–Apr. 1973.

[15] Private communication, June 7, 1974.

[16] J. Terrien, "International agreement on the value of the velocity of light," *Metrologia*, vol. 10, no. 1, p. 9, 1974.

[17] Private communication, Nov. 21, 1973.

ELECTRICAL STANDARDS

From over the world did they roam,
Trading thoughts contained in the dome.
The Ampere and Volt
Were given a jolt;
Then most of them quickly went ohm.

ANON.

The Fundamental Electrical Standards: Present Status and Prospects for Improvement

Robert D. Cutkosky

Institute for Basic Standards, National Bureau of Standards, Washington, D. C. 20234

Absolute measurements of resistance and current have until recently been based on instruments involving carefully constructed and measured single layer solenoids. Minor improvements in technique have resulted in a continuous reduction of measurement uncertainty, but overall uncertainties much smaller than one part in 10^6 are not likely to be achieved without radical changes in design. Some of the principal sources of uncertainty in these experiments are analyzed, and, when possible, alternative measurement systems are proposed which could lead to higher accuracy. Within the time scale appropriate for measurements of this kind, absolute resistance measurements based on calculable capacitors are quite recent, even though the first such measurement was reported in 1961. More recent calculable capacitors have resulted in absolute resistance measurements of higher accuracy than may reasonably be expected from systems utilizing calculable solenoids. The possibility for improvements in absolute current or absolute voltage measurements does not seem quite so clear, but some ideas are presented which are either now being tried or are worth some consideration. An attempt is made to indicate the more important sources of uncertainty in the proposed systems.

Key words: Capacitors; current balances; electrical measurements; electrical standards; electrometers; inductors.

1. Introduction

It is unfortunate that the completion of experimental determinations of physical quantities and of measurements related to them do not always coincide with the convening of an international conference of appropriate stature. In the case of electrical standards, many years commonly elapse between the inception of a particular piece of work and its completion, and in view of the fact that only a few laboratories in the world are involved in such measurements, it may not be surprising that this paper contains no results.

In the short space available I shall quickly summarize the more recent absolute measurements of capacitance, resistance, voltage and current, and give the most attention to the present status of work now underway and to various proposals for improved measurement systems. Some comments on the possible future use of Josephson junctions as maintenance standards of voltage will also be made, although physically the Josephson effect is most useful as a means of accurately measuring e/h.

The starting point for all absolute electrical measurements rests in the extensive body of classical electromagnetic theory, by means of which one can in principle calculate the magnetic fields, inductances, and forces associated with current-carrying conductors, and the electric fields, capacitances, and forces associated with charged conductors, from mechanical measurements of the shapes and positions of these conductors. The task of the metrologist involved in this work is to determine a suitable geometry for his equipment so that the necessary mechanical measurements can be made with a high accuracy, and so that the resultant electrical property has such a magnitude that it can be accurately compared with a set of fixed "maintenance" standards which preserve the unit so obtained. Many compromises must be made in the design of absolute electrical measurement equipment to minimize the uncertainty of the final result. These compromises involve among other things considerations of the relative ease with which various systems can be fabricated and measured.

2. Units of Impedance

Two quite distinct approaches to an absolute ohm measurement are available. One approach begins with an inductor whose inductance can be calculated from its mechanical dimensions, and the other begins with a capacitor whose capacitance can be calculated from its mechanical dimensions. The second method requires a knowledge of the speed of light, which is generally treated as an auxiliary constant.[1] In principle either a calculable inductor or a calculable capacitor can be used to assign a value to a standard resistor using purely bridge methods, and requiring only a measurement of frequency in addition to suitable impedance ratio measurement techniques. Generally these impedance comparisons can be made with substantially better accuracy than is presently achievable in the construction and evaluation of either a calculable inductor or a calculable capacitor.

2.1. The Ohm from Inductance

Calculable self inductors are generally constructed by preparing a grooved cylindrical former of a stable material such as fused silica, and placing a single-layer helical winding of copper wire in the groove. The dimensions of the completed solenoid are measured as precisely as possible and from these measurements the self inductance of the solenoid can be calculated.

Calculable mutual inductors usually contain one precision solenoid similar to that described above, but with one or more gaps in the helical winding, placed so that a region exists exterior to the solenoid in which the magnetic field is very small. The secondary winding is placed in this low-field region, since it is then not necessary for its dimensions or its location to be measured with a high accuracy. Multilayer windings can be used for the secondary without seriously affecting the accuracy with which the mutual inductance can be calculated. Alternatively, a mutual inductor can be constructed by placing a bifilar winding on a single cylindrical former.

At least six absolute ohm determinations based on calculable inductors were reported since 1955. Most of these measurements utilized mutual inductors rather than self inductors, partly because self inductors have larger phase angles than mutual inductors, which complicates the electrical part of the measurement. Two of the recent inductor-based absolute ohm determinations were assigned uncertainties of about 2 parts in 10^6 [1, 2]. In both cases, the uncertainties were almost entirely attributable to the difficulties involved in measuring the mechanical dimensions of the single-layer, wire wound solenoids.

Some reduction in the mechanical measurement uncertainties for solenoids may be possible, but it seems likely that an uncertainty substantially smaller than 1 part in 10^6 will not be achievable with present inductor designs. The reasons for this are first, that even single layer solenoids wound on rigid, grooved formers are slightly compressible, and uncertainties remain even after corrections are applied for the distortion caused by the pressure of the micrometer used in the measurement of solenoid diameter and pitch. Second, oxide films on the wire cause formidable problems; and third, the distortion of the wire caused by winding it tightly on the former cannot be easily determined. Finally, it is necessary to estimate the current distribution in the wire. This depends upon how the resistivity of the wire varies with distance from the axis of the solenoid, and is a function of wire diameter, solenoid diameter, winding tension, and the material chosen for the wire, which is usually copper. Eddy currents within the wires also affect the current distribution,

[1] The vacuum capacitance of a capacitor is equal to a geometric factor times the electric constant ϵ_0, where $\epsilon_0\mu_0 = 1/c^2$. The magnetic constant $\mu_0 = 4\pi \times 10^{-7}$ henry/meter in the SI system.

and are not easy to estimate (eddy currents induced in other metal parts of the system can also cause serious errors if the problem is not recognized).

The current distribution uncertainties discussed above could probably be reduced by reducing the wire diameter; but if carried to an extreme, the wire distortion caused by micrometer pressure would be very large. Additionally, reducing the wire cross section would increase the solenoid resistance, and result in either an increase in power consumption and hence larger temperature uncertainties if the solenoid is in a current carrying part of the electrical circuit, or in increased thermal agitation noise if it is in the potential part of the circuit.

Proposals have been made to produce solenoids by evaporating very thin metal films in a helical pattern on smooth cylindrical forms. There is no doubt that this would result in a reduction of the solenoid diameter uncertainty, but it would be very difficult to determine how the current was distributed over the width of the film. Very small defects in the film could cause significant local variations in the pitch of the solenoid, which could result in substantial errors in the calculated inductance. The relatively large solenoid resistance to be expected with such a system could also be a problem for the reasons cited above. It has been argued that the use of superconducting windings on a solenoid would eliminate many of the above problems, but the current distribution within a superconducting wire is at best ambiguous, and no reasonable way has yet been found for measuring the solenoid dimensions at low temperature.

A completely different geometry for a calculable mutual inductor has been treated theoretically by Page [3]. The proposed system uses a set of eight parallel wires equally spaced around a circle. In this system, the mutual inductances between each pair of wires and every other pair of wires is measured, and these mutual inductances can be related to the length of the wire system. Many of the uncertainties due to small errors in wire placement are of second order, and only the length of the system need be measured to high accuracy. No serious attempt has yet been made to construct such a system, but it seems clear that the problems would be formidable. The mutual inductances are likely to be in the order of 10^{-7} H, which presents serious but not insurmountable electrical measurement problems [4].

2.2. The Ohm from Capacitance

Calculable capacitors have three principal advantages over calculable inductors. Negligible power is lost in a capacitor, so the mechanical dimensions do not change with time due to the resultant change in temperature. The corresponding problem with capacitors has to do with dimensional changes due to the electrostatic forces between the capacitor electrodes, and usually contributes errors smaller than one part in 10^8. The second advantage of capacitors is that the current distribution problem does not exist. In this respect, capacitors are not as pure as might be wished, because dielectric films on the electrode surfaces introduce an analogous uncertainty in the effective electrode spacing. However, the dielectric films are usually quite thin, and the resultant uncertainties are much smaller than the uncertainties resulting from the current distribution in a calculable inductor. The third advantage of calculable capacitors over calculable inductors is that all critical fields are contained within the calculable region, so that the effects of objects external to the calculable instrument can be ignored. This eliminates the need for special nonmagnetic buildings as are generally required for high-precision inductance measurements.

All calculable capacitors now in existence or known to be under construction are of a type called a cross capacitor. This geometry was first proposed by A. M. Thompson and D. G. Lampard, and in practice is usually constructed of four cylindrical electrodes of circular cross section [5]. The axes of the four electrodes are parallel and are located at the corners of a square just slightly larger than the electrode diameter. The two capacitances of interest are the capacitance coefficients between opposite pairs of electrodes. The exterior of the system is completely shielded so that only the region between the four electrodes is of concern.

Provided that reasonable care is taken to obtain the requisite two-dimensional symmetry, all small perturbations from the ideal geometry including those due to dielectric films on the electrode surfaces enter only to second order in the average of the two cross capacitances, leaving only the first order dependence of capacitance upon the overall length of the electrode system. This single critical dimension is measured in the more refined cross capacitors with interferometric techniques.

Several cross capacitors have been described in recent years, but so far only two absolute ohm measurements based on cross capacitors have been completed [6, 7]. The most accurate of these two was the ohm measurement reported by Thompson and making use of the cross capacitor described by Clothier [8]. They reported an overall uncertainty of one part in 10^7 exclusive of the uncertainty in the speed of light. Somewhat smaller uncertainties may be expected soon as improvements are made in the Clothier/Thompson apparatus and as similar systems now under construction elsewhere are completed.

At the present time it appears that capacitor-based absolute ohm measurements are capable of providing much higher accuracy than are inductor-based absolute ohm measurements. The relative accuracies of the two techniques are so disparate that work with calculable inductors could well be abandoned, except that a comparison of measurements made in such completely different ways helps to prevent gross errors. Inasmuch as a capacitor-based absolute ohm measurement requires a knowledge of the speed of light and an inductor-based measurement does not, one can treat the pair of ohm measurements as a speed-of-light measurement, and possibly learn something about the dependence of c upon frequency. No discrepancy attributable to such an effect has

yet been observed, and the continuation of calculable inductor research on this ground might be hard to justify.

3. Units of Voltage or Current

After having established a unit of resistance by means of one of the techniques outlined above, an absolute determination of either the volt or the ampere suffices to establish both units through Ohm's law. In practice it is the unit of voltage that is maintained rather than the unit of current, because of the proven stability of saturated cadmium sulfate standard cells, but in fact all of the precision measurements of this kind made until now have been with current sensitive instruments called current balances. Voltage can also be measured directly with electrometer-type instruments, and some such instruments are now under construction.

From a dimensional standpoint, absolute resistance measurements require only length and time determinations, whereas voltage or current measurements require in addition a determination of mass. The experiments involve a measurement of the torque or force between two current carrying conductors or between two charged electrodes. The electrical force is usually compared with the gravitational force on a known mass, and hence a knowledge of the local acceleration of gravity is also required. These additional complications tend to make absolute voltage or current measurements much more difficult than absolute resistance measurements.

3.1. Current Balances

The most common type of current balance is often called a Rayleigh balance, and contains a fixed center-tapped solenoid having equal currents in each half of the solenoid but of opposite direction, to yield a strong radial component of magnetic field in the center of the system. A relatively short current-carrying solenoid is placed in the center of the system and attached to one arm of a precision balance. Reversing the sign of the fixed-solenoid current while keeping the current in the movable solenoid fixed changes the sign of the force on the movable coil. The balance is then restored to equilibrium by adding a known mass to that arm of the balance. Some Rayleigh balances have a set of coils on each arm of the balance, and the movable solenoid (or solenoids) may be either of larger or smaller diameter than the fixed solenoid. Within the last few years, about four Rayleigh-type current balances have been described, with the smallest reported uncertainties being about 4 parts in 10^6 [9], and about 5 parts in 10^6 [10].

One current balance has been described which involves the torque between two current carrying solenoids whose axes are perpendicular [11]. The torque is measured by attaching one solenoid to a balance beam and restoring the balance equilibrium after reversal of the current in the fixed solenoid by placing a known mass on one pan of the balance. The distance between the knife edge supporting this pan and the central knife edge of the balance must also be measured with this system. Some problems were encountered initially with distortion of the balance beam, but this probably does not constitute a fundamental limitation of the method. The most recent ampere determination with this instrument yielded an uncertainty of 7 parts in 10^6 [12].

The solenoids for all types of current balance are normally constructed and measured using the same techniques as are used for calculable inductors, and all of the problems encountered in calculable inductors also occur in current balances, except that since direct current is used in current balances, eddy current effects do not influence the current distribution in the wires. Since the movable solenoid of a current balance must be kept as light as possible to avoid overloading the balance, the movable solenoid is usually small and quite compressible, and its dimensions are therefore difficult to measure accurately. This is a principal contributor to the uncertainty in a current balance experiment.

A second major problem encountered in current balances is caused by air currents generated by the heated wires, which disturb the balance. Presumably no systematic errors are caused by the air currents, but very erratic balance fluctuations are observed, and long measurement sequences are required in order to obtain a reasonably small uncertainty in the measured force or torque.

Until recently the uncertainty in the local acceleration of gravity contributed substantially to the overall uncertainty of an ampere determination. Recent refinements in gravity measurement techniques have made this source of uncertainty negligible.

A substantial reduction in the uncertainty of an absolute ampere determination would seem to require an improved technique for constructing and measuring the movable solenoid. The fixed solenoid can be made large and rigid enough to allow a relatively accurate determination of its dimensions, and schemes exist for comparing the pertinent electrical properties of one solenoid with another. For example, the ratio of the magnetic fields in the centers of two solenoids carrying equal currents is a function of the relative dimensions of the two solenoids, and may be used in conjunction with a set of mechanical measurements of both solenoids to improve the data obtained for the less precisely known solenoid by a least squares process. Only a small improvement in the calculated force constant of a current balance is likely to result unless the two solenoids are specifically designed to take advantage of this technique.

Another approach to a better ampere determination involves placing the movable solenoid in a much stronger field than can be conveniently obtained from a calculable fixed solenoid, and measuring the ratio of this strong field to the much weaker field of a calculable solenoid using proton gyromagnetic resonance techniques. Forces strong enough to be accurately measured can be obtained with this system using a much simpler and more precisely

measurable movable solenoid, and in fact, the movable "solenoid" usually consists of a winding around the edge of a rectangular insulating form. In this case an evaporated metal "winding" might offer some advantages, since the distribution of current over the width of the conductor is of little concern.

A possible flaw in the above system (sometimes called a Cotton balance) is that one must assume that the proton gyromagnetic ratio is independent of field strength. No contrary evidence exists, but lacking further verification, the results of such an experiment might be subject to question. It is interesting to note that the most direct evidence for the independence of the proton gyromagnetic ratio upon field strength is based on measurements conceptually similar to those described above and on measurements with a conventional current balance. Measurements by Huggins and Sanders of the ratio of the proton resonance frequency to the resonance frequencies of ^{3}H, ^{7}Li, ^{11}B, and ^{19}F at both high and low field intensity indicated that the field dependence of the proton resonance frequency is certainly small, but a slight field dependence cannot be ruled out [13].

3.2. Electrometers

The possibility of obtaining the unit of voltage by measuring the force between two charged electrodes has long been intriguing, because of the absence of the air currents which disturb a current balance. Unfortunately the electrometer geometry appropriate for such a system is not usually amenable to the precise mechanical measurements necessary for determining the force constant with adequate precision directly, and this fact has discouraged work in this direction.

One proposed scheme for constructing a directly calculable electrometer utilizes a pool of mercury with a fixed flat horizontal electrode just above the pool [14]. The distance between the electrode and the pool can be measured interferometrically with and without a voltage between the pool and the electrode. The electrical force between the pool and the electrode can then be inferred from measurements of the density of the mercury and of the local acceleration of gravity.

Problems are expected with this system in measuring the mercury density to an adequate accuracy, and in assuring the cleanliness of and lack of surface films on the mercury. The system appears to be feasible, and preliminary investigations have indicated that the mercury surface can be maintained reasonably stable and ripple-free, but the overall uncertainty likely to result cannot yet be estimated.

An indirect approach to an electrometer system makes use of electrodes in the form of interleaving cylinders, for which the electrical force is constant over a substantial axial displacement of one electrode with respect to the other. The force at a given electrode spacing is proportional to the rate of change of capacitance with respect to distance, and since the force is nearly constant, one can show that the average force over a finite electrode displacement is equal to $\frac{1}{2}V^2\,\Delta C/\Delta l$. It is proposed that the total electrode displacement Δl be measured interferometrically, and that ΔC be measured by comparison with a calculable capacitor. The average force can presumably be determined from a large number of discrete force measurements made with different relative electrode displacements.

The above system seems relatively straightforward at first glance, but some difficult problems remain unsolved. For example, if the voltage between the electrode is dc, the capacitance required for use in the equations is the d-c value, and may differ from the more readily measurable ac capacitance obtained in terms of a calculable capacitor using conventional bridge techniques. Slightly lossy dielectric films on the surfaces of the electrodes would produce such a difference, and hence great care would be necessary to obtain clean electrodes. This problem would be avoided if the electrodes were excited with alternating current, but the substantial double frequency force variation that would then result might prove damaging to the knife edges of the balance, and in addition the measured ac voltage would have to be transferred to dc with a thermal transfer instrument for comparison with the voltage of a standard cell.

Any electrometer would be improved if it could be operated in a vacuum, because the buoyancy corrections for the mass and the dielectric constant correction for air would both be eliminated. The mercury-pool electrometer would probably work well under these conditions, although evaporation of the mercury has been reported to cause some problems. Experiments involving the operation of conventional knife-edge balances in a vacuum unfortunately have not been notably successful. It is expected that occluded surface films on the mass standard would be partially released under vacuum conditions, making an assignment of the vacuum mass a rather difficult task. The magnitude of this effect is at the present time not known.

In view of the many difficult problems that one can foresee in the construction and operation of a precision electrometer, it is not possible at this time to estimate the accuracy likely to be obtained. Judging from some preliminary investigations, it seems to be possible to obtain the unit of voltage from an electrometer with an uncertainty at least as small as can now be obtained by means of a current balance, or a few parts in 10^6.

4. Standards for Maintaining Electrical Quantities

There is little point in investing a great deal of effort in an absolute electrical measurement if there are no adequate standards for maintaining the unit, or for use in comparing the measurements made in different laboratories. The currently accepted standards for maintaining the units of voltage and

resistance appear to introduce uncertainties of a few parts in 10^7. Some possibilities exist for improving these standards, but at present only minor improvements can be foreseen.

4.1. Maintenance Standards for Impedance

The unit of resistance has been maintained by means of 1-Ω, dc resistors for at least fifty years. Proposals have been made to use 10^4-Ω resistors for this purpose because of the valid argument that they are not as strongly influenced by thermal voltages in the measurement circuit, and because of the dubious argument that the optimum source impedances of some recently developed galvanometers are closer to 10^4 Ω than to 1 Ω. Improvements in low-impedance galvanometers in the next few years cannot be ruled out, but the uncertainties caused by varying thermal voltages will always be more significant with smaller resistors. If careful attention is given to the construction of 1-Ω resistors and the associated measurement circuit, one might expect to reduce the uncertainties due to thermal voltages to about one part in 10^8, whereas the limit set by thermal agitation noise is closer to one part in 10^9, and is independent of the resistance. Since a calculable capacitor is inherently a high impedance standard, it is somewhat easier to measure a 10^4-Ω resistor in terms of such a standard than it is to measure a 1-Ω resistor. In practice the transfer from ac impedance to dc impedance is usually made at the 1000-Ω level, and as a result only one less measurement is required if the unit is maintained at 10^4 Ω. A procedure for accurately measuring 1-Ω resistors is required in any case, since current balances normally employ currents of about 1 A, which are measured by comparing the voltage produced by this current passing through a 1-Ω resistor with the voltage of a standard cell.

The effects of thermal voltages could be eliminated by maintaining the unit of resistance by means of ac resistors. Existing ac detectors and matching networks are sufficiently well advanced to allow the measurement of any ac resistor between 1 Ω and 10^5 Ω with an uncertainty limited only by thermal agitation noise in the resistor. Capacitors can also be used to maintain a unit of ac impedance, and measurement uncertainties of about one part in 10^9 can in this case be achieved. The absence of self-heating effects in capacitors makes them especially appealing. Existing capacitors appear to drift less than one part in 10^7 per year, but are not quite as stable as the best 1-Ω resistors.

It is probably too early to recommend a change in the mode of maintaining units of impedance. The most practical solution is for laboratories to maintain separate sets of promising standards for several years, and to periodically intercompare the sets with each other. If a particular type of standard is then found to be more suitable than the others, this fact will emerge from a statistical analysis of the data, and no formal abandonment of any type of standard need be made. The maintained unit could be a weighted average of the units maintained by the different types of standards, with the weighting factors changing with time as stability data accumulates. If the uncertainties associated with intercomparing the different sets of standards were very much larger than the uncertainties associated with comparing the standards within a set with each other, it could be useful to recognize more than one maintained unit for a single quantity, but in this case it would be very important to distinguish between the various units.

4.2. Maintenance Standards for Voltage

The unit of voltage is universally maintained by means of saturated Weston cells. These standards are much more stable than any other known electrochemical systems or semiconductor devices. The voltages of saturated Weston cells unfortunately return to equilibrium very slowly after a thermal disturbance, so that great care is needed when they are transported between laboratories. Because of the large temperature coefficients of voltage characteristics of these cells, and especially because of the very large differential temperature coefficient between the two legs of a cell, very careful temperature control is required.

Recently it has become common to transfer the unit of voltage between laboratories by means of groups of standard cells contained in temperature-regulated enclosures which are maintained at constant temperature during shipment. A significant reduction in the uncertainty assigned to a transferred unit of voltage can be made by means of these systems. Unfortunately, with present enclosures the cell temperatures are not maintained as precisely as could be desired.

A great surge of activity is now taking place in many laboratories to determine whether or not the voltage steps induced by microwave radiation in the d-c current of a Josephson junction can be used to maintain the unit of voltage. Present indications are that Josephson junctions may well prove to be superior to saturated Weston cells for this purpose. An added attraction for this technique is that the use of Josephson junction voltage references would eliminate the need for transporting the unit of voltage between laboratories, since in principle only a published value for e/h and a reference to a time standard are necessary to determine the voltage at a given step of a Josephson junction. The major experimental problem encountered with Josephson junctions is that of accurately comparing their rather small voltages (presently of the order of 10^{-2} V) with the voltages of standard cells. The ability to make this comparison with high accuracy is essential in order to tie the voltage unit maintained with Josephson junctions to the absolute voltage unit obtained by means of a current balance.[2]

[2] The alternative possibility of *defining* the value of e/h would not eliminate the necessity for making measurements with current balances or electrometers, and would in fact degrade the accuracy of the ohm [15].

5. References

[1] Rayner, G. H., An absolute Determination of Resistance by Campbell's Method, Metrologia **3**, No. 1, 12–18 (Jan. 1967).

[2] Linckh, H. E., und Brasock, F., Eine Methode Zur Bestimmung des Widerstandswertes aus der Induktivität, Metrologia **4**, No. 3, 94–101 (July 1968).

[3] Page, C. H., A New Type of Computable Inductor, J. Res. Nat. Bur. Stand. (U.S.), **67B**, No. 1, 31–39 (Jan–Mar 1963).

[4] Homan, D. N., Some Techniques for Measuring Small Inductances, J. Res. Nat. Bur. Stand. (U.S.), **70C**, No. 4, 221–226 (Oct.–Dec. 1966).

[5] Thompson, A. M., and Lampard, D. G., A New Theorem in Electrostatics and its Application to Calculable Standards of Capacitance, Nature **177**, 888 (1956).

[6] Cutkosky, R. D., Evaluation of the NBS Unit of Resistance Based on a Computable Capacitor, J. Res. Nat. Bur. Stand. (U.S.), **65A**, No. 3, 147–158 (May–June 1961).

[7] Thompson, A. M., An Absolute Determination of Resistance Based on a Calculable Standard of Capacitance, Metrologia **4**, No. 1, 1–7 (Jan. 1968).

[8] Clothier, W. K., A Calculable Standard of Capacitance, Metrologia **1**, No. 2, 36–55 (April 1965).

[9] Vigoureux, P., A Determination of the Ampere, Metrologia **1**, No. 1, 3–7 (Jan. 1965).

[10] Driscoll, R. L., and Cutkosky, R. D., Measurement of Current with the National Bureau of Standards Current Balance, J. Res. Nat. Bur. Stand. (U.S.), **60**, No. 4, 297–305 (April 1958).

[11] Driscoll, R. L., Measurement of Current with a Pellat-Type Electrodynamometer, J. Res. Nat. Bur. Stand. (U.S.), **60**, No. 4, 287–296 (April 1958).

[12] Driscoll, R. L., and Olsen, P. T., Unpublished Communication to the Comite Consultatif D'Électricité.

[13] Huggins, R. W., and Sanders, J. H., Nuclear Magnetic Moment Ratios Measured in High and Low Fields, Proc. Phys. Soc. **86**, 53–63 (1965).

[14] Clothier, W. K., A Proposal for an Absolute Liquid Electrometer, Metrologia **1**, No. 4, 181–184 (Oct. 1965).

[15] Page, C. H., Letters to the Editor, Metrologia **1**, No. 2, 73–74 (April 1965).

DISCUSSION

U. Stille: May I just mention one point which touches the general title of our conference, fundamental constants. You mentioned regarding the realization of the ohm differing methods using inductance and using capacitance. There is in effect a difference between these two methods. If you are thinking about accuracies higher than 10^{-8} or in the region of 10^{-8}, then there is a special need. You see, inductance in our system of describing physics to which the SI units are appropriate enters only the magnetic constant which by the definition of the ampere indirectly got a fixed value. But regarding capacitance there enters the electric constant or, in other words, the square of the velocity of light. So then you must know the value of the velocity of light to this accuracy.

R. D. Cutkosky: That is correct.

Comment from the floor: Measure it with frequency. (*Laughter*)

ABSOLUTE VALUES OF ELECTRICAL UNITS - II
Realization of Electrical Units: Quantum Methods

A Test of the Quantum Hall Effect as a Resistance Standard

MARVIN E. CAGE, RONALD F. DZIUBA, MEMBER, IEEE, AND BRUCE F. FIELD, MEMBER, IEEE

Abstract—This paper demonstrates that the quantum Hall effect can be used to monitor a laboratory unit of resistance. A 6453.2-Ω room temperature reference resistor was calibrated relative to two quantum Hall effect devices with a 0.017-ppm (1 σ) uncertainty for each 1 h measurement period. This accuracy was achieved by correcting for a measurement system offset error and for the temperature dependences of each quantum Hall device. Hamon series-parallel resistor networks were then used to calibrate the 6453.2-Ω resistor in terms of the five one ohm resistors which comprise the NBS ohm. The total 1σ accuracy for the transfer between the quantum Hall devices and the 1-Ω resistors was 0.047 ppm.

Manuscript received August 8, 1984. This paper was supported in part by the U.S. Office of Naval Research.

The authors are with the Electricity Division, National Bureau of Standards, Gaithersburg, MD 20899.

I. Introduction

THE HALL resistance R_H of a two-dimensional electron gas is, under certain conditions, quantized in units of h/e^2 [1]:

$$R_H(i) = \frac{V_H}{I} = \frac{h}{e^2 i} = \frac{25812.80}{i} \tag{1}$$

where V_H is the Hall voltage across the sample, I is the current through the sample, h is the Planck constant, e the elementary charge, and i is an integer quantum number. Ultimately one would like to determine the value of R_H in order to verify that it is indeed equal to submultiples of h/e^2 [2] and thus depends only on fundamental constants of nature. If this were proved

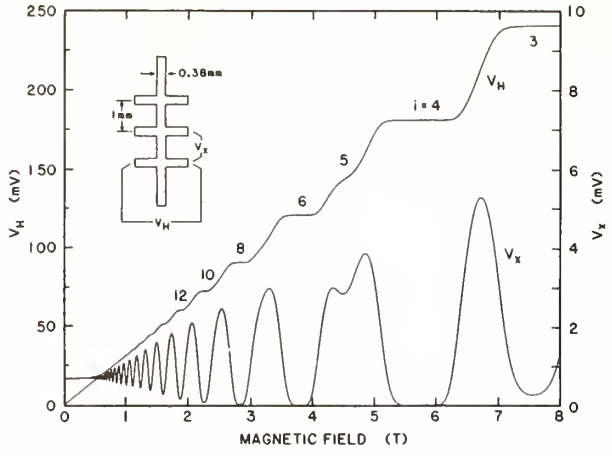

Fig. 1. Recording of V_H and V_x versus magnetic field for a GaAs device cooled to 1.2 K. The current is 25.5 μA.

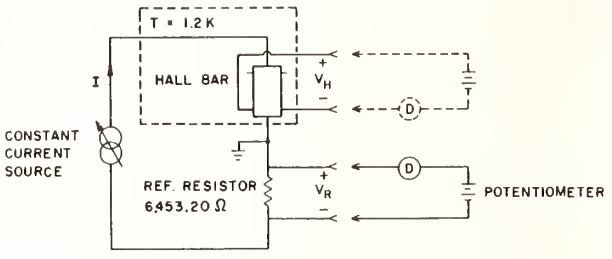

Fig. 2. A simplified schematic of the measurement circuit.

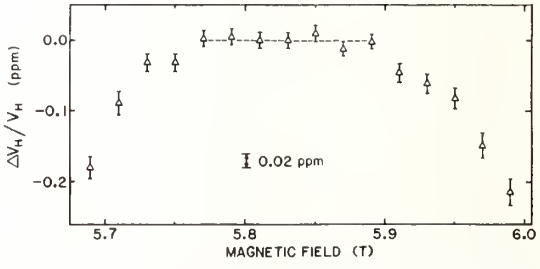

Fig. 3. A 6453.2-Ω GaAs quantum Hall step measured to high precision at 1.2 K, and I = 25.5 μA.

to be correct, then the quantum Hall effect could be used as an absolute resistance standard.

An an intermediate step in achieving this goal it is necessary to demonstrate that the quantum Hall effect can be used as a relative standard to maintain a laboratory unit of resistance based on wire-wound resistors analogous to the way in which the ac Josephson effect is used to maintain a laboratory unit of voltage. To be of practical use this standard would need to be capable of calibrating resistors to a relative accuracy of a few parts in 10^8. We demonstrate that this requirement is indeed achievable.

II. Quantum Hall Effect Measurements

Two high-quality, quantum Hall effect devices were used; both were GaAs-$Al_xGa_{1-x}As$ heterostructures grown by molecular beam epitaxy by A. C. Gossard at AT&T Bell Laboratories, and then prepared into Hall bars and screened by D. C. Tsui at Princeton University, Princeton, NJ. They are 4.6 mm long and 0.38 mm wide, and have three sets of potential probes, with two sets symmetrically displaced ±1.0 mm along the channel from the center set. Their zero magnetic field mobilities were $\sim 10^5$ $cm^2/(V \cdot s)$ at 4.2 K. Both devices were optimized for the $i = 4$ Hall step, where $R_H(4) \approx 6453.2$ Ω. Fig. 1 shows a low-sensitivity recording of V_H and V_x versus magnetic field for one of the devices for a current of 25.5 μA at 1.2 K. The V_H and V_x plots were equally as good for the second device.

The first part of the experiment consisted of making potentiometric comparisons of the quantum Hall voltage V_H with the voltage drop V_R across a series-connected room temperature reference resistor using the measurement circuit indicated in Fig. 2. The wire-wound reference resistors were adjusted to have a resistance within a few parts-per-million (ppm) of R_H. They were then hermetically sealed in silicone-fluid-filled containers and placed in temperature regulated enclosures controlled to within ±0.002°C of a nominal temperature of approximately 28°C.

To measure R_H in terms of a reference resistor, the potentiometer voltage is made almost equal to the voltage drop across V_H or V_R. An electronic detector, D, with an input current less than 10^{-15} A, amplifies the difference-voltage signal. (Note that the potentiometer does not require calibration in this arrangement.) The current source, potentiometer, and electronic detector are all battery operated. Thermally induced voltages and linear drifts in the current source and the potentiometer are cancelled by reversing the current through the device and the reference resistor. A series of reversals in the order + - - + is made for each of two measurements of V_H which bracket in time one measurement of V_R in order to obtain a single data point.

Fig. 3 shows a high resolution mapping of the $i = 4$ Hall step for one of the GaAs devices cooled to 1.2 K with I = 25.5 μA. Each data point was obtained in one hour using the procedure described above, with a ±0.011 ppm random, or type A, measurement uncertainty. This Hall step is flat to within ±0.01 ppm over a range in magnetic field that is 2 percent of the central field value. The $i = 4$ step of the second GaAs sample was equally as flat, had a nearly identical shape, and occurred at 6.02 T central field. Both devices clearly have Hall step shapes that make them suitable for use as resistance standards.

III. Quantum Hall Effect Results

One of the room temperature, 6453.2 Ω, reference resistors was compared with two different Hall probe sets of each of the two GaAs devices for both magnetic field directions over a 12-month time period starting in May 1983. The results are shown in Fig. 4, where $\Delta R/R = (V_H - V_R)/V_R$. For a measurement time of 1 h the data typically had a ±0.011-ppm random uncertainty, and was corrected for a measurement system offset error [3] which was sometimes as large as (0.025 ± 0.013) ppm. This offset error was determined by replacing the Hall device by a second room temperature 6453.2 Ω resistor and then intercomparing the two resistors with the measurement system. Also, a correction for the temperature depen-

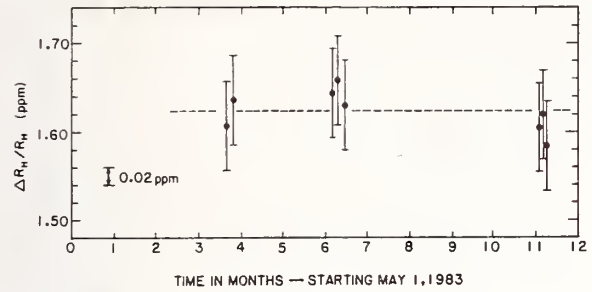

Fig. 4. Relative comparisons as a function of time of a 6453.2-Ω room temperature reference resistor with two different quantum Hall devices.

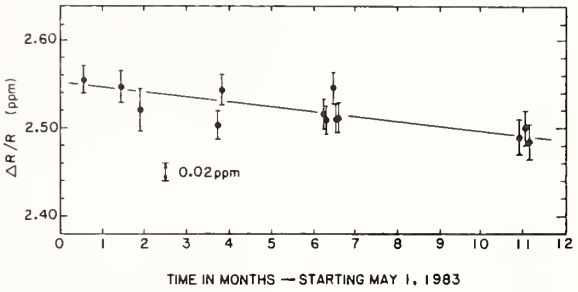

Fig. 5. Monitoring as a function of time the value of R_H expressed as a difference in ppm from a nominal value of 6453.2 Ω_{NBS}.

dence [4] of R_H for each sample was applied to every measurement, the largest correction being (0.026 ± 0.002) ppm. No current dependence [5] was observed for $I \leq 25.5$ μA, so no correction for finite I was required. Our one standard deviation uncertainty, the root-sum-square of the above three uncertainties, is ±0.017 ppm.

The corrected data were independent of the Hall device, the Hall probe set, and the magnetic field direction, so they are not distinguished in Fig. 4. From a least squares fit, these data indicate that the value of the reference resistor is decreasing at the rate of (1.81 ± 0.46) parts in 10^{10} per day or (0.066 ± 0.017) ppm/year.

IV. Step-Down to the NBS Ohm

The second part of the experiment consisted of calibrating the 6453.2-Ω resistors in terms of the set of five one ohm resistors which comprise the NBS ohm. To carry out this calibration we constructed two 6453.2 to 100 Ω series-parallel Hamon resistor networks [6] consisting of eight 800-Ω resistors plus a series-connected 53.2-Ω resistor. The eight 800-Ω resistors in the parallel (100 Ω) configuration, as well as the 53.2-Ω resistor, were each compared with the series (100 Ω) configuration of an existing 100 to 1 Ω Hamon resistor network using a dc current comparator resistance bridge. The 53.2-Ω resistor need only be measured within 1.2 ppm to achieve a 0.01 ppm accuracy for the 6453.2-Ω Hamon network. The transfer from 1 Ω_{NBS} to 6453.2 Ω is estimated to be accurate to within 0.044 ppm (one standard deviation) by this method.

Measurements involving the entire sequence (quantum Hall resistance compared with the 6453.2-Ω resistors and then stepped-down to Ω_{NBS}) have been made since August 1983. Fig. 5 shows the results of these measurements. The total one standard deviation root-sum-squared uncertainty of this sequence is typically ±0.047 ppm, and the mean value of R_H is (1.627 ± 0.047) ppm larger than a nominal value of 6453.2 Ω_{NBS}. (An uncertainty of 0.047 ppm was assigned to the mean value because the resistance step-down errors are mostly systematic, or type B.)

V. Conclusions

Although the precision and reproducibility of these measurements is 0.047 ppm, the inaccuracy with respect to the SI ohm is at least 0.5 ppm due to possible drifts of the NBS ohm since it was determined in SI units in 1974 via a calculable capacitor experiment [7]. Also, many factors such as the temperature [4] and current [5] dependencies must be closely examined and understood before we can confidently use the quantum Hall effect as an absolute resistance standard. Clearly, however, quantum Hall resistance devices can be used to monitor or maintain a laboratory unit of resistance to the level of accuracy required at national standards laboratories.

Acknowledgment

The authors wish to thank A. C. Gossard of AT&T Bell Laboratories for growing the GaAs devices, D. C. Tsui of Princeton University, Princeton, NJ, for preparing and screening the devices, and B. N. Taylor for his continued support and encouragement.

References

[1] K. v. Klitzing, G. Dorda, and M. Pepper, "New method for high-accuracy determination of the fine-structure constant based on quantized Hall resistance," *Phys. Rev. Lett.*, vol. 45, pp. 494–497, Aug. 1980.

[2] D. C. Tsui, A. C. Gossard, B. F. Field, M. E. Cage, and R. F. Dziuba, "Determination of the fine-structure constant using GaAs-Al_x-Ga_{1-x}As heterostructures," *Phys. Rev. Lett.*, vol. 48, pp. 3–6, Jan. 1982.

[3] M. E. Cage, R. F. Dziuba, B. F. Field, R. J. Wagner, D. C. Tsui, A. C. Gossard, and N. N. Tadros, "Progress report on investigations of the quantum Hall effect as a possible resistance standard," *Com. Consult. d'Electricité, Com. Int. Poids Mes., Trav. 16e Sess.*, Doc. CCE/83-32, Mar. 1983.

[4] M. E. Cage, B. F. Field, R. F. Dziuba, S. M. Girvin, D. C. Tsui, and A. C. Gossard, "Temperature dependence of the quantum Hall resistance," *Phys. Rev. B.*, vol. 30, pp. 2286–2288, Aug. 1984.

[5] M. E. Cage, R. F. Dziuba, B. F. Field, E. R. Williams, S. M. Girvin, A. C. Gossard, D. C. Tsui, and R. J. Wagner, "Dissipation and dynamic nonlinear behavior in the quantum Hall regime," *Phys. Rev. Lett.*, vol. 51, pp. 1374–1377, Oct. 1983.

[6] B. V. Hamon, "A 1-100 ohm build-up resistor for the calibration of standard resistors," *J. Sci. Instrum.*, vol. 31, pp. 450–453, Dec. 1954.

[7] R. D. Cutkosky, "New NBS measurements of the absolute farad and ohm," *IEEE Trans. Instrum. Meas.*, vol. IM-23, pp. 305–309, Dec. 1974.

A High-Accuracy Automated Resistance Bridge for Measuring Quantum Hall Devices

BRUCE F. FIELD, MEMBER, IEEE

Abstract—An automated resistance bridge has been constructed specifically to measure the Hall resistance of semiconductor devices which exhibit the quantum Hall effect. The bridge is used to perform a one-to-one comparison of the Hall resistance to a reference resistor of similar value. A measurement accuracy of 0.01 ppm or better is expected.

I. Introduction

THE QUANTUM Hall effect is a phenomenon whereby certain semiconductor devices cooled to near absolute zero and placed in a high magnetic field (≈6 T or greater) produce a resistance, at small currents, that is quantized and in theory is related to fundamental constants via

$$R_H = \frac{h}{e^2 i} \approx \frac{25\,812.8}{i}\,\Omega$$

where R_H is the Hall resistance, h is Planck's constant, e is the electron charge, and i is an integer quantum number [1]. To investigate fully the quantum Hall effect requires a very large number of high-accuracy resistance measurements. Present quantized Hall resistance measuring systems generally require constant attention by an operator [2]-[5]. A fully automated resistance bridge, which consists entirely of room temperature instrumentation, was developed to measure quantum Hall resistances in the range 3-13 kΩ with a measuring current adjustable from 0 to 37.5 μA. The bridge has been constructed with a ratio of one-to-one and will be used to compare with high accuracy the resistance developed in the quantized Hall devices to a room temperature reference resistor of nearly the same value. Such comparisons will allow one to monitor a unit of resistance and to investigate the fundamental characteristics of quantum Hall semiconductor devices. Comparison of the (odd-value) room temperature reference resistor to the as-maintained ohm at the 1-Ω level can be accomplished using a number of methods, including room temperature current comparators, cryogenic current comparators, or series-parallel resistance networks [6].

II. Bridge Design

A simplified schematic of the bridge is shown in Fig. 1. Three electronic detectors (D_1-D_3) are used to compare the voltage drop across the semiconductor device (Hall bar) to a room temperature reference resistor (R_s) constructed to be within a few ppm of the Hall resistance. The isolated outputs of the detectors are fed to three digital voltmeters which are read simultaneously by a desktop computer. Each detector is powered by a separate battery supply to ensure isolation between the detectors, the ac power line, and ground. The current source consists of four mercury batteries and a number of resistors that may be selected to provide a device current between -37.5 and +37.5 μA in steps of 2.5 μA. Resistors $R1$ and $R2$ are approximately 6.4532 kΩ and are closely matched to each other; however their ratio is not exactly known. The interchange switch exchanges the position of $R1$ and $R2$ in the bridge so that the effect of the mismatch of $R1$ and $R2$ may be eliminated from the measurement.

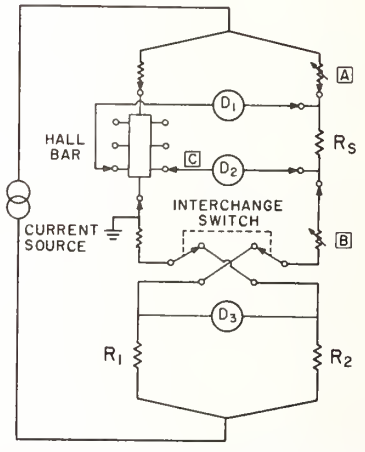

Fig. 1. A simplified diagram of the measuring bridge. D_1-D_3 are electronic detectors with isolated outputs read by digital voltmeters.

At the voltage inputs of the detectors there are no switches which could produce thermal EMF's during the operation of the bridge. British Post Office (BPO) connectors are used to connect the Hall bar and the reference resistor to the bridge so that their position in the bridge may be exchanged to test for systematic errors. This also provides generality, enabling any pair of probes on the Hall bar to be measured. The small longitudinal voltage along the device (V_x) can be measured by connecting either D_1 or D_2 (depending on the probe set and magnetic field direction) directly to the Hall bar and using the detector as a voltmeter. This measurement of V_x is required to permit extrapolation of the Hall resistance to zero temperature [7].

Manuscript received August 1984. This paper was supported in part by the U.S. Office of Naval Research.

The author is with the Electricity Division, National Bureau of Standards, Gaithersburg, MD 20899.

III. Guarding

Not shown in Fig. 1 is the circuitry which is used to guard all the critical bridge components and wiring. Coaxial cable is used for all wiring within the bridge, with the shield of the cable being driven at the same voltage as the inner conductor. Connectors, switches, resistors, and detectors, etc., are mounted within shielded boxes which, so far as possible, are driven at the same voltage as the internal circuitry. These shields are driven by a battery source identical to the main current source so that although the two sources are completely isolated from each other, their outputs track one another with temperature and load current.

Of particular interest are the computer-operated relays used to implement the resistor interchange switch, the current reversing switches (both main and guard currents), and the current magnitude selection switches. Each relay consists of a read-relay surrounded by a continuous copper shield on which the actuating coil is wound. The copper shield is extended as part of the bridge guarding circuitry so that leakage currents generated by the actuating coils are shunted away from the critical cricuitry. By design, thermal EMF's generated by the relays do not affect the bridge reading. At rated power, however, the relays produce thermal EMF's large enough to overload the detectors. Consequently, the relays are actuated with an initial current pulse which is reduced to approximately 25 percent of rated power after 100 ms. This typically reduces the thermal EMF's to 1 μV or less.

IV. Detectors

Three guarded, electronic detectors, powered by separate, guarded, battery supplies, are used to monitor the bridge unbalance simultaneously. The three detectors have transformer-isolated outputs that feed the floating inputs of three 5-$\frac{1}{2}$ digit voltmeters. The detectors are operated near null except for D_2 which measures the entire voltage difference $(R_H - R_S)\,I$, where I is the current through the resistors. The input resistance of each of the detectors was measured and found to be 38 MΩ or more, even when off null. This causes negligible loading (<0.0013 ppm) when the Hall resistance R_H is within ±10 ppm of the reference resistor R_s.

The calibration of the gain of the detectors is done *in situ* by inserting in turn, a small adjustable calibrated voltage source in series with each of the detector inputs. The day-to-day gain uncertainty of the detectors is mostly random and typically 0.024 percent (one standard deviation estimate or 1σ). For especially large differences between R_H and R_s the calibrated source is inserted in series with detector D_2 at C during the measurements to reduce the detector voltage to near zero.

V. Bridge Operation

The computer is programmed to adjust the current source to the desired bridge current and to set the interchange switch to the "up" position. The small trimmer resistors at A and B are manually adjusted to minimize detector readings D_1 and D_3. (The guard voltage is also manually adjusted temporarily using detector D_1 to monitor the difference between the guard voltage and the common-mode detector voltage.) The outputs of the three detectors are then simultaneously integrated for 30 s. The current polarity is reversed and the detector outputs are again integrated. The interchange switch is set to the "down" position and two more measurements are made, first with reversed current and then with the normal current polarity. The current reversal pattern (+, -, -, +) eliminates errors due to both thermal EMF's and detector offset voltages that either remain constant or drift linearly with time. The pattern is repeated again with the interchange switch first in the "down" position and then in the "up" position. This pattern also tends to eliminate errors due to linear drift in the ratio of resistors $R1$ and $R2$.

The interchange and current polarity switches are implemented using four independently controlled single-pole reed relays described earlier, and are operated as make-before-break and break-before-make switches, respectively. Current reversal and resistor interchange can thus be performed with almost no transient voltages appearing at the detectors, and measurements can begin within a few seconds after switching. All relays are in the bridge current paths or are in series with large resistors so thermal EMF's in these switches will not introduce an error in the measured resistance ratio so long as the detector outputs are measured simultaneously. The three digital voltmeters that read the outputs of the detectors are programmed to respond to a single trigger command from the computer and then integrate the outputs for the same length of time.

TABLE I
Difference Between Two Resistors in ppm as Measured with the Manual and Automated Systems

Date	Manual System	New Automated Bridge
4/19/84	0.471 ± 0.011	
4/18/84		0.462 ± 0.016
4/18/84		0.450 ± 0.015
6/1/84		0.449 ± 0.008
6/25/84		0.423 ± 0.008
6/25/84		0.454 ± 0.011
6/26/84	0.429 ± 0.010	
6/27/84		0.441 ± 0.013
Mean	0.450 ± 0.011* ppm	0.447 ± 0.012* ppm
Difference between the manual and automated systems		0.003 ± 0.016 ppm

*These uncertainties are the combined 1σ estimates of the random uncertainties for each measurement.

VI. Results

Comparisons of two 6453.2-Ω resistors were made using the automated resistance bridge and a manual resistance measurement system previously used for quantum Hall resistance measurements [5]. Table I summarizes the results. The uncertainties given for all the comparisons are the 1σ estimates of the random uncertainty only for a measurement time of two hours. Despite an apparent drift in the resistors which is inconsistent with previous data, the results are in good agreement.

The automated bridge was also used to compare a quantum Hall device to a 6453.2-Ω resistor. This resistor had been calibrated previously in terms of the NBS ohm. Eight measure-

ments were made during a one week period with the result $R_H = 6453.2[1 + (1.1594 \pm 0.047) \times 10^{-6}]\ \Omega_{NBS}$ where a 1σ uncertainty of 0.044 ppm has been included for the step-down from 6453.2 Ω to 1 Ω_{NBS}. The value $\Delta R_H/R_H = (1.594 \pm 0.047)$ ppm is the good agreement with previous manual system determinations which gave $\Delta R_H/R_H = (1.624 \pm 0.047)$ ppm [8]. Unfortunately, problems that developed with the manual system prevented a simultaneous comparison of the two systems using a quantum Hall device.

The bridge was tested to verify that thermal EMF's in the relays would not contribute an error to the resistor comparison by measuring the difference between two resistors using zero bridge current on several different days. The difference, which should have been zero, was found to be -0.013 ± 0.008 ppm. This result is not statistically different from zero at a 90-percent confidence level (±0.018 ppm). Another test was performed to estimate the sensitivity of the bridge to the setting of the trim resistors at *A* and *B* in Fig. 1. These were offset in random combinations equivalent to a 30-ppm resistor difference and within statistical fluctuations no change was found in the actual measured difference.

VII. Conclusions

The automated bridge has been used successfully to measure the resistance of a quantum Hall device. Using three detectors simultaneously has introduced no major error or problems in measuring such a device. Preliminary comparisons using both resistors and GaAs quantum Hall devices have indicated agreement with our manual measurement system to within 0.01 ppm. Nevertheless, more testing needs to be done in order to gain full confidence in the new system and to evaluate completely its systematic uncertainty. Specifically, the short-term random measurement error is somewhat larger than expected, probably due to a noisy detector, and there is an as yet unexplained, systematic error in the bridge of 0.018 ppm that can be observed when the positions of the Hall device and reference resistor are exchanged in the bridge.

We emphasize that the bridge is fully automated and will run completely unattended.

Acknowledgment

The author wishes to thank A. V. Gredone for help in constructing the bridge and S. D. Lince for making the tedious resistor comparisons with the manual measuring system.

References

[1] K. von Klitzing, G. Dorda, and M. Pepper, "New method for high-accuracy determination of the fine-structure constant based on quantized Hall resistance," *Phys. Rev. Lett.*, vol. 45, no. 6, pp. 494-497, Aug. 1980.

[2] A. Hartland, "Use of a cryogenic current comparator to determine the quantized Hall resistance in a silicon MOSFET," in *Precision Measurement and Fundamental Constants II*, B. N. Taylor and W. D. Phillips, Eds., NBS, Spec. Publ. 617, USGPO, Washington, DC, Aug. 1984, pp. 543-548.

[3] E. Braun, P. Gutmann, G. Hein, F. Melchert, P. Warnecke, S. Q. Zue, and K. v. Klitzing, "Cryogenic method for the determination of the fine-structure constant by the quantized Hall resistance," in *Precision Measurement and Fundamental Constants II*, B. N. Taylor and W. D. Phillips, Eds., NBS, Spec. Publ. 617, USGPO, Washington, DC, Aug. 1984, pp. 535-538.

[4] G. W. Small, "Comparison of quantized Hall resistance with a 1 Ω standard," *IEEE Trans. Instrum. Meas.*, vol. IM-32, pp. 446-447, Sept. 1983.

[5] T. Endo, Y. Murayama, M. Koyanagi, J. Kinoshita, K. Inagaki, C. Yamanouchi, and K. Yoshihiro, "Measurement system of quantized Hall effect by utilizing a Josephson potentiometer," pp. 323-327, this issue.

[6] D. C. Tsui, A. C. Gossard, B. F. Field, M. E. Cage, and R. F. Dziuba, "Determination of the fine-structure constant using GaAs-$Al_xGa_{1-x}As$ Heterostructures," *Phys. Rev. Lett.*, vol. 18, no. 1, pp. 3-6, Jan. 1982.

[7] M. E. Cage, B. F. Field, R. F. Dziuba, S. M. Girvin, A. C. Gossard, and D. C. Tsui, "Temperature dependence of the quantum Hall resistance," *Phys. Rev. B*, vol. 30, no. 4, Aug. 1984.

[8] M. E. Cage, R. F. Dziuba, and B. F. Field, "A test of the quantum Hall effect as a resistance standard," pp. 301-303, this issue.

1982 Annual Conference

A POSSIBLE QUANTUM HALL EFFECT RESISTANCE STANDARD

M. E. CAGE, R. F. DZIUBA, and B. F. FIELD
National Bureau of Standards
Washington, DC

ABSTRACT

The discovery of the quantum Hall effect by K. V. Klitzing, using semiconductor devices that are cryogenically cooled in large applied magnetic fields has opened up the exciting possibility that this effect could stimulate the discipline of electrical metrology to an extent analagous to that of the Josephson effect. This paper will describe the quantum Hall effect in an attempt to achieve a new resistance standard accurate to a few parts in 10^8, in which the resistance is defined in terms of fundamental constants of nature.

INTRODUCTION

This paper describes a new phenomenon that promises to have the same kind of impact on electrical metrology that the Josephson effect has had. It is called the quantum Hall effect, and it uses specially made semiconductor devices that are cryogenically cooled to temperatures near absolute zero. They are placed in a large magnetic field produced by a superconducting magnet in order to achieve a two-dimensional electron gas in the semiconductor devices. The electrons in this two-dimensional gas can then be made to completely occupy all of the quantum states characterized by a known integer number i. Whenever this condition is achieved the resistance R_H of the device, defined by the ratio of the Hall voltage V_H across the device to the current I through it, is found to have discrete, reproducible values that satisfy the relationship.

$$R_H = \frac{V_H}{I} = \frac{h}{e^2 i} = \frac{25{,}812.80}{i} \ \Omega. \qquad (1)$$

R_H is the quantized Hall resistance, and its value depends upon the quantum integer i, Planck's constant h, and the electron charge e. Thus we have a resistance that can be determined solely in terms of fundamental constants of nature.

This astonishing result was first verified by Klaus vonKlitzing[1] in West Germany about two years ago. He demonstrated that the quantized Hall resistance satisfies Eq. (1) to at least the 10 ppm (parts-per-million) level of accuracy. His work has generated a large amount of excitement in the scientific community, and national metrology laboratories all over the world are starting to investigate this phenomenon.

MOTIVATION

Why are resistance metrologists so interested in this effect when they already have high quality, stable, wire-wound resistance standards? The reasons are two-fold. First, as is well known, wire-wound resistors do not travel well: their values can change due to mechanical and thermal stresses, as well as barometric pressure variations, during transport. The limited data available from international comparisons indicate possible resistance transport shifts in the range 0.05-0.2 ppm for 1 ohm resistors, and significantly larger shifts for higher value resistors. Second, these resistors are artifacts and cannot a priori be expressed in "absolute" (i.e. Système International or SI) units. In the United States, for example, the as-maintained unit of resistance is defined to be the average of five nominal value 1 ohm resistors that are kept at a 25°C mineral oil bath at the NBS. This does not imply, however, that the U.S. unit of resistance is not known in terms of the SI unit. It has been so determined via an extremely difficult measurement based on the NBS calculable capacitor.[2] This measurement was last performed in 1974 and because of its difficulty is only now being repeated. The one standard deviation uncertainty of 0.03 ppm achieved in 1974 is 3 times better than any other attempt. This means that if the quantized Hall resistance is to be used as an SI resistance standard, von Klitzing's original work must be pushed about three more orders of magnitude. We believe that we are now within about a factor of ten of achieving this goal. But do not be alarmed: wire-wound resistors would continue to be used as working standards, with quantum Hall effect resistance standards being maintained in national metrology laboratories and perhaps eventually also in a few primary laboratories. They would be used in much the same way as the Josephson effect is used to maintain the unit of voltage: the national wire-wound resistance standards would periodically be calibrated against the quantized Hall resistance in order to know their time dependences and to assure that they are consistent with the SI units.

QUANTUM HALL EFFECT

With the above as an introduction and the motivation for doing this experiment, let us now investigate the quantum Hall effect in more detail. We first need a suitable semiconductor device. There are two device types which have been successfully used: laboratory versions of silicon MOSFETs (metal-oxide-semiconductor field effect

transistors) and GaAs-$Al_xGa_{1-x}As$ heterojunctions (which are hard to fabricate; to date, no more than a dozen good GaAs heterojunctions have ever been made). We will only briefly describe how our Si MOSFETs are made at the Naval Research Laboratory in a collaboration with R. J. Wagner. We start (see Fig. 1) with a single crystal substrate of p-type silicon and grow a thin SiO_2 layer on the top surface for electrical insulation. A metal film of gold or aluminum is then evaporated over the SiO_2 layer to form a gate and pads for the source and the drain (which electrically contact the substrate via diffused regions of heavily doped n-type material). The devices (see Fig. 2) are 1.3 mm long and 0.2 mm wide and can be seen with the naked eye. In addition to the source and drain pads we have potential probes placed along the device which sample voltages in the channel under the gate.

We ground the source (see Fig. 3) and apply a positive dc voltage to the gate, thereby obtaining a parallel-plate capacitor, with the metal gate being one electrode and the semiconductor substrate the other. The SiO_2 layer is typically 0.1 μm thick, so if the gate voltage is 30 volts this means that the electric field across the insulator is 3×10^6 volts/cm! Therefore, no pinholes can be tolerated in the SiO_2 layer. By increasing the gate voltage we induce more electrons near the top surface of the substrate. But it is not like a normal capacitor because these electrons are bound in a potential well and must therefore obey quantum mechanical laws. This potential well quantizes the electrons in the vertical direction and confines them into a two-dimensional electron gas. The gas is so ner the SiO_2 interface that this surface must literally be atomically smooth, otherwise the electron gas will scatter from the rough surface and destroy the quantum Hall effect. Also, there are always impurity ions present and the electrons will scatter from them; we therefore require state-of-the-art devices to minimize these problems.

By applying an electric field in the vertical direction to a sample cooled to near absolute zero we have quantized the electrons in the vertical direction, forming a two-dimensional electron gas. Let us next apply a magnetic field that is also in the vertical direction. This must be a very large field, so we use super-conducting magnets to produce fields up to 15 T, which is 150,000 gauss (or about 3×10^5 times larger than the Earth's magnetic field). The electrons in the two-dimensional gas form cyclotron orbits about the vertical magnetic field lines, quantizing the electrons in the horizontal plane. The result is a completely quantized, two-dimensional electron gas. By increasing the gate voltage we induce more electrons into allowed cyclotron orbits, and it is possible to completely fill, for example, all of the i = 4 orbits, but none of the i = 5 orbits because the device is so cold, and the current is so low, and the scattering is so small that there is insufficient energy to occupy any i = 5 states.

Now assume that we have just filled the i = 4 states and then pass an electron current through the sample. There is the resulting flow pattern (see Fig. 4): the electrons emerge from one corner of the device and exit at the opposite, the reason being that magnetic forces cause the electrons to pile up in the upper left hand corner and along the top edge. The magnetic forces are exactly balanced by the electrical forces between the electrons within the sample, but there is an escape route at the top right hand corner. The electrons are acclerated at the ends of the device and drift with constant velocity in the interior. If the current is 5 μA and the i = 4 quantum states are just filled, then the source-drain voltage is about 32 mV. Let us next map the potential distribution around the periphery of the sample (as shown in Fig. 4) with the source at zero volts since it is grounded. We can measure voltages within the sample via the potential probes. For example, the voltage drop along the channel, V_x can be obtained with probe sets 1,2 or 3,4 and in both cases $V_x = 0$. The reason is simple: if the i = 4 states are filled and if there is insufficient energy to scatter into any i = 5 states, then there is no scattering. If there is no scattering there is no voltage drop. Thus the voltage drop along the channel becomes very small when all the quantum states are filled. There is, however, a voltage drop across the channel, $V_y = V_H$, and this Hall voltage can be measured with probe sets 1,3 or 2,4. In both cases V_H is about 32 mV. K. v. Klitzing measured V_H more carefully[1] and found in sample after that VH was 32.266 mV. Divide this by 5 A and you get R_H = 6,453.2 Ω, which is precisely the value predicted in Eq. (1) for i = 4!

MEASUREMENT SYSTEM

Can this amazing result be pushed the three more orders of magnitude necessary for use as an SI resistance standard? Here is the measurement system (see Fig. 5) that we are using in our initial attempts to answer this question. The system is battery-operated and consists of a constant current course that supplies current to the Hall device which is cooled to 4.2 K by immersing the device in liquid helium. We can further cool the sample of 1.5 K by pumping on the liquid helium bath. (The Hall sample is, of course, located in the central field of a superconducting magnet.) The current also passes through a room temperature reference resistor constructed to have the same nominal resistance value as the quantum Hall resistance of interest, e.g. 6,453.20 Ω when i = 4. This assures us that $V_H \approx VR$, and that both voltages can be nearly bucked-out by the potentiometer. The electronic detector, D, reads the voltage

differences and its isolated output is either directed into an X-Y recorder or is digitized for computer analysis. If we can assure ourselves that the same current passes through both the sample and the reference resistor, then the current can be eliminated in the equations for V_H and V_R and the quantized Hall resistance RH can be obtained from the ratio V_H/V_R and the calibrated value of the reference resistor RR. (RH will be given in Si units if RR has been determined in SI units via the calculable capacitor experiment.)[2] The current is typically 10 μA, so for a part in 10^8 measurement this requires that any currents shunting the sample or resistor, or leaking to ground, must be less than 10^{-13}A. Another way of stating this condition is that the leakage resistance between the leads, and to ground, must be greater than 10^{12} Ω --except for the gate lead, which must be greater than 10^{14} Ω since it is at a higher voltage. (A fingerprint across terminals can be a short-circuit in this experiment!)

RESULTS

Now for some data. Here are low sensitivity X-Y recordings of V_H and V_x, in mV, versus gate voltage for a silicon MOSFET at 13 tesla obtained at the Naval Research Laboratory (see Fig. 6). The voltage drop along the channel, V_x becomes very small when a quantum level is filled, whereas plateaus or steps simultaneously occur in the Hall voltage because the electrons have insufficient energy to occupy cyclotron orbits with larger quantumnumbers. It is easy to identify the quantum states: for example, a step occurs at about 32 mV; divide that by 5 μA and we have the 6,453.20 Ω step. We have just filled all of the possible i = 4 cyclotron orbits.

We can investigate this step in more detail by bucking-out most of the Hall voltage with the potentiometer and reading the voltage differences with the electronic detector. Here is the Hall step on a scale expanded by 4 orders of magnitude (see Fig. 7). The arrow indicates the minimum V_x. There are large thermally-induced voltages in the leads between the sample at 1.5 K and room temperature; they are eliminated by obtaining a Hall step of the opposite polarity (by reversing the current) and by taking half the difference of the two polarities (since the thermal EMFs do not reverse on current reversal). The resulting Hall step is flat to within at least 1 ppm over a gate voltage range of 0.2 V. It takes about one minute to obtain a Hall step plot at this sensitivity, so we can quickly obtain a lot of information about its overall shape. For precision results, we fix the gate voltage and digitize the data for 1-2 hours.

We have also obtained data on GaAs heterojunctions at Bell Laboratories in a collaboration with D. C. Tsui and A. C. Gossard. Here are high sensitivity plots for three Hall steps (see Fig. 8), two for i = 2 (12,906.40 Ω steps) and one for i = 4 (6,453.20 Ω). (In GaAs heterojunctions we vary the magnetic field rather than the gate voltage to change the quantum state filling factor.) We believe that the different shapes on the sides of the steps are due to inhomogenities in the sample.[3] Our result[4] for these three samples, expressed in SI units, is: RH = 6,453.2004(11) Ω for i = 4, with a one standard deviation uncertainty of ±0.17 ppm. This result is three to eight times more accurate than the other three quantized Hall resistance results obtained by workers in West Germany[5] and Japan.[6,7]

We have also made measurements on silicon MOSFETs, plus direct silicon MOSFET--GaAs heterojunction intercomparisons, at the Naval Research Laboratory (NRL), and find the values of R_H to be sample-independent to at least the 0.1 ppm level of accuracy. However, much to our surprise, there is a problem because the values of R_H obtained at NRL were found to be about 0.8 ppm larger than those we obtained at Bell Laboratories. We currently attribute this discrepancy to rectification of electrical noise in the highly nonlinear samples. This assumption is now being investigated in a much cleaner electrical environment at NBS using an 8 tesla magnet.

SUMMARY

If the results confirm our Bell Laboratories measurements, we will have advanced the experiment two of the three orders of magnitude necessary to achieve an SI resistance standard based upon fundamental constants of nature. What about the final order of magnitude? It will not be easy, but we believe that it is experimentally possible. A new measurement system is under construction for our second generation experiments, and a 15 tesla magnet should be delivered within a year. There are certain to be unexpected problems and surprises along the way but we remain optimistic.

ACKNOWLEDGEMENTS

The authors wish to acknowledge the encouragement of B. N. Taylor and the important contributions of our collaborators: S. M. Girvin and N. N. Tadros of NBS, A. C. Gossard of Bell Laboratories, D. C. Tsui of Princeton University, and R. J. Wagner of the Naval Research Laboratory. The work at NBS is supported in part by the Office of Naval Research and by the Calibration Coordination Group of the Department of Defense.

REFERENCES

1. K. v. Klitzing, G. Dorda, and M. Pepper, "New Method for High Accuracy Determination of the Fine-Structure Constant Based on Quantized Hall Resistance," Phys. Rev. Lett. 45, 494 (1980).

2. R. D. Cutkosky, "New NBS Measurements of the Absolute Farad and Ohm," IEEE Trans. Instrum. Meaa. IM-23, 305 (1974).

3. R. J. Wagner, C. F. Lavine, M. E. Cage, R. F. Dziuba, and B. F. Field, "Measurements of the Quantized Hall Steps in Si at the ppm Level," Surface Sci. 113, 10 (1982).

4. D. C. Tsui, A. C. Gossard, B. F. Field, M. E. Cage, and R. F. Dziuba, "Determination of the Fine-Structure Constant Using GaAs-$Al_xGa_{1-x}As$ Heterostructures," Phys. Rev. Lett. 48, 3 (1982).

5. E. Braun, E. Staben, and K. V. Klitzing, "Experimental determination of h/e^2 by the Quantized Hall Resistance in MOSFETs," PTB Mitteilugen 90, 350 (1980).

6. C. Yamanouchi, K. Yoshihiro, J. Kinoshita, K. Inagaki, J. Moriyama, S. Baba, S.Kawaji, K. Murakami, T. Igarashi, T. Endo, M. Koyanagi, and N.Nakamura, "Hall Effect in Silicon MOS Inversion Layers - For h/e^2 Determination," in Precision Measurement and Fundamental Constants II, ed. by B. N. Taylor and W. D. Phillips (Nat. Bur. Stand. U.S., Spec. Publ. 617, to appear).

7. K. Yoshihiro, J. Kinoshita, K. Inagaki, C. Yamanouchi, J. Moriyama, and S. Kawaji, "Quantized Hall Resistivity in Si-MOSFETs Measured at Liq. ^3He Temperatures," J. Phys. Soc. Japan 51, L5 (1982).

SILICON MOSFET (Side View)

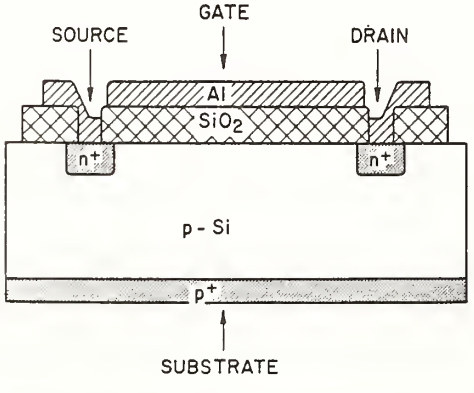

Figure 1

NRL n-CHANNEL SILICON MOSFET

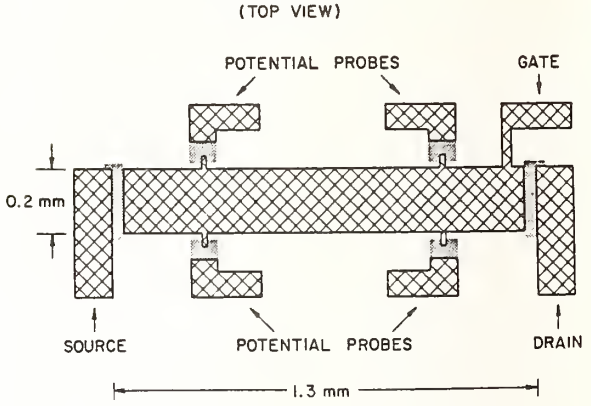

Figure 2

SILICON MOSFET (Side View)

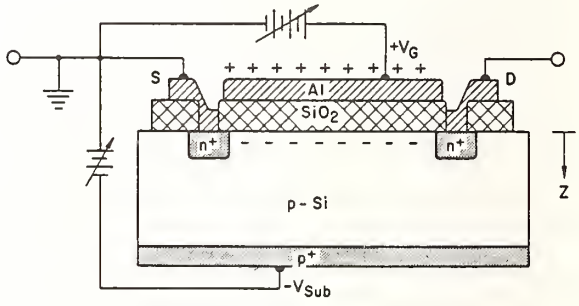

Figure 3

EQUAL-POTENTIAL LINES AND ELECTRON PATHS

$R_H = 6,453.20\ \Omega$

$I_{SD} = +5\ \mu A$

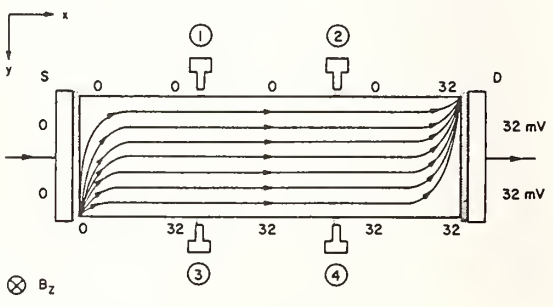

Figure 4

QUANTIZED HALL RESISTANCE MEASUREMENT

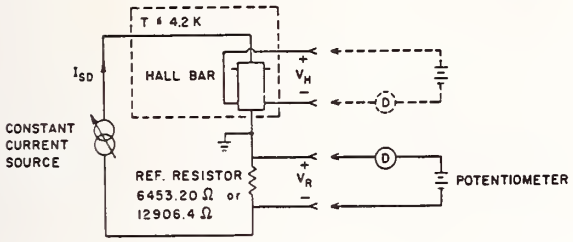

$$V_H = I_{SD} \cdot R_H \qquad V_R = I_{SD} \cdot R_R$$

$$R_H = \frac{V_H}{V_R} R_R$$

Figure 5

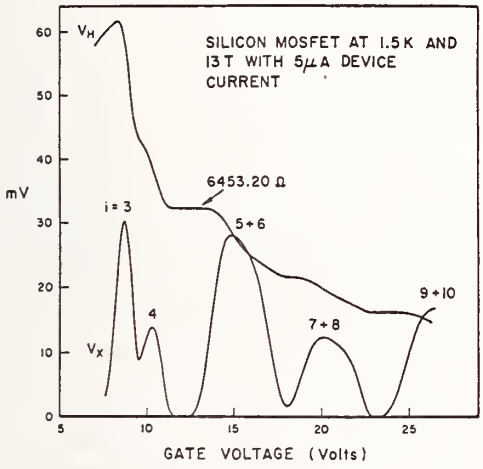

Figure 6

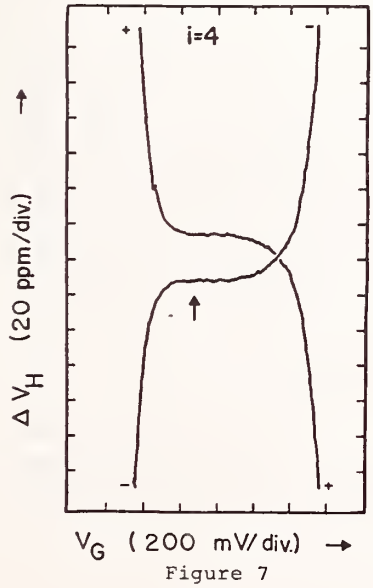

Figure 7

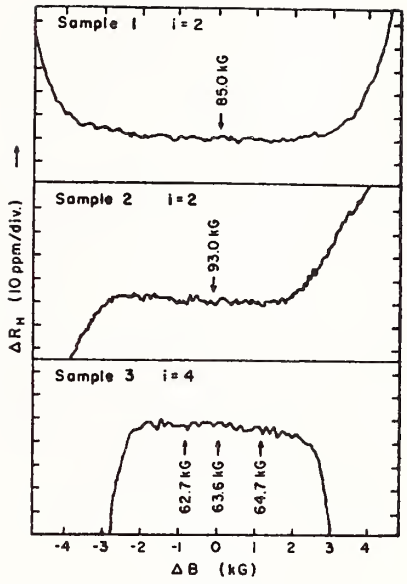

Figure 8

The Quantum Hall Effect. I

The recent surprising observation of a quantization of the Hall resistance in units of h/e^2 in quasi-two-dimensional conductors presents the possibility of obtaining an improved value of the fine structure constant and development of a quantum standard of resistance using a solid state device.

INTRODUCTION

The recently discovered quantum Hall effect has attracted a great deal of interest due to the possibility of obtaining an improved value of the fine structure constant[1] and development of a quantum standard of resistance. The observation of a quantization of the Hall resistance in units of h/e^2 in quasi-two-dimensional conductors has necessitated a major rethinking of our picture of transport in these systems. It is the purpose of this Comment to provide an introduction to this phenomenon and an overview of the important questions in the field which are currently being discussed.

We begin with a brief introduction to the subject of electron inversion layers and the discovery of the quantized Hall resistance. This will be followed by a discussion of the simple theory for the case of no disorder. Next we will consider the theoretical and practical implications of an improved value for the fine structure constant and achievement of a quantum mechanical standard of resistance. We will conclude with a list of questions of specific current interest which will be discussed in more detail in a later Comment.

Comments Solid State Phys.
1983, Vol. 11, No. 1, pp. 1–16
0308-1206/83/1101-0001/$18.50/0

INVERSION LAYERS

One of the features of physical systems which is of great importance is the dimensionality. There has been particular interest in recent years in seeking out and studying quasi-one- and -two-dimensional systems. One of the most versatile and successful examples of such systems is the quasi-two-dimensional electron gas generated in the form of so-called inversion layers at semiconductor interfaces. For a recent comprehensive review see Ando et al.[2] The most common technique involves the use of a device known as a silicon MOSFET (metal-oxide-semiconductor field effect transistor). This is a laboratory version of a commercial device whose structure is shown schematically in Figure 1. The typical length scale of these devices is 1 mm. The inversion layer is formed at the Si–oxide interface by application of a positive (in an *n*-type device) voltage (10–50 V) to the gate. Because the oxide layer is thin, an electric field of order 10^6 V cm^{-1} is generated which bends the Si conduction band downward and attracts carriers to the interface. This is illustrated in the energy level diagram shown in Figure 2. A very nice feature of these systems is that the carrier density is continuously adjustable by means of the gate voltage.

While it is true that the inversion layer charge forms a thin sheet, it is not at all obvious that this system should behave as if it were strictly two-dimensional. This question was first addressed by Schrieffer, who pointed out that the electric field from the gate confines the electrons to such a narrow region (25–50 Å) that quantum mechanical effects are essential to the description (see discussion in Ref. 2). The motion in the direction normal to the interface is quantized into discrete energy levels called electric sub-bands whose splitting is quite large ($\sim$ 20 meV). This energy scale is much larger than any other in the system and so motion in the normal direction is "frozen out" by quantum mechanics. This means that for applied frequencies ω such that $\hbar\omega \ll$ 20 meV the transport properties are those of a mathematically two-dimensional system. This idea was confirmed in a Shubnikov–de Haas measurement by Fowler et al.[3] which showed that the density of states is indeed two-dimensional.

Another inversion layer system which has been developed is the GaAs–$Al_xGa_{1-x}As$ heterostructure[4] which is fabricated by molecular beam epitaxy. Unlike MOSFETs these systems have a fixed carrier

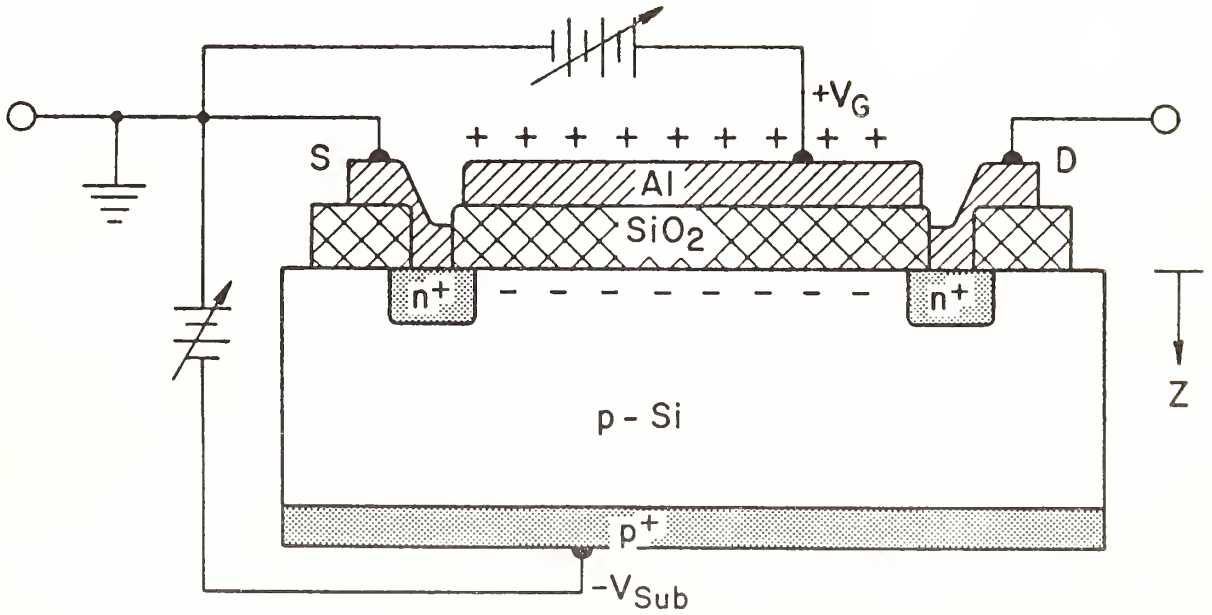

FIGURE 1 Schematic side view of a silicon MOSFET showing the Al gate, the SiO_2 insulator and the Si substrate. The source and drain are the heavily doped n^+ regions. Not shown are other contacts used in determination of the Hall voltage and the longitudinal voltage drop.

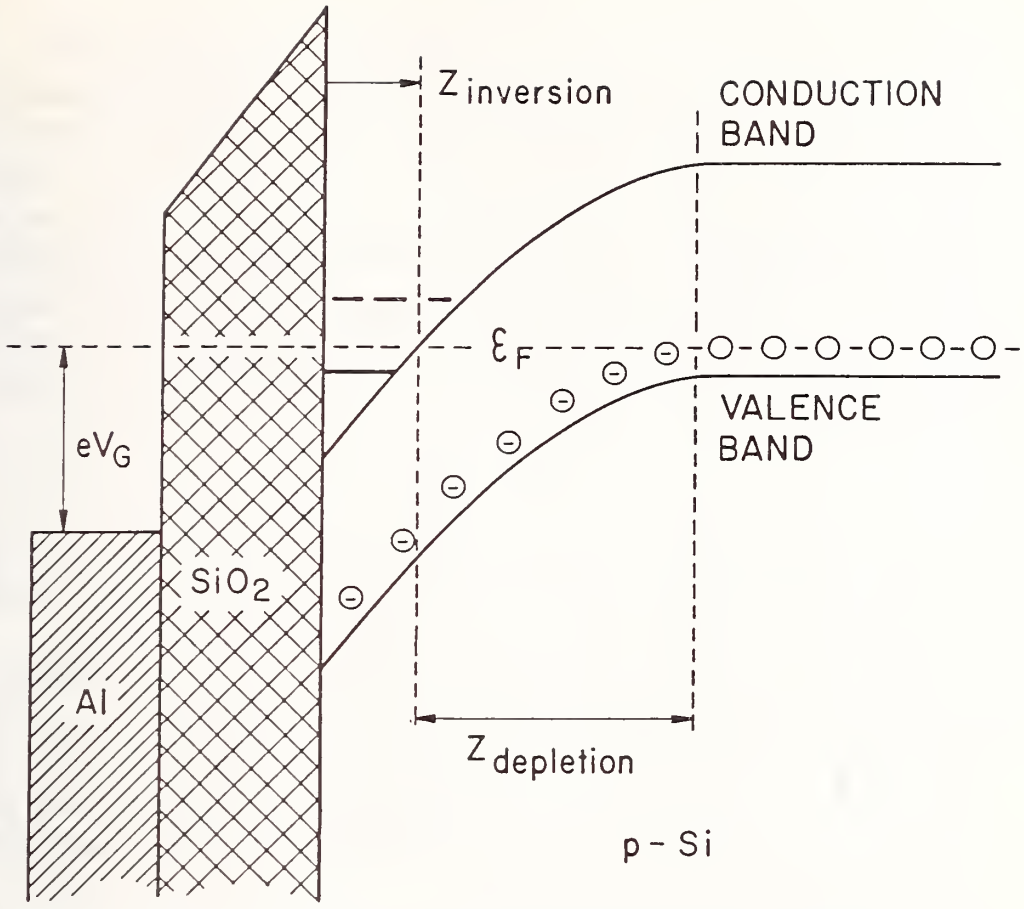

FIGURE 2 Electron energy level diagram showing the effects of a positive gate voltage. When the conduction band is bent down below the Fermi level E_F, the inversion layer is formed at the interface.

density and so the magnetic field must be adjusted to achieve the quantum Hall condition discussed below. Although difficult to construct these devices offer several advantages. The requisite magnetic fields are relatively low ($\sim$ 8 T versus $\sim$ 13 T or more for Si). In addition the electron effective mass is quite low (0.068 m_e versus 0.2 m_e for Si) so that the characteristic magnetic energy is large, allowing one to work at higher temperatures ($\sim$ 4.2 K). Another advantage is the very high mobility that can be obtained since, unlike MOSFETs, the donors provide the inversion layer charge and can be physically separated from the active region.

THE QUANTUM HALL EFFECT

In 1980 von Klitzing et al.[1] reported that under certain conditions the Hall resistance of a MOSFET inversion layer is quantized in units of h/e^2 where h is Planck's constant and $-e$ is the electronic charge. Before delving into this remarkable observation let us briefly review the classical Hall effect. In an ordinary conductor carrying a current density $\mathbf{J}$ the associated electric field $\mathbf{E}$ is given by $\mathbf{E} = \rho\mathbf{J}$ and points in the direction of the current flow. Here ρ is the resistivity. If a magnetic field $B\hat{z}$ is applied normal to the plane, the resistivity becomes a tensor quantity:

$$E_i = \rho_{ij} J_j, \tag{1}$$

so that a component of the electric field appears perpendicular to the current and the magnetic field. This is called the Hall field and the off-diagonal part of the resistivity ρ_{yx} is called the Hall resistivity.

The resistivity tensor is obtained experimentally by establishing a constant current density $\mathbf{J}$ in the $\hat{x}$ (say) direction and measuring the resulting electric field. E_x determines ρ_{xx} and E_y determines ρ_{yx}. In principle one could equally well establish a fixed electric field and measure the resulting current. This would constitute a determination of the conductivity tensor σ defined by

$$J_i = \sigma_{ij} E_j. \tag{2}$$

The conductivity is, as usual, the inverse of the resistivity but because these are tensor quantities it is *not* true that $\sigma_{xx} = 1/\rho_{xx}$. Indeed, in the quantum Hall case where the current is almost perfectly perpendicular to the electric field one has $\rho_{xx} = \sigma_{xx} = 0$. Thus the resistivity and the conductivity both vanish! This paradoxical result is easily understood, however. If an electric field is applied no current flows in the direction of the field. Hence the (diagonal part of the) conductivity vanishes. If on the other hand a current is applied, no field appears in the direction of the current. Hence the (diagonal part of the) resistivity also vanishes. It turns out in this case that the off-diagonal terms are simply related by $\rho_{xy} = -1/\sigma_{xy}$.

The Hall resistivity may be calculated in several different ways, both quantum mechanically and classically, in terms of the Lorentz force

acting on the carriers drifting in the magnetic field. The standard result is

$$\rho_{yx} = \frac{-B}{ne}, \tag{3}$$

where n is the number of carriers per unit volume (or, in the case of two dimensions, per unit area). An important aspect of this expression has to do with the dimensionality. Experimentally, the easiest quantity to measure is the *resistance,* which is the measured Hall voltage divided by the applied current. The quantity given in Eq. (3), however, is the Hall *resistivity*. For a sample of length L in each dimension the connection between the Hall resistance R_H and the Hall resistivity ρ_{yx} is

$$R_H = \rho_{yx} L^{2-d}, \tag{4}$$

where d is the dimensionality. It is fortunate that in two dimensions the length factor drops out so that resistance and resistivity are the same quantity. If this were not the case accurate measurements would entail length scale determinations which would be essentially impossible to perform to high enough accuracy.

Since the inversion layer charge density n is relatively low, one sees a huge Hall voltage ($\sim$ 6 mV/μA). Because the carrier density in a MOSFET is proportional to the gate voltage V_G one expects [from Eqs. (3) and (4)] a smooth hyperbolic dependence of R_H on V_G. Under conditions of high magnetic field ($\sim$ 13 T) and low temperatures ($\sim$ 2 K) startling deviations from this behavior are seen as shown[5] in Figure 3. One sees a series of plateaus now referred to as Hall "steps" where the Hall voltage V_H appears to be essentially constant independent of the gate voltage. The value of the Hall resistance at these plateaus is to a high degree of accuracy (the errors are believed to be less than 1 part in 10^6):

$$R_H = \frac{h}{e^2 i}, \tag{5}$$

where i is a small integer.

This unexpected result is (seemingly) not difficult to understand for the ideal case of no disorder, no Coulomb interactions and zero tem-

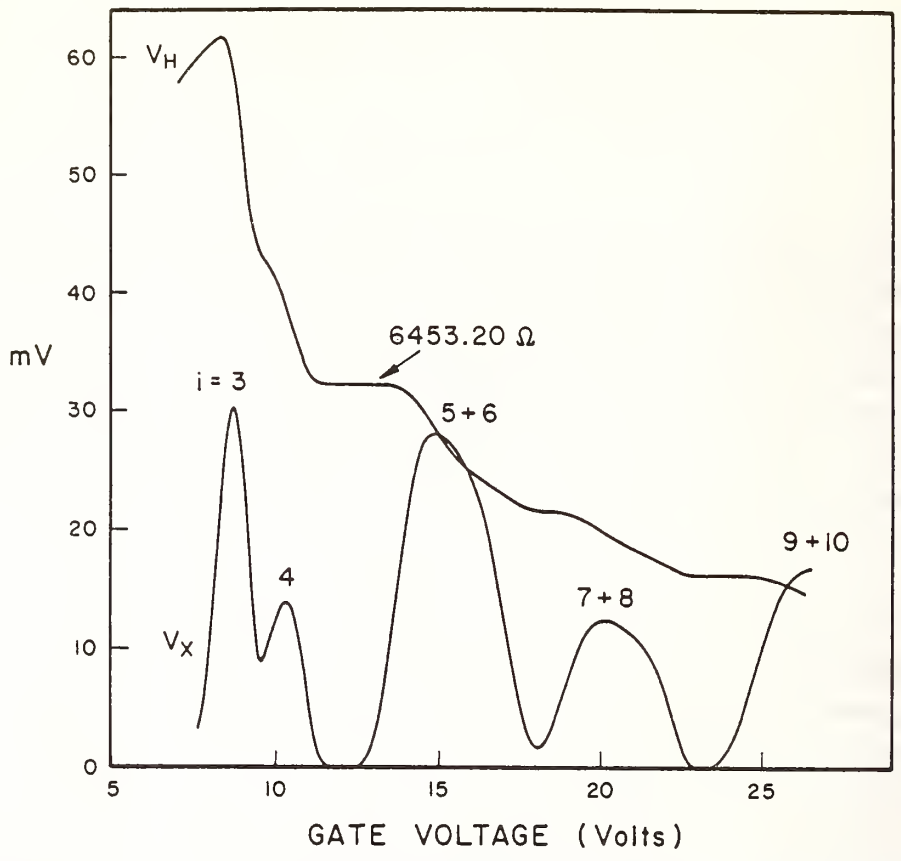

FIGURE 3 Hall voltage (V_H) and longitudinal voltage drop (V_x) in a silicon MOSFET at 1.5 K and 13 T with a constant 5 μA source-drain current. Note that the Shubnikov–de Haas oscillations in V_x are correlated with the plateaus in V_H. The 6453.20 Ω plateau corresponds to $h/4e^2$. The quantum number i appears in Eq. (5).

perature. If we *assume* an effective mass Hamiltonian then we have in the presence of the magnetic field

$$H = \frac{1}{2m^*}(\mathbf{p} + e\mathbf{A})^2, \tag{6}$$

where it is convenient to take the vector potential $\mathbf{A}$ to be in the Landau gauge:

$$\mathbf{A} = \hat{x}\, By. \tag{7}$$

Quite often in atomic and condensed matter physics we make the approximation of keeping in the Hamiltonian only the term linear in B.

Here, however, the magnetic field is so large that the behavior of the system is dominated by the field and it is essential to retain the quadratic term. As shown in Figure 4a the energy levels are quantized into discrete uniformly spaced harmonic oscillatorlike levels $E_n = n\hbar\omega_c$. The magnetic energy is $\hbar\omega_c$ where ω_c is the classical cyclotron frequency.

One can think about the discrete quantization of the energy levels in the following semiclassical picture. As the strength of the magnetic field is increased the radius of the classical Larmor orbit decreases (for a given particle speed). At high enough fields quantum mechanics becomes important because the circumference of the orbit reaches the scale of the de Broglie wavelength. The requirement that the orbit contain an integer number of wavelengths results in the discrete quantization of the energy levels.

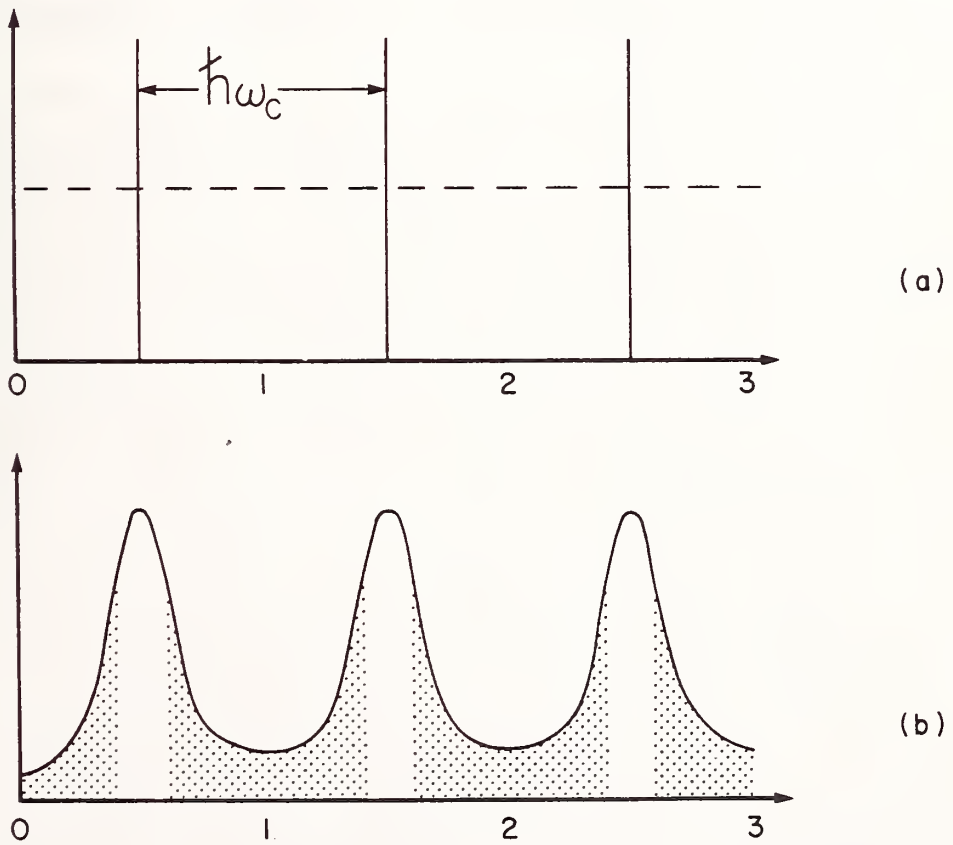

FIGURE 4.(a) Density of states of the ideal two-dimensional electron gas in high magnetic field and zero field (dashed). (b) Broadened density of states in the presence of disorder. Shading indicates regions of localized states.

For a Si(100) inversion layer $\hbar\omega_c = 5.8$ meV at 10 T and for a GaAs heterojunction $\hbar\omega_c = 17$ meV at 10 T. These energies are much larger than characteristic thermal energies ($\lesssim 0.1$ meV at $T \lesssim 1$ K). This is essential to the effect because if the chemical potential lies in the gap between Landau levels then an integer number of levels will be fully occupied and all higher ones will be essentially empty. The essence of the phenomenon is that the density of states per unit area per Landau level is then proportional to the magnetic field:

$$n = \frac{eB}{h}. \tag{8}$$

Putting this into Eqs. (3) and (4) we have the desired result for the quantum Hall resistance:

$$R_H = h/e^2. \tag{9}$$

If i Landau levels are filled this expression is divided by i, yielding the observed result of Eq. (5).

The *sine qua non* of this simple result is the *areal quantization* which produces a density of states per Landau level that is proportional to the applied field and independent of the effective mass. The only quantity which depends on m^* is the energy spacing $\hbar\omega_c$. The first worry that comes to mind is the validity of the effective mass approximation since the bands in semiconductors are never perfectly parabolic and, in addition, the magnetic energy is not small compared to the bandwidth. Onsager's famous argument[6] concerning the de Haas–van Alphen effect for Bloch electrons shows one how to calculate the magnetic energy levels for an arbitrary band. However, this argument is only valid for large magnetic quantum number i and cannot be expected to be valid in the quantum limit where i is small. This is not a problem, however, since the actual Landau level spacing is irrelevant so long as it is much greater than k_BT. The counting argument that gives the density of states per Landau level proceeds in wavevector space and should not (in the absence of random impurities) be dependent on the dispersion relation. Nevertheless, no rigorous proofs along these lines have been developed. In any case the areal quantization in the ideal case is something of a red herring since, as we shall see, it does not apply to the case of strong disorder where some of the states become localized (and ρ_{xy} is nevertheless correctly quantized).

We have already mentioned the lack of length scale dependence of the resistance in two dimensions. A profound implication of this is that in the classical case the measured Hall resistance is completely geometry independent. One can have a variable width or even punch holes in the sample without affecting the Hall resistance.[7] Tsui and Allen[8] have suggested that this classical result is a good point of departure for forming a picture of the quantum Hall effect. Iordansky[9] and Kazarinov and Luryi[10] have used a similar picture in semiclassical considerations of percolation effects in two-dimensional systems with a random potential which is slowly varying on the scale of the magnetic length, $l = (\hbar/eB)^{1/2}$. The essential feature in all these cases that makes the Hall resistance remain constant is that in two dimensions the current not being carried in the insulating regions is compensated by extra current flowing in the conducting regions. The extent to which this applies to the quantum mechanical case with nonsmooth potentials will be discussed briefly below and in more detail in Part II of this series.

SCATTERING AND DISORDER

The most obvious defect of the simple theory presented above is the assumption of no disorder. It is true that in the weak field Boltzmann theory there are no scattering corrections to ρ_{yx} [note that there are corrections of order $(\omega_c\tau)^2$ to σ_{yx}] but there is no reason to expect this result to hold in the present case. We know in fact that the disorder must be quite large because of the anomalously large width of the Hall steps. If there were no disorder then there would be no states in the gap between Landau levels and the chemical potential could not be sustained in the gap for a finite range of magnetic field or gate voltage. The current belief is that there is sufficient disorder (or a combination of disorder and Coulomb interactions) to produce a continuous density of states with no gap. States close to the original Landau level are extended and those further away are expected to be non-current-carrying (zero mobility) localized states (see Figure 4b). Thus, there is a *mobility gap* even though there is no gap in the density of states. This allows the system to keep the chemical potential in the mobility gap over a finite range of electron density or magnetic field. Of course the number of extended current carrying states no longer satisfies Eq. (8) and there is no reason to expect the Hall resistance quantization. The paradox is

that the quantum Hall effect *cannot* be observed *without* disorder, and yet there is no obvious reason to expect it to work *with* disorder. Somehow extra current must be carried by the extended states to compensate for the lack of current in the localized states. This point will be discussed further in Part II.

We will touch only briefly here on one point about the disorder which will show why this system is unique and give a hint as to why disorder does not destroy the quantization. In an ordinary inversion layer system unavoidable disorder produces a finite relaxation time $\tau \sim 10^{-11}$ s. In the presence of low temperature and a high magnetic field, however, the situation is drastically altered if the chemical potential lies in the mobility gap. All the current-carrying states below the Fermi level are filled and, just as in a superconductor, elastic scattering of the carriers cannot occur because of the finite gap. Referring to Figure 3 we see that there are indeed large (Shubnikov–de Haas) oscillations in the diagonal component of the resistance ($R_x = V_x/I$) and that this resistance is very small in the region corresponding to each Hall step.

The resistance becomes so low in fact that it is difficult to measure. A lower limit for the high B field relaxation time τ^* is $10^8\,\tau \sim 1$ ms.[11] The primary limitations in the measurement at present are finite temperature and finite (nonlinear) electric field effects. Measurements of these effects are of great interest since they provide information about the nature of the transport. The scattering rate is so small that the equivalent three-dimensional resistivity is $\leqslant 5 \times 10^{-13}$ Ω-cm[11] which is lower than any other known value except those of superconductors. The resistivity is so low that it might be easier to find the relaxation time directly by measuring the persistence time of current in a closed loop. This can be done for superconductors but would be very difficult in these small devices because the stored energy is very small and in any case is largely capacitive (associated with the applied Hall voltage) rather than inductive.[11]

Another important measure of the scattering rate is $\rho_{xy}/\rho_{xx} = \tan \delta_H$, the tangent of the Hall angle. The Hall angle is defined to be the angle between the electric field and the current, and from the upper limit on ρ_{xx} one finds $\tan \delta_H \gtrsim 10^{10}$, indicating that the dissipation is indeed very low and the current flow very nearly perpendicular to the applied field.

In summary, the peculiar properties of two-dimensional Landau level systems cause the transport to be dissipationless even in the presence

of strong disorder. Thus in principle $\rho_{xx} = 0$ as in the ideal zero-disorder limit. This is not a proof that ρ_{xy} should be unaffected but is a strong hint that there is a fundamental connection between this result and the quantization of the Hall resistance. This connection will be explored in greater detail in Part II.

THE FINE STRUCTURE CONSTANT AND A POSSIBLE RESISTANCE STANDARD

The fine structure constant α is the dimensionless measure of the coupling between matter and the electromagnetic field. It is central to the theory of quantum electrodynamics (QED). The fine structure constant can be related to the quantum Hall resistance by

$$\alpha = \frac{\mu_0 c}{2} \frac{e^2}{h} = \frac{\mu_0 c}{2} \frac{i}{R_H}, \tag{10}$$

where μ_0, the permeability of the vacuum, is by definition exactly $4\pi \times 10^{-7}$ H/m, and c is the speed of light. Because c is very accurately known (and in fact because of a forthcoming redefinition of the meter is soon to be an exactly defined number) one can use the quantum Hall effect (QHE) measurement of $R_H = h/e^2 i$ to determine α. Improvements in our knowledge of α are important as a check on the internal consistency of QED and, if sufficient accuracy is obtained, can also put constraints on modern theories of the weak and strong interactions.

The most accurate experimental determination of α to date is the QED theory-dependent result from measurements of the anomalous magnetic moment of the electron,[12] a_e, with an uncertainty of 0.07 ppm (parts-per-million). One would like to have a value of α that is independent of QED, and this has been obtained by a combined Josephson effect[13] ($2e/h$) - proton gyromagnetic ratio[14] (γ_p') experiment with an uncertainty of 0.11 ppm. The quantum Hall effect experiment also provides a QED-independent value of α, and the accuracies of reported results are approaching the best values: 1.3 ppm,[15] 0.88 ppm,[16] 0.50 ppm,[17] and 0.17 ppm.[18]

Measurements at these levels of accuracy require access to a carefully calibrated set of electrical units. The QHE result for α with the 0.17 ppm uncertainty[18] and the combined $2e/h - \gamma_p'$ value[13,14] for α were

both obtained in terms of the electrical units maintained by the U. S. National Bureau of Standards. It is possible to combine these two results for α in a way which eliminates much of the uncertainty in the calibration of the ohm and thereby obtain a more precise value[18]: $\alpha^{-1} = 137.035965(12)$ (0.09 ppm).

The QHE values of α are in agreement with the a_e and $2e/h - \gamma_p'$ values, within their uncertainties, and seem to be sample independent for both Si MOSFETs[17,19] and GaAs-$Al_xGa_{1-x}As$ heterojunctions.[18,19] It seems reasonable to expect that future QHE experiments will provide even more accurate values of α.

We now turn to the question of a possible resistance standard. As we have seen the quantity h/e^2 has the units of electrical resistance and has a value which is in a convenient range for measurement purposes: $h/e^2 \approx 25\ 812.80\ \Omega$. If the quantized Hall resistance R_H is shown to be sample independent, and if it satisfies the simple relationship given by Eq. (5), then one could use the QHE to achieve an electrical resistance standard in which the resistance is determined in terms of fundamental constants. One advantage of this would be facilitation of international comparison of resistance standards. The present technique involves transport of wire-wound resistors whose resistance values can change due to mechanical and thermal stresses during transport. The limited data available from international comparisons indicate possible resistance transportation shifts in the range 0.05–0.2 ppm for 1-ohm resistors, and significantly larger possible shifts for higher value resistors.

A fundamental problem from the metrology point of view is that the quantities in Eq. (5) are in "absolute" (i.e., Système International or SI) units. The experimentally determined resistance is not R_H but R_H^* which is measured in terms of an as-maintained unit of resistance, Ω^*, and must therefore be converted to the SI unit, Ω, via the equation

$$R_H = R_H^* \left(\frac{\Omega^*}{\Omega}\right). \tag{11}$$

In the United States, for example, the as-maintained unit of resistance $\Omega^* = \Omega_{NBS}$ is defined to be the average of five nominal value 1-ohm resistors that are stored at the National Bureau of Standards in a 25 °C mineral oil bath regulated to within several m°C. Other 1-ohm resistors can be calibrated relative to these as-maintained resistance standards to a one standard deviation accuracy of about 0.01 ppm using a current

comparator bridge.[20,21] The ratio Ω_{NBS}/Ω has been determined to within 0.03 ppm via a calculable capacitor.[22,23] This extremely difficult measurement is about three times more accurate than any other Ω^*/Ω determination,[24] and it means (at least in the U.S.) that if R_H is to be used as an absolute resistance standard, that it should be determined to this same accuracy which is about a factor of five better than the present QHE result[18]: $R_H = 6\,453.2004\ \Omega\ (\pm\ 0.17$ ppm) for $i = 4$.

Resistors will continue to be used as working standards. But, if the values of R_H can be measured to sufficient accuracy and if for a given sample they are shown to be time independent, then it will undoubtedly be used to *maintain* national units of resistance, Ω^*, just as the Josephson voltage is used to maintain the volt; the quantized Hall effect would then become the Josephson effect of the 1980's for electrical metrology. (Note that the Josephson effect does *not* provide a useful *absolute* voltage unit because the SI value of $2e/h$ is not yet known to sufficient accuracy. The present uncertainty is about 2.6 ppm[25]; this uncertainty may soon be lowered to 0.1–0.5 ppm, but a change in the accepted value of $2e/h$ of about 7 ppm[26] can be expected.)

If the value of R_H can be shown to be also sample independent and to satisfy Eq. (5) to sufficient accuracy, then it can become an *absolute* resistance standard. In order to verify that there is no unknown factor involved in Eq. (5), the value of α should be independently determined to higher accuracy. One of the attempts to do this is in progress at NBS via a new γ_p' experiment.[27] Absolute realization of the Ω to the required 0.03 ppm level of accuracy via R_H will not be easy, but should ultimately be possible.

SUMMARY AND UNANSWERED QUESTIONS

We have briefly reviewed the physics of inversion layer systems and the discovery of the quantum Hall effect. If the quantum Hall effect is to be used for an improved determination of the fine structure constant and the realization of a quantum standard of resistance, much more information is needed about the experimental properties of inversion layer devices, and further advances are required in our theoretical understanding of this unexpected phenomenon. The basic questions are: Why do Hall steps exist? Why are they so wide, flat and accurately

quantized despite imperfections in the devices? What are the fundamental theoretical and experimental limitations?

We have already seen how the special properties of two-dimensional Landau level systems cause the transport to be dissipationless ($\rho_{xx} = 0$) even in the presence of disorder. In Part II we shall explore the implications of this important result and will examine progress toward answering the questions listed above.

Acknowledgments

The work at NBS is supported in part by the U. S. Office of Naval Research and the Calibration Coordination Group of the Department of Defense and is being carried out in collaboration with numerous colleagues from several institutions: R. F. Dziuba, B. F. Field, A. C. Gossard, M. Jonson, C. F. Lavine, P. A. Lee, R. W. Rendell, P. J. Stiles, D. Syphers, N. N. Tadros, B. N. Taylor, D. C. Tsui and R. J. Wagner.

M. E. CAGE
Electrical Measurements and Standards Division,
National Bureau of Standards,
Washington, DC 20234

S. M. GIRVIN
Surface Science Division,
National Bureau of Standards,
Washington, DC 20234

References

1. K. von Klitzing, G. Dorda and M. Pepper, Phys. Rev. Lett. **45,** 494 (1980).
2. T. Ando, A. B. Fowler and F. Stern, Rev. Mod. Phys. **54,** 437 (1982).
3. A. B. Fowler, F. F. Fang, W. E. Howard and P. J. Stiles, Phys. Rev. Lett. **16,** 901 (1966).
4. D. C. Tsui and A. C. Gossard, Appl. Phys. Lett. **38,** 550 (1981).
5. Data from R. J. Wagner, C. F. Lavine, M. E. Cage, R. F. Dziuba and B. F. Field, Surf. Sci. **113,** 10 (1982). For the data of von Klitzing see Ref. 1. See also S. Kawaji and J. Wakabayashi, in *Physics in High Magnetic Fields,* Vol. 24, edited by S. Chikazumi and N. Miura, Springer Series in Solid State Sciences (Springer-Verlag, Berlin, 1981), p. 284.

The Quantum Hall Effect II

The recent surprising observation of a quantization of the Hall resistance in units of h/e^2 in quasi-two-dimensional conductors has necessitated a major rethinking of our theoretical picture of transport in these systems. The central problem is understanding why ideal behavior persists even in the presence of strong disorder.

INTRODUCTION

It has recently been discovered[1] that the Hall resistance of the two-dimensional electron gas is, under certain conditions, quantized in units of h/e^2:

$$R_H = \frac{h}{e^2 i}. \tag{1}$$

An introduction to this striking phenomenon was presented in Part I of this Comment.[2] In this second part we will discuss specific theoretical questions of current interest. A consistent theoretical picture of this phenomenon is only just beginning to emerge and there are many open questions presently under active investigation.

THEORY

The quantum Hall effect is a vivid demonstration once again that physics is an experimental science. The unexpected observation of this phenomenon has necessitated a major rethinking of our theoretical picture

Comments Solid State Phys.
1983, Vol 11, No. 2, pp. 47–58
0308-1206/83/1102-0047/$18.50/0

of two-dimensional Landau level systems that is still in progress. We reviewed in Part I the theory of transport in the idealized case of no disorder and no Coulomb interactions. The central theoretical question now facing us is Why do the Hall steps exist and why are they so broad, flat and accurately quantized despite the presence of considerable random disorder in physically realizable devices?

We saw in Part I that the important feature controlling the transport is the existence of a gap in the density of states at the Fermi level, or at least a region of immobile states (a mobility gap) at the Fermi level. At low temperatures all the states below the gap (i.e., below the Fermi level) are filled and those above are empty. This means that there can be no elastic scattering of the carriers and that the current flow is completely dissipationless ($\rho_{xx} = 0$) even in the presence of impurities. It is not at all clear, however, that the Hall resistivity (ρ_{yx}) should be unaffected by the impurities. This is the question we now pursue.

In hindsight a hint of the existence of the quantum Hall effect actually appeared in the theoretical literature even before the experimental discovery. Treating disorder in the self-consistent Born approximation (SCBA), Ando *et al.*[3] found that the Hall resistance is quantized when the chemical potential is in the gap between Landau levels. However, there should be essentially no experimental manifestation of this since the chemical potential cannot be sustained for a finite range of carrier density in a regime with zero density of states. When all the states below the gap are filled, an infinitesimal increase in filling will cause the chemical potential to jump discontinuously across the gap (since states above the gap are now occupied). Thus the Hall step would have zero width and the Hall resistance would be a smooth monotonic function of the magnetic field strength or gate voltage. In short, there would be no quantization of the Hall resistance. In the limit of strong disorder one expects no gap in the density of states—only a mobility gap due to Anderson localization. This means that the region between the Landau levels has a finite density of states but these states cannot take part in the transport because they are localized, non-current-carrying states. The transport would still be dissipationless in this case and so could produce a finite step width (as Ando *et al.*[3] noted) but the SCBA is not valid in this limit, and in any case no longer predicts quantization of the Hall resistivity. Nevertheless, the quantization which was predicted is indeed observed.[4]

Having brought up the question of the plateau width let us deal with it further. A second possible explanation of the width of the plateaus does not require localized states to completely fill the gap between Landau levels. Ando[5] has suggested that if each Landau level is broadened due to some combination of smooth disorder and Coulomb interactions, there may be only a very narrow range of extended states near the center of the level. This picture is consistent with recent discussions within a percolation picture[6,7] and could account for the extremely wide Hall plateaus recently observed in GaAs heterostructures at very low temperatures by Paalanen *et al.*[8] The argument is that the Hall resistance changes with carrier density only when extended states are being filled and remains constant throughout the region of localized states. Another possibility is that Coulomb interactions are so strong that some sort of charge density wave[9] (CDW) or crystallization occurs. Dissipationless charge flow might then occur via some collective phenomenon. This may produce the anomalously wide Hall steps, but our understanding of this phase transition and its effect on the transport is rudimentary at present. A particular puzzle is that the nonlinear transport characteristics are unlike those of known CDW systems. There is no decrease in resistance at higher currents as would be expected for depinning of a CDW. Rather the resistance (ρ_{xx}) increases with increasing current.[8] Still another mechanism, one which involves the tunneling of donor electrons in heterostructures, has been put forth by Baraff and Tsui.[10] This may account for the increased step width in heterostructures relative to MOSFETs.

Having discussed some of the questions associated with the width of the plateaus, let us turn now to the accuracy of the quantization. Does the existence of a mobility gap or a density of states gap imply quantization of the Hall resistance despite the presence of disorder? The first paper to address this question was presented by Prange[11] who solved the case of a single delta-function impurity potential. This can be treated exactly and he showed rigorously that even though the potential binds an electron in a localized state, the Hall current is unaffected. The current-carrying states are modified by the potential in such a way that an extra current is produced which precisely compensates for the loss of one of the charge carriers to the bound state. This result in the quantum case is reminiscent of that for the classical two-dimensional system discussed in Part I.

It seems reasonable that this current compensation can be expected to hold for a finite density of impurities but a general proof is still lacking. Various authors[12–17] have put forth model calculations showing quantization of the Hall resistance. These models have been very instructive, but all put some constraint on the form of the disorder or make some approximation, such as neglecting mixing between Landau levels by the impurity potential.

One of the most interesting ideas concerning the disorder to be put forth is found in the novel and very general approach taken by Laughlin.[18,19] He argues that since the quantization appears to be so good experimentally, it must in fact be exact for a fundamental and simple reason, namely, gauge invariance. Laughlin performs a gedanken experiment in which the Hall current is carried in a ring so that periodic boundary conditions apply. Consider threading a single quantum of flux through the loop. One can show rigorously that the eigenstates and energy eigenvalues are left unchanged by this operation—the states are simply relabeled. It is important to realize that this is not actually a gauge transformation. A gauge transformation modifies the vector potential in a way that produces no physically observable effects. In the present case the electrons feel a transient EMF since the inversion layer is acting as a one-loop transformer secondary. This produces excitations and thereby creates the Hall current. Thus Laughlin's argument does not actually invoke gauge invariance but rather takes advantage of a great simplification which occurs when a single flux quantum is added. Because the eigenstates are precisely the same as they were before the flux addition, the only change can be in the occupation of those states. Laughlin showed that if the flux is added slowly and if the electrons respond to the perturbation adiabatically, then the net effect is to transfer an electron from one edge of the ring to the other. The relationship between the induced current and the Hall voltage then automatically satisfies the condition for quantization of the Hall resistance.

This beautiful argument has given us a good language in which to discuss the transport. Further implications of the picture have been explored by Imry.[20] Laughlin's argument is, however, not completely convincing to some.[21] One question centers on his claim that edge effects pose no difficulty.[19] Let us analyze the situation beginning with the adiabatic assumption. At first sight this would seem to be very bad since we know that adiabatically increasing the flux through an ordinary

transformer (employing say, copper wire) leads to no current at all in the secondary loop. This is because the secondary loop has finite resistance and the current disappears soon after the EMF transient. This objection does not apply to the quantum Hall case: The mobility gap at the Fermi level leads to dissipationless charge flow and so the current should persist even after the EMF disappears. We can also give a well defined meaning to adiabatic: The characteristic frequency ω of the perturbation must be such that $\hbar\omega$ is much less than the energy width of the mobility gap.

There is still a problem, however, because the gap must collapse at the edges of any real sample. Halperin[22] has reformulated Laughlin's argument to emphasize the fact that if ρ_{xx} is truly zero, then the current produced in Laughlin's gedanken experiment will be the result of changes in the current carried in the skipping orbits at the edges of the sample. Halperin shows that ideal (impurity free) edges preserve the quantization and argues (but does not prove) that, even in the presence of disorder, the edge states should be extended current-carrying states which preserve the total Hall current (within his particular model). It must be true, however, that in real devices there is some dissipation at the edges and so the current will not persist indefinitely. In addition, even if there is almost no dissipation at the edges, the lack of a gap implies that no flux change can ever be truly adiabatic. How these points affect the results of actual experiments is unclear at present.

FINITE SIZE EFFECTS

The question of edges brings up finite size effects in general. In a typical Hall device there are only on the order of 10^9 Landau level electrons, and 10^5 of these are in states at the edges. Since there are no errors observed at the 10^{-4} level of accuracy, edge effects must be higher than first order. Another finite size effect results from the peculiar pattern of charge flow in the inversion region. Since ρ_{xx} is never truly zero, the current cannot be strictly concentrated at the edges as in Halperin's model discussed above. A standard macroscopic model[23,24] has ρ_{yx}/ρ_{xx} very large in the inversion layer and relatively small in the source and drain contacts. Because the electrons flow along rather than perpendicular to the isopotential lines, the current entering and exiting the device

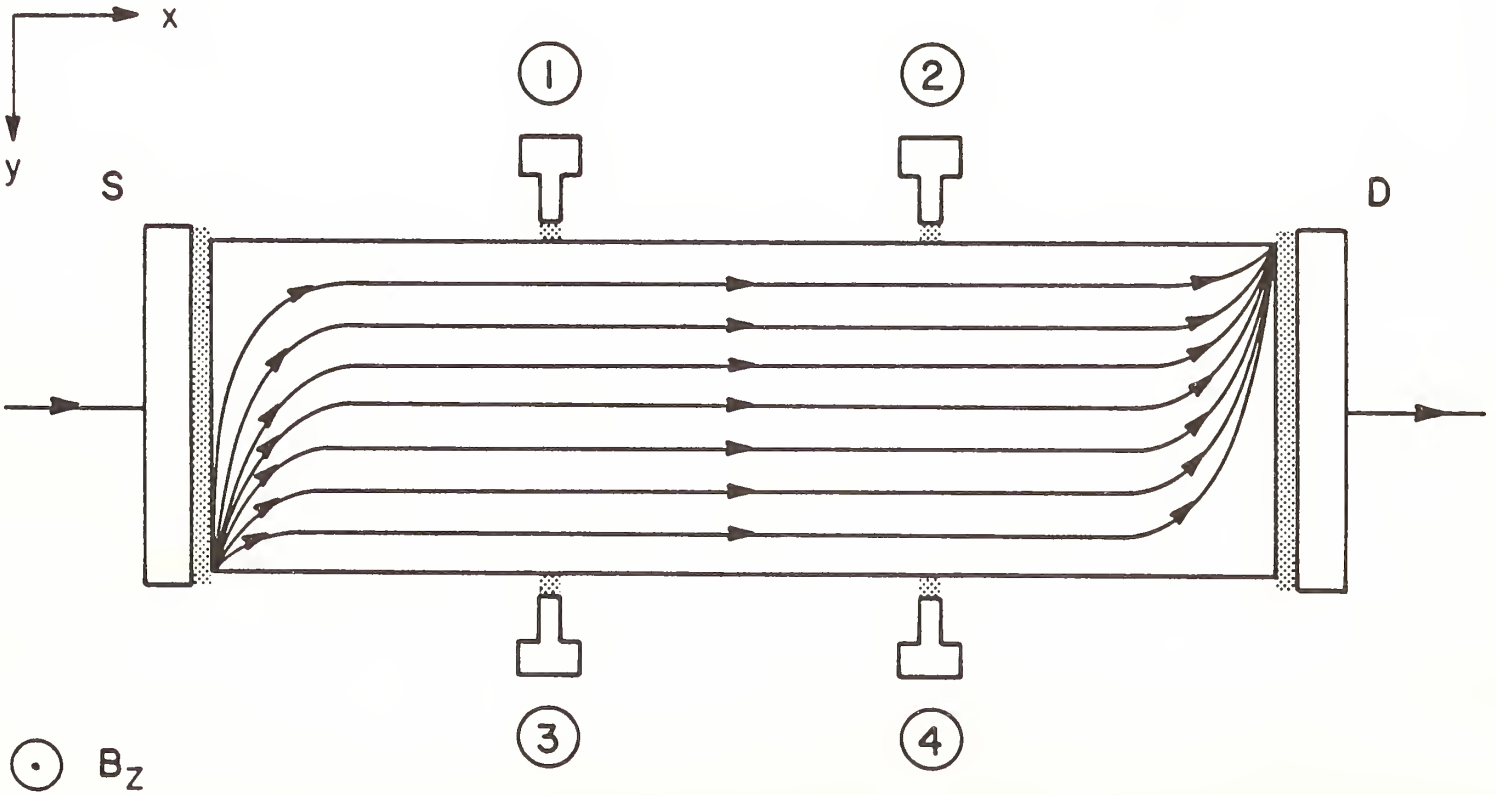

FIGURE 1 Model pattern of electron flow along isopotential lines from source (S) to drain (D) when the Hall step conditions are satisfied. Potential probes one through four are used for measuring the Hall voltage ($V_H = V_y$) as well as the longitudinal voltage drop (V_x).

is concentrated almost entirely in diagonally opposite corners[23,24] as shown in Figure 1. This is a result of the Hall field being shorted in the contacts so that the isopotential lines are forced to curve sharply near the ends. Model calculations[23,24] have shown that this is not a significant source of error in devices of aspect ratio greater than about five. On the other hand this current crowding at the corners may produce electron heating effects. The resulting lack of equilibrium could account for the degradation of the plateau width which typically occurs for currents above about 10 μA. Nothing definite about this phenomenon is known at present.

There is one very important implication of this current crowding in the corners. It leads to a "spraying resistance" for injecting electrons into the device. Thus even though $\rho_{xx} \sim 0$ in the inversion region, there is a large source-drain voltage drop. This is as it should be, of course, since the applied source-drain voltage must exceed (or in this case essentially equal) the induced Hall voltage. Unfortunately there is a similar current crowding at the Hall probe contacts leading to an output impedance for the device equal to the Hall resistance. This rather high output impedance ($\sim$10 kΩ) presents a major inconvenience to the experimentalist attempting low noise, high sensitivity measurements.

COULOMB INTERACTIONS

So far we have talked about the effects of disorder and edges but have largely neglected the role of Coulomb interactions. It is generally supposed that Coulomb effects will not destroy the mobility gap and so the arguments given above will still hold, although again nothing rigorous is known. One possible manifestation of the Coulomb interaction may be found in σ_{xx} when the chemical potential lies in the region of extended states where $\sigma_{xx} \neq 0$. Paalanen *et al.*[8] have observed a logarithmic temperature dependence of σ_{xx} at very low temperatures ($\sim$100 mK) in GaAs devices. The logarithmic singularity may be due to enhancement of Coulomb interaction effects at the Fermi level as a result of the diffusive nature of the electronic motion in the presence of impurities.[25,26] These kinds of studies[27] have proved useful in the "weak localization" regime of metals and semiconductors and seem likely to be important here as well. At small Landau level index ($i < 4$) Paalanen *et al.*[8] see a suppression of σ_{xx} far below the SCBA value, and also

observe an activated temperature dependence for σ_{xx}. These effects are associated with anomalously wide Hall steps and, as mentioned earlier, may be due to overwhelming Coulomb interaction effects which cause a charge density wave (CDW) state to form.

Certainly the most intriguing recent event is the observation by Tsui *et al.*[28] of quantized Hall steps at $R_H = h/e^2 i$ with $i = \frac{1}{3}$ and $\frac{2}{3}$. These steps occur when the lowest spin state of the lowest level is $\frac{1}{3}$ or $\frac{2}{3}$ filled. Related anomalies in σ_{xx} have also been reported by Ebert *et al.*[29] The leading candidate for an explanation of this anomalous quantum Hall effect is a charge density wave formed at $\frac{1}{3}$ and $\frac{2}{3}$ filling. Laughlin has speculated on the properties of this system.[30]

Understanding the highly correlated ground state induced by Coulomb interactions is one of the most difficult and exciting challenges facing us at present. The problem is that Hartree–Fock calculations show CDW formation at all fillings with no preference for $\frac{1}{3}$ or $\frac{2}{3}$. One supposes therefore that the origin of the "commensuration energy" lies in some Coulomb correlation effect neglected by the Hartree–Fock approximation. We believe that it is also fairly clear on physical grounds what the nature of these correlation effects must be. There must be a fluctuation during which the constituents of a ring of three (or more) particles cyclically trade positions. Such processes are familiar from Feynman's roton theory of helium.[31] The quantum amplitude for such a fluctuation event will contain a phase factor $e^{2\pi i\phi}$ where ϕ is the number of flux quanta in the area enclosed by the ring of particles. It is in this way that information concerning the magnetic flux is transmitted to the electrons. The commensuration energy is thus dynamically generated by these fluctuations. The smallest ring that encloses a nonzero area contains three electrons. Shifting each electron to its neighbor's position involves two fermion exchanges giving a net plus sign. At a concentration of $\frac{1}{3}$ the number of flux quanta contained in the electron crystal unit cell is integral (three), so the associated flux phase factor is unity. These points are presumably essential to the fact that $\frac{1}{3}$ is favored.

One other observation from experiment is important at this point: The anomalous Hall steps have finite width. That is, even when the concentration is not precisely $\frac{1}{3}$ or $\frac{2}{3}$, the collective ground state still exists and the correct quantization occurs. This suggests that the $\frac{1}{3}$ and $\frac{2}{3}$ fillings are sufficiently energetically favorable that the system prefers to form domains of concentration $\frac{1}{3}$ or $\frac{2}{3}$ separated by domain walls which make up for the excess (or deficit) of particles. Laughlin[30] has speculated that

such domain walls may be essential to the transport and the quantization at $i = \frac{1}{3}$ and $\frac{2}{3}$.

Developing a complete theory of the dynamic generation of the commensuration energy will be difficult since it appears that no perturbation expansion is possible: The kinetic energy has been quenched by the magnetic field (the unperturbed Landau level is degenerate) and so the Coulomb potential is not small in comparison to the kinetic energy. One saving grace may be that one can probably neglect mixing between the different Landau levels. This is because the observation of Hall steps at both $i = \frac{1}{3}$ and $\frac{2}{3}$ suggests the existence of approximate particle–hole symmetry within the lowest Landau level. Such a symmetry would not be present if there were significant mixing between different levels.

THERMAL VOLTAGES

Another area of transport which is being explored is the thermoelectric response of Landau level systems. It has been shown[32] that on the plateaus the thermopower in an ideal system is thermally activated and so thermal voltages will (fortunately) be an exponentially small source of error in metrology experiments. However, when the chemical potential passes through the Nth Landau level, the thermopower has the peculiar property of rising to a peak whose height is a universal number[32]: $S = \ln 2\ (k_B/e)/(N + \frac{1}{2})$. Thermopower measurements offer us the possibility of gaining new insight into the transport properties of inversion layer systems but unfortunately no data exist at present in this area.

RELATIVISTIC AND QED CORRECTIONS

Finally, we turn to the question of possible relativistic and quantum electrodynamic (QED) corrections to the quantized Hall resistance. The ratio of the magnetic energy $\hbar\omega_c$ to the electron rest energy $m_e c^2$ is $\sim 10^{-8}$, which may eventually be a significant number relative to the experimental precision. QED corrections received a limited investigation in connection with the Josephson effect and its metrological uses, and similar questions need to be asked here.

First it should be noted that the Hall phenomenon is itself a relativistic effect of first order in v/c. One might suppose that there are higher-order effects arising from modification of the electron momentum–energy relation. However these cannot be important in comparison to the severe modification of the momentum–energy relation due to the semiconductor band structure. It is observed experimentally that even the latter has no effect at least at the 10^{-6} level of accuracy.[33,34] Similarly, there may be QED effects arising from coupling to the photon field. The measure of this coupling is the fine structure constant $\alpha = e^2/\hbar c$. There is, however, another boson field present, namely the phonons, for which the coupling is vastly larger; very roughly, $\alpha \sim e^2/\hbar v_s$ where v_s is the speed of sound. Hence vacuum fluctuation effects are negligible in comparison with possible solid state effects. We believe that at zero temperature coupling to the fluctuating phonon field does not destroy the mobility gap, and so one presumes that this effect poses no difficulty, but to what level this persists is not known. Similar considerations apply to vacuum polarization phenomena—the electron gas is vastly more polarizable than the vacuum. In short, it would seem that possible corrections should be sought in solid state effects and not in anything more esoteric.

SUMMARY

In conclusion it has been found that the quantum Hall effect is significant from the point of view of both metrology and fundamental physics. At present it appears that all the metrology will be done on the Hall plateaus where the Hall resistance seems to be universal, whereas all the new physics and new information concerning transport will be obtained between the plateaus where sample and temperature dependent deviations from ideal behavior occur.

Acknowledgments

The work at NBS is supported in part by the U.S. Office of Naval Research and the Calibration Coordination Group of the Department of Defense, and is being carried out in collaboration with a number of colleagues from several institutions: R. F. Dziuba, B.

F. Field, A. C. Gossard, T. Jach, M. Jonson, C. F. Lavine, P. A. Lee, R. W. Rendell, P. J. Stiles, D. Syphers, N. N. Tadros, B. N. Taylor, D. C. Tsui and R. J. Wagner.

S. M. GIRVIN
Surface Science Division,
National Bureau of Standards,
Washington, D.C. 20234

M. E. CAGE
Electrical Measurements and
Standards Division,
National Bureau of Standards,
Washington, D.C. 20234

References

1. K. von Klitzing, G. Dorda and M. Pepper, Phys. Rev. Lett. **45,** 494 (1980).
2. M. E. Cage and S. M. Girvin, Comments Solid State Phys. **11,** 1 (1983).
3. Tsuneya Ando, Yukio Matsumoto and Yasutada Uemura, J. Phys. Soc. Jpn. **39,** 279 (1975).
4. The first observation of Hall steps appears to have been made by S. Kawaji and J. Wakabayashi in *Physics in High Magnetic Fields,* Springer Series in Solid State Sciences 24, edited by S. Chikazumi and N. Miura (Springer, Berlin, 1981), p. 284. However, these authors did not demonstrate the accurate quantization of the Hall resistance and their results did not appear in print until after those of Ref. 1.
5. T. Ando, Surf. Sci., in press.
6. R. F. Kazarinov and Serge Luryi, Phys. Rev. B **25,** 7626 (1982).
7. S. V. Iordansky, Solid State Commun. **43,** 1 (1982).
8. M. A. Paalanen, D. C. Tsui and A. C. Gossard, Phys. Rev. B **25,** 5566 (1982).
9. H. Fukuyama and P. M. Platzman, Phys. Rev. B **25,** 2934 (1982).
10. G. A. Baraff and D. C. Tsui, Phys. Rev. B **24,** 2274 (1981).
11. R. E. Prange, Phys. Rev. B **23,** 4802 (1981).
12. H. Aoki and T. Ando, Solid State Commun. **38,** 1079 (1981).
13. D. J. Thouless, J. Phys. C **14,** 3475 (1981).
14. R. E. Prange and Robert Joynt, Phys. Rev. B **25,** 2943 (1982).
15. T. Ando, Surf. Sci. **113,** 182 (1982).
16. D. J. Thouless, M. Kohmoto, M. P. Nightingale and M. den Nijs, Phys. Rev. Lett. **49,** 405 (1982).
17. P. Streda, J. Phys. C **15,** L717 (1982).
18. R. B. Laughlin, Phys. Rev. B **23,** 5632 (1981).
19. R. B. Laughlin, Surf. Sci. **113,** 22 (1982).
20. J. Imry, J. Phys. C **15,** L221 (1982).
21. J. J. Quinn and B. D. McCombe, Comments Solid State Phys. **10,** 139 (1982).

22. B. I. Halperin, Phys. Rev. B **25,** 2185 (1982).
23. S. Kawaji, Surf. Sci. **73,** 46 (1978).
24. R. W. Rendell and S. M. Girvin, Phys. Rev. B **23,** 6610 (1981).
25. A Houghton, J. R. Senna and S. C. Ying, Phys. Rev. B **25,** 2196, 6468 (1982).
26. S. M. Girvin, M. Jonson and P. A. Lee, Phys. Rev. B **26,** 1651 (1982).
27. B. L. Altshuler, A. G. Aronov and P. A. Lee, Phys. Rev. Lett. **44,** 1288 (1980).
28. D. C. Tsui, H. L. Stormer and A. C. Gossard, Phys. Rev. Lett. **48,** 1559 (1982).
29. G. Ebert, K. von Klitzing, C. Probst and K. Ploog, preprint.
30. R. B. Laughlin, preprints.
31. R. P. Feynman, *Statistical Mechanics* (Benjamin, Reading, Massachusetts, 1972).
32. S. M. Girvin and M. Jonson, J. Phys. C, submitted.
33. D. C. Tsui, A. C. Gossard, B. F. Field, M. E. Cage and R. F. Dziuba, Phys. Rev. Lett. **48,** 3 (1982).
34. K. Yoshihiro, J. Kinoshita, K. Inagaki, C. Yamanouchi, J. Moriyama and S. Kawaji, J. Phys. Soc. Jpn. **51,** L5 (1982).

PROGRESS REPORT ON INVESTIGATIONS OF THE QUANTUM HALL EFFECT AS A POSSIBLE RESISTANCE STANDARD*

Contribution
from the
National Bureau of Standards
Washington, DC USA

This progress report to the Comité Consultatif d'Electricité summarizes our efforts to date (February 1983) to investigate the feasibility of using the quantum Hall effect (QHE) as a new standard of resistance based solely on fundamental constants of nature. Succinctly stated, the results obtained have been encouraging and indicate that the QHE could indeed be used as a resistance standard with parts in 10^8 precision. However, we believe that the full inherent accuracy of the QHE cannot be realized until we overcome a puzzling problem that we have encountered during the course of the work. In this report we present a chronological account of our QHE measurements and our attempts to understand this problem.

It is now well known[1] that the Hall resistance R_H of a two-dimensional electron gas is, under certain conditions, quantized in units of h/e^2:

$$R_H(i) = \frac{(h/e^2)}{i} = \frac{\mu_o c}{2\alpha i} \approx \frac{25{,}812.80}{i} \ \Omega, \qquad (1)$$

where i is a small quantum integer, h is the Planck constant, e is the elementary charge, μ_o is the permeability of vacuum, c is the speed of light in vacuum, and α is the fine-structure constant. These conditions can be obtained by placing special, cryogenically cooled semiconductor devices in large magnetic fields.

R_H, defined as the ratio of the Hall voltage V_H across the device to the current through it, can be potentiometrically compared[2] with a calibrated reference resistor R_R in series with the device. The relationship between the Hall resistance and the series reference resistor is $R_H = (V_H/V_R) \cdot R_R$, where V_R is the voltage drop across R_R, provided the same current passes through both the sample and the reference resistor.

---

* The work summarized in this report has been performed by M. E. Cage, R. F. Dziuba, and B. F. Field of the Electrical Measurements and Standards Division of the National Bureau of Standards in collaboration with these colleagues from other institutions: R. J. Wagner (Naval Research Laboratory), D. C. Tsui (Princeton University), A. C. Gossard (Bell Laboratories), and N. N. Tadros (Guest Worker at NBS during 1982 from the National Institute for Standards, Egypt). The NBS contribution to this work is supported in part by the U.S. Office of Naval Research and the Calibration Coordination Group of the U.S. Department of Defense. This is an informal report not intended for publication.

Our particular measurement approach is indicated in Fig. 1. A constant current is applied to a semiconductor device, cooled to 4.2 K or 1.5 K, and to a room temperature reference resistor. Reference resistors have been constructed with values nominally equal to that of the Hall resistance, i.e., 6,453.2 Ω for i=4 quantum Hall steps and 12,906.4 Ω for i=2 steps. Therefore $V_H \approx V_R$. The potentiometer voltage is made almost equal to the voltage drop across V_H or V_R, and an electronic detector D amplifies the difference voltage signal. The isolated detector output is either displayed on an X-Y recorder or is digitized for further processing by a desktop computer. The current source, potentiometer, and electronic detector are all battery-operated. Thermally induced emfs and linear drifts in the current source and potentiometer are cancelled by reversing the current through the device and the reference resistor. A series of reversals is made for each of two measurements of V_R which bracket in time one measurement of V_H.

In January 1982 we published a value of R_H in a Physical Review Letter[3] based upon measurements on three GaAs-$Al_xGa_{1-x}As$ heterojunction devices. The measurements were made in July 1981 at Bell Telephone Laboratories (BTL) and had an estimated one standard deviation total uncertainty of 0.17 ppm. We then did a similar experiment with four silicon MOSFET devices in September 1981 at the Naval Research Laboratory (NRL). The total uncertainty was again presumably 0.17 ppm, but the September 1981 value of R_H was approximately 0.8 ppm larger than the July 1981 value. Figure 2 shows the results of our subsequent attempts to resolve this disagreement as well as the results of the two series of measurements just described and our first measurements done in May 1981 at BTL. These data represent twenty-one separate measurements over an eighteen month time span on sixteen different samples (seven GaAs devices and nine Si devices). Three of the GaAs measurements involved i=2 Hall steps; all of the other measurements were on i=4 steps. These data were obtained at BTL, NRL, and NBS.

Our battery-operated potentiometric measurement system initially had a 0.2 ppm one standard deviation random or type A uncertainty for measurements with a 25 μA device current. The measurement system was improved until the statistical uncertainty was reduced to 0.025 ppm prior to the October 1982 measurement at NBS. Therefore, six measurements (requiring a total of 66 minutes) now provide a 0.01 ppm statistical uncertainty of the mean. To obtain the error bars assigned in Fig. 2, the appropriate type A uncertainty was root-sum-squared (RSS) with one standard deviation estimates of the known systematic or type B uncertainties, which were as follows: (1) 0.02 ppm due to circuit leakage currents (based upon intercomparison of two resistors in place of the sample and the reference resistor); (2) a 0.05 ppm reference resistor temperature correction uncertainty until November 1981 when each reference resistor was temperature controlled to sufficient precision to reduce this uncertainty to a neglible level; (3) a 0.10 ppm uncertainty in the step-up from Ω_{NBS} (maintained via five 1 Ω resistors) to the reference resistor values; and (4) a 0.10 ppm transportation shift uncertainty for the reference resistors when taken to BTL or NRL, unless the resistor value changed by more than 0.2 ppm between the time that it left NBS and when it was returned (i.e., the before/after values differed by more than 0.2 ppm). Whenever that occurred the most probable resistor value was assumed to be either the before or the after value (depending on our best judgement as based on the calibration data), whereas the error bars were centered about the average of the before/after resistor values, with a transportion uncertainty of half the shift. (This is why the error bars of Fig. 2 are not always symetrically placed about what we consider to be the most probable

values.) Note that the data of Fig. 2 have been expressed in SI units, but that the current 0.08 ppm estimated one standard deviation total uncertainty in the NBS ohm (due in part to a possible drift since its last SI realization[4] via the NBS calculable cross capacitor in 1974) was not included in the error bars. This is because the same Ω_{NBS}/Ω correction was applied to each measurement and we did not want to mask any unknown error sources by an increase in the error bars.

Our measurements began with a preliminary experiment at BTL in May 1981 (see the first two data points at the bottom of Fig. 2). All measurements at BTL were performed using GaAs devices usually cooled to 4.2 K. The May 8 value has a large uncertanty because the 6,453.2 Ω reference resistor 6.45J1 before/after values changed by 0.48 ppm. The May 14 value is also uncertain because leakage currents in the sample holder (due to absorbed moisture) contributed an additional 0.15 ppm uncertainty component to the measurement. The correct value for this sample is likely to be higher. (That was indeed the case when it was remeasured on July 15.) The sample holder was modified by replacing the lead wires with Teflon-coated wire for the July experiment at BTL which we now describe.

In July 1981 two measurements were made on i=2 steps using the 12,906.4 Ω reference resistor 12.9J1, and one measurement on an i=4 step using reference resistor 6.45J1. The i=4 step result is drawn with a dashed line because the step did not appear to be flat on the chart recording. On the same day, July 17, we replaced the GaAs device with two 12,906.4 Ω resistors (12.9J1 and 12.9J2) connected in parallel and compared them with resistor 6.45J1. This comparison indicated a 0.38 ppm discrepancy in the assigned resistor values, even though the before and after calibrations at NBS of all three resistors implied that none of them had significantly changed. Because 12.9J1 and 12.9J2 were also compared with each other at BTL and this comparison agreed with their assigned calibrations, it seemed more likely that resistor 6.45J1 had shifted by 0.38 ppm at BTL rather than both of the 12.9 kΩ resistors. Consequently, the Physical Review Letter results from these data were based upon the calibrations of the two 12.9 kΩ reference resistors and the July 17, 1981 result denoted by the symbol Δ in Fig. 2 was used in Ref. 3 - except that a +0.3 ppm correction (to be discussed later) had not been made.

We next did an experiment at NRL in September 1981 using four different Si MOSFET devices and i=4 steps. The before and after calibrations at NBS of 6.45J1 did not show any significant change, but those for 12.9J1 and 12.9J2 did. Thus the most reliable values were based upon the calibration of 6.45J1 and were about 0.8 ppm larger than those obtained at BTL. This might possibly have been due to a difference between values of R_H for GaAs and Si devices.

To test this possibility, we performed experiments in January and February 1982 at NRL in which we (1) compared two GaAs heterojunctions and five Si MOSFETs with resistor 6.45J1, and (2) compared directly GaAs heterojunctions with Si MOSFETs. The sample versus 6.45J1 comparisons were all in excellent agreement except for those samples in which the Hall step did not appear to be flat in chart recordings for one or both current polarities. The resulting deviations from R_H nominal can have either sign, and this sign appears to be associated with both the slope of the step and with the structure on the side of the step. It is not surprising that such deviations exist for imperfect steps because Eq. (1) holds only for flat

steps (i.e., only when there is an actual mobility gap at the Fermi level). Obviously, one would only use samples as resistance standards for which there was a region that appeared to be flat within the measurement precision.

The two direct GaAs-Si comparisons were done by mounting a GaAs device and a Si device in series on the same sample holder (header) and directly comparing their Hall voltages using a 10 or 20 μA device current. The GaAs device was tilted, via a wedge, with respect to the magnetic field (i.e., the plane of the device and the field were no longer perpendicular) such that when the magnetic field was adjusted to the center of the GaAs i=4 step the field was sufficiently large to obtain a good i=4 step for the Si device (~13T). The Si MOSFET gate voltage was then adjusted to the center of the Si i=4 step.

Unfortunately, the data changed character during the course of the GaAs(5)-Si(5) comparison. The Si(5) gate voltage for the i=4 step was abnormally low that day, and the magnitude and sign of the data shifts are consistent with the Si device re-equilibrating such that the device was no longer biased on the flat part of the Hall step. Using only the initial data, we found $R_H(4)$ for GaAs(5) to be (0.04 ± 0.09) ppm lower than for Si(5) [type A uncertainty only since it was a direct comparison experiment]. We also found the GaAs(6) R_H value to be (0.06 ± 0.06) ppm lower than Si(9). Hence there is no statistically significant difference in $R_H(4)$ between the GaAs and Si devices. We therefore conclude that the 0.8 ppm difference between the BTL and NRL measurements is not due to Si-GaAs device differences. (There may be small non-zero differences in the above comparisons because at 10 μA, 13 T, and 1.5 K the Si steps are much narrower than the GaAs steps. One may very well have to cool Si devices to ~0.5 K if they are to be used as resistance standards at the part in 10^8 level of accuracy.)

Several other tests were also made at NRL in January and February 1982 to try to resolve the 0.8 ppm difference between the BTL and NRL measurements. They were: (1) a verification that the value of reference resistor 6.45J1 had not shifted. This was done by measuring $R_H(4)$ at NRL for the GaAs(5) device (which had a very good Hall step), recalibrating 6.45J1 at NBS (observing no change in its value), and then obtaining the same result for R_H with GaAs(5) at NRL; (2) a check that tilting the GaAs devices did not introduce a change in R_H. This was done by obtaining the same value for GaAs(5) when it was also tilted ~10° about an axis perpendicular to the Hall field direction; (3) verifying that there was no difference in R_H whether samples were mounted either on magnetic or nonmagnetic headers; and (4) checking that the magneto-resistance of the reference resistors was negligible. This was done by moving 6.45J1 closer to the magnet, thereby increasing the magnetic field strength at the resistor by two orders of magnitude.

The laboratory at NRL was thought to be electrically noisy, and we speculated that this noise might couple into the nonlinear devices and introduce a systematic error into the results. Thus we felt that in order to resolve the difference between the NRL and BTL measurements, the experiment had to be done in a quiet environment at NBS. To this end, an 8T superconducting magnet system was installed in a shielded room and the first experiment performed in September 1982 using a GaAs device. The result was in excellent agreement with the values of R_H obtained at NRL.

To further investigate the question of electrical noise, a method was devised to detect noise at the sample and to display it on a spectrum analyzer. We found significant noise at the sample, and therefore constructed a new sample probe with two-stage filters on each lead to the sample. These filters reduced the noise at the sample from all external sources by more than a factor of 100 (to below our detection limit). Additional measurements in October 1982 showed that this 100-fold noise reduction caused no change in R_H to within 0.02 ppm. It was also found that: (1) the value of R_H is independent of the magnetic field direction to within 0.01 ppm; (2) the value of R_H is current independent in this sample over the range 10-25 μA to within at least 0.03 ppm at 1.5 K; (3) the Hall step is flat to within 0.02 ppm over a magnetic field range that is 3% of the central value, as shown in Fig. 3; and (4) the value of R_H when using reference resistor 6.45J1 again agrees with those values obtained at NRL and that this value can repeatedly be reproduced to within 0.02 ppm if the reference resistor is not physically moved. All of these results are very encouraging. They indicate that the quantum Hall effect could indeed be used as a resistance standard to maintain a unit of resistance, and that this standard would probably be much more time-independent than wire-wound resistors. As a matter of fact, we believe that we were able to detect parts in 10^9 day-to-day variations in resistor 6.45J1.

Even though many questions and doubts have been addressed by this work, the 0.8 ppm difference still remains. It might be due to a difference in values of R_H between i=2 and i=4 steps, but this possibility seems highly unlikely because of the excellent agreement found by our Japanese colleagues at ETL for the i=4, i=8, and i=12 steps in Si MOSFETs.[5] We will remeasure R_H for an i=2 step when a sample becomes available just to be certain that our value is not step-dependent.

Since our problem does not seem to be associated with the QHE samples, we are now concentrating our attention on possible problems in the measurement and calibration of the reference resistors. The reference resistors are calibrated at 1 mA with a room temperature current comparator bridge, but are compared with the samples at 10-25 μA. To test the idea that the resistor values might be current-dependent, the QHE measurement system was used to compare resistor pairs over the current range 25 μA - 1 mA. We did observe some changes in the resistor differences on the order of 0.1 ppm when the current was varied from 25 μA to 1 mA. The changes seem to be reproducible for some resistor pairs but not reproducible for other pairs. Thus current-dependent effects could indeed be a problem for measurements below the 0.1 ppm level of accuracy, but do not appear to be a major source of our 0.8 ppm difference.

We also found that there was a (0.025 ± 0.005) ppm offset in our measurement system at 25 μA, and the same offset (with a larger uncertainty) at 1 mA. This offset was discovered by replacing the sample with a resistor, measuring the resistor-reference resistor pair difference, and then interchanging the two resistors in the circuit. Using this technique, we then measured all six pair-wise combinations of three reference resistors (6.45J1, 6.45E1, and 6.45E2) and corrected the results by the 0.025 ppm offset. We obtained loop-closure to within 0.03 ppm at both 25 μA and 1 mA. Because the values of the three resistors differ by -30 ppm to -3 ppm from the nominal value 6,453.2 Ω, these loop-closure measurements check the linearity of our QHE measurement system. However, systematic errors in the system that are proportional to the resistor offset from nominal are not

detected by the loop-closure experiment. This system "gain" error was checked in another experiment in which the same three resistors (6.45J1, 6.45E1, and 6.45E2) were each compared with the GaAs(7) sample and with each other. The results can be interpreted as a 2% "gain" error in the measurement system. These results are very surprising because the null detector used in the system (which would be primarily responsible for such an error) had been calibrated to a much higher accuracy. We are currently investigating this problem. Extrapolating the results for 6.45E1 and 6.45E2 to zero nominal value yields values of R_H that are in excellent agreement with those shown in Fig. 2 for GaAs(7) using 6.45J1 (whose value is within 3 ppm of nominal).

Careful study of Fig. 2 indicates that the observed 0.8 ppm difference could be correlated with the use of either a 6,453.2 Ω resistor or a 12,906.4 Ω resistor as the reference resistor. Indeed, when the two 12,906.4 Ω resistors 12.9J1 and 12.9J2 are individually calibrated on the current comparator bridge and then connected in parallel and calibrated as a 6,453.2 Ω resistor, there is a 0.3 ppm discrepancy between the measured value of the parallel combination and the predicted value based on the individual 12.9 kΩ calibrations. (Measurements of the terminal resistances of 12.9J1 and 12.9J2 indicate that these should alter the predicted value of the parallel combination by only 0.001 ppm.) All results shown in Fig. 2 that involve parallel combinations of 12.9J1 and 12.9J2 (i.e., those denoted by a Θ or by a Δ) have been corrected by+0.3 ppm to agree with the actual parallel calibration.

We plan to check the linearity of the current comparator bridge from 100 Ω to 6,453.2 Ω by constructing a Hamon device that consists of eight 800 Ω resistors plus a 53.2 Ω resistor. (Existing Hamon devices are used to scale the ohm from the Thomas 1 Ω resistors, which define the NBS ohm, to the 100 Ω level, and thence to the 10,000 Ω level.) An independent check is also planned in which we will use purely resistance ratio measurements to scale down from the 10,000 Ω level to calibrate the 6,453.2 Ω and 12,906.4 Ω resistors.

Conclusion

We are presently in the frustrating situation of being able to easily reproduce values of R_H that are in agreement for different samples to a precision of a few parts in 10^8, but with an inaccuracy that may be as large as one part in 10^6. Our immediate goal is to reduce this inaccuracy to one part in 10^7. Only then can we begin the tedious task of achieving the few parts in 10^8 level of accuracy that we seek for an SI quantum Hall effect resistance standard.

References

1. K. v. Klitzing, G. Dorda, and M. Pepper, Phys. Rev. Lett. 45, 494 (1980).

2. M. E. Cage, R. F. Dziuba, B. F. Field, C. F. Lavine, and R. J. Wagner, in Precision Measurement and Fundamental Constants II, Ed. by B. N. Taylor and W. D. Phillips, Natl. Bur. Stand. U.S., Spec. Publ. 617, to appear in 1983.

3. D. C. Tsui, A. C. Gossard, B. F. Field, M. E. Cage, and R. F.

Dziuba, Phys. Rev. Lett 48, 3 (1982).

4. R. D. Cutkosky, IEEE Trans. Instrum. Meas. IM-23, 305 (1974).

5. K. Yoshihiro, J. Kinoshita, K. Inagaki, C. Yamanouchi, J. Moriyama, and S. Kawaji, 16th Int. Conf. on Physics of Semiconductors, Montpellier, France, Sept. 6-12, 1982.

6. L. Bliek, E. Braun, H. J. Englemann, H. Leontiew, F. Melchert, W. Schlapp, B. Stahl, P. Warnecke, and G. Weimann, to be published in PTB-Mitteilugen 93, (1983).

7. E. R. Williams and P. T. Olsen, Phys. Rev. Lett. 42, 1575 (1979).

8. R. S. Van Dyck, Jr., P. B. Schwinberg, and H. G. Dehmelt, in Atomic Physics 7, Ed. by D. Kleppner and F. M. Pipkin (Plenum, New York, 1981), p. 340.

9. T. Kinoshita and W. B. Lindquist, Phys. Rev. Lett. 47, 1573 (1981).

Figure Captions

Figure 1. A simplified schematic of the measurement circuit used to compare the Hall resistance of a semiconducting device to a nominally equal room temperature reference resistor via a potentiometer adjusted to within a few ppm of V_H. The entire system is battery-operated, including the electronic detector, D.

Figure 2. A chronological ordering of precision measurements of R_H using GaAs-$Al_xGa_{1-x}As$ heterojunctions and Si MOSFET samples. These data are plotted as deviations ΔR_H in parts-per-million from the nominal value of R_H (1) $\equiv$25,812.80 Ω. Those data with points represented by the symbol X are for i=4 steps compared with reference resistor 6.45J1; those with the symbol ° are for i=2 steps compared with resistor 12.9J1; those with the symbol • are for i=4 steps compared with resistors 12.9J1 and 12.9J2 connected in parallel; and those with the symbol Δ are derived results for i=4 steps obtained by first comparing the sample with resistor 6.45J1 and then adjusting that result by an amount indicated by a comparison of resistor 6.45J1 with the parallel combination of 12.9J1 and 12.9J2. Also shown are the most recent values of R_H reported by ETL (Ref. 5) and by PTB (Ref. 6), as well as those based upon a γ_p(low) experiment (Ref. 7) and the University of Washington anomalous magnetic moment of the electron experiment (Ref. 8) plus QED calculations (Ref. 9). The measurements with dashed error bars are questionable; see the appropriate comment below.

Comments

(a) This value of R_H could actually be larger because of possible leakage currents in the sample probe.

(b) The step did not appear to be flat in chart recordings, and hence this value of R_H is questionable.

(c) There was no before or after shift in the calibrated value of reference resistor 6.45J1 for this measurement, and thus this is one of our most reliable results.

(d) The gate voltage may have inadvertently been adjusted so that the sample was slightly off of the step.

Figure 3. A high precision mapping of the i=4 step of sample GaAs(7), obtained on October 21, 1982 at 25 μA and 1.5 K. The data points are plotted as deviations of $R_H(4)$ in ppm from the flat region of the step. The larger random or type A uncertainty error bars are for data obtaned in 11 minutes while the smaller error bars are for data obtaned in 22 minutes. The datum point with the open circle is for a different Hall potential probe set on the sample. The actual value of $R_H(4)$ agrees with that given in Fig. 2 for October 13, 1982 to within (0.005 ± 0.012) ppm.

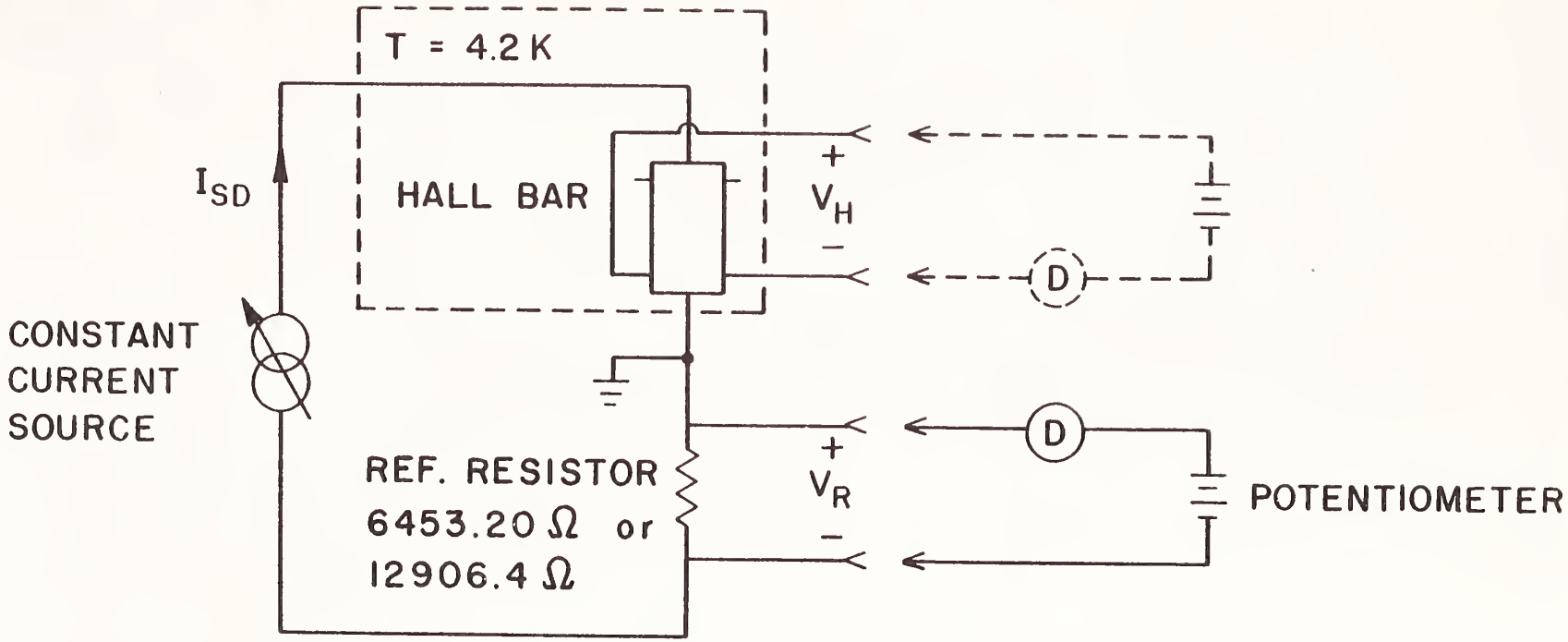
T = 4.2 K
I_{SD}
HALL BAR
+
V_H
−
D
T
CONSTANT
CURRENT
SOURCE
REF. RESISTOR
6453.20 Ω or
12906.4 Ω
+
V_R
−
D
POTENTIOMETER

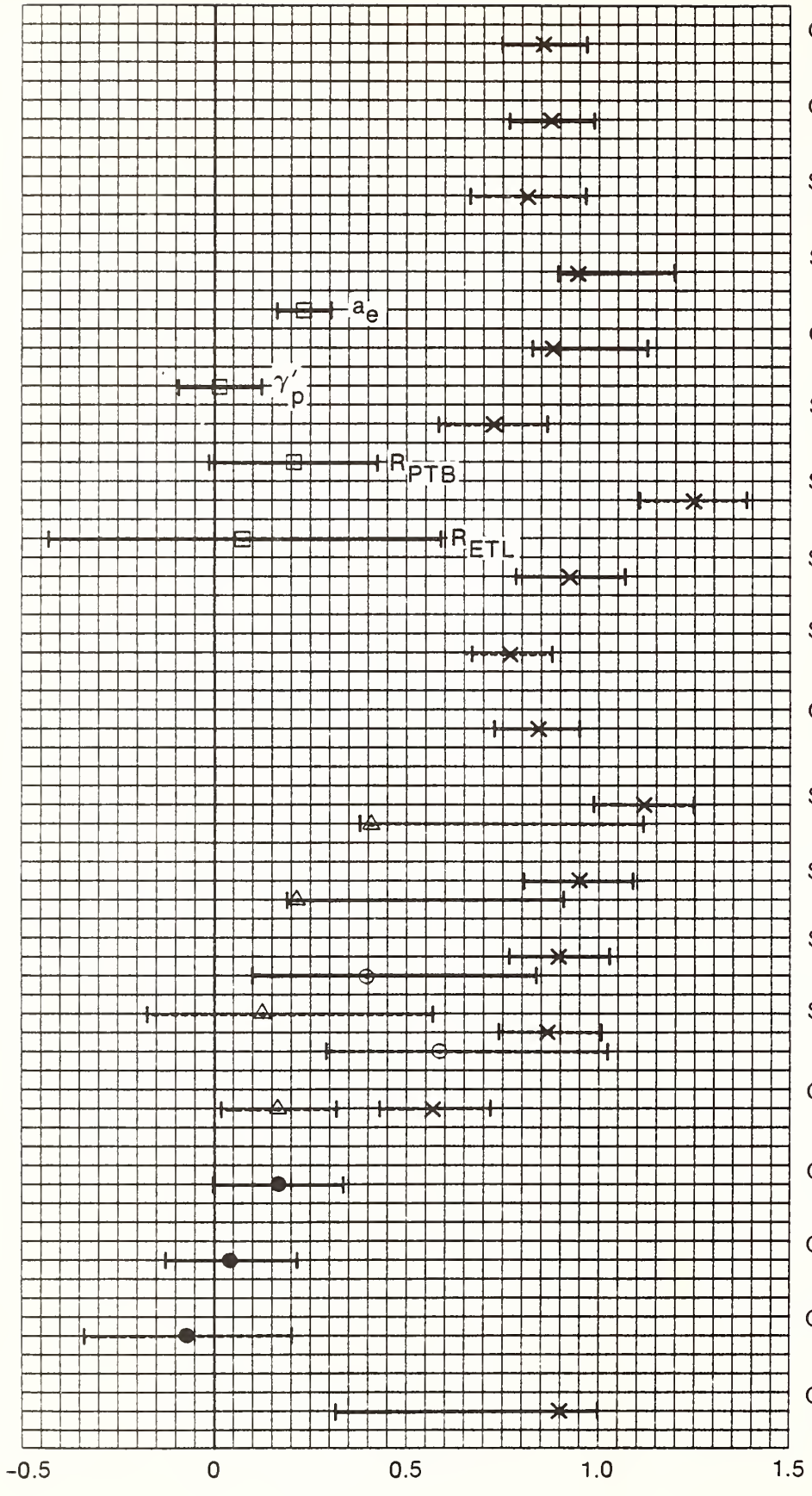

GaAs (7) i = 4 c
10/13/82 @ NBS

GaAs (7) i = 4 c
9/1 - 2/82 @ NBS

Si (8) i = 4 b
2/24/82 @ NRL

Si (9) i = 4
2/16/82 @ NRL

GaAs (6) i = 4
2/16/82 @ NRL

Si (8) i = 4 b
2/9 - 11/82 @ NRL

Si (7) i = 4 b
2/8/82 @ NRL

Si (6) i = 4
1/26/82 @ NRL

Si (5) i = 4 d
1/22/82 @ NRL

GaAs (5) i = 4 c
1/21 - 1/22/82 @ NRL

Si (4) i = 4 b
9/17/81 @ NRL

Si (3) i = 4
9/16/81 @ NRL

Si (2) i = 4
9/15/81 @ NRL

Si (1) i = 4 b
9/14/81 @ NRL

GaAs (4) i = 4 b
7/17/81 @ BTL

GaAs (2) i = 2
7/15/81 @ BTL

GaAs (3) i = 2
7/14/81 @ BTL

GaAs (2) i = 2 a
5/14/81 @ BTL

GaAs (1) i = 4
5/8/81 @ BTL

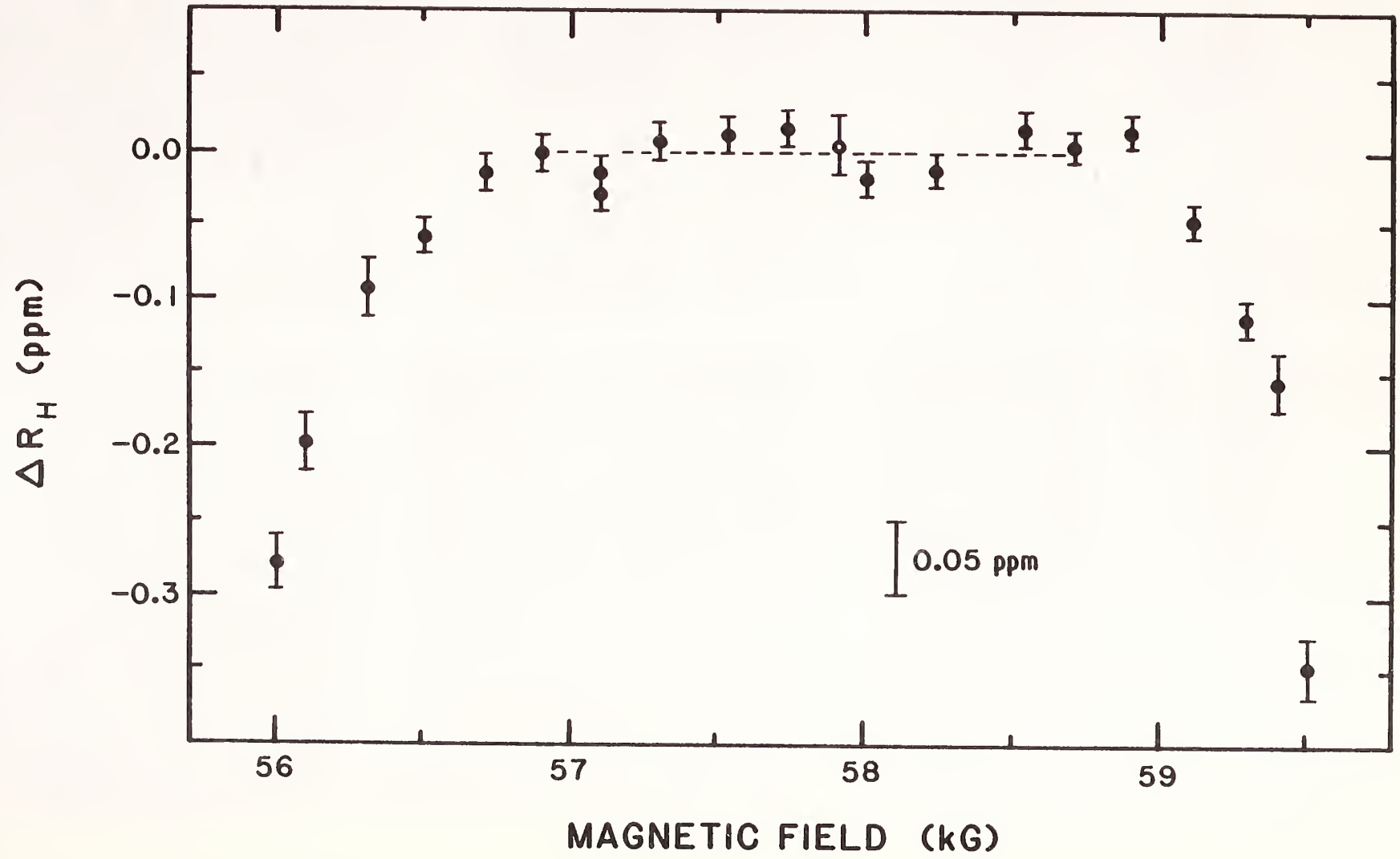
0.0
-0.1
-0.2
-0.3
ΔR_H (ppm)
0.05 ppm
56
57
58
59
MAGNETIC FIELD (kG)

IEEE TRANSACTIONS ON INSTRUMENTATION AND MEASUREMENT, VOL. IM-25, NO. 4, DECEMBER 1976

Laboratory Voltage Standard Based on $2e/h$

BRUCE F. FIELD, MEMBER, IEEE, AND VICTOR W. HESTERMAN

Abstract—**The increased dependence of a standards laboratory on a stable voltage reference has made the maintenance of a "volt" by standard cells a costly and time consuming process. This paper describes an instrument designed to calibrate cadmium-sulfate standard cells directly against a time-invariant superconducting Josephson junction voltage reference, thus replacing the large groups of cells typically used as a voltage reference. An induced voltage of 5.2 mV is produced across the Josephson junction by irradiating the junction with microwaves of a known frequency. A specially designed potentiometer is used to scale this voltage up to 1.01+ V where it can be compared to a standard cell. The overall accuracy (2σ) of the system is 0.4 ppm or better.**

I. Introduction

A PROTOTYPE voltage standard instrument has been developed that is based on the ac Josephson effect in superconductors. Using a Josephson junction as a precise time-invariant voltage reference is a well established technique which is used by many national laboratories [1]–[5]. The junction is used to produce a voltage that is proportional to the frequency of applied microwave radiation, where the proportionality constant $2e/h$ (e is the electron charge, and h is Planck's constant) is independent of individual junction characteristics.

This instrument, similar (but less accurate) than the one used to maintain the NBS Volt, is designed to be used by a secondary standards laboratory to calibrate their standard cells without being dependent on a national laboratory. The system consists of three major parts; the Josephson junction and dewar system, the junction sources, and the potentiometer. A description of each of these parts follows.

II. Josephson Junction

The junctions used with the system are thin-film tunnel junctions with an in-line geometry. The junction devices were developed at NBS by Finnegan [6]. The junction is composed of lead–lead-oxide–lead films deposited on a glass substrate. The junction is coupled to a transmission line formed between the film on the substrate and a ground plane. This in turn is connected to 0.141″ semirigid cable. The resonance frequency of the device is determined by an external microstrip resonator deposited on the substrate as shown in Fig. 1. This permits the resonance to be controlled more accurately during device fabrication. The devices we are using have a resonance frequency of approximately 9 GHz.

Manuscript received June 29, 1976.

B. F. Field is with the Electricity Division, National Bureau of Standards, Washington, DC 20234.

V. W. Hesterman is with Superconducting Technology Inc., Mountain View, CA.

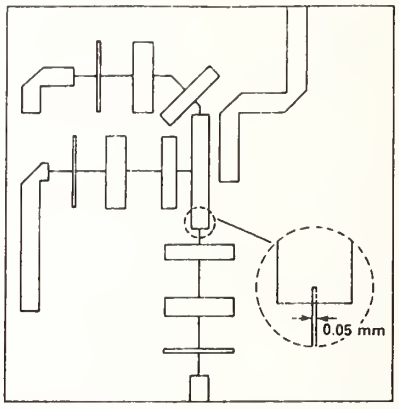

Fig. 1. Josephson junction device geometry. A junction is located at each end of the resonator strip. (Only one is used for the measurements.)

The junction will be used as a fixed voltage reference operating at approximately 5.2 mV. Junctions with resistances of 0.5 to 2.0 Ω have been characterized with current step heights of 100 μA for the low-resistance junctions and 5 μA for the high resistance junctions. We have determined that a current step height of 30 μA is necessary and we have not as yet been able to operate the low resistance junctions at 5.2 mV and 4.2 K. As it is very desirable to operate at 4.2 K, a compromise is needed between current step height and junction resistance.

III. Dewar and Probe

The Dewar used with the system is a 30-l liquid-helium Dewar which is superinsulated and thus requires no liquid nitrogen. It's liquid helium loss rate is less than 2 l/day. This gives a 15 day hold time between refills. This dewar contains three copper radiation shields that are cooled by the cold helium gas venting out the 5-cm diameter neck tube. The all metal design provides electromagnetic shielding for the Josephson junction.

The Josephson junction, a superconducting shorting switch and a ferromagnetic shield are mounted on the bottom end of a simple probe that is immersed in liquid helium in the Dewar.

The top end of the probe has a small SMA connector for the microwave, input, a knob to operate the superconducting shorting switch, a port to allow vacuum pumping of the liquid helium to reduce the temperature, a small pressure gauge to monitor Dewar pressure, a pair of copper leads used for the output EMF of the Josephson junction, and a connector for applying a bias current to the junction.

A 4.2 K mu-metal shield at the bottom of the probe produces a low magnetic field for the junction. A ferromagnetic shield could be used on the outside of the dewar at 300 K but that would add considerable cost and weight. An external shield could also be easily damaged by mechanically straining it.

The superconducting switch consists of a pair of babbit blocks separated by a fiberglass plate. A heavy niobum banana plug can be pushed into a hole in the edge of fiberglass plate thereby producing a superconducting short between the babbit blocks. The banana plug has sharp edges that cut through surface oxide on the babbit blocks. The switch is actuated by a fiberglass rod that extends through an "O" ring seal in the top of the probe.

IV. Microwave Source and DC Bias Supply

The microwave source to be used is a commercially available source consisting of a phase-locked transistor oscillator operating in L band and a frequency multiplier. The output is approximately 9 GHz at up to 50 mW, which is required to irradiate the junction. Additionally, an adjustable attenuator, a dc block (to eliminate ground loops), and an isolator (to absorb reflected power) are placed in series in the output.

The high-stability frequency reference for the source is a temperature controlled 100-MHz crystal oscillator. This oscillator has an initial long term stability of 0.015 ppm/week. Due to the linear voltage to frequency relation of the junction, an error in the frequency is reflected as a proportional error in the measured standard cell voltages. Thus the frequency reference must be checked against WWV (or a suitable frequency standard) and adjusted if necessary.

The dc bias supply provides a stable dc current to keep the junctions at the correct operating point, and contains amplifiers with voltage offsets to permit observation of the IV characteristic of the junction on the oscilloscope. Observation of the junction IV characteristic is necessary to adjust the bias conditions to the proper operating point. A rechargeable sealed lead-acid battery is used as the source in the bias supply, so when measurements of the junction voltage are being made the junction is independent of the ac power lines.

V. Potentiometer

The potentiometer designed for the system has an adjustable ratio of approximately 1/196. Instead of the usual procedure of "fine-tuning" the junction voltage to match the potentiometer output, the potentiometer ratio can be changed (≈0.3 percent) to accommodate both unsaturated and saturated standard cells. A simplified circuit diagram is shown in Fig. 2.

The design of the instrument is based on a method of series and parallel connection of 14 nominally equal resistors. The ratio of the resistances (series connected/parallel connected) is n^2, and the error contributed by the mismatch of the resistors from nominal is second-order.

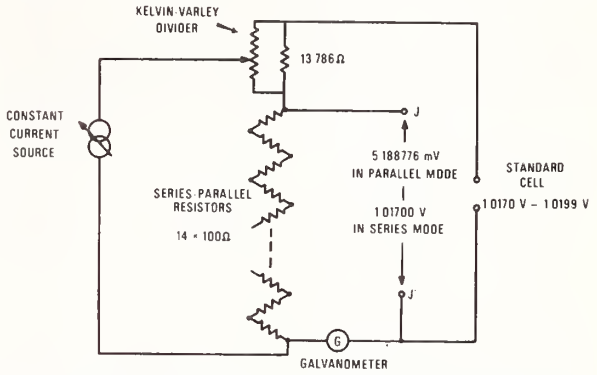

Fig. 2. Simplified circuit diagram of the potentiometer, with the paralleling network for the main resistors omitted for clarity.

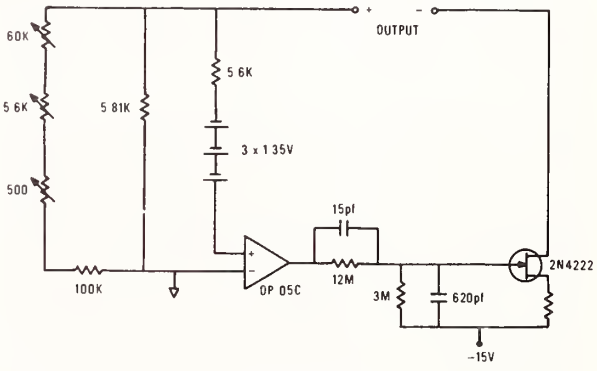

Fig. 3. Circuit diagram of the constant current source for the potentiometer.

The stepup from the junction voltage is accomplished as follows. The 14 resistors are first connected in parallel. Commercal grade rotary switches in series with compensating resistors (fans) are used to obtain a high accuracy ratio. The 14 resistors are permanently connected together using 4-terminal (tetrahedral) connections. The current source in the instrument is adjusted to equate the voltage produced across the parallel connected resistors, to the junction voltage (at $J - J'$), using a photocell galvanometer as a detector. Restoring the resistors to the series connected mode produces a calibrated voltage, across the series–parallel resistors and the Kelvin–Varley divider, that can be compared to a standard cell.

For ease of use it was decided not to require readjustment of the junction voltage and operating current of the instrument for each cell to be calibrated. Instead, a Kelvin-Varley divider shunted by a 13.786-Ω resistor is used to provide a small adjustment of the nominal 1/196 ratio. Thus only periodic "standardization" of the current is needed to compensate for drifts in the current source. The divider dials are arranged to be direct reading in volts with a range of 1.0170 to 1.0199, and with a resolution of 0.1 μV. Because of the limited adjustment range, only moderate accuracy is required of the divider.

The requirements for the constant current source are: it should be unaffected by load changes, have good stability over a 2- or 3-h period, and have low noise output. The

TABLE I
Summary of Sources of Systematic Error in the Potentiometer

Sources	Values ppm (2σ)
1. Main resistor mismatch	<0.01
2. Fan resistor mismatch	<0.02
3. Resistance of tetrhedral junctions	<0.02
4. Main resistor self-heating	<0.10*
5. Potentiometer temperature stability	0.04*
6. Kelvin-Varley divider and shunt	0.20
7. Current source stability	0.08
8. Leakage resistances	<0.04
9. Effects of thermal EMF's	0.02*

*These values are subjective estimates intended to be comparable with statistical 2 σ limits.

circuit diagram of the current source used in the instrument is shown in Fig. 3. The reference for the source is three temperature regulated mercury batteries. The addition of a field-effect transistor at the output of the operational amplifier increases the effective dc loop gain of the system while preserving an adequate phase margin for stability. The source exhibits drift on the order of 0.2 ppm/h which is due almost entirely to drift of the mercury battery reference. Changes in the current due to changing load resistances are less than 0.04 ppm for any setting of the Kelvin–Varley divider or series parallel connection of the resistors. Noise from the source is approximately 0.02 ppm rms in a 10-Hz bandwidth.

VI. Discussion of Errors

The estimated errors in a voltage measurement directly attributable to potentiometer uncertainties are listed in Table I and are discussed briefly below. High quality wirewound resistors were used for the main series–parallel resistors. These resistors had initial resistance matching to better than 100 ppm and matching of temperature coefficients of resistance to better than 2 ppm/°C. The error due to resistance mismatch was measured after the resistors were installed in the instrument. The self-heating error (more power is dissipated in the resistors in the series mode than in the parallel mode) was estimated from measurements made on similar resistors.

The error in the Kelvin–Varley divider and shunt combination is a function of the dial setting of the divider. If corrections were applied to the readings, the uncertainty could be reduced to less than 0.01 ppm. However, it is anticipated that in routine operation corrections will not be applied. For any dial setting the measured worst case error was less than 0.1 ppm.

VII. Results and Conclusions

A system has been developed to permit a standards laboratory to maintain a unit of voltage without time consuming standard cell calibrations in-house or at a national laboratory. The system uses a Josephson tunnel junction as a time invariant voltage reference, and a special potentiometer to scale the 5.2-mV output of the junction to the voltage of a standard cell. An estimate of the uncertainty in a voltage measurement (comparable with statistical 2σ limits), which includes allowances for the potentiometer uncertainties and random measurement uncertainties, would be 0.4 ppm. This uncertainty may be reduced by a factor of three if corrections were determined and applied to the Kelvin–Varley divider readings, and the galvanometer output was time averaged to reduce the random uncertainty. Difficulties in fabricating a junction operable at 4.2 K with large step heights has prevented final measurements from being made at the present time.

Acknowledgment

The authors are grateful to L. B. Holdeman and T. F. Finnegan for numerous suggestions and help in the measurement of the junction characteristics. We would also like to thank J. Toots for fabricating the junctions for the system.

References

[1] I. K. Harvey, J. C. MacFarlane, and R. B. Frenkel, "Monitoring the NSL-standard of EMF using the ac Josephson effect," *Metrologia*, vol. 8, pp. 114–124, 1972.

[2] J. C. Gallop and B. W. Petley, "Recent NPL work on the AC josephson effect as a voltage standard," *IEEE Trans. Instrum. Meas.*, vol. IM-21, pp. 310–314, Nov. 1972.

[3] B. F. Field, T. F. Finnegan, and J. Toots, "Volt maintenance at NBS via $2e/h$: A new definition of the NBS volt," *Metrologia*, vol. 9, pp. 155–166, Mar. 1973.

[4] V. Kose, F. Melchert, W. Engelland, H. Fack, B. Furhrmann, P. Gutmann, and P. Warneck, "Maintaining the unit of voltage at PTB via the ac Josephson effect," *IEEE Trans. Instrum. Meas.*, vol. IM-23, pp. 271–275, Dec. 1974.

[5] G. H. Wood, A. F. Dunn, and L. A. Nadon, "The AC Josephson Effect Monitoring of the Unit of EMF in Canada," *IEEE Trans. Instrum. Meas.*, vol. IM-23, pp. 271–278, Dec. 1974.

[6] T. F. Finnegan, J. Toots, L. B. Holdeman, S. Wahlsten, P. Mukhopadnyay, and T. Claeson, "Coupled Josephson tunnel junctions and microstrip resonators," *Bull. Amer. Phys. Soc.*, vol. 21, no. 3, p. 340, Mar. 1976.

IEEE TRANSACTIONS ON INSTRUMENTATION AND MEASUREMENT, VOL. IM-23, NO. 4, DECEMBER 1974

Cryogenic Voltage Comparator System for 2e/h Measurements

RONALD F. DZIUBA, MEMBER, IEEE, BRUCE F. FIELD, MEMBER, IEEE, AND THOMAS F. FINNEGAN

Abstract—**The design and operation of a cryogenic voltage comparator system for precision $2e/h$ measurements is described. Major improvements embodied in the new $2e/h$ system include the use of 1) a single microstripline-coupled Josephson tunnel junction to obtain usable step voltages up to 10 mV at 10.0 GHz, 2) a cryogenic voltage divider comprised of two resistors whose ratio is calibrated with a low-temperature dc current comparator, 3) a superconducting quantum interference device (SQUID) null detector, and 4) superconducting switching. The accuracy of the present 196:1 divider system is estimated to be about 2 parts in 10^8 on the basis of preliminary tests and is limited by resistor self-heating during calibration.**

I. INTRODUCTION

IN RECENT YEARS the use of the ac Josephson effect to measure $2e/h$ has provided the basis for a new maintenance voltage standard [1], [2]. This low-temperature solid-state physical phenomenon is currently in use at the National Bureau of Standards (NBS) [3] and other standards laboratories throughout the world. Improvements in present prototype $2e/h$ measurement systems to make them more simple, reliable, and portable will permit widespread use of these systems as local laboratory voltage standards and as portable volt transfer standards. The successful realization of rugged compact microwave-coupled Josephson devices and all cryogenic voltage measurements systems are generally regarded as significant steps in this direction.

In this paper, we describe a new cryogenic $2e/h$ system being developed at NBS. In contrast to cryogenic systems previously reported [4], [5] in which the voltage ratio is established via the series-parallel technique, the present system consists primarily of a cryogenic voltage divider comprised of two resistors whose ratio is calibrated with a low-temperature dc current comparator and a single Josephson tunnel junction coupled to external microwave fields via a microstrip transmission line. Superconducting switching and a superconducting quantum interference device (SQUID) null detector complete the major cryogenic portions of the system. The aim of this paper is to describe the design features and the measured performance of this new $2e/h$ system.

In Section II, the Josephson device, which provides the low level voltage for comparison with the 1 V of a standard cell, is discussed. The voltage comparator system, which is operable in two principal configurations (i.e., calibration and measurement), is described in Section III. The results of preliminary testing of a 196:1 voltage divider are presented in Section IV.

Manuscript received July 3, 1974; revised August 9, 1974.
The authors are with the Electricity Division, National Bureau of Standards, Washington, D.C. 20234.

II. JOSEPHSON DEVICES

A Josephson junction can be made in a variety of ways by weakly coupling two superconductors, e.g., via a thin-film oxide, a point contact, or a constriction in a film. When the junction is placed in an applied microwave field of frequency ν, a series of steps can be induced in the current–voltage characteristic at voltages $V_n = nh\nu/2e$, where n is an integer, and the junction can be regarded as a precise frequency-to-voltage transducer. The maximum usable value of V_n depends on the particular device; however, the *tunnel junction* has been applied the most successfully in attaining large voltages, $V_n \geq 5$ mV. By coupling microwave radiation to a series connection of resonant tunnel junctions via X-band waveguide, total Josephson voltages of 10 mV have been regularly obtained and routinely used in $2e/h$ measurements both with in-line [2] and cross-type [3] geometries.

Recently, a new method of coupling microwave radiation to Josephson tunnel junction devices has been developed in which the thin-film tunnel junction is mounted on a ground plane and forms an integral portion of a 50-Ω microstrip transmission line [6]. To be useful in a cryogenic $2e/h$ measurement system, the device should provide a large voltage and the device holder should be compact and well shielded. The microstripline-coupling technique has been refined and used to produce a Josephson device specifically for the $2e/h$ application.

The device itself is composed of a single in-line Pb–Pb oxide–Pb Josephson tunnel junction (1.0 by 0.3 mm) deposited on a glass substrate. The narrow Pb strip (0.3 mm) is deposited first. After thermal oxidation of this film, a second Pb film (2 mm wide) is deposited to form both the junction and a 50-Ω transmission line when the substrate is mounted above a ground plane. Four gold films which had been previously evaporated provide the voltage monitor and "potentiometer" leads. The junction is mounted in a special microwave package as shown in Fig. 1. The microwave fields are coupled to the top of the cryostat via semirigid 50-Ω coaxial cable. The center conductor of the cable and the feedthrough at the end opposite the microstripline launcher are used to feed a dc bias current to the junction. The voltage and potentiometer leads are also connected to feedthroughs which consist of lossy inductors containing iron epoxy filler for filtering.

With devices of this type, usable junction voltages V_n between 5 and 10 mV were readily attained. The relevant $2e/h$ parameters for one of these junctions, resonant at

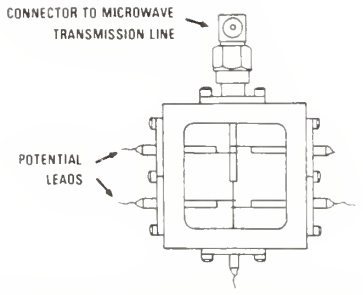

Fig. 1. Microstripline-coupled Josephson junction holder with top cover removed. The junction substrate (2.54 by 2.54 by 0.12 cm) rests directly on a copper ground plane and microwave radiation is coupled into the holder via semirigid cable.

TABLE I
MICROSTRIPLINE-COUPLED $2e/h$ DEVICE PARAMETERS OF AN IN-LINE 0.1-Ω PB–PB OXIDE–PB JUNCTION (ν = 10.0 GHz) AT 1.9 K

V_n (mV)	I_s (μA)	P (mW)	Ratio
5.2	210	20	196:1
7.1	170	35	144:1
10.2	100	75	100:1

Note: The corresponding fixed divider ratio required is also shown.

10.0 GHz, are shown in Table I. The maximum step amplitudes I_s are quite large even at 10 mV. (The external magnetic field is ≤ 0.1 μT.)

The variation in the applied microwave power P between 5 and 10 mV agrees well with that expected from a simple analysis of the Bessel function dependence of the steps (i.e., $P \cong kV_{dc}^2$). This particular device was cycled between cryogenic and room temperatures at least six times with no noticeable change in its characteristics. These results make it clear that compact single-junction devices can be achieved and are practical to use in $2e/h$ measurements.

III. CRYOGENIC COMPARATOR SYSTEM

The cryogenic voltage divider consists essentially of two resistors and an external power supply. The divider ratio N^2:1 is calibrated with a low-temperature dc current comparator (which establishes the ratio N:1) in a two-step procedure by means of an additional auxiliary resistor as shown in Fig. 2(a). The choice of the nominal divider ratio and hence the integer N depends on the ratio of the standard cell voltage to the usable Josephson junction output. The current comparator contains 17 ratio windings enclosed in a superconducting lead sheath wound around a SQUID sensor and is designed to provide any integer ratio up to 15:1. During calibration, each comparator–divider bridge circuit is balanced (with the SQUID null detector) by supplying a known error current to an additional winding.

For voltage comparison measurements with a Josephson junction and standard cell, the cryogenic resistive divider is connected to an external power supply to establish a

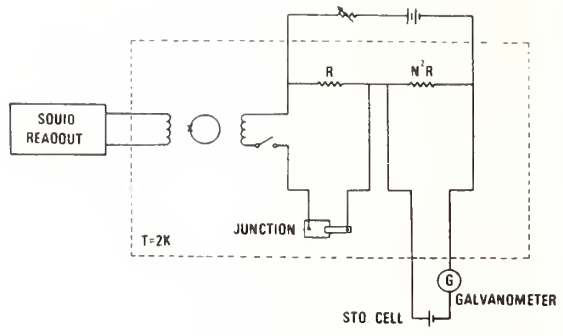

(a)

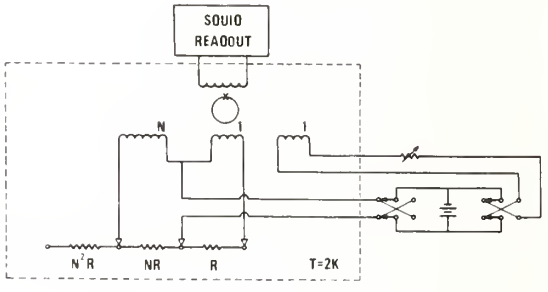

(b)

Fig. 2. Simplified circuit diagram of cryogenic voltage comparator system. (a) Calibration mode. (b) Measurement mode.

voltage ratio (N^2:1) as indicated in Fig. 2(b). With a nominal 7-mV junction, for example, a ratio of 144:1 is suitable. In operation, the voltage ratio of the divider is fixed, and the null detector balances are made by adjusting the current through the divider and the frequency of the applied microwave radiation.

By immersing the critical dc components in a (superfluid) liquid helium bath, the effects of thermal EMF's are reduced, detector sensitivity is increased, and a stable uniform temperature is more easily achieved. The only major parts of the apparatus not at cryogenic temperatures are the microwave generation and frequency measurement equipment, the SQUID readout system, and the power sources.

A. Voltage Divider

In the prototype $2e/h$ system constructed for preliminary testing, a divider ratio of 196:1 was conservatively chosen to measure a voltage of 5.2 mV. The main (two-terminal) resistors of the divider were constructed by loosely winding silicon–copper alloy wire [7] (96-percent Cu, 3-percent Si, 1-percent Zn) on polytetrafluoroethylene formers and have nominal values of 7, 98, and 1372 Ω. The wire for the two lowest value resistors has a diameter of 0.125 mm while that for a 1372-

Ω resistor has a diameter of 0.025 mm (obtained by drawing a portion of the 0.125-mm wire). Terminations between the alloy wire and the superconducting wiring were accomplished via an intermediate copper terminal directly hard-soldered to the resistance wire and are similar to those described by Harvey and Collins [8]. The average fractional temperature coefficient (measured between 2.0 and 4.2 K) of the 7- and 98-Ω resistors was -5.2×10^{-6}/K and that of the 1372-Ω resistor, -6.2×10^{-6}/K. Self-heating measurements indicated a load coefficient of -1×10^{-3}/mW at 4.2 K and about -2×10^{-3}/mW at 2 K.

The divider power supply employs an unloaded mercury battery as the critical regulating element and is similar to that described by Finnegan and Denenstein [9]. The only essential difference in the present system is that the main resistor (~300 Ω) is located in the liquid helium bath to minimize the effects of lead resistance variations caused by changes in the height of the liquid helium level in the Dewar.

An electronic dc temperature control system is used to regulate the temperature of the superfluid bath to ≤ 1 mK at any nominal temperature between 1.5 and 2.1 K. The resistance of a calibrated germanium thermometer is monitored via a dc resistance bridge to determine the temperature, and the amplified bridge output is used to power a resistive heater (1.5-kΩ resistor) located in the liquid helium.

B. DC Ratio Transformer

The current comparator used to calibrate the resistive divider is similar to that described elsewhere [10], [11]. Our comparator, designed to produce any precise integer ratio up to 15:1, has been constructed by enclosing 17 insulated superconducting wires or ratio windings in a superconducting (lead) cable which was then wound around a multihole SQUID sensor. An extra winding is included in order to introduce a small known current for balancing the SQUID detector during calibrations. The number of ratio windings actually used depends on the ratio of the particular resistive divider; e.g., in the preliminary tests described here, 16 of the 17 ratio windings were used to achieve a 14:1 ratio.

The SQUID device and cable containing the ratio windings were shielded with a lead-plated brass can. All connections between and to the ratio windings were made some distance from the SQUID to eliminate end effects. An upper limit on the current ratio accuracy of 2×10^{-9} was obtained by systematically checking 15 of the windings in succession against a reference winding at a current level of 150 mA. The unit winding current sensitivity of this comparator is 6×10^{-11} A.

Calibration of the resistive divider is done in a two-step procedure with an auxiliary resistor as indicated in Fig. 2(a). An inherent limitation of the present method is the self-heating in resistors R and NR, which are calibrated with a current much larger (N times) than that used during measurements.

C. Null Detectors and Switching

The low level junction voltage balances are made with the SQUID system of the current comparator. Its sensitivity in this mode of operation is 2.8×10^{-11}V.

The standard cell balances are made with a conventional photocell-galvanometer amplifier whose isolated output is displayed on a recorder as in regular $2e/h$ measurements [3].

All of the critical switching between the current comparator, resistors, power supplies, junction, and standard cell for calibration and measurement is done with a rotary switch. The switch which has five positions (and eight poles) was rebuilt with fixed Babbitt metal contacts and niobium-clad rotors. Each rotor consists of a phosphor bronze spring with a small piece of niobium foil spot-welded to the contacts to insure a superconducting path between the fixed Babbit contacts. (The contact force was estimated to be 300 g.) The critical current of every switch contact was tested and found to exceed 120 mA. Repeated cycling between 2 and 300 K and over 600 contact closures did not appear to effect either the electrical or mechanical properties of the switch.

IV. RESULTS AND CONCLUSIONS

Although high precision $2e/h$ measurements have not yet been made with the system, a preliminary evaluation of its overall performance has been made by testing the individual components and subsystems. At present the limiting source of uncertainty in the system is the resistor heating during calibration which introduces a deviation of about 2×10^{-7} in the 196:1 ratio. This deviation can be determined to about 2×10^{-8} (1 standard deviation). Changes in the alloy resistors, when repeatedly cycled between liquid helium and room temperature, were usually less than 10^{-5} so that trimming is not a serious problem. Adequate shielding of the various comparator components, particularly the SQUID and tunnel junction, from one another is an essential prerequisite for successful operation of the overall system.

In conclusion, we have designed and built a cryogenic $2e/h$ comparator system with a 196:1 ratio. The overall accuracy with which this system might be used to determine $2e/h$ is about 2×10^{-8} based on the results of our preliminary tests. Also, the successful development of single microstripline-coupled Josephson junction devices with voltage outputs near 10 mV now makes more attractive the application of alternative cryogenic divider techniques such as the series-parallel method for $2e/h$ work.

ACKNOWLEDGMENT

The authors wish to thank D. B. Sullivan, B. N. Taylor, J. Toots, and J. Wilson for useful discussions and valuable assistance.

REFERENCES

[1] B. N. Taylor, W. H. Parker, D. N. Langenberg, and A. Denenstein, "On the use of the ac Josephson effect to maintain standards of electromotive force," *Metrologia*, vol. 3, pp. 89–98, 1967.
[2] T. F. Finnegan, A. Denenstein, and D. N. Langenberg, "AC

Josephson effect determination of e/h: A standard of electrochemical potential based on macroscopic quantum phase coherence in superconductors," *Phys. Rev. B*, vol. 4, pp. 1487–1522, 1971.
[3] B. F. Field, T. F. Finnegan, and J. Toots, "Volt maintenance at NBS via 2e/h: A new definition of the NBS volt," *Metrologia*, vol. 9, pp. 155–166, 1973.
[4] D. B. Sullivan, "Low temperature voltage divider and null-detector," *Rev. Sci. Instr.*, vol. 43, pp. 499–505, 1972.
[5] J. C. Gallop and B. W. Petley, "High-precision measurement of $2e/h$ that uses cryogenic electronic components," *Electron. Lett.*, vol. 9, pp. 798–799, 1973.
[6] T. F. Finnegan, J. Wilson, and J. Toots, "Interactions in small systems of coupled Josephson junctions at microwave frequencies," *Rev. Phys. Appl.*, vol. 9, pp. 199–205, 1974; also "Coupling between Josephson junctions and microstriplines," presented at the Applied Superconductivity Conf., Oakbrook, Ill., Oct. 1974.
[7] D. B. Sullivan, "Resistance of a silicon bronze at low temperatures," *Rev. Sci. Instr.*, vol. 42, pp. 612–613, 1971.
[8] I. K. Harvey and H. C. Collins, "Precise resistance ratio measurements using a superconducting dc ratio transformer," *Rev. Sci. Instr.*, vol. 44, pp. 1700–1702, 1973.
[9] T. F. Finnegan and A. Denenstein, "High accuracy potentiometers for use with ten millivolt Josephson devices. I: Double series-parallel exchange comparator," *Rev. Sci. Instr.*, vol. 44, pp. 944–953, 1973.
[10] I. K. Harvey, "A precise cryogenic dc ratio transformer," *Rev. Sci. Instr.*, vol. 43, pp. 1626–1629, 1972.
[11] D. B. Sullivan and R. F. Dziuba, "Low temperature direct current comparators," *Rev. Sci. Instr.*, vol. 45, pp. 517–519, 1974.

Reprinted by permission from IEEE TRANSACTIONS ON INSTRUMENTATION AND MEASUREMENT
Vol. IM-23, No. 4, December 1974, pp. 264-267

Volt Maintenance at NBS via $2e/h$: A New Definition of the NBS Volt*

B. F. Field, T. F. Finnegan, and J. Toots

Institute for Basic Standards, National Bureau of Standards, Washington, D.C. 20234, U.S.A.

Received: March 16, 1973

Abstract

This paper describes in detail the procedures, methods and measurements used to establish a new definition of the U.S. legal volt via the ac Josephson effect. This new definition has been made possible by the use of thin film tunnel junctions (capable of producing 10 mV outputs) and high accuracy voltage comparators. The Josephson junction is used as a precise frequency-to-voltage converter with a conversion factor equal to $2e/h$. A series of measurements of $2e/h$ has been carried out at NBS referenced to the as-maintained unit of emf based on a large group of standard cells. Measurements made at regular intervals over a one year period (1971 to 1972) indicate that the mean emf of this group of standard cells has decreased about 4 parts in 10^7. Primarily to remove the effects of this drift, on July 1, 1972 a new as-maintained unit was defined by choosing a value of $2e/h$ consistent with the existing unit of emf. The adopted value of $2e/h$ is 483593.420 GHz/V_{NBS}. The precision (one standard deviation) with which the new unit of emf can be maintained with the present techniques and apparatus is about 2 parts in 10^8. The accuracy of the present system is estimated to be 4 parts in 10^8. Comparisons of $2e/h$ systems at different national laboratories have been limited by uncertainties associated with the physical transfer of standard cells. In order to determine the relative agreement of the various $2e/h$ systems with precision better than 1 or 2 parts in 10^7, it appears desirable to compare $2e/h$ systems directly by transporting one of them.

1. Introduction

The ac Josephson effect has made possible the realization of a new voltage maintenance standard at the National Bureau of Standards. Critical to this realization is the role played by a Josephson junction which may be regarded here as a frequency-to-voltage converter, where the frequency-to-voltage ratio is precisely equal to the combination of physical constants $2e/h$ (e is the electron charge and h is Planck's constant). A variety of experimental tests (for material dependence, temperature dependence etc.) [1—5] and theoretical investigations [6—9] of the Josephson relation have been made which indicate that for ordinary Josephson devices (particularly tunnel junctions) with conventional current-voltage lead configurations the ratio is exact to at least a few parts in 10^8. However, further experimental investigation of this question appears desirable.

Since the first high precision measurements of $2e/h$ by Parker, Taylor and Langenberg [10], the potential significance of a precision voltage standard based on $2e/h$ has been recognized throughout the world [1, 2, 11—14]. It was first demonstrated by Finnegan, Denenstein, and Langenberg (FDL) that standard cells could be maintained with a precision of 10^{-7} via a Josephson $2e/h$ apparatus over extended periods of time (5 months) [1]. Establishing a unit of emf based on a fundamental physical phenomenon such as the ac Josephson effect removes many of the inherent difficulties in using a large group of standard cells to maintain a unit of emf. One of the most important of these difficulties is the gradual long term drift characteristic of the emf's of standard cells.

In this paper we present a detailed account of the experiments involved in establishing a working Josephson-effect voltage maintenance standard at NBS. Much of the apparatus and procedures are essentially identical with those described by FDL [1]. Section II contains a description of the Josephson devices and their performance. In Section III, we briefly describe the microwave and Josephson-device bias equipment. Section IV contains descriptions of the two dc voltage comparators including estimates of their respective accuracies. The experimental procedures used to compare a standard cell with the Josephson voltage are described in Section V. This section also contains $2e/h$ data for a local group of standard cells. In Section VI, the history of the NBS voltage maintenance and dissemination program based on standard cells is briefly reviewed. Section VII contains the NBS $2e/h$ results including a discussion of the overall experimental uncertainties. A comparison of recent (1971 to 1972) values of $2e/h$ is presented in Section VIII. Finally in Section IX, the procedures used for the NBS voltage maintenance standard based on $2e/h$ are outlined and its current precision noted.

2. Josephson Device Fabrication and Performance

All of the $2e/h$ measurements made at NBS have utilized resonant thin-film tunnel junctions. These junctions are more difficult to manufacture than point-contact junctions, and couple to the microwave power only over a limited frequency range; however, they can be used to achieve higher step voltages. The ability to use higher dc voltages is a significant advantage since it minimizes the effect of thermal emf's generated in the cryostat and the junction voltage measuring leads, and requires less sensitivity in the voltage null detector. Furthermore, thin-film junctions are permanent structures which require no mechanical adjustment before each experiment nor periodic cleaning and reconditioning.

The junctions we have used are of cross-type geometry with four junctions deposited on a single 2.54 cm square glass substrate, as shown in Fig. 1. The dimensions of the junctions are approximately 1 mm by 0.3 mm with the films approximately 150 nm (1500 Å) thick. This geometric structure has a resonance frequency at about 9 GHz. The junctions used

for the $2e/h$ measurements have been of Pb-Pb oxide-Pb construction. Some Sn-Sn oxide-Sn junctions have been made but usuable steps at the voltage required by our measuring instruments are not easily attained.

The junctions are fabricated with a thermal evaporation system. The first layer of Pb is evaporated on each glass substrate and then oxidized in 1/2 atm of oxygen at a temperature of about 40 °C. (The substrates are heated by radiation from infrared heat lamps external to the vacuum chamber.) The second layer of Pb is evaporated and the junction is overcoated with a layer of photoresist after removal from the evaporator. The junctions are then stored in liquid nitrogen dewars at 77 K.

Shortly after fabrication the dc I-V characteristic and normal-state resistance of the junctions are measured. Junctions with nearly identical I-V characteristics, however, can differ greatly in frequency response, coupling properties, and the rate of decrease of the maximum step height (current amplitude) with increasing dc voltage. Measurements of the dc junction

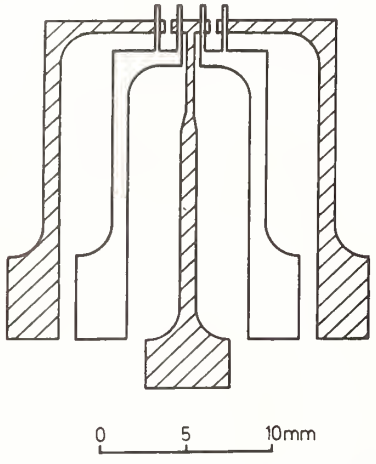

Fig. 1. Josephson-device geometry. The cross-hatched region indicates the oxidized film which is partially covered by the second film to produce four junctions

characteristics are useful in detecting gross defects such as shorts bridging the oxide barrier which can markedly reduce the coupling to external microwave fields.

The normal resistance of the junction is, in theory, inversely proportional to the zero voltage current which in turn is related to the current amplitude of a given step. Therefore the use of low resistance junctions should provide higher step amplitudes. Unfortunately, in going to lower resistance junctions (below 1/3 ohm) the maximum zero voltage current, we observe, increases monotonically, but becomes a significantly smaller fraction of the theoretical limit. Typical junctions with resistances of 0.1 and 0.05 ohm have maximum dc currents of 9 and 12 mA compared to the respective theoretical limits of approximately 20 and 40 mA. Some of this reduction may be attributed to the asymmetric self-field generated by the dc bias current flowing through the junction. In selecting junctions for voltage measurement, one must compromise on the choice of junction resistance; it should be small enough to yield a reasonable zero voltage current and consequently large step amplitudes, and yet be large enough to provide sufficient coupling for operation at reasonable step voltages and applied microwave powers. We have found that the use of junction resistances near 0.1 ohm is a good choice.

When a tunnel junction is irradiated with microwaves, at frequency ν, the I-V characteristic shown in Fig. 2 (a), is modified so that steps appear at discrete voltage intervals given by the relation $2eV_n = nh\nu$. The height of these steps decreases with increasing junction voltage (V_n). As the step amplitude get smaller it becomes progressively more difficult to

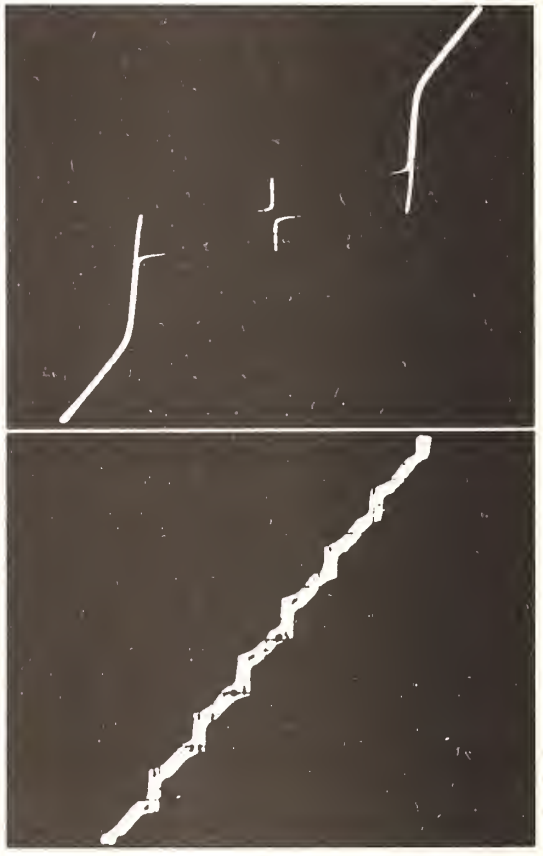

jg. 2. Typical I-V characteristic of a Pb-Pb oxide-Pb tunnel unction. a) With no applied microwaves. Vertical scale: 10 mA/div.; horizontal scale: 1 mV/div. b) With applied microwaves; constant voltage steps induced at 5 mV. Vertical scale: 200 μA/div.; horizontal scale: ≈ 20 μV/div.

remain biased on a step, due to drifts in the dc bias current and microwave power level. For our present apparatus steps smaller than 50 μA are considered unusuable. Our junctions respond to microwave power only near their resonance frequencies. Continuous adjustability of the junction voltages is made possible by the high step numbers used, despite the limited frequency range. The details of the coupling between external microwave fields and our resonant tunnel junctions are not yet clearly understood. Qualitatively better coupling is observed for higher resistance junctions.

In order to get usable step amplitudes at 10 mV we have chosen to operate two junctions in series. For reasonable operating conditions we can tolerate a few tenths of a percent mismatch in the two resonance frequencies. However, a half percent mismatch often means that the junction combination is marginal. When using junctions connected in series in the same microwave field, we have found it advantageous to cascade junctions of nearly equal resistance.

If the induced microwave steps have a finite slope (i.e. $dI/dV \neq \infty$), the Josephson voltage is no longer well defined. The slope of the steps is known to be sensitive to external electromagnetic noise [15, 16] and extensive precautions have been taken (shielded room and equipment) to reduce this noise. The slope is regularly checked by slowly varying the bias current up and down the step and looking for a voltage deflection on the null detector used with the measuring instrument. We have never observed any finite step slope to within the resolution of our null detector (a few parts in 10^8).

3. Microwave and dc Bias Apparatus

In order to obtain an induced step at a desired voltage, sufficient microwave power at a well-defined frequency must be coupled into the junction and a stable dc bias current passed through it.

a) Mircowave Equipment

The microwave apparatus, as indicated in the block diagram in Fig. 3, includes a klystron tube mounted in an oil bath (with air cooling) for microwave stability. The klystron is phase-locked to a continuously-adjustable quartz-crystal oscillator for frequency stability. The short term frequency stability (15 min) is about 1 part in 10^9. The frequency is measured by a frequency counter with an internal converter and a resolution of 1 part in 10^9. The isolator, shown in the diagram adjoining the main attenuator, prevents unwanted reflection of microwave power into the klystron. The microwave generation equipment and the cryostat containing the junction holder are grounded separately, and a dc block is placed in the waveguide to prevent circulating currents.

The accuracy of the counter time base is regularly checked against the U.S. frequency standard. A 100 kHz high stability oscillator is compared to the signal from WWVB using a VLF phase comparator. This oscillator, which is maintained within a few parts in 10^{10} of WWVB, is simultaneously used to check the counter time base. The drift in the counter time base is predictable and changes 2 parts in 10^{10}/day.

b) Junction Holder Description

The glass substrate on which the junctions are evaporated is mounted in the center of a piece of copper X-band waveguide. A slot is milled halfway through the waveguide and the substrate rests in this slot. A close fitting cover holds the substrate in place and provides continuous guide walls. The leads to the junctions are copper magnet wire soldered to the junctions using indium solder. The bias lead wires pass through small grooves in the substrate cover to Teflon standoffs outside the waveguide where they are soldered to leads from a vacuum tight electrical connector mounted in the top of the holder. The voltage leads are from a single spool of copper magnet wire and are kept in close thermal contact by running them to the voltage measuring instrument in a single piece of Teflon tubing. In the cryostat they are enclosed in a length of copper tubing that always crosses the helium level. From the copper tubing to the top of the cryostat the leads are enclosed in a thin-wall stainless steel tube. This arrangement minimized heat transfer and tends to keep the large temperature gradient at one location on the leads.

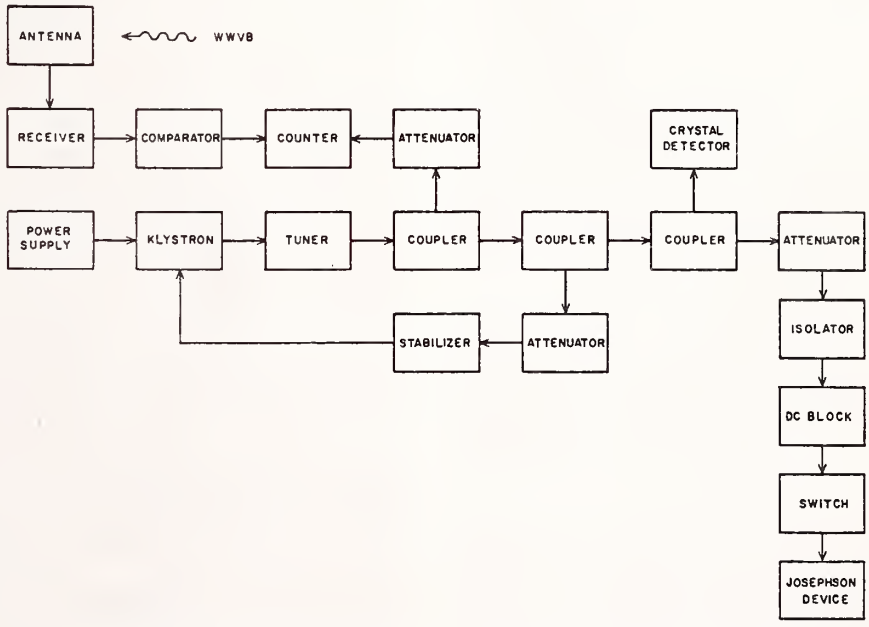

Fig. 3. Block diagram of microwave generation and frequency measuring equipment

In order to maximize the microwave electric field at the junction a shorting plug is placed in the waveguide about 4 cm below the substrate. Since placement of this short is extremely critical, it can be adjusted from the top of the cryostat while observing the step pattern on an oscilloscope. An iris placed above the substrate to form a cavity as described by FDL [1] was not used for our measurements.

c) Bias Circuit

The two junctions used for the $2e/h$ measurements are operated with independent bias current sources, similar to the ones described by FDL [1]. The individual supplies consist of two 14 ampere-hour mercury cells connected in parallel, and adjustable resistors connected in series with the junction to adjust the current. The current is reversible and has separate fine adjustment controls for the forward and reverse current so that small adjustments can be made in the bias current while in one direction without disturbing the settings for the other polarity. An I-V display on an X-Y oscilloscope with differential inputs is provided for each junction by monitoring the voltage across a resistor in the bias circuit and the voltage developed across each individual junction. Adjustable positional offsets in the display circuit are used to suppress the origin of the I-V curve to allow expansion of any portion of the curve for viewing. The offset for the junction voltage is calibrated so the proper step number can easily be determined.

The bias circuit normally supplies dc for use when measuring the junction voltage; however, for viewing the I-V characteristic an ac sweep is extremely useful. Two types of sweep circuits were constructed for use with our bias supply. A separate specially shielded transformer (connected to the 60 Hz power line) can be connected in place of the batteries to provide an adjustable ac sweep which is useful for observing the I-V characteristic with no microwaves applied and determining the critical current. The transformer is disconnected from the bias supply whenever measurements are to be made and a second incremental sweep circuit is used. The second circuit is battery operated and built into the bias supply. This sweep is superimposed on a dc level and is used to observe a small portion of the characteristic. The sweep consists of an oscillator with an active filter to remove all but the fundamental sine wave. During voltage balance both ac sweep circuits and the oscilloscope are completely disconnected from the dc circuitry so that the supply is isolated from grounded equipment with an insulation resistance greater than 10^{11} ohms.

4. Voltage Comparators

Two voltage comparators are presently in use at NBS. Both of these instruments provide a fixed 100 to 1 ratio and rely on the fact that the junction voltage is adjustable to exactly 1/100 of the standard cell voltage. These comparators were built and first used at the University of Pennsylvania and are described in greater detail in reference [1].

The use of a fixed 100/1 ratio comparator reduces the measurement uncertainty by eliminating the need for an adjustable resistance network since the junction voltage can be varied to achieve a null balance. Both instruments can be self-calibrated in less than an hour using no external resistance standards. The use of two instruments operating on different principles with different major sources of systematic error is desirable since it allows us to perform a final check on unsuspected sources of systematic error. The two instruments were periodically compared and were always found to agree within 3 ± 3 parts in 10^8, well within the estimated total instrument uncertainty of 4 parts in 10^8.

a) Series-Parallel Comparator

The design of the first voltage comparator (the one used for the $2e/h$ runs) is based on a method of double series-parallel exchange. If a group of n nominally equal resistors are connected first in series and then in parallel, the ratio of the resistances of the two combinations is n^2 with an error which is second order in the resistor mismatch. Figure 4 is a simplified circuit diagram of the comparator (SPC) showing the two sets of ten matched resistors, one set in series and one in parallel. If the two sets of resistors are exchanged (i.e., the set originally in series is reconnected in parallel, and the other set reconnected in series) and a second set of balances made, the effect of inequality of the total resistance of the two sets of resistors is reduced to second order by averaging the results of the two balances.

Tetrahedral junctions and compensating resistors (fans) for paralleling the network permit the use of commercial grade rotary switches despite their high contact resistance, while maintaining a high accuracy series-parallel transfer. A power supply using mercury batteries and regulated by a mercury battery under essentially no load, supplies stabilized current (1/2 ppm/h) to the resistance networks. The effects of thermoelectric voltages in the circuit are eliminated by reversing the current in the instrument, the standard cell, and the junction bias current. Although the 100/1 ratio can be determined to greater accuracy than that with which the individual resistors can be compared, the power dissipated in the networks changes by a factor of 100 when they are switched from series to parallel. To reduce the error resulting from self-heating the resistors are mounted in a thick walled aluminum can filled with oil. The entire instrument is enclosed in a temperature regulated air enclosure.

The instrument sources of uncertainty in a $2e/h$ measurement for the past year are essentially the same as reported by FDL [1] as the instrument was modified only slightly for use at NBS [12]. These estimated uncertainties are listed in Table 1 and are described briefly below.

a) and b) Checks on the matching of the main and fan resistors were carried out regularly. The uncertainties were estimated from the check data. In the case of the main resistor matching, the second-order corrections to the resistance ratio were calculated. The correction (as a result of periodic trimming of the resistors) was always negligible (<1 part in 10^9). The deviations for the fan resistors were also measured and found negligible. The uncertainties attributed to these two errors are 0.4 and 1 parts in 10^8 respectively.

c) The transfer resistance error due to tetrahedral junction asymmetries introduced a measured uncertainty of 4 parts in 10^9.

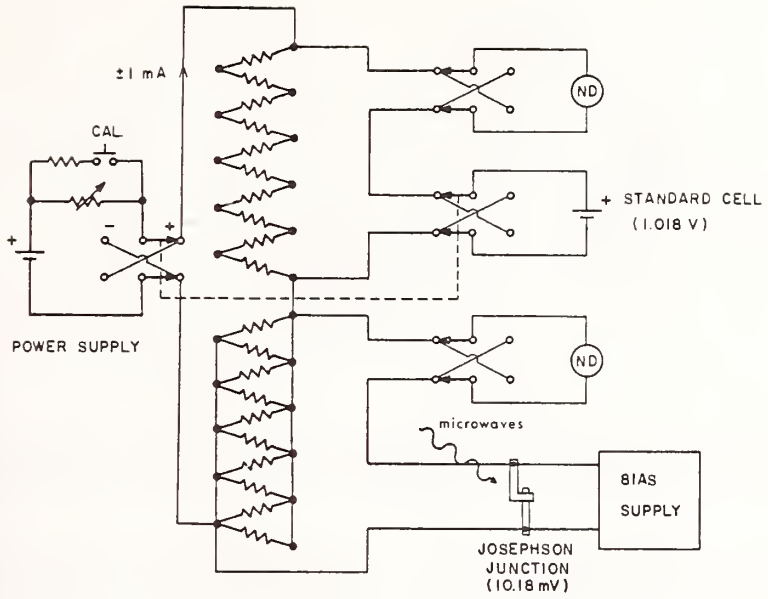

Fig. 4. Simplified circuit diagram of series-parallel voltage comparator

Table 1. Sources of uncertainty in $2e/h$ associated with the series-parallel instrument

	Uncertainty parts in 10^8 (one standard deviation estimates)
a) Main resistor mismatch	0.4
b) Fan resistor mismatch	1
c) Resistance of tetrahedral junctions	0.4
d) Main resistor heating effects	2
e) Comparator temperature stability	0.3
f) Working current stability	0.2
g) Calibrating signal accuracy	1
h) Leakage resistances	1
i) Dielectric polarization	0.2
j) Effects of thermal emf's	0.5
RSS total	2.8

d) The self-heating effects for the main resistors were measured *in situ* using the bridge within a bridge technique [17]. Using this procedure a correction of 3 parts in 10^8 was applied to the data with an uncertainty estimated to be 2 parts in 10^8.[1]

e) Since the series-parallel resistance ratio is not established simultaneously, any change in resistance between the measurements will cause a first order correction. The largest cause of this change is the change in internal temperature of the instrument. The temperature regulated oven changes slightly as ambient temperature changes and thus introduces an uncertainty of 3 parts in 10^9.

f) For the $2e/h$ measurements made before December 1971, a standard cell balance was made after the junction balance and a correction applied for the drift of the power supply. Since December we have begun regularly making standard cell balances both immediately before and after the junction balance and linearily interpolating the results to the time of the junction balance. The uncertainty contributed by non-linear drift in the power supply is estimated to be 2 parts in 10^9.

g) The balancing procedure requires that a calibrating signal be introduced to normalize the null-detector deflections. The uncertainty in calculating this signal is mainly due to resistor aging and results in a measurement uncertainty of 1 part in 10^8.

h) The effects of leakage resistance are estimated by measuring the individual leakage paths directly. The estimated uncertainty from this source is 1 part in 10^8.

i) Small leakage currents are induced in insulators due to a component of the insulator dielectric polarization, and polarization currents are induced due to piezoelectricity caused by mechanical stress on the insulators. The polarization currents were measured using an electrometer and contribute an uncertainty of 2 parts in 10^9.

j) The uncertainty due to the effects of thermal emf's is caused by variations of the thermal emf's in the instrument and non-linear changes in the thermal emf's in the leads from the junction to the instrument. Five parts in 10^9 is estimated for this uncertainty.

The root-sum-square total uncertainty is 2.8 parts in 10^8 and represents the total uncertainty associated with the series-parallel system exclusive of the random uncertainty of a $2e/h$ measurement.

b) Cascaded-Interchange Comparator

The second instrument develops a fixed 100 to 1 ratio by use of a voltbox optimized for self-calibration. A simplified circuit diagram of the cascaded-interchange comparator (CIC) is shown in Fig. 5. The calibration of the voltbox is accomplished by using a second identical voltbox as shown in the figure. With

[1] The instrument is to be modified by replacing the main resistors with better matched, lower temperature coefficient resistors to significantly reduce the error due to self-heating. In addition the fan resistors have been replaced and the temperature control improved.

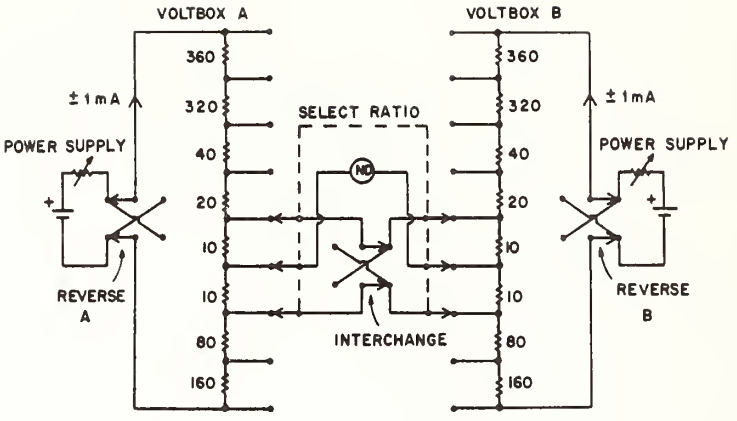

Fig. 5. Simplified circuit diagram of cascaded-interchange voltage comparator shown in the calibrate mode. The voltage developed across any one of the four 10 ohm resistors is 1/100 of the total voltage across the voltbox

Table 2. Sources of uncertainty in $2e/h$ associated with the cascaded-interchange comparator

	Uncertainty parts in 10^8 (one standard deviation estimates)
a) Random uncertainty of calibration measurement	2
b) Switch and power supply variations during calibration	2
c) Trimmer lead resistance error	0.7
d) Comparator temperature stability	0.3
e) Working current stability	1
f) Calibrating signal accuracy	0.5
g) Leakage resistances	0.4
h) Dielectric polarization	0.2
i) Effects of thermal emf's	0.5
RSS total	3.2

the switches set as shown, a 10 ohm equal-arm Wheatstone bridge is formed and the resistors are trimmed until a balance condition is achieved for both positions of the interchange switch. The next position of the "select-ratio" switch then forms a 20 ohm equal arm bridge using the two 20 ohm resistors and the four previously equalized 10 ohm resistors. Calibration is continued in this manner until both boxes are adjusted to a 100 to 1 ratio. By independently powering the voltboxes, the usual need for lead compensation is eliminated. The advantage of this method is that the resistors always operate at the same power so that the self-heating is negligible. However, the calibration procedure must be performed carefully as errors in these measurements contribute first order errors to the $2e/h$ measurement. Table 2 summarizes the sources of uncertainty in $2e/h$ associated with the CIC. Since this instrument was not modified the uncertainties are essentially the same as reported and discussed by FDL [1]. Because the SPC and CIC are of similar construction some of the sources of uncertainty for the CIC are the same as those for the SPC.

c) Null Detector Systems

Two independent null detector systems are used. Both systems consist of photocell galvanometer amplifiers modified to drive a stripchart recorder. The galvanometer amplifiers were: (a) modified to reduce thermal emf variations, (b) shielded electrostatically, and (c) placed on a anti-vibration platform. The amplifier used for the standard cell balance is operated in the series feedback mode and modified for high input impedance to reduce the off-null currents. The amplifier used for the junction balances is operated in the parallel feedback mode to reduce the Johnson noise. In the future we plan to use a superconducting galvanometer (SQUID) to make the junction balances.

d) Standard Cell Comparison System

To compare the standard cells in the $2e/h$ laboratory with other cells, the cells are connected in series opposition (negative leads connected together) and the small voltage difference measured with a commercial potentiometer. The null detector used with the potentiometer consists of a series feedback photocell galvanometer amplifier driving a secondary galvanometer.

The potentiometer system is regularly calibrated and a correction applied to the data. The systematic uncertainty of the correction is estimated to be less than 10 ppm of the voltage difference being measured. When an unsaturated cell is compared to a saturated cell, the difference is about 1000 μV and the systematic uncertainty in comparing the emf's of two cells is less than 0.01 ppm. The potentiometer is used with a resolution of 0.01 μV and the standard deviation of a single observation is about 0.01 μV, however, the use of a redundant statistical design reduces the random uncertainty by at least a factor of two.

5. Experimental Procedure

Prior to a $2e/h$ measurement, junction devices are tested and a suitable one is mounted in the waveguide holder. The device is replaced only if the junctions become defective, otherwise they are left in the cryostat between runs and are kept cold at liquid nitrogen temperatures. On the day of the run the photocell amplifiers are connected to 12 V batteries and allowed to stabilize. Standard cell comparisons are made using the commercial potentiometer, a photocell amplifier, and secondary galvanometer. The com-

parisons of cells are done using a redundant design of the type used in the NBS Volt Transfer Program [18]. Liquid helium is transferred and it is pumped below 2 K. The electrontic equipment is turned on, microwaves and bias current adjusted, and the system is left to stabilize for approximately 1.5 h. Afterwards the bias current and frequency are adjusted to previously selected optimum values and the thermal emf in the measuring leads is checked.

The $2e/h$ working group of cells contains three unsaturated standard cells mounted in a temperature regulated enclosure. On any day's run one of these cells is used throughout the entire run. The 1 V output of the voltage comparator is balanced against the cell and the difference recorded on the strip-chart recorder. The low voltage output of the comparator is balanced against the junction and recorded. During all balances the input to the null detector is reversed. The microwave frequency is measured immediately before and after the voltage balance. The counter is set so that it does not sample during a junction balance as this affects our measurements by disturbing the junctions. Another balance of the cell is then made against the comparator. These balances are interpolated to the time of the junction balance to eliminate the effects

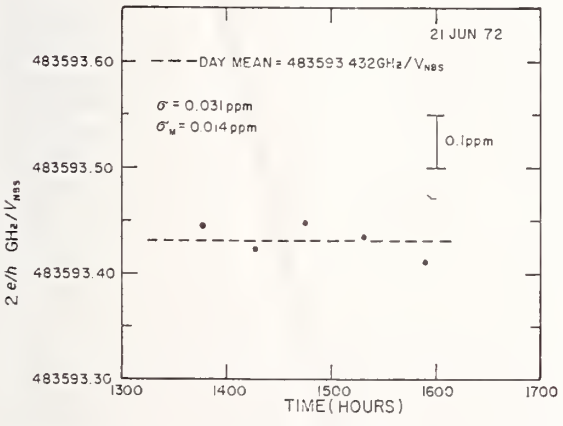

Fig. 6. $2e/h$ results of a typical day's run. Each point consists of four balances against the device voltage to compensate for thermal emf's and series-parallel resistor string inequalities

of the linear drift of the current in the comparator. The polarity of the bias current, the standard cell, and the comparator current is reversed and the procedure is repeated. The series-parallel networks are interchanged and the procedure is repeated for each polarity. The pattern of polarity reversals $(+,-,-,+)$ tends to cancel out the effects of first order drift of the thermal emf's in the measuring leads if the balances are evenly spaced in time. The four junction balances (and associated cell balances) combine to give one independent measurement of the standard cell emf in terms of $2e/h$ (or of $2e/h$ in terms of the standard cell voltage). Typically four or five independent measurements are made during one day's run. During the run small adjustments to the microwave power, microwave frequency, and bias current are made as necessary. At the conclusion of the run additional standard cell comparisons are made between the $2e/h$ working group and the check standards.

The result of a day's run consists of a recording of comparator balances and frequencies. Each balance is adjusted close to null and straight lines can then be fit by eye to the recording traces. A calibration signal is produced by causing a known change ($\simeq$ 1 ppm) in the current in the instrument to determine the normalized deviation. The normalized deviation represents the fractional difference between the 100:1 comparator ratio and the actual standard cell-junction ratio. One set of four comparator balances (including polarity and series-parallel reversals) combines to give

$$(2e/h) \cdot (V_S) = \beta n \nu$$

where V_s is the standard cell voltage, β is the measured voltage ratio V_s/V_j, V_j being the junction voltage, n is the step number, and ν is the microwave frequency. Using this equation, the product $(2e/h \cdot (V_s)$ can be calculated from the $2e/h$ run. If either $2e/h$ or V_s is assumed known then the other can be calculated. A plot of the results of a typical day's run is shown in Fig. 6.

In February 1972 six saturated cells in a temperature regulated enclosure (check standard 1) were placed in the $2e/h$ lab as a local voltage standard to estimate the precision with which a standard can be maintained via $2e/h$ measurements. This enclosure, which was designed by Cutkosky [19], maintains a stable temperature with short-term fluctuations of approximately 20 microdegrees Celsius. The mean emf of the six cells in the enclosure is shown in Fig. 7. (Here a constant value of $2e/h$ has been assumed.) The cell emf's are changing due to the large temperature shock encountered when installed in the box and normal cell aging, however, the emf's are very predictable and the standard deviation of a linear least-squares fitted line to the data in Fig. 7 is less than 0.02 μV.

6. NBS Voltage Maintenance and Dissemination Prior to July 1972

For many decades the U.S. legal volt has been maintained by a large group of standard cells [20]. Over the years groups of cells made at NBS were assembled and called the National Reference Group (NRG). From 1955 to 1969 the NRG consisted of 44 saturated cadmium sulfate (Weston) cells. The mean emf of the 44 cells was assumed to remain constant in time. In 1963, monitoring of a second group of 18 saturated cells designated the Secondary Reference Group (SRG) constructed in 1958 was begun. After the move of NBS from Washington to Gaithersburg in 1966, both groups of cells were put in two stirred temperature-regulated oil baths at 28 °C. In these baths, both groups are exposed to the moving oil, and electrical connections to the cells are made by opening the bath lid and inserting copper stabbers into mercury amalgamated copper cups. The temperature of each oil bath is read with a calibrated platinum resistance thermometer and Mueller bridge. The bridge and thermometer are calibrated monthly, the latter at the triple point of water.

By December 1969 the emf's of several cells in the NRG showed large instabilities due to the formation of gas bubbles. In order to maintain the stability of the legal volt, a new mean for the NRG was calculated

(neglecting the unstable cells) using well established procedure [20].

Measurements of the reference cells were made using the "pivot cell" technique whereby all cells are read against only one cell (the pivot or favorite cell). In May 1970 a different procedure for comparing the reference cells was started. This procedure provides equal precision in determining any cell emf with respect to the mean, as opposed to the pivot cell method which provides high precision in determining the pivot cell and low precision in determining the other cells with respect to the mean. At the same time, a more accurate instrument with better resolution (about 0.01 μV) was used for all comparisons. Both methods of intercomparison were carried out for several months until final conversion to the new method was completed in September 1970. The new method allowed greater flexibility in using any cells of the NRG or SRG for calibration purposes. In practice, the Volt Transfer Program calibrations prior to July 1972 were all made using a subset of 6 cells of the SRG. Since June 1970, *all* calibrations have been related to the NRG via the SRG subset.

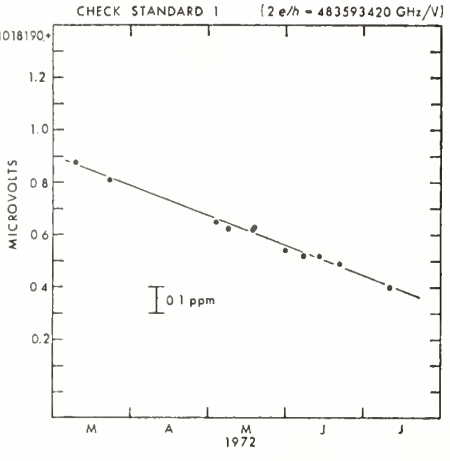

Fig. 7. The mean emf of six saturated cells assigned assuming an arbitrary value of $2e/h$. The cells are mounted in a temperature regulated enclosure located in the $2e/h$ laboratory

Two major improvements were made to one of the oil baths: (a) installation of a new temperature regulating system, and (b) installation of a selector switch for the SRG cells so that the bath lid would not have to be disturbed. These two changes, made in March 1971 by Eicke, lowered the random uncertainty of a standard cell comparison involving these groups by a factor of four [21].

Over the past 60 years, various methods have been employed to place limits on the stability and reproducibility of the NBS volt. The two most meaningful methods used prior to 1970 for determining these limits were (a) the voltage comparisons of national units at the Bureau International des Poids et Mesures (BIPM) conducted every 3 years [22]; and (b) numerous measurements of the gyromagnetic ratio of the proton, γ_p, at NBS since 1958 [23]. Inasmuch as the national units consisted of groups of saturated cells, the international comparisons only gave information on the relative drift of the various groups of cells and not on the absolute stability. Until very recently, the precision of the γ_p experiments permitted checks of the stability of the NBS volt to about 2 ppm. A possible annual drift in the mean emf of the NBS reference cells as large as several tenths of a ppm could have gone undetected. Since 1970, sub-ppm determinations of $2e/h$ at the University of Pennsylvania and NBS have provided checks on the stability of the NBS volt.

7. Determinations of $2e/h$ at NBS (1971—1972)

All determinations of $2e/h$ at NBS have been obtained by relating the Josephson junction voltage to the mean emf of the National Reference Group of standard cells. As discussed in Section V, direct $2e/h$ measurements were made on one of the cells of our working group. The emf of the working cell was related to the mean emf of a second group of standard cells by direct standard cell comparisons before and after each $2e/h$ run. This second group of cells in turn

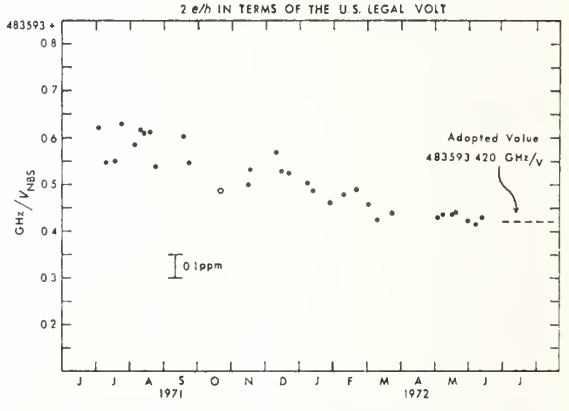

Fig. 8. Values of $2e/h$ measured at NBS referenced to V_{NBS}, the legal volt. Each point represents 1 day's run which usually consists of 3 to 5 independent determinations of $2e/h$. The open circle indicates a run in which the standard cell used for the measurements changed an excessive amount ($>0.1\,\mu V$) during the run. [Error bars indicating within-run standard deviation (~0.04 ppm) have been omitted for clarity.]

was compared to the Secondary Reference Group (which was directly assigned in terms of the NRG). The second group of cells was necessary, since substantial scatter (~0.2 ppm) in the mean emf of the SRG prevented a precise check of possible changes in the working cell during a $2e/h$ run.

A series of 32 $2e/h$ measurements were made at NBS between July, 1971 and July, 1972 to monitor the legal volt (i.e., the mean emf of the NRG) and to obtain sufficient data to permit a redefinition of the U.S. legal volt directly in terms of the ac Josephson effect. These $2e/h$ results are shown in Fig. 8. The within-run standard deviation of the mean of a typical point is about 0.025 ppm. A least-squares linear fit to the data implies an apparent drift of about -0.41 ± 0.03 ppm year in the legal volt during this period. Comparing the results of the last

determination of $2e/h$ at the University of Pennsylvania (May, 1970) with the first reported value at NBS (July to August, 1971), we find an apparent drift of -0.22 ± 0.14 ppm/year in the legal volt for 1970 to 1971 assuming the legal volt alone has changed during this period. The relative agreement of these two numbers suggests that the U.S. legal volt has been decreasing for the period 1970 to 1972.

For the NBS measurements (see Fig. 8), various changes were made from time to time in the procedures used to relate the Josephson volt to the legal volt. These changes primarily involved the use of different standard cells. For runs 1 through 14, the $2e/h$ working cell was one of three saturated cells mounted in a commercial temperature-regulated enclosure at 30 °C. For subsequent runs, the working cell was one of three *unsaturated* cells mounted in the same enclosure. The unsaturated cells were used because changes in emf of the saturated cells, due ostensibly to temperature changes of the enclosure, were limiting the within-run precision of the $2e/h$ measurements. Standard cell comparisons made before and after the $2e/h$ runs indicated a typical change of about 0.04 μV for the saturated cells but a change of only 0.02 μV for the unsaturated cells.

Several different intermediate groups were used to relate the $2e/h$ working group to the Secondary Reference Group of cells. All intermediate groups, the SRG, and the NRG were located in a separate shielded room next to the shielded room in which the $2e/h$ measurements were carried out. For the early $2e/h$ runs (prior to September, 1971), an air enclosure containing four saturated cells was used as the intermediate group. This intermediate group was compared to the SRG weekly but not necessarily on the same days as $2e/h$ runs. Since September 1971, an NBS-built air enclosure containing six saturated cells (which we define as "check standard 2") has been used as the intermediate group. In Fig. 9, we have assumed an arbitrary value of $2e/h$ and plotted the effective mean emf of four of the cells using our $2e/h$ data. The standard deviation of a single point about the fitted line is 0.04 ppm. After January, 1972, comparisons of this intermediate group with the SRG were made on the same day (while the $2e/h$ run was in progress) rather than on arbitrary days.

In order to facilitate the comparisons of large numbers of standard cells, we installed several rotary selector switches which permitted rapid connection of different cells (from the various groups) to the potentiometer. These switches, which were operated in air, were electrostatically and thermally shielded. The thermal emf's present in these switches were on the order of a few nanovolts.

The sources of uncertainty in our $2e/h$ determinations can be divided into two categories: (a) the random and systematic uncertainties associated with the $2e/h$ measurements, and (b) the uncertainties in relating the voltage of the $2e/h$ working cell to the legal volt (i.e., the NRG). A summary of these sources of uncertainty and the corresponding one-standard-deviation estimates is listed in Table 3. The following comments apply. The random uncertainty arises from random variations in the thermoelectric voltages, day-to-day fluctuations in the local and reference

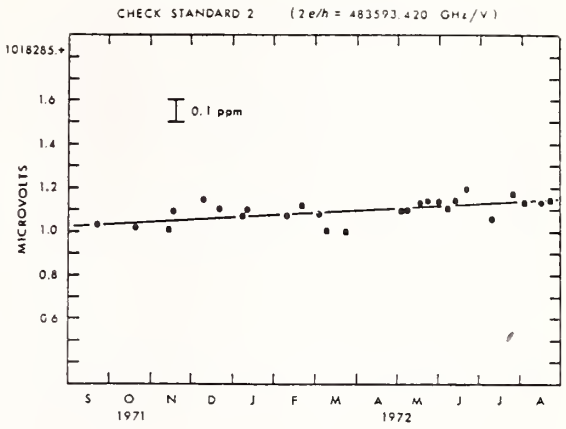

Fig. 9. The mean emf of four cells, assigned assuming an arbitrary value of $2e/h$. This enclosure is located in a separate shielded room containing the NBS reference group of cells

(i.e. the intermediate, SRG, and NRG) groups of cells and any other randomly varying experimental parameters present in a $2e/h$ experiment. The standard deviation for a *single* run referenced to the legal volt (i.e. NRG) was of order 0.04 ppm. The estimated uncertainty in the measurement of the frequency of the applied radiation is 5 parts in 10^9 and thus essentially negligible. The systematic uncertainty in relating the

Table 3. Summary of sources of uncertainty in $2e/h$ for April 1972

	Uncertainty parts in 10^8 (one standard deviation estimates)
1. Measurement uncertainties	
a) Random uncertainty of the predicted value	0.9
b) Frequency measurement and stability	0.5
c) Low-voltage comparison (series-parallel comparator)	2.8
2. Local volt uncertainty in V_{NBS69} (April 1972)	3
RSS total	4

local volt (the $2e/h$ working cell) to the legal volt has been ascribed to thermoelectric emf's in the measuring leads, temperature variations in the standard cell enclosures, and possible undetected changes in the working cell during $2e/h$ measurements.

A value of $2e/h$ based on the first nine runs shown in Fig. 8 has been reported [12]. The result was:

$$(2e/h)_t = 483593.598 \pm 0.024 \text{ GHz}/V_{NBS} \text{ (0.05 ppm)} .$$

The random uncertainty of the mean of these nine measurements was 2.3 parts in 10^8. This determination was related to the results of other workers [2, 13, 14] via direct standard cell comparisons carried out

between NBS and other national laboratories under the auspices of BIPM during the summer of 1971.

In the spring of 1972, a second series of similar volt comparisons was carried out. A value of $2e/h$ referenced to the legal volt for April, 1972 (approximately the central date of this latter series of comparisons) has been obtained by linearly fitting all the $2e/h$ data from January to July, 1972. The result is:

$$(2e/h)_{II} = 483593.444 \pm 0.019 \text{ GHz}/V_{NBS} \text{ (0.04 ppm)} .$$

The random uncertainty of 9 parts in 10^9 (as indicated in Table 3) was obtained by calculating the standard deviation of the interpolated result.

The Josephson voltage is directly proportional to the frequency of the applied radiation with the proportionality constant precisely equal to the physical constant $2e/h$. Since no other method of determining this physical constant with an accuracy comparable to that of the ac Josephson effect exists, we can use it only to establish a very stable and precise voltage standard but not to establish an absolute one. In order to implement such a standard at NBS, we have decided to adopt a value of $2e/h$ consistent with the assumed value of the mean emf of the National Reference Group on July 1, 1972. This value of $2e/h$ was obtained by fitting the $2e/h$ data shown in Fig. 8

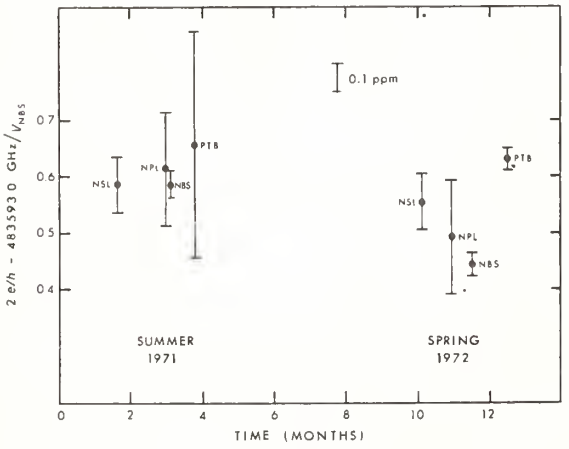

Fig. 10. Values of $2e/h$ as determined by workers at various national laboratories. All values have been expressed in the NBS unit of voltage (V_{NBS}) using the results of direct standard cell comparisons between each laboratory and NBS. (See Ref. [24].)

from January to July, 1972. The (extrapolated) result is:

$$(2e/h)_{III} = 483593.420 \pm 0.019 \text{ GHz}/V_{NBS} \text{ (0.04 ppm)} .$$

The uncertainties in this result are essentially indentical to those of the April value.

8. Comparison of Recent Values of $2e/h$ (1971—1972)

Workers at various nationall aboratories have conducted and reported experimental determinations of $2e/h$ referenced to their particular national unit of voltage. Each of these units has been defined as the mean emf of a different group of standard cells and therefore the relationships between the national units must be determined by comparison experiments. Traditionally these comparison experiments are conducted triennially at BIPM (Sèvres, France). In order to better determine the relationships of the units in laboratories carrying out high precision $2e/h$ experiments, two series of direct volt transfers between NBS and each of these laboratories were completed about 8 months apart. An individual transfer experiment involved the following: (a) calibration of an air enclosure in terms of the NBS reference cells and shipment of the temperature-controlled enclosure to the second laboratory, (b) calibration of the enclosure at the second laboratory and shipment back to NBS, and (c) calibration at NBS. Each transfer experiment lasted about 6 weeks. These transfer experiments provide a good basis for comparing the values of $2e/h$ obtained at the various national laboratories.

In Fig. 10, we have plotted values of $2e/h$ obtained by the various workers applicable to the time[2] of the transfers [2, 13, 14]. The results presented have been normalized to the NBS volt (V_{NBS}) using the data from the direct volt comparisons. Each error bar indicated the one standard deviation uncertainty assigned by the respective workers in determining $2e/h$ relative to their particular national unit of emf. No

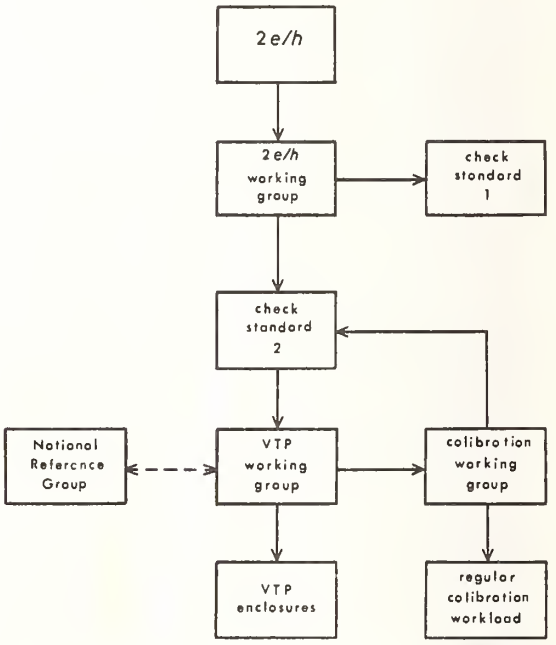

Fig. 11. A block diagram outlining the principle steps in the present (1972) NBS voltage maintenance and dissemination program using $2e/h$ via the ac Josephson effect

additional allowance for the uncertainty of the volt transfers has been added to the workers' estimated

[2] The PTB result shown for the summer of 1971 is based on a $2e/h$ determination made about $^1/_2$ year earlier and is the only reported value available for comparison with the 1971 direct standard cell transfer experiment.

uncertainties. The uncertainty in each of these volt transfer experiments has been estimated to be about 0.2 ppm [24]. The results are in fair to good agreement when the additional uncertainty associated with each volt transfer is included. Critical comparisons of present (1972) determinations are limited by the transfer of standard cell enclosures. The development of an improved portable voltage standard (for example, a portable Josephson standard) should permit meaningful comparisons of $2e/h$ experiments at different laboratories with transfer uncertainties comparable to local $2e/h$ uncertainties of a few parts in 10^8.

9. NBS Volt Maintenance Via the Josephson Effect

In July, 1972, NBS began maintaining and disseminating a unit of emf based on the ac Josephson effect. To define this new unit it was necessary to choose a value of $2e/h$. This new unit was defined to be equal to the apparent mean emf (on July 1, 1972) of the National Reference Group of standard cells. The value of $2e/h$ chosen for this purpose is the NBS $2e/h$ result for July, 1972 previously discussed in section VIII, namely

$$2e/h = 483593.420 \text{ GHz}/V_{\text{NBS}} .$$

Thus, the NBS as-maintained unit of voltage is now directly related by this constant (which is assumed to be exact) to the unit of frequency.

The procedures used to maintain and disseminate the new unit are essentially the same as those used in the $2e/h$ measurements already described in this paper. A diagram indicating the principle steps in the NBS $2e/h$ voltage dissemination program is shown in Fig. 11. Periodically, the Josephson apparatus is used to "calibrate" the emf of one of the standard cells in the $2e/h$ working group. This cell is compared with two other groups of cells (check standards 1 and 2 in Fig. 11) immediately before and after the $2e/h$ measurements. If the observed within-run standard deviation of the $2e/h$ measurement is less than twice the expected value 2σ (presently $\sigma \cong 0.04$ ppm), the assigned emf of the $2e/h$ working cell is used to obtain the emf's of the cells in the two check standards.

The mean emf of each check standard is plotted versus time (as shown in Fig. 7 and 9). The $2e/h$ measurements are made at regular intervals (about every 2 weeks for the data presented here) and mean emf's of check standard 2 and a second (VTP) working group of cells are obtained for use in calibrating the various transport standards and other groups of cells by averaging the respective results of the five most recent $2e/h$ runs. For calibration purposes, values for these mean emf's are calculated for up to several weeks ahead by applying small corrections for the long term (3 to 6 months) drift of the check standard and working group means[3].

[3] Generally, an average of five $2e/h$ runs is used; however, this number may change depending on the time intervals between $2e/h$ runs. The data from a given $2e/h$ run are only used for calibration if the corresponding value for each check standard mean is within 0.1 ppm of the expected value for the mean, and analysis of the individual cell emf's of the check standards shows no anomalous behavior. The small drift corrections (which may be negligible) are applied to the check standard and working group averages (for calibration purposes only) on a weekly basis.

10. Conclusions

The *precision* with which the mean emf of a single group of standard cells can be maintained using the present Josephson apparatus is about 2 parts in 10^8 and is a measure of how reproducibly we can calibrate a group of standard cells over an extended period of time. The accuracy with which the emf's of a group of cells can be determined in terms of a unit based on an adopted value of $2e/h$ is about 4 parts in 10^8 and includes allowances for systematic effects in the present measurement system. This is an estimate of how well the present system would agree with another totally independent $2e/h$ system.

The agreement between the NBS $2e/h$ system and systems in operation at other national laboratories has been tested indirectly via the shipment of standard cells. The results are inconclusive in determining the relative agreement of the various $2e/h$ measuring systems at their current level of precision (< 0.1 ppm). Differences as large as 0.4 ppm between $2e/h$ results and the corresponding cell transfers have been observed. These differences have been attributed primarily to uncertainties in the standard cell transfers.

One way to compare $2e/h$ systems at precisions approaching a few parts in 10^8 is to use a portable $2e/h$ system rather than standard cells. Our present system (particularly the dc instrumentation) is portable and can be used in such a comparison experiment. The application of cryogenic techniques to dc instrumentation (e.g. superconducting galvanometers and cryogenic dividers) and the development of an improved (long lived and durable) Josephson junction should permit the development of a compact cryogenic $2e/h$ system. Finally, with the use of cryogenic instrumentation, it appears that the accuracy of the $2e/h$ voltage ratio measurements can be improved at least an order of magnitude.

Acknowledgements. We would like to thank T. J. Witt for his assistance in setting up the present $2e/h$ system and his collaboration in the initial series of NBS measurements, and D. N. Langenberg and the University of Pennsylvania for the use of several instruments and a standard cell enclosure. We would also like to thank members of the Absolute Electrical Measurements Section, particularly W. G. Eicke, H. H. Ellis, and B. N. Taylor, for assistance.

References

1. Finnegan, T. F., Denenstein, A., Langenberg, D. N.: Phys. Rev. B 4, 1487 (1971).
2. Harvey, I. K., Macfarlane, J. C., Frenkel, R. B.: Metrologia 8, 114 (1972); and private communication.
3. Clarke, J.: Phys. Rev. Letters 21, 1566 (1968).
4. Clarke, J.: Phys. Rev. Letters 28, 1363 (1972).
5. Bracken, T. D., Hamilton, W. O.: Phys. Rev. B 6, 2603 (1972).
6. Bloch, F.: Phys. Rev. Letters 21, 1241 (1968); Phys. Rev. B 2, 109 (1970).
7. Rieger, T. R., Scalapino, D. J., Mercereau, J. E.: Phys. Rev. Letters 27, 1787 (1971).
8. Tinkham, T., Clarke, J.: Phys. Rev. Letters 28, 1366 (1972); Tinkham, M.: Phys. Rev. B 6, 1747 (1972).
9. Fulton, T. A.: Phys. Rev. (to be published).
10. Parker, W. H., Langenberg, D. N., Denenstein, A., Taylor, B. N.: Phys. Rev. 177, 639 (1969).
11. Taylor, B. N., Parker, W. H., Langenberg, D. N., Denenstein, A.: Metrologia 3, 89 (1967).
12. Finnegan, T. F., Witt, T. J., Field, B. F., Toots, J.: In: Proc. 4th Int. Conf. on Atomic Masses and Fundamental Constants, p. 403 (Sanders, J. H., Wapstra, A. H., Eds.). New York: Plenum 1972.

13. Kose, V., Melchert, F., Fack, H., Hetzel, W.: IEEE Trans. Instrum. Meas. IM-21, 314 (1972); and private communication.
14. Gallop, J. C., Petley, B. W.: Metrologia 8, 129 (1972); and private communication.
15. Stephen, M. J.: Phys. Rev. 81, 531 (1969).
16. Kose, V. E., Sullivan, D. B.: J. Appl. Phys. 41, 169 (1970).
17. Wenner, F.: J. Research Natl. Bur. Standards 25, 229 (1940).
18. Volt Transfer Program Instructions. Electricity Division, National Bureau of Standards, 1971; see also Eicke, W. G., Cameron, J. M.: U.S. Nat. Bur. Stand. Technical Note 430 (1967).
19. Cutkosky, R. D. (unpublished).
20. Hamer, W. J.: U.S. Nat. Bur. Stand. Monographs 84 (1965).
21. Eicke, W. G.: Private communication.
22. Terrien, J.: Private communication. See also Metrologia 7, 78 (1971).
23. Driscoll, R. L., Olsen, P. T.: In: Proc. Int. Conf. on Precision Measurement and Fundamental Constants, p. 117 (Langenberg, D. N., Taylor, B. N., Eds.). U.S. Nat. Bur. Stand. Spec. Pub. 343, 1971.
24. Eicke, W. G., Taylor, B. N.: IEEE Trans. Instrum. Meas. IM-21, 316 (1972).

IEEE TRANSACTIONS ON INSTRUMENTATION AND MEASUREMENT, VOL. IM-21, NO. 4, NOVEMBER 1972

Summary of International Comparisons of As-Maintained Units of Voltage and Values of $2e/h$

WOODWARD G. EICKE, JR., AND BARRY N. TAYLOR

Abstract—Using temperature-regulated transportable standard-cell enclosures, the National Bureau of Standards (NBS), under the auspices of the Bureau International des Poids et Mesures (BIPM), during the period June 1971 through June 1972 has carried out a series of direct comparisons of the units of voltage as-maintained by NBS and BIPM, Sèvres, France; the National Physical Laboratory, United Kingdom; the National Research Council, Canada; the National Standards Laboratory, Australia; and the Physikalisch-Technische Bundesanstalt, Germany. The main purpose of these comparisons was to provide a sound basis for intercomparing values of $2e/h$ obtained at the various national laboratories via the ac Josephson effect in superconductors. It was found that when converted to a common unit of voltage, most measured values of $2e/h$ agreed with each other to within the 1 to 2 parts in 10^7 estimated uncertainty (1 standard deviation) of the volt comparisons. This satisfying result would seem to indicate that serious consideration should be given to adopting a single international value of $2e/h$ for use in maintaining units of voltage.

I. Introduction

THE UNIT of voltage is generally maintained in the various national laboratories via large reference groups of saturated standard cells kept at constant temperature and for which the mean emf of the group is assumed constant with time. In order to maintain worldwide consistency in the various as-maintained units of voltage and to provide information on their relative drift rates, the Bureau International des Poids et Mesures (BIPM) conducts, at about three year intervals, international comparisons of the units maintained by the national laboratories. These comparisons are carried out in the following way [1]. Each participating national laboratory sends to BIPM a group of saturated standard cells which have been calibrated in terms of its own as-maintained unit. The cells are sent in nontemperature-regulated containers and are often hand carried. At BIPM, the cells are placed in a common oil bath with the BIPM reference group of cells, allowed to stabilize for several months, and then intercompared among themselves. Finally, they are returned to the originating national laboratories where they are recalibrated in order to determine how much the cells have changed during the overall period, which could be as long as six months or more. Often, changes in individual-cell EMF's as large as 1 or 2 μV are observed; nevertheless, the mean of the cell assignments before and after shipment is taken as the mean EMF of the cells while at BIPM.

Manuscript received June 24, 1972; revised July 14, 1972.
The authors are with the Absolute Electrical Measurements Section, Electricity Division, Institute for Basic Standards, National Bureau of Standards, Gaithersburg, Md.

In early 1967, in cooperation with the U.S. Air Force, the National Bureau of Standards (NBS) undertook a program to improve the interlaboratory transfer of the unit of voltage within the United States. As a result of this program, it was found that the transfer process could be substantially improved by the following.

1) Having NBS ship to the client in question an NBS-owned commercially available standard-cell enclosure with shippable saturated standard cells and maintained under continuous temperature control. (Power is supplied by batteries while in transit.) The cells are calibrated in terms of the NBS unit prior to shipment, compared by the client to the cells he uses to maintain his unit (with the same equipment and methods he uses in his everyday work), and returned to NBS for recalibration, still under temperature control.

2) Carefully controlling the transportation of the enclosure between NBS and the laboratory in question. This may be accomplished via a special shipping container and proper shipping arrangements. (Most enclosures are shipped via air freight.)

3) Using statistically sound experimental designs [2] and procedures for making the intercomparison measurements and for analyzing the resulting data. The standard deviation for a single transfer using these techniques was found to be between 1 and 2 parts in 10^7.

As a result of the success of the initial program, a new calibration service based on the above methods was developed and termed the volt transfer program (VTP). [It is now part of the NBS measurements assurance program (MAP).]

During the development of the VTP within the United States, the question of its use for international comparisons naturally arose. In 1968, NBS explored this possibility with BIPM. Subsequent transfers between NBS and BIPM showed that the vagaries of international flights and zealous customs inspectors not withstanding, VTP techniques could be successfully used to transfer the unit of voltage internationally. Indeed, NBS used the results of such a transfer for the 1970 triennial international comparison at BIPM [1].

During the time period in which the VTP was being developed, many national laboratories began work on the ac Josephson effect in superconductors with the idea of eventually using measurements of $2e/h$ to maintain their unit of voltage. This work has now progressed to the point where $2e/h$ via the ac Josephson effect can be determined in terms of a particular as-maintained unit of voltage to 1 part in 10^7 or better. This level of accuracy significantly exceeds the accuracy of the differences in the units of voltage maintained by the different

TABLE I
SUMMARY OF 1971 AND 1972 INTERNATIONAL VTP TRANSFERS

Lab.	Enclosure Number	Approximate Mean Date at Lab.	EMF's at NBS Before Transit (μV_{NBS})	EMF's at NBS After Transit (μV_{NBS})	Assumed EMF at Lab., E_{NBS} (μV_{NBS})	EMF at Lab. E_{NBS} (μV_{LAB})	$V_{LAB} - V_{NBS}$ (μV_{NBS})
BIPM	1100	30 Nov 71	138.85	138.95	138.90	139.19	−0.28
BIPM	1300	15 May 72	142.91	142.65	142.78	143.01	−0.22
NPL	1100	31 Jul 71	138.61	138.45	138.53	137.38	+1.13[a]
NPL	1300	28 Mar 72	142.74	142.91	142.82	141.75	+1.07
NRC	1400	1 Mar 72	143.35	143.08	143.21	143.72	−0.49
NSL	1100	18 Jun 71	138.44	138.61	138.54	138.07	+0.45[a]
NSL	1500	3 Apr 72	155.66	155.70	155.68	155.29	+0.38[b]
PTB	2200	24 Aug 71	–	–	34.52	34.43	+0.09[c]
PTB	1500	15 May 72	156.22	156.27	156.24	156.29	−0.05[a]

Notes: 1) All EMF's reduced by 1 018 000 μV and corrected to the nominal enclosure temperature.
2) The nominal temperature for all enclosures was 30°C except for 2200 which operated at 32°C.
[a]One cell excluded.
[b]Two cells excluded.
[c]Simple means not applicable due to nonlinear drift.

national laboratories as obtained from the triennial international comparisons at BIPM. Thus, there is no reliable way of assessing the agreement or lack thereof between the several different measurements of $2e/h$, and consequently the potential of the Josephson effect for maintaining units of voltage.

To alleviate this problem, that is, to provide a sound basis for comparing values of $2e/h$ obtained at the various national laboratories, and also to provide further experience to BIPM and other laboratories in using VTP techniques, NBS initiated in 1971, under the auspices of BIPM, an experimental program to apply VTP methods to the international comparison of as-maintained units of voltage. During the period June 1971 through June 1972, transfers were carried out between NBS and BIPM, Sèvres, France; the National Physical Laboratory (NPL), United Kingdom; the National Standards Laboratory (NSL), Australia; the National Research Council (NRC), Canada; and the Physikalisch-Technische Bundesanstalt (PTB), Germany. All of these laboratories participate in the triennial international comparisons and have (or will shortly have) active Josephson $2e/h$ volt-standard programs. Where applicable, the researchers carrying out the Josephson $2e/h$ measurements were encouraged to make $2e/h$ determinations during the period the NBS transport standard was at their laboratory in order to tie together all of the $2e/h$ measurements as closely as possible.

II. Experimental results

Two distinct comparisons were carried out, the first primarily during the summer of 1971, and the second during the spring of 1972. The procedures used were essentially those described in Section I for the NBS VTP except that each national laboratory calibrated the transport standard using its own normal procedures. The transport standards, each containing four cells, were shipped via air freight to and from each laboratory, with the standard remaining at the laboratory from two to four weeks. When a serious problem was encountered with a particular transfer, it was repeated as quickly as possible. The difference between the units was calculated using the relationship

$$V_{LAB} - V_{NBS} = -\frac{\{E\}_{LAB} - \{E\}_{NBS}}{\{E\}_{LAB}} V_{NBS} \qquad (1)$$

where $\{E\}_{LAB}$ and $\{E\}_{NBS}$ are the numerical values only of the EMF assigned at the laboratory and NBS, respectively, and V_{LAB} and V_{NBS} are the respective units of voltage. The results of the two comparisons are summarized in Table I. The assumed standard deviation uncertainty for a single transfer is 0.14 μV, that adopted for the VTP in the United States. On three occasions, erratic cell behavior required doubling the variance (i.e., the assumed uncertainty for PTB 71 and 72 and NSS 72 was taken to be 0.20 μV).

Table II summarizes the relevant $2e/h$ measurements carried out during the period of the direct volt transfers. Two of the participating laboratories, BIPM and NRC, were just getting their $2e/h$ work underway and did not have any results to report. NBS [3]; NPL [4],[5]; NSL [6],[7]; and PTB [8] all had $2e/h$ programs in operation and obtained a value of $2e/h$ in terms of their as-maintained unit during the time the transport standard was in their laboratory. (Unfortunately, a $2e/h$ measurement at PTB could not be completed during the summer of 1971 and the fall 1970 result must be used.) All uncertainties are meant to correspond to 1 standard deviation and are those given by the experimenters involved; generally, they contain both random and systematic components of uncertainty.

The last column in the table gives the change in V_{LAB} from 1971 to 1972 ΔV_{LAB} as implied by the $2e/h$ measurements. In principle, the uncertainty to be assigned a particular ΔV_{LAB} should simply be the root-sum-square of the random uncertainty of the 1971 and 1972 measurements, since the systematic uncertainty is common to both. The reliability of the values for ΔV_{LAB} should, therefore, be significantly better than is implied by the total uncertainty assigned the individual $2e/h$ values. With this in mind, it may be concluded that significant changes in some of the as-maintained national units of voltage have taken place.

Table III summarizes the differences in the units of voltage maintained by the participating national laboratories and NBS

TABLE II
SUMMARY OF $2e/h$ MEASUREMENTS VIA AC JOSEPHSON EFFECT

Lab.	1971 $2e/h$ (GHz/V_{LAB})	1971 Uncertainty (ppm)	1971 Approximate Time Period of Measurements	1972 $2e/h$ (GHz/V_{LAB})	1972 Uncertainty (ppm)	1972 Approximate Time Period of Measurements	Implied Change in V_{LAB} from 1971 to 1972, ΔV_{LAB} (μV_{LAB})
NBS	483 593.589(24)[a]	0.05	July–Aug. 1971	483 593.444(24)[b]	0.05	Apr. 1972	−0.30
NPL	483 594.15(10)[c]	0.2	July 1971	483 594.00(10)[d]	0.2	Apr. 1972	−0.31
NSL	483 593.80(5)[e]	0.1	June–July 1971	483 593.733(48)[f]	0.1	Mar.–Apr. 1972	−0.14
PTB	483 593.7(2)[g]	0.4	Fall 1970	483 593.606(20)[h]	0.04	May 1972	−0.19

Note: Numbers in parentheses are estimated 1 standard deviation uncertainties in last digit(s) of main number.
[a]See [3]. [c]See [5]. [e]See [7]. [g]See [8].
[b]See [10]. [d]See [11]. [f]See [12]. [h]See [9].

TABLE III
SUMMARY OF DIFFERENCES IN UNITS OF VOLTAGE MAINTAINED BY PARTICIPATING NATIONAL LABORATORIES AND NBS

$V_{LAB} - V_{NBS}$	1970 Triennial International Comparison[a] (μV_{BIPM})	1971 Direct Volt Transfers (μV_{NBS})	1971 Via Values of $2e/h$ (μV_{NBS})	1972 Direct Volt Transfers (μV_{NBS})	1972 Via Values of $2e/h$ (μV_{NBS})
$V_{BIPM} - V_{NBS}$	−0.17	−0.28 ± 0.14		−0.22 ± 0.14	
$V_{NRC} - V_{NBS}$	−0.07			−0.49 ± 0.14	
$V_{NPL} - V_{NBS}$	+0.52	+1.13 ± 0.14	+1.16 ± 0.21	+1.07 ± 0.14	+1.15 ± 0.21
$V_{NSL} - V_{NBS}$	−0.17	+0.45 ± 0.14	+0.44 ± 0.11	+0.38 ± 0.20	+0.60 ± 0.11
$V_{PTB} - V_{NBS}$	−0.43	+0.09 ± 0.20	+0.23 ± 0.40	−0.05 ± 0.20	+0.33 ± 0.06

[a]Central date, Feb. 1, 1970; see [1]. Note that V_{BIPM} and V_{NBS} differ by less than $1/10^6$ and therefore small volt differences are for all practical purposes the same whether expressed in terms of V_{BIPM} or V_{NBS}.

as determined via the 1970 triennial international comparisons at BIPM, the direct volt transfers carried out in 1971 and 1972 (Table I), and the $2e/h$ measurements as given in Table II. The $2e/h$ volt differences were calculated from the following readily derived equation which is analogous to (1):

$$V_{LAB} - V_{NBS} = \frac{\{2e/h\}_{LAB} - \{2e/h\}_{NBS}}{\{2e/h\}_{NBS}} V_{NBS} \quad (2)$$

where $\{2e/h\}$ is the numerical value only.[1]

III. Conclusions

At least two important conclusions may be drawn from the data of Table III.

1) The 1971 direct volt transfer differences and those implied by the $2e/h$ measurements are in extraordinarily good agreement (compare columns 3 and 4). In all three cases, the disagreement is significantly less than what would be expected from the assigned uncertainties. For the 1972 transfers, the results are quite consistent with the assigned uncertainties (compare columns 5 and 6), but the agreement is not quite as satisfactory as for 1971. In view of the fact that the transport standards were not as well behaved during the 1972 transfers, this result is not too surprising.

[1]Table III is equivalent to converting all of the $2e/h$ measurements to a common unit of voltage and intercomparing the resulting values. We prefer the present method because the numbers are easier to digest.

2) There is an apparent difficulty with the value for $V_{BIPM} - V_{NBS}$ as obtained via the 1970 BIPM triennial comparison. This becomes evident when, for example, the triennial differences are compared with either the 1971 direct transfer differences or $2e/h$ differences (compare column 2 with either columns 3 or 4). With the exception of the 1971 direct BIPM transfer, there are strong indications that the 1970 triennial result for $V_{BIPM} - V_{NBS}$ is too small by about 0.6 μV. On the other hand, it is difficult to understand why the 1971 (and also 1972) direct transfers between BIPM and NBS do not confirm this apparent discrepancy but rather support the 1970 result. We leave further analysis of the data of Table III for a future publication.

In summary, we may conclude the following from the work reported here.

1) VTP type transfers can be successfully used internationally. The as-maintained units of voltage of different countries may be quickly and reliably compared using shippable standard cell enclosures maintained under continual temperature control. In our opinion, this method of comparison is a significant improvement over the traditional one and should be the technique adopted for use in all future BIPM triennial international comparisons.

2) Measurements of $2e/h$ at the various national laboratories are well in hand.

3) In view of the agreement among the $2e/h$ measurements, serious consideration should be given to adopting a single

international value of $2e/h$ for use by all those laboratories that wish to maintain their units of voltage via the Josephson effect.

4) There is a definite need for developing improved voltage reference and transport standards in order to take full advantage of the inherent accuracy of the $2e/h$ measurements. In our opinion, difficulties alluded to above are due to the inadequacies of these voltage standards. Determinations of $2e/h$ are clearly pushing the existing technology in this area.

Acknowledgment

The results reported here were made possible only by the dedicated efforts of a large number of individuals at the participating laboratories. At the risk of overlooking someone, we should like to gratefully acknowledge the collaboration of the following persons: J. Terrien, Director, BIPM, under whose auspices the transfers were carried out; G. Leclerc, BIPM; J. J. Denton, J. C. Gallop, and B. W. Petley, NPL; A. F. Dunn and G. H. Wood, NRC; R. C. Richardson, I. K. Harvey, J. C. Macfarlane, and R. B. Frenkel, NSL; W. Hetzel, V. Kose, F. Melchert, and H. Fack, PTB; and B. F. Field, T. F. Finnegan, J. Toots, and T. J. Witt, NBS. We are particularly grateful to H. H. Ellis, NBS, for making the hundreds of required measurements on the transport standards. We should also like to thank Miss Thelma Gable of Pan American Airways for her assistance in arranging for the shipment of the standards.

References

[1] G. Leclerc, "Rapport sur la 12ème comparaison des étalons nationaux de force électromotrice," Bur. Int. Poids Mes., Sèvres, France, 1970.
[2] W. G. Eicke, Jr., and J. M. Cameron, "Designs for the surveillance of a small group of standard cells," NBS Tech. Note 430, 1967.
[3] T. F. Finnegan, T. J. Witt, B. F. Field, and J. Toots, "Measurements of $2e/h$ via the ac Josephson effect," in *Proc. 4th Int. Conf. Atomic Masses and Fundamental Constants*, J. H. Sanders and A. H. Wapstra, Eds., to be published.
[4] J. C. Gallop and B. W. Petley, "Recent NPL work on $2e/h$," in *Proc. 4th Int. Conf. Atomic Masses and Fundamental Constants*, J. H. Sanders and A. H. Wapstra, Eds., to be published.
[5] B. W. Petley and J. C. Gallop, "Measurement of $2e/h$ by the Josephson effect," in *Precision Measurements and Fundamental Constants*, D. N. Langenberg and B. N. Taylor, Eds., NBS Spec. Publ. 343, U.S. GPO, Washington, D.C., pp. 227–229, 1971.
[6] I. K. Harvey, J. C. Macfarlane, and R. B. Frenkel, "Determination of $2e/h$ based on the ac Josephson effect," *Phys. Rev. Lett.*, vol. 25, pp. 853–856, 28 Sept. 1970.
[7] ——, "Monitoring the NSL standard of emf using the ac Josephson effect," *Metrologia*, to be published.
[8] V. Kose, F. Melchert, H. Fack, and H.-J. Schrader, "Die Bestimmung von e/h mit hilfe des Josephson-effektes," *PTB Mitt.*, vol. 81, pp. 8–10, Jan. 1971.
[9] V. Kose, PTB, Germany, private communication.
[10] B. F. Field, NBS, Washington, D.C., private communication.
[11] B. W. Petley, NPL, United Kingdom, private communication.
[12] I. K. Harvey, NSL, Australia, private communication.

Reprinted by permission from IEEE TRANSACTIONS ON INSTRUMENTATION AND MEASUREMENT
Vol. IM-21, No. 4, November 1972, pp. 316-319

A FLEXIBLE SYSTEM WITH TWO SELECTABLE RATIOS FOR USE WITH JOSEPHSON DEVICES, David W. Braudaway, IEEE Trans. Instrum. Meas. IM-27, December 1978.

Described is a flexible ratio and detection system for comparing dc voltages developed by means of the ac Josephson effect at either 5 or 10 mV to standard cell voltage. The system is self-calibrating in establishment of the two ratios. A fan-within-a-fan arrangement for current and potential leads is employed to enhance the low value series-parallel resistor combinations. Normal operation is in a deflection mode in which the difference between standard cell voltage and ratio set voltage is read on a high-impedance digital microvoltmeter. Based on root-sum-square combination, the system uncertainty is 5 in 10^8. Also described are the results of an intercomparison between the Sandia 2e/h volt, and the NBS 2e/h volt which indicates no significant difference. Employed in the intercomparison was a specially modified standard-cell air-bath which was shipped by air.

HIGH ACCURACY POTENTIOMETERS FOR USE WITH TEN MILLIVOLT JOSEPHSON DEVICES. II. CASCADED-INTERCHANGE COMPARATOR, A. Denenstein and T. F. Finnegan (Department of Physics and Laboratory for Research on the Structure of Matter, University of Pennsylvania, Philadelphia, PA 19174), Rev. Sci. Instrum. 45, 735-741 (1974).

A potentiometer technique for accurately determining a fixed voltage ratio has been developed which employs a voltbox subdivided for optimum self-calibration. The calibration procedure minimizes the effects of resistor self-heating and interconnection resistances which are commonly limiting factors. The basic theory of the technique and the design and construction of an instrument to compare a Josephson device (10 mV) and a standard cell (1 V) are described. This cascaded-interchange comparator (CIC) was evaluated in conjunction with another instrument, based on the double series-parallel exchange technique, in a series of 2 e/h measurements and direct instrument comparisons. The over-all uncertainty for the CIC was about 3 parts in 10^8 (1σ) and the direct comparisons between the two instruments agreed to within their combined uncertainty of 4 parts in 10^8. The cascaded-interchange technique should also be useful for the accurate measurement of high voltages.

HIGH ACCURACY POTENTIOMETERS FOR USE WITH TEN MILLIVOLT JOSEPHSON DEVICES. I. DOUBLE SERIES--PARALLEL EXCHANGE COMPARATOR, T. F. Finnegan and A. Denenstein (Department of Physics and Laboratory for Research on the Structure of Matter, University of Pennsylvania, Philadelphia, PA 19174), Rev. Sci. Instrum. 44, 944-953 (1973).

High accuracy determinations of 2e/h using the ac Josephson effect require correspondingly accurate measurements of small dc voltages. In the preliminary stages of a determination of 2e/h with substantially improved accuracy, two different potentiometric instruments based on two independent principles of operation were designed and built. Both instruments were used in an extended series of 2e/h measurements at the University of Pennsylvania and subsequently at the National Bureau of Standards where they have been used to realize the U.S. legal volt as recently redefined via the ac Josephson effect. One of these instruments is based on a modified series-parallel technique and is described in detail in this paper. After treating the general theory of the low resistance case, the design and construction of a portable self-checking instrument based on the double series-parallel exchange method is described. This series-parallel comparator (SPC), built to compare a Josephson device (10 mV) and a standard cell (1 V), was evaluated and tested in the course of determinations of 2e/h with one standard deviation (1σ) uncertainties of about 0.1 ppm. The sources of systematic uncertainty are discussed. The uncertainty attributable to the comparator alone is about 3 parts in 10^8 (1σ).

ac-JOSEPHSON-EFFECT DETERMINATION OF e/h: A STANDARD OF ELECTROCHEMICAL POTENTIAL BASED ON MACROSCOPIC QUANTUM PHASE COHERENCE IN SUPERCONDUCTORS, T. F. Finnegan, A. Denenstein, and D. N. Langenberg (Department of Physics and Laboratory for Research on the Structure of Matter, University of Pennsylvania, Philadelphia, PA 19174), Phys. Rev. B 4, 1487-1522 (1971).

An ac-Josephson-effect determination of e/h with significantly improved accuracy is reported. The precision of the measurement is determined by uncertainties associated with the comparison of a Josephson-device voltage with the emf of an electrochemical-standard-cell voltage reference and is about 3 parts in 10^8. This precision was made possible by use of Josephson devices at voltages above 10 mV and design and construction of two special voltage-comparator instruments. The fabrication and operation of the Josephson devices and the design and performance of the voltage comparators are discussed. The $3/10^8$ precision represents the precision with which a drift-free and readily reproducible Josephson voltage standard can be realized in practice using the techniques developed for these experiments. The accuracy of the final result is about 12 parts in 10^8 and is determined primarily by uncertainties associated with the stability of the local electrochemical voltage standard and with establishment of the relationship between the local volt and the volt maintained by the U.S. National Bureau of Standards. Significant improvements in the maintenance of the local-voltage standard which contributed to reduction of the final uncertainty to this value are discussed. During the course of the experiments, the Josephson frequency-voltage realtion was shown experimentally to be independent of magnetic field, temperature, and Josephson-device bias voltage or induced step number to within the accuracy of the final result. The final experimental result and its one-standard-deviation uncertainty are $2e/h = (483.593718 \pm 0.000060)$ MHz/μV_{NBS69} (0.12 ppm) referred to the volt as maintained by the U.S. National Bureau of Standards after January 1, 1969. This result is in excellent agreement with the earlier, less accurate result of Parker, Langenberg, Denenstein, and Taylor, which played an important role in the 1969 adjustment of the fundamental physical constants by Taylor, Parker, and Langenberg. It is in reasonable agreement with values recently reported by several other groups. The significantly improved accuracy of the present result makes possible a small improvement in the accuracy of the derived value of the fine structure constant and clears the way for a larger improvement through more accurate determination of the proton gyromagnetic ratio.

VOLTAGE REFERENCE STANDARDS AND TRANSFER METHODS

A Sub-PPM Automated 1—10 Volt DC Measuring System

BRUCE F. FIELD, MEMBER, IEEE

Abstract—An automated measuring system has been developed for measuring arbitrary-voltage references in the range of 1-10 V with an inherent measurement accuracy of ±0.22 ppm (3σ). This paper discusses the design and uncertainty analysis of the system and presents data obtained on a Zener voltage reference.

I. Introduction

VOLTAGE standards based on solid-state devices are now available with stabilities approaching 1 ppm/year [1]-[4]. These standards typically have their best accuracy at some voltage other than the 1.01-V level of standard cells. In order to separate the performance of the reference device from ensuing buffer amplifiers, it is necessary to measure "peculiar" voltages, for example, 6.583 V. Typically, Kelvin-Varley dividers are used to measure a wide range of voltages in terms of a standard cell. Accuracies better than one ppm are only achieved by frequent, time consuming, manual calibrations of the divider. As an alternative to the Kelvin-Varley method we have constructed a fully automated, self-calibrating measurement system to measure any arbitrary-voltage within the voltage range of 1-10 V. The total measurement uncertainty in comparing a voltage between 5 and 10 V to a 1.018 V standard cell is ±0.22 ppm, three standard deviation estimate (3σ).

Manuscript received August 20, 1984. This paper was supported in part by the Calibration Coordination Group of the U.S. Department of Defense.

The author is with the Electricity Division, National Bureau of Standards, Gaithersburg, MD 20899.

II. System Description

The system to be described is essentially a potentiometric technique which allows voltage measurements to be made without loading the source being measured. Since the system was developed to measure Zener reference units and diodes, we will frequently refer to the voltage source being measured as a Zener reference. Fig. 1 is a simplified diagram of the

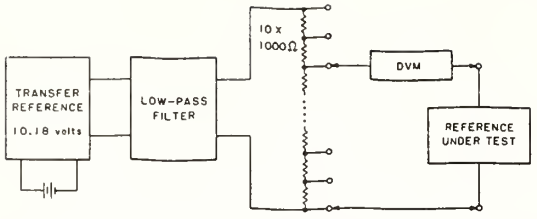

Fig. 1. Block diagram of the measuring system set up to compare a reference-under-test to the calibrated resistor string. Not shown are the crossbar selector switch and desktop computer used to control the switch and DVM.

measuring system. It consists of 10 nominally equal 1000-Ω resistors (resistor string) driven by a 10.18-V battery-operated, solid-state source (transfer reference) with good, short-term stability. The measuring system is used in a two step process. First, the voltage drop across each resistor is determined by comparing it to a standard cell and measuring the microvolt-level difference voltages with a high-accuracy digital voltmeter (DVM). Then the output voltage developed across N of the resistors is compared to the voltage of the unknown Zener reference using the same DVM. Following this, the voltage drops across the resistors are again compared to the standard cell voltage to estimate the drift in the resistor voltages during the comparison. The voltage of the unknown Zener is obtained from the sum of the voltage drops across the N resistors and the digital voltmeter reading. A low-thermal, crossbar selector switch (not shown in Fig. 1) is used to connect the standard cell and Zener references to the measurement system. Up to 60 voltage sources can be selected for measurement. The DVM and the selector switch are both connected to a desktop computer via the IEEE-488 bus so that the whole measurement process is completely controlled by the computer.

With this system the DVM is used to read only a fraction of the unknown Zener reference voltage which reduces the contribution of the DVM uncertainty to the overall measurement uncertainty. Thus

$$U = \frac{V_z - (N)1.018}{V_z} U_{\mathrm{DVM}}$$

where U_{DVM} is the DVM uncertainty expressed as a percentage of reading, V_z is the Zener voltage, N is the number of resistors, and U is the final DVM uncertainty as a percentage of the Zener voltage. For a worst case of $V_z = 5.6$ V, $U = 0.09$ U_{DVM}, and for $V_z = 10$ V, $U = 0.02$ U_{DVM}. Therefore, if the DVM can be calibrated to an accuracy of 1 ppm the worst case error contribution is 0.09 ppm. The gain of the DVM is calibrated during the measurements by periodically measuring the 1.018 V developed across one or more of the resistors. The linearity of the DVM on the 10-V range can be checked by directly measuring the ten voltages, 1.018-10.18 V, developed across the resistors.

III. Transfer Reference

The transfer reference is a commercial solid-state reference that has been modified to produce 10.18 V rather than the 10 V normally supplied. When measurements are being taken, the reference is disconnected from the ac power line and operated from its internal batteries to eliminate coupling to the power line. When the reference is disconnected from the ac power the output voltage is observed to drift down approximately 0.2 ppm during the first hour, apparently caused by temperature changes in the reference. This particular transfer reference has the power transformer in the same enclosure as the reference device and the latter is not temperature controlled. When power is removed from the transformer the internal temperature typically drifts down by about 1°C during the first hour. After a one hour "warm up" time the typical output voltage drift is -0.018 ppm/h. Since the voltage drops across the resistors (and hence the transfer reference), they are calibrated by standard cells before and after Zener measurements, only short-term stability is required of the transfer reference.

IV. Low-Pass Filter

The transfer reference was found to be sensitive to ac noise coupled into it from the output terminals. If any solid-state voltage reference is not properly isolated from external noise sources, nonlinear circuit elements, including the Zener diode, rectify the ac signals and produce a dc shift in the output voltage [5]. Connecting the DVM directly to the transfer reference produced a dc shift in the output voltage of 0.2 ppm. This was determined by monitoring the reference output voltage with a passive measuring system while connecting the DVM. The value of the dc shift was dependent on the position of the DVM in the measuring circuit, and was extremely reproducible from day-to-day. This produced a systematic error in the calibration of the voltage drops of the 10 resistors. A three-stage RC PI low-pass filter with a cutoff frequency of 400 Hz was added between the output of the transfer reference and the resistor string to reduce the ac noise. The filter forms part of a voltage divider (with the resistor string) so wire-wound resistors were used for stability and to reduce thermal EMF's. Installation of the filter reduced the worst case dc shift to 0.039 ppm. However, since similar shifts occur during determination of the resistor voltages and during the unknown Zener measurements, the dc shift error is partially canceled. When necessary, filters are also added to the unknown Zener references under test.

V. Resistor String

The resistor string driven by the transfer reference consists of 10 nominally equal, stable, 1000-Ω wire-wound resistors. We would have preferred to use lower-valued resistors to reduce measurement errors from leakage currents, but the transfer reference is limited to a load current of slightly more than 1 mA. The resistors are mounted in a temperature-controlled air enclosure, with a simple solid-state sensor and dc amplifier controller to maintain the short-term temperature variations to within ±0.01°C.

VI. Crossbar Selector Switch

The crossbar selector switch, a modified commercial product originally intended for telephone applications, permits up to

60 voltage sources to be compared to the voltage drops across the resistors or intercompared with each other and is a variation of that described in [6]. The switch consists of a matrix of switch contacts that are actuated by magnetically latched solenoids to reduce the power dissipated in the switch. Gold contacts on beryllium copper are used exclusively, and the switch is mounted in a temperature-lagged enclosure with all leads to the switch thermally connected to a large aluminum plate. The crossbar switch is interfaced to the desktop computer via the IEEE bus. A universal coupler converts the 488 bus commands to parallel outputs which are boosted by transistor-drivers to actuate the solenoids with the proper timing sequences. Switch reliability has been excellent, no switch problems having been encountered in two years of operation. Thermal EMF's are periodically checked by shorting the input leads and measuring the voltage with the DVM. Unresolved thermal EMF's are less than 0.030 μV.

VII. Digital Voltmeter

A $6\frac{1}{2}$ digit DVM with 0.1-μV resolution on the 0.1-V range is used as the system voltmeter. The voltmeter is programmed by the desktop computer via the IEEE-488 bus. All voltages are measured by the DVM in both the forward and reverse direction to cancel offset voltages in the DVM. The polarity reversal is done by the crossbar switch. The 0.1-V range is used when calibrating the resistor string voltages against standard cells, and an integration time of 9 s for each polarity yields a random measurement uncertainty of 0.034 μV (1σ). For measurements of Zeners (as shown in Fig. 1) the voltmeter is calibrated and used only on the one volt range.

VIII. Desktop Computer

The desktop computer used with the system is programmable only in the Basic language, has 64 kbytes of main memory, and has two 10 Mbyte disks. The large on-line storage capability permits us to maintain a database on measurements made on all the references, examine data, plot control charts, and produce reports as necessary. The system is fully automated with the computer controlling all aspects of the measurement process including operating the crossbar switch, reading the DVM, supplying ac power to the references under test, and reading the temperature of the standard cells.

A number of programs have been developed to automate completely the measurement process. These programs can be used individually or under the control of an interpretative program which calls the programs as overlays (because of limited main memory) and stores the measurement data on a disk. The major tasks include determining the voltage drops across the resistors in terms of a group of standard cells, comparing the voltages across the resistors to a number of unknown Zener references, and producing final calibration reports and control charts on all the Zener references and standard cells.

The interpreter program is very general, permitting any sequence and/or number of measurements to be made based on a set of measurement commands previously stored on the disk. If no changes are to be made to the previous days measurement sequence, performing a complete Zener reference calibration consists of running the program at the start of each day. However, daily changes in the measurement sequence can easily be made, if desired.

The standard cell voltages are compared to the voltages across the resistors using a redundant measurement design. The individual cell and resistor voltages are then determined using a least squares solution to the data. Zener references are identified in the system by a unique serial number with a translation table stored on the disk to equate the serial number to the proper selector switch circuit. Multiple comparisons are made between the Zener reference voltages and the voltages across the resistors to permit estimation of the random measurement uncertainty.

The EMF values assigned the standard cells in terms of the NBS volt are maintained throughout all data files. If later calibrations indicate that small corrections to the cell voltages are necessary, they can be applied to the final Zener voltage results without recalculating all the intermediate data. The latest corrections are maintained on the disk and are applied automatically by the calibration report generator.

IX. Calibration and Sources of Uncertainty

By far the most critical component of the system is the digital voltmeter. However, in this system the DVM offset and gain are calibrated during the measurements. Provision is also made to calibrate automatically the linearity at 10 points on the 10-V range by measuring the 10 voltages 1.018, 2.036, $\cdots$, 10.18 V although periodic linearity measurements at 100 points using a Kelvin-Varley divider have shown that it is not necessary to implement this feature. The system was designed principally to measure Zener diode references in the range 5-10 V. Table I lists the sources of uncertainty in the measuring system extrapolated to the worst case unknown voltage (5.5 V) in the 5-10 V range. The system may be used over the range 1-5 V but with somewhat reduced accuracy when the unknown voltage is not near a cardinal value ($1, 2, 3, \cdots, V$). The uncertainties in Table I are discussed below.

The DVM gain is measured during the course of the Zener measurements (usually four times) by reading the voltages across two or more individual resistors in the resistor string. From these measurements the gain error of the 1 V range can be estimated. Two resistors are used for redundancy and to estimate the errors in measuring voltages above ground.

The DVM linearity is periodically checked on the 10-V range using a calibrated, manual, 7-dial Kelvin-Varley divider. A computer-aided system is used to log the data and typically 100 voltages are measured. Measurements performed when the system was first set up indicated no substantial difference in the linearity of the 10- and 1-V ranges. The linearity error on the particular DVM being used was typically 0.7 ppm at half-scale input. Measurements on three other meters of the same model have confirmed that the linearity error is typically less than 1 ppm of full scale.

The DVM leakage and bias currents and the standard cell leakage currents were measured directly with an electrometer and their effects on the measurement calculated. The ac effects on the transfer reference were estimated by monitoring changes in its voltage using a passive measurement circuit referenced to a standard cell while the DVM was measuring

TABLE 1
UNCERTAINTIES IN THE AUTOMATED MEASURING SYSTEM

Source of uncertainty	1 std. dev. estimate (ppm)
DVM gain uncertainty	0.020
DVM linearity uncertainty	0.062
DVM leakage/bias currents	0.023
Standard cell leakage currents	0.006
AC effects on transfer reference	0.023
Selector switch thermal emfs	0.013
Random uncertainty in calibrating transfer reference	0.007
Random uncertainty in calibrating unknown reference (within day)	0.013
RSS subtotal	0.075
Uncertainty in standard cell assignment	0.11
RSS total	0.133

the resistor string voltages. The selector switch thermal EMF's are periodically measured with the DVM by shorting the input leads and measuring the residual voltages. The random uncertainties in calibrating the transfer reference and the unknown references are estimated from the pooled standard deviations of the measurement designs.

Solid-state voltage references sent to NBS for calibration are now calibrated using this system. In this case an additional uncertainty must be included for the uncertainty of the EMF's of the standard cells used to calibrate the system. The 0.11 ppm uncertainty listed in the table is not indicative of the best obtainable accuracy but is rather an estimate of the uncertainty obtained when the standard cells are calibrated in terms of the NBS volt only three times a year. We have recently installed a cable which will allow more frequent calibration of our cells but it is too early to estimate the improvement in the uncertainty using this method.

As far as is known, all systematic errors listed in Table I are independent of each other. Therefore, they are combined in root-sum-square (RSS) fashion along with the random errors.

X. Results and Conclusions

Measurements of the output of a typical Zener reference are shown in Fig. 2. The reference exhibits a 1 ppm/year drift with a standard deviation of a single observation of 0.07 ppm. We have observed that most references measured by the system showed an unexpectedly high correlation in their voltage fluctuations from day-to-day. This same correlation appeared between references near a cardinal value (i.e., 1.018 V) where the DVM reading is small, and 10 V where the DVM reading is much larger. We concluded that the problem was related to measuring the temperature of our standard cells. Improvements were made to read the temperature automatically at the time of the measurement rather than 1 or 2 h before, and the correlation was reduced.

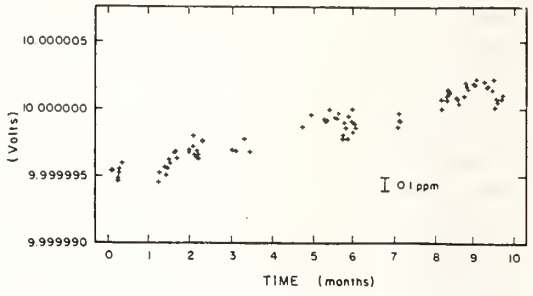

Fig. 2. The measured voltage versus time of a commercial Zener reference standard.

We have developed a fully automated measuring system capable of calibrating an arbitrary-voltage reference with an inherent accuracy of ±0.22 ppm (3σ). It is based on the principle that a properly calibrated digital voltmeter can be used as a transfer device to an accuracy of at least 1 ppm. Using this system we have shown that some solid-state voltage references presently available have drift rates as low as 1 ppm/year, nearly as good as standard cells. We have also found that some Zener references shift in voltage by as much as 2 ppm when connected to a DVM and ac filtering must be used to reduce this offset.

In addition, using the principles developed here, possibly in conjunction with fixed ratio voltage dividers, the voltage range can be extended up to 100–1000 V or down to 100 mV, albeit with reduced accuracy. It is also reasonable to use this system as part of a self-calibrating dc reference in an automatic test equipment (ATE) system, or as a high-accuracy automated DVM calibrator.

Acknowledgment

The author wishes to thank W. G. Eicke for his critical reading of the manuscript and many helpful suggestions.

References

[1] W. Murray and P. Dencher, "High-accuracy voltage transfer using a modified commercial solid-state reference," *J. Phys. E.: Sci. Instrum.*, vol. 17, no. 5, pp. 354-356, 1984.

[2] P. J. Spreadbury and T. E. Everhart, "Ultra-stable portable voltage sources," in *Conf. on Electron. Test and Measuring Instrum.*, IEE Conf. Publ. 174, 1979, pp. 117-120.

[3] K. J. Koep, "The use of a solid state dc voltage transport standard to transfer the dc volt in a regional standard cell MAP program," in *Proc. 1984 Meas. Science Conf.*, 1984, pp.142-146.

[4] L. Huntley, "The Fluke direct voltage maintenance program," in *Proc. 1984 Meas. Science Conf.*, 1984, pp. 147-151.

[5] W. G. Eicke, "The operating characteristics of Zener reference diodes and their measurement," *ISA Trans.*, vol. 3, no. 2, pp. 93-99, Apr. 1964.

[6] D. W. Braudaway and R. E. Kleimann, "A high-resolution prototype system for automatic measurement of standard cell voltages," *IEEE Trans. Instrum. Meas.*, vol. IM-23, pp. 282-286, 1974.

AN AUTOMATED STANDARD CELL COMPARATOR CONTROLLED BY A DESK CALCULATOR: A PRELIMINARY REPORT

Robert E. Kleimann and Woodward G. Eicke, Jr.
Electricity Division
National Bureau of Standards
Washington, D.C. 20234

Abstract

A system is described with which measurements of standard cell differences can be made automatically to an accuracy of one part in 10^7. The system is built using all commercially available equipment and is designed to be a relatively inexpensive easy-to-use instrument for the calibration laboratory. The system is designed around a BASIC-programmable desk calculator and MIDAS, an NBS-developed modular interface, which together control the necessary switching, stimuli and measurements for a set of standard cell difference measurements. The calculator then processes the measurement data using a least-squares fit and prints a calibration report for the cells. The design and construction of the system is described along with an evaluation of the results obtained with the system.

Introduction

Voltage measurements of standard cells are accomplished by connecting a standard cell of known emf value in series opposition with a standard cell of unknown value. This is done for two main reasons. First, by bucking out most of the voltage, the residual voltage need only be measured to a modest accuracy in order to make a high accuracy intercomparison of two cells. For example, a difference of 100 μV, measured by a 0.1% instrument would essentially resolve 0.1 μV or 1 part in 10^7 in terms of the cell emf. Secondly, standard cell performance is significantly degraded by current drawn from or passed through them. A standard cell of typical voltage 1.018 V measured directly by an instrument with 10 MΩ input impedance would, by Ohm's law, result in a current of 101.8 nanoamperes. By measuring a difference of, typically, 100 to 200 μV, the current would be only 10 to 20 picoamperes.

Low-level, high-accuracy voltage measurements require a consideration of some sources of error not significant at higher levels or reduced accuracy. The two major sources of error are thermal emfs and leakage currents.

Thermal emfs are caused by temperature gradients existing in the measurement circuit.[1] The Seebeck effect is a thermal emf caused by a temperature gradient across a junction of dissimilar conductors. The thermal emf is a function of the types of conductors and is directly proportional to the temperature gradient. The Thompson effect is the thermal emf of a homogeneous conductor in a temperature gradient. This thermal emf is also a function of the type of conductor and is directly proportional to the temperature gradient. Thermal emfs in a circuit can be reduced to an acceptable level by using the same or well-matched (in terms of thermoelectric effects) conductors throughout and controlling temperature gradients.

Potential differences existing between conductors in a circuit will cause a current to flow between them, limited by the resistance. If these leakage currents are large enough, they will be a source of error in standard cell measurements because 1) the currents are drawn from the standard cells and 2) the measured emf of the cells will be less than the actual emf by the value of the voltage drop across the internal resistance of the cells. Careful attention to the amount and type of insulation surrounding the conductors and the use of shielded and/or guarded conductors will reduce leakage currents to an acceptable level.[2]

Statistically designed sets of measurements on standard cell groups[3] have reduced the number of measurements required to characterize standard cells while at the same time yielding as results 1) the calculated emf of each cell in the group 2) an estimation of systematic effects caused by thermal emfs and other offsets (the left-right component) 3) the precision of the measurements by the estimation of the standard deviation of a single observation.[3,4] Computer programs for the least-squares fit of measurement data which give the results listed above have been implemented in both BASIC and FORTRAN.[5,6]

The automated standard cell comparator described below was designed to be a relatively inexpensive, easy-to-use instrument for the calibration laboratory. It was designed to have an accuracy of at least one part in 10^7 and uses commercially available equipment as much as possible.

This work was supported by the Calibration Coordination Group of the Department of Defense.

Measuring Circuit Hardware

Standard Cell Selection and Circuit Configuration

The selection of a pair of standard cells whose difference is to be measured and the connection of the measuring instruments in the desired configuration is accomplished by a coordinate-type electromagnetic crossbar switch. This switch has 100-input channels of 6-levels each and 10-output channels of 6-levels each. Each output channel can select any of 10-input channels. Output channels 1, 3, 5 and 7 are wired in parallel to form a left system bus and output channels 2, 4, 6 and 8 are wired in parallel to form a right system bus. Two standard cells are each connected to two input channels, one channel selectable for the left system bus and one channel selectable for the right system bus. (See Figure 1.) Since only 4-levels are needed for two standard cells, the remaining 2-levels are wired to be indicators of the selected cells. Each system bus line, then, by closing one crosspoint, will have two cells selected. The ninth output channel has the two system bus lines as its inputs. By closing one crosspoint on this channel, one cell on the left system bus will be placed in series opposition with one cell on the right system bus with either negative sides common or positive sides common. Thus, any pair of eighty standard cells can be connected, with either positive or negative common, through only two sets of contacts. The tenth output channel is used for selecting a measurement circuit configuration.

To reduce thermal emfs to a minimum, temperature gradients must be carefully controlled. The switch is mounted inside two nested aluminum boxes with a layer of foam insulation between. This makes for a heavier than usual lagging of the switch environment from the laboratory. Magnetic latching actuators are employed on the output channels so that no power is needed to hold the actuators in the operate mode; pulses of 40 - 50 msec duration are sufficient to operate or release the actuators. Essentially, there are no heat sources inside the enclosure. To reduce heat flow along the cell leads and into the switch contacts, a thermal shunt method is employed. Copper wires from the switch terminals are brought through a massive aluminum plate by passing each through a drilled nylon screw. Each wire is then clamped between two copper washers electrically, but not thermally, insulated from the aluminum plate by a beryllium oxide washer. Leads from standard cells are also clamped between the two copper washers to complete the connection to the switch.

Voltage Divider

A voltage divider network used in the measuring circuit (Figure 2) to provide a reverse emf is constructed by the series connection of a precision 10 KΩ card resistor and a precision 4-terminal 1Ω card resistor. The two resistors are mounted inside an aluminum box and are connected to the switch through the same type of thermal tie-downs described above.

Detector

The detector is a commercial low-level digital voltmeter that is capable of resolving 0.01 μV and has a full-scale range of 10 μV on the lowest range. The steady-state input impedance of this instrument is somewhat greater than 10 MΩ. The transient impedance, however, starts at about 8 KΩ but rises rapidly to its final (steady-state) value. Standard cells are not adversely affected by the small amount of energy drawn from them in the transient state. The detector is connected to the switch using thermal tie-downs and has a guarded input. Since the detector is used to measure voltages of 1 μV or less, accuracy requirements are only modest. It is possible to calibrate the detector as required using the automated system.

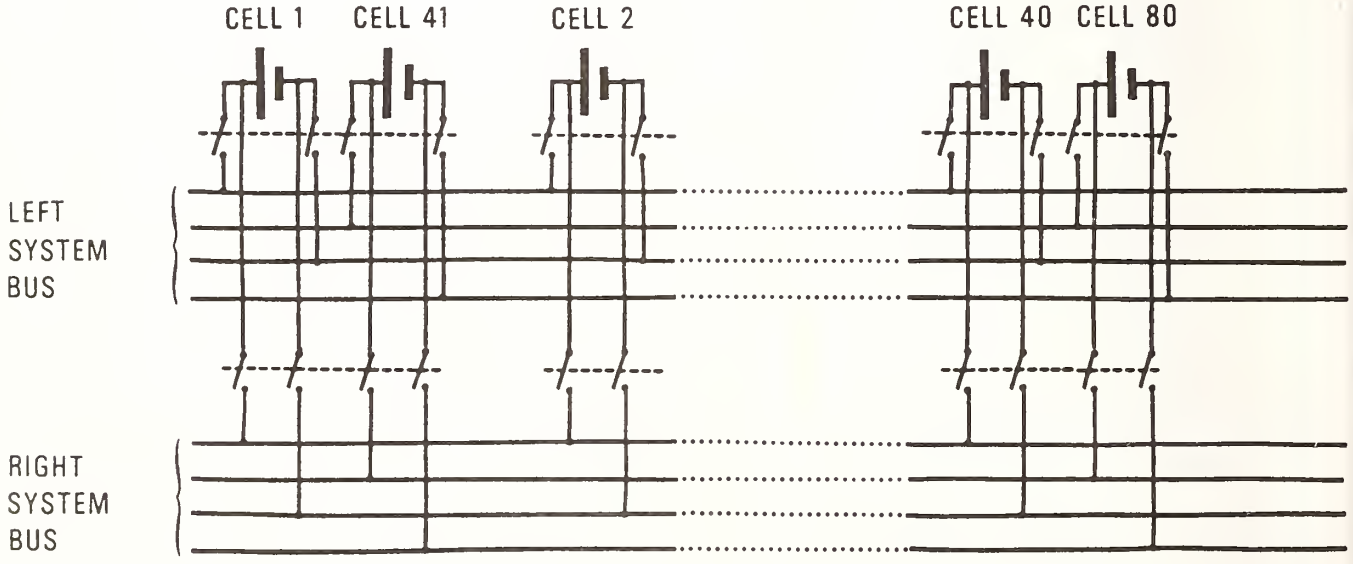

FIGURE 1. STANDARD CELL SELECTION

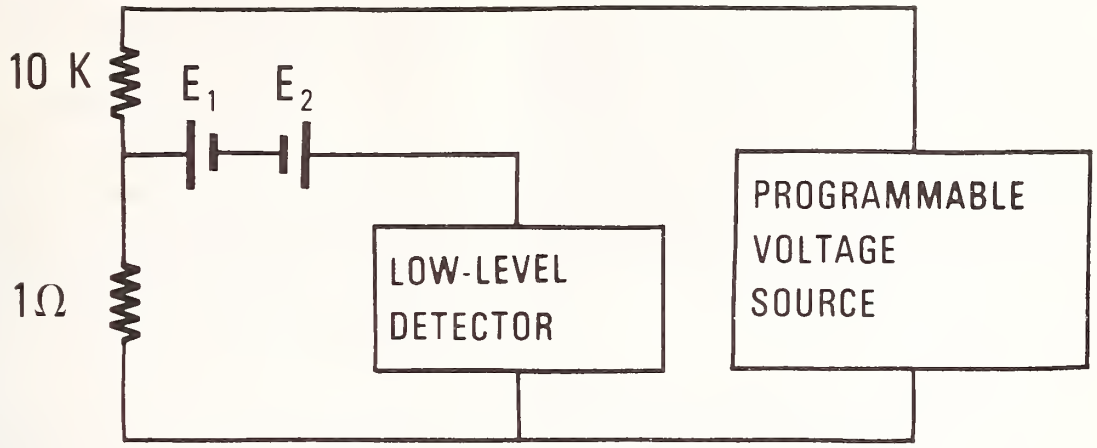

FIGURE 2. MEASUREMENT CIRCUIT

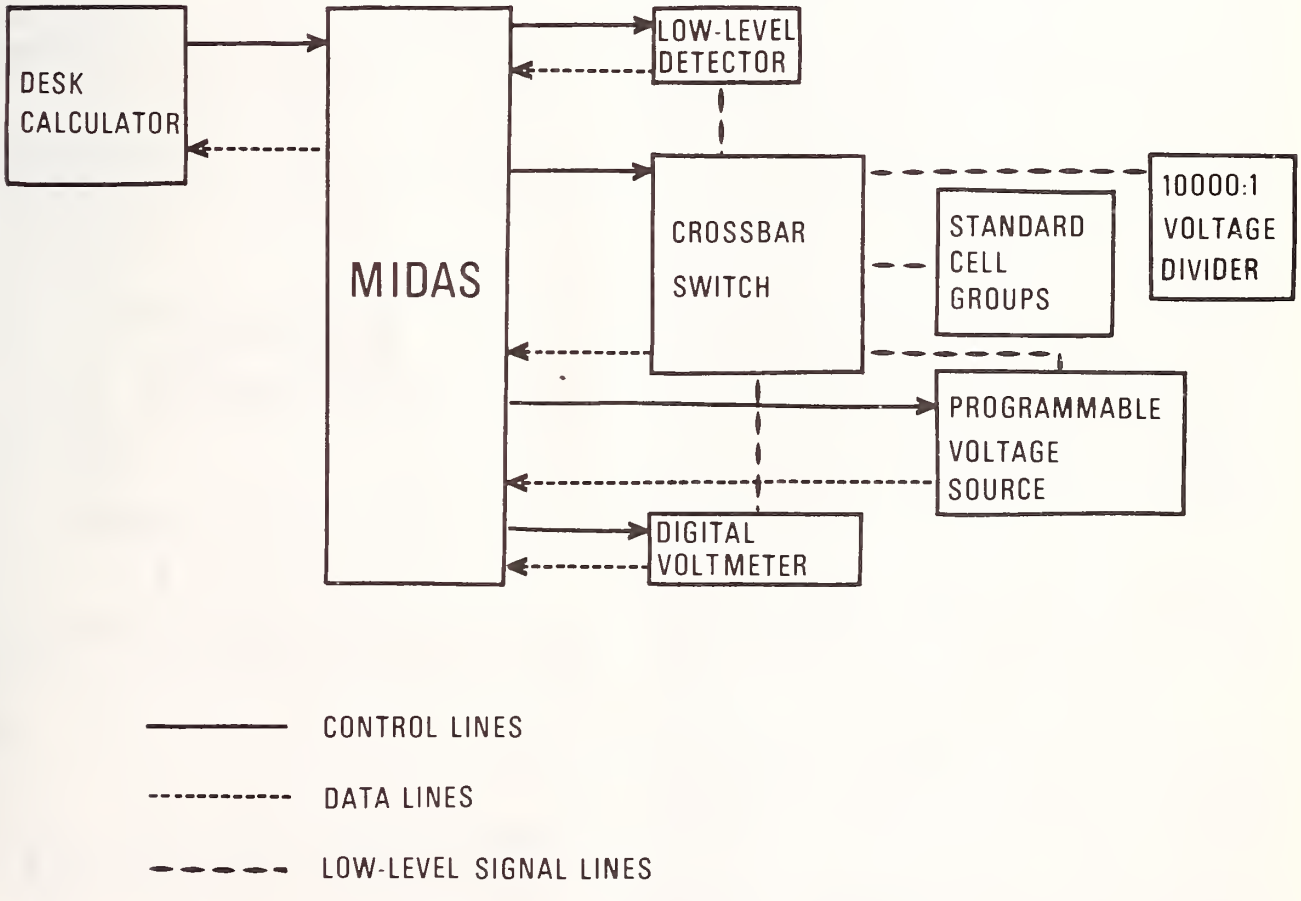

FIGURE 3. BLOCK DIAGRAM OF AUTOMATED STANDARD CELL COMPARATOR

Programmable Voltage Source

A programmable voltage source is used in the measuring circuit to provide a precision reverse voltage across the 1Ω resistor of the voltage divider. It has 5-programmable BCD digits giving a maximum of ± 16.6665 volts at 100 mA maximum current. The accuracy is rated at ± (0.01% + 100 μV) and stability at ± (10 ppm + 20 μV). The programmable voltage source has a guarded output and is connected to the switch using thermal tie-downs. The combination of a 10,000:1 voltage divider and a 16 volt maximum voltage source limits the maximum cell difference measurable to 1600 μV.

Digital Voltmeter

The digital voltmeter is used in the measuring circuit in two ways: 1) to roughly measure large unknown standard cell differences 2) to check the calibration of the programmable voltage source. It is a 5-1/2 digit instrument with lowest range full-scale reading of 0.1 V and resolution of 1 μV. It has a rated input impedance of greater than 1000 MΩ and a guarded input. It, too, is connected to the switch using thermal tie-downs. The guards on all instruments are tied together at the low side of the detector to eliminate ground loops.

Calculator and Digital Circuitry

The programmable desk calculator controls all standard cell and instrument switching, programs and/or reads the instruments, processes the measurement data and prints the results. It is programmable in BASIC, the easiest and most widely known high level language. It has matrix manipulation, string variable and extended input/output capability, 8 K words of read-write memory, line printer, external tape cassette drive and serial I/O (EIA RS-232) interface.

The calculator is interfaced to the switching and instruments through MIDAS[7], an NBS-developed, commercially available, modular interface. (See Figure 3.) All instruments and the crossbar switch are interfaced to individual MIDAS modules. The modules communicate bi-directionally with the MIDAS controller using parallel ASCII and the MIDAS controller communicates bi-directionally with the calculator using serial ASCII. Thus only one I/O slot in the calculator is used to interface to all the various equipment needed for the standard cell comparator.

The major difficulty in interfacing the calculator to MIDAS is a timing problem. Since the calculator is much slower (100 - 1000 times) than a computer, MIDAS responds to a "SEND DATA" command before the calculator is ready to receive the data. At a data rate of 600 baud, a 12-bit long shift register, clocked by the internal MIDAS clock delays the data sufficiently for the calculator to be ready to receive it. Also, the echo-back feature of the calculator's serial interface must be disabled so that MIDAS will not mistake its own data for control commands.

The interfaces from MIDAS to the instruments are straightforward since the detector, programmable voltage source and digital voltmeter have BCD inputs or outputs and MIDAS has the necessary BCD modules.

A MIDAS crossbar controller module is used to control the crossbar switch. The module contains the necessary logic, timing and transistor drivers to close any crosspoint selected. Power for the switch is from an external power supply.

Measurement Design

When two standard cells of emf values E_1 and E_2 are connected in series opposition across a suitable measuring instrument, the measured difference, ΔE should theoretically be $E_1 - E_2$. Realistically, however, there may be thermal emfs, instrument zero offsets or other spurious emfs in the measuring circuit. The actual measured difference would be

$$\Delta E = E_1 - E_2 + E_p \quad (1)$$

where E_p is the sum of all spurious emfs in the circuit. (See Figure 4.) If a second measurement, (Figure 5) with the opposite cell leads common, is taken and assuming the spurious emfs to remain constant, the measured difference would be

$$\Delta E' = -E_1 + E_2 + E_p \quad (2)$$

An estimate of E_p is obtained from the average of the two measurements,

$$E_p = 1/2(\Delta E + \Delta E') \quad (3)$$

and an estimate of $E_1 - E_2$, free of E_p is obtained from the difference average of the two measurements

$$E_1 - E_2 = 1/2(\Delta E - \Delta E') \quad (4)$$

The automated standard cell comparator uses this technique, taking two measurements in opposite polarities, for each cell difference to be obtained.

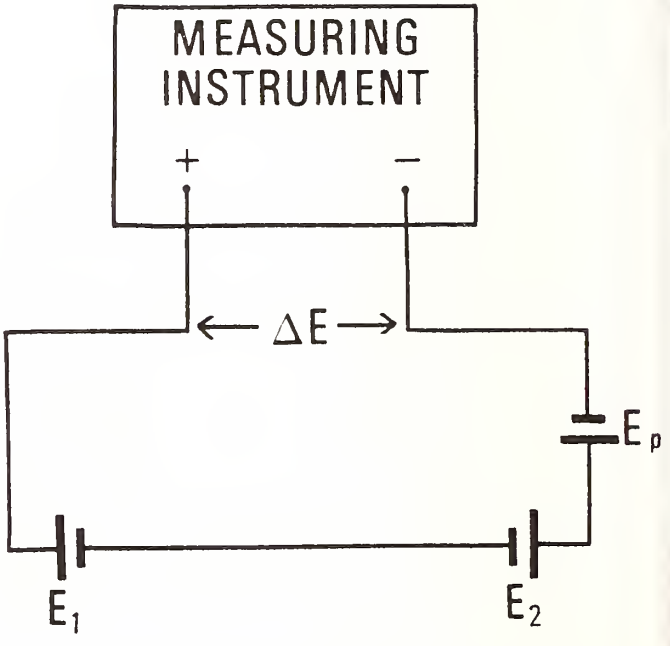

FIGURE 4. FIRST MEASUREMENT

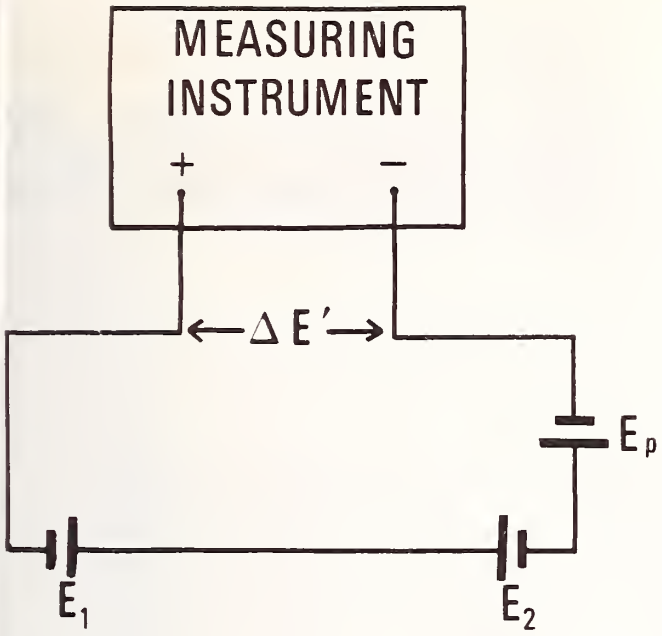

FIGURE 5. SECOND MEASUREMENT

A typical programmed procedure for measuring a standard cell difference is as follows:

1) Connect the selected pair of standard cells in series opposition with negative sides common and wait for settling.

2) Connect digital voltmeter across cells and read digital voltmeter for cell difference.

3) Disconnect digital voltmeter, connect voltage divider, detector and programmable voltage source. (Figure 2)

4) Calculate a setting for the programmable voltage source so that the voltage across the 1Ω arm of the divider will equal the cell difference measured by the digital voltmeter.

5) Set programmable voltage source to calculated value and wait for settling.

6) Read remaining difference with detector.

7) If difference is greater than ± 1 μV, calculate a new setting for the programmable voltage source and go back to step 5; otherwise, continue.

8) Read remaining difference with detector ten times and calculate mean and standard deviation of the ten readings.

9) If the standard deviation exceeds the accepted standard deviation for a single observation then the cells have probably not yet stabilized and step 8 should be repeated; otherwise, continue.

10) Disconnect standard cells; disconnect all instruments; then connect digital voltmeter across programmable voltage source and read digital voltmeter.

11) Disconnect instruments.

12) Calculate cell difference from data obtained.

13) Connect same pair of standard cells in series opposition with positive sides common. Wait for settling.

14) Connect voltage divider, detector and programmable voltage source.

15) Calculate a setting for the programmable voltage source as the same magnitude of the last setting used in the first cell difference measurement but with the opposite polarity.

16) Repeat steps 5) through 12).

17) Calculate $E_1 - E_2$ (free of E_p) from the two calculated cell differences.

The above procedure can be simplified if approximate cell values are known. For example, the detector has a 100% overrange; therefore, if the cell difference is known to be less than ± 20 μV, steps 2) and 3), reading the cell difference with the digital voltmeter could be eliminated. Also, if the approximate cell difference is known, the first setting of the programmable voltage source could be calculated based on that known value. Only if the detector indicated an overrange condition would the digital voltmeter need be used to read the cell difference.

If the programmable voltage source is sufficiently well-calibrated, it would not be necessary to connect the digital voltmeter across it to measure the output; the output could be assumed equal to the known setting.

The calibration of a group of standard cells is usually accomplished by making a set of difference measurements as described above. Each difference measurement involves one cell from a standard or known group and one cell from the group to be calibrated, the unknown group. After all necessary measurements have been made and the data stored in the calculator memory, the calculator processes the data, doing a least-squares fit by means of a matrix inversion technique to obtain emf values for each cell in both groups. These results, along with the other statistics discussed in the introduction are printed as an NBS calibration report. The results can also, if desired, be stored on a data tape for future use or analysis. Alternatively, the original measurement data can be stored on a tape for later processing and another set of difference measurements initiated. In either case, data needed for bookkeeping purposes; e.g., the date, cell serial numbers, run number, etc., can be entered via the calculator keyboard or an input data tape.

Results

The automated standard cell comparator has performed very well as of this writing. The time required for a complete set of 16 measurements to be made, calculations performed and a report printed is about 12 minutes. This compares favorably with the time of 18 - 20 minutes required for only making the same measurements manually. The left-right component, a measure of the systematic effects caused by constant circuit thermal emfs and other offsets, averages between 20 and 30 nanovolts. The observed standard deviation, a measure of the precision of the

calibration, has varied between 10 and 50 nanovolts, apparently depending on the quality of the standard cells. Measurement designs done manually for routine calibration have an average left-right component of about 20 nanovolts and a pooled observed standard deviation of about 25 nanovolts with some as low as 5 nanovolts. In instances where an automated design has been followed by the same design taken manually, or vice versa, the individual cell emfs have agreed to within 0.03 μV and the individual cell difference measurements have agreed to within 0.10 μV. A series of 29 designs involving the same cells, taken over a four-hour period has shown that the automated system is treating the standard cells involved in a measurement very gently. The standard deviation of the 29 calculated cell emfs was no greater than 0.014 μV for any of the standard cells.

Conclusion

The use of a programmable desk calculator as the controller of the system rather than a minicomputer has enabled the design goals of "relatively inexpensive" and "easy-to-use" to be met. The total cost of all materials should not be greater than $30,000. Software costs are low since there is no operating system to deal with; a BASIC interpreter is always available. There are no assembly language drivers to write; functions or subroutines can be easily written to output the necessary MIDAS commands. Since standard cell measurements are inherently slow, the speed obtainable with a minicomputer is not needed. The system is entirely transportable; all equipment, including the calculator, is mounted in a 6-1/2 foot high rack.

At this point, temperature measurements of standard cell enclosures must be made manually and the data entered separately. Modifications to some enclosures are being considered so that the system will be able to measure temperatures automatically.

The system can easily be used as a data acquisition system. Its versatility in this regard is limited only by the ability of interfacing equipment to MIDAS. An extension of the system, adding another crossbar switch and a suitable programmable power supply, will enable automated precision resistance measurements to be done.

References

1. Donald I. Finch, General Principles of Thermoelectric Thermometry, "Temperature: Its Measurement and Control in Science and Industry", Volume 3, Part 2. Reinhold Publishing Corporation, New York, New York, 1962.

2. Norman B. Belecki, A Guarded Shielded Standard Cell Measuring System, ISA Preprint 706-70, (Oct., 1970).

3. W. G. Eicke, Jr. and J. M. Cameron, Designs for Intercomparing Small Groups of Saturated Standard Cells, National Bureau of Standards Technical Note 430, U.S. Government Printing Office, (April, 1967).

4. W. G. Eicke, Jr., The Volt, Yesterday, Today and Tomorrow, ISA Reprint 71-703, (Oct., 1971).

5. J. W. Linnik, Method of Least Squares and Principles of the Theory of Observations Translated from the Russian by Regina C. Elandt. Pergamon Press, New York, 1961.

6. B. F. Field, W. G. Eicke, Jr. and R. E. Kleimann, Unpublished computer programs for reducing standard cell data.

7. Charles H. Popenoe and Mack S. Campbell, MIDAS: Modular Interactive Data Acquisition System - Description and Specification National Bureau of Standards Technical Note 790, U. S. Government Printing Office, (August, 1973).

IEEE TRANSACTIONS ON INSTRUMENTATION AND MEASUREMENT, VOL. IM-25, NO. 4, DECEMBER 1976

A Resistive Ratio Standard for Measuring Direct Voltages to 10 kV

CLIFTON B. CHILDERS, RONALD F. DZIUBA, MEMBER, IEEE, AND LAI H. LEE

Abstract—**A highly accurate guarded voltage-ratio standard has been developed for measuring direct voltages from the range of a standard cell to 10 kV. The ratio standard has a resolution capability of 0.1 ppm for ratios of 1:1 to 10 000:1 with an estimated uncertainty of 0.2 ppm. It is designed for operation at a rating of 2 kΩ/V and consists of an adjustable reference section in series with three resistance groups each containing nine nominally equal sections. The resistance ratios are determined by a self-calibration technique using a 1:1 bridge. A series–parallel mode of calibration provides an additional check on the accuracies of the ratios. The standard is housed in a temperature-controlled oil bath whose oil is filtered to remove moisture and contaminants.**

I. Introduction

THE MEASUREMENT of direct voltages higher than that of a standard cell is achieved by special resistive ratio standards having a limited number of discrete ratios for operation at convenient voltage levels. At NBS, a voltage-ratio standard [1] having ratio accuracies of a few parts in 10^7 is used to calibrate commercial units up to the 1-kV level. Another NBS standard [2], designed for use to 100 kV, provides ratio accuracies of a few parts in 10^5. There have been very few reports [3] of voltage dividers designed specifically for operation at the 10-kV level.

This paper describes a highly accurate, guarded voltage-ratio standard which has been developed for measuring direct voltages from the range of a standard cell to 10 kV: The ratio standard has a resolution capability of 0.1 ppm for ratios of 1:1 to 10 000:1 with an estimated uncertainty of 0.2 ppm. It will provide increased accuracies in the measurement of direct voltages from the 1 to 10 kV range not possible with present NBS standards. An immediate application of this ratio standard is in the absolute volt determination at NBS. In this experiment, the force between the electrodes of an electrometer with high voltage applied will be compared to the force acting on a known mass. Using the ratio standard, the applied voltages in the range of 4 to 9 kV will be measured in terms of one or more standard cells. No auxiliary potentiometer or null balancing circuits are necessary for these measurements because of the fine resolution capability of the ratio standard.

II. Design of Ratio Standard

The basic circuit of the ratio standard without the guarding network is shown in Fig. 1. It consists of an adjustable reference section followed by three resistance groups *A*, *B*, and *C* each containing nine nominally equal sections of 20 kΩ, 200 kΩ, and 2 MΩ, respectively. The reference section has a nominal value of 20 kΩ and is comprised of an 8-decade Kelvin–Varley (K–V) divider of 100-kΩ input resistance shunted by a 25-kΩ section. With the input of the reference section as a base, 27 fixed ratios are available, extending over three decades to a maximum of 1000:1. Since the reference section can resolve 10^{-8} of input, the ratio standard has at least a resolution capability of 0.1 ppm for ratios of 1:1 to 10 000:1.

A. Main Circuit

The main circuit of the ratio standard is constructed from carefully selected card-wound resistors. Each section of groups *A* and *B* is comprised of two resistors, while ten resistors are used for each section in group *C*. Each section of the ratio standard exhibits a temperature coefficient of resistance (TCR) with absolute value less than 0.5 ppm/°C by proper selection and matching of positive and negative coefficients of individual resistors. Initially, the resistance ratios were adjusted to within 2 ppm of nominal by special trimming techniques. At rated voltage, the maximum power dissipation for the resistors (6.4 cm × 2.5 cm) in group *C* is 1.6 mW/cm^2. At this power level, it is estimated that the maximum temperature rise of the resistors in their oil bath will be less than 0.2°C.

B. K–V Divider

The card-wound resistors of the first two decades of the K–V divider are connected to plug-type coaxial terminals. This method of mounting simplifies the guarding of each resistor and provides for easy calibration of these decades. Each section contains its own trimming network that provides adjustment over a 30 ppm range with better than 0.1 ppm resolution. The TCR's of the 10- and 2-kΩ sections are matched to within 0.1 ppm/°C and 0.5 ppm/°C, respectively. A commercial divider of 1 ppm accuracy completes the last six decades of the K–V divider. The K–V divider is housed in its own copper enclosure which is immersed in the oil bath.

C. Guard Circuit

Electrically, the guarding network is the same as the main circuit. It maintains the proper potential on the shields of the coaxial terminals used to mount the resistance sections, including the first two decades of the K–V divider, to the cross-linked polystyrene top piece. The switch housings of the commercial K–V divider are also

Manuscript received June 29, 1976.
The authors are with the Electricity Division, National Bureau of Standards, Washington, DC 20234.

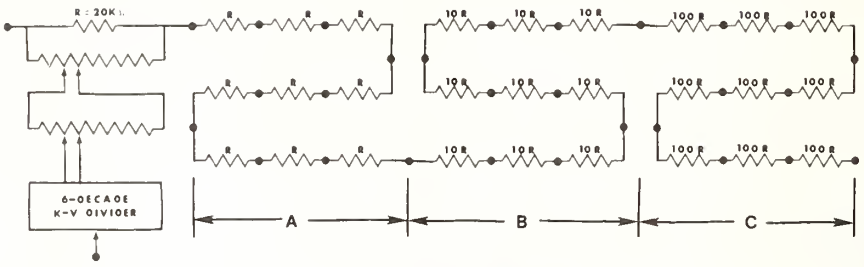

Fig. 1. Circuit diagram (except for guard network) of 10-kV ratio standard.

connected to the guard circuit. In the oil, the main resistors are uniquely guarded and shielded by sandwiching each resistor between two conducting plates of the same size as the resistors and 2.5 cm apart as shown in Fig. 2. With the plates maintained at the proper potential, leakage currents are directed from shield to shield and confined to the guarding network.

D. Oil Bath

The oil bath in which the ratio standard is immersed (75 cm diameter × 40 cm deep) has copper walls about 6 mm thick. Four Peltier units spaced at 90° around the enclosure are operated to supply or extract heat as the bath temperature varies around its set point. Oil flow is directed upward across the resistance units by a central impeller located in the bottom of the tank and operated through a mercury-seal bearing. The return flow of oil is directed along the copper enclosure wall by an acrylic baffle; and a platinum resistor, distributed throughout the annulus between baffle and copper wall, acts as temperature sensor. This sensor and a reference resistor located in the bath form two arms of a bridge whose output is amplified to supply the Peltier units. With 3 in of foam insulation around the bath, temperature control is better than 0.01°C when the divider is operated at 10 kV with a power dissipation of 10 W. The bath oil is filtered to remove moisture and contaminants. The conductivity of the oil is also monitored to determine its quality.

III. Calibration of Ratio Standard

The ratio standard is designed to have negligible errors that result from corona currents or leakage currents through nearby insulation. During operation of the standard, the input and output currents are equal. Consequently, its calibration or the determination of the values of its ratios reduces to measuring differences of resistance and changes of resistance under different load conditions. The ratio of the input voltage V_i to the voltage across the reference section V_R is given by

$$V_i/V_R = N = N'[1 + c_k]$$

where N' is the nominal ratio and c_n is the correction in proportional parts. The output voltage V_o of the reference section can be expressed as

$$V_o = kV_R\,[1 + c_n]$$

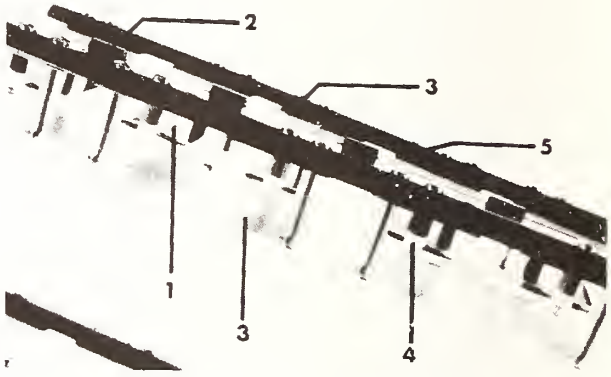

Fig. 2. Guarding of main resistors. (1) Main resistor. (2) Guard resistor. (3) Guard plates. (4) Teflon terminal. (5) Insulating rod.

where k is the dial setting of the K–V divider and c_k is the correction to the dial setting. Therefore, for a particular ratio and dial setting,

$$V_i/V_o = N/k\,[1 + c_n - c_k].$$

Two methods have been used to determine the C_n's of the ratio standard. One is a stepup method whereby a value for every ratio is obtained. The other is a series–parallel method which serves as a check for the 10:1, 100:1, and 1000:1 ratios and provides information concerning the load corrections of the standard.

A. Stepup Method

In the series mode of the ratio standard as shown in Fig. 1, the resistance of each section is nominally equal to either the resistance of the preceding section or to the summation of all preceding sections. Because of this design, the values of c_n can be determined by measuring small differences of resistance of nominally-equal sections. The resistance comparisons are performed using a guarded 1:1 bridge as schematically shown in Fig. 3. Ratio arms A and B of 1 kΩ each comprise a Direct-Reading Ratio Set (DRRS) having a least count of 0.1 ppm. (Interpolation of the detector unbalance extends the resolution of the system.) The R arm indicates the section of the standard under test. Resistor S, depending on the section under test, is nominally equal to 20 kΩ, 200 kΩ, or 2 MΩ. Resistors a, b, r, and s form the guard network which drives the shields of all leads at the proper potential to eliminate errors caused by leakage

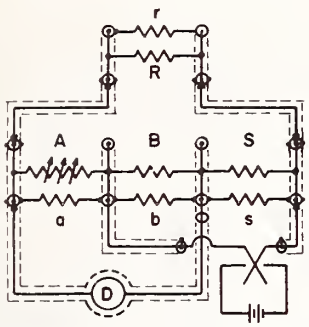

Fig. 3. Bridge circuit for calibrating ratio standard.

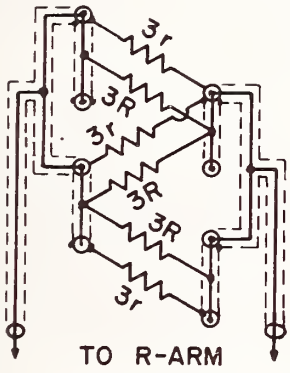

Fig. 4. Series–parallel configuration of a resistance group.

currents. The completely shielded system is immune from external electrostatic interference.

A set of 10 measurement points is obtained for each resistance group in order to compute the values for c_n. Equations for computing these corrections are given in [1]. The measurement of the first section of a group is repeated at the end of the set to check on the stability of resistor S. The total set of 33 measurement points takes approximately one hour to complete. Measurements are performed at rated voltage, i.e., 2 kΩ/V. The detector consists of a photoelectric galvanometer system operating at a sensitivity of 20 nV/mm. Noise in the bridge network limits the useful detector sensitivity to approximately 25 nV or 0.05 ppm.

B. Series–Parallel Method

In addition to the series mode, the nine sections of a given resistance group can be connected into a parallel configuration. A pair of bifurcated leads, as shown in Fig. 4, are used for the series-to-parallel conversion and subsequent connection to the DRRS bridge. The parallel resistance of groups *A*, *B*, and *C* are nominally 20 kΩ, 200 kΩ, and 2 MΩ, respectively. Each group in the parallel configuration is compared to all of the series-connected sections that precede it. A set of six measurement points are obtained for computing the corrections to the 10:1, 100:1, and 1000:1 ratios. Measurements of the parallel-connected sections are performed at ⅓ rated voltage or ⅑ the power level. Consequently, differences between this method and the step-up method will provide data on the load corrections of the standard.

C. K–V Divider

As previously mentioned, all 22 sections of the first two decades of the K–V divider are accessible at the top panel. The linearity of each decade is determined by intercomparing its sections using a bridge circuit similar to the one shown in Fig. 3. To eliminate the need for applying linearity corrections, the trimming networks of each section are adjusted during the measurements to provide a linearity of better than 0.1 ppm. The linearity of the commercial divider, which completes the last six decades of the K–V divider, can be checked by standard calibration techniques [4], [5].

A determination of the end corrections of the K–V divider due to lead and contact resistances is necessary to complete the calibration. This is accomplished by energizing the divider at some convenient voltage and then measuring the voltage between the output terminal and each low terminal with all the dials set at zero; and, measuring the voltage between the output terminal and the high input terminal with all dials set at full scale. The uncertainties that may arise from self-heating are negligible, since maximum power dissipation in the divider is 1 mW and the TCR's are small.

IV. Experimental Results

A number of calibrations have been performed since the ratio standard was immersed in its oil bath in February 1976. An analysis of the data accumulated during the following three months indicated that the values of ratio were correlated with changes in the relative humidity of the laboratory. Differences of ratio as large as 0.5 ppm were observed over a 24-h period when the ambient relative humidity changed from 30 to 60 percent. It should be noted that the top panel of the standard does not make a tight seal with the oil bath and it is very probable that the air space above the bath reflects ambient conditions in the laboratory. In addition, with the oil being stirred, the resistance changes with respect to changes in ambient humidity occur in a relatively short period of time. To correct the situation, a small amount of filtered and dessicant-dried air under pressure is being continually forced above the oil bath.

Table I compares the results between the step-up method and the series–parallel method for a set of 10 complete calibrations taken over a 10-day period started two days after the humidity control system was installed. For comparison, only the 10:1, 100:1, and 1000:1 results are given for the step-up method. Since the measurements were performed, a systematic error of +0.04 ppm was discovered when measuring the 20-kΩ reference section during the series–parallel calibration. This reduces the differences between the two methods to approximately 0.01 ppm. The additional 0.11 ppm difference for the 1000:1 ratio results from loading of the 2-MΩ sections.

TABLE I

Comparison of Step-up (S-U) and Series-Parallel (S-P) Calibration Methods

Ratio	Method	Percent Rated Voltage	Mean c_n (ppm)	Standard Deviation of Mean (ppm)
10:1	S-U	100	+0.84	0.03
	S-P	33 1/3	+0.89	0.02
100:1	S-U	100	+1.25	0.03
	S-P	33 1/3	+1.30	0.03
1000:1	S-U	100	-0.83	0.04
	S-P	33 1/3	-0.68	0.06

TABLE II

Estimates of the Effects of Possible Systematic Uncertainties

Systematic Uncertainties		Estimate* (ppm)
Resistance Comparisons		0.07
K-V Divider Calibration		0.05
Corona Currents		0.03
Leakage Currents		0.01
Load Coefficient		0.04
Interconnections		0.02
Short-term Stability of Resistors		0.03
	direct sum:	0.25
	rss:	0.11

*These values are broad subjective estimates intended to be comparable with statistical 2σ - limits.

Estimates of the effects of possible systematic uncertainties are itemized in Table II. The uncertainties of the resistance comparisons and K–V divider calibration primarily reflect the uncertainty in the calibration of the DRRS and the stability of resistor S of Fig. 3. No visual corona was observed when the ratio standard was energized to 10 kV in air. Since the dielectric strength of the oil is more than 20 times that of the air and the onset of visual corona is within 10 percent of the threshold voltage of significant dark (or precorona) currents, it is estimated that these uncertainties are within 0.03 ppm. The insulation resistance between the main and guard circuits is $>10^{13}\ \Omega$. This resistance is effectively increased by 10^4 with the guard ratios trimmed to 100 ppm of nominal. Thus leakage uncertainties are considered to be negligible. At the 20-kΩ level, interconnection uncertainties due to leads, terminations and cross resistances are within 0.02 ppm. The load coefficient uncertainty only enters in when the standard is operated at a voltage different from its calibration voltages. A 0.03 ppm uncertainty is estimated for the effects of short-term variations of temperature and humidity on the resistance elements. The total rss systematic uncertainty is estimated to be 0.11 ppm.

The imprecision and the estimated systematic uncertainty of the measurement process appear to be of the same magnitude. The overall uncertainty of 0.2 ppm is based on 2σ and the total rss systematic uncertainty. The relatively large standard deviation of 0.05 ppm is due to electrostatic noise in the system resulting from low humidity conditions and the stirring of the oil.

V. Conclusion

Experimental study of this 10-kV ratio standard indicates an uncertainty of its ratio corrections of 0.2 ppm. It will be used for the measurement of high voltage in the determination of the absolute volt. The development of this standard can also lead to a more accurate assignment of ratios and direct voltages to 10 kV. Investigation of the stability of the standard will continue.

Acknowledgment

The authors wish to thank F. K. Harris for contributing ideas regarding the design and construction of the standard.

References

[1] R. F. Dziuba and B. L. Dunfee, "Resistive voltage-ratio standard and measuring circuit," *IEEE Trans. Instrum. Measure.*, vol. IM-19, p. 266, 1970.
[2] J. H. Park, "Special shielded resistor for high-voltage dc measurements," *J. Res. Nat. Bur. Stand.*, vol. 66C, p. 19, 1962.
[3] H. Hirayama, M. Kobayashi, K. Murakami, and T. Kato, "10-kV high-accuracy dc voltage divider," *IEEE Trans. Instrum. Measure.*, vol. IM-23, p. 314, 1974.
[4] A. F. Dunn, "Calibration of a Kelvin–Varley voltage divider," *IEEE Trans. Instrum. Meas.*, vol. IM-13, p. 129, 1964.
[5] D. G. M. Buist, "Calibration of a Kelvin–Varley voltage divider," *A.W.A. Technical Rev.*, vol. 14, p. 323, 1971.

Reprinted by permission from IEEE TRANSACTIONS ON INSTRUMENTATION AND MEASUREMENT
Vol. IM-23, No. 4, December 1974, pp. 282-286

A High-Resolution Prototype System for Automatic Measurement of Standard Cell Voltage

DAVID W. BRAUDAWAY, MEMBER, IEEE, AND ROBERT E. KLEIMANN

Abstract—**The conceptual requirements, the design, and the initial performance of the prototype switching for connecting standard cells to an automatic measurement system are described. Features of the design include random selection of two cells at a time, inversion of connection polarity on command, modular construction for expansion, and less than 10-nV residual uncompensated error voltage.**

Also described briefly are controllers for manual operation of the switches and the rudimentary high-resolution digital potentiometer used to complete the measurement system. Results of tests of the switching and observations of the prototype system performance are presented.

I. INTRODUCTION

SINCE their development late in the nineteenth century by Weston [1], [2], standard cells have been employed in maintaining a standard of voltage throughout the world at the highest attainable levels of accuracy. Testing of these cells has long been the domain of highly skilled and dedicated personnel whose efforts brought the world to the level of the "part-in-a-million" volt. The sheer burden of numbers of cells to be tested in recent years, the desirability of employing advanced test programs with computer aided analysis of the data [3], and the recent development of volt maintenance using the ac Josephson effect [4] have led to the need for automating standard cell measurements. Efforts toward this goal have ranged from the simple obvious use of a high-impedance digital voltmeter to elaborate systems employing scanning and achieving resolution on automatic tests of 1 part in 10^7 [5]–[7].

Recently, a project was initiated at the National Bureau of Standards, Gaithersburg, Md., the long-range objective of which is the automation of all measurements necessary to characterize the performance of both standard cells and their enclosures. Levels of precision and accuracy sought are commensurate with the highest requirement likely to arise in the foreseeable future. The purpose of this paper is to describe the development of the prototype system and to describe the initial experience with the system in testing and use. The goal sought for performance of the prototype system is that the error assignable to it be less than 0.01 μV, or 1 part in 10^8 of standard cell voltage.

II. SWITCHING REQUIREMENTS

Required for any highly precise automated measuring system is the switching necessary for scanning or interconnecting the various parts of the total system load. For

Manuscript received July 3, 1974; revised August 28, 1974. This paper is a contribution of the National Bureau of Standards and not subject to copyright.

D. W. Braudaway is with Sandia Laboratories, Albuquerque, N. Mex., and served as Guest Worker at the National Bureau of Standards, Washington, D. C., during this research.

R. E. Kleimann is with the National Bureau of Standards, Washington, D. C.

a system capable of meeting future needs, not only must a high order of electrical performance be achieved, but also a sufficient flexibility must be provided to satisfy demands imposed by test philosophies yet in the throes of creation. To meet these performance criteria, a list of requirements was established for the prototype switching which are enumerated as follows along with the associated reasoning.

1) Random selection of cells, two at a time, with either a normal or an inverted polarity was required.

Random selection insures maximum flexibility. Pairing of cells permits intercomparison by difference measurement and produces a left–right sense for optimum use of statistically derived measurement patterns [8]. Polarity inversion, suitably interlocked for protection of the cells, permits a cancellation of nearly all unwanted parasitic voltages.

2) Modular construction with a provision for local use of the cells connected to any module without disrupting the system was required.

Modular arrangement, besides permitting the switching function to be accomplished near the cells involved in the test, also permits a simple change of the system size. Cells may be conveniently addressed by their location within the module complement, the module identifier, the output line identifier, and the polarity identifier. This pattern of operation is readily interfaced to computer control, and a simple highly reliable interlock is possible to preclude accidental switching of cells in parallel or with opposite polarity.

3) Simplified connection within the system using only two pairs of guardable coaxial cables was required.

Use of only two lines to interconnect modules and measuring apparatus permits simplified system wiring and minimizes loading of cells by line impedance. Formation of each of the two lines by a pair of coaxial cables adds shielding and permits a further reduction in impedance loading by driving the shields as guards at the center conductor potential. The use of two contacts per line not only isolates cells which are not being tested, but, by proper arrangement of the switches, permits cancellation of most of the thermoelectric voltage generated in switching.

4) There were several miscellaneous performance requirements:

a) uncompensated thermoelectric voltages must be less than 3 nV;
b) leakage resistance must be greater than 10 GΩ;
c) expected life must be greater than 10 years; and
d) cell circuits must open during power failure.

An evaluation of the available switching methods and hardware showed that many switch designs might be adapted to meet a majority of the requirements. However, the multiple-level individually actuated crossbar switch most nearly met the total requirement. The crossbar switch is advantageous in consideration of the actuating power level and offers a life expectancy of 10^7 actuations, which might approach 100 years in this application. Finally, the crossbar switch is amenable to modification to overcome its major fault which is the level of possible thermoelectric voltage.

III. CONSTRUCTION OF THE PROTOTYPE SWITCHING

To demonstrate the feasibility of the selected crossbar switch, a prototype system has been constructed consisting of three modules each capable of servicing 10 cells. One of the modules is expanded to permit use of a local semiautomatic cell selection. These modules employ commercially available crossbar switches that are modified both in the switch structure and in the materials used in the conducting circuit. Fig. 1 is a simplified diagram of the 6-level switching used for each cell. Levels 1 and 3 are used to guard the voltage switched on level 2; similarly, levels 4 and 6 are used to guard the voltage switched on level 5. Cell leads are connected to levels 2 and 5, and the guards are also switched to minimize possible interaction in the system and unwanted noise pickup. Addition of electrically actuated sections to the switch may be employed to expand the switching for a local or special function. There is also a simple local switch that connects the cell lines to output terminals and disables the automatic switching function.

In any system intended for use in scanning standard cell voltages with high precision, consideration of thermoelectric voltage effects is mandatory and is often the limiting criterion on the level of precision achieved. Briefly, the ideal thermoelectrically quiet system would be entirely of copper. Only slightly less elegant would be a system employing copper, silver, and gold, which can produce thermoelectric effects of 100 nV/K and for which a passive thermal shield is normally adequate. Such materials are not available on crossbar switches now made. Thus modification of the switch structure and careful design of the module are necessary to achieve the design requirements.

The crossbar switches employed are modified to use only beryllium–copper conductors and gold–silver–platinum contacts which are thermoelectrically matched to each other with less than 250 nV/K. This modification limits the critical junctions to the two necessary connections to copper lead wires in each circuit. In addition to connecting pairs of switches in a bucking configuration and using cadmium–tin (low thermoelectric voltage) solder, two methods are employed to minimize thermoelectric effects. These may be most readily understood by reference to Fig. 2, which shows the internal switch construction, and Fig. 3, which shows the switch actuators.

The first method employs a heavier than usual lagging of the switch environment against laboratory temperature. Visible behind the 10-cell switch module in Fig. 2 is the containing case formed of two nested aluminum boxes separated by a layer of foam insulation. The thermal masses of these boxes and of the switch mounting plate, and the low conductivity of the foam insulation, are used to reduce thermal gradients that might be troublesome.

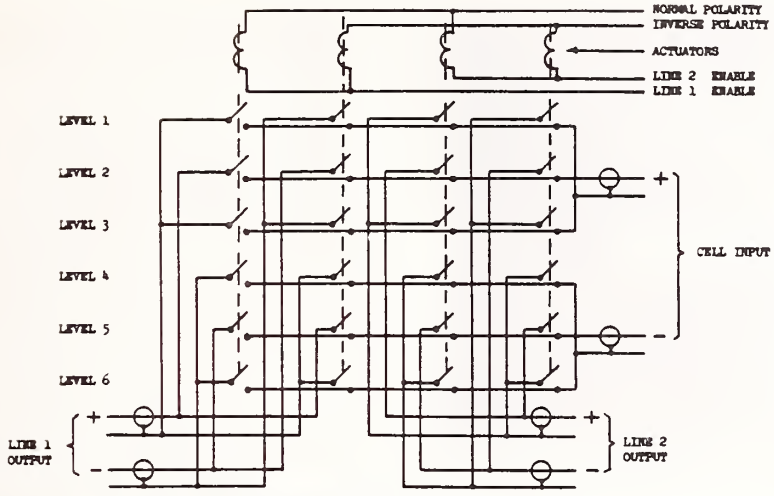

Fig. 1. Simplified switching diagram for each cell.

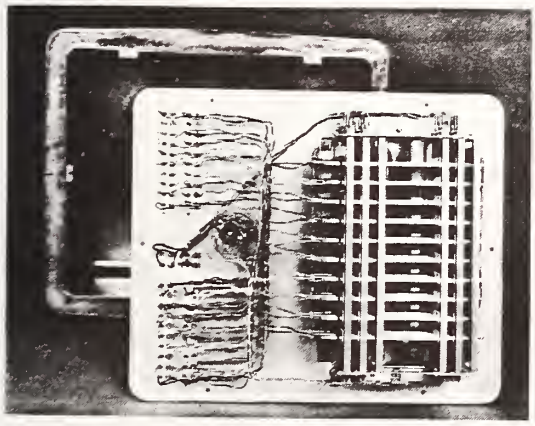

Fig. 2. Internal switch construction.

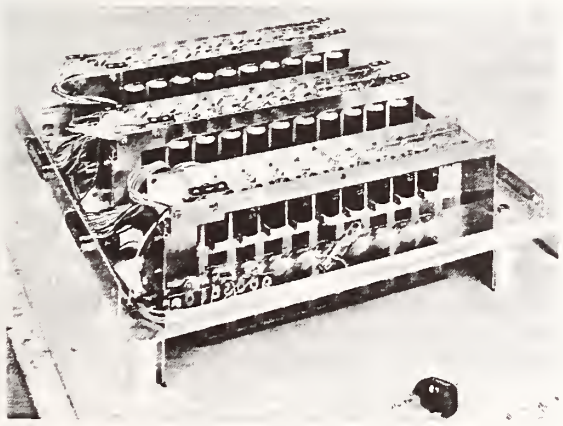

Fig. 3. Switch actuators.

Aiding the filtering action is the high thermal conductivity of the aluminum.

Additionally, critical junctions are heat-sinked inside close-fitting copper sleeves so that the effects of thermal transients are minimized. The added thermal mass also helps to equalize temperatures in the switches. These sleeves can be seen in Fig. 2, as can the rotary switch used to set the local system function of the module.

The final method used is to remove nearby heat sources from the vicinity of the circuitry and to shield them by interposed thermal reflectors. Fig. 3 shows the actuators, which are made remote from the switch proper to minimize heat input from this source. The switch mounting plate and the actuator base plate serve as heat reflectors. Heat from apparatus outside the switch is limited by the lagging and by the physical spacing required by the case. In the particular module shown in Fig. 3, an extra actuator set is used to provide a local/automatic-selection mode.

Fig. 4 shows an assembled switch module. A warning signal is generated when an attempt is made to call a cell and the module has been placed in the local mode. This signal is used to illuminate an indicator light in this particular module. In the local mode, however, an exclusive lockout function is performed and cells cannot be addressed by the system. Shown also are the rows of coaxial connectors used to input the cell voltages to the module, to output these voltages in the local mode, and to interconnect the module to the system. Fig. 5 shows the coaxial connector parts. The core is of copper to minimize thermoelectric voltages, insulation is of Teflon[9] and noncritical parts are of more common materials. The connector is designed to permit direct connection to a coaxial cable and to preserve the guarding feature.

IV. PROTOTYPE SYSTEM

Assembly of the switch modules into a prototype system requires addition of both system controllers and measuring apparatus. To permit operation of the switching, a manually operated system controller and a local controller were constructed. An exclusive lockout is provided so that

[9] Registered trademark of E. I. duPont de Nemours & Co.

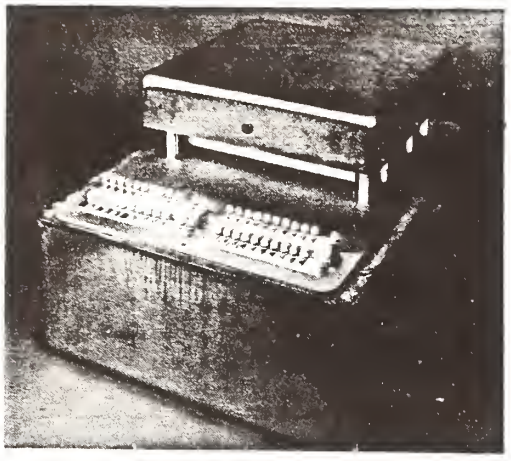

Fig. 4. Expanded 10-cell switch module.

Fig. 5. Guarded coaxial connectors.

when any cell in the system is addressed on a line, no operation. Such a limited life is unacceptable. Thus a additional cell may be addressed on this line until an intentional release has been accomplished. In the manual controllers this function is accomplished by sets of interlocking pushbuttons, but in the computer-controlled operation the exclusive interlock will be generated in the interface.

Logic employed in operation of the prototype system is of the "address-then-wait-and-see" variety. After a cell is addressed, a callback from the switch indicates completion of the switching task. In the manual controller, this callback is used to illuminate an appropriate light. Release of the cell is also indicated as the light extinguishes. Polarity of cells addressed on either line is set by a master polarity switch with a slow-action center-off pattern. All necessary system power is supplied by the controllers. Except for its simpler switching task, the local-automatic controller is identical in operation to the system controller. After assembly of the total automated system, it is anticipated that these controllers will be invaluable in diagnostic testing of individual modules.

The design of a system for high-precision cell voltage measurement entails many considerations, and effort on this phase of the project has been addressed only toward solving some of the more critical problems. One major problem is the switching, which, by the nature of the measurement process, is actuated much more often than that associated with scanning. For example, as might occur in a null-balancing mode of operation, a switch actuated at a rate of 1 per second might exhaust an expected lifetime of 10^7 actuations in only 100 days of measuring logic was chosen in which a null-balance is not obtained and switching is done only to provide 10-μV increments of the voltage difference between the two cells under test. The remaining difference voltage is amplified and digitized directly using a solid-state conversion with an essentially unlimited life expectancy. Such an approach, which is similar to the older deflection methods, requires that the amplifier have a high input impedance to minimize cell loading to a negligible level and provide for accurate measurement.

To complete the prototype of the automated standard cell measuring system, a rudimentary measuring facility was assembled using a precision potentiometer to supply the 10-μV increments. A commercial precision amplifier with digitized output was obtained and modified so that the resolution approaches 10 nV. The input impedance of this amplifier transiently starts at 8 kΩ and rises rapidly to significantly greater than 10 MΩ. This impedance level is sufficient to offer negligible cell loading, lower in fact than can be achieved with a normal light-beam galvanometer and a careful approach to near null-balance.

V. RESULTS

At the time of writing, over a year's experience has been gained in daily use of the prototype standard cell test facility described. Operation has been in the manual mode with visual readout from the digital display because the computer-controller facility is not yet available. During this period, problems have been due to 1) unfamiliarity with the equipment and with provided operational modes, 2) adjustment problems with the crossbar switches associated with the modified structure, and 3) difficulties with ancilliary equipment used to complement the rudimentary measuring system and with cabling interconnections. All of these problems are in the category of expected difficulties, and none has been major.

Estimates of the switching capability based on the testing of component parts indicated that a residual uncompensated thermoelectric voltage level of 1 nV/K had been achieved. Extrapolating to use in a laboratory environment with uncontrolled but modest nearby heat sources indicated that the 3-nV performance level of the design goal had been met. Shown in Fig. 6 is a bar-graph plot of the results of an offset voltage measurement on all active positions of the prototype system in the use condition. Contributions to the plotted figures come from the switching, the interconnecting cabling, and, not insignificantly, the equipment used to perform the special test. It is significant that the mean assignable offset to these measurements is only about 3 nV.

Data obtained using the prototype system indicate that the overall error in measurement that can be assigned to the system proper is less than 10 nV, within the design goal. Also demonstrated in operation of the system is the flexibility of the scanning in fulfilling its intended function. Thus a system can be built which displays measure-

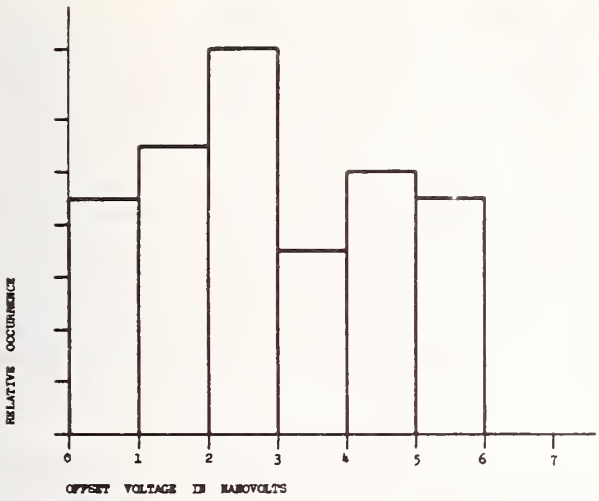

Fig. 6. Magnitude of measured offset voltages in prototype system.

ment capability at the limit of that now envisioned, which is readily flexible, and which is adaptable to new approaches. It should be pointed out that not all of the provisions of the system to ensure measurement excellence have been employed. Specifically, the guarding feature has not been activated and has been employed only as a shield. As the system expands and the workload is increased, however, such a feature can be used to ensure that highest measurement accuracy is maintained.

REFERENCES

[1] G. W. Vinal, *Primary Batteries.* New York: Wiley, 1950, ch. 6.
[2] G. D. Vincent, "Construction and characteristics of standard cells," *IRE Trans. Instrum.*, vol. I-7, pp. 221–234, Dec. 1958.
[3] W. G. Eicke, Jr., Nat. Bur. Stand., Washington, D. C., private communication, unpublished computer programs for reducing standard cell data.
[4] B. F. Field, T. J. Finnegan, and J. Toots, "Volt maintenance at NBS via $2e/h$: A new definition of the NBS volt," *Metrologia*, vol. 9, no. 4, pp. 155–166, 1973.
[5] D. W. Braudaway, *An Automatic Standard Cell Comparator*, Sandia Labs. Tech. Manual SCTM 129-62(24), 1962.
[6] ——, "Automatic testing of standard cells," *ISA Trans.*, vol. 3, no. 5, pp. 211–216, 1966.
[7] H. Hirayama and Y. Murayama, "Automatic measuring system for a control of standard cells," *IEEE Trans. Instrum. Meas.*, vol. IM-21, no. 4, pp. 379–384, 1972.
[8] W. G. Eicke and J. M. Cameron, "Designs for surveillance of the volt maintained by a small group of saturated standard cells," Nat. Bur. Stand. Tech. Note 430, 1967.

IEEE TRANSACTIONS ON INSTRUMENTATION AND MEASUREMENT, VOL. IM-23, NO. 4, DECEMBER 1974

Standard Cell Enclosure with 20-μK Stability

ROBERT D. CUTKOSKY, FELLOW, IEEE, AND BRUCE F. FIELD, MEMBER, IEEE

Abstract—Groups of standard cells are needed to maintain the National Bureau of Standards (NBS) volt between periodic reassignments via $2e/h$. An enclosure to hold six standard cells has been designed and three enclosures have been assembled. The enclosures consist of four concentric aluminum cylinders separated by foamed polystyrene insulation. Two of the four cylinders are controlled, an outer one by a platinum resistance thermometer and dc amplifier and the inner one at 30°C by a second platinum resistance thermometer and an ac transformer-ratio bridge followed by a phase-sensitive detector, a dc amplifier, and a heater. The innermost of the four cylinders is a thermally lagged cell compartment. The temperature excursions over periods of at least several days were found to be less than 20 μK, thus having a negligible effect on the standard cell EMF's.

I. INTRODUCTION

THE NEED FOR a stable and reproducible standard of EMF led to a redefinition of the National Bureau of Standards (NBS) volt in terms of $2e/h$ via the ac Josephson effect. This decision eliminated the dependence of the NBS volt upon the long-term stability of a large group of saturated standard cells. However, the $2e/h$ measurements are relatively difficult and time consuming; thus it is impractical to make measurements frequently (e.g., every day). Groups of standard cells are therefore needed to maintain the volt between periodic $2e/h$ measurements. The EMF's of these group must be predictable to within a few parts in 10^8 for up to several months. For saturated standard cells, such predictability requires that the cell temperature be stable or predictable to about 200 μK and that temperature differences between cell electrodes be constant within 30 μK. Accurately measuring the cell temperature is difficult, because the cell temperature lags the enclosure temperature by some unknown amount. Thus to introduce negligible error due to temperature variations, the total temperature fluctuations should be less than 200 μK. An enclosure to hold six standard cells in air was designed, and three enclosures have been assembled. A double oven system is used with separate proportional controllers for each oven. The mechanical characteristics of the enclosures are described, the controller circuits discussed, and data on the performance of the systems are presented.

II. CONSTRUCTION DETAILS

The enclosures consist of four concentric aluminum cylinders separated by foamed polystyrene insulation (Fig. 1). The outer cylinder thermally lags the enclosure from ambient temperature changes and reduces temperature gradients over the surfaces of the enclosure. The outer oven is heated by resistance wire helically wound on the outside of the cylinder. No heating is applied to either the top or bottom surfaces because the thickness of the aluminum serves to distribute the heat evenly and to minimize temperature gradients. The temperature of the oven is sensed using a miniature platinum resistance thermometer imbedded in the aluminum wall. This oven has two chambers, one in which the inner oven and cells are contained, and another in which temperature-sensitive circuit components and a cell EMF reversing switch are mounted. The inner oven also has a heater that is wound on the cylinder wall only, with no heating applied top or bottom.

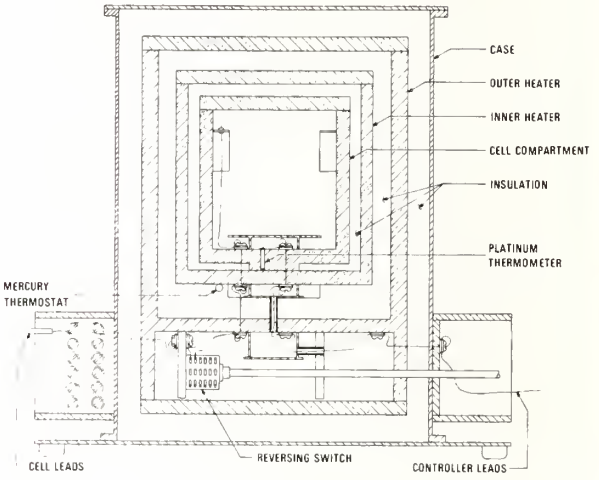

Fig. 1. Side view of 32-cm-diameter enclosure, cut away to show interior cylinders.

The cell compartment is thermally (and mechanically) connected to the inner oven at one point. At this point the cell EMF leads enter the compartment and are thermally tied to the cylinder. Temperature is also sensed at this interface between the two enclosures by a miniature platinum resistance thermometer. The cell compartment and the inner oven are separated by the polystyrene insulation everywhere, except for the one location previously mentioned; therefore, almost all heat flow will be through this interface between the cylinders. By sensing the temperatures at this interface and applying the heat to the inner oven, a condition of zero (negligible) heat flow into the unheated cell compartment is obtained. This condition assures that temperature gradients in the cell compartment are negligible. An auxiliary 25-Ω platinum resistance thermometer is mounted in the cell compartment to permit monitoring the temperature with an external bridge.

Reduction of heat leaks into the cell compartment was of primary inportance. Small-diameter wire (30 gauge)

Manuscript received July 3, 1974; revised August 20, 1974.
The authors are with the National Bureau of Standards, Gaithersburg, Md.

and a series of special thermal tie-downs were used to shunt heat flow along the incoming leads to the more massive aluminum cylinders. Standard cells are noticeably discharged by a resistance across the cell even as large as $10^9\ \Omega$; therefore only tie-downs with very high electrical resistance can be used. The tie-downs consist of a boron nitride washer and a copper washer held firmly to the aluminum surface by a Nylon screw. The wire was wrapped under the head of the screw and then passed through a hole in the screw to the other side of the aluminum surface. This arrangement provides low thermal resistance but high electrical resistance ($10^{12}\ \Omega$) between the wire and the aluminum. Both cell EMF leads and temperature control leads were tied down at several places in the enclosure.

III. CIRCUIT DETAILS

The electronics used to control the temperatures of the two cylinders are housed in a separate package with pilot lamps to indicate the status of the enclosure. There are three controllers, one for the outer oven, one for the inner oven, and a completely independent backup controller for the inner oven. The two main controllers for the ovens are bridges with high gain amplifiers to provide proportional control. Power to the main controllers is normally supplied by a well regulated commerical power supply. Line voltage variations are essentially eliminated and have no effect on the controllers. The backup controller has its own power supply and a mercury thermostat for on–off type control.

Loss of temperature control for only a few hours can cause EMF changes in standard cells for up to several weeks. Control must be maintained even during ac power failures. Mercury batteries have been included that will power the enclosure for two days (in a 23°C ambient) with less than 100 μK change in the cell temperature. Switchover to battery power occurs within milliseconds of a power failure, with large valued capacitors supplying power during the switching time. Transfer back to ac power occurs 10 s after restoration of power to allow power line conditions to stabilize.

The controller for the outer oven consists of a 500-Ω platinum sensor in a Wheatstone bridge and a dc amplifier driving a 60-Ω heater. The dc amplifier is a single low-voltage-offset operational amplifier with a high power output stage. Finite gain of the amplifier causes a temperature change in the oven of 0.002°C for a 1°C change in ambient temperature. Operation is at 29.7°C with 4 W of power required for an ambient temperature of 23°C. Since the amplifier is capable of supplying 15 W to the enclosure, it can maintain temperature control down to −20°C.

The inner oven, with typically 0.1 W applied, is held at a temperature of 30°C, 0.3°C higher than the surrounding outer oven. Requirements for the controller are long-term stability, high sensitivity, low noise, and low sensitivity to ambient temperature changes. A platinum resistance thermometer was chosen as the sensor because of its excellent long-term stability. Power dissipation in the sensor imposes a practical limitation on the maximum signal obtainable from the sensor. As sensor dissipation is increased, the sensor temperature becomes higher than the temperature of the controlled surface. This temperature difference must be maintained constant for best stability of the controlled surface. Thus larger signal output requires higher sensor dissipation, which in turn requires better amplitude stability of the bridge excitation voltage. A compromise of a 100-Ω (at 0°C) thermometer with 1 MA of thermometer current was chosen.

Although several high quality operational amplifiers have very good dc characteristics (low voltage offset, current offset, etc.), these were judged inadequate for this system. It was decided to use ac excitation on the bridge, ac amplifiers, and a phase-sensitive detector. Using ac excitation permits the use of a transformer-ratio bridge instead of a classical Wheatstone bridge. Advantages of this arrangement are that the transformer-ratio arms have a negligibly small temperature coefficient and so do not have to be thermostated. The inclusion of only the reference resistor in the outer oven produces a circuit that is negligibly affected by changes in ambient temperature. A two-stage transformer is used for a four-terminal measurement of the thermometer resistance so that changes in the lead resistance have no effect. The addition of an auxiliary transformer allows for easily adjusting the temperature (a feature used in setting up the enclosure). A 100-Ω standard reference resistor is used with the 110-Ω platinum thermometer (at 30°C).

As noted before, the bridge excitation voltage must remain constant. The circuit diagram of the oscillator used is shown in Fig. 2. A Wein bridge oscillator produces a sine wave of approximately 400 Hz. A dc signal proportional to the average value of the output voltage is generated, and this signal is then compared to the voltage of a temperature-compensated reference Zener diode. The resulting error signal is fed back to the oscillator to stabilize the output voltage at 2.8 V. Observed changes (drifts) of output were less than 0.005 percent with negligible effect from temperature changes. An additional amplifier was added to the circuit to provide two outputs 180 degrees out of phase with each other, because both are needed for the phase-sensitive detector.

The bridge excitation transformer $T1$ is a conventional two-stage device with a toroidal Mumetal shield between stages. Auxiliary transformer $T2$ is coupled to it and provides a means of adjusting the effective transformer ratio, which determines the control temperature. The details of these transformers and the remaining circuitry are shown in Fig. 3.

The low level signal from the bridge is applied to a transformer ($T3$) with a tuned output. This transformer matches the low impedance of the bridge ($\approx 50\ \Omega$) to the optimum sources impedance of the first amplifier ($10^7\ \Omega$). The transformer output is tuned to 400 Hz to reduce 60-Hz noise pickup. The two operational amplifiers that follow have a total gain of 90 dB. This amplified signal is fed to a phase-sensitive detector, then to another operational amplifier. The dc output of this last stage drives the 3000-Ω

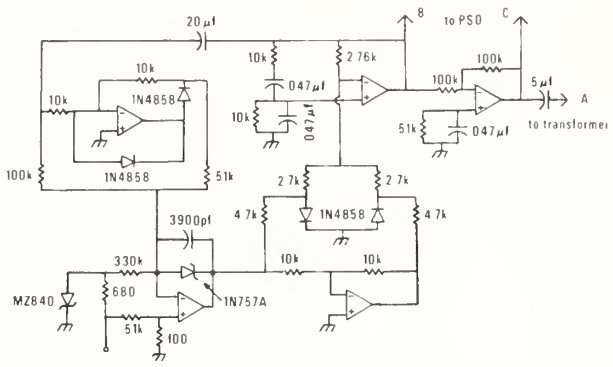

Fig. 2. Circuit diagram of oscillator used to drive transformer ratio bridge for inner oven.

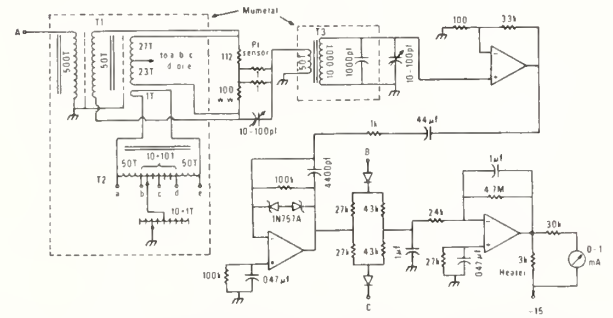

Fig. 3. Complete circuit diagram (except for oscillator) of inner oven controller. (Numbers on transformers indicate number of turns.)

heater on the inner oven, and the heater voltage is indicated on a meter mounted on the front of the electronics package. Since the heater voltage is proportional to the oven temperature, the meter can be calibrated in degrees. For this system the total range of the meter is approximately 1000 μK; thus 10 μK can easily be resolved.

Buffering of ambient temperature by the outer oven ensures that the inner oven operates at almost constant power. Therefore a substantial change of the inner heater voltage can be interpreted as a failure of either or both controllers. The meter that indicates inner heater voltage is a meter relay that can be set to close a switch contact if the voltage changes (equivalent to a temperature change of 300 μK). If this happens, 110 V ac power is removed from both main controllers and applied to the backup controller. This controller has a mercury thermostat in contact with the inner oven. The thermostat opens and closes a sensitive relay that applies half-wave rectified 110-V ac to the 3000-Ω inner heater. Power for the mercury thermostat is from a dc supply independent of the main supply for the other controllers. The backup controller will maintain the temperature to within 0.01°C of nominal until manually reset.

IV. ADJUSTMENT

Several modes of operation are possible to allow initial adjustments of the controllers. First the mercury thermostat controller is used and the operating temperature measured using an external bridge and the 25-Ω platinum thermometer in the cell compartment. The mercury thermostat controller is then disabled and both main controllers are turned on. The temperature of the outer oven is adjusted so that the inner heater operates at 0.1 W. This adjustment is accomplished by shunting one of the arms of the bridge. Trimmer capacitors are added to the two ac amplifiers to make the total phase shift in the amplifiers zero. The trimmer capacitor on the tuned transformer is adjusted for a maximum 400-Hz signal. Additionally, a small trimmer capacitor is shunted across the reference resistance to balance the capacitance in the platinum thermometer. The temperature of the inner oven is adjusted to be within 0.01°C of the mercury thermostat temperature by picking proper taps in the ratio transformer and, if necessary, by shunting the reference resistor with a large valued trim resistor. Once the temperature (heater voltage) stabilizes, the system is reset so that the backup controller will operate if required.

V. PERFORMANCE

The performance of the enclosures was evaluated by monitoring the temperature changes in the enclosure with time, and changes due to ambient temperature changes. An ac resistance thermometer bridge [1] was used to compare the resistance of the 25-Ω thermometer in the cell compartment to a low-temperature-coefficient thermally lagged resistor.

A plot of the cell temperature versus time for one of the enclosures is shown in Fig. 4. During this test the enclosure was in a laboratory environment where ambient temperature fluctuations were less than ±1°C. A check of the temperature two months later showed no change within experimental error (≈50 μK, due to drift of the reference resistor). Temperature drifts this small produce EMF changes in standard cells that are negligible when compared to typical drifts of the EMF's of cells.

To determine the sensitivity of the enclosure to ambient temperature, both the enclosure and electronics package were placed in a temperature-controlled chamber. Temperature was monitored by the ac thermometer bridge which was kept at 23°C. The data obtained are plotted in Fig. 5. The test was started with measurements at 23°C. The chamber temperature was then raised to 29°C, and after allowing the enclosure to stabilize for one day, measurements were made on three different days. The chamber temperature was then lowered to 16°C and another measurement was made after a one-day wait. Similar measurements were made for 19°C and again for 23°C. The test took a total of 10 days and the repeat measurements at 23°C do not indicate any significant drift during the test. The data are reasonably linear; thus the effect of ambient temperature on the enclosure is the slope of the least squares fitted line, or -4×10^{-6}.

A test for sensitivity to temperature gradients was performed by placing a 40-W light bulb in contact with the upper edge of the enclosure. No detectable change was observed during the 8-h monitoring period in either the tem-

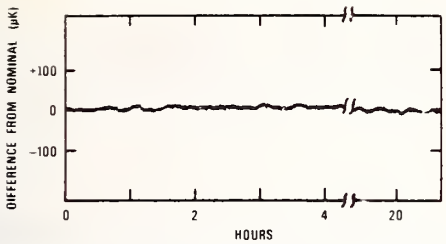

Fig. 4. Deviations of cell temperature from nominal as monitored by independent thermometer bridge.

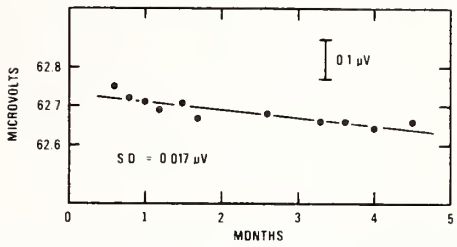

Fig. 6. Mean EMF of six cells in one enclosure minus mean EMF of six cells in second enclosure.

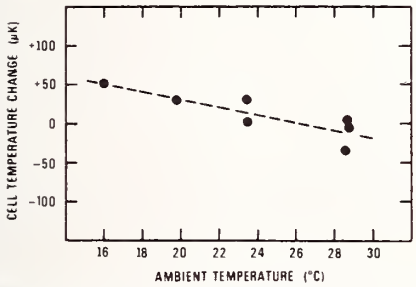

Fig. 5. Temperature change in cell compartment as a function of ambient temperature of enclosure and electronics package.

perature of the auxiliary thermometer within the cell compartment or in the temperature of an additional platinum thermometer temporarily installed near the top of the cell compartment.

To complete the evaluation, standard cells were mounted in the enclosures and regularly compared. Fig. 6 shows the mean EMF of six cells in one enclosure minus the mean EMF of six cells in a second enclosure. The standard deviation of the least squares fitted line is 0.017 μV. The measurements were made potentiometrically with redundant measurements made to evaluate the random error. The typical standard deviation for the difference between the mean EMF's was 0.003 μV. Additional day-to-day random errors are estimated to be 0.007 μV. The root-sum-square total of 0.008 μV is only about one-half the standard deviation observed. Additionally, individual cells occasionally showed unexpected changes as large as 0.06 μV. Temperature fluctuations in the enclosure are too small to account for this, so it is spectulated that residual chemical processes in the standard cells are responsible for the additional "noise."

VI. CONCLUSIONS

It has been demonstrated that an air enclosure can provide outstanding temperature control for a small group of standard cells. The use of a double oven enclosure, ac excitation, and a transformer-ratio bridge eliminate the problems due to ambient temperature changes. A platinum resistance thermometer (while having less sensitivity than some other sensors) is still suitable where long-term temperature stability is desired. The major limitation on the stability of standard cell EMF's has now been shifted from temperature measurement errors to EMF measurement errors and the inherent instabilities in the cell.

REFERENCES

[1] R. D. Cutkosky, "An a-c resistance thermometer bridge," *J. Res. Nat. Bur. Stand.*, vol. 74C, pp. 15–18, Jan. 1970.

Reprinted by permission from IEEE TRANSACTIONS ON INSTRUMENTATION AND MEASUREMENT
Vol. IM-23, No. 4, December 1974, pp. 295-298

IEEE TRANSACTIONS ON INSTRUMENTATION AND MEASUREMENT, VOL. IM-23, NO. 4, DECEMBER 1974

Standard Cell Calibration via Current Transfer

EDWIN R. WILLIAMS, PAUL T. OLSEN, AND BRUCE F. FIELD, MEMBER, IEEE

Abstract—The EMF's of standard cells are now being transferred between laboratories over a 1½-km cable with a precision of 4 parts in 10^8 to provide an instantaneous comparison of the $2e/h$ and γ_p' experiments being carried out at the two facilities. This is accomplished by transferring a constant current that produces a 1-V drop across standard resistors located at both ends of the cable.

I. INTRODUCTION

IN THE Electricity Division of the National Bureau of Standards (NBS), there are three experiments in progress that can be used to monitor the volt, the ohm, and the ampere. The ac Josephson effect has proven extremely useful in monitoring the unit of voltage in terms of the fundamental constant $2e/h$ [1]. The calculable capacitor is now providing an absolute determination of the ohm (Ω_{NBS}/Ω) [2]. And the gyromagnetic ratio of the proton (γ_p') can be used to monitor the unit of current [3]. In addition to providing this essential monitoring service, these three experiments can be combined with a few other fundamental constants to provide an improved value of the fine structure constant α. The following equation shows this relationship [4]:

$$\alpha^{-2} = (1/4R_\infty)(c\Omega/\Omega_{NBS})(\mu_p'/\mu_B)[(2e/h)_{NBS}/(\gamma_p')_{NBS}]$$

where R_∞ is the Rydberg constant for infinite mass, c is the speed of light in vacuum, and μ_p'/μ_B is the magnetic moment of the proton in Bohr magnetons. The subscript NBS implies that $(2e/h)_{NBS}$ is measured in terms of the NBS unit of voltage and that $(\gamma_p')_{NBS}$ is measured in terms of the NBS unit of current. Because these three experiments are being done in a coordinated effort, we can reduce the uncertainties normally introduced in transferring the electrical units. However, the γ_p' experiment is being performed in the nonmagnetic facility which is located 1½ km away from the $2e/h$ and absolute-ohm laboratories. In this paper we describe our efforts to reduce the uncertainty of the voltage transfer so that it negligibly affects the γ_p' experiment. We also suggest how these techniques may be applicable to other problems in the precision electrical standards field.

In the γ_p' experiment the precession frequency of protons in a sample of water (ω_p') is measured via a nuclear magnetic resonance (NMR) experiment, in which $\omega_p' = \gamma_p' B$, where the prime denotes that a spherical water sample is used. A known magnetic field B is produced by passing a 1-A current through a solenoid whose dimensions have been carefully measured. In practice, the 1-A current is produced by making the voltage drop across a precision 1-Ω resistor equal to the EMF of a standard cell. For this experiment the EMF of the cell and resistance of the resistor need to be known in NBS units to determine γ_p' in NBS units. Two different experimental arrangements were used to transfer the cell EMF for comparison with the NBS volt. The first was a 10-mA system with 100-Ω resistors at each end used to transfer the voltage between two standard cells. The second uses a 1-A system to transfer the unit of current directly. This system can also provide a simultaneous voltage transfer. The first system is the one most likely to be useful to others because it is easier to build. We are using the second method because in the γ_p' experiment it is the unit of current that is required. We will describe the present 1-A arrangement first, then describe the 10-mA system because it has a guarding system that should be of general interest.

Manuscript received July 3, 1974; revised August 8, 1974. This work is a contribution of the National Bureau of Standards, and is not subject to copyright.

The authors are with the Electricity Division, National Bureau of Standards, Washington, D. C. 20234.

II. PRESENT METHOD OF TRANSFER

In our present experimental arrangement, we directly transfer current by placing the solenoid in series with the long cable and with the 1-Ω standard resistor R_1 which is located in the $2e/h$ laboratory. (See Fig. 1.) This arrangement does not noticeably affect the quality of the NMR experiment. We need only make sure that the leakage current is sufficiently small. In addition we have a second 1-Ω resistor R_2 in the γ_p laboratory which allows us to do a voltage transfer at the same time that we are doing the NMR experiment.

The experiment is performed by one operator adjusting the constant current source so that the EMF across R_2 is equal to $E_{\gamma_p'}$. A second operator adjusts and reads the frequency of the NMR system. These two operations are being carried out in the same laboratory so that when both are balanced we communicate by intercom to the $2e/h$ laboratory where the EMF across resistor R_1 is measured. Then the current is reversed in the entire system, and the triple balance procedure repeated. This reversal has two purposes. First, any residual earth's field is averaged out in the NMR data and second, any thermal EMF's in the 1-Ω resistors are eliminated. In the NMR part of the experiment, a frequency ω_p' is measured which is proportional to the current I. The ratio E_1/ω_p' is independent of the current I and is the quantity of interest in the γ_p experiment [$\gamma_p' = (\omega_p'/E_1)(R_1/K_c)$, where K_c is the coil constant]. We, therefore, do the transfer using slightly different currents, i.e., different values of $E_{\gamma_p'}$ and the statistical variation in the ratio

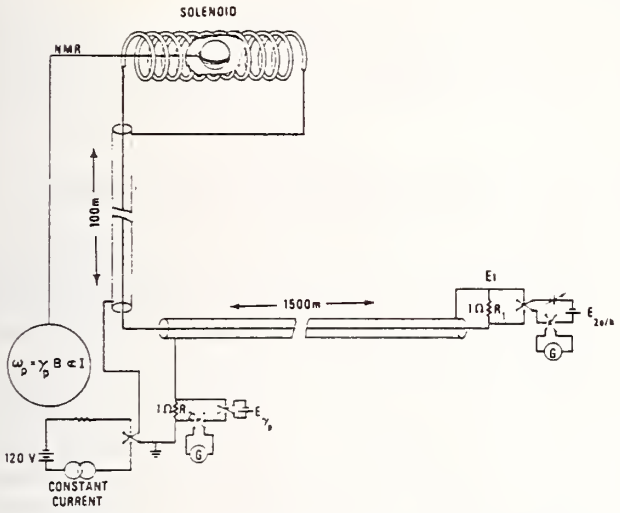

Fig. 1. Current transport system that unites $2e/h$ and γ_p laboratories. Resistors R_1 and R_2 are in series with the solenoid. With 1 A flowing, ω_p' can be measured simultaneously with E_1.

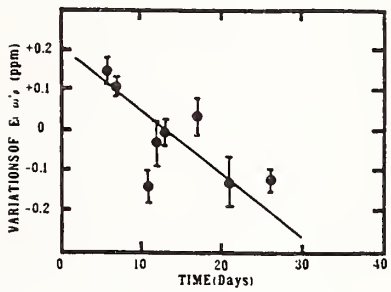

Fig. 2. E_1/ω_p' versus time. The measured quantity E_1/ω_p' is inversely proportional to γ_p'. The error bars represent the 1-standard-deviation uncertainty of each day's transfer. The straight line is the drift rate of -0.0157 ppm/day predicted from dimensional measurements of the solenoid.

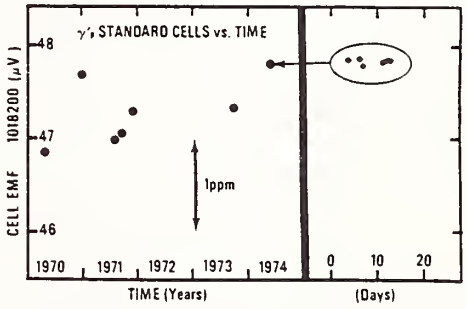

Fig. 3. Average of four standard cells maintained at γ_p' laboratory versus time. The transfers through 1973 were made by direct cell transport taking 3 weeks per point. The June 1974 value is a composite of six transfers taking 30 min a piece.

E_1/ω_p' will give an unbiased measure of the precision of the transfer. The standard deviation of a set of measurements is usually about 0.04 ppm. Fig. 2 shows a composite of recent E_1/ω_p' measurements. The day-to-day variations are larger than would be expected from the uncertainty of each measurement. We feel this is not caused by inadequate transfers, but by systematics in the NMR experiment. Namely, there is presently about a 1 part in 10^7 uncertainty in the way in which we define the center frequency of the NMR signal. This must be done at the start of each day's set of measurements. We expect to reduce this cause of uncertainty in the near future. The straight line shown in Fig. 2 is the drift rate of E_1/ω_p' predicted from early measurements of the coil constant K_c [3]. It is still too early to say if the predicted drift rate is in agreement with this NMR data.

The voltage transfer is also accomplished during the measurement process. We do not need this transfer value for the γ_p' experiment, but it is helpful as a short term standard. For example, if the $2e/h$ laboratory is busy one day, we can still do a γ_p' experiment using these calibrated cells. Or when testing systematic effects in the γ_p' experiments, we need not bother using the $2e/h$ cells.

The value of the γ_p' cells is given by

$$E_{\gamma_p'} = E_1(R_2/R_1).$$

The ratio R_2/R_1 was measured by the resistance calibration section. We also measured it by interchanging R_1 and R_2 and doing another transfer. The ratio we obtained for R_2/R_1 disagreed with the calibrated values by only 0.02 ppm which is within the uncertainty of the measurements. This agreement gives us further confidence that the transfer system is working properly. Fig. 3 shows the EMF of the average of four cells located in the γ_p lab over the past four years. The last point in June 1974 is an average of the six transfers performed by the new technique. The earlier transfers were conventional cell transports which took about 3 weeks to obtain each point, and the results were not always satisfying. In our present scheme each transfer takes 30 min.

III. LEAKAGE CONSIDERATIONS AND GUARDING

In the present configuration (Fig. 1), leakage from the center conductor to the return shield of the two cables is the leakage which affects the γ_p' measurement. There is an average of 11 V across the long cable with 1 A flowing and a leakage resistance of 2×10^{10} Ω. In the 100-m cable there is a 40-V drop because of the solenoid resistance. Again this leakage resistance is about 2×10^{10} Ω. Therefore the correction for leakage current is only about 2 parts in 10^9. In the voltage transfer any leakage from the shield of the coax to ground causes an error. We have a special cable which has one center conductor and three coaxial shields, each electrically insulated from the other. The innermost shield is used to carry the 1-A current because the resistance from it to the next shield is 4×10^9 Ω. The average 4-V drop across this cable produces only a small correction, due to leakage, to the volt transfer. If the cable leakage degrades in time or if higher accuracies

become necessary, a guarded system can be employed to further reduce the leakage in this 1-A system. A guard system was employed in our earlier 10-mA system.

IV. THE 10-mA TRANSFER SYSTEM

This transfer (see Fig. 4) is performed by sending a constant current (10 mA) through two 100-Ω resistors located at either end of the cable. The 1-V drop across each resistor is simultaneously compared with two sets of standard cells located near the two resistors. This simple procedure can be completed with a precision of about 2 in 10^8 in only a few minutes. In this 10-mA system the outputs of both galvanometers are simultaneously recorded, and then the recordings are compared for computation of the double balance condition. This procedure reduces the problem of drift in the galvanometer. In addition, the noise and drift are correlated in both recordings, and with proper analysis, the limitations produced by the noise of the current source can be reduced. For this reason we obtained better precision in the 10-mA system than in the 1-A system.

To prevent leakage of current in the long transfer cable, a dynamic guarded system is used (Fig. 4). The transfer current is sent down the center conductor. The first coaxial shield has a guard current in it such that the potential difference between the guard and the center conductor is less than 0.01 V along the entire length of the cable. This reduces the leakage to less than 2 parts in 10^{10} of the total current. Both currents are returned on a second coaxial shield. A third coaxial shield is grounded to help reduce pickup problems. In this 10-mA setup the accuracy of the transfer is limited to the accuracy with which we measure and maintain the ratio of the two 100-Ω resistors, or about 5 parts in 10^8.

Two inductors (0.3 H each) not shown in the drawing were included at either end of the cable. The capacitance of the cable combined with capacitors placed across the 100-Ω resistors formed a π filter which reduced the noise across the 100-Ω resistors. One must choose inductors that are not saturated by the 10-mA current. In the 1-A system no additional chokes seem necessary.

V. ADVANTAGES OF CURRENT TRANSFER

A current transfer system is preferable to a direct voltage transfer when long cables are involved for the following reasons.

1) The thermal EMF's along the cable have a negligible effect on the transfer; i.e., the thermal EMF's need not be evaluated.

2) The lower impedance of the system reduces the cable leakage problem and reduces the amount of electronic "pickup" noise.

3) A choke can be effective in further reducing any remaining electrical interferance noise before it is "seen" by the standard cell.

With our 1-A system the major advantage is that we need not maintain a high quality voltage standard at the γ_p' laboratory. A large effort is involved in the maintenance of the cells in the $2e/h$ laboratory, for they form the basis of the U.S. legal volt. It is logical to take advantage of this effort by directly using these cells in measuring the current used for the γ_p' experiment. One final advantage is that the EMF developed across the transfer resistors is a very rugged source. Unlike standard cells, it can be shorted without damage or the voltage can be looked at on an oscilloscope without using a very high impedance probe.

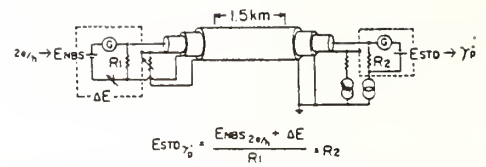

Fig. 4. Diagram of cell comparison by current transport that includes a "dynamic" guard system.

VI. POSSIBLE USES OF THE CURRENT TRANSFER

This transport technique could readily be adapted to a dissemination system which provides a network of substations. Each substation would have continuous calibration via current transfer back to the master reference. Such a system would be useful in standards laboratories or in industrial applications where precise standards are required in a production line environment. Each station could provide any voltage, for example, from 0 to 10 V. The main system could easily be safeguarded against inexperienced operators, and stations having accuracies ranging from 10 ppm to 0.03 ppm could all be on the same system.

A prototype station which provides this type of service is now being maintained in the Electricity Division of NBS at the 10-ppm level of accuracy. It is a self-service unit with a range of 0 to 10 V and is being used for digital voltmeter calibrations by the NBS staff.

Additional uses for our transfer cable at the nonmagnetic facility will be to provide a transfer for the absolute-volt experiment presently in progress at the facility. An absolute-ampere experiment is in the planning stages and this cable will also be used to transfer this measurement to the $2e/h$ laboratory.

VII. CONCLUSIONS

Current transport has increased the accuracy with which we can determine γ_p' in the NBS units and at the same time has reduced the burden of maintaining a high quality voltage standard at the nonmagnetic facility. We can now measure the current in our solenoid with an accuracy on the order of 0.05 ppm in terms of the NBS electrical units as maintained via fundamental constants. This allows us to draw definitive conclusions about the stability of our solenoid dimensions or NMR measuring system.

This system demonstrates the feasibility of transferring precision voltages over even longer cables with accuracies comparable to the present state of the art of maintaining standard cells in terms of $2e/h$.

ACKNOWLEDGMENT

The authors would like to thank T. E. Wells for his measurement of the resistances and the power coefficients of the 1-Ω resistors.

REFERENCES

[1] B. F. Field, T. F. Finnegan, and J. Toots, "Volt maintenance at NBS via $2e/h$: A new definition of the NBS volt," *Metrologia*, vol. 9, p. 155, 1973.
[2] R. D. Cutkosky, "New NBS measurement of the absolute farad and ohm," this issue, pp. 305–309.
[3] P. T. Olsen and E. R. Williams, "A more accurate determination of γ_p' through improved dimensional measurement techniques," this issue, pp. 305–309.
[4] B. N. Taylor, W. H. Parker, and D. N. Langenberg, "Determination of e/h using macroscopic quantum phase coherence in superconductors: Implications for quantum electrodynamics and the fundamental physical constants," *Rev. Mod. Phys.*, vol. 41, p. 491, 1969.

Reprinted by permission from IEEE TRANSACTIONS ON INSTRUMENTATION AND MEASUREMENT
Vol. IM-23, No. 4, December 1974, pp. 299-302

JOURNAL OF RESEARCH of the National Bureau of Standards—A. Physics and Chemistry
Vol. 76A, No. 4, July–August 1972

The EMF-Temperature Coefficient of "Acid" Standard Cells of the Saturated Cadmium Sulfate Type from 15 to 40° C

Walter J. Hamer, Anna Skapars, and Bruce F. Field

Institute for Basic Standards, National Bureau of Standards, Washington, D.C. 20234

(February 9, 1972)

This paper gives the results of new measurements of the effect of temperature on the electromotive force of standard cells of the saturated cadmium sulfate type. Measurements were made over the temperature range of 15 to 40 °C. Twelve cells of NBS manufacture and twenty-four cells supplied by two different commercial manufacturers were used in the studies. Final results were analyzed by the method of least squares using computer programs. The relation between emf and temperature for NBS, company 1, and company 2 cells was found to be given, respectively, by:

$$E_t = E_{20\,°C} - [40.44\,(t-20) + 0.921\,(t-20)^2 - 0.00866\,(t-20)^3] \times 10^{-6}\ \text{V},$$
$$E_t = E_{20\,°C} - [40.14\,(t-20) + 0.888\,(t-20)^2 - 0.00668\,(t-20)^3] \times 10^{-6}\ \text{V},$$
$$E_t = E_{20\,°C} - [39.28\,(t-20) + 0.986\,(t-20)^2 - 0.00943\,(t-20)^3] \times 10^{-6}\ \text{V}.$$

Values for the entropy and heat-capacity changes for the cell reaction in "acid" standard cells are also given.

Key words: EMF-temperature coefficients of standard cells; standard cells; entropy changes in standard cells; heat-capacity changes in standard cells; effect of acid on standard cells.

1. Introduction

In a recent paper [1][1] the thermodynamics of standard cells of the saturated cadmium sulfate type were given. That paper dealt with so-called "neutral" standard cells to which no sulfuric acid is intentionally added when the cell is constructed. The electromotive forces (emfs) were known in terms of the legal volt maintained by the National Bureau of Standards and the emf-temperature coefficient was that derived from the international formula [2, 3, 4] but converted to the V_{69} and t_{68} scales of voltage and temperature [1], respectively.

It is now common practice to add sulfuric acid in small amounts, between approximately 0.03 and 0.1 N (or 0.015 and 0.05 M), to standard cells to reduce the formation of the basic mercurous sulfate, $Hg_2O \cdot Hg_2SO_4$ which is formed in the hydrolysis of mercurous sulfate according to the equation:

$$2\,Hg_2SO_4(s) + H_2O(l) \rightleftharpoons Hg_2O \cdot Hg_2SO_4(s) + H_2SO_4(aq) \qquad (1)$$

where s = solid, l = liquid, and aq = aqueous. Gouy [5] and Hager and Hulett [6] found that the equilibrium concentration of H_2SO_4 formed in the hydrolysis of mercurous sulfate (eq (1)) was 0.002 N while Craig and Vinal [7] found it to be 0.00198 N at 0 °C and 0.00216 N at 28 °C thus showing that it did not change appreciably with temperature. Cadmium sulfate, the solute used to prepare the solution in a standard cell also hydrolyzes to form sulfuric acid, the equilibrium concentration being 0.00092 N at 25 °C [8]. This concentration is insufficient to prevent hydrolysis of mercurous sulfate although sometimes cadmium sulfate, especially if prepared from cadmium nitrate and sulfuric acid or digested with sulfuric acid, contains occluded sulfuric acid in sufficient amount to prevent the hydrolysis of mercurous sulfate and is therefore present through inadvertance. Usually, however, sulfuric acid in small amount is added to the cadmium sulfate electrolyte when the cells are constructed. Solutions 0.03 to 0.06 N with respect to sulfuric acid are generally used because mercurous sulfate exhibits a minimum solubility in the range from 0.04 to 0.08 N. Higher concentrations of acid cause excessive gassing at the cadmium-amalgam electrode.

Although the effect of the addition of sulfuric acid on the emf of saturated standard cells is well known [8, 9, 10, 11, 12, 13] published results do not agree as to the effect of the addition of sulfuric acid on the emf-temperature coefficient. Obata and Ishibashi [14] determined the emf-temperature coefficient of acid cells over a wide range of acidities, namely, 0.078 to 0.756 N and for temperatures from 15.67 to 29.57 °C and concluded that "the use of the acid electrolyte

[1] Figures in brackets indicate the literature references at the end of this paper.

has very little effect on the temperature coefficient of the cell; the cell containing an electrolyte acidified to 0.76 N [too high for emf stability] has a temperature coefficient only 11 percent larger than the neutral one." For 0.078 N their value of -42.5 μV for dE/dT at 20 °C may be compared with -40.64 μV for the neutral cell [1]; it is evident, therefore, that their results even for low acidity show that addition of acid increases the emf-temperature coefficient.

However, Vosburgh and Eppley [15] stated that a cell made with saturated cadmium sulfate to which 0.015 M sulfuric acid was added had the same emf-temperature coefficient as the neutral cell, while they later [16] stated that the change in emf between 25 and 35 °C for *some* cells with electrolytes containing 0.01 mol sulfuric acid per liter of solution is slightly less than that of neutral cells. Also later, Vosburgh [17] after measuring the emf of acid cells from 15 to 40 °C stated that "Wolff's temperature formula was found to hold for all [cells], the presence of acid being found to have little or no effect on the temperature coefficient." Vosburgh had used cells with sulfuric acid concentrations of 0.021, 0.035, 0.048, 0.064, and 0.078 mol per liter. Also the National Physical Laboratory [18] stated that the temperature coefficients of standard cells of acidities from 0.05 to 0.5 N show no particular correlation with the acidity.

At about the same time this latter work was done, the Electrotechnical Laboratory of Japan [12] also investigated the effect of acid on the emf-temperature coefficient of saturated standard cells; acidities ranged from 0.008 to 1.0 N and the temperature range was 15 to 30 °C. Ishibashi and Ishizaki [12] who conducted the investigation found that the emf-temperature coefficients of cells with electrolytes of low acidity were irregular and some of them were smaller than those for neutral cells. They also stated that "the cells acidified up to 0.08 mol/liter (0.16 N) have practically the same temperature coefficient of emf as given by Wolff and Waters' equation, so far as the accuracy of only 0.005 percent is required [i.e., the same as neutral cells]. The coefficient for separate cells, however, must be determined whenever the accuracy of about 0.001 percent is required."

Vigoureux and Watts [19] also measured the emf of "acid" cells as a function of temperature over the range of -20 to 40 °C. The solvent for the electrolyte, $CdSO_4 \cdot \frac{8}{3} H_2O$, in these cells was decinormal sulfuric acid; therefore, the cell acidity was 0.077 N. Vigoureux and Watts did not, however, give comparisons with "neutral" cells except to cite reference [18] to the effect that the acidity of the electrolyte does not affect the temperature coefficient to an appreciable extent.

2. Experimental Detail

Owing to the various results reported above on the emf-temperature coefficients of "acid" standard cells of the saturated cadmium sulfate type and the increased use of "acid" cells it was decided to make new measurements of the emf-temperature coefficient of the "acid" type of cell. Accordingly, 12 cells made at NBS in December 1955 were selected for the study. These cells were made with 10 percent cadmium amalgam, electrolytic mercurous sulfate, and crystals of $CdSO_4 \cdot \frac{8}{3} H_2O$ having a diameter of about 2 to 4 mm. The saturated solution of cadmium sulfate was acidified to 0.021 N by the addition of sulfuric acid. The cells were of the H-form and were assembled as outlined in reference [8]; see also references [20] and [21] for descriptions of the preparations of saturated standard cells at the National Bureau of Standards. These cells were also used in 1966 in the transfer of the "volt standard" from the old NBS site in Washington to the new NBS site in Gaithersburg, Md. [22, 23].

In addition two different manufacturers of standard cells each supplied 12 "acid" saturated standard cells for the study. These are subsequently referred to as commercial 1 cells or C1 cells and as commercial 2 cells or C2 cells. These cells were about 2 years old at the start of the study. They were also of the H-form and were made with 10 percent cadmium amalgam and electrolytic mercurous sulfate. The C1 cells had a stated acidity of 0.061 N (except cell C1B which was replaced by one of acidity of 0.044 N for the measurements in Gaithersburg, Md.; the former one of acidity of 0.061 N was broken in transit from Washington, D.C. to Gaithersburg, Md.) and were made with crystals of $CdSO_4 \cdot \frac{8}{3} H_2O$ of 4, 8, and 10 mm in diameter. The C2 cells had a stated acidity of 0.025 N and the crystals of $CdSO_4 \cdot \frac{8}{3} H_2O$ over the mercurous sulfate paste had a consistency of granulated sugar while those over the amalgam consisted of a mixture of crystals of the consistency of granulated sugar and of larger crystals about 8 mm in diameter. The depth of mercurous paste was about 1.3 cm in NBS cells, 1.5 cm in C1 cells, and 1.7 cm in C2 cells.

Studies of the effect of temperature on the emf of these 36 cells were started in December 1961. The cells were housed in an oil bath maintained within ± 0.001 °C at each of the temperatures used in the study on the day measurements of the emf were made. The temperatures were read with a calibrated Pt-resistance thermometer and the emfs were measured to 0.1 μV with a Brooks comparator [24]. After a change in temperature the cells were maintained at least one week at the new temperature before readings of the emf were taken. At least ten readings over a period of two weeks were made at each temperature. The sequence of the temperatures, the groups of cells used at each temperature, and the time interval from the termination of the last of the initial readings at 28 °C to the time of the last readings at subsequent temperatures are given in table 1.

Various interruptions, most notably the move of NBS from Washington, D.C. to Gaithersburg, Md., in 1966, delayed completion of the study until September,

TABLE 1. *Sequence of measurements*

Sequence of temperatures	Groups of cells	Time intervals (days)* for		
		NBS cells	C1 cells	C2 cells
Washington, D.C.				
28 °C	NBS, C1, C2	0	0	0
32 °C	NBS, C1, C2	42	59	44
35 °C	NBS, C1, C2	108	105	108
38 °C	NBS, C1, C2	147	147	147
40 °C	NBS, C1, C2	190	197	190
35 °C	NBS, C1, C2	253	266	265
28 °C	NBS, C1, C2	351	352	351
20 °C	NBS, C1, C2	506	507	506
20 °C	NBS, C1, C2	625	629	628
25 °C	NBS, C1, C2	741	742	741
Gaithersburg, Md.				
15 °C	C1, C2	.....	1938	1937
25 °C	NBS	2246	.....	.....
20 °C	NBS	2303	.....	.....
15 °C	NBS	2414	.....	.....

*From final date at one temperature to final date at subsequent temperature.

1968. Owing to the time period, about 7 years, consumed in the study, the cells showed slight drifts in emf with time. These were made evident by comparing the mean emf of the 12 cells of each group at those temperatures where second sets of measurements were made. The average changes or drift rates were found to be 3.62×10^{-9} V/day for the NBS cells,[2] 2.71×10^{-9} V/day for the C1 cells, and 9.6×10^{-10} V/day for the C2 cells.

First the observed emfs without drift-rate corrections were fitted to the third-order equation:[3]

$$E_t = E_{20\,^\circ C} + \alpha(t-20) + \beta(t-20)^2 + \gamma(t-20)^3 \tag{2}$$

by the method of least squares using a computer program: $E_{20\,^\circ C}$ is the emf at 20 °C and α, β, and γ are constants. The values of α, β, and γ for the NBS, C1, and C2 cells are given, respectively, in tables 2, 3, and 4. The mean standard deviations are given for α, β, and γ and the uncertainties in the fit, 1σ, are standard deviations of the fit of the data to equation (2). Corrections for drifts in emf with time were then made for each cell. These were obtained from the equation:

$$E'-E=\Delta E=\alpha'(t-20)+\beta'(t-20)^2+\gamma'(t-20)^3 \tag{3}$$

where E' is the corrected emf and $\alpha'=\alpha+\Delta$, $\beta'=\beta+\Delta$, and $\gamma'=\gamma+\Delta$ with Δ being the correction to the constants of eq (2). The final values for the constants for each cell and the averages are given within the parentheses in tables 2, 3, and 4.

Final recommended values for α, β, and γ for each type of cell are given at the bottom of tables 2, 3, and 4; data for cell C2J were omitted in arriving at a final value owing to the large standard deviation of the fit to eq (2). Thus, for NBS cells of 0.021 N acidity,

$$E_t = E_{20\,^\circ C} - [40.44(t-20) + 0.921(t-20)^2 - 0.00866(t-20)^3]\times10^{-6}\text{V} \tag{4}$$

TABLE 2. *Coefficients in the equation:* $E=E_{20^\circ C}+\alpha(t-20)+\beta(t-20)^2+\gamma(t-20)^3$ *for National Bureau of Standards cells*

Cell No.	$E_{20\,^\circ C}$ V	(On V_{69} and t_{68} scales)			
		α μV	β μV	γ μV	σ μV
NBS1157	#[a] 1.0186569(4)	*− 40.4096(.01)	*− 0.9271(.008)	*0.0077(.00070)	1.3194
NBS1158	1.0186598(3)	− 40.4076(.01)	− 0.9498(.003)	.0086(.00061)	1.2891
NBS1159	1.0186597(3)	− 40.4971(.01)	− 0.9304(.007)	.0080(.00069)	1.3941
NBS1160	1.0186599(4)	− 40.4061(.01)	− 0.9260(.005)	.0077(.00063)	1.0890
NBS1161	1.0186619(6)	− 40.7635(.02)	− 0.9221(.010)	.0080(.00136)	1.9925
NBS1162	1.0186507(3)	− 40.2162(.01)	− 0.9216(.003)	.0075(.00060)	1.0133
NBS1163	1.0186528(2)	− 40.3923(.01)	− 0.9194(.002)	.0077(.00054)	1.4056
NBS1164	1.0186580(6)	− 40.6369(.01)	− 0.9221(.008)	.0081(.00099)	1.7193
NBS1165	1.0186529(4)	− 40.6680(.01)	− 0.8893(.008)	.0069(.00070)	1.5041
NBS1166	1.0186549(1)	− 40.7567(0)	− 0.8840(0)	.0067(.00032)	1.3328
NBS1167	1.0186602(6)	− 40.1705(.01)	− 1.0128(.009)	.0114(.00104)	2.3725
NBS1168	1.0186537(2)	−40.1258(0)	− 0.9170(.001)	.0071(.00035)	0.5679
mean	1.0186564(4)	− 40.4542(.01)	− 0.9268(.005)	.0080(.00071)	.....
σ_m	.....	0.0630	0.0093	.00035	1.4847
final	.....	− 40.44	− 0.921	0.00866	1.5

Values within parentheses are negative.
* All values within parentheses are positive corrections for drift in emf with time.
[a] Values in parentheses for this column are corrections for the last decimals in the emf or should be multiplied by 10^{-7}.

[2] Earlier observations, from December 1955 to December 1961 also gave this drift rate for these cells.

[3] Inspections showed that a second-order equation was inadequate whereas a fourth-order equation gave no better fit to the experimental data than a third-order equation.

TABLE 3. *Coefficients in the equation:* $E = E_{20\,°C} + \alpha\,(t-20) + \beta\,(t-20)^2 + \gamma\,(t-20)^3$ *for Company 1 cells*

Cell No.	$E_{20\,°C}$ V	(On V_{69} and t_{68} scales)			
		α μV	β μV	γ μV	σ μV
C1A	# [a] 1.0186005(8)	*−40.1148(0)	*−0.8902(.001)	*0.0061(.00008)	0.4947
C1B	1.0185969(24)	−40.5868(0)	−0.8039(.001)	.0031(.00033)	.4359
C1C	1.0185995(27)	−40.1137(.01)	−0.8963(.001)	.0064(.00035)	.6385
C1D	1.0186021(43)	−40.2768(.01)	−0.8933(.003)	.0065(.00050)	.8085
C1E	1.0185992(45)	−40.4774(.01)	−0.8608(.003)	.0055(.00054)	.6251
C1F	1.0186026(51)	−40.3271(.01)	−0.9174(.004)	.0073(.00058)	.7664
C1G	1.0186006(32)	−40.0042(.01)	−0.9063(.001)	.0067(.00042)	.2867
C1H	1.0186011(61)	−40.1528(.01)	−0.8850(.007)	.0060(.00059)	.3872
C1I	1.0186007(40)	−39.9425(.01)	−0.9064(.002)	.0067(.00050)	.4037
C1J	1.0186000(32)	−39.8191(.01)	−0.9244(.001)	.0072(.00042)	.7741
C1K	1.0185987(37)	−39.9253(.01)	−0.9095(.002)	.0067(.00046)	.7795
C1L	1.0185999(67)	−40.0702(.01)	−0.9015(.008)	.0067(.00062)	.5839
mean	1.0186002(38)	−40.1509(.01)	−0.8913(.003)	.0062(.00044)	.....
σ_m	.....	0.0662	0.0093	0.00029	0.6067
final	.....	−40.14	−0.888	0.00668	0.6

Values within parentheses are negative
*All values within parentheses are positive corrections for drift in emf with time.
[a] Values in parentheses for this column are corrections for the last decimals in the emf or should be multiplied by 10^{-7}.

TABLE 4. *Coefficients in the equation:* $E = E_{20\,°C} + \alpha\,(t-20) + \beta\,(t-20)^2 + \gamma\,(t-20)^3$ *for Company 2 cells*

Cell No.	$E_{20\,°C}$ V	(On V_{69} and t_{68} scales)			
		α μV	β μV	γ μV	σ μV
C2A	[a] 1.0186219(52)	*−38.8723(.01)	−1.0420(.005)	0.0109(.00060)	1.9416
C2B	#1.0186231(21)	−39.6109(0)	−0.9413(.001)	.0075(.00031)	1.1653
C2C	1.0186221(4)	−39.4001(0)	−0.9683(0)	.0084(.00007)	1.5217
C2D	#1.0186220(10)	−40.2280(0)	−0.8616(0)	#.0051(.00018)	0.8837
C2E	1.0186223(31)	−38.9803(.01)	−1.0480(.001)	.0112(.00045)	1.7775
C2F	1.0186214(31)	−39.3767(.01)	−0.9904(.001)	.0095(.00045)	1.3334
C2G	1.0186254(15)	−39.2822(0)	−0.9942(.001)	.0094(.00020)	1.6330
C2H	1.0186199(23)	−38.9568(.01)	−1.0350(.001)	.0106(.00031)	1.8220
C2I	#1.0186169(42)	−40.2187(.01)	−0.8390(.003)	.0040(.00053)	2.0724
C2J	#1.0186041(368)	#−39.9149(1.45)	#−0.7728(.240)	.0008(.00950)	7.2131
C2K	1.0186217(46)	−38.5832(.01)	−1.0853(.004)	.0124(.00054)	2.5660
C2L	#1.0186218(4)	−38.7256(0)	−1.0649(0)	#.0115(.00007)	2.3618
mean	#1.0186202(20)	#−39.3458(.12)	#−0.9702(.019)	.0084(.00035)	.....
σ_m	.....	0.1669	0.0262	.00101	2.7024
mean-C2J	1.0186217(11)	−39.2941(.01)	−0.9882(.002)	.0091(.00029)	.....
σ_m	.....	0.1669	0.0243	.00081	1.7991
final	.....	−39.28	−0.986	.00943	1.8

Values within parentheses are negative.
*All values within parentheses are positive corrections for drift in emf with time unless noted.
[a] Values in parentheses for this column are corrections for the last decimals in the emf or should be multiplied by 10^{-7}.

for C1 cells of 0.061 *N* acidity,

$$E_t = E_{20\,°C} - [40.14(t-20) + 0.888(t-20)^2 - 0.00668(t-20)^3] \times 10^{-6}\text{V} \quad (5)$$

for C2 cells of 0.025 *N* acidity,

$$E_t = E_{20\,°C} - [39.28(t-20) + 0.986(t-20)^2 - 0.00943(t-20)^3] \times 10^{-6}\text{V}. \quad (6)$$

At about the same time covered by this investigation, Froehlich and Melchert, with the assistance of Steiner, in the laboratories of the Physikalisch-Technische Bundesanstalt, also carried out a study of the emf-temperature coefficient of "acid" standard cells over the range of 10 to 30 °C and published their results in April, 1971 [25]. The pH of the electrolyte used in the cells was 1.4 ± 0.2; the hydrogen-ion activity was, therefore, of the order of 0.04. No concentration value was given; from known values of the activity coefficient of saturated cadmium sulfate solution, namely, 0.03641 [1] and of sulfuric acid of the same ionic strength, namely, 0.208 [26], and the density of the saturated solution [27] the normality calculated from the pH value given by Froehlich and Melchert would appear to be about 0.26 *N*. However, the emfs given for 20 °C by Froehlich and Melchert indicate

that the acidity was about 0.03–0.04 N. Ten cells were used in the study, two each of about three, four, five, seven, and nine years old at the time of the measurements. The emfs at 20 °C ranged from 1.0186053 V to 1.0186457 V; no correlation with pH was given, however, a relation between E and dE/dT may be calculated from their data and is shown later.

From the results obtained for the ten cells over a temperature range of 10 to 30 °C and taking cognizance of drifts in emf with time, Froehlich and Melchert [25] arrived at:

$$E_t = E_{20\,°C} - [39.78(t-20) + 0.936(t-20)^2 - 0.0086(t-20)^3] \times 10^{-6}\text{V} \qquad (7)$$

for the relation between emf and temperature.

In table 5, values for dE/dT from 15 to 40 °C are given for NBS, C1, and C2 cells. The standard deviation, σ, of an individual value and the standard deviation of the mean, σ_m, are also given. The values of dE/dT given by the international formula (Int), the equation of Vigoureux and Watts (VW), and of Froehlich and Melchert (FM) are given for comparison. Also the mean emfs are given at the bottom of the table.

Inspection of the data shows that there is no correlation between dE/dT and the normality of the solution. This is clearly shown in figure 1 for values of dE/dT at 20 °C; similar results are found for the other temperatures. It is evident, as was stated earlier by Ishibashi and Ishizaki [12] that the emf-temperature coefficients of cells with electrolytes of low acidity are irregular. Since the emf is decreased by the addition of acid it remains that dE/dT may be a function of the emf. This is shown not to be the case in figure 2 where dE/dT at 20 °C is plotted against the emf at 20 °C; 10.5 μV (see ref. [8] for this factor) were subtracted from the emfs of Ishibashi and Ishizaki to place their emfs on the United States of America base of reference for the volt. It is evident from figure 2 that there is no clear correlation between E and dE/dT over the acidity range of 0 to 0.06 N. As also stated earlier by Ishibashi and Ishizaki for a precision of 0.005 percent the addition of acid has little or no effect on dE/dT while for a precision of 0.001 percent the individual values of dE/dT must be experimentally determined. Furthermore, drift rates must be determined if the highest precision is required.

One point is significant in figure 2, namely, that some of the emf data of NBS and ETL at 20 °C exceed that normally attributed to "neutral" cells and that some of the emfs reported by Froehlich and Melchert are very close to that for the so-called "neutral" cell. The international value of the emf of "neutral" cells was based on the measurements made with cells with chemically prepared and with dc-electrolytic mercurous sulfate. Wolff and Waters [2] showed that dc-electrolytic mercurous sulfate, on the average, gave cells with emfs exceeding by 16.8 μV those made with chemically prepared mercurous sulfate. Since dc-electrolytic mercurous sulfate was used in the cells discussed herein, this value of 16.8 μV was added to the international value and is designated as "corrected emf" in figure 2. With this correction the emfs of the NBS cells approximate that of the so-called "neutral" cell; apparently, the acid in the cells is largely neutralized by the alkaline constituent of the glass container during the aging period (this is exhibited by the upward drift in emf with time, as mentioned earlier in this paper).

Finally in table 6 values of the second derivative, d^2E/dT^2, and in table 7 values of the entropy and heat-capacity changes for the cell reaction in "acid"

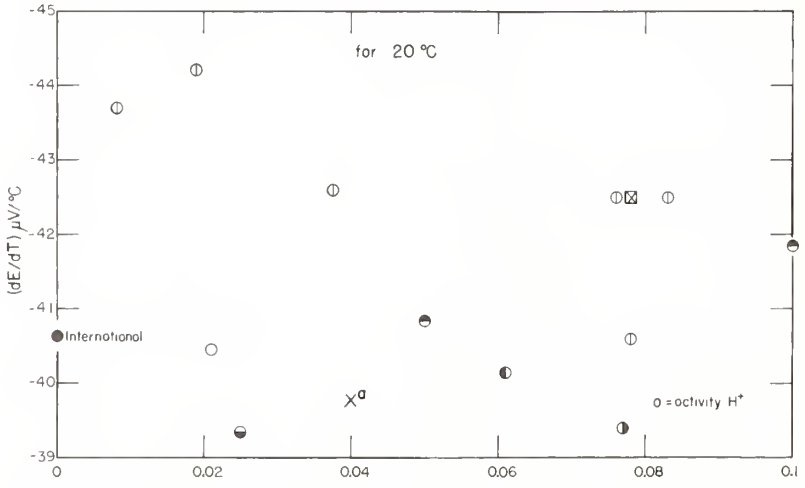

FIGURE 1. *Emf-temperature coefficients of saturated standard cells and the normality of sulfuric acid in the electrolyte in the cell.*

○—National Bureau of Standards [1].
◓—National Physical Laboratory [18].
◑—Electrotechnical Laboratory, Tokyo [12].
×—Physikalisch-Technische Bundesanstalt [25].
◑—Vigoureux and Watts [19].
⊠—Obata and Ishibashi [14].
◐—Company 1.
◒—Company 2.
●—International formula [2,3,4].

TABLE 5. *Emf-temperature coefficients of "acid" standard*

No.*	15 °C			20 °C			25 °C		
	NBS	C1	C2	NBS	C1	C2	NBS	C1	C2
1	−30.60	−30.76	−27.63	−40.42	−40.11	−38.86	−48.98	−48.54	−48.37
2	−30.24	−32.30	−29.62	−40.40	−40.59	−39.61	−49.17	−48.36	−48.43
3	−30.60	−30.64	−29.08	−40.49	−40.10	−39.40	−49.07	−48.55	−48.45
4	−30.56	−30.84	−31.24	−40.40	−40.27	−40.23	−48.98	−48.64	−48.48
5	−30.92	−31.44	−27.63	−40.74	−40.47	−38.97	−49.16	−48.59	−48.57
6	−30.41	−30.59	−28.73	−40.21	−40.32	−39.37	−48.78	−48.86	−48.51
7	−30.59	−30.41	−28.63	−40.38	−39.99	−39.28	−48.94	−48.51	−48.49
8	−30.80	−30.87	−27.79	−40.63	−40.14	−38.95	−49.09	−48.43	−48.47
9	−31.28	−30.35	−31.51	−40.66	−39.93	−40.21	−48.90	−48.44	−48.23
10	−31.39	−30.00	[c](−30.46)	−40.76	−39.81	[c](−41.36)	−49.07	−48.47	[c](−50.72)
11	−29.19	−30.30	−26.79	−40.16	−39.92	−38.57	−49.27	−48.45	−48.42
12	−30.41	−30.58	−27.22	−40.13	−40.06	−38.73	−48.73	−48.45	−48.52
mean	−30.58	−30.76	[c]−28.72	−40.45	−40.14	[c]−39.29	−49.01	−48.52	[c]−48.45
σ	0.557	0.410	1.559	0.216	0.232	0.554	0.159	0.092	0.090
σ_m	.161	.118	.470	.062	.067	.167	.046	.027	.027
Int.		[a]−30.39(.04)			−40.64(.04)			−40.39(.04)	
VW		[b]−29.79(.71)			−39.40(.55)			−48.02(.55)	
FM		[a]−29.78(.06)			−39.78(.05)			−48.50(.03)	
E(NBS)		1.0188353			1.0186572			1.0184331	
E(C1)		1.0187817			1.0186040			1.0183819	
E(C2)		[c]1.0187934			[c]1.0186228			[c]1.0184029	
FM		1.0187982			1.0186238			1.0184026	
Int.		1.0188224			1.0186442			1.0184185	

* Numbers are in sequence for cells NBS, C1, and C2 given in tables 2, 3, and 4.
[a] Values in parentheses are σ_m, standard deviation of the mean.
[b] Maximum uncertainty of deviations from given formula.
[c] Eleven cells only; data for cell No. 10 omitted.
[d] Vigoureux and Watts gave only the differences between emfs at a particular temperature and emfs of reference cells at 20 °C.

TABLE 6. *The second derivative,* d^2E/dT^2

No.*	15 °C			20 °C			25 °C		
	NBS	C1	C2	NBS	C1	C2	NBS	C1	C2
1	−2.090	−1.964	−2.419	−1.838	−1.778	−2.074	−1.586	−1.593	−1.729
2	−2.170	−1.711	−2.115	−1.894	−1.606	−1.881	−1.617	−1.501	−1.646
3	−2.108	−1.993	−2.191	−1.847	−1.791	−1.937	−1.586	−1.588	−1.683
4	−2.092	−1.991	−1.871	−1.842	−1.781	−1.723	−1.592	−1.571	−1.676
5	−2.105	−1.897	−2.444	−1.824	−1.716	−2.094	−1.543	−1.534	−1.745
6	−2.080	−2.063	−2.277	−1.837	−1.827	−1.979	−1.594	−1.590	−1.680
7	−2.082	−2.024	−2.274	−1.835	−1.811	−1.986	−1.588	−1.597	−1.698
8	−2.101	−1.954	−2.395	−1.828	−1.756	−2.068	−1.556	−1.558	−1.741
9	−1.991	−2.025	−1.808	−1.763	−1.809	−1.672	−1.535	−1.593	−1.536
10	−1.979	−2.075	(−2.335)	−1.768	−1.847	(−2.026)	−1.557	−1.618	(−1.717)
11	−2.381	−2.030	−2.551	−2.008	−1.815	−2.163	−1.634	−1.600	−1.774
12	−2.056	−2.004	−2.473	−1.832	−1.787	−2.130	−1.509	−1.570	−1.787
mean	−2.103	−1.978	[c]−2.256	−1.843	−1.777	[c]−1.973	−1.575	−1.576	[c]−1.709
σ	0.088	0.096	0.212	0.058	0.064	0.159	0.036	0.031	0.070
σ_m	.025	.028	.067	.017	.019	.048	.010	.009	.021
Int.		[a]−2.200(.005)			−1.900(.003)			−1.600(.003)	
VW		[b]−2.049(.08)			−1.806(.06)			−1.653(.06)	
FM		−2.130(.007)			−1.872(.004)			−1.614(.007)	

*Numbers are in sequence for cells NBS, C1, and C2 given in tables 2, 3, and 4.
[a] Values in parentheses are σ_m, standard deviation of the mean.
[b] Maximum uncertainty of deviations from given formula.
[c] Eleven cells only; data for cell No. 10 omitted.

cells of the saturated cadmium sulfate type, μV/°C

30 °C			35 °C			40 °C		
NBS	C1	C2	NBS	C1	C2	NBS	C1	C2
−56.28	−56.04	−56.15	−62.32	−62.62	−62.21	−67.10	−68.27	−66.54
−56.57	−55.62	−56.07	−62.58	−62.36	−62.55	−67.22	−68.59	−67.85
−56.35	−55.98	−56.23	−62.32	−62.41	−62.73	−67.00	−67.82	−67.97
−56.32	−55.97	−55.98	−62.40	−62.25	−62.76	−67.24	−67.48	−68.79
−56.18	−55.81	−56.42	−61.79	−62.12	−62.52	−66.00	−67.53	−66.87
−56.15	−56.22	−56.17	−62.30	−62.40	−62.33	−67.23	−67.40	−67.00
−56.08	−55.96	−56.27	−62.34	−62.35	−62.60	−67.19	−67.66	−67.49
−56.18	−55.73	−56.35	−61.91	−62.03	−62.60	−66.28	−67.35	−67.21
−56.00	−55.86	−55.57	−61.97	−62.20	−62.23	−66.79	−67.47	−68.21
−56.33	−55.99	[c](−58.53)	−62.54	−62.37	[c](−64.80)	−67.69	−67.60	[c](−69.52)
−56.50	−55.92	−56.32	−61.88	−62.31	−62.28	−66.75	−67.62	−66.30
−56.21	−55.76	−56.59	−62.58	−61.98	−62.96	−67.83	−67.12	−67.61
−56.26	−55.91	[c]−56.19	−62.24	−62.28	[c]−62.52	−67.03	−67.66	[c]−67.44
0.165	0.160	0.262	0.284	0.179	0.241	0.521	0.405	0.688
.048	.046	.079	.082	.052	.073	.150	.117	.297
	−56.63(.04)			−62.37(.06)			−66.60(.09)	
	[e]−56.10(.63)			[e]−64.08(.70)			[e]−72.41(.70)	
	−55.92							
Electromotive forces [d]								
	1.0181694			1.0178726			1.0175493	
	1.0181205			1.0178246			1.0174994	
	[c]1.0181408			[c]1.0178436			[c]1.0175182	
	1.0181410							
	1.0181528			1.0178547			1.0175317	

[e] Based on four cells only; Vigoureux and Watts considered their results above 28 °C to be less reliable than those for lower temperatures.
Int. International formula [2, 3, 4].
VW Vigoureux and Watts [19].
FM Froehlich and Melchert [25].

for saturated standard cells, μV/°C/°C

30 °C			35 °C			40 °C		
NBS	C1	C2	NBS	C1	C2	NBS	C1	C2
−1.334	−1.408	−1.384	−1.082	−1.222	−1.039	−0.830	−1.037	−0.694
−1.341	−1.396	−1.412	−1.065	−1.291	−1.078	−0.788	−1.186	−0.943
−1.325	−1.386	−1.428	−1.065	−1.183	−1.174	−0.804	−0.981	−0.920
−1.342	−1.361	−1.428	−1.092	−1.151	−1.280	−0.842	−0.941	−1.133
−1.263	−1.353	−1.395	−0.982	−1.172	−1.046	−0.701	−0.991	−0.696
−1.351	−1.354	−1.381	−1.108	−1.118	−1.083	−0.865	−0.881	−0.784
−1.340	−1.383	−1.410	−1.093	−1.170	−1.122	−0.846	−0.956	−0.834
−1.283	−1.361	−1.413	−1.010	−1.163	−1.086	−0.737	−0.965	−0.759
−1.307	−1.377	−1.400	−1.079	−1.161	−1.264	−0.851	−0.945	−1.128
−1.347	−1.390	(−1.408)	−1.136	−1.161	(−1.099)	−0.926	−0.932	(−0.790)
−1.261	−1.385	−1.386	−0.888	−1.171	−0.998	−0.515	−0.956	−0.610
−1.385	−1.353	−1.444	−1.162	−1.136	−1.101	−0.938	−0.919	−0.758
−1.323	−1.392	−1.408	−1.072	−1.177	−1.116	−0.804	−0.974	−0.842
0.038	0.080	0.020	0.068	0.044	0.105	0.113	0.077	0.172
.011	.023	.006	.020	.013	.032	.033	.022	.052
	−1.300(.003)			−1.000(.005)			−0.700(.008)	
	−1.590(.07)			[d]−1.617(.08)			[d]−1.734(.09)	
	−1.356(.013)			.....			.....	

[d] Vigoureux and Watts gave only differences between emfs at a particular temperature and emf of reference cells at 20 °C.
Int. International formula [2, 3, 4].
VW Vigoureux and Watts [19].
FM Froehlich and Melchert [25].

TABLE 7. *Entropy and heat-capacity changes for the reaction in "acid" standard cells of the saturated cadimum sulfate type*

	Acidity N	15 °C	20 °C	25 °C	30 °C	35 °C	40 °C
		Entropy changes, J K^{-1} mol^{-1}					
International [2,3,4]	0.00092	−5.86	−7.84	−9.53	−10.93	−12.04	−12.85
NBS	.021	−5.90	−7.81	−9.46	−10.86	−12.01	−12.94
FM	*	−5.75	−7.68	−9.36	−10.79	.....	.....
C2	.025	−5.54	−7.58	−9.35	−10.84	−12.06	−13.01
C1	.061	−5.94	−7.75	−9.36	−10.79	−12.02	−13.06
VW	.077	−5.75	−7.60	−9.27	[a](−10.83)	[a](−12.37)	[a](−13.97)
Thermochemical [1]	0	.....	.....	−9.58	.....	.....	.....
		Heat-capacity changes, J K^{-1} mol^{-1}					
International [2,3,4]	0.00092	−122.33	−107.48	−92.06	−76.05	−59.46	−42.30
NBS	.021	−116.94	−104.26	−90.62	−77.40	−63.75	−48.59
FM	*	−118.44	−105.90	−92.86	−79.33	.....	.....
C2	.025	−125.45	−111.71	−98.33	−82.37	−66.36	−50.88
C1	.061	−109.99	−101.64	−90.68	−81.43	−69.99	−58.96
VW	.077	−113.94	−102.17	−95.10	[a](−93.02)	[a](−96.15)	[a](−104.79)
Thermochemical [1]	0	.....	.....	−93.72	.....	.....	.....

* pH = 1.4 ± 0.2; $a_{H+} \approx 0.04$.
[a] Based on four cells only [19].

International—International formula [2,3,4].
FM Froehlich and Melchert [25].
VW Vigoureux and Watts [19].

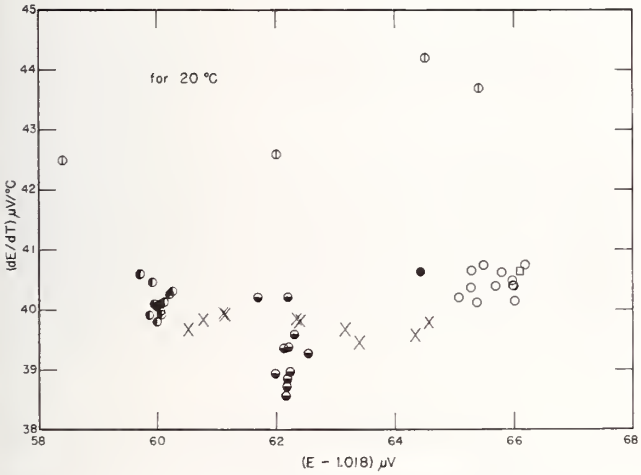

FIGURE 2. *Emf-temperature coefficients of saturated standard cells and the emf of the cell.*

○—National Bureau of Standards [1].
◑—Electrotechnical Laboratory, Tokyo [12].
×—Physikalisch-Technische Bundesanstalt [25].
◐—Company 1.
⊖—Company 2.
●—International formula [2,3,4].
□—Corrected international emf.

standard cells are given. The entropy change for the "acid" cells is in all cases less than those observed for the so-called "neutral" cell while the heat-capacity change for "acid" cells relative to the "neutral" cell is less well defined.

3. References

[1] Hamer, W. J., J. Res. Nat. Bur. Stand. (U.S.), 76A (Phys. and Chem.), No. 3, 185–205 (May-June 1972).
[2] Wolff, W. A., and Waters, C. E., Bull. BS **4**, 70 (1907).
[3] Wolff, W. A., Bull. BS **5**, 309 (1908).
[4] International conference on electrical units and standards, Appendix to report: Notes to the specifications as to the methods adopted in various standardizing laboratories to realize the international ohm and the international ampere, and to prepare the Weston Normal Cell (Darling & Sons, Ltd., London, 1908).
[5] Guoy, M., Compt. rendu. **130**, 1399 (1900).
[6] Hager, O. B., and Hulett, G. A., J. Phys. Chem. **36**, 2095 (1932).
[7] Craig, D. N., and Vinal, G. W., J. Res. NBS **17**, 709 (1936)RP939.
[8] Hamer, W. J., Standard cells, their construction, maintenance, and characteristics, NBS Monograph 84, 1965.
[9] Smith, F. E. (Sir Frank), A Dictionary of Applied Physics, p. 268, Ed. Sir Richard Glazabrook, (Macmillan and Co., Ltd., London, 1911).
[10] Report of Natl. Phys. Lab., Electrician **75**, 463 (1915).
[11] Obata, J., Proc. Math. Phys. Soc. (Japan), (3), **2**, 232 (1920).
[12] Ishibashi, V., and Ishizaki, T., Researches Electrotechnical Lab., No. 318 (1931).
[13] Vosburgh, W. C., J. Am. Chem. Soc. **47**, 1255 (1925).
[14] Obata, J., and Ishibashi, V., Researches Electrotechnical Lab., No. 88 (1921).
[15] Vosburgh, W. C., and Eppley, M., J. Am. Chem. Soc. **45**, 2268 (1923).
[16] Vosburgh, W. C., and Eppley, M., J. Am. Chem. Soc. **46**, 110 (1924).
[17] Vosburgh, W. C., J. Opt. Soc. & Rev. Sci. Instrument **12**, 511 (1926).
[18] Rapport, Comité Consultatif d'Electricité Procès-Verbaux des Séances de 1930, in Procès-Verbaux des Séances, Comité International des Poids et Mesures Deuxième Série-Tome XIV, p. 171, 1931.
[19] Vigoureux, P., and Watts, S., Proc. Phys. Soc. (London) **45**, 172 (1933).
[20] Brickwedde, L. H., Compt. rendus Quatorzième Conférence IUPAC, p. 105, London, 1947.
[21] Hamer, W. J., and Law, C. A., Comité Consultatif d'Electricité, **11**[e] Ses, Doc. No. 5, May 10–12, 1965.
[22] Hamer, W. J., J. Wash. Acad. Sci. **56**, 101 (1966).
[23] Hamer, W. J., Inst. Soc. Am., M2-1-Mestind-67, 1967.
[24] Brooks, H. B., BS J. Res. **11**, 211 (1933).
[25] Froehlich, M., and Melchert, F., with Steiner, O., Metrologia **7**, No. 2, 58 (1971).
[26] Harned, H. S., and Hamer, W. J., J. Am. Chem. Soc. **57**, 27 (1935).
[27] International critical tables **3**, 66 (1928).

(Paper 76A4–723)

JOURNAL OF RESEARCH of the National Bureau of Standards—A. Physics and Chemistry
Vol. 76A, No. 3, May–June 1972

Thermodynamics of Standard Cells of the Saturated Cadmium Sulfate Type

Walter J. Hamer

Institute for Basic Standards, National Bureau of Standards, Washington, D.C. 20234

(December 21, 1971)

This paper gives data on the thermodynamic functions of standard cells of the saturated cadmium sulfate type, as obtained from calorimetric and equilibrium data at 25 °C or from the electromotive forces (emfs) and emf-temperature coefficients of the cell for the temperature range of 0 to 43.6 °C. The functions considered are the changes in Gibbs energy, enthalpy, entropy, and heat capacity for the cell reaction. The electromotive forces are expressed on the V_{69} volt and the t_{68} temperature scale. Results are expressed on the SI and for comparisons with literature data in terms of the defined thermochemical calorie. The effect of expressing the emf-temperature coefficient as a function of temperature in different ways on the values for the changes in entropy and heat capacity for the cell reaction is discussed. Finally, the observed emf of the standard cell at 25 °C is compared with emfs calculated from various values reported for the standard potentials of the cadmium-amalgam and mercury-mercurous sulfate electrodes and the activity coefficient of cadmium sulfate in saturated aqueous solution.

Key words: Emf-temperature coefficients of standard cells; emfs of standard cells; standard potential of standard cells; thermodynamics of standard cells.

1. Introduction

It is the purpose of this paper to present data on the thermodynamic functions of standard cells of the saturated cadmium sulfate type,[1] as obtained from calorimetric and chemical equilibrium data, and to compare these data with those obtained from the electromotive force (emf) and emf-temperature coefficient of the cell. The thermodynamic functions considered are the changes in Gibbs energy (free energy), ΔG; enthalpy (heat content), ΔH; entropy, ΔS; and heat capacity at constant pressure, ΔC_p, where the changes are equal to the differences between the thermodynamic quantities of the products and the reactants of the cell reaction. Thermodynamically, these are given or are related by:

$$\Delta G = \Delta H - T\Delta S = \Delta H + T[d(\Delta G)/dT]_p \quad (1)$$

$$\Delta S = \int_0^T \Delta C_p d \ln T \quad (2)$$

and

$$\Delta C_p = [d(\Delta H)/dT]_p \quad (3)$$

where T is the Kelvin temperature (defined in the thermodynamic scale by assigning 273.16 K to the triple point of water; freezing point of water, 273.15 K [1][2]).

The thermodynamic functions for a galvanic cell (or standard cell) may be obtained from its emf, E, and its emf-temperature coefficient, dE/dT, and are given by:

$$\Delta G = -nEF \quad (4)$$

$$\Delta H = -nEF + nFT(dE/dT) \quad (5)$$

$$\Delta S = nF(dE/dT) \quad (6)$$

and

$$\Delta C_p = nFT(d^2E/dT^2) \quad (7)$$

where n is the number of equivalents involved in the cell reaction (in the present case n is 2) and F is the Faraday. F has a value of 96487 coulombs per gram-equivalent [1, 2, 3, 4] or 23060.9 calories per volt per gram-equivalent.[3] Accordingly, a comparison may be made between the thermodynamics of the overall reaction of a standard cell as determined from calorimetric and chemical equilibrium data or from emf data.

[1] Also referred to as the Weston cell after Edward Weston who invented the cell in 1892.

[2] Figures in brackets indicate the literature references at the end of this paper.

[3] Based on the relation 1 thermochemical calorie (defined) = 4.1840 J [1].

2. The Standard Cell (saturated $CdSO_4$ type)

The conventional standard cell of the saturated cadmium sulfate type,[4] considered here, may be represented by:

$$(-)\mathrm{Cd, Hg}(2p)\left|\mathrm{CdSO_4}\cdot\frac{8}{3}\mathrm{H_2O(s)}\right|\mathrm{CdSO_4(ss)}\left|\mathrm{CdSO_4}\right.$$
$$\left.\cdot\frac{8}{3}\mathrm{H_2O(s)}\right|\mathrm{Hg_2SO_4(s)}\left|\mathrm{Hg(l)}\right.(+)$$

where the vertical lines indicate the interface between two distinct phases (the amalgam consists of 2 phases, one solid and one liquid, but for simplicity vertical lines are not used in designating it), $2p=2$ phases, ss = saturated solution, s = solid (or paste), and l = liquid. The cell reaction is [5]:

$$x\mathrm{Cd}, y\mathrm{Hg}(2p)+\mathrm{Hg_2SO_4(s)}+\frac{8/3}{m-8/3}\mathrm{CdSO_4}$$
$$\cdot m\mathrm{H_2O(ss)}\rightarrow\frac{m}{m-8/3}\mathrm{CdSO_4} \qquad (8)$$
$$\cdot\frac{8}{3}\mathrm{H_2O(s)}+2\mathrm{Hg(l)}+(x-1)\mathrm{Cd}, y\mathrm{Hg}(2p)$$

where x moles of Cd are associated with y moles of Hg in the amalgam and m is the number of moles of water associated with 1 mole of $CdSO_4$ in the saturated solution. Ten percent amalgams are now generally used, although there is now a trend to a return to the use of $12\frac{1}{2}$-percent amalgams as they are more suitable for portable (or shippable) cells. At 25 °C m has a value of 15.089 [6].

The overall reaction for the cell may be considered as the sum of five reactions, namely:

(a) $$\mathrm{Cd(s)}+\mathrm{Hg_2SO_4(s)}\rightarrow\mathrm{CdSO_4(s)}+2\mathrm{Hg(l)} \qquad (9)$$

(b) $$\mathrm{CdSO_4(s)}+\mathrm{H_2O(l)}\rightarrow\mathrm{CdSO_4\cdot H_2O(s)} \qquad (10)$$

(c) $$\mathrm{CdSO_4\cdot H_2O(s)}+\frac{5}{3}\mathrm{H_2O(l)}\rightarrow\mathrm{CdSO_4}\cdot\frac{8}{3}\mathrm{H_2O(s)} \qquad (11)$$

(d) $$\frac{8/3}{m-8/3}\mathrm{CdSO_4}\cdot m\mathrm{H_2O(ss)}\rightarrow\frac{8}{3}\mathrm{H_2O(l)}$$
$$+\frac{8/3}{m-8/3}\mathrm{CdSO_4}\cdot\frac{8}{3}\mathrm{H_2O(s)} \qquad (12)$$

and

(e) $$\mathrm{Cd(10\%\ amalgam)}\rightarrow\mathrm{Cd(s)} \qquad (13)$$

for which, reaction (e) excepted, calorimetric or thermal data are available.

3. Calorimetric and Chemical Equilibrium Data

Reaction (a)

For reaction (a) Cohen, Helderman, and Moesveld [7] obtained -45.346 cal mol^{-1} at 18 °C for the difference between the heats of formation of $CdSO_4$ and Hg_2SO_4; this difference is also equivalent to the heat of reaction (a) since the heats of formation of the elements, Cd and Hg, in their standard states are zero.[5] However, Cohen et al. arrived at their value for the heat of reaction (a) from combined calorimetric and emf data. They obtained their value by combining the value for the heat of solution of $CdSO_4$ in water at 18 °C to give a solution 2.559 percent in $CdSO_4$ with the value for the heat of reaction of an unsaturated standard cell (2.559% in $CdSO_4$) which they obtained from the observed emf of the cell at 18 °C and the measured emf-temperature coefficient of the cell at 18 °C.

For our purpose, however, we need to obtain the heat of reaction (a) directly from calorimetric data. This heat value may be obtained from the heats of reaction of Cd and $CdSO_4$ with other substances and of Hg and Hg_2SO_4 with other substances, as outlined by the following equations (unfortunately, most of the data were obtained many years ago). In these equations, the numbers in parentheses indicate, according to convention, the number of moles of water in which the substance is dissolved. Although, according to convention, the moles of water involved in dilution or solution [eqs (a4) and (a5) under Cd and $CdSO_4$, for example] are not included in representing the reaction they are included here so that the equations balance, but are shown in parentheses with an asterisk to indicate that the heat of formation of water is not used in determining the heat of dilution or solution. Likewise, when the water contains KI or $KI+I_2$, it is also shown in parentheses with a superscript to indicate that the heat of formation of this water, containing KI or $KI+I_2$, is not used in determining the heat of dilution or solution (in the summation of the following reactions this quantity cancels). Also, in each case the values reported in calories were first converted to international joules using the factor used by the individual authors; these were then converted to absolute joules using the factor 1.000167 and these in turn were then converted (for comparison purposes) to calories using the presently accepted thermochemical definition of the calorie (see footnote 3) and are designated by the symbol *cf* meaning conversion factor. Also in the equations that follow, s = solid, l = liquid, and g = gas. The numbers in parentheses after each value for ΔH denote the ± uncertainty, discussed later.

[4] This is the type of standard cell presently used in the maintenance of the unit of emf in National Laboratories.

[5] Calorie is retained for the unit of energy when the literature is cited. More is given on this point including the use of SI later in this paper. The thermochemical calorie is presently defined in terms of the joule by the relation given in footnote 3.

Cd and $CdSO_4$

(a1) $Cd(s) + 2\ HCl(200) \rightarrow CdCl_2(400) + H_2(g)$

$\Delta H_1(20\ °C) = -17{,}230(70)\ cal\ mol^{-1} = -72{,}033(293)\ J\ mol^{-1}$ [8]
$\Delta H_1(18\ °C) = -17{,}290(90)\ cal\ mol^{-1} = -72{,}284(377)\ J\ mol^{-1}$ [8]
$\Delta H_1(18\ °C)^{cf} = -17{,}276(90)\ cal\ mol^{-1} = -72{,}284(377)\ J\ mol^{-1}$

(a2) $CdCl_2(400) + BaSO_4(s) \rightarrow CdSO_4(200) + BaCl_2(200)$

$\Delta H_2(19\ °C) = 5{,}683(55)\ cal\ mol^{-1} = 23{,}742(230)\ J\ mol^{-1}$ [9]
$\Delta H_2(18\ °C) = 5{,}793(60)\ cal\ mol^{-1} = 24{,}201(251)\ J\ mol^{-1}$ [10, 11]
$\Delta H_2(18\ °C)^{cf} = 5{,}784(60)\ cal\ mol^{-1} = 24{,}201(251)\ J\ mol^{-1}$

(a3) $BaCl_2(400) + H_2SO_4(400) \rightarrow BaSO_4(s) + 2\ HCl(400)$

$\Delta H_3(19\ °C) = -9{,}152(55)\ cal\ mol^{-1} = -38{,}234(230)\ J\ mol^{-1}$ [9]
$\Delta H_3(18\ °C) = -9{,}262(60)\ cal\ mol^{-1} = -38{,}694(251)\ J\ mol^{-1}$ [10, 11]
$\Delta H_3(18\ °C)^{cf} = -9{,}248(60)\ cal\ mol^{-1} = -38{,}694(251)\ J\ mol^{-1}$

(a4) $BaCl_2(200) + (200\ H_2O)^* \rightarrow BaCl_2(400)$

$\Delta H_4(18\ °C) = -50(1)\ cal\ mol^{-1} = -209(4)\ J\ mol^{-1}$ [12]
$\Delta H_4(18\ °C)^{cf} = -50(1)\ cal\ mol^{-1} = -209(4)\ J\ mol^{-1}$

(a5) $2\ HCl(400) \rightarrow 2\ HCl(200) + (400\ H_2O)^*$

$\Delta H_5(18\ °C) = 120(2)\ cal\ mol^{-1} = 502(8)\ J\ mol^{-1}$ [12]
$\Delta H_5(18\ °C)^{cf} = 120(2)\ cal\ mol^{-1} = 502(8)\ J\ mol^{-1}$

(a6) $H_2SO_4(222) + (178\ H_2O)^* \rightarrow H_2SO_4(400)$

$\Delta H_6(18\ °C) = -303(3)\ cal\ mol^{-1} = -1{,}268(12)\ J\ mol^{-1}$ [12]
$\Delta H_6(18\ °C)^{cf} = -303(3)\ cal\ mol^{-1} = -1{,}268(12)\ J\ mol^{-1}$

(a7) $CdSO_4(400) \rightarrow CdSO_4(s) + (400\ H_2O)^*$

$\Delta H_7(18\ °C) = 10{,}690(25)\ cal\ mol^{-1} = 44{,}756(105)\ J\ mol^{-1}$ [7]
$\Delta H_7(18\ °C)^{cf} = 10{,}697(25)\ cal\ mol^{-1} = 44{,}756(105)\ J\ mol^{-1}$

(a8) $CdSO_4(200) + (200\ H_2O)^* \rightarrow CdSO_4(400)$

$\Delta H_8(18\ °C) = -206(2)\ cal\ mol^{-1} = -862(8)\ J\ mol^{-1}$ [12]
$\Delta H_8(18\ °C)^{cf} = -206(2)\ cal\ mol^{-1} = -862(8)\ J\ mol^{-1}$

sum: $Cd(s) + H_2SO_4(222) \rightarrow CdSO_4(s) + H_2(g) + (222\ H_2O)^*$

$\Delta H_{1-8}(18\ °C)^{cf} = -10{,}482(69)\ cal\ mol^{-1} = -43{,}858(289)\ J\ mol^{-1}$

Hg and Hg_2SO_4

(a9) $Hg_2SO_4(s) + 2\ KI(694)^{\#} \rightarrow Hg(l) + HgI_2(694)^{\#} + K_2SO_4(694)^{\#}$

$^{\#}$ — contains 5.25 moles of KI

$\Delta H_9(14\ °C) = -44{,}100(560)\ cal\ mol^{-1} = -184{,}236(2339)\ J\ mol^{-1}$ [13]

(a10) $HgI_2(858)^{\phi} \rightarrow Hg(l) + I_2(858)^{\phi}$

ϕ — contains 6.5 moles of KI and 1.0 mole of I_2

$\Delta H_{10}(14\ °C) = 31{,}300(400)\ cal\ mol^{-1} = 130{,}762(1671)\ J\ mol^{-1}$ [13]

(a11) $I_2(858)^{\phi} \rightarrow I_2(s) + (858\ H_2O)^{\phi *}$

$^{\phi}$ – contains 6.5 moles of KI and 1.0 mole of I_2

$\Delta H_{11}(14\ °C) = -200(2)$ cal $mol^{-1} = -835(8)$ J mol^{-1} [13]

sum of (a9), (a10), and (a11): $Hg_2SO_4(s) + 2\ KI(694)^{\#} + HgI_2(858) \rightarrow$
$2\ Hg(l) + HgI_2(1123)^{\alpha} + K_2SO_4(1123)^{\alpha} + I_2(s)$

α – contains 8.5 moles of KI and 0.5 mole of I_2

$\Delta H_{9-11}(14\ °C) = -13{,}000(162)$ cal $mol^{-1} = -54{,}309(676)$ J mol^{-1}
$\Delta H_{9-11}(18\ °C) = -12{,}844(172)$ cal $mol^{-1} = -53{,}658(718)$ J mol^{-1} [10, 11, 14, 15]
$\Delta H_{9-11}(18\ °C)^{cf} = -12{,}825(172)$ cal $mol^{-1} = -53{,}658(720)$ J mol^{-1}

(a12) $HgI_2(1123)^{\alpha} \rightarrow HgI_2(858)^{\phi} + (265\ H_2O)^{\beta *}$

β – contains 2 moles of KI

$\Delta H_{12}(18\ °C) = -2(0.1)$ cal $mol^{-1} = -8(0.4)$ J mol^{-1} [12]
$\Delta H_{12}(18\ °C)^{cf} = -2(0.1)$ cal $mol^{-1} = -8(0.4)$ J mol^{-1}

(a13) $Cl_2(g) + H_2(g) \rightarrow 2\ HCl(g)$

$\Delta H_{13}(18\ °C) = -44.120(24)$ cal $mol^{-1} = -184.644(100)$ J mol^{-1} [16]
$\Delta H_{13}(18\ °C)^{cf} = -44{,}131(24)$ cal $mol^{-1} = -184{,}644(100)$ J mol^{-1}

(a14) $I_2(s) + 2\ HCl(g) \rightarrow 2\ HI(g) + Cl_2(g)$

$\Delta H_{14}(22\ °C) = 55.933(100)$ cal $mol^{-1} = 233{,}985(418)$ J mol^{-1} [17]
$\Delta H_{14}(18\ °C) = 55{,}949(110)$ cal $mol^{-1} = 234{,}053(460)$ J mol^{-1} [10, 18]
$\Delta H_{14}(18\ °C)^{cf} = 55{,}940(110)$ cal $mol^{-1} = 234{,}053(460)$ J mol^{-1}

(a15) $2\ HI(g) + (222\ H_2O)^{*} \rightarrow 2\ HI(111)$

$\Delta H_{15}(18\ °C) = -38{,}344(50)$ cal $mol^{-1} = -160{,}431(209)$ J mol^{-1} [12]
$\Delta H_{15}(18\ °C)^{cf} = -38{,}344(50)$ cal $mol^{-1} = -160{,}431(209)$ J mol^{-1}

(a16) $2\ HI(100) + 2\ KOH(100) \rightarrow 2\ KI(200) + 2\ H_2O(l)$

$\Delta H_{16}(20\ °C) = -27{,}830(20)$ cal $mol^{-1} = -116{,}349(84)$ J mol^{-1} [19]
$\Delta H_{16}(18\ °C) = -28{,}034(29)$ cal $mol^{-1} = -117{,}202(121)$ J mol^{-1} [19]
$\Delta H_{16}(18\ °C)^{cf} = -28{,}012(29)$ cal $mol^{-1} = -117{,}202(121)$ J mol^{-1}

(a17) $2\ KOH(111) + 2\ HI(111) + 2\ KI(200) \rightarrow 2\ KOH(100) + 2\ HI(100) + 2\ KI(222)$

$\Delta H_{17}(18\ °C) = 16(1)$ cal $mol^{-1} = 67(4)$ J mol^{-1} [12]
$\Delta H_{17}(18\ °C)^{cf} = 16(1)$ cal $mol^{-1} = 67(4)$ J mol^{-1}

(a18) $2\ KI(222) + (944\ H_2O)^{\gamma *} \rightarrow 2\ KI(694)^{\#}$

γ – contains 10.5 moles of KI

$\Delta H_{18}(18\ °C) = 115(1)$ cal $mol^{-1} = 481(4)$ J mol^{-1} [12]
$\Delta H_{18}(18\ °C)^{cf} = 115(1)$ cal $mol^{-1} = 481(4)$ J mol^{-1}

(a19) $K_2SO_4(277.5) + 2\ H_2O(l) \rightarrow H_2SO_4(55.5) + 2\ KOH(111)$

$\Delta H_{19}(17\ °C) = 32{,}966(300)$ cal $mol^{-1} = 137{,}930(1255)$ J mol^{-1} [20]
$\Delta H_{19}(18\ °C) = 32{,}907(310)$ cal $mol^{-1} = 137{,}683(1297)$ J mol^{-1} [10, 14, 15]
$\Delta H_{19}(18\ °C)^{cf} = 32{,}907(310)$ cal $mol^{-1} = 137{,}683(1297)$ J mol^{-1}

(a20) $H_2SO_4(55.5) + (166.5\ H_2O)^* \rightarrow H_2SO_4(222)$

$\Delta H_{20}(18\ °C) = -390(10)$ cal mol^{-1} $= -1{,}632(42)$ J mol^{-1} [12]
$\Delta H_{20}(18\ °C)^{cf} = -390(10)$ cal mol^{-1} $= -1{,}632(42)$ J mol^{-1}

(a21) $K_2SO_4(1123) \rightarrow K_2SO_4(277.5) + (845.5\ H_2O)^{\delta *}$

δ – contains 8.5 moles of KI

$\Delta H_{21}(18\ °C) = -195(2)$ cal mol^{-1} $= -816(8)$ J mol^{-1} [12]
$\Delta H_{21}(18\ °C)^{cf} = -195(2)$ cal mol^{-1} $= -816(8)$ J mol^{-1}

sum: $Hg_2SO_4(s) + H_2(g) + (222\ H_2O)^* \rightarrow 2\ Hg(l) + H_2SO_4(222)$

$\Delta H_{9-21}(18\ °C)^{cf} = -34{,}921(135)$ cal mol^{-1} $= -146{,}109(565)$ J mol^{-1}

Cd, $CdSO_4 - Hg_2SO_4$, Hg

sum: $Cd(s) + Hg_2SO_4(s) \rightarrow CdSO_4(s) + 2\ Hg(l)$

$\Delta H_{1-21}(18\ °C)^{cf} = -45{,}403(66)$ cal mol^{-1} $= -189{,}967(276)$ J mol^{-1}
$= -45{,}403(397)$ cal mol^{-1} $= -189{,}967(1661)$ J mol^{-1}

It should be noted here that two uncertainties are given; these are discussed later under overall uncertainties. This value for $\Delta H_{1-21}(18\ °C)^{cf}$ may be converted to a value at 25 °C by using known values of the heat capacities of Cd(s) [10], $Hg_2SO_4(s)$ [14], $CdSO_4(s)$ [21, 22] and Hg(l) [14], as a function of temperature, namely[6]:

$$C_p[Cd(s)] = (5.333 + 0.00294\,T) \text{ cal mol}^{-1} \quad (14)$$

$$C_p[Hg_2SO_4(s)] = (13.8 + 0.060\,T) \text{ cal mol}^{-1} \quad (15)$$

$$C_p[CdSO_4(s)] = (10.771 + 0.0437\,T) \text{ cal mol}^{-1} \quad (16)$$

$$C_p[Hg(l)] = (7.368 - 0.0023\,T) \text{ cal mol}^{-1} \quad (17)$$

$$\Delta C_p[\text{reaction (a)}] = (6.374 - 0.02384\,T) \text{ cal mol}^{-1} \quad (18)$$

all of which may be expressed in J mol^{-1} using the relation given in footnote 3. The heat of reaction (a) at 25 °C is then found to be −45,407 cal mol^{-1} or −189,983 J mol^{-1}. Incidentally, the data of Bichowsky and Rossini [12] for the overall reaction lead to −45,720 cal mol^{-1} at 18 °C or −45,716 cal mol^{-1} at 25 °C (on the presently accepted definition of the calorie) for ΔH for reaction (a); NBS Circular 500 [23] gives −44,021 cal mol^{-1} at 25 °C while revised NBS Circular [24] gives −45,450 cal mol^{-1}; this last value agrees within 43 cal mol^{-1} of the overall sum given above. These latter values [12, 23, 24] are combinations of heat and emf data.

Notes on some of the above reactions should be given here. Richards and Tamaru [8] found that the temperature coefficient of the heat of solution of cadmium in concentrated HCl was −71 cal/°C and believed that even for dilute acid it amounted to as much as −30 cal/°C. Since reaction (a1) is for dilute acid −30 cal/°C is taken for the temperature coefficient; owing to the estimation made by Richards and Tamaru a large uncertainty of ±10 cal/°C is attributed to this value.

Thomsen [9] stated that the temperature of his observations for reactions (a2) and (a3) was 18–20 °C. A mean temperature of 19 °C is taken here, and Thomsen's values were corrected to 18 °C using the known heat capacity of $BaSO_4(s)$ [10] as a function of temperature and the heat capacities of the Ba^{++} and $SO_4^{=}$ ions at 25 °C given by Pitzer and Brewer [11] (these latter values were assumed to be temperature and concentration independent). Since the difference of (a2) and (a3) is taken in arriving at the value for the overall reaction, an error in this temperature correction is negligible.

The temperature correction for the sum of the reactions (a9), (a10), and (a11) was obtained from the known heat capacities of $Hg_2SO_4(s)$ [14], Hg(l) [14], and $I_2(s)$ [10] as functions of temperature and of KI, HgI_2, and K_2SO_4 as functions of concentration and temperature as follows. The heat capacity of HgI_2 was taken equal to that of KI (since it was dissolved in KI solutions) and that of K_2SO_4 as equal to 0.917 times twice the heat capacity of KOH (the temperature coefficient for K_2SO_4 was taken equal to that for KOH). The factor 0.917 is the ratio of the heat capacity of 2KOH and K_2SO_4 at infinite dilution; the value for $SO_4^{=}$ was taken from the compilation of Pitzer and Brewer [11]. The heat capacities of aqueous solutions of KI and KOH at 25 °C, as a function of concentration, were taken from the compilation of Parker [15]. The temperature coefficient for HCl was used for the temperature coefficient of KI and the temperature coefficient of NaOH was used for the temperature coefficient for KOH [15]. These values lead to:

$$\Delta C_p[\text{sum of reactions (a9), (a10), (a11)}] = -579.9 + 2.14\,T \quad (19)$$

[6] Each equation was altered slightly to make it conform with the values in reference [24] at 25 °C.

for the change in heat capacity for the sum of reactions (a9), (a10), and (a11). The estimated uncertainty for equation (19) is ±10 cal/°C.

The temperature correction for reaction (a14) was obtained using the known heat capacities of I_2(s) [10], HCl(g) [18], HI(g) [18], and Cl_2(g) [10] as functions of temperature, or:

$$\Delta C_p\,[\text{reaction (a14)}] = -0.84 - 0.0101\,T - 76000/T^2 \quad (20)$$

An uncertainty of ±10 cal/°C is assigned to this temperature correction.

Richards and Rowe [19] found an average of −50.9 cal/°C for the temperature coefficient for the neutralization of HCl(100) and of HNO_3(100) with LiOH(100), NaOH(100), and KOH(100). This average temperature coefficient is assumed here to also apply to the neutralization of KOH(100) with HI(100) with an uncertainty of ±9 cal/°C, the spread found between the values found for the neutralization of HCl(100) and of HNO_3(100) with KOH(100).

Müller [20] measured the neutralization of H_2SO_4(55.5) with potassium hydroxide of various dilutions (one mole of KOH in 13.508, 27.420, and 51.626 liters of water) at 17 °C. A value for the heat of neutralization of H_2SO_4(55.5) with one mole of KOH in 2 liters of water was obtained by extrapolation of ΔH (neutralization) against $\sqrt{\text{volume}}$; ΔH (neutralization) versus $\sqrt{\text{volume}}$ is a straight line over the range of observations made by Müller. An uncertainty of ± 150 cal/°C per mole of KOH(111) is assigned to this heat of reaction owing to the spread in the three values obtained by Müller. This neutralization value is much higher than the older values of Thomsen [9] and Berthelot [25]. The older values were probably low because of the presence of carbonate in the alkali as has been shown for similar cases by Keyes, Gillespie, and Mitsukuri [26]. The value was corrected to 18 °C, with an estimated additional uncertainty of ±10 cal/°C using the known heat capacity of water [14][7] as a function of temperature and of H_2SO_4, KOH, and K_2SO_4 as functions of concentration and temperature using the procedure discussed above in obtaining the temperature coefficient for the sum of the reactions (a9), (a10), and (a11). These values lead to

$$\Delta C_p\,[(\text{reaction (a19)}] = 574.17 - 1.772\,T \quad (21)$$

for the change in heat capacity for reaction (a19).

For the reactions (a13) and (a14) the uncertainties given in the parentheses are the ± uncertainties given by the experimenters. In the other cases the experimenters were not explicit on their experimental uncertainties. For (a1), Richards and Tamaru [8] stated that the maximum uncertainty if all errors were additive, which would be highly unlikely, would be 70 cal mol^{-1}, and that the probable error was undoubtedly much less. Their maximum uncertainty is retained here and an additional uncertainty of ±10 cal/°C is assigned to the temperature coefficient. The uncertainties assigned to (a2) and (a3) were deduced from the temperature correction, i.e., were taken as one half the correction. For (a7), Cohen, Helderman and Moesveld [7] made eight determinations of the heat evolved; the standard deviation of their mean value is 7 cal mol^{-1}. The average spread in their values is taken, however, as the overall uncertainty. For (a10) Varet gave a general value which differs from that given above for (a10) by 400 cal mol^{-1}; this is taken as the uncertainty and the same percentage uncertainty is assigned to (a9), a reaction also studied by Varet. For (a16) Richards and Rowe stated that the maximum uncertainty in their value was 0.07 percent, and is used here. The estimated uncertainty for (a19) was discussed above. The uncertainties for the other reactions, which are mostly ones for solution or dilution, are estimated ones.

The overall uncertainty value is obtained from the sum of the uncertainties for each reaction taking care of sign. An overall uncertainty may also be taken as the root sum square value of the uncertainties of the 21 reactions, namely 397 cal mol^{-1} or 1661 J mol^{-1} and is the second uncertainty given above. The actual uncertainty probably lies between these two estimates. A root mean square value of the uncertainty is 88 cal mol^{-1} or 368 J mol^{-1}; this value of the uncertainty is close to the first one listed above.

Values for the entropy of Cd(s), Hg_2SO_4(s), $CdSO_4$(s), and Hg(l) at 25 °C are 12.37 [27], 47.96 [24], 29.41 [21], and 18.19 [27] cal K^{-1} mol^{-1}, or 51.75, 200.66, 123.05, and 76.02 J K^{-1} mol^{-1}, respectively. Therefore, ΔS_a for reaction (a) is 5.42 cal K^{-1} mol^{-1} or 22.68 J K^{-1} mol^{-1}. This value combined with the valuc of ΔH_a, given above, gives according to eq (1) −47.023 cal mol^{-1} or −196,745 J mol^{-1} for the Gibbs energy (free energy) change, ΔG_a, for reaction (a). Since $\Delta G = -nEF$ [see eq (4)] E would be 1.0195396 V at 25 °C for the standard cell of the saturated cadmium sulfate type, if the cell reaction were as depicted by reaction (a). Also, since $\Delta S = nF(dE/dT)$ [see eq (6)], dE/dT for the cell at 25 °C would be 0.00011751 V/°C, if the cell reaction were as depicted by reaction (a). Since these values do not agree with the observed ones (see later) it follows that the cell reaction does not correspond to reaction (a).

The heat capacities at 25 °C of Cd(s), Hg_2SO_4(s), $CdSO_4$(s), and Hg(l) are, respectively, 6.21 [24], 31.54 [24], 23.806 [24], and 6.688 [24] cal K^{-1} mol^{-1} or 25.90, 132.00, 99.62, and 27.82 J K^{-1} mol^{-1}; ΔC_p is therefore, −0.580 cal K^{-1} mol^{-1} or −2.427 J K^{-1} mol^{-1}. Stull and Sinke [27] give 6.19 cal K^{-1} mol^{-1} for Cd(s). Papadopoulos and Giauque [21] give 23.806 cal K^{-1} mol^{-1} for $CdSO_4$(s), and Giauque, Barieau and Kunzler [14] give 31.689 and 6.702 cal K^{-1} mol^{-1} for Hg_2SO_4(s) and Hg(l), respectively. These values yield −0.669 cal K^{-1} mol^{-1} or −2.799 J K^{-1} mol^{-1} for ΔC_p(a).

Reaction (b)

The Gibbs energy change for reaction (b) is given by:

[7] Equation given in reference [14] was altered slightly to make equation consistent with the 25 °C value given in reference [22].

$$\Delta G_b = RT \ln \frac{p^*}{p^0} = RT \ln \frac{0.62}{23.7667}$$

$$= -2160 \text{ cal mol}^{-1} = -9037 \text{ J mol}^{-1} \qquad (22)$$

where p^0 is the vapor pressure of water at 25 °C [28], p^* the vapor pressure of the system $CdSO_4 \cdot H_2O - H_2O$, T the Kelvin temperature, and R the gas constant (1.98717 cal K^{-1} mol^{-1} or 8.3143 J K^{-1} mol^{-1} [1]). Ishikawa and Murooka [29] obtained 0.62 mm Hg for p^*. The values in mm Hg may be converted to pascals by the relation 1 mm Hg (0 °C) = 1.333224 $\times 10^2$ pascals.

The entropies for $CdSO_4$(s), H_2O(l), and $CdSO_4 \cdot H_2O$(s) at 25 °C are, respectively, 29.41 [21], 16.71 [24], and 36.82 [21] cal K^{-1} mol^{-1} or 123.05, 69.91, 154.05 J K^{-1} mol^{-1}; therefore, ΔS_b for reaction (b) is -9.30 cal K^{-1} mol^{-1} or -38.91 J K^{-1} mol^{-1}. This value combined with the value for ΔG_b above gives by eq (1) -4.933 cal mol^{-1} or -20.640 J mol^{-1} for ΔH_b, the heat of reaction for reaction (b). Papadopoulos and Giauque [21] measured the heats of solution of $CdSO_4$(s) and $CdSO_4 \cdot H_2O$(s) in 400 moles of water at 25 °C for which they obtained $-10{,}977$ and -6095 cal mol^{-1} or -45.928 and -25.501 J mol^{-1}, respectively. These yield $-4{,}882$ cal mol^{-1} or -20.426 J mol^{-1} for ΔH_b which differs by 51 cal mol^{-1} or 214 J mol^{-1} from that calculated above.

The heat capacities of $CdSO_4$(s), H_2O(l), and $CdSO_4 \cdot H_2O$(s) at 25 °C are, respectively, 23.806 [21], 17.995 [30], and 32.157 [21] cal K^{-1} mol^{-1} or 99.58, 75.29, and 134.544 J K^{-1} mol^{-1}; therefore, $\Delta C_{p(b)}$ for reaction (b) is -9.644 cal K^{-1} mol^{-1} or -40.350 J K^{-1} mol^{-1}.

Reaction (c)

The Gibbs energy change for reaction (c) is given by:

$$\Delta G_c = \frac{5}{3} RT \ln \frac{p^{**}}{p^0} = \frac{5}{3} RT \ln \frac{17.4}{23.7667}$$

$$= -308 \text{ cal} = -1289 \text{ J} \qquad (23)$$

where p^{**} is the vapor pressure of the system $CdSO_4 \cdot \frac{8}{3} H_2O - CdSO_4 \cdot H_2O$ and p^0, T, and R have the same significance as given above. The average of the results of Ishikawa and Murooka [29] and of Carpenter and Jette [31] gives 17.4 mm Hg for p^{**}. Conversion to pascals may be done as stated above.

The entropies for $CdSO_4 \cdot H_2O$(s) and H_2O(l) have been given above. The entropy of $CdSO_4 \cdot \frac{8}{3} H_2O$(s) is 54.89 [21] cal K^{-1} mol^{-1} or 229.66 J K^{-1} mol^{-1}. ΔS_c is, therefore, -9.78 cal K^{-1} mol^{-1} or -40.92 J K^{-1} mol^{-1}. This value combined with the value for ΔG_c given above gives by eq (1) $-3{,}224$ cal or $-13{,}489$ J for ΔH_c, the heat of reaction for reaction (c). Papadopoulos and Giauque [21] measured the heats of solution of $CdSO_4 \cdot H_2O$(s) and $CdSO_4 \cdot \frac{8}{3} H_2O$(s) in 400 moles of water at 25 °C for which they obtained $-6{,}095$ and $-2{,}899$ cal mol^{-1} or $-25{,}502$ and $-12{,}129$ J mol^{-1}, respectively. These yield $-3{,}196$ cal mol^{-1} or $-13{,}372$ J mol^{-1} for ΔH_c which differs by 28 cal mol^{-1} or 117 J mol^{-1} from that calculated above.

The heat capacities of $CdSO_4 \cdot H_2O$(s) and H_2O(l) have been given above. The heat capacity of $CdSO_4 \cdot \frac{8}{3} H_2O$(s) at 25 °C is 50.972 cal K^{-1} mol^{-1} [21] or 213.26 J K^{-1} mol^{-1}. Therefore, $\Delta C_{p(c)}$ for reaction (c) is -11.177 cal or -46.765 J.

Reaction (d)

The Gibbs energy change for reaction (d) is given by:

$$\Delta G_d = \frac{8}{3} RT \ln \frac{p^0}{p^s} = \frac{8}{3} RT \ln \frac{23.7667}{21.17} = 184 \text{ cal} = 770 \text{ J} \qquad (24)$$

where p^s is the vapor pressure of a saturated solution of $CdSO_4 \cdot \frac{8}{3} H_2O$ and p^0, T, and R have the significance given above. Ishikawa and Murooka [29] obtained 21.17 mm Hg for the vapor pressure of the saturated solution at 25 °C; this value may be converted to pascals as described above. Holsboer [32] found that 1,044 calories or 4,368 joules of heat were evolved when one mole of $CdSO_4 \cdot \frac{8}{3} H_2O$(s) was dissolved in enough water to form the saturated solution at 25 °C; for (8/3)/(m − 8/3) mole of salt the heat evolved would be 224 cal or 938 J since $m = 15.089$ [5, 6] at 25 °C and (8/3)/(m − 8/3) = 0.2147. Combining these values for ΔG_d and ΔH_d gives 0.13 cal K^{-1} or 0.544 J K^{-1} for ΔS_d, the entropy change for reaction (d).

Cohen and Moesveld [33] obtained 0.5836 cal g^{-1} or 2.4414 J g^{-1} for the specific heat of a saturated solution of $CdSO_4 \cdot \frac{8}{3} H_2O$ at 19 °C which becomes 0.5823 cal g^{-1} or 2.4359 J g^{-1} at 25 °C based on the higher concentration of the saturated solution at 25 °C and the ratio of the specific heat of water at 25 and 19 °C. Accordingly (8/3)/(m − 8/3) mole of a saturated solution of $CdSO_4 \cdot \frac{8}{3} H_2O$ has a heat capacity of 59.93 cal K^{-1} or 250.705 J K^{-1} at 25 °C; on the present thermochemical calorie the value is 59.92 cal K^{-1} or 250.706 J K^{-1}. Combining this value with the heat capacity of H_2O(l) and $CdSO_4 \cdot \frac{8}{3} H_2O$(s), given above, gives -0.999 cal K^{-1} or -4.180 J K^{-1} for $\Delta C_{p(d)}$ for reaction (d).

The above values are summarized in tables 1 and 2; data are given in SI units in the first section of each table and in defined calories in the second section. Table 1 is based on experimental values for the Gibbs energy changes for reactions (b), (c), and (d) and the enthalpy changes for reactions (a) and (d). Table 2 is based on experimental values for the Gibbs energy change of reaction (d) and the enthalpy changes of reactions (a), (b), (c), and (d). The addition of these values for reactions (a), (b), (c), and (d) gives sum 1 or the values for the reaction in a standard cell of the

TABLE 1. *Thermodynamic data for the reaction in standard cells of the saturated cadmium sulfate type at 25 °C—based on experimental Gibbs energies for reactions (b), (c), and (d) and experimental enthalpies for reactions (a) and (d)*

Reaction	Gibbs energy change	Enthalpy change	Entropy change	Heat-capacity change
	ΔG J mol^{-1}	ΔH J mol^{-1}	ΔS J K^{-1} mol^{-1}	ΔC_p J K^{-1} mol^{-1}
(a).....	#(−196,745)	−189,983	22.68	ϕ−2.427
(b).....	−9,037	(−20,640)	−38.91	−40.350
(c).....	−1,289	(−13,489)	−40.92	−46.765
(d).....	770	937	(0.544)	−4.180
sum 1.....	−206,301	−223,175	−56,606	−93.722
(e)*	9,743	23,764	47.03	0
sum 2[p].....	−196,558	−199,411	−9.576	−93.722
(e)**.....	9,738	21,240	38.58	204.26
sum 3[q].....	−196,563	−201,935	−18.026	110.538
	(cal mol^{-1})[j]	cal mol^{-1}	cal K^{-1} mol^{-1}	cal K^{-1} mol^{-1}
(a).....	(−47,023)	−45,407	5.42	ϕ−0.580
(b).....	−2,160	(−4,933)	−9.30	−9.644
(c).....	−308	(−3,224)	−9.78	−11.177
(d).....	184	224	(0.13)	−0.999
sum 1.....	−49,307	−53,340	−13.53	−22.400
(e)*.....	2,328.6	5,679.8	11.24	0
sum 2[p].....	−46,978.4	−47,660.2	−2.29	−22.400
(e)**.....	2,327.5	5,076.4	9.22	48.82
sum 3[q].....	−46,979.5	−48,263.6	−4.31	26.420

Values in parentheses were calculated from the relation $\Delta G = \Delta H - T\Delta S$.
ϕ See text for alternate value of −2.799 J K^{-1} mol^{-1} or −0.669 cal K^{-1} mol^{-1}.
* Based on data of Hulett [34] and Getman [35].
[p] Sum 1 + (e)*.
** Based on data of Parks and LaMer [39].
[q] Sum 1 + (e)**.
[j] 1 Thermochemical calorie (defined) = 4.184 J [1].

TABLE 2. *Thermodynamic data for the reaction in standard cells of the saturated cadmium sulfate type at 25 °C—based on experimental enthalpies for reactions (a), (b), (c), and (d) and experimental Gibbs energy for reaction (d)*

Reaction	Gibbs energy change	Enthalpy change	Entropy change	Heat-capacity change
	ΔG J mol^{-1}	ΔH J mol^{-1}	ΔS J K^{-1} mol^{-1}	ΔC_p J K^{-1} mol^{-1}
(a).....	#(−196,745)	−189,983	22.68	ϕ−2.402
(b).....	(−8,824)	−20,426	−38.91	−40.350
(c).....	(−1,171)	−13,372	−40.92	−46.765
(d).....	770	937	(0.544)	−4.180
sum 1.....	−205,970	−222,844	−56,606	−93.722
(e)*.....	9,743	23,764	47.03	0
sum 2[p].....	−196,227	−199,080	−9.576	−93.722
(e)**.....	9,738	21,240	38.58	204.26
sum 3[q].....	−196,232	−201,604	−18.026	110.538
	(cal mol^{-1})[j]	cal mol^{-1}	cal K^{-1} mol^{-1}	cal K^{-1} mol^{-1}
(a).....	(−47,023)	−45,407	5.42	ϕ−0.580
(b).....	(−2,109)	−4,882	−9.30	−9.644
(c).....	−280	−3,196	−9.78	−11.177
(d).....	184	224	(0.13)	−0.999
sum 1.....	−49,228	−53,261	−13.53	−22.400
(e)*.....	2,328.6	5,679.8	11.24	0
sum 2[p].....	−46,899.4	−47,581.2	−2.29	−22.400
(e)**.....	2,327.5	5,076.4	9.22	48.82
sum 3[q].....	−46,900.5	−48,184.6	−4.31	26.420

Values in parentheses were calculated from the relation $\Delta G = \Delta H - T\Delta S$.
ϕ See text for alternate value of −2.799 J K^{-1} mol^{-1} or −0.669 cal K^{-1} mol^{-1}.
* Based on data of Hulett [34] and Getman [35].
[p] Sum 1 + (e)*.
** Based on data of Parks and LaMer [39].
[q] Sum 1 + (e)**.
[j] 1 Thermochemical calorie (defined) = 4.184 J [1].

saturated cadmium sulfate type at 25 °C if the anode were made of cadmium metal rather than cadmium amalgam.

Reaction (e)

Calorimetric and chemical equilibrium measurements on reaction (e) have not been made. It is necessary, therefore, to rely on electrochemical measurements for information on reaction (e). Hulett [34] and Getman [35] measured the emf of the cell:

$$(-)\,\mathrm{Cd(metal)}\,|\,\mathrm{CdSO_4(sol)}\,|\,\mathrm{Cd\ amalgam\ (8\text{–}10\%)}\,(+) \quad \text{(A)}$$

at a series of temperatures and obtained:

$$E\ (\text{in volts}) = 0.050487 - 0.0002437\,(t - 25\ ^\circ\mathrm{C}) \quad (25)$$

for the emf as a function of temperature. In cell (A) sol denotes an aqueous solution. Sir Frank Smith [36] showed that 8-percent and 10-percent amalgams have the same electrical potential. Hulett and Getman's emfs, expressed in international volts were converted to absolute volts here using the relation: 1 international volt (USA) = 1.0003384 absolute volts [37, 38]. Their results give 2,328.6 cal mol^{-1}, 5,679.8 cal mol^{-1}, 11.24 cal K^{-1} mol^{-1}, and 0 cal K^{-1} mol^{-1} or 9,742.9 J mol^{-1}, 23,764.2 J mol^{-1}, 47.03 J K^{-1} mol^{-1}, and 0 J K^{-1} mol^{-1} for ΔG_e, ΔH_e, ΔS_e, and $\Delta C_{p(e)}$, respectively, for reaction (e). (Note that reaction (e) is for the reverse reaction of the above cell.) These values are added to sum 1 in tables 1 and 2 to give sum 2 for the thermodynamic data for the reaction at 25 °C in standard cells of the saturated cadmium sulfate type.

Parks and LaMer [39] also measured the emf of the above cell (A) over the temperature range of 0 to 40 °C. They expressed their results by the equation:

$$E\ (\text{in volts}) = 0.055399 - 0.000148\,t - 0.00000385\,t^2 + 0.000000075\,t^3. \quad (26)$$

Their emfs, given in international volts were converted

here to absolute volts using the relation given directly above. Their results lead to 2,327.5 cal mol^{-1}, 5.076.4 cal mol^{-1}, 9,22 cal K^{-1} mol^{-1}, and 48.82 cal K^{-1} mol^{-1} or 9.738.3 J mol^{-1}, 21.239.6 J mol, 38.58 J K^{-1} mol^{-1}, and 204.26 J K^{-1} mol^{-1} for ΔG_e, ΔH_e, ΔS_e, and $\Delta C_{p(e)}$, respectively, for reaction (e) at 25 °C. The value for ΔG_e agrees well with that obtained from Hulett and Getman's data but the values for the other thermodynamic functions do not. These differences are discussed in more detail later. These values are added to sum 1 in tables 1 and 2 give sum 3 for alternate thermodynamic data for the reaction at 25 °C in standard cells of the saturated cadmium sulfate type.

4. Electromotive Force and Emf-temperature Coefficient

The electromotive force of the so-called "neutral" or Normal standard cell was initially determined at 20 °C in terms of the international ohm and the international ampere by an International Committee on Electrical Units and Standards which met at the National Bureau of Standards in 1910.[8] As a result of numerous experiments they arrived at a value of 1.0183 V for the emf of the cell at 20 °C; values derived from this were later assumed to be significant to the fifth, sixth, or seventh decimal as a basis of measurement [5] and subsequent "absolute" measurements of the ohm and ampere confirmed the validity of this process. Somewhat earlier [42, 43, 44] Wolff investigated extensively the emf-temperature coefficient of the "neutral" type of standard cell made with $12\frac{1}{2}$-percent cadmium amalgams. Wolff based his emf-temperature formula (or equation) on the results obtained from 0 to 40 °C, inclusive, on 137 cells, made in various ways, after rejecting the results on 63 cells for a variety of reasons, including cell leakage, abnormal initial emfs, excessive emf-temperature hysteresis, erratic behavior, or chemical instability. Wolff [42] first arrived at the approximate emf-temperature formula:

$$E_t = E_{20\,°C} - 0.0000406(t-20) - 0.00000939(t-20)^2 + 0.000000009(t-20)^3 \quad (27)$$

by the method of least squares on the means of all observations on ten cells selected on the basis of their fast attainment of equilibrium after temperature changes. Using this approximate equation he then determined the residuals for all of the 137 cells at each temperature and calculated the corrections needed for the coefficients in eq (27) above. In this way he arrived at the emf-temperature formula:

$$E_t = E_{20\,°C} - 0.00004064(t-20) - 0.000000942(t-20)^2 + 0.0000000096(t-20)^3 \quad (28)$$

The 137 cells used to obtain eq (28) consisted of seven different groups of cells, namely, (1) 11 cells made with electrolytic mercurous sulfate prepared at low current densities [45], (2) 53 cells made with electrolytic mercurous sulfate prepared at higher current densities [46], (3) 22 cells made with mercurous sulfate prepared chemically in different ways, (4) 19 cells made with various samples of commercial mercurous sulfate, (5) 13 cells made with exchange (gift) samples of electrolytic mercurous sulfate, (6) nine exchange cells (foreign and domestic), and (7) 10 cells made with high current-density electrolytic mercurous sulfate but with different samples of cadmium sulfate synthesized or treated in various ways. Except for group (7) the cadmium sulfate was commercial grade which was recrystallized several times from distilled water.

Wolff [43] later gave a different formula wherein the first, second, and third coefficients in eq (27) or (28) were, respectively, 0.00004075, −0.000000944, and 0.0000000098 (these were uncorrected for residuals, compare data in references [42] and [43]).

The International Conference on Electrical Units and Standards meeting in London in 1908 adopted the formula (since known as the International formula) [47]:

$$E_t = E_{20\,°C} - 0.0000406(t-20) - 0.00000095(t-20)^2 + 0.00000001(t-20)^3 \quad (29)$$

giving weight to Wolff's original (provisional) emf-temperature formula, eq (27) above. It should be noted that practically the same result follows if the data obtained on groups (4) and (6), for which the cells were not well characterized, and on those cells for which the emf-temperature coefficient at 20 °C exceeds one microvolt are eliminated; these eliminations leave 99 cells for evaluation. Using these 99 cells gives:

$$E_t = E_{20\,°C} - 0.00004049(t-20) - 0.000000951(t-20)^2 + 0.00000000962(t-20)^3 \quad (30)$$

Equation (29), the International Temperature Formula, has been confirmed within the experimental uncertainty many times in succeeding years [48–53] for temperatures from 15 to 40 °C. The limits of uncertainty in the equation are discussed later.

Equations (29) and (30) may be given in the alternate forms:

$$E = E_{0\,°C} + 0.0000094\,t - 0.00000155\,t^2 + 0.00000001\,t^3 \quad (31)$$

$$E = E_{0\,°C} + 0.000009094\,t - 0.0000015282\,t^2 + 0.00000000962\,t^3. \quad (32)$$

Vigoureux and Watts [54], Obata and Ishibashi [55], and Ishibashi and Ishizaki [50] also measured the emf-temperature coefficient of standard cells of the saturated cadmium sulfate type. However, their cells were of the "acid" type. i.e., sulfuric acid was added to the cell in small amounts (0.1 *N* for ref. [54] and various amounts for ref. [55] and ref. [50]) and will, therefore, not be considered here. Furthermore, Vigoureux and Watts gave emphasis to measurements below 0 °C.

[8] Some measurements on the emf of standard cells were made earlier (see references [5, 40], and [41]) but these were not standardized internationally in terms of the mechanical units. The term "neutral" cell refers to one in which sulfuric acid, in low concentrations, is not intentionally added to the cell; actually, cadmium sulfate hydrolyzes to give sulfuric acid of 0.00092 N [5].

Obata and Ishibashi made measurements only from 15.6 to 29.6 °C, and Ishibashi and Ishizaki from 15 to 30 °C.

The results of Wolff were expressed in international volts and on the temperature scale based on the constant-volume hydrogen gas thermometer, defined in terms of melting ice (0 °C) and boiling water (100 °C), the hydrogen being taken at an initial manometric pressure of one meter of mercury; realization of the temperature scale was effected through mercurial thermometers calibrated in terms of the gas thermometer [56]. This temperature scale was the same as that adopted as the International Temperature Scale of 1927 [57].

On January 1, 1948 the international volt was replaced by the absolute volt; the change [37] for the United States was 1 international volt (USA)=1.000330 absolute volts. Then on January 1, 1969 another change [38] was made; the factor was: 1 USA volt$_{48}$=1.0000084 USA volt$_{69}$. Accordingly, the total change in going from the old international volt (USA) to the modern absolute volt is: 1 international volt (USA)= 1.0003384 absolute USA volt$_{69}$. In 1948 the International Temperature Scale was revised [57] but differed from the 1927 scale only at temperatures above 630 °C and, therefore, out of the range of work done on standard cells by Wolff. However, in 1968 another revision of the International Temperature Scale was made [58] which did affect the precise value of the emf-temperature coefficient of standard cells; for example, $t_{68}-t_{48}$ is -0.004 °C at 10 °C, -0.007 °C at 20 °C, -0.009 °C at 30 °C and zero at the melting point of ice and the boiling point of water.

In view of the above changes in the basis of reference for the volt and in the International Temperature Scale, changes in the voltage standard and in the results obtained by Wolff on the emf-temperature coefficient become necessary. With these changes eq (29) and the alternate form, eq (31) become, respectively:

$$E = E_{20\,°C} - 0.000004064(t-20) - 0.00000095006(t-20)^2 + 0.000000010034(t-20)^3 \quad (33)$$

and

$$E = E_{0\,°C} + 0.0000094019\,t - 0.0000015521\,t^2 + 0.000000010034\,t^3 \quad (34)$$

In table 3 the thermodynamic data for standard cells of the saturated cadmium sulfate type are given for temperatures from 0 to 43.6 °C [the transition temperature, $CdSO_4 \cdot \frac{8}{3} H_2O(s) = CdSO_4 \cdot H_2O(s)$], inclusive, as calculated from emf data and eq (33) or eq (34). In this table the changes in emf from international to absolute (1948), to absolute (1969), and for the different temperature scales are given. The thermodynamic data given herein are calculated from the most recent values of the emf, i.e., on V_{69} and t_{68}. The emf at 20 °C in column 2 is that recommended by the International Committee on Electrical Units and Standards; it was based on the emf of cells prepared with mercurous sulfate made chemically or by dc electrolysis. Numerous investigations have indicated that mercurous sulfates prepared in different ways, providing they do not contain basic mercurous sulfate or mercuric ions, yield cells of the same emf. However, recent studies to be discussed in a subsequent paper, show that mercurous sulfate prepared by dc electrolysis gives cells with an emf exceeding those in column 5 of table 3 by 16.8 μV. This difference is small and amounts to only 3.24 J mol^{-1} (0.77 cal mol^{-1}) in ΔG and ΔH, see footnote to tables 3, 4, and 10.

The uncertainties listed, 1σ, are mean standard deviations obtained from the data on the 99 cells measured by Wolff, and includes an uncertainty of 5.4 μV[9] arising from the combined uncertainties in the absolute measurement of the ampere and the ohm.

5. Comparisons of Calorimetric and Equilibrium Data With Electrochemical (or Electrical) Data at 25 °C

Comparisons of calorimetric and equilibrium data with electrochemical data are given in table 4 for 25 °C. Insufficient data are available for direct comparisons at other temperatures. Six facts are evident from inspection of the data, namely:

(1) Remarkable agreement is obtained for ΔG, ΔH, and ΔS between the calorimetric and equilibrium data (sum 2) and electrochemical data in Part I if the emf data for cell (A) obtained by Hulett [34] and Getman [35] are used for reaction (e). This agreement may be coincidental in view of the uncertainties in the older heat data or results from a cancellation of errors, but even so it adds weight to the reliability of the postulated chemical reactions for standard cells of the saturated cadmium sulfate type. For example, Harned and Owen [62] state "It should be emphasized . . . that the nature of the chemical reactions, corresponding to a particular electrode, or cell, cannot be determined by electromotive force measurements alone. Cells reactions, no matter how simple and obvious, must be treated as hypothetical until it can be shown that thermodynamic quantities calculated from the electromotive force, $\Delta F[\Delta G]$, ΔH, equilibrium constants, etc. have been checked by other evidence."

(2) The difference of 1.722 J K^{-1} mol^{-1} (0.410 cal K^{-1} mol^{-1}) between the ΔC_p values (sum 2 and electrochemical) may well be accounted for by the data for cell (A) for which ΔC_p is zero. More careful measurements on cell (A) may well show that the emf of this cell as a function of temperature is second- or third-order rather than a linear function.

(3) The data show that the results of Parks and LaMer [39] for cell (A), although they give good agreement with calorimetric data for ΔG, yield

[9] This is a root sum square value. Recently, John Clarke [59] gave the uncertainty as ±2.6 ppm (or μV); this is about one half the root sum square uncertainty in published values for the absolute ampere [60] and the absolute ohm [61].

TABLE 3. *Electromotive forces and thermodynamic data for standard cells of the saturated cadmium sulfate type*

Temperature		Electromotive force, V				Gibbs energy change, ΔG	
°C	Int	Abs_{48} & t_{48}	Abs_{69} & t_{48}	Abs_{69} & t_{68} [b]	$\sigma_m(\mu V)$	(J mol^{-1}) [c]	(cal mol^{-1}) [d]
0	1.0186520	1.0189881	1.0189968	1.0189967	8.14	−196,639.9(4.8)	−46,998.0(1.1)
3	1.0186665	1.0190026	1.0190112	1.0190112	8.12	−196,642.7(4.8)	−46,998.6(1.1)
5	1.0186615	1.0189976	1.0190061	1.0190062	8.10	−196,641.7(4.8)	−46,998.4(1.1)
10	1.0186010	1.0189371	1.0189456	1.0189455	8.08.	−196,630.0(4.8)	−46,995.6(1.1)
15	1.0184780	1.0188141	1.0188226	1.0188224	8.07	−196,606.2(4.8)	−46,989.9(1.1)
18	1.0183773	1.0187133	1.0187219	1.0187216	8.06	−196,586.8(4.8)	−46,985.3(1.1)
20	1.0183000	1.0186360	1.0186445	1.0186442	8.06	−196,571.8(4.8)	−46,981.7(1.1)
25	1.0180745	1.0184105	1.0184190	1.0184185	8.07	−196,528.3(4.8)	−46,971.3(1.1)
28	1.0179195	1.0182554	1.0182639	1.0182634	8.08	−196,498.4(4.8)	−46,964.1(1.1)
30	1.0178090	1.0181448	1.0181533	1.0181528	8.08	−196,477.0(4.8)	−46,959.0(1.1)
35	1.0175110	1.0178467	1.0178552	1.0178547	8.09	−196,419.5(4.8)	−46,945.3(1.1)
40	1.0171880	1.0175236	1.0175323	1.0175317	8.10	−196,357.2(4.8)	−46,930.4(1.1)
43.6 [a]	1.0169446	1.0172797	1.0172886	1.0172878	8.11	−196,310.1(4.8)	−46,919.2(1.1)

Emf-temperature coefficient, $\mu V\ K^{-1}$						Entropy change, ΔS		Enthalpy change, ΔH	
°C	Int	Abs_{48} & t_{48}	Abs_{69} & t_{48}	Abs_{69} & t_{68}	$\sigma_m(\mu V)$	J K^{-1} mol^{-1}	cal K^{-1} mol^{-1}	(J mol^{-1}) [c]	(cal mol^{-1}) [d]
0	9.40	9.40	9.40	9.40	0.14	1.814(.027)	0.433(.006)	−196,147.4(11.8)	−46,880.3(2.8)
3	0.37	0.37	0.37	0.36	.11	0.069(.022)	.017(.005)	−196,624.8(10.4)	−46,994.5(2.5)
5	−5.35	−5.35	−5.36	−5.37	.10	−1.036(.020)	−0.248(.004)	−196,930.1(9.9)	−47,067.4(2.2)
10	−18.60	−18.61	−18.61	−18.63	.06	−3.595(.012)	−0.859(.003)	−197,647.1(7.7)	−47,238.8(2.0)
15	−30.35	−30.36	−30.36	−30.39	.04	−5.864(.008)	−1.402(.002)	−198,295.0(6.6)	−47,393.6(1.7)
18	−36.68	−36.70	−36.70	−36.72	.04	−7.086(.008)	−1.694(.001)	−198,649.3(6.6)	−47,478.2(1.3)
20	−40.60	−40.62	−40.61	−40.64	.04	−7.843(.008)	−1.874(.002)	−198,870.4(6.6)	−47,531.1(1.5)
25	−49.35	−49.37	−49.36	−49.39	.04	−9.531(.008)	−2.278(.002)	−199,370.3(6.6)	−47,650.5(1.6)
28	−53.88	−53.90	−53.89	−53.92	.04	−10.404(.008)	−2.487(.002)	−199,632.2(6.6)	−47,713.1(1.7)
30	−56.60	−56.62	−56.61	−56.63	.04	−10.929(.008)	−2.612(.002)	−199,790.7(6.7)	−47,750.8(1.7)
35	−62.35	−62.37	−62.35	−62.37	.06	−12.036(.012)	−2.877(.002)	−200,128.4(8.0)	−47,831.8(1.8)
40	−66.60	−66.62	−66.59	−66.60	.09	−12.853(.018)	−3.072(.004)	−200,380.6(10.0)	−47,692.1(2.3)
43.6 [a]	−68.73	−68.76	−68.71	−68.72	.13	−13.261(.025)	−3.169(.007)	−200,506.4(12.3)	−47,927.0(3.3)

TABLE 3. *Electromotive etc.*—Continued

°C	Second derivative, d^2E/dT^2, $\mu V\ K^{-1}\ K^{-1}$					Heat-capacity change, ΔC_p	
	Int	Abs_{48} & t_{48}	Abs_{69} & t_{48}	Abs_{69} & t_{68}	$\sigma_m(\mu V)$	J K^{-1} mol^{-1}	cal K^{-1} mol^{-1}
0.....	−3.100	−3.101	−3.102	−3.104	0.010	−163.62(.53)	−39.11(.13)
3.....	−2.920	−2.921	−2.921	−2.924	.008	−155.80(.43)	−37.24(.10)
5.....	−2.800	−2.801	−2.801	−2.803	.008	−150.46(.43)	−35.96(.10)
10.....	−2.500	−2.501	−2.501	−2.502	.006	−136.72(.33)	−32.68(.08)
15.....	−2.200	−2.201	−2.200	−2.201	.003	−122.40(.17)	−29.25(.04)
18.....	−2.020	−2.021	−2.020	−2.021	.001	−113.52(.06)	−27.13(.01)
20.....	−1.900	−1.901	−1.900	−1.900	.001	−107.49(.06)	−25.69(.01)
25.....	−1.600	−1.601	−1.599	−1.599	.001	−92.00(.06)	−21.99(.01)
28.....	−1.420	−1.420	−1.419	−1.418	.002	−82.43(.11)	−19.70(.02)
30.....	−1.300	−1.300	−1.299	−1.298	.003	−75.94(.18)	−18.14(.04)
35.....	−1.000	−1.000	−0.998	−0.997	.006	−59.29(.35)	−14.17(.09)
40.....	−0.700	−0.700	−0.698	−0.696	.008	−42.06(.48)	−10.05(.12)
43.6 [a]...	−0.484	−0.484	−0.481	−0.479	.009	−29.30(.55)	−7.00(.13)

[a] All values at 43.6 °C are extrapolated values.
[b] Based on combined results obtained with chemically-prepared and dc-electrolytic mercurous sulfate; the values are 18.6 μV higher for dc-electrolytic mercurous sulfate alone.
[c] Higher by 3.24 J mol^{-1} for dc-electrolytic mercurous sulfate alone.
[d] Higher by 0.77 cal mol^{-1} for dc-electrolytic mercurous sulfate alone.

results for ΔH, ΔS, and especially ΔC_p (actually of opposite sign) that differ widely from the electrochemical data on standard cells of the saturated cadmium sulfate type. Actually, Parks and LaMer gave too much weight to an apparent curvature in the variation of the emf of cell (A) with temperature.

(4) The enthalpy data of Papadopoulos and Giauque [21] lead to values for ΔG and ΔH that are lower than the electrochemical values by 301.3 J mol^{-1} (71.9 cal mol^{-1}) and 290.0 J mol^{-1} (69.3 cal mol^{-1}), respectively. These differences which amount, respectively, to only 0.16 percent and 0.15 percent, are beyond the uncertainties estimated by Papadopoulos and Giauque. Sometimes cadmium sulfate contains occluded sulfuric acid (especially if digested in sulfuric acid during the purification) which would cause a decrease in ΔG and ΔH for the cell reaction (see conclusions to this paper). Such occlusions could not explain the above differences in ΔG and ΔH between the calorimetric and electromotive force data since the occlusions would have to amount to about 1 molal H_2SO_4 (see conclusions to this paper) which is entirely out of the range of possibility.

(5) If the alternate heat capacity data for reaction (a), discussed above, are used they yield a value for sum 2 which differs more from the electrochemical value than the value given in table 4 (actually, the alternate heat capacity data for reaction (a) yield −94.231 J K^{-1} mol^{-1} (−22.474 cal K^{-1} mol^{-1}) for sum 2 rather than the value shown).

(6) The enthalpy data of Papadoupolos and Giauque [21], if used with the enthalpy data of Bichowsky and Rossini [12], corrected to 25 °C, or the enthalpy data of Circular 500 [23] or the enthalpy data of revised NBS Circular [24, 30] still do not agree with the electrochemical data.

TABLE 4. *Comparison of calorimetric and equilibrium data with electromotive force data*

Part I—Based on table 1: experimental values of ΔG for reactions (b), (c), and (d) and of ΔH for reactions (a) and (b)

Calorimetric and equilibrium data	ΔG J mol^{-1}	ΔH J mol^{-1}	ΔS J K^{-1} mol^{-1}	ΔC_p J K^{-1} mol^{-1}
sum 2	−196,558	−199,411	−9.576	[d] −93.722
sum 3	−196,563	−201,935	−18.026	110.538
Electrochemical data	[a] −196,528.3	[a] −199,370.0	−9.531	−92.00
Calorimetric and equilibrium data	**cal mol^{-1}**	**cal mol^{-1}**	**cal K^{-1} mol^{-1}**	**cal K^{-1} mol^{-1}**
sum 2	−46,978.4	−47,660.2	−2.29	−22.400
sum 3	−46.979.5	−48,263.6	−4.31	26.420
Electrochemical data	[b] −46,971.3	[b] −47,650.5	−2.278	−21.99

TABLE 4. *Comparison etc.*—Continued

Part II—Based on table 2: experimental values of ΔG for reaction (d) and of ΔH for reactions (a), (b), (c), and (d)

Calorimetric and equilibrium data	ΔG J mol^{-1}	ΔH J mol^{-1}	ΔS J K^{-1} mol^{-1}	ΔC_p J K^{-1} mol^{-1}
sum 2	−196,227	−199,080	−9.576	[φ] −93.722
sum 3	−196,232	−201,604	−18.026	110.538
Electrochemical data	[a] −196,528.3	[a] −199,370.0	−9.531	−92.00
Calorimetric and equilibrium data	**cal mol^{-1}**	**cal mol^{-1}**	**cal K^{-1} mol^{-1}**	**cal K^{-1} mol^{-1}**
sum 2	−46,899.4	−47,581.2	−2.29	−22.400
sum 3	−46,900.5	−48,184.6	−4.31	26.420
Electrochemical data	[b] −46,971.3	[b] −47,650.5	−2.278	−21.99

[φ] See tables 1 and 2 for a note on an alternate value.
[a] Higher by 3.24 J mol^{-1} for dc-electrolytic mercurous sulfate.
[b] Higher by 0.77 cal mol^{-1} for dc-electrolytic mercurous sulfate.

6. Range of Precision in Emf Results

In table 3 it is evident that the uncertainties in the data are greater at the two ends of the temperature range. For the emf, these reside in the experimental measurements but for the derived quantities, ΔH, ΔS, and ΔC_p, they may be dependent in addition on the emf-temperature function used to represent the data. Since the emf data available on the standard cell of the saturated cadmium sulfate type are known with high precision they may be used to illustrate the effect an emf-temperature function has on the derived thermodynamic data. Accordingly, the emf data of table 3 were fitted (method of least squares) to second-, third-, and fourth-order equations in the temperature of the form (fourth order shown):

$$E = E_{0\,°C} + \alpha t + \beta t^2 + \gamma t^3 + \delta t^4. \qquad (35)$$

Also, since the literature [11, 62–65] is filled with results on the measurements of the emfs of galvanic cells to only 0.01 mV or 10 μV, and over a range of temperatures, the emf data of table 3 were rounded to 0.01 mV and then fitted (method of least squares) to second-, third-, and fourth-order equations in the temperature of the form of eq (35). The coefficients of the form equations for the several procedures are given in table 5.

Results are given in tables 6, 7, 8, and 9. In table 6 the emfs are given as obtained for fourth-, third-, and second-order equations and for emfs either known to 0.01 μV or rounded to 0.01 mV. Inspection shows that either third- or fourth-order equations may be used to represent the emfs.[10] Inspection also shows that the differences in ΔG are practically negligible between the fourth- and third-order fits. If the precision of the observations is lowered to 0.01 mV (table 7) the errors in ΔG are still practically negligible between the fourth- and third-order fits (see footnote 10). As expected, however, second-order equations are inadequate to represent E and ΔG with either resolutions of 0.1 μV or 0.01 mV in E.

For ΔS and ΔC_p the situation is quite different, see tables 8 and 9. Values of ΔS as given by fourth and third order equations are practically the same, except above 40 °C or at 0 °C for a resolution of 0.1μV in E but differ from 0.013 to 0.179 J K^{-1} mol^{-1} (0.007 to 0.043 cal K^{-1} mol^{-1}) for a resolution of 0.01 mV in E. Particular attention should be given to a comparison, say at 25 °C, between a fourth (or third) order fit to 0.1 μV in E and a *second* order fit to 0.01 mV in E (most common procedure reported in the literature); a difference of 0.607 (0.606) J K^{-1} mol^{-1} (0.145 cal K^{-1} mol^{-1}) is obtained. This difference is large and has mistakenly lead some observers [66–69], under similar cases. to conclude that the emf measurements

TABLE 5. *Coefficients in the equation:* $E = E_{0°} + \alpha t + \beta t^2 + \gamma t^3 + \delta t^4$

(On V_{69} and t_{68} scales)

(to 0.1 μV)

Order	$E_{0°}$	$\alpha \times 10^6$	$\beta \times 10^6$	$\gamma \times 10^9$	$\delta \times 10^{11}$
4th	1.0189968	9.3415	−1.5454	9.7894	0.27990
3d	1.0189967	9.4019	−1.5521	10.034	.....
2d	1.0190260	−1.5507	−0.89411	.....	.....

(to 0.01 mV or 10 μV)

4th	1.01900	9.9747	−1.6498	13.828	−4.2920
3d	1.01900	9.0481	−1.5469	10.082	.....
2d	1.01903	−1.9569	−0.88584	.....	.....

[10] Since the values in table 3 were generated from a third-order equation [see eqs (33) or (34)], the fit of a fourth-order equation would be no better than that of a third-order. However, derived quantities, especially ΔC_p, may be slightly different; actually the difference gives an estimate of the uncertainty in the derived quantity.

TABLE 6. *Results from fourth, third, and second order equations for the emf of standard cells of the saturated cadmium sulfate type as a function of temperature (to 0.1 μV)*

Temperature, °C	Electromotive force, V			Δ *in* Δ*G*,				Δ in Δ*G*,	
				Δ*E*, μV		J mol^{-1}		cal mol^{-1}	
	4th order	3d order	2d order	4–3	4–2	4–3	4–2	4–3	4–3
0	1.0189968	1.0189967	1.0190260	0.1	−29.2	0.02	−5.63	0.005	−1.35
3	1.0190112	1.0190112	1.0190133	0	−2.1	0	−0.41	0	−0.10
5	1.0190061	1.0190062	1.0189959	−0.1	10.2	−0.02	1.97	−0.005	0.47
10	1.0189455	1.0189455	1.0189211	0	24.4	0	4.71	0	1.13
15	1.0188224	1.0188224	1.0188012	0	21.2	0	4.09	0	0.98
18	1.0187217	1.0187216	1.0187084	0.1	13.3	0.02	2.57	0.005	0.61
20	1.0186443	1.0186442	1.0186373	0.1	7.0	.02	1.35	.005	.32
25	1.0184186	1.0184185	1.0184284	0.1	−9.8	.02	−1.89	.005	−0.45
28	1.0182635	1.0182634	1.0182816	0.1	−18.1	.02	−3.49	.005	−0.83
30	1.0181529	1.0181528	1.0181748	0.1	−21.9	.02	−4.23	.005	−1.01
35	1.0178547	1.0178547	1.0178764	0	−21.7	.02	−4.19	.005	−1.00
40	1.0175317	1.0175316	1.0175334	0.1	−1.7	.02	−0.33	.005	−0.08
43.6[a]	1.0172880	1.0172878	1.0172587	0.2	29.3	.04	5.65	.01	1.35

[a] Extrapolated values.

TABLE 7. *Results from fourth, third, and second order equations for the emf of standard cells of the saturated cadmium sulfate type as a function of temperature (to 0.01 mV or 10 μV)*

Temperature, °C	Electromotive force, V			Δ in Δ*G*,				Δ in Δ*G*,	
				Δ*E*, mV		J mol^{-1}		cal mol^{-1}	
	4th order	3d order	2d order	4–3	4–2	4.3	4–2	4–3	4–2
0	1.01900	1.01900	1.01903	0	−0.03	0	−5.79	0	−1.38
3	1.01902	1.01901	1.01902	0.01	0	1.93	0	0.46	0
5	1.01901	1.01901	1.01900	0	0.01	0	1.93	0	0.46
10	1.01895	1.01895	1.01892	0	.03	0	5.79	0	1.38
15	1.01882	1.01882	1.01880	0	.02	0	3.86	0	0.92
18	1.01872	1.01872	1.01871	0	.01	0	1.93	0	.46
20	1.01864	1.01864	1.01864	0	0	0	0	0	0
25	1.01842	1.01842	1.01843	0	−0.01	0	−1.93	0	−0.46
28	1.01826	1.01826	1.01828	0	−0.02	0	−3.86	0	−0.92
30	1.01815	1.01815	1.01817	0	−0.02	0	−3.86	0	−0.92
35	1.01786	1.01785	1.01788	0.01	−0.02	1.93	−3.86	0.46	−0.92
40	1.01753	1.01753	1.01753	0	0	0	0	0	0
43.6[a]	1.01729	1.01729	1.01726	0	0.03	0	5.79	0	1.38

[a] Extrapolated values.

are in error whereas, in fact, the differences arise from a lack of resolution or in imprecision of the instruments employed. For ΔC_p, this situation is even more marked, see table 9. Values of ΔC_p, as given by fourth and third order equations are nearly the same, although the fourth-order results are probably preferable, if the resolution in E is 0.1 μV. However, for a resolution of only 0.01 mV in E, large differences are found between fourth and third order fits, but the third-order fits agree more closely with the fourth and third order fits on 0.1 μV resolution in E; *third-order fits are, therefore, selected as final representations*, in line with eqs (29) and (31) given above. As above for ΔS, particular attention should be given to a comparison, say at 25 °C, between a third-order fit to 0.1 μV in E and a *second* order fit to 0.01 mV in E (most common procedure reported in the literature); a difference of 9.93 J K^{-1} mol^{-1} (2.37 cal K^{-1} mol^{-1}) is obtained. This value is again large and has mistakenly lead some observers [66–69], under similar cases, to conclude that the emf measurements are in error by as much as 1 mV whereas, in fact, the differences rest with the degree of resolution in the measuring equipment.

The situation in regard to both ΔS and ΔC_p is more serious at the extremes of temperature. This is shown in figures 1 and 2. It is obvious from these figures that ΔS and ΔC_p, as determined from emfs of different resolutions and equations of different order differ at the extremes of temperature and that in order to determine them, especially ΔC_p, at 0 °C and 40 °C

TABLE 8. *Entropy changes for reactions in standard cells of the saturated cadmium sulfate type as calculated by different functions*

	(to 0.1 μV in E)			(to 0.01 mV or 10 μV in E)			(to 0.1 μV in E)			(to 0.01 mV or 10 μV in E)		
	J K^{-1} mol^{-1}						cal K^{-1} mol^{-1}					
Temperature, °C	4th order	3d order	2d order	4th order	3d order	2d order	4th order	3d order	2d order	4th order	3d order	2d order
0	1.803	1.814	− 0.299	1.925	1.746	− 0.378	0.431	0.433	− 0.072	0.460	0.417	− 0.090
3	0.065	0.069	− 1.334	0.086	0.008	− 1.403	0.015	0.017	− 0.319	0.021	.002	− 0.335
5	− 1.037	− 1.036	− 2.025	− 1.063	− 1.093	− 2.087	− 0.248	− 0.248	− 0.484	− 0.254	− 0.261	− 0.499
10	− 3.592	− 3.595	− 3.750	− 3.675	− 3.640	− 3.797	− 0.859	− 0.859	− 0.896	− 0.878	− 0.870	− 0.907
15	− 5.861	− 5.864	− 5.475	− 5.937	− 5.896	− 5.506	− 1.401	− 1.402	− 1.309	− 1.419	− 1.409	− 1.316
18	− 7.084	− 7.086	− 6.511	− 7.136	− 7.109	− 6.532	− 1.693	− 1.694	− 1.556	− 1.706	− 1.699	− 1.561
20	− 7.841	− 7.843	− 7.201	− 7.873	− 7.860	− 7.215	− 1.874	− 1.874	− 1.721	− 1.882	− 1.879	− 1.725
25	− 9.532	− 9.531	− 8.926	− 9.508	− 9.532	− 8.925	− 2.278	− 2.278	− 2.133	− 2.272	− 2.278	− 2.133
28	− 10.406	− 10.404	− 9.961	− 10.355	− 10.395	− 9.950	− 2.487	− 2.487	− 2.381	− 2.475	− 2.484	− 2.378
30	− 10.931	− 10.929	− 10.652	− 10.867	− 10.912	− 10.634	− 2.612	− 2.612	− 2.546	− 2.597	− 2.608	− 2.542
35	− 12.036	− 12.036	− 12.377	− 11.975	− 12.000	− 12.344	− 2.877	− 2.877	− 2.958	− 2.862	− 2.868	− 2.950
40	− 12.849	− 12.853	− 14.102	− 12.856	− 12.796	− 14.053	− 3.071	− 3.072	− 3.371	− 3.073	− 3.058	− 3.359
43.6 [a]	− 13.248	− 13.261	− 15.345	− 13.365	− 13.189	− 15.284	− 3.166	− 3.169	− 3.667	− 3.194	− 3.152	− 3.653

[a] Extrapolated values.

TABLE 9. *Heat capacity changes for the reaction in standard cells of the saturated cadmium sulfate type as calculated by different functions*

	(to 0.1 μV in E)			(to 0.01 mV or 10 μV in E)			(to 0.1 μV in E)			(to 0.01 mV or 10 μV in E)		
	J K^{-1} mol^{-1}						cal K^{-1} mol^{-1}					
Temperature, °C	4th order	3d order	2d order	4th order	3d order	2d order	4th order	3d order	2d order	4th order	3d order	2d order
0	− 162.91	− 163.62	− 94.26	− 173.92	− 162.96	− 93.39	− 38.94	− 39.11	− 22.53	− 41.57	− 38.95	− 22.32
3	− 155.29	− 155.80	− 95.29	− 162.82	− 155.08	− 94.41	− 37.12	− 37.24	− 22.78	− 38.91	− 37.07	− 22.57
5	− 150.08	− 150.46	− 95.98	− 155.53	− 149.71	− 95.10	− 35.87	− 35.96	− 22.94	− 37.17	− 35.78	− 22.73
10	− 136.59	− 136.72	− 97.71	− 137.77	− 135.87	− 96.81	− 32.65	− 32.68	− 23.35	− 32.93	− 32.48	− 23.14
15	− 122.44	− 122.40	− 99.43	− 120.72	− 121.45	− 98.51	− 29.26	− 29.25	− 23.77	− 28.85	− 29.03	− 23.55
18	− 113.63	− 113.52	− 100.47	− 110.85	− 112.52	− 99.54	− 27.16	− 27.13	− 24.01	− 26.50	− 26.89	− 23.79
20	− 107.62	− 107.49	− 101.16	− 104.44	− 106.45	− 100.22	− 25.72	− 25.69	− 24.18	− 24.96	− 25.44	− 23.95
25	− 92.12	− 92.00	− 102.89	− 89.02	− 90.87	− 101.93	− 22.02	− 21.99	− 24.59	− 21.28	− 21.72	− 24.36
28	− 82.50	− 82.43	− 103.92	− 80.21	− 81.23	− 102.96	− 19.72	− 19.70	− 24.84	− 19.17	− 19.42	− 24.61
30	− 75.95	− 75.94	− 104.61	− 74.53	− 74.69	− 103.64	− 18.15	− 18.14	− 25.00	− 17.81	− 17.85	− 24.77
35	− 59.09	− 59.29	− 106.34	− 61.05	− 57.94	− 105.35	− 14.12	− 14.17	− 25.41	− 14.59	− 13.85	− 25.18
40	− 41.54	− 42.06	− 108.06	− 48.64	− 40.60	− 107.06	− 9.93	− 10.05	− 25.83	− 11.63	− 9.71	− 25.59
43.6 [a]	− 28.47	− 29.30	− 109.30	− 40.42	− 27.76	− 108.29	− 6.81	− 7.00	− 26.12	− 9.66	− 6.64	− 25.88

[a] Extrapolated values.

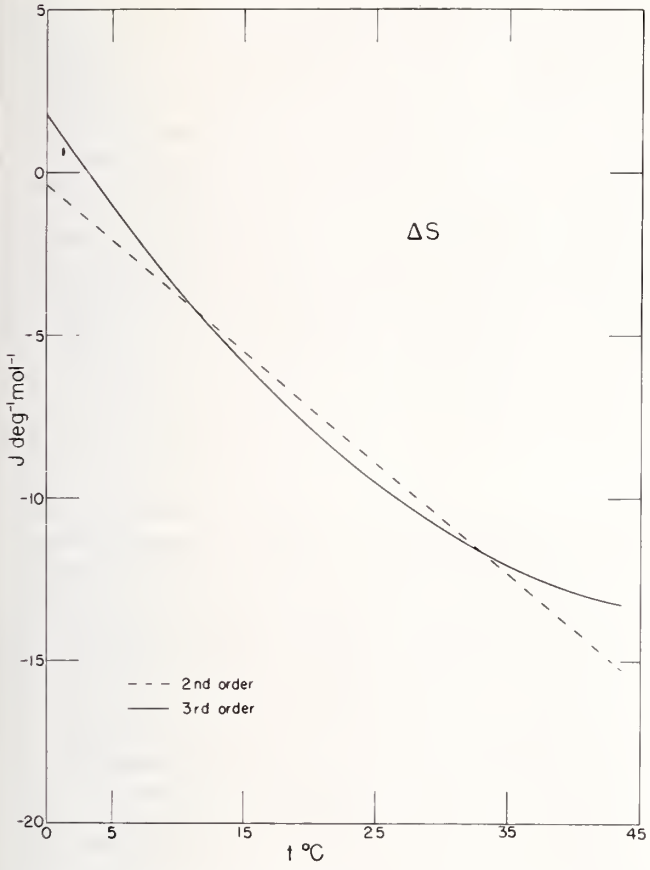

FIGURE 1. *Temperature variations in entropy change for the reaction in standard cells of the saturated cadmium sulfate type, as determined by different functions.*

(Fourth-order function gives nearly the same results as the third-order function and is, therefore, not shown)

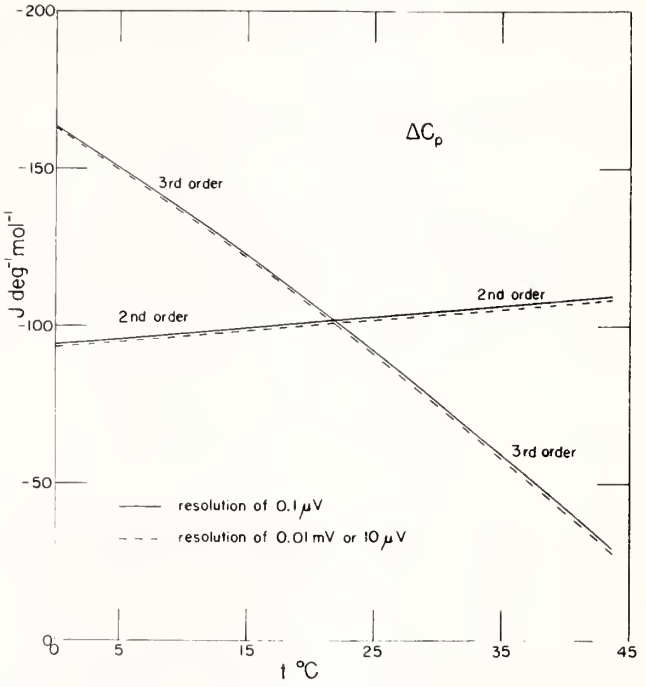

FIGURE 2. *Temperature variations in heat-capacity change for the reaction in standard cells of the saturated cadmium sulfate type, as determined by different functions.*

(Fourth-order function gives slightly different values than the third-order function, see text, table 9, for values).

with the certainty shown at 25 °C, higher resolution in emf and studies over a broader temperature range,[11] if possible, are necessary.

7. Alternate Emf Studies

In the foregoing sections calorimetric and equilibrium data relating to standard cells of the saturated cadmium sulfate type were compared with emf data of such cells. In this section emf data on various cells, which in combination, yield a saturated cadmium sulfate cell, will be compared with the emf of the saturated cadmium sulfate cell. Comparisons are limited to 25 °C where sufficient data are on hand.

Harned and Hamer [70] obtained 0.96495 V (converted to the V_{69} scale) at 25 °C for the emf of the cell:

$$(-)\ \text{Pb-Hg}(2p)\ |\ \text{PbSO}_4(s)|\text{Na}_2\text{SO}_4(\text{sol})|\ \text{Hg}_2\text{SO}_4(s)\ |\ \text{Hg}(l)\ (+) \qquad \text{(B)}$$

LaMer and Parks [71] obtained 0.0013 V for the standard emf, E^0, of the cell:

$$(+)\ \text{Pb-Hg}(2p)\ |\ \text{PbSO}_4(s)\ |\ \text{CdSO}_4(a=1)\ |\ \text{Cd-Hg}\ (11\%)\ (-) \qquad \text{(C)}$$

using the Gronwall, LaMer, and Sandved [72] treatment of interionic attraction to obtain E^0. Here a denotes activity of the solute. On converting to absolute volts and using recent values of the physical constants [1] and the dielectric constant of water [73], it was found that the Gronwall, LaMer, and Sandved treatment did not lead to constant values of E^0 for the emf data of LaMer and Parks at the various concentrations of $CdSO_4$. However, a straight-line extrapolation to $m=0$ to obtain E^0 follows by taking $CdSO_4$ as incompletely dissociated with a dissociation constant of 0.0059 mol kg^{-1} at 25 °C (an ion size of 3 Å was used in the extrapolation). Extrapolations to $m=0$ gives 0.00184 V instead of 0.0013 V, given by LaMer and Parks.[12]

[11] It would appear, at first glance, that Vigoureux and Watts [54] met this criterion, since they carried their measurements to −20 °C thus making possible a good evaluation of ΔC_p at 0 °C. However, the emf goes through a maximum at 3 °C, thus limiting the effectiveness of a second-order equation to a narrow range of 3 °C to −20 °C, thereby not providing sufficient resolution for ΔC_p at 0 °C. In cases where a maximum or minimum in emf did not occur extension of measurements to −20 °C or lower would enhance the evaluation of ΔC_p by a second-order equation. However, higher order equations should be used.

[12] In their 1931 paper LaMer and Parks gave results at 0 and 25 °C. In their 1933 paper (stated to give better results) they gave results of measurments at 0, 10, 20, and 30 °C, but not for 25 °C. Using the above treatment, i.e., taking $CdSO_4$ as incompletely dissociated, E^0 was calculated at these four temperatures which were then fitted to a third-order equation using least squares to give: E^0 (in volts) $= 0.01698 - 0.0003588\ t - 0.000012949\ t^2 + 0.00000012328\ t^3$. At 25 °C this equation yields 0.00184 V, the value given above for E^0; also interpolation of the data for the dissociation constants for these temperatures gives 0.0059 mol kg^{-1} for the dissociation constant for 25 °C.

Combining cells (B) and (C) gives 0.96679 V for the cell:

$$(-)\ \text{Cd-Hg(11\%)}\ |\ CdSO_4(a=1)\ |\ Hg_2SO_4(s)\ |\ Hg(l)\ (+) \qquad (D)$$

which is the cadmium sulfate standard cell but for a $CdSO_4$ solution having an activity of one rather than for a saturated solution of $CdSO_4$. This emf may be converted to that for a saturated solution of $CdSO_4$ using the Nernst equation:

$$E_{\text{standard cell}} = E^0_{\text{standard cell}} - \frac{RT}{F} \ln m_{CdSO_4}\gamma_{CdSO_4} \qquad (36)$$

where

$E^0_{\text{standard cell}} = 0.96679$ V, given above, m is the molality of a saturated solution of $CdSO_4$, 3.6789 [6], γ is the mean stoichiometric activity coefficient of $CdSO_4$, and R, T, and F have the significance given previously in this paper. Harned and Owen [74] and Robinson and Stokes [75] list values of γ from 0.1 to 3.5 molal. Fitting averages of their values above 2 m (γ goes through a minimum at 2.5 m) to an equation of the form:

$$\log \gamma = \frac{-4A\sqrt{I}}{1+1.5\sqrt{I}} + aI + bI^2 + cI^3 \qquad (37)$$

where $A = 0.5108$ [76] and I = ionic strength, gives:

$$\log \gamma = \frac{-2.0432\sqrt{I}}{1+1.5\sqrt{I}} - 0.10780\,I + 0.0091117\,I^2 - 0.00020852\,I^3 \qquad (38)$$

where coefficients a, b, and c were obtained by the method of least squares. This equation yields 0.03646 for γ for a saturated solution of $CdSO_4$ at 25 °C. Substituting this value in eq (36) together with the above values for m and E^0 leads to 1.01840 V for a "neutral" standard cell of the saturated cadmium sulfate type at 25 °C which agrees remarkably well with the observed value, 1.0184185 V, see table 3. This agreement is remarkable since the emfs used in obtaining E^0 were measured to only 0.01 mV.

Another approach to the emf of the standard cell of the saturated cadmium sulfate type may be made using a combination of the three cells:

$$(-)\ \text{Cd-Hg(11\%)}\ |\ CdCl_2(\text{sol})\ |\ AgCl(s)\ |\ Ag(s)\ (+) \qquad (E)$$

$$(+)\ Ag(s)\ |\ AgCl(s)\ |\ HCl(\text{sol})\ |\ H_2(g), Pt\ (-) \qquad (F)$$

$$(-)\ Pt, H_2(g)\ |\ H_2SO_4(\text{sol})\ |\ Hg_2SO_4(s)\ |\ Hg(l)\ (+) \qquad (G)$$

where g = gas and the other symbols have the significance given above. The emfs of these cells were measured for a series of concentrations and temperatures by Harned and Fitzgerald [77], Harned and Ehlers [78], and Harned and Hamer [79], respectively. For the first two cells, the authors obtained the standard potential, E^0, of the cells directly by standard extrapolations using the Debye-Hückel [80] theory of interionic attraction. For the third cell, however, owing to the very high solubility of Hg_2SO_4 in dilute solutions of sulfuric acid, the authors calculated E^0 using values of the activity coefficients of H_2SO_4 obtained from emf measurements of the cell [81]:

$$(-)\ Pt, H_2(g)\ |\ H_2SO_4(\text{sol})\ |\ PbSO_4(s)\ |\ PbO_2(s), Pt\ (+) \qquad (H)$$

The authors measured the emfs of cells (E), (F), (G), and (H) in international volts and for extrapolations to $m=0$ to obtain E^0, used the values of the physical constants then in use [82]; their results were converted here to absolute volts using the factor given above, and the presently recommended values for the physical constants [1] were used in the extrapolations to $m=0$ to obtain values of E^0. For 25 °C, the E^0 values of cells (E), (F), and (G) thus obtained are 0.57399 V,[13] 0.22247 V, and 0.61536 V, respectively. These lead to 0.96688 V for cell (D) whereas the first method using cells (B) and (C) leads to 0.96679 V; this is not a bad agreement considering that the second method involves three different cells, one of which contains an incompletely dissociated electrolyte, $CdCl_2$, and another involves indirect calculations using a combination of results on two cells, cells (G) and (H). This latter value gives 1.01849 V for the emf of the standard cell of the saturated cadmium sulfate type at 25 °C. The agreement here with the observed emf is not as good as in the first case, but is still within the probable error of the measurements; more is given later on this agreement.

The emfs of cells (E), (F), (G), and (H) have been measured by others. Horsch [84], Lucasse [85], Quintin [86], and Treumann and Ferris [87] measured the emfs of cell (E) at a series of concentrations, except that Horsch used a 4.6-percent amalgam and Lucasse, one of unstated percentage. When Horsch's emfs are corrected from 4.6 percent to 11 percent amalgam by adding 0.00293 V, derivable from Smith's [36] measurements, his results agree closely on the average with the results of Harned and Fitzgerald, except below 0.00025 molal where Horsch stated that his results deviated from a smooth curve. Lucasse's amalgams

[13] Harned and Fitzgerald [77] gave 0.57390 international volt for E^0 (a typographical error listed this as 0.57300 international volt) based on a dissociation constant of 0.011 mol kg^{-1} for the equilibrium: $CdCl^+ \rightleftharpoons Cd^{++} + Cl^-$ and 5 Å for the ion-size parameter in treating interionic attraction; they assumed that the dissociation: $CdCl_2 \rightarrow CdCl^+ + Cl^-$ was complete. Their E^0 value becomes 0.57409 absolute volts using the factor between international and absolute volts given above. They stated their experimental accuracy to be of the order of 0.1 mV. Using more recent values for the physical constants [1] and T [1] and the dielectric constant of water [73] it was found that a better fit to their data was obtained using 0.010 mol kg^{-1} for the dissociation constant and 7 Å for the ion-size parameter; these lead to 0.57399 absolute volt for E^0. Incidentally, Reghellato and Davies [83] obtained 0.0101 mol l^{-1} for the dissociation constant from electrolytic conductivity measurements.

apparently were ½ percent in cadmium since, if the difference in the potentials between 1½- and 11-percent amalgams is added to Lucasse's emfs they then agree excellently with those of Harned and Fitzgerald at all concentrations above 0.01 m; however, Lucasse's measurements were not made to sufficiently low concentrations to afford an evaluation of E^0. Quintin's emfs agree closely with those of Harned and Fitzgerald; her emfs yield 0.57395 V for E^0 for cell (E), or 0.04 mV lower than the value obtained from the measurements of Harned and Fitzgerald. Quintin's value for E^0 gives 0.96683 V for cell (D) which yields with the E^0 values for cells (F) and (G) a value of 1.01844 V for the standard cell of the saturated cadmium sulfate type. This value agrees better with the observed emf of a standard cell than the data of Harned and Fitzgerald. However, the standard deviation of the mean of Quintin's measurements is 0.12_8 mV as compared with 0.03_4 mV for Harned and Fitzgerald's results.

The emf of cell (F) has been measured by others in addition to the one cited above. For E^0 at 25 °C Prentiss and Scatchard [88] arrived at a value of 0.22250 V from the earlier measurements excluding those of Harned and Ehlers [78]. MacInnes [89] gave 0.22258 V, Hamer [90] 0.22239 V, Harned and Paxton [91] 0.22239 V, and Bates and Bower [92] 0.22234 V; where necessary these were converted to absolute volts using the factor between international and absolute volts given above. The differences in these values are generally attributed to the differences in the methods of preparation of the silver-silver chloride electrodes or methods of extrapolation to $m=0$ [88]. The average of these values, namely, 0.22244 V agrees within 0.03 mV of the value of Harned and Ehlers, used above. Since Harned and Fitzgerald for cell (E) and Harned and Ehlers for cell (F) used silver-silver chloride electrodes prepared in the same way, the characteristics of the silver-silver chloride electrode should be eliminated if we use their E^0 values in arriving at E^0 for cell (D) since we take the difference of cells (E) and (F) in arriving at E^0 for cell (D).

The emfs of cell (G) have been measured by many in addition to those cited above [79]. Results are listed in table 10. Those marked with a superscript b were calculated here; the authors did not give values for E^0. The value of Harned and Hamer when combined with the E^0 value for the cadmium-amalgam electrode and the m and γ of saturated $CdSO_4$ yields an emf for the standard cell of the saturated cadmium sulfate type that agrees well with the observed emf. The average of the values of Harned and Sturges [98], Randall and Stone [101], Trimble and Ebert [102], Müller and Reuther [104], and Beck et al., namely, 0.61555 V (or 0.61551 V, see footnote e of table 10) agrees within 0.19 (or 0.15) mV of the value of Harned and Hamer.

The recent values for E^0 for cell (G) of Beck, Dobson, and Wynne-Jones [105] and of Covington, Dobson, and Wynne-Jones [69] are not in good agreement, differing by 0.31 mV; the first [105] agrees fairly closely with earlier value of Harned and Hamer [79] whereas the latter [69] agrees fairly well with the very early value of Lewis and Lacey [95]. However, when combined with the E^0 value of the cadmium-amalgam electrode and the m and γ of saturated cadmium sulfate, the E^0 value of Covington et al. for the mercury-mercurous sulfate electrode yields a value for the emf of the standard cell of the saturated cadmium sulfate type which is at great variance (−3.3 mV) from the observed value. There can be little doubt that their E^0 value for the mercury-mercurous sulfate electrode is in error. The value of Beck et al. for E^0 of the mercury-mercurous sulfate electrode leads to a better value for the emf of the standard cell of the saturated cadmium sulfate type than does that of Covington et al., but even so yields a value that is about 0.45 mV above the observed value.

These additional E^0 values for cells (E), (F), and (G) show that the original selection of data [77–79] for these three cells is justified. The slight difference of 0.09 mV in the calculated value of the emf of the

TABLE 10. *Values of the standard potential of the mercury-mercurous sulfate electrode and of the standard cell* (a=1) *and the corresponding electromotive force of the saturated standard cell at 25 °C*

(all values on V_{69} scale)

Date	Experimenters	Hg, Hg_2SO_4	Standard cell	
		E^0	E^0	E(sat.)
		Volt	*Volt*	*Volts*
1910	Brønsted [93]	[a,b]0.6170	0.96843	1.02004
1914	Lewis and Lacey [95]	.6129	.96433	1.01594
1918	Randall and Cushman [94]	[c].6215	.97293	1.02454
1921	Ferguson and France [97]	[b].6199	.97133	1.02294
1925	Harned and Sturges [98]	[b].61534	.96677	1.01838
1926	Åkerlöf [99]	[b].6168	.96823	1.01984
1927	Randall and Langford [100]	[d].6245	.97593	1.02754
1929	Randall and Stone [101]	[b].61550	.96693	1.01854
1933	Trimble and Ebert [102]	[b].6156	.96703	1.01864
1933	MacDougall and Blumer [103]	.6294	.98083	1.03244
1935	Harned and Hamer [79]	.61536	.96679	1.01840
1942	Müller and Reuther [104]	.6155	.96693	1.01854
1960	Beck, Dobson, and Wynne-Jones [105]	[e].61582	.96725	1.01886
1965	Covington, Dobson, and Wynne-Jones [69]	.61251	.96394	1.01555
1969	Gardiner, Mitchell, and Cobble [67]	[f].61251	.96394	1.01555
1970	Sharma and Prasad [107]	.6135	.96493	1.01564

Observed emf of standard cell[g] = 1.0184186

[a] See Randall and Cushman [94]; these authors reported necessary corrections for Brønsted's data and reported some earlier results of Arthur Edgar who, however, measured his emfs only to 1 mV.

[b] Calculated here from emfs for 0.05 to 0.21 m using activity coefficients of sulfuric acid given in reference [79].

[c] Given in Lewis and Randall [96].

[d] Stated to be a provisional value.

[e] Ives and Smith [106] listed this value as 0.61560 V—becomes 0.61561 V on V_{69} scale; reason for discrepancy is unknown.

[f] Selected by these authors in a recalculation of the activity coefficients of sulfuric acid, i.e., the 1965 value.

[g] For dc-electrolytic mercurous sulfate exclusively 1.0184354 V.

standard cell of the saturated cadmium sulfate type as given by cells (B) and (C) on the one hand and by cells (E), (F), and (G) on the other hand can be attributed largely to uncertainties in extrapolations to obtain E^0 values, especially for cell (E) wherein cadmium chloride may show more complex dissociation [108] than assumed by Harned and Fitzgerald. The total uncertainty of 0.09 mV is, therefore, attributed entirely to cell (E), which is within the uncertainty stated by the authors.

The E^0 for the positive electrode of the standard cell is obtained directly from cell (G),[14] while the E^0 for the negative electrode of the standard cell is obtained from the E^0's of cells (B), (C), and (G), or $E_B + E_C - E_G$. These give:

	E^0, V
Positive electrode	0.61536
Negative electrode	−0.35143
Complete cell	0.96679

which give for a saturated solution of cadmium sulfate (assuming that $\gamma_{Cd^{++}} = \gamma_{SO_4} = \gamma_{CdSO_4}$):

	E, V	
Positive electrode	0.64117	0.6411743
Negative electrode	−0.37724	−0.3772443
Complete cell	1.01841	1.0184186
Observed value		1.0184186

As a basis for measurement, the difference of 8.6 μV between the calculated and observed value for the complete cell may be divided between the values for the two electrodes to give the values in the last column.

8. Reproducibility

The good check between calorimetric and equilibrium data and emf data of standard cells of the saturated cadmium sulfate type on the one hand and between emf data on galvanic cells related to the standard cell and the emf of the standard cell itself on the other hand, given above, does not imply that standard cells having the emfs given above to 0.1 μV (see table 3), can be made easily and readily without great care. Cells can be made, however, without extreme care that will agree in emf to 0.01 mV as illustrated by data in table 3.

Various reasons have been advanced why standard cells cannot be made that agree in emf to 0.1 μV. The main reasons are: (1) differences in acidity of the solution, (2) differences in acidity between the two distinct electrodes of the cell, (3) differences in extent of reactions between the solution and the cell container (glass), (4) differences in the size of crystals of both cadmium and mercurous sulfates, (5) undersaturation or oversaturation with cadmium sulfate at either one or both of the electrodes, (6) undersaturation of the solution with mercurous sulfate at the positive electrode, (7) presence of mercuric ions at the positive electrode, (8) amalgam composition, (9) impurities, and (10) cell construction. Of these the ones relating to acidity are the most important; amalgam composition, saturation of the solution with cadmium sulfate at both electrodes and with mercurous sulfate at the positive electrode, crystal size, and amount of mercuric ions can be readily controlled. Also by purification, impurities can be reduced to a minimum; impurities with higher electrical potential than hydrogen must be eliminated. Soluble trace impurities, although they may have no effect on the stability of the cell, may alter the initial emf slightly through a solvent effect affecting the value of the activity coefficient of cadmium sulfate. Thermodynamically, the emf and emf-temperature coefficient are independent of cell construction; however, the rate of attainment of equilibrium after a temperature change can be affected by cell design. The H-form of cell used here and in modern cells permits attainment of temperature equilibrium in relatively short times.

The acidity of the solution and the distribution of the acid throughout the cell affect the emf. Increases in acidity in the cell as a whole decrease the emf of the cell [5, 50, 55, 109, 110]. Increase in acidity at the negative electrode alone increases the emf of the cell while more acid at the positive electrode alone decreases the emf of the cell [36]; these arise from changes in the potential of the acidified electrode and a liquid-junction potential at the interface of the neutral and acid compartments of the cell. If the acid is confined to the region of the mercury-mercurous sulfate paste the liquid-junction potential will differ from that produced if the acid extends to a region above the paste.

Low concentrations of H_2SO_4 (less than 0.1 N) affect only slightly the emf-temperature coefficient of the cell [4, 49, 54, 55]. The relation between the emf-temperature coefficient and the acidity appears to be irregular; more on this will be given in a subsequent paper. Addition of sulfuric acid, through a common-ion effect, decreases the solubility of cadmium sulfate but the total sulfate concentration· ($SO_4^=$ ion from $CdSO_4$ + $SO_4^=$ ion from H_2SO_4) exceeds that of $CdSO_4$ alone. However, the activity coefficient of $CdSO_4$ is decreased by the addition of H_2SO_4, so that the activity of $CdSO_4$ in water or in water-sulfuric acid mixtures is nearly constant. High concentrations of H_2SO_4, of the order of 1 N (or 0.5 M) increase the emf-temperature coefficient of the cell [49, 50]. However, concentrations of H_2SO_4 this high cause excessive gassing at the cadmium-amalgam electrode and are not used for precision cells.

Even though acid affects the initial emf of standard cells, the long-range stability of the cells is affected only slightly. This is evident from the long-range stability exhibited by standard cells of different acidity maintained at the National Bureau of Standards [5, 111] and from international comparisons of cells of various acidities [112]. In the ultimate, stability in emf is the important criterion in the maintenance of the unit of emf, rather than the actual value of the emf. Thermodynamically, however, the value of the emf is all important, in that it gives a measure of the Gibbs energy change or maximum available energy of the cell, and an

[14] As stated earlier, data from cell (H) are required to get E^0 for cell (G).

insight into whether the assigned value is consistent with related thermodynamic quantities.

The author is indebted to Bruce F. Field for writing the computer programs for the emf-temperature equations, to Anna Skapars for making recent checks on the emf-temperature coefficients of standard cells of the saturated cadmium sulfate type, and to Georges Leclerc of the Bureau International des Poids et Mesures for information on the acidity of standard cells submitted to the International Bureau by the various National Laboratories for international comparisons.

9. References

[1] New values for the physical constants—recommended by NAS–NRC, Nat. Bur. Stand. (U.S.), Tech. News Bull. **47**, No. 10. 195 (1963); Consistent set of physical constants proposed. Chem. and Eng. News **41**, No. 46. 43 (Nov. 18. 1963).
[2] Craig. D. N., Hoffman. J. I., Law. C. A., and Hamer. W. J., J. Res. Nat. Bur. Stand. **64A** (Phys. and Chem.), No. 5. 381–402 (Sept.-Oct. 1960).
[3] Hamer. W. J., and Craig. D. N., J. Electrochem. Soc. **111**, 1434 (1964).
[4] Hamer. W. J., J. Res. Nat. Bur. Stand. (U.S.), **72A** (Phys. and Chem.), No. 4. 435–439 (July-Aug. 1968).
[5] Hamer. W. J., Standard cells. their construction. maintenance. and characteristics. Nat. Bur. Stand. (U.S.), Monogr. 84. 40 pages (1965).
[6] Brickwedde. L. H., J. Res. Nat. Bur. Stand. (U.S.), **36**, 377–388 (1946) RP1707.
[7] Cohen. E., Helderman. V. D., and Moesveld. A. L. Th.. Z. physik. Chem. **96**, 259 (1920).
[8] Richards. T. W., and Tamaru. S., J. Am. Chem. Soc. **44**, 1060 (1922).
[9] Thomsen. H. P. J. J., Thermochemische unter suchungen. Vo. I–IV, Barth. Leipzig (1882–86).
[10] Kelley. K. K., Contributions to the data on theoretical metallurgy. XIII. High-temperature heat-content. heat-capacity. and entropy data for the elements and inorganic compounds. Bull. 584. Bur. Mines. 1960.
[11] Pitzer. K. S., and Brewer. L., Lewis and Randall Thermodynamics (McGraw-Hill Book Comp.. Inc.. New York. N.Y., 1961).
[12] Bichowsky. F. R., and Rossini. F. D., The thermochemistry of the chemical substances (Reinhold Publishing Corp.. New York. N.Y., 1936).
[13] Varet. R., Ann. chim. phys. (3) **8**, 79 (1896).
[14] Giauque. W. F.. Barieau. R. E., and Kunzler. J. E., J. Am. Chem. Soc. **72**, 5685 (1950).
[15] Parker, V. B., Thermal properties of aqueous uni-univalent electrolytes. Nat. Stand. Ref. Data Ser. Nat. Bur. Stand. (U.S.), **2**, 69 pages (Apr. 1965).
[16] Rossini, F. D., J. Res. Nat. Bur. Stand. (U.S.), **9**, 679–702 (1932) RP499.
[17] Günther. P., and Wekua. K., Z. physik. Chem. **A154**, 193 (1931).
[18] Kelley. K. K., Contributions to the data on theoretical metallurgy. X. High-temperature heat-content. heat-capacity. and entropy data for the elements and inorganic compounds. Bull. 476. Bur. Mines. 1949.
[19] Richards, T. W., and Rowe, A. W., J. Am. Chem. Soc. **44**, 684 (1922).
[20] Müller, J. A., Bull. soc. chim. (4) **23**, 8 (1918).
[21] Papadopoulos, W. N., and Giauque, W. F., J. Am. Chem. Soc. **77**, 2740 (1955).
[22] Personal calculation using data of reference [21].
[23] Rossini, F. D., Wagman, D. D., Evans, W. H., Levine, S., and Jaffe, I., Selected values of chemical thermodynamic properties, Nat. Bur. Stand. (U.S.), Circ. 500 (1952).
[24] Wagman, D. D., Evans, W. H., Parker, V. B., Halow, I., Bailey, S. M., and Schumm, R. H., (a) Selected values of chemical thermodynamic properties, tables for first thirty-four elements in the standard order of arrangement, Nat. Bur. Stand. (U.S.), Tech Note 270–3, 266 pages (Jan. 1968); (b) Selected values of chemical thermodynamic properties, tables for elements 35 through 53 in the standard order of arrangement, Nat. Bur. Stand. (U.S.), Tech. Note 270–4. 151 pages (1965).
[25] Berthelot, P. E. M., Ann. chim. phys. (4) **29**, 433 (1873).
[26] Keyes, F. G., Gillespie, L. J., and Mitsukuri, S., J. Am. Chem. Soc. **44**, 707 (1922).
[27] Stull, D. R., and Sinke, G. C., Thermodynamic properties of the elements, Am. Chem. Soc., Washington, D.C. (1956).
[28] Wexler, A., and Greenspan, L., J. J. Res. Nat. Bur. Stand. (U.S.), **75A** (Phys. and Chem.), No. 3, 312–230 (May–June 1971).
[29] Ishikawa, F., and Murooka, H., Bull. Inst. Phys. Chem. Res. (Tokyo) **9**, 781 (1933).
[30] Wagman, D. D., Evans, W. H., Halow, I., Parker, V. B., Bailey, S. M., and Schumm, R. H., Selected values of chemical thermodynamic properties, Part 1. Tables for the first twenty-three elements in the standard order of arrangement, Nat. Bur. Stand. (U.S.), Tech. Note 270–1, 127 pages Oct. 1965).
[31] Carpenter, C. D., and Jette, E. R., J. Am. Chem. Soc. **45**, 578 (1923).
[32] Holsboer, H. B., Z. physik. Chem. **39**, 691 (1902).
[33] Cohen, E., and Moesveld, A. L. Th., Z. physik Chem. **95**, 305 (1920).
[34] Hulett, G. A., Trans. Am. Electrochem. Soc. **7**, 333 (1905); **15**, 435 (1909).
[35] Getman, F. H., J. Am. Chem. Soc. **39**, 1806 (1917).
[36] Smith, F. E. (Sir Frank), Proc. Phys. Soc. (London) **22**, 11 (1910); Phil. Mag. **19**, 250 (1910); Natl. Phys. Lab. Coll. Res. **6**, 137 (1910).
[37] Announcement of a change in electrical and photometric units, NBS Circ. 459, 1947.
[38] Nat. Bur. Stand. (U.S.), Tech. News Bull. **52**, 204 (1968); **53**, 13 (1969).
[39] Parks, W. G., and LaMer, V. K., J. Am. Chem. Soc. **56**, 90 (1934).
[40] Hamer, W. J., Inst. Soc. Am., M2–1–Mestind–67, 1967; Proc. Conf. ISA, **22**, Part 1, 1 (1967).
[41] Hamer, W. J., Standard cells, Ch. 12, The primary battery, Ed. G. W. Heise and N. C. Cahoon (John Wiley & Sons, New York, N.Y., 1971).
[42] Wolff, F. A., Trans. Am. Electrochem. Soc. **13**, 187 (1908).
[43] Wolff, F. A., Bull. BS **5**, 309 (1908).
[44] Wolff, F. A., and Waters, C. E., BS Circ. No. 29 (1910).
[45] Wolff, F. A., Trans. Am. Electrochem. Soc. **5**, 49 (1904).
[46] Wolff, F. A., and Waters, C. E., Bull. BS **4**, 70 (1907).
[47] International conference on electrical units and standards, Appendix to the report: Notes to the specifications as to the methods adopted in various standardizing laboratories to realize the international ohm and the international ampere, and to prepare the Weston Normal Cell (Darling & Sons, Ltd., London, 1908).
[48] Vosburgh, W. C., and Eppley, M., J. Am. Chem. Soc. **45**, 2268 (1923).
[49] Vosburgh, W. C., J. Optical Soc. Am. & Rev. Sci. Instr. **12**, 511 (1926).
[50] Ishibashi, Y., and Ishizahi, T., Res. Electrotech. Lab. (Tokyo), No. 318 (1931).
[51] Froehlich, M., Z. Instr. **74**, 216 (1966); private communication, 1969.
[52] Vincent, G. D., IRE Trans. Instr. **I-7**, No. 3 and 4, 221 (1958).
[53] Law, C. A., and Skapars, A., results NBS. 1955–70, unpublished.
[54] Vigoureux, P., and Watts, S., Proc. Phys. Soc. (London) **45**, 172 (1933).
[55] Obata, J., and Ishibashi, Y., Researches Electrotech. Lab. No. 11, 7 (1921).
[56] Waider, C. W., and Dickinson, H. C., Bull. BS **3**, 663 (1907).
[57] NBS Tech. News Bull. **33**, No. 3, 28 (1949).
[58] NBS Tech. News Bull. **53**, 12 (1969).
[59] Clarke, J., Phys. Today **24**, No. 8, 30 (1971).
[60] Driscoll, R. L., and Cutkosky, R. D., J. Res. Nat. Bur. Stand. (U.S.), **60**, 297–305 (1958) RP2846.
[61] Cutkosky, R. D., J. Res. Nat. Bur. Stand. (U.S.), **65A** (Phys. and Chem.), No. 3, 147–158 (May-June 1961).

[62] Harned, H. S., and Owen, B. B., The Physical Chemistry of Electrolytic Solutions, 3rd ed., ACS Monograph Series No. 137 (Reinhold Book Corp., New York, N.Y., 1958) p. 428.
[63] Latimer, W. M., The Oxidation States of the Elements and Their Properties in Aqueous Solutions, 2nd ed. (Prentice-Hall, Inc., Englewood Cliffs, N.J., 1952).
[64] MacInnes, D. A., The Principles of Electrochemistry (Reinhold Publ. Corp., New York, N.Y., 1939).
[65] Ives, D. J. G., and Janz, G. J., Eds., Reference Electrodes, Theory and Practice (Academic Press, New York, N.Y., 1961).
[66] Brackett, T. E., Hornung, E. W., and Hopkins, T. E., J. Am. Chem. Soc. **82**, 4155 (1960).
[67] Gardner, W. L., Mitchell, R. E., and Cobble, J. W., J. Phys. Chem. **73**, 2017 (1969).
[68] Beck, W. H., Singh, K. P., and Wynne-Jones, W. F. K., Trans. Faraday Soc. **55**, 331 (1959).
[69] Covington, A. K., Dobson, J. V., and Wynne-Jones, W. F. K., Trans. Faraday Soc. **61**, 2050 (1965).
[70] Harned, H. S., and Hamer, W. J., J. Am. Chem. Soc. **57**, 33 (1935).
[71] LaMer, V. K., and Parks, W. G., J. Am. Chem. Soc. **53**, 2040 (1931); **55**, 4343 (1933).
[72] Gronwall, T. H., LaMer, V. K., and Sandved, K., Physik. Z. **29**, 358 (1928).
[73] Malmberg, C. G., and Maryott, A. A., J. Res. Nat. Bur. Stand. (U.S.), **56**, 1–8 (1956) RP2641.
[74] Reference [62], p. 565.
[75] Robinson, R. A., and Stokes, R. H., Electrolyte solutions, 2nd ed. (Butterworths Sci. Publ., London, 1959) p. 502.
[76] Hamer, W. J., Nat. Stand. Ref. Data Ser. Nat. Bur. Stand. (U.S.), **24**, 274 pages (Dec. 1968).
[77] Harned, H. S., and Fitzgerald, M. E., J. Am. Chem. Soc. **58**, 2624 (1936).
[78] Harned, H. S., and Ehlers, R. E., J. Am. Chem. Soc. **54**, 1350 (1932); **55**, 652, 2179 (1933).
[79] Harned, H. S., and Hamer, W. J., J. Am. Chem. Soc. **57**, 27 (1935).
[80] Debye, P., and Hückel, E., Physik. Z. **24**, 185, 305 (1923).
[81] Hamer, W. J., J. Am. Chem. Soc. **57**, 9 (1935).
[82] Reference [62], 1st ed., Ch. (5), 1943.
[83] Righellato, E. C., and Davies, C. W., Trans. Faraday Soc. **26**, 592 (1930).
[84] Horsch, W. G., J. Am. Chem. Soc. **41**, 1787 (1919).
[85] Lucasse, W. W., J. Am. Chem. Soc. **51**, 2597 (1929).
[86] Quintin, Mlle M., Compt. Rendus **200**, 1579 (1935).
[87] Treumann, W. B., and Ferris, L. M., J. Am. Chem. Soc. **80**, 5048 (1958).
[88] Prentiss, S. S., and Scatchard, G., Chem. Rev. **13**, 139 (1933).
[89] Reference [64], p. 187, table 1.
[90] Hamer, W. J., Ph.D. Dissertation, Yale University, New Haven, Conn., 1932.
[91] Harned, H. S., and Paxton, T. R., J. Phys. Chem. **57**, 531 (1953).
[92] Bates, R. G., and Bower, V. E., J. Res. Nat. Bur. Stand. (U.S.), **53**, 283–290 (1954) RP2546.
[93] Brønsted, J. N., Z. physik. Chem. **68**, 693 (1910).
[94] Randall, M., and Cushman, O. E., J. Am. Chem. Soc. **40**, 393 (1918).
[95] Lewis, G. N., and Lacey, W. N., J. Am. Chem. Soc. **36**, 804 (1914).
[96] Lewis, G. N., and Randall, M., Thermodynamics and the Free Energy of Chemical Substances (McGraw-Hill Book Co., Inc., New York, N.Y., 1923) p. 407.
[97] Ferguson, A. L., and France, W. G., J. Am. Chem. Soc. **43**, 2150 (1921).
[98] Harned, H. S., and Sturgis, R. D., J. Am. Chem. Soc. **47**, 945 (1925).
[99] Åkerlöf, G. C., J. Am. Chem. Soc. **48**, 1160 (1926).
[100] Randall, M., and Langford, C. T., J. Am. Chem. Soc. **49**, 1445 (1927).
[101] Randall, M., and Stone, H. A., J. Am. Chem. Soc. **51**, 1752 (1929).
[102] Trimble, H. M., and Ebert, P. F., J. Am. Chem. Soc. **55**, 958 (1933).
[103] MacDougall, F. H., and Blumer, D. R., J. Am. Chem. Soc. **55**, 2236 (1933).
[104] Müller, F., and Reuther, H., Z. Electrochem. **48**, 220 (1942).
[105] Beck, W. H., Dobson, J. V., and Wynne-Jones, W. F. K., Trans. Faraday Soc. **56**, 1172 (1960).
[106] Reference [65], p. 405.
[107] Sharma, L., and Prasad, B., J. Indian Chem. Soc. **47**, 379 (1970).
[108] Sahn, G., and Prasad, B., J. Indian Chem. Soc. **46**, 233 (1969).
[109] Vosburgh, W. C. J. Am. Chem. Soc. **47**, 1265 (1925).
[110] Smith, F. E. (Sir Frank), Natl. Phys. Lab. Report 60, 1920; Dic. App. Phys. **2**, 268 (1920).
[111] Hamer, W. J., Brickwedde, L. H., and Robb, P. R., Electrochemical Constants, NBS Circ. 524, ch. 12, 1953.
[112] Leclerc, Georges, private communications, 1971.

(Paper 76A3–716)

Designs for Surveillance of the Volt Maintained by a Small Group of Saturated Standard Cells

W. G. Eicke
Electricity Division
Electrochemistry Section

and

J. M. Cameron
Applied Mathematics Division
Statistical Engineering Laboratory

This technical note describes a procedure for maintaining surveillance over a small group of saturated standard cells. The measurement process is briefly discussed and the principle of left-right balance as a means of eliminating certain systematic errors is developed. Specific designs and their analysis for intercomparing 3, 4, 5 and 6 cells in a single temperature controlled environment are given. Procedures for setting up control charts on the appropriate parameters are given, and a technique is described for detecting certain types of systematic errors.

Key words: Control charts, experiment design, saturated standard cells, standard cells calibration, statistics, voltage standard.

I. INTRODUCTION

At the local level the primary standard of electromotive force is maintained by a group of saturated standard cells, the same type of cell used to maintain the National unit of electromotive force. Many laboratories use groups containing from 3 to 6 cells mounted in either a temperature controlled air or oil bath. The cells are in general calibrated by the National Bureau of Standards at periodic intervals and the mean emf of the group is assumed to remain constant between calibrations. Since such calibrations are done infrequently (at intervals of one year or more) some technique must be employed to maintain surveillance over the local unit between calibrations.

Starting with assigned values for each of the cells of the group as a given set of reference points, one can check on the relative stability of the cells by measuring differences among them. One could measure all possible differences and have equal precision in the knowledge of the values of all cells or one could pick a favorite cell and compare all others with this one (but this leads to high precision in the knowledge of the selected cell and relatively low precision in all others). For small groups it is quite practical to measure all possible differences, but as the group size increases the number of measurements would increase rapidly with N, where N is the group size. As N increases compromise schemes that lead to equal precision in the knowledge of each cell can be used. One such design is given in [1] for a group of 20 cells in which only 40 differences are measured (instead of 190 if all $N(N-1)/2$ were measured).

This note discusses methods for maintaining surveillance of groups containing three, four, five, or six cells in a single temperature controlled enclosure. The procedures suggested are designed to yield information on:

1) the stability of the differences in emf among the group,

2) the components of variability and dependence of the measurement process precision on environmental influences or procedural changes,

3) possible systematic errors and estimation of the accuracy of the process.

Furthermore, they tend to maximize the yield of useful information per measurement.

II. The Measurement Technique

The opposition method [3] is usually employed in the intercomparison of saturated standard cells. In this method the small difference between two cells connected in series opposition is measured using a suitable instrument. The instrument is usually a potentiometer designed for the measurement of very small emfs [2].

In the ideal situation the difference in emf as measured by the potentiometer is:

$$\Delta E = V_1 - V_2 \tag{1}$$

where V_1 and V_2 are the emfs of the two cells being compared.

However in the real situation there may be spurious emfs in the circuit. In general these can be classified into two categories;

1. Those emfs that remain constant, or relatively so, in relation to the interval over which a complete set of measurements is made.
2. Those emfs that vary rapidly (referenced to the interval over which a complete set of measurements is made).

If the emfs are of the second type they will have the effect of decreasing the precision of the process. On the other hand if they are of the first type they will have the effect of introducing a systematic error, thereby making the measurement

$$\Delta E = V_1 - V_2 + P \tag{2}$$

where P is the constant emf. It is possible to estimate P by taking a second measurement

$$\Delta E' = V_2 - V_1 + P \tag{3}$$

and summing the two

$$2P = \Delta E + \Delta E' \tag{4}$$

The difference between eqs. (2) and (3) gives

$$\Delta E - \Delta E' = 2(V_1 - V_2) \tag{5}$$

an estimate of $V_1 - V_2$ free of P. The pair of measurements (eqs. (2) and (3)) are said to be "left-right" balanced. That is if there is a positional effect it is balanced out of the final result. This technique is analogous to that used to eliminate the inequality of balance arms in precision weighing on a two pan equal arm balance. In order to designate the cell positions from the operational point of view they are frequently designated as unknown and reference: Relative to the input terminals of the measuring instrument they are as shown in fig. 1. In the next section the principle of "left-right" balance will be extended to groups containing three or more cells.

III. Designs for Groups of 3, 4, 5, or 6 Cells

Experimental designs of groups of 3, 4, 5, and 6 cells are given in Appendix A. The designs presented have been selected to be (1) efficient from the standpoint of the operators making the measurement (2) statistically efficient, in the sense of minimum standard deviation for the estimated cell values, and (3) relatively easy to analyze using conventional desk calculators. All of the analyses presented are the least square solutions for the associated design assuming that the sum of the differences from the mean of all is zero. For groups of 3, 4, 5, total "left-right" balance has been achieved and the estimate of the "left-right" effect is

$$\hat{P} = 1/n \sum_{i=1}^{n} y_i \tag{6}$$

where n is the number of measurements and y the observed difference in emf between two cells.* For the case of six cells left-right balance is achieved for only the first 12 measurements.

*In terms of the notation of fig. 1 y is the observed ΔE.

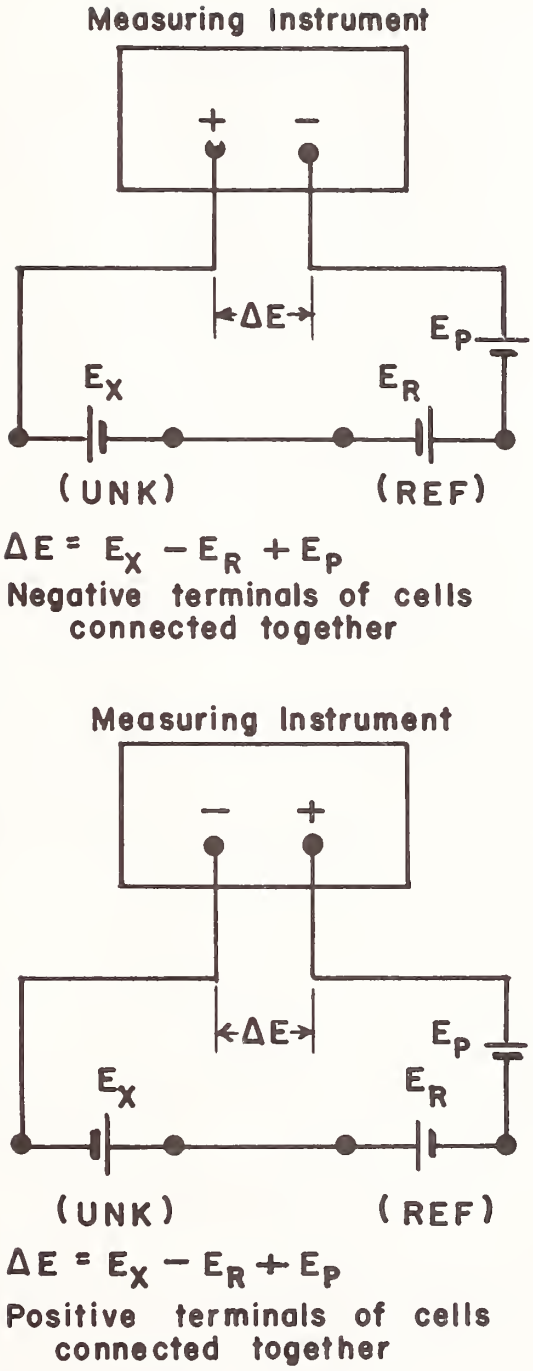

Figure 1

Two ways in which two cells can be connected in series-opposition.

For each size group the design and its analysis are given as a complete entity, with the left half giving the general procedure and the right half a numerical example. The suggested order for making the measurements requires moving one set of leads at a time thereby minimizing the possibility of connecting the wrong cells.

The definitions of the symbols used in the tables are as follows:

Symbol	Definition
V_i	The emf of the ith cell
M	The group mean
M*	The mean of
v_i	The difference V_i-M
y_i	The ith measured difference
$\hat{P}$	The calculated circuit residual
Q_i	A sum of those y's that involve the ith cell
$\hat{v}_i$	The calculated ith v
$\hat{y}_i$	The predicted y_i calculated from $\hat{v}$ and $\hat{P}$
d_i	Deviations, $(y_i - \hat{y}_i)$
s	The standard deviation of a single observation

For all of the designs given in Appendix A the assumption is that the mean of the whole group is known and serves as the restraint in the least square solution. In the next section, procedures for changing the restraint will be given. The analysis produces the following basic information which can be used to monitor the process:

1. The emf of each cell (or the difference from the group mean)
2. The residual emf, $\hat{P}$
3. The standard deviation of a single observation
4. The deviation of each observation from the predicted value

The frequency with which these intercomparisons should be run may vary considerably depending on the particular installation. Once it is established that the process is in a state of control then one intercomparison each week should be sufficient.

IV. Change of Restraint

In the previous section it was assumed that the mean for the whole group was known, such as would be the case if the group had been assigned values by the National Bureau of Standards. Because only differences in emf are measured, this average value is the restraint on the values which provide the "ground zero" to which the cell values are related.

When one or more of the cells show a change so large as to be inconsistent with its assigned value, it becomes necessary to remove these cells from the defining group. Evidence of such changes would be discovered from control charts on either the cell values or control charts on differences between cells (see the next section on control charts).

To illustrate, let us assume that the assigned values for the 5th and 6th cells of the example in Table A-4 had been 1.0182536 and 1.0182501 instead of the values (1.0182416, 1.0182381) given in

section 1 of the table. This is a change of +12.0μV in each cell so that the new emf values for the cells would be as shown in the following table.

Table 1-A

Cell	Assigned values	(Table A-4 Sec. 4) $\hat{v}_i$	Emf of cell $M + \hat{V}_i$	Difference from assigned
1	1.0182605	10.47	1.01826445	3.95
2	2655	15.62	1.01826960	4.10
3	2466	- 3.40	1.01825058	3.98
4	2476	- 2.29	1.01825169	4.09
5	2536*	- 8.37	1.01824561	-7.99
6	2501*	-12.04	1.01824194	-8.16

Average = 1.01825398 = M

*These values differ by 12μV from the data of Table A-4.

The last two cells are obviously inconsistent with their assigned values, so that one would want to remove these from the restraint and establish "ground zero" with the first four cells.

To do this one calculates

(1) $\bar{V}_A$: the average of the assigned value of the cells to be retained in the restraint as shown in column 2 of the table below; and $\bar{v}$: the average of the $\hat{v}$'s to be be retained in the restraint.

(2) $\hat{v}_i$: the cell estimates as given in section 4 and copied into column 3 below; and

(3) adds $\bar{V}_A - \bar{v}$ to each of the $\hat{v}_i$ to give the cell values, $\hat{V}_i$, as shown in column 4.

Table 1-B

Cell	Assigned values	(Table A-4 Sec. 4) $\hat{v}_i$	Emf of cell $\bar{V}_A + v_i = \hat{V}_i$
1	1.0182605	10.47	1.01826042
2	2655	15.62	26557
3	2466	- 3.40	24655
4	2476	- 2.29	24766
	Average = 1.01825505 = V_A	$\bar{v}$ +5.10	
5	1.0182536	- 8.37	24158
6	2501	-12.04	23792

The cell values are now expressed in terms of the average of the "good" cells as the reference point. The misbehaving cells would ordinarily continue to be measured in the hope that they would stabilize at some new value.

V. Control Charts

Control charts [5] [6] on process parameters such as the cell values and standard deviations of a single observation provide an effective means of determining whether or not the process is in a state of statistical control. Control charts for each cell (or difference between cells), process precision (standard deviation of an observation), and the residual emf P should be maintained. These charts provide the verification of that part of the uncertainty statement that deals with bounds for the effect of random error. Such statements say in effect "If this measurement process is used a large number of times, the values obtained for a single quantity will vary within the stated limits." The charts permit one to demonstrate the validity of such statements on current data.

For each run one will have values for each of the cells, the standard deviation, and the residual emf. To check on the state of control of the measurement process and on the stability of the cells, one would study the sequence of values for these parameters. Control charts on the cells can be established on the emf of the cells, the difference between successive cells (e.g. cell 1 - cell 2, cell 2 - cell 3, cell 3 - cell 4, etc.), or both. The former has the difficulty that it is not sensitive to a change in the emf of a single cell. However, by following the differences between successive cells (i.e. 1st minus 2nd, 2nd minus 3rd and so on) one has an easily interpreted set of results even though the successive differences are not independent. A single "bad" cell will show up as out of control on two successive differences, whereas the remaining differences are unaffected.

In order to establish control limits one has to know the precision of the measurement process (see discussion on measurement processes in ref. [7]). However, under the assumption that the standard deviation, σ, of the process is known one can, for a given design, write down the standard deviations of the individual cell emfs, the difference between two cells, and for the residual P. One can use three times the appropriate standard deviation as control limits. For the designs given the values for setting limits are shown in Table 2.

Unfortunately, when starting such surveillance the process precision, σ, is usually not known and must be estimated from the available data. In this case one would pool a number, m, of individual standard deviations using the formula

$$s_p^2 = 1/m \sum_{i=1}^{m} s_i^2 \qquad (7)$$

for a particular design. This might entail making several runs a week for the first month or so to obtain starting control limits. After about 100 degrees of freedom have been accumulated a new value of s_p should be calculated and the control limits revised. For such a large number of degrees of freedom s_p approaches σ very closely. Using s_p and the control limits from the factors in Table 2, a control chart on the standard deviation of the process (i.e. on s as computed in Appendix A) should be constructed.

It is also desirable to maintain a control chart on the residual emf using the limits given in Table 2. Initially the accepted value of P would be taken as zero. However, if after repeated measurements the value of P is other than zero and constant, the central value and control limits should be adjusted accordingly.

The start of each type of control chart is shown in Fig. 2. For the charts on the cells the central values for both cells and difference between cells should be based on the assigned values. The chart can either be kept on a run number or a time basis. The latter has the advantage that one can estimate rate of drift if any cell shows a trend.

Table 2

Factors for Setting the 3σ Control Limits for the Designs in Appendix A

No. of cells Excluded from group mean	Number of Cells in Group			
	3	4	5	6
		Cell Values		
0	1.0000	0.9186	1.2000	1.1260
1*	0.8660 1.500	0.8660 1.2247	1.1619 1.5000	1.1071 1.3512
2*	0. 1.7320	0.750 1.2990	1.0954 1.5492	1.0794 1.3839
3*	--- ---	0 1.5000	.9487 1.6432	1.0000 1.4392
		Residual (P)		
	1.2247	0.8660	0.9487	0.8018
		Successive differences $(\hat{v}_i - \hat{v}_{i+1})$		
	1.7321	1.5000	1.8974	(1)
		Standard deviations		
Upper limit	1.945	1.585	1.737	1.552
Central line	0.888	0.950	0.933	0.963

*The upper figures are for those cells included in the mean and the lower figures are for those cells excluded from the mean.

(1) For differences (1-2)(2-3)(4-5)(5-6) the limit is 1.7321.
For differences (4-5)(6-1) the limit is 1.7525.

To compute control limit multiply σ or pooled s_p by the appropriate factor and add or subtract as required.

If a cell should "go bad" and be removed from the mean, but still kept in the group, then the limits should be altered accordingly (see Table 2). It is important to bear in mind that the control charts on the cells only indicate change in the emf of cells relative to each other. If the whole group is changing it will not show up in any of the charts and can only be ascertained by comparison with other cells whose values are known. This situation does occur because small groups of cells are usually from the same manufacturer and lot, and therefore have similar aging characteristics.

VI. Systematic Errors

Ideally a measurement process should be free of systematic error, however, this is not often the case. In fact, the residual P is a systematic error. Its effect on the values of the cells is readily removed and its magnitude estimated using the suggested designs. Other systematic errors are not so easily detected. Indications of their presence in some cases can be obtained by analysis of deviations from two or more successive designs run on the same group of cells.

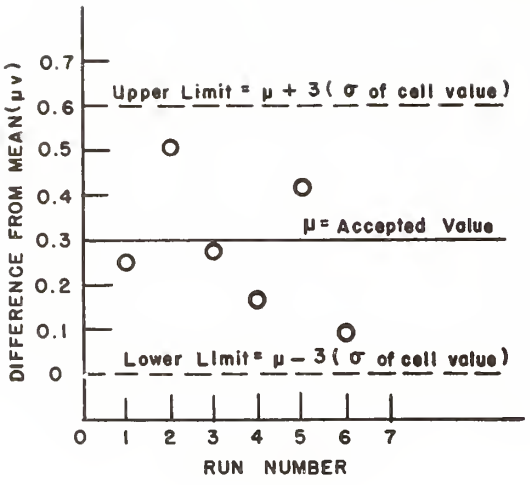

A

Control Chart for value of a cell.

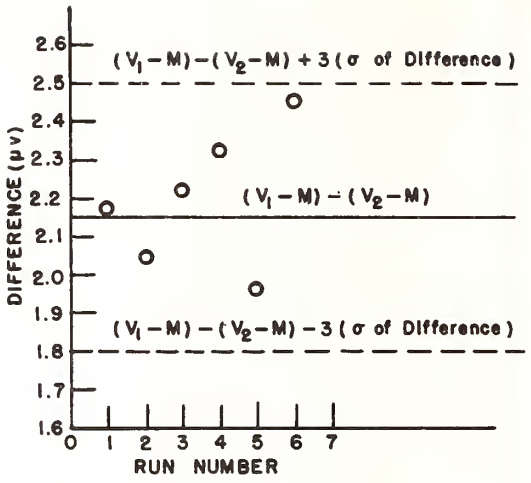

B

Control Chart for the difference between sucessive cells.

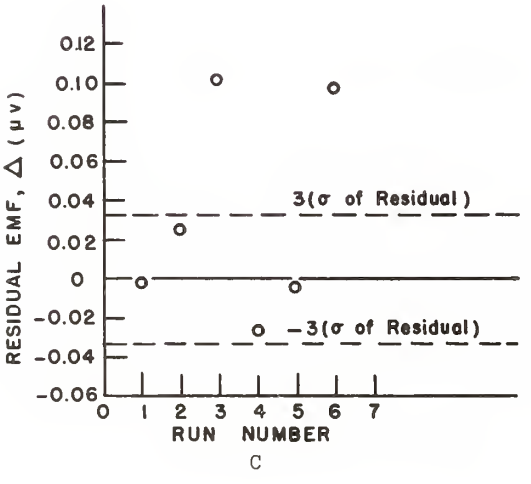

C

Control Chart for residual.

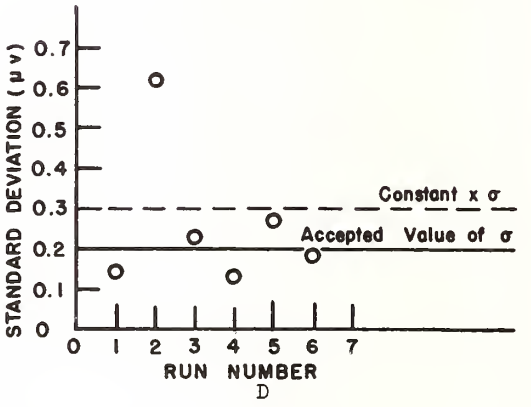

D

Control Chart for standard deviation of a single observation.

Figure 2

Typical control charts for maintaining surveillance over a group of standard cells.

Detection is based on the assumption that the deviations for a particular observation (cell 1 - cell 2, cell 1 - cell 3, etc.) are independent in successive runs.

If the magnitude and sign of corresponding deviations from successive runs tend to agree then one would suspect the presence of a systematic error. Such an analysis can be done on 5 and 6 cell groups graphically by plotting the deviations of one run as a function of the second run. If the deviations tend to fall on a straight line having slope 1 and passing through the origin, then one would suspect a systematic error. If there is none then the points would be distributed randomly. Figure 3 shows an example with no systematic error present. Figure 4 was created from the data of Figure 3 by adding 0.3 μV to the absolute value of each observation to simulate an offset error such as failing to correct for the instrument zero. The presence of such a systematic error will (1) cause the deviations to string along the line, (2) inflate the standard deviation, and (3), introduce a bias into each calculated $\hat{v}_i$. The magnitude of the latter will depend on the particular set of observations. Instead of the model for a single observation being

$$E(y_{ij}) = X_i - X_j + P$$

as in the case of Figure 3, and as assumed in the appendix, it is now

$$E(y_{ij}) = X_i - X_j + P + \frac{y_{ij}}{|y_{ij}|} C$$

where C is the zero offset.

For sets with less than 5 cells one would examine the deviations of successive runs for patterns. If the deviations for a given observation have the same sign and approximately the same magnitude, one would suspect a possible systematic error. Studies are being conducted to develop relatively simple tests that may be used to detect the presence of many types of systematic errors.

The cause or causes of systematic errors will depend on a particular measuring system. Some possible causes are:

1. Failure to make applicable corrections
2. Zero offset
3. Operator reading bias
4. Operator setting bias
5. Leakage currents

This list is by no means complete, but merely suggests some possible causes.

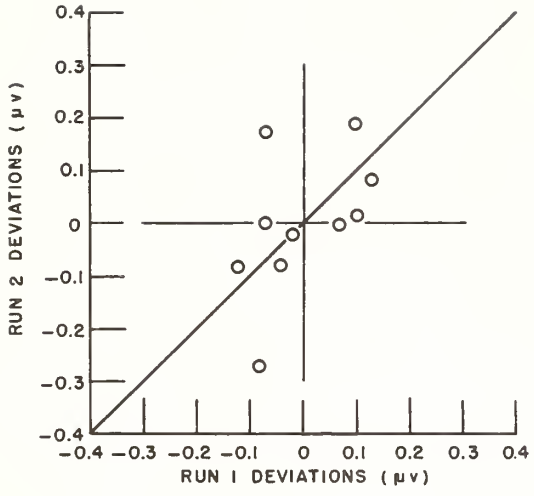

Figure 3

Youden plot for two runs without systematic error.

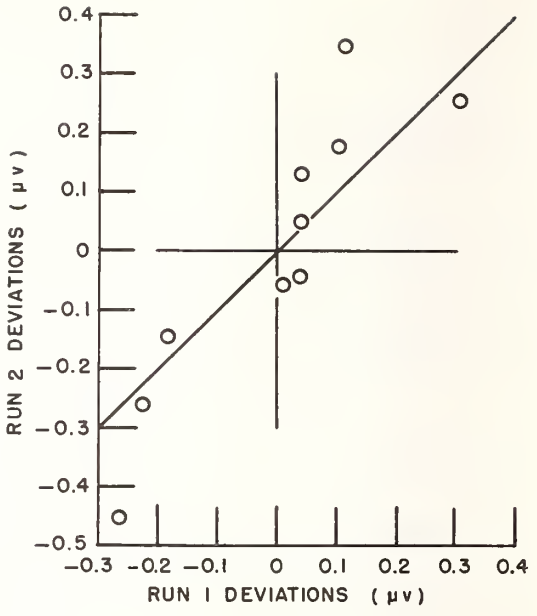

Figure 4

Youden plot for two runs with systematic error.

REFERENCES

[1] Hamer, W. J., "The Volt Standard" Moves To Gaithersburg, Maryland, J. Wash. Acad. of Sci. 56 (1966), pp. 101-108.

[2] Harris, F. K., Electrical Measurements, J. Wiley & Sons (1952), pp. 168-185.

[3] Hamer, W. J., Standard Cells--Their Construction, Maintenance, and Characteristics, NBS Monograph 84 (1965), pp. 8-10.

[4] Hamer, W. J., ibid. pp. 5-8.

[5] ASTM Manual on Quality Control of Materials, Special Technical Publication 15-C, Part 3, January 1951.

[6] Natrella, M. G., Experimental Statistics, NBS Handbook 91 (1963), pp. 18-1, 18-4.

[7] Pontius, P. E., Measurement Philosophy of the Pilot Program for Mass Measurement, NBS Technical Note 288, May 1966.

APPENDIX A

Designs for Groups of 3, 4, 5 and 6 Saturated Standard Cells

APPENDIX A

Designs for Groups of 3, 4, 5 and 6 Saturated Standard Cells

TABLE A-1

THE INTERCOMPARISON OF A GROUP OF THREE SATURATED STANDARD CELLS

	Example
1. Given: The emfs of three saturated standard cells (V_1, V_2 and V_3) are assigned by calibrating them in terms of a known standard of electromotive force. The mean of the group is $M = 1/3 \sum_{i=1}^{3} V_i$ and the difference from the mean of each cell is $v_i = (V_i - M)$	1. From an NBS Report of Calibration: V_1 = 1.0182571 v_1 = -1.2 μV V_2 = 1.0182535 v_2 = -4.8 V_3 = 1.0182643 v_3 = +6.0 Mean = 1.0182583 sum = 0
2. Assuming that there is a small constant emf P associated with the measuring process then the expected value of a single observation is $E(y_i) = V_j - V_k + P$ $j \neq k$; for j and k = 1,2,3. For all possible values of j and k the following schedule of measurements is convenient and requires changing the connections to only one cell at a time.	2. Observations:

Measurement	Cell in UNK position*	Cell in REF position*	
y_1	1	2	y_1 = +4.8 μV
y_2	1	3	y_2 = -6.6
y_3	2	3	y_3 = -10.6
y_4	2	1	y_4 = -3.4
y_5	3	1	y_5 = +7.4
y_6	3	2	y_6 = +10.4

*See Fig. 1 for definition of positions.

3. Estimation of P: $\hat{P} = 1/6 \sum_{i=1}^{6} y_i$	3. $\hat{P}$ = 1/6 (+4.8 -6.6 -10.6 -3.4 +7.4 +10.4) $\hat{P}$ = .333 μV

TABLE A-1 Continued

4. Estimation of v_i: $\hat{v}_1 = \hat{V}_1 - M = 1/6\ (y_1 + y_2 - y_4 - y_5)$ $\hat{v}_2 = \hat{V}_2 - M = 1/6\ (-y_1 + y_3 + y_4 - y_6)$ $\hat{v}_3 = \hat{V}_3 - M = 1/6\ (-y_2 - y_3 + y_5 + y_6)$ Arithmetic Check = $\Sigma\ \hat{v}_i = 0$ (within round-off)	4. $\hat{v}_1 = 1/6\ (4.8 - 6.6 + 3.4 - 7.4) = -.967\ \mu V$ $\hat{v}_2 = 1/6\ (-4.8 - 10.6 - 3.4 - 10.4) = -4.867$ $\hat{v}_3 = 1/6\ (+6.6 + 10.6 + 7.4 + 10.4) = +5.833$ Check = $-.967 - 4.867 + 5.833 = -.001\ \mu V$
5. Calculation of $\hat{y}$'s, the predicted y's: $\hat{y}_1 = \hat{v}_1 - \hat{v}_2 + \hat{P}$ $\hat{y}_2 = \hat{v}_1 - \hat{v}_3 + \hat{P}$ $\hat{y}_3 = \hat{v}_2 - \hat{v}_3 + \hat{P}$ $\hat{y}_4 = \hat{v}_2 - \hat{v}_1 + \hat{P}$ $\hat{y}_5 = \hat{v}_3 - \hat{v}_1 + \hat{P}$ $\hat{y}_6 = \hat{v}_3 - \hat{v}_2 + \hat{P}$ Arithmetic Check = $\Sigma\ \hat{y}_i = 6\hat{P}$	5. $\hat{y}_1 = -.967 + 4.867 + .333 = +4.233\ \mu V$ $\hat{y}_2 = -.967 - 5.833 + .333 = -6.467$ $\hat{y}_3 = -4.867 - 5.833 + .333 = -10.367$ $\hat{y}_4 = -4.867 + .967 + .333 = -3.567$ $\hat{y}_5 = +5.833 + .967 + .333 = +7.133$ $\hat{y}_6 = +5.833 + 4.867 + .333 = +11.033$ Check = $\Sigma\ \hat{y}_i = 1.998$
6. Calculation of the deviations ($d_i = y_i - \hat{y}_i$): $d_1 = y_1 - \hat{y}_1$ $d_2 = y_2 - \hat{y}_2$ $d_3 = y_3 - \hat{y}_3$ $d_4 = y_4 - \hat{y}_4$ $d_5 = y_5 - \hat{y}_5$ $d_6 = y_6 - \hat{y}_6$ Check = $\sum_{i=1}^{6} d_i = 0$ (within round-off)	6. $d_1 = 4.8 - 4.233 = .567\ \mu V$ $d_2 = -6.6 + 6.467 = -.133$ $d_3 = -10.6 + 10.367 = -.233$ $d_4 = -3.4 + 3.567 = +.167$ $d_5 = 7.4 - 7.133 = +.267$ $d_6 = 10.4 - 11.033 = -.633$ $\Sigma d = .002$
7. The standard deviation of a single observation (s) is $s = \sqrt{\frac{\sum_{i=1}^{6} d_i^2}{3}}$ where 3 represents the number of degrees of freedom in this error estimate.	7. $s = \sqrt{\frac{.8933}{3}} \simeq .55\ \mu V$
8. Emf values of the cells The emf's of the cells are calculated by restoring the mean value to give $\hat{V}_i = \hat{v}_i + M$	8. Mean (from Section 1): 1.01825830 $\hat{V}_1 = 1.01825830 - 0.00000097 = 1.01825733$ $\hat{V}_2 = 1.01825830 - 0.00000487 = 1.01825343$ $\hat{V}_3 = 1.01825830 + 0.00000583 = 1.01826413$

TABLE A-2

THE INTERCOMPARISON OF A GROUP OF 4 CELLS

	Example
1. Given: The emfs of four saturated standard cells (V_1, V_2, V_3 and V_4) are assigned by calibrating them in terms of a known standard of electromotive force. The mean of the group is $M = 1/4 \sum_{i=1}^{4} V_i$ and the difference from the mean of each cell is $v_i = (V_i - M)$	1. From an NBS Report of Calibration: $V_1 = 1.0182459$ $v_1 = -4.1\ \mu V$ $V_2 = 1.0182488$ $v_2 = -1.2$ $V_3 = 1.0182526$ $v_3 = +2.6$ $V_4 = 1.0182527$ $v_4 = +2.7$ Mean = 1.0182500 sum = 0
2. Assuming that there is a small constant emf P associated with the measuring process, the expected value of a single observation is $E(y_i) = V_j - V_k + P \quad j \neq k$; for j and k = 1,2,3,4. For all possible values of j and k the following schedule of measurements is convenient, and in most cases requires changing the connections to only one cell at a time.	2. Observations:

Measurement	Cell in UNK position	Cell in REF position	
y_1	1	2	$y_1 = -3.1\ \mu V$
y_2	1	3	$y_2 = -6.9$
y_3	2	3	$y_3 = -3.8$
y_4	2	4	$y_4 = -4.0$
y_5	3	4	$y_5 = -.4$
y_6	3	1	$y_6 = 6.3$
y_7	3	2	$y_7 = 3.3$
y_8	4	2	$y_8 = 3.4$
y_9	4	1	$y_9 = 6.4$
y_{10}	4	3	$y_{10} = -.2$
y_{11}	2	1	$y_{11} = 2.7$
y_{12}	1	4	$y_{12} = -7.0$

3. Estimation of P: $\hat{P} = 1/12 \sum_{i=1}^{12} y_i$	3. $\hat{P} = 1/12\ (-3.1 -6.9 -3.8 -4.0 -.4 +6.3 +3.3 +3.4 +6.4 -.2 +2.7 = 7.0)$ $\hat{P} = -.275\ \mu V$

TABLE A-2 Continued

4. Estimation of v_i:

$$\hat{v}_1 = \hat{V}_1 - M = 1/8\,(y_1 + y_2 - y_6 - y_9 - y_{11} + y_{12})$$

$$\hat{v}_2 = \hat{V}_2 - M = 1/8\,(-y_1 + y_3 + y_4 - y_7 - y_8 + y_{11})$$

$$\hat{v}_3 = \hat{V}_3 - M = 1/8\,(-y_2 - y_3 + y_5 + y_6 + y_7 - y_{10})$$

$$\hat{v}_4 = \hat{V}_4 - M = 1/8\,(-y_4 - y_5 + y_8 + y_9 + y_{10} - y_{12})$$

Arithmetic Check = $\sum_1^5 \hat{v}_i = 0$ (within round-off)

4.

$\hat{v}_1 = 1/8\,(-3.1 - 6.9 - 6.3 - 6.4 - 2.7 - 7.0) = -4.05\ \mu V$

$\hat{v}_2 = 1/8\,(3.1 - 3.8 - 4.0 - 3.3 - 3.4 + 2.7) = -1.088$

$\hat{v}_3 = 1/8\,(6.9 + 3.8 - .4 + 6.3 + 3.3 + .2) = 2.512$

$\hat{v}_4 = 1/8\,(4.0 + .4 + 3.4 + 6.4 - .2 + 7.0) = 2.625$

Check = $-4.050 - 1.087 + 2.512 + 2.625 = 0.001$

5. Calculation of $\hat{y}$'s, the predicted y's:

$$\hat{y}_1 = \hat{v}_1 - \hat{v}_2 + \hat{P}$$
$$\hat{y}_2 = \hat{v}_1 - \hat{v}_3 + \hat{P}$$
$$\hat{y}_3 = \hat{v}_2 - \hat{v}_3 + \hat{P}$$
$$\hat{y}_4 = \hat{v}_2 - \hat{v}_4 + \hat{P}$$
$$\hat{y}_5 = \hat{v}_3 - \hat{v}_4 + \hat{P}$$
$$\hat{y}_6 = \hat{v}_3 - \hat{v}_1 + \hat{P}$$
$$\hat{y}_7 = \hat{v}_3 - \hat{v}_2 + \hat{P}$$
$$\hat{y}_8 = \hat{v}_4 - \hat{v}_2 + \hat{P}$$
$$\hat{y}_9 = \hat{v}_4 - \hat{v}_1 + \hat{P}$$
$$\hat{y}_{10} = \hat{v}_4 - \hat{v}_3 + \hat{P}$$
$$\hat{y}_{11} = \hat{v}_2 - \hat{v}_1 + \hat{P}$$
$$\hat{y}_{12} = \hat{v}_1 - \hat{v}_4 + \hat{P}$$

Arithmetic Check = $\sum \hat{y}_i = 12\hat{P}$

5.

$\hat{y}_1 = -4.050 + 1.088 - .275 = -3.237\ \mu V$
$\hat{y}_2 = -4.050 - 2.512 - .275 = -6.837$
$\hat{y}_3 = -1.088 - 2.512 - .275 = -3.875$
$\hat{y}_4 = -1.088 - 2.625 - .275 = -3.988$
$\hat{y}_5 = 2.512 - 2.625 - .275 = -0.388$
$\hat{y}_6 = 2.512 + 4.050 - .275 = 6.287$
$\hat{y}_7 = 2.512 + 1.088 - .275 = 3.325$
$\hat{y}_8 = 2.625 + 1.088 - .275 = 3.438$
$\hat{y}_9 = 2.625 + 4.050 - .275 = 6.400$
$\hat{y}_{10} = 2.625 - 2.512 - .275 = -0.162$
$\hat{y}_{11} = -1.088 + 4.050 - .275 = 2.687$
$\hat{y}_{12} = -4.050 - 2.625 - .275 = -6.950$

sum = $(-3.237 - 6.837 - 3.875 - 3.988 - 0.388 + 6.287 + 3.325 + 3.438 + 6.400 - 0.162 + 2.687 - 6.950) = -3.300$

6. Calculation of the deviations ($d_i = y_i - \hat{y}_i$):

$$d_1 = y_1 - \hat{y}_1$$
$$d_2 = y_2 - \hat{y}_2$$
$$d_3 = y_3 - \hat{y}_3$$
$$d_4 = y_4 - \hat{y}_4$$
$$d_5 = y_5 - \hat{y}_5$$
$$d_6 = y_6 - \hat{y}_6$$
$$d_7 = y_7 - \hat{y}_7$$
$$d_8 = y_8 - \hat{y}_8$$
$$d_9 = y_9 - \hat{y}_9$$
$$d_{10} = y_{10} - \hat{y}_{10}$$
$$d_{11} = y_{11} - \hat{y}_{11}$$
$$d_{12} = y_{12} - \hat{y}_{12}$$

Arithmetic Check = $\sum d_i = 0$ (within round-off)

6.

$d_1 = -3.1 + 3.237 = .137\ \mu V$
$d_2 = -6.9 + 6.837 = -.063$
$d_3 = -3.8 + 3.875 = .075$
$d_4 = -4.0 + 3.988 = -.012$
$d_5 = -0.4 + .388 = -.012$
$d_6 = 6.3 - 6.287 = .013$
$d_7 = 3.3 - 3.325 = -.025$
$d_8 = 3.4 - 3.438 = -.037$
$d_9 = 6.4 - 6.400 = 0$
$d_{10} = -.2 + .162 = -.038$
$d_{11} = 2.7 - 2.687 = .013$
$d_{12} = -7.0 + 6.950 = -.050$

$(.137 - .063 + .075 - .012 - .012 + .013 - .025 - .038 + 0 - .038 + .013 - .050) = 0$

7. The standard deviation of a single observation (s) is

$$s = \sqrt{\frac{\sum_{i=1}^{12} (d_i)^2}{8}}$$

where 8 represents the number of degrees of freedom in this error estimate.

7.

$$s = \sqrt{\frac{.035}{8}} = .066\ \mu V$$

8. Emf values of the cells

The emf's of the cells are calculated by restoring the mean value to give

$$\hat{V}_i = \hat{v}_i + M$$

8. Mean (from Section 1): 1.01825000

$\hat{V}_1 = 1.01825000 - 0.00000405 = 1.01824595$
$\hat{V}_2 = 1.01825000 - 0.00000109 = 1.01824891$
$\hat{V}_3 = 1.01825000 + 0.00000251 = 1.01825251$
$\hat{V}_4 = 1.01825000 + 0.00000262 = 1.01825262$

TABLE A-3

THE INTERCOMPARISON OF A GROUP OF 5 CELLS

	Example
1. Given: The emfs of five saturated standard cells (V_1, V_2, V_3, V_4 and V_5) are assigned by calibrating them in terms of a known standard of electromotive force. The mean of the group is $M = 1/5 \sum_{i=1}^{4} V_i$ and the difference from the mean of each cell is $v_i = (V_i - M)$	1. From an NBS Report of Calibration: V_1 = 1.0182538 v_1 = .8 μV V_2 = 1.0182531 v_2 = .1 V_3 = 1.0182518 v_3 = -1.2 V_4 = 1.0182532 v_4 = .2 V_5 = 1.0182531 v_5 = .1 Mean = 1.0182530 sum = 0
2. Assuming that there is a small constant emf P associated with the measuring process then the expected value of a single observation is $E(y_i) = V_j - V_k + P \quad j \neq k$; for j and k= 1,2...5 For certain values of j and k a set of 10 measurements having "left-right" balance that is convenient and requires changing the connections to only one cell at a time is	2. Observations.

Measurement	Cell in UNK position	Cell in REF position	
1	1	2	y_1 = .5 μV
2	1	3	y_2 = 1.6
3	2	3	y_3 = .9
4	2	4	y_4 = -.4
5	3	4	y_5 = -1.5
6	3	5	y_6 = -1.3
7	4	5	y_7 = 0
8	4	1	y_8 = -.8
9	5	1	y_9 = -1.0
10	5	2	y_{10} = -.2

3. Estimation of P: $\hat{P} = 1/10 \sum_{i=1}^{10} y_i$	3. $\hat{P}$ = 1/10 (.5 +1.6 +.9 -.4 -1.5 -1.3 +0. -.8 -1.0 -.2) $\hat{P}$ = -.22 μV
4. Estimation of v_i: $\hat{v}_1 = \hat{V}_1 - M = 1/5\ (y_1 + y_2 - y_8 - y_9)$ $\hat{v}_2 = \hat{V}_2 - M = 1/5\ (-y_1 + y_3 + y_4 - y_{10})$ $\hat{v}_3 = \hat{V}_3 - M = 1/5\ (-y_2 - y_3 + y_5 + y_6)$ $\hat{v}_4 = \hat{V}_4 - M = 1/5\ (-y_4 - y_5 + y_7 + y_8)$ $\hat{v}_5 = \hat{V}_5 - M = 1/5\ (-y_6 - y_7 + y_9 + y_{10})$ Arithmetic Check = $\sum_{i=1}^{5} V = 0$ (within round-off)	4. $\hat{v}_1$ = 1/5 (.5 +1.6 +.8 +1.0) = .78 μV $\hat{v}_2$ = 1/5 (-.5 +.9 -.4 +.2) = .04 $\hat{v}_3$ = 1/5 (-1.6 -.9 -1.5 -1.3) = -1.06 $\hat{v}_4$ = 1/5 (+.4 +1.5 +0. -.8) = .22 $\hat{v}_5$ = 1/5 (1.3 +0. -1.0 -.2) = 0.02 Check: $\sum_{i=1}^{5} \hat{v}_i$ = .78 +.04 -1.06 +.22 +.02= 0

TABLE A-3 Continued

5. Calculation of $\hat{y}$'s, the predicted y's:

$$\hat{y}_1 = \hat{v}_1 - \hat{v}_2 + \hat{P}$$
$$\hat{y}_2 = \hat{v}_1 - \hat{v}_3 + \hat{P}$$
$$\hat{y}_3 = \hat{v}_2 - \hat{v}_3 + \hat{P}$$
$$\hat{y}_4 = \hat{v}_2 - \hat{v}_4 + \hat{P}$$
$$\hat{y}_5 = \hat{v}_3 - \hat{v}_4 + \hat{P}$$
$$\hat{y}_6 = \hat{v}_3 - \hat{v}_5 + \hat{P}$$
$$\hat{y}_7 = \hat{v}_4 - \hat{v}_5 + \hat{P}$$
$$\hat{y}_8 = \hat{v}_4 - \hat{v}_1 + \hat{P}$$
$$\hat{y}_9 = \hat{v}_5 - \hat{v}_1 + \hat{P}$$
$$\hat{y}_{10} = \hat{v}_5 - \hat{v}_2 + \hat{P}$$

Arithmetic Check: $\Sigma \hat{y}_i = 10\hat{P}$

5.

$\hat{y}_1 = .78 - .04 - .22 = .52$ μV
$\hat{y}_2 = .78 + 1.06 - .22 = 1.62$
$\hat{y}_3 = .04 + 1.06 - .22 = .88$
$\hat{y}_4 = .04 - .22 - .22 = -.4$
$\hat{y}_5 = -1.06 - .22 - .22 = -1.50$
$\hat{y}_6 = -1.06 - .02 - .22 = -1.30$
$\hat{y}_7 = .22 - .02 - .22 = -.02$
$\hat{y}_8 = .22 - .78 - .22 = -.78$
$\hat{y}_9 = .02 - .78 - .22 = -.98$
$\hat{y}_{10} = .02 - .04 - .22 = -.24$

Check: $\Sigma \hat{y} = -2.20 = 10(-.22) = -2.20$

6. Calculation of the deviations ($d_i = y_i - \hat{y}_i$):

$$d_1 = y_1 - \hat{y}_1$$
$$d_2 = y_2 - \hat{y}_2$$
$$d_3 = y_3 - \hat{y}_3$$
$$d_4 = y_4 - \hat{y}_4$$
$$d_5 = y_5 - \hat{y}_5$$
$$d_6 = y_6 - \hat{y}_6$$
$$d_7 = y_7 - \hat{y}_7$$
$$d_8 = y_8 - \hat{y}_8$$
$$d_9 = y_9 - \hat{y}_9$$
$$d_{10} = y_{10} - \hat{y}_{10}$$

Check = $\sum_{i=1}^{10} d_i = 0$ (within round-off)

6.

$d_1 = .5 - .52 = -.02$ μV
$d_2 = 1.6 - 1.62 = -.02$
$d_3 = .9 - .88 = .02$
$d_4 = -.4 + .4 = 0$
$d_5 = -1.5 + 1.50 = 0$
$d_6 = -1.3 + 1.30 = 0$
$d_7 = 0. + .02 = .02$
$d_8 = -.8 + .78 = -.02$
$d_9 = -1.0 + .98 = -.02$
$d_{10} = -.2 + .24 = .04$

Check = $(-.02 - .02 + .02 + .3(0) + .02 - .02 - .02 + .04) = 0$

7. The standard deviation of a single observation (s) is

$$s = \sqrt{\frac{\sum_{i-1}^{10} d_i}{5}}$$

where 5 represents the number of degrees of freedom in this error estimate.

7.

$$s = \sqrt{\frac{.004}{5}} = .028 \text{ μV}$$

8. Emf values of the cells

The emf's of the cells are calculated by restoring the mean value to give

$$\hat{V}_i = \hat{v}_i + M$$

8. Mean (from Section 1): 1.01825300

$\hat{V}_1 = 1.01825300 + 0.00000078 = 1.01825378$
$\hat{V}_2 = 1.01825300 + 0.00000004 = 1.01825304$
$\hat{V}_3 = 1.01825300 - 0.00000106 = 1.01825194$
$\hat{V}_4 = 1.01825300 + 0.00000022 = 1.01825322$
$\hat{V}_5 = 1.01825300 + 0.00000002 = 1.01825302$

TABLE A-4

THE INTERCOMPARISON OF A GROUP OF 6 CELLS

	Example
1. Given: The emfs of six saturated standard cells (V_1, V_2, V_3, V_4, V_5 and V_6) are assigned by calibrating them in terms of a known standard of electromotive force. The mean of the group is $M = 1/6 \sum_{i=1}^{6} V_i$ and the difference from the mean of each cell is $v_i = (V_i - M)$	1. From an NBS Report of Calibration: V_1 = 1.0182605 v_1 = 10.52 V_2 = 1.0182655 v_2 = 15.52 V_3 = 1.0182466 v_3 = -3.38 V_4 = 1.0182476 v_4 = -2.38 V_5 = 1.0182416 v_5 = -8.38 V_6 = 1.0182381 v_6 = -11.88 Mean = 1.01824998 sum = 0
2. Assuming that there is a small constant emf P associated with the measuring process, the expected value of a single observation is $E(y_i) = V_j - V_k + P \quad j \neq k$; for j and k = 1,2...6 For certain values of j and k a set of 15 measurements, 12 of which are "left-right" balanced, can be made.	2. Observations:

Measurement	Cell in UNK position	Cell in REF position	
1	1	2	y_1 = -5.4 μV
2	1	3	y_2 = 13.7
3	2	3	y_3 = 18.8
4	2	4	y_4 = 17.7
5	3	4	y_5 = -1.3
6	3	5	y_6 = 4.8
7	4	5	y_7 = 5.9
8	4	6	y_8 = 9.5
9	5	6	y_9 = 3.5
10	5	1	y_{10} = -19.1
11	6	1	y_{11} = -22.7
12	6	2	y_{12} = -27.9
13	1	4	y_{13} = 12.5
14	2	5	y_{14} = 23.7
15	3	6	y_{15} = 8.4

3. Create a set of sums Q_i, S and T: $Q_1 = (y_1 + y_2 - y_{10} - y_{11} + y_{13})$ $Q_2 = (-y_1 + y_3 + y_4 - y_{12} + y_{14})$ $Q_3 = (-y_2 - y_3 + y_5 + y_6 + y_{15})$ $Q_4 = (-y_4 - y_5 + y_7 + y_8 - y_{13})$ $Q_5 = (-y_6 - y_7 + y_9 + y_{10} - y_{14})$ $Q_6 = (-y_8 - y_9 + y_{11} + y_{12} - y_{15})$ $S = Q_1 + Q_2 + Q_3$ T = sum of all measurements Arithmetic Check = $\sum_{i=1}^{6} Q_i = 0$	3. $Q_1 = (-5.4 + 13.7 + 19.1 + 22.7 + 12.5) = +62.6$ $Q_2 = (5.4 + 18.8 + 17.7 + 27.9 + 23.7) = +93.5$ $Q_3 = (-13.7 - 18.8 - 1.3 + 4.8 + 8.4) = -20.6$ $Q_4 = (-17.7 + 1.3 + 5.9 + 9.5 - 12.5) = -13.5$ $Q_5 = (-4.8 - 5.9 + 3.5 - 19.1 - 23.7) = -50.0$ $Q_6 = (-9.5 - 3.5 - 22.7 - 27.9 - 8.4) = -72.0$ $S = (62.6 + 93.5 - 20.6) = 135.5$ T = (-5.4 +13.7 +18.8 +17.7 -1.3 +4.8 +5.9 +9.5 +3.5 -19.1 -22.7 -27.9 +12.5 +23.7 +8.4) = 42.1 Check = (62.6 +93.5 -20.6 -13.5 -50.0 -72.0) = 0
4. Calculate $\hat{P}$: $\hat{P} = \frac{3T - S}{42}$	4. $\hat{P} = \frac{126.3 - 135.5}{42} = -.219$ μV

TABLE A-4 Continued

5. Calculate $\hat{v}$'s:

$$\hat{v}_1 = 1/6\ (Q_1 - \hat{P})$$
$$\hat{v}_2 = 1/6\ (Q_2 - \hat{P})$$
$$\hat{v}_3 = 1/6\ (Q_3 - \hat{P})$$
$$\hat{v}_4 = 1/6\ (Q_4 + \hat{P})$$
$$\hat{v}_5 = 1/6\ (Q_5 + \hat{P})$$
$$\hat{v}_6 = 1/6\ (Q_6 + \hat{P})$$

$$\text{Check} = \sum_{i=1}^{6} \hat{v}_i = 0$$

5.

$$\hat{v}_1 = 1/6\ (62.6 + .219) = 10.470\ \mu V$$
$$\hat{v}_2 = 1/6\ (93.5 + .219) = 15.620$$
$$\hat{v}_3 = 1/6\ (-20.6 + .219) = -3.397$$
$$\hat{v}_4 = 1/6\ (-13.5 - .219) = -2.286$$
$$\hat{v}_5 = 1/6\ (-50.0 - .219) = -8.370$$
$$\hat{v}_6 = 1/6\ (-72.0 - .219) = -12.036$$

Check = 1/6 (62.819 +93.719 -20.819 -13.781 -50.219 -72.219) = 0

6. Calculation of $\hat{y}$'s, the predicted y's:

$$\hat{y}_1 = \hat{v}_1 - \hat{v}_2 + \hat{P}$$
$$\hat{y}_2 = \hat{v}_1 - \hat{v}_3 + \hat{P}$$
$$\hat{y}_3 = \hat{v}_2 - \hat{v}_3 + \hat{P}$$
$$\hat{y}_4 = \hat{v}_2 - \hat{v}_4 + \hat{P}$$
$$\hat{y}_5 = \hat{v}_3 - \hat{v}_4 + \hat{P}$$
$$\hat{y}_6 = \hat{v}_3 - \hat{v}_5 + \hat{P}$$
$$\hat{y}_7 = \hat{v}_4 - \hat{v}_5 + \hat{P}$$
$$\hat{y}_8 = \hat{v}_4 - \hat{v}_6 + \hat{P}$$
$$\hat{y}_9 = \hat{v}_5 - \hat{v}_6 + \hat{P}$$
$$\hat{y}_{10} = \hat{v}_5 - \hat{v}_1 + \hat{P}$$
$$\hat{y}_{11} = \hat{v}_6 - \hat{v}_1 + \hat{P}$$
$$\hat{y}_{12} = \hat{v}_6 - \hat{v}_2 + \hat{P}$$
$$\hat{y}_{13} = \hat{v}_1 - \hat{v}_4 + \hat{P}$$
$$\hat{y}_{14} = \hat{v}_2 - \hat{v}_5 + \hat{P}$$
$$\hat{y}_{15} = \hat{v}_3 - \hat{v}_6 + \hat{P}$$

6.

$$\hat{y}_1 = 10.470 - 15.620 - .219 = -5.369$$
$$\hat{y}_2 = 10.470 + 3.397 - .219 = 13.648$$
$$\hat{y}_3 = 15.620 + 3.397 - .219 = 18.798$$
$$\hat{y}_4 = 15.620 + 2.286 - .219 - 17.687$$
$$\hat{y}_5 = -3.397 + 2.286 - .219 = -1.330$$
$$\hat{y}_6 = -3.397 + 8.370 - .219 = 4.754$$
$$\hat{y}_7 = -2.286 + 8.370 - .219 = 5.865$$
$$\hat{y}_8 = -2.286 + 12.036 - .219 = 9.531$$
$$\hat{y}_9 = -8.370 + 12.036 - .219 = 3.447$$
$$\hat{y}_{10} = -8.370 - 10.470 - .219 = -19.059$$
$$\hat{y}_{11} = -12.036 - 10.470 - .219 = -22.725$$
$$\hat{y}_{12} = -12.036 - 15.620 - .219 = -27.875$$
$$\hat{y}_{13} = 10.470 + 2.286 - .219 = 12.537$$
$$\hat{y}_{14} = 15.620 + 8.370 - .219 = 23.771$$
$$\hat{y}_{15} = -3.397 + 12.036 - .219 = 8.420$$

7. Calculation of the deviations ($d_i = y_i - \hat{y}_i$):

$$d_1 = y_1 - \hat{y}_1$$
$$d_2 = y_2 - \hat{y}_2$$
$$d_3 = y_3 - \hat{y}_3$$
$$d_4 = y_4 - \hat{y}_4$$
$$d_5 = y_5 - \hat{y}_5$$
$$d_6 = y_6 - \hat{y}_6$$
$$d_7 = y_7 - \hat{y}_7$$
$$d_8 = y_8 - \hat{y}_8$$
$$d_9 = y_9 - \hat{y}_9$$
$$d_{10} = y_{10} - \hat{y}_{10}$$
$$d_{11} = y_{11} - \hat{y}_{11}$$
$$d_{12} = y_{12} - \hat{y}_{12}$$
$$d_{13} = y_{13} - \hat{y}_{13}$$
$$d_{14} = y_{14} - \hat{y}_{14}$$
$$d_{15} = y_{15} - \hat{y}_{15}$$

7.

$$d_1 = -5.4 + 5.369 = -.031\ \mu V$$
$$d_2 = 13.7 - 13.648 = .052$$
$$d_3 = 18.8 - 18.798 = .002$$
$$d_4 = 17.7 - 17.687 = .013$$
$$d_5 = -1.3 + 1.330 = .030$$
$$d_6 = 4.8 - 4.754 = .046$$
$$d_7 = 5.9 - 5.865 = .035$$
$$d_8 = 9.5 - 9.531 = -.031$$
$$d_9 = 3.5 - 3.447 = .053$$
$$d_{10} = -19.1 + 19.059 = -.041$$
$$d_{11} = -22.7 + 22.725 = .025$$
$$d_{12} = -27.9 + 27.875 = -.025$$
$$d_{13} = 12.5 - 12.537 = -.037$$
$$d_{14} = 23.7 - 23.771 = -.071$$
$$d_{15} = 8.4 - 8.420 = -.020$$

8. The standard deviation of a single observation (s) is

$$s = \sqrt{\frac{\Sigma(d_i)^2}{9}}$$

where 9 represents the degrees of freedom for error.

8.

$$s = \sqrt{\frac{.021590}{9}} = .0490\ \mu V$$

9. Emf values of the cells

The emf's of the cells are calculated by restoring the mean value to give

$$\hat{V}_i = \hat{v}_i + M$$

9. Mean (from Section 1): 1.01824998

$$\hat{V}_1 = 1.01824998 + 0.00001047 = 1.01826045$$
$$\hat{V}_2 = 1.01824998 + 0.00001562 = 1.01826560$$
$$\hat{V}_3 = 1.01824998 - 0.00000340 = 1.01824658$$
$$\hat{V}_4 = 1.01824998 - 0.00000229 = 1.01824769$$
$$\hat{V}_5 = 1.01824998 - 0.00000837 = 1.01824161$$
$$\hat{V}_6 = 1.01824998 - 0.00001204 = 1.01823794$$

MEASUREMENT ASSURANCE PROGRAMS IN A FIELD ENVIRONMENT

Woodward G Eicke, Jr.[1], Thomas F. Leedy[2]
Brian R. Moore[3], and Charles F. Brown[3]

ABSTRACT

To date most measurement assurance programs have been carried out between the National Bureau of Standards and various standards laboratories in the U.S. For the most part, these have been conducted at the highest accuracy levels. In the spring of 1982 the Army Missile Command and NBS conducted two special, lower accuracy, measurement assurance programs (S-MAP) at a field location at Redstone Arsenal, Alabama, in the areas of dc voltage, dc current dc resisitance, ac voltage, and ac current. This paper describes the experiments performed, presents the results, and discusses them in light of a number of externally imposed constraints.

INTRODUCTION

The extensive use of automatic test equipment (ATE) and precision electronic instruments and equipment in the United States has necessitated new concepts to ensure measurement accuracy. This new generation of equipment, unlike early instrumentation, is characterized by complexity. It is often comprised of numerous sophisticated electronic instruments operating as an integral unit, often under computer control, and is frequently used in field locations where the environment is uncontrolled. Traditionally, in order to support the accuracy requirements of such equipment it is calibrated in the standards laboratory; however, such calibrations may be meaningless when the instrument is returned to its normal operating environment. To obtain a meaningful calibration it is often necessary to calibrate the instrument in its normal operating environment. Such an on-site calibration requires that standards, auxilary equipment and personnel from the standards laboratory be transported to the site, perform the necessary measurements, analyze the data, and report the results. In addition they must measure the transport standards to insure that they have not changed during the calibration interval. This process is essentially that of a

---

(1) Electrical Measurements and Standards Division, National Bureau of Standards, Washington, DC 20234.
(2) Electrosystems Division, National Bureau of Standards, Washington, DC 20234.
(3) Electrical Standards and Development Laboratory, U.S. Army TMDE Support Group, Redstone Arsenal, AL 35898.

measurement assurance program (MAP). Unfortunately, most MAPs are operated among NBS and standards laboratories, are aimed at the highest levels of accuracy attainable for a given measurement area, and are usually limited to certain specific values of standards. Such MAPs employ sophisticated transport standards, are labor intensive, and require extensive data analysis. Because of their complexity, present MAP techniques are not readily applicable to modern electronic equipment requiring many calibration points or to calibration equipment which is located in less than an ideal environment. Therefore an extension of the present MAP techniques is needed to serve as a link between the standards laboratory and equipment requiring field calibration. MAPs for this type of activity should be efficient, require a minimum of equipment and manpower, be tailored to the particular instruments and locale, and should provide calibration results in real time (on-site).

Early in 1982 NBS and the U.S. Army Missile Command (MICOM) at Redstone Arsenal, Alabama, as a part of a larger project, carried out special measurement assurance programs in five electrical measurement areas: dc voltage, dc current, dc resistance, ac voltage, and ac current. The nature of the NBS involvement provided an ideal opportunity to explore the possibility of developing MAPs between the standards laboratory and instruments located in a field environment. The objectives, within the available resources, were to (1) investigate the feasibility of carrying out on-site calibrations, (2) identify measurement problems, (3) make preliminary assessment of uncertainties of such calibrations, and (4) investigate the use of desk-top computers for on-site data aquisition and processing.

At Redstone Arsenal (RSA), most of the work described was carried out at a field site on the arsenal grounds. The building had only limited temperature and humidity control, and no control over the electrical environment. In addition it was necessary to frequently move the measuring equipment from one location to another within the building. Short term temperature variations were as large as 6 deg. C and relative humidity exceeded 65 percent on several occasions. NBS hand-carried transport standards, digital mulitmeters, and auxilary equipment to and from Redstone on two occassions: in late March and in mid-May 1982. All measurements at Redstone had to be made within a specific time frame and had to be integrated into a larger on-going Army program at the field site. The NBS transport standards, with one exception, were measured in terms of local standards at the field site which were provided and calibrated by the Electrical Standards and Development Laboratory, U.S. Army TMDE Support Group. All NBS transport standards were calibrated by NBS before and after each trip. At Redstone measurements were performed using the procedures described in this paper. The results of all measurements described in this paper are expressed as the differences, d.d, in parts per million, between the measured values at RSA and NBS obtained from the equation

$$\frac{X_{RSA} - X_{NBS}}{X_{NBS}} \times 10^6 = d.d \text{ ppm},$$

where X_{RSA} and X_{NBS} are the measured values in terms of local Army standards and the NBS standards respectively. In this paper we will present an overview of the experiments, pertinent results, and give some conclusions.

DC MEASUREMENTS

The NBS dc measurement package contained (1) a temperature-controlled standard cell enclosure with four cells, (2) a voltage divider, (3) standard resistors, (4) six-digit digital multimeters (DMM), and (5) auxilary equipment which included a desk-top computer, low thermal leads, and switches. The DMMs had 0.1 microvolt resolution, an input impedance in excess of 100 megohms, were IEEE-488 bus compatible, and were used as the measuring instrument for all dc measurements at Redstone. In order to minimize the effect of parasitic emfs in the measuring instruments and some of the leads two observations were taken, one with the DMM connected normally and the other with its input leads reversed. Typically the observed differences rarely exceeded 2 ppm. At NBS the linearity of the DMMs was determined to be approximately within ±3 ppm over the full scale. For the lower three digits the linearity was within ±1 ppm or less.

DC VOLTAGE: Two different experiments were conducted to determine dc voltage. The first was a direct intercomparison of the RSA local voltage standard and the NBS transport standard, the other a comparison of two measuring systems at nominally 1, 10, and 100 volts. Using standard Volt Transfer Program techniques (VTP) the four cells in the RSA standard cell enclosure were directly compared to the NBS transport standard using a DMM to measure the differences between the cells connected in series opposition. From the measurements at Redstone and NBS the following results were obtained:

March 1982	$E_{RSA} - E_{NBS} = 0.8$ ppm
May 1982	$E_{RSA} - E_{NBS} = 0.7$ ppm.

The observed differences are consistent with those of the normal VTP even though the settling time was short and only one set of measurements were made at Redstone. The estimated uncertainty at the three standard deviation level of this experiment is no greater than 1.5 ppm.

The second experiment consisted of RSA and NBS making concurrent voltage measurements using stable voltage sources on several days. RSA and NBS each used a precision voltage divider and a DMM as the measuring system. The voltage dividers were connected to the source and the divider output (at the 1 volt level) was

measured with a DMM having 1 ppm resolution. Using their respective standard cells as the reference the RSA and NBS DMMs were calibrated in terms of the local units of voltage. RSA and NBS each calculated a voltage in terms of their respective standards and the differences in these calculated voltages are summarized below.

Nominal Voltage (V)	Difference ($E_{RSA} - E_{NBS}$) in ppm			
	Day 1	Day 2	Day 3	Mean
1	+0.2	+0.2	+0.7	+0.37
10	-3.1	-2.7	-0.7	-2.17
100	-0.5	-7.1	-3.1	-3.57

At the 1 volt level the results are consistent with the differences from the cell comparison. At the other two voltages there is clearly an offset which may be voltage dependent. This technique is very simple, can be carried out quickly, and could lend itself to automation.

DC CURRENT: A traditional approach to measuring dc current was used and consisted of simply measuring the voltage drop across calibrated resistors mounted in a temperature controlled oil bath. RSA and NBS each concurrently measured nominal currents at the 10 A, 0.1 A and 0.0001 A levels in terms of their local standards (resistance and voltage). Current measurements were made in March and May using several stable current sources. The results of these measurements are summarized below.

10 A level	$I_{RSA} - I_{NBS} = +42$ ppm
0.1 A level	$I_{RSA} - I_{NBS} = +9$ ppm
0.0001 A level	$I_{RSA} - I_{NBS} = +14$ ppm

The large difference at the the 10 A is attributable to the self-heating of the 0.1 ohm resistors. The difference at 0.1 A, in as far as can be determined at this time, was mostly caused by thermals at the potential terminals and temperature gradients in the resistor caused by problems with temperature control and oil level. At the 0.0001 A level a 10 k ohm resistor was used as the shunt. From other work we concluded that leakage problems in the oil bath could cause differences of the magnitude observed. Certainly if more accurate current measurements are required then self heating, leakage, and thermal problems must be addressed.

DC RESISTANCE: Resistance intercomparisons were conducted at the 1 ohm, 10 k ohm, and 10 M ohm levels. The NBS transport standards were two Rosa type 1 ohm, two Rosa type 10 k ohm, and two NBS constructed 10 M ohm resistors which were intercompared with the RSA local standards. All resistors except the two 10 M ohm were in an oil bath operated at a nominal temperature of 25 deg. C. At the one ohm level the resistors were measured by applying a constant current of 100 mA to the three resistors connected in series (one RSA and two NBS) and measuring the voltage drop with the DMM. For the other two values the DMM was used in the ohmmeter mode. In each case the value of the transport standards was calculated from the relationship

$$R_x = R_s(E_x/E_s)$$

where the subscripts s and x designate the RSA standards and the NBS transport standard, respectively, E the DMM reading, and R the resistance. The May measurements were performed when the bath temperature sometimes exceeded 25 deg. C. The results are summarized below.

Nominal	$R_{RSA} - R_{NBS}$ in ppm	
Resistance	March 1982	May 1982
1 ohm	+0.2	+4.7
10 K ohm	-0.6	-0.5
10 M ohm	+39	+58

During March, measurements were made when temperature conditions were relatively stable there was little variability among the runs, and the measurement process was well behaved. In May, temperature and humidity conditions were far more variable and there was much more variability in the results. In all cases the measured differences were consistent with the estimated uncertainties for the measurements made. The difference between the two NBS transport standards, at the 10 M ohm level, when measured using the DMM, at both Redstone and NBS, consistently differed from those obtained by the normal NBS calibration process.

AC MEASUREMENTS

AC VOLTAGE: The NBS transport standard was an unmodified commerical ac-dc thermal transfer standard which was hand-carried between NBS and Redstone. Two types of measurements were made at Redstone: (1) the direct measurement of the ac-dc differences of the transport standard and (2) a comparison of the Army field site measuring system and the NBS transport standard. In both March and May, the ac-dc differences of the transfer standard were measured directly in terms of the Army standards in their

standards laboratory rather than at the field site. Because of time restrictions it was necessary to limit the number of measurements of ac-dc differences to two voltage levels, 5 and 500 volts, at each of three frequencies, 60, 400 and 6000 Hz. At NBS, the transfer standard was also measured at the same voltages and frequencies before and after transport. The results are summarized below in the form:

$$D_{RSA} - D_{NBS}$$

where the D's are the mean ac-dc differences measured by the respective laboratories.

Transport Standard	Date	$D_{RSA} - D_{NBS}$ ppm	Std. Dev. ppm
NBS	March 1982	+2.7	6.3
RSA*	March 1982	-5.0	2.2
NBS	May 1982	+2.0	5.6

* In March the Army also measured their own transport standard and it was hand carried to NBS where it was also measured.

The mean of the three is -0.1 ppm and the pooled standard deviation is 5.0 ppm. The agreement of ac-dc difference is remarkable considering the fact that the NBS uncertainty assignment for this type of calibration is 50 ppm. Furthermore the NBS transport standard remained quite stable over the whole period of the work. These results suggest that a MAP service for ac-dc difference might easily be developed.

The May comparisons at the field site of the RSA measuring system and the NBS transport standard were performed at the same voltages and frequencies as were used in March. However, the May observations included measurements at the 50 volt level. Measurements were made as nearly concurrently as practical using the two systems and stable ac and dc voltage sources. After applying the appropriate corrections to the measurements the difference

$$V_{RSA} - V_{NBS}$$

was calculated for each measured value. The mean difference for all voltage observations was +23.2 ppm and the standard deviation of a single observation was 7.5 ppm. Although well within the NBS assigned uncertainty of 50 ppm the observed difference is larger than can be accounted for by the standard deviation of the measurements made. It was not possible, within the time available, to investigate the the orgin of this difference.

AC CURRENT: The measurement of ac current was performed using the ac-dc transfer standard and three current shunts designed to operate with the unit. In May the transport standard and the 3 A, 0.1 A, and .01 A shunts were calibrated as a unit in terms of the Army primary standards . Except for the 3 A shunt the applied current was the rated shunt current. In the 3 A case, the Army used 2 A and NBS used 3 A. The mean difference between the Army and NBS corrections was +7.7 ppm and the standard deviation was 8.2 ppm. Although the uncertainty is somewhat larger than than obtained for voltage, these results are in good agreement with the voltage data.

Comparisons of the measurement system at the field site and the NBS transport standard were conducted in both March and May. The mean difference in the measured currents was -3 ppm with a range of 58 ppm. Again time constraints prevented further investigation of the sources of the observed differences. However, it was observed that certain of the equipment was very temperature sensitive. Since it was designed to operate in a standards laboratory environment, this observation is not surprising.

AUTOMATED MEASUREMENTS AND DATA PROCESSING

Automation of the NBS electrical measurements described in the preceeding sections provided a logical and practical means of increasing the efficiency of taking measurement data. Specifically, automation afforded several advantages over manual methods. First, automation improved the integrity of the data taken. Since the data was in machine-compatible form, it was possible to record, print and analyze the measurement results during the measurement process. This eliminated the manual data recording process in which errors are highly likely. Second, automation increased the speed at which data was taken. The NBS experience in two field tests at RSA consisted of performing similar tests both with and without the aid of an automated system. The automated measurements permitted much more data to be taken in approximately 30 percent less time. This increased efficiency and allowed more measurements to be made, thus increasing the experimenter's confidence in their data. The third benefit that was realized by automation was the consistency of performance of a measurement. Each time the measurement program was run, the same action took place. In our case, the measurement procedure coded into the software was simple. It consisted of the commands to set a digital mulitmeter to the desired function, to wait for a specified length of time, and to print the results. By having these commands in software, errors introduced by the operator in setting up and using the instrument and in the recording the data were virtually eliminated. The final advantage of automation realized in this work was to provide a documentation of the procedures used to make the measurements. The software provided an unambiguous record of the sequence of events that occured during the

measurement process. This may be valuable, especially in field tests such as reported here here, where further data analysis depends on the knowledge of the details of measurements made.

In fairness, it should be pointed out that there were some disadvantages to automating the measurements. Foremost, care must be exercised to assure that the software operates properly. This was accomplished by writing software in modular form, proper documentation throughout the software with remarks and comments on what was being calculated, and proper testing of the software under all conditions of data input.

For the implementation of automation techniques in measurement systems, it is desirable that the test instrumentation be easily interfaced to the controller being used. The approach used in this work was to use an IEEE-488 (1978) interface among all instruments. The IEEE-488 bus is a "party-line" bus in which instruments are attached in parallel to all the wires of the bus all of the time. Thus, only one instrument can be sending data at any given moment. Software in the controller determines the sequence of messages that will be transferred on the bus. In the NBS experiments, the most used software program was a simple routine, written in BASIC, which issued instructions to the digital mulitmeter to make ten readings average the readings, and print the average, standard deviation of the measurements, and the highest and lowest readings in the group of ten. Additionally, a time was printed which could establish the order of of the measurements should the need arise. The results were printed on a thermal-paper printer integral to the controller. These records then provided the raw data that was further evaluated using the controller as a simple calculator. By processing the data promptly, a potentially serious problem with one of the NBS procedures was discovered immediately. This procedure was then modified, the measurements repeated, and satisfactory results were obtained. The next logical step to further improve the system described would be to record the measurement data directly onto magnetic tape or disk files and to immediately process the data and display the corrected results. Such a procedure would give virtually real-time information on the calibration of complex equipment.

SUMMARY AND CONCLUSIONS

For the most part no uncertainties have been assigned to the particular measurements because of the complexity of the overall measurement processes involved. Any assigned uncertainty must include an error analysis and assignment of uncertainties to the NBS transport standards, the NBS measurements of the Army primary standards, the Army surveillance process, the local Army standards at the field site, variability of the voltage and current source, effects of the local environment on the

measurement process, and, above all, the measurement processes used by both the Army and NBS for this work. As of this writing the differences reported seem to be consistent with the preliminary estimates of the uncertainties for the various measurements. It is heartening to note that we were able to conduct a series of measurements between two metrology laboratories and obtain the quality of agreement reported in this paper. In closing, the following tentative conclusions have been drawn based on this work.

1. There is a need to develop standards that can operate in the type of environment that was encountered in this work.

2. In the area of ac measurements there is a need to develop tranfer standards that will reduce the time required to make the necessary measurements. It was found that the ac measurements were the most labor intensive of all the measurements made.

3. It is essential that calibrations of the type described in this paper be carried out in real time so that problems can be resolved as they occur rather than simply be identified after the fact. NBS experience in these experiments indicates that the microcomputers are useful for this purpose because they provide on-site data analysis and may be used for control of the calibration process.

4. Finally, this work, even though limited, shows that (a) field calibrations are one alternative to returning the equipment to the standards laboratory; and (b) that such calibrations can be carried out to a high accuracy and over a broad range of values for different electrical quantities using a relatively small number of standards and instruments.

68-608

TRANSFER OF THE UNIT OF VOLTAGE

Presented at the 1968 ISA Annual Conference and Exhibit
October 28-31, 1968
NEW YORK CITY

INSTRUMENT SOCIETY of AMERICA
530 William Penn Place
Pittsburgh, Pennsylvania 15219

68-608
TRANSFER OF THE UNIT OF VOLTAGE

Norman B. Belecki
Physicist
2802 Inertial Guidance and Calibration Group
Newark, Ohio

ABSTRACT

In January 1967 a joint project was established between the United States Air Force Calibration and Metrology Division and the National Bureau of Standards to investigate the problem of transferring the unit of voltage at the highest accuracy levels. After ascertaining the relative stability of the voltage standards in the two laboratories various types of transfer devices were evaluated including saturated and unsaturated standard cells and Zener diodes in various environments. Statistical measurement schemes were employed to eliminate average residual emf's in the measurement system and to provide estimates of the system precision. The details and results of this project will be discussed at length.

INTRODUCTION

Starting in the first month of 1967, the USAF Calibration and Metrology Division and the National Bureau of Standards undertook a joint project to study the problems associated with the inter-laboratory transfer of the unit of voltage. The primary objectives of the study were these:

(a) To reduce the uncertainty of assignment of the unit of voltage

(b) To reduce the time, and hence the expense, required to make an assignment

(c) To develop and use statistical procedures for maintaining surveillance over the unit

In order to pursue these objectives, every aspect of the problem had to be considered. Various types of transportation were considered. Techniques were developed for the handling and processing of the data taken.

STATISTICAL DESIGNS

Statistical measurement designs were used throughout the program. The solutions of such designs give one the value of each cell relative to the mean value of any cell or cells within the group, the standard deviation of a single measurement, the mean left-right component, and the difference of each observation from the value predicted by the values of the cells. Physically, the left-right component can be a detectable thermal emf within the measuring circuit or a scale shift in the potentiometer used to measure the difference between two cells. Components of the standard deviation of an observation are:

(a) Short term instability of the cell emf's

(b) Lack of perfect linearity of the measuring device

(c) Lack of infinite resolution of the measuring device

(d) Instability of the left-right component with time

These designs were suggested for use by Mr. Joseph Cameron, Chief of the Statistical Engineering Section of N.B.S., and were used throughout the program. One is for the comparison of a group of nine cells with a group of three in three sets of eighteen observations each. The other two designs are used to intercompare a group of six cells with a group of four or another group of six. Each of these designs requires twenty four observations. Data garnered in these designs is processed by the N.B.S. on a time shared computer using a program written by Mr. Eicke of the Electro-chemistry Section of N.B.S.

DEFINITION OF LOCAL STANDARDS

For the purposes of this experiment, local standards were defined both at N.B.S. and NAFS. At the N.B.S., the nine N.B.S. made cells of the Secondary National Reference Group defined as the local standard are housed in a center N.B.S. temperature mineral oil bath maintained at 20°C. This bath has a thermistatic (on-off) controller and has a short term temperature stability of about .01°C. Differences in emf of the various cells are measured using a commercial standard cell comparator and electronic null detector. The resolution is 0.1 microvolts.

In the USAF Primary Electrical Standards at Newark Air Force Station, Ohio, the local standard was defined to be nine commercial saturated standard cells. These cells are contained in a commercial oil bath maintained at 35°C. The temperature control unit has proportional, rate, and reset capabilities. The short term temperature stability is of the order of 0.0005°C. Due to problems created by the large difference between the bath temperature and ambient ($25° \pm .5°$) temperature, the cells are permanently connected to a mercury cup switch located in an oil filled aluminum box. This box is contained in a larger aluminum box located in

an instrument console beside the oil bath. The boxes, leads, and the conduit through which the leads run form the basis of a guarded, shielded measuring system. Leads are provided in this system for seventeen three cell enclosures and one four-cell enclosure. Enclosures are attached to the system upon arrival and remain physically undisturbed throughout the tests. Differences between cell emf's are measured using a potentiometer of 0.1 microvolt resolution. Null Detection is by means of a photocell amplifier which drives a mechanical galvanometer.

STANDARD CELL TRANSPORT UNITS

A representative sample of commercially available portable standard cell enclosures were utilized in this program. Preliminary studies were also made of Zener diode units and unsaturated cells.

The table shows the types of enclosures used. Temperature fluctuations could be monitored in each enclosure by means of a thermister bridge with a readout dial on the face of the device. In addition, one of the thirty degree baths and both of the twenty eight degree baths have provisions made for the insertion of a platinum resistance thermometer. All units have provisions for a battery standby power supply. The twelve cell 28 degree bath was a modification of a commercial bath. There was a massive aluminum block added for thermal bulk, and four groups of three cells each were installed with a guard circuit. There were two groups of portable saturated cells and two groups of shippable unsaturated cells. The modification was unowrkable due to the lack of geometric symmetry of the block and the location of the control sensor. The four cell 35 degree bath was modified because of leakage to the oven from the cell leads. The modification consisted of TFE sleeved, pure copper leads with a driven guard.

carrying by an aircraft, hand carrying by automobile (using the car's electrical system), and by air freight. All Three of these methods were utilized. For the third, arrangements were made with one of the major airlines for a monitored shipment by reserve air freight in a heated cargo space. Special fiberglas packing cases with polyurethene foam solution around the enclosure and its batteries were procured. The entire transportation process was tightly scheduled with the enclosure held at the airport of the destination for personal pickup by laboratory personnel. In transfers between NAFS and the N.B.S., this system worked well at all times despite inadequate instructions given the carrier on one occasion. In cases involving a change of aircraft enroute, some difficulties were encountered. Evidently, the enclosures received a severe beating during the transfer.

TRANSFERRING THE UNIT

It was decided at the beginning of the program that the best method to handle the information was to monitor the differences in assignments to transport units of the two laboratories. The resultant plot (voltage differences vs. time) would be a band ideally centered about zero with a zero shape. The distribution of the points about the center curve of the band and the shape of the band itself determine the final accuracy of assignment. As long as the points added to this plot remain within the acceptable bounds from the center curve, the same value is used for the mean of the local cells. The process is then said to be in a state of statistical control. If, however, a point is plotted which is out of bounds, the process is then said to be out of control. At this point, some sort of validation of the out of control point is required. Unless there is obvious reason to believe the transport unit is faulty, the transfer must be accomplished again. If subsequent transfers are also out of control, of course, the former statement of uncertainty no longer applies, and either a new local value is required or a new accuracy statement, or both.

TABLE I. Types of Transport Units

No. of Enclosures	No. of Cells	No. of Ovens	Nom. Cell Temp.	Type of Temp. Cont.	Typical Short Term Stab. *
2	3	2	35	Proportional	.4 - .5
2	4	2	30	Proportional	.2 - .3
1	3	2	32	Proportional	.3 - .4
1	12 (6 Unsat.)	1	28	Proportional	.5 - 1.0
1	8 (4 Unsat.)	1	28	On-Off	.5 - .8
1	41	2	35	Proportional	.3 - .4

* Average per cell 3 sigma for two weeks readings

In view of the second objective of the program, it was necessary to maintain the temperature integrity of the enclosures at all times. This precludes all modes of transportation but three, due to the bulk of batteries. The three are hand

TABLE II. NAFS Standard Disturbances

Date	Occurrence
25 May 1967	Mechanical failure, Loss of temperature
22 Jun 1967	Power Failure, 5 Deg. loss in temperature.
9 Aug. 1967	Electrical difficulty in measuring circuit, at mercury cups.
7 Oct. 1967	Power failure, Loss of temperature; Cells placed in aluminum cans in bath.
17 Nov 1967	Cells lowered in oil bath.
22 Dec 1967	Mylar sleeves placed in aluminum cans.
22 Jan 1968	Emergency power system installed, 0.1 Deg. loss in temperature.
12 Feb 1968	Removed excess cans from bath; Sleeved positive leads with TFE.
26 Apr 1968	Excess items removed from bath.

The value of the local standard at N.B.S. was determined by inter-comparing the nine cells with cells from the National Reference Group. Figure One shows the value of the mean of the group during the first fourteen months of the experiment. The calibration points are shown as data. However, it is important to note that the average mean value as represented by the solid line was in all cases taken to be the value of the group mean. As seen in the seventh month, the cell responsible for the downward shift of the mean emf was removed and another substituted. From this point, the assignment has remained constant.

The average value of the group of nine in the Air Force laboratory was assigned as the result of two interchanges during which two portable standard cell enclosures were carefully hand carried between Gaithersburg and Newark while under power and or prior data taken on these two enclosures (the first enclosures in Table One).

At this point, the use of the various types of transport devices was begun. The graph (Figure Two) shows the control chart kept for the first sixteen months of the program. For the first fourteen months of the project, the points (representing complete transfers) are within control. One of the observations made is that Box 100 (represented by crosses) always seems to have a lower difference in assignment than Box 200 (represented by the dots). A similar relationship exists between Boxes 1100 and 1200 (the boxes represented by squares and triangles). After the fourteenth month, the entire picture is shown out of control as the result of some changes made in the bath containing the nine cells.

The local standard at Newark was disturbed a number of times during the experiment. Table Two lists the major difficulties encountered in the system during the experiment. As the October power failure resulted in the return of the cells to room temperature, it was decided to mount them in aluminum cans to remove the effects of oil turbulence. The resulting recovery to stability of the mean of these cells is shown in Figure Three. It is interesting to note that internal differences alone would have indicated stability in two to three weeks during which time the actual mean value would have been high in excess of a microvolt. On the other hand, the internal differences indicated some types of disturbance at about sixty-five days. At that time, the mean was relatively stable. This indicates the folly of relying on internal measurements alone to determine the validity of a standard, especially if all of the components are similar and in the same environment.

THE I.B.M. - NAFS - N.B.S. TRANSFER

Two additional experiments were attempted involving a third laboratory, that of I.B.M. in San Jose, California. The two thirty degree enclosures were used, one being shipped to NAFS and the other to I.B.M. from N.B.S. At the end of a two week period of testing, the laboratories exchanged boxes. The end of another two week test period saw both boxes returned to N.B.S. As shown in Table Three, the enclosures each experienced a real change in emf during the interchange between I.B.M. and NAFS.

It is to be noted that all shipments to I.B.M. and the return trip from I.B.M. to Gaithersburg involved power failures of the two enclosures. It was also noticed that the enclosures received at NAFS were at a higher temperature than nominal, undoubtedly due to the extra insulation afforded

Mean of Nine N.B.S. Cells

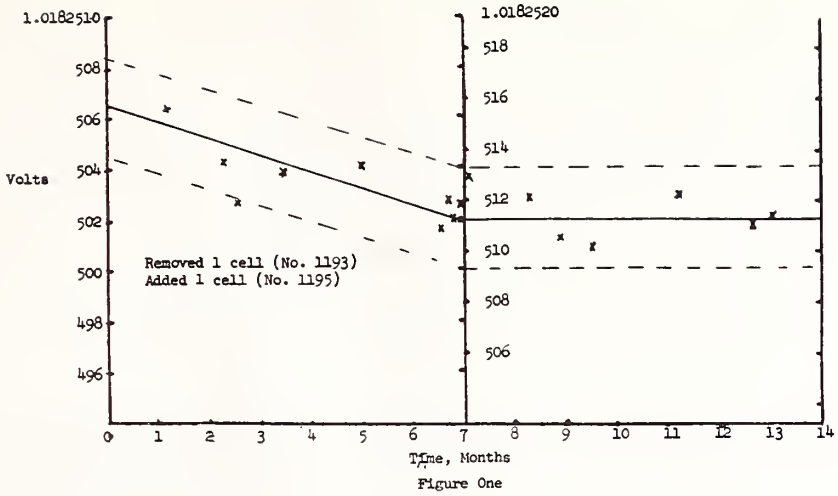

Figure One

NAFS
Control Chart

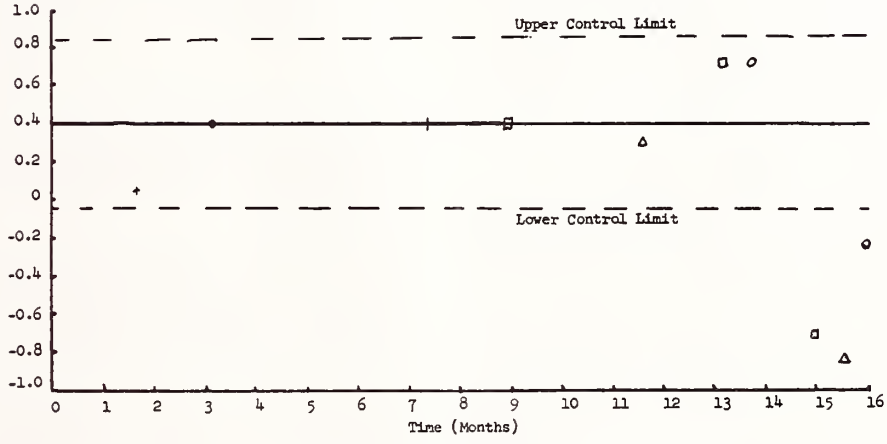

Figure Two

THIRTY FIVE DEGREE
BATH RECOVERY

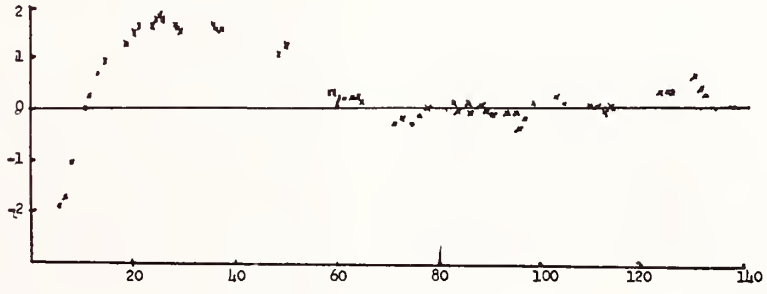

TIME (Days)

FIGURE THREE

TABLE III. Interlaboratory Differences

Enclosure	Difference in Microvolts
1100	V(NBS 1) - V(NBS 2) = -1.2
	V(NBS 1) - V(IBM) = +.3
	V(NBS 2)-- V(NAFS) = -.7
1200	V(NBS 1) - V(NBS) = +1.8
	V(NBS 1) - V(NAFS) = -.3
	V(NBS 2) - V(IBM) = -.9

by the packing case.

The experiment was repeated at a later date. The results of the second experiment were inconclusive due to extreme mishandling of the enclosures again between I.B.M. and Newark, and due to problems in the measurement system at Newark. In this instance, physical damage was actually done to the shipping cases of one enclosure. This experiment will be repeated, soliciting extra care on the part of the carrier and involving at least one enclosure at thirty five degrees.

UNSATURATED CELLS AS TRANSFER DEVICES

The use of unsaturated cells for the transfer of the unit was partially investigated. Each of the two twenty eight degree baths contain unsaturated cells. Although the twelve cell bath was a failure, preliminary tests on the eight cell enclosure indicate that the standard deviation of the measured points from the predicted emf at any time was 0.3 microvolts, indicating that these cells may be potentially used to transfer the unit with an uncertainty of one microvolt. This information assumes a least square fit of a straight line through the data taken during the duration of a normal transfer. A further test of the use of unsaturated cells is currently under way between the two laboratories and other tests are planned by the USAF.

ZENER DIODES

Preliminary tests have also been made on the use of self contained Zener diode packages. It has been shown that the emf of the units at any time is predictable to within about three microvolts without a transfer. One transfer has been made utilizing eight Zener diodes. The results have been varied enough to permit no firm conclusions. More work will be undertaken in the future.

RESULTS AND CONCLUSIONS

The primary unit of D.C. voltage of the USAF has been certified to have an uncertainty of 0.5 microvolts at Newark Air Force Station. Formerly, cells were certified accurate to one microvolt at N.B.S. with the responsibility for transporting, maintaining, and proving the uncertainty left to the using laboratory.

Thirty five degrees centigrade is too high a temperature for the maintenance of cells to be used on a permanent local standard. The recovery time from temperature loss is sixty five days as compared to about a week or two for cells at 28°C.

The standard deviation for a single observation was shown to be 0.08 microvolts at Newark Air Force Station while it is 0.18 microvolts at the N.B.S. The increased precision at NAFS is surmised due to the superior temperature control made possible by the proportional, rate, and reset controller.

Standard cell enclosures which operate at higher temperatures are seen to be effected less by the variety of ambient conditions encountered in a transfer. This was illustrated by the overheating of the two thirty degree boxes in transit.

The recovery time for saturated cell enclosures transported maintaining temperature integrity is of the order of a few hours. Readings taken immediately upon the arrival of the enclosure generally tend to be four or five tenths of a microvolt from their final value. Data taken twenty four hours after arrival usually is within 0.1 microvolts of the average value.

ACKNOWLEDGEMENTS

The author wishes to acknowledge Henry Ellis and Ann O'Toole of N.B.S. and John Donahue and Gerald Howard of NAFS for making the observations upon which this paper is based. Thanks of the author go to the I.B.M. standards laboratory and its chief, Mr. DeWayne Sharpe, for their participation. Without the efforts of Mr. Woodward G. Eicke of N.B.S. in handling the logistics, data, and many of the details, this program would not have been the success it was.

KEY WORDS

Saturated Standard Cell, Unsaturated Standard Cell, Zener Diode, Standard Cell Enclosure, Standard Deviation, Control Charts

IEEE TRANSACTIONS ON INSTRUMENTATION AND MEASUREMENT, VOL. IM-23, NO. 4, DECEMBER 1974

Regional Maintenance of the Volt Using NBS Volt Transfer Techniques

WOODWARD G. EICKE, JR., MEMBER, IEEE, AND LAUREL M. AUXIER

Abstract—**In cooperation with five industrial standards laboratories, the National Bureau of Standards (NBS) studied the feasibility of establishing a regional volt maintenance and surveillance program in the greater Los Angeles, Calif., area. The objectives were to improve surveillance, to reduce dependence on NBS, and to have each laboratory maintain its unit of voltage to within 1 ppm of the U.S. legal volt. A two-phase program was established, the first to characterize the five laboratories and the second to carry out the surveillance. After 3 years all laboratories were found to be maintaining their unit to within better than 1 ppm of the U.S. legal volt.**

I. INTRODUCTION

THE U.S. legal volt is disseminated by the National Bureau of Standards (NBS) to several hundred private and public facilities throughout the United States via either unsaturated or saturated standard cells submitted by NBS clients for calibration. In late 1967 it became obvious that the services offered did not meet the accuracy requirements of a small but important group of users. To alleviate this problem, NBS, in cooperation with the U.S. Air Force, undertook a program to improve the interlaboratory transfer of the unit of voltage. As a result of this work a new service, the NBS Volt Transfer Program (VTP), was developed and made fully operational in early 1971 [1], [2]. This technique reduced the uncertainty of the transfer of the unit of voltage from approximately 2 ppm using the normal methods to 0.4 ppm.

In early 1970 the authors discussed the possibility of extending the VTP technique to the establishment of a regional volt surveillance program in the Los Angeles, Calif., area with the goals of improving local volt surveillance and reducing the dependence of the participating laboratories on NBS. As a result, five industrial laboratories in the greater Los Angeles area established the Southern California Standard Cell Interchange Program (SCSCIP) to work with NBS on a study of the feasibility of setting up a regional volt maintenance program. Participating were the Autonetics Division of Rockwell International, Inc., Beckman Instruments, Inc., Electrical Standards Repair Service, Inc., Lockeed-California Company, and TRW Systems Group. Since no one had previously undertaken such an endeavor, a two-phase program was formulated first to establish the feasibility of such a program, and second to develop an operational plan to carry out, on a continuing basis, a regional volt maintenance program. After discussions with the participating laboratories we set, as a goal, 1 part in 10^6 as the maximum difference between any participant's as-maintained unit and the U.S. legal volt.

Manuscript received July 3, 1974; revised August 21, 1974. This paper is a contribution of the National Bureau of Standards and not subject to copyright.

W. G. Eicke, Jr., is with the Absolute Measurements Section, Electricity Division, National Bureau of Standards, Washington, D. C. 20234.

L. M. Auxier is with Beckman Instruments, Inc., Fullerton, Calif.

II. FEASIBILITY STUDY

A. Experiment Plan

Each of the five laboratories maintained their local volt via saturated standard cells, kept under close temperature control, and each intercompared its cells using the series opposition method. However, no two laboratories were identical; some maintained their reference cells in oil baths, while others used temperature-controlled "air baths." In addition, instrumentation, operating procedures, and stastistical techniques also varied among the participants. It was clear from a study of the operating procedures of the various laboratories that all were comparable; hence, no major changes in their method for maintaining their volt were required at that time.

Therefore, it was decided that as-maintained units of voltage would be best compared using the NBS VTP techniques. Furthermore, since each laboratory had a transport standard available, five transport standards would be employed simultaneously. In this way the desired measurements of the differences between as-maintained units of voltage could be carried out in 12–15 weeks. The design of the experiment showing the five laboratories, designated A through E, and the ten transfers is depicted in Fig. 1. The arrows indicate the laboratory supplying the transport standard for each path. For example, for path 1, laboratory A sends its transport standard to laboratory B. All the data were sent to NBS for processing and analysis as they were obtained.

The actual technique used to measure the differences in the units is essentially that reported in [1] and [2]. Briefly, the home laboratory calibrates its transport standard in terms of its as-maintained unit of voltage V_H and then transports the enclosure under power to the designated laboratory. There, it is calibrated in terms of that laboratory's as-maintained unit V_{LAB}. Finally, it is returned to the home laboratory where it is recalibrated. If $E_{H(1)}$ and $E_{H(2)}$ are the assigned EMF's at the home laboratory in terms of V_H, and E_{LAB} is the EMF in terms of V_{LAB} at the receiving laboratory, then the difference in

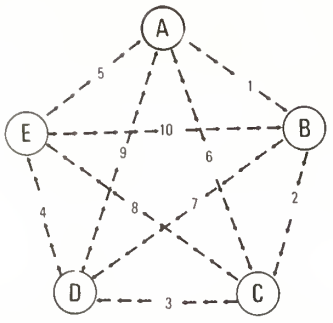

Fig. 1. Design for Phase I experiment. Arrows indicate the laboratory furnishing the transport standard for that leg of the experiment.

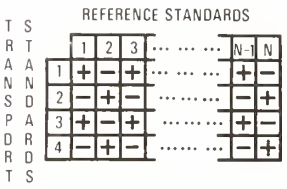

Fig. 2. Experiment design used to intercompare reference standards and transport standard. Signs indicate relative position in the measuring circuit.

the as-maintained units is

$$V_{\text{LAB}} - V_H = -\frac{\{E\}_{\text{LAB}} - \{E\}_H}{\{E\}_H} V_H \qquad (1)$$

where the $\{E\}$'s are the numerical values only of the EMF's assigned by a given laboratory and

$$E_H = \tfrac{1}{2}(E_{H(1)} + E_{H(2)}). \qquad (2)$$

The timing of the experiment was such that any linear drift in the EMF of the cells in the transport standard was automatically eliminated from the final result given by (1).

The procedures used to intercompare the transport standards and the reference standards were those used in the VTP, and the experiment designs were those shown in Fig. 2, where the signs + and − indicate the position in the circuit. All transport standards contained either three or four cells, and intercomparisons were made between the reference and transport standards 2 to 4 times per week, with measurements extending over a 2- to 4-week period.

B. Experimental Results

The experiment was begun on November 9, 1970, and completed February 15, 1971, according to the schedule of Table I. The planned schedule called for completing the experiment by January 22, 1971, but several minor problems including the Los Angeles earthquake caused slippages of a few days each, while the Christmas holiday caused a 1-week delay. It was also found that approximately 3 weeks at each stage yielded much better results, because a number of enclosures showed some instability for the first week, even though they were carefully transported under power less than 80 km by automobile. Results from the individual daily runs were combined and the average EMF of the cells in the transport standard for each stage was calculated. These results are summarized in Table II.

Although the data of column 10, Table II, are in terms of the home laboratory V_H, we can view the data as being referenced to a single unit of voltage because the interlaboratory differences are small. This single unit is taken as the unit of voltage for SCSCIP, V_{SC}. We, therefore, define V_{SC} as the mean unit of voltage for the five laboratories. Now the difference between the ith laboratory's unit V_i and V_{SC} can be readily calculated using the method of least squares. Using the procedure for 5 cells given by Eicke and Cameron [4] one obtains the results presented in Table III.

From the data of Table III the predicted observations and deviations (observed minus predicted) were calculated (columns 11 and 12 of Table II). In addition, the lack of closure was estimated to be $-0.09\ \mu$V as shown at the bottom of column 10. The standard deviation of a single difference was found to be $0.35\ \mu$V for 5 degrees of freedom.

Laboratory A had also participated in two NBS VTP experiments that bracketed this work. The data showed their unit of voltage was constant to within the experimental error of the VTP and had been adjusted to make $V_A - V_{\text{NBS}} = 0$ to within experimental error. Therefore, V_{SC} was set equal to V_{NBS} and the results are shown in the second column of Table III. From the individual designs carried out by each laboratory, one obtains the left–right component, an estimate of the precision of a single observation, the precision of the assignment of the transport standard in terms of the reference group, and some information on individual transport standards. This information is also summarized in the last three columns of Table III. The left–right component is an estimate of the residual constant EMF's in the measuring circuit. In two cases they were on the order of 0.1 to 0.2 μV. Since they remained constant during any run their effects on the calculated data are eliminated by means of the experiment design. For each laboratory, the standard deviation of a single observation is given in the next to the last column. Each figure is an estimate of the precision of the laboratories measurement process and most are comparable to data obtained from the regular VTP [4]. The last column gives information on the day-to-day performance of the process. Based on these data, participants were able to make a number of minor changes in their process that improved their overall capability. Using the data in the third column of Table III, the units were all adjusted to make $V_{\text{LAB}} - V_{\text{NBS}} = 0$ to within experimental error.

III. PHASE II. ROUTINE REGIONAL SURVEILLANCE

Because the Phase I program was far too complex and time consuming to be used for routine surveillance, a simpler method had to be devised. The obvious method for setting up a routine program was to use one laboratory as a pivot as shown in Fig. 3. Using this scheme, each laboratory submits a calibrated transport standard to the pivot

TABLE I
SCHEDULE FOR PHASE I EXPERIMENT

From	To	Transport Standard Calculated at: Home	Transport Standard Calculated at: Designated Laboratory	Numer of Days
November 9, 1970	November 20, 1970	×		12
November 21, 1970	December 11, 1970		×	20
December 12, 1970	January 8, 1971	×		27
January 9, 1971	January 29, 1971		×	21
January 30, 1971	February 15, 1971	×		16

Note: Average time at each laboratory was about 3 weeks.

TABLE II
SUMMARY OF PHASE I INTERCHANGE

Path Number	EMF's Reduced by (μV)	Laboratory	Home Laboratory: $E_{H(1)}$ (μV_H)	Home Laboratory: $E_{H(2)}$ (μV_H)	Home Laboratory: Assumed Mean[a] (μV_H)	Home Laboratory: Standard Deviation of Assumed Mean	Receiving Laboratory: Laboratory ID	Receiving Laboratory: E_{LAB} (μV_{LAB})	Difference in Units: (μV_H)	Difference in Units: Predicted $V_{LAB} - V_H$ (μV)	Difference in Units: Deviation (μV)
1	1018100	*A*	37.35	37.38	37.36	0.015	*B*	36.03	+1.31	+1.57	−0.26
2	1017600	*B*	93.34	95.99	94.66[b]	[c]	*C*	96.56	−1.86	−1.22	−0.64
3	1018100	*C*	36.13	36.05	36.09	0.040	*D*	35.65	+0.43	+0.32	+0.11
4	1017600	*D*	93.01	93.11	93.06	0.050	*E*	93.58	−0.51	−0.77	+0.26
5	1018100	*E*	44.75	45.31	45.03	0.280	*A*	45.28	−0.24	−0.17	−0.07
6	1018100	*A*	37.38	37.46	37.42	0.040	*C*	36.86	+0.55	+0.26	+0.29
7	1017600	*B*	95.99	97.51	96.75[b]	[c]	*D*	97.49	−0.73	−0.99	+0.26
8	1018100	*C*	36.05	36.06	36.05	0.005	*E*	36.71	−0.64	−0.36	−0.28
9	1018100	*D*	93.11	93.45	93.28	0.170	*A*	94.03	−0.74	−0.85	+0.11
10	1017600	*E*	45.31	45.13	45.22	0.090	*B*	43.64	+1.55	+1.49	+0.06
						$s = 0.123$					

[a] Assumed mean at receiving laboratory.
[b] Cells in this enclosure showed a relatively linear drift. The assumed mean took this drift into account to eliminate confusion with $E_{H(1)}$.
[c] Standard deviation not calculated because of drift.

TABLE III
SUMMARY OF DIFFERENCES IN AS-MAINTAINED UNITS AND OTHER PERTINENT LABORATORY DATA

Laboratory	Difference in Units: $V_{LAB} - V_{SC}$ (μV_{SC})	Difference in Units: $V_{LAB} - V_{NBS}$ (μV_{NBS})	Left–Right Component (μV)	Standard Deviation[a] Single Observation (μV)	Standard Deviation[b] Assignment Between Days (μV)
A	−0.57	0	0.021	0.071	0.057
B	+1.09	+1.66	−0.017	0.131	0.082
C	−0.22	+0.35	0.065	0.063	0.200
D	+0.19	+0.76	0.161	0.09	0.098
E	−0.49	+0.08	−0.028	0.23	0.183

[a] Standard deviation of a single observation corresponds to the within day standard deviation.
[b] This quantity is calculated from the individual runs.

laboratory; at the same time NBS supplies a transport standard. The pivot laboratory intercompares the NBS transport standard with its laboratory reference group and all of the transport standards, a process requiring 3–4 weeks. All of the daily data are forwarded to NBS for processing. Upon completion of the measurements all transport standards are returned to their respective laboratories where they are again measured over a 2–4-week period. After all the data have been processed by NBS, results are analyzed and reports of the test are sent to each laboratory, which give the difference V_{LAB}-V_{NBS}, recommended adjustments to the local unit, and other process data. The pivot laboratory assignment is based only on the comparison between their reference group and the NBS transport standard. For each transfer a different pivot laboratory was selected so that in the long run all laboratories in SCSCIP are treated in the same manner. After each experiment, if required, the units of voltage are adjusted to make V_{LAB}-$V_{NBS} = 0$ to within experimental error.

To date a total of three such transfers have been carried out and the results are summarized along with other pertinent data in Table IV. Lines 1 and 3 give results of regular transfers between laboratory *A* and NBS, and line 2 gives the normalized data from the Phase I experiment,

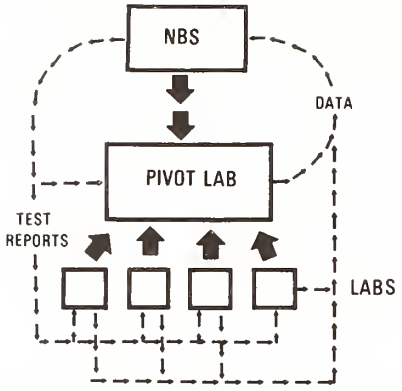

Fig. 3. Phase II showing by means of large arrows the movement of transport standards. Flow of data and results are also shown.

TABLE IV
SUMMARY OF PHASE II EXPERIMENTS

Pivot Laboratory	Date	Laboratory A		Laboratory B		Laboratory C		Laboratory D		Laboratory E		SCSCIP[c]
		Observed[a]	Adjusted[b]	Observed[a]	Adjusted[b]	Observed[a]	Adjusted[b]	Observed[a]	Adjusted[b]	Observed[a]	Adjusted[b]	
A[d]	July 1970	0	+0.80	—	—	—	—	—	—	—	—	—
A[e]	Dec. 1970	−0.10	+0.52	−0.10	+0.52	−0.10	+0.52	−0.10	+0.52	−0.10	+0.52	−0.10
A[d]	Apr. 1971	−0.18	+0.31	—	—	—	—	—	—	—	—	—
C	Oct. 1971	−0.38	−0.09	−0.55	−0.27	−0.36	−0.08	−0.08	−0.20	+0.35	+0.63	−0.20
A	Oct. 1972	−0.27	−0.27	+0.24	−0.31	−0.30	−0.66	−0.26	−0.16	+0.28	+0.07	−0.06
D	Nov. 1973	−0.05	−0.05	+0.22	−0.08	−0.69	−1.35	−0.24	−0.40	0.00	−0.07	−0.15

[a] Observed difference experimentally determined.
[b] Difference in the units normalized to the Phase I experience.
[c] All units were adjusted to make $V_{LAB} - V_{NBS} = 0$ using the two VTP experiments with Laboratory A. It was assumed that V_A was constant; however, later data showed a slight drift.
[d] Regular VTP transfers between NBS and Laboratory A.

while lines 4, 5, and 6 summarize the Phase II transfers from October 1970 to November 1973. The data of this table constitute a complete history of the SCSCIP data going back to July 1970. For each laboratory two values are given. The first is the actual measured difference between the laboratory and NBS. The second is normalized to December 1970 (except laboratory A whose base date is July 1970), in order to show changes with respect to time in the as-maintained units as a result of changes in the EMF's of the reference cells. The normalization takes into account the drift in the U.S. legal volt prior to July 1972 and the adjustments to the local unit as the result of previous intercomparisons. Field *et al.* [5] reported that the U.S. legal volt as maintained using saturated cells drifted at the rate of about $-0.41\ \mu$V per year relative to the assigned value of $2e/h$ from July 1971 to July 1972. Assuming this relationship was valid for the 12 months prior to July 1971, all data prior to July 1972 were adjusted accordingly. The last column of the table gives $V_{SC} - V_{NBS}$. This latter quantity is simply the mean of the 5 measured differences. The observed differences represent, within experimental error, the changes from one calibration to the next of the local units as preserved by means of saturated cells. In some cases the actual constitution of the laboratories' reference group was changed between transfers. For three of the five laboratories (A, C, and D) the normalized differences show definite time dependence, as is shown in Fig. 4, which is typical of other VTP data [4]. In the case of the other two laboratories no such dependence was detected. Analysis of the data from individual designs and changes in EMF of the transport standard as a result of transport indicated that the various processes were similar to those of the VTP. Therefore, the overall standard deviation of a single transfer between each laboratory and the pivot laboratory was taken as that of the NBS VTP, or 0.14 μV. Since two transfers were involved the standard deviation of a transfer between NBS and all but the pivot laboratory is 0.20 μV.

IV. DISCUSSION OF RESULTS

The Phase I study clearly demonstrated the feasibility of establishing a relatively simple volt maintaince program using the basic VTP techniques with only slight modification. Further, for the first time, to the authors' knowledge, it provided quantitative data on a *closed loop* experiment comparing several units of voltage. Phase II results showed a definite improvement in both the maintenance of the local units and the performance of the transport standards. It is our opinion that the repeat of the Phase I experiment would result in a standard deviation

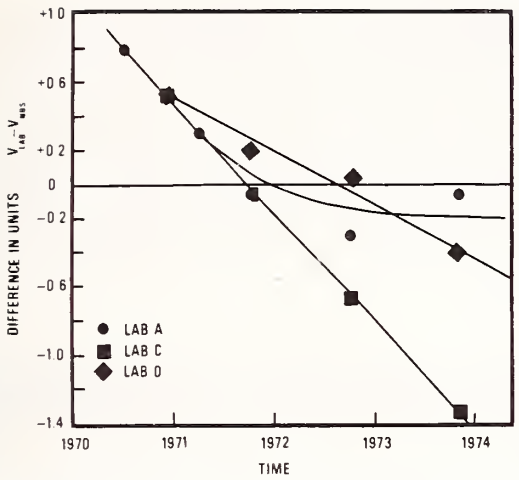

Fig. 4. Behavior of the reference standards for the five laboratories showing the drift of their standards relative to the U. S. legal volt. (See text.)

substantially less than the observed 0.35 μV. Even so, the results are still in excellent agreement with those obtained via the regular VTP. Furthermore, the Phase I technique can be readily extended to other size groups without unduly increasing the amount of work to be done. The Phase I experiment also identified problems heretofore unknown to the laboratory personnel, most being readily solved prior to starting Phase II.

All of the laboratories had received their initial assignments from NBS using the conventional service which required sending *their* standards to NBS for calibration. It is heartening to note that the largest observed difference in units (1.66 μV) was well within the expected range (2 to 4 μV) when allowances are made for long-term drift and transport. From the initial assignment in early 1971 to the last transfer all laboratories have shown changes of less than 1 ppm per year. Neglecting any adjustments for drift, the magnitude of the change in the units is only 0.28 μV per year with a 3 standard deviation uncertainty of 0.53 μV. In addition, Phase I type of experiments, by themselves, provide a powerful tool for evaluating a group of laboratories simply and quickly. In fact, this approach would be a very useful tool, when conducted between national laboratories, to unravel the unresolved discrepancies in measuring the difference in as-maintained units of voltage reported at the 1972 Conference on Precision Electromagnetic Measurements by Eicke and Taylor [1]. Finally, the results to date demonstrate the feasibility of establishing regional volt maintenance programs. In fact such techniques can and are now being extended to areas such as resistance capacitance.

ACKNOWLEDGMENT

The results reported here and the success of the experiment were made possible by the dedicated efforts of a large number of individuals at the participating laboratories. At the risk of overlooking someone, we gratefully acknowledge the collaboration of the following persons: B. Morton of Beckman Instruments Co., R. Wangerin and R. Stromquist of Electrical Standards Repair Service, D. Buck and R. Englander of Lockeed–California Co., F. Woodsmall and H. Buehrle of Rockwell International, and R. Stodola and G. Davidson of TRW Systems Group. Special thanks are due B. F. Field of NBS for coordinating the Phase I experiment, R. E. Kleimann and G. Free of NBS for coordinating the Phase II experiments. We are particularly grateful to H. H. Ellis of NBS for the hundreds of measurements required on the transport standards.

REFERENCES

[1] W. G. Eicke, Jr., and B. N. Taylor, "Summary of international comparisons of as-maintained units of voltage and values of $2e/h$," *IEEE Trans. Instrum Meas.*, vol. IM-21, pp. 316–319, Nov. 1972.
[2] "NBS offers new calibration service for the volt," Nat. Bur. Stand., Washington, D. C., NBS Special Publ. 250, Users Bull. no. 1, Mar. 1971.
[3] W. G. Eicke and J. M. Cameron, "Designs for the surveillance of small groups of saturated standard cells," Nat. Bur. Stand., Washington, D. C., Tech. Note 430, 1968.
[4] ——, "NBS test reports for the volt transfer program," unpublished.
[5] B. F. Field, T. F. Finnegan, and J. Toots, "Volt maintenance at NBS via $2e/h$: A new definition of the NBS volt," *Metrologia*, vol. 9, no. 4, pp. 155–166, 1973.

Reprinted by permission from IEEE TRANSACTIONS ON INSTRUMENTATION AND MEASUREMENT
Vol. IM-23, No. 4, December 1974, pp. 290-294

A COORDINATED SYSTEM OF MAINTAINING AND DISSEMINATING THE VOLT, Robert M. Shaw, IEEE Trans. Instrum. Meas. IM-29, December 1980.

Groups of standard cells may be used to maintain the volt with an uncertainty of 1/4 parts per million (ppm) using a separate transportable group of cells to transfer the value from the National Bureau of Standards (NBS). An enclosure to hold 24 standard cells has been designed in which temperature control is better than 100 μK in an environment varying as much as 3 K. The volt thus maintained is transferred over coaxial cables to service groups about 1/2 km away. This is done by generating a constant current that produces a 1-V drop across standard resistors located at both ends of each cable group. Accuracy of the transferred volt is about 1 ppm.

THE RESPONSE OF STANDARD CELLS TO ALTERNATING CURRENTS IN THE FREQUENCY RANGE 10-10^5 Hz, G. J. Sloggett (National Measurement Laboratory, CSIRO, University Grounds, City Road, Chippendale, Australia 2008), Metrologia 13, 57-61 (1977).

Measurement of the effects of passing alternating currents in the frequency range 10-10^5 Hz through a group of saturated standard cells showed that their internal resistances declined with increasing frequency at a mean rate of 25 Ω/decade. AC caused the emf's of certain cells to decrease, whereas only increases have been previously reported. For most cells, this effect became very small for frequencies above 1 kHz. Also, a previously unreported phenomenon, the generation of an emf at twice the ac frequency, has been observed. A simple relationship between the magnitude of this effect and that of emf change is suggested.

AUTOMATIC INTERCOMPARISON OF STANDARD CELLS, Andrew F. Dunn, IEEE Trans. Instrum. Meas. IM-23, December 1974.

A system is described whereby precise intercomparisons of standard cells are accomplished under full computer control. The results obtained indicate accuracies (one standard deviation) of ±10 nV from which the individual values of the standard cells in a maintaining group of ten cells are estimated to be accurate to ±20 nV. The major source of indeterminacy continues to be the variation of standard cell EMF due to temperature, mechanical vibration, etc.

INTERNAL COMPARISON OF A LARGE GROUP OF STANDARD CELLS, J. Wilbur-Ham, IEEE Trans. Instrum. Meas. IM-22, September 1973.

Equipment is described for comparing any number N of standard cells which constitute a standard of electromotive force. The scheme is economical, needing only 2N measurements. The cells are disposed in a ring, and there is simple switching to compare each cell with its four neighbors. The calculations are done by a program on a desk calculator. They give the value of each cell with respect to the mean of the group. They also give the rms error, which is typically less than 0.02 μV for one cell in a group of 22. There are safeguards for identifying a spurious measurement and a false keyboard entry.

AUTOMATIC MEASURING SYSTEM FOR A CONTROL OF STANDARD CELLS, Hiroyuki Hirayama and Yasushi Murayama, IEEE Trans. Instrum. Meas. IM-21, November 1972.

The automatic measuring system developed in the Electrotechnical Laboratory to monitor standard cells requiring a lot of measurements is described. It is composed of a scanner, an integrating-type digital voltmeter, a programmer or minicomputer, etc., and carries out the data acquisition and processing for a maximum of 200 cells. The difference in EMF of two cells is measured precisely. To reduce the effect of the induced EMF in the scanner, a delay unit is provided, and procedures minimizing errors and evaluating random errors have been adopted. In the on-line version of system, a great part of the data processing is done during the delay and integrating time of digital voltmeter. Applying this system to the measurement of standard cells, a precision of the order of 0.1 μV has been obtained.

MAINTENANCE OF A LABORATORY UNIT OF VOLTAGE, Andrew F. Dunn, IEEE Trans. Instrum. Meas. IM-20, February 1971.

Many of the problems involved in maintaining a laboratory reference group of standard cells with a reliability better than one part per million are outlined and solutions suggested. Methods are presented for reducing the number of measurements by approximately 40 percent from the ideal without seriously reducing the accuracy achieved, and procedures for assessing the quality of the group are indicated. Suggestions are given for preferred methods to be used for groups of 4, 8, or 12 cells, and as an example of these procedures the 20-month history of a new group of standard cells is illustrated.

TRULY TRANSPORTABLE STANDARD-CELL AIR BATH, David W. Braudaway, IEEE Trans. Instrum. Meas. IM-19, November 1970.

Dissemination of the volt is complicated by the complex temperature response of standard cells. Described are the design and performance characteristics of an experimental standard-cell air-bath specifically optimized for transportable voltage-dissemination service. Salient features of this bath are 1) ±0.001°C control of the cell temperature in the laboratory, ±0.02°C maximum variation around 28°C in shipment; 2) exposure capacity from over 8 hours at 0°C or 45°C to over 72 hours in moderate temperatures; 3) shipping package weight 14.5 kg, size 20.3 x 22.9 x 30.5 cm; and 4) electrical power drain 0.8-0.2 watt.

Cell temperature is determined primarily by an ambient-temperature-biased on-off heater system. Immunity to external environment is achieved by a unique secondary control, which employs the energy storage capacity of two heat-of-fusion alloys, which are reset simply by exposure to laboratory temperature.

Experience with this bath has shown that the average value of cell voltage is reproducible to 0.1 μV within a few hours following shipment. This time delay is significantly shorter than the days-to-weeks for most air baths and the weeks-to-months for cells shipped without temperature control.

THE APPLICATION OF THE DIRECT CURRENT COMPARATOR TO A SEVEN-DECADE POTENTIOMETER, Malcolm P. MacMartin and Norbert L. Kusters, IEEE Trans. Instrum. Meas. IM-17, December 1968.

The design and construction of a self-balancing direct current comparator for use in a seven-decade potentiometer is described. The comparator generates an output current whose value, as a proportion of a constant input current, is determined to a very high accuracy by the ratio of the numbers of turns of two windings on a magnetic core. A linear, adjustable voltage scale is obtained by passing this output current through a resistor whose value does not vary with current. Since the voltage adjustment is made by varying turns on a magnetic core and not by means of a resistive divider, the usual problems of contact resistance and thermal electromotive forces associated with this adjustment in conventional potentiometers are avoided.

The main sources of error in the comparator and the design techniques used to keep the errors less than the smallest step of the output current is discussed. A self-checking feature whereby the linearity of each step of the output current can be checked quickly and easily is described. The performance of the prototype model is given. The normal range of the potentiometer is from zero to 2 volts in steps of 0.1 μV.

THE CONSTRUCTION AND CHARACTERISTICS OF STANDARD CELLS, George D. Vincent (Director, Standard Cell Dept., The Eppley Laboratory, Inc., Newport, RI) IRE Transactions on Instrumentation I-7, 221-234 (1958).

In order to maintain standards of the electrical units, two of the three quantities interconnected by Ohm's Law must be represented by stable reference standards. The best standard of EMF now known is the cadmium standard cell. The saturated cadmium standard cell, carefully made and maintained, as a reproducibility and stability in the order of one or two ppm, which is about one order of magnitude better than the accuracy at present attainable in the measurement of the absolute dimensions of the electrical units. Probably in the not-too-distant future, refinement in the determination of the electrical units in terms of fundamental standards, or of a natural constant, will require even more stable standards of reference.

RESISTANCE AND RESISTANCE APPARATUS

Automated NBS 1-Ω Measurement System

KENNETH R. BAKER, STUDENT MEMBER, IEEE, AND RONALD F. DZIUBA, MEMBER, IEEE

Abstract—**A microcomputer-controlled measurement system has been developed for calibrating stable, 1-Ω standard resistors. It consists of a direct current comparator potentiometer, a self-balancing detector circuit, and special switching networks. The measurement system is capable of comparing resistors to a precision of better than 0.01 parts per million (ppm).**

I. Introduction

THE UNIT of resistance is maintained at the National Bureau of Standards by a group of five Thomas-type 1-Ω resistors. A dc current comparator potentiometer is used to compare the NBS reference group to other 1-Ω resistors under test [1]. Fifteen resistors, five of which comprise the reference group along with two control resistors and eight unknown resistors, can be connected in series with the primary circuit of the dc current comparator. The value of any resistor in the string can be determined by indirectly comparing its voltage drop to the mean voltage drop of the reference group via a stable "dummy" resistor in the secondary circuit of the comparator. The resistors in the primary circuit are measured at a current level of 0.1 A (0.01 W/resistor); therefore, a detector resolution of 1 nV is required in order to measure a resistance change of 0.01 parts per million (ppm). The Thomas-type resistors are hermetically sealed in double-walled enclosures and are very stable after being fully annealed; however, because they are constructed of manganin they exhibit significant temperature and pressure coefficients. Thus to achieve accuracies of the order of 0.01 ppm, the operator must monitor the bath temperature of the resistors along with the ambient conditions, primarily the barometric pressure. The operation of the system in the manual mode is limited to a resolution of 0.025 ppm, which corresponds to an interpolation of one-half of the last dial setting. Automation of the system has been a high priority not only because of the large work load in the calibration of 1-Ω standards and the ease with which a computer can monitor the significant test parameters, but also because of the possibility of improving the resolution and accuracy of the system.

An earlier attempt was made to automate the system by using a digital nanovoltmeter as a detector in the critical part

Manuscript received September 8, 1982; revised October 29, 1982.

K. R. Baker is at the National Bureau of Standards with the Co-operative Engineering Education Program, University of Maryland, College Park, MD 20742.

R. F. Dziuba is with the Electrical Measurements and Standards Division, National Bureau of Standards, Washington, DC 20234.

of the dc current comparator circuit [2]. This detector could be readily interfaced to a computer; however, it proved unsatisfactory due to excessive ac output from the comparator which introduced noise greater than 50 nV rms in the detector circuit. The present automated system has alleviated these problems and has achieved a resolution of better than 0.01 ppm in the comparison of stable 1-Ω resistors. At this resolution, the practical measurement range of the automated system is ±500 ppm; however, it can easily be extended to wider ranges at slightly reduced accuracies. Over 95 percent of the Thomas-type resistors measured at NBS have deviations within ±50 ppm from 1 Ω. A few resistors constructed prior to 1948, whose values were based on the "international" units, have deviations at the ±500-ppm level. Thus the ±500-ppm range of the automated system satisfies the measurement needs of NBS in this area.

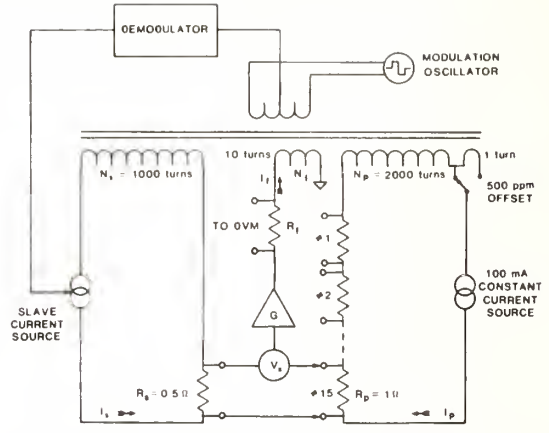

Fig. 1. Schematic diagram of dc comparator potentiometer circuit.

II. System Description

A. Comparator

The heart of the measurement system is the dc current comparator as shown in Fig. 1. In the dc current comparator, a condition of magnetic balance in the core is detected by modulating the permeability of the core by a square-wave modulation current. The output of the demodulator is proportional to the magnitude and polarity of the ampere-turn imbalance and it is used to correct the slave current source to obtain a zero flux condition in the core [3]. The comparator is a commercially available unit having an adjustable 2000-turn primary, 1000-turn secondary, and a fixed 0.1-A primary current source. In the automatic mode, the primary winding is set at 2000 turns and a relay with mercury-wetted contacts is used to insert a unit winding as a 500-ppm calibration signal.

B. Resistors

The 1-Ω resistors in the primary circuit are connected in series on a mercury ring stand which is totally immersed in a specially designed circular oil bath with temperature maintained at 25.000 ± 0.003°C. A modified crossbar switch selects the appropriate potential terminals of a resistor in the primary circuit whose voltage drop is to be compared to the voltage drop of the 0.5-Ω resistor in the secondary circuit. The 0.5-Ω resistor or "dummy" is a specially designed resistor having a low load coefficient and a negligible drift during the period of a test run.

C. Detector and Feedback Circuit

The voltage difference V_x between the dummy and test resistor is detected by a photocell-galvanometer amplifier (PGA). The PGA has been modified by mounting a pair of cadmium-sulfide (CdS) photoconductive cells adjacent to the original set of photocells in order to provide an isolated output [4]. The CdS cells form two arms of a Wheatstone bridge, as shown in Fig. 2. The output of this bridge yields a sensitivity of 0.067 V/ppm. This output voltage is buffered by an operational amplifier, A_1 and then amplified by a factor of 5 by A_2. Since a 1-ppm change of resistance corresponds to a voltage change of 0.1 μV, the open-loop gain of the system G at this point is equal to 3.35×10^6. It was observed that any further amplification will lead to oscillations in the feedback circuit. Amplifier A_3 provides a feedback current I_f through the 10-turn winding N_f. This 10-turn winding is normally used to provide adjustable standardization settings to make the dc current comparator potentiometer direct reading. The current I_f is monitored by measuring the voltage drop across a 100-Ω resistor with a digital voltmeter (DVM). A 1-μF capacitor of PTFE dielectric connected across the 100-Ω resistor provides sufficient filtering of electrical noise in the system. The feedback system is similar to the one described in [5].

At zero flux in the core

$$N_p I_p = N_s I_s + N_f I_f \tag{1}$$

and at detector balance

$$R_p I_p = R_s I_s. \tag{2}$$

The value of resistor R_p can then be expressed as

$$R_p = R_s \frac{N_p}{N_s}\left[1 - \frac{N_f}{N_p}\frac{I_f}{I_p}\right]$$

The difference in value between resistors 1 and 2 in the primary circuit can be expressed in terms of the difference in their respective feedback currents at balance, i.e.,

$$\Delta R_p = R_{p2} - R_{p1} = R_s \frac{N_f}{N_s}\frac{(I_{f1} - I_{f2})}{I_p}.$$

Since the feedback current difference can be expressed as the voltage difference ΔV across the feedback resistor R_f then

$$\Delta R_p = \frac{R_s}{R_f}\frac{N_f}{N_s}\frac{\Delta V}{I_p} \tag{3}$$

and

$$\frac{\Delta V}{(\Delta R_p/R_p)} = \frac{N_s}{N_f}\frac{R_f}{R_s} R_p I_p \tag{4}$$

which gives a sensitivity of 20 μV/0.01 ppm.

Amplifier A_3 is capable of supplying ±10 mA which would correspond to a measurement range of ±500 ppm using this feedback circuit. A booster amplifier could be used to increase the measurement range of the system.

It is essential to examine whether the system has sufficient

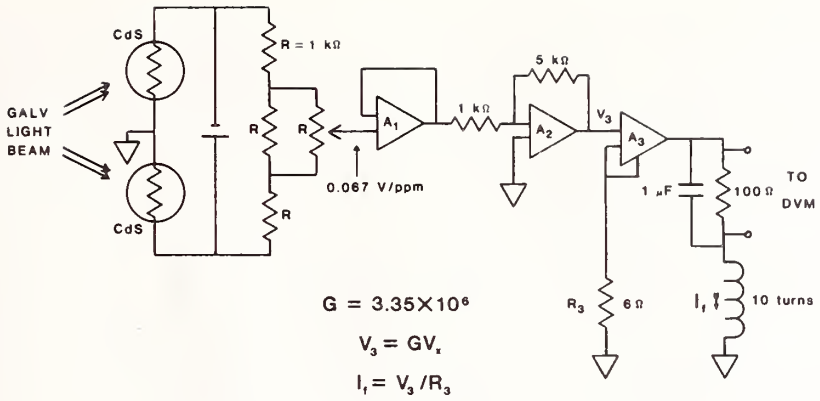

Fig. 2. Schematic diagram of detector and feedback circuits.

gain to provide the necessary feedback control for large resistance changes. As shown in Fig. 2, the feedback current can be expressed as

$$I_f = \frac{GV_x}{R_3} \tag{5}$$

where R_3 is the controlling element of current amplifier A_3. A change in R_p is reflected as a change in V_x, i.e.,

$$\Delta R_p = \frac{\Delta V_x}{I_p}. \tag{6}$$

Substituting (1) and (5) into (6) and then dividing by R_p gives

$$\frac{\Delta R_p}{R_p} \approx -\frac{N_p}{N_f}\frac{R_3}{GR_p}\frac{\Delta I_s}{I_s} \tag{7}$$

where $\Delta I_s/I_s$ represents the normalized measurement range and $\Delta R_p/R_p$ indicates an apparent offset caused by insufficient gain in the feedback system.

The offset for a measurement range of 150 ppm is 5×10^{-8}, calculated from the values given in Figs. 1 and 2. This offset can be seen as a deflection on a secondary galvanometer that is connected to the nonisolated output of the PGA. It has been observed experimentally that a 150-ppm change results in a 1-mm deflection on the secondary galvanometer. This deflection corresponds to an offset of 4×10^{-8} which is in reasonably good agreement with the calculated value. For a measurement range of 2800 ppm, the offset would be 1 ppm which corresponds to a 25-mm deflection on the secondary galvanometer.

The offset problem can be eliminated if the change of current in the feedback circuit is measured for a known change in ratio. This is accomplished by measuring the change in voltage across the 100-Ω resistor in the feedback circuit before and after inserting a unit winding in the primary circuit. For a 2000-turn primary, this corresponds to a 500-ppm change in ratio. Then the offset will not result in a measurement error if the detector output is linear and the system gain is constant. Measurements indicate that these factors contribute less than a 5-percent error for an offset of 1 ppm or less. Thus for measurements of 1-Ω resistors over the range of 0 ± 500 ppm, the resulting error due to insufficient gain in the feedback circuit would be less than 0.01 ppm. The error would increase to 0.05 ppm for resistors that deviate from nominal by 2800 ppm.

D. Microcomputer

The microcomputer is a disk-based system with an 8-bit microprocessor and 64K of RAM. It utilizes the S-100 bus and comprises eight parallel input/output ports, an IEEE-488 controller port, a 12-bit A/D converter port, two RS-232 ports, and a clock board. Basic I/O is accomplished with a CRT terminal and a printer via the RS-232 ports. The microcomputer is completely dedicated to running the 1-Ω measurement system. A block diagram of how the computer interacts with the other parts of the system is shown in Fig. 3.

Interfacing of the resistor selection switch, detector sensitivity switch, ambient temperature and humidity sensors, as well as the barometric pressure transducer was done via the eight parallel I/O ports. Ambient temperature and humidity are monotired by a digital thermometer/hygrometer instrument that is interfaced to the computer through two of the I/O ports.

The barometric pressure is monitored with a transducer whose frequency output is proportional to the input pressure. Transducer temperature is determined indirectly by measuring the voltage drop across a calibrated diode that is mechanically attached to the tranducer body. The pressure sensitivity of the system is 0.1 mmHg (13.3 Pa) and the corresponding accuracy is checked periodically against a calibrated aneroid barometer. The pressure transducer has been tracking the aneroid barometer to within 0.3 mmHg which is sufficient accuracy for applying pressure corrections to 1-Ω resistors. The transducer outputs are measured by a timer/counter/DVM that is controlled by the microcomputer through a single port. The DVM, which measures the feedback current, communicates along the 488 bus. A platinum resistance thermometer (PRT) bridge monitors the oil bath temperature. The recorder output of this bridge is interfaced to the microcomputer by the 12-bit A/D converter. This approach provides a temperature measurement range of 25.000 ± 0.010°C with a resolution of 0.1 mK.

E. Critical Switching

The critical switching area in this automated measuring system is that necessary to select and connect the potential circuits of the resistors to the PGA detector. Although the

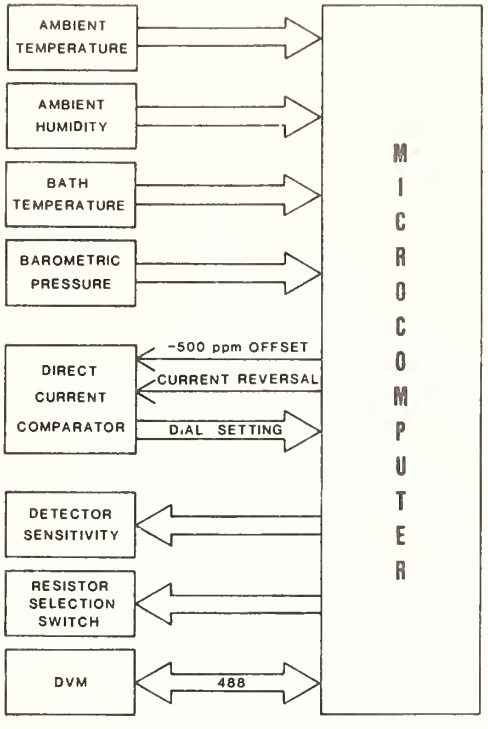

Fig. 3. Block diagram of microcomputer-controlled measurement system.

reversal technique used for achieving a balance condition cancels the effect of constant thermoelectric voltages generated in switching this part of the circuit, it is desirable to minimize the magnitude of these voltages in order to reduce the effects of varying thermal EMF's. A proper sequence of data taking can cancel the effects of thermal EMF's that are varying linearly.

The resistor selection is of crossbar type having low thermal contacts and is similar to the one described in [6]. The activating coils of the switch are separated from the switch mechanism to reduce heat transfer to this critical area. The switch mechanism is housed in a heavy aluminum box to suppress thermal gradients.

The detector sensitivity switch consists of four latching-type low thermal relays. The relays are sealed in a heavy aluminum box filled with silicone fluid and the box is immersed in the oil bath that contains the resistors. When operating in the manual mode, all four sensitivity positions are needed to adjust the primary turns of the comparator for a balance condition. In the automatic mode, only the highest sensitivity relay is required since the feedback circuit protects the PGA detector by servoing it to a null condition. Even if the potential terminals were connected mistakenly in the wrong polarity the offset voltage at the PGA would not be enough to do permanent damage.

F. Software

The computer program is written in BASIC language using multiple subroutines to handle the data taking and data processing. The flowchart shown in Fig. 4 indicates the specific operations performed by the microcomputer.

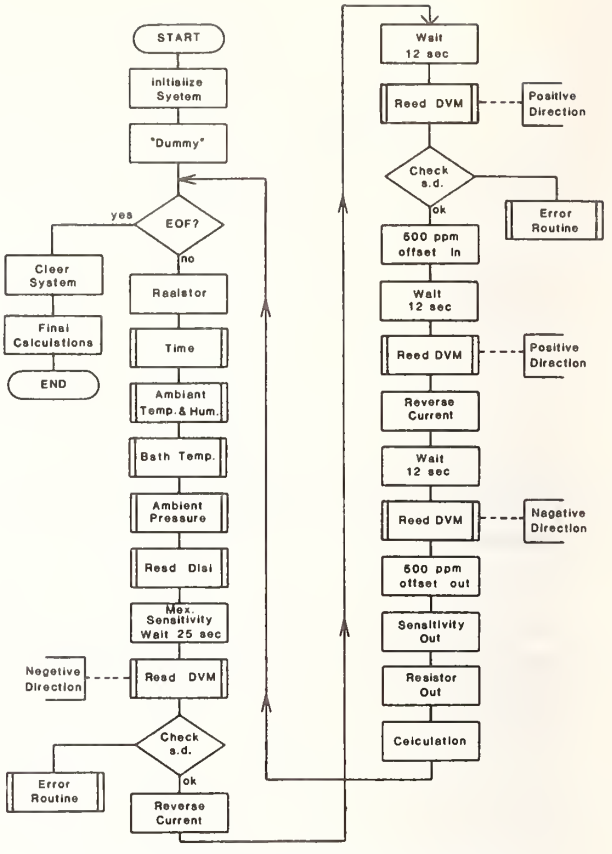

Fig. 4. Flowchart of the routine for 1-Ω measurements.

III. System Performance

The data in Table I are given to show the level of precision that is available with the automatic system. The same set of resistors were measured four times within a single day and the differences from the mean of these four series of measurements for individual resistors are listed in the table. The number of DVM readings that were taken and averaged per resistor was varied from 8 to 20 readings. The table lists the DVM readings according to the actual time sequence in which the data were taken. When a resistor was measured one-half of the total DVM readings was taken for one particular current direction, then the current direction was reversed, and after an approximate 12-s delay, the remaining half of the DVM readings was taken. The integration time per reading was 10 s. The larger imprecision for data using the 20 DVM readings is probably caused by varying thermal EMF's. No significant improvement is obtained if several reversals are performed for each resistor. The measurement range was <40 ppm.

The data in Table II indicate the differences in parts per million between the automatic and manual measurement modes. For the manual mode, an operator varies the primary turns to achieve a null balance with the PGA detector. Four measurements are taken on each resistor in the manual mode with a resolution of 0.025 ppm for each measurement. Since the automatic system is more precise, the differences are mainly due to the lower precision and operator bias in the

TABLE I
PRECISION OF AUTOMATIC SYSTEM
(Differences from mean value in parts per million.)

RESISTOR	MEAN VALUE	NUMBER OF DVM READINGS 12	10	8	20
C93	33.1908	-.001	-.001	-.001	.003
S66	18.4700	-.001	-.002	.002	.001
S69	3.0070	.001	-.004	-.001	.004
S70	-3.9908	-.003	-.000	-.002	.005
S72	1.2134	-.003	-.002	-.001	.006
S83	17.0494	-.001	-.003	-.005	.009
C84	6.1205	-.004	.002	-.005	.008
#8	34.0921	-.002	.001	-.002	.004
#9	28.0882	-.001	.002	-.002	.001
#10	33.1591	-.001	.001	-.001	.000
#11	33.5714	.003	-.000	-.004	.001
#12	33.4628	-.004	.007	-.002	-.002
#13	2.1992	-.003	-.004	-.002	.009
#14	35.4442	-.002	.004	.000	-.002
#15	32.4392	.001	.002	-.002	-.001
	mean	-.0014	.0002	-.0019	.0031
	s.d.	.0020	.0030	.0018	.0038

TABLE II
DIFFERENCES BETWEEN MANUAL AND AUTOMATIC MEASUREMENT MODES
(Differences in parts per million.)

RESISTOR	5/28/82	6/01/82	6/03/82	6/07/82
C93	-.001	-.006	-.020	-.008
S66	.005	.013	.011	.003
S89	.013	-.017	-.014	-.005
S70	-.029	.012	.013	.000
S72	.018	.015	.008	-.009
S83	-.007	-.022	-.018	.011
C84	.040	.039	.024	-.027
#8	-.010	-.040	-.018	-.029
#9	.003	.007	.011	-.002
#10	.011	.018	.025	-.005
#11	.018	.025	.012	-.047
#12	.025	.033	.028	.023
#13	.020	.027	.020	.007
#14	.019	.028	-.000	.020
#15	.028	.029	-.005	.007
mean	.010	.011	.005	-.004
s.d.	.017	.023	.017	.019

manual mode. The random nature of the differences indicates no measurable systematic error between the two measurement modes.

IV. Future Plans

Future plans include an evaluation of systematic error of the automatic system and then a re-evaluation of the uncertainty [0.08 ppm (3σ)] that is presently assigned to 1-Ω measurements at NBS [1]. The automated system has improved the precision in comparing 1-Ω resistors. With an increase in the number of measurements and the improved monitoring of test parameters that the automated system provides, it should be possible to obtain a better estimate of the possible systematic errors in the measurement process. It is planned to have the microcomputer transfer the data to a time-shared minicomputer where the data will be permanently stored and a more complex data analysis performed.

With this system it is possible to measure resistors that are located in a separate oil bath with no apparent degradation of precision or accuracy. Measurements have been made successfully on resistors in a variable-temperature oil bath with current and potential leads over 7 m long. Thus it is possible to compare resistors at any temperature against the NBS reference group maintained at 25°C. This capability is important because many international laboratories maintain their standards at 20°C and consequently it is desirable to compare standards at their working temperature. Unfortunately, the present thermometer bridge does not have the capability for computer control over a wide range of temperatures. An automatic resistance thermometer bridge [7], which can be readily interfaced to the microcomputer, is being built to measure PRT resistances over the range 0–100 Ω. Another feature of this capability is that it now becomes possible to automatically determine the temperature coefficients of resistance for standard resistors.

V. Conclusion

The automatic system has improved the precision of comparing 1-Ω standard resistors. It is expected that, after a re-evaluation of the uncertainties in the measurement process, an improvement of the accuracy level of these measurements will be demonstrated. Another advantage is that the automatic system relieves the operator from tedious repetitive measurements using a light-beam galvanometer.

Acknowledgment

The authors wish to thank R. Pederslie and D. Prather for assisting in the experimental work. The authors are also grateful to T. M. Sounders for helpful discussions on current comparators and to B. Field for suggestions on analog and digital circuits for the system. Last, but not least, the authors wish to thank R. Fronk for his assistance is solving their software problems and for his continued help in developing the necessary software required to interface the microcomputer with the minicomputer.

References

[1] T. E. Wells and E. F. Gard, "An integrated system for the precise calibration of four-terminal standard resistors," *IEEE Trans. Instrum. Meas.*, vol. IM-20, pp. 253–257, Nov. 1971.

[2] J. J. Morrow, "NBS automated one-ohm resistance measurements," *Quality Progress*, pp. 22–25, Nov. 1976.

[3] P. McMartin and N. L. Kusters, "The application of the direct current comparator to a seven-decade potentiometer," *IEEE Trans. Instrum. Meas.*, vol. IM-17, pp. 263–268, Dec. 1968.

[4] T. F. Finnegan, "AC Josephson effect determination of e/h: A standard of electrochemical potential based on macroscopic phase coherence in superconductors," B.S. thesis, Univ. of Pennsylvania, 1971.

[5] H. van Kemper, H. W. Heyenhuisen, and J. H. J. M. Ribot, "Semiautomatic bridge for high-precision dc resistance measurements on pure metals at low temperatures," *Rev. Sci. Instrum.*, vol. 50, pp. 161–164, Feb. 1979.

[6] D. W. Braudaway and R. E. Kleimann, "A high-resolution prototype system for automatic measurement of standard cell voltage," *IEEE Trans. Instrum. Meas.*, vol. IM-23, pp. 282–286, Dec. 1974.

[7] R. D. Cutkosky, "An automated resistance thermometer bridge," *IEEE Trans. Instrum. Meas.*, vol. IM-29, pp. 330–333, Dec. 1980.

A New Switching Technique for Binary Resistive Dividers

ROBERT D. CUTKOSKY, FELLOW, IEEE

Abstract—**A binary resistive divider network has been found which utilizes N cascaded DPDT reversing switches plus one SPDT switch for an N-bit divider. The network features a simple and accurate method for internal calibration. With a fixed divider input voltage the power dissipated in each resistive element is independent of switch setting.**

I. Introduction

MANY OTHERWISE satisfactory resistive dividers are found in practice to be very difficult or time consuming to calibrate. This problem is most effectively handled during the design of the instrument, at which time much future frustration can often be eliminated. The resistive divider described here contains its own internal calibration circuitry, but it would probably be an impractical device if it were not coupled to a microprocessor. It is hoped that the technique contains enough advantages to make this additional complexity worthwhile.

II. Basic Circuit

The network shown in Fig. 1 is proposed for use as a binary resistive divider. It can be seen that with no output load, the resistance of the network to the right of each DPDT reversing switch is always 2 (arbitrary) units of resistance, so that with V_{in} fixed, the power in each resistance element is independent of all switch settings. It also can be seen that if all switches are on "0" (as represented in Fig. 1), $V_{out} = 0$; if S_1 is on "1" and all other switches are on "0", $V_{out} = V_{in}$. All intermediate output voltages representable by an N-bit binary code can be obtained by two different settings of the cascaded switches. This redundancy can be used to provide the divider with a self-calibration facility.

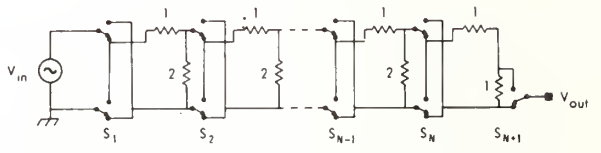

Fig. 1. An N-bit binary resistive divider. Relative resistances are indicated.

Consider the network with all switches on "0" except S_{N+1} (switch code 0—001). Then, $V_{out}/V_{in} = 1/2^N$. If the switch code is now changed to 0—011, one again has $V_{out}/V_{in} = 1/2^N$. The effect of the operating switch N is to interchange the dropping resistor and the load resistor to the right of S_N. If V_{out} is observed to change, the difference can be retained as a correction for the Nth divider.

In a similar way, one can measure the change in V_{out} when the switch code changes from 0—0010—0 ($(k + 1)$th switch set) to 0—0110—0 (kth and $(k + 1)$th switch set) to obtain the correction to the kth divider. Note that $V_{out}/V_{in} = 1/2^k$ and that the load resistor for the kth divider contains all of the resistance elements to the right of stage k; since this resistance is independent of all switch settings, however, no error will occur when the individual corrections are combined. It is therefore sufficient to make N difference measurements ($2N$ individual measurements) to completely calibrate the binary divider.

The N difference measurements required in the above scheme could be performed with ease if a fixed voltage

Manuscript received June 5, 1978; revised July 27, 1978.
The author is with the Electrical Standards Division, National Bureau of Standards, Washington, DC 20234.

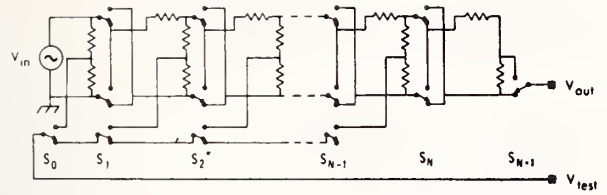

Fig. 2. An N-bit divider with enhanced self-calibration capability. All resistances are nominally equal.

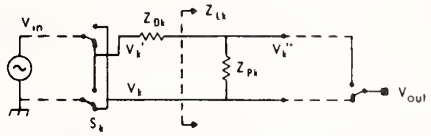

Fig. 3. The kth stage of a binary divider with voltages and impedances labeled. The load resistance Z_{Lk} is made up of all successive resistors in the chain. Z_{Dk} is the dropping resistance.

source were available which provided constant output voltages programmable to approximate each of the N voltages to be compared. An ordinary N-bit uncalibrated divider could be used for this purpose provided it had the requisite stability.

Several ways can be found for generating the required reference voltages within the divider itself, one of which is shown in Fig. 2. To calibrate the kth divider, first set switches $k-1$ and $k+1$ to "1", and set all other switches to "0". Measure the ideally zero voltage, $V_{out} - V_{test}$. Second, set switch k to "1", leaving the other switches as they were. Any change in $V_{out} - V_{test}$ can be attributed to an error in the kth divider.

III. Ratio Calculations

In the following analysis, let S_k be the logical value of the kth switch; that is, $S_k = 0$ if the kth switch is "down" as shown in the figures, and $S_k = 1$ if it is reversed. Using the nomenclature of Fig. 3, neglecting switch and wiring resistances and writing $\varepsilon_k = (Z_{Lk} - Z_{Dk})/(Z_{Lk} + Z_{Dk})$, one has $V_1/V_{in} = S_1$, $V_1'/V_{in} = 1 - S_1$, and

$$V_1''/V_{in} = 1/2 + (1 - 2S_1)\varepsilon_1/2.$$

More generally, V_k' is obtained by replacing S_k by $1 - S_k$ in the expression for V_k, and $V_k'' = (V_k' + V_k)/2 + (V_k' - V_k)\varepsilon_k/2$. The recursion formula

$$V_{k+1}/V_{in} = V_k/V_{in} + (S_{k+1}/2^k)\prod_{p=1}^{k}(1 - 2S_p)(1 + \varepsilon_p)$$

can be readily verified, from which it follows that

$$\begin{aligned} V_{N+1}/V_{in} = {} & S_1 + S_2(1 - 2S_1)(1 + \varepsilon_1)/2 + S_3(1 - 2S_2) \\ & \cdot (1 - 2S_1)(1 + \varepsilon_1)(1 + \varepsilon_2)/4 + S_4(1 - 2S_3) \\ & \cdot (1 - 2S_2)(1 - 2S_1)(1 + \varepsilon_1)(1 + \varepsilon_2) \\ & \cdot (1 + \varepsilon_3)/8 + \cdots. \end{aligned}$$

For calibration of the kth ratio, measure $V_{N+1}/V_{in} = V_{out}/V_{in}$ first with $S_k = 0$, $S_{k+1} = 1$, and then with $S_k = 1$, $S_{k+1} = 1$, in each case with all $S_p = 0$ for $p > k + 1$. The difference between these ratios is given by

$$\Delta_k = \frac{\varepsilon_k}{2^{k-1}}\prod_{p=1}^{k-1}(1 + \varepsilon_p) \approx \varepsilon_k/2^{k-1}$$

for $2 \le k \le N$, and $\Delta_1 = \varepsilon_1$. Note, however, that the sign to be attached to the Δ_k's must be reversed if during calibration an odd number of the switches to the left of the kth switch are logically true.

Ignoring terms of the order ε^2 and higher, we have finally

$$\begin{aligned} V_{N+1}/V_{in} \approx {} & S_1 + S_2(1 - 2S_1)(1 + \Delta_1)/2 + S_3(1 - 2S_2) \\ & \cdot (1 - 2S_1)(1 + \Delta_1 + 2\Delta_2)/4 \\ & + S_4(1 - 2S_3)(1 - 2S_2) \\ & \cdot (1 - 2S_1)(1 + \Delta_1 + 2\Delta_2 + 4\Delta_3)/8 + \cdots \end{aligned}$$

If each of the voltage measurements involved in the calibration of the divider has an uncertainty of σ_i, then each Δ_k will be uncertain by $\sigma_i\sqrt{2}$. The total uncertainty in the corrected value for V_{N+1}, σ_T, may be calculated from the preceeding equation. It is found that for an N-bit divider, the maximum uncertainty in V_{N+1}, $\max(\sigma_T)$, occurs when all of the switches are up ($S_k = 1$ for all k). To a very close approximation, $\max(\sigma_T) \approx \sigma_i\sqrt{2}\sqrt{N + 1/3}$. Although these assertions about $\max(\sigma_T)$ are made without proof, they may be readily verified for realistic values of N.

IV. Practical Considerations

Resistive dividers achieve their highest accuracy when the resistances are chosen so that the uncertainties due to switch resistance variations are about equal to those due to leakage resistance variations. If conventional switches or relays are used, 100 000-Ω resistors are about optimum and should yield divider accuracies around 1 part in 10^7. It is expected that a commercial solid-state digital-to-analog converter would be used in the low-order end of a practical divider to reduce the number of relays to a minimum. A 17-bit DAC combined with an 8-bit binary divider is being considered for voltage measurements up to 20 V.

NBS Automated One-Ohm Resistance Measurements

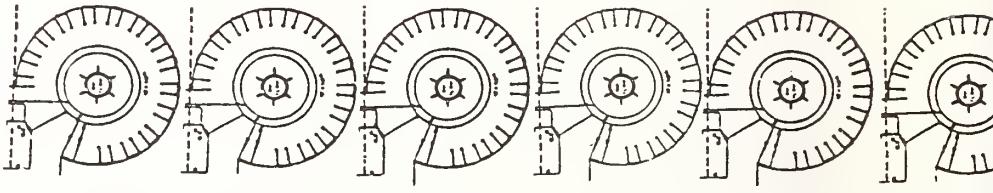

* **Jerome J. Morrow**
Physicist, Electricity Division
U.S. National Bureau of Standards

Automation of the U.S. National Bureau of Standards' one-ohm resistance measurement system is part of a program of automating all systems used in calibration of electrical reference standards. Automating these systems allows more measurement redundancy in both number and type of test, and will provide the opportunity for the NBS staff to gain experience in automated systems which are rapidly replacing manual systems in all parts of the measurement world.

In automating the NBS one-ohm manual system it was necessary to preserve the manual system and to minimize the need for new analog and digital hardware. While these limitations are rather severe, this approach offers several distinct advantages. The automation activity may be pursued with minimum interruption to ongoing calibration work. Considerable saving in captial equipment money may be realized by utilizing the manual equipment to the largest extent possible. Finally, parallel construction allows the evaluation of critical components, such as switching, to be done by direct substitution.

The manual system shown in Figure 1 consists basically of a dc current comparator potentiometer with resistors and their switches in an oil-bath whose temperature is stable to better than ± 0.001 degree Celsius. The following is based on a simplistic view of the operation of the current comparator. Manual measurements consist of balancing the IR drops across the "dummy" resistor in the secondary circuit and those of the unknown and standard resistors in the primary circuit by changing the primary number of turns. Each balance provides an equation of the form:

$$R_i = (N_{pi}/N_s)R_D$$

where R_i = resistor in primary circuit
N_{pi} = primary number of turns for R_i
N_s = secondary number of turns (constant for all balances)
R_D = dummy resistor

Since N_s and R_D are constant and five of the resistors are standards, it is possible to determine the unknown resistors in terms of the mean of the five standards.

In order to automate and preserve such a system, it was decided to place a modified cross-bar switch in parallel with the existing manual rotary switch (for the primary resistors) and to add a switch to

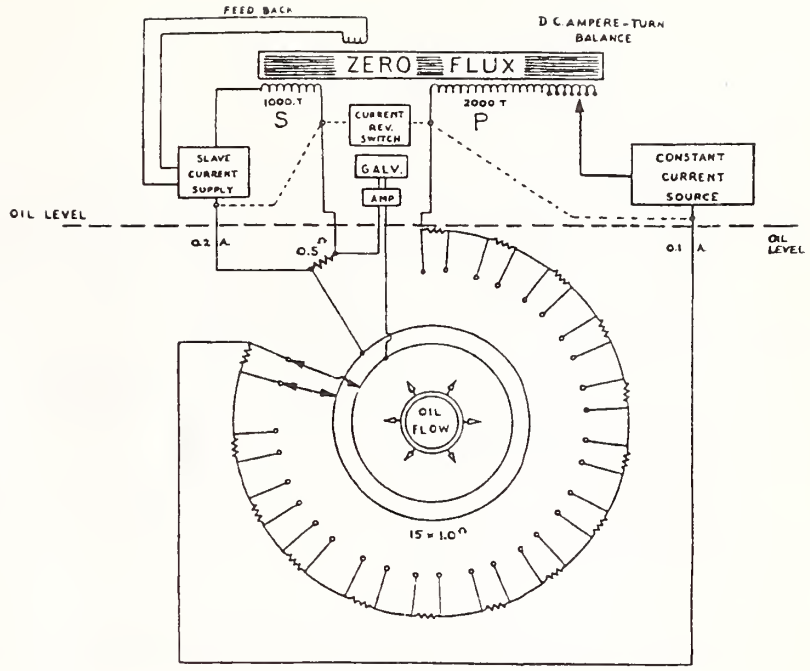

FIGURE 1:
Circuit for comparison of one-ohm resistors.

the galvanometer circuit so that the photo-cell galvanometer could be replaced by a digital nanovolt meter (DNM). The system would then be operated in an unbalanced state, i.e. the primary turns are not changed and the DNM would measure the difference in IR drops across the dummy resistor and the resistors in the primary circuit. The stability of the cross-bar switch's thermal emfs and of the DNM had to be several nanovolts or less in order to compete with the manual system.

From previous work in switching standard cells, it was known that some commercial independent-select cross-bar switches could be made suitable by separating the electro-magnetic coils from the switch mechanism. The switch mechanism is placed inside a heavy aluminum box and the coils outside. The push rods from coil to switch point are extended by plastic rods. This type of separation reduces heat transfer from coil to switch point sufficiently, and the heavy aluminum box effectively eliminates thermal gradients within the box. In addition all lines entering the box are thermally coupled to the box by means of one mil Mylar. Since the cross-bar is in parallel with the manual rotary switch immersed in the oil bath, it is possible to compare the magnitudes and stabilities of their thermal emfs. By manually switching in a resistor and noting the deflection and noise on the photo cell galvonometer for each direction of current, and repeating this with the other switch, it was concluded that there were no significant differences between the two switches. In addition, measurements of the same resistors with both switches yielded no significant differences.

Automating the Manual System

The DNM is a commercial item capable of resolving one nanovolt with two nanovolts peak-to-peak noise for the loads and voltages (10 microvolts or less) of the system. In terms of one-ohm resistors, one nanovolt equals 0.01 ppm. However, all noise must be kept to a very low level because of the low normal mode rejection of 70 db and common mode of 180 db inherent in the DNM. It was found necessary to isolate the system from the power lines, to use coaxial cables for all lines between the current comparator and oil bath and, as far as was possible, connect all grounds to the input ground of the DNM. Without these measures the DNM output varies by hundreds of nanovolts. The presence of pump motors and temperature controllers are probably responsible for most of the residual noise. It also has been apparent that line voltage fluctuations are responsible for some of the noise. This noise is also present in the manual system and appears to correlate with the noise in the automated system. At present the peak-to-peak noise in the automated system is usually ten nanovolts or less, and it is possible to reduce the noise by taking nine or more readings and averaging it out if nine or more readings are taken.

Resistance measurements in the automated system consist basically of measuring the difference of the IR drops between the "dummy" resistor and the resistors in the primary circuit. The primary and secondary number of turns and their currents are constant throughout all measurements. These measurements lead to equations of the form:

$$I_S R_D - I_p R_i = v_i$$

where I_S = current in secondary circuit
R_D = dummy resistor
I_p = current in primary circuit
R_i = resistor in primary circuit
v_i = voltage measured by the DNM

It should be noted that in the equations for an unbalanced system the current directions and polarity of the DNM must be known. The voltage, v_i, is half of the difference of the voltages for both current directions. This difference eliminates thermal emfs and the DNM "zero" provided they are constant within the time required for the voltage measurements.

If such an equation for an unknown and a standard resistor are subtracted from one another, the result is:

$$R_S - R_X = (v_X - v_S)/I_p$$

In order to obtain R_X, I_p must be measured. This is accomplished by switching a short in place of the "dummy" resistor. The DNM will then read the voltage across the standard from which one can calculate the primary current. It should be noted that the primary current measured need not be very accurate since it is divided into a relatively small quantity. Also note that the errors which are constant for all measurements will be reduced further by the subtraction of the two voltages. If the drift rate of the DNM "zero" is con-

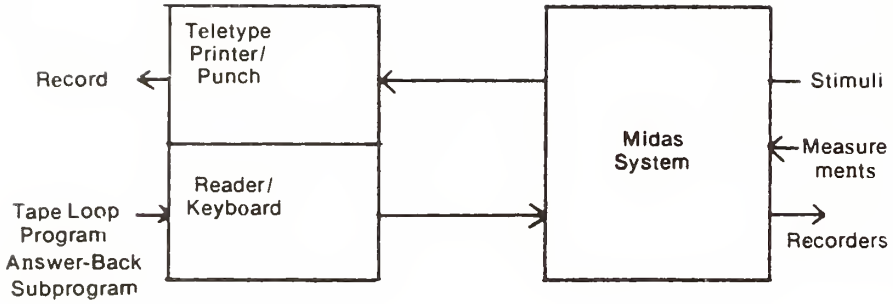

Figure 2. MIDAS and teletype configuration.

```
 R #H60*R F6949*  5832109*  5832109*  5832109*
  5832109*  5832109*  5832109*  5832109*
  5832109*  583210$ Z
N  #B05=$#H60*R F6949*  5832109*  5832109*  5832109*
  5832109*  5832109*  5832109*  5832109*
  5832109*  583210$ ZZ
 N #B765#H60*R F6949*  5832109*  5832109*  5832109*
  5832109*  5832109*  5832109*  5832109*
  5832109*  583210$ Z
R #B05=$ #H60*R F6949*  5832109*  5832109*  5832109*
  5832109*  5832109*  5832109*  5832109*
  5832109*  583210$ ZZ
```

FIGURE 3: Sample MIDAS paper-type program.

stant, the resultant "offset" error will b
eliminated. Errors such as voltage meas
urements on different DNM ranges woul
not be reduced adequately. The one-ohn
resistor values measured by this systen
differ from nominal by less than 50 ppm o
five microvolts. Therefore, the DNM range
need not be changed.

The settling time of the automated sys
tem was found to range from 45 to 5
seconds. The former is for a resisto
change and the latter is for a current re-
versal. The settling time for the DNM fo
these same voltage changes with essen-
tially no input noise is about 30 seconds.
The settling time for the manual system is
no more than two seconds with the auto-
matic switch. These large settling times
are a real disadvantage of the automated
system. If one ppm resolution is specified,
then the settling time would be six
seconds or less.

Control of the automated system was
accomplished by a modular programable
digital interface system developed at
NBS. This system has been given the acro-
nym MIDAS. In general, MIDAS consists
of a crate and power supply with a control-
ler and modules which directly interface
any device with TTL levels. The program
source and data logger can be any device
which transmits and receives standard 7-
bit parallel USASCII code format.

In the system considered here a stand-
ard Teletype served as this device. Con-
figuration of the MIDAS is shown in
Figure 2. The operating rate of the sys-
tem is limited by the Teletype of ten char-
acters per second. This limitation was of
no consequence except on recording DNM
output. The A/D conversion rate is about
two readings per second and there are five
digits per reading plus several command
characters. Consequently about every
other reading was recorded. If the DNM
output is "flip-flopping" as a result of
noise, it is possible to record only one side
of the variations, or considerably more of
one side than the other. In addition, re-
cording time constitutes a considerable
portion of the total run time. Another
limitation of this configuration is that any
program must be sequential. This elim-
inates any possibility of change in the se-
quence, decision making, or determining
variable parameters such as settling time
and noise during a run. Coupling this lim-
itation with the fact that no program could
be a tape loop because of the need to
switch resistors in the primary circuit in
and out, experimentation with the sytem
required a large number of very long pro-
grams. In the very near future, the
MIDAS will be controlled by a minicompu-
ter and such limitations will be eliminated.

Differences between duplicate measurements in ppm.

Resistor Position	4/11/75	4/15/75	4/15/75	4/18/75	5/1/75	5/14/75	5/14/75
1	0.00	0.02	0.01	-0.02	-0.01	0.02	-0.09
2	0.05	0.01	-0.02	-0.02	0.27	-0.02	-0.08
3	0.08	0.01	-0.02	-0.03	-0.04	-0.04	-0.04
4	-0.02	0.00	-0.03	-0.02	0.04	-0.01	-0.03
5	0.02	0.03	0.02	0.03	-0.03	-0.03	-0.02
6	0.00	0.04	0.04	-0.02	0.00	-0.03	-0.01
7	0.00	-0.01	-0.01	-0.01	0.02	0.02	0.00
8	-0.01	0.01	-0.01	0.00	0.01	0.00	0.05
9	-0.01	0.07	-0.03	0.00	-0.01	0.03	-0.01
10	0.00	0.01	-0.02	-0.01	-0.08	-0.02	-0.03
11	0.00	0.00	-0.04	0.00	-0.06	0.00	-0.05
12	0.00	0.02	-0.01	0.00	-0.09	-0.04	-0.05
13	0.00	0.01	-0.01	0.01	-0.07	0.00	-0.02
14	0.00	0.00	-0.02	-0.02	-0.07	-0.03	-0.03
15	0.00	0.04	0.01	0.00	-0.07	0.02	-0.01

A portion of a tape program is shown in Figure 3. The basic sequence for the measurements for one resistor is, in this case, a set of six lines in the figure. In terms of Teletype lines, it is a set of two. The first line prints the current direction (R); inhibits the MIDAS for 60 seconds to allow for settling of all components; and then prints overflow, range, and three DNM readings. Each reading is printed after a conversion pulse is received from the DNM. The second and third lines print six more DNM readings. The fourth line prints the new current direction, the current reversal relay is actuated and the remainder is the same as the first line. The fifth and sixth lines are identical to the second and third. The seventh line is the same as the first except that the old resistor is switched out and a new one switched in.

Evaluation

The stability of the automated system has been measured by making duplicate measurements. As seen in Figure 4, there are only two differences greater than 0.1 ppm. Each day's measurements were made in the following order: 1 through 15 and then 15 through 1. Therefore the time lag between both measurements of resistor 1 can be quite long. Depending upon the program, it ranged from 1.5 to 1.1 hours. In the manual system a three sigma difference of 0.056 ppm or less is acceptable. In the automated system some differences larger than this are simply due to noise. In other cases, it is due to a shift in the measured voltages. These shifts can be detected by finding the change in the measured voltages for each current direction for both measurements of each resistor. These changes indicate that there is generally a very slow drift with time, usually less than a nanovolt from one resistor to another. However, sudden erratic changes of ten nanovolts or more occur. If they occur between the voltage measurements for both current directions, they will not be subtracted out. It has not been possible to ascertain the cause of the shifts. Thermal emf shifts can be ruled out.

The accuracy of the automated system can be evaluated by comparing its measured resistance values with those from the manual system. With one exception, differences between resistor values from the automated and manual systems are 0.1 ppm or less.

A least squares fit of a straight line to the nominal value corrections for 59 resistors from both systems yielded the following line.

$$C_a = -0.008 + 1.00013\ C_m$$

where C_a = correction in ppm as measured on the automated system

C_m = correction in ppm as measured on the manual system

The residual standard deviation of the fit was 0.023 ppm. If both systems gave identical results, then the equation would be

$$C_a = 0.0 + 1.\ C_m$$

The difference between the two equations for the resistors considered here is no more than 0.01 ppm.

In addition, a least squares fit of a straight line was made to the differences of duplicate measurements from both systems. Ideally one would expect no correlation between the differences; i.e., the slope of the line should be close to zero. The least squares fit yielded the following line.

$$D_a = 0.03 - 0.31\ D_m$$

where D_a = difference in ppm of duplicates from the automated system

D_m = difference in ppm of duplicates from the manual system

The residual standard deviation was 0.021 ppm and the standard deviation of the slope was 0.277 ppm.

In addition, a fit was made of a zero slope line and the following resulted.

$$D_a = 0.024$$

The residual standard deviation was 0.021 ppm.

These results indicate that there was no correlation between the differences from both systems and that differences of the automated system are larger than those of manual systems by 0.02 ppm at the one sigma level.

LCS 700:70:991 ASQC 11/76-245

References

(1) Wells, T.E., and Gard, E.F., "An Integrated System for the Precise Calculation of Four-Terminal Standard Resistors," IEEE Trans. on Istr. and Meas., Vol. 1M-20, No. 4, (Nov. 1971).

(2) Natl. Bur. Stand (U.S.), Tech. Note 990, 42 pages (Aug. 1973).

Acknowledgements

Construction of the crossbar switch by R.E. Long, programing and data reduction by D.E. Bruch, and R.C. Fronk, assistance in making measurements by L.R. Cooke, and valuable suggestions and criticism by N.C. Belecki and T.E. Wells are gratefully acknowledged.

Reprinted by permission from IEEE TRANSACTIONS ON
INSTRUMENTATION AND MEASUREMENT
Vol. IM-20, No. 4, November 1971

An Integrated System for the Precise Calibration of Four-Terminal Standard Resistors

THOMAS E. WELLS AND EARL F. GARD, MEMBER, IEEE

Abstract—A description is given of the system currently in use at the National Bureau of Standards for measurements of 1-Ω standard resistors of the Thomas type. A tenfold improvement in accuracy over the former method has been realized. Resistors of this type are now reported to eight decimal places with a total uncertainty of 0.08 ppm. The latter figure includes a three-standard-deviation limit for random errors plus an estimate of systematic errors [1].

The new system is not only more rapid in operation than the old one (fewer man hours required), but has consistently produced data of superior resolution while operating with a lower test power in resistors. A dc current-linkage balance is used to determine the standard–unknown differences while both are connected in series and totally immersed in a specially designed circular oil bath, which remains completely covered during all tests. Bath temperature is maintained constantly at 25 000°C (±0.003°C) in a unique manner.

Manuscript received May 27, 1971; revised July 9, 1971.
The authors are with the Electricity Division, National Bureau of Standards, Washington, D. C.

Introduction

IN 1963, as reported to the clients of the National Bureau of Standards, the precision of the resistance of double-walled 1-Ω resistors was increased from 1 to 0.1 part/million (ppm). Since this precision was near the limit obtainable on the bridge in use at that time (the Wenner bridge [2]), it seemed prudent to plan a new resistance measurement system capable of meeting expected demands for increased precision. It was planned that this new system would not only be capable of greater precision but, if possible, would be faster and easier to use.

In developing a new system, the following recognized limitations of the old system were kept in mind: 1) the requirement for manually made lead adjustment in the ratio-arm connections; 2) disturbance of the temperature

equilibrium by handling of the resistors when performing interchange; 3) generation of transient thermal EMF's when changing potential connections to the resistors; 4) uncompensated errors in the ratio set itself caused by unequal power coefficients of certain ratio resistors; 5) temperature-control difficulties partially inherent in the original bath design such as its rectangular shape and placement of heater lamps close to the measured resistors. Lack of a cooling element rendered the bridge inoperative when the ambient room temperature rose above 24.0°C. Temperature control was ±0.01°C at best, but frequently averaged ±0.02°C; and 6) electrostatic disturbance caused by charged objects, e.g., people moving around the room and electromagnetic disturbance caused primarily by the heater lights in the bath turning on and off.

Although most of these limitations of the old Wenner bridge system could have been eliminated by the construction of a modified bridge system, it was decided to use a potentiometric system. This method seemed attractive due to the development of the direct current comparator by Kusters and others at the National Research Council of Canada [3], [4].

Integrated System

Constant Temperature Bath

A tank was constructed large enough to accommodate a circular mercury stand holding 15 Thomas-type resistors in a series ring.

Salient features of this bath are the following.

1) It is cylindrical in shape with approximately 550-l capacity. The radial oil flow is produced by a belt-driven propellor located in the bottom center of the tank. The oil flow moves horizontally between two cylindrical screens, a central one (15 cm diameter) of fine mesh capped at the top and an outer very coarse mesh screen (Fig. 1). The oil return path to the propellor is via a false bottom containing coiled tubing designed to form a heat exchanger. The oil circulation is superior to that obtained in the rectangular tank of the Wenner bridge.

2) The resistor ring stand is positioned so as to place all resistors at the same middepth oil level and also equidistant from the central oil distribution screen.

3) No electrical heaters or coolers are installed in the 550-l bath. Temperature control is obtained by regulating the circulation of cooling oil pumped from a smaller (110-l) auxiliary bath through the heat-exchanger tubing located in the bottom of the larger tank. This cooling oil carries away the heat produced by the stirring of the oil in the large bath. It was found that variations of 0.02°-0.03°C in the temperature of the auxiliary bath would be reflected by variations 1/10 or less as large in the larger bath.

The temperature of the bath can be controlled manually by varying the flow of cooling oil by adjusting a needle valve in the oil pipeline. Alternatively, the needle valve can be set high enough to assure cooling of the bath and the flow of oil can then periodically be interrupted by a valve in the cooling oil circulating line that is controlled by an electronic sensor in the large bath.

Current Comparator

The direct current comparator operates on the principle that when two magnetomotive forces imposed on a magnetic core by currents in two windings are equal and opposite, the flux in the core is zero. This balance condition can be detected by a modulation detector. The detector circuit can be used to control the output of a current source, connected into one of the windings so as to automatically maintain the condition of zero flux in the core. How the current comparator can be used to compare resistors can be seen from the equation developed below, with reference to Fig. 2.

The basic equations are as follows when

N_p, N_s primary and secondary number of turns;
I_p, I_s primary and secondary currents;
R_D, R_x, R_s resistances of "dummy," unknown and standard.

At flux balance in the transformer core,

$$N_s I_s = N_p I_p$$

or

$$I_s/I_p = N_p/N_s \tag{1}$$

At voltage balance the IR "drop" across the "dummy" (secondary) resistor R_D and the IR drop across the selected unknown resistor R_X in the primary circuit results in

$$R_x I_p = I_{sx} R_D$$

where I_{sx} is the secondary current at balance or

$$R_x = (I_{sx}/I_p) R_D.$$

Substituting turns for current, from (1) we have

$$R_x = (N_{px}/N_s) R_D \tag{2}$$

where N_{px} is the number of turns in the primary winding at balance.

Similarly when a resistor of known resistance R_s is being measured we have

$$R_s = (N_{ps}/N_s) R_D. \tag{3}$$

Dividing (2) by (3) we then have

$$R_x = (N_{px}/N_{ps}) R_s. \tag{4}$$

Measurement Technique

Briefly, the technique is one in which the voltage drop across each of the client's resistors is compared indirectly (via a stable dummy resistor) with the voltage drop across each resistor in a reference group while all are connected in series and totally immersed in the oil bath

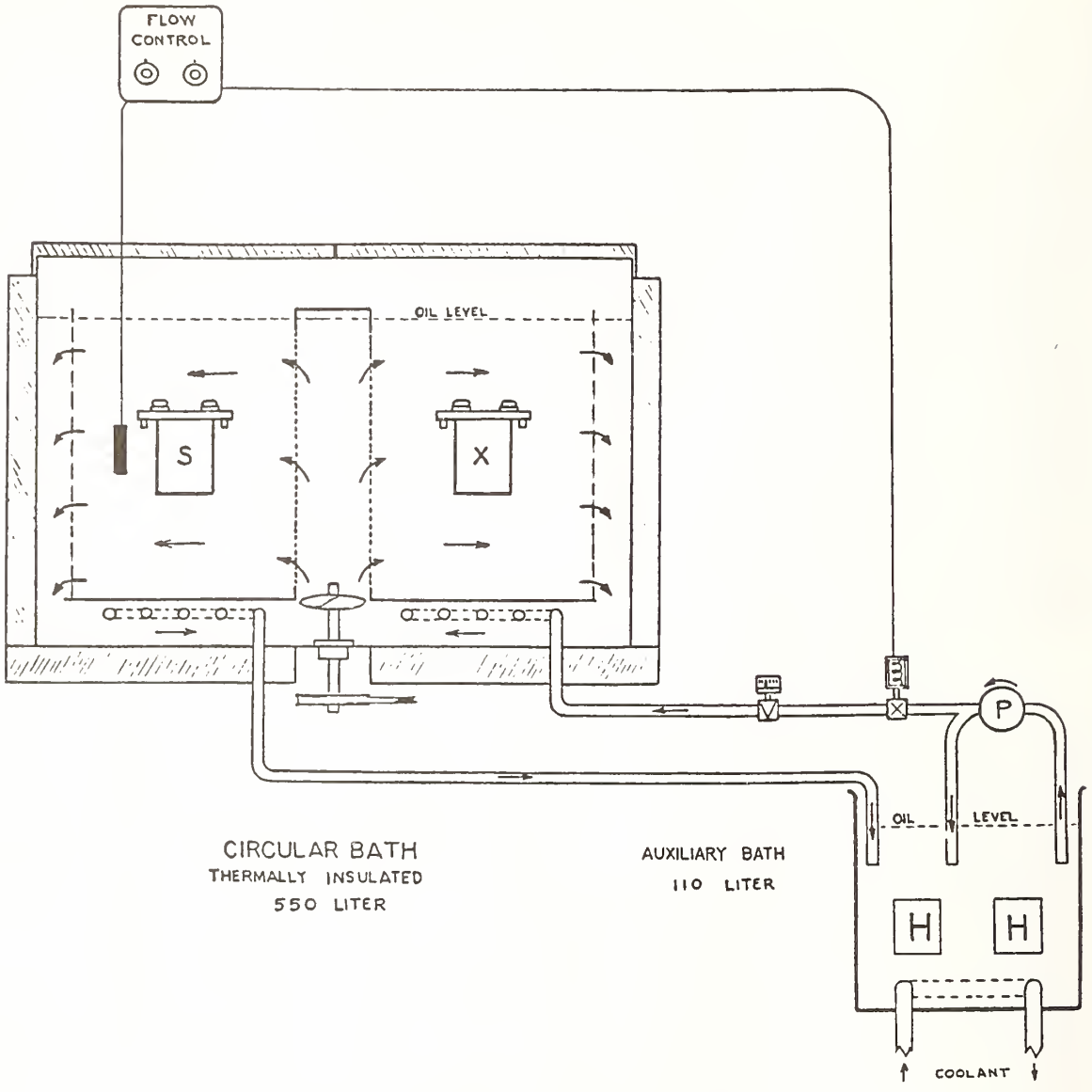

Fig. 1. Two-stage temperature control system.

maintained at 25.000°C ± 0.003°C. The dc-current comparator (ampere-turn balance) is used for making the comparisons while all the standard and unknown resistors are carrying the continuous test current of 0.1 A (0.01 W/Thomas resistor). The comparator is usually used near the maximum setting of the balance dials (2000 turns of the primary winding) and the circuit "trimmed" in such a manner that only the last three or four dials are changed in balancing. Final balance settings of the seven decade controls are recorded and utilized solely to obtain accurate standard–unknown differences.

A series of balances between the 0.5-Ω dummy and each of the standard and unknown resistors in turn is made by adjusting the seven dials controlling the turns of the primary winding. Sensitivity is sufficient to readily discern 0.5 step of the seventh dial. As the first dial has 20 steps and all balances in this instance are made with it at the twentieth step, the 0.5 step is 0.025 ppm.

With the 0.1-A dc primary current automatically controlled and the slave supply tracking it at 0.2-A dc (the zero flux feedback ensures this condition), the series of balances between the 0.5-Ω dummy and of the standard and unknown resistors in turn can be made as rapidly as the technician can operate the potential selector switch and adjust the seven dials controlling the taps to the primary winding using the standard technique of reversing the currents to eliminate the effect of "parasitic" EMF in the detector circuit.

Standard operating procedure at NBS is as follows.

1) The bath is "loaded" with a maximum of eight clients' resistors on the day preceding measurements, oil depth checked, cover replaced, and 0.1-A current

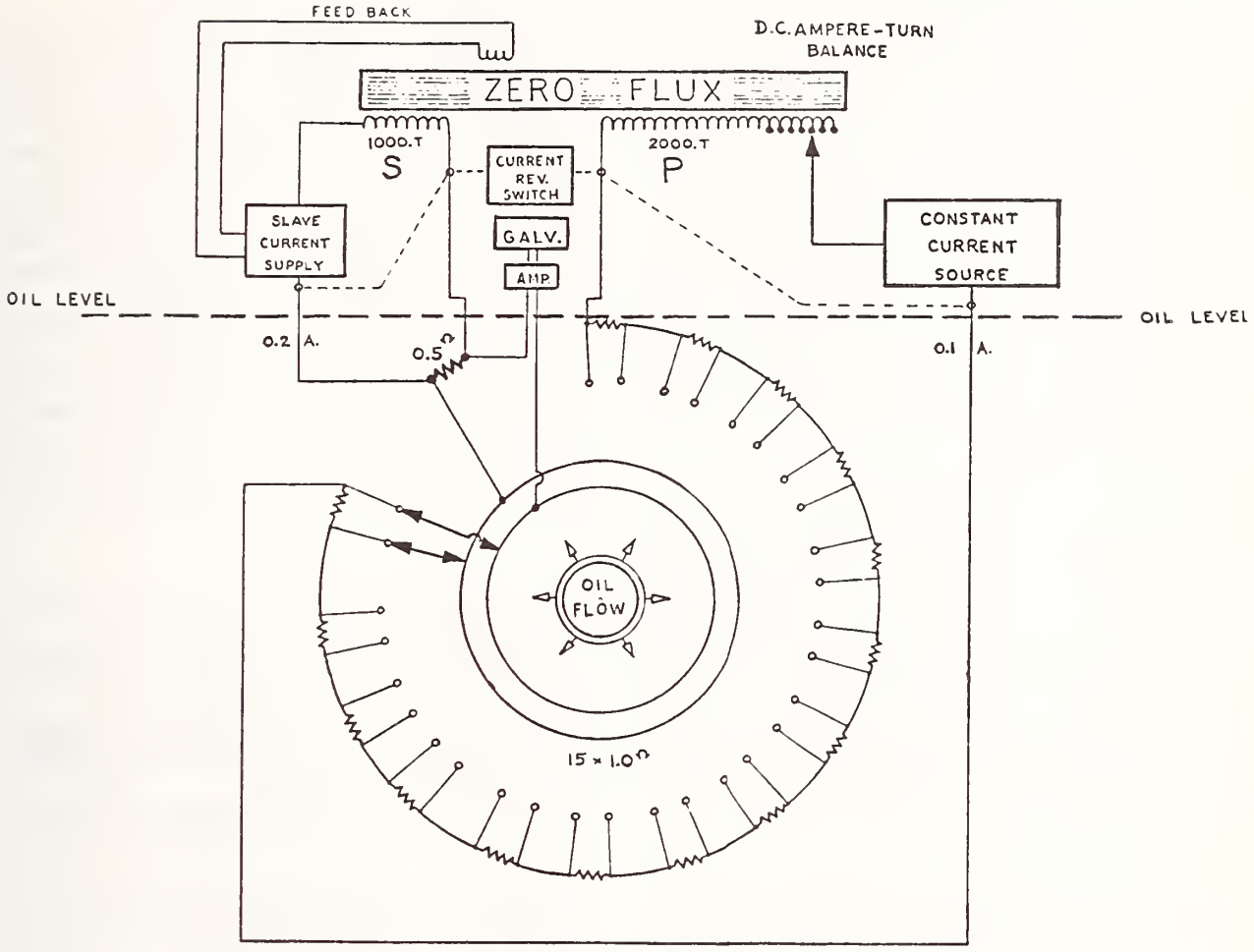

Fig. 2. Circuit for comparison of 1-Ω resistors.

switched on. Note that the bath is in constant temperature control with continuous stirring even when not in use.

2) On the following day, the bath temperature is checked, trimmed slightly if necessary, and the temperature recorder started for the calibration run.

3) Balances are then made as described for each of the 15 selector switch positions, 1–15, and dial readings recorded.

4) Room barometer is read and pressure recorded along with room temperature.

5) Repeat balances are then made in reverse order, 15–1.

6) Approximately five hours later, without opening the bath, steps 2–5 are repeated entirely by another technician.

7) Test current is turned off; bath is opened and unloaded.

We now have four balances for each switch position. Averaging these and knowing the average correction of the five NBS reference resistors, only simple arithmetic is necessary to arrive at the proper corrections for each of the unknown resistors. The value of the dummy 0.5-Ω resistor is unimportant as it does not enter into the calculations. However, its resistance must remain constant during a given run. A low power coefficient is desirable for the 0.5-Ω resistor although in this case the secondary current is essentially constant because only small changes are made in the primary turns setting.

In addition to the five reference standard resistors, there are always present in the series an extra pair of NBS Thomas 1-Ω resistors that are measured and serve as controls in the data analysis.

Resistors of the double-walled type such as these are affected slightly by pressure variations [5], [6]. Therefore, if maximum use is to be made of the reported values, the effect of pressure must be considered. Although the temperature and oil-immersion depth are held constant, the ambient air pressure will naturally vary; therefore, before a mean value for the correction of the five can be utilized, it must be adjusted back to the 101 325 N/m^2 pressure

base, from the total pressure as measured in a given calibration run.[1] Pressure coefficient tests were carefully made on each of the reference resistors at NBS. Results have shown the effect to be positive and linear with no appreciable hysteresis.

Clients' resistors whose individual pressure coefficients are not known in most cases are simply reported at the total pressure existing during the testing period. An approximate figure for commercial units is 0.000 015-ppm decrease in resistance per newton per square meter decrease in pressure on resistor (multiply pressure in millimeters of mercury by 133.32 to obtain pressure in newtons per square meter). For a user located at an altitude of one mile the resistance of this type resistor will be about 0.3 ppm less than the value at the altitude of the NBS Gaithersburg Laboratory.

System Performance

The resistance values of Thomas-type standard resistors submitted to NBS for calibration prior to July 1, 1970, were reported to 0.1 ppm with an uncertainty of ±1.0 ppm. Since that date, using the new system the values have been stated to 0.01 ppm with an uncertainty of only 0.08 ppm. The latter figure includes a three-standard-deviation value for random error due to minute temperature, pressure, resistance fluctuations, and lack of resolution plus estimated amounts for the uncertainty in temperature and pressure measurements, the only known sources of systematic errors.

The test power, formerly 0.05 W/resistor (intermittent) is now 0.01 W (continuous). The performance of the oil bath now permits specification of temperature at which the calibrations are performed as 25.00° rather than 25.0°C, as was previously the case. The new reports state the total pressure on the resistor during calibration.

Additional advantages of the new system include: elimination of the tedious and time consuming lead balances that were necessary with the Kelvin double-ratio circuitry; and elimination of a secondary or working group of NBS standards. Clients' resistors are now compared directly with the National Reference Group of standards.

This measurement system was completed in 1969 and has been in successful operation since that time. The initial circuitry was designed solely for 1-Ω comparisons of Thomas-type standard resistors. Experiments indicate that with proper modifications the same type of system can be extended to perform one to one comparisons of resistors in the range 0.1–100 Ω and such extension is contemplated.

[1] Total pressure existing at the level of the surfaces of the amalgamated current terminals when the resistor is immersed so as to place the terminal surfaces 60 mm below the oil level.

References

[1] Nat. Bur. Stand. "Improved accuracy in Thomas-type one-ohm standard resistor calibration," *Tech. News Bull.*, vol. 54, 1970, p. 188.

[2] F. Wenner, "Apparatus and procedures for the comparison of precision standard resistors," *J. Res. Nat. Bur. Stand.*, vol. 25, 1940, p. 229; also reprinted in *NBS Handbook,* vol. 77, 1961, p. 1.

[3] M. P. MacMartin and N. L. Kusters, "A direct-current-comparator ratio bridge for four-terminal resistance measurements," *IEEE Trans. Instrum. Meas.*, vol. IM-15, Dec. 1966, pp. 212–220.

[4] N. L. Kusters and M. P. MacMartin, "The application of the direct current comparator to a seven-decade potentiometer," *IEEE Trans. Instrum. Meas.*, vol. IM-17, Dec. 1968, pp. 263–268.

[5] J. L. Thomas, "Stability of double-walled Manganin resistors," *J. Res. Nat. Bur. Stand.*, vol. 36, 1946, p. 107.

[6] Nat. Bur. Stand., "General information of standard resistors. (Elec. Ref. Stand. Sec. 211.01), Dec. 1970.

Reprinted by permission from IEEE TRANSACTIONS ON
INSTRUMENTATION AND MEASUREMENT
Vol. IM-19, No. 4, November 1970

NRC 11548

Resistive Voltage-Ratio Standard and Measuring Circuit

RONALD F. DZIUBA AND BERNADINE L. DUNFEE, SENIOR MEMBER, IEEE

***Abstract*—This paper describes a highly stable, guarded dc voltage-ratio standard and the measuring network and techniques used to establish the values of its ratios to an accuracy of 0.2 ppm. The entire system is housed within a dry-air enclosure whose temperature is maintained at 23 ± 0.05°C. Discrete ratios from 1:1 to 1000:1 are provided, with maximum rated voltage set at 1000 volts. The design of the standard was chosen so that a redundancy of measurement could be incorporated in the system. Thus each successive ratio is measured by a substitution or "bootstrap" method and by satisfying the conditions of the series-parallel principle, the 10:1, 100:1, and 1000:1 ratios are measured by a second independent method. The design also admits additional checks on the validity of the measurements. An analysis of measurement errors and a discussion of their possible origin are included. Since the intent also was to design the ratio standard for low-frequency operation some preliminary data are included on its ac performance.**

INTRODUCTION

RECENT years have brought challenges to the scientific and technological communities that were barely discernible a few decades ago. Advances made in meeting these have been possible only through the more precise and accurate measurement of physical quantities that often are interweaved within vast complex measuring systems and often cover a range of magnitudes of several decades. Measurement of dc voltage from the 1-volt level of the standard cell to 1 or 2 kV is a case in point—a necessary and important link in the system. Extension from the approximate 1-volt level is realized through ratio networks that most generally are built up from resistive elements. Those that can be more aptly classed as ratio standards contain a limited but adequate number of discrete ratios and are most often used in comparison circuits to assign values to working standards of somewhat lower accuracy class.

The ratio standard that for many years performed this function at NBS was a Silsbee design [1]. It featured a separate guarding network for the more critical sections, exhibited only small changes with self-heating, and admitted to a self- or step-up calibration process. The stability and the accuracy to which its ratios were known were of the order of 5 ppm of ratio. Some degradation in accuracy followed when using it in a comparison network to assign values to other types of ratio networks.

The need for an improved standard, with a more accurate assignment to its ratios has become evident. Voltage supplies of constant known output and digital voltmeters for monitoring voltage are approaching claimed accuracies of 10 or 20 ppm. These must be evaluated through ratio networks, leading ultimately

Manuscript received June 4, 1970.
The authors are with the Electricity Division, National Bureau of Standards, Washington, D. C.

to an assignment in terms of the national standard of EMF. Thus, ratios must be known with increasing accuracy at each higher echelon of measurement thereby placing stringent requirements on those ratio measurements at the national level.

To help provide the increased accuracies required in such a chain of measurements, the intent at NBS was to design a more versatile standard of improved stability and with ratios more closely equal to their nominal values, together with a measuring network and technique for assigning those values of ratios to an accuracy better than 0.5 ppm of the output (5×10^{-10} of the 1000-volt input).

During this study and prior to the final design described in this paper, several ratio networks were considered. One, which looked promising, was developed and examined as an experimental model DD-2 before it was rejected for practical reasons. Theoretically, the design admits errors only of second order but the problems encountered in its construction, operation, and in the assignment of its errors outweighed the advantage predicted by theory. However, the basic design, although not new, might be useful in some applications and provide high accuracy where a model of limited range or one with few ratios is desired. For this reason, a brief discussion is included in Appendix I.

Rejection of this design led to the one described that is simpler in construction, more versatile, and includes a redundancy of measurement feature. Study of an experimental model (DD-3) built in 1967 proved its feasibility and furnished the guidelines for its design for both dc and low-frequency ac operation. Further advantage was gained by providing the ratio standard with its own measuring network so that the combination would serve as a measurement system. This paper describes the measurement system, identified as model DD-4, and includes an analysis of the measured ratios that led to an estimate of 0.2 ppm for the uncertainty.

It is interesting to note that a similar basic design for a ratio standard was being explored simultaneously and independently by Ohlon [2].

Basic Circuits

The measurement system as regarded in this application includes two networks housed within the same enclosure. One is the ratio standard, the second is the main bridge array used to measure its ratios. Each is electrically separate from the other and either is available for use with external circuitry. The voltage supply, detector, and connecting leads are the only external accessories required. The system is shown schematically in Fig. 1 and its physical arrangement appears in Fig. 2.

Ratio Standard

The "working" branch of the ratio standard designed for 1000 Ω/V is indicated in the schematic circuit of Fig. 3. Carefully selected resistance elements are arranged singly or in combination to form 28 sections. Taking the first section as the reference with a nominal value of $R = 1$ kΩ, the remaining sections divide into three groups A, B, and C, each containing nine sections. Those of group A have a nominal value of 1 kΩ while those of groups B and C have nominal values of 10 kΩ and 100 kΩ, respectively.

In the series mode as shown, 27 ratios (referred to the first section) are available, extending over three decades to a maximum of 1000:1. The resistance of each section is nominally equal to either the resistance of the preceding section or to the summation of all preceding sections. As stated in [1], this satisfies the criterion by which such a network is judged to be self-calibrating. Thus, the bootstrap technique described in [1] is applicable and requires only the measurement and appropriate summations of small differences between nearly equal quantities.

In addition to the series mode, the nine sections comprising a given group are geometrically arranged for easy transfer to a parallel configuration [3]. Links, or their equivalent (indicated by dotted lines), from a to b and from c to d reduce group A to a parallel resistance of 1 kΩ, nominal; similarly, those bridging groups B and C reduce these groups to nominal values of 10 and 100 kΩ, respectively. Inclusion of the paralleling feature increases the number of available ratios with some convenient duplications, but more important, it makes possible an intended redundancy of measurement so that more accurately known ratios are assured.

The ratio standard also carries a "guard" chain of 200 Ω/V arranged and mode operated in similar fashion to that of the working branch. Operating in parallel with the working branch, its function is twofold: 1) it maintains the proper potentials on metal shields that surround the critical parts of the working branch and prevents the loss of current through the insulation, 2) it completes the shielding network of the measuring circuit and, through its accessible terminals, maintains the branches of this network at the proper potentials, so that leakage paths through insulation are diverted from the measuring circuit.

Measuring Circuit

The measuring network, although accessible for external use, is designed as an integral part of the system for the ready calibration of the ratio standard. With suitable connecting leads, it accomodates the ratio standard in either its parallel or series mode and can be used entirely or partially depending on the calibration method employed. The circuit as it would be used for either mode of the standard is indicated schematically in Fig. 4. Ratio arms A and B operate on the principle of the direct-reading ratio set (DRRS) [4]. Resistor B and resistor A, when at midscale setting, have nominal values of 1 kΩ, with A adjustable by 50 ppm on either side to a least count of 0.1 ppm. (Interpolation extends the resolution to 0.01 ppm.) Three resistance elements having nominal values of 1, 10, and 100 kΩ are separately

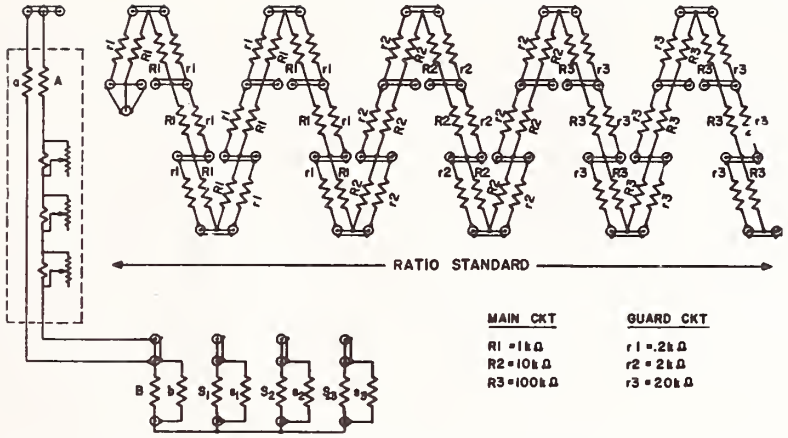

Fig. 1. Model DD-4 voltage ratio standard and measuring circuit.

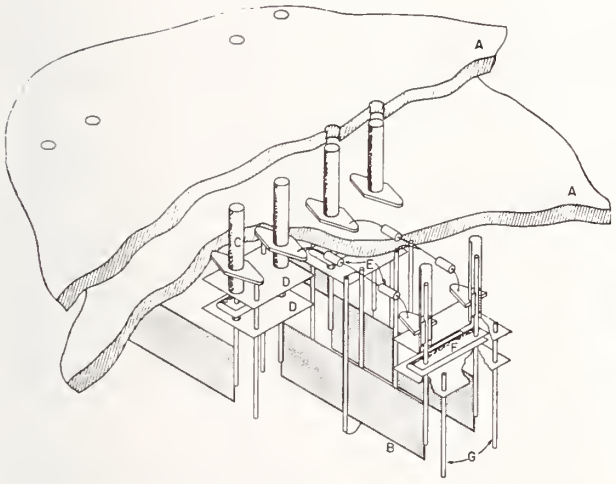

Fig. 2. Physical arrangement of DD-4. *A*—Plexiglass top pieces. *B*—Card-type resistor. *C*—Coaxial terminal. *D*—Brass guarding plates. *E*—Guard resistors. *F*—Folded Cu 4-terminal junction. *G*—Brass guarding rods.

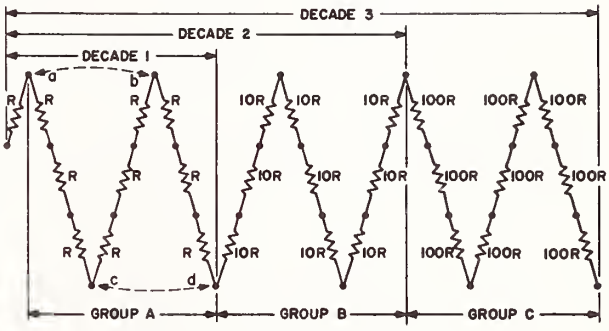

Fig. 3. "Working" branch of DD-4.

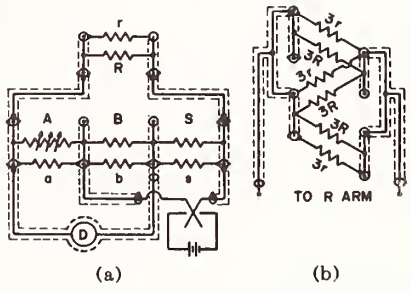

Fig. 4 (a) Simplified measuring circuit for a single section (b) for a series-parallel array.

available as *S*. The *R* arm is occupied in sequence by the sections of the standard whose differences are being determined. Since the bridge measures only small differences between nearly equal quantities, only moderate accuracy of measurement is required.

The guarding network is essentially a mirror image of the main bridge. With the shields maintained at proper potentials, leakage currents are directed from shield to shield and confined to the guarding network.

Design Parameters

Ratio Standard

The performance of this type of ratio standard is governed in great measure by the behavior and structure of the resistance elements that comprise the working branch. These were carefully selected to reduce the largest sources of error to manageable size.

Special effort was made to acquire elements with the lowest possible temperature coefficient. Measurements and proper selection assured a temperature coefficient less than 0.5 ppm/°C for the 1 and 10 kΩ elements. Thus, each section of groups *A* and *B* (Fig. 3) comprises a single element. A similar selection provided 100-kΩ elements with temperature coefficients not exceeding 1 ppm/°C. Allotting four elements to each section of group *C* and arranging them in a series-parallel network with some matching of positive and negative coefficients reduced the temperature coefficient per section to less than 0.5 ppm/°C.

A related and equally troublesome source of instability and uncertainty arises from temperature changes produced

in the elements when under load. This can be alleviated by designing for the lowest power consumption except that an upper limit is imposed on the value of resistance that can be chosen. Leakage currents and their control become paramount problems so that some compromise is required. The design for 1000 Ω/V offers a low operating current without placing too stringent demands on the guarding system, the sensitivity of detection, and the stability of the resistors. Further reduction of uncertainties associated with heat flow was assured by selecting single-layer card-type elements of Evanohm with each having a radiating area of 16 cm^2 per surface. Each element is suspended between its respective terminals with its two surfaces exposed to the coolant and removed sufficiently from neighboring elements to alleviate problems from proximity heating.

The nine elements comprising a given group were closely matched (adjusted if necessary) to satisfy the requirement that the proportional correction to the resistance of a group when in the parallel mode be identical to that when in the series mode within the accuracy sought.

The high accuracy and stability prescribed for this system dictated that complete guarding along the working resistance chain be provided. The departure of each guard section from its nominal value of resistance does not exceed 0.01 percent so that the guarding sleeves and the working terminals they enclose are essentially at the same potential. Thus, with guarding and high insulation resistance, errors caused by leakage currents are less by several orders than the accuracy prescribed for the measurement process. To prevent heat generated in the guard from influencing the working circuit, the guard chain is mounted in an upper channel external to the enclosure and open to the outside.

Measuring Circuit

The DRRS, although available to external circuits, was essentially tailored to the application at hand. The adjustable arm is a small and compact commercial unit with Waidner–Wolff circuitry and card-type resistance elements. The resistor that forms the B arm and those that occupy the S arm (Fig. 1) in sequence are also the card type having been selected by the same criteria and mounted in the same fashion as those of the ratio standard.

Additional Considerations

Terminal Junctions

Proper selection and arrangement of elements that satisfy design criteria neither guarantee that the values assigned to the ratios are conclusive nor that they are valid when the standard is used to calibrate other ratio networks. Unless other precautions are taken, values obtained by two or more independent methods of equal precision could differ by significant amounts with no assurance, which, if any, represents the value of the ratios as used in calibration. Thus, special attention was given to the design of the terminal junctions and provision was made so that effects from their interconnections and their connections to both internal and external measuring circuits could be predicted and verified experimentally.

An ideal junction is four terminals, designed and adjusted so that all four-terminal resistances are zero [5]. This is the preferred junction, since, if four-terminal techniques are used to measure a chain of nominally equal resistance elements, it defines each resistance precisely. Furthermore, through the use of compensating fans or their equivalent, it permits the parallel arrangement of these elements without introducing spurious resistances through the paralleling process. This subject has been covered quite thoroughly in the literature [6], particularly the use and analysis of compensating fans as proposed by Page [7]. If the ideal junction and compensating fans were applied to the circuitry discussed in this paper as indicated in Fig. 5, no discrepancies would exist between the identity of the measured ratios and those in use.

However, a study of the preliminary experimental model (DD-3) indicated that strict adherence to the geometry of the ideal junction (three terminals symmetrical to a fourth) was not necessary even though the measuring technique selected would not be strictly four terminal. For these and practical reasons, each junction is a small thin copper plate with its terminals located at the four corners of a square (see Fig. 2). The plug-type coaxial terminals are silver-plated brass with polytetrafluoroethylene (PTFE) insulation. The plug-socket resistance of a connection is approximately 450 $\mu\Omega$, and the contact resistance is repeatable to within ± 10 $\mu\Omega$.

The four-terminal resistances of each junction measured 5.5 ± 0.5 $\mu\Omega$ for both the direct and cross resistances. The maximum uncertainty from junction effects and from possible variations in lead and connector resistances was estimated at less than 0.05 ppm. Appendix II indicates how this estimate was approached. The results and their analysis in Appendix III indicate the experimental verification.

Detection System

The detection system consists of a photoelectric galvanometer amplifier (PGA) whose unbalance signal is further amplified and displayed by an electronic detector. To provide proper negative feedback for the PGA, a 500-ohm resistor is connected across its output terminals. The system is operated at a sensitivity of 30 nV/mm. The noise level is less than 40 nV peak-to-peak during the time period for a single measurement. By visually integrating the signal voltage over a time period of approximately 3 seconds, it is possible to detect 0.01-ppm changes in the bridge circuit at the 1-mA level.

The metal cases of the amplifier and electronic detector as well as the shields of all leads in the detection system are driven at the appropriate guard potential. Thus, the integrity of the insulation is maintained and effects

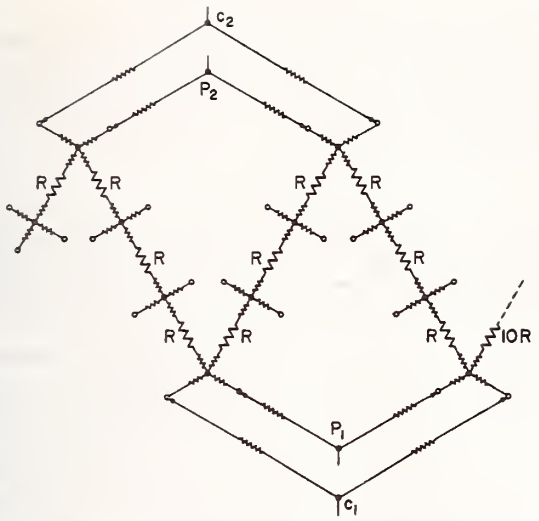

Fig. 5. The parallel mode of the ratio standard, emphasizing ideal junctions and their interconnections. The unlabeled resistance elements are lead and junction resistances.

caused by leakage are reduced to a negligible level. In addition, electrostatic interference is suppressed. The detection system is isolated from the 60-Hz power circuits to reduce noise problems.

During a measurement operation, the DRRS is adjusted while the bridge current is periodically reversed until a null condition results.

Controlled Enclosure

The ratio standard and the measuring network are immersed in a dry-air bath maintained at a temperature of 23 ± 0.05°C. Heat transfer occurs by forced convection using two fans that provide laminar flow across the resistance elements. The thermally lagged bath of approximately 0.1 meter^3 consists of two aluminum boxes separated by 2.5 cm of foam polystyrene and two plexiglass top pieces separated by a 2.5-cm air space.

The temperature control system consists of 1) a thermoelectric heat-pump assembly that extracts a constant amount of heat and 2) a proportional control circuit that regulates the power input of two (0–15 watts) heater elements. Twelve copper-constantan thermocouples strategically located within the bath monitor the temperature to within ±0.05°C.

A recently installed regenerative drying system holds the humidity constant at 4 percent relative humidity. A small amount of filtered and desiccant-dried air under pressure is continually forced into the bath while two small ports located at the opposite end of the bath serve as the exhaust.

Methods of Measurement

Four essentially independent methods were used during the period of evaluation and several lead assemblies were introduced for each method. Two of these were considered as the principal methods while the others served as occasional checks. The one identified as the bootstrap method is regarded as primary since values are obtained for each consecutive ratio. The other identified as series–parallel serves as the redundant method, providing additional values for the 10:1, 100:1, and 1000:1 ratios. Although both techniques utilize the built-in measuring circuit they are sufficiently different to be regarded as independent.

Bootstrap

The circuit of Fig. 4(a) shows the exact arrangement of leads and shielding as used in the bootstrap method with one section of the standard (e.g., the reference section), in the R arm. The 1-kΩ sections, beginning with the first or reference section, are introduced in the R arm in rapid succession and the bridge is balanced for a null on the detector. The balance equation for each k section is of the form

$$R_{1,k} = S_1[1 + D_{1,k} - D_0] \tag{1}$$

where S_1 has the same nominal value as $R_{1,k}$. The reading on the DRRS stated in proportional parts is $D_{1,k}$ while D_0 corresponds to the reading that would exist for an *exact* 1:1 ratio of $A:B$. (The derivation of (1) appears in [1].) The correction to each successive ratio through 10:1 is obtained by taking differences between each equation and the reference equation and averaging their successive sums. The summation $\sum_{k=1}^{k=10} R_{1,k}$ is the resistance of the first decade that is nominally equal to the resistance of each section in group B (Fig. 3). A comparable set of 10 balances is then made beginning with the first decade and continuing through the B group with S_1 changed to $S_2 = 10$ kΩ. A third set of similar balances carries the measurements through the 1000:1 ratio. Under rated conditions each measurement is made with 1 mA through each section. The general equation from which any ratio (referred to the first section) can be computed is

$$\frac{S_{m,k}}{R_{1,1}} = k10^{m-1}\left[1 + \frac{\left(\sum_{k=1}^{k=10} d_{1,k} \cdots + \sum_{k=1}^{k=10} d_{m-1,k}\right)}{10} + \sum_{k'=1}^{k'=k} \frac{d_{m,k'}}{k'}\right] \tag{2}$$

where $S_{m,k}$ is the sum of all resistances up to the kth tap of decade m, and $R_{1,1}$ is the reference section. Each term in the parenthesis is the sum of all the measured differences throughout a decade while the last term accounts for the measured differences up to the k section of interest. (The derivation of (2) is similar to the one appearing in [1].) Since $k10^{m-1}$ is the nominal ratio, (2) is of the form

$$N = N_n[1 + c]$$

where c is the correction to a ratio in proportional parts.

It is important to emphasize that a systematic error that might exist in each measurement is not cumulative within a decade since it, like the differences, partakes of the averaging process. Any accumulation occurs only when passing from one decade to another.

Series–Parallel

This method provides corrections to ratios 10:1, 100:1, and 1000:1 and requires six measurements in contrast to the 30 of the previous method. In each successive set of two measurements, each group (A, B, and C) is converted, in turn, into its parallel mode and compared against *all* the series-connected sections preceding it. Thus in the first set of two balances, the reference section occupies the R arm and is followed by group A connected in its parallel mode, as shown in Fig. 4(b). In the second set, with group A returned to its series connection, the first decade followed by group B in its parallel mode occupies the R arm. A similar sequence repeated once again carries the measurements through the 1000:1 ratio. For each successive set, S takes on the values 1, 10, and 100 kΩ. Three sets of differences and the average of their successive sums with the series–parallel principle applied yield values for the three ratios. The general equation for any ratio (referred to the first section) is

$$N_m = 10^m\left[1 + \frac{9}{10}\sum_{p=1}^{p=m} d_p\right]$$

where m is the number of the decade and

$$\sum_{p=1}^{p=m} d_p.$$

is the sum of the measured differences.

Two principal lead assemblies were used. In the one case the paralleling of groups was effected by using both current and potential fans. In the other only one pair of compensating fans was used. No difference in the results was noted so that the simpler arrangement was preferred. This is further indicated in Fig. 9 of Appendix II where the connections for both the reference section and the parallel array are shown.

Additional Methods

The two "check" methods alluded to earlier are identified as the "interchange" and "Kelvin bridge" methods. In the former, only arms A and B of the internal bridge are used. The other two arms of the bridge are occupied in turn by two adjacent sections with each pair advancing by one section. Since decade (m) forms the first section of decade ($m + 1$) the process can be carried forward through the remaining sections. In this kind of measurement, D_0 must be determined by the usual interchange technique. The measuring process is similar to that of the bootstrap method in that a value is obtained for each ratio.

The second method, as the name implies, is a four-terminal measurement. The step-by-step procedure of the bootstrap method is followed but the sections are measured as four-terminal resistances using a Kelvin bridge. This method was used only for the 1-kΩ decade where effects from terminal junctions and lead arrangements would be greatest.

Results

An analysis of all dc data accumulated from December 1968 to November 1969 is contained in Appendix III. Data taken since the completion of the analysis and too late for inclusion continue to substantiate the conclusions as stated.

The dc data obtained by the two principal methods covered 50–60 *complete* sets of measurements for each of two applied voltages. (Additional complete or partial sets obtained on occasion from the two supplementary methods totalled 14). The initial study covering about six months was made at 50 percent rated voltage. When evidence indicated that the measuring system was sufficiently stable and that measurements probably could be made to better than the 0.5 ppm anticipated, the system was moved to a location where ambient influences could be better controlled. The concentrated study continued for 4 months with measurements made at the reduced voltage over a 2-month period followed by those at rated voltage.

Analysis of the data at rated voltage shows that for a 99 percent confidence interval no difference greater than 0.1 ppm exists between the two methods. This excellent agreement between two independent methods makes it very unlikely that a systematic error greater than 0.1 ppm has gone undetected.

Additional information is available from Fig. 11 where the results at rated voltage are plotted against elapsed time for the 10:1, 100:1, and 1000:1 ratios. Fig. 11(c) is interesting since it appears to indicate a difference approaching 0.3 ppm between the two methods. However, as shown in the appendix, about 0.2 ppm arises because the power level at which each section operated was appreciably different for the two methods. Hence, this portion of the observed difference simply reflects a difference in test conditions and can not be regarded as a systematic error that lies hidden in one method or the other. Furthermore, the load conditions on the sections at rated voltage for the bootstrap method are essentially the same as those that would exist when in use, so that this difference could be regarded as a systematic error only if the series–parallel method were used alone to assign values at so-called rated voltage. Adjustment of the values to account for the known change with load led to the assignment of 0.1 ppm as the systematic error through the 1000:1 ratio.

As justified in Appendix III, greater weight was accorded the values obtained at rated voltage. The stability of the system improved after its transfer to the inner room and the subsequent analysis indicated that the standard deviations at 50 percent rated voltage were reduced, the change being appreciable on the 1000:1

ratio, and were more consistent with those at rated voltage. Also toward the end of the measurement series at reduced voltage, when the values were scrutinized more closely, it became evident that humidity effects, though small, could no longer be considered negligible. These are discussed more fully in the appendix; however, they are evident in Fig. 11 where the changes in the drying agent are noted along the abscissa. Evidence indicates that much of the random behavior arises from this cause. Data accumulated after an improved humidity control was installed have produced no evidence to the contrary. There are two known mechanisms that could produce the humidity effects observed: 1) surface leakage across the resistance elements and 2) forces on the fine wire caused by dimensional instability of the wire insulation or mica former. Leakage across the insulation between the guard and working circuit appears negligible. An estimate of σ for the first decade where effects from humidity are least is 0.05 ppm. This includes not only the random error of the measurement process but also any random changes in the ratio standard over a period of about 2 months. Taking this value as applying also to the other decades (under dry conditions), an uncertainty is assigned at 0.2 ppm, based on a 3σ confidence limit for random errors with a 0.1-ppm estimate for the residual systematic error.

AC Characteristics

Several features were incorporated in the design of the ratio standard for operation at 100 Hz or below. These include:

1) the use of single-layer card-type resistors having small residual inductances and shunt capacitances;

2) the use of air as the heat-exchange fluid for the bath instead of oil or a similar fluid having a larger dielectric constant;

3) the design of junctions that could be guarded easily, along with the use of guarded connectors as the terminations of these junctions;

4) a low guard resistance (200 Ω/V) to minimize the effect of external shunt capacitances on the guard ratio and thus further reduce their effect on the main ratio [8];

5) the use of brass rods, connected to appropriate guard-circuit taps, at various points to suppress errors caused by capacitive currents from the resistors to their surroundings.

The ratio standard was calibrated at 100 Hz by the substitution method using an inductive voltage divider. The output of an auxiliary inductive voltage divider connected to the common point of the guard-circuit resistors in the bridge provided for the phase adjustment. The calibration procedure is similar to that described previously in the bootstrap method. Results of these tests compared to the dc values agree to 0.1 ppm for ratios 1:1–10:1, 0.2 ppm for ratios 10:1–100:1, and 2.5 ppm for ratios 100:1–1000:1. The good agreement of the lower ratios further substantiates the accuracy of the dc values. The larger disagreement of the 100-kΩ sections is due probably to the uncompensated residual shunt capacitances and to significant dielectric absorption of the mica winding form of the resistors. The above ac data are only preliminary and further study is planned.

Summary

A stable voltage-ratio standard with extremely small errors and the networks for measuring its dc ratios to an accuracy of 0.2 ppm were described. Preliminary study of the standard at 100 Hz indicates a comparable performance can be expected at low ac frequencies. Investigation of the ac performance will continue. This development can lead to a more accurate assignment of ratios and relatively large dc voltages throughout the entire chain of measurements.

Appendix I

In the experimental model DD-2, a "base" element, which provides a reference ratio, contains two sets of n nominally equal resistors connected in series [9]. Each set is arranged so that its n resistors can be connected either in series or parallel. Two ratios are possible. A ratio $N_1 \approx 1 + n^2(1 + \alpha_s - \beta_p)$ is obtained by connecting the α set in its series mode and the β set in its parallel mode. A second ratio $N_2 \approx 1 + n^2(1 + \beta_s - \alpha_p)$ is formed when each set is reconnected for its alternate mode and the two are interchanged in position. (The α and β terms are small corrections to the resistance of the respective sets as they occupy the series or parallel position.) If the series–parallel principle is satisfied $\alpha_s = \alpha_p$ and $\beta_p = \beta_s$ and the mean ratio $N \approx 1 + n^2$. Thus a reference ratio is provided that, theoretically and to first order, is a function only of the number of elements. Extension of the principle to higher ratios is effected by adding sections whose resistances could be adjusted to the mean value of the base element.

Appendix II

This section outlines the procedure that was used to predict from circuit considerations the uncertainty introduced in a measurement of the combined effects from 1) the finite resistance of the four-terminal junction, 2) the changes in connections when transferring from a series to a parallel mode, and 3) the variations in lead and contact resistance as each section is introduced into the bridge. Since the uncertainties would be greatest for the lowest valued sections, only the first decade was considered.

Three circuits must be examined. Two of these duplicate the networks associated with the two principal methods of measurement while the other identifies the standard as its ratios appear in use. It is necessary that the ratios measured be identical to those in use or that a correction be applied to compensate for the discrepancy.

A four-terminal junction that departs from the ideal configuration has the equivalent circuit of Fig. 6 [6]. As applied to the junctions of the DD-4, the six resistances are calculable from the plug resistance of the connectors,

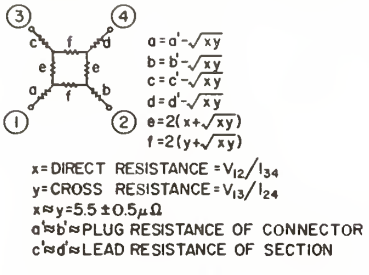

Fig. 6. Equivalent circuit of a four-terminal junction.

the lead resistance of the sections and the readily measureable direct and cross resistances X and $Y (X \approx Y = 5.5 \pm 0.5\ \mu\Omega)$. Fig. 7(a) identifies the circuit of DD-4 when it is *used* in the NBS ratio comparator to measure an unknown ratio. (The 10:1 ratio is indicated in the figure.)

Making the appropriate Δ-Y transformations reduces the circuit to that of Fig. 7(b). The ratio in use

$$N_u = \frac{\sum_{k=1}^{k=n} R_k}{R_1} = N_u[1 + c_n]$$

where $R_k = R_k' + Y_k + d_k' + c_{k+1}'$.

The problem now reduces to a similar examination of the two measuring networks to determine the extent to which the measured ratios differ from those in use.

The measuring network for the bootstrap method is indicated in Fig. 8(a) and simplified in (b), where g_k(or h_{k+1}) is the sum of the socket and contact resistances and l_k(or m_{k+1}) is the lead resistance.

Applying the latter network to each successive measurement through the decade gives a defining equation of the form

$$\frac{\left[\sum_{k=1}^{k=n} R_k\right]_{\text{bootstrap}}}{R_1} = n\left[1 + \sum_{k=1}^{k=n} d_k/n - \sum_{k=1}^{k=n} \frac{(\epsilon_{1k} + \epsilon_{2k} + \epsilon_{3k})}{n}\right]$$

where

$$\epsilon_{1k} = [(X_k - X_1) + (X_{k+1} - X_2)]1/R_1$$

$$\epsilon_{2k} = [(a_k' - a_1') + (a_2' - a_{k+1}') + (g_k - g_1) + (h_2 - h_{k+1})]1/R_1$$

$$\epsilon_{3k} = [(l_k - l_1) + (m_2 - m_{k+1})]1/R_1$$

and

$$\frac{\sum_{k=1}^{k=n} d_k}{n} = c_n.$$

From an experimental study of the junctions, connectors, and connecting leads, it is unlikely that the sum of the

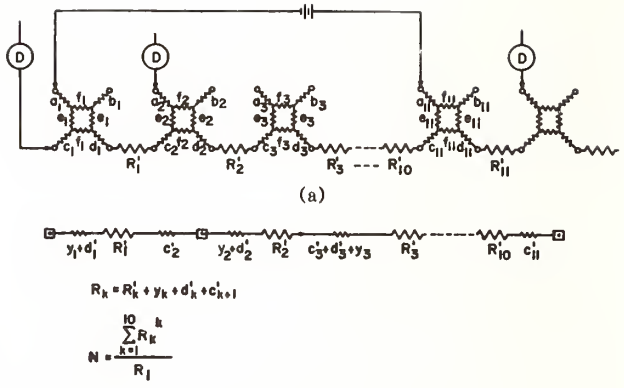

Fig. 7. Circuit of DD-4 (a) and its equivalent (b) when in *use*.

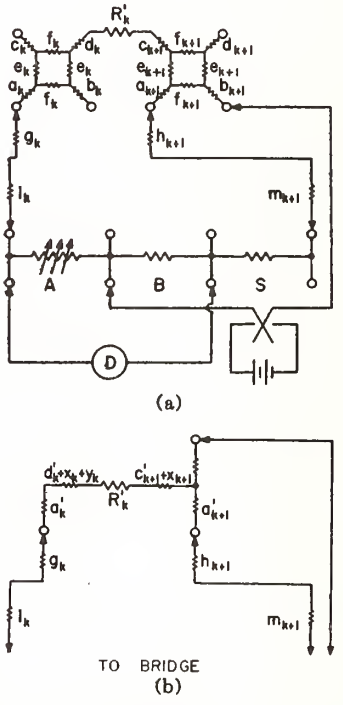

Fig. 8. Circuit and its equivalent for DD-4 when measured by bootstrap method.

ϵ terms would exceed 0.03 ppm. It appears that the ratio measured and the ratio when used are identical to well within the accuracy assigned.

The circuits for the series-parallel method are shown in Fig. 9 and refer to the connections when the reference section and the parallel array of the first decade occupy the R arm.

All resistances are identified as before except for two pairs of compensating resistors (u_1—u_2) and (v_1—v_2). Resistors u_1 and v_1 are adjusted to bring points p_1 and p_2 to the same potential. Resistors u_2 and v_2 are adjusted to bring points p_3 and p_4 to the same potential. Since the u leads, in contrast to the v leads, carry current to or from *two* branches, their resistances are half those

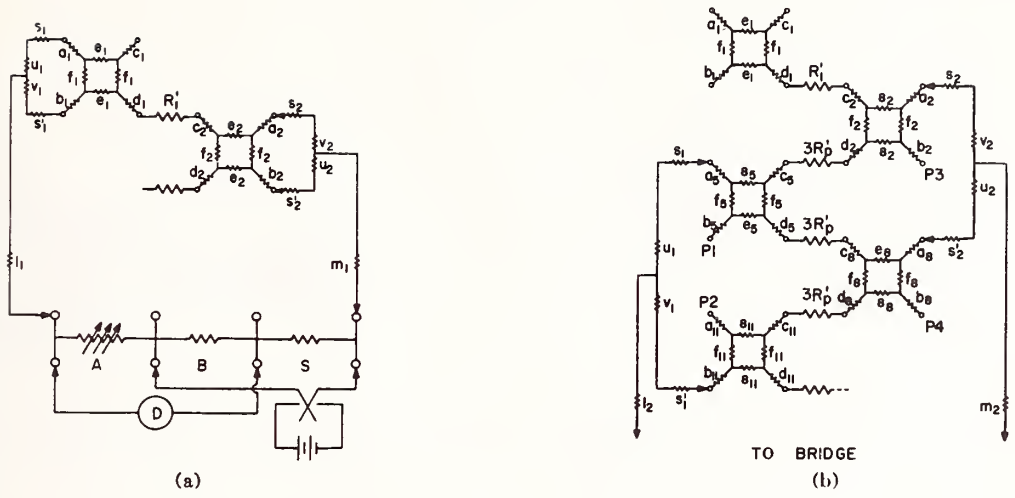

(a) (b)

Fig. 9. Circuits for DD-4 when measured by series–parallel method.

of the v leads. The corresponding simplified circuits are shown in Fig. 10.

The balance equation when the first section occupies the R arm is

$$S[1 + D_1 - D_0] = R_1\left[1 + \frac{1}{R_1}\left(l_2 + m_2 + X_2 + \frac{\alpha_1\beta_1}{\alpha_1 + \beta_1} + \frac{\alpha_2\beta_2}{\alpha_2 + \beta_2}\right)\right]$$

where R_1 is that portion of the section that is identical to the section when in use and the $\alpha\beta$ terms are the resistances of the parallel arrays at the two ends. The balance equation when the parallel group occupies the R arm is

$$S[1 + D_p - D_0] = R_p\left[1 + \frac{1}{R_p}\left(l_2' + m_2' + \frac{X_{11}}{9} + \frac{\alpha_1'\beta_1'}{\alpha_1' + \beta_1'} + \frac{\alpha_2'\beta_2'}{\alpha_2' + \beta_2'}\right)\right]$$

From these two equations and making the parallel-to-series conversion, the defining equation for the 10:1 ratio is

$$\frac{\left[\sum_{k=1}^{k=10} R_k\right]_{S-P}}{R_1} = 10\left[1 + \frac{9}{10}\,d_p + \frac{9}{10}\,(\epsilon_1' + \epsilon_2' + \epsilon_3')\right]$$

where

$$\epsilon_1' = (X_{11} - 9X_2)1/9R_1$$

$$\epsilon_2' = [(l_2' - l_2) + (m_2' - m_2)]1/R_1$$

$$\epsilon_3' = \left[\left(\frac{\alpha_1'\beta_1'}{\alpha_1' + \beta_1'} - \frac{\alpha_1\beta_1}{\alpha_1 + \beta_1}\right) + \left(\frac{\alpha_2'\beta_2'}{\alpha_2' + \beta_2'} - \frac{\alpha_2\beta_2}{\alpha_2 + \beta_2}\right)\right]1/R_1$$

and

$$\frac{9}{10}\,d_p = c_{10}.$$

The sum of the ϵ' terms is calculated to be about 0.02 ppm. From this value and that given for the ϵ term of the bootstrap method a difference no greater than 0.05 ppm would be expected between the two methods. This is in good agreement with the value of 0.02 ppm deduced from experiment for the 10:1 ratio.

Appendix III

The *principal* argument of the analysis deals with the results obtained for the 10:1, 100:1, and 1000:1 ratios by the bootstrap and series–parallel methods, since these were more apt to disclose junction and connection uncertainties as well as uncertainties arising from environmental influences. Results for the intermediate ratios that are available only from the bootstrap method provide additional information. The supplementary methods further substantiate the argument.

Data from the first series of measurements obtained at 50 percent rated voltage for each of the three ratios are analyzed separately from those of similar sets obtained subsequently at rated voltage. The principal argument covers data obtained after the system was relocated in a room environment that was more easily controlled. This required the deletion of only three pairs of measurements for each ratio.

All results are stated as *corrections* to the nominal ratios in ppm.

Range

To first provide a feel for the data and the magnitudes involved, *all* data, irrespective of elapsed time, method, or innovation were plotted as histograms (not included) for each of the ratios at the two voltages. The values at *rated voltage* for each ratio approximate a normal distribution and the same is true for the values at reduced voltage when a few of the initial and relatively extreme outliers are deleted. Under this condition, the average

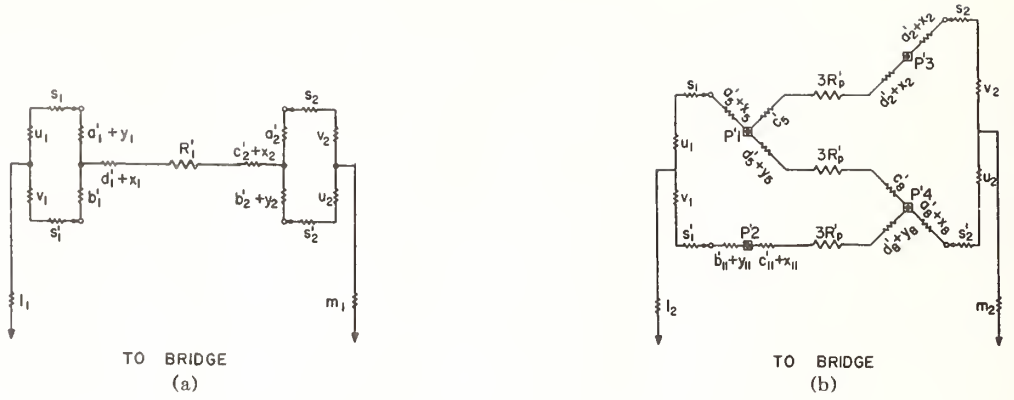

Fig. 10. Equivalent circuits for DD-4 when measured by series–parallel method. In text,

$\alpha_1 = u_1 + s_1 + a_1' + Y_1$ $\quad \beta_1 = v_1 + s_1' + b_1'$

$\alpha_2 = v_2 + s_2 + a_2'$ $\quad \beta_2 = u_2 + s_2' + b_2' + Y_2$

$\alpha_1' = u_1 + s_1 + a_5' + X_5$ $\quad \beta_1' = v_1 + s_1' + b_{11}' + Y_{11}$

$\alpha_2' = v_2 + s_2 + a_2' + Y_2$ $\quad \beta_2' = u_2 + s_2' + a_8' + X_8.$

TABLE I
RANGES FOR ALL MEASURED VALUES AND THEIR AVERAGES (PPM)

Ratio	Percent Rated Voltage	n	Correction Average (ppm)	Range (ppm) Maximum	Minimum
10:1	50	57	−0.072	+0.13	−0.30
	100	59	+0.199	+0.28	+0.08
100:1	50	46	+0.528	+0.96	0.00
	100	59	+1.012	+1.26	+0.56
1000:1	50	43	+1.432	+1.89	+0.84
	100	53	+1.456	+1.73	+1.14

TABLE II*

Ratio	Percent Rated Voltage	n	$\bar{d}$	s_d	Confidence Interval Estimates
10:1	50	13	+0.042	0.089	−0.033 → +0.117
	100	28	−0.008	0.033	−0.025 → +0.009
100:1	50	13	+0.101	0.082	+0.031 → +0.171
	100	28	−0.047	0.036	−0.066 → −0.028
1000:1	50	13	+0.056	0.211	−0.123 → +0.235
	100	28	−0.250	0.044	−0.273 → −0.227

* The 99 percent confidence interval estimates of the average difference between the two principal methods with the averages and the standard deviations of the differences included.

and range have the values given in Table 1, where n specifies the number of measurements. Inclusion of the outliers increases each range at reduced voltage by about 1 ppm. The corresponding effect on the averages is no greater than 0.2 ppm.

t Test

This portion of the analysis is an examination for any difference between the two principal methods. A sufficient number (n) of measurement pairs extending over the 4-month period were available for which a value by the one method was obtained within 1 hour of the other. The 99 percent confidence interval estimates of the average difference between the methods are given in Table II along with the averages $\bar{d}$ and the standard deviations s_d of the differences. The difference was taken as the bootstrap value less the series–parallel value.

The following facts and *apparent* inconsistencies are to be noted.

1) There is strong evidence at *rated* voltage of a negative difference between the methods that is essentially negligible for the 10:1 ratio but which increases to almost 0.3 ppm for the 1000:1 ratio, i.e., for the 100:1 and 1000:1 ratios, the limits $[\bar{d} - (ts_d/\sqrt{n})] < 0 < [\bar{d} + (ts_d/\sqrt{n})]$ are not satisfied.

2) A consistent set of limits is lacking at 50 percent rated voltage, and the intervals are wider.

3) The standard deviations at rated voltage are essentially equal and small in magnitude but exhibit perhaps a slight upward trend with increase in ratio.

4) The corresponding standard deviations at reduced voltage are inhomogeneous in magnitude with s_d at the 1000:1 ratio being unduly large. The set lacks the self-consistency feature exhibited by that at rated voltage.

The data and associated test conditions warranted further examination.

Data at Rated Voltage

Further examination of the data and the graphs of Fig. 11 indicates that $\bar{d}$ and the confidence interval for the 1000:1 ratio at rated voltage are more negative than would be expected. Several known factors could account for the apparent difference between methods, but these are equally applicable at the lower ratios and at reduced

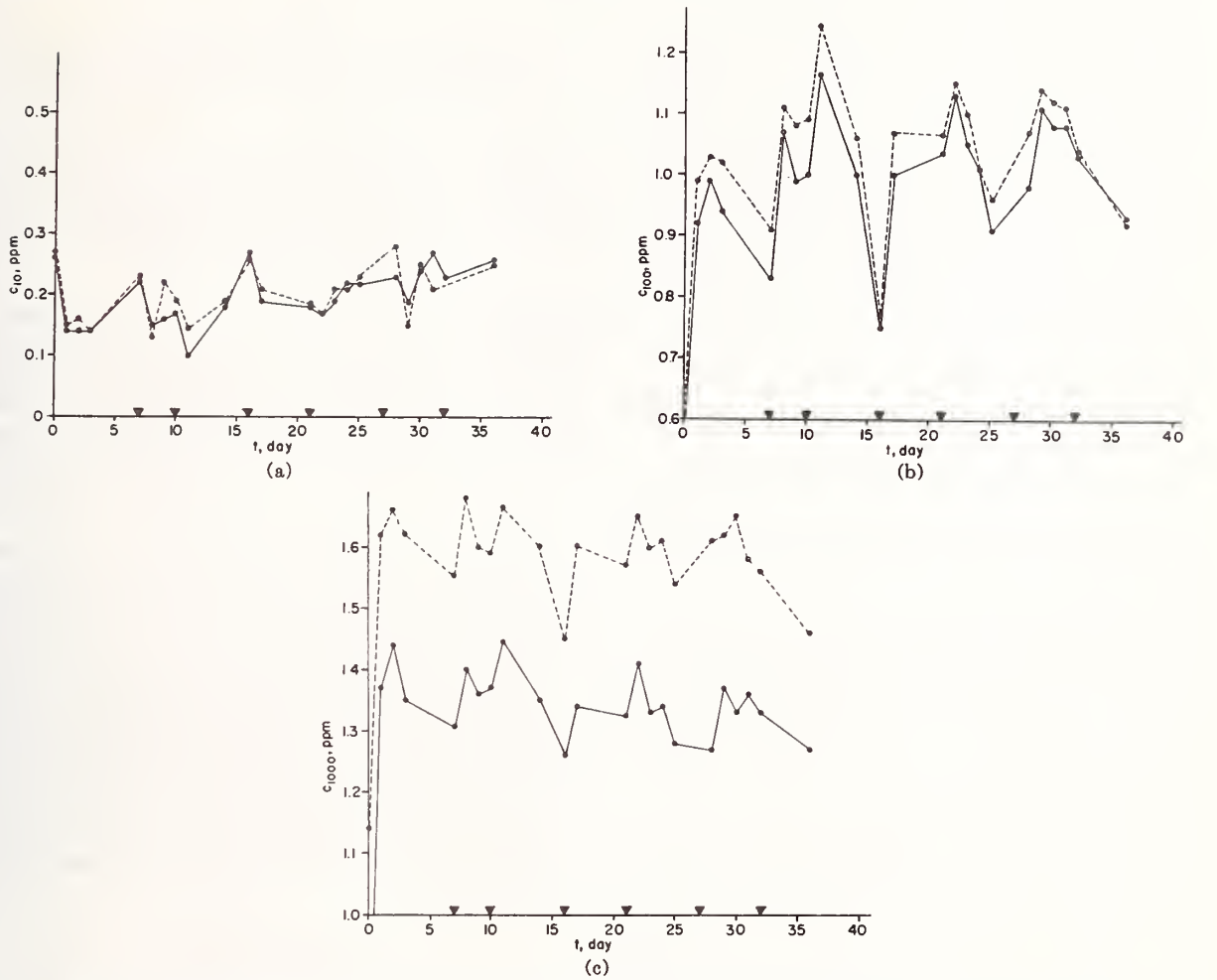

Fig. 11. Corrections to the ratios at rated voltage in ppm versus elapsed time. Solid line indicates bootstrap method; dashed line indicates series–parallel; arrows indicate desiccant was changed after the given measurement. (a) 10:1 ratio. (b) 100:1 ratio. (c) 1000:1 ratio.

voltage, with one notable exception. The power dissipated in the resistance elements in the bootstrap technique is nine times that in the series–parallel, and any contribution to the difference from this source would be magnified at the higher voltage.

The temperature coefficient of ratio is negative for all ratios and attains, with the bootstrap technique, a maximum of −0.6 ppm/°C for the 1000:1 ratio. Consideration of the power per centimeter squared of radiating surface with the resistive elements in contact with the circulating air leads to an estimated temperature rise at the surface of about 0.3°C at rated voltage. This would account for an equivalent change in the 1000:1 ratio of about −0.17 ppm. It is reasonable to assume a negligible heating effect for the parallel mode. With this assumption, it would be expected that values by the bootstrap method for the 1000:1 ratio would be more negative by the above amount than those by the series–parallel method.

If the bootstrap values are adjusted upwards (or series–parallel downwards) to eliminate the difference arising from heating effects, the confidence interval becomes (−0.103 → −0.057) in contrast to (−0.273 → −0.227) given in the table. A similar treatment of the data for the 100:1 ratio reduces the limiting values given in the table by about 0.010. Thus, the evidence supplied by the data at *rated* voltage would indicate a real difference approaching 0.1 ppm between the two methods.

Data at Reduced Voltage

An equivalent concinnity among the data at reduced voltage would be expected unless spurious influences, not present to the same extent at rated voltage, were affecting the measurement. Two obvious factors must be considered—an inherent instability in the ratio standard and effects from humidity. Since the series of measurements at reduced voltage preceded those at rated voltage, either or both might exist. However, since the two series were immediately consecutive, an inherent instability in the standard appears a less likely cause.

Furthermore, with self-heating greatly reduced, changes in the resistance of the elements would be reflected in both methods unless the instability were of an unusual nature, e.g., a steady but rapid drift. No evidence of this behavior existed. It is more logical to suppose that a humidity not under careful control would be the more likely cause for the discrepancies in Table II, since its effect on the response of resistive networks is difficult to predict. This conclusion is reached in the next section.

Table III completes the present argument and introduces the section that follows. It includes the standard deviations s_b and s_p for the bootstrap and series–parallel methods, respectively, and the ratios of their squares F. The values at rated voltage are included for comparison.

There is no evidence from the F values that the precision differs for the two methods at either applied voltage. As indicated later, it is probable that the poorer agreement between the standard deviation pairs s_b and s_p at reduced voltage arises from insidious humidity effects.

TABLE III
INDIVIDUAL STANDARD DEVIATIONS FOR THE TWO PRINCIPAL METHODS AND THE RATIO OF THE VARIANCES SQUARED

	50 Percent Rated Voltage				Rated Voltage			
Ratio	n	s_b	s_p	F	n	s_b	s_p	F
10:1	13	0.093	0.062	2.25	28	0.048	0.045	1.15
100:1	13	0.151	0.123	1.51	28	0.134	0.134	1.00
1000:1	13	0.100	0.165	0.37	28	0.110	0.107	1.05

Humidity Influence

No attempt was made to control the humidity within the enclosure during the measurement series at reduced voltage. The small effects from this parameter were given attention during the measurement series at rated voltage when it appeared that an accuracy of 0.2 ppm or better was achievable.

During the latter period, changes were effected in the humidity condition by replenishing a drying agent at suitable intervals. These changes are entered in Fig. 11 where the arrows along the abscissa indicate that the drying agent was replaced after the corresponding reading on the ordinate. The humidity effect is evident in all cases, and no trend with elapsed time of any significance is apparent. Changes in ratio following replacement of the desiccant are in the same direction for the two methods and agree to 0.1 ppm or better.

An examination of values obtained for *all* nominal ratios by the bootstrap method disclose with one exception the following behavior.

1) On the $X1$ range, corrections for all ratios go more negative with a maximum at 0.2 ppm.

2) On the $X10$ and $X100$ ranges, corrections for all ratios go more positive with maximum at 0.3 and 0.2 ppm, respectively.

3) As to the exception and for no apparent reason, the signs of the changes are reversed to those given in 1) and 2).

In contrast to Fig. 11, similar curves for the data at reduced voltage (omitted from the paper) exhibit downward trends for the two highest ratios. The maximum apparent drift amounts to about 0.3 ppm for the series–parallel method on the 1000:1 ratio and about 0.2 ppm for all others. Furthermore, the effects from the first recorded change in the drying agent, made near the end of the series, are appreciable. The changes in values for the respective methods differ by 0.2 ppm but have a maxima of 0.6 and 0.4 ppm for the 100:1 and 1000:1 ratios.

Omission of the data at reduced voltage in assigning an uncertainty of measurement is based on the facts and argument presented. These indicate that the measurement process was not under statistical control during operation at reduced voltage.

On the basis that the relative humidity is now closely controlled, the standard deviation σ is taken as the average of s_p and s_b as given for the 10:1 ratio. The uncertainty of measurement is then estimated at 0.2 ppm, based on the 3σ confidence limit for random errors, and 0.1 ppm for the systematic error. Occasional values obtained by the two "check" methods substantiate the above conclusion.

REFERENCES

[1] B. L. Dunfee, "Method for calibrating a standard volt box," *J. Res. Nat. Bur. Stand., Sec. C*, vol. 67, pp. 1–13, January–March 1962.
[2] R. Ohlon, "A new type of volt box," *Metrologia*, vol. 5, pp. 21–25, 1969.
[3] "Metrology catalog," Electro Scientific Industries, Inc., Portland, Ore., 1970–1971.
[4] F. K. Harris, *Electrical Measurements*. New York: Wiley, 1952, p. 272.
[5] F. Wenner, "Methods, apparatus and procedures for the comparison of precision standard resistors," *J. Res. Nat. Bur. Stand.*, vol. 25, pp. 279–285, August 1940.
[6] J. C. Riley, "The accuracy of series and parallel connections of four-terminal resistors," *1965 IEEE Internat. Conv. Rec.*, pt. 2, vol. 13, pp. 136–146.
[7] C. H. Page, "Errors in the series–parallel buildup of four-terminal resistors," *J. Res. Nat. Bur. Stand., Sec. C*, vol. 69, pp. 181–189, July–September 1965.
[8] F. B. Silsbee, "A shielded resistor for voltage transformer testing," *Sci. Papers Nat. Bur. Stand.*, vol. 20, pp. 489–514, December 1925.
[9] "AC calibration—A systems concept," Holt Instrument Laboratories, Oconto, Wis., March 1962.
[10] J. J. Hill, "Calibration of dc resistance standards and voltage-ratio boxes by an ac method," *Proc. Inst. Elec. Eng.*, (London) vol. 122, pp. 211–217, January 1965.

JOURNAL OF RESEARCH of the National Bureau of Standards—A. Physics and Chemistry
Vol. 65A, No. 3, May–June 1961

Evaluation of the NBS Unit of Resistance Based on a Computable Capacitor

Robert D. Cutkosky

(January 16, 1961)

An evaluation of the unit of resistance maintained at the National Bureau of Standards, based on the prototype standards of length and time, is described. The evaluation is based on a nominally one-picofarad capacitor whose value may be calculated from its mechanical dimensions to high accuracy. This capacitor is used to calibrate an 0.01-microfarad capacitor. A frequency-dependent bridge involving this capacitor establishes the value of a 10^4-ohm resistor. Comparison of that resistor with the bank of one-ohm resistors maintaining the NBS unit of resistance establishes that this unit is

$$\Omega_{BU} = 1.000002_3 \text{ ohms} \pm 2.1 \text{ ppm}.$$

The indicated uncertainty is an estimated 50 percent error of the reported value based on the statistical uncertainty of the measurements and allowing for known sources of possible systematic errors other than in the speed of light, assuming that the speed of light $c = 2.997925 \times 10^{10}$cm/sec.

1. Introduction

The United States national standard of resistance is maintained at the National Bureau of Standards by a group of 1-ohm manganin resistors. Values of resistance are assigned to the 1-ohm reference standards by techniques based ultimately upon the national prototype standards of length and time.

The most accurate methods which have been used for this purpose in the past made use of either self-inductors or mutual inductors whose inductances were computable from their mechanical dimensions. In principle, it is then straightforward to compare the impedance of the computable inductor at a known frequency with that of the 1-ohm reference standard resistors. In practice, this comparison is likely to involve several steps, and may not even make use of sinusoidal currents through the inductor.

An alternative method for assigning values to the reference resistors involves constructing a capacitor whose capacitance may be calculated from its mechanical dimensions. By comparing the impedance of the capacitor at a known frequency with that of the reference standard resistors one may establish the values of the reference resistors in terms of the prototype standards.

Within recent years the development of an improved computable capacitor [1, 2, 3, 4] [1] and improved methods for the precise comparison of capacitances [5, 6] have made the latter process appear to be the more fruitful.

The method involves stepping up from a 1-pf three-terminal computable capacitor to two 0.01-μf three-terminal capacitors. The step-up is made in four steps, using a transformer whose nominally 10:1 ratio may be accurately measured. The average admittance of the two 0.01-μf capacitors at an angular frequency of 10^4 radians per second is compared with the average admittance of two 10^4-ohm shielded a-c resistors using a bridge network to be described. These measurements serve to assign values to the 10^4-ohm a-c resistors in terms of the prototype standards.

A conventional d-c step-down from these 10^4-ohm a-c resistors to the 1-ohm NBS reference resistors provides an absolute calibration of the 1-ohm resistors. A small correction must be applied to the results so obtained because of the a-c–d-c differences of the 10^4-ohm resistors. This correction is determined by comparison with a special transfer resistor.

2. Computable Cross Capacitor

Computable capacitors of the traditional guard-ring or guard-cylinder design require, in general, the measurement of several dimensions. For example, with the guard-ring type, area, plate separation, flatness of electrodes, parallelism, and proper location of the guarded island are of major concern. Most of these dimensions have to be measured to a higher accuracy than the required overall accuracy of the computed capacitance.

The development by A. M. Thompson and D. G. Lampard of a device called by them a computable cross capacitor [1] has made possible the construction of a capacitor whose value may be computed from dimensional measurements with an accuracy considerably higher than that attainable with any previous design.

[1] Figures in brackets indicate the literature references at the end of this paper.

585402—61——2

A cross capacitor consists of a cylindrical arrangement of four electrodes, with cross section as shown in figure 1. Electrodes 1, 2, 3, and 4 are separated from each other by very small insulating gaps. Let C_1/L be the direct capacitance per unit length (perpendicular to the plane of the drawing) between electrodes 1 and 3 with electrodes 2 and 4 grounded, and let C_2/L be the direct capacitance per unit length between electrodes 2 and 4 with electrodes 1 and 3 grounded. It may be shown that in *cgs*, esu,

$$e^{-4\pi^2 C_1/L}+e^{-4\pi^2 C_2/L}=1, \text{ or in MKS units,}$$

$$\overline{C}=\frac{1}{2}(C_1+C_2)=\epsilon_o L(\ln 2/\pi)[1+0.087(\Delta C/\overline{C})^2]$$

$$+\mathcal{O}\{(\Delta C/\overline{C})^4\}] \text{ farads} \qquad (1)$$

where $\epsilon_o=1/\mu_o c^2$, c is the speed of light, and $\Delta C=C_2-C_1$. The notation "$\mathcal{O}$" means that all remaining terms in eq (1) are fourth order or higher in $\Delta C/\overline{C}$, and their sum approaches zero as $K(\Delta C/\overline{C})^4$ as $\Delta C/\overline{C}$ tends to zero. This relationship allows $\overline{C}$ to be calaculated from a single measured length L. One finds that if $C_1 \approx C_2$, then $\overline{C}/L \approx 2$ pf/meter $\approx$ 0.05 pf/in.

The requirements that both $\overline{C}$ and L be easily measurable have led to the use at NBS of two cross capacitors in parallel, each about 10 in. long, to produce a capacitance of about 1pf [6]. Figure 2 shows the cross section of the NBS 1-pf computable cross capacitor, which is housed in an evacuated chamber. Electrodes 1, 2, 5, and 6; and electrodes 2, 3, 6, and 7 of the two cross capacitors are steel bars ⅞ in. in diameter supported with accurately ground glass slips and disks, shown dotted in the figure, resting on a precision granite surface plate. The bottom row of bars is held together with a phosphor-bronze coil spring between bars 4 and 8 at each end of the assembly. The glass spacers are all located within guard sections at the ends of the capacitor, so that no solid dielectric appears between the bars within the active length of the capacitor. Figure 3 shows a side view of electrode 6, which is similar to electrode 2. The assembly is constructed of precision gage blocks having circular cross sections, with wrung joints between the 10-in. bar and its adjacent 2-in. bars, and insulated with firmly cemented 0.002-in. mica spacers between each pair of 2-in. bars. The outer 2-in. bars constitute the guard sections, and are grounded. The composite 14-in. central section defines the length of the cross capacitor, and extends roughly between the centers of each insulated gap. Electrodes 1, 3, 5, and 7 are approximately 18 in. long, and so extend well beyond the active sections of bars 2 and 6.

Additional shields not shown in figure 2 eliminate capacitive coupling between electrodes around the outside of the grounded electrodes. This is essential, since (1) deals only with the capacitance associated with the region in the interior of the electrode system.

One capacitance measurement is made, with electrodes 1, 3, and 6 grounded, of the direct capacitance between electrodes 5 and 7 in parallel and the central section of electrode 2. Another measurement is made, with electrodes 5, 7, and 2 grounded, of the capacitance between electrodes 1 and 3 in parallel and the central section of electrode 6. If we neglect, for the moment, the small second order correction $0.087(\Delta C/\overline{C})^2$ in eq 1, the average of these two capacitances is equal to $2\times\epsilon_o L'\ln 2/'\pi$; where L' is the average length of the two central sections of electrodes 2 and 6, or approximately 14 in. If the 10-in. gage blocks are removed from electrodes 2 and 6 and the 2-in. bars on either end are wrung directly together, a new cross capacitor is formed with a length differing

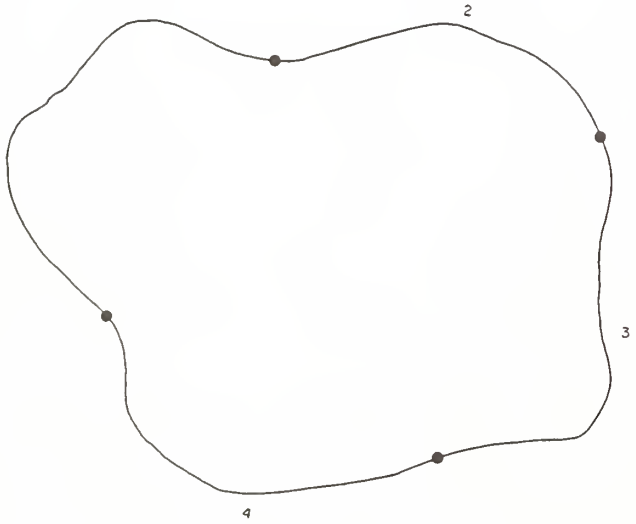

FIGURE 1. *Cross section of a general cross capacitor.*

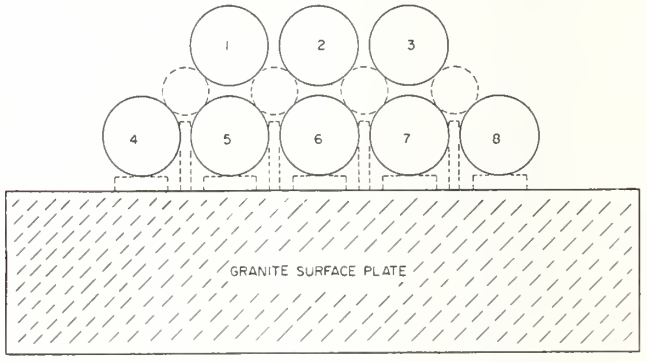

FIGURE 2. *Cross section of the NBS cross capacitor.*

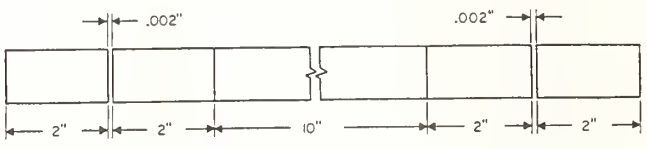

FIGURE 3. *Side view of the NBS cross capacitor detector electrodes.*

from the first by twice the average length of the 10-in. bars, or about 20 in. The difference between the two cross capacitances so measured is not affected by irregularities or lack of perfect centering of the bars near the insulated gap, provided that the end sections are not rotated or otherwise disturbed when the 10-in. bars are removed or replaced.

The small discontinuities caused by the slightly-rounded ends of the gage blocks produce only second-order errors in the capacitance computed from eq (1). These errors have been investigated experimentally by introducing additional discontinuities on the bars.

Between May 12 and May 18, 1960, and again between July 21 and July 27, 1960, two series of measurements with the NBS computable cross capacitors were made to establish the value of a fixed, 1-pf, air-dielectric, three-terminal, reference capacitor; NBS 89790–B. This capacitor was maintained in an oil bath at a constant temperature near 25 °C.

A transformer ratio-arm bridge was used for this purpose with the circuit shown in figure 4. The cross capacitor with the 10-in. bars in place has a capacitance slightly under 1.4 pf so that the bridge may be balanced with a small adjustable capacitance p as shown, and a small adjustable conductance not shown, which may be placed on either side of the bridge. The bridge components have been described in detail elsewhere [6] and will not be elaborated upon here.

The bridge circuit for the measurement with the 10-in. bars removed is similar to figure 4 except that the cross capacitance is now about 0.4 pf, so the 1-pf capacitor in the lower portion of the circuit must be removed. The 4-pf capacitor consists of 4 one-pf capacitors which may each be compared directly with the 1-pf standard, and then connected in parallel. Since the adjustable capacitor has a relatively high reading, it is also necessary to calibrate it for each measurement.

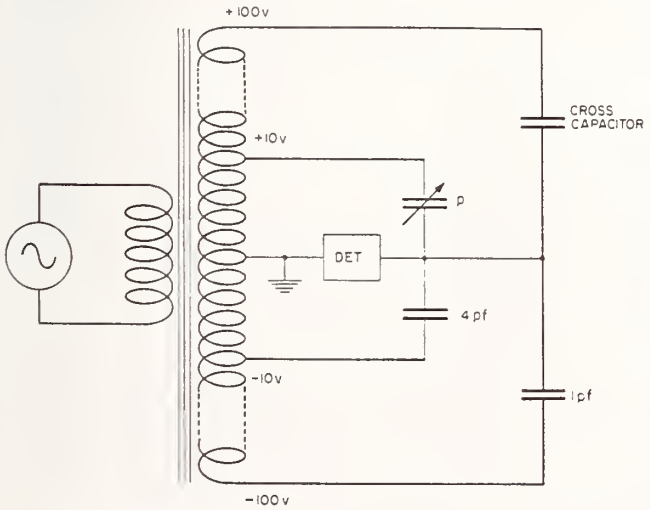

FIGURE 4. *Inductively coupled ratio arm bridge used with the NBS cross capacitor.*

All of the above steps are straightforward and can be done in a symmetrical fashion (calibration, cross-capacitor measurement, and recalibration) in less than 30 min by an experienced operator.

Before and after the determination, the 1-pf capacitor used is compared with the 1-pf reference capacitor in the oil bath.

Although small direct (three-terminal) capacitances are much easier to measure than small two-terminal capacitances because of the virtual elimination of connection problems, a particularly troublesome source of error arises when capacitance to ground is very high, as is the case with the NBS cross capacitor. Figure 5 shows a three-terminal capacitor with direct capacitance C_1 connected to a bridge with leads of inductance L_1, L_2, and L_3. It may be shown that the effective capacitance seen by the bridge is given by

$$C_{eff} \approx C_1[1-\frac{\omega^2(C_2C_3)}{C_1}L_1+\omega^2C_3L_2+\omega^2C_2L_3+ \omega^2C_1(L_2+L_3)].$$

For C_1, C_2, and C_3 all less than 1000 pf, the important error, expressed as an additive term, is $-\omega^2L_1C_2C_3$; which is independent of C_1 and hence relatively more important for a very small C_1. Thompson [5] has shown that if the capacitor is treated as a four-terminal network as in figure 5 with a high perme-

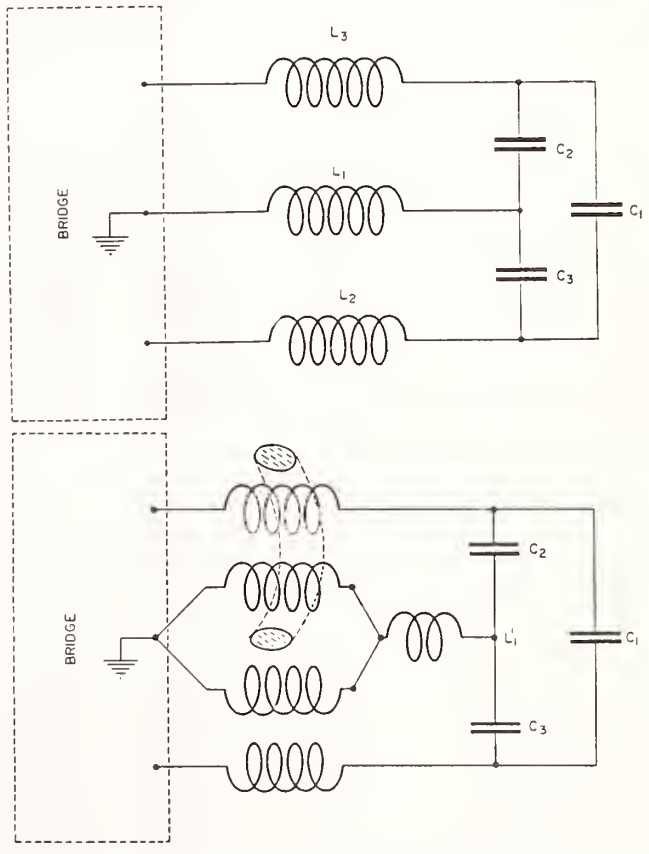

FIGURE 5. *Three-terminal capacitor C_1 connected to a bridge with three leads, with four leads and using a high permeability core (See text).*

ability core linking one ground lead with one active electrode lead, the troublesome error term is eliminated. This technique has been used throughout the measurements reported here. It is impossible with the NBS cross capacitor to completely eliminate all common ground lead inductance in this way, and a small inductance L_1' remains in the cross capacitor circuit. We have found it necessary to measure C_{eff} as a function of frequency and extrapolate to zero frequency under the assumption that the error is proportional to ω^2. With most of L_1 eliminated by the use of high permeability cores, the factor $\omega^2 L_1' C_2 C_3$ is very small, and the d-c value may be determined to high accuracy.

Table 1 shows the results of two complete series of measurements on the NBS computable cross capacitor, based on the assumption that the reference capacitor in the oil bath was exactly 1 pf.

The correction term in the measured capacitance $0.087(\Delta C/C)^2$ is less than two parts in 10^7 and has been neglected. The calculated cross capacitance also appears in table 1, based on the measured lengths of the 10-in. gage blocks, and taking the speed of light $c=2.997925\times10^{10}$ cm/sec as adopted recently by the IGGU and the URSI. Combining these figures we obtain true values for the reference capacitor at the time of measurement. The difference between the May and July figures reflects a shift in the temperature of the oil bath which occurred some time in June, and has no effect on the final results quoted in this paper. The stability of the reference capacitor and the closeness of temperature regulation during each of the determinations was sufficient to reduce any error arising from the variability of the reference capacitor considerably below 1 ppm.

TABLE 1. *Capacitance of cross capacitor*

Based on 1-pf reference capacitor #NBS 89790-B.

Time and date (1960)	Nominal length	Frequency	Measured capacitance	D-c capacitance
	in.	*c/s*	*pf*	*pf*
11:00 a.m. May 12.	14	1592	1.3898231	1.3898241
8:55 a.m. May 13	14	1592	1.3898224	1.3898234
9:40 a.m. May 13	14	1592	1.3898222	1.3898231
2:05 p.m. May 13	14	1000	1.3898229	1.3898233
2:50 p.m. May 13	14	1592	1.3898220	1.3898229
1:20 p.m. May 16	4	1592	0.3973528	0.3973532
2:00 p.m. May 16	4	1592	.3973531	.3973535
2:55 p.m. May 16	4	1000	.3973536	.3973538
10:45 a.m. May 18	14	1592	1.3898201	1.3898210
11:35 a.m. May 18	14	1000	1.3898211	1.3898215
12:20 p.m. May 18	14	1592	1.3898198	1.3898208

Measured cross capacitance difference=0.9924687 pf.
Computed cross capacitance difference=0.9924151 pf.
True value of reference capacitor=1-pf −54.0 ppm (May 1960).

Based on 1-pf reference capacitor #NBS 89790-B.

Time and date (1960)	Nominal length	Frequency	Measured capacitance	D-c capacitance
	in.	*c/s*	*pf*	*pf*
9:22 a.m. July 21	14	1592	1.3898177	1.3898187
10:15 a.m. July 21	14	1000	1.3898177	1.3898180
12:45 p.m. July 21	14	1000	1.3898171	1.3898175
1:15 p.m. July 21	14	1592	1.3898164	1.3898174
9:45 a.m. July 25	4	1592	0.3973511	0.3973515
11:20 a.m. July 25	4	1000	.3973511	.3973513
1:00 p.m. July 25	4	1000	.3973512	.3973514
1:43 p.m. July 25	4	1592	.3973507	.3973511
9:15 a.m. July 27	14	1592	1.3898154	1.3898164
10:05 a.m. July 27	14	1000	1.3898165	1.3898168
12:52 p.m. July 27	14	1000	1.3898155	1.3898169
1:15 p.m. July 27	14	1592	1.3898165	1.3898175

Measured cross capacitance difference=0.9924661.
Computed cross capacitance difference=0.9924151.
True value of reference capacitor=1-pf −51.4 ppm (July 1960).

3. Capacitance Step-Up

The bridge for comparing capacitive reactance with resistance, to be described in a later section, requires the use of two 0.01-μf capacitors. These capacitors must be calibrated in terms of the 1-pf reference capacitor. A transformer ratio-arm bridge with a nominally 10:1 ratio is used for this calibration in the circuit of figure 6.

The balance conditions are, to a sufficiently close approximation,

$$C_2=10\ C_1(1+\alpha)-p, \text{ and } g_2=10\ g_1-10\omega C_1\beta-q,$$

where p and q are small adjustable admittances for balancing the bridge. One may connect p and q to point "B" instead of "A" to change their apparent signs if this is needed to obtain a balance.

Shielding completely surrounds each of the capacitors in the circuit in such a way that the measurement compares the direct capacitances C_1 and C_2. This technique allows the direct capacitance of the 10-pf capacitor to be determined relative to the 1-pf reference capacitor. The 10-pf capacitor is in turn compared with a 100-pf capacitor, to reach after four such steps the 0.01-μf mica capacitors used in the resistance bridge. All of the step-up capacitors are located in a regulated oil bath. The 0.01-μf capacitors as well as the 1000-pf capacitor are sufficiently large to require correction for the equivalent series inductances of the transformer. The total inductance correction was found to be two parts in 10^7 for each 0.01-μf capacitor [6].

It was desired that the total uncertainty in the step-up be less than one part in 10^7, which requires that the transformer ratio $10(1+\alpha+j\beta)$ be known to

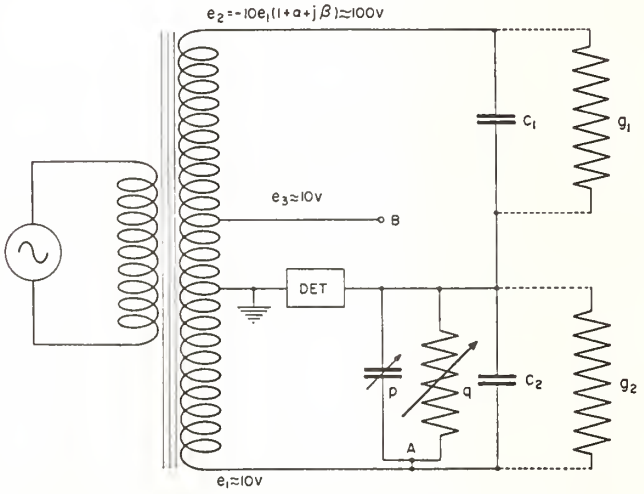

FIGURE 6. *Ten-to-one inductively-coupled ratio arm bridge for stepping up from 1 pf to 0.01 μf in four steps.*

an accuracy of about two parts in 10^8. A procedure for calibrating such a transformer to the required accuracy has been described [7] which involves the use of 11 nominally equal three-terminal capacitors having their detector electrodes connected together. Provision is made for switching any one of the capacitors to the high voltage side of the transformer while the other 10 are in parallel on the low voltage side. The bridge was balanced with a small admittance on one side or the other of the bridge with each of the 11 capacitors in turn on the high voltage transformer winding. After applying small corrections for lead impedances one obtains from this series of measurements values for α and β in the expression for the transformer ratio.

4. Resistance-Capacitance Bridge

Several bridges capable of being used for the comparison of resistance with capacitive reactance have been used in the past, one of the most popular being the Wien bridge. The Wien bridge, like many frequency dependent bridges, is difficult to shield against stray pickup. The difficulty comes from the fact that one arm of the bridge contains a resistor and a capacitor in series. If this arm is shielded, leakage currents from their common point to the shield produce errors which are difficult to evaluate with high accuracy.

4.1. Bridge Equations

In theory it is simple to compare resistance with capacitive reactance provided that one may obtain two a-c voltage sources exactly 90° out of phase and exactly equal in magnitude. Figure 7 shows two such sources used to compare a capacitance C with a conductance G. The balance condition is $G=\omega C$. The components may be readily shielded as shown with dotted lines; leakage paths to ground are either across the detector, which at balance has no voltage on it; or across one of the generators, which is assumed to have a very low impedance. Although it has not been possible to construct voltage sources with the required phase and magnitude relationships, accurate low impedance voltage sources equal in magnitude and 180° apart in phase are readily procurable from a center-tapped transformer.

A double bridge using the principles of figure 7 may be constructed with the circuit of figure 8, which shows all voltages referred to one generator as reference.[2] The voltages $+1$ and $-1(1+\alpha+j\beta)$ are approximately equal and 180° out of phase, with α and β representing magnitude and phase angle errors respectively. The voltage $j(1+z)$ is approximately 90° out of phase with each of the other generators. The small complex number z represents the departure of the generator from its nominal value.

Figure 8 also shows the residual leakage conductances g_1 and g_2 of the main capacitors C_1 and C_2, and the stray capacitances c_1 and c_2 of the main conductance standards G_1 and G_2.

[2] Bridge networks of this type were investigated at the National Standards Laboratory in Sidney, Australia, in 1952 but the findings were not published. The network described in this paper was subsequently developed independently.

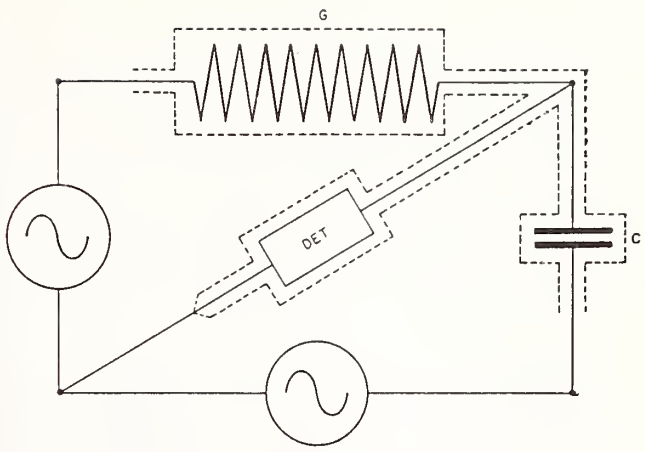

FIGURE 7. *Basic bridge for comparing conductance with capacitive susceptance.*

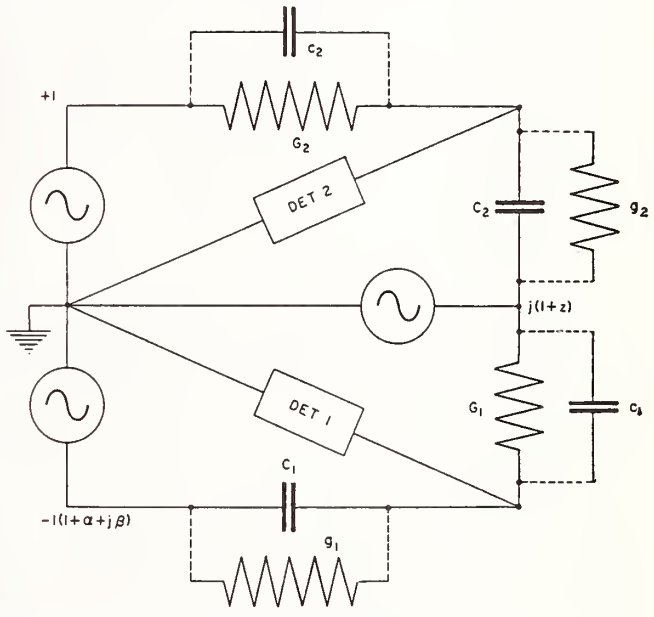

FIGURE 8. *Double bridge for comparing conductance with capacitive susceptance.*

This circuit is used with $C_1 \approx C_2 \approx 0.01$ μf, $G_1 \approx G_2 \approx 10^{-4}$ mhos, and $\omega \approx 10^4$ radians per second (about 1592 c/s).

With both bridges balanced we have the conditions

$$j\omega c_2+G_2=-j(1+z)(j\omega C_2+g_2)$$

and

$$(1+\alpha+j\beta)(j\omega C_1+g_1)=j(1+z)(j\omega c_1+G_1).$$

Eliminating z from these equations we have

$$(j\omega c_2+G_2)(j\omega c_1+G_1) = -(1+\alpha+j\beta)(j\omega C_2+g_2)(j\omega C_1+g_1).$$

Separating real and imaginary parts we find

$$G_1G_2=(1+\alpha)\omega^2C_1C_2+\beta(\omega C_1g_2 + \omega C_2g_1)-(1+\alpha)g_1g_2+\omega^2c_1c_2,$$

and

$$\omega[c_1G_2+c_2G_1]+(1+\alpha)\omega[C_1g_2+C_2g_1]=\beta\omega^2C_1C_2-\beta g_1g_2.$$

It may be shown that if all residual parameters are small, we may write approximately

$$\overline{G}=(1+\tfrac{1}{2}\alpha)\omega\overline{C} \tag{2}$$

and

$$\omega\overline{c}\overline{G}+\omega\overline{C}\overline{g}=\tfrac{1}{2}\beta\omega^2\overline{C}^2 \tag{3}$$

where bars over letters signify the average of the two values involved.

The voltage appearing at the terminals of detector 1 may be reduced to zero by making either C_1 or G_1 and either c_1 or g_1 adjustable, and similarly for detector 2. One finds that even if z is zero, either c_1 or g_1 and either c_2 or g_2 must be negative. As shown in figure 9, this is accomplished by connecting an adjustable conductance q_1 from point A to D_1 and an adjustable capacitance p_1 from point B to D_2. The main capacitors C_1 and C_2 consist of the 0.01-μf mica capacitors in parallel with adjustable capacitors having ranges of 1 pf. With these provisions eq (3) is replaced by

$$\omega\overline{c}\overline{G}+\omega\overline{C}\overline{g}-\tfrac{1}{2}(\omega p_1\overline{G}+\omega\overline{c}q_1)=\tfrac{1}{2}\beta\omega^2\overline{C}^2. \tag{4}$$

It is apparent from figure 9 and the above equations that C_2 is the effective capacitance including the correction resulting from self inductance between junctions C and D_2, and G_1 must include the series resistance correction between junctions C and D_1. If the open circuit transformer-ratio parameters α and β are used, C_1 and G_2 must include the effects of impedances ζ_1 and ζ_2, measured from junctions D_1 and D_2 respectively, through the transformer to the ground point G. To avoid the problems of accurately measuring the transformer impedances, we have found it profitable to measure the loaded rather than the open circuit transformer ratio between A and B to G while the bridge is balanced. Using the values so obtained for α' and β', the required values of G_2 and C_1 include impedances only to junctions A and B.

The loaded transformer ratio is easily measured with a third bridge involving C_3, C_4, and detector 3 on the left of figure 9. This bridge is balanced with the circuit as shown and rebalanced after interchanging C_3 and C_4. The readings of p_2 and q_2 are called p_2' and q_2' before interchanging, and p_2'' and q_2'' after interchanging. The transformer parameters α' and β' are calculated from the formulas

$$\alpha'=-\frac{p_2'+p_2''}{C_3+C_4} \text{ and } \beta'=\frac{q_2'+q_2''}{\omega(C_3+C_4)}.$$

The signs of p_2 and q_2 are positive if connected to B as shown, and negative if connected to A. It is found that for this bridge, with the loading shown in figure 9, $\alpha'\approx+17\times10^{-6}$ and $\beta'\approx-16\times10^{-6}$.

4.2. Physical Bridge Arrangement

In order to minimize current loops and localize the junction points A, D_2, C, D_1, B, and D_3, a hexagonal bridge center was constructed of copper as shown in figure 10. Each segment consists of five coaxial connectors with their shields bolted to a ¼-in. copper top plate and their inner conductors connected by means of a copper plate. These six connecting plates shown dotted in the figure, are shielded from each other so that capacitance and conductance between segments arises only from external elements that are connected between pairs of coaxial connectors in the various segments. The intersections of the arms of the copper connecting plates define the junction points referred to in the discussion of figure 9. The bridge center is located just above the liquid level in the middle of a large temperature-regulated oil bath.

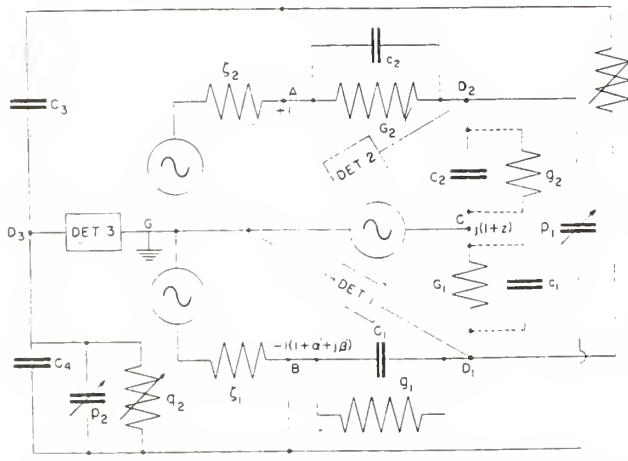

FIGURE 9. *Complete bridge with auxiliary components.*

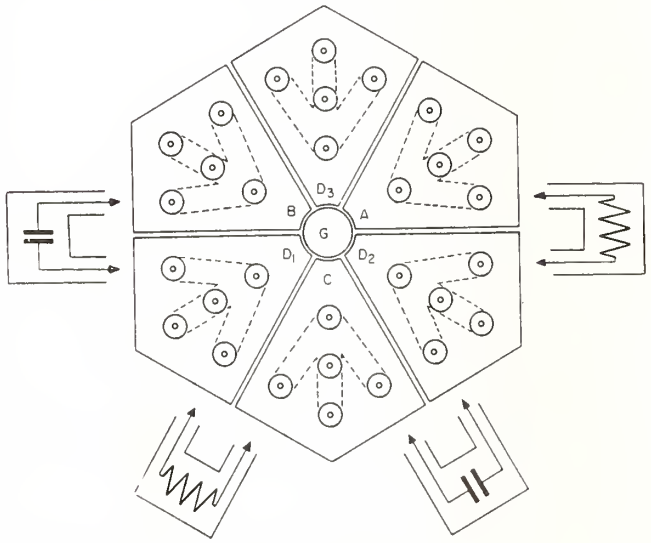

FIGURE 10. *Diagram of bridge center.*

The voltage sources are connected to the bridge center points A, B, and C, by heavy wires passing through a tube that is welded to the bottom of the oil bath tank and extends above the liquid level beneath the center. The 10^4-ohm resistors and the 0.01-μf capacitors, hermetically sealed and immersed in the oil to maintain them at a constant temperature, are connected to the center with rigid coaxial leads positioned as in figure 10.

Coaxial detector leads run from the connectors at D_1, D_2, and D_3, upwards through an eye-level shelf to filters, amplifiers, and visual detectors.

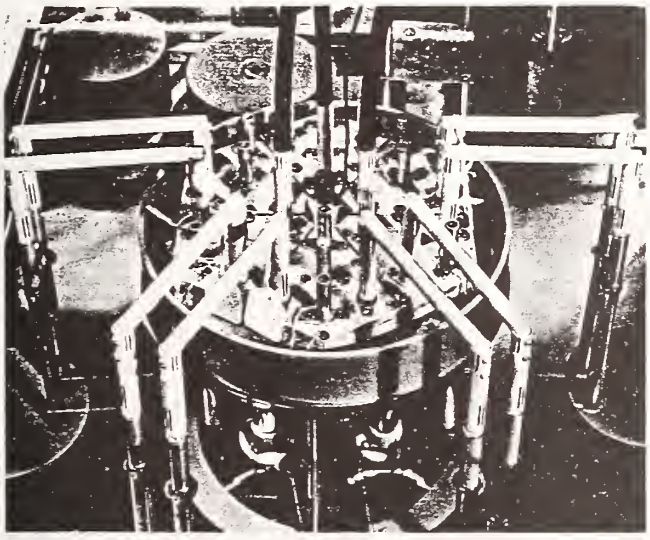

FIGURE 11. *Photograph of components shown in figure 10.*

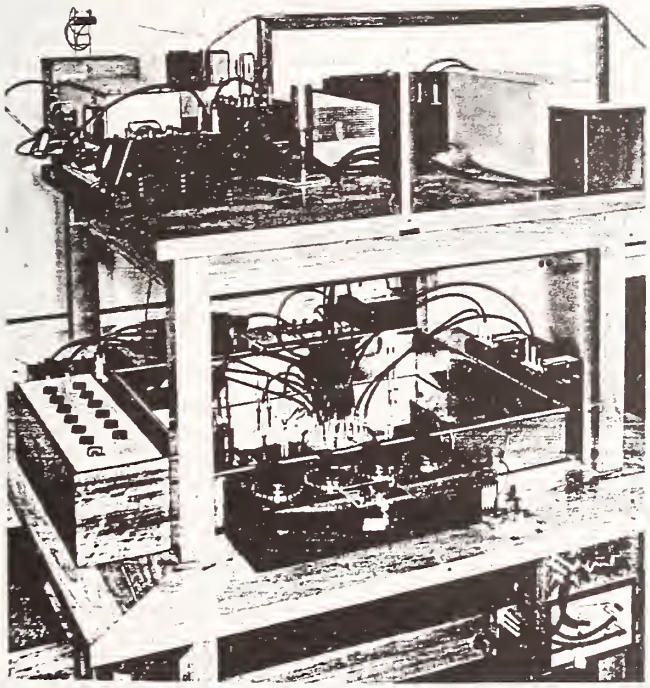

FIGURE 12. *Photograph of bridge assembly for comparing conductance with capacitive susceptance.*

Figure 11 shows the principal features of the bridge arrangement, and figure 12 shows the auxiliary admittances in place for balancing the bridge.

Although the two voltage sources derived from a transformer are easily procurable, the third source 90° out of phase with them presented some design problems. Our equipment uses a passive phase-shifting network driven by a separate winding on the main transformer to produce this voltage. The phase-shifting network is adjustable to allow the complex components of z to be varied in small increments and set within a few parts in a million of zero.

The assumptions leading to the bridge equations require only that the proper voltage at junction C be produced and maintained, and place no restriction on the equivalent series impedance of the 90° source. However, if its impedance is too large, variation of one balancing component such as C_1 in figure 9 changes not only the voltage at D_1, but also the voltage at junction C and hence at D_2. This mutual dependence between the two bridges makes it very difficult to balance both bridges simultaneously unless the impedance of the 90° source is less than $\frac{1}{10}$ the impedance of the bridge arms, or in this case less than 1000 ohms. Based on these considerations, the circuit of figure 13 was chosen to provide the three sources for the bridge. With A, B, and C connected to the bridge. the voltage at C may be adjusted, with the controls provided, to the proper value.

Power for driving the bridge is provided by a commercial tuning fork oscillator driving a power amplifier as shown in figure 14. The filter is designed to reduce harmonic content of the signal. The tuning fork frequency is adjustable in a small range around $\omega = 10^4$.

4.3. Frequency Measurement

The frequency is measured with the circuit of figure 15. The pulse former preceding the preset counter proper is part of the preset counter assembly. The sharp pulse produced therein goes through the gate when the preset counter registers the desired

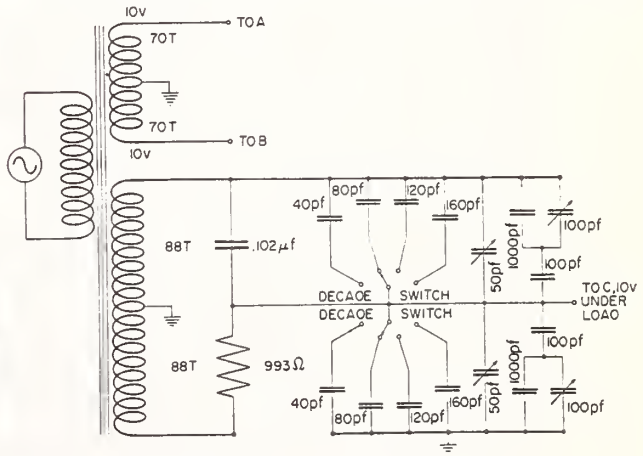

FIGURE 13. *Bridge voltage sources.*

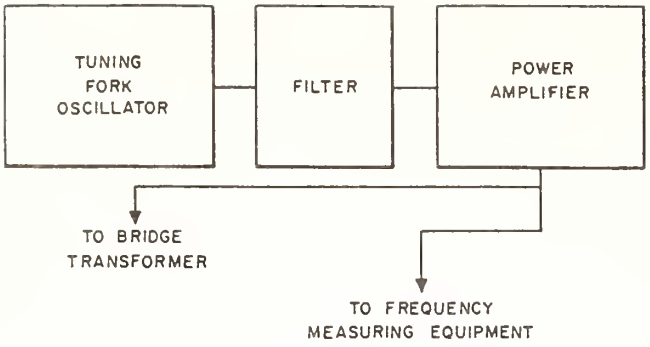

FIGURE 14. *Bridge power supply.*

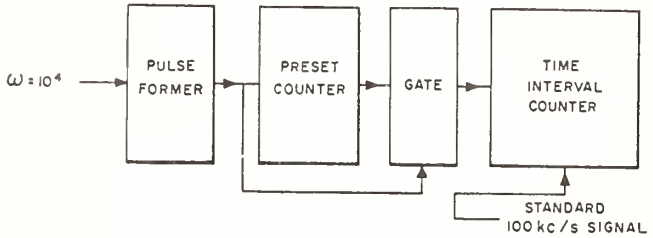

FIGURE 15. *Frequency measuring system.*

number of counts, and the time interval counter measures the time between two such pulses. The preset counter is automatically reset after 10^4 cycles at the input. For $\omega = 10^4$ the time interval between pulses reaching the time interval counter is 2π sec, during which time a 10-Mc/s signal derived from the 100-kc/s standard frequency source is counted and displayed by the time interval counter. The system may be checked for internal consistency by using it to measure 10^4 periods of a standard 1000-cycle signal. This equipment monitors the tuning fork output while the bridge is in use, and allows the frequency to be measured with an accuracy better than 5 parts in 10^8.

4.4. Detectors

Since the bridge balance is strongly frequency dependent, the harmonics of the driving frequency may have relatively high signal levels at the detector inputs. Sharp tuning of the detectors is not sufficient to eliminate trouble from this source, since two or more harmonics may mix in the nonlinear first stages of the amplifiers to produce apparent fundamental frequency signals [8].

Figure 16 shows the circuit of filters which precede the electronic amplifiers used with detectors D_1 and D_2. With the exception of the input transformer, all inductors are 0.1-henry commercial dust-core toroidal inductors. The input transformer must have a very high Q to preserve high signal strength, and was constructed from a similar inductor by removing a few turns and adding a primary; the turns ratio being chosen to give a good impedance match between the bridge and the filter. The filter forms a bridge which is balanced at the second harmonic

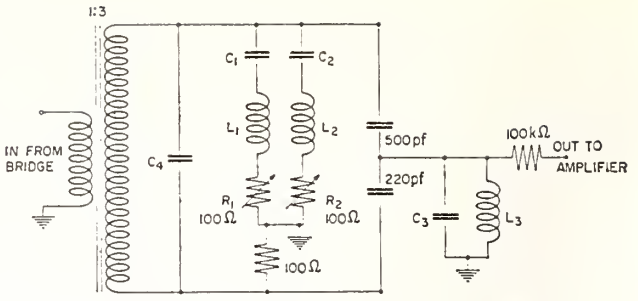

FIGURE 16. *Filters for harmonic rejection.*

by adjusting C_1 so that C_1 and L_1 resonate, and by adjusting R_1. Also, C_2 and R_2 are adjusted to produce balance at the third harmonic. Tuning the input transformer with C_4 and the output circuit with C_3 to the fundamental completes the adjustment of the doubly-tuned filter which attenuates harmonics higher than the third sufficiently for our purposes. The filters are housed in boxes constructed of $\frac{1}{16}$ in. sheet steel for magnetic shielding.

It has been found that with these filters, second and third harmonic signal levels are attenuated 140 db with respect to the fundamental, and all higher harmonics by at least 95 db. Experimentation with filter orientation shows that stray pickup to the filters cannot produce an error as large as one part in 10^7.

The effectiveness of the filters has been investigated by greatly increasing the harmonic content of the power signals reaching the bridge. For this purpose a diode rectifier was placed between the tuning-fork filter and the power amplifier. Harmonic levels at the bridge center were measured with and without this diode. It was found that although the levels of all measured harmonics were greatly increased, the bridge balance change was less than one part in 10^7.

Following the detector filters, commercial tuned amplifiers are used, which drive the vertical deflection plates of cathode-ray tubes. The horizontal plates of the cathode-ray tubes are driven by constant amplitude sinusoidal voltages derived from the tuning-fork oscillator but passing through variable phase shifters. At balance a straight horizontal line appears on the cathode-ray tube, and the phase shifter may be adjusted so that an unbalance in a main component (C_1 or C_2) opens the line into an ellipse, and an unbalance in phase (q_1 or p_1) tilts the line. This provides a phase sensitive detection scheme which allows the bridge to be balanced with a minimum of time consumed. The detector sensitivity is sufficient to observe unbalances of one part in 10^7 in magnitude or 10^{-7} radians in phase angle.

4.5. Resistance Comparisons

The bridge system described allows the mean of two a-c conductances G_1 and G_2 to be measured in terms of a measured frequency and two capacitors C_1 and C_2 whose values are obtained from a computable capacitor. The conductance standards G_1 and

G_2 each consists of a commercial 10^4-ohm woven-wire resistor mounted in a shielded hermetically-sealed box and placed in the oil bath. The reciprocal of their measured conductance values is a resistance, which must be stepped down and compared with the bank of 1-ohm reference resistors which maintain the unit of resistance [9].

The conductance standards G_1 and G_2 are completely shielded, and are measured in the a-c bridge as direct conductances. In section 5 we will describe measurements performed to evaluate the difference between their conductances as measured with 1592 c/s alternating current, and their conductances as measured with direct current. This difference may be expected to be small, and will certainly remain constant over long periods of time. We will, at this time, tentatively assume that the difference is zero, and apply a correction later.

The d-c direct conductances of G_1 and G_2 are compared with the resistance of a stable 10^4-ohm d-c resistor in the circuit of figure 17, which shows the provision for eliminating the effect of leakage resistances R_3 and R_4 to the shield. The bridge is balanced first with point (1) grounded, which shorts R_4 and places R_3 in parallel with G_1; and then with point (2) grounded, which places R_4 across the battery and places R_3 across the 10^4-ohm standard $R\#505$. Neither balance depends upon R_4, and a large R_3 affects the two balances equally with opposite sign; hence the average balance gives the ratio[3]

$$\frac{r_4+1/G_1}{r_3+R\#505}=\frac{B}{\overline{A}_1}$$

Interchanging the link and standard, moving the galvanometer to D_1, and repeating the two balances gives

$$\frac{r_4+R\#505}{r_3+1/G_1}=\frac{B}{\overline{A}_2},$$

so that to the accuracy desired $R\#505=1/G_1(\times[1+(\overline{A}_1-\overline{A}_2)/2B]$, which allows the resistance of G_1 to be compared with the resistance of the d-c standard. The measurement is made with G_1 connected to the bridge center, and measurements are made between the same junctions used in the a-c measurement. A similar measurement of G_2 allows the 10^4-ohm d-c standard to be measured in terms of $\overline{G}=\frac{1}{2}(G_1+G_2)$, which is obtained from the a-c bridge. The measurement method involves the well-known double substitution technique with provision for eliminating the errors which might be caused by leakage resistance.

The variable arm A is constructed from a 100-ohm direct reading ratio set with a smallest step of one ppm, but is connected in series with a 900-ohm resistor to give a smallest step of one part in 10^7.

[3] This relationship is actually an approximation, and depends upon R_3 being large compared with $R\#505$. Since the two values of A_1 differed in our measurements by only a few parts per million, the approximation introduces no significant error.

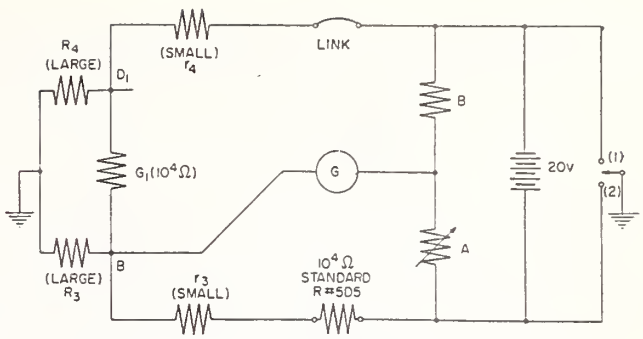

FIGURE 17. *Circuit for three-terminal d-c resistance measurement.*

This 900-ohm resistor, a 10^3-ohm resistor B, the 10^4-ohm standard, and the link rest on a mercury stand in the oil bath.

Table 2 shows the results of several comparisons of the 10^4-ohm d-c resistor with the 1-pf reference capacitor, using the frequency-dependent bridge. Recalling that the reference capacitor was measured in terms of the computable capacitor in May and July 1960, it will be noted that groups of runs were made immediately preceding and immediately following each cross capacitor measurement.

Each set of one cross capacitor measurement and two groups of resistance-capacitance bridge runs constitutes an evaluation of the resistance of the 10^4-ohm standard $R\#505$.

5. Frequency Dependence of Bridge Resistors

The measurements of the a-c–d-c resistance differences of G_1 and G_2 were made by comparing them with a standard resistor of simple geometry having predictable frequency characteristics, using both direct current and 1592 c/s alternating current. Figure 18 shows the cross section of such a standard

TABLE 2. *Resistance of 10^4 ohm d-c resistor #505*

Based on 1 pf reference capacitor #NBS 89790-B neglecting a-c–d-c differences

Date (1960)	$R\#505$	Average phase angle of 10^4 ohm a-c resistors
		Microradians
May 5	10^4 ohms −73.6 ppm	+15.0
May 10	−73.4	+15.4
May 11	−74.3	+14.8
May 19	−74.1	+15.4
May 20	−74.0	+15.2
Average	−73.9 ppm	+15.2

True value of 1 pf reference capacitor=1 pf −54.0 ppm.
Resistance of $R\#505=10^4$ ohms −19.9 ppm.

Date (1960)	$R\#505$	Average phase angle of 10^4 ohm a-c resistors
		Microradians
July 18	10^4 ohms −72.2 ppm	+14.7
July 19	−71.8	+15.0
July 28	−72.5	+14.8
July 29	−71.6	+14.7
Average	−72.0 ppm	+14.8

True value of 1 pf reference capacitor=1 pf −51.4 ppm.
Resistance of $R\#505=10^4$ ohms −20.6 ppm.

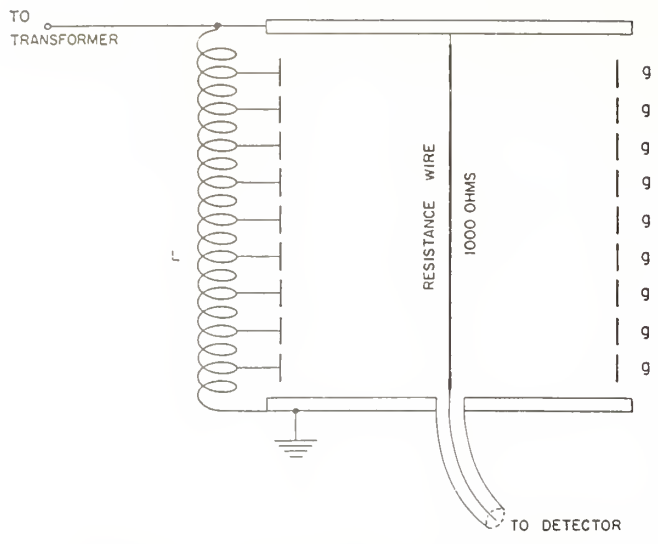

FIGURE 18. *A-c–d-c resistance transfer standard.*

whose resistance element consists of a single straight wire 0.0008 in. in diameter and 9.5 in. long having a resistance of 1000 ohms. The structure is cylindrical with the resistance wire down the center. The large phase angle expected from a conventional coaxial line resistor is eliminated by the use of a set of guard rings, g, about 4 in. in diameter, which surround the resistance wire. The potentials of the guard rings are defined with a tapped inductor L placed between the line terminal and ground. The inductor taps are placed to provide a uniform potential gradient down the center of the cylinder in the absence of the resistance wire.[4]

When a bridge containing the transfer resistor is balanced with the resistance wire in place, the detector voltage is zero, and the potential gradient along the wire is still uniform. Since the wire does not change the electric field within the resistor assembly, we may expect no capacitance contribution to the resistor phase angle and a-c–d-c resistance difference. The effectiveness of the guard rings may be checked by connecting adjacent guards in parallel to cut the effective number of them in half, and by suitably reconnecting them to the tapped inductor. If the apparent resistance and phase angle measured in these two ways are the same, we may assume that the number of guard rings is sufficient to eliminate the effects of capacitance within the resistor. In practice it is found that even with all of the guard rings grounded, the measured a-c resistance is equal to the a-c resistance with all guards connected properly to the tapped inductor, and the phase angle change between the two-guard arrangements is less than 3 microradians.

The inductance of the standard resistor was measured by replacing the fine resistance wire with a larger low resistance wire and measuring, with a Maxwell-Wien bridge, the inductance including that of the coaxial leads between the junction points

[4] Similar arrangements applied to high voltage transformer testing have been described by Silsbee [10] and Weller [11].

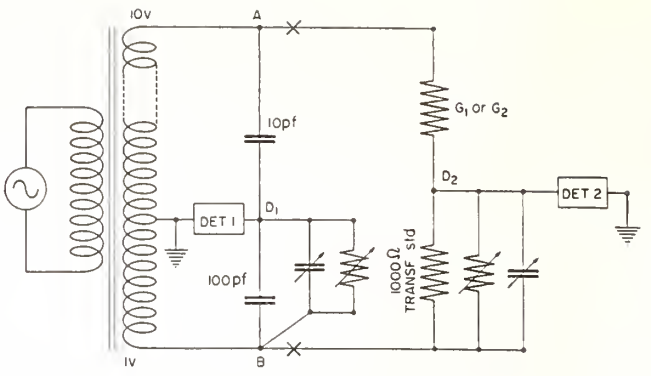

FIGURE 19. *Circuit for comparing the transfer resistor with the bridge resistors, using ac.*

of the bridge center used in the measurements to be reported below. A simple computation [12] yields the difference between the inductances of the fine wire and the low resistance wire. We find for the series inductance of the resistor attached to the bridge center $L=1.1$ microhenries. This inductance has a negligible effect on the a-c resistance, but produces a phase angle of 11 microradians.

Figure 19 shows the bridge used for the a-c comparison of the 1000-ohm transfer resistor, R_T, with G_1 or G_2. The 10:1 transformer is the one used for the capacitance step-up, and has a known ratio. A balance is observed on detector 1 with the resistors disconnected at "X" to compare the 100-pf capacitor with the 10-pf capacitor. When the resistors are placed in the circuit and both bridges are balanced, a change in the balance at detector 1 indicates a change in the transformer ratio between the junctions A and B, and allows the loaded voltage ratio between these points to be calculated. This figure combined with the readings of the admittances required to balance detector 2 allows the a-c ratio of the resistances of G_1 or G_2 to the resistance of the 1000-ohm transfer standard to be determined, and also allows the phase angles of G_1 and G_2 to be determined from the known phase angle of the transfer standard.

Figure 20 shows the bridge used for comparing the d-c resistance of the transfer standard with G_1 or G_2. Since the tapped inductor of the transfer resistor presents a low d-c impedance to ground, it must be removed from the circuit for the d-c measurement. With this done, the leakage resistances R_1, R_2, and R_3 are all high. Series resistances r_1 and r_2 in connecting wires are small. Two balances are made with points 1 and 2 grounded in turn. The direct reading ratio set readings are called A_1 and A_2, respectively.

The bridge is then connected as in figure 20, where R_1' and R_3' are low resistance "shorts." The bridge is balanced with the galvanometer connected to 3 and 4 in turn; the readings of the DRRS are called A_3 and A_4, respectively. An analysis shows that for G_1,

$$R_T G_1 = \frac{R\#400}{R\#505}\left[1+\frac{100(A_1-A_3)}{11B}+\frac{10(A_2-A_4)}{11B}\right].$$

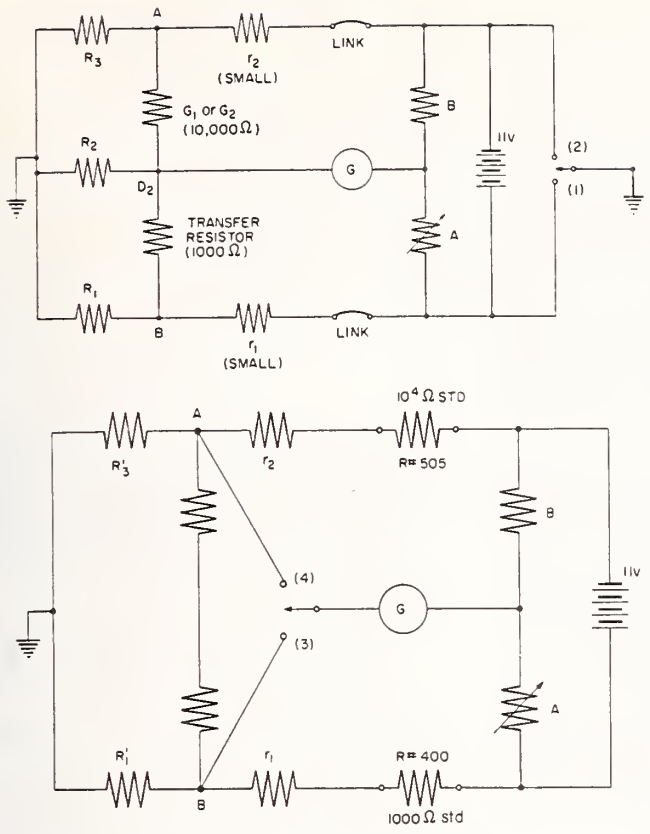

FIGURE 20. *Circuits for comparing the transfer resistor with the bridge resistor, using dc.*

Provided that the resistance ratio of the d-c standards is known, measurements of this form yield the a-c–d-c differences of both G_1 and G_2. Since the 10^4-ohm resistor #505 was used for both this measurement and for the direct d-c comparison between it and G_1 and G_2 in connection with the frequency dependent bridge, one finds that resistor #505 serves only to maintain the unit between the two measurements, and that in effect the 10:1 transformer is used five times to step up the impedance of the 1-pf standard capacitor to the 1000-ohm transfer resistor. The d-c step-up is then needed only from the bank of one-ohm reference resistors to the 10^3-ohm d-c standard resistor #400. An error in the d-c step-up from 10^3 ohms to 10^4 ohms would cause no error in the final value assigned to the one-ohm reference resistors, but would only cause an error in the measured a-c–d-c differences of G_1 and G_2, which in this sense is not needed for our work. In fact, the only reason for including 10^4-ohm #505 in the measurements is that it is much more stable than G_1, G_2, and the transfer resistor. The use of 10^4-ohm #505 allows the complete determination to be broken up into smaller steps which may be completed more quickly and with higher accuracy. Subject to the above comments, we find that G_1 and G_2 have identical a-c–d-c differences and that their a-c resistances are 0.85 ppm higher than their d-c resistances. The average of their phase angles is found from the a-c measurement using the phase angle calculated for the transfer resistor to be 16.6 microradians (capacitive).

6. Conclusion

Combining the results of table 2 with the measured a-c–d-c difference of G_1 and G_2 we find $R\#505 = (10^4 \text{ ohms} - 19.4 \text{ ppm})$. Comparison of this resistor with the NBS bank of one-ohm reference standards yields the value (10^4 ohms -21.7 ppm) in terms of the ohm as adopted in 1948 [13] and as maintained at NBS. Our measurements therefore indicate that the NBS unit of resistance is 1.000002_3 ohms.

Two values have been obtained for the phase angles of the 10^4-ohm woven-wire resistors; 16.6 microradians from the computed phase angle of the straight wire a-c–d-c transfer resistor and 15.0 microradians based on the assumption that the 1-pf reference capacitor has no phase angle. The discrepancy of 1.6 microradians may be ascribed to the actual phase angle of the 1-pf capacitor, an error of 0.16 microhenry in the measurement of the transfer resistor series inductance, or a combination of these two effects. The agreement is considered satisfactory in view of the uncertainties in these measurements.

Table 3 summarizes the steps of this determination and lists the estimated uncertainties associated with each step. The estimates are in most cases little more than guesses, since they must include allowances for possible systematic errors. The estimates are in all cases given as "50 percent errors," meaning that in the experimentor's judgment the chances of the error being greater or less than this amount are approximately equal. It is judged to be almost certain that the error is less than four times the stated 50-percent error. No allowance is made for the possibility of error in the assigned value of the speed of light, which is taken as a predetermined constant, $c = 2.997925 \times 10^{10}$ cm/sec.

With the exception of the speed of light, all measurement uncertainties may be reduced with suitable refinements in measurement techniques. It is believed that with the development of an improved cross capacitor and with minor changes in the rest of the equipment, the measurement uncertainties not including the contribution from the speed of light may be reduced below 1 ppm.

TABLE 3. *Uncertainties associated with steps followed in this determination*

	50% error
	ppm
Measurement of the reference capacitor in terms of the computable capacitor, neglecting the contribution from the uncertainty in the speed of light	2.0
Instability of the reference capacitor	0.3
Ten-to-one step-up using alternating current (times 5)	.1
Frequency dependent bridge	.3
Dependence of bridge resistors upon frequency	.3
Step-down from 10^3 ohms to 1 ohm using direct current	.3
Measurement uncertainty neglecting the uncertainty in the speed of light	2.1

7. Comparision With Other Determinations

In order to compare several recent evaluations of the 1948 resistance unit with each other, it is necessary to know the relative values of the units in terms of which these evaluations were made. Figure 21 shows the results of comparisons made at the International Bureau of Weights and Measures (BIPM) of resistors embodying the units as maintained by NBS (Ω_{EU}), NRC (Ω_{Ca}), and NPL (Ω_{GB}) in terms of the unit as maintained at the International Bureau (Ω_{BIPM}) [14, 15, 16, 17].

No information is yet available concerning the 1960 intercomparisons, so it is impossible to compare the present work with Ω_{BIPM} at this time. For this reason and for consistency in the table to follow, all measurements will be referred to the unit as maintained at NBS, Ω_{EU}.

Table 4 contains values assigned to Ω_{EU} by several recent investigations [18, 19, 20]. The values have been adjusted to allow for the difference between Ω_{EU} and the units used for the measurements. The results obtained by Thomas et al have been referred to Ω_{EU} instead of the international ohm, and also revised upwards by 3 ppm. This revision represents the results of a new evaluation of the current distribution in the primary winding of the mutual inductor, and is based on measurements of the dependence of resistivity upon strain in a sample of the wire used for the winding. These measurements were made in 1956 by Wells [21]. The revised current distribution correction was also calculated by him, but the result was not published.

The National Bureau of Standards was fortunate in receiving a visit in April and May of 1960 from Mr. G. H. Rayner of the National Physical Laboratory in England. Mr. Rayner helped perform the May measurements reported in this paper, and contributed greatly to the early success of this method. His contributions are gratefully acknowledged.

Others contributing substantially to the work described in this paper were Mr. John C. Clark, Mr. Lai H. Lee, Mr. John Q. Shields, and Mr. Thomas E. Wells.

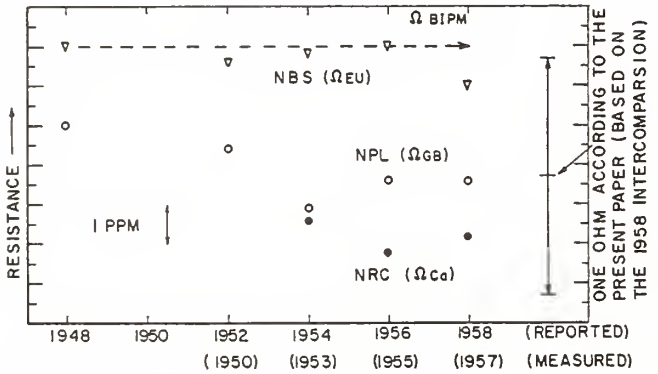

FIGURE 21. *Resistance units maintained by NBS, NPL, and NRC in terms of the unit maintained at the International Bureau of Weights and Measures* (Ω_{BIPM}).

TABLE 4. *Values assigned to the resistance unit maintained at NBS* (Ω_{EU}) *by several recent investigations*

(See text.)

Date of measurements	Reference	Laboratory	Value of the resistance unit Ω_{EU} maintained at NBS
1938 to 1949	Thomas, Peterson, Cooter, & Kotter	NBS	0.999997
1951	Rayner	NPL	1.000004
1957	Romanowski & Olson	NRC	.999996
1960	Present paper	NBS	1.000002_3

8. References

[1] Thompson, A. M., and Lampard, D. G., A new theorem in electrostatics and its application to calculable standards of capacitance, Nature, **177**, 888 (1956).

[2] Lampard, D. G., A new theorem in electrostatics with applications to calculable standards of capacitance, Proc. I.E.E.. Mono. No. 216M, January 1957.

[3] Thompson, A. M., The cylindrical cross capacitor as a calculable standard, Proc. I.E.E., Vol. 106, Pt. B, No. 27, May 1959.

[4] Lampard, D. G., and Cutkosky, R. D., Some results on the cross capacitances per unit length of cylindrical 3-terminal capacitors with thin dielectric films on their electrodes, Proc. I.E.E., Mono. No. 351M, January 1960.

[5] Thompson, A. M., The precise measurement of small capacitances, I.R.E. Trans. Instr., vol. **I–7**, Nos. 3 and 4, December 1958.

[6] McGregor, M. C., et al, New apparatus at the National Bureau of Standards for absolute capacitance measurement, ibid.

[7] Cutkosky, R. D., and Shields, J. Q., The precision measurement of transformer ratios, Paper presented at the 1960 Conference on Standards and Electronic Measurements at Boulder, Colorado, IRE Trans. Instr. **I–9**, 243 (1060).

[8] Johnson, G. J., and Thompson, A. M., Intermodulation in bridge detector amplifiers, Proc. I.E.E., Mono No. 210M, November 1956.

[9] Thomas, J. L., Precision resistors and their measurement, NBS Circular 470, 1948.

[10] Silsbee, F. B., A shielded resistor for voltage transformer testing. Scientific Papers NBS No. 516, 1925.

[11] Weller, C. T., A 132-KV shielded potentiometer for determining the accuracy of potential transformers, A.I.E.E. **48**, 1929.

[12] Grover, F. W., Inductance Calculations, Van Nostrand Co., Inc., New York, N.Y., 1946.

[13] Comité International des Poids et Mesures, Procès-Verbaux Deuxième Serie, **TXX**, 1945–1946.

[14] Comité International des Poids et Mesures, Procès-Verbaux Deuxième Serie, **TXXIII**, 1952.

[15] Comité International des Poids et Mesures, Procès-Verbaux Deuxième Serie, **TXXIV**, 1954.

[16] Comité International des Poids et Mesures, Procès-Verbaux Deuxième Serie, **TXXV**, 1956.

[17] Comité International des Poids et Mesures, Procès-Verbaux Deuxième Serie, **TXXVI**, 1958.

[18] Thomas, J. L., et al, An absolute measurement of resistance by the Wenner method, NBS Research Paper 2029, 1949.

[19] Rayner, G. H., An absolute measurement of resistance by Albert Cambell's bridge method, I.E.E., Mono. No. 95, 1954.

[20] Romanowski, M., and Olson, N., An absolute determination of resistance, Can. J. Phys., **35**, 1957.

[21] Wells, T. E., Measurement of the resistance-strain relation and Poisson's ratio for copper wires, Proc. Instr. Soc. Am., **11**, 1956.

(Paper 65A3–97)

NATIONAL PHYSICAL LABORATORY
TEDDINGTON, ENGLAND

SYMPOSIUM ON PRECISION ELECTRICAL MEASUREMENTS

17th - 20th November 1954

PAPER NO. 14

Alloys for Precision Resistors

by

C. Peterson
(National Bureau of Standards, USA)

14. Alloys for Precision Resistors

by

Chester Peterson

National Bureau of Standards U.S.A.

SUMMARY

The National Bureau of Standards has always been vitally interested in the properties of metals and alloys suitable for use in precision resistors and has developed standards known as the Rosa-Type and the Thomas-Type. This paper is a condensation of a longer unpublished manuscript which was intended to serve as an historical summary and bibliographical guide for other workers in the field. During the decade 1930-40 Thomas did much valuable work on resistance alloys which should be continued and expanded. One object of such a continuing programme is to produce stable standards, 10 ohms and higher, having little temperature dependence in the range 20° to 30°C. The present paper summarizes the performance of 15 Thomas-type 1ohm resistors constructed in 1933; the unit of resistance in the United States is maintained by ten of these standards.

INTRODUCTION

When applied to resistors the word "precision" has a double connotation. In the electronics field it signifies a resistor accurate to better than a few percent, whereas in the electrical measurements field it means a resistor adjusted within 0.01% of its nominal value, and of such quality and stability as to maintain this value over long periods of time. In this paper we shall deal only with alloys suitable for use in the latter field although a few of these alloys have also found application in the broader electronics and communications fields.

Nearly a century has passed since Matthiessen conducted his classical researches on alloys suitable for the construction of resistance standards. During the intervening years numerous workers have investigated various phases of the problem and new alloys adapted to particular uses have been developed. Intermittently during a period of over 25 years one of the most indefatigable workers in this field was an Englishman, labouring in the United States, whose results were best publicized by the Germans. This was Edward Weston who developed for use in current shunts an alloy which later became known as "manganin". This alloy deservedly enjoys much favour, although to this day it is not fully understood what makes "good" manganin for precision standards.

This paper does not attempt to cover all aspects of the field. The prime objectives here are to assemble a key bibliography, to present chronologically highlights in the development of the art, and to point out gaps in our knowledge where further work might advantageously be undertaken. This paper deals primarily with resistance alloys, although some discussion of resistance standards is inextricably involved.

REQUIREMENTS FOR PRECISION RESISTORS

To be useful in precision resistors, alloys should possess the following properties:

(a) They should have a low temperature coefficient of resistance over as wide a temperature range as possible.

(b) They should, particularly for d.c. applications, have low thermoelectric power against copper.

(c) They should be stable over long periods of time.

(19649)

(d) They should be workable by conventional wire and rolling mill practices.

(e) They should be easily soldered and welded.

In order to evaluate a given alloy with respect to the above properties it is necessary to construct with it a resistor of some sort, be it a heavy four-terminal rod or a coil of fine insulated wire wound on any one of a number of different coil-form materials. Herein lies one of the difficulties in comparing the results of one investigation with another, because the results obtained may depend to a noticiable degree upon the form of the resistor and the distribution of stresses in the alloy. Frequently differences of opinion between producer and purchaser can be traced to these circumstances. It is known, for example, that if two resistors are constructed using fine wire, one on a brass spool and the other on a steel spool, but otherwise identical in construction, the former may have a positive temperature coefficient, whereas the latter may have a negative coefficient. The effect is due to the differences in thermal expansion of brass, steel, and the alloy in question. The point here simply is that some uniformity of procedure should be adopted whenever possible when comparing the resistance properties of various alloys.

CHRONOLOGICAL DEVELOPMENT

The copper-nickel-zinc alloy known as "German-silver" is probably the oldest alloy to have been used in the construction of resistance apparatus. It has a mean temperature coefficient of resistance of about 450 parts per million per ^{o}C (ppm/^{o}C) between the ice and the steam point; it has considerable thermal e.m.f. against copper and is not very stable in its resistance properties. It was the standard of comparison with respect to which early workers sought to find improvements, and continued to be used until about the turn of the century. It was eventually shown that the element zinc was objectionable in this alloy.

Literature published before the year 1900 frequently mentioned an alloy called "Platinoid". This trade name was misleading because the material contained no platinum. The alloy was essentially German-silver with small amounts of tungsten added.

The first worker to make a systematic investigation of the suitability of various alloys for use in resistance standards was A. Matthiessen who did much of his work under the auspices of the British Association Committee on Standards of Electrical Resistance. Matthiessen published a number of papers on the electrical properties of metals and alloys during the decade 1855-65, of which two *(refs.1,2)* may be cited here. Much of Matthiessen's work on resistance alloys is also published in appendices to reports of the B.A. Committee *(ref.3)*. The best alloy developed had a composition 2/3 silver and 1/3 platinum. This alloy had a temperature coefficient of about 325 ppm/^{o}C and was the alloy which the committee adopted for use in constructing the British Association type of standard resistor. The work of Matthiessen can be summarized by quoting his concluding remarks at the end of Appendix B in the Second B.A. Report (1863) as follows: "It will be observed that I have not yet been able to find an alloy whose conducting power decreases between 0^{o} and $100^{o}C$ less than that of the alloy of silver with 33.4%. platinum; and from results obtained in this direction in conjunction with Dr. Vogt, I am of the opinion that there will be great difficulty in doing so. We have already tested upwards of 100 alloys, and it is curious how few we have found whose conducting power varies less than that of German-silver between 0^{o} and $100^{o}C$."

In reptrospect one wonders why Matthiessen did not hit upon a combination which had a temperature coefficient lower than 325 ppm/^{o}C, but it should perhaps be borne in mind that metals such as manganese and chromium, even in impure form, were a rarity in his day. Furthermore, Matthiessen seems to have laboured under the misapprehension *(ref.4)* that no practical binary alloy could have a temperature coefficient much smaller than the minimum values he observed.

(19649)

To Edward Weston belongs the credit for producing the first resistance alloy having substantially a zero temperature coefficient. At the time this was a remarkable achievement, particularly when it is recalled that, in that day, metals by definition were materials which always had positive temperature coefficients of resistance. Unfortunately for posterity, Weston was never inclined to publish the results of his researches. It is known that his interest in resistance alloys covered a period of 25 or more years extending from about 1886 to at least 1910. His most intense effort on alloys was made in the years immediately following the establishment of his private research laboratory in Newark, New Jersey, in 1886. His interest in alloys, arose out of some practical difficulties in connexion with the development of his portable indicating instruments. He needed a resistance material for voltmeter multipliers and ammeter shunts which did not vary in resistance with changes in temperature. Early shunts were made with German-silver. A simple calculation shows that energy dissipation sufficient to produce a 40°C temperature rise will change the resistance of such a shunt by almost 2%, an amount clearly intolerable when the overall accuracy sought was a fraction of 1%. Weston and his assistants systematically compounded hundreds of alloys *(ref.5)* among which was found an alloy of copper and nickel which actually had a negative coefficient. The firm of Basse & Selve, of Altena, Germany, later coined the name "Konstantin", and hence our name "Constantan", for this low temperature coefficient alloy having the composition 60 copper-40 nickel. This alloy was not entirely satisfactory because of its large thermal e.m.f. against copper. Eventually Weston produced alloys containing manganese which proved superior. Two brief news items appearing in the technical press in 1888 *(refs.6,7)* described these as zero temperature coefficient alloys having the compositions 70 copper-30 ferromanganese, or 65 copper-25 to 30 ferromanganese - 2.5 nickel. No further details were given.

The word "Manganin" was coined by the Germans to describe a copper-nickel-manganese alloy of rather specific composition. The Physikalisch-Technischen Reichsanstalt (P.T.R.) was founded in 1887 and within a year after its establishment a definite programme for the development of resistance standards was under way. The precise relation between Weston's work and the investigations of the P.T.R. is difficult to unravel at this late date, but in 1888 Weston's name was well known in electrical industry throughout the world and German technicians were aware of his researches on resistance alloys. In his papers on resistance alloys published in 1889 and 1892 Feussner *(refs.8,9)* makes brief mention of Weston's alloys. In the latter paper Feussner states that an electrical manufacturer in Berlin attempted to make an alloy in accordance with Weston's patent specifications using ferromanganese, but the product was brittle and could not be drawn to wire. Feussner was of the opinion that iron was responsible for the brittleness.

The Isabellen Metal Works* in Dillenberg, Germany, had for some time used a copper-manganese alloy for certain machine parts. Feussner ordered from this company samples of that alloy with and without additions of nickel. In his 1889 paper Feussner gave preliminary values for the electrical properties of these alloys. For nominal compositions 70 copper-30 manganese, and 73 copper-24 manganese-3 nickel, Feussner reported temperature coefficients of +40 and -30 ppm/°C respectively. The chemical composition of these alloys was not determined by analysis; consequently the amount of iron and other impurities was not known. Historically speaking, the situation is beclouded by the fact that Weston was reputedly dissatisfied with the inability at that time of American wire mills to draw his copper-nickel alloy ("constantan") to the fine gauges he wanted. According to Woodbury [loc. cit. p. 168] Weston employed German mills for this purpose and the Isabellen works may have been one of those so employed. This company coined the name "Westonin" for the copper-nickel-manganese alloy made to P.T.R. specifications, but later the more descriptive name "Manganin" was adopted. Whatever the precedence of development may have been, no less a person than von Helmholtz stated in 1892 [loc. cit. p.179] that "the discovery of a metal whose resistance diminishes with temperature was made by an American engineer" (Weston).

---

* This firm is still in business under the name Isabellen-Hütte Heusler K.-G., (16) Dillenburg (Hessen) Germany.

(19649)

The remark by von Helmholtz quoted above was made at the nineteenth meeting of the B.A. Committee in Edinburgh, 1892. He and other representatives from Germany, France, and the United States were present by invitation to consider the problem of establishing identical electrical standards in various countries. Lindeck presented a paper on wire standards of resistance describing some of his work at the P.T.R. This paper appeared in English as an appendix *(ref.10)* to the report covering that meeting.

In 1895 the P.T.R. published in its own journal a paper *(ref.11)* summarizing all the work done on wire standards since the beginning of the project in 1888. That paper was a landmark in the history of resistance alloys and standards, and merits some consideration at this point. The paper consisted of four major parts, of which only the first and the last are of interest here. The first part discussed the alloys investigated and the last part gave data on the stability of standards constructed at the Reichsanstalt. The alloys investigated were divided into two groups: (a) the commercially available alloys platinum-iridium, platinum-silver, german-silver, nickelin, and patentnickel; (b) new alloys identified by the names "manganin" and "constantan". Platinum-iridium was not actively considered because of its cost and high temperature coefficient; the authors had a poor opinion of Matthiessen's platinum-silver alloy because the samples they had were inhomogeneous and brittle. Considerable attention was paid to the last three alloys in group (a), particularly "patentnickel". This last-named material was a coinage alloy (essentially 75 copper-25 nickel) used by the German mint, and with it a temperature coefficient of resistance as low as +170 ppm/°C was obtained. The authors recognized that the principal limitation on the accurate measurement of resistance was the temperature coefficient of the resistance alloy used. They observed that alloys of copper and nickel without zinc had stable properties and that lower temperature coefficients were obtained with increasing amounts of nickel. Accordingly they directed their further researches to binary copper-base alloys containing various amounts of nickel or related elements. They were aware of the fact that Weston had obtained negative coefficients with alloys involving copper and manganese. For their investigation on new alloys they obtained a series of copper-manganese alloys from the Isabellen works, and a series of copper-nickel alloys from the firm Basse and Selve. In the first alloy series they found that a manganese content of seven or more percent gave low temperature coefficients and a small negative thermal e.m.f. against copper. In the second series they found that negligible coefficients were obtained with nickel contents between 40 and 60%; the thermal e.m.f. of these alloys was about 40 μV/°C with respect to copper. The authors therefore probably reasoned that by adding a small amount of nickel to the copper-manganese alloy a material might be had which would possess a low temperature coefficient of resistance and negligible thermal e.m.f. against copper. The proportions finally adopted were approximately 84 copper-12 manganese-4 nickel. The alloy of this rather specific composition made by the Isabellen works for the P.T.R. is the alloy which became known as "manganin".

The last part of Feussner and Lindeck's paper gave observations on the stability of 45 standard resistors having decimal values ranging from 0.1 ohm to 10 000 ohms. These were constructed according to the authors' design and became known as the "Reichsanstalt Type" of standard resistor. In this group of resistors 25 changed less than 0.01% during a period of 1½ to 3 years. The stability measurements referred ultimately to mercury standards on which the P.T.R. concurrently did much work.

The P.T.R. actively pursued its work on manganin resistors and set up working standards covering the range 0.001 to 10 000 ohms. Most of these standards were manufactured to P.T.R. specifications by Otto Wolff* who limited his efforts to the production of standard resistors and resistance apparatus only, and achieved in this field an international reputation for the quality of his workmanship. Reports on the stability of these standards are contained in papers by Jaeger and Lindeck *(ref.12)*.

---

* Otto Wolff senior died of natural causes during World War II. The business of the firm is carried on by a son, also named Otto Wolff. The firm is located in the Western Sector of Berlin and their present address is: Abbe-Strasse 12, Berlin-Charlottenburg 2, Germany.

(19649)

As a result of the thoroughness of the P.T.R. investigations and the excellence of Wolff's manufacture, manganin standard resistors of the Reichsanstalt type became firmly established in scientific and testing laboratories throughout the world. When the National Bureau of Standards was organized in 1901 it acquired Wolff resistors with Reichsanstalt certification as rapidly as funds permitted. During the period 1907-1909 *(ref. 13)* the unit of resistance in the United States was maintained with a group of ten 1ohm and seven 0.1ohm standard resistors of this type. After May, 1909, the unit was preserved with a sealed type of resistor developed by Rosa. Twice in the history of the N.B.S. improved resistance standards have been developed by changes in design and fabrication procedures rather than by changes in the resistance alloy employed. The first improvement was the development of the N.B.S. type of sealed resistor alluded to above, and described in a paper by Rosa *(ref. 14)* in 1908. The second improvement was the development of the double-wall type of resistor by Thomas around 1930, regarding which more will be said in a subsequent portion of this paper. In each case the alloy used was manganin.

Before World War I, instrument manufacturers in the United States imported practically all their constantan and manganin from Germany. When this source of supply was cut off, the stocks on hand were eventually depleted and domestic sources of supply had to be developed. The essential difficulty was not inability of domestic producers to make sound wire; the problem was more one of specifications. The foreign product varied considerably in its properties and users differed in their opinion regarding desired requirements. This situation stimulated a number of investigations among which may be mentioned the work of Hunter and Bacon at Rensselaer Polytechnic Institute *(ref. 15)* and F. E. Bash at the Leeds and Northrup Company *(refs. 16, 17)*. The results of these investigations showed that the peak of the resistance-temperature curve for manganin could be placed near 25°C if the total iron content of the alloy was raised somewhat above that which resulted from the unavoidable iron content of the impure manganese employed. However, in comparing the results of Hunter's work with those of Bash, there seems to be some conflict of opinion regarding the effect of iron. Hunter states that the samples to which no extra iron was added had maximum resistance around 40°C, and that with increasing additions of iron the maximum resistance is reached at lower temperatures. Bash states that with small amounts of iron the maximum of the resistance-temperature curve occurs at low temperature, and that increasing amounts of iron up to 1.5% raise the location of the peak; iron beyond 1.5% apparently brought the peak down again. The situation may be affected by the amount of silicon or other impurity present, but in any event both authors agreed that a total of 1.0 to 1.5% iron placed the peak of the curve near 25°C. Most manganin manufactured domestically after 1920 therefore contained extra iron, particularly if intended for use in precision resistors as distinguished from current shunts.

It should be noted that the manganese used before about 1937 usually contained several percent of impurities; this might account for some of the discordant results reported by Hunter and Bash.

In 1925 Pilling published a paper *(ref. 18)* presenting the results of a more or less cursory examination of some electrical properties of the copper-nickel-manganese series of alloys, tracing the major effects of composition on resistivity, temperature coefficient and thermoelectric power. Pilling covered a large portion of the ternary diagram and verified that alloys with zero or negative temperature coefficient could be obtained over a broad range of compositions, involving about half the area of the diagram. However, when consideration was limited to workable alloys having low thermal e.m.f. against copper, the alloys of interest centered around two fields: (1) a group containing less than 10% of nickel, with from 10 to 35% of manganese; (2) a group containing about 50% of nickel and 30% of manganese. The first of these groups includes the manganin-type alloys; the second was marginal in workability and has apparently never been studied in detail.

No survey of the present type would be complete without reference to the investigations of J. O. Linde made in Sweden at the Tekniska Högskola, Stockholm, during the period 1928-38. Linde was interested in the electrical properties of the binary solid solutions formed when pure gold, silver or copper were diluted with small amounts of other elements. His results were expressed as the proportional increase in resistance per atom percent of diluent, and the data were arranged to show how these numerical values depended upon the

relative location of the solvent and diluent metals in the periodic table of the elements. The effect of temperature was included in the investigation. Most of Linde's work is published in Annalen der Physik, to which one reference may be made here *(ref.19)*. In 1939 all of Linde's work in this field was assembled and published (in German) in a paper-bound volume *(ref.20)*. Although Linde included only a few percent of diluent metal in most cases, his work was of great value because it provided the stimulus for later practical development work on gold-chromium alloys in the N.B.S. by Thomas, and on silver-manganese alloys by Schulze at the P.T.R.

In 1928, Thomas began an investigation at the N.B.S. aimed at determining the cause of erratic variations in the values of the standards used to maintain the unit of resistance. Since May, 1909, the unit in the United States had been preserved with a group of 10ohm sealed resistors of the Rosa type. Although these resistors were of high quality, experience with them during the ensuing decades revealed that individual resistors might change several ppm/ year with respect to the average of a group of ten. Manganin coils for these standards were insulated with silk and were prepared and baked according to the methods used at the P.T.R. and described in the papers of Feussner and Lindeck of that organization. Because of the silk insulation the baking temperature was limited to 140°C. This baking procedure was necessary in order to dry the shellac and to help stabilize the resistance; no significant annealing of the wire took place, although some partial stress relief undoubtedly occurred. From Bridgeman's work *(ref.21)* it is known that resistivity is influenced by stress. Thomas reasoned that if he annealed the wire at a temperature sufficiently high to remove all stress better stability would be obtained. Accordingly he used bare manganin and annealed it in vacuum at 550°C *(ref.22)*, supporting the coil on a steel mandrel of the same diameter as the spool on which the finished coil was to be mounted. The annealed coil was anchored to a silk-insulated tube with linen thread, after which it was coated with shellac and baked for an hour at about 80°C. The finished coil was sealed in a double-walled container. These resistors gave very encouraging results; Thomas then modified the design slightly by increasing the size of the wire and the container. A group of these large double-walled resistors was made at the N.B.S. in 1933 and a review of their performance was published 13 years later. *(ref.23)*. These resistors proved to be superior to any previously developed; consequently the unit of resistance in the United States was preserved with this type of standard exclusively, beginning in 1939. With respect to the mean of ten the value of any individual standard changed only a few parts in ten million per year. To carry forward the performance data given in Tables 1 and 2 of *ref.23* the observations made since 1945 have been assembled in *Table* 1 below. This table has been prepared on the same basis as that employed by Thomas in the reference cited, *i.e.* it is assumed that the average value of the 10 resistors maintaining the unit had remained constant. As noted, some resistors have met with accidents, yet the average change of all 15 without regard to sign was only 1.5 ppm over a period of 21 years.

(19649)

TABLE I

Stability of 1ohm double-walled manganin resistors. (In this table the effect of change in units on January 1, 1948, is omitted.)

Standard No.	Change in resistance, in microhms, from 1933 until -									
	1933	1945	1946	1947	1948	1949	1950	1951	1952	1954
68	0	+0.1	-0.1	-0.4	-0.4	-0.6	-0.6	+3.7(a)	+3.6	+3.7
70	0	+0.3	+0.5	+0.4	+1.0	+0.9	+0.8	+0.9	+1.0	+1.1
74	0	-0.7	-0.3	-0.6	-0.8	-0.7	-0.8	-1.1	-1.2	-1.4
77	0	-1.0	-1.1	-1.1	-1.1	-1.1	-1.3	-1.3	-1.4	-1.3
78	0	+1.0	+1.1	+1.3	+1.5	+1.5	+1.6	+1.7	+1.8	+1.8
81	0	-0.9	-0.6	-0.6	-0.5	-0.7	-0.7	-0.7	-0.7	-0.9
82	0	-0.4	-0.0	+0.2	+0.1	+0.4	+0.2	+0.1	+0.2	+0.1
84	0	+0.6	+0.6	+0.3	+0.6	+0.4	+0.6	+0.4	+0.6	+0.5
89	0	+0.1	-0.2	-0.1	-0.6	-0.2	-0.4	-0.3	-0.3	-0.5
90	0	+0.5	+0.7	+1.1	+0.8	+0.8	+1.0	+1.1	+0.9	+1.2
67	0	-1.5	-1.4	-1.0	-0.8	-1.0	-1.5	-1.3	-1.6	-1.7
69	0	+1.9	—	+4.7(b)	+4.6	+4.5	+4.4	+4.4	+4.3	+4.3
72	0	+0.4	+0.4	—	—	—	+2.8	+2.7	+2.5	+2.6
73	0	-0.9	—	—	—	—	-1.2	-1.5	-2.0	0.0(c)
83	0	-2.1	—	—	—	—	-1.5	-1.5	-1.9	-1.3

Notes: (a) This resistor was accidentally dropped in January 1951, which caused a sudden increase in resistance of about 4 microhms; its value has remained constant since that date.

(b) (c) These resistors were employed in international intercomparisons immediately preceding the date noted. In 1953 Nos.72, 73, and 83 made a round trip to France by air via diplomatic mail pouch; in each direction of travel they journeyed in 3 separate flights and were not given preferential treatment. The resistance of No.73 increased 1.3 microhms during its absence from Washington.

The manganin employed in these large double-walled resistors has been of much interest and the source of numerous inquiries. The wire was obtained from the Driver-Harris Company in 1933 and was manufactured before the advent of electrolytic manganese. It was known that the 550°C anneal would raise the temperature coefficient; the producer was therefore requested to supply, if possible, manganin wire which had a slightly negative coefficient. Two lots of wire were supplied; the wire appeared to be quite soft, and as received had a zero temperature coefficient at about 20°C. The finished standards had small coefficients, varying from zero to +3ppm/°C at 25°C. The chemical analysis of this wire is given in *table* 2 overleaf. Samples A and B were from lots 1 and 2 respectively, and were analyzed at the N.B.S. in 1933. Sample C came from the remains of lot 1 or 2 used by Thomas in 1933, and was given to the Leeds and Northrup Company in 1947, which organization redetermined the composition. Their results are included to show silicon content.

(19649)

TABLE 2

Analyses of Manganin Used in N.B.S. Double-Walled Standards*

Sample	A	B	C
Copper	82.2	82.7	82.38
Manganese	13.2	12.1	12.98
Nickel	4.2	4.6	4.22
Iron	0.3	0.5	0.246
Silicon	-	-	0.042

* All values are in percent by weight

During the decade 1930-40 Thomas investigated the resistance properties of the following alloys: gold-chromium *(ref.24)*, gold-cobalt *(ref.25)*, and copper-manganese-aluminium *(ref.26)*. A brief summary of the resistance properties of these alloys will be given here, but the interested reader should refer to the original papers for further details.

The investigation of the gold alloys was suggested by Linde's work referred to above. Thomas found that the resistivity of a gold-chromium alloy containing 2.1% chromium by weight could be made independent of temperature to less than 1 part in a million in the range 20° to 30°C. This was achieved by a suitable baking procedure. Most alloys exhibit an increase in temperature coefficient at 25°C and a decrease in resistivity when baked at elevated temperatures. Gold-chromium behaves in an unusual fashion inasmuch as baking produces the opposite effect in that the resistance increases and the temperature coefficient decreases on baking. For alloys of the proportions mentioned it was found that a linear relationship existed between the increase in resistance and the decrease in coefficient when baked at 150°C. A 1% increase in resistance was accompanied by a decrease of 26 ppm/°C in the temperature coefficient. By employing this relationship, the coefficient could be adjusted to zero with comparatively few determinations of its value because the resistance changes were large and could be measured and followed with ease. The general shape of the resistance-temperature curves of these alloys is well illustrated in figure 3 of a later paper by Godfrey *(ref.27)*. The thermal e.m.f. of gold-chromium against copper is 7 or 8 μV/°C at 25°C as compared with 2 or 3 μV/°C for manganin against copper. Gold-chromium alloy shows to best advantage when used for constructing standards of 10 ohms or more. Two 1ohm standards have been made using heavy wire mounted in the large-type double-walled containers. Over a period of 4 years the resistance of one has decreased 6.6 ppm while the other has increased 1.6 ppm; the stability of these is apparently no better than the best manganin double-walled resistors, and may in fact be not quite as good. The advantage of gold-chromium alloy lies in the fact that the resistance of coils made with the small wire sizes appropriate to nominal values in the range 10 to 100 ohms can be manipulated by baking, so that the temperature coefficient can be made substantially zero over the interval 20° to 30°C.

Linde's work indicated that 2% by weight of cobalt in gold would give an alloy having zero temperature coefficient around 25°C. Thomas therefore prepared a series of gold-cobalt alloys having from 0.75 to 5% cobalt. He found that 10-ohm coils when baked for 18 hours at 140°C would have zero temperature coefficients if the cobalt content was about 2.2% by weight. The thermo-electric power of this alloy against copper is very high, being about 45 μV/°C. The stability of a few resistors made with this alloy indicated that the general performance was inferior to gold-chromium.

Alloys similar to manganin, but with the nickel replaced with about the same weight percent of aluminium, first came to the attention of the National Bureau of Standards around 1910. At that time Wilbur B. Driver donated samples of such an alloy which he had developed as an electrical-resistance material. This material had a very low thermal e.m.f. against copper and was of the type which later became known as "Therlo". The composition of Driver's material was approximately 84 copper-12 manganese-4 aluminium, with

traces of iron and nickel. A number of resistance standards were made from these samples and kept under observation and in regular use for more than 20 years. The alloy used in these standards was not physically sound inasmuch as inclusions and imperfections were readily visible. The performance of these standards was sufficiently good, however, to warrant a more complete investigation of the resistance properties of alloys of this type. Such an investigation was finally made by Thomas in the early 1930's. Thomas made a series of alloys containing from 80 to 95% copper with varying proportions of manganese and aluminium, and he worked out a procedure for making sound material in small quantities. The resistivity and temperature coefficient of these alloys were quite appreciably influenced by heat treatment. Baking at 140°C for 18 hours changed the resistivity by over 10% in some cases. A number of compositions were found which gave substantially zero temperature coefficient after baking. Of these alloys, that alloy which gave the lowest thermoelectric power against copper was found to be 85 copper-9.5 manganese-5.5 aluminium. Compared to manganin this alloy had approximately the same resistivity; its temperature coefficient could be made zero at 25°C; the change of the resistance with temperature was about half that of manganin; and the thermoelectric power against copper was only 10% that of manganin. The structure of this alloy was evidently complex because the wire would become harder if it were heated at too high a temperature in the attempt to anneal it during the swaging process. Ductile cold-worked wire, after mounting on the insulated spool for the finished coil, would become brittle after the 140°C baking procedure. These effects may have been caused by a precipitation hardening phenomenon; some metallographic work should be included in any future work on alloys of this type.

During the period 1933-41 Alfred Schulze in Germany did considerable work on alloys for standard resistors at the P.T.R.; some of his work paralleled and confirmed that of Thomas, particularly on the high-temperature treatment of manganin *(ref.28)* and on gold-chromium alloys *(ref.29)*. Of more interest here, however, are two other papers of Schulze's, the first of which *(ref.30)* is a summary of the properties of certain resistance materials suitable for use in constructing standard resistors. That paper is divided into three parts: (1) resistance materials based on copper-manganese; (2) gold-chromium; (3) peculiarities in physical behaviour of resistance materials. In part I the author reviews the properties of manganin as a function of annealing temperature, and he includes data on three aluminium-bearing copper-manganese alloys. Two of these were commercial German alloys known as "Isabellin" and "Novokonstant", while the third, called "A-Legierung", was intended to duplicate the composition adopted by Thomas in his paper *(ref.26)* on copper-manganese-aluminium alloys. In agreement with Thomas, Schulze found that these aluminium-bearing alloys had resistance properties which were quite sensitive to heat-treatment. He found that the alloy "Isabellin" (84 copper-13 manganese-3 aluminium) had a temperature coefficient of about -38 ppm/°C in the cold-worked condition, but that after heating for 75 to 85 hours in a neutral atmosphere at 500°C the coefficient could be made very small. Small coefficients could also be obtained with the other two alloys by following a similar baking process. Schulze made experimental resistors from all three alloys and obtained stable coils from "Isabellin" and "Novokonstant" in most cases. However, with Thomas' alloy (85 copper-9.5 manganese-5.5 aluminium) Schulze was unable to produce stable resistors. This result is not in agreement with results obtained at N.B.S. and is further evidence that alloys of this type possess some metallurgical peculiarities which are not fully understood. Alloys of this type ("therlo") have many desirable features and it appears that further study is warranted.

In part II of the paper under discussion *(ref.30)*, the author makes brief reference to gold-chromium resistors containing 2.05% chromium by weight. These were baked at about 200°C for 16 to 20 hours to reduce temperature coefficients to low values. Their behaviour was entirely in accord with the observations of Thomas and Godfrey in the United States. In part III the author discusses the effect of atmospheric humidity on the resistance of coils attached to supporting spools with shellac and describes a new form of resistor employing a sealed container, a type of construction not heretofore used extensively in Germany. The early work of Rosa at the N.B.S. demonstrated the necessity for sealing precision resistors against the effect of atmospheric humidity, and in this country precision resistors of 1ohm and higher have been enclosed in sealed containers for the

(19649)

past 40 years. Indeed, experience in the United States has shown that the beneficial effect of the high temperature anneal of manganin is largely lost if the resistors are left open and exposed to the atmosphere.

The second of Schulze's papers to which particular reference will be made here deals with the use of silver-base resistance alloys *(ref.31)*. That paper is of great interest because Schulze demonstrated that certain silver alloys could be made which had very small temperature coefficients around room temperature, and which had other desirable properties making them useful in the construction of precision resistance standards. From Table 8 in Linde's book *(ref.20)* it is apparent that silver alloyed with 7 to 17 atomic % of manganese would have substantially a zero temperature coefficient. A few resistors using alloys of this type have been made at the N.B.S. during recent years; no systematic study has as yet been made here, but the results support the conclusions of Schulze and indicate that further investigation of silver-manganese alloys would be profitable. It is interesting to note that although Matthiessen never succeeded in producing an alloy having lower temperature coefficient than about +325 ppm/°C obtained with his silver-platinum alloy, Schulze was able to produce silver alloys having the largest negative coefficients ever observed in metallic solid solutions as far as the author knows. Schulze studied five alloys consisting of silver alloyed with from about 9 to 22% of manganese and tin in various proportions. The alloy containing least silver had a composition 78 silver - 13 manganese - 9 tin, and although its electrical properties were very good, the alloy had such poor mechanical properties as to render it unsatisfactory for extensive use. Three of the five alloys were found to be particularly useful in the construction of standard resistors. Their properties are summarized in *Table 3* below.

TABLE 3

Electrical Properties of Three Silver Alloys
(From data by Schulze)

Alloy	Nominal Composition	Resistivity, microhm-cm C.W.	Resistivity, microhm-cm H.T.	α, C.W.	Finished Resistors α_{20}	Finished Resistors β	de/dT
A	8.78 Mn, bal Ag	32	28	-40×10^{-6}	-0.85×10^{-6}	-0.04×10^{-6}	+2.5
B	10 Mn 8 Sn 82 Ag	55	51	-36×10^{-6}	$+1.70\times10^{-6}$	$+0.23\times10^{-6}$	+0.5
C	17 Mn 3 Sn 80 Ag	58	46	-105×10^{-6}	$+0.49\times10^{-6}$	$+0.05\times10^{-6}$	+2

Notes: Data taken from *ref.31*. C.W. = cold worked. H.T. = heat treated. α and β are constants in the quadratic resistance-temperature equation. de/dT = thermoelectric power against copper, in $\mu V/^{o}C$, in the vicinity of 25°C.

The properties of these three alloys depended greatly upon their mechanical and thermal treatment. The very large negative temperature coefficient of the cold-worked wire could be changed to substantially zero by heating it in accordance with a schedule which varied with the composition. Alloys A, B, and C were given the following respective heat treatment: 12 hours at 250°C, 10 hours at 175° C and 18 hours at 270°C. The finished resistors referred to were open coils on porcelain spools, of 1-ohm nominal value, using wire of 0.5 and 0.6 mm diameter. No data are available regarding the long-time stability of these resistors, but data taken over a period of 1 to 10 months indicated that they remained constant within a few ppm. Schulze's work on silver alloys may be summarized by stating that alloys of this type can be prepared which are responsive to heat treatment, and which can be processed in such a manner as to make their temperature coefficients extremely small. The resistance-temperature curve is much flatter than in the case of

(19649)

manganin; in this regard the alloy compares favourably with gold-chromium. The thermoelectric power against copper is not greater than that of manganin.

In recent years two new resistance alloys of a modified nickel-chromium type have been introduced in the United States. They are produced by the Wilbur B. Driver Company and the Driver-Harris Company under the respective trade names "Evanohm" *(refs.32,33)* and "Karma". They contain approximately 74 nickel and 20 chromium, the balance being aluminium plus iron or copper. The thermoelectric power of these alloys against copper is about the same as that of manganin, but their resistivity is higher by a factor of 2.5 to 3 times. By a suitable annealing and baking process the 25°C temperature coefficient can be made to fall in the range ±20 ppm/°C. The resistance-temperature curve of these materials is fairly flat over a wide temperature interval.

Mention should also be made of a new alloy sold by the C. O. Jelliff Mfg. Corp., known as "Jelliff Alloy 800". This alloy has a resistivity of approximately 800 ohms (circular mil, ft), and is composed of substantial amounts of nickel, chromium and manganese, together with smaller amounts of molybdenum; it can be made to have a temperature coefficient of ±20 ppm/°C in the vicinity of room temperature. The thermoelectric power against copper is about twice that of manganin. This material, like the modified nickel-chromium alloys mentioned above, has greater strength than the copper-base alloys and consequently fine wire can be handled with relative ease in automatic winding machines employed for manufacturing wire-wound resistors used in considerable quantities in the communications and semi-precision instrument fields. The three new alloys mentioned are frequently used in constructing high-valued wire resistors. A limited number of precision standard resistors have been made in the N.B.S. using these new alloys. They have satisfactory temperature coefficients but no great amount of data on long-time stability has been accumulated. Some difficulty due to hysteresis effects have been experienced with the alloys containing aluminium. These alloys are of sufficient interest to warrant further study.

RECAPITULATION

In this paper reference has been made to the principal resistance alloys that have at one time or another been used in the construction of precision resistors. It is a tribute to the excellent qualities of manganin when one considers that this alloy still finds wide favour after 60 years of use, although to some extent it is being displaced by the new high-resistivity alloys of the modified nickel-chromium type. Many studies of manganin-type alloys have been made, yet there is no adequate explanation for the instability that has occasionally been observed in some lots of this material. The effect of residual iron and silicon in this alloy is not fully understood. Unpublished results of studies by Thomas on alloys of the manganin type made with electrolytic manganese indicate that the exact proportions of copper, nickel, and manganese are not critical. A series of alloys of this type can be made with copper in the range 70 to 85% and all with substantially zero temperature coefficient. In this series of alloys the thermoelectric power against copper and the curvature of the resistance-temperature graph have values depending on the composition; Thomas was unable to adjust the composition so as to simultaneously obtain negligible values for these properties. An investigation currently under way in the N.B.S. aims to complete this work.

The work of Schulze on silver alloys indicates that further investigation of modified silver-manganese alloys should be made. Alloys with very little temperature dependence, comparable to gold-chromium, appear to be attainable.

Alloys of the therlo type have long been of interest because of their low thermoelectric power and because their resistance-temperature curve has less curvature than that of manganin. More work needs to be done on these alloys to determine why they sometimes become brittle and show instability.

(19649)

A few standard resistors have been made in the N.B.S. using the high-resistivity alloys Evanohm, Karma, and Jelliff Alloy 800. Further studies are required in order to determine their suitability for the needs of national standardizing laboratories.

References

1. A. MATTHIESSEN, On the electric conducting power of alloys, *Trans. Roy. Soc.* (London) 1860, **150**, 161.

2. A. MATTHIESSEN and C. VOGT, On the influence of temperature on the electric conducting power of alloys, *Trans. Roy. Soc.* (London) **154**, 167 (1864). 1864, **154**, 167.

3. British Association Reports on Electrical Standards. (Reprinted 1913 by Cambridge Univ. Press.)

4. First B.A. Report (1862). appendix A. (See ref.3).

5. DAVID O. WOODBURY, A measure for greatness, p.168. McGraw-Hill, 1949.

6. Weston's new alloys for electric conductors. *Elec. World*, 1888, **12**, 39.

7. Alloys for electrical resistances with no temperature coefficient, *Science* 1888, **12**, 156. See also U.S. patents 381304 and 381305.

8. FEUSSNER and LINDECK, Metallegierungen fur elektrische widerstande, *Zeits. fur Instrumentenkunde*, 1889, **9**, 233.

9. FEUSSNER, Neue materialien fur elektrische messwiderstande, *Elektrotechnische Zeits.* 1892, **13**, 99.

10. STEPHAN LINDECK, On wire standards of electrical resistance, 19th B.A. Report (1892), appendix IV. (See ref. 3).

11. FEUSSNER and LINDECK, Die elektrischen normal-draht-widerstande der Physikalisch-Technischen Reichsanstalt, *Wiss, Abh. der P.T.R.* 1895, **2**, 503.

12. JAEGER and LINDECK, Ueber die konstanz von normal-widerstanden aus manganin, *Zeits. fur Instrumentenkunde*, 1898, **18**, 97; 1908, **26**, 15.

13. F. B. SILSBEE, Establishment and maintenance of the electrical units, *N.B.S. Circular* C475 (1949). See p. 6.

14. E. B. ROSA, A new form of standard resistance, Bul. BS, 1908-9, **5**, 413, S107.

15. M. A. HUNTER and J. W. BACON, Manganin, *Trans. Am. Electrochem. Soc.*, 1919, **36**, 323.

16. F. E. BASH, Manufacture and electrical properties of constantan, *Am. Inst. Mining and Met. Engrs.*, 1921, **64**, 239.

17. F. E. BASH, Manufacture and electrical properties of manganin, *Am. Inst. Miningand Met. Engrs.*, 1921, **64**, 269.

18. NORMAN B. PILLING, Some electrical properties of copper-nickel-manganese alloys, *Trans. Am. Electrochem. Soc.*, 1925, **48**, 171.

19. J. O. LINDE, Elektrische eigenschaften verdunnter mischkristallegierungen, *Ann. d. Physik*, 1932, **407**, 219.

(19649)

20. J. O. LINDE, Elektrische widerstandseigenschaften der verdunnten legierungen des kupfers, silbers und goldes. *Gleerupska Univ.-Bokhandeln*, Lund, Sweden, (1939).

21. P. W. BRIDGEMAN, The electrical resistance of metals under pressure, *Proc. Am. Acad. Arts & Sci.*, 1917, **52**, 537.

22. J. L. THOMAS, A new design of resistance standard, *BS J. Research*, 1930, **5**, 295, RP 201.

23. J. L. THOMAS, Stability of double-walled manganin resistors, *BS J. Research*, 1946, **36**, 107, RP 1692.

24. J. L. THOMAS, Gold-chromium resistance alloys, *BS J. Research*, 1934, **13**, 681, RP 737.

25. J. L. THOMAS, Gold-cobalt resistance alloys, *BS J. Research*, 1935, **14**, 589, RP 789.

26. J. L. THOMAS, Electrical-resistance alloys of copper, manganese, and aluminium, *BS J. Research*, 1936, **16**, 149, RP 863.

27. T. B. GODFREY, Further data on gold-chromium resistance wire, *BS J. Research*, 1939, **22**, 565, RP 1206.

28. ALFRED SCHULZE, Elektrische und thermische untersuchungen an manganin, *Physik. Zeits.* 1937, **38**, 598, **39**, 300 (1938).

29. ALFRED SCHULZE, Uber die gold-chrom-widerstandslegierung fur normalwiderstande, *Wiss. Abh. der P.T.R.* **24**, 51 (1940), 1940, **24**, 51.

30. ALFRED SCHULZE, Uber widerstandswerkstoffe fur normalwidetstande, *Wiss. Abh. der P.T.R.* 1940, **24**, 91.

31. ALFRED SCHULZE, Uber die verwendung von silberlegierungen als widerstandswerkstoffe, *Wiss. Abh. der P.T.R.*, 1941, **25**, 1 1941, **25**, 121.

32. New alloy has improved electrical resistance properties, *Materials and Methods*, 1948, **28**, (No.2), 62.

33. C. P. MARSDEN, Jr., Three design considerations in selecting resistance alloys, *Elec. Mfg.*, 1948, **42** (No.2), 116.

(19649)

THE ERROR DUE TO THE PELTIER EFFECT IN DIRECT-CURRENT MEASUREMENTS OF RESISTANCE, C. G. Kirby and M. J. Laubitz (National Research Council of Canada, Division of Physics, Ottawa, Canada), Metrologia 9, 103-106 (1973).

The recent development of ac bridges for precise resistance determinations has brought on the not altogether unexpected discovery of significant differences between dc and ac measurements. In this article, we discuss one such difference, observed in germanium resistance thermometers, and show that it can be unequivocally ascribed to the Peltier effect, the dc measurement in this case being in error. This conclusion is based on a thermal model of the resistor which predicts accurately the magnitude and frequency variation of the observed effect, both for 2- and 4-terminal measurements. The applicability of this model to other devices is briefly discussed.

RESISTANCE COMPARISONS AT NANOVOLT LEVELS USING AN ISOLATING CURRENT RATIO GENERATOR, L. Crovini and C. G. M. Kirby (National Research Council of Canada, Ottawa, Canada), Rev. Sci. Instrum. 41, 493-497, (1970).

A circuit has been developed for the generation of isolated current having precisely defined ratios. It can be used to compare resistances with accuracies up to 0.03 ppm and with sensitivities as low as 1 nV. When comparisons are made using low frequency currents, thermal emf's are eliminated. Several variations of the circuit which can be made easily in the laboratory are described.

CAPACITORS AND INDUCTORS

Transportable 1000 pF Standard for the NBS Capacitance Measurement Assurance Program

George Free and Jerome Morrow

Electrical Measurements and Standards Division
National Bureau of Standards
Washington, DC 20234

U.S. DEPARTMENT OF COMMERCE, Malcolm Baldrige, Secretary
NATIONAL BUREAU OF STANDARDS, Ernest Ambler, Director

Issued October 1982

National Bureau of Standards Technical Note 1162
Natl. Bur. Stand. (U.S.), Tech. Note 1162, 15 pages (Oct. 1982)
CODEN: NBTNAE

U.S. GOVERNMENT PRINTING OFFICE
WASHINGTON: 1982

For Sale by the Superintendent of Documents, U.S. Government Printing Office, Washington, D.C. 20402.
Price $2.75
(Add 25 percent for other than U.S. mailing.)

TRANSPORTABLE 1000 pF STANDARD FOR THE NBS CAPACITANCE MEASUREMENT ASSURANCE PROGRAM

George Free and Jerome Morrow
Electrical Measurements and Standards Division
National Bureau of Standards
Washington, DC 20234

Abstract

A capacitance transport standard has been constructed for use in the National Bureau of Standards Measurement Assurance Program. The transport standard was designed so that variations in ambient temperature and mechanical shock would have a minimal effect on the value of the internal reference capacitors. A significant improvement in stability of 1000 pF capacitors during shipment and in the laboratory has been achieved through this design.

Key words: calibration; measurement assurance; measurement assurance programs; reference standards; standard capacitors; standard qualification; transfer standards.

Introduction

The National Bureau of Standards Measurement Assurance Program (MAP) in electrical units has been in existence for several years. In this program, NBS transport standards are shipped to customer laboratories and calibration of the customer's reference standards is done in place. The accuracy of the calibration procedure depends on the degree of knowledge of the value of the NBS transport standard while it is at the customer's laboratory; this is optimized by analysis of measurements made at NBS before and after the period of time the standard is at that laboratory. If the value of the transfer standard is known accurately, the advantages to the laboratory are threefold: reduction of down-time due to the absence of reference standards, greater confidence in the values of laboratory standards, and documentable verification of the customer's measurement process through the test procedure.

For the capacitance MAP, it was necessary to develop a transport standard which would behave predictably over an extended period during which the internal capacitors would be subjected to both mechanical and thermal shock. Due to customer needs, the transport standard would have to be at the 1000 pF level (the most common reference standard in most laboratories).

At the 1000 pF level, the most stable, commercially-available standards are nitrogen dielectric capacitors. The values of these capacitors vary due to temperature (with coefficients of about 2 ppm/^{o}C), temperature hysteresis, and mechanical stress. The reduction of instability from these sources were planned through design of the transport box and minor modifications to commercially available capacitors.

The goals for the construction of the transport package were as follows:

- The package should provide a transportable temperature controlled environment with a maximum departure from nominal temperature of 0.01 ^{o}C under normal laboratory conditions.

- The package should provide for a minimum amount of change due to handling.

- The package should be of simple design and construction so that it may be duplicated by laboratories interested in increasing the stability of their standards.

Construction

The most important limitation in the performance of the transport standard is the quality of the capacitor used. Tests were devised by which the mechanical stability of capacitors could be systematically evaluated (1) and the results were used to select the four "best" capacitors available for inclusion in the standard. The method of testing and the results are discussed in the Appendix. These tests were also used to evaluate 10 pF and 100 pF standards.

Before placing the capacitors in the transport box, their outer enclosures were removed. Since the stability of the trimmer in these capacitors is unknown and difficult to analyze, it was also removed and electrical connection to the inner enclosure was made through a special head. The head was designed to eliminate stray capacitance between the leads coming out of the capacitor and to guarantee good electrical contact between the cable shield and the enclosure, thus making the capacitor more closely meet the requirements for three-terminal devices with a negligible amount of stray capacitance.

The capacitors were placed in an aluminum box (see Figure 1) 25.4 cm (10 inches) on a side, with sufficient soft-sponge packing material surrounding them so that they were effectively fixed in position with no rigid connections. The capacitors were insulated from each other by plastic sheets, thereby reducing the possibility of electrical ground loops during measurements. Heaters, consisting of many turns of magnet wire, were positioned to cover the total surface of each side of the box and were attached to the box with adhesive tape (adhesive agent on both sides). Additional tape (of the type used to seal heating air ducts) was tightly wrapped on top of the heater wires to assure good thermal contact with the box and prevent motion of the wire. An outer box was made out of plastic and wood, its dimensions allowing for at least 7.6 cm (3 inches) of insulation between it and the inner box. The aluminum box was then foamed in place with rigid polyurethane. Coaxial leads from the inner box to the outside were placed so as to assure good thermal contact with the inside aluminum box, reducing temperature variations transmitted through the leads. The coaxial leads are RG316/U 50 ohm cable. The small cross-section of metal in the inner conductor and shielding reduces the heat path to the outside.

The temperature control circuit for the standard (see Figure 2) consists of a thermistor bridge and a very simple operational amplifier circuit. The temperature-sensitive components of the control circuit (resistors and amplifier) are placed inside the aluminum box in a section separated from the capacitors by an aluminum plate. The less sensitive components, such as the power supply and the power transistor for the heating coils, are in a small control box separate from the transport standard. The control thermistor is wrapped in aluminum foil and placed under the adhesive tape between the heater wires and the aluminum enclosure.

A temperature measuring device consisting of a thermistor bridge with variable decade resistors in one arm was constructed. The thermistor was placed on top of and taped to one of the capacitors.

The control circuit was designed to operate from 110 VAC or a 12 VDC primary power source. When operated from a DC power source, the circuit needs an additional $\pm$15 VDC battery to provide current for the operational amplifier.

Performance

As the standard was too large to fit in available environmental chambers, the temperature-variation performance could be studied only with respect to changes in the laboratory environment. The temperature variation tests were carried out over a relatively narrow range of temperatures.

For a temperature range of 3.9 ^{o}C in the laboratory, i.e., from 19.9 ^{o}C to 23.8 ^{o}C, the measured variation in box temperature was 0.011^{o}C while, for a temperature variation of 1.3 ^{o}C from 19.9 ^{o}C to 21.2 ^{o}C, the measured variation was 0.005^{o}C. These two tests were carried out in different laboratory environments.

Tests correlating change in capacitance with temperature variations were first carried out using the measurement system described in (1). The standards were intercompared with 100 pF fused silica dielectric capacitors which were in a temperature controlled air bath. The small apparent changes in value of the transport standard could not definitely be attributed to the transport standard alone due to possibilities of error in the rest of the system.

The reported measurements of temperature dependence were obtained using the measurement system described in (2) and 100 pF quartz dielectric capacitors in an oil bath as the reference standard. The results of the stability test are shown in Table 1. The period during which measurements were made was one month (31 days). There were 17 intercomparisons and the time-of-day of measurement was varied in order that the full range of laboratory temperatures, i.e., 19.9 to 21.1 ^{o}C, was included. The

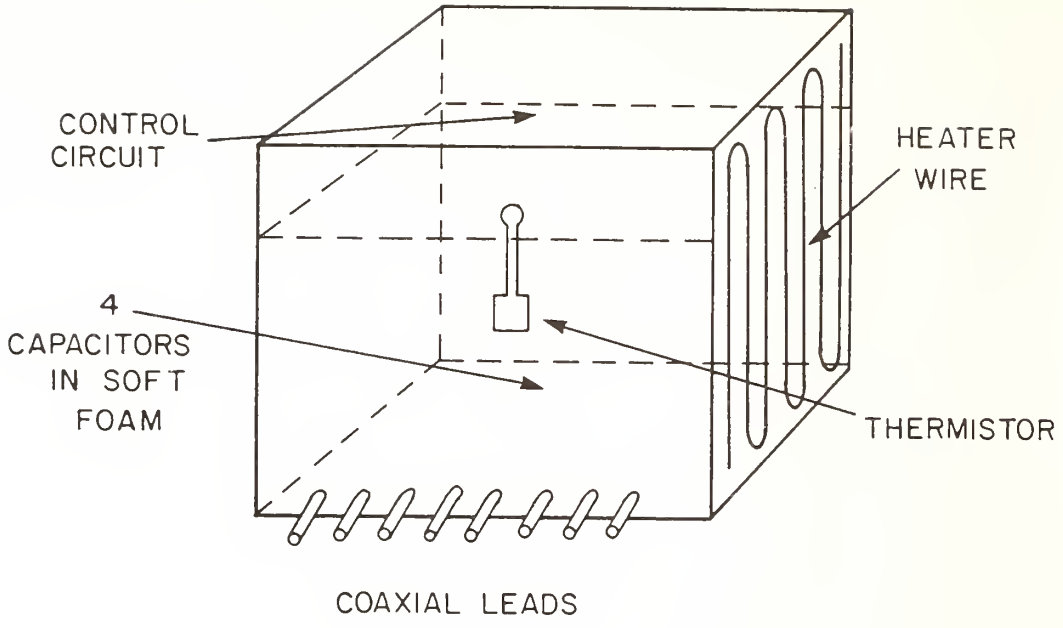

FIG. 1 Schematic diagram of the aluminum box for housing the 1000 pF transportable standard.

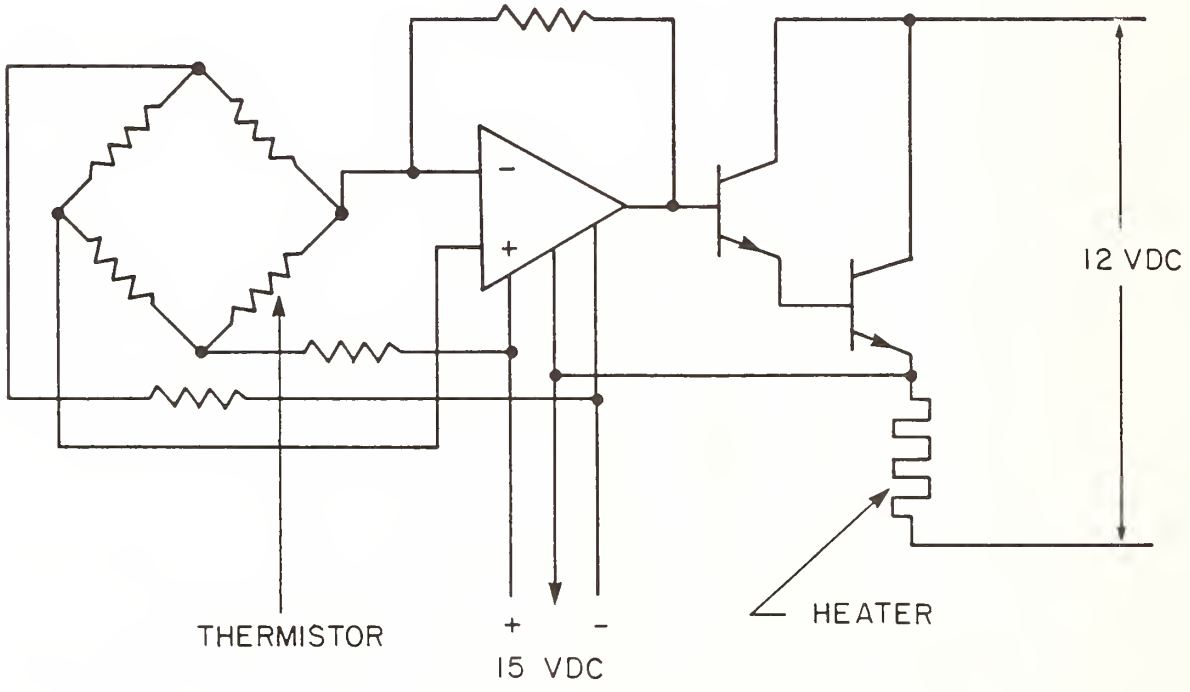

FIG. 2 Schematic diagram of heater control circuit.

resolution of the measuring system is ±0.001 ppm. The range of capacitance change, C(MAX)-C(MIN), for each standard is given in the first row of the table.

Table 2 is based upon the same data as Table 1 but the measured values are represented by the equation $y = \alpha + \beta t + \gamma \Delta T$ using a least squares fit. In this equation y is the departure from the nominal capacitance value (in ppm) after a time t (in days), and for the temperature increment ΔT (degrees celsius) which is the departure of the box temperature from the nominal control temperature, or $\Delta T = T_{Box} - 30.00\ ^{o}C$. The paramters α, β, and γ are, respectively, the residual capacitance offset (ppm), the daily drift rate (ppm/day), and the temperature coefficient (ppm/^{o}C).

Comparisons of the residual standard deviation σ(RES) with the standard deviation of an individual measurement σ(Ind. Meas.) of Table 1 indicates that this equation fits the performance of the capacitors quite well. The range of temperature variations of the standards during this test was 0.005 ^{o}C. The similarity of σ (MEAN) in Table 1 and σ(RES) in Table 2 indicates that over a short period of time (one month) the values of the standards could be calculated either from the mean of a set of measurements or by using a linear fit.

The methods used to test mechanical stability of individual capacitors could not be applid to the entire transport standard because of its size and weight. Mechanical stability was determined through actual shipment of the box to laboratories. In this evaluation the capacitors were shipped five times to various parts of the United States. All shipping was by air freight with hand carried delivery service to and from the airports. The transport standard was shipped under battery power for temperature control. No care was taken to ensure that the shipping container received special handling by the airlines. With data from shock recorders on similar boxes it was surmised that the container might well experience forces exceeding 45g during transport. Table 3 indicates the effects of travel on the standards.

The numbers given are absolute values, the sign of the change being disregarded. Actual changes were both positive and negative, thus the change in the box mean is generally less than the changes in individual capacitors. The columns indicate changes due to one complete round trip. Each change was calculated as $C_B - C_A$ = change, where C_B is the value before shipment and C_A is the value after shipment. The last row of the table indicates the changes $C_B - C_A$, where C_B is the value of each standard at the start of testing and C_A is the value of each capacitor nine months later. As a general rule, the larger changes occurred in all capacitors on the same transfer.

TABLE 1.

Parameter	Capacitors A1 (ppm)	A2 (ppm)	A3 (ppm)	A4 (ppm)	Mean (ppm)
Range	0.022	0.080	0.064	0.036	0.046
σ(Individual Measurement)	0.009	0.020	0.020	0.012	0.015
σ(Mean)	0.003	0.007	0.007	0.004	0.005

TABLE 2.

DAILY VALUES FITTED TO $\alpha + \beta t + \gamma \Delta T$

	A1	A2	A3	A4
α(ppm)	-147.290	-270.115	-325.593	-172.455
β(ppm/day)	-0.0012	-0.0030	-0.0027	-0.0021
γ(ppm/^{o}C)	3.2667	2.8826	2.6822	3.8676
σ(RES)(ppm)	0.006	0.004	0.006	0.004

t = time in days $\qquad \Delta T = T_{box} - 30.00\ ^{o}$

TABLE 3.

CHANGES IN CAPACITANCE DUE TO SHIPMENT

	A1 (ppm)	A2 (ppm)	A3 (ppm)	A4 (ppm)	Mean (ppm)
Min. Change	0.071	0.047	0.030	0.020	0.009
Max. Change	0.388	0.162	0.209	0.111	0.180
Ave. Change	0.194	0.104	0.083	0.061	0.069
Change for 9 Months	0.123	0.426	0.193	0.081	

In one shipment, capacitor A3 changed 1.24 ppm. This value was not included in Table 3, since in a normal MAP procedure, this change would be sufficient to cause this capacitor to be excluded from all calculations.

Conclusion

Calibrations using the transport standard appear to offer significant improvement over the normal method of shipping capacitors to NBS. At present, a 5-ppm uncertainty in value must be assigned to capacitors shipped to NBS for calibration; a major portion of this uncertainty is an allowance for changes due to shipping. Using the transport standard, this uncertainty can be reduced by approximately one order of magnitude.

There are several improvements that will be made on future transport standards. For example, the enclosure is too heavy and bulky for easy handling. Thus a reduction in both weight and size will be attempted.

The capacitors used were not initially tested for frequency response. Since they have varying degrees of frequency dependence, their range of applicability is limited. The conductances of these capacitors are higher than normal indicating that greater care must be taken in the assembly of the package on future versions.

The temperature coefficients and drift rates of the capacitors were calculated for a period of time between shipments. A further study will be carried out to see if these coefficients remain unchanged over the time interval of two measurement periods with shipment of the standards in between. If the coefficients do remain constant, a further reduction in the uncertainty of predicted values for the standards will be justified.

Acknowledgements

The authors would like to thank Mr. Robert E. Long and Mr. Charles Levy for their help in the construction and testing of the transport standard.

References

(1) Cutkosky, Robert D. Capacitance bridge-NBS type 2. Nat. Bur. Stand. Report No. 7103, 1961.

(2) Cutkosky, Robert D. Actual and passive direct reading ratio sets for comparison of audio-frequency admittances. J. Res. Nat. Bur. Stand., 68(4):227-236; 1964 October. Vol. 68C, No. 4, October 1964.

Appendix

Capacitors are exposed to a variety of mechanical shocks during use in the laboratory or during shipment. Great care in packing standard capacitors will, at most, reduce the intensity of the shock incurred in shipment; in the laboratory, a capacitor receives some degree of shock every time it is moved. Capacitors of the type used in the transport box have parallel plates fixed in position by support rods. Mechanical shock tends to change the geometry of the plates or the position of the plates relative to the enclosure.

The mechanical stability of the standards was of utmost importance since it was intended that they be shipped from six to ten times annually. Therefore, six tests of stability were devised to select those standards most suitable for shipment. Since only a limited number of capacitors were available as candidates for testing the transport box, absolute limits of performance could not be established. Instead, those capacitors of the available groups which appeared to be "best" were chosen.

The six tests used were designated as ORIENTATION, SMALL ANGLE, TILT, SOFT KNOCK, HARD KNOCK and DROP TESTS. The test protocols and the changes of capacitance measured are outlined below.

ORIENTATION: The capacitor is measured while in an upright (vertical) position and while in the four posible horizontal positions. The maximum difference with all measurements considered is determined. Any change greater than 10 ppm is usually evidence of a faulty capacitor. This test was used to determine gross instability.

SMALL ANGLE: The capacitor is measured in the upright position and on a 3^{o} inclined plane. Four measurements are made on the inclined plane with the capacitor being rotated 90^{o} (around the vertical axis) after each measurement. The maximum difference with all measurements considered is determined. Since most laboratory tables are not exactly horizontal, the offset from horizontal would cause error if the capacitor were excessively sensitive. Differences of several tenths of a ppm were evident in some capacitors. Only those with a negligible change were used in the box.

TILT: After measurement of capacitance in the upright position the capacitor is tilted 90^{o} and returned to the upright position for the second measurement. The test is repeated for each side and the bottom of the capacitor, i.e., five tests in all. The net difference $C(UPRIGHT)_1 - C(UPRIGHT)_2$ is determined. Since changes with position should be completely reversible for a good capacitor, any measurable net change was cause for rejection.

SOFT KNOCK: The capacitor is measured before and after being struck by the head of a pendulum. The head is covered with

soft rubber. The force generated by the pendulum is roughly equivalent to that generated by a mild wrist action motion of the human hand. The force is in a horizontal plane and it is applied to the four sides and corners of the capacitor. The differences C(BEFORE) - C(AFTER) are determined. A minimum change was the criterion for selection of capacitors from those available as candidates.

HARD KNOCK: The test procedure is the same as that for SOFT KNOCK with the exception that the soft rubber head is replaced by a hard plastic head. In the SOFT KNOCK test the force has a relatively long duration with a gaussian-like shape; in the HARD KNOCK the force tends to be impulsive with a more abrupt rise and fall.

DROP TEST: The capacitor is measured in the upright position. A 2" plate is inserted under one side of the capacitor raising that side off the table. The plate is quickly removed allowing the capacitor to drop back in its initial upright position and the capacitance is measured again. Differences $C(UPRIGHT)_1$ - $C(UPRIGHT)_2$ are determined for tests repeated for the four sides of the capacitor. The applied impulse is in the vertical direction. Capacitors were chosen on the basis of minmum change in this test.

The results of these six tests for a large number of 1000 pF capacitors are shown in Figures 3-8. Many capacitors not specifically considered for the transport standard are included and, therefore, these graphs indicate the general performance of the 1000 pF capacitors.

The graphs are histograms for the various tests. The Y axis gives the percentage of capacitors which fall into specific ranges of maximum change given by the X axis. The X axis has a limit of either 20 ppm (Figure 3) or 2 ppm (Figures 4-8). The tests revealed a few capacitors with changes far beyond these limits. In these cases the position of the mark on the graphs relative to the limiting value indicate only that they are beyond the limit and are not intended to show the actual change measured.

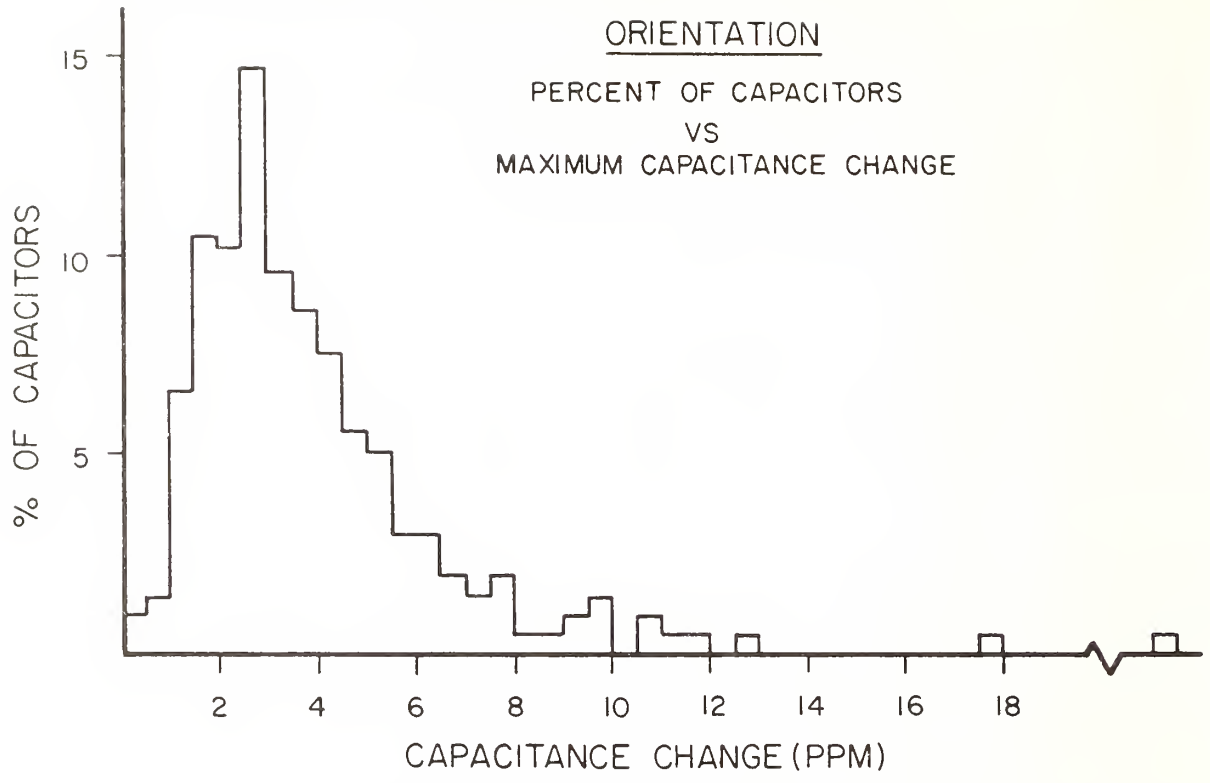

FIG.3 Histogram of the fractional numbers of capacitors for which different values of maximum capacity change were caused by the Orientation Test.

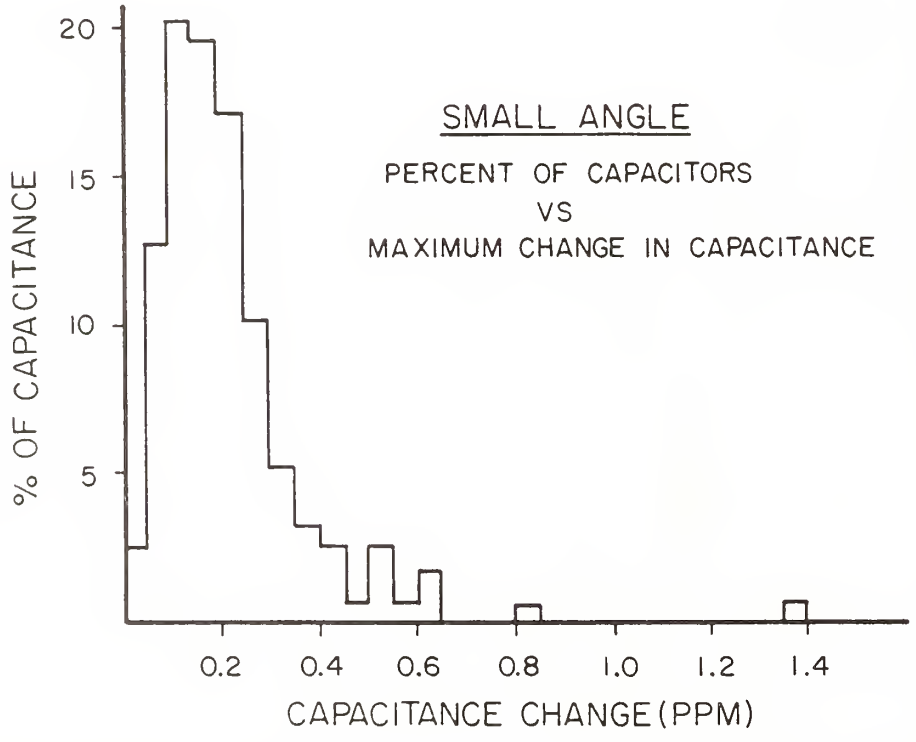

FIG.4 Histogram of the fractional numbers of capacitors for which different values of maximum capacity change were caused by the Small Angle Test.

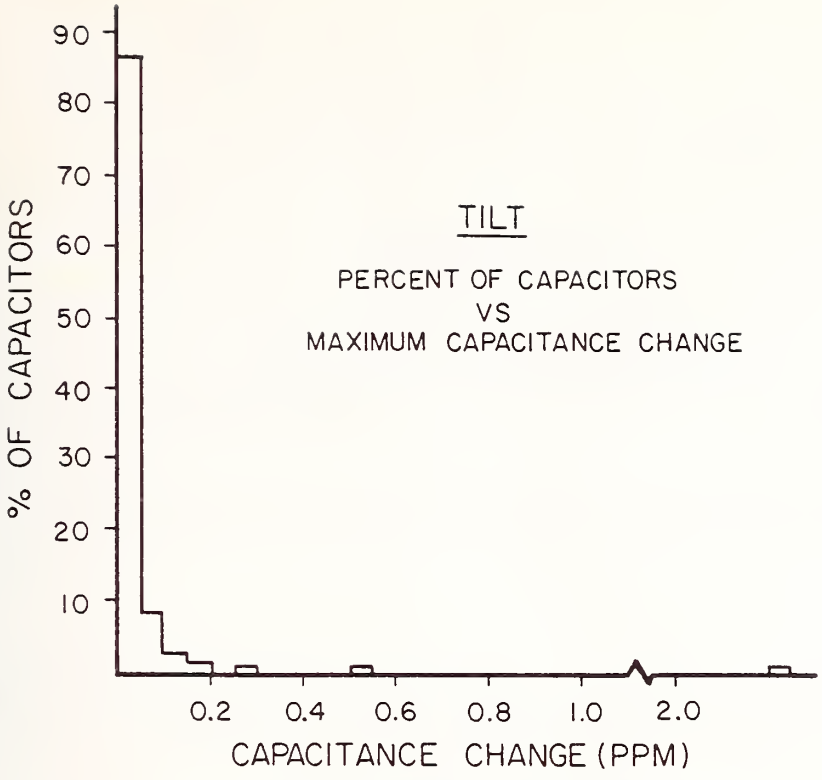

FIG. 5 Histogram of the fractional numbers of capacitors for which different values of capacity change were caused by the Tilt Test

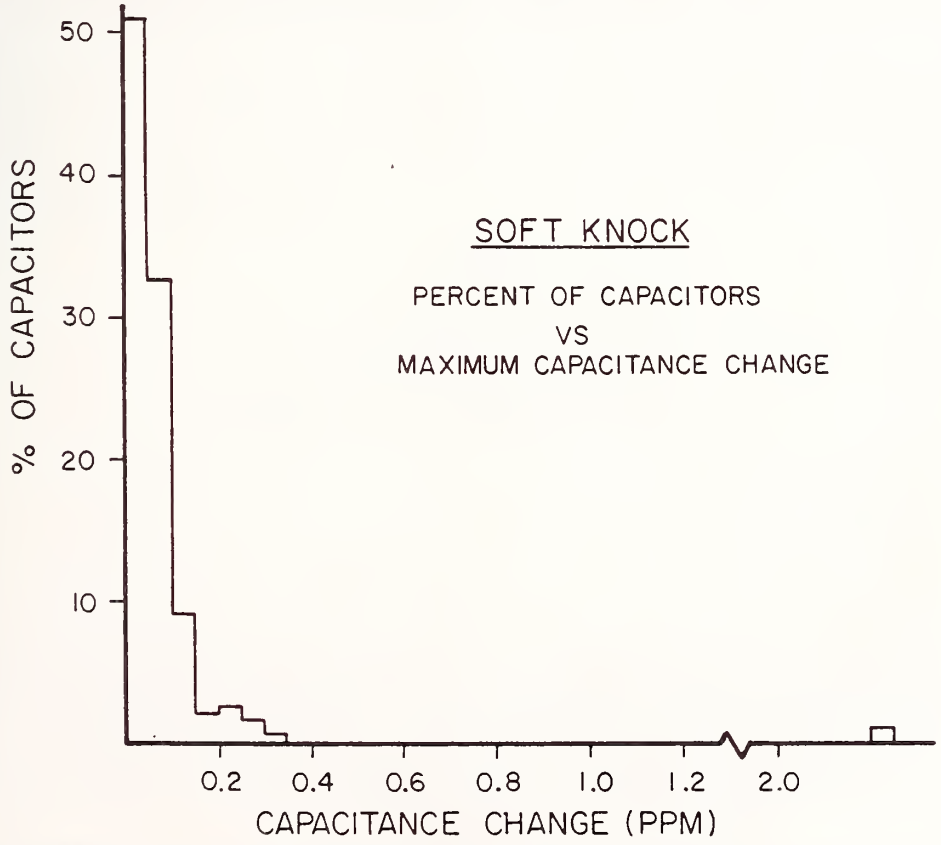

FIG. 6 Histogram of the fractional numbers of capacitors for which different values of maximum capacity change were caused by the Soft Knock Test.

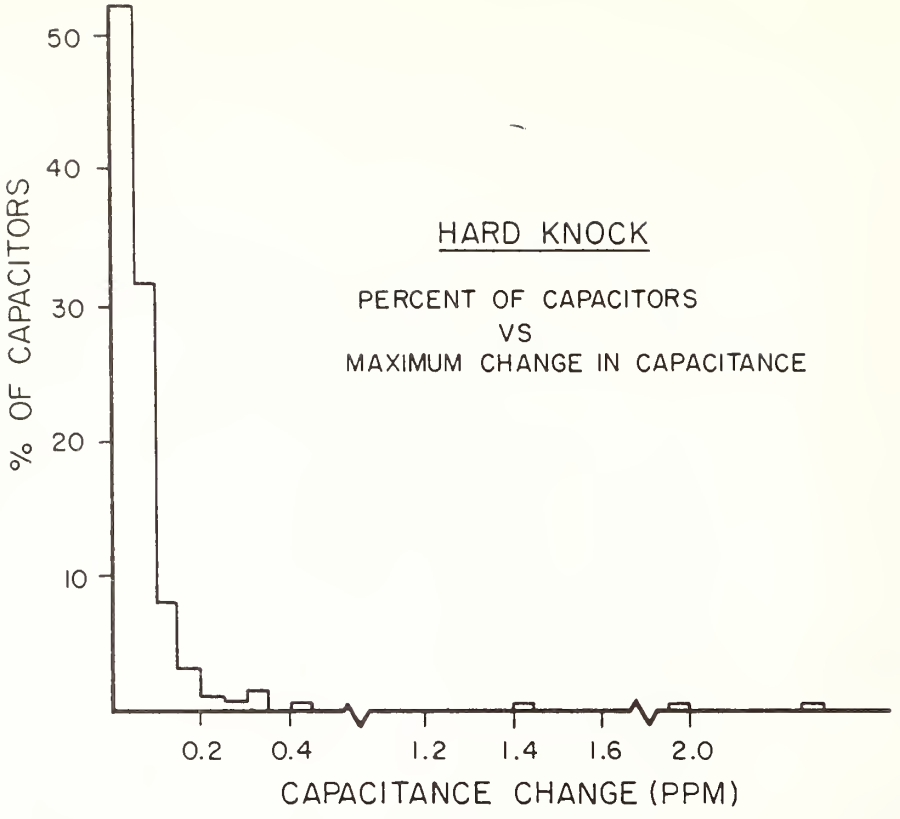

FIG. 7 Histogram of the fractional numbers of capacitors for which different values of maximum capacity change were caused by the Hard Knock Test.

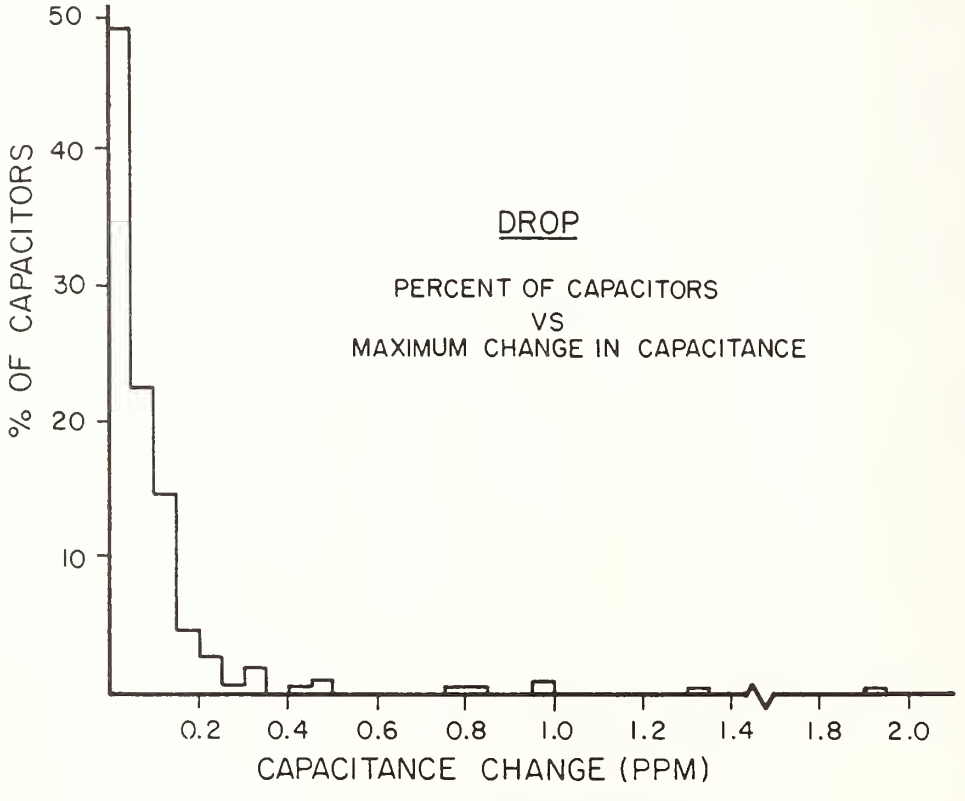

FIG. 8 Histogram of the fractional numbers of capacitors for which different values of maximum capacity were caused by the Drop Test.

NBS-114A (REV. 2-8C)

U.S. DEPT. OF COMM. BIBLIOGRAPHIC DATA SHEET (See instructions)	1. PUBLICATION OR REPORT NO. NBS TN 1162	2. Performing Organ. Report No.	3. Publication Date October 1982

4. TITLE AND SUBTITLE

Transportable 1000 pF Standard for the NBS Capacitance Measurement Assurance Program

5. AUTHOR(S)
George Free and Jerome Morrow

6. PERFORMING ORGANIZATION (If joint or other than NBS, see instructions)

NATIONAL BUREAU OF STANDARDS
DEPARTMENT OF COMMERCE
WASHINGTON, D.C. 20234

7. Contract/Grant No.

8. Type of Report & Period Covered
~~XXXX~~ Final

9. SPONSORING ORGANIZATION NAME AND COMPLETE ADDRESS (Street, City, State, ZIP)

same as #6

10. SUPPLEMENTARY NOTES

☐ Document describes a computer program; SF-185, FIPS Software Summary, is attached.

11. ABSTRACT (A 200-word or less factual summary of most significant information. If document includes a significant bibliography or literature survey, mention it here)

A capacitance transport standard has been constructed for use in the National Bureau of Standards Measurement Assurance Program. The transport standard was designed so that variations in ambient temperature and mechanical shock would have a minimal effect on the value of the internal reference capacitors. A significant improvement in stability of 1000 pF capacitors during shipment and in the laboratory has been achieved through this design.

12. KEY WORDS (Six to twelve entries; alphabetical order; capitalize only proper names; and separate key words by semicolons)
calibration; measurement assurance; measurement assurance programs; reference standards; standard capacitors; standard qualification; transfer standards.

13. AVAILABILITY

☒ Unlimited
☐ For Official Distribution. Do Not Release to NTIS
☒ Order From Superintendent of Documents, U.S. Government Printing Office, Washington, D.C. 20402.
☐ Order From National Technical Information Service (NTIS), Springfield, VA. 22161

14. NO. OF PRINTED PAGES
15

15. Price
$2.75

USCOMM-DC 6043-P80

Testing to Quantify the Effects of Handling of Gas Dielectric Standard Capacitors

Charles R. Levy

Electrical Measurement and Standards Division
Center for Absolute Physical Quantities
National Measurement Laboratory
National Bureau of Standards
Washington, DC 20234

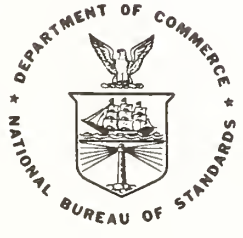

U.S. DEPARTMENT OF COMMERCE, Malcolm Baldrige, Secretary
NATIONAL BUREAU OF STANDARDS, Ernest Ambler, Director

Issued October 1982

CONTENTS

LIST OF FIGURES

ACKNOWLEDGMENT

I acknowledge with appreciation Dr. Arthur O. McCoubrey for his expertise, time, and effort in the editing of this paper.

TESTING TO QUANTIFY THE EFFECTS OF HANDLING OF GAS DIELECTRIC STANDARD CAPACITORS

by Charles R. Levy

1. Abstract

A test method known as the "Handling and Stability Test" is currently being used at NBS as part of the requirement for the five-part-per-million calibration of gas dielectric standard capacitors. This test is used to achieve qualitative information on the effects of mechanical shock from shipping and handling on standard capacitors and to rank them quantitatively with respect to these effects.

2. Introduction

Nitrogen dielectric capacitors are used as the reference standards for measurements of capacitance in many metrology laboratories in the United States, as well as in many other parts of the world. Since the most common standard used has a capacity of 1000 picofarads, this report is based on tests of capacitors of this value, but an equivalent test is performed on 10 and 100 pF capacitors as well.

Recognizing the range of mechanical shocks which these capacitors may receive in service or in transport, NBS devised tests to confirm the mechanical integrity of the units before calibration and to determine the magnitude of any related effects [1]. Such effects may then be taken into account quantitatively in the systematic error portion of the uncertainty statement. The results of the handling test were also expected to be useful to guide the user concerning changes in capacitance to be expected as a result of transport and normal handling. The use of standard gas filled capacitors in transport service is rapidly becoming a more important basis for the intercomparison of reference standards among calibration laboratories. A similar approach, based upon the use of a compressed gas capacitor (specifically designed for high voltage) in transport service, has also been investigated in connection with the intercomparison of high voltage capacitance measurements [2].

The test procedure has also been used for the development of a very stable, transportable capacitance standard. In particular, the results of these tests were used in the selection of capacitors and in the design of a suitable transport box for shipping the capacitors.

If the procedures described within this paper are used, gas dielectric capacitors not normally shipped to a primary reference facility may be tested to identify possible handling problems that may not otherwise be detected. In some metrology laboratories, step-up or step-down methods are used (3, 4, 6, 7, 8) to compare capacitors having a range of value with a high

quality (e.g., fused silica) reference capacitor. In such cases, the uncertainties assigned to the measurements should include appropriate allowances for capacitance changes associated with normal laboratory handling. The handling test procedures are an effective tool for this purpose and, in those laboratories having the necessary facilities and data analysis skills, there is a significant possibility for reducing the cost of traceability to primary standards. Such cost savings may result from a reduction in the number of reference standards in inventory to replace those taken out of service for calibration at a remote facility, a reduction of the cost of a larger number of such calibrations, and a reduction in the risks of shipping fragile devices.

3. Methodology

Tests simulating the acceleration forces during various types of handling had to be defined. Some guidance in this regard was obtained from the manufacturers' specifications. On the basis of these tests, specialized equipment, relatively simple in design, was developed by Jerome Morrow and George Free of NBS [1]. This equipment and the procedures used to affect these tests are described in later portions of this document. In addition, dimensions of the equipment are given in Appendix 2 as an aid to those who wish to duplicate it.

The tests which have been developed address many of the common handling problems users may encounter. The test names and their purposes are:

- CONNECTOR TEST - Determines looseness of either or both connectors and associated parts. Also used to determine conductance problems that may be due to poor bonding of the connector to the case of the capacitor standard, poor solder joints, or loose inner pins of the connectors.

- ORIENTATION TEST - Used to determine the change in capacitance due to a ninety-degree rotation of the capacitor from its upright position; i.e., to a position of lying on its side. The capacitor is tested six times, once to each side. Excessive changes may indicate looseness of fasteners within the capacitor housing.

- ANGLE 3 DEGREES - Most lab table surfaces vary from the horizontal and this test was planned [1] on the basis of the estimated worst case in normal calibration laboratory operations considering a survey within NBS. The value of three degrees does not reflect a sampling of other laboratories. The change in measured capacitance allows the user to relate errors to surface differences of lab tables.

- TILT TEST - This test was devised to check for movement of component parts within the capacitor housing that may not be detected by measurement of the standard capacitor in its normal resting position.

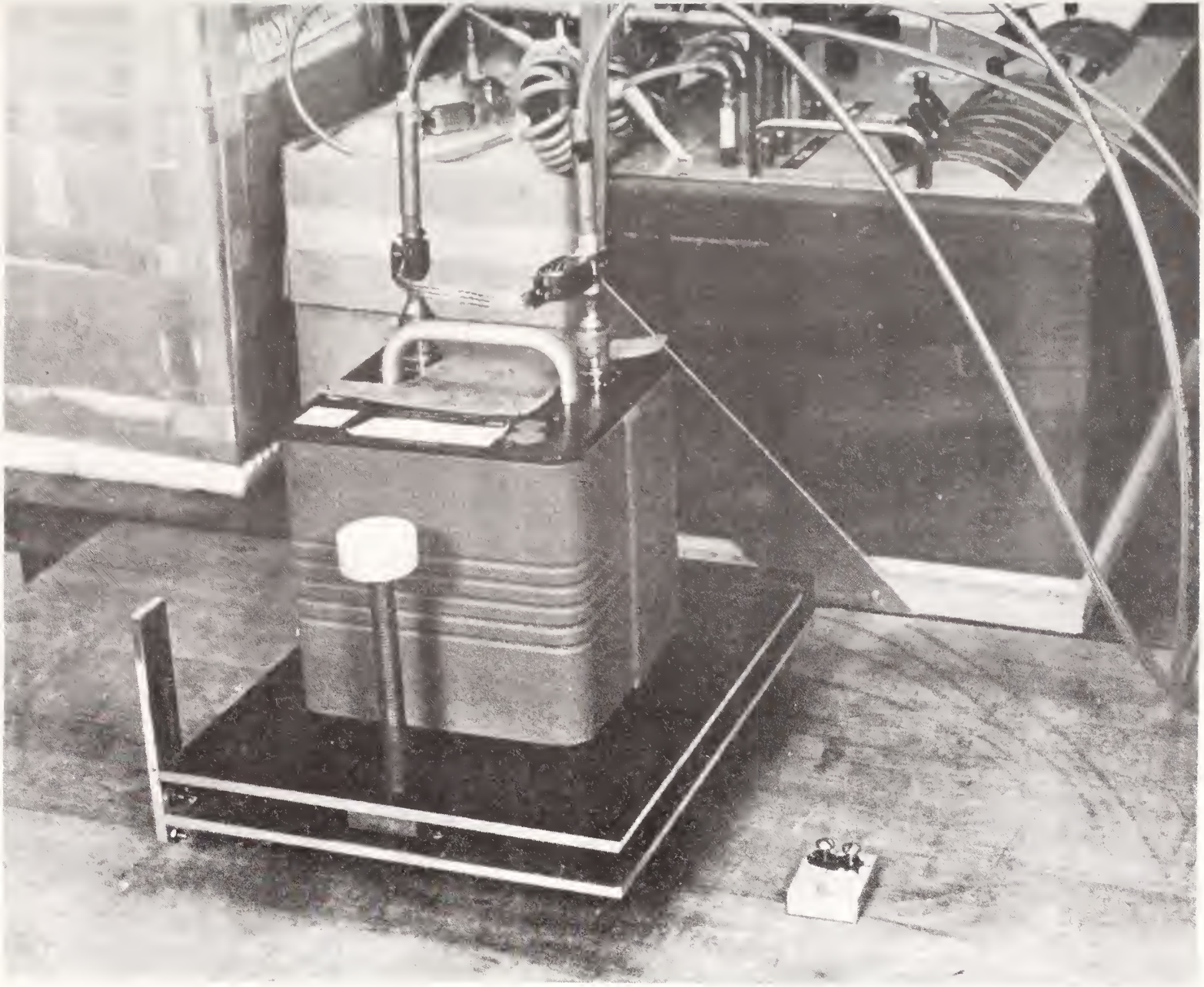

Figure 1. Tilting table for angle test.

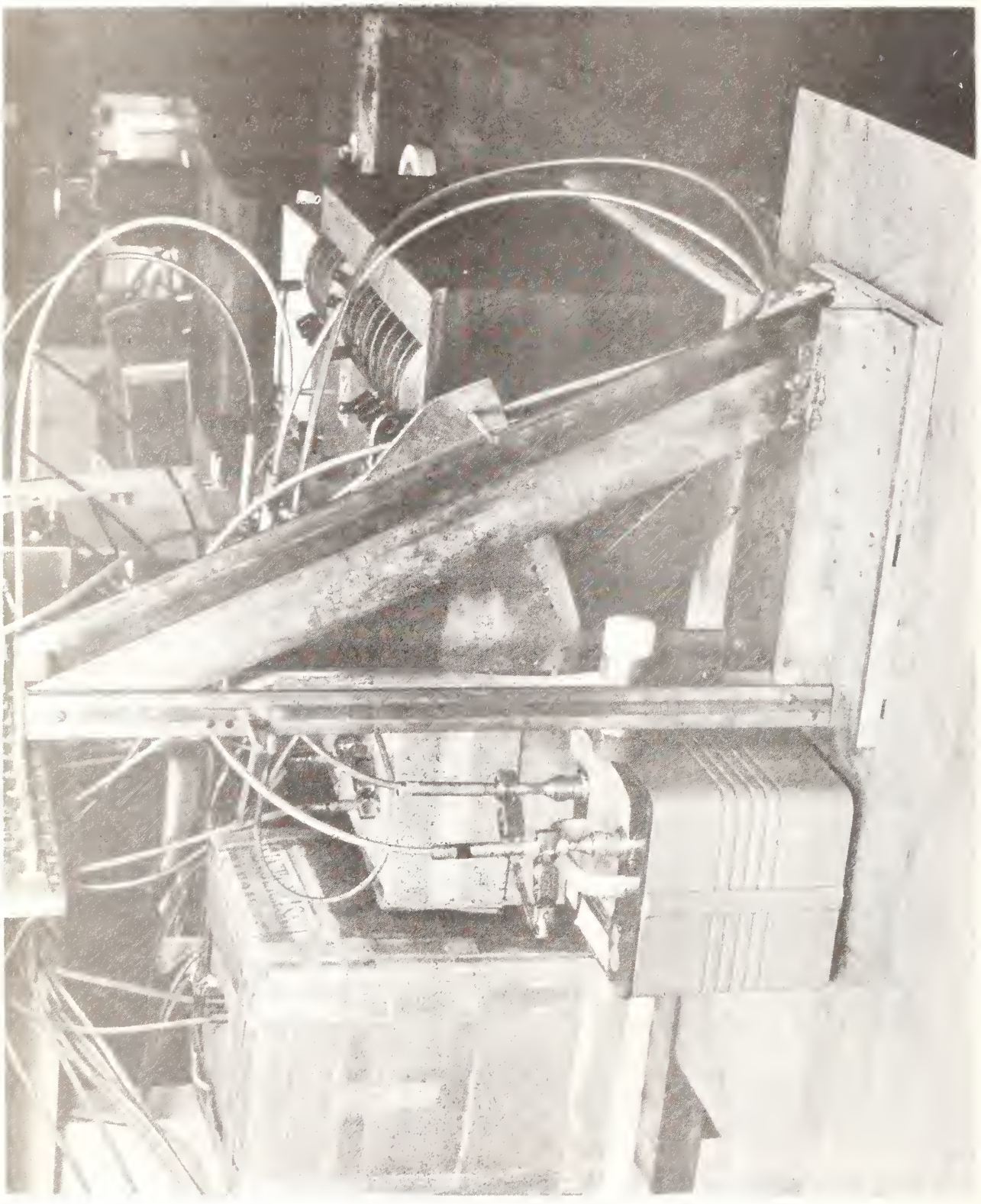

Figure 2. Special fixture for knock test.

- KNOCK SOFT OR HARD TEST - To simulate impacts the standard capacitor receives while in transit or through rough handling in the lab.

- DROP TEST - Designed to simulate the capacitor standard being dropped during transport or excessively rough handling within the users' lab or shipping facility.

4. Equipment Fabricated for Tests

Special equipment was constructed at NBS to accomplish the tests described in this paper. For the convenience of those interested in reproducing this equipment, drawings are included following the text.

For the angle test, a tilting table was built consisting of a platform supporting a hinged plate that can be tilted in half degree increments. Three adjustable feet are used to level the platform. To adjust the angle of the tilting plate, an adjustable screw rod with a large knob is provided as shown in figure 1. This knob can vary the angle of the adjustable plate from zero to three degrees or more as required. However, as an angle of three degrees was selected as the most useful test angle and to save time in adjustment of the elevated table, a removable block with an adjustable screw was fashioned and fixed in the three degree position.

For the knock tests, a stand was made to support a hammer with interchangeable heads. Referring to figure 2, an angle plate on the side of the stand was marked off in increments of 10, 15, 20, 25, and 45 degrees. A stop is used to prevent the hammer from going back further than the desired angle. The plate is movable in the vertical plane to accommodate taller capacitors without affecting the desired striking angle.

The hammer selected was manufactured by the Nicholson File Co., Providence, R. I., and is designated as No. 155. The two detachable heads used are manufactured by J. H. Williams and Company, United Greenfield Division of TRW, Inc., Buffalo, N. Y.; they are designated as HSF-15-SS (soft head) and HSF-15-N (hard plastic head)[1].

In the case of the drop test, a block of wood having dimensions 3.8 cm (1.5 inches) by 8.9 cm (3.5 inches) was used. By inserting this block with the smaller dimension under one of the capacitor sides and then quickly removing it, one drops the capacitor to that side. This test simulates dropping a capacitor contained within an appropriate shipping container on one of its sides or corners.

---

[1] Certain commercial equipment, instruments, or materials are identified in this paper in order to adequately specify the experimental procedure. Such identification does not imply recommendation or endorsement by the National Bureau of Standards, nor does it imply that the materials or equipment identified are necessarily the best available for the purpose.

5. Testing Procedure and Results

To produce uniform results, a systematic method of testing was developed. The results collected over the years have, therefore, consistent significance and may be examined for indications of impending problems, or to predict the direction in which the value of the capacitor may change. They also provide a history of the handling and stability of the standard. Furthermore, the test results can be used to screen capacitors not suitable for precision measurements and to select capacitors for a bank.

A long set of coaxial leads was connected to the test capacitor and to the appropriate transformer tap on the NBS-TYPE 2 Bridge (8, 9). A known capacitance standard was connected to the appropriate tap on the standard side of the bridge as outlined in Table 1.

Table 1. Connection of test unit (unknown) and standard reference capacitor to NBS-type 2 bridge

Test Capacitor		Standard Capacitor	
Nominal Value	Bridge Transformer Tap	Nominal Value	Bridge Transformer Tap
1000 pF	+ 1 Fx	100 pF	- 1 Fs
100 pF	+ 1 Fx	100 pF	- 1 Fs
10 pF	+ 1 Fx	10 pF	- 1 Fs

The procedure adopted at NBS provided for testing the capacitors in a specific order: connector, orientation, angle three degrees, tilt, knock soft, knock hard, and finally the drop test (1). The detailed description of each is given later in this paper.

A uniform method of identifying the sides of the capacitor was established as specified in figure 3. Throughout this report, mention will be made to the reference position. Referring to figure 3, the reference position in the case of all tests except the knock test is that position of the capacitance standard resting upright on the lab table with Side A facing the operator. In the case of the knock tests, Side A faces the striking force (refer also to figure 2).

The long coaxial leads to the capacitor are used to allow for complete movement of the capacitor within the testing area as needed. The capacitor in all tests is connected to the bridge with the capacitance standard selected using Table 1 and in accordance with NBS procedures outlined in references (3), (4), and (5). All measurements start with the capacitor in the reference position and a return to the reference position after all movements associated with a particular test are accomplished.

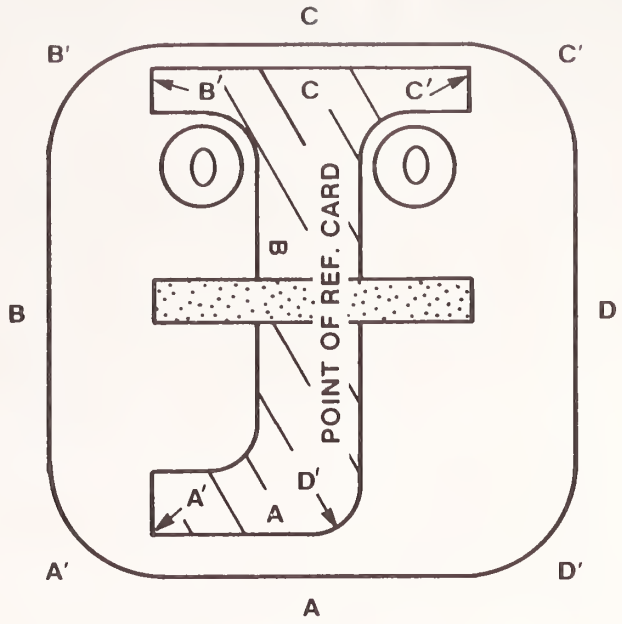

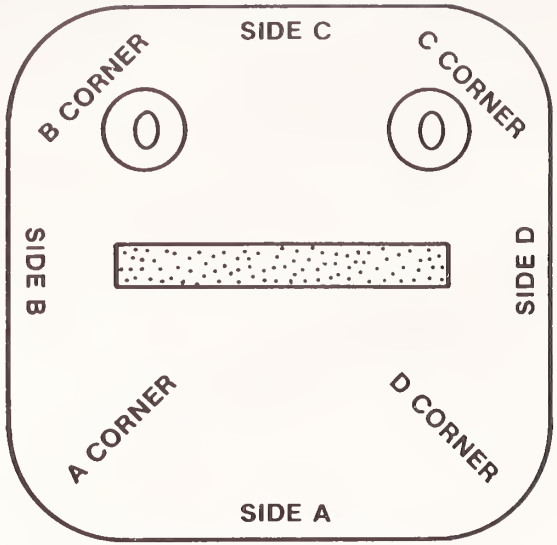

FIGURE 3 REFERENCE POINTS - ALL TESTS

The long leads to the unit under test do not affect the accuracy of these measurements because only changes from the initial values are significant.

6. Connector Test

This test was devised to detect several common problems experienced with capacitors received for calibration at the NBS. Such problems are not necessarily related to transportation effects. Many standards arrive with loose connectors, loose connector inner conductors, or broken or damaged connector parts; for example, a leaf may be missing from the inner conductor of the GenRad 874 connectors, those most commonly used.

Repairs made at the user's lab have been found to create significant problems due, particularly, to improper soldering techniques. Unacceptably high or unstable conductances are often the result of cracked or cold solder joints at the inner pins of the connectors or at points of connection to the capacitor; likewise such faults may be associated with a loose inner conductor in either or both connectors. Modifications of the unit often lead to similar problems (6).

The procedure to determine if a connector defect exists is to apply a gentle force in a rotary fashion to each lead connector. The bridge must be balanced prior to this test. Any changes in capacitance or conductance are noted. Then, with the source oscillator voltage to the bridge off (to avoid transients in the bridge circuits), each connector is disconnected and then reconnected. Repeat, recording any difference observed. Changes greater than 0.05 ppm capacitance or 10^{-5} micromhos conductance are cause for concern. If a problem is apparent, check the points mentioned above to see if improvement can be achieved. In some cases, the rotation procedure will improve the readings without doing anything to the connector; this suggests dirt or oxidation on the connector surfaces or one of the other problems mentioned earlier. In such cases, the test should be repeated in an effort to obtain consistent results.

7. Orientation Test

This test is a good indicator of looseness in the web assembly (refer to figure 4), the case components, and possible problems within the sealed capacitor assembly.

The most frequent fault detected is a loose web assembly (refer to figure 4). Web assembly screws loose by one or more turns have been found to cause changes of several tenths of a part per million. Defects within the sealed capacitor, such as strains and mechanical displacement of the capacitor plates, may also be detected (6).

The procedure for this test is quite simple. The test capacitor is first placed with Side A facing the operator (refer to figure 3) and the capacitance bridge is balanced. This is the

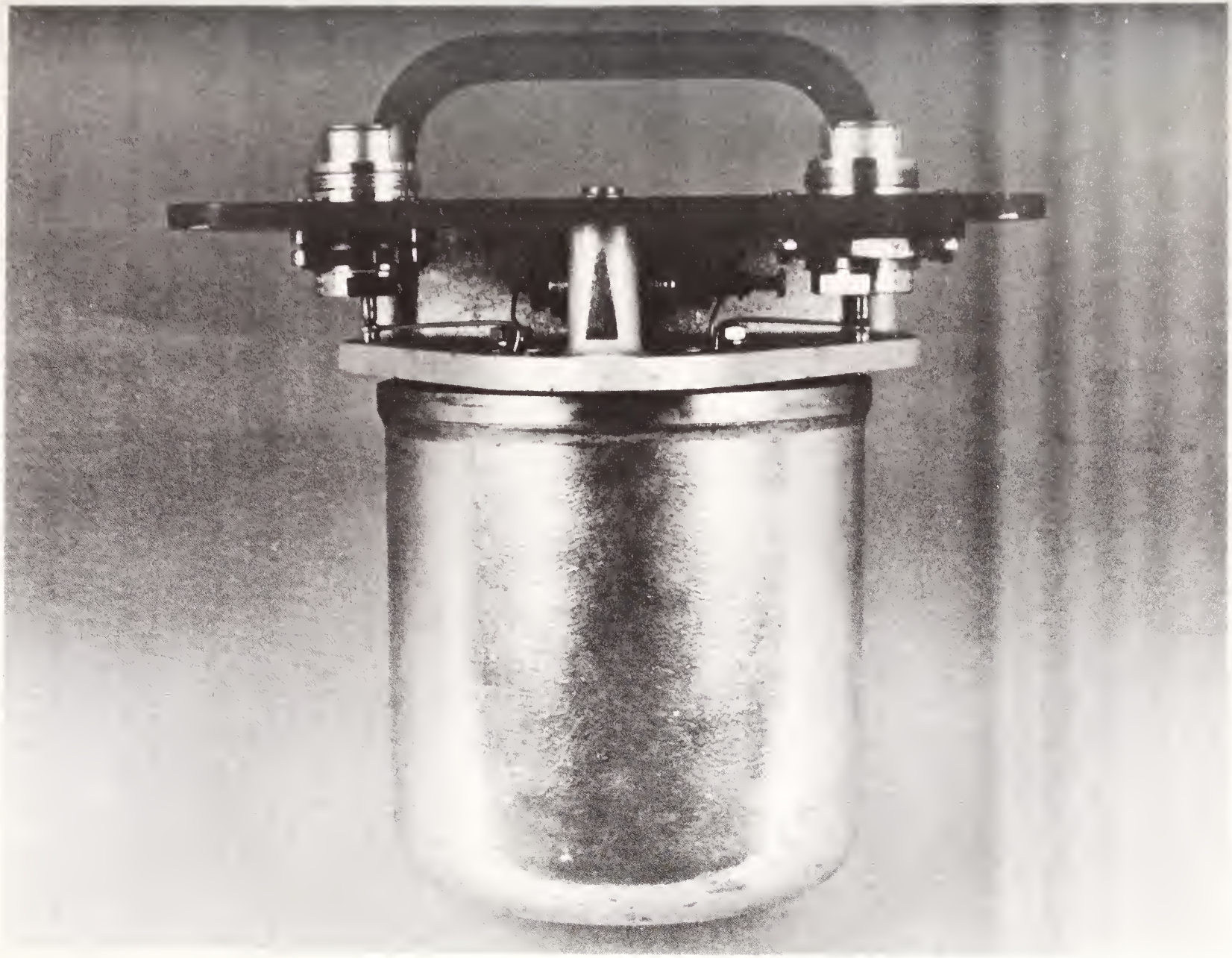

Figure 4. View showing web assembly.

reference position. Then the capacitor is moved from the upright position to a position of rest on Side A (refer to figure 5), the bridge rebalanced, and the capacitance value recorded. Without bringing the capacitor to the upright position, it is turned successively to positions of rest on Sides B, C, and D, the capacitance value for each position being recorded. After capacitance values for positions on all sides have been measured, the capacitor is returned to the upright position facing Side A (reference position) and a final measurement is made. The last reading, identified as ref2, is used to check the first (ref1) for drift (ref1-ref2=drift). Should the difference between the reference value and the value associated with any position be greater than ten ppm, the test should be repeated to determine whether or not the change is consistent or erratic. Two or more tests are desirable to reduce the possibility of a reading or recording error. Always use the last reference point in a series of measurements. If the capacitance value changes are not consistent from test to test, it is advisable to check the capacitor for defects such as loose screws, nuts, etc., including, in particular, those associated with the trimmer capacitor contained inside the outer enclosure and adjacent to the sealed capacitor assembly.

As indicated earlier, capacitors supplied from two different sources were evaluated. In the case of the models involved, the manufacturer's published specifications for maximum capacity changes under the conditions of the tests ranged from 1 ppm to 10 ppm. Changes greater than manufacturer's published specifications were considered as evidence of a defective capacitor.

8. Small Angle Test

This test was originally done for changes from zero to one, zero to two, and zero to three degrees. However, this series of tests was time consuming, and a single test for a change from zero to three degrees was found to be just as useful. The angle of three degrees was selected as the worst case by measuring a number of laboratory tables and finding that surfaces are usually within plus or minus two degrees of the horizontal. The change in capacitance due to small changes in angle of tilt is generally found to be a linear function of the angle within the zero to three degree limits. A worst-case acceptable value of 0.2 ppm per degree of angle change has been established for capacitors in satisfactory condition [1].

The procedure for this test is not difficult. However, the placement of the capacitor, adjustment of the elevated table, and provisions to avoid movement of the laboratory table or the elevated table are all important for consistent results (refer to figure 6). Be sure the adjustable table is horizontal (zero degrees). Then place the capacitor in the center of the tiltable plate on the adjustable table upright with Side A facing the operator. The measured capacitance under these conditions becomes the reference value and should be recorded as such. Use the adjustable knob to increase the angle to three degrees or, alter-

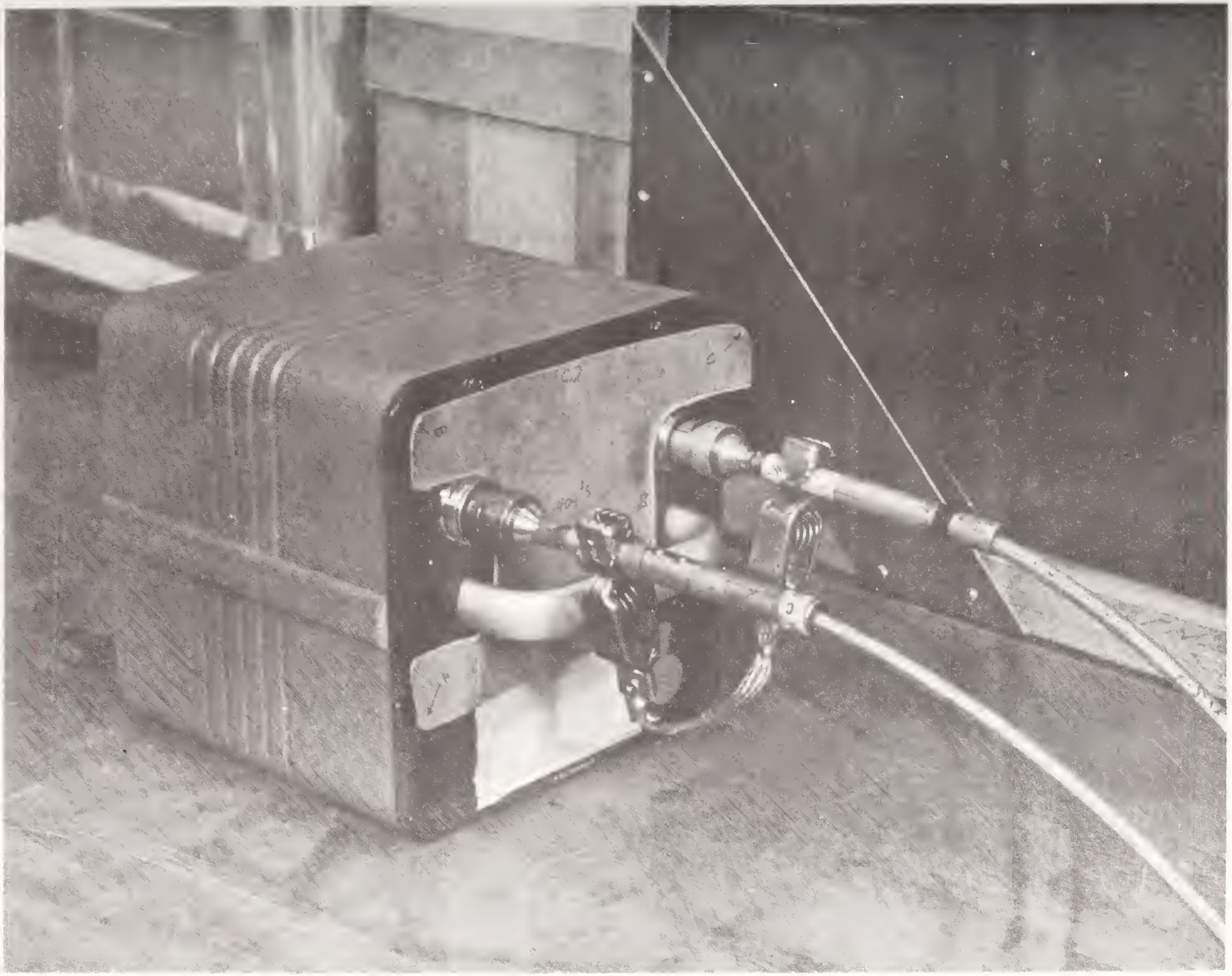

Figure 5. Orientation test - side A.

nately, use the special block made for three degrees, located securely in a suitable slot to avoid error in the elevation of the table. (Refer to figure 6). Measure the capacitance values with Sides A, B, C, and D facing the operator. Differences greater than 0.2 ppm between the reference value and the value associated with any other position indicates that the test should be repeated. If the results of a second series of measurements are similar to those of the first run, the changes probably reflect a characteristic of the particular capacitor. If the test is repeated, and the results are significantly different from those of the first test, subtract the smallest change from the largest change and record one half the result; this value should not be greater than 0.2 ppm. If it is larger, check for looseness in the web assembly.

9. Tilt Test

The tilt test (rotation through angles of 90 degrees, 180 degrees and return) serves several purposes. The geometry of parallel plate capacitors is such that movement of the plates will cause changes in capacitance. For example, shifting of the capacitor plates by only a few thousandths of an inch will cause changes ranging from a few tenths of a part per million to several parts per million. If all accessible fasteners holding the capacitor to the web assembly are tight and a sudden change in capacitance can be detected upon tilting and it does not disappear within plus or minus 0.1 ppm when the capacitor is placed back in the upright position on the table, it may be assumed that a problem exists within the sealed capacitor assembly.

The testing procedure is as follows. First, place the capacitor in the reference position on the table with leads connected as in previous tests. Balance the capacitance bridge as usual. Then grasp the handle of the capacitor and by balancing the weight of the capacitor in the other hand (refer to figure 7), turn (gently) the capacitor to a position with Side A in the horizontal plane. Note any erratic changes of the detector reading as you place the capacitor in the upright position on the table. Record any change observed. Repeat the test for Sides B, C, and D. Finally, repeat the test for the inverted position (refer to Figure 8). Grasp the capacitor and turn it upside down again observing the detector for changes as you return the capacitor to the normal orientation and place it back on the table.

Changes greater than 0.2 ppm between any two measurements of the capacitance of the upright capacitor indicate the possibility of a problem and the test should be repeated at least once. If the change is greater than 0.2 ppm, and consistent with the previous test, the test may be considered to reflect a characteristic of the capacitor. If changes during a second test are significant and do not repeat the results of the first test, check for looseness in the web assembly and capacitor assembly mounting parts. In the worst case, you might hear a distinct

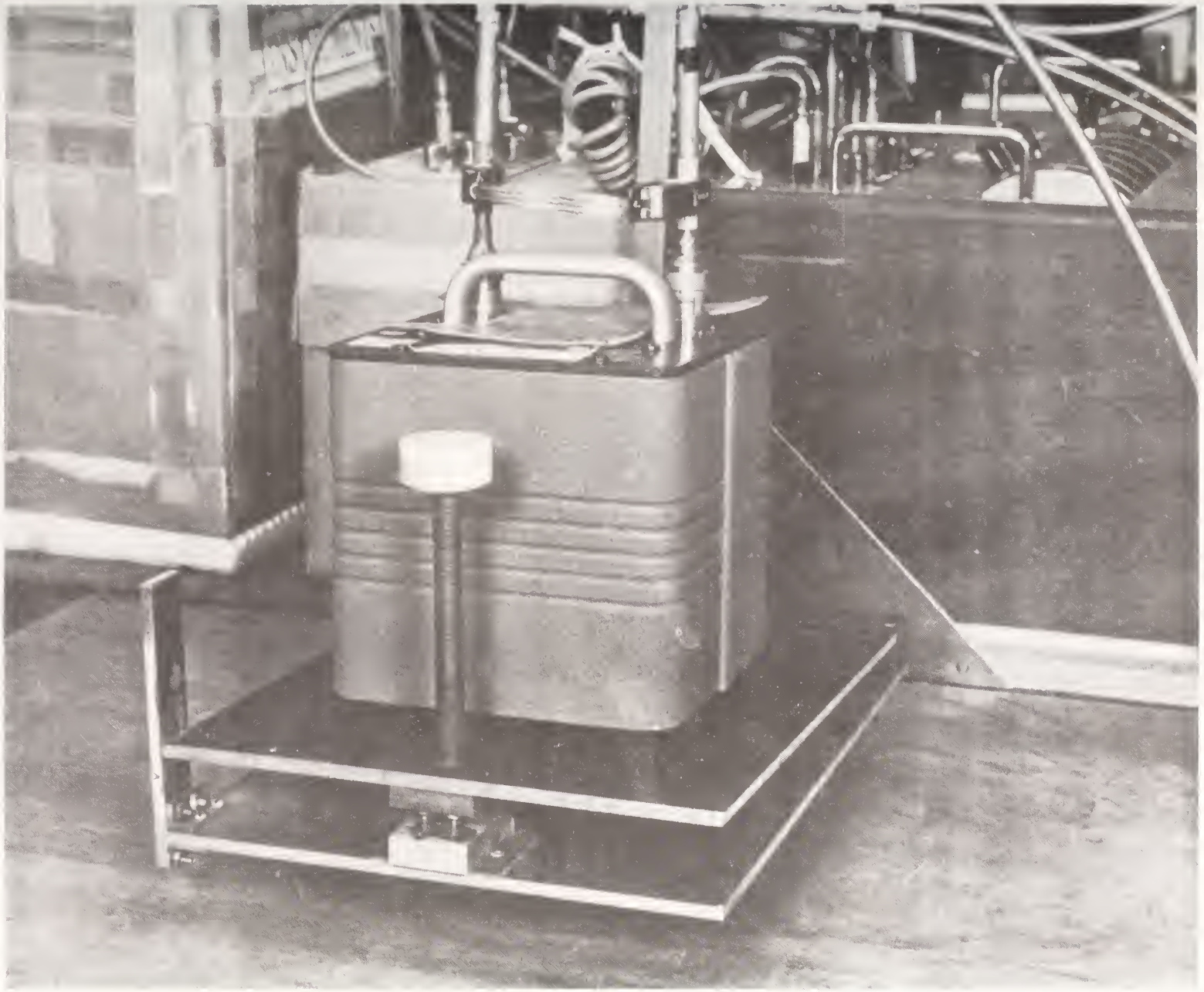

Figure 6. Angle test - special block for 3 degrees in place.

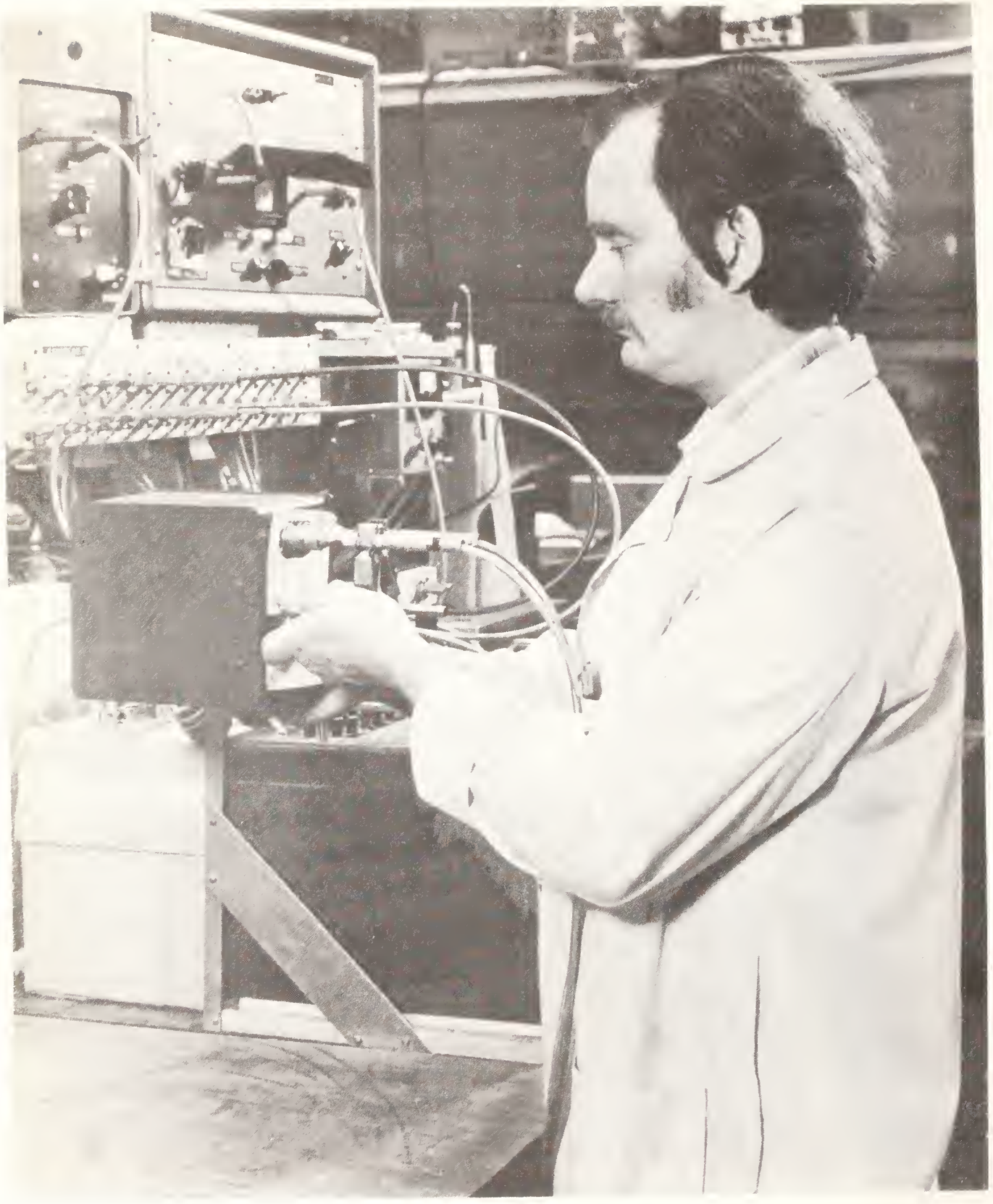

Figure 7. Tilt test in progress - side A horizontal.

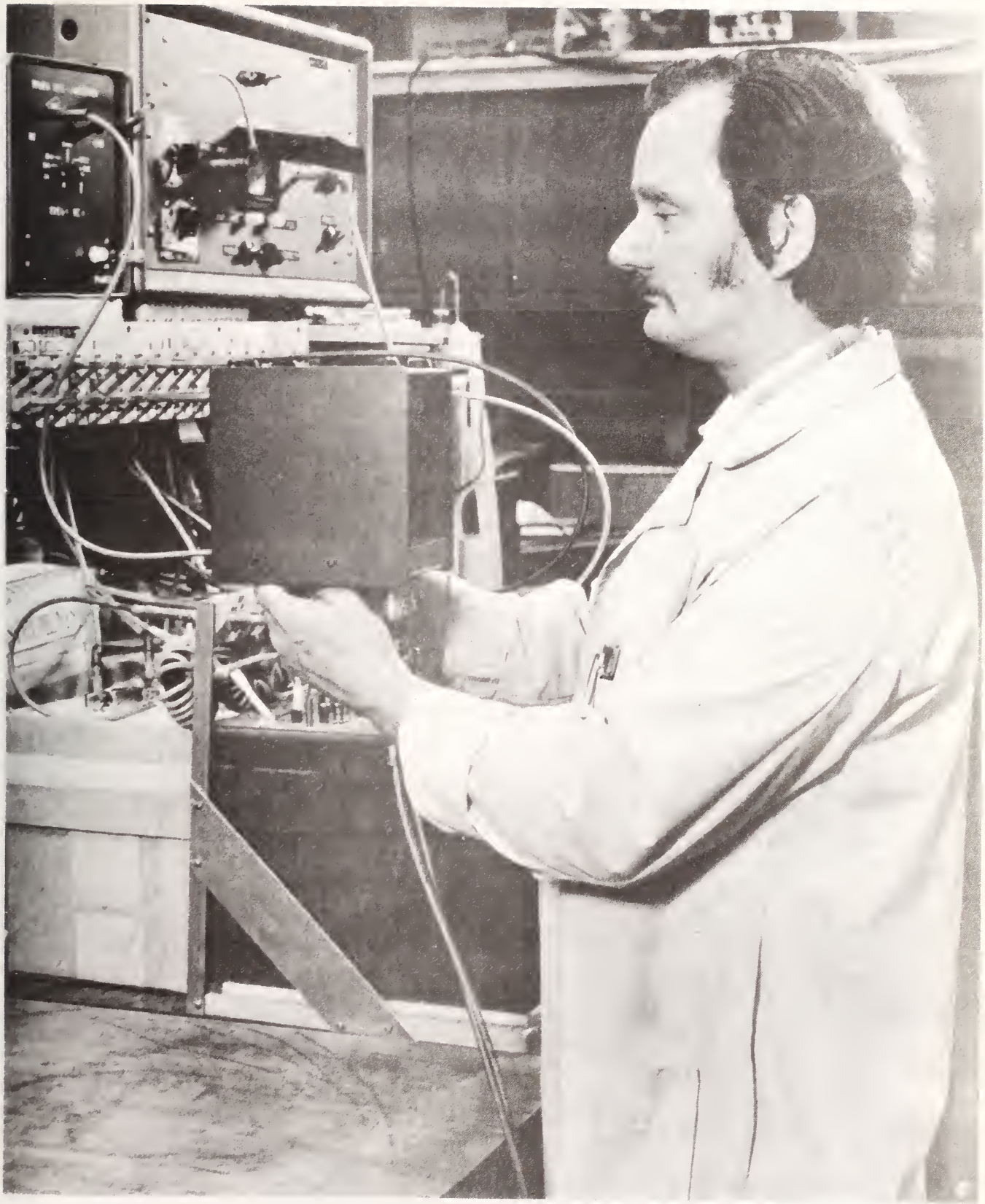

Figure 8. Tilt test in progress - test unit inverted.

"clunk" as you invert the capacitor indicating that the capacitor assembly within the case will probably be found to be loose.

Visual observation of the detector during this test is essential. Erratic behavior, indicated by a sudden change in the detector zero point, may be evidence of problems such as movement within the capacitor. This should be recorded to determine, in the future, if the quality of the capacitor degrades with time. It is also suggested that such a capacitor be calibrated more frequently as behavior of this nature is generally a sign of impending deterioration. Before reaching a conclusion that the capacitor is faulty, be sure to check all fasteners previously mentioned as well as connection points and cables. In many cases, a correctable fault can be eliminated.

10. Knock Soft Test

The mechanical shock in the knock soft test is approximately equal to a mild, wrist-action motion of one's hand against the side of the capacitor. The test is a controlled impact of a soft rubber-tipped hammer swung, in the vertical plane, from a position of 45 degrees. The hammer strikes the test unit on a side, just below the horizontal plane of the top surface, and midway between adjacent sides.

This test may reveal several conditions. For example, defects within the sealed capacitor enclosure, or looseness of fasteners in the web assembly of the capacitor, may be responsible for shock-induced changes of capacitance.

During transit, the capacitor is generally subjected to larger mechanical forces than this test will produce. However, small impulsive forces often create more noticeable changes within a capacitor than larger, less impulsive forces. This test is intended to simulate a typical impulsive force that a well-packed capacitor may receive during handling in transit. There are no specified manufacturers' limits for such shocks.

For the test, use the stand with the soft tip end of the hammer head toward the face of Side A of the capacitor. Balance the bridge and record the reading. This capacitance value is the reference value. The hammer is then drawn back to the 45 degree position and released to strike the capacitor (refer to Appendix 2, Figures 2 and 4). However, it is not allowed to strike a second time following rebound. Again the capacitance value is recorded. The capacitor is moved to position A Corner (refer to figure 3) for a hammer strike. The measurement is repeated through all sides and corners in the order: Side A, Corner A, Side B, Corner B, Side C, Corner C, Side D, Corner D.

If changes are greater than 0.2 ppm between any two tests in this series, it is suggested that the series be repeated. If the relative changes between a first series and a second series is noted to be approximately the same, subsequent tests are not necessary.

11. Knock Hard Test

This test is similar to the knock soft test. The differences are that the hammer swing is limited to fifteen degrees and the hard tipped head strikes the capacitor. The object of this test is to simulate shocks received by the test capacitor when, in being lifted from a work bench, it accidentally strikes another object. Mechanical shock in transit may, under some conditions, be similar to this type of shock. This test is particularly effective for detecting problems associated with the trimmer capacitor.

Changes larger than 0.2 ppm should be recorded, particularly when two sets of readings do not repeat. Changes greater than 0.5 ppm are cause for concern and the capacitor should be carefully checked for correctable defects. If there are no loose components, the excesssive capacitance change may be a result of stress changes within the sealed capacitor enclosure.

12. Drop Test

The drop test was devised to simulate a shock which may occur in service, for example, due to a drop from the hand to a table surface. It may also simulate, to some extent, the dropping of the standard in its shipping container during handling in transit. Short-duration forces in the vertical direction may cause various movements of plates or support rods. Intermittent electrical shorts between plates may sometimes be found using this method.

Testing the unknown capacitor requires a block of wood having measurements of 3.8 cm (1.5 inches) x 8.9 cm (3.5 inches) and from 10 to 15 cm (4-6 inches) long (refer to figure 9). Balance the capacitance bridge with the capacitor normally resting on the table, being sure that all four feet of the capacitor are in contact with table surface. Then place the block of wood under Side A (smallest dimension vertical) and carefully, but swiftly, pull out the block. After the block of wood has been removed and the capacitor has struck the table, record any changes in capacitance value. The test is repeated raising each side of the capacitor sequentially (Side A, B, C, and D). Changes greater than 0.2 ppm between any two capacitance values, or between the reference value and any other value should be recorded. Changes greater than 1 ppm indicate the possibility of a problem capacitor.

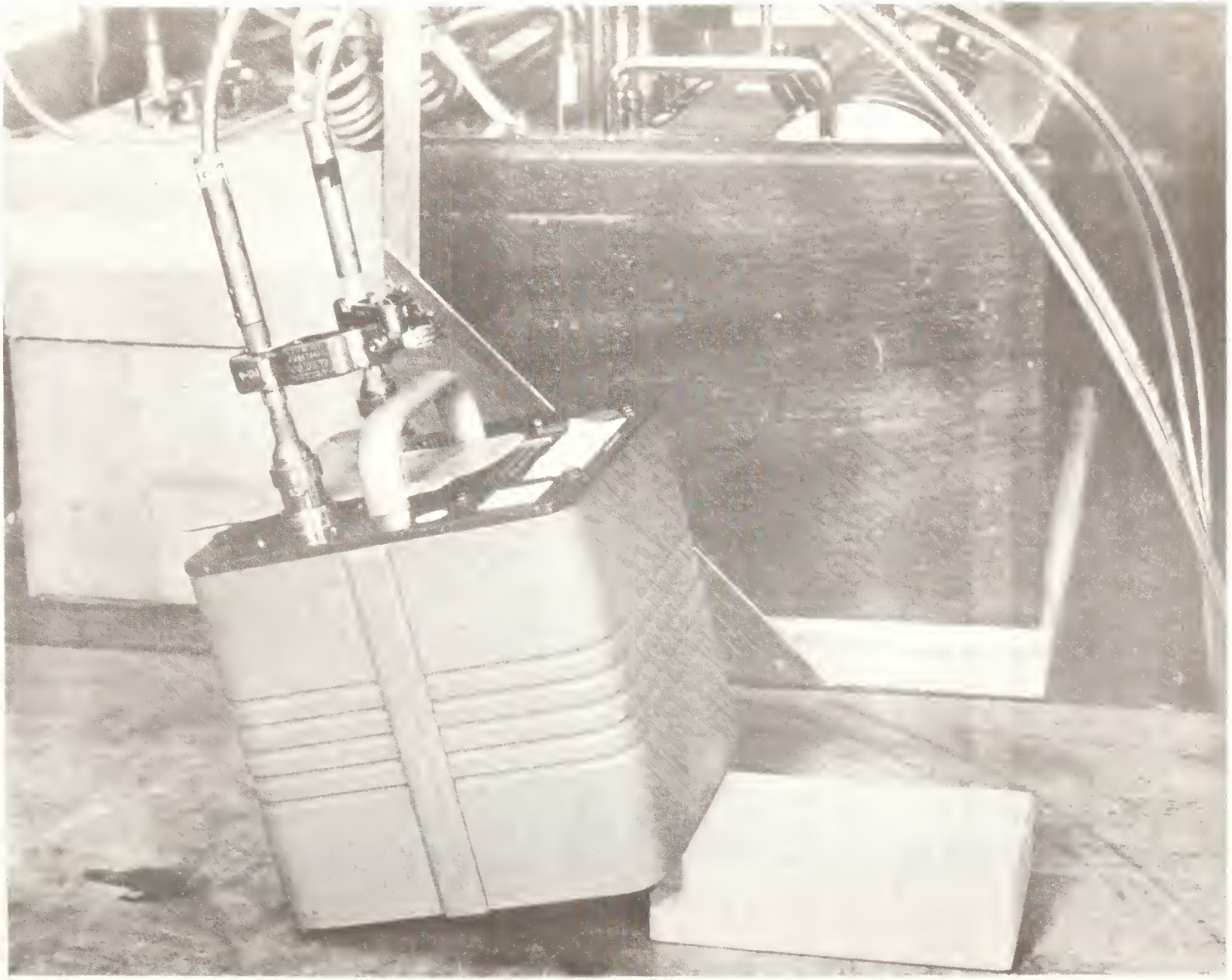

Figure 9. Set-up for simulated drop test.

13. General Considerations

All of the tests described in this document should be performed in a systematic manner. No test should be discontinued until all specified sides, corners, etc. have been included. The specified order of tests, connectors, orientation, small angle, tilt, knock soft, knock hard, and drop test should be followed to eliminate possible confusion in comparing results with those of earlier or later tests. This order was determined to give the most reproducible results. There is one caution that should be mentioned. If any fasteners are suspected of being loose, either tighten all fasteners before the handling test is undertaken, or wait until all tests are completed. Otherwise, it will not be possible to know if the repairs caused or cured the problem(s).

It is not necessary to complete a series of tests in one day; it is only important that the tests be done in the proper sequence. This is the only way to obtain a repeatable characterization of the standard.

Capacitors determined to be faulty should be retested before any repairs are attempted in order to eliminate the possibility of other factors such as improper hook-up, faulty electrical leads, bridge problems, or faulty connections within the test system being used.

The use of two reference standards, having known characteristics, to which the unit under test is compared, one during the first half of the test series and the other during the second half, may help reveal problems external to the test capacitor. Such problems might include intermittent faults in a reference capacitor, improper hook-up, bridge malfunction, faulty leads, or faulty connectors.

14. Data Reduction

The data for any of the test series described in the previous sections of this document may be represented by a string as follows:

ref, rdg_1 rdg_2 ..... rdg_n,

where ref=initial reference value which appears only at the beginning of a string for all positions to be tested, and rdg_i=reading for a particular side or corner.

Successive differences or changes would then be as follows:

$dif_1 = rdg_1 - ref_1$

$dif_2 = rdg_2 - rdg_1$

$dif_3 = rdg_3 - rdg_2$

$\vdots$

$dif_n = rdg_n - rdg_{n-1}$,

where dif = difference, rdg_i = reading at position i, and ref = reference.

The range between any two values is used for two reasons. In the first place, most laboratories only need to know the maximum change expected. In the second place, if changes were nearly equal but opposite in sign, the average would underestimate possible changes. Changes noted for each side or corner in a string usually will not be randomly distributed, particularly when significant changes are experienced.

For the tests listed, the following data should be obtained:

ORIENTATION: Minimum of six data points required - ref1, Side A, Side B, Side C, Side D, ref2

ANGLE 3 DEGREES: Minimum of six data points required - ref_1, Side A, Side B, Side C, Side D, ref_2

TILT: Minimum of six data points required - ref, side A, side B, Side C, Side D, upside down, rightside up

KNOCK SOFT OR HARD TEST: Minimum of nine data points required - ref, Side A, Corner A, Side B, Corner B, Side C, Corner C, Side D, Corner D

In the orientation and angle tests, drift can be determined from the difference between the first reference and last reference in a given string. If the test is completed with minimal time between measurements (less than a half hour), drift in excess of 0.2 ppm should be recorded. Most excessive drift will be observed during the first few minutes of testing. In some cases, drift may continue for several minutes or as long as a half hour. Such drift may be caused by changes in temperature of the capacitor under test or changes in temperature of the standard used as the reference. While the latter may be placed in a lag box to reduce the effects of rapid temperature fluctuations, it may not be practical to do so for the capacitor

being tested. Therefore, these tests should each be carried out rapidly to minimize temperature-created anomalies in the data (which one would have a difficult time sorting out from the effects of defects) and take place in a relatively well-controlled room.

Except for the results of the orientation test, the magnitude of changes caused by handling tests should be included in the uncertainty of calibration results as a systematic error. This is particularly important if any of the changes are greater than 0.5 ppm. In the case of capacitance standards which are not kept continuously within the metrology laboratory or are otherwise exposed to unusual handling conditions, experience at NBS suggests that the calibration uncertainty should be increased by the addition of half the largest change induced by the handling tests described in this document [1].

The stresses described in this document are believed to be small compared to those that are encountered in normal shipping and handling; therefore, unusual effects due to shipping should be determined by using the results of control measurements made in the user laboratory before and after shipping in addition to the results of these tests at NBS.

15. Unusual Problems

Gas dielectric capacitors have two sources of capacitance change which are not repairable by the user; in the first place, all gas dielectric capacitors manufactured in the United States use a trimmer capacitor to bring the value of the capacitor close to its nominal value. Many users adjust this capacitor to meet specific needs. Two types of trimmers are in use, one having an adjustable core and the other having interleaved plates similar to a radio tuning capacitor. The plate type is rarely found to be a problem unless it becomes loose. Since this type is generally exposed within the capacitor housing, a loose part, such as a nut or screw, falling between the blades of the trimmer capacitor may cause an electrical short or mechanical damage to the plates. Such faults may cause capacitance changes of greater than 100 ppm. Changes in placement of the leads to the trimmer may also affect the capacitance by several ppm in either direction without any change in the trimmer adjustment.

The coaxial adjustable-core type of capacitor trimmer has been known to short, or worse, fall apart due to extreme abuse in transit. If there is a possibility of an electrical short, the trimmer must be replaced because excessive current will be drawn through the measuring system. Malfunction of the trimmer may cause a capacitance change of several hundred ppm.

Removal of either type of trimmer will result in capacitance changes of up to 300 ppm (determined for the capacitors selected for the NBS portable transport box). If such departures from

nominal value are acceptable, it is suggested that the trimmer capacitor be removed to eliminate a possible cause of instability.

A second, less frequent, problem involves hermetic seal leakage. The hermetic seals of capacitors manufactured in the United States are generally trouble free unless undue pressure is applied on the electrical feed-through connection points or they are overheated. Cracked seals are not common; however, if this is suspected, temperature cycling will reveal the fault. Cooling to freezing followed by warming to approximately forty degrees Celsius and returning to lab temperature should be sufficient to verify seal leakage. A capacitor that is cycled will not retrace to the previous value within the tolerance stated by the manufacturer unless the seals are intact. There may be problems within the sealed capacitor other than those associated with the seals. However, any capacitor that cannot be cycled without significant changes should not be considered satisfactory as a working standard.

16. Conclusion

A review of the graphs for the various test procedures will disclose the utility of handling tests described in this document. The overall results of a number of such tests conducted at NBS are summarized in table 2, following:

Table 2. Summation of tests

TEST	ACCEPTABLE LIMITS* (PPM)	% FAILED
Orientation	10	23
Angle 3 Degrees	0.2	48
Tilt	0.2	5
Knock Soft	0.2	14
Knock Hard	0.2	13
Drop	0.2	14

*Acceptable limits excluding orientation test for which one half the largest change in any test should be added to the uncertainty of calibration.

The tables and graphs (Appendix 1) in this document are derived from the results of tests carried out on 200 capacitors during the period 1972-78. The method of evaluation involved collection of data from all capacitors received for testing the first time in order to establish a basis unbiased by the selection criteria and to reflect a good cross-section of all capacitors received. Data are selected randomly from all

capacitors received for test in order to avoid disclosure of differences between the products of different manufacturers. Data from succeeding years were also selected randomly for capacitors not used in previous data evaluations in order to obtain an overall balance.

Data from the first year of testing were compared with data from succeeding years with very convincing results. In more than 80% of the cases compared, the results of the capacitors repeated to within 0.2 ppm of those from the previous year for each particular test. Most capacitors with changes greater than 0.2 ppm had been subjected to rough treatment. For fewer than 10% there was no discernible reason for the changes noted.

Referring to the summary of tests, it is apparent that the orientation and three degree angle tests were failed more often than the other tests. If a capacitor shows poor results on the tilt test, the problem can, in principle, be overcome by using a level table. In the case of the orientation problem, there is not much that can be done other than use the capacitor in the upright position. It should be recognized that excessive changes during these tests suggest a lack of mechanical integrity within the standard capacitor and reliabilty during service is open to question.

It will be noted that there is no graph in Appendix 1 for the connector test. Generally, the changes during this test are small and when a problem with a connector is corrected, there is generally no remaining concern.

17. Additional Observations

The care with which a gas dielectric capacitor is packed for shipping can, to a large extent, determine its useful life. Manufacturers in the United States ship standard capacitors in protective reusable containers, which should also be placed in an outer box containing at least 10 cm (4 inches) of shock-absorbing material on all sides for added protection.

Exposure of the capacitor to abnormal temperatures, such as those found in the trunk of a car on a hot day, should be avoided. The time for the capacitor to stabilize after being exposed to excessively low or high temperatures depends on the design of the capacitor. A similar consideration applies following a long period of storage with the capacitor resting on a side; a period of recovery in the normal upright position is necessary before its use or before calibration at NBS.

Checking all screws, nuts, etc., for looseness before the capacitor is shipped for calibration will reduce the possibility of damage due to the movement of parts during transit. Loose connectors should be properly positioned and tightened before tests are started.

Handling the capacitor in the laboratory or field is as important as care in shipping if long term stability is essential. Capacitors receiving rough treatment, such as impacts against other equipment or furniture, may be damaged in terms of loosened parts or more serious mechanical changes.

It is important to document values and abnormal changes found in the handling tests. Both can guide the user in avoiding problems and removing from service a faulty capacitor; many hours of needless measurements can, thereby, be saved.

All maintenance and repairs should be performed after completing the series of tests described in this document unless a definite problem is detected. In this way, problems discovered during tests may be evaluated as correctable or otherwise identified as an intrinsic characteristic of the unit under test.

The material contained within this paper is intended to serve as a guide; it is not suggested that the problems discussed are the only problems the user will experience. However, the handling tests described have been found to disclose the most frequent problems encountered at NBS. All known causes of capacitance change should be documented fully and the capacitor should be monitored systematically if it is to be used at the five ppm level of uncertainty.

18. References

[1] Free, G. and Morrow, J., Transportable 1000 pF capacitance standard. Nat. Bur. Stand. (U.S.) Tech. Note 1162; 1982.

[2] Anderson, W. E., Davis, R.S., Petersens, O., and Moore, W. J. M., An International Comparison of High Voltage Capacitor Calibrtions, IEEE Trans. Power Appar. Syst. PAS-97(4), pp. 1217-1223 (1978).

[3] Thompson, A.M., The precise measurement of small capacitances. IRE Trans. Instrum. I-7(3-4):245-255; 1958 Dec.

[4] Cutkosky, R.D., Four-terminal pair network as precision admittance and impedance standards. IEEE Trns. Commun. Electron. 70:19-22, 1964 Jan.

[5] Homan, D. N., Application of coaxial chokes to a-c bridge circuits. J. Res. Nat. Bur. Stand. 72C(2):161-165; 1968 April-June.

[6] A highly stable reference standard capacitor. GR Experimenter. 37(8); 1963 August.

[7] Thoma, P., Absolute calorimetric determination of dielectric loss factors at = $10^4 s^{-1}$ and application to measurement of loss factors of standard capacitors at room temperature. IEEE Trans. Instrum. Meas. IM-29(4); 1980 Dec.

[8] McGregor, M. C., Hersh, J. F., Cutkosky, R.D., Harris, F. K., and Kotter, F. R., New apparatus at NBS for absolute capacitance measurements. IRE Trans. Instrum. I-7:253-261; 1958 Dec.

Appendix 1

Histograms of the Effects of Handling and Stability Tests on Standard Capacitors

The following histograms are based upon the results of performing each of the Handling and Stability Tests on each capacitor of the test group. The maximum capacitance change value caused by a given test performed a number of times on each capacitor was used to determine the numbers of capacitors for which such change values fell within the ranges indicated in the histograms.

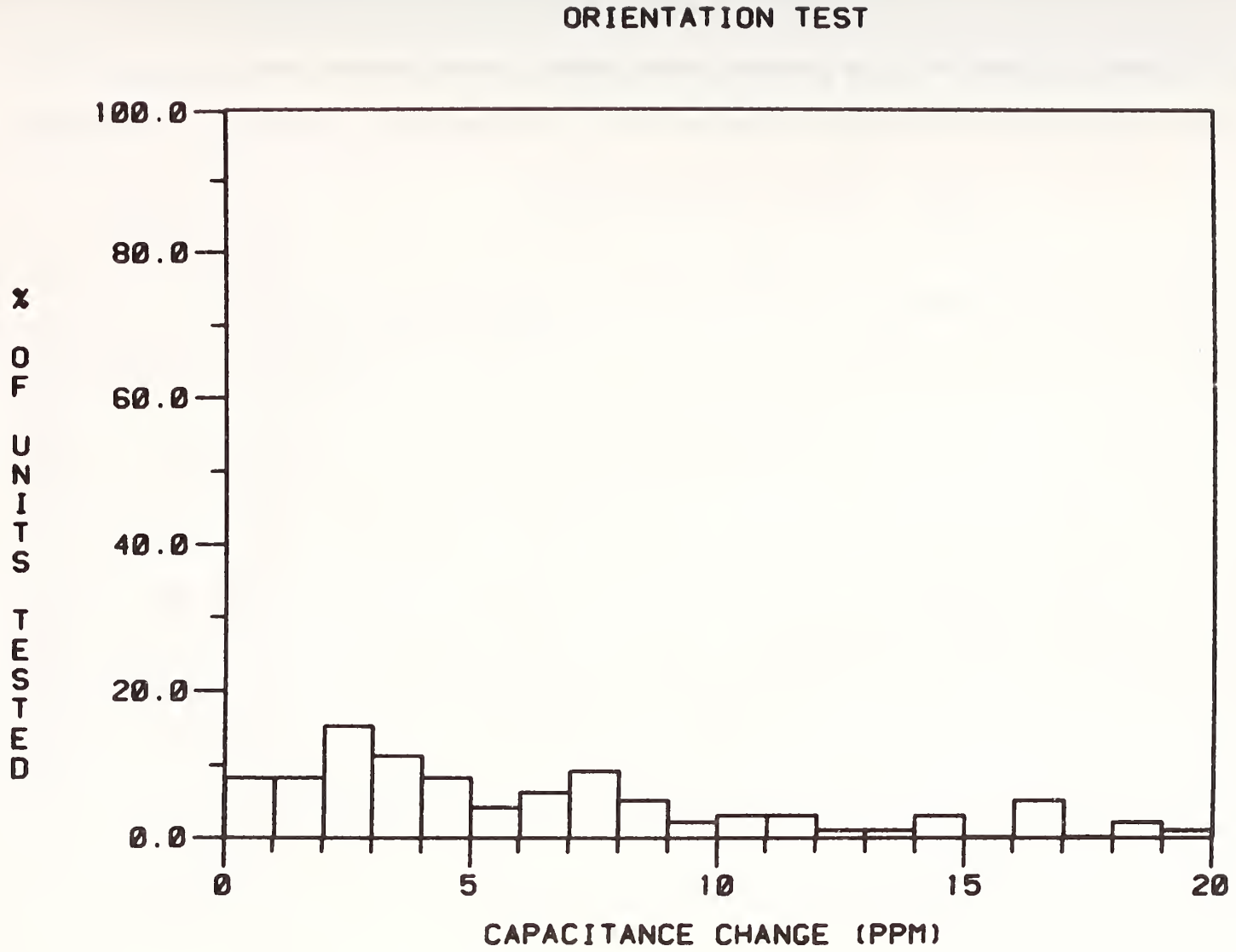

Appendix 1, Figure 1. Histogram of the fractional numbers of capacitors for which different values of maximum capacitance were caused by the Orientation Test.

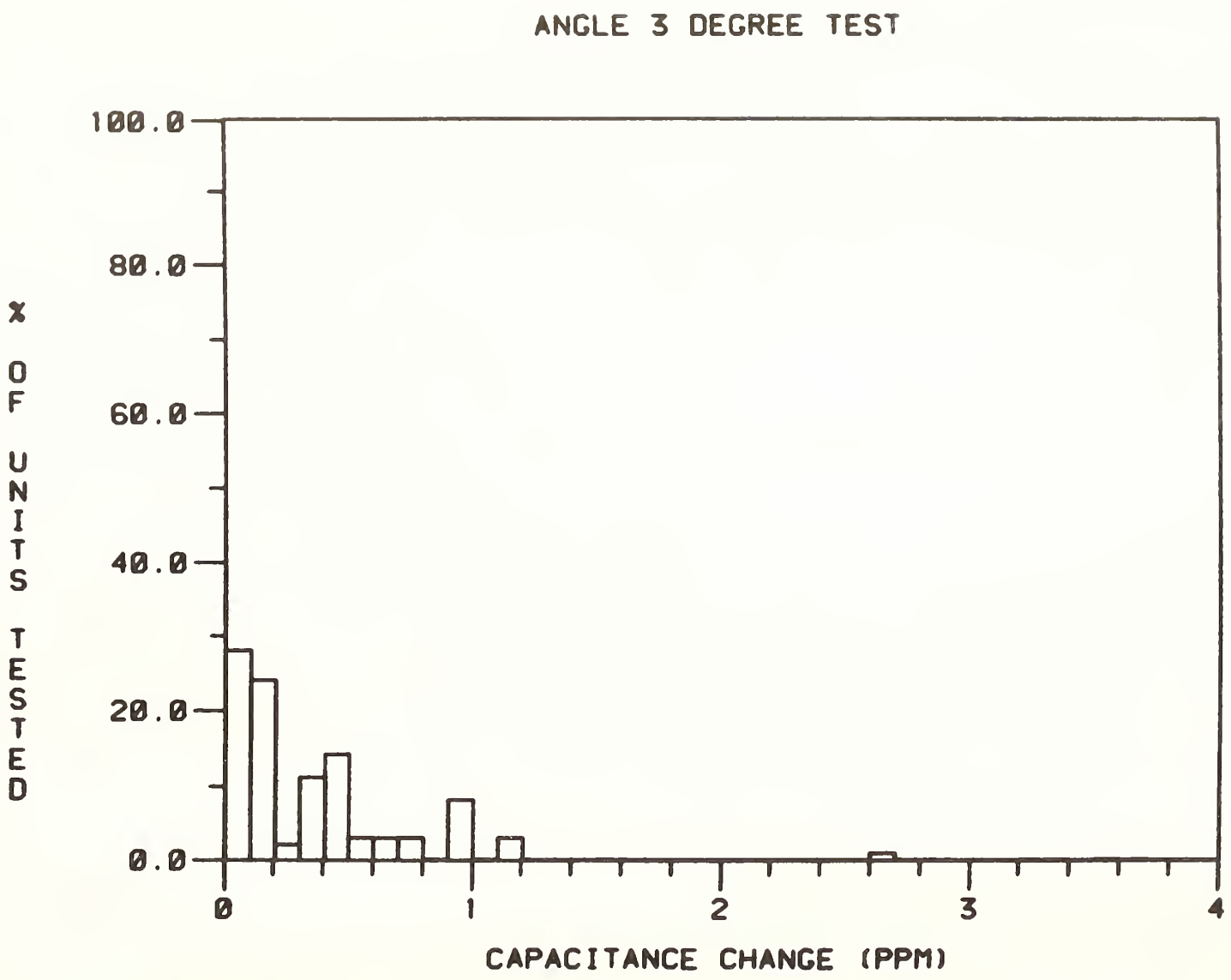

Appendix 1, Figure 2. Histogram of the fractional numbers of capacitors for which different values of maximum capacitance change were caused by the Angle 3 Degree Test.

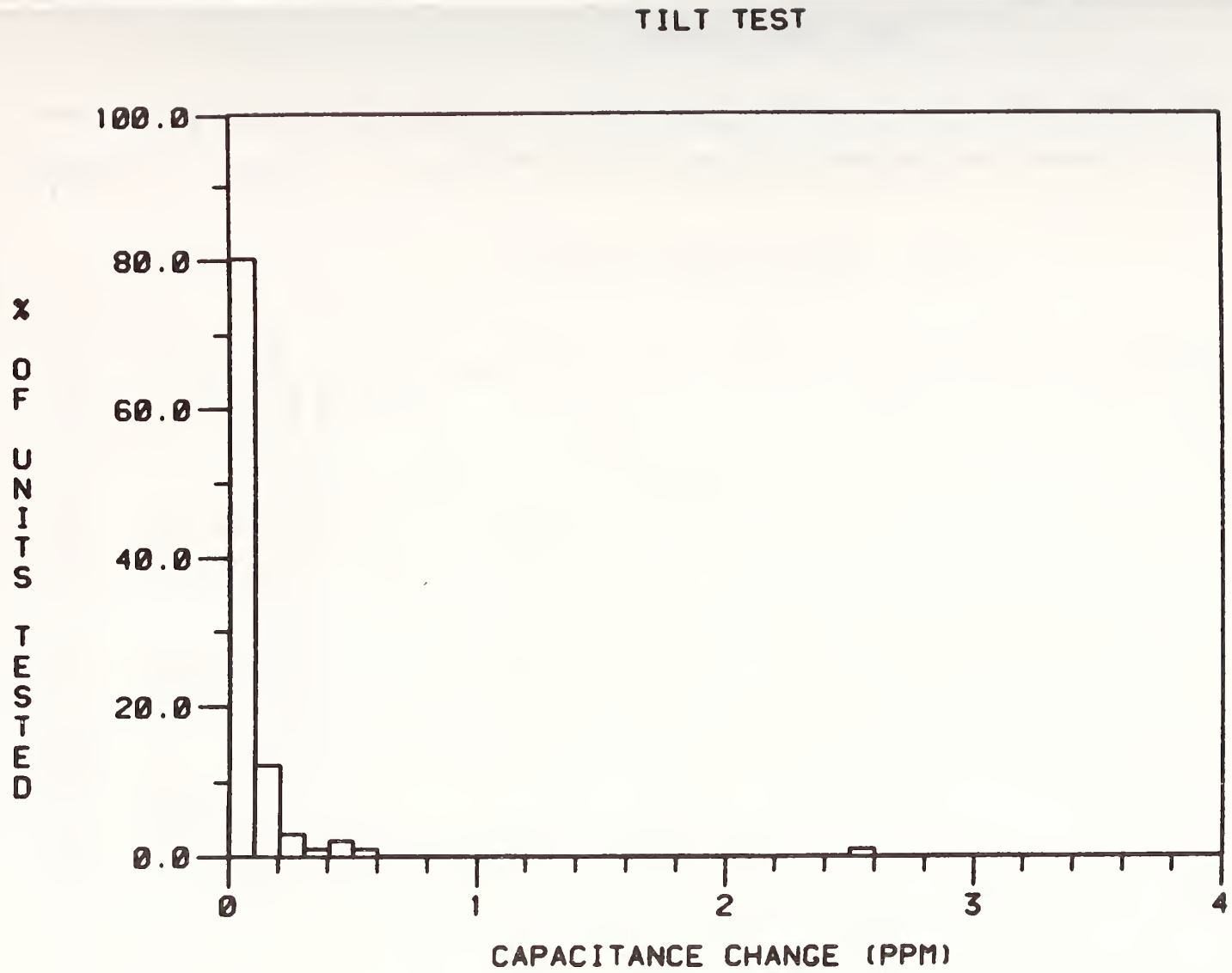

Appendix 1, Figure 3. Histogram of the fractional numbers of capacitors for which different values of maximum capacitance change were caused by the Tilt Test.

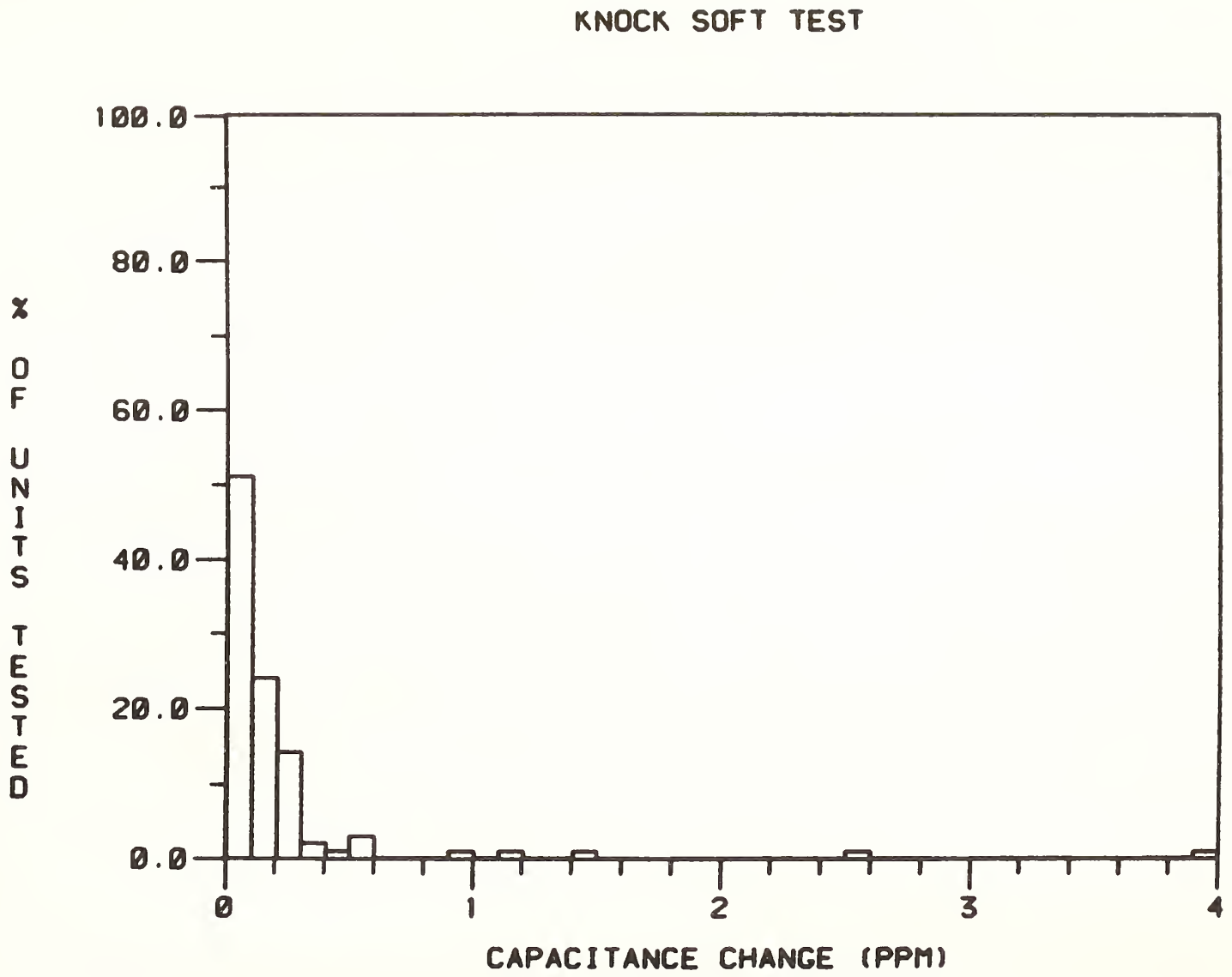

Appendix 1, Figure 4. Histogram of the fractional numbers of capacitors for which different values of maximum capacitance change were caused by the Knock Soft Test.

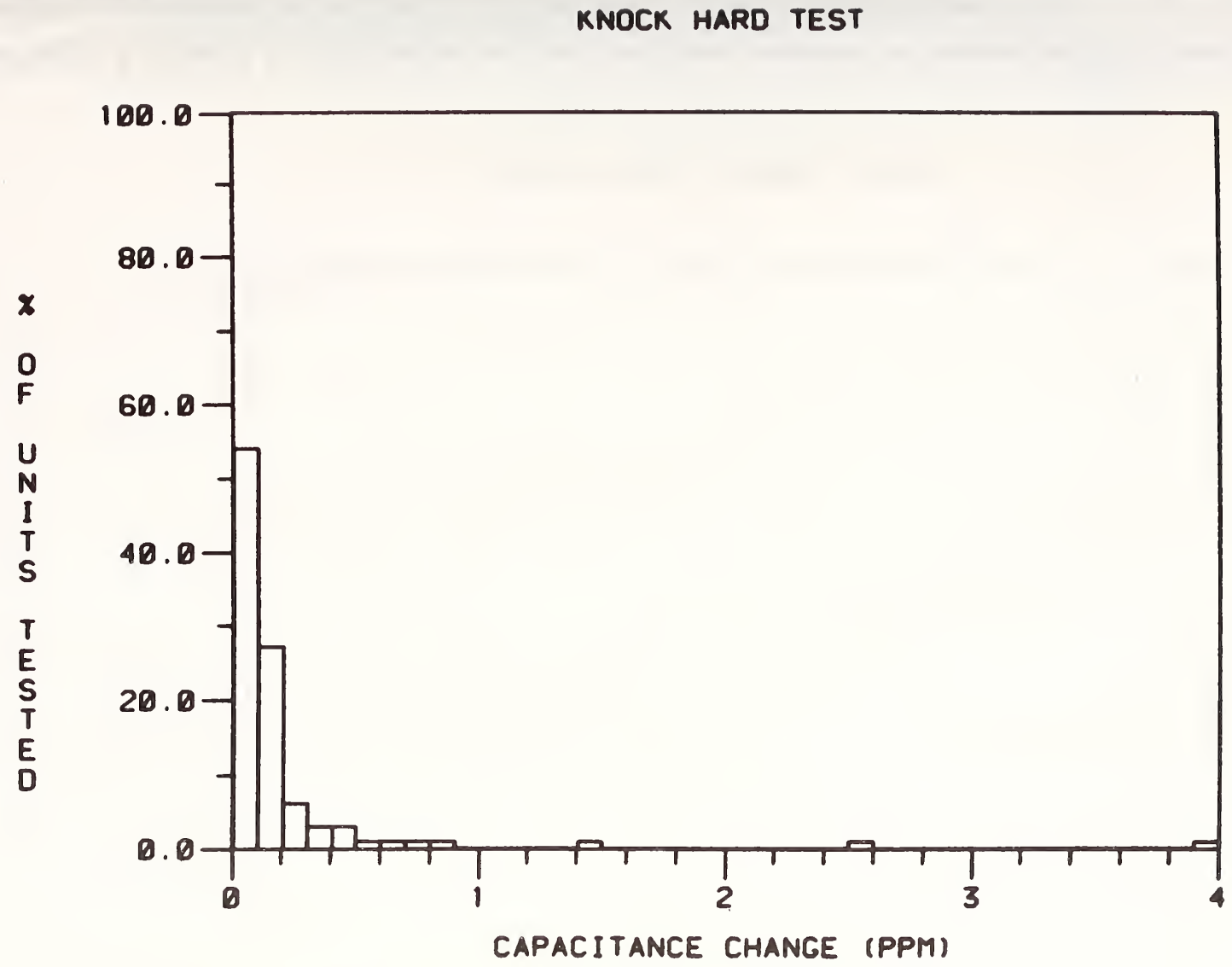

Appendix 1, Figure 5. Histogram of the fractional numbers of capacitors for which different values of maximum capacitance change were caused by the Knock Hard Test.

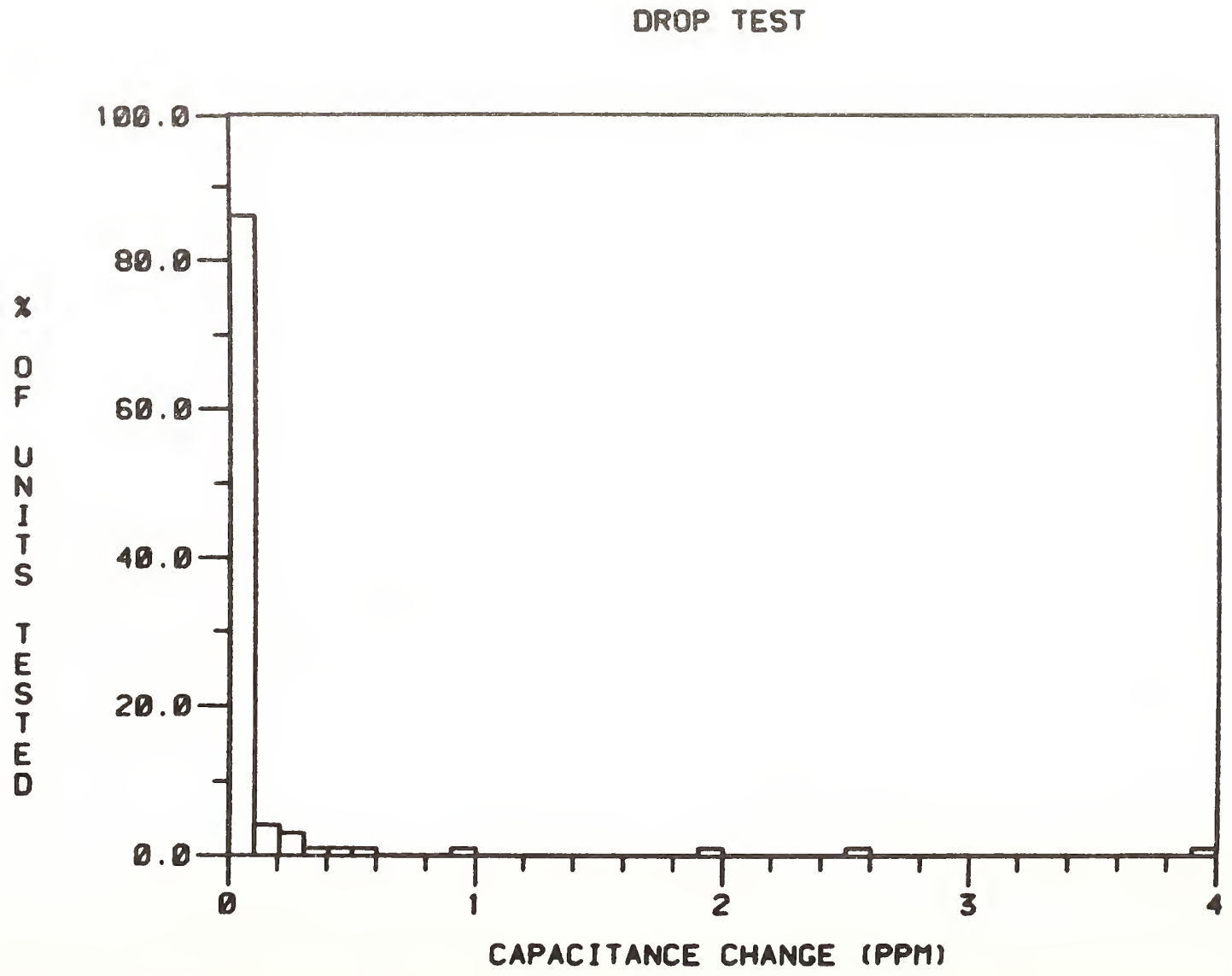

Appendix 1, Figure 6. Histogram of the fractional numbers of capacitors for which different values of maximum capacitance change were caused by the Drop Test.

Appendix 2

Drawings of Test Apparatus

The following drawings represent the apparatus used at the National Bureau of Standards for the tests described in this publication. Dimensions are given in metric units and customary units used in the United States.

Appendix 2, Figure 1.

KNOCK STAND ANGLE PLATE PATTERN

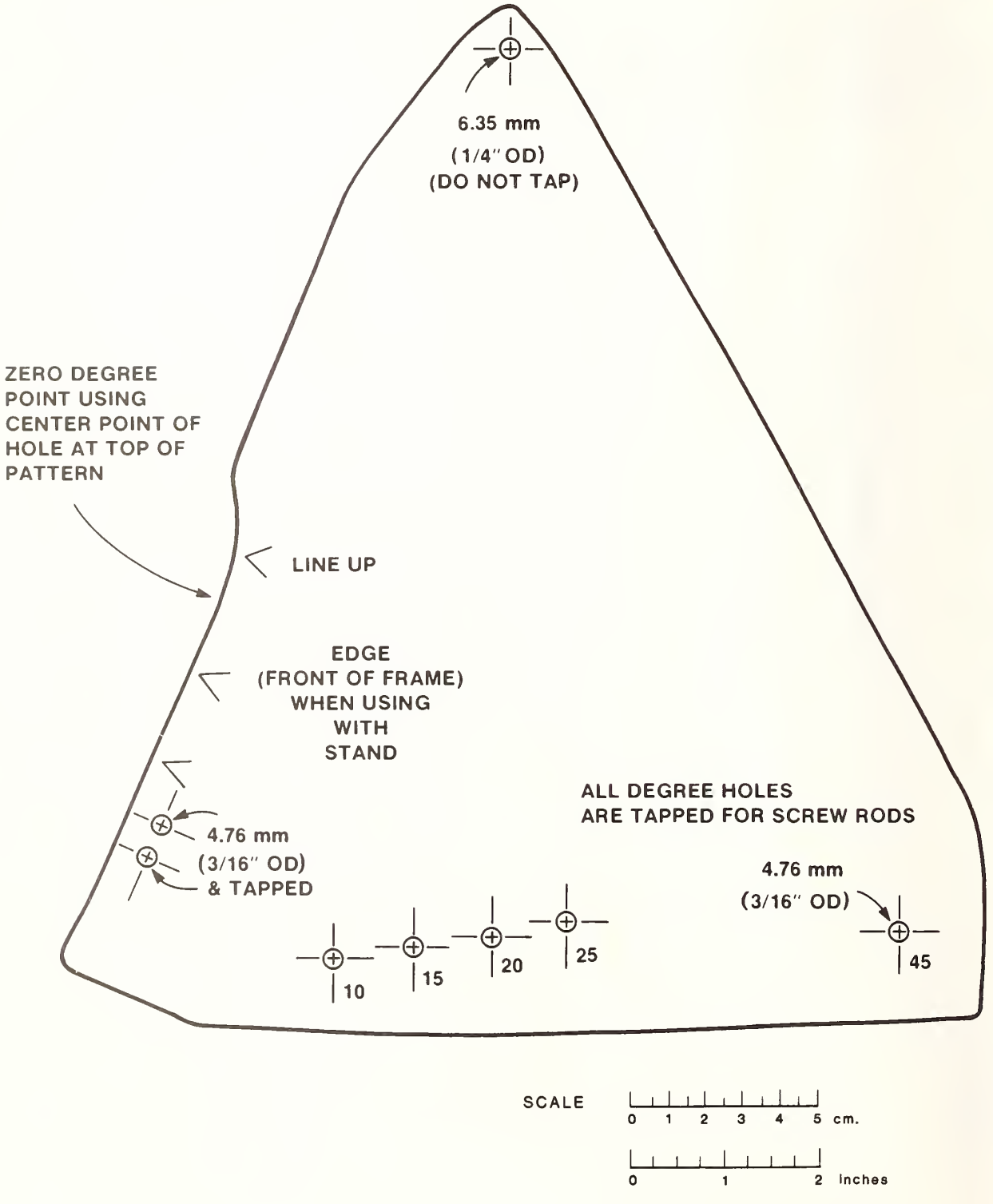

Appendix 2, Figure 2.
Hammer for use with Knock Stand (see following figure)

	grams	lbs.
HARD RUBBER HEAD	41.03	.09
SOFT RUBBER HEAD	46.70	.10
HAMMER-HEADS	441.14	.97
TOTAL Wt. OF HAMMER	528.87	1.16

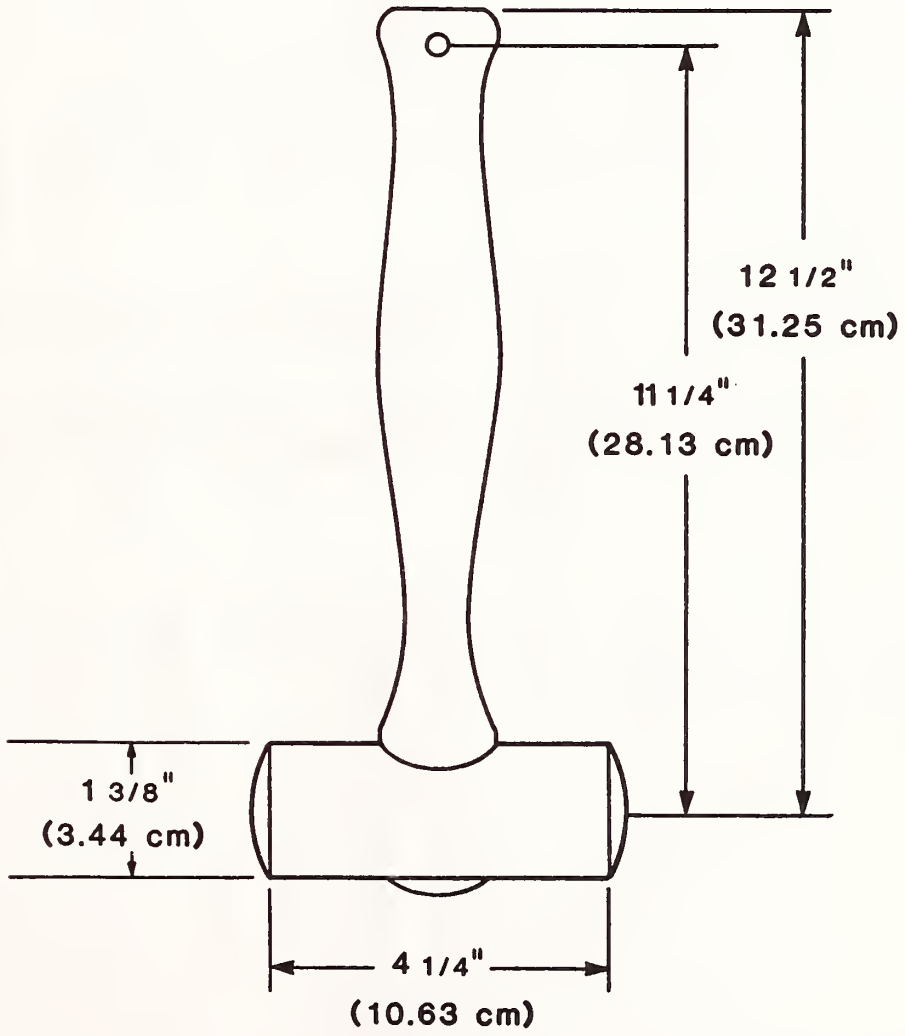

Appendix 2, Figure 3.

KNOCK STAND
(SKETCH NOT TO SCALE)

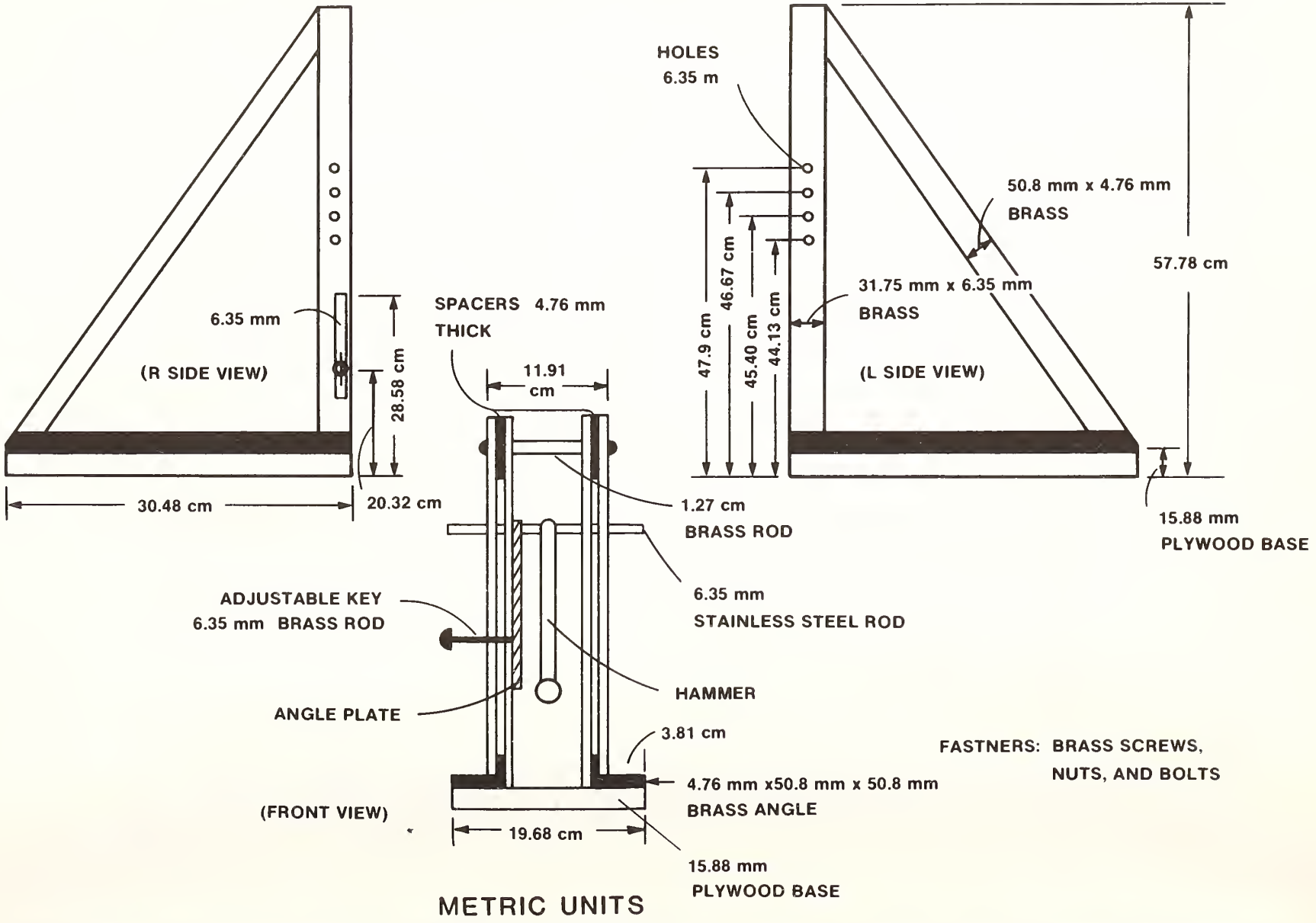

FASTNERS: BRASS SCREWS,
NUTS, AND BOLTS

METRIC UNITS

Appendix 2, Figure 3.

KNOCK STAND
(SKETCH NOT TO SCALE)

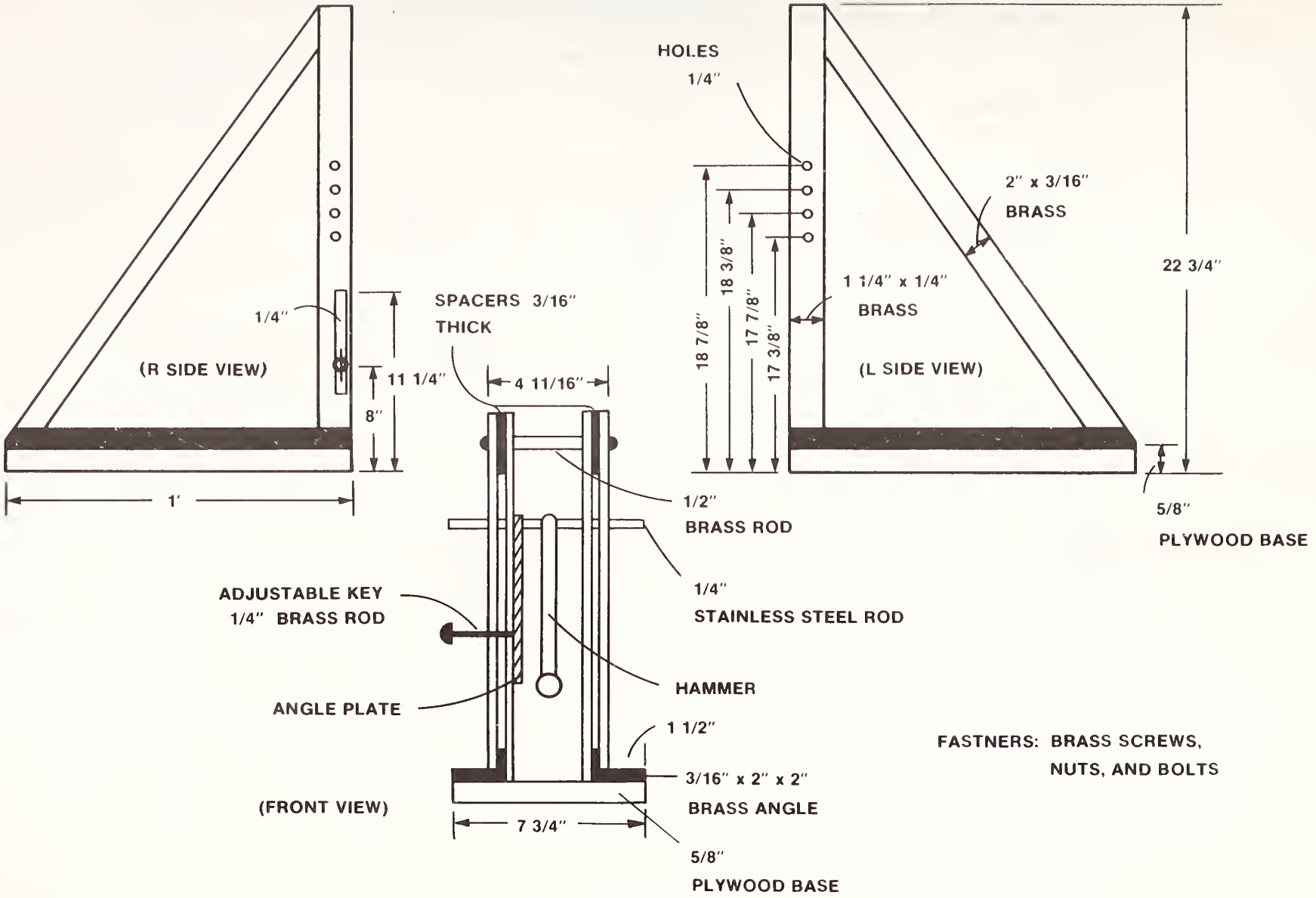

FASTNERS: BRASS SCREWS,
NUTS, AND BOLTS

UNITS IN INCHES

Appendix 2, Figure 4.

ELEVATED TABLE FOR ANGLE TESTS
(SKETCH NOT TO SCALE)

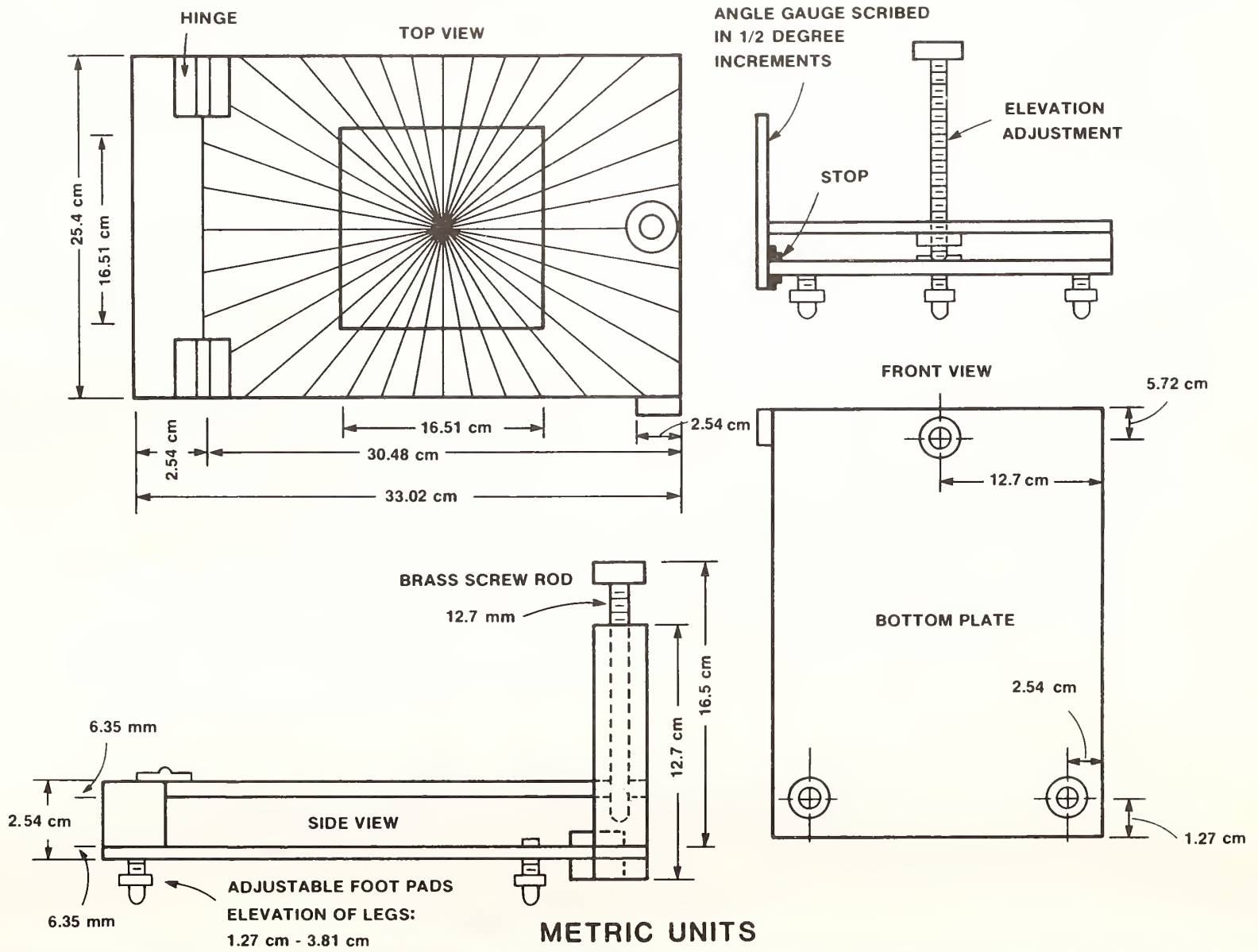

Appendix 2, Figure 4.

ELEVATED TABLE FOR ANGLE TESTS
(SKETCH NOT TO SCALE)

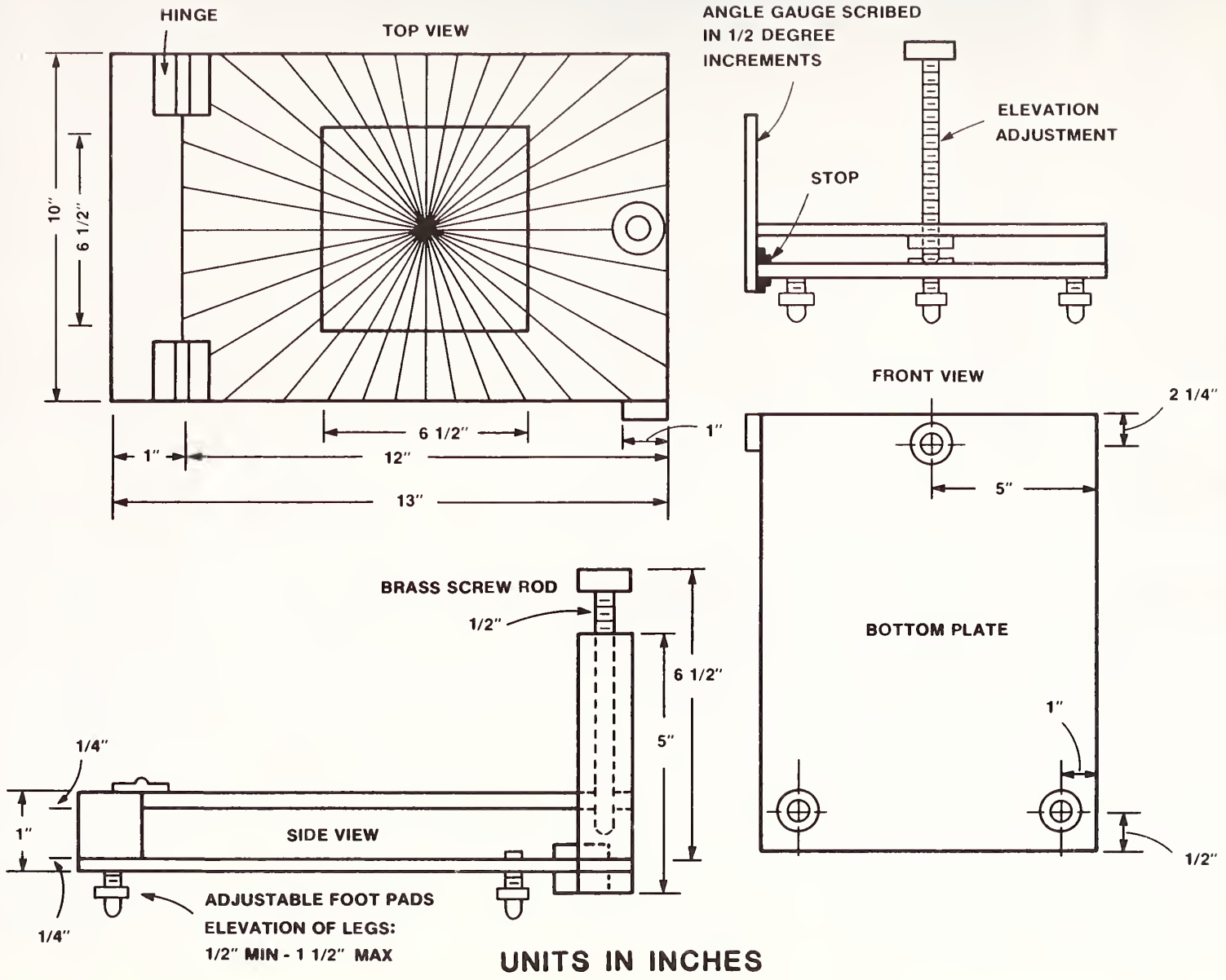

UNITS IN INCHES

NBS-114A (REV. 2-8C)

U.S. DEPT. OF COMM. BIBLIOGRAPHIC DATA SHEET (See instructions)	1. PUBLICATION OR REPORT NO. NBS TN 1161	2. Performing Organ. Report No.	3. Publication Date October 1982

4. TITLE AND SUBTITLE

Testing to Quantify the Effects of Handling of Gas Dielectric Standard Capacitors

5. AUTHOR(S)

Charles R. Levy

6. PERFORMING ORGANIZATION (If joint or other than NBS, see instructions)

NATIONAL BUREAU OF STANDARDS
DEPARTMENT OF COMMERCE
WASHINGTON, D.C. 20234

7. Contract/Grant No.

8. Type of Report & Period Covered

9. SPONSORING ORGANIZATION NAME AND COMPLETE ADDRESS (Street, City, State, ZIP)

same as #6

10. SUPPLEMENTARY NOTES

☐ Document describes a computer program; SF-185, FIPS Software Summary, is attached.

11. ABSTRACT (A 200-word or less factual summary of most significant information. If document includes a significant bibliography or literature survey, mention it here)

A test method known as the "Handling and Stability Test" is currently being used at NBS as part of the requirement for the five-part-per-million calibration of gas-dielectric standard capacitors. This test is used to achieve qualitative information on the effects of mechanical shock from shipping and handling on standard capacitors and to rank them quantitatively with respect to these effects.

12. KEY WORDS (Six to twelve entries; alphabetical order; capitalize only proper names; and separate key words by semicolons)

calibration; measurement assurance; reference standards; standard capacitors; standard qualification.

13. AVAILABILITY

☒ Unlimited
☐ For Official Distribution. Do Not Release to NTIS
☒ Order From Superintendent of Documents, U.S. Government Printing Office, Washington, D.C. 20402.
☐ Order From National Technical Information Service (NTIS), Springfield, VA. 22161

14. NO. OF PRINTED PAGES

44

15. Price

$4.75

IEEE TRANSACTIONS ON INSTRUMENTATION AND MEASUREMENT, VOL. IM-28, NO. 4, DECEMBER 1979

Losses in Electrode Surface Films in Gas Dielectric Capacitors

EDDY SO, MEMBER, IEEE, AND JOHN Q. SHIELDS

Abstract—**The surface characteristic of a number of electrode materials including stainless steel, brass, brass with various plated surfaces, aluminum, and anodized aluminum has been examined over a wide range of humidity. The measurements of surface characteristic, expressed in microradian millimeters, have an estimated uncertainty of 0.01 μrad · mm.**

I. Introduction

ONE STEP in studying the properties of a dielectric material is to use it as the dielectric of a capacitor and to determine its loss angle relative to a reference capacitor. Thus the behavior of the reference capacitor provides the bound of the measurement; and it becomes important to establish the limits within which its loss angle can be specified. In the absence of solid dielectric from the direct capacitance of a parallel-plate guard-ring capacitor, its loss is a function of its electrode-surface films and of electrode separation, and this property can be expressed in terms of loss-angle and separation [1], as the product microradian · millimeters.

The effect of electrode surface films on the loss in a 3-terminal gas-dielectric capacitor has been studied for a variety of surfaces and surface conditions at 1592 Hz, using a state-of-the-art transformer-ratio-arm bridge and a specially constructed test capacitor. The test capacitor consists of a parallel-plate guard-ring capacitor whose electrode separation can be adjusted while maintaining a vacuum or constant gas condition. The electrode mounting system provides auxiliary adjustments for making the electrodes concentric, coplanar, and parallel.

In order to find the product of loss angle and electrode separation of an electrode material, it is necessary that the absolute surface loss of the electrode material for a given electrode separation be known. This was accomplished by measuring the losss angle differences between a reference capacitor and the test capacitor at different electrode separations. After applying corrections for the bridge system and for lead resistance and voltage dependence associated with the test capacitor, the linear relationship between loss angle differences and corresponding values of capacitance was used to calculate the absolute loss angles of the test capacitor and reference capacitor.

Manuscript received June 15, 1979; revised July 2, 1979.

E. So was a Guest Worker at the National Bureau of Standards, Washington, DC. He is with the National Research Council of Canada, Ottawa, Ont. K1A OR 8. Canada.

J. Q. Shields is with the Electrical Measurements and Standards Division, National Bureau of Standards, Washington, DC 20234.

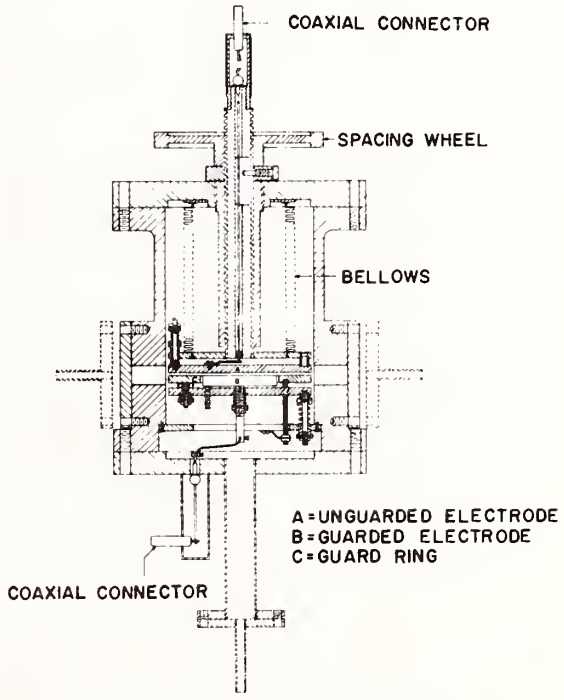

Fig. 1. Cross section of test capacitor.

The absolute measurements described were made with stainless steel electrodes in a dry gas condition. Measurements at only one setting of the test capacitor (100 pF) were subsequently required to calculate the surface characteristics for other electrode materials and relative humidity conditions.

II. Test Capacitor

A cross section of the test capacitor is shown in Fig. 1. The figure is drawn approximately to scale with the guarded electrode (*B*) having a diameter of 6.10 cm and the guard ring (*C*) having diameters of 6.35 cm and 11.75 cm.

The vacuum housing consists of a heavy cylindrical case constructed entirely of stainless steel. The top and bottom of the housing can be removed to expose the electrode surfaces. Aluminum gaskets are used for making it air tight. Two windows are provided so that the electrodes can be viewed from the side and air can be blown through it to clean the electrodes of dust or lint. The side covers with pipes shown beside the windows are used to make a closed system for

circulating air with a certain relative humidity through the electrode system.

The central guide rod of the movable electrode (A) extends through the top of the housing. The upper end of the guide rod is threaded (10 threads per inch), and a large diameter knurled nut (spacing wheel) is used on this to set the spacing between the electrodes. This nut works against the collar of a brass bushing. A bronze pin in the collar fits into a slot in the guide rod and this prevents the rotation of the movable electrode assembly. The rim of the spacing wheel is divided into 100 slots and a large diameter screw with fine threads (40 threads per inch) mounted on top of the case (not shown in Fig. 1) is used to rotate the spacing wheel (pushing against one of the slots).

The movable electrode (A) is mounted on a metal disk attached to the guide rod by three screws spaced 120° apart. The electrode is insulated from the metal disk and the case by small cylindrical insulators. A metal bellows is attached to the mounting disk and to the top lid of the case, which fits over the brass bushing.

The guarded electrode (B) and guard-ring (C) are also mounted on a metal disk. The mounting of the guard ring is such that it is insulated from the metal disk at a fixed distance. The guarded electrode is supported by three screws spaced 120° apart. Using these three screws adjustment for coplanarity with the guard ring can be made. The guarded electrode is held in place by a cylindrical rod at the center of the electrode, tightened against the metal disk by a spring and a nut. The hole in the center of the metal disk is made a bit larger than the rod so that adjustment can be made for eccentricity of the guarded electrode with respect to the guard ring. This whole assembly is again mounted on another metal disk (see Fig. 1) by three long screws spaced 120° apart, supported by springs. These screws are used for adjusting the parallelism of the upper and lower electrodes.

The deviation from perfect alignment which could be tolerated for each of the mechanical adjustments was determined from theoretical and experimental results. The theoretical calculations were based on earlier work [2] which showed that conductance resulting from a thin dielectric surface film is proportional to the rate of change of capacitance with displacement of the surface. The experimental determinations consisted of changing the electrode misalignment by measurable amounts while at the same time increasing the effective dielectric film loss through the use of vinyl tape applied to the electrode surfaces.

The above techniques were also used to show that one half of the loss angle contribution from dielectric surface films is attributable to the unguarded electrode. This result makes the investigation of different electrode materials much easier since only the unguarded electrode needs to be changed.

III. Absolute Measurement

In order to find the product of loss angle and electrode separation of an electrode material under certain conditions of measurement, it is necessary that the absolute surface loss of the electrode material for a given electrode separation be known. The technique used for determining absolute loss is basically the same as that described by Astin and others [3], [4]. It uses a parallel-plate guard-ring capacitor with variable electrode separation in one arm of the bridge and a standard capacitor in the other arm. The absolute loss angle of the guard-ring capacitor at different electrode separations is determined indirectly by first determining the absolute loss of the standard capacitor. Successive bridge measurements are made with the standard capacitor (C_s) alone or in parallel with auxiliary capacitors (nominal values equal to the standard capacitor C_s and their differences in loss with respect to C_s known from other measurements) while the capacitance of the guard-ring capacitor is set at C_s, $2C_s$, $3C_s$, etc. (in an equal-arm bridge) or $10C_s$, $20C_s$, $30C_s$, etc. (in a 10:1 ratio-arm bridge) by changing the separation between its electrode. The loss angle differences at these settings with respect to the standard capacitor can then be calculated from the measurements. When the resulting loss angle differences are plotted against the corresponding values of the guard-ring capacitance, the points are found to lie on a straight line. If this line be extended until it intercepts the axis (guard-ring capacitance = 0), the intercept gives the absolute loss angle of the fixed standard capacitor. This value can then be used in conjunction with the loss angle differences to calculate the absolute loss angles of the guard-ring capacitor.

The linear relationship described above is based on the assumption that the loss angle of the guard-ring capacitor is due entirely to electrode surface losses. In the present work significant contributions to the loss angle of the guard-ring capacitor (test capacitor) were found to result from lead resistances and voltage dependence. These contributions were evaluated and removed from the loss angle differences by means of appropriate corrections.

The bridge used to measure loss angle differences is a transformer ratio-arm bridge [5] having a nominal voltage ratio of 10:1, adjustable over the range ± 500 ppm (least count of 1×10^{-9}) and ± 50 μrad (least count of 1 nrad) [6]. The test capacitor was used on the low voltage side of the bridge (10 V) and balanced against a 10-pF standard capacitor on the high voltage side (100 V). Bridge balances were obtained for three different settings of the test capacitor corresponding to capacitances of 100 pF, 200 pF, and 300 pF, thus requiring two 10-pF auxiliary capacitors which could be used in parallel with the standard capacitor on the high voltage side.

One of the 10-pF fused silica capacitors that maintain the NBS unit of capacitance [7], designated as number 127, was used as the standard capacitor. Two others, designated as numbers 114 and 109, were used as auxiliary capacitors. If δ_{127}, δ_{114}, and δ_{109} denote the loss angles of the three fused silica capacitors and δ_{100}, δ_{200}, and δ_{300} denote the loss angles of the test capacitor at settings corresponding to 100 pF, 200 pF, and 300 pF, respectively, then the bridge balances described previously yield values for the following loss angle differences: $\delta_{100} - \delta_{127}$, $\delta_{100} - \delta_{114}$, $\delta_{100} - \delta_{109}$, $\delta_{200} - (\delta_{127} + \delta_{109})/2$, and $\delta_{300} - (\delta_{127} + \delta_{114} + \delta_{109})/3$, from which a simple calculation yields values for the desired

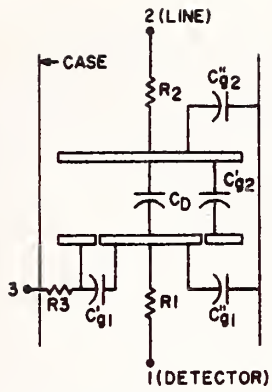

Fig. 2. Schematic diagram of test capacitor.

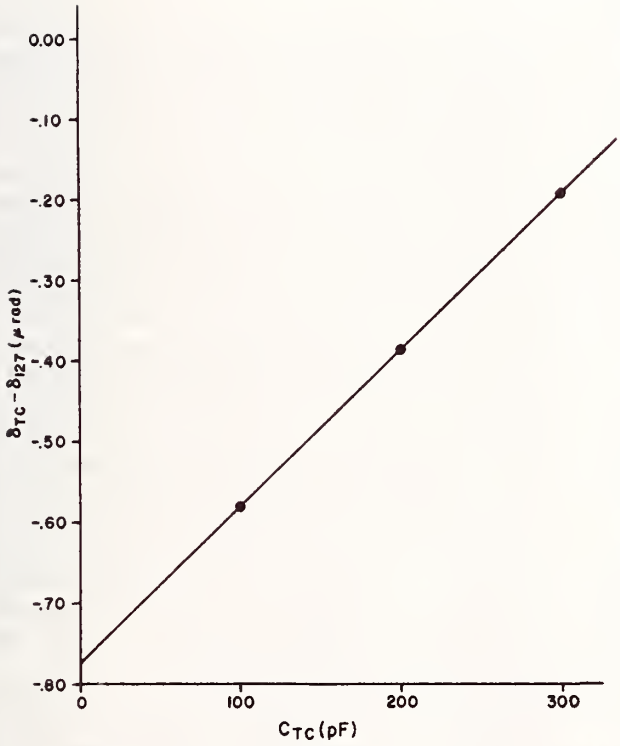

Fig. 3. Difference between the loss angle of the test capacitor δ_{TC} and that of the reference capacitor δ_{127} as a function of the capacitance of the test capacitor C_{TC}.

loss angle differences $\delta_{100} - \delta_{127}$, $\delta_{200} - \delta_{127}$, and $\delta_{300} - \delta_{127}$.

The loss angle differences measured by the bridge refer to loss angles as defined at coaxial tees connected to the line and detector terminals of each capacitor (four-terminal pair definition [8]). This results from the method used to obtain loading corrections, i.e., a special extrapolation technique involving the use of matched cables and connectors [9].

As mentioned previously, corrections are required for loss angle contributions from internal lead resistances and voltage dependence. The corrections for internal lead resistances are calculated from measurements of each of the

TABLE I
ESTIMATES OF THE EFFECTS OF POSSIBLE SYSTEMATIC ERRORS ON THE MEASUREMENT OF δ_{127}

Sources of Possible Systematic Error	Estimate* (μrad)
1. Loading corrections	0.004
2. Lead resistance corrections	0.005
3. Voltage dependence corrections	0.003
4. Effect of capacitance drift	0.005
5. Bridge calibration and stability	0.005
Direct sum:	0.022
rss:	0.010

*These values are subjective estimates intended to be comparable with statistical 2 σ limits.

capacitances and resistances shown in Fig. 2. The only significant distributed capacitance (not shown) was that associated with R_2. One half of this capacitance was included in C''_{g2} and an appropriate systematic uncertainty assigned. The resistances were measured as four-terminal resistances at 1592 Hz. Small spring contacts inserted through the side windows of the housing provided two points of contact for each electrode. Corrections for voltage dependence were calculated from measurements using previously established standards of voltage dependence [10].

The final corrected values for the loss angle differences are

$$\delta_{100} - \delta_{127} = -0.580\ \mu\text{rad} \quad (1)$$

$$\delta_{200} - \delta_{127} = -0.385\ \mu\text{rad} \quad (2)$$

$$\delta_{300} - \delta_{127} = -0.192\ \mu\text{rad}. \quad (3)$$

The values shown are the averages from eight measurements involving the use of three dry gases: N_2, CO_2, and SF_6. There was no statistically significant difference with respect to the choice of gas dielectric. Stainless steel electrodes were used for all measurements. The linear relationship between loss angle differences and the corresponding values of capacitance is illustrated in Fig. 3 where the calculated value of the y intercept is

$$\delta_0 - \delta_{127} = -0.774\ \mu\text{rad}. \quad (4)$$

Assuming that the values of δ_{100}, δ_{200}, and δ_{300} in (1), (2), and (3) result entirely from surface losses, i.e., assuming that we have successfully identified and corrected for all other loss angle contributions, then the value of δ_0 corresponding to zero capacitance (infinite electrode separation) is zero and from (4)

$$\delta_{127} = 0.774\ \mu\text{rad}.$$

The standard deviation of δ_{127} is 0.005 μrad, thus pointing out the fact that individual measurement results deviate significantly from Fig. 3. Estimates of the effects of possible systematic errors on the measurement of δ_{127} are listed in Table I. Items 1 through 3 account for uncertainities in the corrections previously described. Item 4 accounts for uncertainty in the quadrature balance due to capacitance drift (as a result of temperature effects) in association with imperfect

adjustment of the phase-sensitive detector. Item 5 is due mainly to uncertainty in the 10:1 voltage ratio of the bridge transformer which was measured using a modified version [9] of the permutation method [11].

The value obtained for the absolute loss of standard capacitor 127 was found to agree with the value measured in terms of a toroidal cross capacitor [12] within a few nanoradians. The agreement between measured values provides a valuable check on both absolute measurements. A second area of agreement is in the value obtained for the surface characteristic of stainless steel under dry gas condition.

IV. Surface Characteristic Measurements

The surface characteristic (SC) of stainless steel under dry gas condition can be calculated from the results of the previous section. Substituting the value obtained for δ_{127} into (1) yields

$$\delta_{100} = 0.194\ \mu\text{rad}.$$

Multiplying 0.194 μrad by 0.269 mm, the electrode separation of the test capacitor at 100 pF yields

$$\text{SC} = 0.05\ \mu\text{rad} \cdot \text{mm}.$$

The surface characteristics of stainless steel under different relative humidity conditions (to be described shortly) were calculated in the same manner with the only changes being the numerical values in (1). Thus each relative humidity condition requires but one additional bridge balance with the test capactitor remaining fixed at 100 pF.

The above procedure was also used to determine the surface characteristics of different electrode materials. However, because only the unguarded electrode was changed, one additional calculation was required, e.g.,

$$(\text{SC})_{\text{AA}} = 2(\text{SC})_{\text{AS}} - (\text{SC})_{\text{SS}}$$

where $(\text{SC})_{\text{AA}}$ is the surface characteristic that would have been obtained if all electrodes were made of aluminum, $(\text{SC})_{\text{AS}}$ is the value obtained when the unguarded electrode is made of aluminum and the other electrodes are of stainless steel, and $(\text{SC})_{\text{SS}}$ is the value obtained under the same relative humidity condition when all electrodes are made of stainless steel.

It should be noted that the value of δ_{127} does not actually enter into the calculation of surface characteristic, i.e., substituting the expression used to calculate δ_{127} into (1) results in a formula for δ_{100} which is independent of δ_{127}. This is consistent with the more direct calculation of δ_{100} in which (1) is subtracted from (3) and the result divided by 2 yielding

$$\delta_{100} = (\delta_{300} - \delta_{100})/2 = 0.194\ \mu\text{rad}$$

which agrees with the value obtained previously.

Thus the one requirement for δ_{127} is that its value, whatever it may be, not change during the measurements, and similarly for the transformer voltage ratio whose value does not enter into the surface characteristic calculations. A third quantity which must remain constant throughout the measurements is the surface loss of the stainless steel reference electrodes consisting of the guarded electrode and guard ring. An estimate of the overall stability of these quantities was obtained by periodically remeasuring the original system, i.e., all electrodes of stainless steel and under dry gas condition.

TABLE II
Surface Characteristics of Different Electrode Materials Under Dry Gas Condition

Electrode Material	Surface Characteristic (μrad-mm)
Stainless steel	0.05
Silver-plated brass	0.06
Gold-plated brass	0.06
Nickel-plated brass	0.06
Rhodium-plated brass	0.08
Brass	0.12
Aluminum	0.10

As previously mentioned, surface characteristics were measured over a wide range of humidity. A convenient method using a saturated salt solution exists for establishing atmospheres of known relative humidity which depend upon the equilibrium vapor pressure of water when a chemical is dissolved in it [13], [14]. A closed circulating air system incorporating a suction-pressure pump was used in conjunction with five different saturated salt solutions to obtain relative humidities of 14, 33, 54, 75, and 92 percent.

Table II shows the surface characteristics of different electrode materials under dry gas (N_2) conditions. Fig. 4 shows the surface characteristics of stainless steel, brass, and of silver, gold, nickel and rhodium-plated brass under different relative humidity conditions. A semilog scale is used in Fig. 5 to show the surface characteristics of aluminum and of a particular specimen of anodized aluminum under the same relative humidity conditions; stainless steel is included for comparison purposes.

Possible systematic errors in the surface characteristic determinations are the same as those listed in Table I but with each having a numerical estimate of 0.002 μrad · mm or less. An overall uncertainty of 0.01 μrad · mm was assigned to the surface characteristic measurements based on the estimates of possible systematic error (root-sum-square = 0.004 μrad · mm) and a standard deviation of 0.003 μrad · mm. It is important to realize that these uncertainties apply only to the measurement process and that the quantities being measured are dependent upon surface conditions which can be difficult to control or specify.

It should be noted that cleaning the electrodes and keeping them clean was quite necessary for consistent results. Small quantities of dust were especially troublesome. The electrodes were prepared by first degreasing them using acetone and methanol, then washing them in soapy water (using a detergent) and rinsing them with distilled water. To avoid water spots methanol was again used and dry air was then blown over the surface of the electrodes.

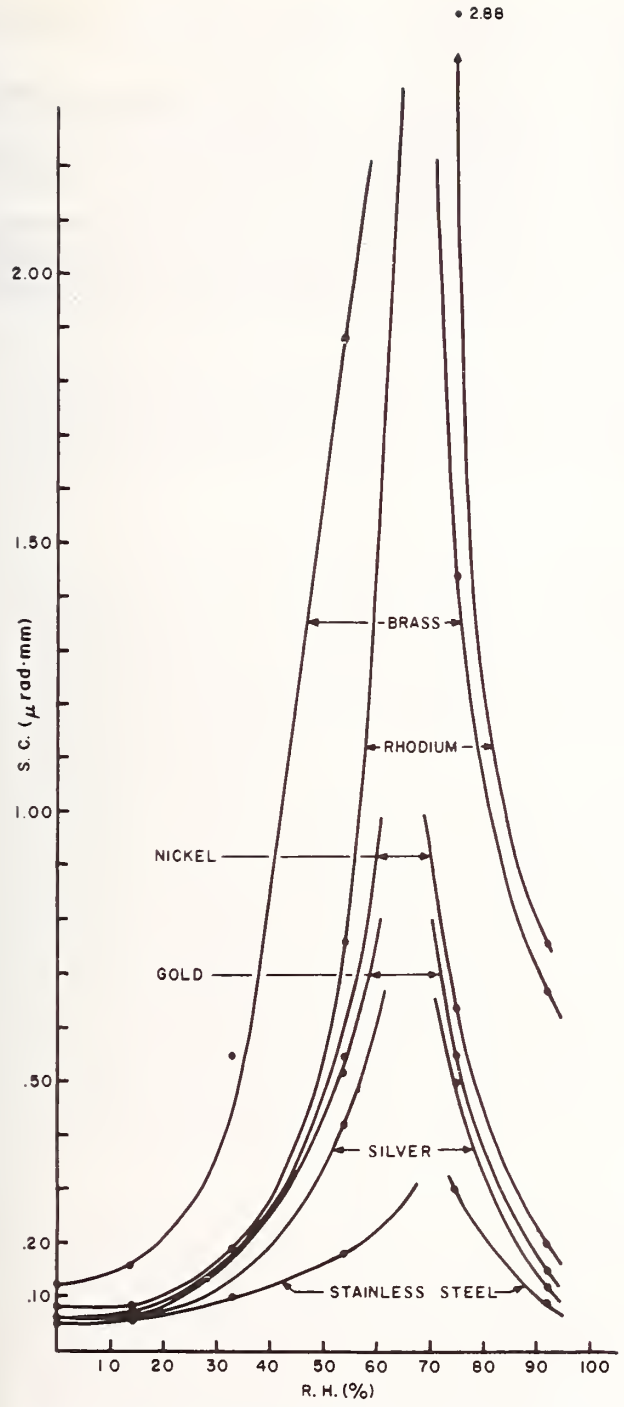

Fig. 4. Surface characteristics (SC) of stainless steel, brass, and of silver, gold, nickel, and rhodium-plated brass as a function of relative humidity (RH).

V. Conclusion

Stainless steel (type 304) seems to have the best surface characteristic as compared to the other electrode materials under dry conditions as well as under moisturized conditions. The surface characteristic of stainless steel under dry gas condition is 0.05 μrad · mm, while the surface characteristics of the silver, gold and nickel-plated brass are only slightly higher at 0.06 μrad · mm. Thus under dry conditions these four materials are recommended for use as electrodes in low-loss reference standards. Even though aluminum under dry conditions is slightly better than unplated brass, aluminum would be a questionable choice as the electrode material of a capacitor which is to serve as a low-loss reference standard. In the presence of moisture the surface losses of aluminum increase much more rapidly than for the other measured electrode materials. In addition, it was found that the surface of aluminum releases absorbed moisture less readily than the surfaces of the other materials studied.

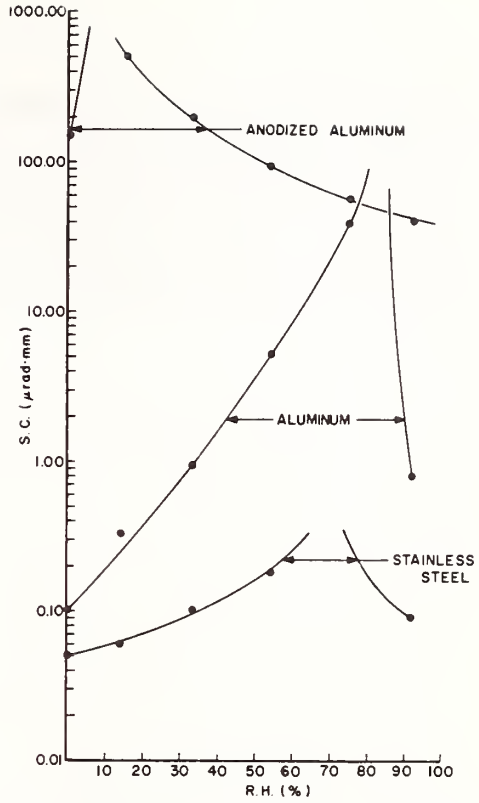

Fig. 5. Surface characteristics of aluminum, anodized aluminum, and stainless steel as a function of relative humidity (semilog scale).

References

[1] A. V. Astin, "Nature of energy losses in air capacitors at low frequencies," *J. Res. Nat. Bur. Stand.*, vol. 22, p. 673, June 1939, RP1212.

[2] J. Q. Shields, "Phase-angle characteristics of cross capacitors," *IEEE Trans. Instrum. Meas.*, vol. IM-21, pp. 365–368, Nov. 1972.

[3] A. V. Astin, "Measurement of relative and true power factors of air capacitors," *J. Res. Nat. Bur. Stand.*, vol. 21, p. 425, Oct. 1938, RP1138.

[4] W. B. Kouwenhoven and E. L. Lotz, "Absolute power factor of air capacitors," *AIEE Trans.*, vol. 57, p. 766, 1938.

[5] A. M. Thompson, "The precise measurement of small capacitances," *IRE Trans. Instrum.*, vol. I-7, pp. 245–253, Dec. 1958.

[6] R. D. Cutkosky, "Active and passive direct-reading ratio sets for the comparison of audio-frequency admittances," *J. Res. Nat. Bur. Stand.*, vol. 68-C, no. 4, pp. 227–236, Oct.–Dec. 1964.

[7] R. D. Cutkosky and L. H. Lee, "Improved ten-picofarad fused silica dielectric capacitor," *J. Res. Nat. Bur. Stand.*, vol. 69-C, pp. 173–179, July–Sept. 1965.
[8] R. D. Cutkosky, "Four-terminal pair networks as precision admittance and impedance standards," *Commun. Electron.*, vol. 70, pp. 19–22, Jan. 1964.
[9] J. Q. Shields, "Measurement of four-pair admittances with two-pair bridges," *IEEE Trans. Instrum. Meas.*, vol. IM-23, pp. 345–352, Dec. 1974.
[10] ———, "Voltage dependence of precision air capacitors," *J. Res. Nat. Bur. Stand.*, vol. 69-C, no. 4, pp. 265–274, Oct.–Dec. 1965.
[11] R. D Cutkosky and J. Q. Shields, "The precision measurement of transformer ratios," *IRE Trans. Instrum.*, vol. I-9, pp. 243–250, Sept. 1960.
[12] J. Q. Shields, "Absolute measurement of loss angle using a toroidal cross capacitor," *IEEE Trans. Instrum. Meas.*, vol. IM-27, pp. 464–466, Dec. 1978.
[13] A. Wexler and S. Hasegawa, "Relative humidity—temperature relationships of some saturated salt solutions in the temperature range 0° to 50°C," *J. Res. Nat. Bur. Stand.*, vol. 53, no. 1, July 1954, RP2512.
[14] A. Wexler and W. G. Brombacher, "Methods of measuring humidity and testing hygrometers," NBS Circular S12, Sept. 28, 1951.

IEEE TRANSACTIONS ON INSTRUMENTATION AND MEASUREMENT, VOL. IM-27, NO. 4, DECEMBER 1978

A Programmable Phase-Sensitive Detector for Automatic Bridge Applications

ROBERT D. CUTKOSKY, FELLOW, IEEE

Abstract—**A phase-sensitive detector is described which features programmable gain, digital output, and a resolution of 0.02 μV. The instrument suppresses harmonic sensitivity through the use of analog circuitry which multiplies the signal by constant amplitude sine and cosine waves derived from an external reference of arbitrary voltage and frequency.**

I. Introduction

AN AUTOMATIC audio frequency bridge is now under construction at the National Bureau of Standards (NBS). Although this instrument is intended mainly for calibrating capacitors, ac resistors, and inductive dividers in conjunction with the NBS calibration service, it also serves as a convenient vehicle for investigating techniques for achieving rapid convergence of bridges containing multiple auxiliary balance circuits.

Conceptually the bridge is balanced by measuring the complex voltages at a number of points with a phase sensitive detector or voltmeter, and by adjusting the main and auxiliary bridge variables until all of these voltages are nulled, or are sufficiently small. This process may be iterative, and is performed under computer control.

Many commercial phase sensitive detectors are available for use with manually balanced bridges, but none were found which combined programmable gain and digital output with either very low intrinsic harmonic sensitivity or a means of automatically tuning the signal channel to suppress harmonic sensitivity. The instrument described here was designed to meet these requirements.

II. Design

This instrument was intended for use with a nominally frequency-independent bridge driven by a frequency synthesizer with a reasonably pure sine-wave output. The harmonic rejection requirements of such a system are not especially severe, but the use of switching type demodulators, which are highly sensitive to odd harmonics, would have required the use of a tuned signal amplifier. This complication was avoided by using analog multipliers for the in-phase and quadrature demodulators (see Fig. 1). The signal amplifier is untuned, and connected to the x inputs of both multipliers. The y input of the first multiplier is driven with a sine wave having a peak voltage of 5 V derived from the reference oscillator; the y input of the second multiplier is driven with a cosine wave having a peak voltage of 5 V derived from the same oscillator. The output of each multiplier is integrated for one second and these averaged values are converted to digital form upon reception of a local or remote conversion command with a pair of 8-bit analog to digital converters. Use is thereby made of the orthogonality of the sine and cosine functions to suppress harmonic sensitivity.

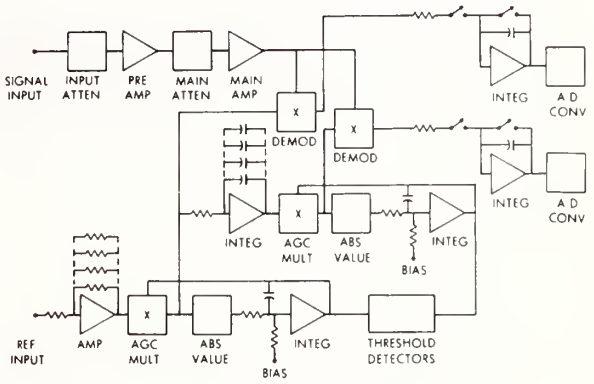

Fig. 1. Block diagram of phase sensitive detector.

The integration time was chosen to be one second in our instrument in order to achieve an adequate signal to noise ratio. A capability for selecting a shorter integration time when less than maximum sensitivity was required would have resulted in a generally faster instrument, but in addition to the increased complexity entailed, an integration time shorter than one second would have caused averaging uncertainties at low frequencies.

The constant amplitude sine wave is obtained through the use of an automatic gain control circuit in which the gain control element is an analog multiplier. The difference between a dc reference voltage and the absolute value of the output sine wave is integrated and applied to the y input of the multiplier for level control. In order to accommodate reference input voltages from 0.06 V to 40 V, one of five discrete ranges is automatically selected dependent upon the states of upper and lower threshold detectors fed by the integrator.

The constant amplitude cosine wave is obtained by integrating the constant amplitude sine wave and using the same gain control circuitry described above, except that the

Manuscript received June 5, 1978.

The author is with the Electrical Measurements and Standards Division, National Bureau of Standards, Washington, DC 20234.

threshold detectors select different integrating capacitors to yield a useful frequency range of 10 Hz to 50 kHz.

If one of the thresholds is crossed, the appropriate status is displayed, and signaled to the computer if in "remote" mode. Then, an internal one-second clock shifts resistors or capacitors into or out of the appropriate circuit as required, until both integrators are within their prescribed limits. After a further delay to provide adequate settling, the status indication is cleared.

The signal amplifier consists of a preamplifier containing a low-noise field effect transistor [1], a programmable attenuator with a range of 75 dB and a post amplifier. An additional 60 dB of attenuation can be obtained by switching a 1000:1 divider into the circuit before the preamplifier. A TTL decoder is provided so that the attenuation can be programmed in standard binary code, the least significant bit representing 5 dB. Maximum gain is 135 dB, which gives a resolution of 0.02 μV. At minimum gain (0 dB), full-scale indication represents about 10 V.

The instrument is housed in a 5¼" relay rack module, which includes a double mu-metal shield for the preamplifier, the necessary power supplies, the logic circuits to provide timing, decoding and status information, and the LED indicators for local display of gain, output, and status.

References

[1] S. Harkness, "Low noise FET amplifiers for low loss capacitative sources," NPL Report DES 41, National Physical Laboratory, Teddington, England, June 1977.

Reprinted by permission from IEEE TRANSACTIONS ON INSTRUMENTATION AND MEASUREMENT
Vol. IM-23, No. 4, December 1974, pp. 345-352

Measurement of Four-Pair Admittances with Two-Pair Bridges

JOHN Q. SHIELDS

***Abstract*—The purpose of this paper is twofold: 1) to show how extrapolation techniques can be used to obtain well-defined and versatile measuring systems; and 2) to apply such techniques to the measurement of four-pair admittances with two-pair bridges. When four-pair admittances are large, measurements with two-pair bridges have limited precision, but with reasonably small admittances, measurement precision is essentially equal to that attained with four-pair bridges.**

INTRODUCTION

ALTHOUGH a major portion of the present paper will be devoted to the measurement of four-pair admittances with two-pair bridges, this represents but one example of the use of extrapolation techniques which are applicable to a variety of situations. Basically, extrapolation techniques provide a means for adapting existing measuring systems to changing needs while at the same time, retaining well-defined measuring conditions. The paper illustrates this, to a degree, by including applications which are not restricted to four-pair admittances, e.g., the elimination of the effects of matched cables, and a double permutation method for measuring transformer ratios. When the applications are restricted to four-pair admittances, it is important to keep in mind that any two-pair admittance is easily converted to a four-pair admittance by the addition of two coaxial tees. The reader is referred to earlier papers [1], [2] by Cutkosky for a discussion of the advantages of four-pair admittances as precision standards.

When four-pair admittances are large, measurements with two-pair bridges have limited precision, but with reasonably small admittances, measurement precision is essentially equal to that attained with four-pair bridges. For example, measurements of four-pair capacitance standards in the range from 10 to 1000 pF at $\omega = 10^4$ can be made with uncertainties on the order of 1 or 2 parts in 10^9 using either four-pair bridges or two-pair bridges.

The author has attempted to write the paper in a manner that would be useful to practitioners of precision measurements at many levels. As a result, there is a detailed description of the direct-reading ratio set and two-pair bridges at one extreme, and, at the other extreme, the term "defining transformers,"[1] is used here with only a reference for descriptive purposes. The reader's discretion is encouraged.

THEORY

The four-pair admittance, as originally described by Cutkosky [1], [2], is shown in Fig. 1. The parameter of interest is defined as the ratio of the current at pair 3 to

Manuscript received July 3, 1974; revised August 22, 1974.
The author is with the Electricity Division, National Bureau of Standards, Washington, D. C. 20234.

[1] The auxiliary balances of the four-pair DRRS are such that four-pair admittances are defined at "defining transformers" [2] rather than at connectors. This change in defining conditions was easily accounted for by adding 2.35 pF to the measured values of the two-terminal admittances which were extrapolated to zero.

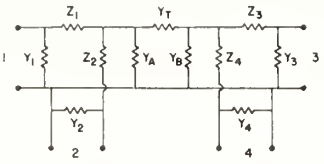

Fig. 1. Complete circuit of four-pair admittance standard.

the open-circuit voltage at pair 2, subject to the condition that both the voltage and current at pair 4 are zero. This parameter has the dimensions of admittance and may be written

$$P_{32}{}^{14} = \frac{i_3}{e_2}\bigg| i_2 = i_4 = 0, \qquad e_4 = 0. \tag{1}$$

Using Fig. 1, it can be shown that

$$P_{32}{}^{14} = Y_T(1 + Y_2Z_2)(1 + Y_3Z_3). \tag{2}$$

In comparison, the corresponding two-pair admittance is defined as the ratio of the short-circuit current at pair 3 to the voltage at pair 2, with the implicit condition that pairs 1 and 4 are open-circuited (capped if necessary–otherwise ignored). This may be written

$$Y_{32} = \frac{i_3}{e_2}\bigg| e_3 = 0. \tag{3}$$

If admittances are added to pairs 1 and 4, the value of Y_{32} will be changed, but $P_{32}{}^{14}$ will remain unchanged. This applies even if the terminals of pairs 1 and 4 are modified in the process.

It can be shown that if the admittances added to pairs 1 and 4 are correctly chosen, then

$$Y_{32} = P_{32}{}^{14}.$$

The correct admittances are those which will result in $Y_{22} = Y_{33} = 0$ where

$$Y_{22} = \frac{i_2}{e_2}\bigg| e_3 = 0 \tag{4}$$

and

$$Y_{33} = \frac{i_3}{e_3}\bigg| e_1 = 0. \tag{5}$$

Y_{22} is the easily measured two-terminal admittance at pair 2 with pair 3 shorted. For most purposes, Y_{33} can be measured in a similar manner, i.e., as the two-terminal admittance at pair 3 with pair 2 shorted. This changes the condition $e_1 = 0$ in (5) to $e_2 = 0$ and results in

$$Y_{32} = P_{32}{}^{14} + \text{terms in } (YZ)^2 \text{ and higher}. \tag{6}$$

It is not generally practical to adjust $Y_{22} = Y_{33} = 0$, but fortunately, it is sufficient to add an admittance to pair 1, note the corresponding changes in Y_{22} and Y_{32}, and effectively extrapolate Y_{22} to zero by means of appropriate corrections to Y_{32}. A corresponding sequence is used to effectively extrapolate Y_{33} to zero.

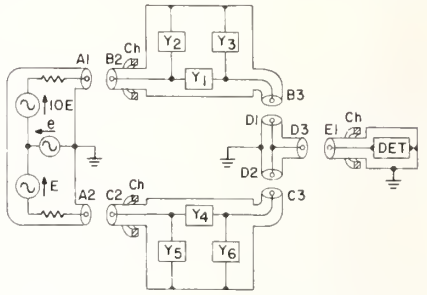

Fig. 2. Comparison of two-pair admittances using the two-pair direct-reading ratio set.

APPLICATIONS

Although the basic concepts presented in the previous section should be applicable to a variety of measuring systems, the examples presented in this paper have been limited to measurements using the transformer ratio-arm bridge [3], [4] with adjustable ratio. This type of bridge is commonly termed an ac direct-reading ratio set [5] and will henceforth be referred to simply as a DRRS. In Fig. 2, the equivalent circuit of a DRRS is represented by the component having coaxial connectors $A1$ and $A2$. The bridge is balanced by adjusting the voltage ratio at connectors $A1$ and $A2$ by means of a small adjustable voltage designated e in Fig. 2. The voltage e consists of two components, α and β, which provide adjustments to both the real and quadrature components of the voltage ratio. Typically, α and β would each consist of six decades providing a range of ± 500 ppm and ± 500 μrad, respectively, and a least count of 1×10^{-9} and 1 nrad, respectively.

The complete circuit of Fig. 2 is typical of the type of circuit used to compare precision two-pair admittances whose nominal values are in a ratio of 10:1. Net currents in the cables are reduced to negligible amounts by the use of coaxial chokes [3], [6], which are designated *Ch* in Fig. 2. The component having connectors $B2$ and $B3$ represents the equivalent circuit of a two-pair admittance defined at connectors $B2$ and $B3$, and similarly for the component having connectors $C2$ and $C3$. It will be assumed for the present that the coaxial tee is ideal, i.e., the voltage at $D1$ and $D2$ is zero when the voltage at $D3$ is zero.

A. Four-Pair Measurements

Fig. 3 is identical to Fig. 2 if all adjacent connectors are joined. If $F1$ and $F2$ are disconnected, the component having connectors $B1$, $B2$, $B3$, and $B4$ can be considered as a pictorial representation of a four-pair admittance (henceforth termed four-pair admittance P_B) whose complete circuit would be similar to that shown in Fig. 1 with pairs 1, 2, 3, and 4 corresponding to connectors $B1$, $B2$, $B3$, and $B4$, respectively. Similar considerations can be applied to the component having connectors $C1$, $C2$, $C3$, and $C4$ (henceforth termed four-pair admittance P_c).

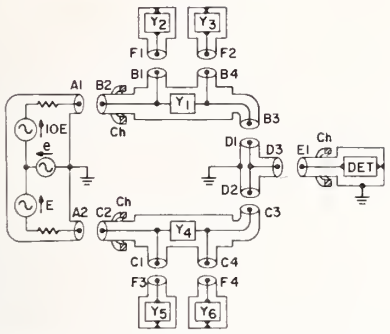

Fig. 3. Comparison of two-pair admittances having adjustable shunt admittances Y_2, Y_3, Y_5, and Y_6.

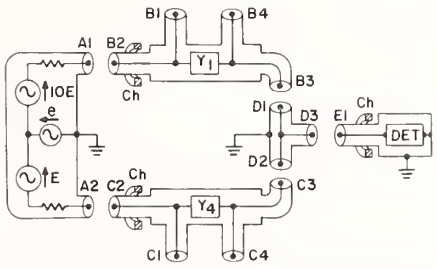

Fig. 4. Four-pair admittances connected into a two-pair bridge.

It is important to bear in mind that when all connectors are joined, Y_1, Y_2, and Y_3 represent the lump-sum admittances of the equivalent circuit of a two-pair admittance, and, similarly, for Y_4, Y_5, and Y_6. If Y_2, Y_3, Y_5, and Y_6 have been adjusted so that $Y_2 = Y_3 = -Y_1$ and $Y_5 = Y_6 = -Y_4$, with all connectors joined, then, referring to (4), (5), and (6), it can be seen that the value of e required to balance the bridge will yield a measure of the ratio of Y_1 to Y_4 which is the same[2] as the ratio of four-pair admittance P_B to four-pair admittance P_c, as would be obtained with a regular four-pair bridge. Note that when the bridge is balanced, there is no current between $A1$ and $B2$ or between $A2$ and $C2$. This not only satisfies one of the defining conditions of a four-pair admittance, but also eliminates the need to account for the equivalent lead impedances in the DRRS.

As pointed out in the section on theory, it is not necessary to reduce the current between $A1$ and $B2$ to zero. It is sufficient to change the current, note the corresponding change in e required to rebalance the bridge, and effectively extrapolate the current to zero by means of appropriate corrections to e. Details of the complete extrapolation are more easily described using Fig. 4 and the equation

$$e_x = e_N + (-Y_{B2}/Y_L)(e_{B1} - e_N) + (-Y_{B3}/Y_L)(e_{B4} - e_N) + (-Y_{C2}/Y_L)(e_{C1} - e_N) + (-Y_{C3}/Y_L)(e_{C4} - e_N) \quad (7)$$

where e_x is the value of e which yields a measure of the ratio of four-pair admittance P_B to four-pair admittance P_c, e_N is the value of e required to balance the bridge in the normal condition shown in Fig. 4 (unused connectors may require caps which are not shown), Y_L is a two-terminal admittance defined at a connector which is joined to connectors $B1$, $B4$, $C1$, and $C4$ (each in turn), e_{B1}, e_{B4}, e_{C1}, and e_{C4} are the corresponding values of e required to balance the bridge, Y_{B2}, Y_{B3}, Y_{C2}, and Y_{C3} are two-terminal admittances measured at connectors $B2$, $B3$, $C2$, and $C3$, respectively, with a short at connectors $B3$, $B2$, $C3$, and $C2$, respectively.

For practical usage, (7) must be separated into real and imaginary parts yielding two equations, one for α_x and one for β_x, where α and β correspond to the real and quadrature components of e as previously described. However, for simplicity, (7) will be used in the discussion which follows.

Note that the last four terms of (7) are simply corrections which are applied to e_N. In general, the corrections do not need to be determined to high accuracy, e.g., $\pm 1 \times 10^{-3}$ is sufficient for many applications. If Y_L is chosen to be many times larger than Y_{B2}, Y_{B3}, Y_{C2}, and Y_{C3}, then the measurements of $(e_{B1} - e_N)$ and $(e_{C1} - e_N)$ will be above the noise level of the system; the effect on the measurements of $(e_{B4} - e_N)$ and $(e_{C1} - e_N)$ will depend on the particular circuit being used. Y_L should obviously not be a component which reduces the signal-to-noise ratio unnecessarily.

B. Two- and Three-Pair Measurements

If the third and fourth correction terms in (7) are eliminated, e_x will yield a measure of a two-pair admittance in terms of a four-pair admittance. If the second and fourth correction terms in (7) are eliminated, e_x will yield a measure of the ratio of two three-pair admittances. The latter is particularly useful for comparing the main ratios of different transformer ratio-arm bridges (including four-pair bridges which are adaptable to a three-pair configuration).

C. Elimination of Cable Effects

In all of the examples thus far presented, the admittances have been defined at the ends of cables connected to the admittance standards. This can cause problems under certain circumstances, especially since the cables containing coaxial chokes are of necessity quite long (often approaching 3 m in length).

Fig. 5 is intended to illustrate two four-pair admittance standards, P_B and P_C, whose defining pairs are coaxial connectors ($B1$, $B2$, $B3$, $B4$, and $C1$, $C2$, $C3$, $C4$) which are permanently attached to the housings of the standards. The component having connectors $G1$, $G2$, and $G3$ represents a cable with a permanently attached coaxial tee (henceforth termed cable G) and similarly for the component having connectors $H1$, $H2$, and $H3$ (henceforth

[2] Neglecting the effect of terms in $(YZ)^2$ and higher. The remainder of the paper is subject to the preceding condition wherever applicable.

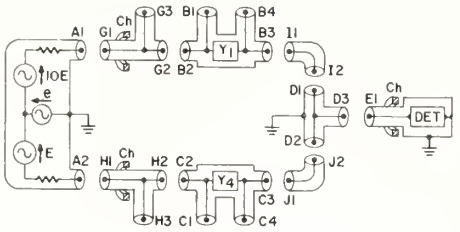

Fig. 5. Circuit for illlustrating how to eliminate the effects of coaxial cables and coaxial tees used to connect the admittance standards to the bridge.

termed cable H). The other cables will be termed cable I and cable J. The coaxial tee ($D1$, $D2$, $D3$) will no longer be assumed to be ideal.

It can be shown that the effects of cables G, H, I, and J, coaxial tee ($D1$, $D2$, $D3$), and the equivalent lead impedances of the DRRS can all be eliminated by extrapolation techniques. Details of the extrapolation are more easily described using the equation

$$e_x = e_N + (-Y_{B2}/Y_L)(e_{B1} - e_N) + (-Y_{B3}/Y_L)(e_{B4} - e_N) + (-Y_{C2}/Y_L)(e_{C1} - e_N) + (-Y_{C3}/Y_L)(e_{C4} - e_N) + (-Y_{G1}/Y_L)(e_{G3} - e_N) + (-Y_{H1}/Y_L)(e_{H3} - e_N). \quad (8)$$

Note that with the exeeption of the two extra terms at the end of (8), it is identical to (7). These two terms are correction terms similar to the four eorreetion terms which precede them, with e_{G3} and e_{H3} being the values of e required to balance the bridge when the defining connector of Y_L is joined to conneetors $G3$ and $H3$, respectively. Y_{G1} and Y_{H1} are the two-terminal admittances measured at connectors $G1$ and $H1$, respectively, with connectors $G2$ and $H2$ open-circuited.

One result of applying the correction terms is that, in effeet, no current flows between $A1$ and $G1$, between $G2$ and $B2$, between $A2$ and $H1$, or between $H2$ and $C2$. This means that only the lead impedances and shunt admittances associated with cables G and H affect the ehanges in voltage from $A1$ to $G2$ and from $A2$ to $H2$, and these changes are proportional to the voltages. If cables G and H are matched cables, i.e., if they have identical electrical characteristics, then the ratio of the voltage at $G2$ to the voltage at $H2$ will be the same as the ratio of the voltage at $A1$ to the voltage at $A2$.

A similar effect occurs at the detector end of the circuit, only this is related to proportional changes in current rather than voltage. The result is that if eables I and J are matched cables, and if the eoaxial tee is such that $D1$ and $D2$ are electrically symetrical with respect to $D3$, then they will have no effect on the bridge balance. It is interesting to note that matched cables yield equal lead impedances, whereas with ordinary unshielded bridges having 10 to 1 ratio arms, the lead impedances would need to be in the ratio of 10 to 1 with respect to each other if they were to have no effect on the bridge balance. If the eables are not matched, and if the coaxial tee is not symmetrieal, then we can interchange cables G and H, eables I and J, and rotate the coaxial tee. This will result in a new value of e_x. It can be shown that the average of the two values of e_x will yield a correet value for the ratio of the two four-pair admittances.

D. Cable Effects in Other Circuits

The extrapolation techniques for eliminating the effects of cables G and H are not limited to the circuit shown. For example, if the two four-pair admittances are connected into a regular four-pair bridge, we can still add admittanee Y_L to $G3$ and to $H3$, note the corresponding changes in the bridge balance, and apply eorrection terms similar to those described previously.

If the components containing $Y1$ and $Y4$ represent two-pair admittances, then the effects of cables G and H can only be partially eliminated. In general, however, if the junctions of $G3$ and $H3$ are close to $G2$ and $H2$, respectively, then the effeets not eliminated will be quite small compared to those eliminated, which include the effects of the equivalent series impedances of the DRRS. When Y_L is added to $G3$, the admittance to be extrapolated to zero is the sum of Y_{G1} and Y_{B2} (as previously defined) and similarly for the other side of the bridge. If the effects of cables I and J are large, eoaxial tees ean be joined to $I1$ and $J1$, thus permitting an extrapolation process similar to the preceding.

E. Parallel Admittance Measurements

Fig. 6 shows two nominally-equal four-pair admittances in parallel being compared to a third four-pair admittance. Although the auxiliary balances associated with regular four-pair bridges are usually not adaptable to this type of comparison, the comparison by means of extrapolation techniques is the same as described previously, with the six resulting correction terms similar to the four correction terms in (7). If matched cables are used (not shown in Fig. 6), the extrapolation process results in nine correetion terms which are similar to the six eorrection terms in (8).

If the eables are not perfeetly matched and if the coaxial star ($M1$, $M2$, $M3$, $M4$) is not perfectly symmetrical, then the cables and the star can be permuted to obtain a total of three different values of e_x. It can be shown that the average of the three values will yield a correct measure of the sum of two four-pair admittances in terms of a third four-pair admittanee.

In order to better understand the permutation process, imagine that three cables similar to G in Fig. 5 are inserted between $A1$ and $B2$, between $A2$ and $K2$, and between $A3$ and $L2$, and that each cable is used to join a different pair during each of the three different measurements. The other half of the extrapolation process, which is carried out simultaneously, is more easily understood by imagining that $M1$, $M2$, and $M3$ are connectors at the ends of three cables which have been permanently joined to a coaxial star, and that each of these connectors is joined to a different four-pair admittance during each of the three

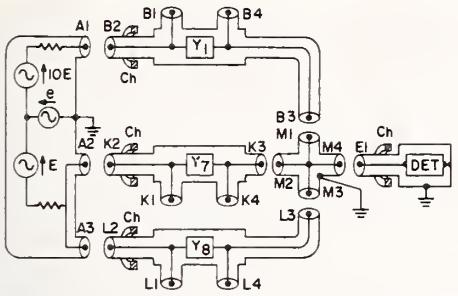

Fig. 6. Circuit for measuring the sum of two four-pair admittances in terms of a third four-pair admittance.

measurements. It is assumed that any difference in the open-circuit voltages at connectors $A2$ and $A3$ has been accounted for.

The techniques just described are not limited to the circuit shown in Fig. 6. These techniques can be extended to circuits where the two four-pair admittances containing $Y7$ and $Y8$ in Fig. 6 are replaced by three or more four-pair admittances in parallel. Furthermore, it is not necessary that all of the four-pair admittances in parallel be nominally equal to each other. The most important application of this is where one of the four-pair admittances is a small adjustable admittance which is used to balance the bridge. Thus the DRRS used in the examples throughout this paper can be replaced by a regular bridge transformer having a fixed voltage ratio.

F. Transformer Ratio Measurements

Fig. 7 shows part of the circuit used at NBS for measuring the nominally 10 to 1 ratio of precision bridge transformers. The remainder of the circuit consists essentially of the bridge transformer whose ratio is to be measured, plus eleven nominally-equal capacitors. The method to be used is a modification of the permutation method which was described in an earlier paper [7], and the reader is referred to this paper for further details.

Fig. 7(a) and (b) shows two different views of the same setup. The component in the lower right-hand corner of Fig. 7(b), having eleven toggle switches, is termed a load adjuster. The load adjuster consists of eleven metal boxes, each having two coaxial connectors, one on the top and one on the bottom. In practice, the load adjuster is mounted on the edge of a table so that cables can be attached to the bottom coaxial connectors. Each metal box contains a trimmer capacitor and a relatively large capacitor which are, in effect, connected between the inner and outer conductors of the cables. Each of the large capacitors, which correspond to Y_L in the previous discussion, can be removed from the circuit by means of the appropriate toggle switch.

Each of the eleven coaxial connectors on the bottom of the load adjuster is joined to a coaxial cable (not shown in Fig. 7) which contains a coaxial choke and is joined to one of eleven 10-pF fused silica capacitors. The eleven detector cables from the capacitors are joined together with a twelfth cable, which is connected to a phase sensitive detector. There are no special requirements for joining the detector cables [7].

The eleven cables from the top of the load adjuster are plugged into eleven of the twenty-two double-ended coaxial connectors, which, together with the bakelite board on which they are rigidly mounted, is termed a plug board. Looking at the other side of the plug board (Fig. 7(a)), note that the cables on the top row are joined to eleven coaxial connectors symmetrically placed near the outside edge of one of the hollow metal disks. The cables on the bottom row are joined to eleven connectors similarly placed on the other disk. Each disk has two additional coaxial connectors which are centrally located, one on the top and one on the bottom. The center conductors of all thirteen coaxial connectors are soldered to a thin metal disk located inside the hollow disk. The resulting component consists of thirteen coaxial connectors whose inner conductors are joined together by means of a solid metal disk and whose outer conductors are joined together by means of a hollow metal disk. This will henceforth be referred to as a coaxial star.

Note that the four darker colored cables are joined to the centrally-located coaxial connectors of the coaxial star. In practice, the connectors at the ends of the two shorter cables are rigidly mounted to some solid object so as not to disturb the other cables, and it is at these connectors that additional two-terminal admittances are added, i.e., similar to Y_L in the previous discussion. The connectors at the ends of the two longer cables are joined to the bridge transformer DRRS whose ratio is to be measured.

For illustrative purposes, we will assume that the connectors are joined to connectors $A1$ and $A2$ of the DRRS, which has been used in the figures throughout this paper. Measuring the ratio of the DRRS actually amounts to finding e_o, where e_o is the value of e which will result in a perfect 10 to 1 open-circuit voltage ratio at connectors $A1$ and $A2$.

The basic permutation method consists of eleven bridge balances where each capacitor, in turn, is connected to the high-voltage side of a 10 to 1 transformer, and the other ten capacitors are connected to the low-voltage side. Note that in Fig. 7(b), capacitors 1–10 are plugged into connectors 1–10 of the bottom row of the plug board, and capacitor eleven is plugged into connector eleven of the top row of the plug board. This corresponds to one of the eleven bridge balances referred to previously. In the second of the eleven balances, capacitors 1–9 are plugged into connectors 1–9 of the bottom row of the plug board, capacitor ten is plugged into connector ten of the top row of the plug board, and capacitor eleven is plugged into connector eleven of the bottom row of the plug board. Proceeding in the same manner, we obtain eleven values of e required to balance the bridge in each of the eleven configurations.

It can be shown that the average of the eleven values of e is equal to e_o, provided that lead impedances and the

equivalent series impedances of the DRRS are negilgible and the voltage dependence of the capacitors has been accounted for [8]. If the impedances are not negligible, we can obtain the same result by using matched pairs of coaxial star/cable combinations, while, at the same time, extrapolating the current to zero at connectors $A1$ and $A2$ of the DRRS and also at the capacitor end of each of the plug-board connectors. The star/cable combinations include all of the circuit shown in Fig. 7, with the exception of the load adjuster and the eleven cables connected to it.

If the star/cable combinations are not matched, they then can be interchanged, the measuring procedure repeated, and a second value of e_o determined. It can be shown that the average of the two values of e_o will yield a correct value of e_o. Interchanging the star/cable combinations amounts to interchanging the connectors joined to $A1$ and $A2$ of the DRRS and, of necessity, changing the plug-board connections so that ten capacitors are plugged into the top row of connectors and one capacitor is plugged into the bottom row of connectors.

In practice, the two star/cable combinations were found to be better matched than had been anticipated. The two values of e_o differed by less than 1 part in 10^9. More specifically, the two values of α_o (the real component of e_o) differed by less than 1 part in 10^9 and the two values of β_o (the quadrature component of e_o) differed by less than 1 nrad.

In addition to the star/cable combinations being well matched, the design and construction of the stars was such that the effects of mutual impedances associated with the extra currents in the low-voltage star were both small and uniform. As a result, it was found that the load adjuster could be eliminated from this particular circuit since it was not necessary to extrapolate the currents to zero at the plug-board connectors, nor was it necessary to use the trimmer capacitors in the load adjuster. Stating the same thing in a slightly different manner, the extrapolation of currents to zero at the plug-board connectors results in a correction to α_o of 2 parts in 10^{10} and a correction to β_o of 1×10^{-10} rad, and, since the corrections result from mutual impedances in the stars, the corrections are applicable with or without the use of the load adjuster.

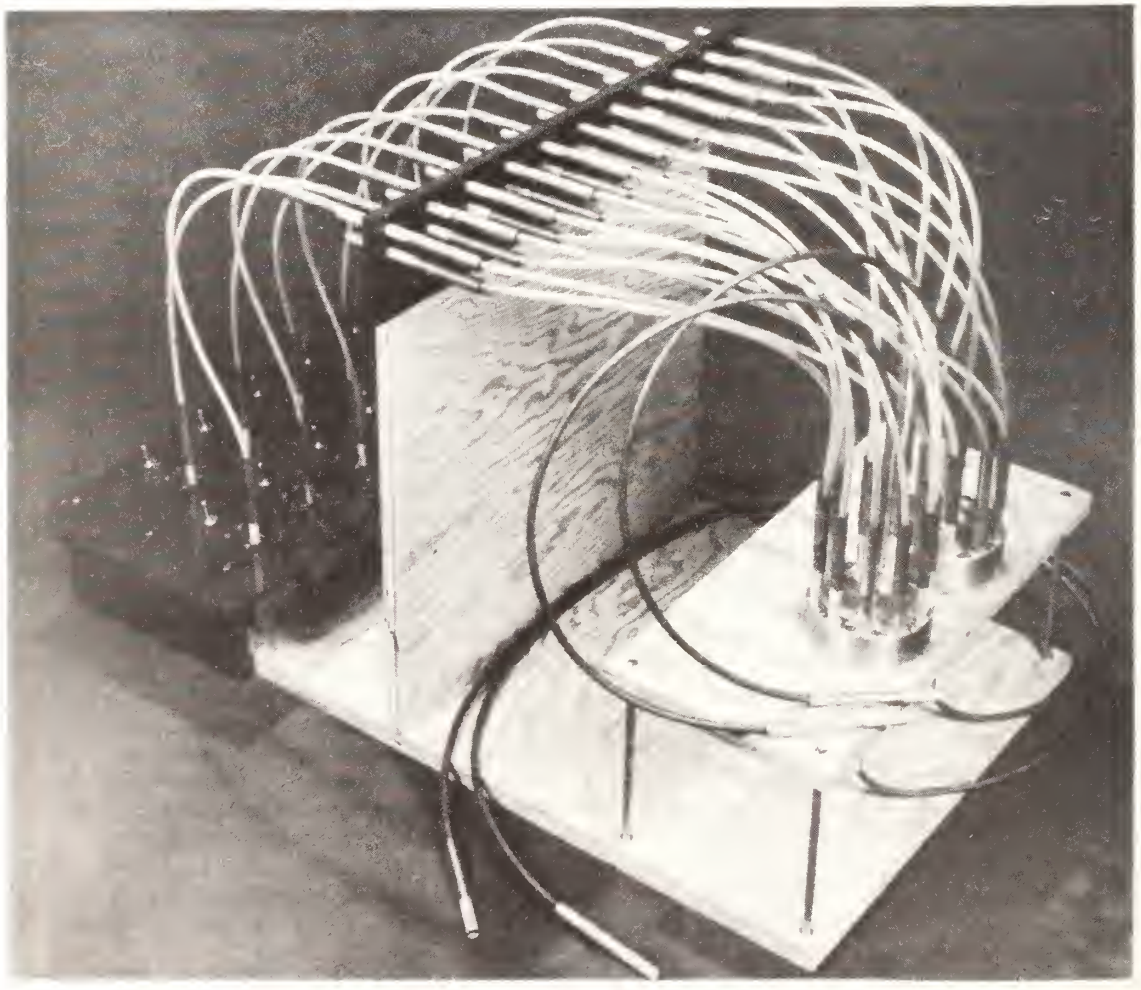

(a)

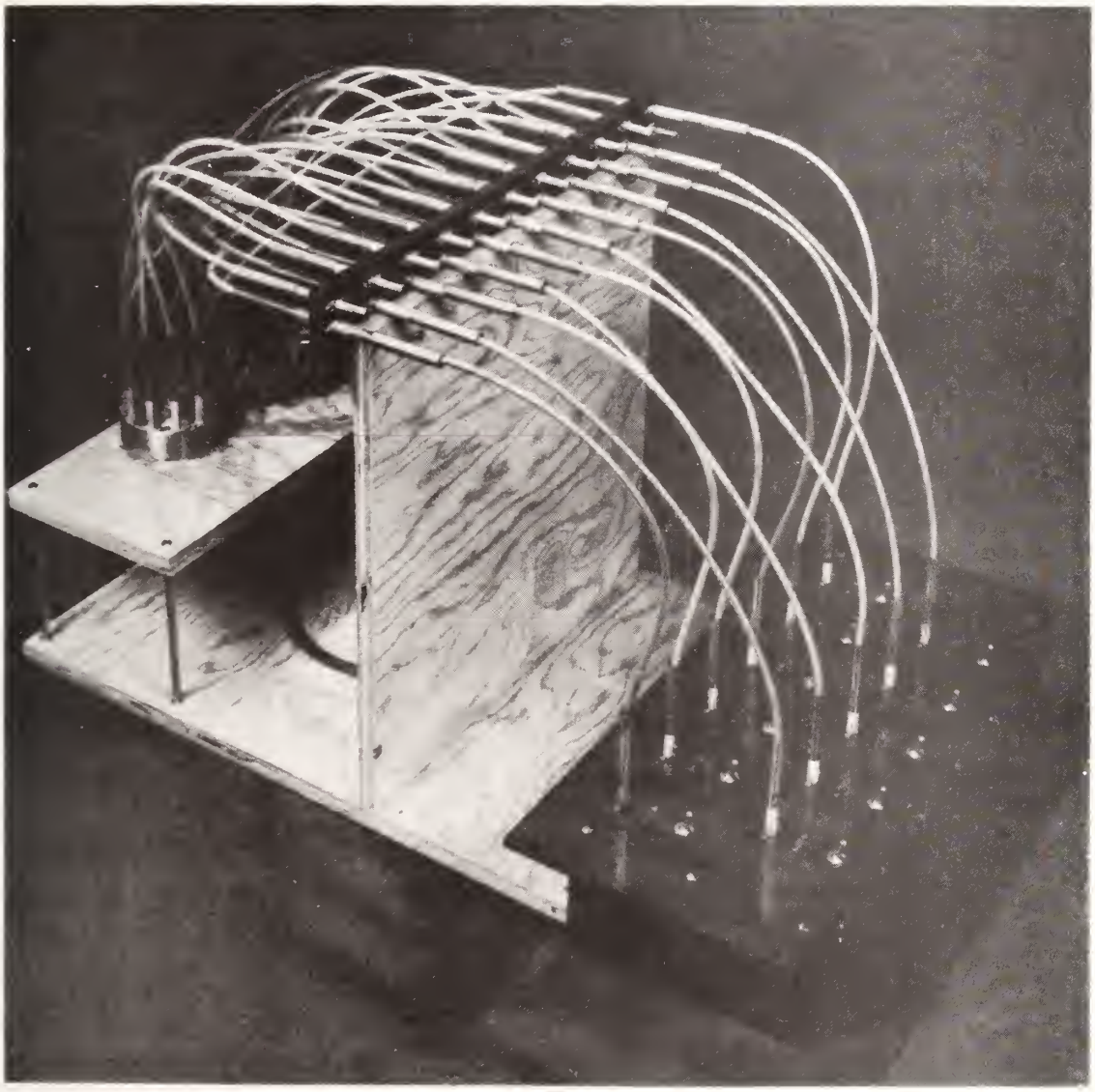

(b)

Fig. 7. Part of the circuit used to measure the 10 to 1 ratio of a bridge transformer or DRRS (two-pair or four-pair). Two views of the same setup are shown.

The circuit of Fig. 7 was also used to measure the 10 to 1 ratio of a four-pair DRRS [2] whose current cables were joined to the centrally-located connectors on the top of the stars and whose potential leads were joined to the bottom connectors of the stars. The only corrections required were for mutual impedances as described previously.

G. Comparison of Measuring Systems

As a check on extrapolation techniques in general, four-pair capacitance standards in the range from 10–1000 pF were compared at $\omega = 10^4$ using both the four-pair DRRS[2] and the two-pair DRRS. Maximum discrepancies between the two types of comparisons were 2 parts in 10^9 for the capacitance and 2 nrad for the phase angle. All discrepancies could be accounted for by sensitivity and stability of the various components.

CONCLUSION

The use of extrapolation techniques to provide well-defined and versatile measuring systems has been illustrated by means of a number of applications. Note that bridge transformer ratios are measured (application F) in the same manner in which they will later be used to measure admittance ratios (applications A and B). The admittance ratios so determined can, in turn, be used to measure the main ratios of other bridges, or of the same bridge, when its defining connectors have been changed by the addition of cables and/or stars. A change in the value of an admittance standard resulting from a change

in its defining connectors can be measured in a similar manner provided that the admittances to be extrapolated to zero are properly accounted for.

Note also that "application E" provides a second method for measuring precision transformer ratios. This method should be of special interest when precision transformers are available, but large numbers of nominally equal admittances, as required in "application F," are not available.

It is hoped that four-pair admittanced will have a more practical appeal and receive wider usage now that they can be measured with two-pair bridges (including commercial bridges). At the other extreme, as pointed out by Cutkosky, combining extrapolation techniques with four-pair bridge techniques provides exciting possibilities for data acquisition and automation at the highest levels of precision.

REFERENCES

[1] R. D. Cutkosky, "Four-terminal pair networks as precision admittance and impedance standards," *Commun. Electron.*, vol. 70, pp. 19–22, Jan. 1964.
[2] ——, "Techniques for comparing four-terminal pair admittance standards," *J. Res. Nat. Bur. Stand.*, vol. 74C (Eng. and Instr.), No. 3 and 4, pp. 63–78, July–Dec. 1970.
[3] A. M. Thompson, "The precise measurement of small capacitances," *IRE Trans. Instrum.*, vol. I-7, pp. 245–253, Dec. 1958.
[4] M. C. McGregor *et al.*, "New apparatus at the National Bureau of Standards for absolute capacitance measurement," *IRE Trans. Instrum.*, vol. I-7, pp. 253–261, Dec. 1958.
[5] R. D. Cutkosky, "Active and passive direct-reading ratio sets for the comparison of audio-frequency admittances," *J. Res. Nat. Bur. Stand.*, vol. 68C (*Engr. and Instr.*), no. 4, Oct.–Dec. 1964.
[6] D. N. Homan, "Applications of coaxial chokes to ac bridge circuits," *J. Res. Nat. Bur. Stand.*, vol. 72C (Eng. and Instr.), no. 2, pp. 161–165, Apr.–June 1968.
[7] R. D. Cutkosky and J. Q. Shields, "The precision measurement of transformer ratios," *IRE Trans. Instrum.*, vol. I-9, pp. 243–250, Sept. 1960.
[8] J. Q. Shields, "Voltage dependence of precision air capacitors," *J. Res. Nat. Bur. Stand.*, vol. 69C (Eng. and Instr.), no. 4, pp. 265–274, Oct.–Dec. 1965.

Reprinted by permission from IEEE TRANSACTIONS ON INSTRUMENTATION AND MEASUREMENT
Vol. IM-21, No. 4, November 1972, pp. 365-368

Phase-Angle Characteristics of Cross Capacitors

JOHN Q. SHIELDS

Abstract—It has been found that under proper conditions thin dielectric films on the electrodes of certain types of cylindrical cross capacitors tend only to produce equal and opposite contributions to the phase angles of the two cross capacitances. To a lesser degree, this same type of cancellation effect has been found to be associated with toroidal cross capacitors.

Manuscript received June 26. This work was supported in part by the National Bureau of Standards.
The author is with the Absolute Electrical Measurements Section, Electricity Division, Institute for Basic Standards, National Bureau of Standards, Washington, D.C. 20234.

I. Introduction

NORMALLY, the greatest uncertainties in a determination of the true phase angle of a three-terminal air capacitor result from the effects of thin dielectric films on the electrode surfaces. In addition to the difficulty in evaluating

the contribution of these films to the phase angle of the capacitor, the stability of such films must be determined by periodic reevaluations.

It is with regard to thin dielectric films that cross capacitors were found to have unusual phase angle characteristics. Specifically, it was found that if the addition of a thin dielectric film to one of the electrodes produced an increase in the phase angle of one of the cross capacitances, it correspondingly produced a decrease in the phase angle of the other cross capacitance. With certain types of cross capacitors, and under proper conditions, it was found that thin dielectric films on the electrode surfaces tend only to produce equal and opposite contributions to the phase angles of the two cross capacitances. A cylindrical cross capacitor that comes close to meeting these conditions is illustrated in Fig. 1. One limitation is that films near the defining ends of the capacitor may not behave as described unless electrical measurements are made before and after a mechanical manipulation of the electrodes.

The toroidal cross capacitor shown in Fig. 2, having cross capacitances C_{TB} and C_{OI}, is not subject to this limitation since it has no defining ends. Although the cancellation of film effects with this capacitor is not as complete as with the capacitor shown in Fig. 1, the cancellation is of a sufficient degree for this type of capacitor to be suitable as a standard of phase angle for precision air capacitors.

Two capacitors of the type shown in Fig. 2 have been constructed and are presently under investigation. Results thus far indicate that the contribution of thin films to the phase angle of the average cross capacitance is probably between one and two orders of magnitude below the bridge sensitivity of $\pm 1 \times 10^{-8}$ rad. All work has thus far been limited to 1592 Hz.

II. Cylindrical Cross Capacitor

Let the two cross capacitances in Fig. 1 be designated as C_{AC} and C_{BD}, their sum as C_T, and let $C_{AC} = C_{BD} = C_O$ when physical symmetry is present and dielectric films are absent. It has been well established [1], [2] that if one of the electrodes is displaced slightly so that $C_{AC} \neq C_{BD}$, then

$$C_T = 2C_O \left[1 + \frac{\ln 2}{8}\left(\frac{C_{AC} - C_{BD}}{C_O}\right)^2 + \cdots\right]. \quad (1)$$

It has also been established [3] that if a thin dielectric film is added to one of the electrodes so that $C_{AC} \neq C_{BD}$, then $(C_{AC} - C_O) \approx -(C_{BD} - C_O)$. By speculating that the second-order term contained in (1) might also be applicable to changes produced by thin dielectric films and by including the loss component of the dielectric, (1) can be rewritten as

$$Y_T = 2(j\omega C_O)\left[1 + \frac{\ln 2}{8}\left(\frac{Y_{AC} - Y_{BD}}{j\omega C_O}\right)^2 + \cdots\right], \quad (2)$$

which yields

$$\theta_T \approx \frac{\ln 2}{4}\left(\frac{C_{AC} - C_{BD}}{C_O}\right)(\theta_{AC} - \theta_{BD}), \quad (3)$$

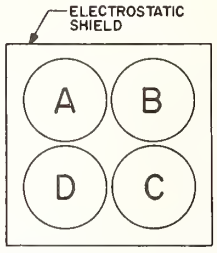

Fig. 1. Cross section of cylindrical cross capacitor constructed from four bars.

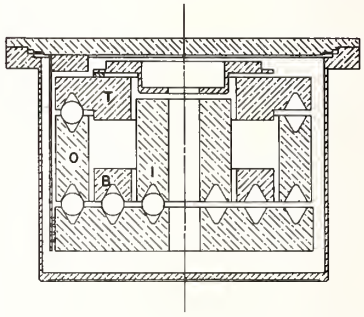

Fig. 2. Cross section of a toroidal cross capacitor.

where θ_T, θ_{AC}, and θ_{BD} are phase angles corresponding to C_T, C_{AC}, and C_{BD}.

The validity of (3) was checked by applying various types and thicknesses of dielectric materials to the electrodes of a capacitor of the type shown in Fig. 1. A sampling of results obtained for one thickness of vinyl tape is given in Table I. Agreement between measured and calculated values of θ_T is within the uncertainties of the measurements.

The following points regarding Table I should be noted: 1) as predicted by (3), θ_T is small when either $(C_{AC} - C_{BD})/C_O$ or $\theta_{AC} - \theta_{BD}$ is small; 2) discontinuities at the ends of the tape required relatively small corrections; 3) $(C_{AC} - C_{BD})/C_O$ is independent of its source, i.e., the tape on electrodes A and B contribute approximately 0.04 and -0.04, respectively, to $(C_{AC} - C_{BD})/C_O$; deviations from these values result from deliberate changes in the physical symmetry of the electrodes; 4) (3) is applicable to relatively thick dielectrics, i.e., $t = 0.38$ mm $= 0.012\ r$ where t is the tape thickness and r is the minimum distance between electrodes A and C; 5) with greater thicknesses of vinyl tape, a third-order term in t can be observed as differences between the measured and calculated values of θ_T; 6) with materials having different dielectric constants, the third-order term becomes significant at somewhat smaller or larger thicknesses. Dielectric constants of the materials measured were between 1.1 and 5.8; thicknesses were between 0.1 and 2.9 mm.

It is also possible to calculate θ_T directly from the dielectric properties. The equations needed for these calculations are derived from basic equations for C_{AC} and C_{BD} when dielectric films are absent, i.e.,

$$C_{AC} = C_O[1 + k_1 t + k_2 t^2 + \cdots] \quad (4)$$

TABLE I
COMPARISON OF THE MEASURED VALUE OF θ_T WITH THE VALUE CALCULATED FROM (3), $\theta_T \approx (\ln 2/4)[(C_{AC} - C_{BD})/C_O]\,(\theta_{AC} - \theta_{BD})$

With Vinyl Tape	$\frac{C_{AC} - C_{BD}}{C_O}$	θ_{AC} (μrad)	θ_{BD} (μrad)	$\theta_T \approx \frac{\ln 2}{4}\left(\frac{\Delta C}{C_O}\right)(\Delta\theta)$ Measured (μrad)	Calculated (μrad)
A	+0.0402	+466	−472	+6.5	+6.5
B	−0.0384	−448	+442	+5.6	+5.9
B	+0.0638	−425	+434	−9.3	−9.5
B	−0.0048	−442	+441	+0.6	+0.7
A and *B*	+0.0304	+2	−1	+0.2	0.0

$$C_{BD} = C_O[1 - k_1 t - (k_2 - k_1^2 \ln 2)\,t^2 + \cdots], \tag{5}$$

where t is the thickness of a metal film on electrode A. If the metal film is replaced by a dielectric film having a thickness t and a dielectric constant ϵ, then

$$C_{AC} = C_O\{1 + k_1 t[f_1(\epsilon)] + k_2 t^2\,[f_3(\epsilon)] + \cdots\} \tag{6}$$

$$C_{BD} = C_O\{1 - k_1 t[f_2(\epsilon)] - (k_2 - k_1^2 \ln 2)\,t^2\,[f_4(\epsilon)] + \cdots\}. \tag{7}$$

It has previously been shown [3] that from theoretical considerations $f_1(\epsilon) = f_2(\epsilon) = [1 - (1/\epsilon)]$ provided that t is small compared with the length of the lines of force terminating at the dielectric. Experimental results indicate that the preceding can be extended to the second-order terms so that $f_3(\epsilon) = f_4(\epsilon) = [f_1(\epsilon)]^2 = [f_2(\epsilon)]^2 = [1 - (1/\epsilon)]^2$. If $t[1 - (1/\epsilon)] \equiv t' - jt''$, then

$$C_{AC} - j\frac{G_{AC}}{\omega} \approx C_O[1 + k_1(t' - jt'') + k_2(t' - jt'')^2] \tag{8}$$

$$C_{BD} - j\frac{G_{BD}}{\omega} \approx C_O[1 - k_1(t' - jt'') - (k_2 - k_1^2 \ln 2) \cdot (t' - jt'')^2], \tag{9}$$

where G_{AC} and G_{BD} are the effective parallel conductances. Thus, to second order, a thin dielectric film on the preceding capacitor can be replaced by a metal film of thickness t' and an imaginary component of equivalent thickness t''.

Separating real and imaginary parts yields

$$\frac{G_{AC}}{\omega} \approx \frac{\partial C_{AC}}{\partial t'}\,t'' \tag{10}$$

$$\frac{G_{BD}}{\omega} \approx \frac{\partial C_{BD}}{\partial t'}\,t''. \tag{11}$$

Within limitations, a general form of (10) and (11) has been found to be applicable to other capacitors, i.e.,

$$\frac{G}{\omega} \approx \frac{\partial C}{\partial t}\,t'', \tag{12}$$

where t relates to an actual or effective change in electrode dimension. Thus,

$$\theta_T \approx (\ln 2)\,k_1^2 t' t'' \tag{13}$$

and when physical asymmetry is accounted for

$$\theta_T \approx \frac{\ln 2}{4}(2k_1 t' + 2k_3\tau)\,(2k_1 t''), \tag{14}$$

where τ is the displacement of electrode A from its position of symmetry. A comparison of (14) with (3) shows that $(C_{AC} - C_{BD})/C_O = (2k_1 t' + 2k_3\tau)$ and $(\theta_{AC} - \theta_{BD}) = (2k_1 t'')$.

The preceding relationships were checked experimentally using a variety of dielectric materials. Agreement was within the controllability of the various materials. Values of t' and t'' were determined experimentally using a guard-ring parallel-plate capacitor.

In the practical case of clean dry metal surfaces and reasonable asymmetry, t' can be neglected since $\tau \gg t'$. Assuming that τ is adjusted to $\pm 5 \times 10^{-6}$ m, (14) yields

$$\theta_T/t'' \approx \pm 1 \times 10^{-11} \text{ rad/equivalent nm.} \tag{15}$$

Values of t'' for a variety of metal surfaces were determined by Astin [4], i.e., a microradian-millimeter as listed by Astin is equal to 0.5 equivalent nanometers on each surface. Most dry metal surfaces are listed below 1 μrad-mm. Thus, the magnitude of θ_T can be expected to be less than 1×10^{-11} rad. Since the other three electrodes are likely to have similar films, the resultant magnitude of θ_T can be expected to be further reduced. As mentioned earlier, the preceding results are not directly applicable to films near the defining ends of the capacitor.

III. Toroidal Cross Capacitor

Two capacitors of the type shown in Fig. 2 have been constructed of stainless steel. Each of the main electrodes, I, O, T, and B, is supported by two glass balls and one glass spacer. The assembly is suspended from the top plate by three straps and enclosed by a vacuum housing.

The preceding contains three important capacitances: C_{TB}, C_{OI}, and C_{TI}. C_{TB} and C_{OI} are 0.5-pF cross capacitances. C_{TI} is a 10-pF capacitance, which serves essentially as a means for evaluating t''. Let $C_{TB} + C_{OI} = C_S$ and let θ_{TB}, θ_{OI}, θ_S, and θ_{TI} be the phase angles corresponding to C_{TB}, C_{OI}, C_S, and C_{TI}.

The values of θ_{TB}/t'', θ_{OI}/t'', and θ_S/t'' listed in Table II are applicable when dielectric films are thin and $(C_{TB} - C_{OI})/C_S \ll 1$. Values were determined theoretically using (12) and checked experimentally with dielectric materials as previously described.

The contribution of second-order terms to θ_S was found to be approximately the same as with the preceding cylindrical cross capacitor and can be neglected when clean metal surfaces are present. Thus, from Table II

$$\theta_S/t'' \approx 3 \times 10^{-9} \text{ rad/equivalent nm} \tag{16}$$

assuming that identical films are present on all electrodes. In a

TABLE II
EFFECTS OF A STANDARD FILM ON THE TOROIDAL CROSS CAPACITOR'S ELECTRODES

Electrode	θ_{TB}/t'' (n rad/ equivalent nm)	θ_{OI}/t'' (n rad/ equivalent nm)	θ_S/t'' (n rad/ equivalent nm)
T	+113	−112	+1
O	−127	+104	−12
I	−103	+130	+13
B	+113	−112	+1
Total	−4	+10	+3

similar manner it was found that

$$\theta_{TI}/t'' \approx 6 \times 10^{-7} \text{ rad/equivalent nm.} \quad (17)$$

The significant fact here is that $\theta_{TI}/\theta_S \approx 200$. Combining this ratio with the value of $\theta_{TI} - \theta_S$ obtained from a bridge comparison of C_{TI} and C_S yields values for the true phase angle of each capacitor.

It is assumed in the preceding calculations that uniform films are present on all active electrode surfaces. Since it is unlikely that θ_{TI} will be more than one order of magnitude above the estimated uncertainty ($\pm 2 \times 10^{-8}$) in the measurement of $\theta_{TI} - \theta_S$, a substantial allowance can be made for possible nonuniform films with no significant reduction in accuracy.

IV. Conclusion

Thin dielectric films on the line or detector electrodes of a three terminal capacitor tend to produce positive contributions to the phase angle; thin dielectric films on the grounded electrodes tend to produce negative contributions. The symmetry associated with cross capacitors indicates that thin dielectric films should produce approximately equal and opposite contributions to the phase angles of the two cross capacitances. This has been confirmed experimentally as previously described.

It is planned that the two toroidal cross capacitors will become permanent standards of phase angle. Sources of error associated with the realization of these standards will be described in a future paper.

References

[1] D. G. Lampard, "A new theorem in electrostatics with applications to calculable standards of capacitance," *Proc. Inst. Elec. Eng.* (London), mono. 216M, Jan. 1957.
[2] A. M. Thompson, "The cylindrical cross capacitor as a calculable standard," *Proc. Inst. Elec. Eng.* (London), vol. 106, pt. B, May 1959.
[3] D. G. Lampard and R. D. Cutkosky, "Some results on the cross capacitances per unit length of cylindrical 3-terminal capacitors with thin dielectric films on their electrodes," *Proc. Inst. Elec. Eng.* (London), mono. 351M, Jan. 1960
[4] A. V. Astin, "Nature of energy losses in air capacitors at low frequencies," *J. Res. Nat. Bur. Stand.*, vol. 22, June 1939.

JOURNAL OF RESEARCH of the National Bureau of Standards—C. Engineering and Instrumentation
Vol. 74C, Nos. 3 and 4, July–December 1970

Techniques for Comparing Four-Terminal-Pair Admittance Standards

R. D. Cutkosky

Institute for Basic Standards, National Bureau of Standards, Washington, D.C. 20234

(June 26, 1970)

Some of the advantages of four-pair admittance standards and some of the special problems encountered in their measurement are pointed out. Detailed descriptions of three distinct types of four-pair bridges and some of their limitations are presented. These three bridges form a vital part of a very precise absolute measurement of resistance based on a calculable capacitor being undertaken at the National Bureau of Standards, but are believed to be of more general usefulness.

Key words: AC direct-reading ratio set; ac measurements: bridge; coaxial chokes: defining transformers; equal power bridge: four-pair standards: frequency-dependent bridge; quadrature bridge.

1. Introduction

The quest for improved accuracy in the measurement of audiofrequency admittances has led from the now universally accepted practice of utilizing two pair standards, such as so-called three-terminal capacitors for high-impedance devices and such as mutual inductors for low-impedance devices, to a composite system combining the advantages of both techniques. A theoretical justification of this composite system in which the standards are provided with four pairs of terminals was published in 1964 [1][1], but with the exception of a paper by Homan [2] which was limited to measurements on fairly small impedances, no systematic investigation of four-pair admittance measurements has yet been described. The process of converting to four-pair measurement systems has been underway at the National Bureau of Standards for several years, during which time many of the special problems involved in their use have been investigated. This paper is an attempt to describe some of the techniques which have evolved, and to indicate the order of precision that may be obtained.

The techniques described in this paper are of general applicability but were developed for the specific purpose of comparing the reactances of capacitors having nominal values of 10 pF with the resistance of a special 1000-Ω resistor having a negligible frequency dependence [3]. The three basic types of bridges used for making this comparison are described here in some detail. It is intended to calibrate the 10-pF capacitors by means of a calculable capacitor now under construction at NBS. A dc comparison of the 1000-Ω resistor with the bank of 1-Ω resistors presently maintaining the NBS unit of resistance will then complete an absolute measurement of the ohm.

Because of the large number of intervening steps between the calculable capacitor and the bank of 1-Ω resistors, very elaborate precautions are necessary to maintain a high level of accuracy. Using the techniques outlined here, it is expected that the principal uncertainties in the measurement sequence will be due to mechanical imperfections in the calculable capacitor.

Although a rather complex sequence of auxiliary balances is required with the bridges described in this paper, they are not prohibitively time-consuming for the limited number of comparisons needed in an absolute ohm determination. These techniques would be considerably less attractive for a bridge in constant use, but this would be less of a drawback in a computer-operated system. It is considered that techniques similar to those described in this paper are essential if uncertainties must be kept smaller than 1 part in 10^8 over a large range of impedances at audiofrequencies.

The equivalent circuit of a four-pair admittance standard is shown in figure 1a, taken from the paper cited above [1], and in an abbreviated form, in figure 1b. The standard may be viewed as a device in which the ratio of current in pair 3 to the open circuit voltage at pair 2, subject to the condition that both the voltage and current at pair 4 are zero, is the parameter of interest. This parameter has the dimensions of admittance and may be written

$$P_{32}^{14}=\frac{i_3}{e_2}\bigg|i_2=i_4=0,\quad e_4=0. \tag{1}$$

It may be shown using figure 1a that

$$P_{32}^{14}=Y_t(1+Y_2Z_2)(1+Y_3Z_3). \tag{2}$$

[1] Figures in brackets indicate the literature references at the end of this paper.

An interesting reciprocity theorem also exists, which shows that $P_{32}^{14} = P_{23}^{41}$ for any four-pair network.

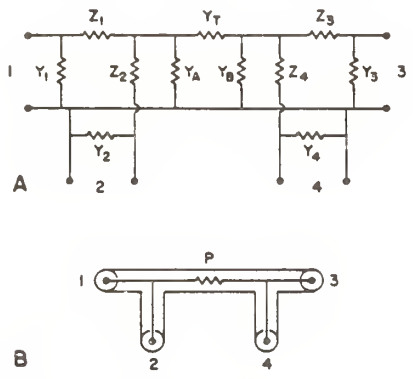

FIGURE 1. *Four-pair admittance standards:* (a) *Complete circuit.* (b) *Pictorial representation.*

Some properties of four-pair admittance standards which make them particularly useful are their relative insensitivities to variations in series impedances and shunt admittances in the leads as is implicit in (2), and the fact that standards of either very small or very large admittance may be constructed in such a way that their four-pair admittances are nearly identical with their ordinary two-pair admittances obtained by either open circuiting or short circuiting the two extra terminal pairs. These properties are discussed in the reference cited above [1].

Ordinarily the relationship between the four-pair admittance of a standard and its admittance when treated as a two-pair standard is of interest only when the standard is some kind of absolute or calculable instrument, and it is necessary to determine the difference between the calculated admittance at some internal and inaccessible location, and the effective four-pair admittance at the external connection points. Examples of this type of standard are calculable capacitors, calculable inductors, and resistors having calculable phase angles or ac-dc differences. Such devices are outside the scope of this paper, which is restricted to the problem of comparing four-pair admittance standards with each other.

Implicit in the adoption of either a four-pair or a two-pair approach is the requirement that the connections are indeed treated as pairs, and that there is no net current from one terminal pair to another. Many advantages result from grouping the terminals of a standard in pairs. Consider the simple case of a three-terminal capacitor provided with two coaxial connectors and with a permanent connection between the shields of these connectors. Conceptually the measurement of the capacitor consists of applying a voltage, e, to one connector pair and measuring the short circuit current i at the other connector pair. The transfer admittance of the device is then given by

$$Y = j\omega C + G = \frac{i}{e}.$$

The transfer admittance defined in this way is a function of the impedance in the connection between the shields of the coaxial connectors, but there is no ambiguity in the definition as there would be if a single ground connection of unspecified placement were used for both the input and output.

One of the principal reasons for defining the standards in terms of isolated coaxial connector pairs as sketched above is that under these conditions there is exactly the same current but with reversed sign in the inner wire of each cable as there is in the surrounding coaxial shield, and therefore the magnetic field exterior to both cables is zero. This eliminates possible mutual inductive couplings between the cables used to interconnect a number of components together to form a bridge. Likewise, even if stray magnetic fields were present in the vicinity of the coaxial cables, no induced voltages would be produced by these fields to affect the measurement. Although these arguments pertain only to the connecting leads of the devices, the devices themselves can be quite easily isolated from each other by providing them with individual mu-metal shields when this is needed.

Four-pair admittance standards are constructed with four coaxial connectors, and the advantages gained by preventing net currents from flowing between the four connector pairs are very great, as this eliminates external magnetic fields and their effects on the measurement. In this respect, the practice of dealing with five terminal standards having a single, common ground connection cannot be recommended.

It is necessary to maintain the conditions of zero net currents in the cables of components defined as outlined above when they are interconnected to form a bridge circuit. Coaxial chokes were developed for dealing with this problem [4], and are effective in attenuating the net currents in the cables by a factor of several hundred. Unfortunately the net currents are not completely suppressed by coaxial chokes. A method for estimating the errors caused by incomplete suppression of net currents by coaxial chokes is described later in this paper.

Most of the bridge circuits appearing in this paper show explicitly the coaxial nature of the components. This was done to emphasize the importance of considering the return currents in the shields. After some practice in dealing with circuits drawn in this way, they are much easier to relate to the physical bridge setup than are the conventional textbook bridge circuits. Some difficulty may be experienced at first in translating the still useful and important body of classical bridge theory to the coaxial form of presentation. It may be an aid in understanding some of the circuits in this paper to redraw them with a common ground point. If this is done, the similarities between many of the auxiliary balance systems used here and common classical techniques, such as yoke and lead balancing in Kelvin double bridges, and the use of Wagner and conjugate Wagner arms in ac bridges, can be readily seen. Redrawing the circuits in this way must be thought of purely as an aid to understand-

ing, because any attempt actually to construct a circuit without proper attention to the details of the shield return circuits would result in large and erratic errors dependent upon the accidental arrangement of the leads.

A final but important introductory point about comparisons of four-pair admittances, or indeed any other kind of admittances, is that even though the standards are defined subject to certain constraints on the currents and voltages, it is not necessary when comparing two such standards to satisfy *any* of the defining conditions; it is merely required that the same result be obtained for the ratio of the four-pair admittances being compared as would have been obtained *if* the conditions had all been satisfied. This observation opens up a very wide range of possibilities in the design of bridge circuits, and is related to the techniques described by Thompson for dealing with bridges involving multiple balances [4]. The Kelvin bridge for comparing four-terminal dc resistors also makes use of this principle, since currents exist in the potential leads of the resistors, but cause no errors.

2. Basic Comparison Circuits

Figure 2 shows four four-pair admittances connected in a bridge circuit involving six generators and six detectors. The balance procedure consists (for example) of arbitrarily fixing one generator, and then adjusting the other five generators and one of the four

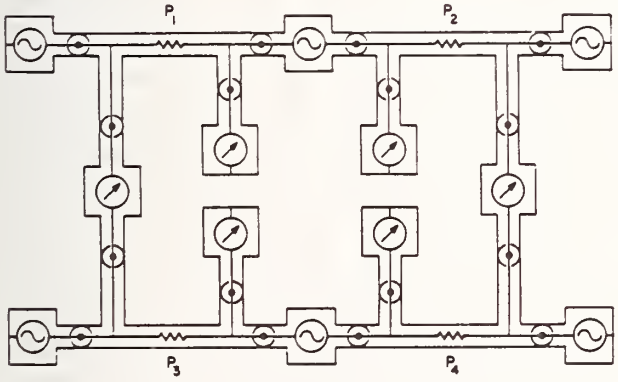

FIGURE 2. *Elementary four-pair bridge.*

four-pair admittances until all six detectors are balanced. The balance condition is $P_1P_4=P_2P_3$. If all generators and detectors are interchanged, the bridge network retains its form, and it may be shown, using the reciprocity theorem for four-pair networks, that the balance condition is unchanged.

The scheme of figure 2 contains a number of drawbacks, chief among which is the difficulty in simultaneously nulling six detectors, all of which are affected in various ways by the six adjustable parameters. This problem is solved in principle by mixing the various null detector responses in a suitable combining network to obtain six new null detector responses, each of which is a weighted average of the six original null detector inputs. The combining network parameters are chosen so that the matrix relating the new detector responses to the adjustable parameters is diagonal [4.5]. In this case, only the detector which responds to the adjustable four-pair admittance, called the main detector, is of interest, and the others need to be balanced only if the non-diagonal elements of the matrix are not exactly zero.

A more fundamental problem encountered in realizing figure 2 has to do with shunt admittances to ground associated with the detectors which compare the open circuit voltage of one standard with that of another, and with shunt admittances to ground associated with the generators between the current leads of two adjacent standards. By the reciprocity theorem the effects of these sets of leads are similar, and any solution found for one problem may be immediately applied to the other. The nature of the problem and the order of magnitude of the possible errors likely to occur may be seen from (2), which shows that the effect of admittance to ground in the potential lead is to load the leads joining the internal junction points of the standard with the point at which the open circuit potential is to be measured. The effect of admittance to ground at the current lead is to shunt some of the current to ground before it enters the adjacent standard.

The lead effects described above are unlikely to exceed a few parts in 10^7 at audiofrequencies, unless interconnecting cables longer than several meters are used. Even with very long cables, no errors result provided that these cables are treated as part of the standard, so that their effects are the same when the standard is calibrated as when it is used for calibrating another standard. However, the stabilities of the series impedances and shunt admittances of the cables must be considered.

The network used to interconnect the ends of the two cables and the null detector or generator is in principle a three-pair network, since the interaction of the null detector or generator terminal pair must be included in the matrix description of the network. This network must be carefully constructed so that the admittances shunting the cables from the standards are small, equal, and measurable; and so that the interaction of the null detector or generator with the other two terminal pairs is simple to analyze. An ideal three-pair circuit for accomplishing the desired objectives would provide a direct, completely reproducible connection between the two coaxial cables, except for an infinitesimal gap between their inner conductors, and with provision for connecting a null detector or generator across this gap. A network electrically equivalent to the above is employed at NBS which we call a defining transformer, shown pictorially in figure 3. A particular advantage of this network is that one side of the detector or generator terminal pair is at ground potential.

When used in the potential leads of the bridge shown in figure 2, the potential leads from the two standards are connected to terminals A and B of the defining transformer. The direct internal connection between the inner conductors, in connection with the

return through the outer shield, provides a one-turn loop around the high-permeability core shown shaded. A detector is connected to a 100-turn winding on this core via the coaxial connector C, and indicates a null

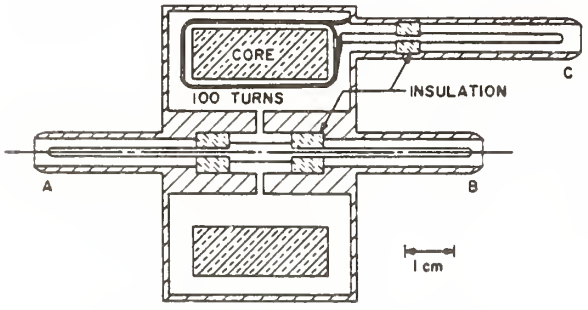

FIGURE 3. *"Defining transformer" for terminating current and potential leads of four-pair standards.*

if the potentials at A and B are equal. Capacitance between the 100-turn winding and the connection between the inner connectors of A and B could cause substantial errors. An internal shield with a thin air gap as shown eliminates this problem. Incomplete shielding can be detected by interchanging A and B.

When using defining transformers in a bridge, the potential leads are considered to terminate at the center of the device, in the region of the insulated gap in the inner shield. A number of nearly identical defining transformers have been built such that they may be used interchangeably to terminate the potential leads of the standards without changing the loads on the leads. These devices are used in the current leads also, in which case a generator may be substituted for the null detector.

Some objection may be made to the use of these devices, in that the standard is no longer an entity in itself, but has a definition dependent upon a termination; which might more properly be considered as part of the measuring instrument. Precedents do exist for this type of procedure, an example being the use of a precision coaxial connector on a two-terminal capacitor, for which a correct measurement requires a mating precision connector. In practice a very substantial simplification of our measurements was found to result from the introduction of defining transformers.

The technique which we use for measuring the effects of net currents between one terminal pair and another in a bridge containing coaxial chokes is rather cumbersome, but provides a reliable measure of the errors caused by non-ideal coaxial chokes. It is first assumed that every ground loop in the system to be investigated contains a coaxial choke, and that the minimum possible number of chokes to accomplish this purpose is used. This does not imply that one cannot add as many ground loops as may be desired, but simply that in the final circuit all ground loops are interrupted with a minimum number of coaxial chokes. Singling out a particular choke for investigation, a single turn of wire is wrapped around the core of the choke and connected to an auxiliary detector. The deflection of this detector is a measure of the voltage tending to drive current through the choke.

A quantitative measure of this voltage may be obtained using the voltage insertion transformer shown in figure 4. This device consists of a high permeability

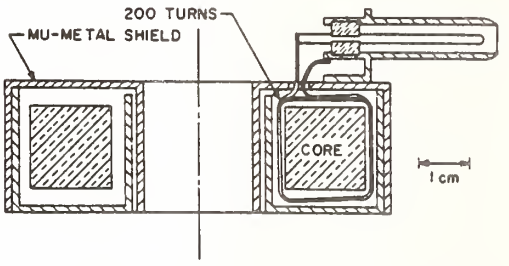

FIGURE 4. *Voltage insertion transformer for investigating errors caused by net currents in coaxial cables.*

toroidal core wrapped with 200 turns of wire connected to a coaxial connector. A toroidal mu-metal shield surrounds the core and winding, so that negligible magnetic fields exist outside of the shield when the 200-turn winding is excited. In use, the cable leading to the choke selected for testing is passed through the hole in the shield of this device, forming a 200:1 transformer. A voltage source derived from the same oscillator supplying the bridge, and adjustable in both real and imaginary components, is connected to the 200-turn winding. We find that an operational amplifier circuit described in an earlier paper [6] is convenient for this purpose.

The voltage source is adjusted until the auxiliary detector monitoring the voltage across the coaxial choke registers a null. The real and imaginary parts of the adjustable voltage required to obtain this null are recorded. The next step is to remove the auxiliary detector and to change the adjustable voltage by an amount large enough to yield sufficient sensitivity but not large enough to drive the choke into a nonlinear region. The real and imaginary parts of the change in balance point of the bridge caused by this change in applied voltage are recorded. A straightforward manipulation of the various complex quantities obtained by this scheme allows one to calculate the real and imaginary parts of the error caused by incomplete suppression of net current by the coaxial choke.

All of the coaxial chokes in the system are evaluated in this way. An algebraic addition of the individual errors then gives the total error, which is applied as a correction to the raw results of the measurement.

The technique sketched above could be generalized for a system with M chokes by providing each of the M chokes with voltage insertion transformers, and by bringing all of the choke voltages simultaneously to a null as indicated by M auxiliary detectors. In this case no net currents with their attendant errors would exist, and there would be no corrections to apply to the bridge balance. The complete system applied in the circuit of figure 2 could then be viewed as one with

$M+6$ adjustable parameters and with $M+6$ null detectors. One could conceivably construct a combining network to diagonalize the matrix relating these two vector quantities to make the effects of net choke currents less important. This has not yet been required for our purposes, since the residual errors due to net currents through the chokes are small enough to be measured with adequate precision using the extrapolation technique sketched above.

It is very important that one uses the minimum number of chokes necessary to break all ground loops when the normal loop voltages are measured by balancing them out as indicated above. If two chokes of equal impedance were in series in a particular loop, the method described would assign the total loop voltage to each choke, when in reality each choke would have across it only half of the total voltage. A simple test for multiply choked loops is to measure the voltages at each choke produced by exciting each loop in turn with a voltage insertion transformer. If the nondiagonal terms of the resultant matrix are much smaller than the diagonal terms, no multiply choked loops exist.

It is found in measuring the effects of the chokes in a given system that they can often be placed in categories according to the amount of voltage driving the loop, and according to the effect of a loop voltage on the bridge balance. The measurement error caused by a coaxial choke having insufficient impedance is large only if the loop voltage driving a choke is large *and* if a voltage in this loop has a strong effect on the bridge balance. It is usually possible to arrange a bridge in such a way that no choke has both undesirable characteristics. This usually requires the addition of extra ground connections with an extra choke for each added connection. The procedure for accomplishing this is at this time largely empirical.

Coaxial chokes do not provide the only means for suppressing net currents in coaxial cables. Isolation transformers are used in some cases, and net currents can then result from unbalanced interwinding capacitances. If the interwinding capacitances are very poorly balanced, the effective ground loop voltage can be quite high, and the accurate measurement of the errors due to the resultant ground loop current is rather difficult. In such cases it is usually best to measure the current directly, for example by converting the voltage insertion transformer to a current sensor by connecting a phase-sensitive voltmeter in parallel with a low impedance load to the 200-turn winding.

About the only other errors likely to occur in a four-pair bridge are those caused by stray couplings between the various components. These effects can usually be made negligible with electrostatic and electromagnetic shields, and tests for the effectiveness of these shields are not difficult to perform. Eccentric coaxial cables usually cause no serious problems, but must be considered. In some cases acoustic couplings can be troublesome, particularly if the generator and detector circuits both contain partially magnetized transformers. The 100:1 bridge described in section 5 suffered from this effect initially, but after the cores were carefully demagnetized and after the addition of some acoustic insulation, the errors due to acoustic coupling were reduced to a few parts in 10^{10}. The mechanism responsible for the acoustic coupling involves magnetostriction in the core of the transformer in the generator circuit. If the core is partially magnetized, the acoustic output of the core will contain a component at the same frequency as the generator in addition to the expected but less troublesome components at the even harmonics of the generator frequency. The resultant mechanical excitation of the transformer in the detector circuit causes no trouble unless the detector transformer is also partially magnetized, in which case a fundamental frequency component of current can be generated.

Some care must be taken when adjusting the meters of the null detector to zero deflection in the absence of a signal. It had been the practice at NBS to disconnect the admittance standards of a bridge from the voltage transformer to which they were normally connected and to zero the meters with the voltage transformer excited. This technique eliminates most of the errors due to magnetic coupling from the oscillator and voltage transformer to the detector, and also eliminates some of the errors caused by imperfect coaxial chokes. When the choke errors are measured independently as sketched above, this procedure could result in a double correction for some of the choke errors.

3. Quadrature Bridge

As the first example of an actual four-pair bridge, we will use a type of frequency-dependent bridge of which two-pair versions have been in existence for some time [4, 7, 8, 9]. The circuit is basically the same as that described by Thompson [4] and uses the twin-tee detector coupling network proposed by him. The NBS bridge contains two 10^5-Ω four-pair resistors and two 1-nF four-pair capacitors, and operates at an angular frequency of 10^4 rad/s, which corresponds to a frequency of about 1592 Hz. Figure 5 shows a partial schematic of the NBS four-pair quadrature bridge, in which D_1 through D_8 are null detectors, T_5 through T_9 are defining transformers, and P_1 through P_4 are the four-pair admittance standards. Seven of the eight complex adjustments required to balance the eight null detectors are indicated by either admittances or generators with arrows through their symbols. These seven adjustments are required only for realizing the defining conditions for the four-pair admittances, and may be uncalibrated. The eighth complex adjustment required to balance the bridge is made through the use of two seven-dial inductive voltage dividers T_2 and T_3, which drive small fixed capacitors labeled Y_5 and Y_6. This complex pair of adjustments serves to indicate the relationship between P_1, P_2, P_3, and P_4. Using the notation indicated on figure 5, we have when all detectors are balanced

$$i_1 = e_a P_1 + e_d Y_5 \approx -e_c P_2$$

and

$$i_2 = e_b P_4 + e_f Y_6 \approx -e_e P_3.$$

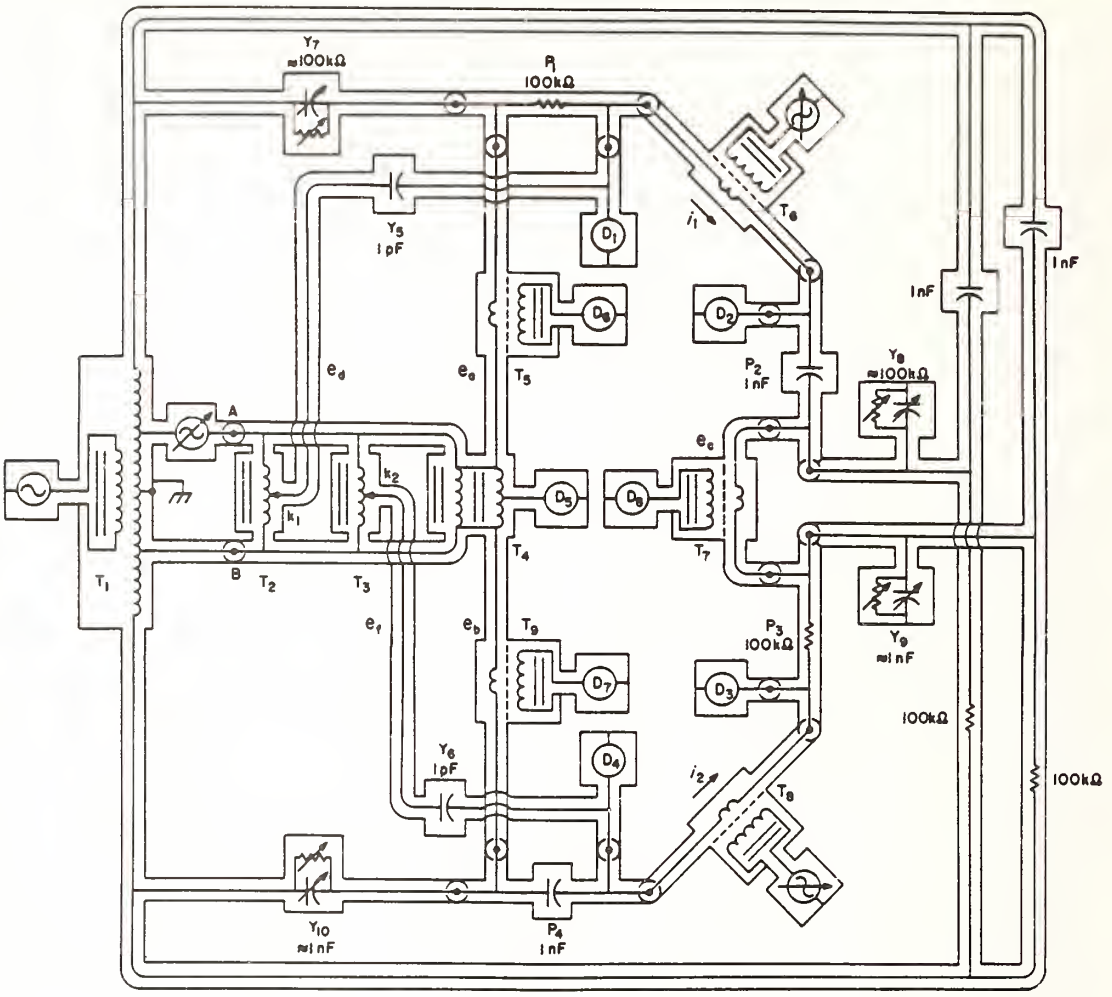

FIGURE 5. *Four-pair quadrature bridge with detector combining network deleted.*

If we represent the ratio of T_4 by $e_b = -e_a(1+\delta)$ with δ complex and $|\delta| \ll 1$, and since $e_d \approx e_a(2k_1-1)$ and $e_f \approx -e_b(2k_2-1)$, we have the balance condition

$$P_3[P_1+Y_5(2k_1-1)] \approx -P_2(1+\delta)[P_4-Y_6(2k_2-1)]. \tag{3}$$

A repeat measurement is made with the connections interchanged at points A and B, and with the connections between T_4 and the defining transformers T_5 and T_9 interchanged. This reverses the sign of δ to first order, and also reverses T_2 and T_3, so that

$$e_d' \approx e_a(1-2k_1') \qquad \text{and} \qquad e_f' \approx -e_b(1-2k_2').$$

The resultant balance condition is

$$P_3[P_1+Y_5(1-2k_1')] \approx -P_2(1-\delta)[P_4-Y_6(1-2k_2')]. \tag{4}$$

Averaging (3) and (4) we have

$$P_3[P_1+Y_5(k_1-k_1')] \approx -P_2[P_4-Y_6(k_2-k_2')]. \tag{5}$$

If we let $P_n = G_n + j\omega C_n$, $Y_5 = j\omega C_5$ and $Y_6 = j\omega C_6$ and assume that $G_1 \approx G_3 \approx \omega C_2 \approx \omega C_4$ and that $\omega C_1 \ll G_1$, $\omega C_3 \ll G_3$, $G_2 \ll \omega C_2$ and $G_4 \ll \omega C_4$, we may separate real and imaginary parts of (5) to obtain

$$\frac{G_3 G_1}{\omega^2 C_2 C_4} \approx 1 + \frac{C_6}{C_4}(k_2 - k_2') \tag{6}$$

which relates the main components of the four-pair admittances, and

$$\frac{\omega C_1}{G_1} + \frac{\omega C_3}{G_3} + \frac{G_2}{\omega C_2} + \frac{G_4}{\omega C_4} \approx \frac{G_5}{C_2}(k_1' - k_1) \tag{7}$$

which relates the phase angles of the four-pair admittances.

The approximations made in deriving (6) and (7) cause no errors exceeding 2 parts in 10^{10} for the NBS four-pair quadrature bridge. Under less ideal conditions, the second-order correction terms might be required.

The nominally 1 : 1 transformer T_4 in figure 5 is of two-stage construction [6, 10], with a mu-metal shield between the first and second stages, and with another mu-metal shield surrounding the entire transformer. It can be seen that when the null detectors D_6 and D_7 are balanced, the output terminal pairs of T_4 are subject to open circuit conditions as defined at the central reference planes of the defining transformers T_5 and T_9. The voltages e_a and e_b in the equations above are referred to these reference planes in a manner analogous to the definitions of the open circuit voltages of the four pair standards. Reversal of T_4 is accomplished by reconnecting the cables at the points of entry to T_5 and T_9, which has a negligible effect on the open circuit ratio.

Three of the eight null detectors shown in figure 5 are not operated on by the combining network used with the bridge. The detectors labeled D_6, D_7, and D_8 connected to T_5, T_7, and T_9 are brought to a null one at a time by adjusting Y_7, Y_{10}, and either Y_8 or Y_9, after which these detector terminals are shorted to reduce the effect on the main detector of a slight error in these auxiliary balances. This technique works very well for adjusting Y_7 and Y_{10}, but some convergence problems exist with the balance of Y_8 or Y_9. Ideally, one would like to null the detector D_8 connected to T_7 by adjusting $Y_8 - Y_9$ while keeping $Y_8 + Y_9$ fixed. One of the other balance conditions turns out to involve $Y_8 + Y_9$ but not $Y_8 - Y_9$. In practice, we have been able to achieve fast convergences of these two auxiliary balances without the elaboration of ganged switches by manually tracking Y_8 with Y_9.

The guiding principle behind the combining network used with the bridge (see fig. 6) is to combine the various detector terminal pairs two at a time and further to combine the new detector terminals so formed until only one detector terminal pair remains. We begin by combining the detector terminals D_1 and D_2 of P_1 and P_2 to form a single detector terminal D_9 which does not respond to excitation of T_6, and by similarly combining the detector terminals D_3 and D_4 of P_3 and P_4, to form a single detector terminal D_{10} which does not respond to excitation of T_8. The initial combining network linking the detector terminals D_1 and D_2 can be understood by letting $e_a = e_c = 0$ in figure 5 and observing that the circuit between T_6 and D_9 in figure 6 is a Schering bridge, for which a complex balance may be obtained by adjusting the two variable capacitors C_{11} and C_{12}. The circuit is adjusted by actually connecting the bridge generator to the input lead of T_6 rather than to the input of T_1. After C_{11} and C_{12} are adjusted, the input terminal of T_6 is shorted. The result is that although the voltage at neither D_1 nor D_2 is exactly nulled, these voltages are very small; and since changing the excitation on T_6 does not change the voltage at D_9, no error results from failure to adjust this excitation to obtain individual nulls on the detector pairs D_1 and D_2. The combining network between the detector terminals of D_3 and D_4 is identical with that described above, and is adjusted by varying C_{13} and C_{14}. The relative sizes of the admittances are chosen to produce a minimal effect on the bridge sensitivity and on the operation of the twin-tee combining network linking D_9 and D_{10}.

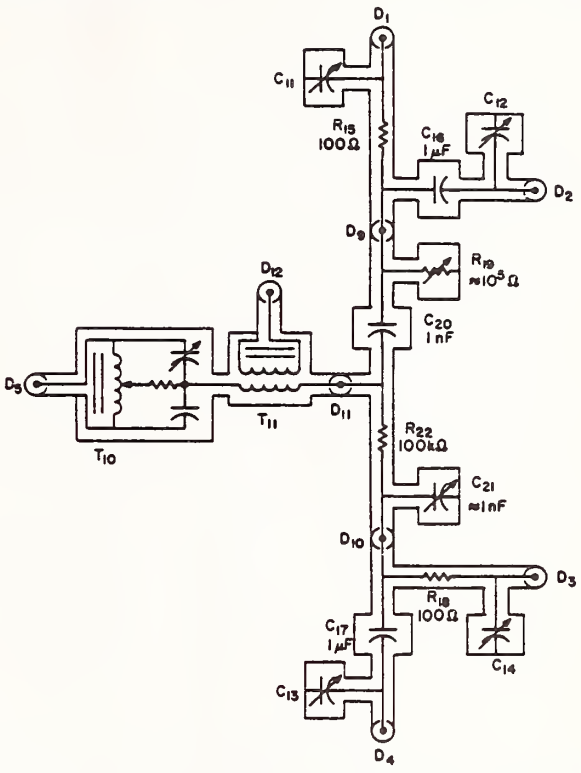

FIGURE 6. *Detector combining network for quadrature bridge.*

The network linking D_9 and D_{10} may be understood by letting all generators in figure 5 be zero and by assuming that a generator is inserted to make $e_c \neq 0$. The network can be recognized as a twin-tee circuit in which a null can be produced at D_{11} by adjusting R_{19} and C_{21}. After making this balance, the voltage at D_{11} is independent of the auxiliary adjustment $Y_8 + Y_9$. In practice the twin-tee is adjusted so that changing $Y_8 + Y_9$ produced no change in the detector voltage at D_{11} and $Y_8 + Y_9$ is adjusted so that changing the twin-tee setting produces no change in the detector voltage at D_{11}.

Although a twin-tee combining network is convenient for a quadrature bridge, a detailed noise calculation shows that it rather greatly augments the thermal agitation noise already present in P_1 and P_3. With 4 mW dissipated in P_1 and P_3, one has difficulty in detecting an unbalance smaller than one or two parts in 10^9. A substantial improvement could be made by maintaining the combining network at low temperature, or by separately amplifying the voltages at D_9 and D_{10} before coupling them together.

The final combining network links D_{11} and D_5 with D_{12}. It is adjusted by means of the decade inductive voltage divider T_{10} and the associated phase-shifting network so that inserting a 5-Ω resistor in one of the cables joining T_1 with T_2, T_3, and T_4 to simulate the generator shown in figure 5 does not change the detector voltage at D_{12}. After making this adjustment the 5-Ω resistor is removed.

The sequence of adjustments outlined above is easier to perform than to describe. The entire bridge can be adjusted in 10 minutes, and the auxiliary adjustments have been found to drift in a week by less than that required to yield an error of 1 part in 10^9.

The complete quadrature bridge consisting of figures 5 and 6 contains 25 coaxial chokes, each of which was checked using the techniques described in section 2. The largest individual error was found to be 1 part in 10^{10}, and the total error resulting from the existence of net currents in all chokes, the algebraic sum of the individual errors, was about 2 parts in 10^{11}.

Some special problems are encountered in a quadrature bridge simply because the balance is frequency-dependent. One especially important problem is caused by intermodulation distortion in the bridge detector between adjacent harmonics of the bridge fundamental frequency. These distortion products may have components at the fundamental frequency, which would cause a substantial error. The individual harmonic components entering the detector of a frequency-dependent bridge are not nulled with the fundamental as they are in a frequency-independent bridge, and may be of rather high amplitude. We use a special filter between T_{11} of figure 6 and the detector amplifier to reject all harmonics of the bridge fundamental frequency before the signals reach any strongly nonlinear elements. The filter contains a bridge network to obtain a zero transfer admittance for the second and third harmonics of the fundamental frequency, and a doubly tuned circuit to attenuate all higher harmonics. The circuit is similar to that used in an earlier quad bridge [7] but has been modified to yield a smaller noise figure.

The need for a good filter is indicated by the fact that removing the filter results in an apparent change in the bridge balance of several parts in 10^6. With the filter in, tests indicate that the error due to intermodulation distortion is less than 1 part in 10^9. A convenient check on the effectiveness of the filter is to augment each of the harmonics present at the detector terminal D_{12} by injecting an additional current into D_{12} with a small capacitor connected to an auxiliary oscillator tuned to the appropriate harmonic. Other tests using two auxiliary oscillators confirm that the effect is indeed due to intermodulation distortion. The technique is very sensitive, and can be used to detect distortion products resulting from nonlinear mixing of frequencies up to at least the 15th harmonic. The technique gives only an upper bound to the error and would probably not be reliable for determining corrections.

If a frequency-dependent bridge is balanced at an angular frequency $\omega = \omega_0$, then for $\omega \approx \omega_0$, the detector input voltage will be given by $e_d = k_1(\omega - \omega_0)e_g$ where k_1 is a complex constant and e_g is the bridge generator voltage. If the detector contains a sharply tuned single section filter (6 dB/octave) having a bandwidth $2\omega_d$, then for frequencies near ω_0 the detector output voltage will be of the form

$$e_0 = \frac{k_2(\omega - \omega_0)e_g}{1 + \frac{j(\omega - \omega_0)}{\omega_d}}. \tag{8}$$

The power transfer function between the bridge input terminals and the detector is then given by

$$TF_1 \propto \frac{(\omega - \omega_0)^2}{1 + \left(\frac{\omega - \omega_0}{\omega_d}\right)^2} = \frac{\Delta\omega^2}{1 + \left(\frac{\Delta\omega}{\omega_d}\right)^2}. \tag{9}$$

If a two section filter were used (12 dB/octave), the power transfer function would be

$$TF_2 \propto \left(\frac{\Delta\omega}{1 + \left(\frac{\Delta\omega}{\omega_d}\right)^2}\right)^2. \tag{10}$$

TF_1 and TF_2 are plotted in figures 7 and 8 for several values of ω_d. In both cases, oscillator noise components with frequencies very near ω_0 are strongly attenuated, and those at the edge of the filter pass band are the least attenuated.

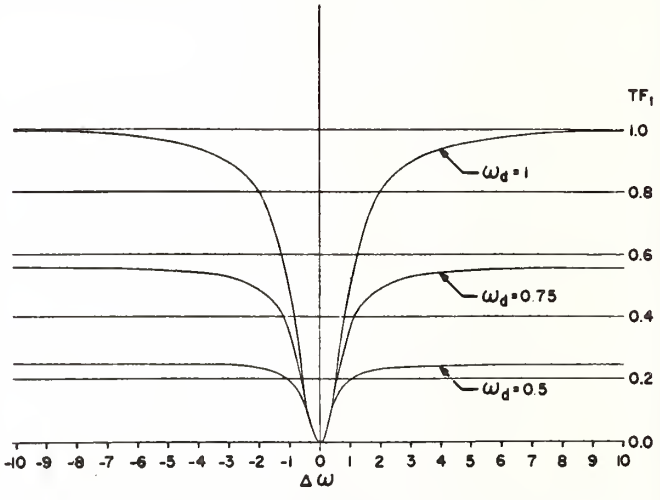

FIGURE 7. *Power transfer functions for a frequency-dependent bridge followed by a single section filter.*

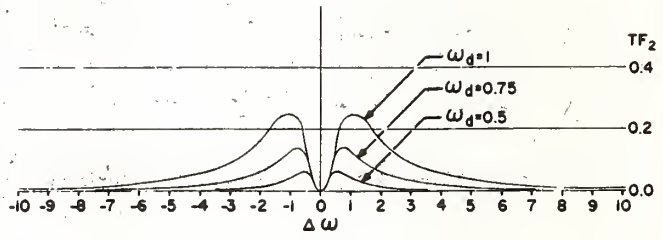

FIGURE 8. *Power transfer functions for a frequency-dependent bridge followed by a double section filter.*

The total noise power reaching the detector depends upon the noise spectrum of the oscillator. This is not known a priori, but in general is highest near ω_0. We will assume arbitrarily that the noise spectrum is of constant amplitude, in order to simplify the calcula-

tions. In this case, the total noise power with a single section filter would be of the form

$$W_1 \propto \int_0^\infty \frac{(\omega-\omega_0)^2}{1+\left(\frac{\omega-\omega_0}{\omega_a}\right)^2}\, d\omega \to \infty \qquad (11)$$

and for a two-section filter,

$$W_2 \propto \int_0^\infty \left[\frac{\omega-\omega_0}{1+\left(\frac{\omega-\omega_0}{\omega_a}\right)^2}\right]^2 d\omega \to \frac{\pi\omega_a^3}{2}. \qquad (12)$$

The expression (11) for W_1 is not realistic because (9) is correct only for $\omega \approx \omega_0$. In general TF_1 would decrease when $\Delta\omega$ is very large and would not remain constant, so that W_1 would be very large but finite.

The advantage of using a two-section filter is obvious from figures 7 and 8 and from (11) and (12), and in addition the very strong dependence of W_2 on the filter bandwidth can be seen. If the oscillator noise spectrum had a peak at $\omega = \omega_0$, the exponent of ω_a in (12) would be reduced, but in practice the observed detector noise due to oscillator noise decreases faster than that due to ordinary thermal agitation noise in the bridge components when the detector bandwidth is decreased. We find with the NBS quadrature bridge connected to a reasonably clean oscillator that the use of two cascaded filters with time constants of 0.3 s makes the portion of the detector noise due to oscillator noise about equal to that due to thermal agitation noise in the bridge components. Filters with 3-s time constants are normally employed, in which case the effect of oscillator noise is negligible.

The above discussion deals with noise power and makes no distinction between the different effects of FM and AM noise. If a frequency-dependent bridge is connected to a two-phase phase sensitive detector adjusted so that the first channel responds only to the "real" part of the bridge balance and the second channel responds only to the "phase" part of the bridge balance, then the effect of FM noise on the oscillator is to give noise only on the first or real channel of the phase-sensitive detector, as might be expected. It can also be shown that the effect of AM noise on the oscillator is to give noise only on the second or "phase" channel of the detector. The latter effect is not usually anticipated. One consequence of this effect is that when the power level of the bridge is being changed, the phase channel of the detector is thrown off balance, usually by enough to saturate the detector and to require a short wait before the detector recovers. The separation of FM and AM noise with a frequency-dependent bridge can be helpful in the study of oscillator noise.

The main components, P_1, P_2, P_3, and P_4 of the NBS quadrature bridge are maintained at 25±0.001 °C in an oil bath. The precision of the bridge is limited by the temperature variations in the bath and by the load coefficients of P_1 and P_3. The sum of all other errors, including that due to thermal agitation noise, is believed to be less than 1 part in 10^9.

4. Four-Pair Direct-Reading Ratio Set (DRRS)

The bridge to be described next was actually the first four-pair admittance bridge to be completed at NBS, and is in some ways not as well conceived as the more recent quadrature bridge described above. It is nevertheless a highly accurate and wide range instrument, and has received much use in the last few years. The bridge has a number of rather complex features, making it difficult to understand without prior experience with four-pair bridges. It is for this reason that its description follows that of the quadrature bridge.

The four-pair direct-reading ratio set was intended to provide a means of comparing two four-pair admittances whose ratio is nominally 10:1. It was designed so that it could also be used to compare ordinary two-pair standards. Fewer auxiliary balances are required with the two-pair configuration, so this usage will be described first.

An elementary schematic of the bridge is shown in figure 9. The two admittances to be compared are labeled Y_1 and Y_2, and are connected to three star connectors as indicated. The star connectors are constructed in accordance with a design first described by

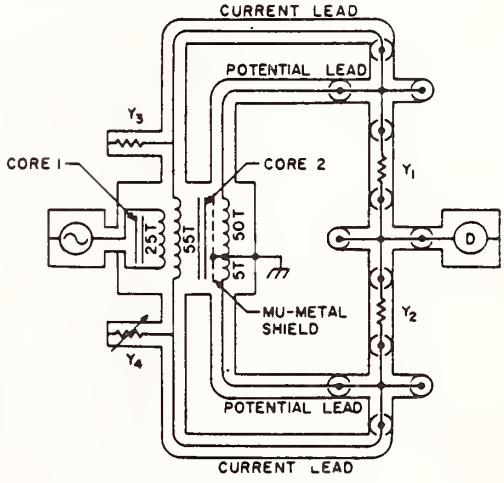

FIGURE 9. *Elementary 10:1 bridge using a two-stage transformer.*

Hamon [11] for dc junctions, but are provided with ground potential shields to allow their use with alternating current. The equivalent circuit of an ideal four-pair star connector consists of five impedances linking the five terminals to an inaccessable internal junction point. The impedance to ground is typically much larger than the other four. With this system, the admittances under test are considered to terminate at the internal junction points of the star connectors, rather than at the ends of the coaxial cables leading to the standards. The discrepancy between the two

definitions of a standard is small if its admittance is small, but could be accounted for to first order.

The transformer in figure 9 is a two-stage device in which the 25-turn primary and the 55-turn current winding are wound around core 1 only. The 50-turn and 5-turn potential windings are wound around both cores and are isolated from the inner windings and the two cores by a mu-metal shield.

If there were no capacitance between windings or to ground, there would be very little current in the potential leads to Y_1 and Y_2, and a detector connected to the star connector between Y_1 and Y_2 would register a null when Y_1/Y_2 equalled the open circuit ratio of the potential windings. Because of loading effects, both in the potential winding circuit and in Y_1 and Y_2 and the associated cables, two auxiliary balances are required to obtain zero current in both potential leads. The first auxiliary balance can be conveniently obtained by means of an adjustable admittance to ground Y_4 so that Y_3 and Y_4 serve as a conventional Wagner circuit, and the second balance can be obtained by means of an auxiliary winding around core 2 only (not shown), whose excitation is adjustable and derived from a high impedance source. It may be noted here that one anticipates that only a very small excitation will be required on core 2, to drive current through the interwinding capacitance of the transformer potential windings, and that very little voltage will appear across the auxiliary winding on core 2 because of the two-stage construction. Ideally, an adjustable current source could be used to drive core 2.

The balance procedure for the system of figure 9 would be first to adjust Y_1 or Y_2 to achieve a null on the detector: second, to disconnect both potential leads between the transformer and the star connectors and to adjust Y_4 to restore the null (a balance which is completely independent of the excitation of core 2): and third, to reconnect one of the potential leads and to restore the null by adjusting the core 2 excitation. The process is repeated until the adjustment of Y_1/Y_2 converges to a fixed ratio, which is equal to the open circuit ratio of the transformer potential windings.

A fast convergence of this series of balances is obtained if the equivalent impedences in series with the potential windings are very small with respect to the impedences of the second core excitation circuit and of the Wagner circuit. A technique for eliminating the impedance in series with the high-voltage secondary winding of a three-winding transformer at the expense of slightly increasing the impedence in series with the low-voltage secondary winding has been described [6]. This technique is illustrated by the equivalent circuits based on ideal transformers shown in figures 10a and 10b. The circuit of figure 10a is equivalent to the circuit of figure 10b, with $z_1' = z_1 - 9z_3$ and $z_2' = z_2 + 0.9z_3$ for a transformer with a 10:1 ratio. The unlabeled impedences and turns ratio are not precisely equal in the two figures, but this is not important. The significant result is that z_3 can be adjusted to make $z_1' = 0$.

A technique for making the effective impedance in series with the low potential winding also equal to zero is shown in figure 11. If there is no current in the low potential winding, there will be no voltage across transformer T_2, and hence no current through the

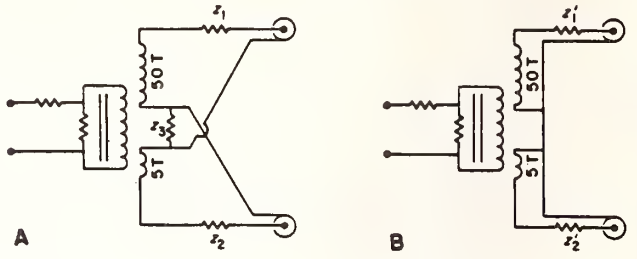

FIGURE 10. *Equivalent circuits for showing the effect of* z_3 *on* z_1' *(see text).*

auxiliary admittance Y_2'. However, if there is a current in the potential winding, T_2 will be excited, producing a compensating current in Y_2'. In the worst case, suppose the potential lead of Y_2 is shorted. Then if $z_2'' = z_2'$, the voltage on the 100-turn winding of T_2 will be $e_1/2$, and the voltage applied to Y_2' will be equal to e_1. The drastic measure of shorting the potential lead of Y_2 would then cause no deflection of the null detector provided $Y_2' = Y_2$. An argument based on the circuit linearity indicates that smaller currents in the low potential lead would likewise cause no deflection of the null detector.

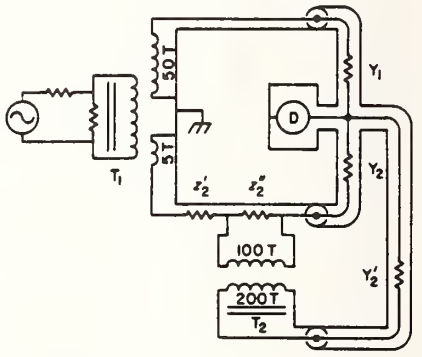

FIGURE 11. *Compensation scheme for eliminating the effect of* z_2.

Applying the concepts of figures 10 and 11 to the basic circuit of figure 9 we have a system in which the currents in both potential leads can be adjusted to zero, but in which the bridge balance condition is not strongly dependent upon either auxiliary balance. In order to make the potential lead impedances definite so that z_3 and z_2'' need only be adjusted once during construction of the bridge, we have elected to plug the star connectors directly into the potential terminals on top of the bridge. The adjustments of z_3 and z_2'' then serve to make the effective impedances from the internal junction points of the star connectors to the equivalent voltage generators of the transformer potential windings equal to zero, using an auxiliary admittance $Y_2' = Y_2$. It is to be noted that when this

bridge was designed, the special defining transformers described in section 2 had not yet been invented and the potential leads were open circuited by simply unplugging them. This technique is adequate in this particular case since the potential lead equivalent series impedances are very small. When the junctions between the current and potential leads are located remotely from the bridge, as is the case when measuring four-pair admittances, the lead impedances are not small, and the Wagner and second core excitation adjustments are very critical. The shunt capacitance uncertainties caused by unplugging the coaxial connector could then cause substantial errors.

In order to make a direct reading ratio set out of the circuit of figure 9, a means must be provided for adjusting the ratio of the potential winding in accurately divided steps. The adjustment of the magnitude of the ratio is straightforward, and can be accomplished in principle by means of a step-down transformer T_4 and a six-decade inductive voltage divider T_3 magnetically coupled to the potential windings of T_1 as shown in figure 12. Although T_3 and T_4 are represented as being ordinary single-stage transformers, they are actually both two-stage devices. The first stage of T_3 is coupled to the first stage of T_1 only, and is used to excite the first stage of T_4. The switching of the first and second stages of T_3 are ganged, which improves the accuracy of the voltage division, and results in a negligible interaction with the core 2 excitation adjustment for T_1.

Constructing an accurate quadrature adjustment for a direct-reading ratio set is much more difficult than constructing an equally accurate magnitude adjustment. At the heart of the problem is the requirement for a 90° phase-shifting circuit. The conflicting requirements of small output impedance, relatively large output voltage, and reasonably small power dissipation tend to limit the accuracy and range of most passive quadrature balance circuits.

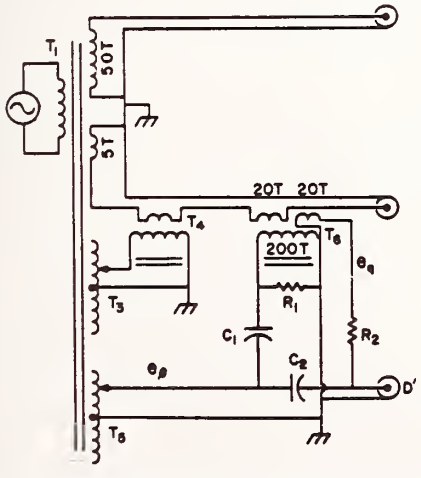

FIGURE 12. *Circuitry for adjusting the real and quadrature components of a transformer ratio.*

In the quadrature balance system shown in figure 12, the output of a phase shifting circuit consisting of a 0.01-μF capacitor C_1 and a 10-Ω resistor R_1 is connected to the primary of the three-winding transformer T_6. One secondary of T_6 is in series with the low potential winding of T_1. R_1 is small compared to the input impedance of T_6, and since $\omega R_1 C_1 \ll 1$, the voltage e_q added to T_1 by T_6 is nearly orthogonal to the voltage across T_5 and nearly of the desired magnitude. A test of the voltage added to T_1 by T_6 can be made by setting up a bridge using a precision 1-nF capacitor C_2 and a precision 10-Ω resistor R_2. A detector connected to terminal D' will register a null when $e_\beta j\omega C_2 = e_q/R_2$. A small complex adjustment of the excitation to the primary of T_6 may be made to give a null at D', so that $e_q = e_\beta j\omega C_2 R_2$. Divider T_5 is a six-decade, two-stage device similar to T_3, and in fact has separate windings on ganged switches to separate the coarse output tap connected to C_1 from the precision output tap connected to C_2. Resistor R_2 may at this stage be considered to include the equivalent series impedance of the winding on T_6 to which it is connected, but in the final design an extra winding was put on T_6 to provide a four-terminal connection for R_2.

When the circuits of figures 9, 10, 11, and 12 are combined, the result is a system with two sets of detector terminals. The advantages of combining the two to give a single detector whose response is essentially independent of the excitation of T_6 is by now quite apparent. The NBS bridge has been designed so that connecting an auxiliary admittance $Y_2'' = Y_2$ from D' to the main null detector D indicated in figure 9 achieves the desired effect. Rather than using two equal auxiliary admittances Y_2' and Y_2'', a single admittance is used for both purposes by connecting the 200-turn output winding of T_2 in figure 11 between terminal D' in figure 12 and the auxiliary admittance. This serves to add the compensating voltage produced in the quadrature balance circuit of figure 12 to that produced in the load compensation circuit of figure 11.

The complete four-pair direct-reading ratio set contains all of the features described above, and some special compensation circuits for obtaining a quadrature adjustment which is precisely proportional to frequency. The only critical impedances required in the bridge are the capacitor C_2 and the resistor R_2 involved in the quadrature adjustment circuit.

The bridge was a test bed for a number of previously untried ideas, and as such it grew in a rather haphazard manner. It is felt that the bridge could be greatly improved if it were rebuilt, and while this is not contemplated at this time, a complete circuit of the existing bridge would be more exposing than revealing, and therefore no such circuit appears in this paper. It is perhaps useful to point out that the key to achieving highly accurate and stable ratios in critical transformers and inductive dividers is to make generous use of multi-stage transformers with magnetic shielding between stages. The principal errors in such transformers are due to capacitive loading effects working on their output impedances. Both the interwinding

capacitances and the output impedances are minimized by minimizing the number of turns on the transformer. The optimum number of turns on a shielded two-stage transformer designed for audiofrequencies is believed to be less than 100 turns, which is much smaller than the number normally employed in a single-stage design.

The calibration of the bridge was in some ways even more formidable than its construction. The first step was to check the linearity of the bridge dials at several frequencies by an external calibration technique in which a fixed admittance was repeatedly added in parallel with one side of the bridge for various settings of an auxiliary admittance in parallel with the other side. Both magnitude and quadrature balance linearities of all dials were checked in this way. A resolution of 1 part in 10^{10} was obtained at 1592 Hz, and of 1 part in 10^9 at all other frequencies.

The second step was to determine the actual bridge settings which would produce an exact 10:1 ratio. A modification of the permutation method described in an earlier paper [12] was used for this purpose.

The last step in the calibration was to determine the actual magnitudes and phase angles corresponding to changes of the real and quadrature dials of the bridge over their entire ranges. A quadrature bridge and a system for comparing admittances in a 1000:1 ratio are needed for this step. Three step-ups using the 10:1 ratio of the bridge under test provided the 1000:1 ratio with ample accuracy.

The bridge accuracy is optimum at 1592 Hz. at which frequency the ratio is adjustable over a range of ± 5 parts in 10^4 in steps of 1 part in 10^9 for both real and quadrature components. A complete calibration using the procedure outlined above disclosed that the bridge readings are linear at 1592 Hz over the entire range of the dials within an estimated uncertainty of 3 parts in 10^{10}. The actual changes in both real and imaginary parts of the bridge ratio produced by changing the dials over their entire ranges differ slightly from the values indicated on the dials. The discrepancies are never greater than 5 parts in 10^9, even when the bridge dials are at the limits of their ranges. Corrections for linear errors of this form are relatively easy to apply.

At 159.2 Hz, the range of the bridge quadrature balance control decreases to ± 5 parts in 10^5, and at 15920 Hz it increases to ± 5 parts in 10^3. The first decade of the quadrature balance control is somewhat nonlinear above 10 kHz, but if the bridge is not used for comparing admittances for which the quadrature component of their ratio exceeds ± 5 parts in 10^4, no errors exceeding 5 parts in 10^9 exist from 159.2 Hz to 15920 Hz.

The additional circuitry needed when using the bridge for comparing four-pair standards, P_1 and P_2, is shown in figure 13. The critical leads to the standards P_1 and P_2 are terminated at the reference planes of the defining transformers T_7, T_8, and T_9, and the leads between these transformers and the standards are treated as part of the standards. The combining network involving T_{10} and the associated phase-shifting network, which joins the detector terminals D_1 and D_2 of the two standards, is adjusted to obtain a null on D_6 when an oscillator is connected to the 100-turn input winding of the defining transformer T_8. Then the input winding of T_8 is shorted and the oscillator is reconnected normally. Alternatively, this adjustment can be made by leaving the oscillator connected normally, and adjusting the network so that D_6 does not respond when the short on T_8 is removed.

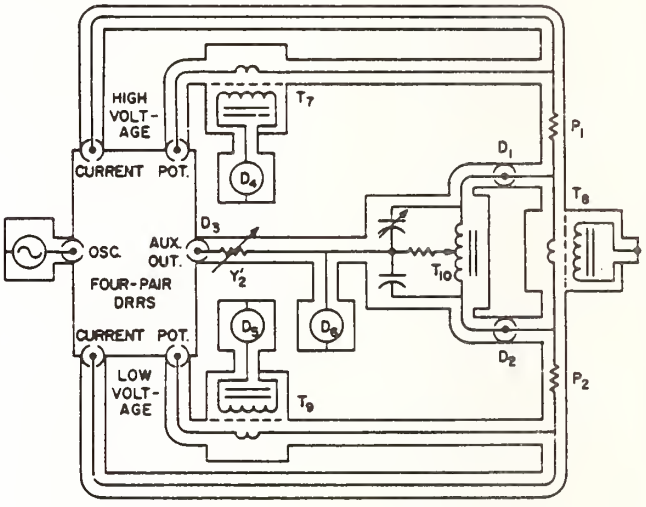

FIGURE 13. *Comparison of four-pair admittances with the four-pair DRRS.*

The Wagner balance and second core excitation of the four-pair bridge are adjusted to obtain nulls on detectors connected to points D_4 and D_5 of defining transformers T_7 and T_9 rather than by disconnecting the potential leads to the bridge. With this system the bridge ratio is defined at the reference planes in T_7 and T_9, and differs from the ratio defined at the potential terminals of the bridge. Techniques for comparing the ratios defined in these two ways can be easily developed, or alternatively the permutation method for measuring the bridge ratio [12] can be modified to give the ratio at the reference planes of T_7 and T_9 directly. A standard pair of cables for connecting T_7 and T_9 to the potential terminals of the bridge is obviously required.

The circuit of figure 13 is not easy to operate directly, partly because the deflections of the auxiliary detectors connected to D_4 and D_5 both change when either the bridge Wagner Balance or the second core excitation is changed, and partly because these balances are both much more critical than they are when comparing two-pair admittances. The criticalness is caused by the extra equivalent impedances in series with the bridge potential terminals resulting from the added cables between these terminals and the internal junctions of P_1 and P_2. A network with the double purpose of combining the output of D_5 with the main detector and of providing two auxiliary detector outputs, one of which responds to each bridge auxiliary balance, is shown in figure 14.

The 100-turn windings of both T_7 and T_9 are terminated with 50-Ω resistors, which when referred to the

1-turn input windings yields a very small impedance. The voltages across the 100-turn windings are thus proportional to the currents in T_7 and T_9. The output voltage at terminal D_8 is proportional to the sum of these two currents, and responds to changes in the

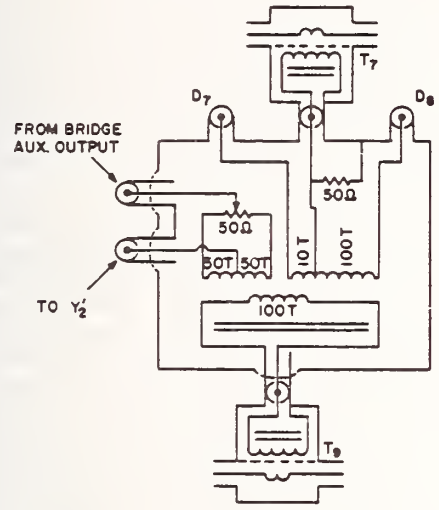

FIGURE 14. *Combining network for assuring fast convergence of DRRS auxiliary balances.*

Wagner balance but not to changes in the second core excitation. The output voltage at terminal D_7 is proportional to the current in T_7 minus 1/10 of the current in T_9. It responds to changes in the second core excitation, but not to changes in the Wagner balance. A very rapid convergence of the auxiliary balances can thus be obtained.

A complete combining network for joining the two auxiliary detector points D_7 and D_8 with the main detector D_6 would require two complex adjustments for a total of four adjustable parameters. The simple combining network of figure 14 contains only one adjustable resistor and does not give perfect compensation. It is adequate at 1592 Hz and below because the reactances of the bridge cables are much smaller than their resistances at this frequency, because the impeddance of the high-voltage potential lead is only one-tenth as important as the impedance of the low-voltage potential lead, and because a factor of 10 reduction in the criticalness of the auxiliary balances was found to be sufficient.

A detailed calculation to verify the above conclusions is not appropriate to this paper. The analysis can be carried out with the aid of the equivalent circuit for the bridge potential circuit shown in figure 15, in which i_1 represents the second core excitation, i_2 represents the effect of changing the Wagner balance, i_3 and i_4 are the currents in the potential leads, i_d is the short circuit current at the main detector, and Y_1 and Y_2 are the admittances under test. The voltage generator in the current leads of the bridge is represented by e_1, and can be set equal to zero when analyzing the behavior of the auxiliary balances.

The use of an auxiliary admittance Y_2' as indicated in figure 13 for combining several null detectors causes no appreciable reduction in bridge sensitivity when the admittances under test are capacitors, but when one is measuring ac resistors this technique substantially increases the thermal agitation noise appearing at the detector. The alternative combining network shown in figure 16 avoids this problem, and works well when the smaller of the resistors under test is $10^4\ \Omega$ or less. The alternative combining network has been

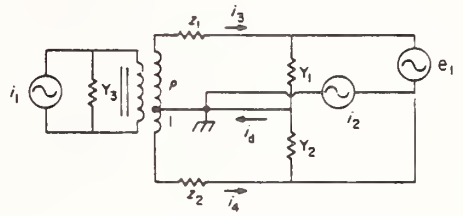

FIGURE 15. *Equivalent circuit representing the DRRS auxiliary balances and their effects.*

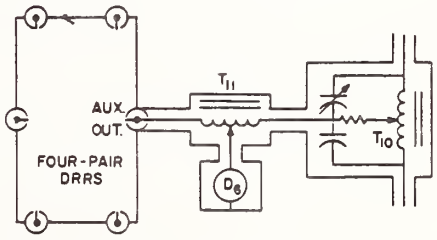

FIGURE 16. *Alternative combining network for use when* $Y_2 \geq 10^{-4}$ *siemen.*

found to be more convenient than the circuit of figure 13 for the measurement of all admittances for which $|Y_2| \geq 10^{-4}$ siemens. The circuit of figure 13 is usually easier to adjust when $|Y_2| \leq 10^{-5}$ siemens, because it is not as strongly affected by admittances to ground at the junction of Y_1 and Y_2 and in the combining network involving T_{10}. The circuit of figure 14 works equally well with either combining network.

Although no coaxial chokes are shown in any of the circuits for this bridge, they are obviously essential for proper operation. They are inserted where needed to break ground loops, and tested in accordance with the principles laid out in section 2.

5. Equal-Power 100 : 1 Resistance Bridge

The comparison of two resistors whose ratio substantially differs from unity is usually made either by connecting them directly in series and comparing their voltages, or by applying equal voltages to them and comparing their currents. As a result, the powers dissipated in the two resistors differ greatly, and if the load coefficients of the two resistors are about equal, the excitation of the bridge is limited by the load coefficient of the resistor which dissipates the most power. In this case, the bridge sensitivity is much less

than would be obtained with a unity ratio bridge containing resistors of comparable load coefficients.

Using a voltage transformer bridge such as the direct-reading ratio set described above, the larger resistor dissipates ten times as much power as the smaller resistor. Using a current transformer bridge such as the conjugate bridge obtained by interchanging generators and null detectors, the smaller resistor dissipates ten times as much power as the larger resistor.

If a bridge contains a voltage transformer of ratio N_1 *and* a current transformer of ratio N_2, then the balance condition is $R_1 = N_1 N_2 R_2$; and the powers dissipated in the two resistors are equal if $N_1 = N_2$. The bridge sensitivity in this case is equal to that of a unity ratio bridge for comparing equal resistors. The technique is only applicable for resistors whose ratio is a perfect square, but this is not a fundamental limitation since a rational number can be found that is arbitrarily close to any irrational number.

For the very important case in which the two resistors to be compared have a ratio of 100, each transformer must have a ratio of 10. The bridge described in section 4 above contains all of the components required of the voltage transformer in such a system, and in principle another bridge exactly like it but with a subtractive rather than an additive ratio could be used for the current transformer. Fortunately the current transformer part of the bridge need not be provided with an adjustable ratio, and is therefore much easier to build. A quite different approach to an equal-power, four-terminal (but not four-pair) impedance bridge has been developed by Henry Hall of the General Radio Company.[2] Both two-pair and four-pair equal-power bridges have been described in the literature [12], but the operation of the four-pair version is not clear unless two-stage transformers are employed.

[2] A paper describing this work was presented at the 1970 Conference on Precision Electromagnetic Measurements at Boulder, Colorado. The text of this paper will be published in an issue of the IEEE Transactions on Instrumentation and Measurement.

The 100:1 bridge used at NBS for comparing a 10^3-Ω four-pair resistor with a 10^5-Ω four-pair resistor at 1592 Hz is shown in figure 17. It is convenient for the purpose of analyzing the behavior of this circuit mentally to interchange all generators and detectors and to work with the conjugate bridge. Although the circuit could of course be described directly without making use of the fictitious interchange, and although this would seem a more natural approach to people familiar with current comparators, the interchange is helpful here because it allows the use of the same terminology as was developed for describing the direct reading ratio set of section 4.

If we consider then that a generator is connected to terminal B in figure 17, it can be seen that the second core excitation circuitry is identical with that described in section 4, but that the Wagner circuitry is much more complex. The Wagner circuit combines a 10:1 voltage transformer T_{15} with a 10:1 current transformer T_{16} to obtain simultaneously nearly the correct 10:1 voltage ratio and 10:1 current ratio in the two resistors under test. Note that the ratio of currents in the two windings of T_{16} is nominally equal to the turns ratio, so that very little voltage appears across either winding. The two auxiliary adjustments then provide only the small corrections necessary to meet exactly the required conditions of zero current in the defining transformers T_{12} and T_{13}.

Although a much simpler Wagner balance system involving resistors could have been used, the circuit chosen is superior because it leads to a negligible augmentation of the thermal agitation noise appearing at a detector connected at point B. This consideration is of no importance in the Wagner circuit of the voltage transformer part of the bridge, and the use of R_3 to extend the limited range of the internal Wagner adjustment of the direct-reading ratio set is perfectly satisfactory.

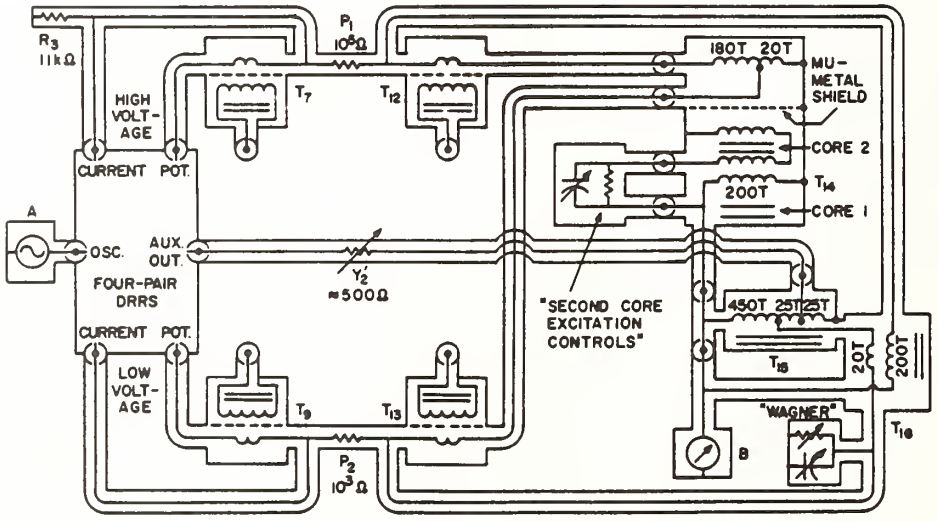

FIGURE 17. *A 100:1 equal power bridge making use of the four-pair DRRS.*

The auxiliary resistor required for proper operation of the quadrature balance controls of the direct-reading ratio set would most conveniently consist of a 10^4-Ω resistor connected between the auxiliary output terminal of the bridge and the detector point B. This would produce an unacceptably large thermal agitation noise. The use of a 500-Ω auxiliary resistor for Y_2' which is connected to a tap on T_{15} eliminates this problem. This does not interfere with the use of the circuit of figure 14 to reduce the criticalness of the direct-reading ratio set auxiliary balances.

A circuit similar to that of figure 14 and connected to defining transformers T_{12} and T_{13} is used to reduce the criticalness of the current transformer auxiliary balances and to provide a means of quickly making the current transformer auxiliary balances. This circuit is shown in figure 18. An auxiliary admittance Y_3 (not shown) is connected between this circuit and the generator terminal A on the direct-reading ratio set.

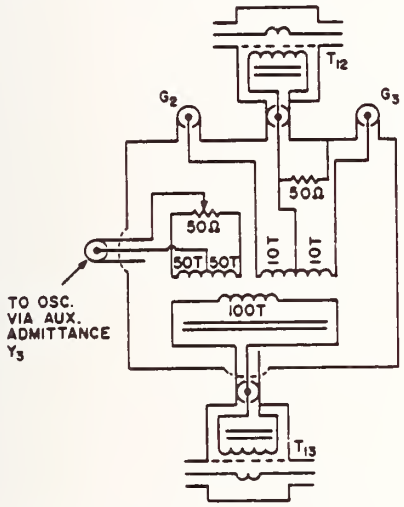

FIGURE 18. *Combining network for assuring fast convergence of current transformer auxiliary balances.*

The circuit of figure 18 is complimentary to the circuit of figure 14. In use, the current transformer auxiliary balances are adjusted so that temporarily connecting a generator to either G_2 or G_3 produces no change in the detector connected to terminal B in figure 17. The adjustable 50-Ω resistor in figure 18 or the auxiliary admittance Y_3 is set so that these auxiliary balances are not critical.

It was necessary to compromise in choosing the number of turns for transformer T_{14} in figure 17 in order to achieve a reasonably stable ratio without unduly augmenting the thermal agitation noise due to excessive shunt conductance in the transformer. With 200 turns on T_{14}, the shunt conductance measured at point B with P_1 and P_2 removed was found to be 1.8×10^{-5} siemens which is only slightly less than the 2×10^{-5} siemens conductance contributed by the resistors under test. With 4×10^{-3} W dissipated in each resistor (20 V on P_1), the sensitivity is sufficient to resolve 1 part in 10^9 using a phase-sensitive detector followed by a recorder, which is considered to be adequate.

The easiest way to measure the ratio of the current transformer T_{14} is to interchange the connections with respect to the direct-reading ratio set so that a balance is obtained when P_1 is nominally equal to P_2. Interchanging P_1 and P_2 and rebalancing allows the current transformer ratio to be determined from the known ratio of the direct-reading ratio set. A slight change in the Wagner circuit of the current transformer is also required. This consists of interchanging the windings of T_{16}. Resistors cannot be used for P_1 and P_2 because of their large load coefficients, so a pair of 1-nF capacitors is used instead. The voltages on the two capacitors change from 20 V to 200 V in the course of the measurement, so their voltage dependencies must be accurately known. Techniques for measuring the voltage dependencies of capacitors to the required accuracy have been described by Shields [14].

6. Conclusions

The series of bridges described above were built to provide the admittance comparisons necessary for an absolute ohm determination, as sketched in the introduction. It has been found that all of the comparisons necessary for this work can be made with an overall uncertainty of a few parts in 10^9 using these bridges. In practice, the largest source of uncertainty results from instabilities in the admittance standards used in the measurements. This problem can be handled only be carefully controlling the temperature of the standards.

7. References

[1] Cutkosky, R. D., Four-terminal-pair networks as precision admittance and impedance standards, commun. and Electronics **70**, 19–22 (Jan. 1964).

[2] Homan, D. N., Some techniques for measuring small mutual inductances, J. Res. Nat. Bur. Stand. (U.S.), **70C** (Eng. and Instr.), No. 4, 221–226 (Oct.–Dec. 1966).

[3] Haddad, R. J., A resistor calculable from DC to $\omega = 10^5$ rad/s, Master's thesis, School of Engineering and Applied Science, The George Washington University, Washington, D.C., 1–57 (Apr. 1969).

[4] Thompson, A. M., AC bridge methods for the measurement of three-terminal admittances, IEEE Trans. Instr. Meas. **IM-13**, No. 4, 189–197 (Dec. 1964).

[5] Kavanagh, R. J., Noninteracting controls in linear systems, Trans. AIEE **76**, part 2, 95–100 (May 1957).

[6] Cutkosky, R. D., Active and passive direct reading ratio sets for the comparison of audio-frequency admittances, J. Res. Nat. Bur. Stand. (U.S.), **68C** (Eng. and Instr.), No. 4, 227–236 (Oct.–Dec. 1964).

[7] Cutkosky, R. D., Evaluation of the NBS unit of resistance based on a computable capacitor, J. Res. Nat. Bur. Stand. (U.S.), **65A** (Phys. and Chem.), No. 3, 147–158 (May–June 1961).

[8] Thompson, A. M., An absolute determination of resistance based on a calculable standard of capacitance, Metrologia **4**, No. 1, 1–7 (Jan. 1968).

[9] Millea, A., and Ilie, P., A class of double-balance quadrature bridges for the intercomparison of three-terminal resistance, inductance and capacitance standards, Metrologia **5**, No. 1, 14–20 (Jan. 1969).

[10] Brooks, H. B., and Holtz, F. C., The two-stage current transformer, AIEE Trans. **41**, 382–393 (1922).

[11] Hamon, B. V., A 1–100 Ω build-up resistor for the calibration of standard resistors. J. Sci. Instr. **31**, 450–453 (1954).
[12] Cutkosky, R. D., and Shields, J. Q., The precision measurement of transformer ratios. IRE Trans. Instr. **I-9**, No. 2, 243–250 (1960).
[13] Clark, H. A. M., and Vanderlyn, P. B., Double-ratio AC bridges with inductively-coupled ratio arms. Proc. IEE **96**, Pt. 3, 189–202 (1949).
[14] Shields, J. Q., Voltage dependence of precision air capacitors. J. Res. Nat. Bur. Stand. (U.S.), **69C** (Eng. and Instr.), No. 4, 265–274 (Oct.–Dec. 1965).

(Paper No. 74C3&4–299)

A VARACTOR NULL DETECTOR FOR AUDIO FREQUENCY CAPACITANCE BRIDGES

BY

R. D. CUTKOSKY

Reprinted from IEEE TRANSACTIONS
ON *INSTRUMENTATION AND MEASUREMENT*
Volume IM-17, Number 4, December, 1968
pp. 232-238

A Varactor Null Detector for Audio Frequency Capacitance Bridges

ROBERT D. CUTKOSKY, MEMBER, IEEE

Abstract—A two-varactor, double-sideband up-converter pumped at 30 MHz has been constructed. Operated at room temperature with a signal frequency of 10^4 rad/s, the device has an optimum source resistance of 10^5 ohms and a minimum noise figure of 0.01 dB. Immersed in liquid N_2, minimum noise figures below 0.001 dB referred to a room temperature source have been measured. The device is particularly useful as a null detector for audio frequency capacitance bridges. At 10^4 rad/s, a signal current of 10^{-14} amperes through a capacitance of 1000 pF can be detected in less than one second with this instrument. Techniques for suppressing microphonics and other extraneous sources of noise are described.

I. Introduction

BRIDGE circuits commonly used with calculable capacitors may be viewed at their detector terminals as a signal current source of 10^{-14} amperes at an angular frequency of 10^4 rad/s (1592 Hz) shunted with a 1000-pF capacitance and a 10^{-9}-reciprocal-ohm conductance. Thermal agitation noise is produced by the conductance, and is given by $i_n \approx 4 \times 10^{-15}$ ampere for a bandwidth of 1 Hz. Since this noise current is considerably smaller than the signal current, detection of the signal would seem to be a simple matter of matching the source to a detector having a noise figure smaller than a few dB.

Although conventional detectors are available with noise figures below 1 dB, the capacitive source cannot be correctly matched to these detectors without greatly increasing the thermal agitation noise. For example, a 10-henry inductor will correctly tune out the 1000-pF capacitance at 10^4 rad/s, but even if it has a Q of 500, it will augment the noise current in a 1-Hz bandwidth by an amount $i_n \approx 1.8 \times 10^{-14}$ ampere, and in addition, the tuning will require readjustment whenever the source capacitance changes.

If the detector noise is sufficiently small, it is preferable to connect the source directly to the detector with no matching network. A detector with an optimum source impedance of 10^5 ohms and a noise figure of about 0.0025 dB is called for in this application if a 1-Hz bandwidth is used, and a detector with a noise figure of 0.01 dB would give a performance comparable with that obtained using a matching inductor having a Q of 500, but retuning would not be required to compensate for changes in source capacitance.

Manuscript received June 17, 1968. This paper was presented at the 1968 Conference on Precision Electromagnetic Measurements, Boulder, Colo.

The author is with the National Bureau of Standards, Washington, D. C. 20234.

Varactor amplifiers are extensively used at microwave frequencies in very low noise detector systems. Audio frequency varactor amplifiers have not been as extensively investigated, but noise figures below 0.1 dB have been reported for an amplifier designed for the range 2 to 50 Hz [1]. An investigation made at NBS indicated that it should be possible to construct audio frequency varactor amplifiers with noise figures below 0.01 dB. This paper describes recent progress toward realizing these theoretical predictions.

Although very low noise amplifiers are of critical importance for capacitance bridges, other uses for the system described here may be found. One possible field of application is the detection of signals from very low temperature resistive sources.

II. Circuit Description

The circuit investigated in our laboratory contained a pair of varactor diodes in a balanced circuit pumped at 30 MHz. An audio frequency input signal results in the production of sidebands separated from the 30-MHz carrier by the signal frequency. A commercial 30-MHz amplifier intended for use as an intermediate-frequency amplifier in a superheterodyne receiver (IF amplifier) amplifies these sidebands, which are then detected in a phase-sensitive detector whose reference voltage is obtained from the 30-MHz oscillator. A dc component in the output of this detector indicates a lack of balance in the varactor pair, and is returned as feedback to the bias circuits to eliminate the carrier from the output. This precaution prevents saturation of the IF amplifier, and helps to stabilize the overall system.

The audio frequency output of the 30-MHz phase-sensitive detector contains the amplified signal at its original frequency, and is usually passed after further amplification through a second phase-sensitive detector whose reference is obtained from the oscillator which drives the audio frequency bridge. The original signal has at this point been reduced to direct current, and is easily filtered to reduce the bandwidth of the detector system, thereby reducing the noise.

The construction of the system is illustrated in Figs. 1–7. The varactor head, Fig. 2, is contained in an evacuated chamber, Fig. 4. This chamber is immersed in liquid N_2 contained in a 4-liter Dewar. The Dewar is enclosed in a rectangular mu-metal box visible in Figs. 6 and 7.

The operation of the varactor head, Fig. 2, is as follows. A 30-MHz-pump input drives the two varactors

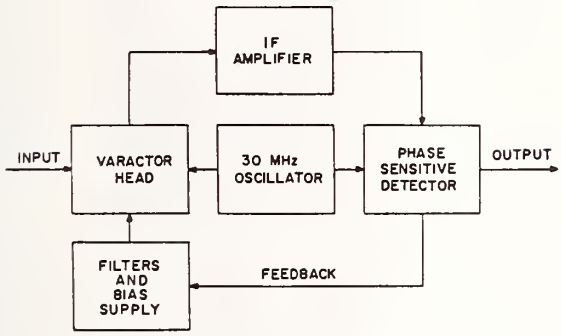

Fig. 1. Block diagram of varactor amplifier.

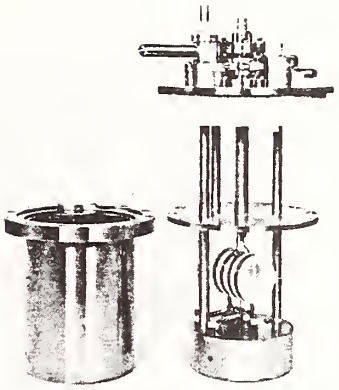

Fig. 4. Interior of varactor head.

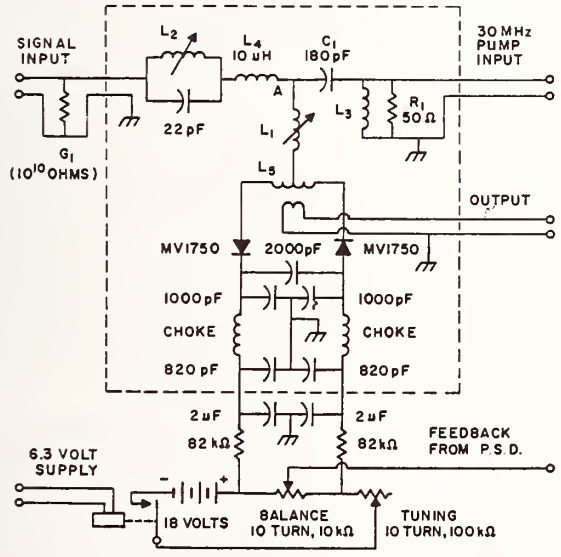

Fig. 2. Varactor head and bias supply circuits. Section within dotted lines is maintained at 77K.

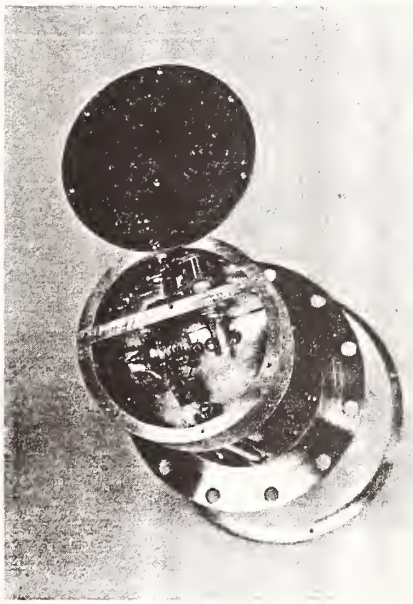

Fig. 5. Bottom view of varactor head showing L_1, L_2, L_3, and L_4.

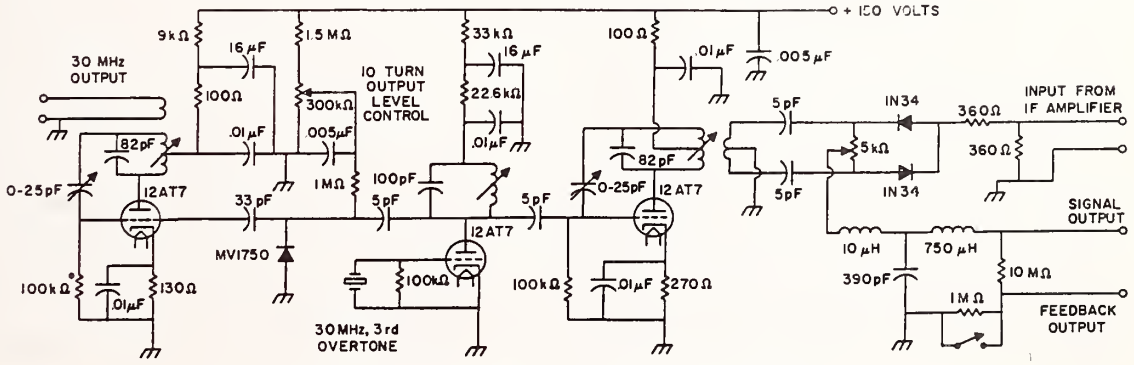

Fig. 3. Pump oscillator–phase-sensitive detector circuit.

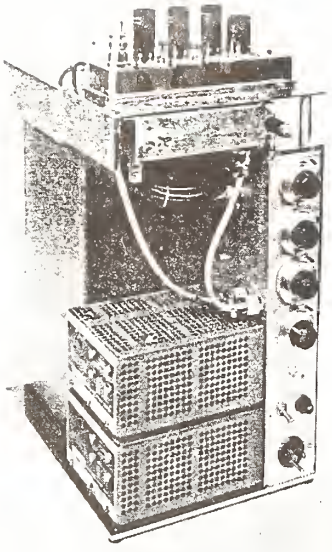

Fig. 6. Front view of varactor amplifier.

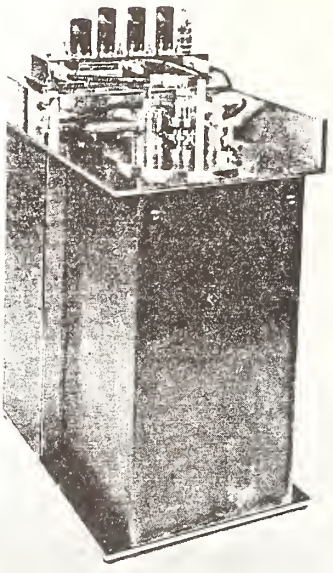

Fig. 7. Rear view of varactor amplifier.

symmetrically to vary their capacitances at 30 MHz. Inductor L_1 is adjusted to resonate with the parallel combination of the two varactors, and minimizes the magnitude of the 30-MHz voltage appearing at point A for a given varactor excitation voltage. Inductor L_3 resonates with the 180-pF capacitor C_1 connected to it, and as a result the pump line is teminated with the 50-ohm resistor R_1. This was done so that variations in the length of the 50-ohm pump line would not affect the varactor excitation voltage. The phase shift in the 30-MHz circuit may then be adjusted by varying the pump line length. The choke L_4 and the 30-MHz trap involving L_2 suppress the high-frequency voltages that would otherwise appear at the signal input terminals. If these filters were not present, the behavior of the system would depend upon the impedances of the signal input circuit at multiples of 30 MHz.

The bias voltages are adjusted to balance the 30-MHz pump currents passing through the two varactors, and to produce a 30-MHz resonance in the circuit containing L_5 and the series combination of the two varactors. Under these conditions, the output voltage induced in the one-turn coupling loop associated with L_5 is zero when the audio frequency input signal is zero, but due to the reversed polarity of the two varactors, the presence of a signal voltage results in an unbalance in the varactor bridge and in the appearance of an output voltage. A mechanism for adjusting the coupling loop position is accessible from outside the Dewar–varactor head assembly, hence the match between L_5 and the IF amplifier can be optimized with the system in operation.

The signal input and bias circuits are designed to minimize the contributions to the output signal of the thermal agitation noise voltages produced in their resistive components. The low-frequency series resistance of the combination L_1, L_4, and L_2 is less than 1 ohm, and is negligible compared with the measured amplifier equivalent noise resistance R_{eq} (see Table I). Likewise, the low-frequency equivalent series resistances of the bias circuits were reduced below 1 ohm above 1 kHz by the use of high-Q, 2-μF bypass capacitors.

Current noise generators operative at audio frequencies include shot noise in the varactor diodes, and thermal agitation noise in G_1. The varactor leakage currents are below 10^{-14} ampere at liquid N_2 temperature (77K), and the resulting shot noise is not significant. However, this source of noise would not have been negligible at room temperature. The 10^{-10}-reciprocal-ohm conductance G_1 is needed to maintain the dc voltage levels in the circuit at their proper values, but is unfortunately a large source of current noise. The measured conductance of this element at 1592 Hz was found to be 3.1×10^{-10} reciprocal ohm, which is close to the measured amplifier equivalent noise conductance of 5.2×10^{-10} reciprocal ohm (see Table I). It would be desirable to maintain G_1 at 77K in a new construction.

Much has been published on the theory of varactor amplifiers [2], [3]. The following first-order analysis leaves much to be desired in elegance, but has been found particularly useful in the unusual case of an unmatched signal source.

A varactor pumped at an angular frequency ω_p ex-

TABLE I

EXPERIMENTALLY DETERMINED AMPLIFIER NOISE PARAMETERS BASED ON THE EQUIVALENT CIRCUIT OF FIG. 9

Frequency (Hz)	R_{eq} (Ω)	G_{eq} (reciprocal Ω)	G_s^{opt} (reciprocal Ω)	F_{min}' (dB)
90	400	1.1×10^{-10}	5.2×10^{-7}	1.8×10^{-3}
160	180	4.7×10^{-10}	1.6×10^{-6}	2.5×10^{-3}
400	100	4.0×10^{-10}	2.0×10^{-6}	1.7×10^{-3}
1000	35	5.1×10^{-10}	3.8×10^{-6}	1.2×10^{-3}
1592	23	5.2×10^{-10}	4.8×10^{-6}	0.95×10^{-3}
4000	14	2.3×10^{-9}	1.3×10^{-6}	1.6×10^{-3}
10000	14	1.2×10^{-8}	2.9×10^{-5}	3.6×10^{-3}
16000	16	2.7×10^{-8}	4.1×10^{-5}	5.7×10^{-3}
40000	50	6.5×10^{-8}	3.6×10^{-5}	16×10^{-3}
100000	140	6×10^{-7}	6.5×10^{-5}	80×10^{-3}

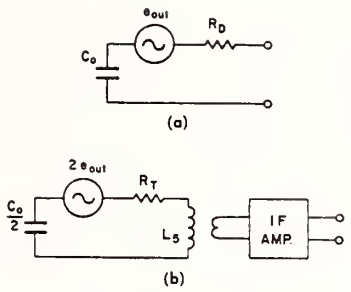

Fig. 8. Varactor equivalent circuits at output frequency. (a) An individual varactor. (b) Complete output circuit, in which $2\,e_{out} = -2\,e_s(\Delta C/C_0)\sin\omega_p t$ (see text).

hibits a time-dependent capacitance $C = C_0 + \Delta C \sin \omega_p t$, where C_0 is the average capacitance, and ΔC is the peak capacitance excursion from C_0 and depends upon the pump voltage.

If the varactor is open-circuited at the output frequency, we have

$$i = \frac{d}{dt}(Ce_{var}) = 0,$$

where e_{var} is the varactor voltage. If follows that $Ce_{var} = \text{constant} = C_0 e_s$, where e_s is the signal voltage, and hence

$$C_0\left(1 + \frac{\Delta C}{C_0}\sin\omega_p t\right)e_{var} = C_0 e_s,$$

and

$$e_{var} = \frac{e_s}{1 + \frac{\Delta C}{C_0}\sin\omega_p t} \approx e_s - e_s\frac{\Delta C}{C_0}\sin\omega_p t,$$

or

$$e_{out} \approx -e_s\frac{\Delta C}{C_0}\sin\omega_p t, \qquad (1)$$

where e_{out} is the high-frequency part of e_{var}. This expression is strictly true only if e_s is a constant, but is also valid when e_s is a slowly varying signal voltage.

The varactor equivalent circuit at the output frequency may then be represented as in Fig. 8(a), where R_D is the varactor series resistance. Because of the reversed polarity of the two varactors, their output voltages add, and the complete output resonance circuit takes the form of Fig. 8(b), where $R_T = 2R_D + R_L$, and R_L includes the series resistances of L_5 and the 1000- and 2000-pF bypass capacitors shown in Fig. 2.

Thermal agitation noise e_n in R_T is given by $e_n^2 = 4kT_N R_T \Delta f$ where $T_N \approx 77$ K. To this must be added the IF amplifier noise, which under conditions of optimum matching has the effect from the noise standpoint of adding a resistance R_{amp} at a temperature $T_{std} = 290$K to the circuit of Fig. 8(b). R_{amp} is given by $F = 1 + R_{amp}/R_T$, where F is the amplifier noise figure, or $R_{amp} = R_T(F-1)$. The total noise voltage in the circuit is then given by $e_n^2\,(\text{total}) = 4kT_N R_T \Delta f + 4kT_{std}(F-1)\Delta f R_T$.

Using (1), it can be seen that the total noise is equivalent to that which would be produced by thermal agitation noise in a resistor R_{eq} at $T_{std} = 290$K at the signal input terminals given by

$$4kT_{std}R_{eq}\Delta f \cdot \lim_{\tau\to\infty}\int_0^\tau\left(2\frac{\Delta C}{C_0}\sin\omega_p t\right)^2 dt \cdot \frac{1}{\tau} = 4kT_N R_T\Delta f + 4kT_{std}R_T(F-1)\Delta f,$$

or

$$R_{eq} = \frac{R_T\left(\frac{T_N}{T_{std}} + F - 1\right)}{2\left(\frac{\Delta C}{C_0}\right)^2}. \qquad (2)$$

For the IF amplifier used here, $F = 1.26$ (1 dB), and since $T_N/T_{std} \approx 0.26$ we have

$$R_{eq} = \frac{0.26R_T}{\left(\frac{\Delta C}{C_0}\right)^2}.$$

A measurement of the Q of the resonant circuit yielded $R_T = 0.4$ ohm. $\Delta C/C_0$ was estimated from the varactor characteristics and the pump voltage to be $\Delta C/C_0 = 0.1$, yielding $R_{eq} = 10$ ohms, in reasonable agreement with the measured results listed in Table I.

Several observations are in order regarding (2). First, the strong dependence upon $\Delta C/C_0$ suggests that an effort should be made to make this ratio as large as possible. In practice, when $\Delta C/C_0$ is much larger than 0.1 the second- and higher-order terms which were neglected in the analysis above become very important, and (2) requires modification. In fact, the amplifier described here oscillates when $\Delta C/C_0 > 0.14$.

Second, R_T enters the expression directly, and should be made as small as possible. Part of R_T is due to the varactor resistances, and is a prime consideration in

their selection. The remaining part is due to the series resistances of L_5 and of the bypass capacitors, and this leads indirectly to the choice of a high pump frequency, since a smaller number of turns are then required for L_5. The resistance R_T is also affected by temperature, and this was a factor in deciding to operate at 77K.

Third, since $T_N/T_{std} \approx F-1$, no more than a factor of two can be gained by either reducing the varactor temperature assuming R_T is constant, or reducing the IF amplifier noise figure; a substantial reduction in R_{eq} requires reducing both terms.

Fourth, neither the varactor capacitance nor the pump frequency enters directly into (2). This is not inconsistent with the Manley–Rowe equations, which govern the varactor power relationships. The effect of increasing the pump frequency is to allow the reduction of the series resistance of L_5, to provide an increased bandwidth $\Delta\omega$, and to reduce the Q of the resonant circuit, which simplifies tuning. We have for the circuit of Fig. 8 (b),

$$\frac{\Delta\omega}{\omega_p} = \frac{1}{Q} = \omega_p R_T \frac{C_0}{2}$$

or, neglecting R_L,

$$\frac{\Delta\omega}{\omega_p} = \frac{1}{Q} = \omega_p R_D C_0,$$

so that

$$\Delta\omega = \frac{\omega_p}{Q} = R_D C_0 \omega_p^2 \quad \text{and} \quad Q = \frac{1}{\omega_p R_D C_0}.$$

For the amplifier described here, $f_p = 3 \times 10^7$ Hz and $Q = 250$, so $\Delta f = f_p/Q \approx 10^5$ Hz. The tuned circuit should therefore pass both sidebands generated by signals with frequencies up to 50 kHz.

In practice, the advantages of using a pump frequency appreciably higher than 30 MHz would be partially offset by the larger noise figures that are usually associated with amplifiers designed for these frequencies.

When the varactor head was first operated in liquid N_2, a very large current noise was observed. This was traced to a microphonic sensitivity stimulated by the boiling nitrogen. The microphonic effect was principally due to the use of a polytetrafluoroethylene (PTFE) insulated wire for the signal lead entering the varactor head. Static charges on the PTFE induced currents into the signal lead when the lead moved with respect to the ground potential tube in which it was contained. The wire was replaced with an uninsulated length of thin-wall stainless steel tubing securely anchored at both ends, and the remaining PTFE insulators in the varactor head were deionized by passing a flame quickly over their surfaces. Although a rather large piece of PTFE was used to support inductor L_5 (see Fig. 4), it is in rigid contact with the inductor, and is a considerable distance from other ground potential objects. The deionization procedure and the reconstruction of the input lead seem to have eliminated the microphonic effects.

The 30-MHz pump oscillator–phase-sensitive detector circuit shown in Fig. 3 is conventional and needs no discussion. The filament voltages for it and for the IF amplifier are obtained from a 6.3-volt negative dc supply to minimize interference from power line harmonics. This supply is also used to power the IF amplifier gain control circuit.

The amplifier system requires about two hours to cool from room temperature to 77K, and was found to be quite stable and easy to adjust. Only the tuning of the circuit involving L_5 and the varactors is critical, and this is done in a way which minimizes the equivalent noise resistance R_{eq} at 1592 Hz.

III. Measured Noise Parameters

Most of the experimental work on this amplifier was done with a signal frequency of 1592 Hz. Several measurements were made of the correlation capacitance at this frequency using a 1000-pF source admittance (see Appendix), and it was found to be about 300 pF, which was equal to the measured input capacitance of the amplifier. This is the expected result based on the analysis in Section II of this paper. At all other frequencies the above result was assumed to be true, but was not verified. No measurements of the correlation conductance were made, and it is assumed to be zero.

All noise measurements were made at the selected spot frequencies by the use of tuned postamplifiers having bandwidths of a few hertz, and with a thermocouple–dc voltmeter combination. The postamplifier noise was small in most cases, but was not subtracted from the quoted results.

Considerable interference from power line harmonics was observed below 1 kHz. A narrower passband postamplifier would have avoided this problem, but the thermocouple response would then have been more difficult to interpret. Better magnetic shielding of the varactor head would probably reduce this interference.

Table I lists the pertinent noise parameters for the amplifier, using the equivalent circuit of Fig. 9.

An attempt was made to measure R_{eq} at 400 kHz. Although the results were not conclusive, R_{eq} appeared to be about 1000 ohms. This result and the data in Table I are consistent with the 50-kHz passband estimation made in Section II of this paper.

The dependence of G_{eq} upon frequency is partially attributable to the increased ac conductances of G_1, C_1, and the associated leads inside the varactor head at higher frequencies. A reduction in G_{eq} would therefore result if these conductances were reduced, or if the temperature of G_1 were reduced. R_{eq} increases as expected at high frequency, due to the bandwidth limitation of the 30-MHz tuned circuit. The behavior of R_{eq}

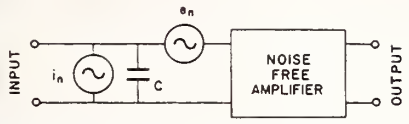

Fig. 9. Equivalent circuit of amplifier as deduced from measurements made at 1592 Hz. $C=305$ pF, $i_n^2=4kTG_{eq}\Delta f$, and $e_n^2=4kTR_{eq}\Delta f$, with G_{eq} and R_{eq} given in Table I.

at low frequencies seems to have the character of flicker noise ($R_{eq} \propto 1/f$), but power line interference may have given abnormally high noise readings.

When this amplifier was initially operated at room temperature, a minimum noise figure of 0.01 dB was measured at 1592 Hz. Unfortunately, after operation at 77K, the varactor leakage currents at room temperature were very much larger than before, resulting in an unacceptable level of shot noise at room temperature.

Appendix

A noisy amplifier may be represented by a number of equivalent circuits, including those shown in Fig. 10, where the e's and i's represent current and voltage noise generators.

An arbitrary amplifier may be represented by Fig. 10(a) only if a correlation between the current and voltage noise generators is postulated [4]. The noise current i_a may then be separated into an uncorrelated part i_a' and a correlated part $i_a-i_a'=Y_a'e_a$, where Y_a' is the (complex)correlation coefficient. Fig. 10(b) shows a circuit by means of which an arbitrary noisy amplifier may be represented in terms of uncorrelated current and voltage noise generators. An inspection shows the correspondence between Figs. 10(a) and 10(b) to be given by:

$$\begin{aligned} i_b &= i_a' \\ e_b &= e_a \\ Y_b &= Y_a' \qquad \text{(correlation admittance)} \\ Y_b + Y_b' &= Y_a. \end{aligned}$$

The significance of this breakdown is that the correlation coefficient needed with Fig. 10(a) appears in Fig. 10(b) as a real admittance, and its effect may be readily analyzed. In particular, it is clear from Fig. 10(b) that shunt capacitance in the input cable of the amplifier adds directly to Y_b, and hence that the input terminals to which the circuit parameters are referred must be carefully specified, even for audio frequency amplifiers. This physical interpretation of the correlation admittance Y_b makes Fig. 10(b) especially useful for representing high-impedance amplifiers.

Fig. 10(c) is the dual of Fig. 10(b). It too uses uncorrelated current and voltage noise generators, yet can represent an arbitrary amplifier. Its use would be indicated for describing low-impedance amplifiers.

Fig. 11 shows the circuit of Fig. 10(b) connected to a source consisting of an admittance $Y_s=G_s+jB_s$ shunted

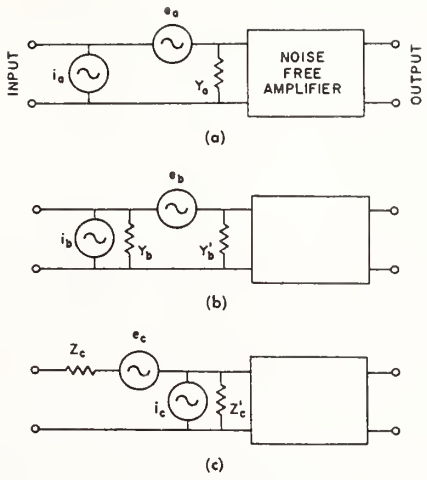

Fig. 10. Three possible representations for a noisy amplifier.

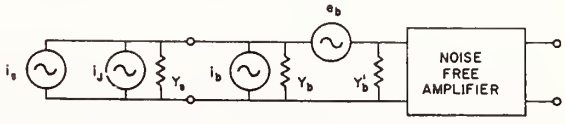

Fig. 11. A noisy amplifier connected to a source, with source noise $i_J^2=4kTG_s\Delta f$.

with a signal current generator i_s. Thermal agitation noise in the source is given by $i_J^2=4kT_sG_s\Delta f$, where T_s will be assumed to be standard temperature, 290K.

Since all of the generators are uncorrelated, we have

$$e_{out}^2 = \frac{A^2}{|Y_s+Y_b+Y_b'|^2} \cdot [e_b^2|Y_b+Y_s|^2+i_s^2+i_J^2+i_b^2], \tag{3}$$

where A is the voltage amplification factor of the system. Representing the voltage noise by an equivalent noise resistance R_{eq} given by $e_b^2=4kTR_{eq}\Delta f$ and the current noise by an equivalent noise conductance G_{eq} given by $i_b^2=4kTG_{eq}\Delta f$, we have

$$e_{out}^2 = \frac{A^2}{|Y_s+Y_b+Y_b'|^2} \cdot \{i_s^2+4kT\Delta f[R_{eq}|Y_b+Y_s|^2+G_s+G_{eq}]\}. \tag{4}$$

The noise figure of the system is given by

$$F = \frac{G_s+R_{eq}|Y_b+Y_s|^2+G_{eq}}{G_s}.$$

Letting $Y_s=G_s+jB_s$ and $Y_b=G_b+jB_b$ and differentiating with respect to G_s and B_s, we find F is minimum when $B_s=-B_b\equiv B_s^{opt}$, and

$$G_s = \sqrt{\frac{G_{eq}}{R_{eq}}+G_b^2} \equiv G_s^{opt}.$$

Under the special condition that $G_b = 0$, we have the interesting results:

$$G_s^{\text{opt}} = \sqrt{\frac{G_{eq}}{R_{eq}}}$$

and

$$F_{min} = 1 + 2\sqrt{G_{eq}R_{eq}}.$$

If the term on the right is much smaller than 1, F_{min}', the minimum noise figure in decibels is obtained from a first-order expansion of the logarithm of F_{min}:

$$F_{min}' \approx 8.68\sqrt{G_{eq}R_{eq}} \text{ (dB)}.$$

When Y_s is greatly different from Y_s^{opt}, and in particular when $B_s + B_b \gg G_s + G_b$, the description of the circuit in terms of noise figure is very awkward, and a direct reference to (3) or (4) leads to much simpler results. In the latter case, (4) reduces to

$$e_{out}^2 \propto i_s^2 + 4kT\Delta f[R_{eq}(B_s + B_b)^2 + G_s + G_{eq}] \quad (5)$$

where $4kT = 1.6 \times 10^{-20}$ W/Hz, and the smallest signal i_s detectable with a bandwidth Δf may be directly inferred from measurements of R_{eq}, G_{eq}, B_b, B_s, and G_s.

The following method for measuring the noise parameters of an amplifier is specifically directed toward use with the exceptionally low-noise amplifier described in the body of this paper, for which the approximations made introduce no appreciable errors. The method is not likely to be useful at high frequencies, or with very noisy amplifiers. Since the input admittance of the amplifier $Y_{in} = Y_b + Y_b'$ was found to be almost purely capacitive throughout the useful frequency range, the analysis will be restricted to the case in which $Y_b + Y_b' = jB_{in}$. An instrument is assumed available for measuring relative values of e_{out}^2 over a selected constant frequency band.

Let $e_{out}^2|_{sc}$ be the value of e_{out}^2 with $Y_s = \infty$ (short circuit). Then from (4), $e_{out}^2|_{sc} = A^2 \cdot 4kT\Delta f\ R_{eq}$. If a source resistance $R_s \equiv 1/G_s$ is inserted such that $e_{out}^2 = 2e_{out}^2|_{sc}$ and if $Y_b \ll G_s$, $Y_{in} \ll G_s$, and $G_{eq} \ll G_s$,

$$e_{out}^2 = A^2 \cdot 4kT\Delta f(R_{eq} + R_s)$$
$$= 2A^2 \cdot 4kT\Delta f R_{eq}, \quad \text{or} \quad R_{eq} = R_s.$$

The equivalent noise resistance is then simply the value of that source resistance which makes e_{out}^2 double its short circuit value.

Let $e_{out}^2|_{oc}$ be the value of e_{out}^2 with $Y_s = 0$ (open circuit). Then

$$e_{out}^2|_{oc} = A^2 \cdot 4kT\Delta f\left[R_{eq}\frac{G_b^2 + B_b^2}{B_{in}^2} + \frac{G_{eq}}{B_{in}^2}\right],$$

so that

$$\frac{e_{out}^2|_{oc}}{e_{out}^2|_{sc}} = \frac{G_b^2 + B_b^2 + \dfrac{G_{eq}}{R_{eq}}}{B_{in}^2} \equiv N_1. \quad (6)$$

Let $e_{out}^2|_B$ be the value of e_{out}^2 with a selected, measured source admittance $Y_s' = G_s' + jB_s'$, with $|B_s'| \gg G_s'$. Then

$$e_{out}^2|_B = A^2 \cdot 4kT\Delta f\left[R_{eq}\frac{G_b^2 + (B_b + B_s')^2}{(B_{in} + B_s')^2} + \frac{G_s' + G_{eq}}{(B_{in} + B_s')^2}\right]$$

and

$$\frac{e_{out}^2|_B}{e_{out}^2|_{sc}} = \frac{G_b^2 + (B_b + B_s')^2 + \dfrac{G_s' + G_{eq}}{R_{eq}}}{(B_{in} + B_s')^2} \equiv N_2. \quad (7)$$

Combining (6) and (7), we have

$$B_b = \frac{(B_{in} + B_s')^2 N_2 - B_{in}^2 N_1 - (B_s')^2 - \dfrac{G_s'}{R_{eq}}}{2B_s'}. \quad (8)$$

In principle, (8) allows the determination of B_b from readily measurable parameters. In practice, the admittance Y_s' must be carefully chosen to minimize the measurement uncertainties.

A technique for measuring G_b can be similarly developed with the use of a source admittance $Y_s'' = G_s'' + jB_s''$, with $|B_s''| \ll G_s''$. Unfortunately, the source temperature would have to be very low indeed to prevent its thermal agitation noise from completely masking the amplifier noise.

After measuring G_b and B_b as outlined above, G_{eq} may be obtained from (6).

References

[1] J. R. Biard, "Low-frequency reactance amplifier," *Proc. IEEE*, vol. 5, pp. 298–303, February 1963.

[2] H. E. Rowe, "Some general properties of nonlinear elements. II. Small signal theory," *Proc. IRE*, vol. 46, pp. 850–860, May 1958.

[3] P. Penfield and R. P. Rafuse, *Varactor Applications*. Cambridge, Mass.: M.I.T. Press, 1962.

[4] IRE Subcommittee 7.9 on Noise, H. A. Haus, Chairman, "Representation of noise in linear twoports," *Proc. IRE*, vol. 48, pp. 69–74, January 1960.

ISA TRANSACTIONS: 3 (238-242) 1964

Comparison Calibration of Inductive Voltage Dividers*

RAYMOND V. LISLE†
RCA Service Company
Missile Test Project
Patrick Air Force Base, Florida
and
THOMAS L. ZAPF‡
Radio Standards Laboratory
National Bureau of Standards
Boulder, Colorado

▶ Calibrated inductive voltage dividers serve as excellent standards of voltage ratio for use in the comparison calibration of other AC voltage dividers. Differences in phase angles in the dividers can be accommodated by the production of a voltage in the detector circuit in quadrature with the reference voltage. This paper discusses the comparison circuit, the handling of stray impedances, guarding, measurement procedures, quadrature voltage production, and errors. The comparison method described can be used in standardizing laboratories for the calibration of inductive voltage dividers and other voltage ratio equipment.

INTRODUCTION

Inductive voltage dividers may be described as tapped inductors wound on high-permeability cores. The relatively recent metallurgical development of ferromagnetic core material having extremely high magnetic permeability has made possible the construction of inductive voltage dividers having excellent stability and loading characteristics. The effects of internal loading are inherently small in such inductive voltage dividers, and errors in voltage ratios are frequently less than 1×10^{-6} in the low audio-frequency range. The absolute measurement of voltage ratios with uncertainties less than this is difficult. However, known voltage ratios embodied in an inductive voltage divider may be preserved as a standard and re-established again and again. The accurate initial establishment of voltage ratio for the calibration of inductive voltage dividers[1-4] is not discussed here, but a method of calibrating an inductive voltage divider by comparing it with a standard is presented. The comparison method, essentially as described herein, has been used at the National Bureau of Standards for several years and appears worthy of general use in standardizing laboratories. This method provides efficient, accurate calibration of inductive voltage dividers using common laboratory equipment with a standard inductive voltage divider. Comparison circuits have been mentioned in several publications[4-7] without detailed elaboration. This paper discusses in considerable detail a particularly successful type of comparison circuit.

*Presented at the 18th Annual ISA Conference and Exhibit, September 9-12, 1963, Chicago, Illinois.
†Standards Engineer.
‡Physicist, Radio Standards Engineering Division; Member—ISA Denver Section.

THE COMPARISON CIRCUIT

A simple bridge circuit for comparing inductive voltage dividers is shown in Figure 1. The standard inductive voltage divider is the divider for which the corrections are known. The unknown inductive voltage divider is the divider for which the corrections are to be obtained.

Other elements of the circuit are the guard divider and shielding circuit, flexible coaxial cables to the detector transformer, the detector, a resistor and capacitor for the introduction of a quadrature voltage in the detector circuit, and several fuses. The dashed lines indicate the connections of a capacitor that may be used to reduce loading.

The input terminals of the unknown and standard dividers are joined together by short, heavy leads having low impedance to reduce voltage drops between the

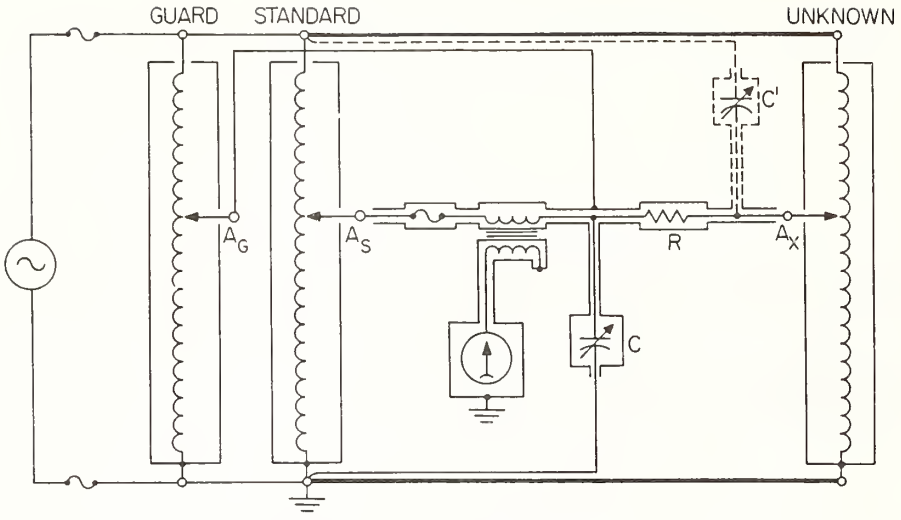

Figure 1. Bridge circuit for the calibration of an inductive voltage divider by comparison with a standard.

dividers. The electrical connection to the case of the standard divider should duplicate the connection used when the standard divider was calibrated. Similarly, the electrical connection to the case of the unknown divider should duplicate the connection to be used in subsequent work. In Figure 1 the cases are shown connected to the common terminals. These connections fix, in a reproducible manner, the stray capacitances from the windings to the case of each divider. Connecting the case to the output terminal is not recommended, as this would not fix the stray impedances from the case (and output terminal) to the surroundings, which are often quite uncertain and variable. The output of the guard divider is connected to the shield around the detector circuit. When comparing an unknown inductive divider with the standard, the guard divider is set at the same setting as the other dividers and drives the shield at nearly the same instantaneous potential as that of the conductors within. The guard divider may be either inductive or resistive because its only function is to maintain the proper potential on the shield. The guard circuit minimizes current leakage through the stray impedances of the detector circuit.

Usually there is a relatively large stray capacitance to ground from the detector transformer shield and the capacitor case. The current in this stray capacitance to ground must not be allowed in the shield of the flexible coaxial cables going to the output terminals of the dividers because a current in the shield can induce a voltage in the inner conductor. To minimize this error, the connection between the detector transformer shield and the capacitor case should be made as short as possible, and the output of the guard divider should be connected to the shield at some point in this vicinity. The major components of stray capacitive current then are conducted directly to the guard divider. The deleterious effect that is avoided by this procedure may be observed by increasing the length of the leads in the detector circuit and connecting the lead from the guard divider to a different point on the shield. If all leads are short the error may be insignificant.

It should be noted that, with the circuit shown in Figure 1, the guard circuit and the capacitor case are at a potential somewhat above ground, and care should be exercised in touching the shields to avoid hazardous shocks. Alternatively, the circuit may be grounded at the output of the guard divider, but the cases of the dividers will then be at a high potential. With this connection it may be necessary to use an isolation transformer between the power supply and the bridge circuit to avoid double grounding. Regardless of the grounding system selected, it is good practice to provide an outer covering of insulation for the shielding wherever needed to prevent accidental short circuits.

Many inductive dividers are provided with two "common" terminals connected together and to one extremity of the winding by a wire of low impedance so that one terminal may be used with the input circuit and the other may be used to make connections to the load. In the circuit shown in Figure 1 the inductive dividers are treated as three-terminal dividers, i.e., the common output terminal is ignored. A small voltage drop in the internal connection between the two common terminals would make the three-terminal measurements differ from four-terminal measurements in which both common terminals are used. However, the difference is usually small and often insignificant. Fuses are inserted in the circuit as shown in Figure 1 to prevent damage to components in the event of inadvertent short circuits. The fuse in the detector circuit prevents damage to the resistor, R, if a large unbalance of the bridge circuit is encountered.

VOLTAGE RATIO MEASUREMENT

Let $D + d$ represent the dial reading of an inductive voltage divider, where D is the reading of the decades to be calibrated (usually the highest three decades) and d is the reading of the lower decades. In most calibrations D will be a step setting of one of the highest three decades with the other two set to zero. The true ratio, A, can then be represented by $D + d + c$, where c is the

TABLE I

Voltage ratio						Phase angle		
D_s	d_s	c_s	d_x	c_x	Ratio$_x$	γ_s, μrad	$\Delta\gamma$, μrad	γ_x, μrad
	$\times 10^{-6}$	$\times 10^{-6}$	$\times 10^{-6}$	$\times 10^{-6}$				
0.900	0.0	+0.4	+0.1	+0.3	0.900 000 3	−2	0	−2
0.500	0.0	0.0	+0.4	−0.4	0.499 999 6	+4	+1	+5
0.100	0.0	−0.1	+0.1	−0.2	0.099 999 8	+49	+3	+52
0.090	+0.1	−0.5	0.0	−0.4	0.089 999 6	+36	+4	+40
0.050	0.0	−0.3	0.0	−0.3	0.049 999 7	+42	+4	+46
0.010	0.0	0.0	0.0	0.0	0.010 000 0	+70	+20	+90
0.009	0.0	0.0	0.0	0.0	0.009 000 0	+60	+10	+70
0.005	+0.1	−0.1	0.0	0.0	0.005 000 0	+80	+30	+110
0.001	0.0	0.0	0.0	0.0	0.001 000 0	+330	+130	+460

correction to the setting D. For all practical purposes c is independent of d. At balance

$$D_x + d_x + c_x = D_s + d_s + c_s \tag{1}$$

where the subscripts x and s denote the unknown and the standard, respectively. Solving for the correction to the unknown divider and realizing that $D_x = D_s$, one obtains

$$c_x = c_s + d_s - d_x \tag{2}$$

Ordinarily, d_x would be set to zero. Under this condition

$$c_x = c_s + d_s \tag{3}$$

However, if $c_x < c_s$ and if the standard divider cannot be set to a negative d_s, the lower decades of the unknown divider, d_x, can be used to obtain the balance. If d_s is set to zero the ratio balance equation is

$$c_x = c_s - d_x \tag{4}$$

Typical data and results for a calibration at 100 V and 1000 cps are shown in Table I.

PHASE-ANGLE MEASUREMENT

A true voltage null at the detector can be obtained if a quadrature voltage is introduced into the circuit to compensate for the phase-angle difference between the unknown and the standard inductive voltage dividers. The RC combination in Figure 1 is used to develop and introduce a voltage in quadrature with the output of one of the dividers. If the capacitive reactance of C is made considerably larger than the resistance, R, the current in R will lead the voltage across the impedance $R - jX_c$ by nearly $\pi/2$ radians and will cause the quadrature voltage to appear across R. At balance the current in the detector is zero, and the voltage at the junction, of R and C is E_s, as indicated in Figure 2a. An expression for the current in R and C can be written

$$i = E_s / X_c \tag{5}$$

The quadrature voltage, e, is the product of i times R,

$$e = iR \tag{6}$$

and

$$e = E_s R / X_c = E_s \omega RC \tag{7}$$

From Figure 2a, γ_s and γ_x are the phase angles associated with the standard and the unknown inductive voltage dividers, respectively, and $\Delta\gamma$ is the phase-angle difference between the unknown and the standard dividers. An expression for $\Delta\gamma$ can be written from inspection of Figure 2a as

$$\tan \Delta\gamma = e / E_s \tag{8}$$

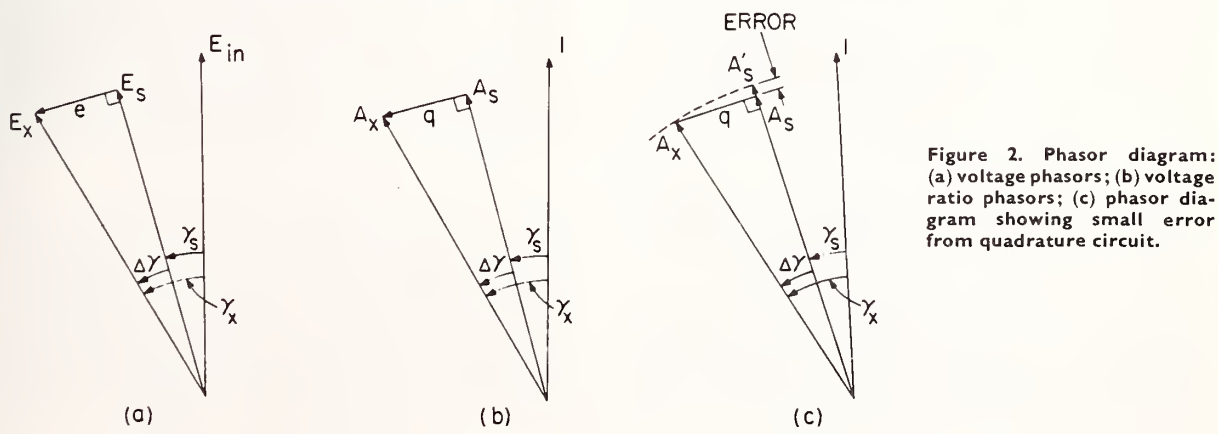

Figure 2. Phasor diagram: (a) voltage phasors; (b) voltage ratio phasors; (c) phasor diagram showing small error from quadrature circuit.

Combining the last two equations yields

$$\tan \Delta\gamma = \omega RC \tag{9}$$

For small angles $\tan \Delta\gamma \approx \Delta\gamma$, and

$$\Delta\gamma \approx \omega RC \tag{10}$$

This equation provides a design formula for the RC combination in the detector circuit. For any test frequency ω a variable capacitor can be chosen in combination with a resistor so that $\Delta\gamma$ in microradians is a multiple-of-ten times the reading of the variable capacitor in picofarads. Various multiplying factors can be obtained using resistors differing by multiples of ten. As an example, at a frequency of 1000 cps, resistors having values of 1592, 159.2, and 15.92 Ω, will produce multipliers of 10, 1, and 0.1, respectively. Thus a 0–100 pF variable air capacitor can be used to cover a wide range of phase-angle differences.

In the above discussion with reference to Figure 2a, it has been assumed that the phase angle of the unknown inductive voltage divider is larger than that of the standard inductive voltage divider. Under these conditions, $\Delta\gamma$ is positive, and the phase angle of the unknown inductive divider can be obtained from the equation

$$\gamma_x = \gamma_s + \Delta\gamma \tag{11}$$

If the difference $\gamma_x - \gamma_s$ is negative, the comparison circuit can be balanced by putting the RC combination on the other side of the detector with R connected to the standard divider. Under these conditions, the phase-angle balance equation would be

$$\gamma_x = \gamma_s - \Delta\gamma \tag{12}$$

Typical data and results from phase-angle measurements are shown in Table I.

DISCUSSION OF ERRORS

If errors from incorrect connections, incorrect frequency, or incorrect applied voltage (i.e., errors arising from conditions different from those under which the standard was measured) are precluded, the ponderable systematic errors, such as those arising from the assumptions made in the derivation of the equations, are of very small magnitude. These will now be investigated.

The error introduced by the approximation that $\tan \Delta\gamma \approx \Delta\gamma$ can be evaluated from the trigonometric expansion of the tangent, namely,

$$\tan \Delta\gamma = \Delta\gamma + \frac{\Delta\gamma^3}{3} + \frac{\Delta\gamma^5}{15} + \ldots \tag{13}$$

The second term, $\Delta\gamma^3/3$, evaluated for $\Delta\gamma = 300\ \mu$rad would be of the order of 1×10^{-11} rad, which is negligible, and higher order terms are smaller yet.

It is convenient to consider a phasor diagram of voltage-ratio phasors, as shown in Figure 2b, rather than one formed of voltage phasors, as in Figure 2a. The diagram in Figure 2b is formed by normalizing the voltage phasors by dividing the circuit voltages by the input voltage magnitude. The voltage ratio A of an inductive voltage divider is then $E_0/|E_{in}|$, and the quadrature component, $q = e/|E_{in}|$.

A small error in ratio from the voltage drop across R is illustrated in Figure 2c in which the angles have been grossly exaggerated to illustrate the error. In this diagram A_s is the apparent ratio at balance, smaller than the true ratio A'_s because the phasor q is added at right angles to the phasor A_s by means of the RC circuit. The error, $A'_s - A_s$, can be evaluated from the trigonometric series expansion for $\cos \Delta\gamma$, namely,

$$\cos \Delta\gamma = 1 - \frac{\Delta\gamma^2}{2!} + \frac{\Delta\gamma^4}{4!} - \ldots \tag{14}$$

From Figure 2c,

$$A_s = A_x \cos \Delta\gamma \approx A_x\left(1 - \frac{\Delta\gamma^2}{2!}\right) \tag{15}$$

The error in ratio is represented by the term $A_x(\Delta\gamma^2/2!)$. In comparing two good-quality inductive voltage dividers at a frequency of 1000 cps a $\Delta\gamma$ of 100 μrad would be experienced only at the lower values of ratio below about $A = 0.01$. The error in ratio would be approximately 5×10^{-11}. An error of this magnitude would be negligible in most cases.

Another source of error in both magnitude of voltage ratio and phase angle is the loading on the unknown divider by the capacitor C. To determine the magnitude of these errors in practical work, the difference in voltage ratio and phase angle can be observed when another capacitor having the same value as C is connected from the output terminal of the unknown divider to ground in the circuit in Figure 1 (i.e., across R and C). The observed differences may be subtracted from the original readings to yield the values of ratio and phase angle with no load. Alternatively, the loading may be eliminated by adding a capacitor as shown by the dashed lines in Figure 1: C' and C form a capacitive divider to reduce the loading of C on the output circuit of the inductive divider. The magnitude of C' must be adjusted depending on the ratio being measured and, in particular, must have a value equal to $CA_s/(1 - A_s)$.

The power source should have a reasonably low harmonic content, and the null detector should be tunable to suppress harmonics in the quadrature voltage, which would otherwise prevent the attainment of a precise null. To understand the need for a tunable null detector, consider that harmonic components exist in both E_s and E_x having a frequency $n\omega$, equal amplitude hE_s, and the same phase. The total voltage across R is

$$e = e_\omega + e_{n\omega}\ (\text{phasor sum}) \tag{16}$$

where e_ω is the fundamental component and $e_{n\omega}$ is the harmonic component as shown in Figure 3. The phasor $e_{n\omega}$ rotates n times faster than e_ω, and its magnitude can be expressed in terms of the phase-angle difference of the fundamental output voltages, $\Delta\gamma$. The expression is similar to that for equation (7), except the harmonic current is hE_s/X_c and the angular frequency is $n\omega$; thus

$$e_{n\omega} = hE_s n\omega RC = nhE_s\Delta\gamma \tag{17}$$

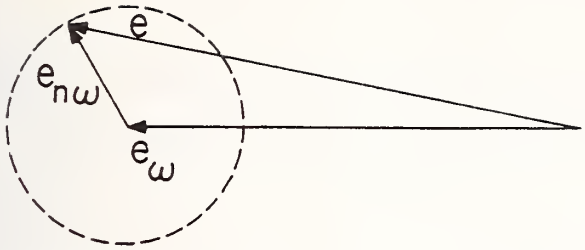

Figure 3. Phasor diagram showing effect of a harmonic in the quadrature voltage.

If this component is not suppressed by the detector, it would not by itself create a systematic error, but it would result in a limitation on the attainment of a null equivalent to a voltage-ratio uncertainty

$$u_A = \frac{e_{n\omega}}{|E_{\text{in}}|} = \frac{e_{n\omega}}{E_s/A} = A\frac{e_{n\omega}}{E_s} = Anh\Delta\gamma \qquad (18)$$

and a phase-angle uncertainty

$$u_\gamma = \frac{e_{n\omega}}{E_s} = nh\Delta\gamma \text{ [radians]} \qquad (19)$$

In a typical measurement at 1000 cps, where $A = 0.1$, $n = 3$, $h = 0.01$, and $\Delta\gamma = 20$ μrad, it is found that $u_A = 0.06 \times 10^{-6}$ and $u_\gamma = 0.6$ μrad. It is evident that a tuned indicating amplifier that suppresses the third harmonic by a factor of 10 would be sufficient to permit the discrimination of ratio to within $\pm$ 0.01 $\times$ 10^{-6} in this case.

It should be noted that if a detector is used that has a linear response to small signals, it is possible to use it to interpolate between steps on the lowest decade of the divider.

MEASUREMENT VERIFICATION

A simple partial check on the bridge circuit and the calibration results can be performed by reversing the leads to the unknown divider and measuring the complement of the ratio.[4] Caution should be exercised because the case of the unknown divider will now be at a high potential if it has been connected to the common terminal. It can be seen that $1 - A_x$ is now to be compared with A_s. With this connection $c_x = -(c_s + d_s + d_x)$. The correction, c_x, obtained in this way may be compared with that obtained in the normal way.

The corrections to both inductive voltage dividers for the setting of $A = 0.5$ can be obtained from the complementary ratio measurements without prior knowledge of either of these corrections. If d_s is the reading of the standard for the normal circuit as shown in Figure 1, and d'_s is the reading of the standard with the unknown divider connections reversed, then

$$c_s = -(d_s + d'_s)/2 \quad \text{and} \quad c_x = (d_s - d'_s)/2 \qquad (20)$$

By a somewhat analogous method a check on the phase-angle measurements can be made. The formula for phase angle can be derived simply from the phasor diagrams of voltage ratio for the reversed connection. The phase angles of both inductive voltage dividers set at $A = 0.5$ can be obtained by the method of complementary measurements without prior knowledge of either of these phase angles.

CONCLUSION

If care is exercised in setting up the circuit, using good shielding practices, and a detector having adequate amplification and harmonic suppression is employed, the voltage ratios and phase angles of two good-quality inductive voltage dividers may be compared with negligible loss in accuracy. Several systematic errors in the circuit, for which corrections could be made, have been discussed and found to be negligible under the typical conditions described. The precision of the comparison is limited primarily by the resolution and stability of the standard and unknown dividers. The existence of a method for accurate comparison makes possible the use of calibrated inductive voltage dividers as standards for the calibration of other dividers and these, ultimately, for the very accurate measurement of voltage ratio and impedance ratio.

REFERENCES

1. Sze, W. C., *Trans. A.I.E.E., Part* I 76, 444, 1957.
2. Harris, F. K., and W. C. Sze (NBS Washington), unpublished communications to the authors.
3. Zapf, T. L., *J. Res. NBS* 66C, 25, 1962.
4. Engineering Bulletin No. 1 (Ratio Tran), Gertsch Products Inc., Los Angeles, California.
5. Engineering Bulletin No. 4 (Ratio Tran), Gertsch Products Inc., Los Angeles, California.
6. Morrison, N. E., Engineering Bulletin No. 20, Electro Scientific Industries, Portland, Oregon.
7. Morgan, M. L., Engineering Bulletin No. 29, Electro Scientific Industries, Portland, Oregon.

JOURNAL OF RESEARCH of the National Bureau of Standards—C. Engineering and Instrumentation
Vol. 68C, No. 4, October–December 1964

Designs for Temperature and Temperature Gradient Compensated Capacitors Smaller Than Ten Picofarads

Robert D. Cutkosky

(July 22, 1964)

A theoretical study is made of the dependence of capacitance upon electrode temperature in an air dielectric capacitor. The possibility of constructing a three-terminal standard whose capacitance depends only upon the temperature of one electrode is pointed out, and some practical capacitors utilizing the principle are described. The temperature sensitive electrodes of these capacitors are constructed of fused silica, which results in temperature coefficients of capacitance near 0.5 ppm/°C. The temperature independent electrodes of these capacitors may be constructed of any stable metal, facilitating adjustment to nominal value.

1. Introduction

One of the problems encountered in the construction of standard air dielectric capacitors is that of reducing the dependence of capacitance upon temperature. The best technique seems to be to construct the capacitor entirely of materials which have very small mechanical temperature coefficients. Then provided that the electrode distortions and displacements caused by temperature dependences of the elastic coefficients of the electrodes and electrode supports are not significant, the capacitance temperature coefficient will also be small. Materials of small mechanical temperature coefficient which have been used for the construction of capacitors are fused silica and Invar. Fused silica is difficult to form and mount, and must be metalized to provide electrodes. Its exclusive use in a capacitor with air dielectric results in temperature coefficients of capacitance around 0.5 ppm/°C. Invar is somewhat unstable and must be carefully heat treated. When treated for optimum stability, temperature coefficients around +2 ppm/°C are typical.

The disadvantages of fused silica and Invar are often avoided by the use of two or more materials of different but relatively high temperature coefficients in an arrangement that provides temperature compensation. Temperature compensated capacitors using two metals have been built in many ways and with varying degrees of success. One simple but somewhat unsatisfactory design makes use of coaxial cylinders in which the outer cylinder has a higher temperature coefficient than the inner. The dimensions of the capacitor are chosen so that the capacitance between the cylinders is independent of temperature, provided that no temperature differential exists between the two cylinders.

Since the temperatures of the various elements in a capacitor are not generally equal but vary with the room or bath temperature with possibly different time lags, quite large temperature differentials and capacitance changes can result. The cylindrical design is particularly objectionable from this standpoint, since the outer cylinder is often in more intimate contact with the surroundings than the inner cylinder, and hence responds to temperature changes more rapidly.

A temperature compensation technique often used for capacitors larger than 100 pF involves stacking plates between spacers having a higher temperature coefficient than the plates. A second similar stack of plates is interleaved with, but insulated from, the first set of plates. Since the dissimilar metals are in intimate thermal contact, temperature differentials between plates and spacers remain relatively small, and the capacitance between the two stacks is not strongly affected by temperature fluctuations.

A more elaborate system of temperature compensation may be developed by considering the effect on the direct capacitance caused by independent variations in the temperatures of the separate electrodes. This procedure is found to be most useful for capacitors smaller than a few picofarads in which the temperature of the ground electrode may also be important.

2. Partial Capacitance-Temperature Coefficients

Consider a three terminal capacitor whose direct capacitance is given by $C=C(t_1, t_2, t_3)$ where the t's are the temperatures of the three electrodes. Then for small departures from the reference temperature,

$$C=C_0+\frac{\partial C}{\partial t_1}\Delta t_1+\frac{\partial C}{\partial t_2}\Delta t_2+\frac{\partial C}{\partial t_3}\Delta t_3,$$

or

$$C=C_0\left(1+\frac{1}{C_0}\frac{\partial C}{\partial t_1}\Delta t_1+\frac{1}{C_0}\frac{\partial C}{\partial t_2}\Delta t_2+\frac{1}{C_0}\frac{\partial C}{\partial t_3}\Delta t_3\right)$$

$$=C_0(1+\alpha_1\Delta t_1+\alpha_2\Delta t_2+\alpha_3\Delta t_3). \quad (1)$$

The terms $\frac{1}{C_0}\frac{\partial C}{\partial t_1}=\alpha_1$ etc., are the partial capacitance-temperature coefficients of the three electrodes.

If we let l_1 be a characteristic length of electrode 1, we may write

$\alpha_1=\frac{l_1}{C_0}\left(\frac{\partial C}{\partial l_1}\right)\cdot\frac{1}{l_1}\left(\frac{\partial l_1}{\partial t_1}\right)$. We recognize $\frac{1}{l_1}\left(\frac{\partial l_1}{\partial t_1}\right)=\beta$ as the thermal expansion coefficient of electrode 1, and write

$$\alpha_1=P_1\beta_1 \text{ where } P_1=\frac{l_1}{C_0}\frac{\partial C}{\partial l_1}, \text{ etc., and obtain}$$

$$\frac{C}{C_0}=1+P_1\beta_1\Delta t_1+P_2\beta_2\Delta t_2+P_3\beta_3\Delta t_3. \tag{2}$$

If $\beta_1=\beta_2=\beta_3$ and $\Delta t_1=\Delta t_2=\Delta t_3$, we know from geometrical considerations that $\frac{C}{C_0}=1+\beta\Delta t$, and hence $P_1+P_2+P_3=1$, but no other restrictions on the P's exist.

Equation (2) suggests the possibility of designing capacitors with $P_2=P_3=0$ so that $P_1=1$. Then if β_1 is small, C will be relatively independent of Δt_1, Δt_2, and Δt_3. This can be done by constructing electrode 1 of fused silica and choosing a suitable geometry. Such a capacitor may be adjusted by machining operations on electrodes 2 and 3, which may be of any stable metal, and the principle objection to the use of fused silica is eliminated.

The above analysis is correct if no temperature gradients exist in any electrode, and if the capacitance changes caused by motions of the electrodes with respect to each other are not appreciable. The first criterion can be partially satisfied by avoiding the use of long, thin electrodes. The second criterion can be satisfied by locating the electrodes at saddle points in the capacitance-displacement function.

Experimentally it is often convenient to set one of the P's, say $P_2=0$, by a geometrical consideration, and then either to adjust $P_3=0$ or $P_1=1$ by observing the capacitance changes brought about by changing the dimensions of electrode 1 or electrode 3. The easiest approach will be determined by the capacitor configuration.

3. Guard-Cylinder Capacitor

Consider a guarded cylindrical capacitor whose inner electrode has a radius a_1 and whose outer electrode and guards have a radius a_2. If the length of the outer electrode is l and if ϵ is the permittivity of the dielectric, the direct capacitance of this system is given by

$$C=\frac{2\pi\epsilon l}{\ln\left(\frac{a_2}{a_1}\right)}. \tag{3}$$

Differentiation yields

$$\frac{C}{C_0}=1+\frac{1}{\ln\left(\frac{a_2}{a_1}\right)}\frac{\Delta a_1}{a_1}-\frac{1}{\ln\left(\frac{a_2}{a_1}\right)}\frac{\Delta a_2}{a_2}+\frac{\Delta l}{l}. \tag{4}$$

For a uniform expansion of the outer cylinder, $\frac{\Delta a_2}{a_2}=\frac{\Delta l}{l}$, and C is independent of the temperature of the outer cylinder if $\ln\frac{a_2}{a_1}=1$, or $\frac{a_2}{a_1}=e$. This relationship results in temperature compensation for the outer cylinder, but only if the guard expands at the same rate as the guarded electrode; and results in a capacitor whose temperature coefficient of capacitance is equal to the thermal expansion coefficient of the inner cylinder.

Although independent compensation for guard and guarded electrode temperature changes cannot be achieved with the simple guard cylinder capacitor, some insight into the behavior of more complicated cylindrical systems is derived from the results obtained. The critical ratio of radii, which is e for the simple guard cylinder capacitor, is found to be quite close to this value for a large variety of completely compensated cylindrical designs.

4. Practical Compensated Capacitors

After some model studies, an experimental 5 pF capacitor was constructed as shown in figure 1. The inner electrode was a metallized fused silica cylinder. The guard electrodes were set back as illustrated to reduce the influence of their temperatures upon the direct capacitance of interest. It was found experimentally that small changes in the length of electrode 2 did not appreciably affect the compensation, so that adjustment to nominal value is simple.

Tests of the completed capacitor showed an overall temperature coefficient less than 1 ppm/°C and no appreciable overshoot when subjected to a rapid temperature change.

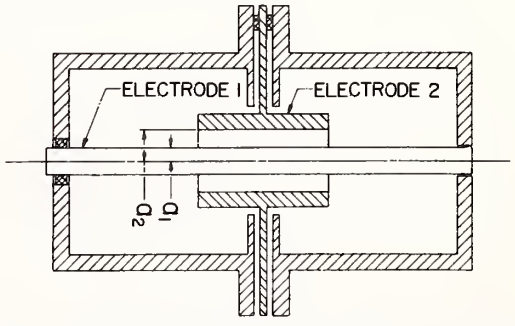

FIGURE 1. *An experimental 5 pF completely temperature compensated capacitor drawn roughly to scale for correct compensation, $a_2/a_1\approx 2.5$.*

It is found that the design of figure 1 is not easily modified to yield either much larger or much smaller capacitance. Other designs have been investigated, however, which may be useful for the construction of arbitrarily small completely compensated capacitors. One such design is sketched in figure 2. It makes use of a cylindrical shield between the two capacitor electrodes. The inner electrode is once again constructed of metalized fused silica. Holes in the cylindrical shield may be varied in sizes to provide a range of capacitances between the inner and outer electrodes. The outer electrode is automatically temperature compensated by virtue of its shape. Any increase in its temperature will increase the spacing between it and the cylindrical shield, but will not change the position of the critical conical surfaces. The outer ends of the cones must of course be truncated, but it is found that this can be done without greatly upsetting the compensation. Experimentally it is found that the critical ratio of cylindrical shield radius to inner electrode radius is somewhat dependent upon the size and shape of the holes in the shield, but remains remarkably close to e.

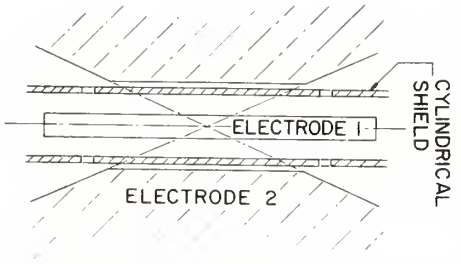

FIGURE 2. *A completely temperature compensated capacitor for values smaller than 0.1 pF.*

5. Conclusions

Most practical capacitors are found to be not greatly dependent upon temperature differentials. However, complete disregard for the principles of partial temperature compensation can result in capacitors which are unduly sensitive to rapid temperature changes. It is possible at least in principle to design capacitors which depend only upon the temperature of one element; and if this element has a small thermal expansion coefficient, very close temperature control is not necessary. The technique seems most practical for capacitors smaller than 10 pF.

(Paper 68D4–177)

NATIONAL BUREAU OF STANDARDS

Technical Note 201

Issued November 5, 1963

A TECHNIQUE FOR EXTRAPOLATING THE 1 KC VALUES OF SECONDARY CAPACITANCE STANDARDS TO HIGHER FREQUENCIES

R. N. Jones
Radio Standards Laboratory
National Bureau of Standards
Boulder, Colorado

For sale by the Superintendent of Documents, U. S. Government Printing Office
Washington, D.C. 20402

Contents

A TECHNIQUE FOR EXTRAPOLATING THE 1 KC VALUES OF SECONDARY CAPACITANCE STANDARDS TO HIGHER FREQUENCIES

A simple technique is described for extrapolating the 1 kc values of certain two-terminal capacitors to higher frequencies without incurring serious losses in accuracy. The method is intended for use with air capacitors having binding post or banana plug type connectors. Because of inherent errors, such connectors are not appropriate for measurement where the highest accuracy is required. For this reason, it is recommended that calibration of this type be performed by secondary laboratories and not be submitted to the National Bureau of Standards.

1. INTRODUCTION

With the establishment of requirements that military contractors show traceability to the National Bureau of Standards in all areas of measurement, increasing demands for new and improved types of calibration services have appeared. Included in these demands is the entire area of high frequency impedance measurements. Prior to the increased demand for traceability there was little requirement for impedance standards and calibration services at frequencies much above 1 kc, and as a result there existed almost no commercially available standards which were designed for high frequency applications. Consequently, NBS has been requested to perform high frequency calibrations of standards which were primarily intended for use at dc and low frequencies. Such requests have presented difficulties because NBS does not possess appropriate standards to use for comparison, nor is it practical to attempt to develop them.

A limiting factor in the accuracy of impedance measurements is associated with the connector systems which are employed as a part

of the instrumentation set-up. This is true to a varying degree at all frequencies, but in general, as the frequency of measurement is increased, the importance of connectors must be given added consideration. There are certain minimum requirements which should be satisfied by any connector system in order to assure accurate results in impedance measurements. First, the connector should be coaxial for purposes of self-shielding so as to avoid any influence of surrounding objects upon the measurement result. This requirement is an important one even at the very low frequencies, especially when small values of capacitance are to be determined. Two other requirements are a well defined plane of electrical reference and a voltage standing wave ratio (VSWR) as nearly 1.0 as possible. These are most important at the higher frequencies where short wavelengths are encountered and measurement accuracy depends upon the degree of impedance matching within the connector.

Many of the impedance standards submitted to NBS for calibration at frequencies above 30 kc employ banana plug connectors and are, therefore, subject to connection errors which render them inappropriate for use where highest accuracy is desired. Of particular interest here are capacitance standards which are equipped with banana plug connectors of either the plug or jack type.

Because the calibration methods employed at NBS for standards of this type do not depend upon any national reference standard, it is possible for a laboratory to perform its own high frequency calibrations of such capacitors and avoid the necessity of submitting them to NBS. By employing accepted techniques to calibrate such secondary standards, mutual benefits can accrue both to NBS and to the laboratories requiring calibration services. NBS, by limiting services to only the

highest quality standards, can devote increased effort to research and, as a result, provide better services. On the other hand, other standards laboratories can save money and time and avoid the perils of transporting standards by utilizing as many such self-calibration techniques as possible.

The measurement technique to be described is not new, nor is it complicated. It is presented as an aid to overall efficiency, and while it does contain several sources of error, they are not out of reason when compared with the general accuracy to which standards to this type may be considered reliable.

2. PROCEDURE FOR DETERMINING HIGH FREQUENCY VALUE

Let us assume that we have a two-terminal air capacitor, with binding post or banana plug connectors, whose known low frequency (1 kc) value in farads is C_o, and that we have an application requiring that we know the capacitance value, C_e, at some higher angular frequency, $\omega = 2\pi f$, where f is in cycles per second. Inherent in any capacitor is a certain amount of conductance, series resistance, and series inductance. All of these contribute to the effective value of the capacitor at any given frequency, but, in this case, it is only the series inductance which is considered significant. This is especially true for high Q capacitors. Consider the simplified equivalent circuit for the capacitor as shown on the right in figure 1.

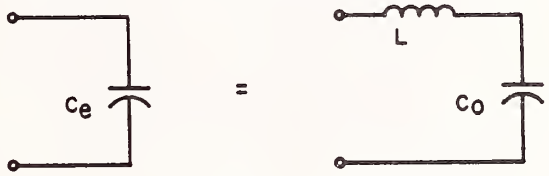

Figure 1

Simplified Equivalent Circuit

Here L is the residual series inductance of the capacitor in henries and C_o is the low frequency (1 kc) value of the capacitor in farads. At some angular frequency, we wish to find the effective value C_e. Equating the reactances of these two circuits gives:

$$\frac{1}{\omega C_e} = \frac{1}{\omega C_o} - \omega L$$

and

$$C_e = \frac{C_o}{1-\omega^2 L C_o} \qquad (1)$$

To arrive at a value for C_e, it is necessary to evaluate the residual series inductance, L. This is easily done by short circuiting the terminals of the capacitor and employing a grid-dip meter to ascertain the angular frequency, $\omega_r = 2\pi f_r$, at which the resulting circuit resonates. The residual series inductance of the capacitor is then given by the expression:

$$L = \frac{1}{\omega_r^2 C_o} - L_s \qquad (2)$$

where C_o is again the low frequency value of the capacitor and L_s is the inductance of the device used to short circuit the terminals. The effective capacitance is then obtained by substituting the value for L into (1). A typical set-up for determinations of this type is shown in figure 2.

The solid line in figure 3 indicates the percentage correction, as a function of frequency, for a 1000 picofarad capacitor having a residual series inductance of 0.050 microhenry. This is a typical value for the inductance of a good capacitance standard and may be expected to be nearly the same for all capacitors of the same general type of construction and comparable physical size. With this in mind,

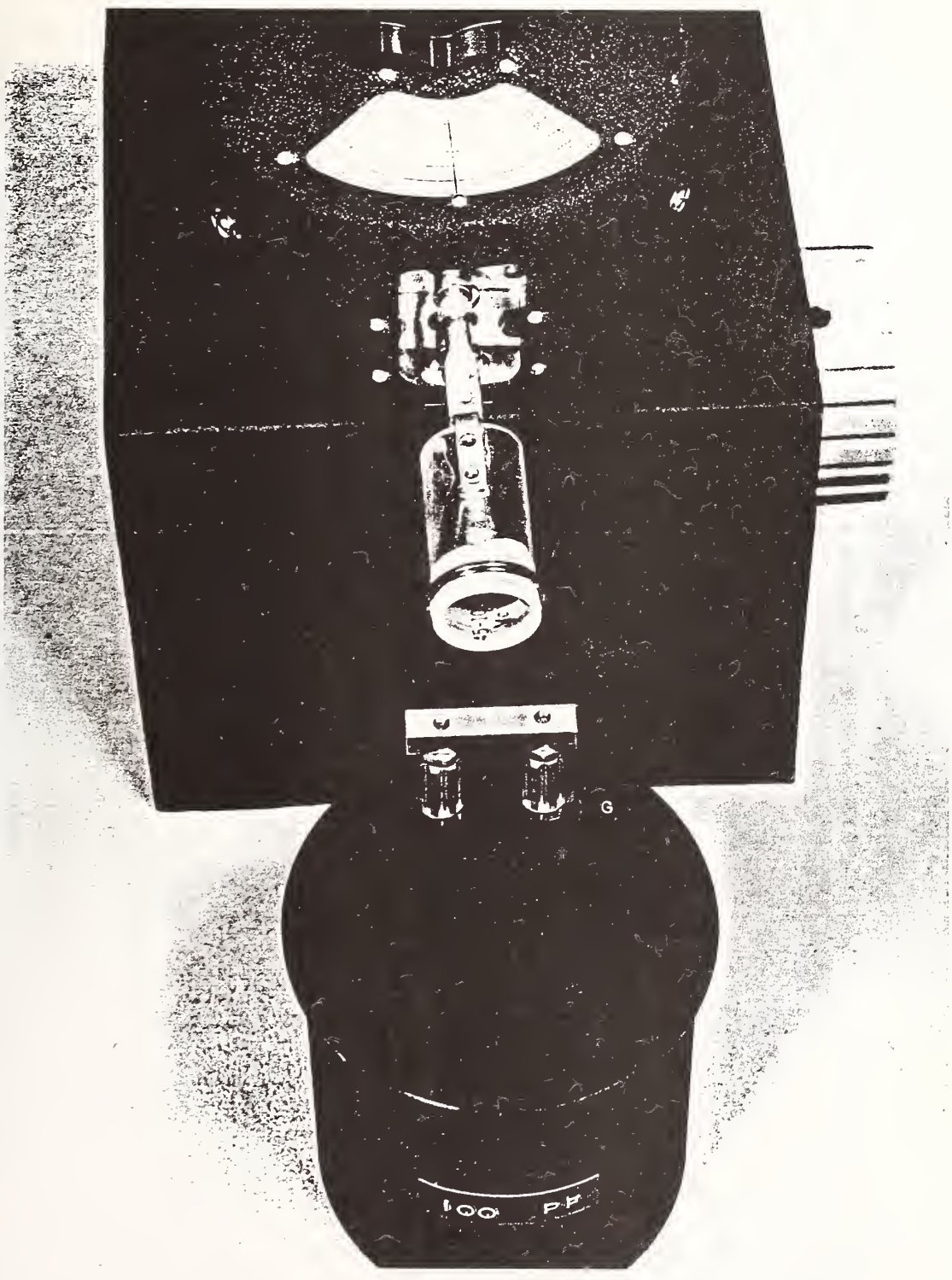

Figure 2

Grid-Dip Meter Arrangement Used to Determine the Resonant Frequency of a Short-Circuited Capacitor.

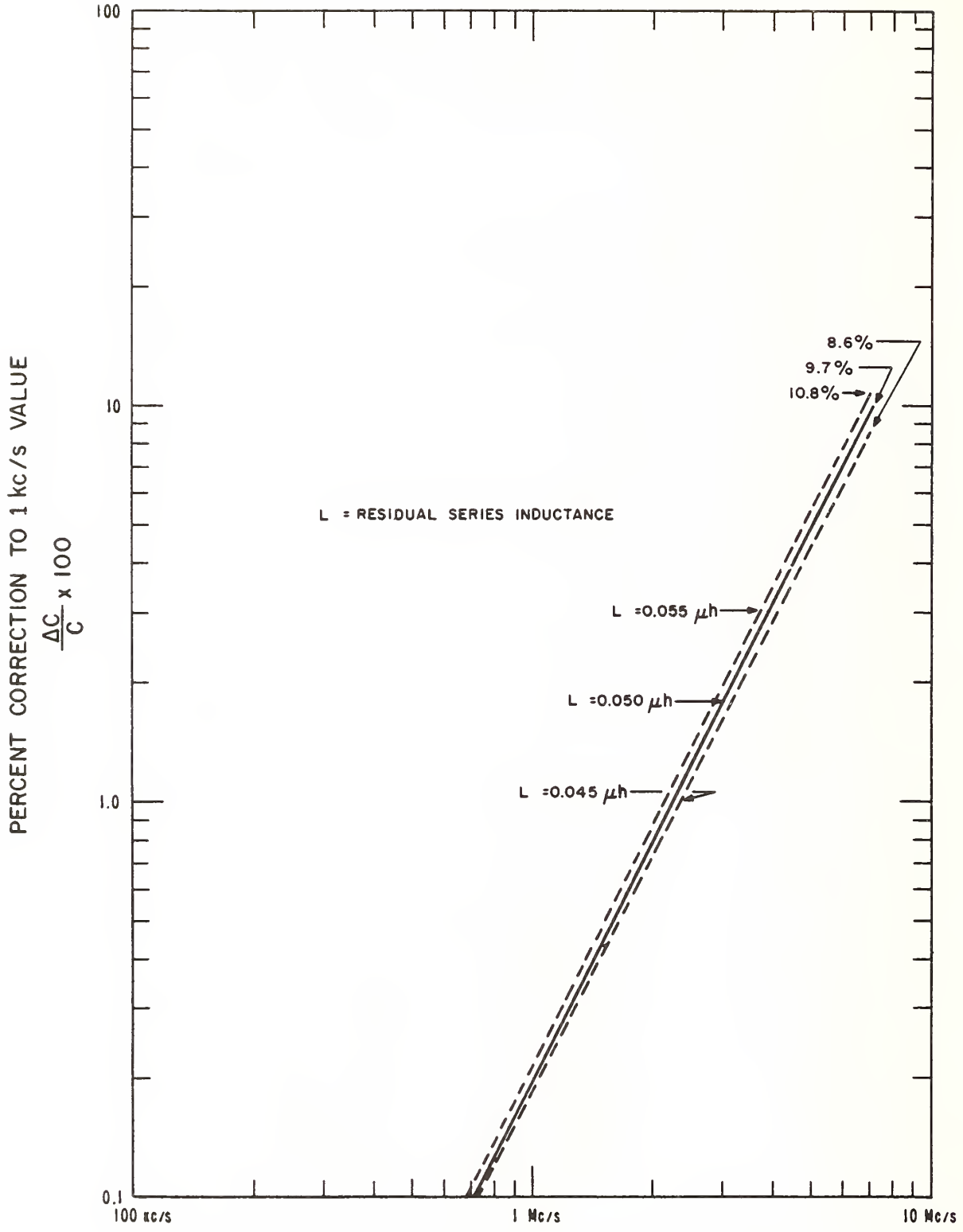

PERCENT CORRECTION VERSUS FREQUENCY FOR A 1000 pf CAPACITOR HAVING A RESIDUAL INDUCTANCE OF 0.050 MICROHENRY

Figure 3

it should be noted that the larger the value of the capacitor being considered, the more the effective value will rise for a given frequency.

3. SOURCES OF ERROR

Four principal sources of error associated with this measurement procedure are as follows: (a) inaccuracy in the determination of the resonant frequency of the short-circuited capacitor, (b) mutual coupling between the shorting device and the grid-dip meter coil, (c) the inductance of the shorting device, and (d) the equivalent circuit used to represent the capacitor. In examining these sources of error it is necessary to generalize in a number of instances because of the absence of a convenient geometrical arrangement upon which to base a rigorous analysis. This is especially true in the latter three instances where current distributions in conductors and the resulting fields are extremely complex and true representations of actual circuit conditions are almost impossible to realize.

In measuring the resonant frequency of the short circuited capacitor, the grid-dip meter indication is very distinct because the capacitor and short constitute a high Q circuit. This condition makes in possible to achieve repeatability which is beyond the resolution of the frequency scale on the grid-dip meter oscillator. Either of two methods may be employed to improve this resolution. The frequency of the radiated signal of the oscillator may be measured with a hetrodyne frequency meter, or the signal may be amplified and fed into a frequency counter. In this manner, it is possible to achieve repeatability well within one percent. Assuming that the accuracy is also of this order, the effect on the accuracy of the total circuit inductance would be approximately two percent. For frequency accuracies within a few

percent, the accuracy in inductance is given by the expression:

$$\frac{\Delta L}{L} \approx \frac{\Delta \omega}{\omega}$$

where ΔL and $\Delta \omega$ represent the errors in inductance and angular frequency respectively.

The error due to mutual coupling between the short and the grid-dip meter coil is evidently very small because no distinct change in the resonant frequency is caused by varying the distance between them. Any change in the resonant frequency resulting from an increase or decrease in the separation is probably of the same order as the stability and setability of the grid-dip meter oscillator. In any event, the coupling error may be minimized by maintaining a separation of an inch or more between them.

Probably the largest source of error is in the value used to represent the self-inductance of the short. It is possible to improve the situation by making a judicious choice of the size and configuration of the device used so as to permit the use of available formulas [Terman,1943] to calculate the self-inductance. Even so,there remains a margin of uncertainty due to the geometry of the current path,and such formulas may not be expected to yield accuracies better than ten to fifty percent. However, since the inductance of the short is usually only a small portion of the total inductance of the resonant circuit, this does not represent a serious degradation of the value obtained for L in equation (2). Figure 4 is a photograph showing two shorting bars which are convenient to use. These are brass bars fitted with banana plugs or jacks appropriately spaced to fit the capacitor terminals.

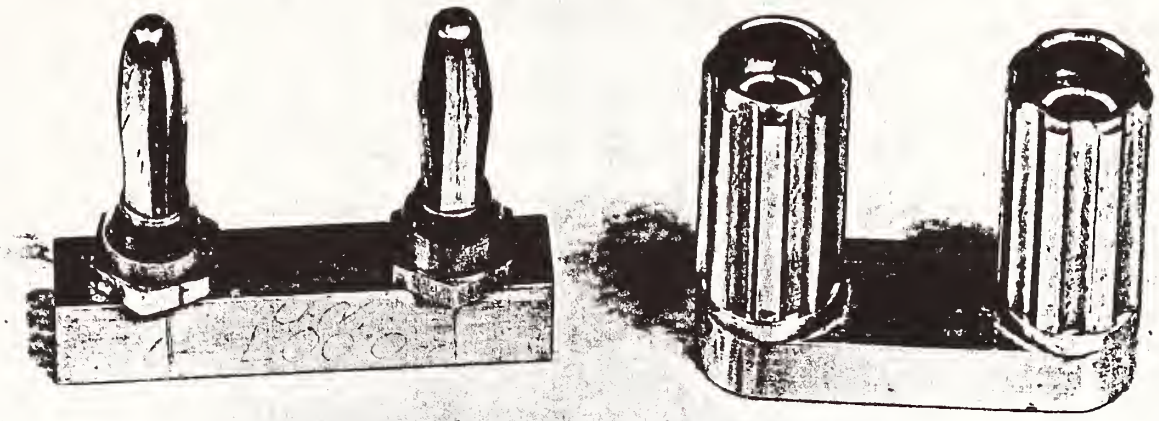

Figure 4

Shorting Bars

Finally, we must consider the equivalent circuit used to represent the capacitor. The circuit of figure 1 may be criticized because, in actuality, the inductance and capacitance probably do not exist as shown. Depending upon the physical details of the construction, the capacitor may be more accurately represented by other equivalent circuits. As an example, consider the equivalent circuit of figure 5.

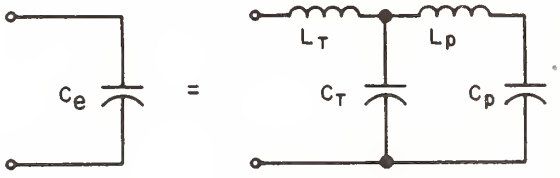

Figure 5

High Frequency Equivalent Circuit

Here the inductance and capacitance, instead of being lumped together at one point, are separated into fractional parts of the total and arranged in a manner which more nearly approximates the actual situation. C_t is the capacitance between the case and the high potential lead passing through it, and C_p is the capacitance in the stack of plates. L_t and L_p are the lead inductances arranged as they may appear in relation to C_t and C_p. Problems arise, however, because it is difficult to estimate the values to assign these components, and also because complex circuits are cumbersome to handle mathematically. To illustrate the importance of the equivalent circuit, consider a capacitor having a 1 kc value of 1000 picofarads and a residual series inductance of 0.050 microhenry. Using the equivalent circuit of figure 1, the value at 1 Mc is 1001.98 picofarads. The circuit of figure 5 gives a value of 1001.96 picofarads if we let $L_t = L_p = 0.025$ microhenry, $C_t = 10$ picofarads, and $C_p = 990$ picofarads. At this frequency the difference is essentially negligible,

but at 15 Mc the values are 1799.00 picofarads for the circuit of figure 1 and 1786.32 picofarads for the circuit of figure 5, using the same values for L_t, L_p, C_t, and C_p. Thus it is seen that the equivalent circuit assumes increasing importance at the higher frequencies.

Because of the sources of error, it is believed that the reliability of the value obtained for the residual series inductance by the method described is not better than ten percent. Again referring to figure 3, the broken lines indicate the upper and lower limits of the corrections which result from this ten percent uncertainty in the inductance value. In general, it may be said that the effective capacitance may be determined by this method to accuracies of one percent or better up to frequencies where the correction amounts to ten percent of the 1 kc value.

4. CONCLUSION

With the advent of improved rf connector systems, many standards and instruments using the older type connectors are no longer appropriate for use at the level of primary standards. NBS has developed and does maintain standards which are only appropriate for use with the improved type of coaxial connectors [Jones and Nelson,1962]. Because it is impractical for NBS to attempt to maintain standards for a wide variety of connector configurations, secondary standards laboratories are urged to employ this calibration procedure where possible and when compatible with traceability requirements.

5. REFERENCES

1. Jones, R. N., and R. E. Nelson (1962). "The Role of Capacitance in the National Reference Standards of High Frequency Impedance," Proceedings of the Instrument Society of America, Paper No. 18.1.62.

2. Terman, F. E. (1943). Radio Engineers Handbook, First Ed., pp. 48-51 (McGraw-Hill Book Co., Inc., New York, N. Y.).

GPO 837 - 107

Four-Terminal-Pair Networks as Precision Admittance and Impedance Standards

R. D. CUTKOSKY
MEMBER IEEE

THE DEVELOPMENT of suitable standards for the maintenance of impedance and admittance has been along two separate lines. One of these lines is based on the concept of 4-terminal measurement, which requires a standard to be provided with two current and two potential terminals. This technique has long been used with low d-c resistances, and may be applied directly to the measurement of small mutual inductances. The technique results in the elimination of uncertainties caused by variations in contact impedances. The other line of approach is applicable to very high impedances in which case even a very low stray admittance between the terminals could change appreciably the apparent impedance of the standard. The effect of stray admittances is eliminated by shielding the standard and making measurements in such a way that stray admittances to the shield are not included in the measurement. The technique is most often applied to the measurement of low capacitances; this standard is called a 3-terminal capacitor. The technique is also feasible for use with very high d-c resistances.

An interesting point is that if neither 4-terminal construction nor shielding is provided, the most reliable measurements are made in a middle range of impedance in which errors due to contact impedance and shunt admittance are about equal. However, precision attainable in this range may not be as high as desired.

The provision of current and potential terminals results in an improvement of precision for very low impedances, with very little improvement in the middle- and high-impedance range. The use of shielded or 3-terminal construction results in an improvement of precision for very high impedances, with very little improvement in the middle- and low-impedance range. Neither system alone substantially improves the measurement precision in the middle-impedance range.

The purpose of this paper is to develop a theoretical basis for measurement techniques involving both shielding and current and potential terminals, and to show that the generalized impedance standard so defined reduces to the 4-terminal impedance when it is very low and to a shielded (3-terminal) admittance when its impedance is very high. Partial solutions to the problem have been described in the literature,[1,2] but without sufficient attention to the details of ground connections. Some concepts and techniques of modern network theory are used in the analysis.[3]

Refinement of 3-Terminal Capacitors

For many years 3-terminal capacitors have been widely used as low-value capacitance standards. Three-terminal construction greatly reduces errors due to stray and variable capacitances between the terminals. Careful analysis of the behavior of such devices shows that, although the uncertainty caused by variations in lead geometry is rather small, it is not negligible when the capacitances are high, or if extremely high accuracy is desired.

Three-terminal admittances are usually constructed with two coaxial connectors as terminals, and with the outer members of the coaxial connectors joined with a low-impedance conductor. Since this conductor has a finite impedance, the standard has in reality four terminals, and its current response to applied voltages must be described by the six independent elements of its three-by-three admittance matrix. To reduce the number of variables, it is common practice to treat the standard as a 2-terminal-pair device, whose current response to voltages at the pairs of terminals may be described with only three independent admittances. This approach assumes first, that we are interested only in the loop currents at the 2-terminal pairs caused by voltage applied across these pairs; and second, that either currents in all other external loops are identically zero or, equivalently, that

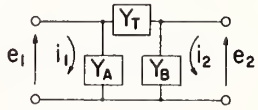

Fig. 1. Two-terminal-pair admittance

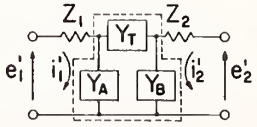

Fig. 2. Two-terminal-pair admittance with series lead impedances

Paper 63-928, recommended by the IEEE Fundamental Electrical Standards Committee and approved by the IEEE Technical Operations Committee for presentation at the IEEE Summer General Meeting and Nuclear Radiation Effects Conference, Toronto, Ont., Canada, June 16–21, 1963. Manuscript submitted March 18, 1963; made available for printing April 26, 1963.

R. D. CUTKOSKY is with the United States Department of Commerce, National Bureau of Standards, Washington, D. C.

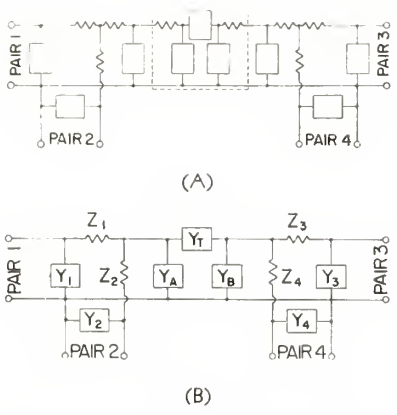

Fig. 3. Four-terminal-pair admittance

A—As constructed
B—Simplified circuit

the current into the inner member of each coaxial connector is exactly equal to the current out of its outer member. Mathematically, this approach allows the impedance between the coaxial connector's outer members to be suppressed when the device is represented by an equivalent circuit.

An equivalent circuit for a 2-terminal-pair admittance is shown in Fig. 1. If

$$i_1 = e_1 Y_{11} + e_2 Y_{12}$$

and

$$i_2 = e_1 Y_{21} + e_2 Y_{22}$$

then

$$Y_{11} = Y_A + Y_T$$

$$Y_{22} = Y_B + Y_T$$

and

$$Y_{12} = Y_{21} = -Y_T$$

Fig. 1 is clearly similar to the usual equivalent circuit for a 3-terminal capacitor, in which $Y_T = j\omega C$, where C is the direct capacitance.

This analysis implies that there may be conditions under which an "ordinary" measurement of a 3-terminal capacitor may be uncertain by an amount dependent upon net current from one coaxial terminal pair to the other, and upon the internal construction of the standard. It is thus suggested that the transfer admittance of a 2-pair network

$$Y_{21} = \left.\frac{i_2}{e_1}\right|_{e_2 = 0}$$

may be a more precisely defined parameter than the loosely defined 3-terminal admittance.

If net current between terminal pairs is suppressed and if all leads are coaxial, the current then also will be coaxial and no magnetic fields will exist outside of the cables. This astatic condition reduces the errors that otherwise might be produced by stray fields. Carried to an extreme, one can see that the admittance standards themselves should be as astatic as possible. Although this condition is usually fairly difficult to achieve, it may be improved by the use of eddy currents or magnetic shields, as they are needed.

When lead impedances becomes significant, the network of Fig. 1 must be modified as in Fig. 2. An analysis shows that if

$$Y_{11} = Y_A + Y_T$$

$$Y_{22} = Y_B + Y_T$$

and

$$Y_{12} = Y_{21} = -Y_T$$

$$\left.\frac{i_2'}{e_1'}\right|_{e_2' = 0} \equiv Y_{21}' = \frac{Y_{21}}{1 + Z_1 Y_{11} + Z_2 Y_{22} + Z_1 Z_2 (Y_{11} Y_{22} - Y_{12}^2)} \quad (1)$$

If all terms of the form $(Z1')$ are much smaller than unity,

$$Y_{21}' \simeq Y_{21}(1 - Z_1 Y_{11} - Z_2 Y_{22})$$

If $Z_1 = Z_2 = 10^{-2}$ ohms and $Y_{11} = Y_{22} = 10^{-4}$ mhos, the expression $Z_1 Y_{11} + Z_2 Y_{22}$ represents an error term in the measurement of Y_{21} with a value of two parts per million.

In practice, it is found that one may work conveniently with Y_{21}' instead of Y_{21} for intercomparison purposes. Even if Y_{11} and Y_{22} are constant, accuracy is limited by the repeatability of Z_1 and Z_2. These impedances include, for the system under study, the resistance of the coaxial connectors used to make contact with the standard; for good connectors, they will be uncertain by less than 10^{-4} ohms. If Y_{11} and Y_{22} are about 10^{-4} mhos, Y_{21}' will be measurable to a few parts in 10^8. Special connectors could no doubt be constructed to reduce the contact uncertainty, but if Y_{21} is very high, a limit will be reached beyond which uncertainties due to lead variations cannot be reduced conveniently.

This difficulty may be circumvented by the use of 4-terminal techniques, such as those used for low-value standard resistors. In our case, the 2-pair network is then replaced by a 4-pair one. Some properties of general 4-pair networks are derived in the Appendix, but these properties unfortunately do not have a simple physical interpretation.

One logical extension of the 2-pair network can be constructed by extending and splitting each coaxial pair with a permanently attached coaxial T-connector,

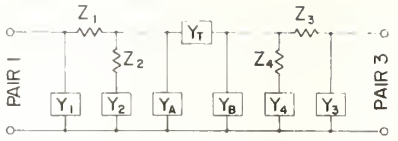

Fig. 4. Four-terminal-pair admittance with two pairs ignored

as in Fig. 3(A). Using suitable Y–delta transforms, this may be simplified to Fig. 3(B).

If we constrain $i_2 = 0$, $i_4 = 0$, and $e_4 = 0$ in Fig. 3(B) by placing suitable generators at terminal pairs 1 and 3, we find the following equation results:

$$\frac{-i_3}{e_2} = Y_t(1 + Y_3 Z_3)(1 + Y_2 Z_2) \quad (2)$$

which we define to be the 4-pair admittance P_{32}^{14}. Z_2 and Z_3 will typically be the impedances of a few inches of coaxial line, and Y_2 and Y_3 the shunt admittances of the same lines. Hence $Y_2 Z_2$ and $Y_3 Z_3$ will be very small at audio frequencies. Numerically, we may expect that if $Z_2 = Z_3 = 10^{-2}$ ohms at $Y_2 = Y_3 = 10^{-7}$ mhos (10 picofarads if $\omega = 10^4$ radians/second), then $Y_2 Z_2 = Y_3 Z_3 = 10^{-9}$. If Z_2, Z_3, Y_2, and Y_3 are each constant and repeatable to 1%, P_{32}^{14} will be defined with a connection uncertainty of a few parts in 10^{11}.

Lastly, it should be noted that a very small 4-pair admittance for which all (YZ) products are negligible reduces to the normal 2-pair transfer admittance if terminals 2 and 4 are ignored (open circuit). In this case Fig. 3(B) may be redrawn as Fig. 4. The transfer admittances of this 2-pair circuit may be calculated to be

$$\left.\frac{-i_3}{e_1}\right|_{e_3 = 0} = -Y_{31} = \frac{Y_T}{1 + Z_1(Y_T + Y_X) + Z_3(Y_T + Y_Y) + Z_1 Z_3(Y_T Y_X + Y_T Y_Y + Y_X Y_Y)} \quad (3)$$

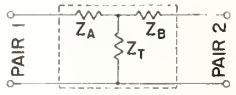

Fig. 5. Two-terminal-pair impedance

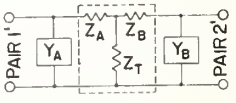

Fig. 6. Two-terminal-pair impedance with shunt lead admittances

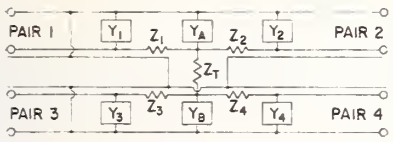

Fig. 7. Four-terminal-pair impedance

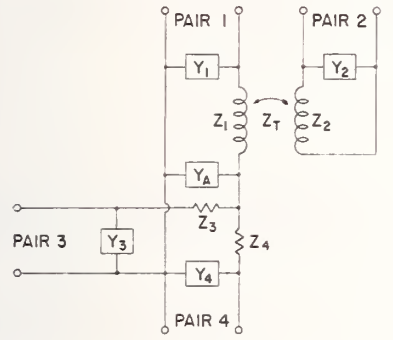

Fig. 8. Special 4-terminal-pair impedance constructed with a mutual inductor

where

$$Y_X = Y_A + \frac{Y_2}{1+Z_2Y_2}$$

and

$$Y_Y = Y_B + \frac{Y_4}{1+Z_4Y_4}$$

In the limit as all YZ products become negligible, equations 2 and 3 reduce to the following:

$$P_{32}{}^{14} = -Y_{31} = Y_T$$

Refinement of Mutual Inductors

Four-pair networks may be constructed in many ways for use at low-impedance levels. A complete survey of possible construction practices will not be attemped here. Discussion will be limited to one special case in which the 4-pair impedance has the highly desirable property of reducing in the low-impedance limit to the ordinary 2-pair transfer impedance.

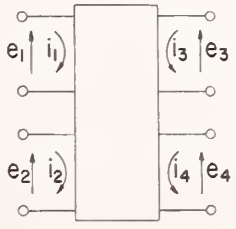

Fig. 9. General 4-terminal-pair network

Fig. 5 represents a general 2-terminal-pair (4-terminal) impedance. We may write

$$e_1 = i_1Z_{11} + i_2Z_{12}$$

and

$$e_2 = i_1Z_{21} + i_2Z_{22}$$

with

$$Z_{11} = Z_A + Z_T$$

and

$$Z_{22} = Z_B + Z_T$$

where $Z_{12} = Z_{21} = Z_T$ is called the transfer impedance.

As with the 2-terminal-pair transfer admittance of Fig. 1, net current from one pair to the other of the network must be suppressed or its effect on the apparent transfer impedance investigated. Otherwise, Fig. 5 is not a valid equivalent circuit.

If the shunt admittances of the leads are taken into account, Fig. 5 must be replaced by Fig. 6. Analysis shows that

$$\left.\frac{e_2'}{i_1'}\right|_{i_2'=0} \equiv Z_{21}'$$

$$= \frac{Z_{21}}{1 + Y_AZ_{11} + Y_BZ_{22} + Y_AY_B(Z_{11}Z_{22} - Z_{12}{}^2)} \tag{4}$$

If all YZ products are small, so that terms of the form $(YZ)\,(YZ)$ are negligible, we have $Z_{21}' \simeq Z_{21}(1 - Y_AZ_{11} - Y_BZ_{22})$. We may work with this Z_{21}' instead of Z_{21} for intercomparison purposes, but accuracy is still limited by the repeatability of Y_A, Y_B, Z_{11}, and Z_{22}. The arguments are similar to those associated with equation 1, which resembles in form equation 4.

Elimination of errors due to shunt admittance may be achieved by the use of shields around each individual terminal. This may be compared with shielding a 2-terminal capacitor to produce a 3-terminal one. Fig. 7, which shows such a shielded transfer impedance, is identical with Fig. 3(B) if

$$Y_T = \frac{1}{Z_T}$$

We may hope to use the same conditions $i_2 = i_4 = 0$ and $e_4 = 0$, so that

$$\frac{e_2}{i_3} \equiv Q_{32}{}^{14} = \frac{1}{P_{32}{}^{14}} = \frac{Z_T}{(1+Z_2Y_2)(1+Z_3Y_3)} \tag{5}$$

and find a meaningful interpretation for $Q_{32}{}^{14}$ in the limit as all Z including Z_T become small. That this may be done for the special case of a mutual inductor will now be shown.

Consider a mutual inductor constructed as in Fig. 8. For this circuit

$$Q_{32}{}^{14} = \frac{Z_T}{(1+Z_2Y_2)(1+Z_3Y_3)} \tag{6}$$

If terminal pairs 3 and 4 are short-circuited, we may calculate the mutual impedance between the remaining terminal pairs 1 and 2 to be

$$\left.\frac{e_2}{i_1}\right|_{i_2=0} = Z_{21}$$

$$= \frac{Z_T}{(1+Z_2Y_2)[1+Y_1(Z_1+Z_x)] - Z_t{}^2Y_1Y_2} \tag{7}$$

where

$$Z_x = \frac{Z_3Z_4}{Z_3+Z_4+Z_3Z_4Y_A}$$

If all YZ products are negligible, equations 6 and 7 reduce to $Z_{21} = Q_{32}{}^{14} = Z_T$, the desired correspondence.

General Considerations

It has been shown that it is theoretically possible to construct 4-terminal-pair devices having properties dimensionally equivalent to admittance or impedance, and that these suitably defined properties are relatively independent of the properties of the leads connected to the network. The technique is expected to be useful as an aid in designing a wide range of impedance standards which may be intercompared and used to calibrate other standards. Four-pair standards will have the same physical meaning at very low and very high impedances as presently existing standards. In the middle-impedance range, they may be used as well-defined elements in an impedance step-up chain. They may also be used to measure ordinary 2-, 3-, or 4-terminal standards with accuracies limited only by the ordinary standards.

Construction of 4-terminal-pair devices may follow the existing techniques for constructing ordinary standards. Capacitors, resistors, and self- or mutual inductors are expected to be useful. Regardless of the construction, 4-pair ad-

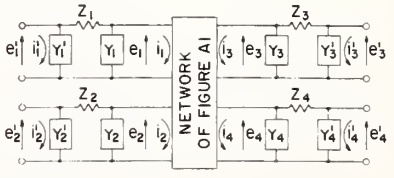

Fig. 10. General 4-terminal-pair network with leads

mittances must be carefully designed to be astatic; that is, they must neither produce stray field nor be susceptible to pickup from existing stray fields. This is particularly important with very low impedances. Search coils may be used to investigate standards for this effect.

The preceding discussion has centered around a particular type of 4-pair network. Unfortunately, the conclusions do not hold for general 4-pair networks. For this reason, it is essential to test a completed standard to determine whether or not the required conditions of this paper can be met. Varying lead lengths and noting the result may be one test. The appendix, which treats a general 4-pair network, may be used as an aid in developing appropriate tests. Just as important is an experimental determination of the effectiveness of the methods used to suppress unwanted loop currents between terminal pairs.

It is not the purpose of this paper to describe techniques for measuring 4-terminal-pair admittances. However, experimental work has been done to verify some of the conclusions made here. Measurement techniques will be discussed in a subsequent paper.

Appendix

If the network of Fig. 9 is linear, we may write

$$i_1 = e_1 Y_{11} + e_2 Y_{12} + e_3 Y_{13} + e_4 Y_{14}$$

$$i_2 = e_1 Y_{21} + e_2 Y_{22} + e_3 Y_{23} + e_4 Y_{24}$$

$$i_3 = e_1 Y_{31} + e_2 Y_{32} + e_3 Y_{33} + e_4 Y_{34}$$

$$i_4 = e_1 Y_{41} + e_2 Y_{42} + e_3 Y_{43} + e_4 Y_{44}$$

If we require that $e_4 = 0$, $i_2 = 0$, and $i_4 = 0$, we find

$$\frac{-i_3}{e_2} = -\left[Y_{32} + \frac{Y_{21} Y_{33} Y_{42} + Y_{31} Y_{43} Y_{22} - Y_{31} Y_{42} Y_{23} - Y_{33} Y_{22} Y_{41}}{Y_{23} Y_{41} - Y_{43} Y_{21}} \right]$$

which we define to be the 4-pair admittance $P_{32}{}^{14}$. It is seen that if reciprocity holds, $P_{23}{}^{41} = P_{32}{}^{14}$.

An expression for the error due to series impedance and parallel admittance of leads may be calculated by considering the circuit of Fig. 10. A calculation yields for $i_2' = i_4' = 0$ and $e_4' = 0$,

$$\frac{-i_3'}{e_2'} \equiv (P_{32}{}^{14})' = \left[P_{32}{}^{14} + \frac{(Y_{31} Y_{43} - Y_{33} Y_{41}) Y_A + (Y_{21} Y_{42} - Y_{41} Y_{22}) Y_B - Y_{41} Y_A Y_B}{Y_{43} Y_{21} - Y_{41} Y_{23}} \right] K$$

where

$$Y_A = \frac{Y_2 + Y_2' + Y_2 Y_2' Z_2}{1 + Z_2 Y_2'}$$

$$Y_B = \frac{Y_3 + Y_3' + Y_3 Y_3' Z_3}{1 + Z_3 Y_3'}$$

and

$$K = (1 + Z_2 Y_2')(1 + Z_3 Y_3')$$

This is of a form which may be treated experimentally by varying Y_A and Y_B and observing the change which is brought about in $(P_{32}{}^{14})'$.

References

1. A Design for Resistors of Calculable AC/DC Resistance Ratio, **D. L. H. Gibbings.** *Proceedings*, Institution of Electrical Engineers, London, England, vol. 110, Feb. 1963, pp. 335–47.

2. Evaluation of the NBS Unit of Resistance Based on a Computable Capacitor, **R. D. Cutkosky.** *Journal of Research*, National Bureau of Standards, Boulder, Colo., vol. 65A, no. 3, May–June 1961, pp. 147–58.

3. Introductory Circuit Theory (book), **E. A. Guillemin.** John Wiley and Sons, Inc., New York, N. Y., 1953.

A reprint from **COMMUNICATION AND ELECTRONICS**, published by The Institute of Electrical and Electronics Engineers, Inc.

January 1964 issue

621.319.42

The Institution of Electrical Engineers
Monograph No. 351 M
Jan. 1960

SOME RESULTS ON THE CROSS-CAPACITANCES PER UNIT LENGTH OF CYLINDRICAL THREE-TERMINAL CAPACITORS WITH THIN DIELECTRIC FILMS ON THEIR ELECTRODES

By D. G. LAMPARD, M.Sc., Ph.D., and R. D. CUTKOSKY, B.Sc.

(*The paper was first received* 1*st April, in revised form* 17*th July, and in final form* 18*th August*, 1959. *It was published as an* INSTITUTION MONOGRAPH *in* January, 1960.)

SUMMARY

The effect on the cross-capacitances per unit length of cylindrical 3-terminal capacitors of thin dielectric films on the capacitor electrodes is discussed.

It is assumed that the cross-section of such dielectric films remains constant throughout the length of the capacitor. Some conformal transformations of basic cylindrical capacitor cross-sections are given. When these are applied to a symmetric cylindrical capacitor with a thin dielectric film on its electrodes, the results suggest that the mean capacitance per unit length may remain constant to the first order despite the presence of the dielectric film. The same methods also suggest that the individual cross-capacitances per unit length may remain constant to the first order provided that the dielectric film is disposed symmetrically with respect to the capacitor symmetry plane.

Further support for these conjectures is given by the results of a detailed calculation of the cross-capacitances per unit length of a parallel-plate cylindrical capacitor with a thin uniform dielectric film on one electrode. In the last Section, a lemma concerning the existence of an equivalent dielectricless capacitor is given and this is followed by the proof of general results of the type suggested by the previous working.

(1) INTRODUCTION

A new approach to the design of calculable 3-terminal capacitance standards has recently been made possible as a consequence of a general theorem[1] concerning cross-capacitances of certain cylindrical electrode systems. This theorem enables a capacitor to be constructed such that only one precision length measurement is necessary to compute its capacitance to a high order of accuracy.

A proof of this general theorem, together with detailed calculations of cross-capacitances of cylindrical systems with a variety of cross-sections, has been given in a recent paper.[2] In that paper the effects of various perturbations which could occur in practice were considered, but an important practical perturbation, namely the presence of spurious thin dielectric films on the capacitor electrodes, was dealt with only in one special case.

Such dielectric films can be present, for example, in a precision calculable cylindrical capacitor, where it may be difficult to avoid surface contamination of the electrodes with oil films, adsorbed vapours, etc. They can also arise in connection with the direct experimental determination (by capacitance measurement of a cylindrical capacitor) of the permittivity of vapours, where a thin film of condensed vapour on the capacitor electrodes may constitute a serious source of error.

In the paper we examine further the effects of thin dielectric films in cylindrical capacitors, the assumption being made that the cross-section of the dielectric film remains constant throughout the length of the capacitor. To facilitate the discussion of these dielectric effects, a number of conformal transformations are given in Section 2 by means of which a cylindrical capacitor of arbitrary cross-section can be mapped into a cylindrical parallel-plate capacitor. This procedure provides a simple alternative proof of the main theorem on cylindrical capacitors in a more generalized form.

In Section 3 it is shown how some uniform dielectric distributions behave under the transformations of Section 2, while in Section 4 both cross-capacitances per unit length of the cylindrical parallel-plate capacitor of Section 2, with a highly asymmetric dielectric distribution on its electrodes, are calculated in detail. The calculations of Section 3 and 4 suggest some general results, which are established in Section 5, concerning the effect of thin dielectric films.

(2) GENERALIZATION OF THE THEOREM ON CYLINDRICAL CAPACITORS

Consider a conducting cylindrical shell whose right cross-section, Fig. 1(*a*), is the arbitrary closed curve S. Let this shell be divided into four parts by infinitesimal gaps at α, β, γ and δ.

By means of an existence theorem due to Riemann,[3] in the theory of conformal transformations, the interior of the cross-section S can be mapped into the interior of a circle, Fig. 1(*b*), and with a suitable choice of a co-ordinate system the point α can be mapped on to the origin and the centre of the circle taken on the real axis.

The mapping $\omega = 1/z$ transforms the interior of the circle of Fig. 1(*b*) onto the right-hand half-plane of Fig. 1(*c*), where the distances $\beta\gamma$ and $\gamma\delta$ have been arbitrarily called b and a, respectively.

By means of simple rotations and translations, the right half-plane of Fig. 1(*c*) can be mapped into the upper half-plane of either Fig. 1(*d*)(i) or (ii).

Finally, the mapping $v = \log_\varepsilon u$ transforms the upper half-planes of Fig. 1(*d*) into the strip spaces of Fig. 1(*e*).

The configuration of Fig. 1(*e*)(i) is that of the usual guarded parallel-plate capacitor. The capacitance per unit length can be computed by assuming electrode $\alpha\beta$ to be at unit potential and all other electrodes at zero potential. In this case, all lines of force are parallel to the imaginary axis and the capacitance per unit length, C_1, between electrodes $\alpha\beta$ and $\gamma\delta$ is simply

$$C_1 = \frac{1}{4\pi} \frac{\log_\varepsilon (a+b) - \log_\varepsilon b}{\pi} \quad . \quad . \quad . \quad (1)$$

$$= \frac{1}{4\pi^2} \log_\varepsilon \left(1 + \frac{a}{b}\right) \quad . \quad . \quad . \quad . \quad . \quad (2)$$

Similarly, the capacitance per unit length, C_2, between electrodes $\alpha\delta$ and $\beta\gamma$ is,* from Fig. 1(*e*)(ii),

$$C_2 = \frac{1}{4\pi^2} \log_\varepsilon \left(1 + \frac{b}{a}\right) \quad . \quad . \quad . \quad . \quad (3)$$

* Note that eqns. (2) and (3) agree with eqn. (75) of Reference 2.

Correspondence on Monographs is invited for consideration with a view to publication.

Dr. Lampard is in the Division of Electrotechnology of the Commonwealth Scientific and Industrial Research Organization, Australia, and Mr. Cutkosky is at the National Bureau of Standards, Washington, D.C., United States.

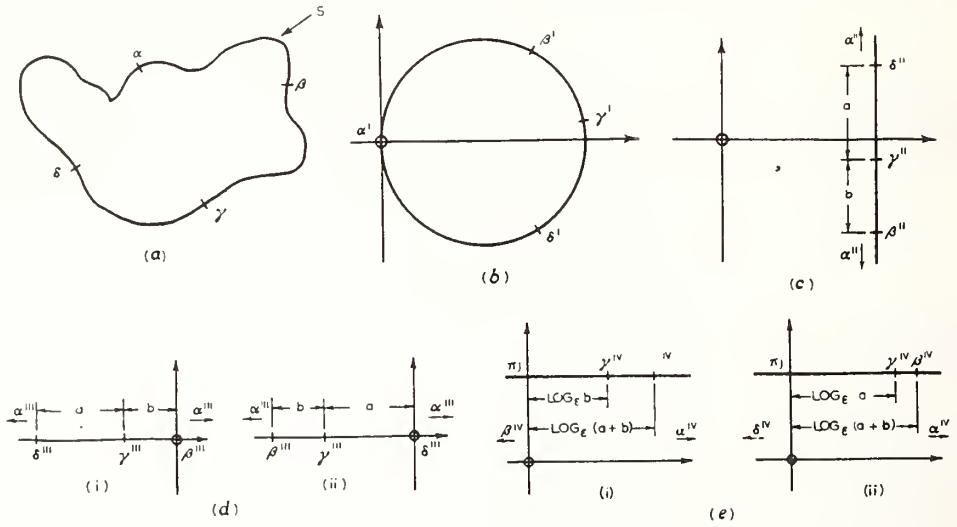

Fig. 1.—Transformed cross-sections of general cylindrical capacitor.

(*a*) Cross-section.
(*b*) Transformation into *z*-plane.
(*c*) Transformation into *w*-plane.
(*d*) Transformation into *u*-plane.
(i) Orientation 1. (ii) Orientation 2.
(*e*) Transformation into *v*-plane.
(i) Orientation 1. (ii) Orientation 2.

If we introduce a parameter $\tau = a/b$ we see that the two cross-capacitances per unit length for any cylindrical capacitor can always be written in the form

$$C_1(\tau) = \frac{1}{4\pi^2} \log_\varepsilon (1 + \tau) \quad . \quad . \quad . \quad (4)$$

$$C_2(\tau) = \frac{1}{4\pi^2} \log_\varepsilon \left(1 + \frac{1}{\tau}\right) \quad . \quad . \quad . \quad . \quad (5)$$

Eliminating τ between these two equations,

$$\varepsilon^{-4\pi^2 C_1} + \varepsilon^{-4\pi^2 C_2} = 1 \quad . \quad . \quad . \quad . \quad (6)$$

This identity was given as eqns. (32) and (71) of Reference 2 in connection with cylindrical capacitors of square and circular cross-section, respectively, but its complete generality was not noticed until some time later (Lampard[4] and more recently van der Pauw[5]).

It follows immediately from eqn. (6) that, if $C_1 = C_2$,

$$C_1 = C_2 = \frac{1}{4\pi^2} \log_\varepsilon 2 \quad . \quad . \quad . \quad . \quad . \quad (7)$$

It is clear that a sufficient, but not necessary, condition for the equality of C_1 and C_2 is the existence of an axis of symmetry of the capacitor cross-section, which passes through a pair of non-adjacent electrode gaps. This was the form in which the theorem was originally stated. It will be clear that the cross-section of any cylindrical capacitor whose cross-capacitances per unit length are equal can always be mapped into a cross-section having this symmetry property, and hence, in the paper, any such cylindrical capacitor will be referred to as *electrically symmetric*. The non-necessity of the physical symmetry condition has been pointed out by Thompson.[6]

On differentiating eqn. (6),

$$\varepsilon^{-4\pi^2 C_1} dC_1 = - \varepsilon^{-4\pi^2 C_2} dC_2 \quad . \quad . \quad . \quad (8)$$

and, in particular, when $C_1 = C_2$,

$$dC_1 = - dC_2 \quad . \quad . \quad . \quad . \quad . \quad . \quad . \quad (9)$$

We shall make use of this result in a later Section to prove some general results concerning the effects of thin dielectric films.

(3) CONFORMAL MAPPING OF DIELECTRIC DISTRIBUTIONS

The way in which two simple uniform dielectric distributions behave under the conformal transformations of Section 2 will be examined. Thus consider the physically symmetrical system of Fig. 2(*a*). This system was analysed in Reference 2, where

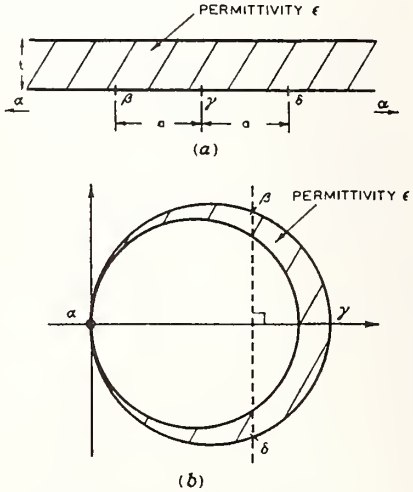

Fig. 2.—Infinite-plane cylindrical capacitor with dielectric film.

(*a*) Cross-section.
(*b*) Transformation into *z*-plane.

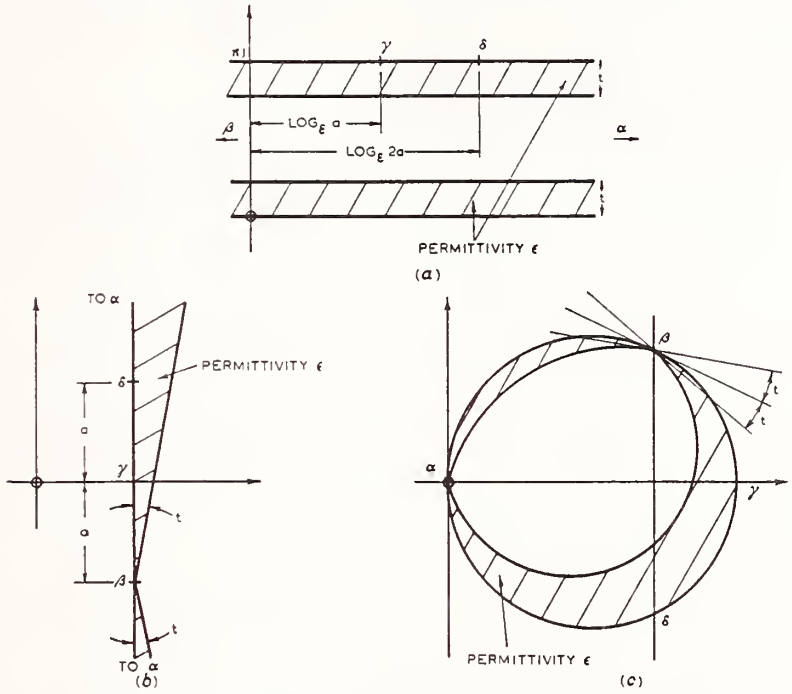

Fig. 3.—Parallel-plate cylindrical capacitor with dielectric film.

(*a*) Cross-section.
(*b*) Transformation into *w*-plane.
(*c*) Transformation into *z*-plane.

it was shown that the cross-capacitance per unit length between electrodes $\alpha\beta$ and $\gamma\delta$ is given, when the dielectric thickness is small, by

$$C = \frac{1}{4\pi^2}\log_\epsilon 2 + \frac{3}{16\pi^2}\left(\frac{t}{a}\right)^2\left(1 - \frac{1}{\epsilon^2}\right) + \text{terms in } \left(\frac{t}{a}\right)^2 \text{ and higher} \quad (10)$$

If we transform this system [which is to be compared with that of Fig. 1(*d*)(ii)] back into a circular cross-section by the methods of the previous Section, we obtain the system of Fig. 2(*b*), where the dielectric is still symmetrically distributed with respect to the capacitor symmetry plane but is no longer of constant thickness.

From eqn. (10) it can be seen that for this system each cross-capacitance per unit length is increased by an amount proportional to the square of the dielectric thickness when this thickness is small.

Now consider the electrically symmetrical system of Fig. 3(*a*), which may be compared with Fig. 1(*e*)(i) (with $a = b$). Transforming the system back by the methods of Section 2, we obtain the physically symmetrical systems of Fig. 3(*b*) and (*c*), respectively. It will be seen that the dielectric in the transformed systems is neither symmetrically disposed with respect to the capacitor symmetry plane nor of constant thickness.

A simple calculation on the original system of Fig. 3(*a*) shows that, in this case, the cross-capacitance per unit length between $\alpha\beta$ and $\gamma\delta$ is

$$C = \left(\frac{1}{4\pi^2}\log_\epsilon 2\right)\left[1 + 2\frac{t}{\pi}\frac{\epsilon - 1}{\epsilon} + 4\left(\frac{t}{\pi}\right)^2\left(\frac{\epsilon - 1}{\epsilon}\right)^2 + \ldots\right] \quad . \quad . \quad . \quad . \quad (11)$$

i.e. the cross-capacitance per unit length between $\alpha\beta$ and $\gamma\delta$ is increased by an amount directly proportional to the dielectric thickness when the thickness is small.

These results suggest that, for small dielectric thickness, the cross-capacitance per unit length of a symmetric cylindrical capacitor may be written as a Taylor series in terms of the dielectric thickness, in which the coefficient of the linear term is zero, provided that the dielectric is disposed symmetrically with respect to the capacitor symmetry plane. That this is so will be demonstrated in Section 5.

Up to this point we have been concerned only with the individual cross-capacitances per unit length. It would be of considerable interest to know what happens to the mean capacitance per unit length of a symmetrical cylindrical capacitor when its electrodes have a thin dielectric film distributed on them asymmetrically. Thus in the system of Fig. 3 it may be conjectured that the cross-capacitance per unit length between $\alpha\delta$ and $\beta\gamma$ will be reduced by the same amount, to the first order, as the increase in the cross-capacitance per unit length between $\alpha\beta$ and $\gamma\delta$. As will be seen in the next Section, such a result is certainly true for the system discussed there (a slightly simplified version of the system of Fig. 3), and in Section 5 it is shown that this result is true in general.

(4) THE PARALLEL-PLATE CYLINDRICAL CAPACITOR WITH A UNIFORM DIELECTRIC FILM ON ONE ELECTRODE

By the methods of Section 2 any cylindrical capacitor can be transformed into an equivalent parallel-plate cylindrical capacitor. When the original capacitor cross-section may be transformed into one having symmetry about a line passing through a pair of non-adjacent electrode gaps, the dimensions of the equivalent parallel-plate capacitor have been shown to be such

that each cross-capacitance per unit length is given by $C = (1/4\pi^2)\log_e 2$.

In this Section we analyse the general parallel-plate cylindrical capacitor with the additional complication of a dielectric film of constant thickness on one electrode. The capacitor cross-section, together with the co-ordinate system that will be used in the analysis, is shown in Fig. 4.

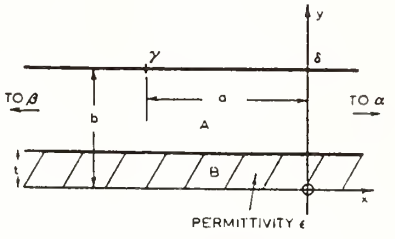

Fig. 4.—Cross-section of parallel-plate cylindrical capacitor with dielectric film on one electrode only.

The working of this Section will be given in some detail, since the system of Fig. 4 appears to be one of the few general asymmetric cases in which both cross-capacitances per unit length can be fairly readily evaluated analytically.

(4.1) Cross-Capacitance per Unit Length from $\alpha\beta$ to $\gamma\delta = C_1(\epsilon)$

Electrode $\alpha\beta$ may be placed at unit potential, all other electrodes at zero. The lines of force are parallel to the y-axis and the dielectric boundary is an equipotential. Thus the required capacitance per unit length may be regarded as arising from two capacitors in series:

$$[C_1(\epsilon)]^{-1} = \left[\frac{a}{4\pi(b-t)}\right]^{-1} + \left(\frac{\epsilon a}{4\pi t}\right)^{-1} \quad . \quad . \quad (12)$$

and hence

$$C_1(\epsilon) = \frac{a}{4\pi b}\left[1 - \frac{t}{b}\frac{(\epsilon-1)}{\epsilon}\right]^{-1} \quad . \quad . \quad . \quad . \quad . \quad . \quad (13)$$

$$= \frac{a}{4\pi b}\left[1 + \frac{t}{b}\frac{(\epsilon-1)}{\epsilon} + \left(\frac{t}{b}\right)^2\left(\frac{\epsilon-1}{\epsilon}\right)^2 + \ldots\right] \quad (14)$$

In particular, for the symmetrical cylindrical capacitor,

$$\left.\begin{aligned} a &= \log_e 2 \\ b &= \pi \end{aligned}\right\} \quad . \quad . \quad . \quad . \quad . \quad . \quad (15)$$

and substituting eqn. (15) in eqn. (14) and denoting the particular value of C_1 by C_1^*,

$$C_1^*(\epsilon) = \left(\frac{1}{4\pi^2}\log_e 2\right)\left[1 + \frac{t}{\pi}\frac{(\epsilon-1)}{\epsilon} + \left(\frac{t}{\pi}\right)^2\left(\frac{\epsilon-1}{\epsilon}\right)^2 + \ldots\right]$$
$$. \quad . \quad . \quad . \quad (16)$$

(4.2) Cross-Capacitance per Unit Length from $\alpha\delta$ to $\beta\gamma = C_2(\epsilon)$

The calculations here are considerably more difficult. It is convenient to take electrode $\alpha\delta$ at unit potential and all other electrodes at zero. In region B, with the co-ordinate system shown, the particular solution of Laplace's equation which vanishes when $y = 0$ is

$$V_B(x, y) = \int_{-\infty}^{+\infty} B(k)\varepsilon^{jkx}\sinh ky dk \quad . \quad . \quad . \quad (17)$$

and, in region A, is

$$V_A(x, y) = \int_{-\infty}^{+\infty}[A_1(k)\cosh ky + A_2(k)\sinh ky]\varepsilon^{jkx}dk \quad (18)$$

with the boundary conditions

$$V_A(x, t) = V_B(x, t) \quad . \quad . \quad . \quad . \quad . \quad . \quad . \quad (19)$$

$$\frac{\partial V_A(x, y)}{\partial y} = \epsilon\left[\frac{\partial V_B(x, y)}{\partial y}\right]_{y=t} \quad . \quad . \quad . \quad . \quad (20)$$

These two boundary conditions, together with Lerch's theorem on the uniqueness of Fourier transforms, serve to determine the two functions $A_1(k)$, $A_2(k)$ in terms of $B(k)$:

$$A_1(k) = \tfrac{1}{2}B(k)(1-\epsilon)\sinh 2kt \quad . \quad . \quad . \quad . \quad . \quad (21)$$

$$A_2(k) = \tfrac{1}{2}B(k)[(1+\epsilon) - (1-\epsilon)\cosh 2kt] \quad . \quad (22)$$

On substituting eqns. (21) and (22) in eqn. (18),

$$V_A(x, y) = \tfrac{1}{2}\int_{-\infty}^{+\infty}\{(1-\epsilon)\sinh 2kt\cosh ky$$
$$+ [(1+\epsilon) - (1-\epsilon)\cosh 2kt\}\sinh kyB(k)\varepsilon^{jkx}dk \quad (23)$$

Setting $y = b$ and using the boundary condition

$$\left.\begin{aligned} V_A(x, b) &= 1 \quad x > 0 \\ &= 0 \quad x < 0 \end{aligned}\right\} \quad . \quad . \quad . \quad . \quad (24)$$

we obtain, on inverting the Fourier transform of eqn. (18),

$$\tfrac{1}{2}B(k)\{(1-\epsilon)\sinh 2kt\cosh kb + [(1+\epsilon) - (1-\epsilon)\cosh 2kt]\sinh kb\}$$
$$= \frac{1}{2\pi}\int_0^{\infty}\varepsilon^{-jkx}dx \quad . \quad . \quad . \quad . \quad . \quad . \quad (25)$$

$$= \frac{1}{2\pi}\left[\frac{1}{jk} + \pi\delta(k)\right] \quad . \quad . \quad . \quad . \quad (26)$$

where $\delta(k)$ is the unit impulse or Dirac delta function.

Using eqn. (26) in eqn. (23) and writing

$$m = \frac{1+\epsilon}{1-\epsilon} \quad . \quad . \quad . \quad . \quad . \quad . \quad (27)$$

we find the complete solution for the potential function in region A, namely

$$V_A(x, y) = \frac{1}{2\pi}\int_{-\infty}^{+\infty}\left[\frac{1}{jk} + \pi\delta(k)\right]\varepsilon^{jkx} \times$$
$$\times \frac{\sinh 2kt\cosh ky + (m - \cosh 2kt)\sinh ky}{\sinh 2kt\cosh kb + (m - \cosh 2kt)\sinh kb}dk \quad (28)$$

Now, the charge density on the upper electrode is given by

$$\sigma(x) = -\frac{1}{4\pi}\left[\frac{\partial V_A(x, y)}{\partial y}\right]_{y=b} \quad . \quad . \quad . \quad . \quad . \quad . \quad (29)$$

$$= -\frac{1}{8\pi^2}\int_{-\infty}^{+\infty}\left[\frac{1}{jk} + \pi\delta(k)\right]k\varepsilon^{jkx}F[k, b, t]dk \quad (30)$$

where

$$F[k, b, t] = \frac{\sinh 2kt\sinh kb + (m - \cosh 2kt)\cosh kb}{\sinh 2kt\cosh kb + (m - \cosh 2kt)\sinh kb} \quad (31)$$

It seems impossible to evaluate eqn. (30) in closed form, so we content ourselves with an expansion in powers of t, the dielectric thickness. This procedure is reasonable as we are primarily concerned with the effects of thin dielectric films. Thus,

expanding eqn. (31) in powers of t, and substituting the resulting expansion in eqn. (30),

$$\sigma(x) = -\frac{1}{8\pi^2}\int_{-\infty}^{+\infty}\left[\frac{1}{jk}+\pi\delta(k)\right]k\varepsilon^{jkx}\frac{\cosh kb}{\sinh kb}dk$$
$$-t\left(\frac{2}{1-m}\right)\frac{1}{8\pi^2}\int_{-\infty}^{+\infty}\left[\frac{1}{jk}+\pi\delta(k)\right]k^2\varepsilon^{jkx}\frac{1}{\sinh^2 kb}dk$$
$$-t^2\left(\frac{2}{1-m}\right)^2\frac{1}{8\pi^2}\int_{-\infty}^{+\infty}\left[\frac{1}{jk}+\pi\delta(k)\right]k^3\varepsilon^{jkx}\frac{\cosh kb}{\sinh^3 kb}dk$$
$$+\text{ terms in } t^3 \text{ and higher} \quad . \quad . \quad . \quad . \quad . \quad . \quad . \quad . \quad (32)$$

The three integrals occurring here are readily evaluated, for negative x, by contour integration. Results are given in Appendix 8.1. On using these results in eqn. (32) we have, finally,

$$\sigma(x)=\frac{1}{4\pi b}\left\{\frac{\varepsilon^{\pi x/b}}{(1-\varepsilon^{\pi x/b})}+\frac{t}{b}\frac{(\epsilon-1)}{\epsilon}\left[\frac{\varepsilon^{\pi x/b}}{1-\varepsilon^{\pi x/b}}+\frac{\frac{\pi x}{b}\varepsilon^{\pi x/b}}{(1-\varepsilon^{\pi x/b})^2}\right]\right.$$
$$\left.+\frac{1}{2}\left(\frac{t}{b}\right)^2\left(\frac{\epsilon-1}{\epsilon}\right)^2\left[\frac{2\varepsilon^{\pi x/b}}{1-\varepsilon^{\pi x/b}}+\frac{4\frac{\pi x}{b}\varepsilon^{\pi x/b}}{(1-\varepsilon^{\pi x/b})^2}+\frac{\left(\frac{\pi x}{b}\right)^2(1+\varepsilon^{\pi x/b})\varepsilon^{\pi x/b}}{(1-\varepsilon^{\pi x/b})^3}\right]\right\}$$
$$+\text{ terms in } (t/b)^3 \text{ and higher} \quad (33)$$

Here we have reintroduced ϵ by the relation

$$\frac{2}{1-m}=\frac{\epsilon-1}{\epsilon} \quad . \quad . \quad . \quad . \quad . \quad . \quad (34)$$

The cross-capacitance per unit length, $C_2(\epsilon)$, is just the total charge on electrode $\beta\gamma$, namely

$$C_2(\epsilon)=\int_{-\infty}^{-a}\sigma(x)dx \quad . \quad . \quad . \quad . \quad . \quad . \quad (35)$$

We now substitute eqn. (33) in eqn. (35), and carry out the integration, making use of the results given in Appendix 8.2.

$$C_2(\epsilon) = -\frac{1}{4\pi^2}\log_\varepsilon(1-\varepsilon^{-\pi a/b})$$
$$-\frac{1}{4\pi^2}\left(\frac{t}{b}\right)\left(\frac{\epsilon-1}{\epsilon}\right)\frac{\pi a}{b}\frac{\varepsilon^{-\pi a/b}}{1-\varepsilon^{-\pi a/b}}$$
$$+\frac{1}{4\pi^2}\left(\frac{t}{b}\right)^2\left(\frac{\epsilon-1}{\epsilon}\right)^2\frac{1}{2}\left[\left(\frac{\pi a}{b}\right)^2\frac{\varepsilon^{-\pi a/b}}{(1-\varepsilon^{-\pi a/b})^2}-2\frac{\pi a}{b}\frac{\varepsilon^{-\pi a/b}}{1-\varepsilon^{-\pi a/b}}\right]$$
$$+\text{ terms in }\left(\frac{t}{b}\right)^3 \text{ and higher} \quad . \quad . \quad . \quad . \quad . \quad . \quad . \quad . \quad (36)$$

Of particular interest is the case of the symmetrical cylindrical capacitor for which

$$a=\log_\varepsilon 2 \quad b=\pi \quad . \quad . \quad . \quad . \quad (37)$$

For this case, denoting the particular value of $C_2(\epsilon)$ by C^*,

$$C_2^*(\epsilon)=\frac{1}{4\pi^2}\log_\varepsilon 2\left[1-\frac{t}{\pi}\frac{\epsilon-1}{\epsilon}-\left(\frac{t}{\pi}\right)^2\left(\frac{\epsilon-1}{\epsilon}\right)^2(1-\log_\varepsilon 2)\right.$$
$$\left.+\text{ terms in }\left(\frac{t}{\pi}\right)^3 \text{ and higher}\right] \quad (38)$$

We note that the linear terms in eqns. (16) and (38) are equal in magnitude and opposite in sign, so that the change in the mean capacitance per unit length is only of the second order in the dielectric thickness. Specifically

$$\frac{C_1^*(\epsilon)+C_2^*(\epsilon)}{2}=\frac{1}{4\pi^2}\log_\varepsilon 2\left[1+\left(\frac{t}{\pi}\right)^2\left(\frac{\epsilon-1}{\epsilon}\right)^2\frac{\log_\varepsilon 2}{2}\right.$$
$$\left.+\text{ terms in }\left(\frac{t}{\pi}\right)^3 \text{ and higher}\right] \quad (39)$$

This example thus supports the conjecture that, in the case of a thin dielectric film asymmetrically distributed on the electrodes of a cylindrical capacitor, the mean capacitance per unit length remains constant to the first order.

Finally let us briefly consider the results for the general parallel-plate cylindrical capacitor with no dielectric film. Setting $t=0$ in eqns. (14) and (36) we have (on dropping the arguments of C_1 and C_2)

$$C_1=\frac{a}{4\pi b} \quad . \quad . \quad . \quad . \quad . \quad . \quad . \quad . \quad . \quad (40)$$

$$C_2=-\frac{1}{4\pi^2}\log_\varepsilon(1-\varepsilon^{-\pi a/b}) \quad . \quad . \quad . \quad (41)$$

As a partial check on the fairly complicated calculations of this Section we note that the introduction of a parameter

$$\tau=\varepsilon^{\pi a/b}-1 \quad . \quad . \quad . \quad . \quad . \quad (42)$$

enables eqns. (40) and (41) to be written in the standard parametric form of eqns. (4) and (5).

(5) GENERAL RESULTS CONCERNING DIELECTRIC FILMS IN CYLINDRICAL CAPACITORS

In this Section we give proofs of the following general results, which have been suggested by the working of Sections 3 and 4.

(*a*) In an electrically symmetric cylindrical capacitor, an arbitrary thin dielectric film on the capacitor electrodes produces only a second-order change in the mean capacitance per unit length.

(*b*) In a physically symmetric cylindrical capacitor, a thin dielectric film on the capacitor electrodes, which is disposed symmetrically with respect to the capacitor symmetry plane, produces only a second-order change in each cross-capacitance per unit length.

Before proceeding to the proof of these results we establish a preliminary lemma. This lemma states that, given any cylindrical capacitor with a thin dielectric film on its electrodes, there exists an equivalent cylindrical capacitor containing no dielectric,* whose electrodes lie wholly within the space occupied by the dielectric film, such that the electric fields, at all points in the dielectricless region of the two capacitors, are equal to the first order.

The significance of this lemma is that it shows, for dielectric films whose thickness is small, that the perturbation required to obtain the equivalent electrode system is both small, of the same order as the dielectric thickness, being in fact bounded by the dielectric itself, and independent of the field configuration, i.e. independent of the individual electrode potentials.

Thus consider the cross-section of an arbitrary cylindrical capacitor and, in particular, a small region near electrode $\alpha\beta$, say (assumed at zero potential without loss of generality), as shown in Fig. 5.

* Throughout the paper the term dielectric is used in the sense of a material substance.

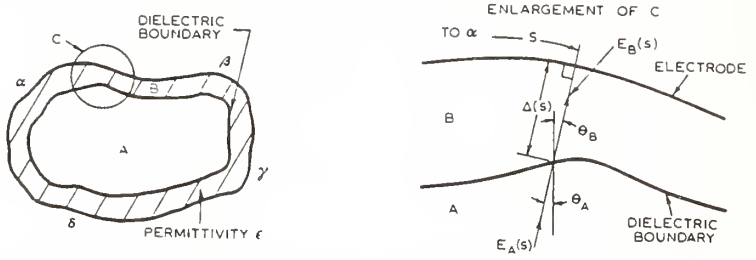

Fig. 5.—Cross-section of general cylindrical capacitor with arbitrary thin dielectric film.

In the following discussion we assume that:

(i) $\Delta(s)$ is small compared with the length of the line of force terminating at s.

(ii) $\Delta'(s)$ is such that the field is almost normal to the dielectric boundary.

With these assumptions, the field $E_B(s)$ in the dielectric can be regarded as essentially constant for a given s and, on equating normal components of electric displacement,

$$E_A(s)\cos\theta_A = \epsilon E_B(s)\cos\theta_B \quad . \quad . \quad . \quad . \quad . \quad (43)$$

i.e.
$$E_B(s) = \frac{1}{\epsilon}E_A(s)\sqrt{\frac{1+\tan^2\theta_B}{1+\tan^2\theta_A}} \quad . \quad . \quad . \quad (44)$$

Using the identity

$$\epsilon\tan\theta_A = \tan\theta_B \quad . \quad . \quad . \quad . \quad . \quad (45)$$

and noting that for small $\Delta'(s)$

$$\tan\theta_B = \Delta'(s) + o[\Delta^2(s)] \quad . \quad . \quad . \quad . \quad (46)$$

we have

$$E_B(s) = \frac{1}{\epsilon}E_A(s)\left\{\sqrt{\frac{1+[\Delta'(s)]^2}{1+\left[\frac{\Delta'(s)}{\epsilon}\right]^2}} + o[\Delta^2(s)]\right\} \quad (47)$$

$$= \frac{1}{\epsilon}E_A(s)\{1 + o[\Delta^2(s)]\} \quad . \quad . \quad . \quad . \quad . \quad (48)$$

Thus for small $\Delta(s)$ the potential function at the dielectric boundary is

$$V(s) = \frac{1}{\epsilon}\Delta(s)E_A(s) + o[\Delta^2(s)] \quad . \quad . \quad . \quad (49)$$

Now consider the same region of the capacitor but with the dielectric removed and the electrode surface at s advanced a distance $x\Delta(s)$ towards the former position of the dielectric boundary. The potential at the dielectric boundary is now simply

$$V^*(s) = (1-x)\Delta(s)E_A^*(s) + o[\Delta^2(s)] \quad . \quad . \quad (50)$$

where asterisks have been used to denote the values of $V(s)$ and $E_A(s)$ in this situation.

Clearly, if $V(s) = V^*(s)$ for all s, then so must the electric fields in region A also be equal; in particular we must have $E_A(s) = E_A^*(s)$ for all s. Equating the two expressions for $V(s)$ and solving for x,

$$x = \frac{\epsilon-1}{\epsilon} + o[\Delta(s)] \quad . \quad . \quad . \quad . \quad (51)$$

which result is independent of s to the first order and also independent of the way in which the field arises.

Thus we have shown that the electric field in the region unoccupied by dielectric remains constant to the first order, if the dielectric and electrode systems are replaced by a perturbed electrode system (without dielectric) such that each new electrode element is a distance $\Delta(s)(\epsilon-1)/\epsilon$ from the corresponding original electrode position. Since $(\epsilon-1)/\epsilon < 1$, the perturbed electrode system of the equivalent dielectricless capacitor lies wholly within the region formerly occupied by the dielectric, which proves the lemma.

Finally, the capacitance per unit length between electrodes $\alpha\beta$ and $\gamma\delta$, say, can be computed by assuming that electrode $\gamma\delta$ is at unit potential and all other electrodes are at zero potential. Hence

$$C_1 = \int_\alpha^\beta \sigma(s)ds \quad . \quad . \quad . \quad . \quad . \quad (52)$$

where $\sigma(s)$, the charge density per unit length, may be written in terms of the electric displacement at the electrode surface. To the first order, this electric displacement is identical with the normal component of the electric field at the dielectric, and hence

$$\sigma(s) = \frac{1}{4\pi}E_A(s)\left\{1 + \left[\frac{\Delta'(s)}{\epsilon}\right]^2\right\}^{-1/2} + o[\Delta(s)] \quad (53)$$

$$= \frac{1}{4\pi}E_A(s) + o[\Delta(s)] \quad . \quad . \quad . \quad . \quad . \quad . \quad (54)$$

We have already seen that the electric field $E_A(s)$ remains constant to the first order in the equivalent dielectricless capacitor, and so, on using eqn. (54) in eqn. (52), it is clear that the same conclusion applies to the capacitance per unit length, C_1, and by similar working to the other cross-capacitance per unit length, C_2.

As an example of the use of this lemma we may compute the first-order changes in the cross-capacitances per unit length for the system of Fig. 4 due to the presence of the dielectric film. Then, according to the lemma, the equivalent dielectricless capacitor would have the same disposition, but the distance b between the electrodes must now be reduced by an amount $t(\epsilon-1)/\epsilon$. Thus, using eqns. (40) and (41),

$$C_1(\epsilon) = \frac{a}{4\pi\left(b - t\frac{\epsilon-1}{\epsilon}\right)} \text{ to the first order} \quad . \quad . \quad . \quad (55)$$

$$C_2(\epsilon) = -\frac{1}{4\pi^2}\log_\epsilon\left[1 - \exp\left(-\frac{\pi a}{b - t\frac{\epsilon-1}{\epsilon}}\right)\right]$$

to the first order (56)

On expanding eqns. (55) and (56) in powers of $t(\epsilon-1)/\epsilon$,

$$C_1(\epsilon) = \frac{a}{4\pi b}\left(1 + \frac{t}{b}\frac{\epsilon-1}{\epsilon} + \text{higher terms}\right) \quad . \quad . \quad (57)$$

$$C_2(\epsilon) = -\frac{1}{4\pi^2}\log_\epsilon(1-\varepsilon^{-\pi a/b}) - \frac{1}{4\pi^2}\frac{t}{b}\frac{\epsilon-1}{\epsilon}\frac{\pi a}{b}\frac{\varepsilon^{-\pi a/b}}{1-\varepsilon^{-\pi a/b}} + \text{higher terms} \quad (58)$$

which of course agree with eqns. (14) and (36), to the first order.

To prove the first general result, mentioned at the beginning of this Section, consider an electrically symmetric cylindrical capacitor with an arbitrary thin dielectric film on all its electrodes. By the lemma and its subsequent discussion it follows that there is an equivalent dielectricless capacitor, with the same cross-capacitances per unit length to the first order, but whose electrodes lie wholly within the region formerly occupied by dielectric. The change in the mean capacitance per unit length, C_M, is then given by

$$\delta C_M = \delta\left(\frac{C_1 + C_2}{2}\right) \quad . \quad . \quad . \quad . \quad . \quad . \quad . \quad . \quad . \quad (59)$$

$$= \tfrac{1}{2}(dC_1 + dC_2) + \text{terms of higher degree} \quad . \quad (60)$$

But for the electrically symmetric cylindrical capacitor ($C_1 = C_2$) we have, from eqn. (9),

$$dC_1 = -\,dC_2 \text{ (if } C_1 = C_2) \quad . \quad . \quad . \quad . \quad (61)$$

and so $$\delta C_M = 0 \text{ (to the first order)} \quad . \quad . \quad . \quad (62)$$

which proves the first result.

To prove the second general result, consider a physically symmetric cylindrical capacitor C with a thin dielectric film on all its electrodes, which is disposed symmetrically with respect to the capacitor symmetry plane. The dielectric in such a capacitor may be considered to be introduced in two steps as shown in Fig. 6.

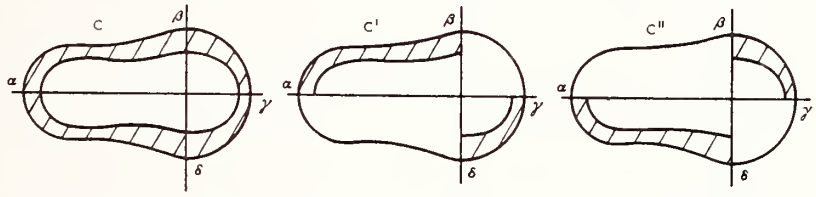

Fig. 6.—Sequential placement of dielectric film in a physically symmetric cylindrical capacitor.

When we consider the equivalent dielectricless capacitors, which exist by the lemma above, we have, on making use of eqn. (9),

$$\delta C_1' = -\,\delta C_2' \text{ (to first order)} \quad . \quad . \quad . \quad . \quad (63)$$

$$\delta C_1'' = -\,\delta C_2'' \text{ (to first order)} \quad . \quad . \quad . \quad . \quad (64)$$

Also, because of the symmetry of the dielectric film,

$$\delta C_1' = \delta C_2'' \quad . \quad . \quad . \quad . \quad . \quad . \quad . \quad (65)$$

$$\delta C_2' = \delta C_1'' \quad . \quad . \quad . \quad . \quad . \quad . \quad . \quad (66)$$

On superposing the two sets of equations to obtain results for the whole capacitance, C,

$$\delta C_1 = \delta C_1' + \delta C_1'' = 0 \text{ (to first order)} \quad . \quad . \quad (67)$$

$$\delta C_2 = \delta C_2' + \delta C_2'' = 0 \text{ (to first order)} \quad . \quad . \quad (68)$$

which proves the second general result, namely that in this case the individual cross-capacitances per unit length remain constant to the first order.

Alternatively we may note that, by the lemma, the equivalent dielectricless capacitor is also physically symmetrical, and hence to the first order the individual cross-capacitances per unit length are both $(1/4\pi^2)\log_e 2$ and thus remain constant to the first order, which proves the second general result.

(6) CONCLUSION

The application of conformal-transformation methods to certain types of cylindrical 3-terminal capacitors, whose electrodes carry thin dielectric films, has suggested some general results concerning the effects on the cross-capacitances of such dielectric films. The detailed computation of the cross-capacitances of a parallel-plate cylindrical capacitor (with a thin, highly asymmetric dielectric film on its electrodes) has further substantiated these conjectures, and proofs are given in the final Section.

It should be realized that the results of the paper apply only to dielectric films which maintain a constant cross-section throughout the length of the capacitor. More generally, dielectric films will be distributed in a 3-dimensional pattern over the electrode surfaces. In this case the potential problem is correspondingly 3-dimensional and hence the powerful methods of conformal transformation are no longer available for its solution. Such problems require further study.

(7) REFERENCES

(1) THOMPSON, A. M., and LAMPARD, D. G.: 'A New Theorem in Electrostatics and its Application to Calculable Standards of Capacitance', *Nature*, 1956, **177**, p. 888.

(2) LAMPARD, D. G.: 'A New Theorem in Electrostatics with Applications to Calculable Standards of Capacitance', *Proceedings I.E.E.*, Monograph No. 216 M, January, 1957 (**104** C, p. 271).

(3) COPSON, E. T.: 'Theory of Functions of a Complex Variable' (Oxford, 1948).

(4) LAMPARD, D. G.: C.S.I.R.O. Division of Electrotechnology, Internal Report, March, 1957.

(5) VAN DER PAUW, L. J.: 'A Method of Measuring Specific Resistivity and Hall Effects of Discs of Arbitrary Shape', *Philips Research Reports*, 1958, **13**, p. 1.

(6) THOMPSON, A. M.: 'The Cylindrical Cross-Capacitor as a Calculable Standard', *Proceedings I.E.E.*, Paper No. 2887 M, May, 1959 (**106** B, p. 307).

(8) APPENDIX

(8.1) Values of Integrals occurring in Eqn. (32)

The integrals occurring in eqn. (32) may be evaluated (for negative x) by summing residues at the poles $k = -jn\pi/b$ with $n = 0, 1, 2 \ldots$ The results are:

$$\frac{1}{8\pi^2}\int_{-\infty}^{+\infty}\left[\frac{1}{jk} + \pi\delta(k)\right]k\varepsilon^{jkx}\frac{\cosh kb}{\sinh kb}dk = -\frac{1}{4\pi b}\sum_{n=1}^{\infty}\varepsilon^{\pi nx/b} \quad (69)$$

$$= -\frac{1}{4\pi b}\frac{\varepsilon^{\pi x/b}}{1-\varepsilon^{\pi x/b}} \quad (70)$$

$$\frac{1}{8\pi^2}\int_{-\infty}^{+\infty}\left[\frac{1}{jk}+\pi\delta(k)\right]k^2\varepsilon^{jkx}\frac{1}{\sinh^2 kb}dk$$

$$=-\frac{1}{4\pi b^2}\sum_{n=1}^{\infty}\left(1+\frac{\pi nx}{b}\right)\varepsilon^{\pi nx/b} \qquad (71)$$

$$=-\frac{1}{4\pi b^2}\left[\frac{1-\varepsilon^{\pi x/b}}{\varepsilon^{\pi x/b}}+\frac{\dfrac{\pi x}{b}\varepsilon^{\pi x/b}}{(1-\varepsilon^{\pi x/b})^2}\right] \qquad (72)$$

$$\frac{1}{8\pi^2}\int_{-\infty}^{+\infty}\left[\frac{1}{jk}+\pi\delta(k)\right]k^3\varepsilon^{jkx}\frac{\cosh kb}{\sinh^3 kb}dk$$

$$=-\frac{1}{8\pi b^3}\sum_{n=1}^{\infty}\left[\left(\frac{\pi nx}{b}\right)^2+4\left(\frac{\pi nx}{b}\right)+2\right]\varepsilon^{\pi nx/b} \qquad (73)$$

$$=-\frac{1}{8\pi b^3}\left[2\frac{\varepsilon^{\pi x/b}}{1-\varepsilon^{\pi x/b}}+4\frac{\dfrac{\pi x}{b}\varepsilon^{\pi x/b}}{(1-\varepsilon^{\pi x/b})^2}+\frac{\left(\dfrac{\pi x}{b}\right)^2(1+\varepsilon^{\pi x/b})\varepsilon^{\pi x/b}}{(1-\varepsilon^{\pi x/b})^3}\right] \qquad (74)$$

(8.2) Values of Integrals occurring in Eqn. (35)

When carrying out the integration of eqn. (35), with $\sigma(x)$ given by eqn. (33), the following results are needed:

$$\int_{-\infty}^{-a}\frac{\varepsilon^{\pi x/b}}{1-\varepsilon^{\pi x/b}}dx=-\frac{b}{\pi}\log_\varepsilon(1-\varepsilon^{-\pi a/b}) \qquad (75)$$

$$\int_{-\infty}^{-a}\frac{\dfrac{\pi x}{b}\varepsilon^{\pi x/b}}{(1-\varepsilon^{\pi x/b})^2}dx=-\frac{b}{\pi}\left[\frac{\dfrac{\pi a}{b}\varepsilon^{-\pi a/b}}{1-\varepsilon^{-\pi a/b}}-\log_\varepsilon(1-\varepsilon^{-\pi a/b})\right] \qquad (76)$$

$$\int_{-\infty}^{-a}\frac{\left(\dfrac{\pi x}{b}\right)^2(1+\varepsilon^{\pi x/b})\varepsilon^{\pi x/b}}{(1-\varepsilon^{\pi x/b})^3}dx$$

$$=\frac{b}{\pi}\left[\frac{\left(\dfrac{\pi a}{b}\right)^2\varepsilon^{-\pi a/b}}{(1-\varepsilon^{-\pi a/b})^2}+\frac{2\dfrac{\pi a}{b}\varepsilon^{-\pi a/b}}{(1-\varepsilon^{-\pi a/b})}-2\log_\varepsilon(1-\varepsilon^{-\pi a/b})\right] \qquad (77)$$

Printed in Great Britain by
UNWIN BROTHERS LIMITED, WOKING AND LONDON

A COMBINED TRANSFORMER BRIDGE FOR PRECISE COMPARISON OF INDUCTANCE WITH CAPACITANCE, Andrzej Muciek, IEEE Trans. Instrum. Meas. IM-32, September 1983.

A combined transformer bridge, composed of two alternately balanced transformer bridges, designed for precise comparison of inductance with capacitance standards has been analyzed. A number of possible sources of error have been studied and experimentally examined in a constructed model of the combined bridge. The experimental results confirmed an ability to measure inductance in reference to capacitance with an accuracy up to 10 parts per million (ppm) in the frequency band 0.16-2 kHz.

AC/DC TRANSFER STANDARDS AND INSTRUMENTS

A Dual-Channel Automated Comparator for AC–DC Difference Measurements

EARL S. WILLIAMS AND JOSEPH R. KINARD, SENIOR MEMBER, IEEE

Abstract—An automated ac-dc difference calibration system is described. The system incorporates a new electronic comparator which determines ac-dc differences of thermal voltage converters (TVC's) by simultaneously measuring the difference between nearly equal ac and dc voltages with both the test and standard instruments. The comparator consists essentially of two practically identical channels each containing a digital-to-analog converter balancing circuit, an operational amplifier to amplify voltage imbalance, and an integrator circuit in which a capacitor is charged during an accurately controlled 10-s period. The difference between the ac and dc voltages applied to the test and standard TVC's is computed from differences in capacitor voltages, and the ac-dc difference is derived from the variation between the test and standard channel indications of this voltage difference. Measurements are made in about half the time required for our manual procedures.

I. Introduction

AC AND DC voltages are compared using a thermal voltage converter (TVC) which responds nearly equally to ac and dc voltages. Those discussed here are electrothermic. Typically, they consist of ranging resistors and a thermoelement—a vacuum bulb containing a heater wire with a thermocouple attached to its midpoint. The output, E, of the thermocouple is usually 7-12 mV with rated heater current. The TVC is connected alternately to an ac voltage, V_a, and to both polarities of a dc reference voltage, V_d. V_a is measured relative to V_d by observing the output EMF, E, of the TVC and changes in output, E_a-E_d, where E_a is observed with V_a applied, and E_d is observed with V_d applied. When the difference between V_a and V_d is small, the proportional difference can be computed from (1):

$$\frac{(V_a - V_d)}{V_d} = \frac{(E_a - E_d)}{nE} + \delta. \tag{1}$$

The factor n relates small changes in TVC heater current to corresponding changes in output EMF, E. It is near 2.0 (a square-law response) at very low heater currents, but is usually 1.7-1.9 at rated heater current. δ is the ac-dc difference of the TVC. It is negligible at low frequencies, but becomes significant at frequencies of 20 kHz and higher in most TVC's.

The ac-dc difference correction for a TVC is determined by comparing it to a similar standard instrument whose correction, δ_s, is known [1]. Ac and dc voltages are applied to both TVC's in parallel, and in most procedures, the ac and dc voltages are adjusted for equal outputs from the test TVC, i.e., $E_a = E_d$ (1). The test instrument thus indicates that $V_a = V_d$. The actual proportional difference between the ac and dc voltages is then measured by observing E and changes in E from the standard TVC. The correction to the test TVC, δ_t, is computed using an equation similar to (1):

Manuscript received August 23, 1984. This work was supported by the Calibration Coordination Group of the U.S. Department of Defense.

J. R. Kinard is with the Electricity Division, National Bureau of Standards, Gaithersburg, MD 20899.

E. S. Williams (retired) was with the Electricity Division, National Bureau of Standards, Gaithersburg, MD 20899.

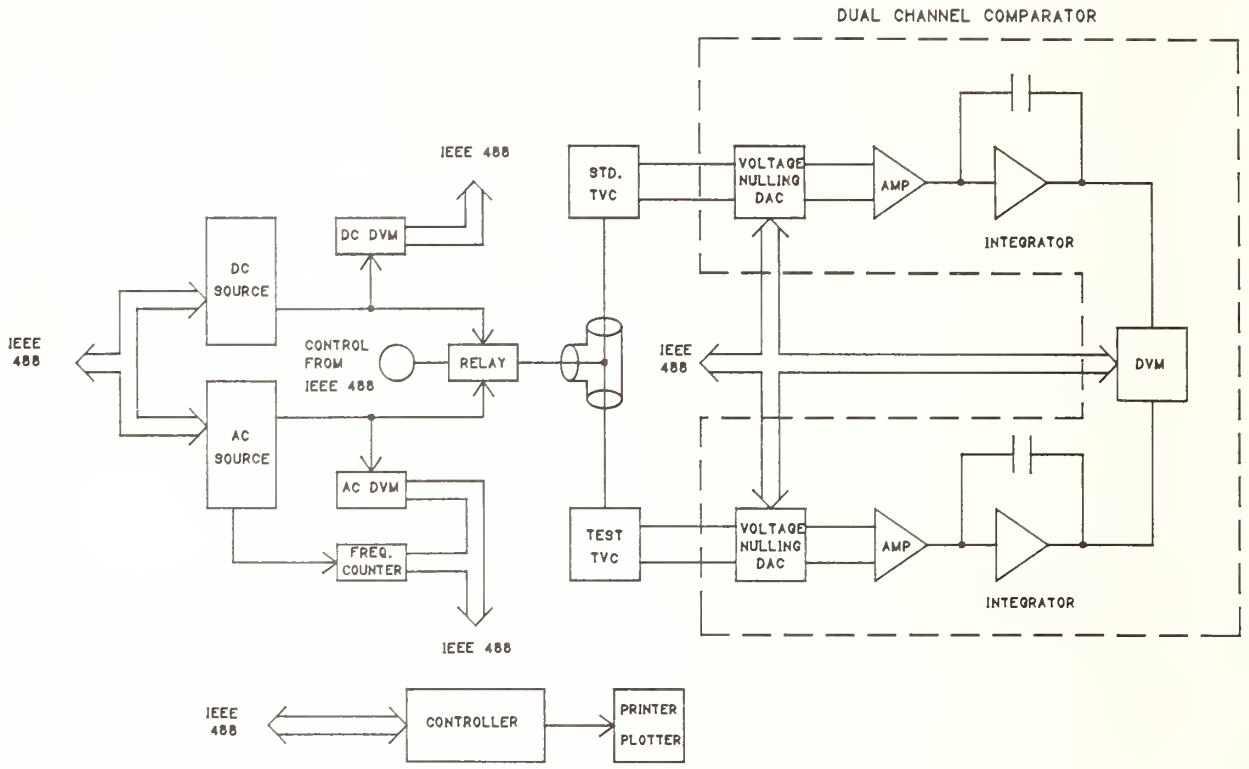

Fig. 1. Block diagram of automated ac–dc difference calibration system.

$$\delta_t = (E_a - E_d)/nE + \delta_s \tag{2}$$

where subscripts t and s refer to test and standard.

With a manual comparator, the precise adjustments of ac and dc voltages for equal outputs from the test TVC are tedious and a skilled operator is necessary [2]. These adjustments have been made automatically but the process is slowed significantly [3]. In the alternative procedure used in the new comparator, data is collected more quickly because the ac and dc voltages are set nearly equal and not further adjusted during one determination. The ac voltage is trimmed automatically after each determination to compensate for drift and to avoid the difficulty, discussed below, of a large difference between ac and dc applied voltages. In this new approach the difference between the unequal ac and dc voltages is measured by both the test and standard TVC's, and, therefore,

$$\frac{(V_a - V_d)}{V_d} = \frac{(E_{as} - E_{ds})}{n_s(E_s)} + \delta_s = \frac{(E_{at} - E_{dt})}{n_t(E_t)} + \delta_t. \tag{3}$$

Eliminating the first expression and solving the remaining two for δ_t, we have

$$\delta_t = \frac{(E_{as} - E_{ds})}{n_s(E_s)} - \frac{(E_{at} - E_{dt})}{n_t(E_t)} + \delta_s. \tag{4}$$

II. Automated System

The entire automated ac–dc difference calibration system is shown in block diagram form in Fig. 1. A photograph of the equipment appears in Fig. 2. The system contains programmable ac and dc voltage sources, a high-voltage relay for switching between ac and dc, voltmeters and frequency counters, a desktop computer to provide IEEE-488 bus control, and the two-channel comparator itself. The two-channel comparator circuit is sketched in Fig. 3. It uses elements from a commercial data acquisition system (DAS) including programmable digital-to-analog converters (DAC's), programmable relays (K1 to K6 and K9), and an auto-ranging voltmeter (VM). An additional board was assembled containing the DAC balancing circuits, amplifiers A1 to A4 and their related resistors and capacitors.

The DAC's supply up to 10 volts to Lindeck-type circuits with 5-kΩ total circuit resistance. With only one range, the 12-bit resolution is insufficient for an appropriate null. A two-pole four-position input switch allows the operator to select either a 5- or 10-Ω resistance in the divider circuit, thus providing either a 10- or 20-mV range.

The measurement procedure is as follows. The operator provides ranges, voltages, frequencies, and record-keeping information to the controller interactively. The ac and dc supplies are then programmed to the appropriate values, and dc is applied to the TVC's. With the DAC set to zero and K3 closed, the standard TVC output, E_{ds}, is measured by the voltmeter, and a DAC voltage is computed and supplied to null the input to amplifier A1. The output of A1, with gain of 10 000, is then measured by closing relay K2, and the DAC signal is trimmed in several steps until the amplifier output is less than 20 mV. The same balancing procedure is followed in the test channel. When both balances have been completed, $n_s(E_s)$ and $n_t(E_t)$ are computed and printed along with other test parameters.

Fig. 2. Automated ac-dc difference calibration system.

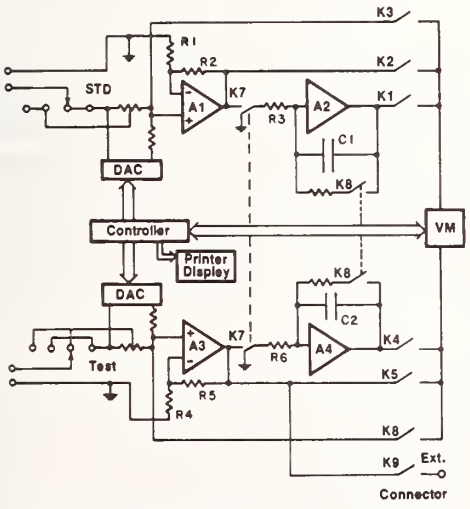

Fig. 3. Dual-channel ac-dc difference comparator.

Voltages are then applied to both TVC's in the test sequence (ac, dc+, dc−, ac), and after each one has stabilized, the relay K7, with a contact in each channel, is closed to charge the two capacitors during an accurately measured time interval of 10 s. The capacitor voltages, four from each channel for a single measurement, are then measured with the voltmeter by closing relays K1 and K4 in turn, after which the capacitors are discharged by closing two-pole relay K8. Providing they are stable over the time required for one determination, amplifier offsets cancel because the results are collected in paired sums and differences.

For the standard channel, the relation between the voltage, e_{in}, at the input to A1 and the voltage, e_{out}, on the integrator capacitor is

$$e_{out} = -\frac{1}{R3C1}\int \frac{R1 + R2}{R1}\, e_{in}\, dt = -\bar{e}_{in} \times 10^5 \qquad (5)$$

with R1 = 10 Ω, R2 = 100 kΩ, R3 = 1 MΩ, C1 = 1 μF, and an integration time of 10 s. Nominally equal values of resistance and capacitance are used in the standard and test channels, so the same nominal relations apply. If the eight voltage readings are reversed in sign and set equal to e_2, e_4, e_6, and e_8 in the standard channel, and e_3, e_5, e_7, and e_9 in the test channel, then using (5), (4) may be written as

$$\delta_t = \frac{5 \times (e_2 - e_4 - e_6 + e_8)}{n_s E_s \cdot 10^6} - \frac{5 \times (e_3 - e_5 - e_7 + e_9)}{n_t E_t \cdot 10^6} + \delta_s. \qquad (6)$$

The numerator in (6) gives twice the actual change in EMF, so the constants are adjusted appropriately. These constants are also adjusted slightly to compensate for departures from nominal in the integrators and amplifiers. The test TVC correction is computed using (6), with the appropriate ac-dc difference correction, δ_s, determined from an equation devised to simulate the standard TVC correction curve.

Since this two-channel method requires the knowledge of n for both test and standard, any uncertainty in either n contributes to uncertainty in the final ac-dc difference. Should either or both terms in (4) become large due to inequality between applied ac and dc voltages, the calculation contains the difference of two large terms each involving an n. Since the n value can only be determined to 1 or 2 percent, a constraint is added to system that the 1st term in (4) be 50 ppm or less to limit the uncertainty contributed by n to 1 ppm, or less. With this constraint the procedure places an upper limit of about 50 ppm on the difference between the applied ac and dc voltages.

Equally satisfactory results are obtained by a "two-voltmeter"

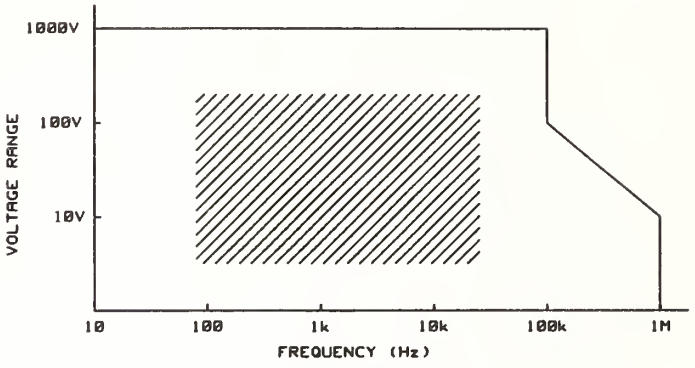

Fig. 4. Voltage and frequency limits of calibration system.

method similar to that used by Inglis in a semi-automatic system [4]. Instead of the analog integrators, an external digital voltmeter connected to relay K9, and the voltmeter located in the DAS, are used to measure the amplified voltage imbalances. After the DAC balances are made, relays K2 and K9 are closed and remain closed while the ac and dc voltages are applied. The voltmeters are read alternately and the two sums are accumulated. If ten readings are summed for each channel with the measurement sequence ac, dc+, dc−, ac, and the sums set equal to e_2 through e_8 and e_3 through e_9, then δ_t can still be obtained from (6) with no change.

III. Other Measurements

Measurements of the response characteristic, n, and comparisons of ac and dc voltages are two types of measurements made using only one channel of the comparator. For these cases, each EMF measurement is the average of 10 voltmeter readings taken in about 10 s.

A. Measurements of n

The factor n is ordinarily measured at 10 percent intervals from 50 to 110 percent of rated voltage. For instruments to be calibrated at rated voltage, however, n is usually determined at 80, 90, and 100 percent. In the middle voltage range, small accurate voltage steps are easily made and the stability of the system is optimum. Tests are made, therefore, most conveniently on the 100-V range of multirange TVC's, and the resulting n values are usable with any range when related to the TVC output, E. Low-voltage single-range TVC's are usually tested with additional resistance in series, so that 50–100 V may be applied. The output of the TVC is connected to the "STD" channel, and the operator enters the lowest and highest voltages applied. After the TVC has stabilized at the measurement voltage, the DAC balance is made as described above, and relay K2 is closed connecting the amplifier to the voltmeter. The TVC input is increased and decreased alternately by 0.1 V, ΔV, and the resulting changes in TVC output are computed from voltmeter readings.

With only dc applied, the relationship between small changes in input voltage, ΔV, and changes in the output voltage, ΔE, can be given by rewriting (1) as

$$\Delta V/V = \Delta E/nE \quad \text{or} \quad n = (\Delta E/E)/(\Delta V/V). \tag{7}$$

As in the two-voltmeter method, 10 voltmeter readings of the output are averaged to obtain one measured value. One ΔE is calculated from measurements taken in the sequence (V, $V + \Delta V$, V). The last reading with V applied from the previous set is then taken as the first reading in the next set. Four values of n are computed from four values of ΔE requiring nine voltmeter measurements. These data are then used to determine constants for a straight line from which the appropriate value of n can then be found for any value of E.

B. Comparison of AC and DC Voltages

AC voltage, such as from an ac calibrator, can be measured relative to a dc-reference voltage by a procedure similar to that used for the determination of n. The system applies dc+, ac, dc−, to a TVC in that order, and its output is monitored by the "STD" channel with the DAC balance and voltmeter readings performed as described above. Computations are made using (1) with $(E_a - E_d)$ computed from three voltage readings—e_1, e_2, e_3—so that

$$2(E_a - E_d) = e_1 + 2e_2 - e_3$$

where e_1 and e_3 correspond to the two directions of dc voltage, and e_2 to the ac voltage. Again, four values of EMF difference are computed from nine voltages—each being the average of 10 voltmeter readings. When low voltages are being compared, the voltage drops along the leads from the sources to the TVC may become significant. Dedicated cables are provide with total inner and outer resistance equal for both ac and dc. These connections also permit voltage sensing of the dc if required.

IV. Results

A significant reduction in the time required to perform routine calibrations is achieved with this system. Four determinations, for one set of test conditions, are made and averaged in about half the time required with our manual procedures. The voltage and frequency operating ranges, shown in Fig. 4, are determined primarily by the availability and cost of a programmable ac voltage source. The region between 100 kHz and 1 MHz represents a maximum volt-Hertz product of 10^7. Test

results taken over the operational region rarely differ by more than 10 ppm from data obtained manually. The standard deviation is generally less than 5 ppm in the middle-voltage and middle-frequency region indicated approximately by the cross-hatched region in Fig. 4. For well-constructed single-range TVC's, standard deviations of 2 ppm or less are achieved. At extreme voltages and frequencies standard deviations are usually less than 10 ppm. Although this system was built as a research tool for investigation of new thermal voltage conversion techniques and instruments, it has been used for some routine calibrations. Another system, of very similar design and dedicated to routine calibration work, is under construction. These automatic systems are expected to fulfill most of our TVC calibration requirements.

Acknowledgment

The authors would like to thank F. L. Hermach for his helpful suggestions.

References

[1] F. L. Hermach and E. S. Williams, "Thermal converters for audio-frequency measurements of high accuracy," *IEEE Trans. Instrum. Meas.*, vol. IM-15, pp. 260–268, Dec. 1966.

[2] E. S. Williams, "Thermal voltage converters and comparator for very accurate ac voltage measurements," *J. Res. Nat. Bur. Stand.*, vol. 75C, pp. 145–154, 1971.

[3] ——, "A thermoelement comparator for automatic ac–dc difference measurements," *IEEE Trans. Instrum. Meas.*, vol. IM-29, pp. 405–409, Dec. 1980.

[4] B. D. Inglis, "Evaluation of ac–dc transfer errors for thermal converter-multiplier combinations," *Metrologia*, vol. 16, pp. 177–181, 1980.

IEEE TRANSACTIONS ON INSTRUMENTATION AND MEASUREMENT, VOL. IM-32, NO. 1, MARCH 1983

An Automatic System for AC/DC Calibration

K. J. LENTNER, MEMBER, IEEE, AND DONALD R. FLACH, MEMBER, IEEE

Abstract—**An automatic ac/dc difference calibration system using direct measurement of thermoelement EMFs is described. The system operates over a frequency range from 20 Hz to 100 kHz, covering the voltage range from 0.5 V to 1 kV. For all voltages, the total uncertainty (including the uncertainty of the specific reference thermal converters used) is 50 ppm at frequencies from 20 Hz to 20 kHz, inclusive, and 100 ppm at higher frequencies up to 100 kHz. In addition to ac/dc difference testing, the system can be used to measure some important characteristics of thermoelements, as well as to calibrate ac voltage calibrators and precision voltmeters. Results of intercomparisons between the new system and the manual NBS calibration system, using single-range, coaxial-type, thermal voltage converters as transfer standards, are reported. The results indicate that the ac/dc differences measured are accurate to well within the combined total uncertainty limits of the two systems.**

Introduction

UNTIL RECENTLY, techniques for performing precision ac/dc difference measurements generally made use of manual testing methods which utilize photocell preamplifiers and light-beam galvanometers as voltage detectors, in conjunction with manually balanced comparators [1], [2]. Careful attention to the reduction of systematic and random uncertainties in measurement methods, thermoelements (TEs), and thermal voltage converters (TVCs) has resulted in sufficient confidence in test data to allow results to be reported with total uncertainties at the 10–100-ppm level (or better, in special cases) over wide voltage and frequency ranges [3], [4]. These manual test methods, however, are very time consuming and subject to errors due to operator fatigue and lack of skill. More recent work [5], [6] overcame some of the deficiencies of manual test methods. However, the referenced systems still require the use of a TE voltage comparator which is not available commercially. Because of the need to custom build it, the comparator adds to a system's cost and complexity.

Stringent requirements are placed on the measurement system to resolve low-level voltages (about 10 nV), and to overcome the effects of large temperature coefficients and dc reversal differences of the TEs, as well as instabilities of the voltage sources. However, with the advent of stable and accurate analog voltage amplification techniques in combination with digital electronics, digital voltmeters are available with stability, linearity, resolution, and accuracy sufficient to meet the requirements of automated ac/dc difference measurements. Programmable ac and dc voltage sources which lend themselves to adaption for automatic testing are also available. Advances in analog/digital interfaces have improved the ease with which computers can be used to control these instruments.

The system to be described in this paper was designed to overcome the deficiencies of present test methods by taking advantage of the technological advances described above. Specifically, some objectives were to: 1) utilize a desk-top computer; 2) use commercially available programmable instruments whenever possible; 3) eliminate as much operator intervention as possible in order that testing could be done completely automatically at one fixed voltage range of the test unit; 4) eliminate the additional cost and complexity of using a TE voltage comparator; 5) use test procedures which assure that the test TE's output EMF is held as constant as possible; 6) eliminate the effects of operator fatigue and lack of skill; and 7) achieve about the same level of uncertainty as is presently possible for general purpose ac/dc difference manual testing methods.

The system operates over a frequency range from 20 Hz to 100 kHz, covering the voltage range from 0.5 V to 1 kV. For all voltages, the total uncertainty (including the uncertainty of the reference TVCs used) is 50 ppm at frequencies from 20 Hz to 20 kHz, inclusive, and 100 ppm at higher frequencies up to 100 kHz. In addition to performing ac/dc difference tests, the system can be used to calibrate ac voltage calibrators or precision voltmeters. Furthermore, as will be discussed later, automatic measurements of a TE's dc reversal difference, response time, and the value of the exponent "n" in the expression relating a TE's heater current and output EMF can also be made.

System Hardware

The new system differs from most present techniques for ac/dc difference measurements in that no TE voltage comparator is used. Eliminating the comparator places additional requirements upon the stability of the system's ac and dc voltage sources, the digital voltmeter (DVM) which measures a TE's output EMF, and the switches which select a voltage to be measured by the DVM. The hardware development problem of obtaining low-thermal-EMF switches which could be automatically controlled was solved during previous work [5]. Manually operated low-thermal-EMF switches were modified by linking them to solenoids with 24-V operating coils energized by means of programmable relays.

TE voltages of about 10 mV must be measured to within about 10 nV to achieve 1-ppm comparison precision, and the

Manuscript received September 24, 1982. This work was partially funded by the Calibration Coordination Group of the U.S. Department of Defense.

The authors are with the Electrosystems Division, National Bureau of Standards, Washington, DC 20234.

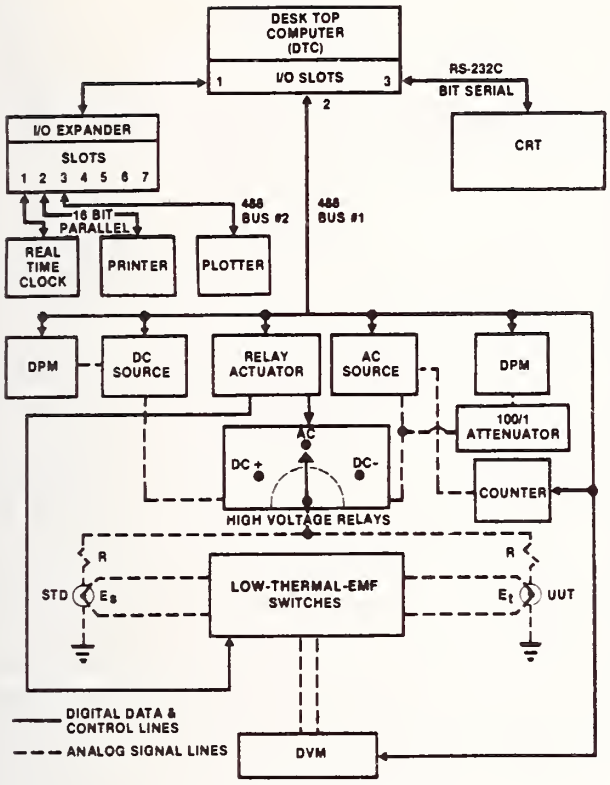

Fig. 1. System block diagram.

DVM used to measure these voltages has the resolution necessary to make such a voltage measurement when extensive averaging of data is used. The DVM has an input resistance of about 10 GΩ, a 60-Hz common-mode noise rejection >140 dB, and a dc common-mode noise rejection >150 dB. On its most sensitive (10-mV) range, the peak-to-peak low-frequency (dc to about 10 Hz) noise of the DVM, with its input shorted, was measured to be about 50 nV.

The dc voltage source has 10-V, 100-V, and 1-kV ranges with six-digit voltage setting capability on each range. Its specified accuracy is 50 ppm of setting to 10 V, and 100 ppm above 10 V. The ac voltage source also has six-digit voltage setting capability for voltage ranges of 1 V, 10 V, 100 V, and 1 kV, with specified accuracies in the range of about 0.02 to 0.1 percent depending on voltage and frequency ranges. Some typical results of stability tests of these sources will be discussed later.

A block diagram of the system is shown in Fig. 1. The desk-top computer serves as the system controller and has about 60 kbytes of user-available memory. Magnetic tape cartridges are used for program and data storage. A video display terminal (CRT) is used for data display during testing and also as an aid during software development. Since the computer only has three input/output slots, an I/O expander is needed to accomodate the required instrumentation. The real-time clock is used for precise control of the time interval between applications of ac or dc voltages during a test, and the printer and plotter provide test records.

As indicated in Fig. 1, communication between the computer and the stimulus and measurement instrumentation is via the IEEE-488 bus. The digital panel meters (DPM's) monitor the voltage outputs from the dc and ac sources. During testing, readings of both the dc and ac source's output voltages are obtained by the DPMs. These voltage readings are made before the voltages are applied to the test circuit. If the measured voltages differ by more than 0.5 percent from the programmed values, the test is automatically aborted. High accuracy in these voltage readings is not necessary, since TVCs can readily withstand an applied voltage which is 120 percent of rated value. For the ac source, the output voltage is attenuated by a factor of 100 before being connected to the DPM. The attenuation is necessary in order to overcome the voltage-frequency product limitation of the DPM. The counter shown in Fig. 1 monitors the frequency of the ac source. If the counter reading differs by more than about 10 percent from the programmed frequency, the test is automatically aborted. The relay actuator is used to apply 24-V dc to the operating coils of the high-voltage relays as well as to the coils of the solenoids which operate the low-thermal-EMF switches. These switches select the output voltage of the standard TE (E_s) or the unit-under-test TE (E_t). The voltages, E_s and E_t, are applied directly to the input of the DVM, and the DVM voltage readings are then stored in the computer's memory for later processing.

AC/DC Test Procedure

One of the advantages of using a TE voltage comparator is that, since small differences between the standard and test TE EMFs are measured directly, the output EMF of the test TE can be allowed to drift slightly from its reference EMF value when ac, +dc, or −dc voltages are applied [2], [6]. In this new system, since no TE voltage comparator is used, the requirement for holding the test TE's EMF constant is quite stringent. However, with automation and the rapid response time of the voltage sources (typically 50 μs for the dc source and a few milliseconds for small voltage changes for the ac source), the constant output requirement can be readily satisfied. The techniques used will be discussed in this section.

For a TVC with response defined by $E = KV^n$, where E is the output EMF of the TE in the TVC, V is the voltage applied, and K and n are parameters characteristic of the particular TVC, the ac/dc difference is defined as

$$\delta = \frac{V_a - V_d}{V_d} \tag{1}$$

where V_a is the applied ac voltage, and V_d is the average of the two polarities of dc voltage; i.e.,

$$V_d = \frac{V_+ + V_-}{2}. \tag{2}$$

V_a, V_+, and V_- are voltage values which give the same output EMF of the TE. In a manual test system using a TE voltage comparator, the voltage difference $V_a - V_d$ is determined by a second TVC, the standard. If the standard's response is defined as

$$E_s = K_s V_s^{n_s} \tag{3}$$

it can be shown [2] that the ac/dc difference of the test TVC is

$$\delta_t = \frac{E_{sa} - E_{sd}}{n_s E_{sd}} + \delta_s = \frac{dE_s}{n_s E_{sd}} + \delta_s \tag{4}$$

where E_{sa} is the standard TE's EMF when the voltage V_a is applied, E_{sd} is the standard TE's average EMF when voltages V_+ and V_- are applied (cf. (2)), n_s is the standard's dimensionless characteristic n, and δ_s is the ac/dc difference (in parts per million) of the standard determined as described in [1], [2]. Equation (4) is consistent if dE_s is in nanovolts, E_{sd} in millivolts, and the "δ's" are in parts per million. During a test, V_a, V_+, and V_- are adjusted until the same EMF of the test TVC is obtained in each case when these voltages are applied in sequence.

In the automated system, the test TVC's output EMF is held constant in the following manner. With a dc voltage applied to the test TVC, an output EMF, E_{set}, is measured which is called the "set-point" voltage. In all subsequent applications of ac and dc voltages to the test circuit of Fig. 1, the computer is used to adjust the voltage applied so that the test TVC has an output very nearly equal to E_{set}. A four-step procedure is used for making ac/dc difference measurements. The procedure consists of applying a sequence of ac, +dc, −dc, and ac voltages to the unit under test at approximately equal time intervals. The following operations are performed for each step in the procedure presently used with the system.

First, the nominal ac or dc voltage is applied, the test EMF, E_t, is measured, and a difference voltage, dE_t, is calculated as

$$dE_t = E_{\text{set}} - E_t. \tag{5}$$

If the difference voltage is not sufficiently small, as discussed below, a voltage correction, dV_t, is calculated from

$$dE_t/n_t E_t = dV_t/V_t. \tag{6}$$

Hence

$$dV_t = dE_t V_t/n_t E_t. \tag{7}$$

The correction, dV_t, is added to the nominal voltage, V_n, and a "reset" voltage, $V_r = V_n + dV_t$, applied. The test EMF, E_t, is measured again, and a second voltage correction, dV_2, is calculated using (5) and (7). The output EMF of the standard TE, E_s, is now measured. A correction for the EMF of the standard TE, dE_s, is calculated, using dV_2 to compensate for any deviation of the actual EMF of the test TE from the set point E_{set}; i.e.,

$$dE_s = (n_s E_s dV_2)/V_r. \tag{8}$$

The corrected EMF for the standard TE is then

$$E_{s1} = E_s + dE_s. \tag{9}$$

After completing the sequence of four steps by applying successively ac, +dc, −dc, and ac voltages, the ac/dc difference of the test TVC, δ_t, is calculated as

$$\delta_t = \frac{E_a - E_d}{n_s E_{sd}} + \delta_s \tag{10}$$

where E_a is the average of the standard's corrected EMFs determined for the two applications of ac voltage; E_{sd}, n_s, and δ_s are as defined in (4); and E_d is

$$E_d = \frac{E_{s1+} + E_{s1-}}{2} \tag{11}$$

where E_{s1+} is the corrected EMF calculated as in (9) when +dc is applied, and E_{s1-} is the corrected EMF when −dc is applied.

In the computations previously discussed, account is taken of the finite resolution of the ac and dc voltage sources. The voltage setting remains unchanged if the EMF output of the test TVC is close enough to the set-point voltage (E_{set}) that a least significant digit change in the voltage source's output will provide no decrease in the magnitude of the calculated difference dE_t.

A test run consists of four determinations of ac/dc difference, and the average of the four determinations is calculated and printed on the system's printer. In general, three runs are normally made at each test voltage and frequency.

In order to increase the reliability of the EMF measurements made by the DVM, ten readings are automatically taken and the standard deviation of an observation of the ten readings is calculated. If the deviation is >300 nV, the average EMF value is discarded and the series of ten readings is repeated. Up to ten attempts are made to obtain an average EMF value with a standard deviation ≤300 nV, and the test is aborted if the tenth attempt is unsuccessful.

As the preceding equations show, the values of the exponent n for both the test and standard TVCs must be known. The exponent varies with applied voltage, and its variation can be determined by doing "n tests." These tests will be discussed in the next section. For the standard TEs, the coefficients in the equation expressing the value of n as a function of output EMF are stored in a data file in the system software. Once the operator has specified which standard TE is being used, the standard TE's output EMF is measured with a +dc voltage applied, and the value of n_s is automatically computed. The values of the test TE's coefficients for n must be manually typed into the computer at the beginning of a test. To guard against mistakes in entering data, the computed values of n for the test TE must be within the limits 1.4 to 2.1.

An additional safeguard is contained in the ac/dc difference program to avoid application of voltages great enough to damage the TEs. When the reset voltage, V_r, is calculated, its value must be less than 120 percent of the rated voltage of the TVC. If the calculated reset voltage is outside this limit, the program aborts.

Other System Capabilities

As mentioned above, the system can readily be used to calibrate ac voltage calibrators using TVCs with known ac/dc differences. The output voltage of the test calibrator replaces the output voltage of the system's ac source, and the test calibrator's correction can be determined in terms of a calibrated

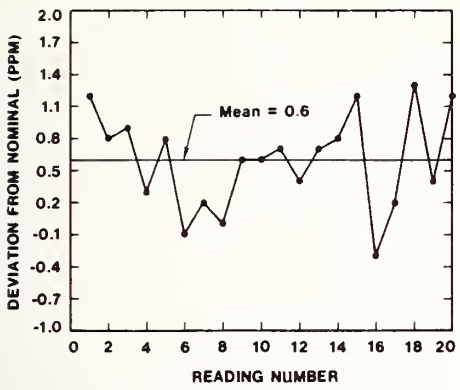

Fig. 2. DC voltage source stability, 10 V.

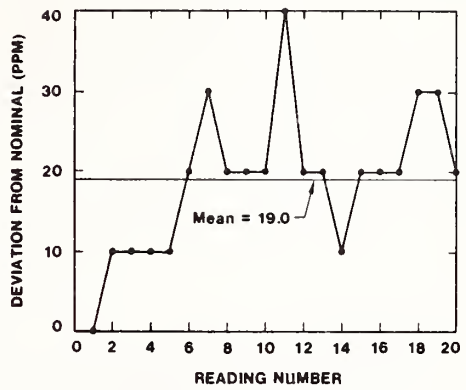

Fig. 3. AC voltage source stability, 10 V—20 kHz.

dc source and the known ac/dc differences of the standard voltage converters used.

The correction to the test calibrator (in ppm) is

$$C_t = \frac{E_a - E_d}{n_s E_d} + \delta_s + C_{dc} \tag{12}$$

where E_a is the measured EMF of the TVC with ac voltage applied, E_d is the average EMF with direct voltage of both polarities applied, n_s is as previously defined, δ_s is the correction (in ppm) to the standard, and C_{dc} is the correction (in ppm) to the dc voltage source's nominal output obtained from calibration data. As in the case of ac/dc difference tests, the correction is in parts per million if $E_a - E_d$ is in nanovolts and E_d in millivolts.

To control the variability in the test data, it is important to make sure that the voltage sources are quite stable. Thus a program was written which uses the system's DVM to measure the stability of the voltage sources with time.

Fig. 2 illustrates typical stability test data for the dc source. At a nominal setting of 10 V, 20 voltage readings were taken over a time interval of about 20 min. The deviation of the measured voltage (in ppm) from the nominal voltage is defined as

$$\frac{\Delta V}{V} = \frac{V_1 - V_2}{V_2} \times 10^6 \tag{13}$$

where V_1 is the measured value, and V_2 is the nominal value. The maximum deviation measured was 1.3 ppm and the mean deviation was 0.6 ppm. The standard deviation of an observation was 0.5 ppm, and the 3σ limits for the mean were ± 0.3 ppm. These results indicate that the dc source has acceptable stability and is well within its specified accuracy of 50 ppm.

Typical results for a test of the ac source's stability are shown in Fig. 3. Again, 20 readings were obtained during a 20-min time interval. The test voltage was 10 V at a frequency of 20 kHz. Here the range of deviations was 40 ppm with the mean being 19 ppm. The standard deviation of an observation was 9 ppm, and the 3σ limits for the mean were ± 6 ppm. The discrete 10-ppm steps in the plotted data are due to the fact that the DVM's resolution on its 10-V range is limited to 10 ppm.

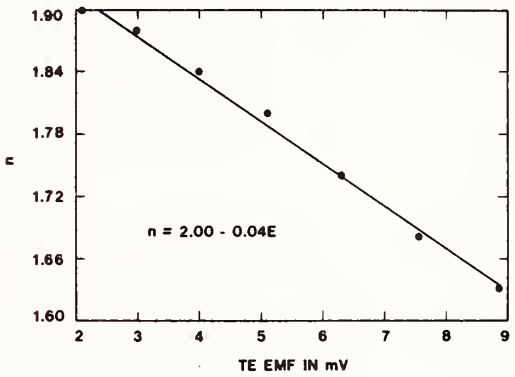

Fig. 4. Typical n-test data.

As mentioned in the previous section, one important test that is readily performed automatically is that of determining a TVC's "n" characteristic. Typical results for a 2.5-mA, VHF-type TE which was tested with a nominal 3-V range resistor are illustrated in Fig. 4.

The characteristic n is defined by

$$n = \frac{\Delta E/E}{\Delta V/V} \tag{14}$$

where ΔE is the measured change in output EMF for small changes in applied voltage ΔV, V is the nominal test voltage for the TVC, and E is the measured EMF at the nominal test voltage. ΔV is programmed to be ± 0.5 percent of nominal test voltage V. Sufficient time is allowed after each voltage change for the TE to reach its final EMF value.

For the results shown in Fig. 4, the TVC was tested from 50 to 110 percent of rated voltage. The total elapsed time to obtain the seven data points was about 1.25 h.

Each value of n is computed as the average of four determinations at any given voltage. A least squares analysis of the data provides the option of obtaining a fitted curve using up to a fourth-degree polynomial. An analysis of variance table and residual standard deviation are computed and printed so that the "goodness of fit" of the computed equation for n as a function of TE output EMF can be determined. The printed

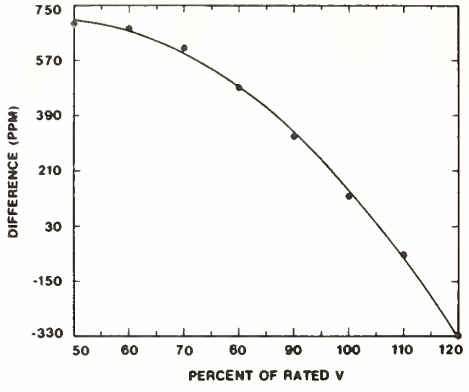

Fig. 5. Constant input reversal difference, Δ.

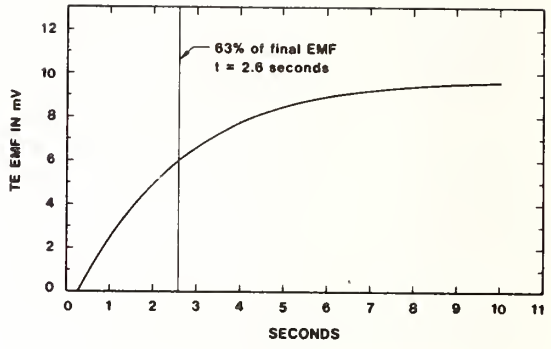

Fig. 6. Typical response time of a TE.

data sheet also shows the values of n(measured) − n(computed). The figure shows an example of a linear fit which, in most cases, provides sufficent accuracy. The coefficients 2.00 and −0.04 are either stored in the computer's data file (for a standard TE) or are typed by the operator into the computer program for the TE under test at the beginning of an ac/dc difference test.

The dc reversal difference (DCRD) of a TE can also be readily determined. DCRD is defined as the difference in applied values of both polarities of dc voltage required to produce an equal output EMF (or "constant output") of the test TE [7]. In order to facilitate DCRD measurements, a "constant input" EMF, Δ, is actually measured. This Δ is related to the DCRD by a factor of $1/n$ as

$$\text{DCRD} = (1/n)(\Delta) = (1/n)\left\{\frac{E_+ - E_-}{\left(\frac{E_+ + E_-}{2}\right)}\right\} \qquad (15)$$

where E_+ and E_- are the TE output EMFs with equal +dc and −dc (or "constant input") voltages applied, and n is as previously defined.

During acceptance tests of some TEs, the data showed much greater variation of DCRD from unit to unit than had been expected. The only information available indicated that the DCRD should reach a maximum value between 70 to 80 percent of rated heater current and should approach a zero value close to 100 percent of rated current. The results obtained did not substantiate this information. Hence, a program was written to determine the DCRD as a function of applied voltage. Typical results for a 5-mA, UHF-type TE tested with a 60-V range resistor are shown in Fig. 5. In this test, the voltage was varied from 50 to 120 percent of its rated value in 2-percent increments. For the sake of clarity in the figure, not all of the actual 36 data points are shown. It should be noted that the plotted data show Δ; hence, the DCRD values referred to a constant output EMF would be smaller by the factor of n (see (15)). In this test, the maximum Δ was about 700 ppm at 58 percent of rated voltage, and the minimum was about −330 ppm at 120 percent of rated voltage.

At the time the DCRD testing program was developed, the information on DCRD variation was limited. However, in the intervening time Inglis [8] has published a substantial amount of information in this area. Investigations at NBS have not been as extensive as those of Inglis, but, in general, the results obtained are in agreement with his published data.

The response time of a TE is also a characteristic which can readily be measured using the automatic system. Response time is obtained by making measurements of a TE's EMF when full rated voltage is suddenly applied to the TE. The calculated response time t is the time taken for the output EMF to reach $1 - (1/e)$ of its final value. Typical results for a 2.5-mA, VHF-type TE are shown in Fig. 6.

Measurement Results and Uncertainties

Manual calibration systems have been in operation for many years at NBS, and their uncertainties have been documented [1]-[3]. DC reversal difference, self-heating and ambient temperature effects, drift effects due to nonequal time intervals between the EMF measurements, unbalanced lead impedances, induced voltages from electromagnetic fields, and operator fatigue and lack of skill are some of the more common sources of error. The process of determining an estimated total uncertainty for a system is based upon 1) a history of measurement results; 2) careful measurements of standards with accurately known corrections; 3) theoretical analysis of sources of errors, along with, preferably; 4) intercomparison tests using two independent test methods [3]. A combination of 2) and 4) was used for the initial evaluation of the automated system. The primary emphasis was placed on comparison of results obtained with a well-characterized manual system and those obtained with the new system.

A single-range (3-V), coaxial-type TVC was tested using established manual techniques, followed by tests on the automated system. The results obtained from the two test systems are shown in Table I.

For the automatic system, the values reported are the average of 12 determinations of the transfer standard's ac/dc difference. The random uncertainty was calculated as three times the standard deviation of the mean of the 12 observations, with the result that $3\sigma = 21$ ppm for the worst case. In each case, the differences between the results obtained with

TABLE I
3-V TVC AC/DC DIFFERENCE (ppm)

Frequency kHz	Manual	Automatic	Difference
0.02	0	2	-2
20	1	-9	10
50	-1	-9	8
100	-1	-4	3

TABLE II
10-V TVC AC/DC DIFFERENCE (ppm)

Frequency kHz	Manual	Automatic	Difference
20	-4	-17	13
50	-3	-7	4
100	-1	6	-7

TABLE III
50-V TVC AC/DC DIFFERENCE (ppm)

Frequency kHz	Manual	Automatic	Difference
5	29	26	3
10	56	52	4
20	121	121	0
50	320	310	10

the two test methods are less than the total uncertainty of the manual test system, which is 20 ppm for all voltages for frequencies in the range 0.02–20 kHz, 30 ppm for 20–50 kHz, and 50 ppm for 50–100 kHz (the lower uncertainty applies at the crossover frequencies).

A second test was made using a 10-V range TVC as a transfer standard. The test results are listed in Table II.

Both the 3-V and 10-V TVC transfer standards had small ac/dc differences. Therefore, a third intercomparison test was conducted using a transfer standard with large, but accurately known differences. The results of this test are listed in Table III.

The test results summarized in the three tables suggest a possible systematic uncertainty since the automatic system gave lower values for all but three test frequencies. Further investigation is required to evaluate whether or not this uncertainty is significant, and a multirange transfer standard is presently being evaluated.

Conclusions

The results indicate that it is feasible to make fully automatic precision ac/dc difference measurements at one voltage. The principal advantage of the system is the elimination of the need for any type of manually or automatically balanced TE comparator, permitting the system to be assembled using commercially available instrumentation, except for the switching modules. This approach, therefore, should make automation attractive to many calibration laboratories faced with the need to make ac/dc difference measurements. Moreover, the system can be used as a nearly self-calibrating meter calibration system. Measurements can be done with minimal operator intervention, eliminating tedious and fatiguing manual operations. Hence, personnel presently engaged almost exclusively in manual ac/dc difference tests can be freed to do other work. Experience obtained during many years of testing with manually operated systems at NBS has shown that the precision of the test results is dependent upon operator skill. The automatic system's precision is independent of operator skill, eliminating this variable in the experimental uncertainty.

Acknowledgment

The authors are indebted to M. S. Carter who wrote much of the software and solved many difficult programming problems encountered in developing the system. S. G. Tremaine, L. Freeman, and E. V. Byland also made valuable contributions to some of the programs which have become part of the total system software. C. B. Childers helped greatly by doing the measurements on the manual system. Acknowledgment goes to B. A. Bell for his conceptual ideas and continuing support in the development of this system.

References

[1] F. L. Hermach and E. S. Williams, "Thermal converters for audio-frequency voltage measurements of high accuracy," *IEEE Trans. Instrum. Meas.*, vol. IM-15, pp. 260–268, Dec. 1966.

[2] E. S. Williams, "Thermal voltage converters and comparator for very accurate ac voltage measurements," *J. Res. Nat. Bur. Stand.* (U.S.), vol. 75C, pp. 145–154, Dec. 1971.

[3] F. L. Hermach, "AC-DC comparators for audio-frequency current and voltage measurements of high accuracy," *IEEE Trans. Instrum. Meas.*, vol. IM-25, pp. 489–494, Dec. 1976.

[4] R. S. Turgel, "A comparator for thermal ac-dc transfer standards," *ISA Trans.*, vol. 6, no. 4, pp. 286–292, 1967.

[5] K. J. Lentner *et al.*, "A semiautomatic system for ac/dc difference calibration," *IEEE Trans. Instrum. Meas.*, vol. IM-29, pp. 400–405, Dec. 1980.

[6] E. S. Williáms, "A thermoelement comparator for automatic ac-dc difference measurements," *IEEE Trans. Instrum. Meas.*, vol. IM-29, pp. 405–409, Dec. 1980.

[7] "American national standard for ac-dc transfer instruments and converters," ANSI C100.4—1973, Amer. Nat. Stand. Inst., Inc., 1430 Broadway, New York, NY 10018.

[8] B. D. Inglis, "Errors in ac-dc transfer arising from a dc reversal difference," *Metrologia*, vol. 17, pp. 111–117, 1981.

AC VOLTAGE CALIBRATIONS FOR THE 0.1 Hz TO 10 Hz FREQUENCY RANGE

Howard K. Schoenwetter

The development of voltmeters to meet the need for rms voltage measurements in the infrasonic frequency range is discussed as well as the need to trace these measurements to the U.S. legal unit of voltage. A new method for supporting voltage measurements in the 0.1 Hz - 10 Hz range was described in a 1979 paper and is discussed further. The principles of the method are embodied in detailed procedures given for calibrating sine-wave voltage standards and rms voltmeters over the 0.1 Hz - 10 Hz frequency range, using the NBS AC Voltmeter/Calibrator. The sine-wave calibrator of this instrument, used for these calibrations, has an accuracy of 0.020 percent over the 0.5 mV - 7 V range.

Key words: ac voltage calibrations; ac voltage calibrators; ac voltage standards; infrasonic voltage measurements; low-frequency voltage measurements; rms voltmeters.

1. INTRODUCTION

Calibrated vibration transducers are required in laboratories and test facilities to determine the acceleration of vibration exciters, tables, and fixtures. They are also used to measure the vibrations in many other types of machines and structures, including prototype models of military, space, and commercial vehicles undergoing qualification testing. In past years, calibrations of these transducers at frequencies below 2 Hz were either omitted or performed with uncertain accuracy. This was because the voltmeters available for measuring the transducer outputs at these frequencies had questionable accuracy and excessively long response times (15 to 20 periods of the measured voltage).

In 1976, an rms digital voltmeter (DVM) was developed at the National Bureau of Standards (NBS) to support vibration measurements over the 0.1 Hz - 50 Hz range.[1] It was designed to measure voltages from 2 mV to 10 V with an uncertainty of approximately 0.1 percent of reading. The maximum response time of 40 seconds corresponds to four periods of the lowest frequency signal that can be measured. Since the means for calibrating the voltmeter to the required accuracy did not exist, a voltage calibrator was developed and incorporated

[1]This work was supported, in part, by the DC and Low Frequency Calibration Coordination Working Group of the Department of Defense.

into the same instrument. This calibrator, providing bipolar dc voltages and sine-wave voltages at frequencies of 0.1, 0.2, 0.5, 1, 2, 10, and 50 Hz, was intended not only for calibration of the companion voltmeter but also for the calibration of other low-frequency voltmeters.

During the 1976-77 period, the NBS AC Voltmeter/Calibrator was used at the Metrology and Calibration Centers of Redstone Arsenal (Army) and Newark Air Force Base, as well as the Vibration Section at NBS, to measure vibration transducer outputs and to calibrate other ac voltmeters [1][2]. Except for the need of a 5-Hz calibration frequency,[3] the instrument met all present and expected future requirements for support of voltage measurements at very low frequencies.[4] Consequently, a detailed instruction manual and an archival paper were written to facilitate reproduction of the instrument [2]. A commercial instrument based on the NBS design later became unfeasible because the ac voltmeter portion utilizes a multi-junction thermal converter (MJTC), which has been available only in limited quantities from one manufacturer. Subsequent to the development of the NBS AC Voltmeter/Calibrator, at least two other instruments have been developed which can measure voltages at infrasonic frequencies. NBS has developed a Low Frequency AC Samping Voltmeter which has approximately 0.1 percent uncertainty and a nominal maximum response time of two periods of the lowest frequency signal (0.1 Hz) that can be measured [3,4].[5] Also, a large instrumentation manufacturer has developed a multimeter with a sampling voltmeter, operable down to 0.1 Hz or lower. However, the accuracy and response time of the voltmeter depend upon the frequency of the measured voltage.

As the number of ac voltage measurements in the 0.1 Hz - 10 Hz range increases, because of the greater availability of suitable voltmeters, the need increases for tracing these measurements to the U.S. legal unit of voltage. Selecting the best method for effecting this traceability is discussed next.

---

[2]Numbers in brackets refer to the literature references listed at the end of this report.

[3]This calibration frequency was added later.

[4]Commercial voltage calibrators operate at frequencies down to 10 Hz and can be calibrated using conventional ac-dc transfer measurements. Also, a number of commercial voltmeters function satisfactorily above 10 Hz; therefore, the voltage measurement and calibrator capability above 10 Hz were not considered vital.

[5]Six of these units have been made by NBS, and supplied to each of the DoD metrology laboratories. They were calibrated by using the NBS AC Voltmeter/Calibrator as a reference standard.

2. A METHOD FOR INFRASONIC VOLTAGE MEASUREMENTS

Standards laboratories calibrate ac voltage standards against dc voltage standards, using thermal voltage converters (TVCs) to make the ac-dc voltage comparisons. Calibrations of the dc voltage standards and TVCs are traceable to reference standards maintained by NBS. Theoretical and practical limitations arise in calibrating TVCs (measuring their ac-dc difference), and employing them to make calibrations at the lower infrasonic frequencies [5].[6] These limitations cause the calibrations to be slow, costly, and inaccurate, particularly at frequencies below ~2 Hz. For these reasons, a new method was proposed in [5] for supporting ac voltage measurements below 10 Hz, which supplements the existing method as shown in figure 1. The primary objective of the new procedure is to make it feasible to equip standards laboratories with easily calibrated multi-range sine-wave standards, which operate at frequencies of 0.1, 0.2, 0.5, 1, 2, 5, and 10 Hz. These voltage sources would be used mostly to calibrate voltmeters at these frequencies over the voltage range of approximately 0.5 mV - 7 V rms.[7]

The proposed equipment and procedures for testing a multi-range voltage source are described in sections IV and V of [5]. Central to the method is a single voltage level sine-wave reference source with frequencies of 0.1, 0.2, 0.5, 1, 2, 5, and 10 Hz, whose amplitude variation with frequency (frequency response) is calibrated and has excellent long-term stability. This unit serves as a voltage transfer standard. By adjusting the output of the multi-range source to be approximately the same as the voltage level of the reference, the frequency response of the source can be determined from ac-ac comparisons, using an rms transfer voltmeter. Following this step, the voltage level at each frequency is established by calibrating the unit at 10 Hz, using a dc voltage standard and a TVC to make an ac-dc transfer measurement.

Except for the rms voltmeter contained in the NBS AC Voltmeter/Calibrator, existing rms voltmeters do not have the necessary high resolution and small differential nonlinearity to make ac-ac comparisons for calibration work.[8] Until rms voltmeters suitable

---

[6] For convenience, reference 5 is included at the end of this report.

[7] Present commercial ac voltage calibrators either have insufficient accuracy over this voltage range or only operate above 10 Hz.

[8] A transfer voltmeter must be able to measure voltage differences as small as 20 ppm of the measured value, both voltages being of the same frequency. The ac-dc difference and accuracy of the voltmeter are not critical, however.

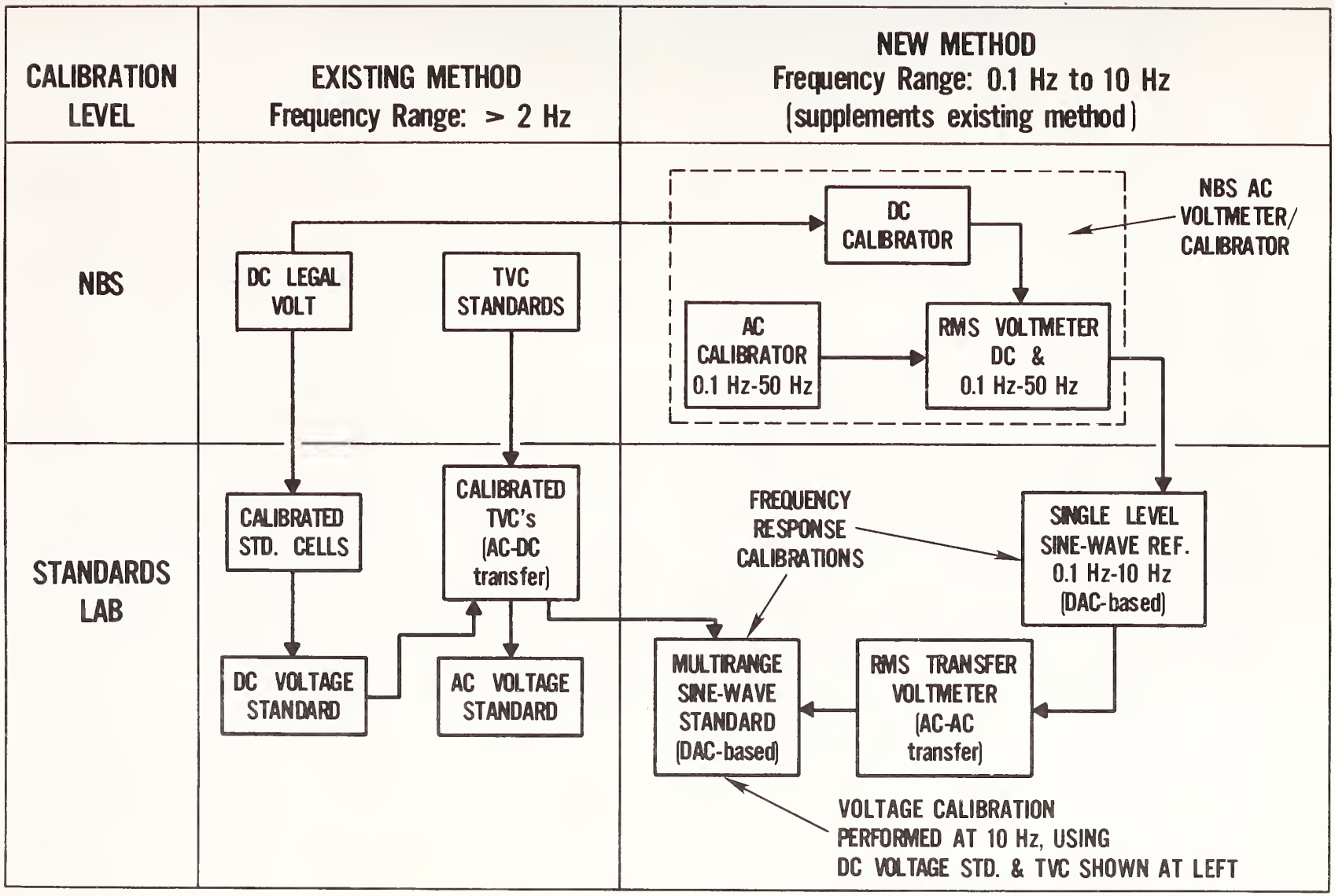

Figure 1. New method for supporting ac voltage measurements at frequencies below 10 Hz.

for this work become available, calibration of multi-range sine-wave voltage sources[9] and rms voltmeters will be performed at NBS. Procedures for these calibrations are discussed in sections 4 and 5.

Since the ac calibrator portion of the NBS AC Voltmeter/Calibrator (see fig. 1) would be a suitable multi-range voltage standard for use by standards laboratories, the detailed design of this circuit is given in appendix B. The methods used to calibrate the unit are included in the calibration procedure described in the next section.

3. CALIBRATION OF NBS AC VOLTMETER/CALIBRATOR

As described in [2] and [5], the NBS AC Voltmeter/Calibrator consists of an rms digital voltmeter and a calibrated voltage source which can function as either a dc or ac voltage calibrator. The rms voltmeter consists of an input amplifier, rms/dc converter, and dc DVM.

The ac voltage calibrator is used to calibrate ac voltmeters and is used in conjunction with the rms voltmeter to calibrate ac voltage sources. The procedure used to calibrate the ac voltage calibrator is shown in figure 4 of [5]. To perform this calibration, the frequency response of the ac calibrator and the ac-dc difference of the rms/dc converter must be known from prior measurements. All of these calibrations are listed below and are discussed in this section.

(1) Frequency response and voltage calibrations of the ac voltage calibrator.

(2) Calibration of the laboratory dc voltage standard (standard cell).

(3) Calibration of the dc calibrator.

(4) AC-DC difference calibration of the rms/dc converter.

The errors associated with the items listed above all contribute to the estimated uncertainty assigned to the ac calibrator voltage and will be summarized after these calibrations have been described.

Several refinements were made recently to simplify the task of calibrating the AC Voltmeter/Calibrator and to improve its overall performance. These changes are also discussed in this section.

---

[9]Assuming that the voltage standards employ a D/A converter for the sine-wave generation, a frequency response (relative voltage) calibration is preferable to a conventional voltage calibration.

3.1 Calibration of AC Voltage Calibrator

Calibration of the ac voltage calibrator consists of two calibrations: (1) a frequency response calibration in which the calibrator voltages at 5, 2, 1, 0.5, 0.2, and 0.1 Hz are compared with the voltage at 10 Hz, and (2) a voltage calibration at 10 Hz.

3.1.1 Frequency Response Calibration of AC Calibrator

The frequency response of the ac calibrator was originally determined using peak-to-peak and rms measurements, the latter being made with the rms voltmeter and limited to the 1 Hz - 10 Hz range [2]. Average-value measurements were later combined with the above results [5]. Since the peak-to-peak method uses a storage oscilloscope to exhibit the voltage peaks, the measurements are somewhat subjective and are considered less reliable than the average-value measurements; therefore, only the latter (along with limited rms measurements) are now used for the frequency response calibrations. The precision rectifier-filter circuit used for these measurements is represented by figure 5 of [5]. This circuit and associated power supply are contained in a separate shielded enclosure. The justification for basing the rms frequency response of the ac voltage calibrator on average-value (or peak-to-peak) measurements is given in [5].

Figure 2 shows the front panel operating controls of the NBS AC Voltmeter/Calibrator. The 5 Hz and 0.1 Hz frequencies are selected with the CAL FREQ switch in the 10 Hz and 0.2 Hz positions, respectively, using the rear panel "5 Hz-10 Hz" and "0.1 Hz-0.2 Hz" switches (see fig. 3). For average-value measurements, the precision rectifier circuit is connected between the CAL OUT terminals and the AVE. VOLT. IN terminals (rear panel) with the PREC RECT-INTERNAL switch in the PREC RECT position. In this switch position, the rms/dc converter is disconnected and the output of the precision rectifier is connected to the input (point o) of the voltmeter's low pass filter (see fig. 2 of [5]). A dc voltage level of 5 V (nominal) at this terminal corresponds to a full-scale indication of the voltmeter. Therefore, the full-scale voltmeter reading is normalized to whatever range is selected by the V-RANGE-MV switch. Since full-scale readings of 10000.0, 5000.0, 2000.0, 1000.00, --- result from range selections of 10, 5, 2, 1, --- volts, it is seen that the best resolution is obtained with the 10, 1, 0.1 or 0.01 V ranges. (Unless indicated otherwise, the PERIOD is set to 10 for all measurements.) The 10 V range has been arbitrarily selected for the frequency response measurements. Because the rms/average ratio for a sinewave is ~1.11, the ac calibrator should be set to approximately 5.55 V to yield a full-scale output of 5 V from the rectifier-filter circuit. (The "÷100" attenuator switch, not shown in fig. 2, should be kept in the OUT position. Also, the FUNCTION switch should be in the MEAS position.)

Figure 2. Front panel view of NBS AC Voltmeter/Calibrator.

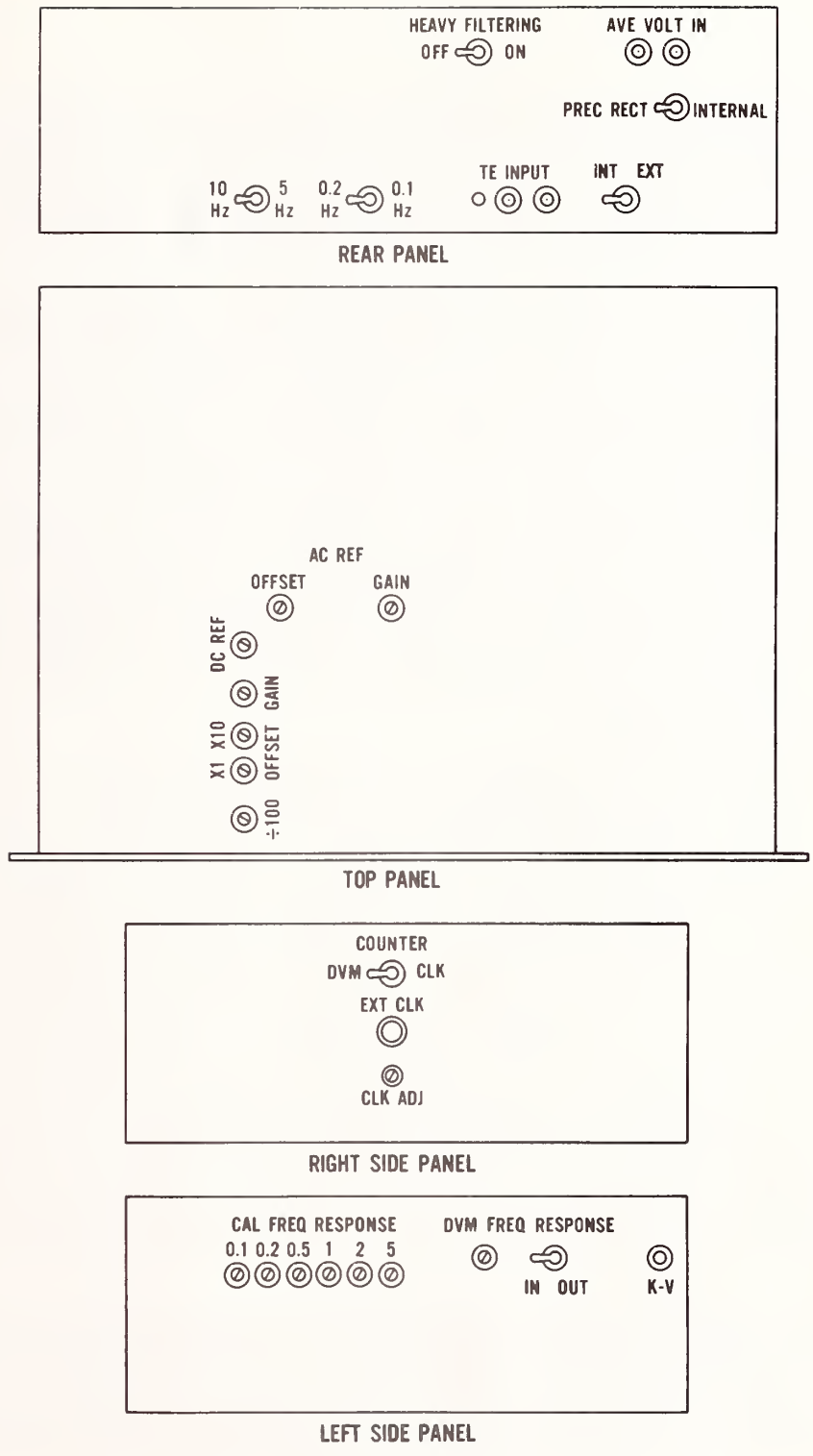

Figure 3. Controls and connectors on rear, top, and side panels of AC Voltmeter/Calibrator.

The dc DVM employed in the rms voltmeter of the NBS AC Voltmeter/Calibrator (fig. 2 of [5]) consists of a V/F converter and a counter-timer which counts the output pulses from the V/F converter over periods of 1 s or 10 s (PERIOD set to 1 or 10), determined by a crystal-controlled oscillator. An integrating voltmeter was used to effectively reduce the ripple in the output voltage from the low-pass filter, to minimize fluctuations in the displayed voltage. The frequency of the ripple voltage in the outputs of both the rms/dc converter and the precision rectifier circuit is twice the frequency of the input voltage to these circuits. If the counter period (integration period) includes an integral number of ripple periods, the ripple in the dc voltage applied to the dc DVM will integrate to zero [2].[10] Therefore, fluctuations in the indicated voltage from ripple are zero for frequencies of 0.05, 0.1, 0.15, --- Hz, which include the nominal values of the calibrator frequencies. (An integration period of 10 s must be used for frequencies of 0.5 Hz and less.) To allow for some deviation from these frequencies by the AC Voltage Calibrator, ripple filtering in the low-pass filter and rms/dc converter can be increased (with respect to the original design) using the HEAVY FILTERING switch on the rear panel of the AC Voltmeter/Calibrator.

The effect of this filtering on rms measurements will be discussed later. When the precision rectifier is used, the additional filtering limits the measured peak-to-peak ripple voltage to ±0.30 percent of the dc voltage applied to the dc DVM when the input frequency is near 0.1 Hz. (The ripple voltage is much less near the higher calibrator frequencies.) The computed maximum peak-to-peak fluctuation in the DVM readings is approximately ±30 ppm for each percent deviation in frequency from 0.1 Hz. For all calibration work, the calibrator frequencies should be held within ±0.05 percent of their nominal values so that the effect of ripple on DVM readings is negligible (±1.5 ppm or less, based on the preceding statements). The calibrator frequencies are at their nominal values when the clock frequency, from which they are derived, is 6400 Hz. The clock frequency is easily held with ±0.05 percent of 6400 Hz, since observed daily frequency variations are usually less than ±2 Hz (±0.03%). The frequency can be adjusted by the CLK ADJ pot and is displayed by the counter-timer when the COUNTER switch is in the CLK position (see fig. 3).

Worst-case DVM reading errors caused by ripple voltage can be avoided by using the average of several successive readings instead of a single reading, since the ripple integrations in the dc DVM will vary in size and usually are of both polarities. Therefore, the average value is more accurate than the worst-case single reading

[10] In other words, the ripple voltage integrates to zero if a time interval equal to two counter periods includes an integral number of input signal periods.

value. Unless indicated otherwise, maximum filtering (FILTER FREQ switch in position L and the HEAVY FILTERING switch on) should be used for all calibration work. With maximum filtering, the DVM settling time to within 5 ppm is about 2 minutes. This response time must be considered when devising the measurement procedure for determining the calibrator frequency response.

Table 1 shows a typical set of average-value measurements which was used to evaluate the frequency response of the ac calibrator. The DVM readings are represented by V_f or V_{10}, where the subscripts denote the frequency of the voltage being measured. Calibrator frequencies are switched approximately every 3 minutes, allowing 2 minutes for voltmeter settling and 1 minute for recording six readings. If the first-recorded value is not repeated, it should be discarded, since this probably indicates lack of complete settling by the DVM. Successive numbers represent the least significant digit of successive DVM readings. The 0.5, 0.2, and 0.1 Hz measurements are compared with the succeeding 10 Hz measurement to minimize the time periods between readings that are compared, thus minimizing the effect of voltmeter drift.

Table 1. Typical set of average-value measurements used to evaluate the frequency response, $V_f - V_{10}$, of the ac voltage calibrator. The nominal value of V_f and V_{10} is normalized to 1000 units.

Elapsed time(min)	Frequency(f)	DVM reading(V_f)[a]	Mean value	$V_f - V_{10}$
0	10 Hz	1000.47,8,8,8,8,7	1000.477	
3	5	1000.48,8,8,8,8,8	1000.480	+0.003
6	2	1000.48,8,8,8,8,8	1000.480	+0.003
9	1	1000.48,8,8,7,8,8	1000.478	+0.001
12	0.5	1000.48,8,9,8,9,8	1000.483	+0.005
15	0.2	1000.48,8,8,9,8,8	1000.482	+0.004
18	0.1	1000.48,7,7,7,8,8	1000.475	-0.003
21	10	1000.48,8,7,8,8,8	1000.478	

[a]Successive numbers represent the least significant digit of successive readings.

Erratum: Third line, third paragraph should be 12 degrees of freedom instead of 2 degrees

For routine calibrations of the frequency response, it is planned to use the averages $\overline{(V_f - V_{10})}$ from two sets of measurements like those shown in table 1. In order to hold the magnitude of $(V_f - V_{10})$ near zero, frequency response adjustments have been added recently. If $\overline{(V_f - V_{10})}$ exceeds ±10 ppm for any frequency, the appropriate CAL FREQ RESPONSE pot should be adjusted to minimize the voltage difference (see fig. 3).

The estimated standard deviation of the measurement process is based on 15 sets of measurements, divided evenly among three groups. One group of measurements was made after the frequency response adjustments were added. A second group was made before the adjustments were provided. The third group of sets was obtained from the Naval Air Test Center, Patuxent River, MD (NATC) calibrator, which is based on the NBS design without frequency response adjustments. The maximum magnitude of $(V_f - V_{10})$ was approximately 5, 27, and 12 ppm, respectively, for the first, second, and third groups of sets. Although the statistical populations corresponding to the three groups have different values of $(V_f - V_{10})$, their standard deviations should be approximately equal, since all three calibrators had nearly identical electrical and mechanical designs. Therefore, a worst-case pooled estimate of the standard deviation (s_p), based on these three groups (15 sets) of measurements, will be used as the estimated standard deviation of a $(V_f - V_{10})$ measurement. The largest pooled estimate of the standard deviation is 4.4 ppm and occurs for a frequency equal to 0.5 Hz.

The estimated imprecision in $\overline{(V_f - V_{10})}$, obtained from N sets of measurements, can be expressed by $(s_p/\sqrt{N})t$, where t is Student's t, based on 2 degrees of freedom and a selected confidence level of 0.99. If $\overline{(V_f - V_{10})}$ is determined from two sets of measurements, the calculated imprecision is approximately 10 ppm. As mentioned previously, V_f will be readjusted if $\overline{(V_f - V_{10})}$ is larger than ±10 ppm. A control chart (fig. 4) will be kept showing calibration dates and the value of $\overline{(V_f - V_{10})}$ before being reset.

3.1.2 Voltage Calibration of AC Calibrator

The voltage level of the ac voltage calibrator is established by comparing the ac calibrator voltage at 10 Hz with the dc calibrator voltage, using the rms voltmeter as a transfer standard. For these ac-dc comparisons, the PREC RECT-INTERNAL switch is set to the INTERNAL position, HEAVY FILTERING is switched to OFF, and the FILTER FREQ switch set to L. Also, the PERIOD is set to 10 to yield maximum voltmeter resolution, and the DVM FREQ RESPONSE switch should be in the OUT position.

Before making ac-dc comparisons, the dc offset voltage of the calibrator buffer amplifier should be adjusted to a minimum value as follows. Set the CAL VOLTS dial to all zeros, the RANGE switch to 1 and the FUNCTION switch to INT AC CAL. Then, using a sensitive null

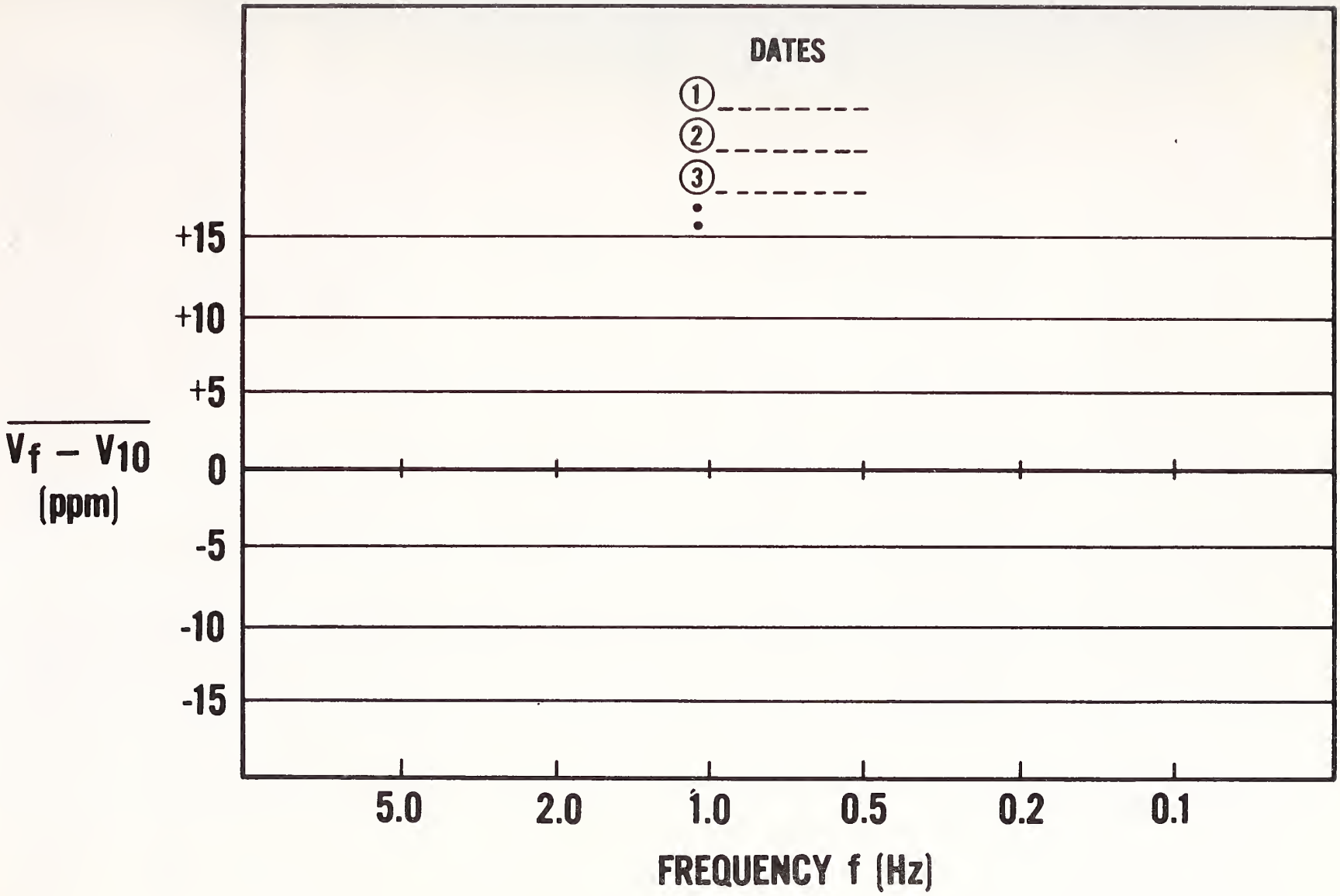

Figure 4. AC calibrator frequency response calibrations from average-value measurements. Calibrator voltages, V_f, at 5, 2 ---- Hz are compared with 10 Hz value. If $\overline{(V_f - V_{10})}$ exceeds ±10 ppm for any frequency, adjustment is made to minimize value.

detector, adjust the X1 OFFSET for a minimum voltage (<1 μV) at the CAL OUT terminals. With the RANGE at 10, adjust the X10 OFFSET for a minimum voltage (<10 μV). Following these adjustments, set the CAL FREQ to 10 Hz, CAL VOLTS to 5.000000, and the V-RANGE-MV switch to 10 V. Also, connect the CAL OUT terminals to the TE INPUT terminals with a coaxial cable and set the TE switch to EXT. Compare the ac calibrator voltage with the dc calibrator voltage (average of both polarities) as shown in table 2.

Table 2. A comparison between ac and dc calibrator voltages, applied directly to the rms/dc converter (TE INPUT). The FUNCTION and CAL columns are switch positions on the AC Voltmeter/Calibrator. The averages of ac and dc mean values are used for V_{ac} and V_{dc}. The nominal value of the DVM readings is normalized to 1000 units.

Elasped time(min)	FUNCTION INT CAL	CAL	DVM readings	Mean value	$V_{ac} - V_{dc}$
0	AC		1006.64,4,4,4,3,4	1006.638	
3	DC	+	1006.64,4,4,4,3,3	1006.637	0.6365-0.6235 = 0.013
6	DC	-	1006.61,1,1,1,1,1	1006.610	
9	AC		1006.64,3,4,3,4,3	1006.635	

For routine ac-dc difference calibrations, it is planned to use the average $\overline{(V_{ac} - V_{dc})}$ from three comparisons like the one shown in table 2. If $\overline{(V_{ac} - V_{dc})}$ exceeds ±20 ppm, the AC REF GAIN should be adjusted for a minimum difference. The estimated standard deviation s, of a comparison, is 7.0 ppm, obtained from 13 comparisons. Using the expression $(s/\sqrt{N})t$ to calculate the imprecision of $\overline{(V_{ac} - V_{dc})}$ yields approximately 12 ppm, where N is 3 and Student's t is based on 12 degrees of freedom and a confidence level of 0.99. Since $\overline{(V_{ac} - V_{dc})}$ will be readjusted if it is larger than ±20 ppm, the maximum estimated systematic error is ±20 ppm. A control chart (fig. 5) will be kept showing calibration dates and the value of the ac-dc difference before the AC REF GAIN is readjusted.

The dc offset of the function generator used in the sine-wave reference should be checked approximately every three years. It can be measured at pin 11 of the function generator with the DPDT switch in the ZERO position (see fig. B-2). The switch and offset adjustment

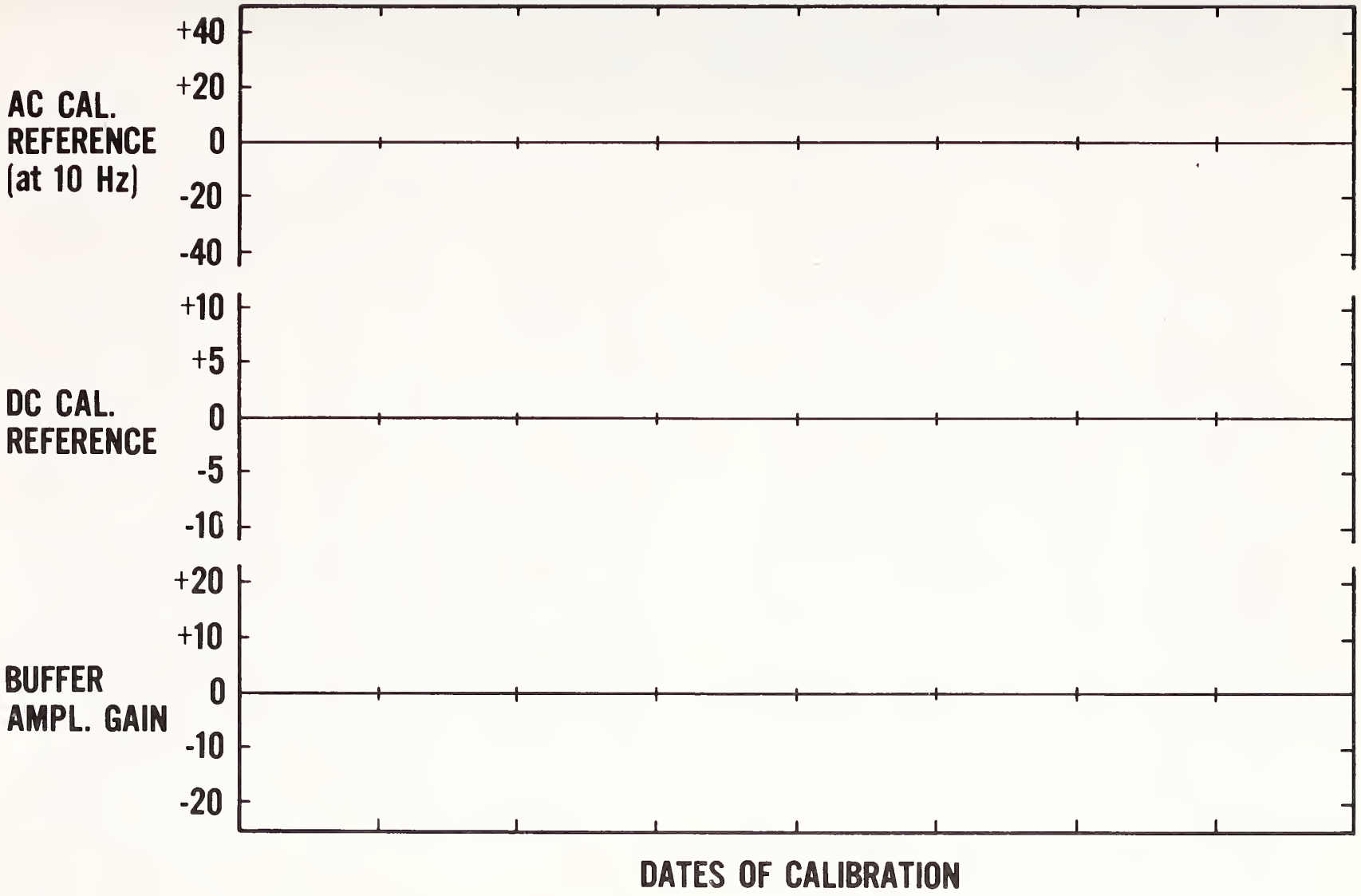

Figure 5. Drift (ppm) between calibrations of ac and dc calibrator references and buffer amplifier gain (X10 range). The ac voltage reference is not readjusted unless its drift exceeds ±20 ppm.

(R21) are accessed by removing the top panel. Adjustment of the offset is non-critical and is seldom required. Measurements show that an offset as large as ±200 μV contributes less than ±1 ppm to the rms value of the 1 V ac reference. A dc offset has a much larger effect on the average value of a sine wave; however, an offset voltage affects all calibrator frequencies the same and has no affect on frequency response measurements.

The measured temperature coefficient of the ac voltage reference is approximately +3 ppm/°C. Therefore, the imprecision for a 2°C range is ±6 ppm.

3.2 Calibration of the Standard Cells

The basic laboratory voltage standard to be used for calibrating the dc voltage calibrator is a set of four saturated standard cells, housed in a temperature-controlled standard cell enclosure and located near the AC Voltmeter/Calibrator. The cell voltages are fed to the NBS Volt Facility via a cable to facilitate in situ calibration. It is planned to calibrate the cells at least once a year. Calibrations performed in January and November of 1982 show a maximum drift of 0.4 ppm for this 10-month period.

3.3 Calibration of the DC Calibrator

The voltage of one of the calibrated standard cells (approx. 1.01815 V) is transferred to a "working" reference, using a null detector for the voltage comparison. A stable, 10 V laboratory reference with seven decade resolution (1 μV) is suitable for the working reference. The null detector should have approximately 140 dB common mode rejection and at least 1 MΩ input impedance. The detector is used for all voltage comparisons and offset voltage (zero) measurements described in this section.

A laboratory Kelvin-Varley (K-V) divider is used to "step" the reference voltage to the appropriate level for calibrating the dc reference, buffer amplifier, and ÷100 attenuator of the calibrator. The K-V divider should have seven-digit resolution and a linearity of 0.1 ppm of input for dial settings between 1.0 and 0.1.

To calibrate the dc reference and buffer amplifier gain, set the CAL VOLTS dial to 0000000 and the FUNCTION switch to INT AC CAL. With the RANGE at 1, adjust the X1 OFFSET for minimum voltage (<1 μV) at the CAL OUT terminals. With the RANGE at 10, adjust the X10 OFFSET for minimum CAL OUT voltage (<10 μV). Return the RANGE to 1 and set the FUNCTION switch at INT DC CAL, CAL at + and CAL VOLTS at .99999910 (last digit set to 10). Set the K-V divider to the reciprocal of the standard cell voltage (approx. .9821700) and connect its input to the laboratory reference. Then, adjust the DC REF pot so that the calibrator voltage equals the K-V divider output

voltage. The gain of the buffer amplifier is adjusted with RANGE at 10, CAL VOLTS at 5.000000, and the K-V divider set to the ratio of the standard cell voltage to 5 V (approx. .2036300). With the K-V divider input connected to the CAL OUT terminals, adjust the X10 GAIN so that the divider output voltage equals the laboratory reference voltage.

In order to minimize errors in the ac and dc calibrator voltages at small signal levels (< 50 mV) caused by extraneous signal and noise pickup, voltage offsets and Kelvin-Varley divider (see fig. 2 [5]) nonlinearity, an attenuator has been provided which attenuates both ranges of the dialed voltage by a factor of 100. This precision resistive attenuator has a 50 Ω output impedance and is inserted between the buffer amplifier output and the CAL OUT terminals when the attenuator switch is in the "÷100" position. When calibrator voltages larger than 50 mV are desired, this switch should be in the OUT position. If required, calibration of the ÷100 attenuator should immediately follow the preceding calibrations. The calibrator control positions are not changed, except for putting the attenuator in the ÷100 position. The laboratory K-V divider input is connected to the laboratory reference and set to the ratio of 0.05 V to the standard cell voltage (approx. .0491090). The ÷100 pot is then adjusted so that the calibrator voltage equals the K-V divider output voltage.

The uncertainty in transferring the standard cell voltage to the laboratory voltage reference at the 1.01815 V level is less than ±2 ppm. The uncertainties in stepping the reference voltage down to 1.000000 V (calibration of dc reference) and up to 5.000000 V are 4 and 10 ppm, respectively. These uncertainties are caused mostly by varying thermal voltages at connectors, circuit noise, and lack of resolution in adjustments. The 10 ppm uncertainty includes 1 ppm systematic error, caused by the nonlinearity of the laboratory K-V divider. The measured temperature coefficients of the dc reference and buffer amplifier (on X10 range) are -6 ppm/°C and +2 ppm/°C, respectively. The corresponding imprecisions for a 2°C range are ±12 ppm and ±4 ppm.

The expected maximum temperature coefficient for the attenuator is ±3 ppm/°C (±6 ppm uncertainty for a 2°C range). Tests show that thermal voltages up to ±0.7 μV are generated at the CAL OUT terminals when the voltage applied to the ÷100 attenuator is zero. This corresponds to ±14 ppm of the 50 mV output from the attenuator when it is being calibrated. Also, the nonlinearity of the laboratory K-V divider at the .0491090 setting may contribute 2 or 3 ppm error to the calibration of the attenuator. Finally, the adjustment of the attenuator has an uncertainty of about 2 ppm. Therefore, a systematic error of 3 ppm (from K-V divider) and an imprecision of 22 ppm have been assigned to the ÷100 attenuator calibration.

Based on a linearity comparison with the laboratory K-V divider, the K-V divider employed in the calibrator can cause up to 25 ppm error in the ac calibrator voltage (V_c). It is planned to check this unit against the laboratory standard approximately once a year.

Control charts (fig. 5) will be kept which show the changes in the ac and dc reference voltages and the buffer amplifier gain that occur between calibrations. Based on measurements and manufacturer's specifications, the yearly drift rates of the standard cell, ÷100 attenuator, and the K-V divider are expected to be less than 2, 2, and 3 ppm, respectively. Since these systematic errors are very small compared with the expected uncertainty of the ac calibrator voltage, no control charts are planned for these components.

3.4 AC-DC Difference Calibration of RMS/DC Converter

The ac-dc difference of the rms/dc converter used in the rms voltmeter was calibrated at NBS in April 1981. The reference thermal voltage converter (TVC), employed in the calibration test set, consisted of model FE reference thermal element and model F.10V (#1) multiplier range resistor. This thermal element, consisting of four single junction thermal elements in series, was designed to have negligible ac-dc difference for frequencies down to 10 Hz or below. Ten comparisons were made between the rms/dc converter and reference TVC involving four measurements each (ac, dc, dc reverse, ac), yielding an average ac-dc difference of ±0.25 ppm. The standard deviation of a comparison was 5.83 ppm, so that the standard error of the mean was 1.84 ppm. If the selected confidence level is 0.99, Student's t is 3.3 and the imprecision in the calculated ac-dc difference is ±6 ppm.

The only known source of systematic error in the ac-dc calibration is the uncertainty in the ac-dc difference of the reference TVC. This unit has been intercompared with several other reference TVCs, with an ac-dc difference of less than 1 ppm [6]. These units are maintained at NBS and are believed to have zero ac-dc difference to within 1 or 2 ppm for frequencies as low as 10 Hz. If ±2 ppm uncertainty is allowed for the reference TVC, the estimated ac-dc difference of the rms/dc converter is 0 ±8 ppm.

It is recommended that multi-junction thermal converters (MJTCs) be re-calibrated every five years. This re-calibration interval should also apply to the rms/dc converter, since its ac-dc difference is determined by the ac-dc difference of the MJTC employed.

3.5 Summary of Calibration Errors of AC Voltage Calibrator

Table 3 lists the estimated uncertainties which limit the calibration accuracy of the ac calibrator. Item 9 of this table 3 shows that, following a frequency response calibration, the $(V_f - V_{10} = 0)$ with an uncertainty of ±20 ppm. It should be emphasized

Table 3. Estimated systematic error and imprecision components of the uncertainties which limit calibration accuracy of ac voltage calibrator. Estimated components of uncertainties less than 0.5 ppm are rounded to zero.

		Systematic error	Imprecision
(1)	Standard cell uncertainty	2 ppm	0 ppm
(2)	Standard cell lab reference transfer	0	2
(3)	Step-down to 1 V level in dc reference	0	4
(4)	Step-up to 5 V level in dc calibrator	1	9
(5)	Temperature coefficient of dc reference (-6 ppm/°C) for a 2°C range	0	12
(6)	AC/DC comparisons (calibration of ac calibrator at 10 Hz)	20	12
(7)	AC-DC difference uncertainty of rms/dc converter	2	6
(8)	Temperature coefficient of ac reference (+3 ppm/°C) for a 2°C range	0	6
(9)	Calibration of (V_f-V_{10})	10	10
(10)	Maximum error from calibrator K-V divider	25	0
(11)	Maximum K-V drift between calibrations	3	0
(12)	Temperature coefficient of buffer amplifier on X10 range (+2 ppm/°C) for a 2°C range	0	4
(13)	Calibration of the ÷100 attenuator	3	22
(14)	Maximum attenuator drift between calibrations	2	0
	Sub-totals	68	33 (rss)
Total uncertainty of ac calibrator voltage V_c			±101 ppm

that when frequency response calibrations are made of a customer's voltage source or voltmeter, only the uncertainty of (V_f-V_{10}) needs to be known. Table 3 also shows that the estimated uncertainty of the ac calibrator voltage V_c is ±101 ppm, following a complete calibration of the dc and ac calibrator circuits.

Although periodic calibration intervals cannot be established for these circuits until control chart data are available, it is believed that a specified maximum uncertainty of ±200 ppm for the ac calibrator will allow calibration intervals approaching one year for the dc reference voltage, buffer amplifier gain, and (V_f-V_{10}). A somewhat shorter calibration interval is expected for the ac reference. The corresponding error budget for (V_f-V_{10}) alone is ±35 ppm. Therefore, the calibration intervals will be chosen to ensure that the maximum uncertainties of (V_f-V_{10}) and V_c are less than ±35 ppm and ±200 ppm (0.020%), respectively.

Although considerable reliance will be placed on control chart data to anticipate future drifts in calibrator circuits, accurate checks on circuit performance can be made at any time using shortened procedures. Using only one set of measurements as shown in table 1 to determine (V_f-V_{10}), instead of the average of two sets, decreases the measurement time from 48 minutes to 24 minutes. The imprecision increases from ±10 ppm to ±14 ppm and the allowable value of (V_f-V_{10}) should be increased from ±10 ppm to ±14 ppm before being readjusted. Using one set of measurements as shown in table 2 to determine $(V_{ac}-V_{dc})$, instead of the average of three sets, decreases the measurement time from 36 minutes to 12 minutes. The imprecision increases from ±12 ppm to ±21 ppm and the allowable value of $(V_{ac}-V_{dc})$ should be increased from ±20 ppm to ±35 ppm before being readjusted. Substituting these values into table 3 (items 6 and 9) yields maximum uncertainties of ±28 ppm and ±125 ppm for (V_f-V_{10}) and V_c, respectively. The time required to calibrate the dc reference, buffer amplifier gain, and ÷100 attenuator is 13 minutes. (These procedures cannot be shortened.) Therefore, the total calibration time of the dc and ac calibrators, using the shortened procedures, is approximately 50 minutes.

3.6 Frequency Response of the RMS Voltmeter

The ac calibrator can be used to calibrate voltage standards at frequencies other than the nominal calibrator frequencies, if the frequency response of the rms voltmeter (DVM) is known. The response of the DVM decreases as the frequency of the input signal is decreased below ~2 Hz, because of increasing ripple voltage in the rms/dc converter and lack of square law response by the MJTC of this circuit [2]. The effect from ripple is minimized, however, by the HEAVY FILTERING circuit which is used for most calibration work (see sec. 3.1.1). Five (V_f-V_{10}) comparisons were made using the ac calibrator voltage as the input signal. The mean values of these comparisons and the standard deviation of a comparison for each frequency are shown in table 4.

Table 4. Frequency response of the rms voltmeter with corrections applied for variations in the ac calibrator voltage, used for the input signal. The mean values and standard deviation, s_f, were obtained from five (V_f-V_{10}) DVM comparisons.

Frequency (f)	$\overline{(V_f-V_{10})}_{DVM}$	s_f
5 Hz	0 ppm	6.1 ppm
2	-2	6.5
1	-13	4.5
0.5	-49	6.5
0.2	-109	5.5
0.1	-208	2.7

The voltmeter response as a function of input signal frequency can be approximated by second degree equations of curves that pass through the values of $\overline{(V_f-V_{10})}_{DVM}$ at frequencies of 2, 1, 0.5 Hz and at 0.5, 0.2, and 0.1 Hz. The equation that is applicable to the 0.5 to 2 Hz range is

$$(V_f-V_{10})_{DVM} = -105.33 + 133.00f - 40.67f^2. \quad (1)$$

The equation for the 0.5 to 0.1 Hz range is

$$(V_f-V_{10})_{DVM} = -346.50 + 1582.50f - 1975.00f^2. \quad (2)$$

These equations are used to plot the curves in figure 6.

As indicated previously, the lack of flatness in the DVM response is attributed to the rms/dc converter response. Since applying corrections from the curves in figure 6 or the preceding equations is quite tedius, an effort was made to improve the DVM frequency response sufficiently so that corrections usually are not necessary. This was accomplished by employing frequency-dependent negative feedback circuits in a section of the input amplifier, as shown in figure 7. With these circuits, the amplifier response approximately complements the rms/dc converter response. Components R1, C1, and R2, C2 provide

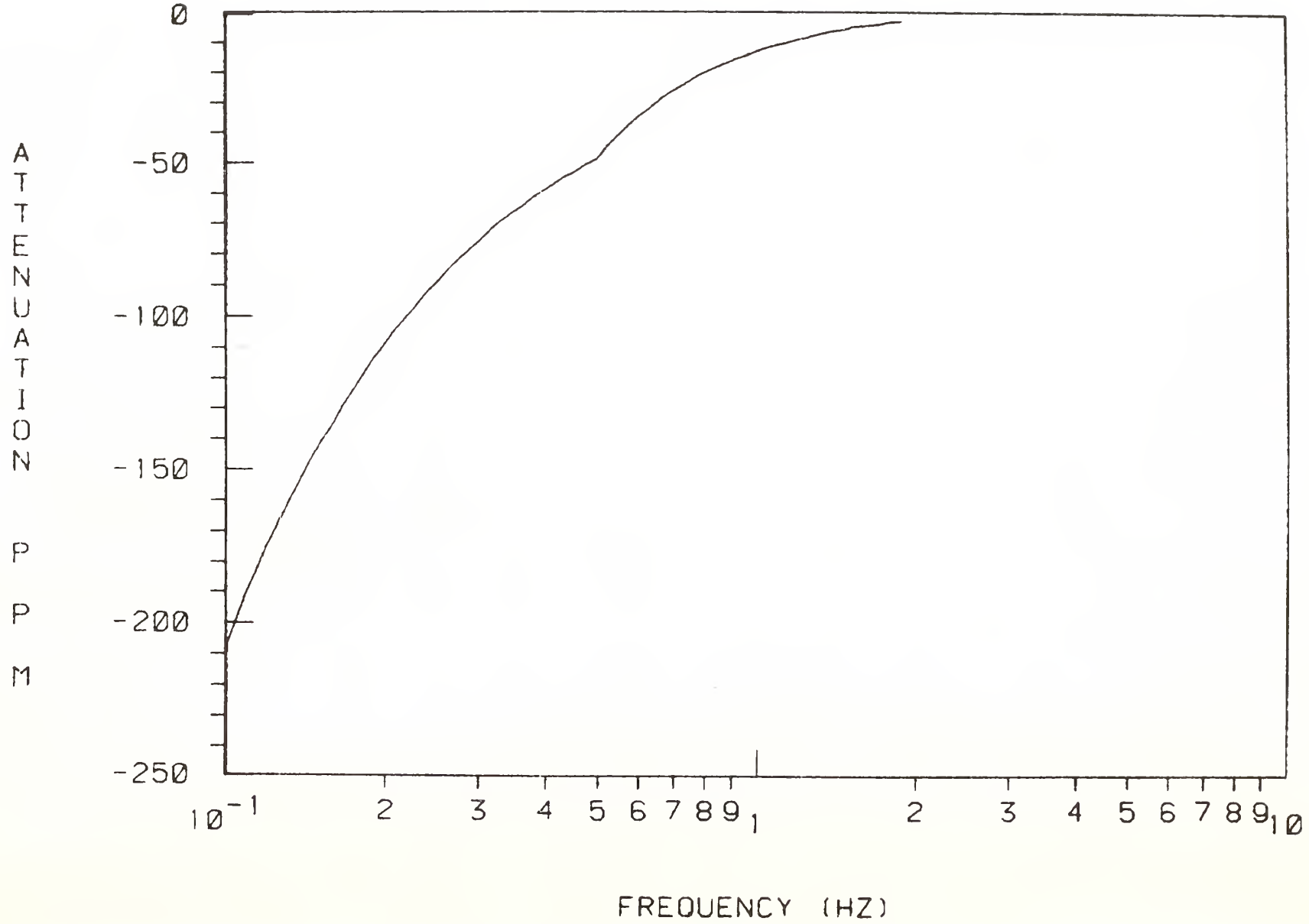

Figure 6. Plot of DVM frequency response, using equations 1 and 2.

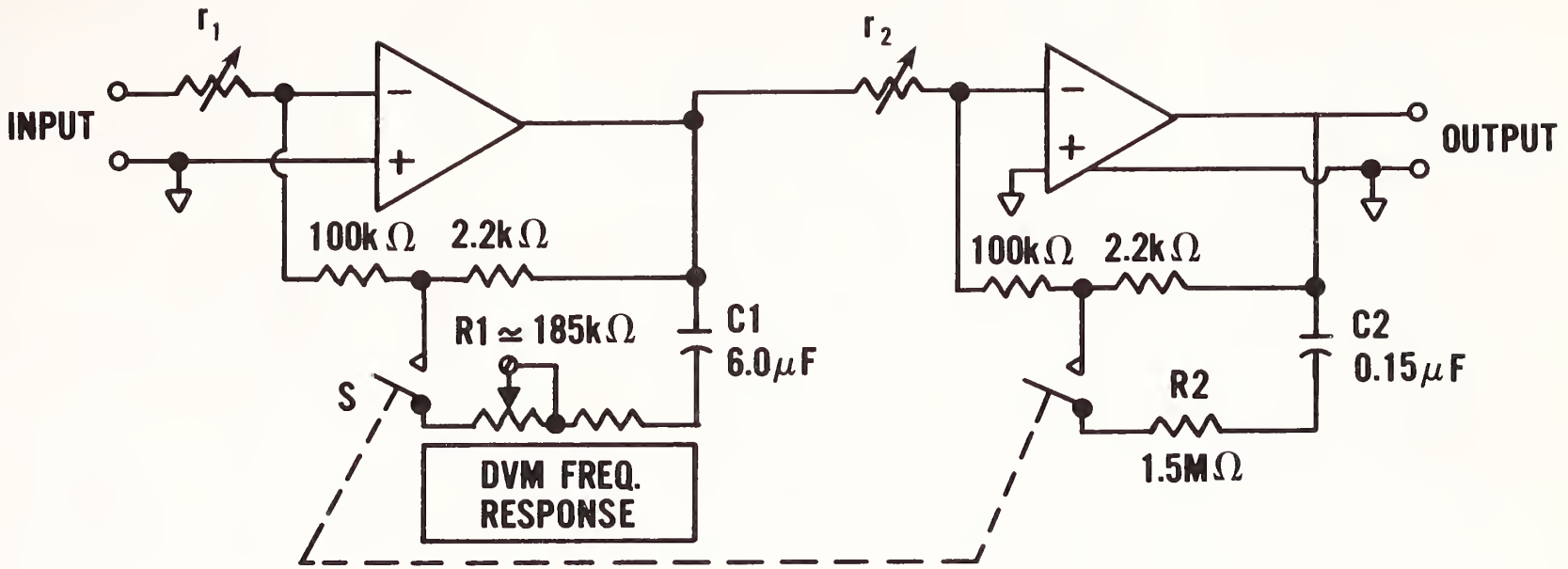

Figure 7. Section of input amplifier used to compensate for decrease in DVM response at low frequencies.

high-frequency attenuations of approximately 250 and 30 ppm, respectively. The corresponding corner frequencies are 0.14 and 0.71 Hz. The frequency response of the circuit which has the higher attenuation is adjustable over a small range by the DVM FREQ RESPONSE pot. Figure 8 is a plot of the amplifier transfer characteristic with the DVM FREQ RESPONSE circuit switched in (switch S closed). Resistances r_1 and r_2 were arbitrarily assigned the value of 100 kΩ; however, measurements show that the frequency response is essentially independent of the values of r_1 and r_2 selected by the V-RANGE-MV switch (see fig. 2).

The frequency response of the circuit shown in figure 7 was combined with the responses of eqs. 1 and 2 and plotted in figure 9. This response curve shows that the maximum values of $(V_f-V_{10})_{DVM}$ occur at 0.5 Hz and approximately 0.14 Hz. A good estimate of the outside limits of $(V_f-V_{10})_{DVM}$ can be obtained by measuring this quantity at 0.1, 0.2, and 0.5 Hz, using the ac calibrator. Table 5 shows the DVM response at the lowest four calibrator frequencies, obtained from 13 measurements. Corrections were made for the measured frequency response of the calibrator (systematic error), leaving only the imprecision of these measurements (±6.0 ppm) as the uncertainty of the calibrator voltages. (The frequency response and estimated standard deviation of the ac calibrator were based on 5 and 13 measurements, respectively - see section 3.1.1.) Using the maximum estimated standard deviation of the measurement process represented by table 5 (6.4 ppm) and a confidence level of 0.99, the imprecision of these measurements is 5.4 ppm. Combining this imprecision with the calibrator imprecision gives ±8.1 ppm as the maximum uncertainty of $(V_f-V_{10})_{DVM}$. Therefore, the outside limits of $(V_f-V_{10})_{DVM}$, measured at 0.1, 0.2, 0.5, and 1 Hz, are approximately +20 and -19 ppm.

Table 5. Measured DVM frequency response with input amplifier compensated. The average values of $(V_f-V_{10})_{DVM}$ and estimated standard deviations, s_f, are based on 13 measurements.

Frequency (f)	$\overline{(V_f-V_{10})_{DVM}}$	s_f
1 Hz	+1 ppm	3.0 ppm
0.5	-11	4.2
0.2	+12	6.4
0.1	-7	5.0

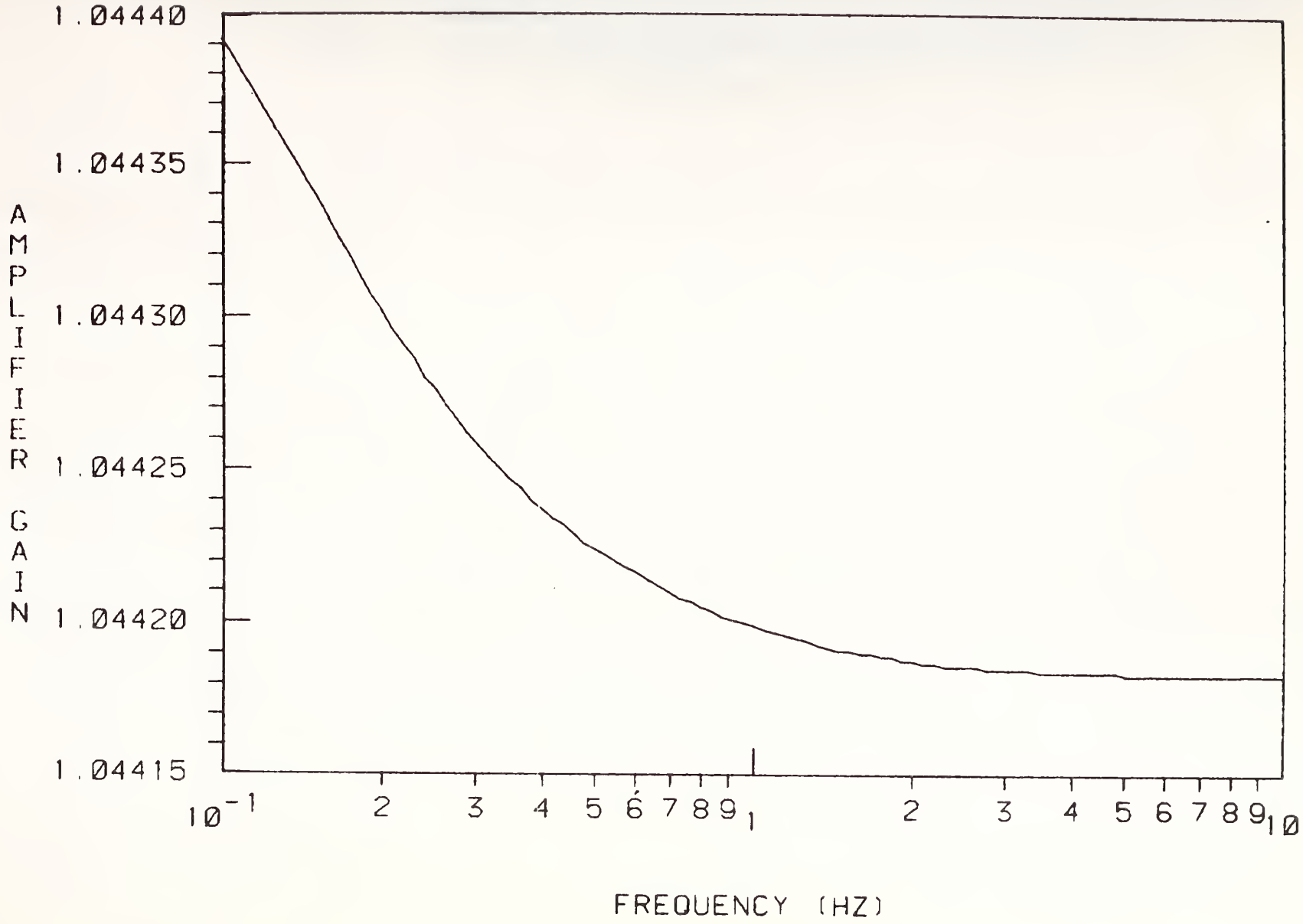

Figure 8. Transfer characteristic of input amplifier with DVM FREQ RESPONSE circuit switched in (see fig. 7).

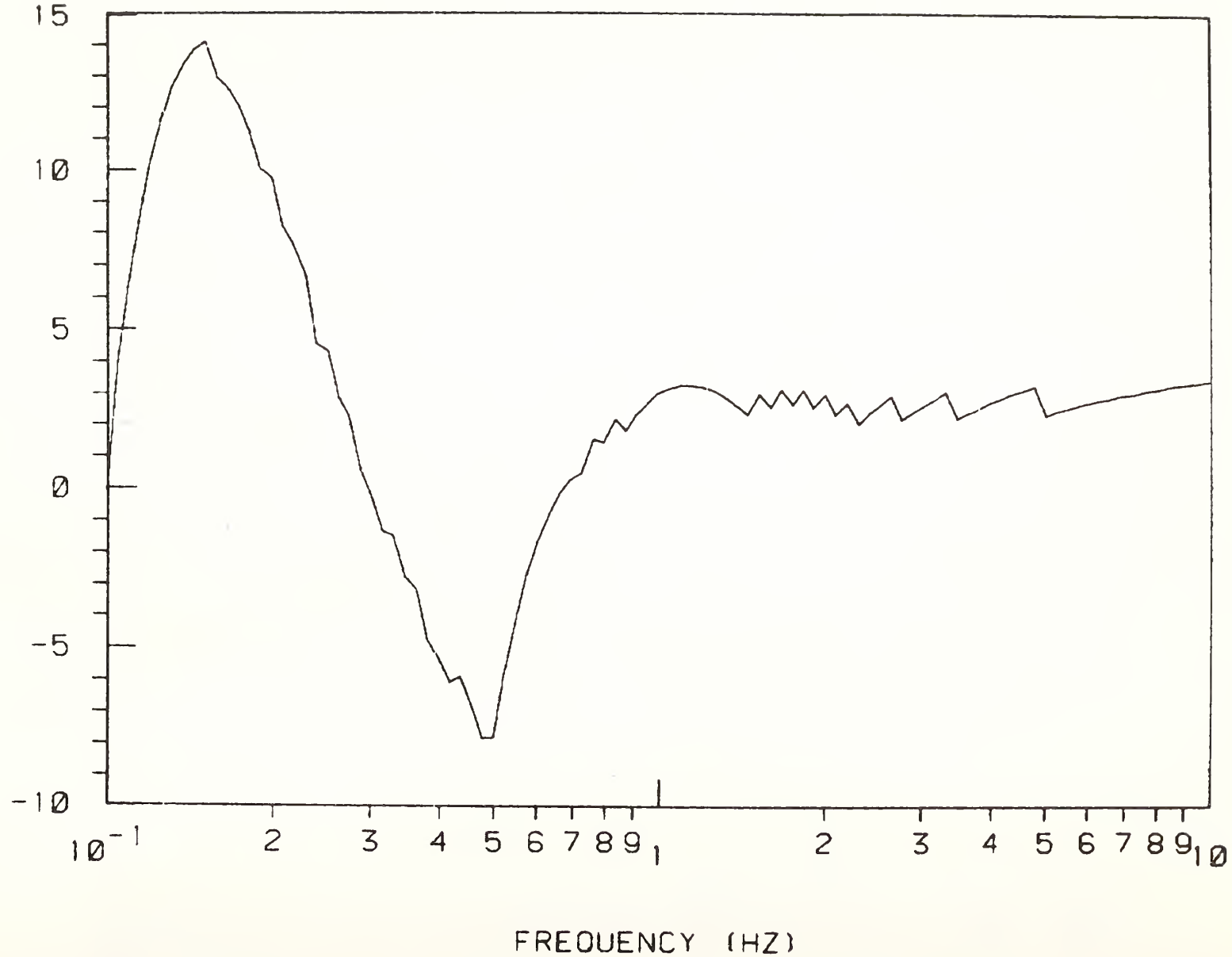

Figure 9. Theoretical DVM response with input amplifier frequency compensated.

These limits result from using 5 and 13 measurements to establish the frequency response of the calibrator and DVM, respectively. For routine calibrations of the DVM frequency response, it is planned to use three measurements. Assuming that the calibrator response is also obtained from three measurements, the DVM and calibrator imprecisions will be 11.3 and 7.8 ppm, respectively. Combining these quantities gives 13.7 ppm, an increase of 5.6 ppm over the imprecision applicable to the frequency response values in table 5. To obtain the maximum expected values of $(V_f-V_{10})_{DVM}$, using three DVM and three calibrator measurements, the maximum frequency response values in figure 5 should be increased by 5.6 ppm, yielding +17.6 and -16.6 ppm. Adding the corresponding imprecision to these quantities gives estimated uncertainty limits of +31.3 and -30.3 ppm to $(V_f-V_{10})_{DVM}$. The response curve in figure 9 indicates that $(V_f-V_{10})_{DVM}$ is approximately 4 ppm larger at 0.14 Hz than at 0.2 Hz. Also, any uncertainty in the difference between $(V_{.14}-V_{10})_{DVM}$ and $(V_{.2}-V_{10})_{DVM}$ in figure 6 carries over to figure 9. The computed value of this difference is approximately 55 ppm. It is believed that the uncertainty in this difference should not exceed 10 percent or 6 ppm. Adding this uncertainty and the 4 ppm difference mentioned above to the uncertainty limits for the measured frequency response yields +41.3 and -30.3 ppm as the uncertainty limits of $(V_f-V_{10})_{DVM}$ for any frequency. Since the attenuation caused by the feedback circuits of the input amplifier is small at 0.1 Hz but increases with frequency, the DVM response curve (fig. 9) can be effectively rotated about the 0.1 Hz point of the curve by adjusting the DVM FREQ RESPONSE pot. Therefore, this control can be used to adjust the +41.3 and -30.3 limits to approximately ±36 ppm. Drift in $(V_f-V_{10})_{DVM}$ that cannot be removed by adjusting the DVM FREQ RESPONSE pot, estimated to be less than 2 ppm in five years, can be compensated by trimming the values of R2 and C2 in figure 7. However, to obviate the trimming, the frequency response will be specified as 0 ±40 ppm to allow some margin for drift of this type.

It is useful to estimate the uncertainty that the DVM response causes if two voltages are compared which have frequencies differing by no more than 5 percent. Figure 9 shows that the maximum rate of change of $(V_f-V_{10})_{DVM}$ with frequency occurs over the frequency range of 0.1 Hz to 0.14 Hz, approximately. Assuming that $(V_f-V_{10})_{DVM}$ changes by no more than two-thirds of the specified limits of ±40 ppm over this frequency range (a 40% change in frequency), a 5 percent uncertainty in frequency corresponds to a maximum uncertainty in $(V_f-V_{10})_{DVM}$ of approximately ±7 ppm.

4. CALIBRATIONS OF VOLTMETERS

Calibrations are performed on rms-responding ac voltmeters using the ac voltage calibrator of the NBS AC Voltmeter/Calibrator. AC voltmeters can be calibrated at frequencies of 10, 5, 2, 1, 0.5, 0.2, and 0.1 Hz at any voltage level between 0.5 mV and 7 V.

The total uncertainty of a calibration is $\pm(\varepsilon_C + \varepsilon_r)$, where ε_C is the uncertainty of the ac voltage calibrator voltage and ε_r is the imprecision of the calibration process. The estimated uncertainty of the ac voltage calibrator is ±0.020 percent, as described in section 3.5. The imprecision for a given calibration point is $ts/\sqrt{N}$, where t is Student's t for the selected confidence level, s is the standard deviation for a measurement, and N is the number of measurements (test runs) used to obtain the mean values of the measured quantities (voltmeter readings).

Unless otherwise requested by the customer, a single accuracy of calibration will be given for the corrections to the calibration points, based on a confidence level of 0.98 and the largest standard deviation encountered. It is expected that the value of N, requested by the customer, will generally be 3, 4, or 5. Assuming a selected confidence level of 0.98, values of t corresponding to N equal 3, 4, and 5 are approximately 7.0, 4.5, and 3.7, respectively.

5. CALIBRATIONS OF VOLTAGE STANDARDS

Voltage calibrations are performed on precision ac sources using the ac voltage calibrator and rms voltmeter of the NBS Voltmeter/Calibrator. The rms voltmeter is used as a transfer voltmeter to compare the voltages (of the same nominal level) from the test unit and the ac calibrator. Voltage calibrations can be made at any frequency in the 10 Hz to 0.1 Hz range and are usually made near the full-scale level of the DVM ranges (2, 5, 10, 20, 50 mV, and 0.1, 0.2, 0.5, 1, 2, 5 V).

If the voltage standard is of a design which has inherently stable voltage with respect to frequency, a frequency response (relative voltage) calibration may be preferable to a conventional voltage calibration. The user then establishes the voltage levels by calibrating the voltage at 10 Hz. Since the rms voltmeter has a frequency response that is flat to within ±40 ppm, it is used to determine the frequency response of voltage sources. Frequency response calibrations can be made at any frequency in the 10 Hz to 0.1 Hz range and are usually made near the full-scale level of the DVM ranges (2, 5, 10, 20, 50 mV, and 0.1, 0.2, 0.5, 1, 2, 5, 10 V).

5.1 Voltage Calibrations

For each calibration point, the rms voltmeter (DVM) is used to compare the voltage V_T from the standard under test with the voltage V_C of the same nominal level from the ac voltage calibrator, choosing the calibrator frequency closest to that of the voltage being measured. After the test runs are made, the average $\overline{(V_C - V_T)}$ is formed for each calibration point, yielding corrections to the nominal voltage values of the test unit.

If the uncertainty of the calibrator voltage and the uncertainty caused by the DVM frequency response are denoted by ε_c and ε_m, respectively, the total uncertainty of a calibration point is given by $\pm(\varepsilon_c + \varepsilon_m + ts/\sqrt{N})$, where s is the standard deviation of a $(V_c - V_T)$ comparison and N is the number of comparisons (test runs). If the frequencies of the voltages being compared are within 5 percent of each other, ε_m is ±7 ppm. If the frequency difference is larger, the worst case value of ε_m, ±40 ppm, is used. The value assigned to ε_c is ±200 ppm (±0.02%); however, if the highest calibration accuracy is required by the customer, ε_c can be decreased to ±125 ppm by a special calibration of the NBS instrument.

Unless otherwise requested by the customer, a single accuracy of calibration will be given for the corrections to the calibration points, based on a confidence level of 0.98 and the largest standard deviation encountered. It is expected that the value of N, requested by the customer, will be 3, 4, or 5.

5.2 Frequency Response Calibrations

These calibrations are made using the DVM to compare test unit voltages of frequency f with the 10 Hz value. After N comparisons, the quantities $\overline{(V_f - V_{10})}$ are computed for each test frequency, yielding the frequency response. The uncertainty of these calibration points is $\pm(\varepsilon_m + ts/\sqrt{N})$, where ε_m is ±40 ppm, the frequency response of the DVM, and s is the standard deviation of a comparison.

Unless otherwise requested by the customer, a single accuracy of calibration will be given for the frequency response, based on a confidence level of 0.98 and the largest standard deviation encountered. It is expected that the value of N, requested by the customer, will be 3, 4, or 5.

6. ACKNOWLEDGMENTS

The author is grateful for the valuable suggestions made by Barry A. Bell, Group Leader for Electronic Instrumentation and Metrology, and the CALCOM subcommittee members who reviewed this document. The members of this subcommittee were: David W. Berning, Ronald F. Dziuba, Dr. James A. Lechner, and John D. Ramboz. Special thanks are due Mr. Ramboz, who served as chairman of the CALCOM subcommittee, and Dr. Lechner, who provided assistance on the statistical aspects of the measurements. The very helpful suggestions by Jenny Palla, the typing of Bonnie L. Smith, and the editorial assistance of Betty A. Oravec, in preparing this manuscript, are also gratefully acknowledged.

7. REFERENCES

[1] AC Voltmeter/Calibrator Developed, NBS DIMENSIONS, Dec. 1977.

[2] H. K. Schoenwetter, "An RMS Digital Voltmeter/Calibrator for Very Low Frequencies," IEEE Trans. Instrum. Meas., Vol. IM-27, pp. 259-268, Sept. 1978.

[3] B. F. Field, "A Fast Response Low-Frequency Voltmeter," IEEE Trans. Instrum. Meas., Vol. IM-27, pp 368-372, Dec. 1978.

[4] B. A. Bell, B. F. Field, and T. H. Kibalo, "A Fast Response Low Frequency Voltmeter," Nat. Bur. Stand. (U.S.) Tech Note 1159 (Aug. 1982).

[5] H. K. Schoenwetter, "NBS Provides Voltage Calibration Service in 0.1 - 10 Hz Range Using AC Voltmeter/Calibrator," IEEE Trans. Instrum. Meas.. Vol. IM-28, pp. 327-331, Dec. 1979.

[6] F. L. Hermach, "An Investigation of Multijunction Thermal Converters," IEEE Trans. Instrum. Meas., Vol. IM-25, pp. 524-528, Dec. 1976.

APPENDIX A

Calibration Forms

Several forms have been prepared to facilitate the calibrations of rms voltmeters and the voltage and frequency response calibrations of ac voltage standards. These are:

(1) LOG SHEET

(2) WORK SHEET

(3) TABLE OF CALIBRATIONS

(4) REPORT OF TEST

These forms, as well as a brief description of the calibration procedure, are given in the following sections for each type of calibration. Items 3 and 4 and the summarized calibration procedure are sent to the customer, following a calibration.

Department of Commerce
National Bureau
of Standards

LOG SHEET

Date_____Test No._____

VOLTMETER CALIBRATIONS USING NBS AC VOLTMETER/CALIBRATOR

Equipment Mfr._____

Submitted by:_____

Model No._____ Ser. No._____

Time	Frequency	Voltage range	Voltmeter readings (V_m)	Mean value		

Department of Commerce
National Bureau
of Standards

WORK SHEET

Date_____Test No._____

VOLTMETER CALIBRATIONS USING NBS AC VOLTMETER/CALIBRATOR

Equipment Mfr._____Model No._____Ser. No._____

Submitted by: _____

Frequency	Voltage range	$\bar{V}_{vm}$	V_c	Correction $V_c-\bar{V}_{vm}$	Standard deviation (s)	Number of readings (N)	Imprecision $\epsilon_r=ts/\sqrt{N}$	Uncertainty of V_c (ϵ_c)	Total uncertainty $\pm(\epsilon_c+\epsilon_r)$	Confidence level used for t	

Calibration of Voltmeters

Calibrations are performed on rms-responding ac voltmeters using the ac voltage calibrator of the NBS AC Voltmeter/Calibrator. AC voltmeters can be calibrated at frequencies of 10, 5, 2, 1, 0.5, 0.2, and 0.1 Hz at any voltage level between 0.5 mV and 7 V.

The total uncertainty of a calibration is $\pm(\varepsilon_C + \varepsilon_r)$, where ε_C is the uncertainty of the ac calibrator voltage and ε_r is the imprecision of the calibration process. The estimated maximum uncertainty of the ac voltage calibrator is ±0.020 percent. The imprecision for a given calibration point is $ts/\sqrt{N}$, where t is Student's t for the selected confidence level, s is the standard deviation for a measurement, and N is the number of measurements (test runs) used to obtain the mean values of the measured quantities (voltmeter readings).

Unless otherwise requested by the customer, a single accuracy of calibration will be given for the corrections to the calibration points, based on a confidence level of 0.98 and the largest standard deviation encountered.

Department of Commerce
National Bureau
of Standards

TABLE OF CALIBRATIONS

Date________Test No.________

VOLTMETER CALIBRATIONS USING NBS AC VOLTMETER/CALIBRATOR

Equipment Mfr.________________________________

Submitted by:________________________________

Model No.____________________Ser. No.__________

Frequency	Voltage range	Average of voltmeter readings $\overline{V}_{vm}$	Correction to $\overline{V}_{vm}$	Number of readings (N)	Total uncertainty	Confidence level used for t

FORM NBS-259
(3-66)

U.S. DEPARTMENT OF COMMERCE
NATIONAL BUREAU OF STANDARDS
WASHINGTON, D.C. 20234

REPORT OF TEST

LOW FREQUENCY VOLTMETER

Manufacturer_____
Model No._____
Serial No._____

Submitted by

_____
_____

This voltmeter was tested using the ac voltage calibrator of the NBS AC Voltmeter/Calibrator at a room temperature of 23 ±1 °C.

The test points, average voltmeter readings, corrections,and total uncertainty are shown in the attached TABLE OF CALIBRATIONS. Also shown is the confidence level upon which the imprecision is based. The ac calibrator voltage uncertainty is treated totally as a systematic error. Unless otherwise indicated, the total uncertainty is based on the largest standard deviation encountered for any of the test points. Measurements on the test unit were made over a period of time which was too short to yield long-term stability information.

For the Director
National Engineering Laboratory

Barry A. Bell, Group Leader
Electronic Instrumentation and Metrology
Electrosystems Division

Test No. 722/_____
Order No._____
Date: _____
Attn: _____

Department of Commerce
National Bureau
of Standards

CALIBRATIONS OF VOLTAGE STANDARD USING NBS AC VOLTMETER/CALIBRATOR

Equipment Mfr._____ Model No._____ Ser. No._____

LOG SHEET

Submitted by:_____

Date_____ Test No._____

Time	Nominal voltage	Frequency		Test unit		Calibrator			
		Test unit	Calibrator	DVM readings	Mean	DVM readings	Mean		

Department of Commerce
National Bureau
of Standards

WORK SHEET

Date_____Test No.

CALIBRATIONS OF VOLTAGE STANDARD USING NBS AC VOLTMETER/CALIBRATOR

Equipment Mfr._____Model No._____Serial No._____

Submitted by:_____

Nominal voltage	Frequency		Average of comparisons $\overline{V_C - V_T}$	DVM frequency response (ε_m)	Uncertainty of V_C (ε_C)	Standard deviation (s)	Number of comparisons (N)	Imprecision $\varepsilon_r = ts/\sqrt{N}$	Total uncertainty $\pm(\varepsilon_C + \varepsilon_m + \varepsilon_r)$	Confidence level used for t	
	Test unit	Calibrator									

Calibration of Voltage Standards

For each calibration point, the rms voltmeter (DVM) is used to compare the voltage V_T from the standard under test with the voltage V_C of the same nominal level from the ac voltage calibrator, choosing the calibrator frequency closest to that of the voltage being measured. After the test runs are made, the average $\overline{(V_C - V_T)}$ is formed for each calibration point, yielding corrections to the nominal voltage values of the test unit.

If the uncertainty of the calibrator voltage and the uncertainty caused by the DVM frequency response are denoted by ε_C and ε_m, respectively, the total uncertainty of a calibration point is given by $\pm(\varepsilon_C + \varepsilon_m + ts/\sqrt{N})$, where s is the standard deviation of a $(V_C - V_T)$ comparison and N is the number of comparisons (test runs). If the frequencies of the voltages being compared are within 5 percent of each other, ε_m is ±7 ppm. If the frequency difference is larger, the worst case value of ε_m, ±40 ppm, is used. The value assigned to ε_m is ±200 ppm (±0.02%); however, if the highest calibration accuracy is required by the customer, ε_C can be decreased to ±125 ppm by a special calibration of the NBS instrument.

Unless otherwise requested by the customer, a single accuracy of calibration will be given for the corrections to the calibration points, based on a confidence level of 0.98 and the largest standard deviation encountered.

Department of Commerce
National Bureau
of Standards

TABLE OF CALIBRATIONS

Date_____Test No._____

CALIBRATIONS OF VOLTAGE STANDARD USING NBS
AC VOLTMETER/CALIBRATOR

Equipment Mfr._____

Submitted by:_____

Model No. Ser. No.

Nominal voltage of standard	Frequency of standard	Correction to nominal voltage	Number of comparisons (N)	Total uncertainty	Confidence level used for t	

FORM NBS-259
(3-66)

U.S. DEPARTMENT OF COMMERCE
NATIONAL BUREAU OF STANDARDS
WASHINGTON, D.C. 20234

REPORT OF TEST

LOW FREQUENCY VOLTAGE STANDARD

Manufacturer_____
Model No._____
Serial No._____

Submitted by

_____
_____

This voltage standard was tested using the ac voltage calibrator and rms voltmeter (DVM) of the NBS AC Voltmeter/Calibrator at a room temperature of 23 ±1°C.

The test points (nominal voltage and frequency), corrections, and total uncertainty are shown in the attached TABLE OF CALIBRATIONS. Also shown is the confidence level upon which the imprecision is based. The uncertainty of the ac calibrator voltage and the uncertainty caused by the DVM frequency response are treated as systematic errors. Unless otherwise indicated, the total uncertainty is based on the largest standard deviation encountered for any of the test points. Measurements on the test unit were made over a period of time which was too short to yield long-term stability information.

For the Director
National Engineering Laboratory

Barry A. Bell, Group Leader
Electronic Instrumentation and Metrology
Electrosystems Division

Test No. 722/_____
Order No._____
Date_____
Attn:_____

Department of Commerce
National Bureau
of Standards

LOG SHEET

Date_____Test No._____

FREQUENCY RESPONSE CALIBRATIONS OF VOLTAGE STANDARD USING NBS AC VOLTMETER/CALIBRATOR

Equipment Mfr._____Model No._____Ser No._____

Submitted by: _____

Time	Nominal voltage	Frequency	Voltage standard		Voltage standard			
			DVM readings	Mean	DVM readings	Mean		

Department of Commerce
National Bureau
of Standards

WORK SHEET

Date_____Test No._____

FREQUENCY RESPONSE CALIBRATIONS OF VOLTAGE STANDARD USING NBS AC VOLTMETER/CALIBRATOR

Equipment Mfr. _____ Model No._____Ser. No._____

Submitted by:_____

Nominal voltage	Frequency	Test unit response $(V_f - V_{10})$	DVM frequency response (ϵ_m)	Standard deviation of comparison (s)	Number of comparisons (N)	Imprecision $\epsilon_r = t/s\sqrt{N}$	Total uncertainty $\pm(\epsilon_m + \epsilon_r)$	Confidence level used for t			

Frequency Response Calibrations

These calibrations are made using the DVM to compare test unit voltages of frequency f with the 10 Hz value. After N comparisons, the quantities $\overline{(V_f - V_{10})}$ are computed for each test frequency, yielding the frequency response. The uncertainty of these calibration points is $\pm(\varepsilon_m + ts/\sqrt{N})$, where ε_m is ± 40 ppm, the frequency response of the DVM, and s is the standard deviation of a comparison.

Unless otherwise requested by the customer, a single accuracy of calibration will be given for the frequency response, based on a confidence level of 0.98 and the largest standard deviation encountered.

Department of Commerce
National Bureau
of Standards

TABLE OF CALIBRATIONS

Date_____Test No._____

FREQUENCY RESPONSE CALIBRATIONS OF VOLTAGE STANDARD
USING NBS AC VOLTMETER/CALIBRATOR

Equipment Mfr._____

Submitted by:_____

Model No._____Ser. No._____

Nominal voltage	Frequency	Frequency response $\frac{(V_f - V_{10})}{}$	Number of comparisons (N)	Total uncertainty	Confidence level used for t	

FORM NBS-250
(3-66)

U.S. DEPARTMENT OF COMMERCE
NATIONAL BUREAU OF STANDARDS
WASHINGTON, D.C. 20234

REPORT OF TEST

LOW FREQUENCY VOLTAGE STANDARD

Manufacturer_____
Model No._____
Serial No._____

Submitted by

_____
_____

This voltage standard was tested for frequency response using the rms voltmeter (DVM) of the NBS AC Voltmeter/Calibrator at a room temperature of 23 ±1°C.

The test points (nominal voltage and frequency), corrections, and total uncertainty are shown in the attached TABLE OF CALIBRATIONS. Also shown is the confidence level upon which the imprecision is based. The uncertainty caused by the DVM frequency response is treated as a systematic error. Unless otherwise indicated, the total uncertainty is based on the largest standard deviation encountered for any of the test points. Measurements on the test unit were made over a period of time which was too short to yield long-term stability information.

For the Director
National Engineering Laboratory

Barry A. Bell, Group Leader
Electronic Instrumentation and Metrology
Electrosystems Division

Test No. 722/_____
Order No. _____
Date_____
Attn:_____

APPENDIX B

Detailed Design of Voltage Calibrator

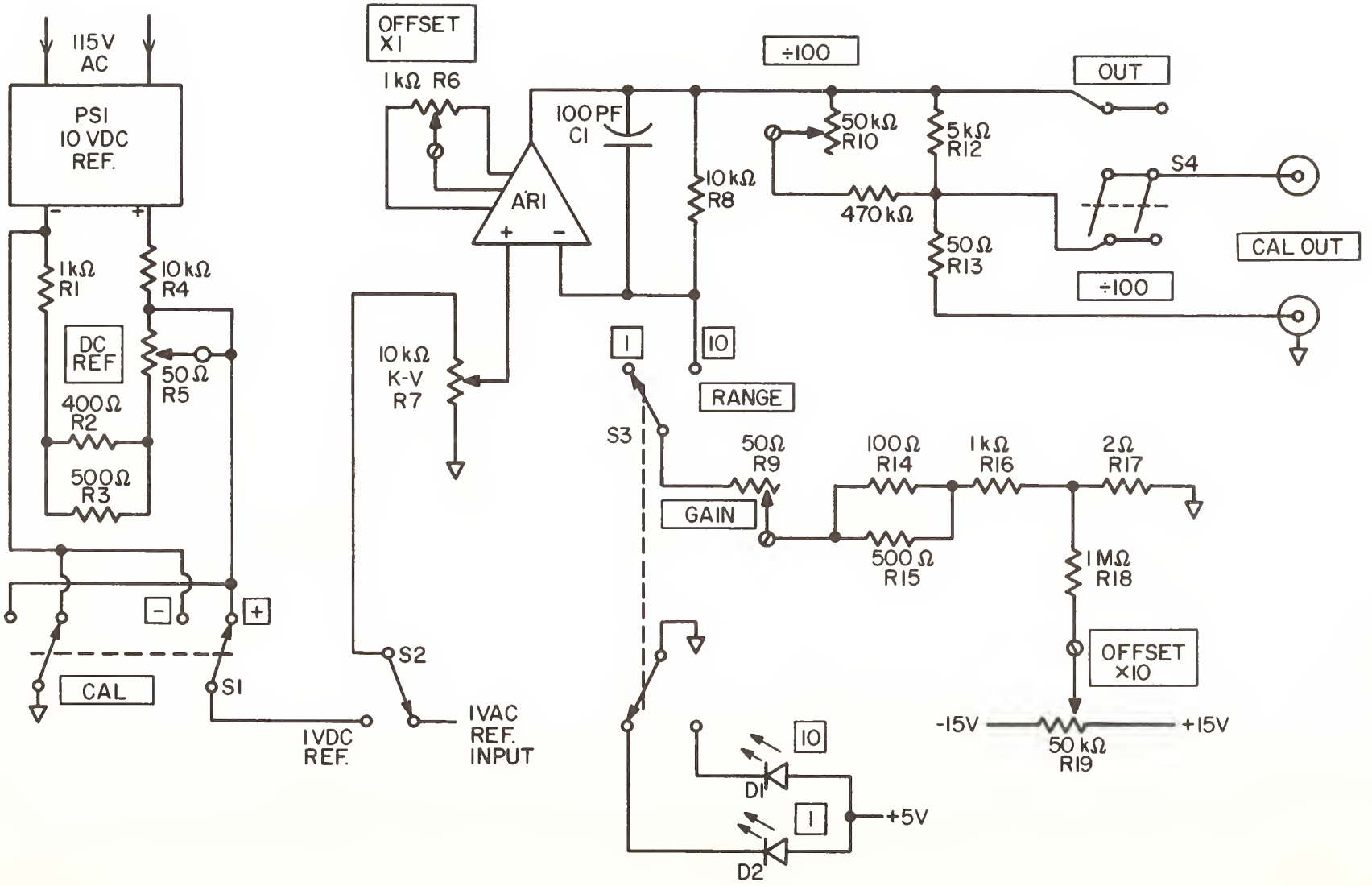

Figure B-1. Voltage calibrator. The 1 VAC reference is shown in figure B-2.

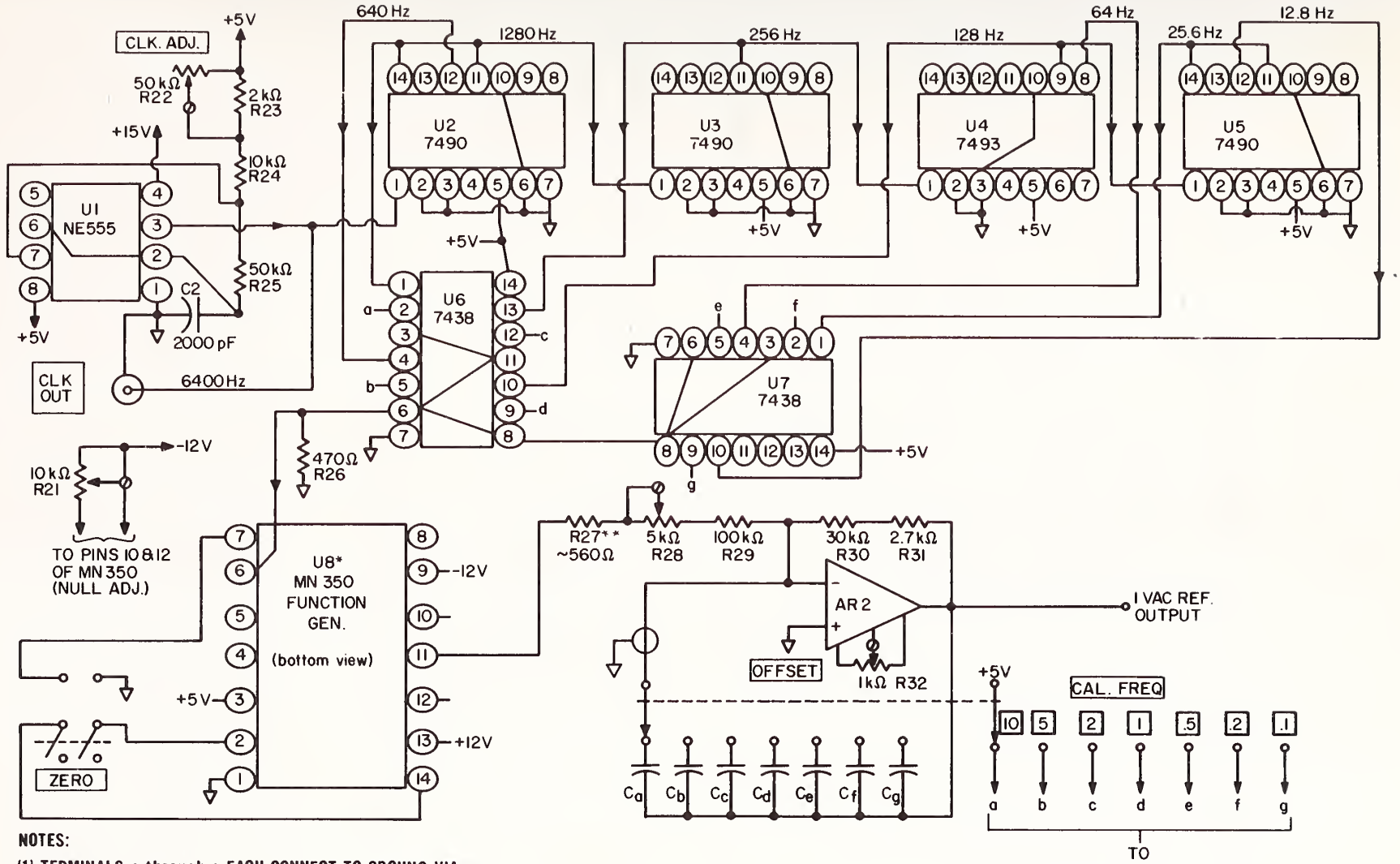

NOTES:

(1) TERMINALS a through g EACH CONNECT TO GROUND VIA 470Ω, SHUNTED BY 0.1μF

*MOUNTED ON 3×4×¼ in. Cu HEAT SINK VIA STEEL SPRING CLAMP

**TEMPERATURE COMPENSATING RESISTOR

Figure B-2. AC (sine-wave) reference.

Description of Components Used in Voltage Calibrator

Amplifiers AR1 and AR2 are Analog Devices Type 52K.[1]

Capacitors C1 and C2 are 5 percent silver mica types. Capacitor C2, or associated timing components, may need trimming to yield the desired clock frequency. The capacitors associated with AR2 should be trimmed so that (capacitance)(calibrator frequency) = constant, to within ±0.2 percent. Nominal values (μF) are: C_a = 0.025, C_b = 0.05, C_c = 0.125, C_d = 0.25, C_e = 0.5, C_f = 1.25, and C_g = 2.5. These polycarbonate capacitors have a rating of 100 V, 5% tolerance and ±0.1%/°C temperature coefficient. They were shunted with smaller capacitors (mica or polycarbonate) to obtain the desired capacitance ratios.

The function generator (U8) is Micro Networks Corporation Type MN350.

The dc reference (PS1) should have a dc stability of better than ±5 ppm/year.

Resistors R12 and R13 are 1W precision wirewound resistors with ±0.01% tolerance and temperature coefficients matched to within 2 ppm/°C. Two parallel 100 Ω resistors may be used for R13. All trimpots are 1W, 25 turn, panel mount type with ±150 ppm/°C temperature coefficient. Resistors R1 - R4, R8, R14 - R16, R23 - R25 and R28 - R30 are Vishay Resistive Systems Group Type 5102C. A non-inductive wirewound resistor was used for R17. R27 is a sensistor from Texas Instruments, whose value is determined from temperature tests. R7 is a general resistance Type DV-4007A K-V divider.

Switches S1 - S4 should have plastic sleeves on their handles to minimize thermal voltage generation at the switch contacts.

---

[1] Certain commercial equipment, instruments or materials are identified in this report in order to adequately specify procedures or special circuits. In no case does such identification imply recommendation or endorsement by the National Bureau of Standards, nor does it imply that the material or equipmment identified is necessarily the most suitable for the purpose.

APPENDIX C

Shipping and Fee Information

General shipping instructions are given in the latest issue of NBS Special Publication 250, "Calibration and Related Measurement Services of the National Bureau of Standards." Shipments of voltmeters and voltage sources for calibrations should be directed to

National Bureau of Standards
Electrosystems Division, MET B162
Rt. 270 and Quince Orchard Road
Gaithersburg, MD 20878 .

Current information on calibration fees is given in the NBS Special Publication 250 Appendix, which is updated every six months.

THE PRACTICAL USES OF AC-DC TRANSFER INSTRUMENTS

Earl S. Williams

ABSTRACT

Alternating currents and voltages are measured most accurately at this time when they are compared with nominally equal and known dc currents and voltages. The comparisons are usually made with thermal transfer instruments which respond nearly equally to ac and dc quantities. Practical information and recommended procedures are given for using these instruments along with diagrams of apparatus and examples of typical data and calculations. Methods for minimizing difficulties caused by dc reversal differences, thermal drift, energy picked up from local electromagnetic fields, and the deviation from square-law response of these instruments are considered. Causes of ac-dc differences are discussed, and methods for measuring them and applying corrections are also described.

Key words: ac current measurements; ac voltage measurements; ac-dc comparator; ac-dc difference; thermoelement.

1.0 Introduction

The basic units for electrical measurements are derived at the National Bureau of Standards in absolute terms from the units of mass, length, and time. The standards primarily used to transfer these units for direct current measurements from NBS to other users, and to preserve them in the standards laboratories, are the saturated standard cell (the volt) and the standard resistor. With these and a variety of shunts and resistance ratio instruments for range extension, direct current and voltage can be measured with high accuracy.

Since there is no ac counterpart to the standard cell, measurements of alternating current, voltage, and power are made relative to these same standards. The chain of measurements is extended to these alternating quantities by ac-dc transfer instruments, which have a flat and known frequency response and hence may be calibrated on direct current and then used for alternating current measurements. They provide an accurate transfer from direct voltage and current standards to alternating current and voltage measurements, hence the name.

Electrodynamic instruments have been used to transfer voltage, current, and power; however, they are limited in frequency to a few thousand hertz due to their relatively high inductance. Electrostatic moving systems are usable to higher frequencies, but they have severe low voltage limitations. Instruments which respond to peak and average values of ac voltage have been employed successfully over certain voltage and frequency ranges (see section 3.8). The instruments most widely used for voltage and current transfer measurements, and the ones to be discussed here, are electrothermal. They are usually called thermal voltage converters (TVCs) and thermal current converters (TCCs) to distinguish them from other types of transfer instruments [1].

2.0 Thermoelements

The key component in these transfer instruments is a thermoelement (TE), consisting of a heater which carries the current to be measured and a thermocouple attached to its midpoint. The output from the thermocouple is relatively low (7 to 12 mV); however, heater current differences, and differences between ac and dc currents, as small as one part-per-million (ppm) can be detected, if changes in the output are monitored with a sensitive detector--a galvanometer or microvoltmeter. Thermoelements for currents from 1 to 1000 mA are available with evacuated glass-bulb enclosures and with insulation (a small ceramic bead) between the thermocouple and heater (fig. 1). TEs are available for currents up to at least 20 amperes, but vacuum enclosures are not feasible at these currents because the elements require heavy copper conductors which are very difficult to pass through a vacuum seal. Insulation is not generally available in TEs for currents greater than one ampere. They are difficult to construct, and the demand for them is not great. Most current comparisons are made with special ac shunts in parallel with low-range TEs (see section 8).

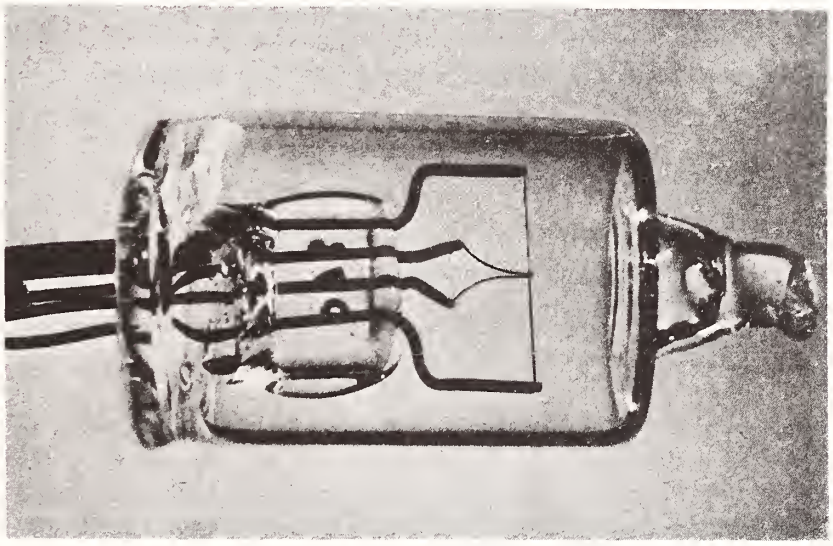

Figure 1. Vacuum thermoelement. (Heater and thermocouple wires retouched.)

The TE heater is short and straight thus having minimal reactance, and the insulation of the thermoelement prevents any appreciable interaction between the ac current and the read-out instrument. TEs are therefore well suited to measurements at audio and higher frequencies. They are used with series resistors in multirange TVCs up to 100 kHz on most ranges and to 1 or 2 MHz at low voltages. Single-range units with carbon or metal film resistors coaxially mounted in tubular casings are used up to 100 MHz.

Multijunction thermoelements [2,3,4,5], with a relatively low heater temperature and 50 to 200 thermocouples in series distributed evenly along the heater, are capable of higher accuracy in transfer measurements, and their structure minimizes most of the thermoelectric effects that cause errors in

other types of TEs. However, they are difficult to construct, and therefore expensive and not readily available.

2.1 Output Characteristics

The thermocouple output of the TE is a function of the power dissipated in the heater, and therefore varies approximately as the square of the heater current. However, the device does deviate significantly from a square-law response as the heater current approaches the rated value. The relationship of the output, E, to the heater current, I, may be expressed as

$$E = kI^n. \tag{1}$$

The response appears to be nearly square-law (i.e., n=2) at very low currents, but n is usually 1.6 to 1.9 at rated heater current. The factor k varies somewhat with large changes in heater current, but this is not a constraint. The TE is a substitution device, and not normally used to measure ac current as a function of thermocouple output. The factor k is constant over a narrow range where nearly equal ac and dc currents are compared.

The relationship between a small change in TE heater current (ΔI) and the corresponding change in output (ΔE) is expressed as

$$\Delta I/I = \Delta E/nE. \tag{2}$$

If the thermoelement is in a TVC,

$$\Delta V/V = \Delta E/nE. \tag{3}$$

It is often advantageous to make measurements of n and use the data in calculations as suggested in sections 3.2 and 6.2. The measurements are not difficult, and the values are quite permanent. Methods for measuring n are described in section 7.

2.2 DC Reversal Difference

DC reversal difference is generally (and in this document) defined as the percentage difference between the dc current and its reversed counterpart, when they both produce the same output from a TE. This difference is not necessarily constant and may increase in some TEs as the heater current is lowered. A low dc reversal difference is, of course, advantageous. The difference between ac and dc voltage and current is often measured by observing the change in indication of an instrument which responds to changes in TE output as ac and dc are applied. If the dc reversal difference is large, it may be necessary to reduce the sensitivity of the read-out instrument to keep all readings on scale.

It is recommended that both directions of dc be used in the procedures described here. However, it is not often necessary to have an explicit measurement of dc reversal difference. A measurement may be desirable sometimes, as for instance when making sure that new TEs conform to specifications. A low-range TE can be connected in series with a resistance of 50 to 200 kΩ, and the appropriate voltage applied for rated heater current. The value of the two direct voltages which give equal output can be read from a

calibrated source or measured with a digital voltmeter. Common current-measuring equipment, usually a potentiometer or a digital voltmeter and a shunt, is used to measure currents in higher range TEs. In any method, it is advisable to use a test sequence which will minimize the effect of drift in the TE output. Readings should be taken with DC+, DC-, DC+ after time intervals which are about equal. The average of values obtained with the two positive dc voltages should be used in the calculations.

DC reversal difference can also be measured conveniently with a second or reference TE of about the same range and with known n values. The two heaters are connected in series through a switch which reverses the test TE input but not that of the reference one (fig. 2). Direct and reversed currents are adjusted for equal output from the test TE (null on detector D1). The emf of the reference TE (E) is read from its potentiometer (Pot'r) and changes in emf (ΔE) are computed from readings taken from the detector (D2), which must be a microvoltmeter or a calibrated galvanometer. DC reversal difference, $\Delta I/I$, is then computed from eq. (2).

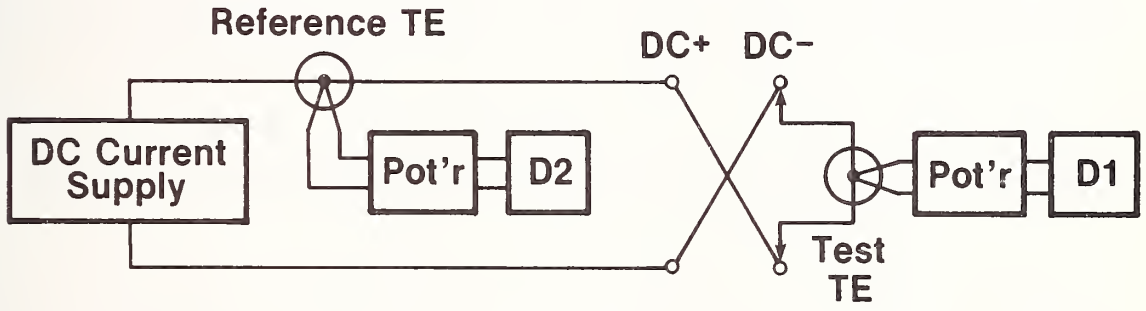

Figure 2. Circuits for dc reversal difference measurements.

As pointed out in the previous section, a TE output varies approximately as the square of the heater current. If dc reversal difference were to be defined as the percentage difference between emfs obtained with equal currents in opposite directions, the figure would be about twice as large.

DC reversal differences range from near zero to several hundredths of a percent. They are largely due to Peltier heating and cooling at the ends of the heater, and to Thomson heating in the two halves of the heater [6,7]. Both of these effects cause asymmetry in the temperature rise of the heater. The asymmetry is affected when the current is reversed, and therefore the temperature at the point where the thermocouple is attached is changed. DC reversal difference is minimized by placing the thermocouple at the thermal center of the heater. If the heater wire is not quite uniform, this may not be the exact mechanical center. DC reversal difference is therefore not easily controlled. Some manufacturers sort TEs according to dc reversal difference and market those with low dc reversal difference as a premium product.

DC reversal difference rarely changes with use, and the few changes that have been observed are believed to be due to the heater having been overloaded. One possible explanation for this is that one-half of the heater was stressed more than the other, and its thermal center was shifted relative to the thermocouple's position. If this model is correct, the dc reversal difference could be either increased or decreased by an overload.

2.3 Temperature Coefficient

The temperature coefficient of most TEs (percentage change in output for a temperature change of 1 °C with constant heater current) is relatively high--often 0.1%/°C. Elements should therefore be mounted in a thermally lagged enclosure to minimize the effect of ambient temperature changes. The output of a TE can be very stable at a fixed temperature if the heater is carrying a constant current for several hours. However, if the instrument is switched back and forth between ac and dc after a brief warm up, as it is in most measurements, the output will usually drift. The drift may be negligible during the short time required for a measurement, especially at low voltages. However, on many ranges where there is some self-heating effect, the drift rate is apt to be quite constant but significant. Accurate and consistent measurements can be made under these circumstances, if readings are taken at time intervals that are about equal and in a sequence which tends to average out the effect of drift (e.g., [a] +DC, AC, -DC or [b] AC, +DC, -DC, AC).

2.4 AC-DC Difference

Thermoelements, as well as TVCs and TCCs, sometimes have a significant ac-dc difference, δ, particularly at higher frequencies,

$$\delta = (V_a - V_d)/V_d \ ,$$

where V_a and V_d are the ac voltage and the average of the two directions of dc voltage required for equal response, or output emf. For voltage measurements,

$$V_a = V_d\,(1 + \delta). \qquad (4)$$

Similarily, for current converters, $I_a = I_d\,(1 + \delta)$.

AC-dc differences, methods for measuring them, and the application of corrections are discussed in sections 5.0 to 6.5.

2.5 Radio Frequency Interference

Thermoelements have a frequency response which extends to 100 MHz or more, and measurements made with them can therefore be affected by local electromagnetic fields. Interference from television stations can be particularly troublesome with low-current TEs, because the length of leads used in calibration laboratories often makes them an effective antenna. Energy picked up by a measurement circuit can usually be detected by shorting the TVC input terminals with all connections in place as in normal use, but with the power supplies off. Any change in the indication of a detector in the TVC output circuit as the short is opened and closed will indicate a pick up problem. Interference can usually be avoided by using coaxial leads and shielded circuit components. In extreme cases it may be necessary to work in a shielded room.

3.0 Voltage Measurements

AC voltage is measured most accurately at this time by comparison with a nominally equal dc reference voltage using a thermal voltage converter. The TVC may consist simply of a series resistor and a thermoelement mounted coaxially in a tubular casing, usually a plated brass tube, with input and output connectors [8]. As noted earlier, this configuration is well suited to rf measurements. In another arrangement, the resistor is mounted in one tube and the TE in another. The TE can then be attached to any one of a set of resistors to make a TVC with the desired voltage range [9]. The number of resistors in a set can be reduced to about half, by using two TEs with different current ratings (e.g., 2.5 and 5 mA). Each resistor is then used for two ranges [10]. These sets, which are commercially available, have two distinct advantages. The ac-dc difference corrections are very small, and they can be determined relative to any one range, which has known corrections, by a step-up or step-down intercomparison of adjacent ranges.

Multirange TVCs usually contain 10 to 14 ranges between 0.5 and 1000 volts, and ranges are selected with a rotary switch which connects the TE in series with one of the ranging resistors. Some commercial models also incorporate an ac-dc switch, as well a null detector, and a balancing emf source for monitoring the TE output. (The "balancing emf" referred to here and elsewhere usually consists of the voltage across a fixed resistor with current supplied by a battery and adjusted with a resistive divider or series resistors. The circuit may be quite similar to the Lindeck potentiometer shown in fig. 3, but without the milliammeter. It balances, but does not measure, the emf.) If these components are not included in the TVC, the relatively simple Lindeck potentiometer (fig. 3) can be used with a detector, which may be either a microvoltmeter or a galvanometer, to monitor the TE output.

The detector can be simply used as a null detector when an ac voltage is adjusted to be equal to a reference dc voltage (3.1), or a calibrated detector can be used to measure the changes in TVC output emf as ac and dc voltages are applied alternately. The difference between the ac voltage and the dc reference is then computed from the emf differences (3.2). Provisions are made, and instructions furnished, by some manufacturers for using either method.

3.1 A Null Method

In the "null" procedure, the ac voltage to be measured is applied to the TVC and the balancing emf is adjusted for a detector null. The two polarities of dc voltage are then applied in turn, and each one is adjusted to produce a null indication on the detector. The two voltages are measured (or read from a calibrated source), corrected, and averaged. The average is corrected for the ac-dc difference, δ, of the TVC to give the RMS amplitude of the ac voltage. For example, from eq. (4), with δ = -0.012%, V_d+ = 200.012 V, and V_d- = 199.960 V,

$$V_a = [(200.012 + 199.960)/2] + (V_d \times -0.012/100)$$
$$= 199.986 - 0.024$$
$$= 199.962 \text{ V}.$$

AC voltage should be reapplied after the two dc voltage measurements, to evaluate any significant drift from the original null position. To find the magnitude of the drift, the detector can be calibrated by making a small change in the dc voltage, observing the change in detector indication, and computing the scale sensitivity in percent per division. If the drift is large, a longer warm up period should be allowed, or the "deflection method" (3.2) may be used.

In the example above, a small part of the 0.026 percent difference between the two dc voltages may be due to drift in the TVC output, but most of it is due to the dc reversal difference. These measurements are sometimes carried out with only one direction of dc voltage, and a correction equal to half the dc reversal difference is then applied. This must be done very cautiously. If the correction is applied with the wrong sign, the error is twice as large as with no correction. Of course, if the dc reversal difference is small relative to the desired accuracy, satisfactory measurements may be made using only one direction of dc current flow.

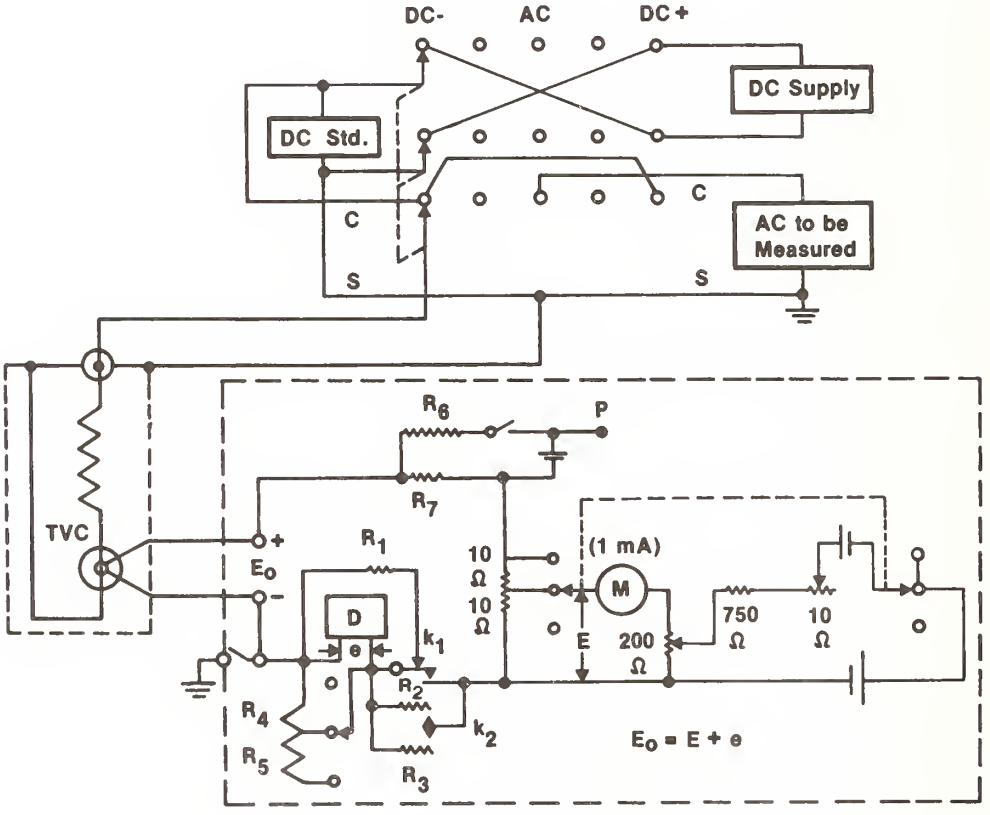

Figure 3. AC-dc switching, TVC and potentiometer for ac-dc comparisons.

NOTES:

The "DC Supply" may be a calibrator and serve as both source and standard, or the voltage may be measured with a "DC Std."--a digital voltmeter or a volt box and a potentiometer.

R_4 and R_5 (see section 3.3) and R_6 and R_7 (section 3.6) are optional. They are used to adjust and measure the detector sensitivity, respectively.

The null procedure has certain disadvantages which should be kept in mind: (A) If the dc standard is one of the widely used five or six dial calibrators, adjusting it for a detector null may be tedious and time consuming; (B) the wear on the lower two or three control switches will be accelerated; (C) the calibration of the dc standard may be in some question if a number of readings are obtained above and below the round-number value where a calibration test was made; (D) if the TVC output drift is significant during the time required for the null adjustment, it may be difficult to obtain consistent results. Where the drift rate is constant, and the measurements are made in equal time spans, the results may be consistent but in error; and (E) if the dc voltage is supplied by a power supply and measured with a volt box and potentiometer, the time required for the two adjustments (the voltage adjustment for a TVC null and then the potentiometer balance) may be even longer. The two adjustments can be made in less time if two operators work together.

3.2 A Deflection Method

A calibrated detector may be used with a TVC to measure the difference between a dc reference voltage and an ac voltage. The difference can be applied as a correction, C, to the dc voltage to obtain the value of the ac voltage.

$$V_a = V_d\,(1 + C) \qquad (4A)$$

(see section 3.5, Calculations)

This procedure will largely avoid the problems listed above. It should also save time, as the adjustments are fewer and less tedious. The data and calculations may be a bit more complicated; however, once routine procedures are established, this method can be used with confidence. If the correctness of the results is in question, they can be verified by relatively simple extra tests, as described in section 3.5.

In the deflection method, the dc voltage is adjusted to a round-number value which is nominally equal to the ac voltage to be measured. The TVC is connected to the dc voltage (see fig. 3), and the balancing emf (or potentiometer) is adjusted for a near null on the detector. The TVC is then switched to the ac and dc voltages in the sequence indicated in fig. 3 (DC+, AC, DC-), and the small emf variations are read from the detector directly or computed from the detector readings,* as explained below. The difference between the ac and dc voltages is computed from these readings.

An equation very much like (3) in section 2.1 is used. Instead of a simple change in TVC input voltage ($\Delta V/V$), the difference between the ac voltage (V_a) and the corrected dc voltage (V_d) is measured by observing the change in TVC output. Therefore, ΔE in eqs. (2) and (3) becomes $E_a - E_d$, the emfs corresponding to the voltages V_a and V_d. The eq. (4A) above may therefore be written

---

* The detector should be connected so the indication increases, or deflects up scale, when the input voltage to the TVC is increased.

$$V_a = V_d\,(1 + C) = V_d\,(1 + \frac{E_a - E_d}{nE} + \delta),$$

where, as before, n is the exponent in eq. 1, E is the output of the thermoelement, and δ is the ac-dc difference correction to the TVC.

The emfs E_a and E_d are the TVC outputs (E_o, fig. 3) with ac voltage and the two directions of dc voltage applied to the TVC. However, all but a small fraction of these emfs are balanced by the emf source or the potentiometer. The difference between the two emfs can be computed from imbalance emfs, e, read from a microvoltmeter.

The procedure is probably most straightforward when a digital microvoltmeter is used. Emfs are indicated directly in volts (μV or nV). AC and dc voltages should be applied, and emf readings taken, in time intervals which are about equal. Apply DC+, AC, and DC-, read e_1, e_2, and e_3, and compute

$$E_a - E_d = e_2 - (e_1 + e_3)/2.$$

The complete calculation is discussed in section 3.5. The digital microvoltmeter indicates both positive and negative readings with the sign displayed, but mistakes are less likely to occur if the balancing emf is adjusted so that all readings have a positive sign.

Emfs may also be read directly from a deflecting microvoltmeter. However, it is recommended that readings be made in divisions, a deflection change, ΔD, computed, and the emf difference $E_a - E_d$ be computed from the deflection change. Techniques for reading detector scales are described in section 3.7, and multiplying factors, K, for converting ΔD to emf differences are also discussed. Calculations from data taken by this procedure are shown in table 1, column 5, where

$$E_a - E_d = (D_2 - (D_1 + D_3)/2) \times K\ .$$

Emf differences may also be measured by a calibrated galvanometer.

3.3 Electronic Galvanometers

An electronic galvanometer with appropriate sensitivity may be used to measure an emf difference, if a method is provided to determine its voltage sensitivity, K, as described in section 3.6. Electronic galvanometers are available with continuously adjustable gain control over a wide range, and this feature provides a significant advantage. The sensitivity can be adjusted for maximum resolution for each measurement. On the other hand, a deflecting microvoltmeter's sensitivity drops typically by about 60 percent if the range is increased (e.g., from 10 to 30) to keep all readings on scale.

Table 1. Examples of Calculations

In these examples, data are listed in columns 3 and 5 and identified in columns 1, 2, and 4. Test parameters are listed in the first eight lines. An emf difference, ave ΔE, is computed from emf readings e_1 to e_5 in column 3 and from deflection readings D_1 to D_5 in column 5. See text for further explanation.

1	2	3	4	5
Freq	kHz	50	Freq	50
Range	test inst.	200	Range	200
V_d	DC voltage(V)	200.006	V_d	200.006
TVC	range	200	TVC	200
E	TVC emf (mV)	8.8	E	8.8
n		1.83	n	1.83
nE		16.1	nE	16.1
μVm	range	10	μVm	10
			K	2×10^{-4}
e_1	dc	6.5	D_1	23
e_2	ac	4.4	D_2	36
e_3	dc (rev)	7.1	D_3	73
e_4	ac	4.1	D_4	35
e_5	dc	5.8	D_5	20
ΔE_1 *	μV	-2.4	ΔD_1	-12
ΔE_2 *	μV	-2.3	ΔD_2	-11
ave ΔE	mV	-0.0024	ave ΔE	-0.0024 ($\Delta D \times K$)
$\frac{100\ \Delta E}{nE}$	percent	-0.015	$\frac{100\ \Delta E}{nE}$	-0.015
δ	TVC corr %	+0.003	δ	+0.003
C	Final corr %	-0.012	C	-0.012

Notes: $*\Delta E_1 = e_2 - (e_1 + e_3)/2$ and $\Delta E_2 = e_4 - (e_3 + e_5)/2$

e_1 and e_5 differ because of drift in the TVC output. e_1 and e_3 differ partly because of drift but mainly due to dc reversal difference in the TVC. In the statements above, substitute D for e where the readings are in divisions.

If a "one-range" instrument intended mainly as a null detector is used, an arrangement to adjust its sensitivity is often desirable. Such detectors can be shunted by resistors, such as R_4 and R_5 in fig. 3. When the potentiometer is balanced, the detector responds to currents through these resistors. The switch, which must have contacts with very low noise and thermal emfs, may select one or several shunting resistors. The resistor values should be chosen experimentally, depending on the basic sensitivity of the instrument and the sensitivity desired. Difference ratios of 2/1 or 3/1 between sensitivities are recommended. These instruments may be calibrated as suggested in section 3.6, and the scale reading techniques of section 3.7 are useful also.

3.4 D'Arsonval Galvanometers

D'Arsonval (permanent magnet, moving coil) galvanometers are often considered to be quaint, if not obsolete, by electronically oriented metrologists, and buying one for these measurements is not recommended. However, if an appropriate galvanometer is readily available, as is often the case, it should not be rejected out of hand. It is probably superior to most electronic instruments in two important respects--noise rejection and zero stability. Its sensitivity will probably be quite low unless a photoelectric galvanometer amplifier is used to increase its input voltage. However, some galvanometers may be sufficient for certain measurements where the voltage differences are large, or where there is less need for accuracy.

It is advisable to test a galvanometer for linearity if a deflection method is to be used by applying small equal changes to the potentiometer input and seeing that the resulting changes in indication are about equal on all portions of the scale. Some instruments may be nonlinear at the extreme ends, but satisfactory over most of the middle portion.

3.5 Calculations

Table 1 is intended to illustrate data logging and calculations and to suggest a data sheet format. Different data arrangements and line labels may be preferred by some users, but it is advisable to develop a more or less standardized data sheet for each type of measurement. The line labels in column 1 are brief to conserve space ($E_a - E_d$ is abbreviated to ΔE as in eqs. (2) and (3)), but they should be sufficient for a practical data sheet. Labels are further explained or defined in column 2.

In column 3, a correction, C, is determined for a test instrument indicating 200.000 V at 50 kHz. The measurements are made relative to a corrected dc reference voltage of 200.006 V. Two emf differences, ΔE_1 and ΔE_2, are computed from five readings of a digital microvoltmeter. The average ΔE is changed to millivolts to be in the same units as the TVC output, E, before being divided by nE. (Measurements and plots of n are discussed in section 7.0.) $\Delta E/nE$ is multiplied by 100 to obtain a percentage value, and the ac-dc difference correction to the TVC (δ) is added to determine the correction, C, to be applied to the dc voltage to obtain the ac value.

The same test is repeated in columns 4 and 5, but the data are read in divisions from a deflecting microvoltmeter. The line labels in columns 1 and 4 are very similar. Deflections D_1 to D_5 are read rather than emfs, ΔD_1 and ΔD_2 are computed, and the average is multiplied by conversion factor $K = 2 \times 10^{-4}$ (from table 2) to find the average ΔE in millivolts. The rest of the calculation is the same as in column 3. If data in ppm are preferred, the average ΔD can be multiplied by K=200 from table 2 to obtain -2400 nV. Then

$$\Delta E/nE' + \delta = -2400/16.1 + 30 = -120 \text{ ppm} .$$

The correction, C, expressed in percent, can be applied to the reference voltage, V_d, in two ways, as illustrated below, to obtain the measured value of ac voltage, V_a. The calculation on the right may be preferable where a machine calculator is not used.

$$V_a = V_d (1 + C/100)$$
$$= 200.006 (1 + (0.01 \times -0.012))$$
$$= 200.006 (.99988)$$
$$= 199.982 \text{ V}$$

$$V_a = V_d + (V_d/100 \times C)$$
$$= 200.006 + (2 \times -0.012)$$
$$= 200.006 - 0.024$$
$$= 199.982 \text{ V}$$

where C is expressed in percent

*** If the accuracy of the procedure or the correctness of the sign is in question, it can be verified as follows: Increase the dc voltage by 0.020 percent after a measurement, and repeat the procedure and calculation. The correction, C, should be 0.020 percent more NEGATIVE than in the first measurement.

3.6 Galvanometer Calibration

An obvious method for calibrating a galvanometer scale in these test circuits is to introduce a small measured change in the TVC input, observe the resulting change in indication, and compute a multiplying factor, K, for converting changes in indication to voltage differences (e.g., percent/div or ppm/mm). This method has certain advantages. No n data are required, and the TVC output, E, need not be measured. It is also quite feasible in voltage measurements if the small voltage change can be measured with the dc standards being used. The change should be large enough for good resolution, but of course, the galvanometer must not deflect off scale.

This calibration method is, however, more tedious and time consuming than some alternate methods. It may also require additional equipment in ac-dc difference measurements (see 6.2) where no dc standards are ordinarily used.

Several calibration methods have been developed to introduce a known change in emf directly in the detector circuit. In one of these, a change in resistance (ΔR) in the balancing emf circuit produces a change in current and hence a change in emf. However, this requires a rather sophisticated circuit with practically constant resistance (except for the ΔR) at all emf levels.

A relatively uncomplicated calibration circuit, which requires its own battery, is shown in fig. 3. It consists of R_6 and R_7, an on-off switch and a 2400-mAh mercury battery. A computable emf, e, is inserted across R_7 (a one percent, 1-ohm resistor is recommended) by closing the switch. A round-number emf of 10 μV (R_6=135 kΩ) will be satisfactory in many instances; however, the calibrating emf should be commensurate with the detector sensitivity. A rotary switch with several contacts can be used to connect any one of several resistors in the R_6 position. It may be desirable to have more than one calibrating emf if the sensitivity of the detector is adjustable over a wide range.

A multiplying factor, K, (μV/div) is computed from the deflection observed when the voltage is inserted. The deflection change, ΔD, (sections 3.2, 6.2 and 8.0) resulting from differences between ac and dc voltages or currents, is multiplied by K to obtain the emf difference, $E_a - E_d$. This factor K is equivalent to K in table 1 (column 5). But in that example the detector is a microvoltmeter, and K is obtained from table 2.

Table 2. Conversion Factors K

Microvolts	Divisions	μV	K (x by) for 100-div scale		
μV range	(full scale)	(full scale)	div to millivolts	div to microvolts	div to nanovolts
30	60	60	6×10^{-4}	0.6	600
10	100	20	2×10^{-4}	0.2	200
3	60	6	6×10^{-5}	0.06	60
1	100	2	2×10^{-5}	0.02	20

The current drawn by the battery is, of course, minimal, and the mercury cell maintains a nearly constant voltage for most of its useful life. A new battery should last a year unless it is inadvertently left on for an extended period. It is advisable to check its voltage occasionally by connecting a voltmeter between the positive input connection and the test point "P" (fig. 3). The potentiometer switch may be either on or off.

3.7 Reading Deflecting Detectors

The scales on most suitable microvoltmeters and galvanometers have the zero indication at the center, so that positive and negative readings can be made to the right and left. Microvoltmeters with intermediate ranges--3, 30, 300, etc.--usually have scales with 30 divisions to either side of zero as well as 50-division scales for the decade ranges. This arrangement is convenient for most measurements and for null detectors. However, it is very desirable to have the zero at the far left for the procedures described here. Typical microvoltmeter scales are shown in fig. 4, but with a number plate in front of the 50-division scale. The substitute numbers are engraved on a plastic plate and filled with black wax. A similar plate can be made by cementing cut-out numbers on a transparent plate. The instrument is read with zero at the left and a full scale range of 100 divisions. It can be read in microvolts; however, some conversion to other units will probably be advantageous in the

calculations. It is probably more straightforward, and mistakes are less likely, if readings are recorded in divisions. A deflection difference, ΔD, can be computed in divisions and then converted to an emf difference, ΔE, using the appropriate factor, K, from table 2 below.

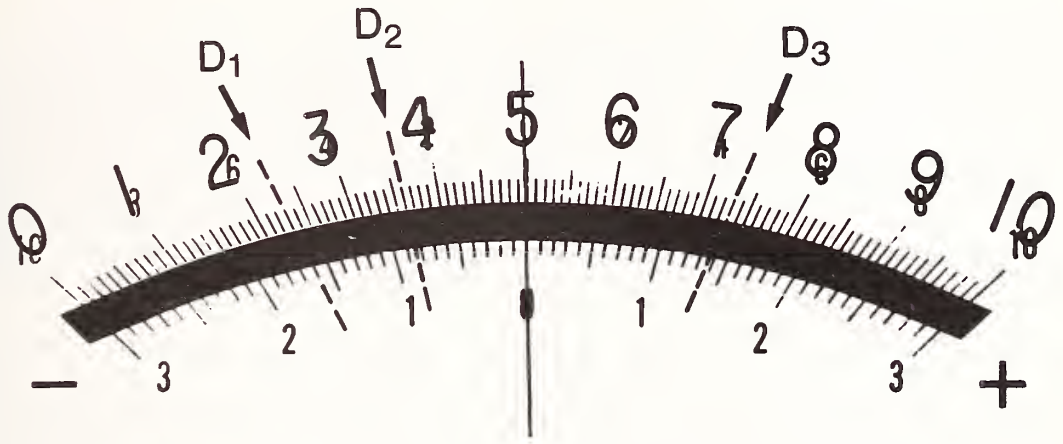

Figure 4. Typical microvoltmeter scales with three deflections marked.

Three readings are marked on the scale in fig. 4 at 23, 36, and 73 divisions as an illustration. If the reading at 36 divisions corresponds to an ac voltage or current and the others to direct and reversed-dc, then

$$\Delta D = D_2 - (D_1 + D_3)/2 = 36 - (23 + 73)/2 = -12 \text{ div.}$$

Of course, the same result is obtained when the regular scale is read, but the sign must then be observed very carefully. The readings are -27, -14, and +23, and

$$\Delta D = -14 - (-27 + 23)/2 = -12 \text{ div.}$$

Obviously, mistakes are less likely with the substitute numbers, where all readings are positive.

The scales shown in fig. 4 are typical of several instruments in which the zero and full scale indications on either scale coincide. It is feasible--and advantageous--to read the 100-division scale with any range on most of these instruments. The same substitute numbers can be used with any range, and the reading precision is better with 100 divisions. The feasibility of this procedure must, of course, be verified for any particular instrument. In the example in fig. 4, the indications marked on the 100-division scale are extended to the 60-division scale and read as 14.0, 21.5, and 43.5. Then ΔD = 21.5 - (14 + 43.5)/2 = -7.25 div. The emf difference is -7.25 μV on the 30-μV range (60 div full scale). If the corresponding reading of -12 divisions on the 100-division scale is multiplied by 0.6 from table 2, essentially the same result is obtained.

The table gives factors, K, for converting deflection changes to mV, μV, and nV for the four most-used ranges. As indicated in the text, a conversion to mV is preferred for results in percent while nV are more convenient for ppm.

3.8 Peak and Average Responding Instruments

Peak and average responding instruments are widely used for certain applications, and their principles can be adapted for ac-dc comparisons. They are not electrothermic and are therefore outside the intended scope of this writing. However, since at least one peak comparator [11], a peak calibration method [12], and one average responding ac-dc comparator [13] have been developed, they are noted here and referenced. The accuracy of these comparators is sufficient for many applications; however, they are more limited in voltage and frequency range than electrothermic instruments. These comparators are not commercially available at this time.

4.0 Switches and Potentiometers

As noted earlier (3.0), some commercially available multirange TVCs have provisions for ac-dc switching as well as an adjustable emf source and a detector for monitoring the thermoelement output. If these components are not included, or if single-range TVCs, thermoelements or TCCs are to be monitored, the equipment described in this section is not difficult to build, and the parts are readily available. The circuits are shown in some detail in fig. 3, and of course, variations can be made to meet particular needs. The diagram of the potentiometer includes two optional features, as noted below the caption, which were discussed in previous sections.

4.1 AC-DC Switches

The ac-dc switch shown in fig. 3 connects the TVC to either direction of dc voltage, or to the ac voltage to be measured, in the order suggested in section 3.2. Other switch arrangements, such as reversing dc with a separate switch, should be satisfactory also. The ac input to the switch, and the cable connection to the TVC, should be coaxial to minimize electromagnetic interference and circuit impedance. The switch and the potentiometer should be in separate shielded enclosures, and the cable to the detector, D, input should also be shielded.

The dc voltage may be supplied by a calibrator which serves as both source and standard, or a separate standard (a volt box and potentiometer or a digital voltmeter) may be connected at the terminals for "DC Std." The standard should not be appreciably affected by changing the polarity of the applied voltages. At very low voltages, where the voltage drop across the line resistance may be significant, the dc voltage should be monitored at the "DC Std." terminals. The cables with conductors c and shields s (fig. 3) should have equal resistance (identical cables are preferable) to equalize the voltage difference between the ac and dc voltage terminals and the comparison points at the switch contacts.

The ac-dc circuit should have only one ground point, usually, but not necessarily, at the ac source. The switching circuit shown in fig. 3 provides

a direct connection from the TE to ground. It is preferable to have no switch in this part of the circuit. If a switch is used, and if it opens an instant before the switch contact in the input side, the insulation between the thermoelement heater and the thermocouple will probably be punctured by an excessive voltage.

4.2 Lindeck Potentiometers

A two-range (10- and 20-mV) potentiometer is shown in fig. 3. It is powered by a 1.35-V mercury battery and controlled by two helical resistors, which may be either the 3- or 10-turn devices currently available. If the "deflection method" proposed in section 3.2 is used, the fine (10-ohm) control need not have resolution sufficient for an exact null. The controls are adjusted for a detector indication in the portion of the scale where the first reading (e_1, section 3.2) should be made.

If the 1-mA meter (M) is omitted, the instrument is a balancing emf source which cannot measure the TE output. However, as noted earlier (3.2), the emf can be measured by the detector if the detector is a microvoltmeter. Select a range to measure 10 mV or more, turn the balancing emf off, and close the key (k_1).

As noted in the caption (fig. 3), the resistors R_4 and R_5 (section 3.3) and R_6 and R_7 (section 3.6), and their associated switches, are used to adjust and measure the sensitivity of the detector, D. These components may be omitted if the detector is a microvoltmeter, or if a null method (3.1) is used.

The potentiometer and detector should be grounded, preferably at the negative input to the detector. This is sometimes done by linking the detector input to ground through the detector's power cord. A few instruments may have the negative output connected to the instrument casing which is grounded. However, it is preferable to connect the circuits to the grounded potentiometer shield by closing the switch at the negative input terminal (fig. 3), or by some other link at this point.

4.3 Detector Keys

The detector keys k_1 and k_2, and the three associated resistors (fig. 3), are typical of those used in these procedures. Key k_1 should have low-thermal contacts and low contact resistance. A two-position lever switch is recommended for k_2. The contacts should be good, but a quality less than that of k_1 should be satisfactory. The resistor R_1 is always in parallel with the detector, unless k_1 is closed for a detector reading. This keeps the detector "quieter" when the key is open. R_1 also serves to reduce the detector sensitivity when k_2 is closed for preliminary balance adjustments. It should not be necessary to switch a multirange detector to a higher range for preliminary balances with this key configuration. An R_1 of 100 ohms is satisfactory for most high-impedance detectors. R_2 and R_3 should be chosen experimentally, depending on the range most often used and individual preference. However, 20 kΩ and 100 kΩ, respectively, may be useful as values to start with.

5.0 AC-DC Difference

The ac-dc difference in a thermal voltage converter is nearly all due to reactance in the ranging resistors, the range selector switch, and other switches and connections in the ac-dc circuit. Series inductance will impede the ac current, so that more ac than dc voltage is required for equal TE current--and thermocouple output. The sign of the correction is, by eq. (4), positive in this case. A positive correction can also result from ac current being lost to ground by capacitance. However, capacitance between resistors connected in series, or between turns of wire in a wire-wound resistor, will increase the TE current for a given ac voltage and result in a negative correction. Compensation for this effect is sometimes provided by adding capacitors to ground which bypass the TE and part of the series resistors.

5.1 AC-DC Difference Corrections

AC-dc difference corrections can be plotted conveniently on a semilog scale as in fig. 5, and such a plot can be used to find good estimates of corrections at frequencies where determinations were not made. Fig. 5 illustrates a typical set of correction curves where the specified error limits are +a to -a. Low-voltage ranges in a multirange TVC usually have small corrections (curves A, B, and C). Intermediate and high-voltage ranges are often limited to lower frequencies (curves D and E), because the effects of reactive components are larger and more difficult to control. The useful frequency range at high voltage is often extended by adding compensating elements as mentioned above. Optimum compensation (curve F) will sometimes result in a change in direction (and sign) of the correction, and the change in magnitude is usually rapid after the sign change.

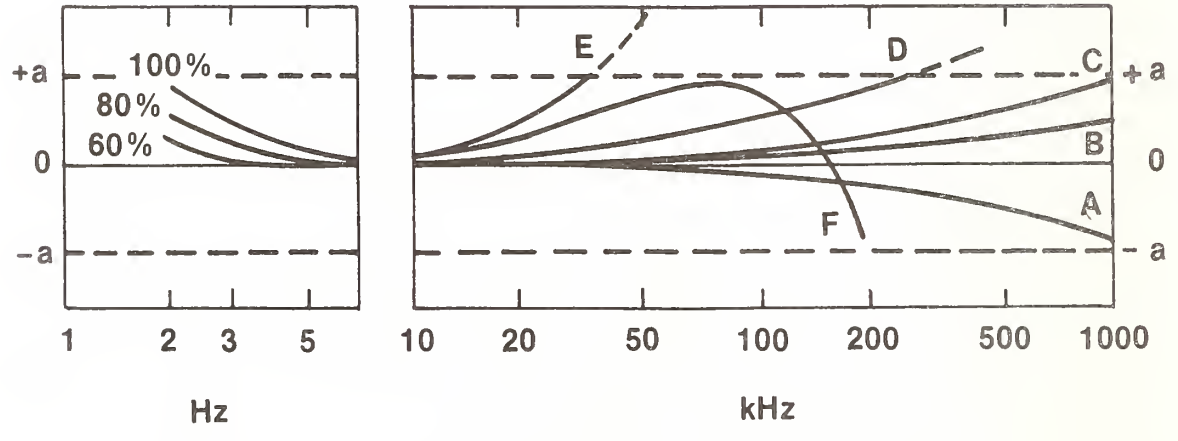

Figure 5. AC-dc difference correction curves.

It is usually sufficient to make only one determination of ac-dc difference at low and intermediate-voltage ranges. This determination should be at the highest frequency of interest. If the instrument is used only at audio frequencies, a test at 20 kHz is often sufficient, even on high-voltage ranges. The correction curve can be expected to approach zero rapidly, and if the instrument is designed for use at 50 to 100 kHz, the correction should be quite negligible at 10 kHz and lower. Where corrections are relatively large, or if there is evidence of a curve such as F (fig. 5), additional determinations should be made.

5.2 AC-DC Difference in Thermoelements

The low-range thermoelements used in TVCs (2.5 to 10 mA) rarely add significantly to the ac-dc difference of the instrument. The TE response to ac current is affected by two or three thermoelectric phenomena which, incidentally, are quite independent of frequency. However, the result of these effects is less than 5 ppm for most low-current TEs. It should not be necessary to redetermine the ac-dc difference of a TVC after a TE is replaced, and new TEs furnished by the instrument manufacturer should not require ac-dc difference tests before being installed. However, if they are tested, they should be treated as current converters (i.e., tested in series with a standard TE), as they respond to the current through the series resistors. The TE acts more as a voltage converter on very low ranges where its impedance is a large part of the total.

AC-dc difference in higher-range vacuum TEs is larger due to skin effect in the current conductors leading to the heater. The copper-coated nickel alloy widely used to pass current conductors through glass seals is sufficiently magnetic to cause a small increase in impedance. Therefore, more heating is produced with ac current than with equal dc current. AC-dc difference resulting from skin effect usually varies from about 0.005 percent at 200 mA to between 0.01 and 0.02 percent at 1 ampere--the highest range now available in vacuum bulbs. The effect in the low-current TEs used in TVCs is nearly always negligible. However, it may account for very small positive corrections in some 0.5- and 1-volt ranges, and in the low-voltage TVCs (0.3 to 1 volt) used with ac shunts for current measurements. The shunt and TVC combination is ordinarily tested and used as a unit. However, the ac-dc difference of the TVC can be determined and appropriate corrections applied (see section 8.0 and reference [16]).

TEs for currents of 10 amperes and higher sometimes have a tubular heater, or a heater with a C-shaped cross section made from a flat material. The heater is mounted between heavy copper support blocks with terminals at either end. The ac-dc difference of these elements can be very much dependent on the location of other conductors, particularly the return conductor, which is usually placed close to, and more or less parallel to, the TE heater. AC current will distribute itself for minimum reactance, and may therefore be concentrated close to, or away from, the thermocouple which is attached to the side or top of the heater. This nonuniform current distribution can cause ac-dc differences as large as 0.03 percent. The ac-dc difference of these TEs can be made constant by mounting both terminals on one end of the

device and connecting a rigid copper conductor between one terminal and the heater support at the other end. This conductor can also be placed, relative to the heater, for minimum ac-dc difference.

Practically all low-frequency (below 60 Hz) ac-dc differences in thermoelectric transfer instruments are due to the thermoelement [9]. At most frequencies the heater temperature, and therefore the TE output, are essentially constant. However, at low frequencies the heater is cooled slightly between peaks of ac current by conduction through the heater supports and the thermocouple wires. This effect is greater in high-current TEs and may be detected up to about 60 Hz on some ampere-range TEs. However, in 2.5- to 10-mA TEs used in TVCs the effect usually occurs below 5 or 10 Hz. It also decreases sharply as the heater current is reduced on all current ranges. Correction curves for three current levels in one TE are illustrated in the left-hand portion of fig. 5.

6.0 AC-DC Difference Measurements

AC-dc difference corrections to a transfer instrument (TVC or TCC) under test, δ_t, are determined relative to a similar standard whose corrections, δ_s, are known. Corrections to a standard or reference TVC or TCC are determined at the National Bureau of Standards and other laboratories. Measurements of $\delta_t - \delta_s$ may be made by either of the two methods outlined below. Fig. 6 shows a typical test arrangement for comparing two TVCs. AC and the two directions of dc voltage are connected to the TVCs successively by the ac-dc switch. Note that both TEs are connected directly to ground as in fig. 3. The switch shown in fig. 3 can also be used in ac-dc difference measurements. However, the switching sequence indicated in fig. 6 may be preferable, and the switch is a bit simpler. The TVC outputs are monitored with detectors (D) after being balanced by the emf sources (B), each of which may be a potentiometer, as in fig. 3.

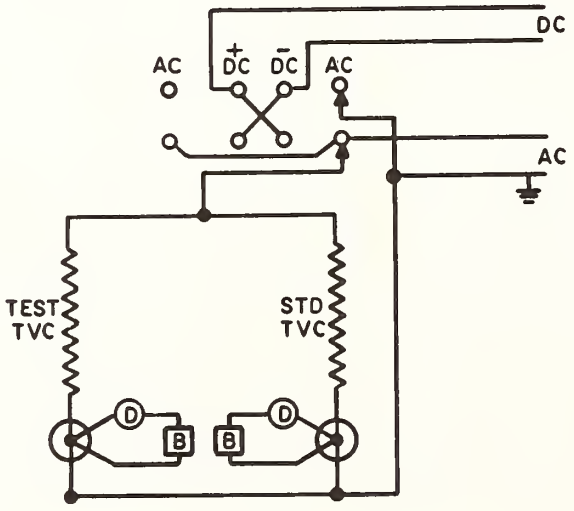

Figure 6. Circuit for ac-dc difference measurements.

The power supplies need not be calibrated; however, if the "null method" is used, provisions must be made to measure the dc voltage. The dc supply must have fine controls, with resolution of a few ppm, for adjusting the input to the test TVC for equal output on both directions of dc voltage. AC voltage may be supplied by an oscillator, amplifier, and appropriate transformers. Fine control for the ac voltage is necessary if the deflection method is used. Control circuits are discussed in section 6.4.

6.1 A Null Method

AC-dc difference can be measured using a procedure in which only null readings are made on the detectors used with the TVCs. This method is similar to the "null method" described in section 3.1 for voltage measurements. In this procedure, ac voltage is applied first, and both balancing emfs are adjusted to null the detectors. DC voltage is then applied, adjusted for a null on the test TVC detector, and measured (or read from a dc calibrator). The dc voltage is then readjusted for a null on the standard TVC detector and measured. In the example below, these voltages are listed on the line labeled "DC+." DC voltage of the opposite polarity is then applied, adjusted for the two nulls, and measured as before. ("DC-" in the example.) The ac voltage should then be reapplied, and any drift from the original null position on either detector should be evaluated for significance. If either TVC output is drifting appreciably, more warm-up time should be allowed, or the deflection method (6.2) may be used.

The relative ac-dc difference between the two TVCs in volts is equal to the difference between the average of the dc voltages required for nulls on the standard TVC and those required for nulls on the test TVC. The difference is usually converted to percent (or ppm) as in the following example.

Voltage	Voltages required for detector nulls	
	Test TVC (V_t)	Std. TVC (V_s)
DC+	200.000	199.952
DC-	200.032	200.010
Ave DC	200.016	199.981
$\Delta V = V_s - V_t$		-0.035 V
Relative ac-dc difference		-0.018%
δ_s(Std.) known		+0.003%
δ_t(Test)		-0.015%
		or -150 ppm

This procedure requires no galvanometer calibration or measurements of n. However, the adjustments are tedious and time consuming, dc standards are necessary, and the disadvantages discussed earlier (3.1) are present here also.

6.2 A Deflection Method

The deflection method for making ac-dc difference measurements is similar to the one described in section 3.2 for making ac-dc voltage comparisons. DC

voltage is applied to both TVCs, and the balancing emfs are adjusted to null both detectors. AC and the two directions of dc voltage are adjusted in turn to obtain a null indication on the detector used with the test TVC. The corresponding indications on the standard TVC's detector are recorded, and an emf difference, $E_a - E_d$, is computed as in section 3.2. The ac-dc difference of the test TVC, δ_t, (defined in section 2.4) is determined by evaluating $E_a - E_d/nE$ and applying a correction for the ac-dc difference of the standard TVC, δ_s.

$$\frac{V_a - V_d}{V_d} = \frac{E_a - E_d}{nE} + \delta_s = \delta_t$$

In this application, V_a and V_d are the ac and dc voltages required for equal response from the test TVC. The emf difference, $E_a - E_d$, can be computed from readings taken from a digital microvoltmeter or a deflecting detector, as discussed in section 3.2, and the scale reading techniques described in section 3.7 are useful here also. The reading sequence suggested for voltage measurements (DC+,AC,DC-) may be used for ac-dc difference measurements. However, it is probably advantageous to take four readings in the sequence suggested in fig. 6 (AC,DC+,DC-,AC). Either sequence will minimize the effects of drift in the TVC outputs, if the readings are taken at time intervals that are about equal. The second reading with ac voltage should increase the reproducibility.

A measurement made with a deflecting detector can be illustrated using the indications from fig. 4. If it is assumed that there is no appreciable drift, so that both readings on ac voltage are equal (i.e., 36 divisions), then

$$\Delta D = (D_2 - D_1 - D_3 + D_2)/2 = (36-23-73+36)/2 = -12 \text{ div.}$$

If nE = 16.1 mV, δ_s = +0.003% and K = 2×10^{-4} mv/div (10 μV range--table 2), then

$$\delta_t = -0.015 + 0.003 = -0.012\%.$$

6.3 TE Comparators

Stable power supplies are necessary for accurate measurements, and instability is probably the major cause of nonreproducibility in ac-dc difference comparisons. This difficulty can be largely overcome by using a TE (thermoelement) comparator. The instrument is not commercially available at this time; however, it is not difficult to build. A brief description of the general principle and advantages is given below. A more complete discussion is left to the referenced papers. TE comparators have been built in at least three configurations [9,10,14], but they all employ a divider circuit to which the emfs from the test and standard TVCs are connected. The divider is adjusted, nulling a detector, and at this point the divider setting corresponds to the ratio of the emfs.

The comparator sketched in fig. 7 shows a typical circuit. The potentiometer (Pot'r) is used, with key k_1, to measure both emfs and to monitor the test TVC output. The divider (DIV) is a two-dial Kelvin-Varley, the second dial being a ten-turn helical resistor. The lower emf, which may be either from the test or standard TVC, is balanced against a portion of the higher emf by adjusting the divider. A balance is indicated by a null reading on the microvoltmeter (μVm) with key k_2 closed. After this preliminary balance, the ac and dc voltages are applied in the sequence indicated, and each voltage is adjusted to give a test TVC output equal to the Pot'r emf. Then with key k_1 open, k_2 is closed and an emf is read from the μVm. These emfs differ because of ac-dc difference and dc reversal difference. If both directions of dc voltage are used, the ac-dc difference can be computed from them.

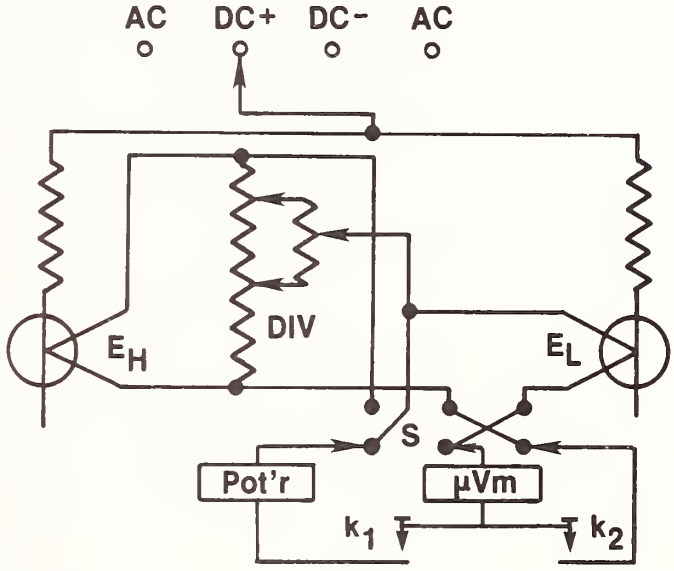

Figure 7. TE comparator with two TVCs and ac-dc switch.

Small fluctuations in the power supply output will produce nearly equal proportional changes in the emfs, and the divider balance will not be affected appreciably. The stabilizing effect is greater if the TEs have well-matched time constants and response characteristics (n values), but even if they are not quite matched, the effect usually affords a significant advantage. A second advantage is that the ac and dc voltages do not have to be adjusted for equal output from the test TVC so exactly as in other test methods. Actually, if the test and standard TEs were quite similar, and the dc reversal differences were small, it should not be necessary to adjust or monitor the test TVC output at all, once the ac and dc voltages are adjusted to be nearly equal. However, TEs usually differ enough to make adjustments to near equal output necessary for accurate measurements of ac-dc difference.

An automated model of this comparator is described in reference [15].

6.4 Voltage Control Circuits

Measurements of ac-dc difference require very fine voltage adjustments to produce equal output from the test TVC. Fine controls are required for dc

voltage in the null method, and for both ac and dc in the deflection method. AC and dc voltages are often supplied by five- and six-dial calibrators. The lower two or three dials can be adjusted for a detector null; however, this method is not very satisfactory. The knobs are often small, close together and not easily turned. An exact null may not be obtainable with the resolution available, and it is sometimes difficult to place the supply within easy reach of the operator.

The series resistance control shown in fig. 8 is recommended as a substitute fine control for voltages from 1 to 1000 V. It is placed between the dc supply and the ac-dc switch for dc voltage control, or between this switch and the TVCs to control both ac and dc voltage. The voltages are set to be nearly equal with the regular controls, and the final fine adjustments are made with this control. It can be built into a shielded box and connected into the line by a two-conductor shielded cable. It can then be placed where most convenient for the operator. It is important to remember that the control carries the test voltage which is often high enough to be dangerous. The casing must therefore be well insulated, and the shield firmly grounded. This control can, of course, be used with other power supplies which do not have sufficient fine controls. The voltage across the control, and hence the voltage at the TVC terminal, is adjusted with the ten-turn, 1-kΩ, helical resistor R_1. The sensitivity is adjusted by shunting R_1 with any one of 10 resistance values R_2. The value of R_2 is selected by a rotary switch, and is increased as the voltage increases. A resistor R_3 of about 250 ohms prevents R_2 from being shorted and improves the linearity. The most appropriate setting for R_2 depends not only on the voltage level and user preference, but on the current drawn by the TVCs--usually 5 to 20 mA. The recommended value of resistance for each switch setting is listed in table 3 below. Each successive step increases R_2 by 50 to 70 percent.

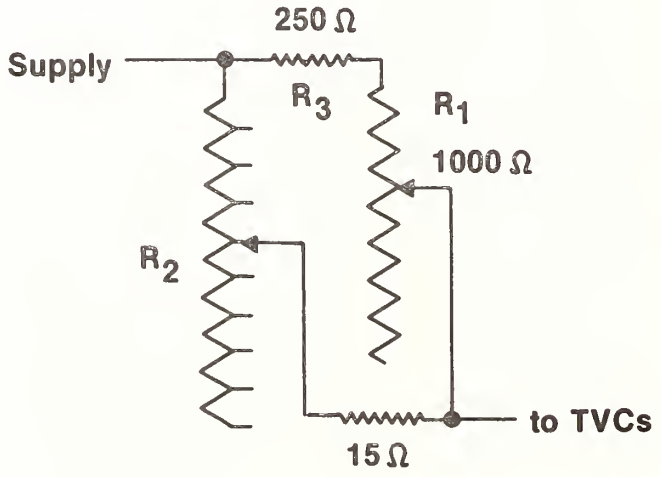

Figure 8. Series resistance fine control for ac and dc voltages.

Table 3. (see fig. 8)

Switch position	Resistance of R_2 (ohms)	Switch position	Resistance of R_2 (ohms)
1	15	6	150
2	25	7	250
3	40	8	400
4	60	9	650
5	100	10	1000

* * * * *

AC voltage and current from an oscillator-amplifier supply can be controlled with the circuit shown in fig. 9, which regulates the input signal to the amplifier. Resistor R_1 is a ten-turn helical resistor for coarse control, and adjusts the amplifier input from zero to near the oscillator output voltage. The control is less coarse if this resistor is operated near full range. The oscillator gain should therefore be set for an amplifier output only slightly higher than that necessary for the desired output voltage. An R_1 of 1 kΩ is suitable for most oscillators, but 10 kΩ may be necessary for those with relatively high output impedance.

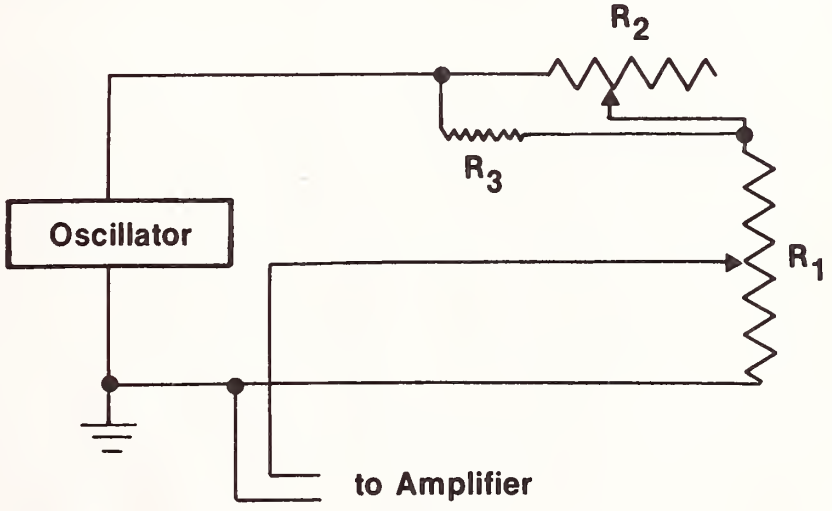

Figure 9. Control for an amplifier input.

Fine control is provided by a ten-turn helical resistor R_2 of 100 ohms and a shunt R_3 which regulates the sensitivity. The value of R_3 depends on several factors in addition to personal preference, but 20 to 50 ohms is usually satisfactory. The control assembly should be well shielded. If it is connected to the oscillator and amplifier through a shielded three-conductor cable, it can be moved around and placed conveniently for the operator.

6.5 Verifying AC-DC Difference Corrections

AC-dc difference corrections are primarily due to reactance in the switches and resistors in the TE circuit (see section 5.0). They are not likely to change, if these components are rigidly mounted and spaced so that capacitance between components, and between components and ground, is not excessive. Changes are probably more likely, if fixed and adjustable capacitors are added for frequency compensation. This is often done in multirange TVCs for the higher voltage ranges. If repairs or alterations are made that might affect these circuits, the ac-dc difference corrections should be redetermined.

If there is no reason to suspect that a change has occurred, then recalibration at NBS or other laboratories can be several years apart. (Five-year intervals are reasonable.) However, it is advisable to make periodic comparisons between TVCs within a laboratory to detect any changes that might have occurred. Such tests are especially valuable at high voltages and frequencies where changes are most likely.

Tests are made most easily between adjacent ranges in a set of single-range TVCs, or between members of two sets. If these tests are made accurately, it should not be necessary to send the entire set to another laboratory for recalibration. A few ranges, perhaps a low, medium, and high range, would serve as a basis for determining corrections to the other ranges by intercomparison. Of course, other sets and multirange instruments can be compared with such a set.

If two multirange TVCs are available, one can be calibrated relative to the other. Such periodic comparisons will assure that no changes have occurred as long as the results are the same from one test to the next. It is very unlikely that both instruments will change equally and simultaneously.

If only one multirange TVC is available, no intercomparisons can be made. However, the procedure outlined below should be useful in detecting any significant changes in the ac-dc difference corrections. It consists of measuring the difference between a constant ac voltage and the average of the two polarities of a constant dc voltage at rated voltage on a given range and then immediately with the same voltages on the next higher range (e.g., 50 volts on the 50-volt and the 100-volt ranges). If the voltages are stable during the test, the difference between the ac-dc difference corrections of the two ranges ($\delta_1 - \delta_2$) can be computed. The voltage difference can be determined by evaluating $(E_a - E_d)/nE$ as in section 3.2, and from the equation in section 6.2,

$$\frac{V_a - V_d}{V_d} = \frac{E_a - E_d}{nE} + \delta.$$

Then, since $(V_a - V_d)/V_d$ is the same,

$$\delta_1 - \delta_2 = \frac{E_{a2} - E_{d2}}{n_2 E_2} - \frac{E_{a1} - E_{d1}}{n_1 E_1},$$

where the subscripts 1 and 2 refer to the two ranges.

This procedure is more likely to be used on instruments with built-in detectors and balancing emf circuits, so that E and n values may not be known. However, the detector can be calibrated directly by making a small change in the dc voltage, observing the resulting deflection change, and computing a multiplying factor, K, (ppm/div) as suggested in section 3.6, first paragraph.

In the example of actual data below, multiplying factors K_1 and K_2 were determined for the 50- and 100-volt ranges of a typical multirange TVC. The sensitivity of the 100-volt range was, of course, low (38 ppm/div) as only 50 percent of rated voltage was applied. AC voltage at 100 kHz and the two polarities of dc voltage were then applied in the sequence DC+,AC,DC-,AC,DC+,AC,DC-, and seven deflections, D_1 to D_7, were observed. Then

$$D_a = D_2 - (D_1+D_3)/2, \quad D_b = D_4 - (D_3+D_5)/2, \quad D_c = D_6 - (D_5+D_7)/2 ,$$

and "ave ΔD" is the average of the three. K is in ppm/div and

$$\delta_1 - \delta_2 = (\Delta D_2 \times K_2) - (\Delta D_1 \times K_1) ,$$

where the subscripts 1 and 2 refer to the 100- and 50-volt ranges, respectively.

Range	D_1	D_2	D_3	D_4	D_5	D_6	D_7	ave ΔD	K	ΔD x K
100	23.0	14.0	25.0	14.0	23.0	13.5	25.0	-10.2	38	-390
50	27.0	12.5	23.5	12.0	25.0	12.0	22.5	-12.2	8.6	-100

The ac-dc differences of the 100- and 50-volt ranges at 100 kHz were +210 and -90 ppm, respectively, when measured by conventional methods. These corrections differ by 300 ppm, and the voltage comparisons indicate a difference ($\delta_1 - \delta_2$) of 290 ppm. This agreement is closer than in most of these tests; however, changes on the order of 50 ppm should be detected readily enough by this method.

Accurate knowledge of the ac and dc voltages is not necessary, and the need for equality is only that all readings be within the range of the readout detector. It is necessary, of course, to ensure that neither voltage changes significantly during the few minutes required for a measurement. Changes are more likely when the TVC range, and hence the load on the supplies, is changed. However, the loads are very small--usually 2.5 and 5 mA--and most ac and dc calibrators are well enough regulated to remain stable during these changes. An additional load resistor can be inserted in parallel with the TVC for a few seconds to roughly double the current drawn. No significant change in the TVC detector balance should be observed. A repeat test after a few minutes with consistent results will indicate that one voltage is not drifting relative to the other.

If stable calibrators are not available, the voltages may be monitored with digital voltmeters. However, most ac DVMs currently available are limited to 4-1/2 digits, and this resolution is marginal at best in this application.

7.0 Measurements of n

The measurements described thus far are made to determine small voltage and current differences by evaluating $(E_a-E_d)/nE$. As noted earlier (2.1), the factor n is near 2 at very low currents, but usually 1.6 to 1.9 at rated currents. The expression above can be evaluated if n is predetermined in a special test using dc voltage or current. Values of n corresponding to any value of E can be found, if a curve is plotted of n versus E. Four or five determinations between 50 and 110 percent of rated heater current are sufficient.

From eqs. (2) and (3),

$$n = \frac{\Delta E}{E\ (\Delta I/I)} \quad \text{, and for a TVC,} \quad n = \frac{\Delta E}{E\ (\Delta V/V)}$$

Measurements of n are made by introducing small measured proportional changes in TE heater current ($\Delta I/I$) and measuring the resulting output, E, and changes in output, ΔE. Current changes should be large enough for good resolution, but small enough to keep all detector readings on scale. Changes of a few tenths to about one percent are usually convenient.

These tests are probably made more conveniently on the 100-V range of a multirange TVC, and n values obtained on one range can be used with any range, if they are correctly related to the TE output. Low-voltage, single-range TVCs can be placed in series with additional resistance, and more manageable voltages can then be applied. Low-range TEs (2.5 to 10 mA) may be connected in series with 50 to 200 kΩ and appropriate voltage applied for the desired heater currents. The voltages may be supplied, and small voltage changes "dialed in," from a dc calibrator. Or the voltage may be supplied by a stable dc power supply with fine controls, and small changes measured with a digital voltmeter or a volt box and potentiometer.

In the example below, one determination of n is made by applying 90.000 and 90.500 volts for a proportional change of 0.00556, and E = 8.51 mV. Imbalance emfs, e, are read from a digital microvoltmeter, and three emf changes are computed from seven readings.

$$\Delta E_1=e_2-(e_1+e_3)/2, \quad \Delta E_2=e_4-(e_3+e_5)/2, \quad \Delta E_3=e_6-(e_5+e_7)/2$$

Successive readings are made at the alternate voltages--90.0 and 90.5. The average of the three emf changes (80.4 μV) is converted to 0.0804 mV for the calculations.

V	ΔV	E	e_1	e_2	e_3	e_4	e_5	e_6	e_7	ave ΔE	ΔV/V	n
90	0.5	8.51	12.3	92.8	11.4	91.2	10.8	90.8	10.4	0.0804	0.00556	1.70

Current changes can also be introduced in a TVC, or in a TE in series with a high resistance, by inserting a known resistance change in the TE circuit. A relatively low resistance, with a switch for shorting it, is placed in series with a TVC or TE, and as the switch is opened and closed, $\Delta I/I=-\Delta R/R$. The power supply must, of course, be well regulated, and the resistance ratio $\Delta R/R$

should be known to about one percent. The calculations are simplified, as $\Delta I/I$ is the same at all voltage levels. The change can, of course, be a round number. A 400-Ω resistor in series with a 40-kΩ ,5-mA, 200-V TVC will introduce a change of 0.01 (one percent) at all voltage levels.

Currents higher than 10 mA are usually measured with a potentiometer and a shunt in series with the TE.

The TE output emf, E, can be measured with a Lindeck potentiometer (fig. 3), or it can be measured by the detector, if a microvoltmeter with a 10-μV range is used, by turning the potentiometer off and closing key k_1. Emf changes, ΔE, are measured by the detector as described in section 3.2.

It is difficult to measure n with an accuracy better than about one percent. However, that accuracy is sufficient, as errors in n have a second-order effect on the end result. A one percent error will result in an equal error in measuring a difference, say of 0.05 percent, between an ac voltage and a dc reference voltage. However, this will affect the ac voltage measurement by only 0.0005 percent (5 ppm).

8.0 Current Measurements

Thermoelements are sometimes used as thermal current converters (TCCs), and they are usually excellent up to about 100 mA. They have ac-dc differences at higher currents, as discussed in section 5.2, which can be evaluated, and corrections can be applied. However, TCCs usually consist of a set of special ac shunts and a low-voltage (0.3 to 1 volt) TVC. In some commercial models, the shunt output is connected to the TE in a multirange TVC through a special connector. These TVCs include a balancing emf source and a detector for monitoring the output of the TE. Instructions for using these instruments are, of course, furnished by the manufacturers.

Shunts can also be connected to a low-voltage, single-range TVC, and its output can be monitored with an emf source or a potentiometer like the one shown in fig. 3. The detector may be any one of the four instruments discussed in 3.2, 3.3, and 3.4. Techniques for galvanometer calibration (3.6) and detector readings (3.7) are also useful with TCCs.

AC current may be measured, and ammeters calibrated, with the equipment and circuit shown in fig. 10. The procedure is very much like the deflection method described in section 3.2 for voltage measurements. DC current is adjusted to be nominally equal to the ac current, and the balancing emf or potentiometer (P) is adjusted for a near null indication on the detector (D). The indication, e_1, of the detector is recorded. The TCC is then switched to ac current, the ac supply is adjusted for the desired indication on the instrument under test (Test AM--fig. 10), and the detector indication, e_2, is recorded. Reversed-dc current is then applied to the TCC, adjusted to the nominal value, and e_3 is recorded. The difference between the ac and dc currents is then computed from the equation,

$$\frac{I_a - I_d}{I_d} = \frac{E_a - E_d}{nE} + \delta_s \ ,$$

where δ_s is the ac-dc difference correction to the TCC, and

$$E_a - E_d = e_2 - (e_1 + e_3)/2.$$

If the detector is a deflection instrument,

$$E_a - E_d = (D_2 - (D_1 + D_3)/2) \times K.$$

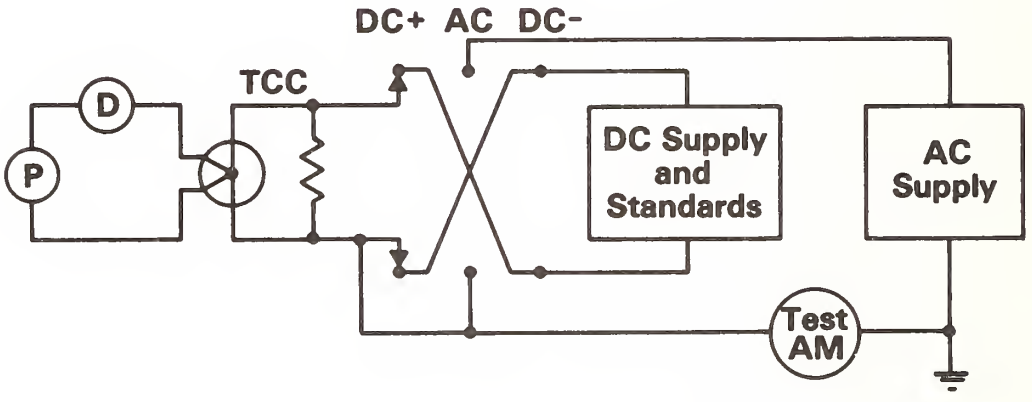

Figure 10. Circuit for current measurements using a thermal current converter (TCC).

The calculations illustrated in 3.5 are then practically the same as those for current measurements. I is substituted for V, and TCC for TVC, in table 1.

The ac-dc difference of a TCC can be determined, relative to a standard instrument, with the circuit shown in fig. 11. The equipment and switch may be the same as those in fig. 10, but no dc standards are required. The switching sequence may be as shown (DC+, AC, DC-), although the sequence suggested in 6.2 (AC, DC+, DC-, AC) may yield greater reproducibility. The switch shown in fig. 6 may be used if the current-carrying capacity is sufficient.

Each TCC output is monitored with a balancing emf, or potentiometer (P), and detector (D). A method similar to that suggested in 6.2 may be used. The ac and dc currents are adjusted for equal response (output emf) from the test TCC, and imbalance emfs are read from the detector used with the standard TCC. If four readings are taken, e_1 and e_4 are read with ac current, and e_2 and e_3 with the two directions of dc current. Then

$$E_a - E_d = (e_1 - e_2 - e_3 + e_4)/2,$$

or

$$E_a - E_d = ((D_1 - D_2 - D_3 + D_4)/2) \times K,$$

and

$$\frac{I_a - I_d}{I_d} = \frac{E_a - E_d}{nE} + \delta_s = \delta_t$$

where δ_t and δ_s are the ac-dc difference corrections to the test and standard TCCs.

If the shunts have shields or casings (dashed lines in fig. 11), it is recommended that they be connected as shown in fig. 11. If one shield were attached between the shunts, a small capacitive current might flow between that shield and ground. This current would flow through one shunt, but not the other, causing an error.

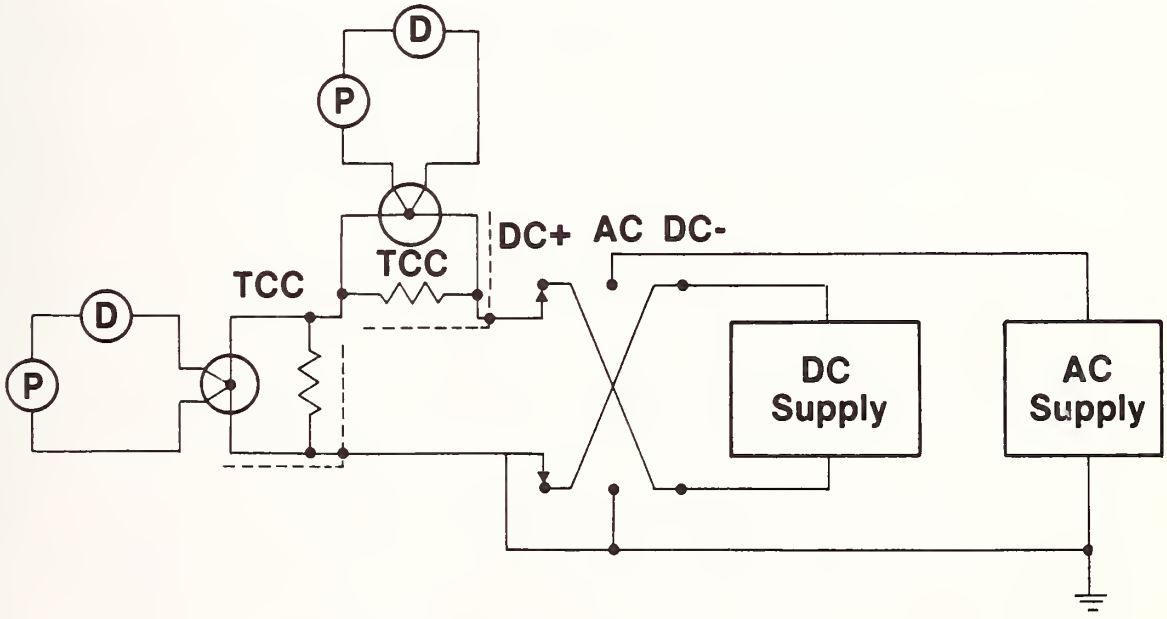

Figure 11. Circuit for ac-dc difference tests of thermal current converters (TCC).

Additional suggestions for building and using TCCs are found in reference [16] where the following are discussed:

(A) Members of a set of shunts can be intercompared very much as TVCs are (see sections 6.0 to 6.5), and corrections determined for each shunt and TE combination relative to two or three ranges which have known corrections.

(B) A "short set" of shunts can be built in which each shunt in the set is used with two TVCs (0.3 and 0.6 V) to form two current ranges. Thus the two

TVCs and six shunts provide 14 ranges. It is, of course, necessary in this arrangement that the TVC correction be negligible or that a correction, δ_T, be applied. AC-dc difference in low-voltage TVCs is mainly due to skin effect in the input leads to the thermoelement heater (5.2). This effect can be practically eliminated by using TEs with platinum lead-in wires. Such elements are available from one or two manufacturers upon special request, and at a reasonable price.

(C) If the TVC corrections are appreciable, they can be determined relative to other TVCs with known corrections. Then, at high and middle ranges, the ac-dc difference of the shunt and TVC combination, δ_C, is practically equal to the sum of the ac-dc differences due to the admittance of the shunt, δ_S, and the impedance of the TVC, δ_T. As discussed in the referenced paper, this separation of correction components is not feasible at low currents (less than 0.25 A in most cases) where the TVC carries a substantial portion of the total current. These low-range TCCs should be tested and used as shunt-TVC combinations.

References

[1] "AC-DC transfer instruments and converters," American National Standard C100.4, ANSI, 1430 Broadway, New York, NY 10018, 1973.

[2] F. J. Wilkins, T. A. Deacon, and R. S. Becker, "Multijunction thermal convertor and accurate ac-dc transfer instrument," Proc. Inst. Elec. Eng., Vol. 112, No. 4, pp. 794-805, 1965.

[3] F. J. Wilkins, "Theoretical analysis of the ac-dc transfer difference of the NPL multijunction thermal convertor over the frequency range dc to 100 kHz," IEEE Trans. Instrum. Meas., Vol. IM-21, pp. 334-340, 1972.

[4] F. L. Hermach and D. R. Flach, "An investigation of multijunction thermal converters," IEEE Trans. Instrum. Meas., Vol. IM-25, pp. 524-528, 1976.

[5] Manfred Klonz and F. J. Wilkins, "Multijunction thermal converter with adjustable output voltage/current characteristics," IEEE Trans. Instrum. Meas., Vol. IM-29, pp. 409-412, 1980.

[6] F. L. Hermach, "Thermal converters as ac-dc transfer standards for current and voltage measurements at audio frequencies," J. Res. Nat. Bur. Stand., Vol. 48, pp. 121-138, 1952.

[7] F. C. Widdis, "Theory of Peltier- and Thomson-effect errors in thermal ac-dc transfer devices," Proc. Inst. Elec. Eng., Vol. 109, Pt. C (Monograph 497 M), pp. 328-334, 1962.

[8] F. L. Hermach and E. S. Williams, "Thermal voltage converters for accurate voltage measurements to 30 megacycles per second," Trans. AIEE (Communication and Electronics), Vol. 79, Pt. I, pp. 200-206, 1960.

[9] F. L. Hermach and E. S. Williams, "Thermal converter for audio-frequency voltage measurements of high accuracy," IEEE Trans. Instrum. Meas., Vol. IM-15, pp. 260-268, 1966.

[10] E. S. Williams, "Thermal voltage converters and comparator for very accurate ac voltage measurements," J. Res. Nat. Bur. Stand., Vol. 75C, pp. 145-154, 1971.

[11] P. Richman, "A new peak-to-dc comparator for audio frequencies," IRE Trans. Instrum., Vol. I-11, pp. 115-122, 1962.

[12] D. R. Flach and L. A. Marzetta, "Calibration of peak ac to dc comparators," ISA Conference Report No. 14.2-3-65, 1965.

[13] L. A. Marzetta and D. R. Flach, "Design features of a precision ac-dc converter," J. Res. Nat. Bur. Stand., Vol. 73C, pp. 47-55, 1969.

[14] R. S. Turgel, "A comparator for thermal ac-dc transfer standards," ISA Trans., Vol. 6, No. 4, pp. 286-292, 1967.

[15] E. S. Williams, "A thermoelement comparator for automatic ac-dc difference measurements," IEEE Trans. Instrum. Meas., Vol. IM-29, pp. 405-409, 1980.

[16] E. S. Williams, "Thermal current converters for accurate ac current measurement," IEEE Trans. Instrum. Meas., Vol. IM-25, pp. 519-523, 1976.

Other papers not specifically cited:

F. L. Hermach, J. E. Griffin, and E. S. Williams, "A system for accurate direct and alternating voltage measurements," IEEE Trans. Instrum. Meas., Vol. IM-14, pp. 215-224, 1965.

F. L. Hermack, "AC-dc comparators for audio-frequency current and voltage measurements of high accuracy," IEEE Trans. Instrum. Meas., Vol. IM-25, pp. 489-494, 1976.

*U.S. GOVERNMENT PRINTING OFFICE:1982 360-997/2265 1-3

IEEE TRANSACTIONS ON INSTRUMENTATION AND MEASUREMENT, VOL. IM-29, NO. 4, DECEMBER 1980

A Thermoelement Comparator for Automatic AC–DC Difference Measurements

EARL S. WILLIAMS

Abstract—**AC–DC differences in thermal voltage converters (TVC's) are determined relative to a similar instrument, from imbalance EMF's measured in a divider circuit to which both instrument outputs are connected. These EMF's are more stable than the input voltages to the converters, because input voltage fluctuations produce nearly equal proportional changes in the converter outputs. The divider balance is therefore affected only slightly. The divider and a Lindeck potentiometer for monitoring the test instrument output are driven by stepping motors and balanced automatically. AC and DC voltages are applied by programmable power supplies whose outputs are adjusted, in response to imbalance EMF's in the potentiometer circuit, to produce equal output from the test instrument. The system automatically calibrates one voltage range at one or more frequencies, but requires an operator to change ranges and to enter the test parameter at a computer terminal.**

Introduction

AC VOLTAGE IS measured most accurately at the present time when it is compared directly with a dc reference voltage using a thermal voltage converter (TVC). These instruments, which are also called thermal transfer voltmeters, consist essentially of ranging resistors and a thermoelement (TE), a short straight electrical heater whose temperature is sensed by a thermocouple or a thermopile. Multirange TVC's usually include a balancing EMF source and a null detector for monitoring the TE output.

The reference voltage V_d is usually an accurately measured "round number" value which is nominally equal to the ac voltage V_a to be measured. The proportional difference between the two voltages $(V_a - V_d)/V_d$ is measured by observing the output E of the TVC, and changes in output as the TVC is connected alternately to the two voltages. Both polarities of dc voltage are generally used because the TE in most TVC's has a significant reverse dc difference. When the difference between the ac and dc voltages is small

$$\frac{(V_a - V_d)}{V_d} = \frac{(E_a - E_d)}{nE}. \tag{1}$$

E_a is the EMF observed when ac voltage is applied to the TVC, E_d is the average of EMF's observed when the forward and reverse dc voltage is applied, and the factor n relates small changes in TE heater current to the corresponding changes in output EMF.

Ideally the TE has a square-law response with $E = kI^n$ ($n = 2$ and k constant for small changes in I). However, the value of n deviates from 2 as the heater current is increased and is usually in the range of 1.7 to 1.9 at the rated current of the TE. Values of n must be determined at several levels by applying known voltage changes $\Delta V/V$ to the TVC and observing the output E and changes in output ΔE. The equation is very much like (1) above:

$$\Delta V/V = \Delta E/nE \tag{2}$$

or

$$n = \frac{\Delta E/E}{\Delta V/V}. \tag{3}$$

AC voltage measurements, as described above, usually require the application of a correction (δ) for the ac–dc difference of the TVC. Such corrections are needed due to inductance in the ranging resistors and range selecting switches and

Manuscript received June 28, 1980.

E. S. Williams is with the National Bureau of Standards, Washington, DC 20234.

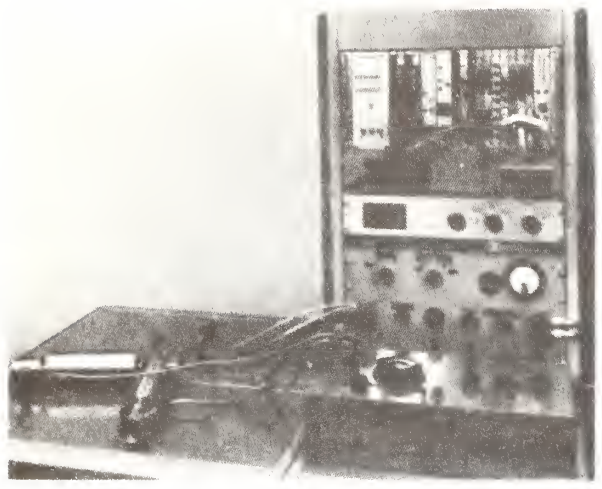

Fig. 1. Automatic test system with comparator in the foreground.

to capacitance between these components and ground. The TE rarely contributes significantly to the ac–dc difference except at very low frequencies. AC–DC difference corrections of a TVC under test δ_t are determined by comparison with a standard TVC whose corrections δ_s are known. Measurements of $\delta_t - \delta_s$ are made by applying the same ac and dc voltages to the two TVC's, adjusting the voltages for equal output from the test instrument, and observing the changes in response of the standard. The output ot the test TVC is usually balanced by an adjustable EMF source and monitored by a detector which may be a microvoltmeter or a calibrated galvanometer.

TE (thermoelement) comparators have been developed at NBS [1], [2] and elsewhere which have certain advantages over other methods for making these measurements. The system described here is built around a new automatic comparator which utilizes a digital millivoltmeter to measure TVC outputs EMF and a digital linear amplifier (DLA) to measure imbalance EMF's as small as 10 nV. Both instruments have BCD outputs. The system is interfaced with a minicomputer by a Modular Interactive Data Acquisition System (MIDAS) which was developed at NBS [3]. Similar programming for another interface scheme, such as the IEEE 488 standard bus for instrument control [4], should present no particular problem.

Fig. 1 is a photograph of the console showing the comparator, on the right table top, connected to two TVC's. Equipment in the rack are, from top to bottom, the MIDAS interface, a panel containing the millivoltmeter and certain relays, the DLA and the ac–dc switching circuits. Not shown in the photograph are the power supplies, a cathode ray computer terminal (CRT), and a teletype (TTY) for printing test results.

TE Comparator Principle

The automatic comparator is similar to the NBS manual model described in reference [2]. Both comparators consist essentially of a 1000-Ω divider and a Lindeck potentiometer. In the manual comparator (Fig. 2), the higher EMF is connected to the two-dial Kelvin–Varley divider through the E_H input and the lower through E_L. The potentiometer may be connected to either input by switch S, and both EMF's are measured by adjusting the potentiometer for a zero reading on the microvoltmeter ($\mu V \cdot m$) with key k_1 closed. The potentiometer is then connected to the test TVC output, which may be either lower or higher than the standard output. The divider is adjusted to balance the lower EMF, as indicated by a zero reading on the $\mu V \cdot m$ with key k_2 closed. Then, as ac and dc voltages are applied to the TVC's and adjusted for equal output from the test instrument (zero reading on the $\mu V \cdot m$ with k_1 closed), imbalance voltages in the low EMF circuit are measured by the $\mu V \cdot m$, and

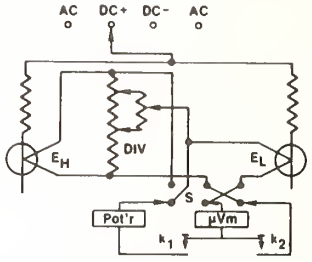

Fig. 2. Manual TE comparator circuit with TVC's.

$$\delta_t - \delta_s = \frac{(E_d - E_a)}{n_s E_L}. \tag{4}$$

E_a and E_d are the readings on the $\mu V \cdot m$ obtained with ac voltage and the average of the readings with two polarities of dc voltage, E_L is the lower EMF, and n_s is the n characteristic of the standard TVC at its output EMF. Switch S has two additional poles which reverse the connection to the $\mu V \cdot m$. This is necessary to maintain a consistent sign convention for the EMF difference $E_d - E_a$ [2].

Imbalance voltages in the divider circuit (key k_2 closed) are not affected appreciably by changes or fluctuation in the input voltage to the TVC's. Such changes will produce nearly equal proportional changes in the two EMF's, and the divider balance is affected only slightly. This stabilizing effect accounts for the two advantages of the comparator: The input voltage instability is less troublesome, and the requirement that the voltages be adjusted for equal output from the test TVC is less severe. If the response characteristics of the TE's in the TVC's are identical, or nearly so, equal output from the test converter may not be necessary. Most elements are similar enough to give the comparator a considerable advantage. However, if both the reverse dc difference and the n characteristic differ at the same time, as they often do, a significant error in the ac–dc difference determination can be expected unless the voltages are adjusted for equal output from the test TVC.

Automatic Comparator

The divider in the automatic comparator is connected to either input, TEST or STD, by switch S (Fig. 2), which is turned by a 30° stepping motor, SM1. A 3½ digit millivoltmeter (mV · m) is connected across the divider by closing the 2-pole relay k_1, and it measured the standard TVC output E_s

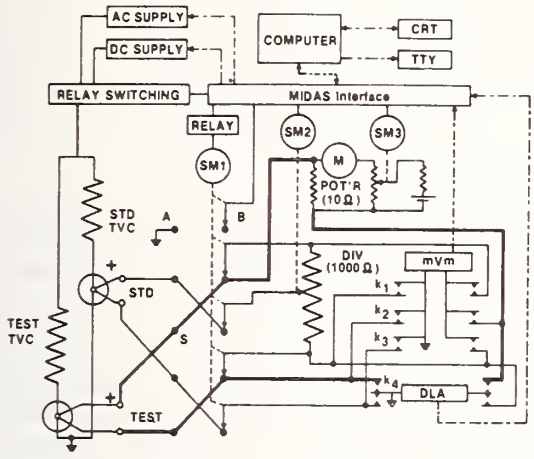

Fig. 3. Diagram of automatic system with comparator.

in switch position A and the test TVC output E_t in position B. The denominator in (4) ($n_s E_L$) is computed using the lower EMF, and n_s is computed from a equation which relates the values of n_s to the output of the standard TVC. The divider is then connected to the higher EMF. The position of switch S is determined by the MIDAS which detects a ground in the "A" position of the switch. In this way, the EMF's E_s and E_t are distinguished from one another, and the sign of the EMF difference $E_d - E_a$ (4) is also determined.

The 15-mV potentiometer is used only to monitor the output of the test TVC, and it is therefore permanently connected to the TEST input, as shown in heavy lines in Fig. 3. The potentiometer current is supplied by a mercury battery and adjusted by a ten-turn helical 3-terminal resistor for a near balance with one direction of dc voltage applied to the TVC's. The control resistor is driven by stepping motor SM3 (Fig. 3) with 200 steps per revolution. The resolution is not high (about 8 μV); however, an exact balance is not necessary because the ac and dc voltages are adjusted during the measurement procedure for a balance between the test TVC output and the potentiometer. The steps necessary for a near balance are computed from voltages measured by the mV · m with relay k_2 closed. Below 20 μV, additional adjustments are computed for a balance within ±4 μV from measurements made by the DLA. The DLA is connected into the potentiometer circuit for these measurements by relay k_4, a low-noise key-type switch which is closed in either of two directions by small solenoids.

A two-dial Kelvin–Varley divider (Fig. 2) is used in the manual comparator to provide sufficient fine adjustment to be compatible with the narrow range and linearity limitations of the microvoltmeters or galvanometers used with that system. The wider (40-μV) range of the DLA permits the use of a single ten-turn resistor as a divider in the automated system. The resistor must of course have a low-thermal low-noise moving contact. However, as no movements are made during the actual measurements, the resistors currently available have been adequate. The divider is balanced by stepping motor SM2 in procedures similar to the one used with the potentiometer. The required steps for a near null are computed from imbalance voltages measured by the mV · m with relay k_3 closed.

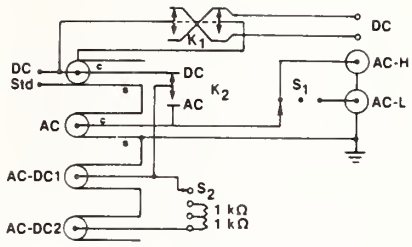

Fig. 4. AC–DC switching circuit.

When the imbalance voltage is sufficiently small, the DLA is connected into the divider circuit by relay k_4, and additional adjustment are computed from its measurements of the residual imbalance voltage.

Voltage Switching and Control

AC and DC supply voltages are connected to the TVC's by the circuit shown in Fig. 4. Up to 100 V are supplied by the AC-L terminal by a programmable ac calibrator, and a companion high-voltage amplifier provides voltage at AC-H from 100 to 1000 V. The input to be used is selected manually by switch S_1. The TVC's are connected to the AC–DC 2 terminal, where the circuit can be opened by switch S_2, and a resistance of 1000 or 2000 Ω can also be added to the circuit. The resistance permits the power supplies to run in the range of 10 to 40 V where they are more stable and controlled more readily, while supplying less than 10 V to the TVC's. The terminals DC-Std, AC, and AC-DC1 are used for voltage measurements with one TVC. Relay k_1 reverses the dc voltage to the TVC's, and k_2 connects them to ac or dc voltage. These relays are shown in the unenergized position with dc voltage applied to the TVC's. The relays are activated by 26-V dc which is connected to the relay coils by programmable switches in the MIDAS controller.

The power supplys are remotely programmed and turned on in response to the test voltage and the frequency (in kHz) which are entered at the CRT along with other test conditions. The alpha-numeric "string" codes which activate the power supplies are either stored in the computer or computed by it. Zeroes are added to the value of test voltage to extend it to seven digits for the dc supply which is a seven-dial calibrator and to five digits for the five-dial ac calibrator. Both calibrators have several ranges but only the 10-, 100-, and 1000-V ranges are used. The codes for range selection are found by executing three Basic language statements which relate the code to the desired voltage range.

The ac calibrator supplies frequencies from 10 Hz to 100 kHz in four decade ranges with eleven settings (0 to 10) in each range. Thus there are 44 discrete frequencies available, and each one is designated by a two-digit code. The code numbers are computed from one of four equations which is selected according to the required frequency range.

When the "round number" ac and dc voltages are applied to the TVC's, both voltages usually require small adjustments to make the test TVC's output equal to the potentiometer EMF. The potentiometer setting is established as outlined previously, using one direction of dc voltage as input to the

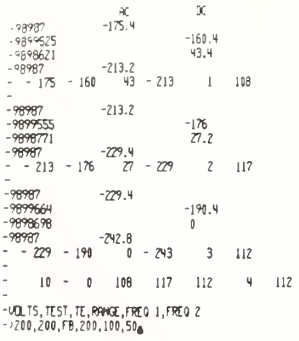

Fig. 5. Calibration data as displayed by the computer terminal.

TVC's. The test TVC often has a significant reverse-dc difference which then requires readjustment. The ac voltage may need adjustment because of the ac–dc difference and also because the ac supply voltage may not be equal to the voltage at the TVC terminals due to reactance in the conductors, in the relay k_2 (Fig. 4), and in the switches S_1 and S_2. The voltages are adjusted in response to EMF E_1 measured by the DLA while it is connected into the potentiometer circuit by relay k_4 (Fig. 3). The adjustment ΔV is computed using an adaptation of (2) which may be written

$$\Delta V = -(\Delta E/nE)V. \tag{5}$$

A nominal value of 1.8 is substituted for n, E is the EMF of the test TVC, and the negative sign gives the voltage change the proper direction. The numerical value of the voltage change is calculated to give an EMF change ΔE equal to E_1 and thus reduce E_1 to near zero. It is then suitably formatted by the controller to reset the five-digit ac supply or the seven-digit dc supply. Unless the initial change is large, a single adjustment is usually sufficient for a balance within 1 μV.

Fig. 5 is a photograph of the CRT display of actual test results. The data appears on the screen one line at a time as the test proceeds. The left-hand column shows the adjusted value of voltage (five digits for the ac supply and seven for the dc supply), and opposite each voltage is the EMF measured by the DLA in the divider circuit. The first four EMF readings are repeated on the fifth line, and the first value of ac–dc difference 108 is listed. The last EMF reading in the first determination is used as the first reading for the next determination. Thus three values of ac–dc difference are computed from 10 EMF readings. The three values are listed on the last line of data—10, 0, 108, 117, 112, 4, 112—and these data are also printed on a TTY under appropriate columns. These figures are, from left to right, the frequency in kHz, the ac–dc difference correction (in ppm) to the standard TVC (computed from an equation which was devised to simulate the correction curve for the standard in use), the three values of ac–dc difference, the standard deviation of the three, and the average of the three with the standard TVC correction applied. If the standard deviation is larger than 10 ppm, additional determinations are made. When one range is completed, parameters for the next range are requested at the next line (Fig. 5) and entered on the last line. If only one frequency is to be used, the last entry on the line is 0.

Other Measurements

Measurements of n

Measurements of n are made automatically by connecting a TVC to the AC-DC1 terminal and entering into the CRT the lowest and highest voltage to be applied. Tests are usually made on a 100-V range at 10-V intervals from 60 to 100 V; however, this can be varied. Data obtained on one range of a multirange TVC are usable on any range if the values of n are correctly related to output EMF of the TE. At each voltage level the TVC output E is measured, and the potentiometer is nearly balanced. However, a small imbalance is deliberately programmed into the routine to obtain a negative DLA reading. The input voltage is then increased by a 0.1-V step so that a positive reading is obtained and then reduced by the same step for a repeat of the negative reading. This procedure is repeated three more times and four values of ΔE are computed. The average of the four is used as ΔE, and $\Delta V/V$ is computed with $\Delta V = 0.1$. A value of n is thus computed at each voltage level using (3) and printed on the TTY along with the voltage, EMF, and the DLA readings. The values of n are plotted, a straight line is fitted to the upper two-thirds of the curve, and the parameters of that line are stored in the computer. Values of n can then be approximated by the computer with sufficient accuracy by evaluating the straight-line equation of any value of E.

In an alternative procedure, a certain percentage change in TE heater current is introduced by connecting a resistor in series with a TVC and alternately opening and closing a relay which short circuits the resistor. A 40-Ω resistor is shorted to introduce a 0.1-percent change at any voltage level in a 40-kΩ 200-V TVC. This procedure can be used after merging thirteen substitute lines into the software described above.

Comparison and AC and DC Voltages

AC and DC voltages may be compared by connecting the ac voltage to the AC terminals (Fig. 4), with switch S_1 in the center or OFF position and an appropriate TVC at AC-DC1. AC and the two polarities of dc voltage are connected to the TVC by relays k_1 and k_2. The EMF E of the TVC is measured, and the potentiometer is balanced. Changes in the imbalance EMF in the potentiometer circuit are computed from DLA readings, and the difference between the ac and dc voltage is computed using equation (1), but with the TVC correction δ applied. A dc calibrator may be connected to the DC terminals (Fig. 4) and used as both supply and standard, or a separate standard (volt box and potentiometer or digital voltmeter) can be used at the DC-Std terminals. The standard should not be affected significantly by changing the polarity of the applied voltage.

At very low voltages, where the voltage drop across the line resistance may be significant, it is necessary to monitor the dc voltage at the DC-Std terminals. The cables with conductors c and shields s (Fig. 4) are identical to equalize the voltage

drop between these terminals and the comparison points at relay k_2. These cables can be seen on the left rear table on the photograph of the console (Fig. 1).

Conclusion

A thermoelement comparator has been developed with a self balancing potentiometer and a divider, and it has been integrated into an automatic calibration system for measurements of the ac+dc difference of a TVC relative to a similar standard instrument. The potentiometer is also used in automatic measurements of the n characteristic of thermoelements and ac–dc voltage comparisons. The system requires an operator to make the electrical connections and to select the ranges, as few if any TVC's have provisions for automatic range selection. The operator also enters the test parameters at a computer terminal (see last two lines, Fig. 5). The system proceeds automatically beyond that point; however, it will stop at a number of points if instability or other conditions prevent a DLA reading or a balancing operation with a specified time.

More expert maintenance is required than for manual systems, but data transcription errors are very unlikely and data storage for further reduction, pooling, analysis, and automatic test report generation is feasible. As presently written, the software accommodates input instructions for only one or two test frequencies; however, provisions could be made for a table of frequencies if a comprehensive scan were required.

The system saves time in the preliminary balances, frequency changes, and in data processing. However, due to the settling time required for the thermoelements in the TVC's, it proceeds at about the same rate as manual operations when ac and dc voltages are being alternately applied to the instruments. A major advantage is that the operator is largely relieved of a task that is probably more tedious and fatiguing than those of most other types of calibrations.

References

[1] F. L. Hermach and E. S. Williams, "Thermal converters for audio frequency voltage measurements of high accuracy," *IEEE Trans Instrum. Meas.*, vol. IM-15, pp. 260–268, Dec. 1966.

[2] E. S. Williams, "Thermal voltage converters and comparators for very accurate Ac voltage measurements," *J. Res. Nat. Bur. Stand.*, vol. 75C, pp. 145–154, 1971.

[3] C. H. Popenoe and M. S. Campbell, "Modular interactive data acquisition system—description and specifications," NBS Tech. Note 790, 1973.

[4] IEEE Std. Digital Interface for Programmable Instrum., IEEE Std. 488, 1978.

An International Comparison of Thermal Converters as AC-DC Transfer Standards

O. P. GALAKHOVA, S. HARKNESS, FRANCIS L. HERMACH, FELLOW, IEEE, H. HIRAYAMA, P. MARTIN, T. H. ROZDESTVENSKAYA, AND EARL S. WILLIAMS

***Abstract*—The ac-dc differences of 4 sets of thermal current and voltage converters were determined at 40 Hz, 20 kHz, and 50 kHz with reference to the standards of the national metrology laboratories of the United Kingdom, Japan, the Soviet Union, and the United States. For each voltage and current range and at each frequency, the average ac-dc difference determined by each laboratory for the 4 sets differed from the average of all laboratories by less than 10 ppm.**

INTRODUCTION

THERMAL converters (each consisting of a conductor heated by a current and one or more thermocouples to sense the temperature rise) are the basic standards for all ac current and voltage measurements at audio frequencies. Extensive research in several national laboratories has indicated that ac quantities can be determined in terms of dc standards to 10 ppm or better with converters of proper design and construction [1]. Such accuracies are needed to support recent developments in electronic instruments and calibrators. New types of multijunction thermal converters (MJTC's) show evidence of even better accuracies.

INTERNATIONAL TESTS

Because of the importance of converters as fundamental standards of ac-dc difference, an international comparison of the standards of four national metrology laboratories (Institute of Metrology (IMM), Leningrad, USSR; Electrotechnical Laboratory (ETL), Tokyo, Japan; National Bureau of Standards (NBS), Washington, DC and National Physical Laboratory (NPL), Teddington, UK) was agreed upon at the 1968 meeting of the Consultative Committee on Electricity (CCE) of the International Committee on Weights and Measures. NBS served as the coordinating laboratory. Each laboratory furnished a set of five converters with ratings (ranges) of 10 and 30 mA and 10, 30, and 100 V, and evaluated all 4 sets at 40 Hz, 20 kHz, and 50 kHz. (Regrettably, NBS inadvertently omitted making 40-Hz measurements.) The ac-dc differences δ were reported for each converter. [$\delta = (Q_{ac} - Q_{dc})/Q_{dc}$ where Q_{dc} is the average of the two directions of the dc quantity (current or voltage) required to produce the same output Electromotive Force (EMF) as the ac quantity Q_{ac}.] The tests were made by IMM, ETL, NBS, NPL, and IMM in that order. After the tests of each laboratory were completed, the results of all previous tests were forwarded to that laboratory.

Because of the time required in each laboratory for the construction and preliminary testing of the converters comparisons did not actually begin until 1972. Because of the delays and damages in shipment and the pressure of other tasks, they were not completed until 1977.

TABLE I
ESTIMATED OVERALL UNCERTAINTIES μ IN PPM (INCLUDING THE STANDARD DEVIATION OF THE MEAN σ AND THE SYSTEMATIC ERROR ϵ)

Laboratory	Quantity	μ (ppm) 40 Hz - 20 kHz	μ (ppm) 50 kHz	See Note ℓ
IMM	voltage	15	15	1
ETL	current	10	10	2
	voltage	15	25	2
NBS	current	5	7	3
	voltage	10	15	3
NPL	current	3 to 4	4	4
	voltage	3 to 7	4 to 8	4

Notes:

(1) $\mu = \epsilon + \sigma$
(2) $\sigma < 1$ ppm
(3) $\mu = \epsilon + 3\sigma$. $3\sigma = 2$ ppm
(4) $\sigma = 1$ to 2 ppm

NATIONAL STANDARDS AND MEASUREMENTS

General

Brief descriptions of the ac-dc transfer standards and of the methods and equipment for comparing them in each of the 4 laboratories are given in this section. The accuracies claimed by each laboratory in the evaluation of the interlaboratory (traveling) converters are shown in Table I.

National Bureau of Standards

The NBS primary standards for ac-dc transfer at frequencies up to 50 kHz consist of a group of single-junction thermoelements (TE's), with Evanohm or Karma heaters to

Manuscript received July 21, 1980.

O. P. Galakhova and T. H. Rozdestvenskaya are with the Mendeleev All Union Institute of Metrology (IMM), USSR.

S. Harkness and P. Martin are with the National Physical Laboratory (NPL), UK.

F. L. Hermach and E. S. Williams are with the National Bureau of Standards (NBS), Washington, DC.

H. Hirayama is with the Electrotechnical Laboratory (ETL), Japan.

minimize Thomson errors (which are calculated to be less than 2 ppm), and MJTC's [2].

Each thermal voltage converter (TVC) consists of one or more thin-film cylindrical resistor, mounted coaxially in a metal cylinder and connected in series with a 5-mA TE. Twelve resistors give ranges from 1 to 1000 V [2]. With 2 TE's, adjacent ranges may be compared in a step-up or build-up process. The results have verified that reactance errors (which can be calculated roughly from the geometry) are less than 2 ppm for ranges below 200 V. The ac-dc differences of higher ranges are assigned from these comparisons.

To increase the precision of ac-dc current comparisons, the heaters of two TE's are connected in series, and the outputs are connected to an "EMF comparator" which balances the 2 outputs [2]. Changes in input current cause proportional changes in the EMF's, with little resulting change in the balance. The ac, dc, dc reversed, and ac currents are applied in succession for equal time intervals to reduce errors from drifts in the TE's, and each current is adjusted to obtain the same output from one TE. The difference between the 2 ac-dc differences $\delta_1 - \delta_2$ is determined from the resulting readings of a balance detector (nanovoltmeter). To compare TVC's in the same way, their input circuits are connected in parallel. The NBS interlaboratory standards are similar in construction to the basic ac-dc standards.

National Physical Laboratory

The NPL comparisons are made using a bridge circuit similar to that used at NBS. A semiautomatic system was developed, the switching between ac, dc forward, and dc reverse being made by mercury-wetted relays in an automatically timed sequence. A single measurement of ac-dc difference is obtained from 10 measurements of the bridge output when successively energized from ac, dc forward, dc reverse, etc. The bridge output is measured by an NPL-modified photocell-galvanometer amplifier to form a high input-resistance voltmeter having a most sensitive range of ± 1 μV, a linearity of ± 0.2 percent, and a peak-to-peak noise of 4 nV with a 250-Ω source. The output is recorded using conventional data-logging equipment. This data is analyzed by computer, using a curve-fitting technique [3], to determine an ac-dc difference relatively unaffected by nonlinear drifts present during the measuring period.

Over the range 0.5 to 100 V the NPL maintains its ac voltage capability by means of build-up measurements using resistors of 200, 900, 3000, and 10 000 Ω in conjunction with separate 5- and 10-mA thermal converters, each adjusted to have 100-Ω heater resistance. The linearity of all resistors, which is vital to the buildup, has been checked using third-harmonic testing. On theoretical grounds it is assumed that the 900-Ω resistor has negligible frequency error.

The thermal converters have platinum leadouts, rather than the conventional Dumet, to avoid ac losses which would cause errors in high-frequency low-voltage measurements. With the exception of the 30-mA converter, which has a Nichrome heater, all other converters have Evanohm heaters. The latter were constructed by a method which is believed not to impair the Thomson coefficient of the heater material. These converters were compared with the NPL Wilkins-type MJTC's, and those with the best relative transfer errors were selected. The MJTC's were assigned zero transfer error at low and medium frequencies.

The NPL interlaboratory standards consisted of 10-mA and 30-mA thermal converters for current measurements and a 5-mA thermal converter to be used in conjunction with 2000, 6000, and 20 000-Ω resistors to provide voltage ranges of 10, 30, and 100 V. The higher value resistors were known to have a voltage-dependent frequency response, believed to be due to the dielectric loss of the protective coating. A frequency-independent error of about 10 ppm, probably attributable to the Nichrome heater, was known to exist in the 30-mA converter.

Electrotechnical Laboratory

As reported previously [4], the ETL primary standards have been built up from 10-mA converters according to the following procedures:

1) After preliminary experiments on single and multijunction-type converters, the most appropriate construction was decided upon.

2) Three 10-mA single-junction vacuum-thermocouple current converters (Nikrothal heater and Chromel-Constantan couple) were selected, considering their characteristics and stability with time. Applying a theoretical formula, the ac-dc differences for individual converters and then their mean -5.1 ppm was calculated. This mean has been assumed to be constant up to 100 kHz. The ac-dc differences of other current converters were determined by comparison with these 3 standards. This method is different from that for determining ac-dc difference in other national laboratories. The effect of the assignment of -5.1 ppm is partially evident in the results of the international comparisons.

3) The ac-dc differences of 30-mA converters were determined by comparison with three 10-mA converters in parallel.

4) The frequency dependencies of 1-kΩ, 3-kΩ, and 100-kΩ series resistors were determined on the basis of a calculable single-wire resistor. Then the ac-dc differences of 10, 30, and 100-V voltage converters and their frequency dependencies were determined by combining the ac-dc difference of the 10-mA current converter with the frequency dependencies of the resistors.

For ac-dc measurements, a comparator [4] of 0.1-ppm resolution and accuracy better than 1 ppm up to 100 kHz is used. The standard deviation of a single measurement is normally better than 1 ppm.

For the international comparison, detailed measurements at 40 and 1592 Hz and at 20, 50, and 90 kHz were made on the ETL interlaboratory standards during 1973, and measurements to check their stability with time were made in 1978. The stability was within 10 ppm for 5 years except for converters with faults. From ETL's experience, the development of converters more resistant to shocks and vibration during transportation is desirable.

Mendeleev All Union Institute of Metrology

For the comparisons of current converters at IMM, a standard which reproduces the unit of ac current in the frequency range from 40 Hz to 100 kHz is used [5]. For the comparisons of voltage converters, a standard which reproduces the unit of ac voltage in the frequency range from 20 Hz to 30 MHz is used [6]. The main elements of these State Standards include specially developed and studied noncontact current and VTC's [7]. The voltage standard comprises 8 low-frequency (20 Hz to 100 kHz) and high-frequency (100 kHz to 30 MHz) converters with nominal values of voltage from 0.3 to 10 V.

The units of ac current and voltage are realized at different frequencies, using the State Standards, by the method of sequential comparison of ac current (or voltage) with dc current (or voltage) which produces an equivalent effect in an appropriate thermal converter. Theoretical analysis of the method and investigation of these standard thermal converters, developed at IMM, have been carried out. They showed that the equality of the thermal EMF's, generated by a converter, when its heater is alternately connected in dc and ac circuits, corresponds with high accuracy to the equality of the effective value of the measured ac current (or voltage) and dc current (or voltage) [8].

Each of the NBS, NPL, and ETL interlaboratory current and voltage converters was compared with an IMM standard converter by connecting the two converters in the ac circuit, then in the dc circuit whose polarity was then reversed, and then in the ac circuit again. Each time the thermal EMF of an interlaboratory converter was measured by means of a dc potentiometer, the thermal EMF of the IMM standard converter being kept constant. The error of the transfer was determined as the difference of mean values of the thermal EMF's of the interlaboratory converter obtained when the converter was connected in the ac and dc circuits.

Results and Discussion

The ac-dc differences in ppm assigned to each interlaboratory converter by each laboratory in terms of its national standards are given in Table II.

The most significant result of an interlaboratory comparison is an indication of the agreement among the laboratories. In the present comparison, this is most readily shown by averaging, for each laboratory, at each frequency, the results of the tests of all 4 converters of a given range, since the effects of random errors and changes in individual converters are thereby reduced. These averages are shown in Fig. 1. Because the ETL converters were not available then, none of the results of the first test at IMM are included in the figure or in Table II.

The converters were reasonably stable during the tests in any one laboratory. However, shipment did cause problems: ETL had to return the NPL TVC's for repairs, and IMM noted a 10-ppm change in its 100-V converter at 50 kHz between its first and second tests. The change probably occurred in transit after the NPL tests. There may also have been a change in the 10-mA converter after the first IMM test. The average change for all of the other converters between the two IMM tests was less than 1 ppm.

TABLE II
The AC-DC Differences in ppm of Each Converter as Determined by Each Laboratory

Measuring Laboratory ETL	NBS	NPL	IMM	Interlab Standard	Range	Frequency
0.7	-	0.9	8	NPL	10 V	40 Hz
- 5.1	-	- 5.9	3	ETL		
- 8.8	-	-12.0	0	IMM		
- 3.4	-	- 4.7	4	NBS		
0.0	-	0.3	9	NPL	30 V	40 Hz
- 4.3	-	- 5.6	6	ETL		
- 8.6	-	-13.0	0	IMM		
- 4.0	-	- 4.1	5	NBS		
4.3	-	- 0.5	8	NPL	100 V	40 Hz
- 4.8	-	- 8.9	3	ETL		
- 5.1	-	- 9.5	0	IMM		
- 0.1	-	- 4.9	5	NBS		
- 5.8	-	- 5.4	5	NPL	10 mA	40 Hz
- 4.9	-	- 4.5	5	ETL		
-13.7	-	-15.9	0	IMM		
- 2.5	-	- 2.8	15	NBS		
-14.6	-	-11.1	-9	NPL	30 mA	40 Hz
- 7.8	-	- 4.6	-3	ETL		
- 6.0	-	- 1.8	0	IMM		
- 7.2	-	- 2.3	-1	NBS		
- 4.5	0	- 0.8	7	NPL	10 V	20 kHz
- 4.2	- 2	- 3.7	6	ETL		
- 4.5	- 4	- 5.9	0	IMM		
- 1.7	- 1	- 1.1	6	NBS		
- 6.3	- 2	- 1.9	7	NPL	30 V	20 kHz
- 5.5	0	- 3.9	7	ETL		
-10.2	- 7	- 9.7	0	IMM		
- 4.6	- 1	- 1.4	7	NBS		
- 4.0	- 7	- 6.0	3	HPL	100 V	20 kHz
- 4.8	- 4	- 7.0	6	ETL		
- 6.4	- 9	- 9.3	0	IMM		
0.1	- 2	- 1.4	7	HBS		
- 2.5	- 2	- 3.4	-3	NPL	10 mA	20 kHz
- 5.1	- 1	- 4.3	-3	ETL		
- 1.9	4	2.1	0	IMM		
- 2.8	- 2	- 2.5	4	NBS		
-15.6	-11	-11.1	-9	NPL	30 mA	20 kHz
- 8.8	- 4	- 4.5	-5	ETL		
- 5.6	0	1.8	0	IMM		
- 7.2	0	- 1.5	-2	HBS		
- 5.3	2	0.0	-5	NPL	10 V	50 kHz
- 3.7	- 2	- 1.9	-4	ETL		
6.1	6	4.1	0	IMM		
- 0.4	3	- 0.1	-4	NBS		
-10.5	- 3	- 3.7	1	NPL	30 V	50 kHz
- 6.0	1	- 1.5	6	ETL		
- 9.6	- 4	- 7.1	0	IMM		
- 4.9	0	- 0.6	5	NBS		
-15.2	-19	-14.2	-10	NPL	100 V	50 kHz
- 6.2	- 2	- 7.3	1	ETL		
-11.0	-12	-11.4	-10	IMM		
- 0.3	- 2	- 1.3	4	NBS		
- 4.6	- 3	- 1.6	-4	NPL	10 mA	50 kHZ
- 5.6	0	- 3.3	-5	ETL		
- 3.5	8	8.8	0	IMM		
- 4.0	0	- 1.9	4	NBS		
-16.0	-14	-11.0	-1[illegible]	NPL	30 mA	50 kHz
- 9.0	- 3	- 5.5	-5	ETL		
- 6.9	0	1.9	0	IMM		
- 8.0	0	- 1.0	-2	NBS		

As shown in Fig. 1, the differences between the averages obtained by the laboratories for the 4 converters of a given range at a given frequency were very small. The largest difference between any one of these laboratory averages and the mean of the 4 laboratory averages at the same range and frequency was less than 9 ppm. The average of these differences (without regard to sign), taken over all laboratories, ranges, and frequencies, was less than 3 ppm.

Since the same 4 converters of each range were evaluated at each laboratory, it is possible to test the hypothesis that any offset (systematic difference) between 2 laboratories is masked by the imprecision of the measurements; i.e., that the differ-

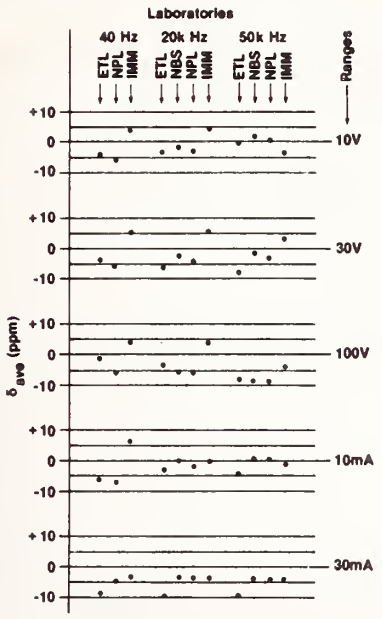

Fig. 1. Average ac-dc differences in ppm as determined by each of the 4 laboratories.

ences between the averages shown in Fig. 1 are not significant because of the random differences between the results of tests of individual converters. For 4 laboratories there are 6 such calculations for each range and frequency. To reduce the number, one laboratory can be used as a reference.

Experience indicates that the random error in comparing converters is not strongly dependent on range or frequency but may differ for different laboratories. There are also random changes in the converters between tests by two laboratories. On the basis that they are also roughly independent of range and frequency, the precision of testing the hypothesis can be increased by computing a pooled standard deviation s_0 for each pair of laboratories from all of the comparisons between them. If s_i is the standard deviation of the differences between the pairs of measurements in two laboratories for the 4 converters of a given range at a given frequency, and there are k such subsets of $n = 4$ pairs each, then

$$s_0^2 = \left(\sum_{i=1}^{k} s_i^2\right) \Big/ k.$$

The results of a series of such calculations are shown in Table III, with NPL as the reference. NPL was chosen because its results are generally centrally located in Fig. 1 and because it made measurements at all frequencies. A "yes" in Table III indicates that $3s_0/\sqrt{n} < |d_a|$, where d_a is the difference between the averages obtained by the 2 laboratories for the subset, because we can then decide that there is an offset (statistically significant difference), and we reject the hypothesis that it is masked by measurement imprecision. A dash indicates that $3s_0/\sqrt{n} > |d_a|$, so that there is no evidence of an offset. Although the table shows offsets in about one third of the cases, it should be emphasized that the differences between laboratories actually observed were much smaller than the assigned uncertainties shown in Table I.

TABLE III
EVALUATION OF DIFFERENCES BETWEEN LABORATORIES WITH NPL AS REFERENCE

	Evidence of Offset							
	40 Hz		20 kHz			50 kHz		
Range	ETL	IMM	ETL	IMM	NBS	ETL	IMM	NBS
10 V	-	yes	-	yes	-	-	-	-
30 V	-	yes	-	yes	-	yes	yes	-
100 V	yes	yes	-	yes	-	-	yes	-
10 mA	-	yes	-	-	-	yes	-	-
30 mA	yes	-	yes	-	-	yes	-	-

The pooled standard deviations s_0 were 2.10 ppm for ETL–NPL, 2.59 ppm for IMM–NPL ($k = 15$), and 2.07 ppm for NBS–NPL ($k = 10$). The distributions of the differences between NPL and the other laboratories were reasonably normal. In only one case did the pair of tests on an individual converter in 2 laboratories differ from d_a by more than $3s_0$, possibly indicating a change in that converter.

CONCLUSIONS

It is apparent that the agreement among the laboratories is much better than the uncertainties estimated in Table I. In most cases the differences between the averages obtained by the laboratories are not statistically significant because of the scatter of the measurements. The primary ac-dc transfer standards of the 4 laboratories are all thermal converters, but are of different types of construction. The methods and equipment for comparing converters are also different. Further, the primary converters were studied independently and thoroughly in each laboratory. It is extremely unlikely that all of them could be afflicted with an ac-dc difference of the same magnitude and sign. The excellent agreement in these careful international tests provides valuable assurance of the absence of significant systematic errors in the primary standards and the comparison apparatus. It is thus highly significant. There is now a very firm basis for international concordance of the ac-dc transfer to better than 10 ppm at audio frequencies.

REFERENCES

[1] F. L. Hermach, "AC-DC comparators for audio frequency current and voltage measurements of high accuracy," *IEEE Trans. Instrum. Meas.*, vol. IM-25, pp. 489–492, Dec. 1976.
[2] F. L. Hermach and E. S. Williams, "Thermal converters for audio-frequency voltage measurements of high accuracy," *IEEE Trans. Instrum. Meas.*, vol. IM-15, pp. 260–268, Dec. 1966.
[3] S. Harkness and R. B. D. Knight, "Computer correction of errors due to instrumental drift by curve fitting," Natl. Phys. Lab., Eng. DES Memo No. 20, Nov. 1975.
[4] S. Iwamoto and H. Hirayama, "AC-DC thermal converters of the ETL," *IEEE Trans. Instrum. Meas.*, vol. IM-23, pp. 326–329, 1974.
[5] O. P. Galakhova, E. K. Dranishnikova, and M. S. Belayeva, "Special state standard of the AC current unit in the range from 40 Hz to 100 kHz," *Izmer. Tekh.*, pp. 42–44, Mar. 1976.
[6] T. B. Rozhdestvenskaya R. F. Aknaev, and O. P. Galakhova, "Special state standard of the AC voltage unit in the range of frequencies from 20 Hz to 30 MHz," *Izmer. Tekh.*, pp. 44–46, Mar. 1976.
[7] R. F. Aknaev, O. P. Galakhova, and T. B. Rozhdestvenskaya, "Methods and instruments of assurance of the uniformity of AC voltage measurements," *Izmer. Tekh.*, pp. 66–71, Apr. 1976.
[8] R. F. Aknaev and T. B. Rozhdestvenskaya, "Analysis of errors introduced by thermal converters when comparing AC and DC current and voltages," Trudy Metrology Inst. SSSR, 138(198), 1972.

IEEE TRANSACTIONS ON INSTRUMENTATION AND MEASUREMENT, VOL. IM-29, NO. 4, DECEMBER 1980

A Semiautomatic System for AC/DC Difference Calibration

KEITH J. LENTNER, MEMBER, IEEE, CLIFTON B. CHILDERS, AND SUSAN G. TREMAINE

Abstract—**A semiautomatic ac/dc difference calibration system is described. The system operates over a frequency range of 20 Hz to 100 kHz, covering the voltage range from 0.5 V to 1 kV. For all voltages at frequencies in the range from 20 Hz to 20 kHz, the total uncertainty is 50 ppm and 100 ppm for voltages at frequencies between 20 kHz and 100 kHz. In addition to ac/dc difference testing, the system can be readily adapted to calibrate precision ac digital voltmeters or ac calibrators. Results of extensive intercomparison testing of the new system against a manual test system, using a multirange thermal transfer instrument as a transport standard, are reported, and the results indicate that the differences obtained are well within the combined total uncertainty limits of the two systems.**

INTRODUCTION

TECHNIQUES for performing precision ac/dc difference testing, not only at the National Bureau of Standards (NBS) but also in other national and industrial or governmental metrology laboratories, generally make use of manual testing methods which utilize photo-cell preamplifiers and light-beam galvanometers as voltage detectors, in conjunction with manually balanced voltage comparators [1], [2]. Careful attention to the elimination or reduction of systematic and random uncertainties in testing methods and thermoelements (TE's) has resulted in sufficient confidence in test data to allow results to be reported with total uncertainties at the 10–100 ppm level (or better, in some cases) over wide voltage and frequency ranges [3], [4]. These manual test methods, however, are very time consuming and subject to errors due to operator fatigue. To overcome these deficiencies, and to expedite test report generation, a semiautomatic ac/dc calibration system was developed.

Because of the low-level voltages that must be resolved (10 nV or less), large temperature coefficients of TE's, ac or dc source instabilities, and dc reversal differences of TE's, stringent requirements are placed upon the measurement system. In addition, light-beam galvanometers suffer the disadvantage of not being easily adaptable to automation. However, with the advent of digital electronics, low-level digital voltmeters (DVM's) are available with resolution and accuracy sufficient to meet the requirements of precision automatic ac/dc difference testing. Programmable ac and dc voltage calibrators are also available which lend themselves to adaption for automatic testing. Advances in analog/digital interfaces have greatly improved the ease with which computers can be used to control these instruments.

The system, to be described in this paper, was designed to overcome the deficiencies of manual test methods by taking advantage of the electronics advances discussed above. Specifically, some objectives were to: 1) use commercially available programmable instruments whenever possible; 2) eliminate the need of manual data entry into a computer for data reduction; 3) eliminate the frequent data checks and cross checks required in manual tests; 4) eliminate as much operator intervention as possible during the testing procedure; 5) closely control the time interval between application of both ac and dc voltages to the test circuit in order to minimize drift effects; 6) provide as much computer-operator interaction as possible to simplify the testing procedure; and 7) achieve the same level of uncertainty as is presently possible with manual testing methods.

The system operates over a frequency range of 20 Hz to 100 kHz, covering the voltage range from 0.5 V to 1 kV. For all voltages at frequencies in the range from 20 Hz to 20 kHz, the total uncertainty is 50 ppm and 100 ppm for voltages at frequencies between 20 kHz and 100 kHz. In addition to ac/dc difference testing, the system can be readily adapted to calibrating precision ac digital voltmeters or ac calibrators.

SYSTEM HARDWARE

The hardware implementation emulates that used in manual systems at NBS. The prinicpal instrumentation difference is the use of an electronic voltage detector. Also, almost all the instruments are programmable. The major problem in hardware development was obtaining low-thermal-noise switches which could be automatically controlled. TE voltages of about 10 mV need to be measured to within 1 ppm (10 nV), and solid-state relays were found to be unsuitable since most of these devices have thermal noise of the order of 1 μV. The problem was solved by modifying manually operated low-thermal-noise switches. Solenoids with 24-V operating coils were mechanically linked to the low-thermal-noise switch, and are energized by programmable relays.

Experience gained at NBS throughout many years of manual testing was used to design the remainder of the system. The switches which apply the ac or dc voltages to the test circuit are relays capable of switching up to 5 kV. The 24-V operating coils of these relays are supplied in turn by means of programmable relays.

Manuscript received July 24, 1980. This work was partially funded by the U.S. Department of Defense Calibration Coordination Group.

The authors are with the Electrosystems Division, National Bureau of Standards, Washington, DC 20234.

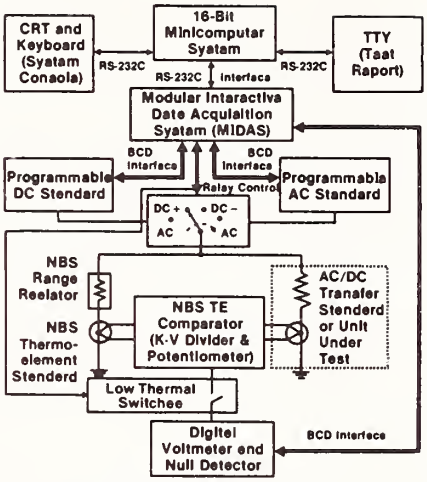

Fig. 1. Simplified system block diagram.

Fig. 2. Photograph of system.

A simplified block diagram of the system configuration is shown in Fig. 1, and a photograph of the system in Fig. 2. The 16-bit minicomputer serves as the system controller and has 64 kbytes of core memory with a dual floppy-disk system for program and data storage. The system console (CRT), the teletypewriter (TTY), and the Modular Interactive Data Acquisition System (MIDAS) [5] are connected to the computer by means of interfaces which conform to the EIA RS-232-C [6] standard. MIDAS is a user-oriented digital interface system for data acquisition and experiment control. Its hardware is based on the CAMAC [7] standard and is composed of several functional modules which may be plugged into slots in a standard crate. A MIDAS power supply and controller are the only two additional items of equipment necessary to make MIDAS operational. Communication between the MIDAS controller and individual modules is in accordance with the ASCII [8] standard code for information interchange.

As indicated in Fig. 1, the programmable ac and dc sources and the voltage detector are controlled by binary-coded-decimal (BCD) MIDAS modules. The sequence of applying voltages to the test circuit, as indicated in Fig. 1, is ac, dc+, dc−, ac, and the ac or dc source voltage relays are controlled by means of a MIDAS relay module. The choice of this par-

ticular voltage application sequence has been fully discussed in reference [2] and will not be reiterated here. The NBS-developed TE comparator (consisting of a Kelvin–Varley voltage divider and Lindeck potentiometer) has been described in the same reference. The low-thermal-noise switches, controlled by a MIDAS relay module, are solenoid actuated switches which select the proper voltage output from the TE comparator. The detector obtains readings of the proper voltages and passes these readings in BCD format to the computer where they are stored for later processing. The voltage detector is a digital voltmeter which has a steady-state input impedance of about 10 MΩ and is capable of 1-nV resolution on its most sensitive (10-μV) range. The Kelvin–Varley divider in the TE comparator is used to adjust the difference between the output voltages of the standard TE and the unit under test (UUT) to within 500 nV.

A typical programming sequence will be described in more detail in the next section. For simplicity in Fig. 1, two digital panel meters which monitor the voltage outputs of the dc and ac programmable standards are not shown. Also not shown is a counter used to monitor the ac standard's frequency. This equipment is visible in the system photograph (Fig. 2). The large instrument on the left of the test console table is an ac calibrator under test.

As was mentioned previously, the system can be readily adapted as well to the tasks of calibrating precision digital voltmeters or ac calibrators. In this case, the testing procedure and balance equation differ slightly from those described in reference [2]. For example, the corrections to the nominal output voltage dial settings of an ac calibrator can be determined by using the system's dc programmable standard voltage source (set to the same nominal value as the ac calibrator) and a thermal voltage converter (TVC), both having known corrections. For this case, only the Lindeck potentiometer portion of the TE comparator is used. The correction to the UUT in ppm (whether that of an external ac calibrator or the system's programmable ac standard) is given by

$$C_t = \frac{V_a - V_d}{n_s V_s} + \delta_s + C_{\mathrm{dc}}$$

where δ_s is the ac/dc difference correction of the TVC at the test frequency, V_a is the reading of the detector (DVM) with ac voltage applied (i.e., the difference between the TE's output emf and the fixed voltage of the Lindeck potentiometer), V_d is the average of the detector readings with direct voltage of both polarities applied, n_s is a dimensionless factor equal to 2 if the TE has a square-law response, V_s is the standard TE's output EMF at the applied test voltage, and C_{dc} is the correction to the dc voltage standard's nominal output.

System Software

In order to reduce the effort involved in making routine tests of TE's and TVC's, the software for the system was designed to provide as much interaction between the system console (the CRT) and the operator as possible. This interaction was used to reduce the possibility of damage to either the standard TVC or the UUT when either software or hardware failures occur. Also, by progressing logically through the first portions of the test routines, the operator, when necessary, can take whatever corrective actions might be required. A significant advantage of the software design is that sufficient warm-up time is automatically provided between application of the various test voltages so that the effects of errors due to the warm-up drifts of the TE's are reduced. In addition, the computer can closely control the time intervals between DVM readings; hence, the effects of linear drift in the ac or dc sources are minimized.

The programs written in Basic language for this system provide the means for automatically setting the ac or dc source voltages and ac frequency, operating the voltage relays and low-thermal switches, triggering the DVM to obtain voltage readings, and storing these readings in the computer memory. About thirty programs have been written with six constituting the major testing software package. Program ACDCLV is used for making ac/dc difference tests at voltages from 0.5 to 95 V, and ACDCHV is used for similar tests at voltages greater than 105 V up to 1 kV. NTSTF is used to determine a TE's dimensionless factor n [1], [2] and includes provision to perform a linear least squares fit of the experimental data. ACCAL is a program used to calibrate an ac calibrator, a precision ac-digital voltmeter, or the ac source of the system in terms of a standard TVC and the system's calibrated dc supply, as discussed in the previous section.

Stability of the system's dc and ac sources can be checked by using programs called STABLV and STABHV. These programs are used at voltage ranges similar to those for ACDCLV and ACDCHV. These stability tests are useful to determine whether or not the supplies are functioning properly. Occasionally, test results appear to be erratic and the stability tests are a convenient method to ascertain whether the erratic results may be due to the ac or dc sources. Stability of the sources is measured by using a programmable 6½ digit DVM whose function, ranges, and reading rates are remotely controlled.

Initial stability test parameters for voltage, frequency, time between readings, and total number of readings are entered into the computer. The program then exercises complete automatic control over the ac and dc sources, the voltage relays, and the DVM. At completion, stability data including the values of minimum, maximum, range, average, standard deviation of the mean, and three times the standard deviation of the mean for both ac and dc voltage readings are printed on the TTY.

Operation

Since the major application of the work described in this paper has been directed toward ac/dc difference testing, a typical sequence of operations for this type of testing will be described. ACDCLV is a program which provides partial automatic control of ac/dc difference testing. The program is "partially automatic" in that an operator must manually input test parameters, switch the TE comparator to select proper TE's, and must manually balance the TE comparator's Lindeck potentiometer and Kelvin–Varley voltage divider.

Basically, ACDCLV contains three general sections. The first section provides program initialization and documenta-

tion. The midsection includes a network of subroutines that interact with the operator. Instructions displayed on the CRT prompt the operator to: 1) key in test parameters which set ac and dc voltages and frequency; 2) switch the TE comparator to determine whether the standard TVC or UUT has the greater TE output, ensuring that the TE's are connected to the proper input terminals of the TE comparator; 3) balance one TE's output with the Lindeck potentiometer; then 4) balance the Kelvin–Varley divider. Repeatedly accessed subroutines then close and open the appropriate relays, and obtain the DVM voltage readings for four determinations of ac/dc difference at each test point. Finally, in the third section, statistical calculations are performed, and the results are printed on the TTY. Options are provided, and the operator can choose whether to stop, repeat a test, or change parameters (either voltage or frequency) and run another test. This program is used for voltages ≤ 95 V.

Since the MIDAS interface does not have isolated analog and digital grounds, it was necessary to develop a separate software package for high-voltage testing. At high voltages, it was found that the opening or closing of either the ac or dc voltage relays introduced transient voltage surges into the MIDAS digital circuitry. The MIDAS controller interpreted these surges as voltage level changes identical to programmed input commands. The result was that incorrect relays might be opened or closed, the voltage detector might be falsely triggered to obtain a reading, or any other of a series of unwanted events might occur. Hence, the ACDCHV program was developed to ensure that no high-voltage supplies are turned on whenever a voltage relay is opened or closed. The specific procedures include:

1) Input test number, voltage, frequency, observer's name, and code for the standard TVC used.

2) Visually check to see that both software and hardware are operating correctly by checking the system's digital panel meters and frequency meter for correct readings of the outputs from the ac and dc sources. If the outputs are incorrect, try again.

3) Manually set the TE comparator to its high TE voltage position and switch the voltage detector to its 10-mV range. The program automatically closes the dc voltage relay and a low-thermal-noise switch, turns on the dc supply, and triggers the detector to obtain the TE voltage output reading.

4) Switch the TE comparator to its low TE voltage input position.

The program then commands the detector to read the voltage. The values of the high- (from the previous step) and low-voltage readings are compared. If the values are incorrect, the operator is instructed to interchange the two TVC inputs after the dc voltage has been turned off. The program automatically stores the value of E_{low}, since that value is used in the balance equation [2, appendix].

5) Switch the TE comparator to the high TE input position, turn on the Lindeck potentiometer, change the detector to its 10-μV range, and manually balance the potentiometer.

6) The first low-thermal-noise switch is opened and a second closed. The operator now manually balances the Kelvin–Varley divider for a near null reading on the detector. The dc source is automatically turned off, and the dc voltage relay opened.

7) The ac voltage relay is closed, the ac supply turned on, and its voltage is automatically incremented or decremented until the UUT's TE output voltage is ≤ 1 μV of its value with dc voltage applied as in step 6.

8) At this point, the manual initialization process is complete, and the test proceeds automatically under program control. A sequence of near null voltage readings is obtained by the null detector when ac, dc+, dc−, and ac voltages are applied to the standard TVC and UUT. These four voltage readings are each obtained from the average of ten readings of the DVM. The standard deviation of the ten readings is computed and, if this value is <200 nV, the program continues. If the standard deviation is ≥ 200 nV, due to drifts in either the standard TVC or the UUT, or the ac or dc sources, or any of these effects combined, the series of ten readings is repeated. After five attempts, if the DVM readings have not stabilized, the test is aborted.

9) The sequence of readings with ac, dc+, dc−, and ac voltages applied constitutes one determination of the ac/dc correction to the UUT. The process is continued for four determinations; the average value of four determinations is computed and printed on the TTY. The operator then may elect to repeat the test, change voltage range or frequency, or stop the test.

The system was intended to calibrate high-quality TVC's, and it was not necessary to add additional balancing steps to eliminate uncertainties due to large dc reversal difference (i.e., difference between the dc direct and reverse voltages required for the same TE EMF output of the UUT). For the worst case, using 2.0 and 1.6 as the two extremes of the characteristic n which may occur for the standard and UUT TE's, it can be shown [4] that systematic uncertainties of less than one-fourth the UUT's dc reversal difference will occur. Minor software changes can eliminate this systematic source if large reversal differences are anticipated. The changes would amount to adjusting the ac voltage (cf. step 7 above) for a TE output equal to that when dc reversed voltage is applied to the test circuit. The only penalty for such a change in the operating procedure would be an increase in testing time of perhaps one or 2 min (for four determinations of ac/dc difference).

There is also the possibility of a systematic uncertainty if the ac or dc voltage sources drift during a sequence of four determinations. However, for the same extremes of n, the uncertainty is only 10 ppm if either source drifts by as much as 100 ppm. The STABLV and STABHV programs readily provide information about the stabilities of the sources.

Measurement Results and Uncertainties

There are many error sources which determine the uncertainty of ac/dc difference measurements of the type described in this paper. Similar manual systems have been in operation for many years at NBS and their uncertainties have been documented [1]–[3]. DC reversal difference of a TE, self-heating and ambient temperature effects, drift effects due to nonequal time intervals during the voltage measurements, unbalanced lead impedances, and induced voltages from

TABLE I
RANGE OF AC/DC DIFFERENCES FOR TRANSPORT STANDARD (ppm)

Voltage Range	Test Voltage Volts	Test Frequency (kHz) 20	50	100
0.25-0.5	0.5	18	19	23
0.5 - 1	1	9	2	4
1 - 2	2	1	6	9
2 - 4	3	2	0	0
4 - 8	8	0	1	3
8 - 16	16	8	15	3
16 - 32	30	8	10	9
32 - 64	50	3	3	10
64 - 125	98	2	6	12
125 - 250	200	4	2	14
250 - 500	500	4	50	39
500 - 1000	500	22	54	147
500 - 1000	1000	17	70	--

electromagnetic fields are some of the more common sources of error. The process of determining an estimated total uncertainty for a system is based upon experience with the system, careful measurements of standards with accurately known corrections, or intercomparison tests of two independent test methods [3]. The latter procedure, involving comparison of a well-characterized manual system with the new one, was followed, since the uncertainty sources are believed to be the same in both systems.

The system performance was verified by an extensive testing procedure which involved the use of a multirange thermal voltage converter instrument as a transport standard. The transport standard was first tested for ac/dc difference corrections at various combinations of applied voltages and frequencies using the MIDAS-based system. It was then tested, at similar voltages and frequencies with the same standard TVC, using the manual testing techniques which have been used for many years at NBS. A third test was performed, again using the MIDAS system. Finally, the MIDAS system was disassembled, physically relocated, reassembled, and tested for proper operation. Then the transport standard was tested a fourth time, again using the MIDAS system. It should be noted that not all voltage range-frequency combinations were tested for all four tests. However, in those cases where fewer than four tests were performed, the results indicated sufficiently small differences between at least two independent test methods to establish that further testing was not warranted. The results of these independent intercomparison tests are summarized in Table I. In evaluating these results, it must be remembered that, for calibrating multirange instruments like the transport standard, the manual test system has uncertainties of the same magnitude as the semiautomatic system. Hence, combined total uncertainties of the order of 100 and 200 ppm are possible depending upon the test frequency.

In Table I, the column listing "Voltage Range" refers to the input voltage range of the transport standard, the "Test Voltage" is the actual test voltage applied, and the different columns for frequency are the actual test frequencies used. The numbers listed under the frequency columns are the maximum differences (in ppm) of the calibrated ac/dc difference corrections for the transport standard as determined for at least two, and up to a maximum of four, of the test conditions described above. That is, the numbers reported are the range (magnitude of the maximum minus the minimum) of the ac/dc difference corrections calculated for each test voltage and frequency. The total elapsed time between the first and final tests of the transport standard was about eight weeks.

From the test results at 20 kHz, the average value of the range of ac/dc differences for all voltages is only 8 ppm. At 50 kHz the average value of the range is 19 ppm, and at 100 kHz, where skin effects and stray capacitance effects predominate, the largest difference (at 500 V) was 147 ppm. However, this large range is within the expected combined total uncertainty of 200 ppm for the two systems. Even with this one range greater than 100 ppm, the average value of the range at 100 kHz is still only 23 ppm. No intercomparison results were obtained at 1000 V, 100 kHz since the high-voltage amplifiers in both systems could not supply sufficient power at that voltage-frequency combination.

CONCLUSIONS

The results of the work reported in this paper indicate that it is possible to measure ac/dc differences semiautomatically with uncertainties about the same as those obtained with manual testing techniques. The major advantage of the system appears to be the elimination of most of the tedium involved in manual testing, in which deflections of light beam galvanometers must be observed and recorded.

For future work, it appears that improvements in system operation can be obtained by development of self-balancing TE comparators. Beyond that, it may be possible, by taking advantage of improvements in voltage detector resolution, desktop computers, and system components whose operation is compatible with new digital/analog interfaces, to make readily available the hardware and methodology for improved ac/dc difference testing techniques.

ACKNOWLEDGMENT

The authors are indebted to E. S. Williams for his many valuable contributions to the work reported in this paper. He designed and built the voltage and low-thermal-noise switch modules and provided much of the initial software which eventually became part of the total programming package required for system operation. R. E. Kleimann, S. C. Bailey, and W. C. Caterisano each contributed portions to some of the computer programs.

REFERENCES

[1] F. L. Hermach and E. S. Williams, "Thermal converters for audio-frequency voltage measurement of high accuracy," *IEEE Trans. Instrum. Meas.*, vol. IM-15, pp. 260-268, Dec. 1966.

[2] E. S. Williams, "Thermal voltage converters and comparator for very accurate ac voltage measurements," *Nat. Bur. Stand. J. Res.*, vol. 75C,

pp. 145–154, Dec. 1971.
[3] F. L. Hermach, "AC-DC comparators for audio-frequency current and voltage measurements of high accuracy," *IEEE Trans. Instrum. Meas.*, vol. IM-25, pp. 489–494, Dec. 1976.
[4] R. S. Turgel, "A comparator for thermal ac-dc transfer standards," *ISA Trans.*, vol. 6, no. 4, pp. 286–292, 1967.
[5] C. H. Popenoe, M. S. Campell, "MIDAS Modular Interactive Data Aequisition System—description and specifications," *Nat. Bur. Stand. Tech. Note 790*, U.S. Gov. Printing Office, Washington, DC 20402 (Aug. 1973).
[6] "Interface between data terminal equipment and data communication equipment employing serial binary data interchange," *EIA RS-232-C, Electron. Ind. Ass.*, 2001 Eye St., N.W., Washington, DC 20006 (Aug. 1969).
[7] "IEEE standard modular instrumentation and digital interface system (CAMAC)—computer automated measurement and control," *IEEE Stand. 583—1975*, IEEE, 345 E. 47 St., New York, NY 10017.
[8] "American National Standard Code for Information Interchange," *ANSI X3.4—1977*, Amer. Nat. Stand. Inst., Inc., 1430 Broadway, New York, NY 10018.

IEEE TRANSACTIONS ON INSTRUMENTATION AND MEASUREMENT, VOL. IM-27, NO. 3, SEPTEMBER 1978

An RMS Digital Voltmeter/Calibrator for Very-Low Frequencies

HOWARD K. SCHOENWETTER, SENIOR MEMBER, IEEE

Abstract—**A portable rms digital voltmeter (DVM) has been developed at NBS to support vibration measurements over the ranges of 0.1 to 50 Hz and 2 mV to 10 V. A self-contained calibrator provides for self-calibration and may be used for calibrating other VLF voltmeters. The calibrator basically consists of a Kelvin–Varley divider fed by a reference voltage (either dc or sinewave generated by a ROM–DAC combination). A multijunction thermal converter (MJTC) was selected as the sensing device in the rms/dc converter of the DVM since its low ac/dc difference facilitates calibration of the ac calibrator. Factors affecting accuracy and response time are analyzed. The DVM response time is 40 s for the lowest input frequency. Its accuracy (percent of reading) is 0.1 percent above 0.5 Hz and 5 mV and 0.2 percent below these values. The ac calibrator accuracy is 0.02 percent. Measurement accuracy improves by a factor of about 4 for transfer measurements (comparing input voltages with ac calibrator voltages). Means for extending this accuracy to 0.01 percent are discussed.**

I. Introduction

CALIBRATED vibration transducers (accelerometer–amplifier systems) are required in calibration laboratories and test facilities to determine the acceleration of vibration exciters, tables and fixtures. At very-low frequencies (VLF's), particularly below 10 Hz, the major source of error in calibrating these transducers (both reference standards and test items) has been the error in measuring the output voltage from the transducer [1], [2]. This is because the measurement error of the few commercial voltmeters (that measure VLF's) ranges from a few tenths of a percent to over 1 percent, depending upon the voltage and frequency. Furthermore, calibration of these voltmeters is difficult since no commercial ac voltage calibrator operates below 10 Hz. Voltage measurement errors are very significant since their contribution to transducer calibration uncertainty is added at each level of the calibration hierarchy.

To meet present and expected future requirements of vibration and other very low frequency measurements, a portable rms digital voltmeter (DVM) was designed to measure voltages from 2 mV to 10 V over the frequency range of 0.2 Hz to 50 Hz.[1] Since the means for calibrating the voltmeter to the required accuracy below 10 Hz did not exist, an ac voltage calibrator was also developed and incorporated into the same instrument. This calibrator, covering the frequency range of 0.2 Hz to 50 Hz,[2] is intended not only for calibration of the companion voltmeter but also for the calibration of other voltmeters. In addition, the calibrator facilitates transfer measurements.

Manuscript received February 20, 1978. This work was supported in part by the Calibration Coordination Group of the Department of Defense.

The author is with the Electricity Division, National Bureau of Standards, Washington, DC 20234.

[1] The design was later modified to extend the range to 0.1 Hz.

Fig. 1. RMS digital voltmeter used in ac voltmeter/calibrator.

The accuracy objective for the voltmeter was 0.1 percent of reading above 2 Hz and 5 mV and 0.25 percent of reading for lower frequencies and voltages. As explained in the next section, the minimum response time obtainable in rms voltmeters is directly proportional to the period of the input voltage. Commercial rms DVM's require 15–20 periods for a response to within ±0.1 percent of the input change. This extrapolates to 150–200 s for 0.1 Hz. Since slow response limits an instrument's usefulness, the design objective also was to decrease the response time below these figures as much as was practicable.

II. RMS Voltmeter Design

A. Design Considerations

The rms voltmeter designed for this instrument follows the conventional approach shown in Fig. 1. In describing the operation of this circuit and the following circuits, rms and instantaneous values will be represented by upper and lower case letters, respectively. The ac input voltage E_i is amplified to a voltage level E_o suitable for the rms/dc converter and converted to a unidirectional voltage E_o. The converter transfer characteristic E_o/E_o is ideally a constant, adjustable to unity.[3] Since the input voltage to the converter e_o is sensed by a square-law device, the converter output e_o consists of a dc component E_{dc} and a ripple component e_r whose rms value is E_r; hence,

$$E_o = \sqrt{E_{dc}^2 + E_r^2} \simeq E_{dc}(1 + E_r^2/2E_{dc}^2). \quad (1)$$

If the amplifier gain is G and $E_o/E_o = 1$, then $E_o = E_o = GE_i$. For accurate measurement of E_i, the voltmeter reading should be E_o/G; however, the dc DVM responds to E_{dc} (since it is average-responding) and displays the value E_{dc}/G. Therefore, it is seen from (1) that the ripple value E_r causes a fractional error of $E_r^2/2E_{dc}^2$ in the displayed voltage.

[2] The design was later modified to extend the range to 0.1 Hz.

[3] In practice, E_o/E_o varies somewhat with the frequency of the input voltage. This rms/dc conversion error will be discussed in later sections.

Thus ripple filtering is required in the converter to limit this rms/dc conversion error to an acceptable level. This constraint still allows a relatively large peak-to-peak value of e_r and would, if not reduced, cause intolerable fluctuations in the displayed voltage. These fluctuations, in effect, reduce the DVM accuracy. Therefore, a low-pass (LP) filter is used to reduce the peak ripple (in e_M) to an acceptable level.

If the input voltage e_i is a waveform with a crest factor greater than 1 (e.g., a sinewave), the time constants in the converter and LP filters must be increased in direct proportion to the period of e_i in order to maintain acceptable ripple levels. Consequently, the minimum rms voltmeter response time is proportional to the period of e_i. For a given frequency (and a given voltmeter design), response time can only be decreased by decreasing the filter time constants, resulting in increased voltmeter error (including fluctuations in the displayed voltage). Thus a tradeoff exists between minimum response time and minimum voltmeter error.

B. Error Budget

The error budget of 0.1 percent above 2 Hz was allocated as follows:

rms/dc conversion error	0.02%
calibration errors	0.03%
temperature effects/°C	0.02%
gain-offset drift/30 days	0.03%

The error budget of 0.25 percent below 2 Hz included the above items, plus the following:

rms/dc conversion error from ripple (E_r)	0.05%
rms/dc conversion error from sensing element	0.05%
peak fluctuations in displayed voltage	0.05%

Much smaller fluctuations (0.01–0.02 percent) in the displayed voltage are desirable when using the voltmeter for ac/ac transfer measurements where the input voltage is measured by comparison with a calibrator voltage of approximately the same frequency. The gain-offset error budget was not considered critical since corrections are readily made (2 adjustments) using the voltage calibrator.

C. Detailed Design

1) Input Amplifier: The input amplifier is direct-coupled and has gains from 0.5 to 2500, selectable in 12 ranges of 1–2–5 gain sequence. The amplifier consists of two cascaded low-noise low-drift operational amplifiers with buffering to provide high-input impedance and power capability with low distortion at its output. The sequence of voltage ranges limits the nominal input range over which the rms/dc converter must operate from 2 to 5 V. Reed relays in DIP configuration are used for range switching. The frequency response for all gain ranges is flat from dc to 50 Hz to within 0.01 percent or better.

2) RMS/DC Converter:[4]

a) General description: The rms/dc converter in this instrument (Fig. 2) is a feedback type, employing a differential multijunction thermal converter (MJTC) for the sensing element.[5] The differential MJTC contains two matched MJTC's connected so that the dc components of their outputs oppose each other. The outputs $e_1(t)$ and $e_2(t)$ have dc components E_{d1} and E_{d2} proportional to the input power to heater elements H_1 and H_2, respectively. Therefore,

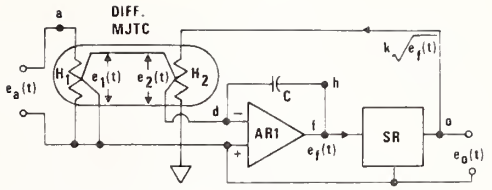

Fig. 2. Functional block diagram of rms/dc converter.

$$E_{d1} = K_1 E_a^2/r_1 \quad \text{and} \quad E_{d2} = K_2 E_o^2/r_2 \tag{2}$$

where E_a and E_o are the rms values corresponding to $e_a(t)$ and $e_o(t)$, K_1 and K_2 are constants of proportionality and r_1 and r_2 are the resistance values of H_1 and H_2. It will be shown later that the circuit is constrained to allow only negative feedback, i.e., the voltage fed back to H_2 always tends to decrease the difference between E_{d1} and E_{d2}. If the loop gain is very large, $E_{d1} - E_{d2} \simeq 0$. Equating the expressions in (2), $E_o^2 \simeq K_1 r_2 E_a^2/K_2 r_1$ or

$$E_o \simeq \sqrt{K_1 r_2/K_2 r_1}\, E_a. \tag{3}$$

Hence, E_o is proportional to E_a, the rms value of the input voltage $e_a(t)$. To simplify later discussions, it is assumed that $K_1/r_1 = K_2/r_2 \equiv B$, i.e., $K_1 r_2/K_2 r_1 = 1$.

Equation (3) is also valid if square-rooting circuit SR is omitted and point f connected to point o. However, omitting circuit SR causes the rms/dc converter circuit to be nonlinear, since the MJTC in the feedback loop has a nonlinear transfer characteristic ($E_{d2} = BE_o^2$). This nonlinearity, in turn, causes the response time of the converter to be different for input step increases than for input step decreases [7], [8]. This effect can be removed by placing a squaring amplifier between points f and h [8], [9], or by linearizing the converter circuit using circuit SR, as shown in Fig. 2. The latter method has the advantage of maintaining constant dc loop gain, independent of E_o.

b) Detailed description: Circuit details of the rms/dc converter are shown in the upper part of Fig. 3. As explained in the next section, resistor $R1$, matched to the resistance of heater H_1 (~ 1 kΩ), is used to reduce the low-frequency ac/dc difference of the MJTC input section.[6] Resistor $R2$ is added to equalize the rms values of the input and output voltages. Adding these resistors decreases the effective value of B by a factor of 4. (See statement following (3) for definition of B.)

Amplifier AR1 is a low-noise chopper-stabilized amplifier which provides high loop gain. The circuit SR (Fig. 2)

[4] Bibliographies on rms/dc converters may be found in [3] and [4].

[5] The MJTC is described in [5]. Differential MJTC's have been used previously in rms/dc feedback converters operating above 50 Hz [6].

[6] The ac/dc difference is defined as $\delta = (Q_a - Q_d)/Q_d$ where Q_a and Q_d are the ac and dc inputs which produce the same thermal converter output (dc component only).

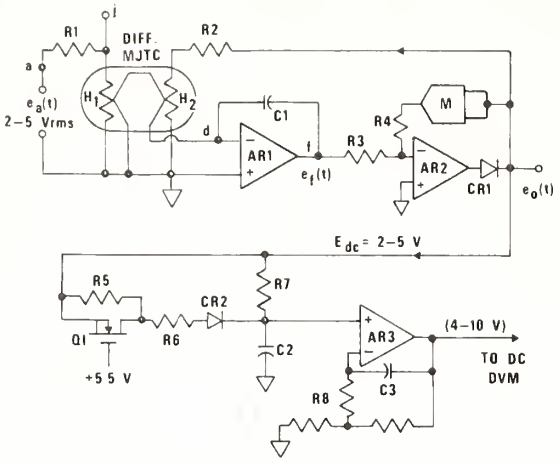

Fig. 3. RMS/dc converter and signal conditioner.

consists of amplifier AR2 and multiplier M, which functions as a squaring circuit in the AR2 feedback loop. The constant k of the SR circuit's transfer characteristic ($e_0 = k\sqrt{e_f}$) is adjusted by the value of $R3$. Diode CR1 restricts the feedback voltage $e_0(t)$ to positive values (negative feedback only).

c) Sensing element: An MJTC was selected for the sensing element of the rms/dc converter because of its negligible ac/dc difference over a large part of the 0.1–50 Hz frequency range. It will be shown later that this factor is important for the calibration of the ac calibrator.

For input frequencies sufficiently high that negligible temperature variation of the thermal converter heater occurs during a cycle (because of the heater thermal time constant), deviation from square-law response has no effect on δ and the ac/dc difference is very small. At very-low frequencies (VLF's), the heater temperature varies with instantaneous input power and external filtering is necessary to smooth the output voltage. Lack of square-law response now increases δ. It is shown in Appendix I that the low-frequency ac/dc difference of a thermal converter (TC), caused by lack of square-law response, is

$$\delta_m = b'I^2m^2/4 \tag{4}$$

where I is the rms value of the input current and m is the ratio of peak to average value of the output electromotive force (EMF) (before external filtering is applied). Constant b' is a measure of the TC's deviation from a square-law response, may be of either sign, and can be determined from dc measurements (see (A.3) and (A.12)).

Resistor $R1$ (Fig. 3), matched to the resistance of heater H_1, reduces δ_m in two ways: 1) It minimizes the dependence of input power on small cyclic resistance changes [10] which decreases b', and 2) it reduces δ_m by decreasing I to a full-scale value of 2.5 mA (rated current for the MJTC is 5 mA). The value of b' should be specified so that $\delta_m \leq 0.1$ percent for $m = 1$. For the MJTC used in this instrument, m is approximately 0.6 and 0.1 at 0.1 and 1 Hz, respectively. Therefore, $\delta_m \leq 0.04$ percent at 0.1 Hz and causes and equivalent error in rms/dc conversion, which is within the allocated error budget. At 1 Hz, $\delta_m \leq 10$ ppm and decreases to zero below 10 Hz. The ac/dc difference from other causes (such as Thompson and Peltier effects) is less than 1 ppm up to 10 kHz [10], [11], and is expected to be constant over the voltmeter's frequency range.

The rms/dc converter has essentially the same ac/dc difference as the MJTC if its output ripple is negligible (maximum filtering used). Consequently, the ac/dc difference of the rms voltmeter (input applied to the TC DIRECT terminals) changes less than 10 ppm from 1 to 10 Hz and is negligible above 10 Hz. This voltmeter characteristic is very useful in calibrating the ac calibrator.

In the following discussions, each section of the differential MJTC is treated as a device with a single time constant, represented by the 0–63 percent step response. The MJTC used in this instrument has time constants of approximately 1 s for each section, represented by the symbol τ_1. Therefore, the transfer characteristics for the MJTC may be written

$$e_1(t) = Be_a^2(t)/(1 + \tau_1 p) \tag{5}$$

and

$$e_2(t) = Be_0^2(t)/(1 + \tau_1 p) \tag{6}$$

where $p \equiv d/dt$ and B is a dimensional constant defined earlier (see statement following (3)).

d) Accuracy and response time: Since it is most difficult to meet the accuracy and response time objectives at the lowest frequencies, the converter design requirements will be examined at 0.1 Hz. The transfer characteristics for the circuit of Fig. 2 are derived in Appendix II-A for the critically damped and overdamped cases. These cases correspond to circuit conditions of $\omega_0^2 = b^2$ and $\omega_0^2 < b^2$, where $b \equiv 1/\tau_1$, $\omega_0^2 \equiv Bk^2/\tau_1 RC$, R is the MJTC output resistance, and C is the integrating capacitance.

The response of the critically damped circuit to an input $e_a(t) = \sqrt{2}\,V_i \sin \omega t$ is given in (A.21). The transient and steady-state parts of that equation are

$$e_0(t)_t \simeq \tfrac{1}{2}bte^{-bt}V_i \tag{7}$$

and

$$e_0(t)_{ss} \simeq \left(1 - \frac{X^2}{16} - \frac{X}{2}\cos 2\omega t\right)V_i \tag{8}$$

where

$$X \equiv b^2/(b^2 + 4\omega^2) \quad \text{and} \quad \omega \equiv 2\pi f.$$

The second term of (8) represents the rms/dc conversion error caused by ripple and is 0.12 percent at 0.1 Hz. The response time is obtained by equating (7) to $0.0005V_i$ and is 18.2 s.[7]

The error budget of 0.05 percent for conversion error from ripple can be met by decreasing ω_0^2 (increasing C or decreasing k), resulting in an overdamped circuit. The response of the overdamped circuit to $e_a(t) = \sqrt{2}\,V_i \sin t$ is given in

[7] Unless stated otherwise, "response time" refers to the time required for the output voltage to reach its final value ±0.05 percent of the voltage change.

(A.23) (applicable for $\omega_0 < 0.95b$). The transient and steady-state parts of that equation are

$$e_0(t)_t \simeq \frac{\omega_0^2 \exp\{-[b - \sqrt{b^2 - \omega_0^2}]t\}}{4\sqrt{b^2 - \omega_0^2}[b - \sqrt{b^2 - \omega_0^2}]} V_i \qquad (9)$$

and

$$e_0(t)_{ss} \simeq \left(1 - \frac{Y^2}{16} - \frac{Y}{2}\cos 2\omega t\right) V_i \qquad (10)$$

where $Y \equiv \omega_0^2/[2\omega\sqrt{4b^2 - 2\omega_0^2 + 4\omega^2}]$. The second term of (10) represents conversion error from ripple.[8] Equating this term to $0.0005V_i$ yields $\omega_0^2 = 0.67b^2$ at 0.1 Hz, the value of ω_0^2 which will reduce the conversion error to 0.05 percent. Substituting this value for ω_0^2 into (9) and equating it to $0.0005V_i$ give 34 s for the response time. Since this increase in response time was considered unacceptable, a circuit was designed to compensate for ripple error, thus making it feasible to use the critically damped converter. This ripple error compensating circuit is part of the signal conditioner circuit described later.

3) Low-Pass Filter: The filtering following the converter must reduce the peak ripple to 0.05 percent and should have less than 0.05 percent transient overshoot for input voltage steps to the rms/dc converter. In the worst case of $f = 0.1$ Hz, the ripple from the converter must be reduced by a factor of 136. These are minimum requirements (see error budget) and can be met by 1) LP filtering, 2) integration over an integral number of periods of ripple or 3) by a combination of LP filtering and fixed period integration. Method 2) was considered to be somewhat beyond the scope of this project.[9] Comparison of the other two methods (Appendix II-B) was limited to filters whose poles are all real and equal. The comparison shows that method 1) has the shorter response time if the filter has 5 or more poles. However, method 3) is more appropriate for ac/ac transfer measurements, since the fluctuations in the voltage indication are zero for frequencies of 0.05, 0.1, 0.15, ⋯, Hz (includes calibrator frequencies) and are less for most other frequencies. For this reason, method 3) was used to perform the filtering and consists of a 2 pole LP filter and an integrating dc DVM. The filter is part of the signal conditioner circuit, described next.

4) Signal Conditioner: The signal conditioner (lower half of Fig. 3) consists of a 2-pole LP filter, a ripple error compensating circuit, and a voltage follower (AR3) with a gain of 2. The output of the rms/dc converter $e_0(t)$, consisting of dc and ripple components E_{dc} and e_r, is applied to the signal conditioner for attenuation of e_r and correction and amplification of E_{dc}.

The attenuation factor of the LP filter (sections $R7$–$C2$ and $R8$–$C3$) is[10]

$$\frac{4\omega^2 + \alpha^2}{\alpha^2} \qquad (11)$$

where $\alpha \equiv 1/(R7)(C2) = 1/(R8)(C3)$. As indicated in Appendix II-B2, a maximum ripple attenuation factor of 11.7 is required in the LP filter at $f = 0.125$ Hz (ripple frequency = $2f$). This corresponds to $\alpha = 0.48$. Larger α (smaller time constants) are used for $f > 0.5$ Hz.

The ripple error compensating circuit consists of $Q1$, $R5$, $R6$, and $CR2$. This circuit compensates for rms/dc conversion error (from excessive ripple e_r) by injecting a positive charge on $C2$ during the positive half cycles of e_r. The amplitude of e_r is proportional to E_{dc}. Therefore, because of the nonlinear $V - I$ characteristic of diodes, $CR2$ presents an increasing impedance to ripple as E_{dc} decreases. This effect is compensated by $Q1$ which is biased so that its drain-source resistance decreases as E_{dc} decreases. The compensating circuit reduces conversion error at the lowest frequencies to well below the 0.05-percent objective.

In addition to functioning as an active filter, AR3 serves to amplify E_{dc} to the 4–10 V level required for the dc DVM. The overall temperature coefficient of the rms DVM is compensated to within ± 0.015 percent/°C by using a Sensistor in the feedback circuit of AR3.

5) DC Digital Voltmeter: The dc digital voltmeter consists of a voltage-to-frequency (V/F) converter and a frequency counter with digital display. The V/F converter has an input voltage range of 0 to 10 V (only the 4–10 V range is used) and a transfer characteristic of 1000 Hz/V. Since the number displayed by the frequency counter must be proportional to the input voltage, the pulse rate output of the V/F converter is effectively scaled inversely to the gain (scaling) of the input amplifier and the integration period (either 1 or 10 s). This is accomplished by pulse rate scaling of 1, 2, and 5 (using a counter) and decimal point selection. The ripple attenuation factor (versus frequency) of the integrating dc DVM, and its effective response time are given in Appendix II-B2.

III. Calibrator Design

The error budget for the rms DVM allocated 0.03 percent for calibration errors. Since up to 0.01 percent calibration uncertainty results from lack of resolution in the displayed voltage, 0.02 percent was the accuracy objective for the ac calibrator.

The voltage calibrator consists of a compact 7-digit Kelvin–Varley (K–V) divider fed by a reference voltage of 1 V (either ac or dc) and buffered at its output by a voltage follower with selectable gains of 1 and 10. The frequency response of the K–V divider (set to all fives) and buffer amplifier is flat to within 0.005 percent through 50 Hz. The measured nonlinearity of the K–V divider is 0.005 percent for a dial setting of 0020000 (2-mV output), decreasing to 0.002 percent or less at 1000000 and above. The 1-V dc reference is derived from a precision 10-V reference supply.

The ac (sinewave) reference is shown in Fig. 4. The sinewave is generated by a 7-bit counter–ROM–DAC combination so that 128 input pulses are required per sinewave cycle. The necessary input frequencies are obtained using a clock frequency of 6400 Hz and scaling it 5, 25, 50, 100, 250, and 500 times using a series of counters. The amplifier is designed to have an output of 1-V rms and sufficient filtering to reduce the contribution of all harmonics generated by the

[8] The second term of (8) and (10) corresponds to the second term of (1).

[9] A long-range program is underway at NBS to develop an all-digital system for measuring and analyzing VLF waveforms in time periods approaching the theoretical minimum.

[10] Attenuation factor is defined here as the reciprocal of the transfer characteristic.

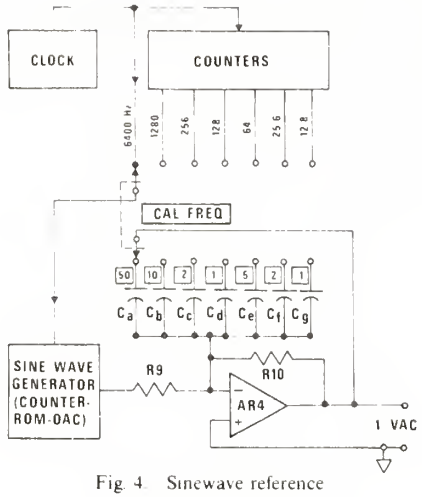

Fig. 4. Sinewave reference

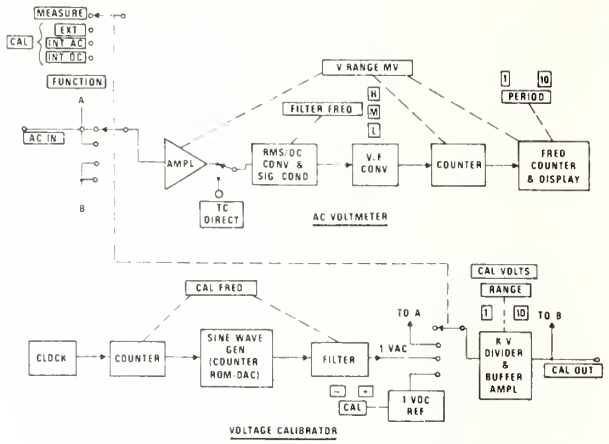

Fig. 5. Simplified block diagram of ac voltmeter/calibrator.

digital-to-analog converter (DAC) to less than 20 ppm. Capacitances C_a, C_b, $\cdots$ are chosen so that capacitance $\times$ frequency = a constant (to within 0.2 percent). Therefore, attenuation of the fundamental and harmonic components remains constant for all calibrator frequencies. Also, the phase shifts of the harmonics are essentially the same for all calibration frequencies. The circuit was designed to have a small output amplitude sensitivity to a change in capacitance or frequency and is approximately 27 ppm per percent change.

The flatness (constancy) of the ac calibrator voltage with frequency was determined by using the ac voltmeter (input connected to the TC DIRECT terminals) to measure 1, 2, 10, and 50-Hz calibration voltages at the 5-V level. The voltage indications for 1, 2, and 10 Hz fell within a 20 ppm range; however, each reading had an uncertainty of 20 ppm because of lack of resolution. As described earlier, the change in the ac/dc difference of the voltmeter over this range is < 10 ppm. Therefore, the worst case difference between the 1, 2, and 10-Hz calibration voltages is 70 ppm. The voltage indication for 50 Hz was 40 ppm less than for 10 Hz, probably because of the finite risetimes and small glitches between steps in the DAC output. Since the range of measured amplitudes for 1, 2, and 10 Hz was less than 70 ppm, these factors evidently have little effect on the calibrator output in this frequency range. More important, there is no reason to believe that these factors or any others have a more adverse effect from 0.1 to 1 Hz than in the 1–10 Hz range. Hence, it is unlikely that the calibration voltages from 0.1 to 10 Hz fall outside a 70 ppm range. Since the ac/dc difference of the ac voltmeter is too large to accurately compare the calibrator voltages from 0.1 to 1 Hz, a special "viewing circuit" developed for another project [12] was used to compare the peak-to-peak values of the calibrator voltages from 0.1 to 10 Hz. The measured values fell within a 38-ppm range, adding confidence to the 70-ppm range assigned above. Basing differences between the rms values of voltages on the differences between the peak-to-peak values appears to be valid since all necessary precautions were taken to insure that the wave shape is the same for all frequencies. The calibration voltage at 50 Hz is easily trimmed (by decreasing C_a of Fig. 4 slightly) to be the same as at 10 Hz. Thus since the ac calibrator voltage is essentially independent of frequency, it is sufficient to calibrate it at only one frequency.

Fig. 6. AC voltmeter/calibrator.

The ac calibrator is temperature compensated to within ± 0.005 percent/°C, using a Sensistor in series with $R9$ of the amplifier. For dc voltages, the calibrator temperature coefficient is within ± 0.0025 percent/°C (average of both polarities). Calibration and overall accuracy of the calibrator will be discussed in a later section.

IV. Voltmeter/Calibrator Description

A. Operation

Fig. 5 is a functional block diagram of the ac voltmeter/calibrator and Fig. 6 is a photograph of the instrument showing the front panel controls and connectors.

When the FUNCTION switch is in the MEASURE mode, the instrument functions as a voltmeter and measures voltages applied to the AC IN terminals. The same is true in the CAL-EXT position, except that now the input voltage is also applied to the K-V divider; therefore, this voltage can be multiplied by any factor up to 10 and outputed at the CAL OUT terminals. This mode of operation permits wave shapes and frequencies other than those provided in the internal calibrator to be used as a reference. With the FUNCTION switch set to either the CAL-INT AC or CAL-INT DC positions, calibration voltages determined by the K-V divider and associated RANGE switch appear at

the CAL OUT terminals and are applied to the input of the voltmeter. The calibration voltages are limited to ±10-V dc or 7-V ac. Selection of the calibration frequency is by the CAL FREQ switch. The dc calibrator is intended to be used primarily as a means of calibrating the ac calibrator and is very accurate at 1 V and larger. Offsets in the direct-coupled amplifiers of the voltmeter and calibrator limit the smallest dc voltage at which they can be used with good accuracy to 0.1 V.

Measurement accuracy is determined by the accuracy of the voltmeter when it is used to measure voltages directly. However, measurement accuracy approaches the accuracy of the ac calibrator when the voltmeter is used as a transfer device (i.e., the voltmeter is used to compare the input voltage with the calibrator voltage at the nearest frequency—two measurements). For example, if the indicated value E_i' of the input voltage is dialed into the calibrator, yielding an indicated value E_c', the correct value of the input voltage is $2E_i' - E_c'$.

The FILTER FREQ (H, M, L) switch selects appropriate filtering for different frequency ranges and the PERIOD (1, 10) switch selects the integrating period. It is shown in Appendix II-B2 that maximum filtering results in a response time of about 37 s. With minimum filtering (including a 1-s integration period), the response time is approximately 19 s. This response was thought to be acceptable for general use; however as shown in Appendix II-C, it can be shortened by modifying the converter circuit.

B. Calibration

Use of low-drift film resistors and other components eliminates the need for frequent calibrations of the instrument. However, the self-contained calibrator makes it a simple matter to recalibrate the instrument any time the accuracy is in question.

The dc calibrator serves as the basic voltage reference for the instrument. It is calibrated against laboratory standards at the 1- and 5-V levels of the 1- and 10-V ranges, respectively.[11] The average of both polarities is used. Since the ac/dc difference of the MJTC (and the rms/dc converter) is very small at 1 Hz and above (< 10 ppm), the ac voltmeter (input connected to the TC DIRECT terminals) can be used as a transfer voltmeter to compare ac and dc calibrator voltages. Calibration of the ac calibrator is performed at 10 Hz, and consists of adjusting the ac reference so that the ac and dc voltages are equal at the 5-V level. The ac calibrator is then used for adjusting the gain and offset of the signal conditioner and the gain ranges of the input amplifier.

C. Overload Protection

The input amplifier is given instantaneous protection against peak voltages in excess of ±16 V by diode-coupled current sinks of 5-A capacity. Sustained overdrive blows a fuse, disconnecting the amplifier. Applying calibrator voltages to the thermal converter (via the TC DIRECT terminals) cannot damage it. However, the voltmeter can be used for high frequency measurements if driven at the TC DIRECT input by an external wide band amplifier. For this reason, the current sinks were also diode-coupled to point j of Fig. 3. Sustained overdrive may damage or open resistor $R1$ but will not damage the MJTC.

D. Performance Specifications

A brief list of the ac voltmeter/calibrator performance specifications follows.

Input signal range: 2 mV to 10 V in 12 ranges (1–2–5 sequence)

Frequency range: 0.1–50 Hz

Accuracy, percent of reading (23 ± 1°C): 0.1 percent for 0.5–50 Hz, 5 mV–10 V; 0.2 percent for 0.1–50 Hz, 2 mV–10 V

Response time (see footnote 7): Approximately 40 s for 0.1–0.5 Hz range, decreasing to 20 s for 2 Hz and above (see Appendix II-C)

Temperature coefficient of voltmeter: ±0.015 percent/°C

Calibration voltages: 0 to 7-V ac and 0 to ±10-V dc, with 7 place resolution

Calibration frequencies: 50, 10, 2, 1, 0.5, 0.2, 0.1 Hz

Calibration accuracy (23 ± 1°C): For dc voltages in range of 1–10 V, ±0.005 percent (average of both polarities). For ac voltages, ±(0.02 percent + 0.4 μV)

Temperature coefficient of calibrator: For dc voltages, ±0.0025/°C (average of both polarities). For ac voltages, ±0.005 percent/°C

Transfer accuracy: Voltmeter accuracy is improved by a factor of 4.

V. Conclusions

An rms DVM has been developed for measuring VLF's which represents an improvement of 4 to 5 times over existing equipment with respect to response time and worst case accuracy. Extensive circuit analysis (Appendix II) facilitated the choice and design of the circuits employed.

A self-contained calibrator, providing both ac and dc calibration voltages, is used for 1) calibration of the companion DVM, 2) calibration of other very low frequency voltmeters, and 3) very-high accuracy measurements, using the DVM as a transfer instrument. After initial calibration against a laboratory standard, the dc calibrator serves as the basic voltage standard for the instrument. The calibration of the ac calibrator is based on three methods: a) the transfer of the dc calibrator accuracy to the ac calibrator, using the DVM as an ac/dc transfer instrument, b) theoretical considerations, and c) peak-to-peak amplitude measurements. Theory is developed in Appendix I which relates the ac/dc difference of a TC to its lack of square-law response and the measured output ripple. Using this theory, it is shown that the ac/dc difference of the DVM is less than 10 ppm above 1 Hz but increases rapidly as the frequency is decreased. Therefore, method a) is used from 1 Hz to 50 Hz and b) below 1 Hz. Method c) is applicable to the entire frequency range and is used as an independent check on the other two methods.

The ac calibrator accuracy is 0.02 percent of dialed voltage + 0.4 μV; DVM accuracy (percent of reading) is 0.1 percent above 0.5 Hz and 5 mV and 0.2 percent below these

[11] Trim adjustments facilitate calibration of all circuits.

values. However, when the input voltage is measured by comparison with a calibrator voltage of approximately the same frequency (ac/ac transfer measurement), measurement accuracy improves by a factor of about 4.

By upgrading or changing a few components, it appears feasible to increase the ac calibrator accuracy to 50 ppm and the accuracy of ac/ac transfer measurements to 0.01 percent or better.

The DVM has a very-high input impedance (input impedance of FET voltage follower) for all ranges except the 10-V range (for which it is 200 kΩ). Therefore, it is a simple matter to extend the DVM voltage range using an external, single ratio, resistive voltage divider. Using a 1000/1 divider extends the range to 5 kV and changes the displayed voltage from millivolts to volts. Transfer measurements (ac/ac) are made the same way as before; however, their accuracies are derated by the uncertainty of the divider ratio.

Appendix I
Thermal Converter Characteristics

The transfer characteristic of a TC can be represented by a power series in I^2

$$E = \sum a_n I^n, \qquad n = 2, 4, 6, \cdots \tag{A.1}$$

on dc and ac for frequencies sufficiently high that temperature rise θ does not vary during a cycle. If the frequency is so low that $e(t)$ follows $[i(t)]^2$ without significant delay or attenuation, then

$$e = \sum a_n i^n. \tag{A.2}$$

The temperature coefficients of electrical resistivity and thermal conductivity, and the variation of the EMF versus θ characteristic cause a_4 to be significant. The a_6 and higher terms are usually smaller. Thus at VLF's,

$$e \simeq ai^2 + ab'i^4 = ai^2(1 + b'i^2). \tag{A.3}$$

For multijunction TC's, $b'i^2 \ll 1$. If $i = \sqrt{2}\, I \sin \omega t$, (A.3) becomes

$$e = a(I^2 - I^2 \cos 2\omega t) + \frac{ab'I^4}{2}(3 - 4 \cos 2\omega t + \cos 4\omega t) \tag{A.4}$$

The average value of e over one cycle of i (i.e., a period $T = 2\pi/\omega$) is

$$E_a = \frac{1}{T}\int_0^T \left(aI^2 + \frac{3ab'I^4}{2} + \text{cosine terms}\right)dt$$

$$= aI^2 + \frac{3ab'I^4}{2}. \tag{A.5}$$

With dc applied, $E_d = aI^2 + ab'I^4$. Therefore, for the same I,

$$\frac{E_a - E_d}{E_d} = \frac{ab'I^4/2}{aI^2 + ab'I^4} \simeq \frac{b'I^2}{2}. \tag{A.6}$$

The conventional ac–dc difference δ is defined by

$$\delta = \left.\frac{I_a - I_d}{I_d}\right]_{E_a = E_d} \text{ which equals } \left. -\frac{1}{2}\frac{E_a - E_d}{E_d}\right]_{I_a = I_d} \tag{A.7}$$

from which[12]

$$\delta_l = -\frac{b'}{4} I^2 \tag{A.8}$$

where δ_l denotes the limiting low frequency ac/dc difference caused by lack of square-law response.

The constant b' can be evaluated from dc measurements. Let a dc of rated value (I_r) be applied to the TC. Its measured output EMF E_{dr} can be equated to

$$aI_r^2(1 + b'I_r^2) = E_{dr}. \tag{A.9}$$

Let the applied current be reduced to $I_r^2/\sqrt{2}$. If the TE has a perfect square-law characteristic, the output voltage is now $E_{dr}/2$. This is numerically equal to

$$\frac{aI_r^2}{2}(1 + b'I_r^2) \equiv E_s. \tag{A.10}$$

The actual measured voltage, however, should be equated to

$$\frac{aI_r^2}{2}\left(1 + \frac{b'I_r^2}{2}\right) \equiv E_d. \tag{A.11}$$

Therefore,[13]

$$b' \simeq \frac{2(E_s - E_d)}{E_d I_r^2}. \tag{A.12}$$

When a low-frequency sinewave is applied to a TC, the ratio m of peak ripple to average output EMF ranges (approximately) from 1 at very low frequencies to zero at high frequencies. Lack of square-law response has no effect on the ac/dc difference δ when $m = 0$ and a maximum effect when $m = 1$. (Equation (A.8) represents the case of $m = 1$.) The effect on δ for the case $0 < m < 1$ is considered next.

Equation (A.3) may be written as

$$e = ai^2 + ab'i^4 \equiv e_1 + \frac{b'}{a} e_1^2 \tag{A.13}$$

where $e_1 \equiv ai^2$. If $i = \sqrt{2}\, I \sin \omega t$ and τ is the TE time constant, it can be shown that

$$e_1 = aI^2(1 - m \cos 2\omega t) \tag{A.14}$$

where $m \equiv 1/\sqrt{1 + 4\omega^2\tau^2}$. Substituting (A.14) into (A.13) and following the same procedure as in (A.5) to (A.8) yields

$$\delta_m \simeq -\frac{b'm^2}{4} I^2 \tag{A.15}$$

where δ_m designates the low-frequency ac/dc difference (as a function of m) caused by lack of square-law response.

Appendix II

A. Transfer Characteristics of RMS/DC Converter

From Fig. 2

$$Cpe_f(t) = \frac{e_1(t) - e_2(t)}{R} \tag{A.16}$$

[12,13] These derivations were suggested by F. L. Hermach, NBS, in a private communication.

and

$$e_0(t) = k\sqrt{e_f(t)}. \tag{A.17}$$

Substituting (A.17) into (6) and then (5) and (6) into (A.16) gives

$$\tau_2 p e_f(t) = \frac{Be_a^2(t)}{1+\tau_1 p} - \frac{Bk^2 e_f(t)}{1+\tau_1 p}, \tag{A.18}$$

where $p \equiv d/dt$, B, and k are dimensional constants, τ_1 is the time constant for each thermal converter section, R is the output resistance of the thermoelement, and $\tau_2 \equiv RC$. Rearranging (A.18)

$$\left(p^2 + \frac{1}{\tau_1} p + \frac{Bk^2}{\tau_1 \tau_2}\right) e_f(t) = \frac{B}{\tau_1 \tau_2} e_a^2(t). \tag{A.19}$$

Let $2b \equiv 1/\tau_1$ and assume the system is critically damped, i.e., $1/4\tau_1^2 = Bk^2/\tau_1\tau_2$. Then, if an input voltage $e_a(t) = \sqrt{2}\, V_i \sin \omega t$ is applied at $t = 0$ and the initial conditions are zero,[14] the solution to (A.19) is

$$e_f(t) = \frac{V_i^2}{k}\left[1 - (1+bt)e^{-bt} + \frac{b^3 t e^{-bt}}{(b^2+4\omega^2)} - \frac{b^2(4\omega^2 - b^2)e^{-bt}}{(b^2+4\omega^2)^2} - \frac{b^2}{b^2+4\omega^2}\cos(2\omega t + \phi)\right] \tag{A.20}$$

where $\omega = 2\pi f$ and $\phi = \tan^{-1} 4b\omega/(b^2 - 4\omega^2)$. All of the transient terms except $bt \exp(-bt)$ can be omitted without causing significant error in the calculated response time (see footnote 7 for definition). Also, the phase angle is not needed. Applying these simplifications to (A.20), substituting in (A.17) and using a binomial series approximation yields[15]

$$e_0(t) \simeq V_i\left[1 - \frac{b^4}{16(b^2+4\omega^2)^2} - \tfrac{1}{2}bte^{-bt} - \frac{1}{2}\frac{b^2}{b^2+4\omega^2}\cos 2\omega t\right]. \tag{A.21}$$

The second term is the rms/dc conversion error caused by ripple.

If $Bk^2/\tau_1\tau_2 < 1/4\tau_1^2$, the circuit of Fig. 2 is overdamped and the solution to (A.19) contains transient terms in both $\exp(-b + \sqrt{b^2 - \omega_0^2})t$ and $\exp(-b - \sqrt{b^2 - \omega_0^2})t$, where $\omega_0^2 \equiv Bk^2/\tau_1\tau_2$. If ω_0 is less than about $0.95b$, the $\exp(-b - \sqrt{b^2 - \omega_0^2})t$ terms have little effect on the response time and can be omitted. Retaining only the largest transient term as before, the solution to (A.19) for an input $e_a(t) = \sqrt{2}\, V_i \sin \omega t$ is

$$e_f(t) \simeq \frac{V_i}{k}\left[1 - \frac{\omega_0^2 \exp[-(b - \sqrt{b^2-\omega_0^2})t]}{2\sqrt{b^2-\omega_0^2}(b - \sqrt{b^2-\omega_0^2})} - \frac{\omega_0^2 \cos 2\omega t}{2\omega\sqrt{4b^2 - 2\omega_0^2 + 4\omega^2}}\right] \tag{A.22}$$

Substituting (A.22) into (A.17) and approximating as before,[16]

$$e_0(t) \simeq V_i\left[1 - \frac{\omega_0^4}{64\omega^2(4b^2 - 2\omega_0^2 + 4\omega^2)} - \frac{\omega_0^2 \exp[-(b^2 - \sqrt{b^2-\omega_0^2})t]}{4\sqrt{b^2-\omega_0^2}(b - \sqrt{b^2-\omega_0^2})} - \frac{\omega_0^2 \cos 2\omega t}{4\omega\sqrt{4b^2 - 2\omega_0^2 + 4\omega^2}}\right]. \tag{A.23}$$

B. Ripple Filtering and Response Time

1) LP Filtering: As mentioned in the text, filtering must reduce the ripple in $e_0(t)$ by a factor of 136 at $f = 0.1$ Hz. The tradeoffs between number of poles and response time will be examined for LP filters whose poles are all real and equal.

If a unit voltage step is applied to an n-pole filter whose transfer function is $\alpha^n/(s+\alpha)^n$, the transient term which largely determines the response time for $\alpha t > 10$ is[17]

$$\frac{(\alpha t)^{n-1}}{(n-1)!} e^{-\alpha t}. \tag{A.24}$$

The response time is obtained by equating this expression to 0.0005. The attenuation factor for this filter[18] is

$$\frac{[(4\omega^2 + \alpha^2)^{1/2}]^n}{\alpha^n}. \tag{A.25}$$

Using (A.24) and (A.25), and adjusting α to hold the attenuation factor constant at 136, the calculated response times are 35, 30, 27, 26, and 25 s for n equal to 4, 5, 6, 7, and 8, respectively. Corresponding values for α are 0.385, 0.51, 0.62, 0.72, and 0.81.

The overall response time of the rms/dc converter plus filter will be computed for the 4 and 5 pole filters. Using the transient term in (A.21) as the forcing function, the response of the 4 pole filter is

$$\mathcal{L}^{-1}\left\{\frac{1}{2}\frac{b}{(s+b)^2}\cdot\frac{\alpha^4}{(s+\alpha)^4}\right\} \simeq \frac{b\alpha^4}{12}\frac{[(b-\alpha)^3t^3 - 6(b-\alpha)^2t^2 + 18(b-\alpha)t - 24]e^{-\alpha t}}{(b-\alpha)^5} \tag{A.26}$$

where $b = 0.5$ and $\alpha = 0.385$. For the 5-pole filter, the response is

$$\mathcal{L}^{-1}\left\{\frac{b\alpha^5}{2(s+b)^2(s+\alpha)^5}\right\} \simeq \mathcal{L}^{-1}\left\{\frac{\alpha^6}{2(s+\alpha)^7}\right\} \simeq \frac{(\alpha t)^6}{2(6)!}e^{-\alpha t} \tag{A.27}$$

[14] For response time determinations, initial conditions can be considered zero if the input has been zero for at least 20 s.

[15] This approximation is acceptable for the ranges of t and ω applicable to response time and rms/dc conversion error (or ripple) calculations, respectively.

[16] This approximation is acceptable for the ranges of t and ω applicable to response time and rms/dc conversion error (or ripple) calculations, respectively.

[17] Symbol s is the Laplace transform variable.

[18] Reciprocal of its transfer function. See footnote 10.

where $\alpha = 0.51$. The computed response times using the 4 and 5 pole filters are 38 and 34 s, respectively.

2) LP Filtering Plus Integration: A second approach to the filtering requirement is to perform part of the filtering by integration in the dc voltmeter. If the integration period is T_i, perfect filtering of the ripple frequency ($2f$) occurs for input frequencies of $f = n/2T_i$, where $n = 1, 2, 3, 4, \cdots$. Minimum filtering occurs for $f = (n + \frac{1}{2})/2T_i$ and, depending upon the phase of the ripple relative to the start of the integration period, approaches a minimum attenuation factor of $2\pi f T_i$. If $T_i = 10$ s, its minimum value is 7.85 at $f = 0.125$ Hz. (It is convenient to use integration periods of 1 and 10 s in the dc DVM.) Using (A.21), the peak ripple from the converter at 0.125 Hz is $V_i/21.74$. Therefore, the attenuation factor required for the LP filter is $2000/(7.85)(21.74) = 11.7$. According to (A.25), a 2 pole filter with $\alpha = 0.48$ meets this requirement. A good approximation to the overall response time t_f of the converter plus this filter results if we average their time constants ($b = 0.50$, $\alpha = 0.48$) and equate (A.24) to 0.0005.

$$\frac{1}{2}\frac{(0.49t_f)^3}{6}e^{-0.49t_f} = 0.0005 \tag{A.28}$$

from which $t_f = 26$ s. The factor of $\frac{1}{2}$ is introduced by the SR circuit. (See (A.21).)

The integrator can start integrating at some time t_1 prior to t_f without exceeding a residual transient value of 0.05 percent. Integrating the most significant transient in the filter output over a 10-s period (starting at $t = t_1$), taking its average and equating to 0.0005:

$$T(t_1) \equiv \frac{1}{10}\int_{t_1}^{t_1+10}\frac{(\alpha t)^3}{12}e^{-\alpha t}\,dt = 0.0005$$

$$T(t_1) = \frac{1}{10}\cdot\frac{\alpha^3}{12}\left\{-\frac{e^{-\alpha t}}{\alpha^4}\left[(\alpha t)^3 + 3(\alpha t)^2 + 6(\alpha t) + 6\right]_{t_1}^{t_1+10}\right\}. \tag{A.29}$$

Only the highest degree term for the lower integration limit needs to be retained, yielding

$$T(t_1) \simeq \frac{1}{10\alpha}\left[\frac{(\alpha t_1)^3}{12}e^{-\alpha t_1}\right] = 0.0005. \tag{A.30}$$

Setting α equal to 0.49 and solving for t_1 gives 21.6 s. There is no simple method of synchronizing the integrator with t_1. If integration starts at t_1, the ac voltmeter response time is $22 + T_i = 32$ s. If it starts before t_1, two integration periods are required and the response time approaches 42 seconds. Therefore, the average response time is 37 s.

C. Improved Converter Response Time

For the upper decade or so of input frequencies, response time is limited by the time constant τ_1 of the MJTC. This can effectively be shortened by placing a resistance r in series with capacitance C (Fig. 2). Equation (A.16) now becomes

$$\frac{Cp}{1 + rCp}e_f(t) = \frac{e_1(t) - e_2(t)}{R}. \tag{A.31}$$

Substituting (A.17) into (6) and then (5) and (6) into (A.31) gives

$$CRpe_f(t) = (1 + rCp)\frac{Be_a^2(t)}{(1 + \tau_1 p)} - \frac{Bk^2 e_f(t)}{(1 + \tau_1 p)}. \tag{A.32}$$

Rearranging (A.32) and letting $\tau_2 \equiv RC$ and $\tau_3 \equiv rC$,

$$\left[p^2 + \frac{1}{\tau_1}\left(1 + \frac{Bk^2\tau_3}{\tau_2}\right)p + \frac{Bk^2}{\tau_1\tau_2}\right]e_f(t) = \frac{B}{\tau_1\tau_2}(1 + \tau_3 p)e_a^2(t). \tag{A.33}$$

Let $2b \equiv (1/\tau_1)(1 + [Bk^2\tau_3/\tau_2])$, $\omega_0^2 \equiv Bk^2/\tau_1\tau_2$ and assume that $b^2 = \omega_0^2$. Also, let $e_a(t)$ in (A.33) be a unit step. Then, solving for $e_f(t)$ and substituting into (A.17) yields[19]

$$e_0(t) \simeq 1 - \tfrac{1}{2}(1 + bt - b^2\tau_3 t)e^{-bt}. \tag{A.34}$$

If $\tau_3 = 0$ (i.e., $r = 0$), equation (A.33) reduces to (A.19). Let $e_a(t)$ be a unit step and solve (A.19) for $e_f(t)$. Substituting this result into (A.17) gives[20]

$$e_0(t) \simeq 1 - \tfrac{1}{2}(1 + bt)e^{-bt}. \tag{A.35}$$

The circuits represented by (A.34) and (A.35) have response times largely determined by the factor $\exp(-bt)$. However, the b in (A.34) is $(1 + Bk^2\tau_3/\tau_2)$ times larger than the b in (A.35). Therefore, adding a resistance r in series with capacitance C (Fig. 3) shortens the response time by nearly a factor of $(1 + Bk^2\tau_3/\tau_2)$.

Let $e_a(t) = \sqrt{2}\,V_i \sin \omega t$ in (A.33). Solving for the steady-state value of $e_f(t)$ and substituting into (A.17) results in[21]

$$e_1(t)_{ss} \simeq \left(1 - \frac{Z^2}{16} - \frac{Z}{2}\cos 2\omega t\right)V_i \tag{A.36}$$

where $Z \equiv b^2\sqrt{1 + 4\omega^2\tau_3^2}/(4\omega^2 + b^2)$. This equation shows that adding r moves the -3-dB point of the ripple attenuation versus ripple frequency characteristic up by at least a factor of $(1 + Bk^2\tau_3/\tau_2)$, and changes the slope of the attenuation characteristic from -12 dB/octave to -6 dB/octave. (Compare (A.36) with (8).)

Acknowledgment

The author is grateful to B. A. Bell for helpful suggestions on the manuscript and to F. L. Hermach for helpful discussions on thermal converters.

References

[1] R. S. Koyanagi, "Development of a low-frequency-vibration calibration system," *Experimental Mechanics*, vol. 15, no. 11, p. 3, Nov. 1975.

[2] R. S. Koyanagi and J. D. Pollard, "Piezoelectric accelerometer low-frequency response by signal insertion methods," NBSIR 74-597, pp. 3–4, May 1975 (Final Report).

[3] F. L. Hermach, "ac–dc comparators for audio-frequency current and voltage measurements of high accuracy," *IEEE Trans. Instrum. Meas.*, vol. IM-25, pp. 489–494, Dec. 1976.

[4] *Nonlinear Circuits Handbook*. Norwood, MA: Analog Devices, Inc., 1974.

[5] F. J. Wilkins, T. A. Deacon, and R. S. Becker, "Multijunction thermal

[19,20,21] See footnote 15.

converter," *Proc. Inst. Elec. Eng.*, vol. 112, no. 10, Oct. 1965.
[6] L. G. Cox and N. L. Kuster, "An automatic rms/dc comparator," *IEEE Trans. Instrum. Meas.*, vol. IM-23, pp. 322–325, 1974.
[7] H. Handler, "A hybrid circuit rms converter," in *IEEE Int. Solid State Circuit Conf. Dig.*, vol. 14, p. 190, Feb. 1971.
[8] W. E. Ott, "A new technique of thermal rms measurement," *IEEE J. Solid State Circuits*, vol. SC-9, pp. 374–380, Dec. 1974.
[9] J. B. Folsom, "Measuring true rms ac voltages to 100 MHz," *Hewlett-Packard J.*, vol. 23, no. 7, p. 17, Mar. 1972.
[10] F. L. Hermach, "An investigation of multijunction thermal converters," *IEEE Trans. Instrum. Meas.*, vol. IM-25, pp. 524–528, Dec. 1976.
[11] F. J. Wilkins, "Theoretical analysis of the ac/dc transfer difference of the NPL multijunction thermal converter over the frequency range of dc to 100 kHz," *IEEE Trans. Instrum. Meas.*, vol. IM-21, pp. 334–340, Nov. 1972.
[12] H. K. Schoenwetter, "A high speed, low noise 18 bit digital-to-analog converter," to be published.

S ON INSTRUMENTATION AND MEASUREMENT, VOL. IM-27, NO. 4, DECEMBER 1978

A Fast Response Low-Frequency Voltmeter

BRUCE F. FIELD, MEMBER, IEEE

Abstract **A sampling voltmeter implemented with a microprocessor has been developed to perform as a true rms voltmeter and waveform analyzer. The instrument measures to 0.1 percent accuracy the true rms voltage of approximately sinusoidal inputs at voltages from 2 mV to 10 V and frequencies from 0.1 to 120 Hz. The major feature of the instrument is fast response time, with a total autoranging, settling, and measurement time of two signal periods for frequencies below 10 Hz.**

Manuscript received May 30, 1978; revised July 24, 1978. This work was supported in part by the Coordination Calibration Group of the Department of Defense under CCG Project 77-111.

The author is with the Electrical Measurement and Standards Division, National Bureau of Standards, Washington, DC 20234.

I. Introduction

COMMERCIAL voltmeters presently available are generally not capable of measuring with high accuracy the true rms value of voltages at frequencies below 10 Hz. A new instrument has been developed and tested which is capable of measuring the true rms voltage of approximately sinusoidal waveforms from 2 mV to 10 V with frequencies between 0.1 to 120 Hz. An earlier ac voltmeter/calibrator, employing a multijunction thermal converter device for rms-to-dc conversion had been developed at NBS [1]. However, this new instrument is designed to have a very short settling time as well as providing measurements of the rms value of the ac

component of the signal, the frequency, and the harmonic distortion of the signal, features which are not available on the previous instrument.

A research and development program at the National Bureau of Standards (NBS) has recently been concerned with developing and testing improved vibration accelerometers [2], [3]. The major motivation for improved accelerometers has been due to interest in accurately predicting the mean-time-between-failure and failure modes of equipment subjected to mechanical vibration. Previously, the largest source of uncertainty in calibrating these accelerometers has been in the low-frequency voltage measurements. Also, studies performed to evaluate new accelerometer designs have produced inconclusive results because of the voltage measurement uncertainties. The present instrument was developed to fulfill the following requirements of vibration accelerometer calibration systems:

1) frequency range—0.1 to 120 Hz fundamental + approximately the first 10 harmonics;
2) input voltage range—2 mV to 10 V;
3) accuracy—0.1 percent of reading (2σ);
4) minimal calibration in an easy-to-use portable instrument;
5) fast response time, i.e., the measurement should require no more than 2 periods at the lowest frequency;
6) some measure of the harmonic distortion of the waveform should be made.

It should also be noted that in many cases vibration accelerometers produce slowly drifting dc offsets which are added to the ac component. It is awkward to manually compensate for a changing offset thus it is necessary that the instrument provide for measuring the ac component of the signal.

II. Instrument Design

Traditional measurement methods for ac waveforms all rely on some square-law device (thermal converter, log amplifier, etc.) to provide a true rms indication. For this application, squaring modules based on log amplifiers do not provide sufficient accuracies at low frequencies. Thermal converters generally have large time constants due to the thermal mass of the heater and thermoelement. Although improvements in thermal converter time constants can be made, increased ac ripple on the dc output results requiring additional filtering or smoothing. Thus if optimized for low-frequency measurements, the response time of such an instrument becomes excessively large. In addition, these methods do not provide any means for measuring the distortion in the waveform.

The general approach used to implement this new voltmeter system is to use an analog-to-digital (A/D) converter for digitizing the input signal. The digital values are transferred to a microcomputer for calculation of the desired results. A simplified block diagram of the entire instrument is shown in Fig. 1.

The preamplifier is a differential-input instrumentation amplifier with an external gain setting resistor that can be changed by the microcomputer. Four decade gain settings are available to accommodate the wide range of possible input signals. A data acquisition system consisting of a sample-and-hold amplifier, a second instrumentation amplifier, and an A/D converter are physically contained in one hybrid module. This second amplifier is normally wired to provide only one of three input voltage ranges for the A/D converter, 2.5, 5, or 10 V. However, external relays have been added to allow the range to be set by the microcomputer, thus a total of twelve gain settings is possible using combinations of preamp gain and A/D range. All these gain settings are necessary to obtain adequate resolution for all specified inputs. The A/D converter is a 12-bit (11 bits plus sign bit) successive-approximation converter with a conversion time of 12 μs.

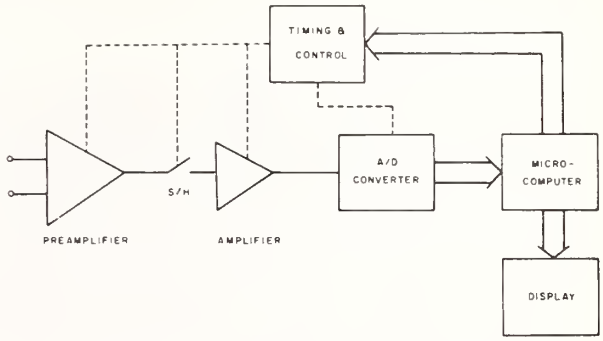

Fig. 1. A simplified block diagram of the sampling instrument.

The timing and control section has two functions. The first is a hardware clock that may be programmed by the microcomputer to output a pulse at regular intervals. This pulse is used to trigger the A/D converter to make a conversion, thus a series of A/D readings uniformly spaced in time are generated irrespective of the operation of the microcomputer which may be busy with other calculations. The second function of this section is to route control signals generated by the microcomputer to the gain-controlling relays for the preamplifier and the A/D converter.

The microcomputer used is a National Semiconductor IMP-16.[1] This is a 16-bit word length multichip microcomputer. It was chosen mainly for the powerful arithmetic instructions in its instruction set. All peripherals (display, A/D converter, etc.) are treated as memory locations and the instruction program (2048 16-bit words) is stored in ultraviolet erasable programmable READ-ONLY memories (EPROM's). A small amount of READ-WRITE memory is provided on the microcomputer board for temporary storage of input values and program variables.

III. Measurement Algorithms

A combination of algorithms is used to implement the voltmeter and harmonic analysis functions. The harmonic distortion is calculated by determining the discrete Fourier transform (DFT) coefficients using a fast Fourier transform

[1] The use of this product does not constitute an endorsement by NBS; other products may also be suitable for this application.

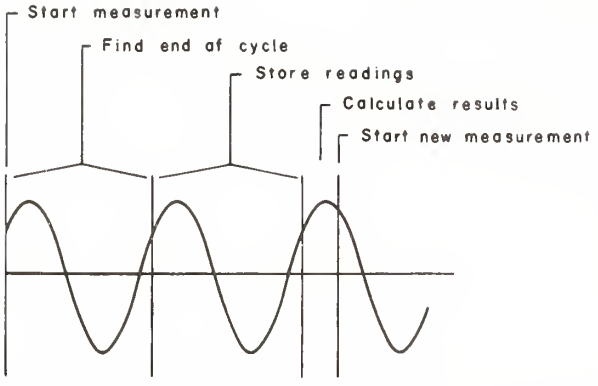

Fig. 2. Timing sequence of the measurement in relation to a typical sinusoidal input.

algorithm. Although the DFT coefficients can be used to calculate the rms value, serious errors result when the signal is frequency modulated. Thus the rms value is determined directly by numerically integrating the signal over one period, producing a result that is unaffected by frequency modulation. For both of these methods the period must first be accurately determined. Fig. 2 shows the measurement sequence and timing relationships of the software and a typical input signal.

When starting a measurement sequence on an unknown waveform, the frequency may be as low as 0.1 Hz or as high as 120 Hz. Sampling at a fast enough rate to capture a possible 120-Hz signal would produce an unreasonable number of samples if a 0.1-Hz signal were present. A preliminary decision based on the slope of the signal at the start of the measurement is used to determine the proper sampling rate. All input voltages are scaled to roughly the same amplitude by the preamplifier and the value of the slope (the decision point is approximately equivalent to 5 Hz) determines whether a fast (8-kHz) or slow (500-Hz) sampling rate should be used. Sampling continues, and the number of samples is counted until the sample values obtained are similar to the initial values. This provides an approximate measure ($\approx$ 1–2-percent accuracy) of the period. Problems that can occur when starting the measurement sequence at a signal peak are eliminated by delaying slightly the start of the measurement until the peak has passed. Advantages of this method are that the measurement process does not need to wait for a zero crossing of the signal; indeed, this algorithm does not require any zero crossing. The algorithm performs well with a noisy signal, and for low frequencies, gain changing (i.e., autoranging) may be accomplished between measurement samples without disturbing the continuity of the overall measurement. A disadvantage of this algorithm is the failure to operate with a square-wave input; however, this is outside the intended operation of the instrument.

Once the end of the signal period is found, the preamplifier gain and A/D range are set to optimum values, the sample rate clock is set to 128 times the measured frequency, and sample values spanning the next period are stored in memory. It should be noted that the measured frequency previously determined is of low accuracy, because of limited resolution imposed by the calculation time required between samples.

In order to correctly calculate the rms value of the input signal, the period must be known to approximately the same accuracy as is desired of the rms value. Thus a second calculation using the stored sample values is performed to determine the period more accurately. The method chosen to determine the period accurately must provide some way of reducing the effect of noise. Basing any measurement or decision on one or even a few input samples is likely to cause a serious error. For this reason, an autocorrelation technique based on several samples is used to determine the maximum point of correlation with respect to the period between the beginning and end of the waveform. The algorithm chooses an initial period (an integral number of samples, N) and computes the following sum from the stored sample values (E_i):

$$\text{error function} = \sum_{i=1}^{16} |E_i - E_{i+N}|.$$

The sum is calculated for different values of N until a minimum is found. However, due to the limited number of readings stored, the period is not determined with sufficient accuracy using only integral values for N. To provide more resolution, the two smallest sums are used to linearly interpolate to the minimum point between them.

Computer simulations have shown that numerical integration by the midpoint method provides good reproducibility for the value of the integral when measuring a noisy sinusoid. Therefore, the rms value of the input is calculated in a straightforward manner from the set of stored samples. The sample values are squared and summed using 32-bit precision arithmetic. When the period is not an integral number of samples, a small end correction is applied.

One feature of the instrument is an "ac only" function which removes any dc offset from the signal. In this case, the true rms value is calculated normally by squaring and summing the input samples. After dividing this sum by the number of samples in the period, the square of the average of the input samples is subtracted from the sum and then the square root is taken. This produces the rms value of only the ac component.

A 64-point radix 2, fast Fourier transform algorithm is used to compute the DFT of the input signal [4], [5]. The total execution time is typically 400 ms. For highest accuracy, this algorithm requires that 128 stored samples exactly span one signal period; therefore, after each measurement the sample rate clock is reset to keep it "locked" to the signal frequency. Although for some applications the measurement of the individual coefficients is required, usually the operator wants a "figure of merit" or "how close is it to a sine wave?". For this requirement, a total harmonic distortion (THD) value is calculated. This consists of dividing the rms value of the harmonic content by the total rms value. The THD of the waveform is then displayed on the front panel in percent of the rms value of the input voltage.

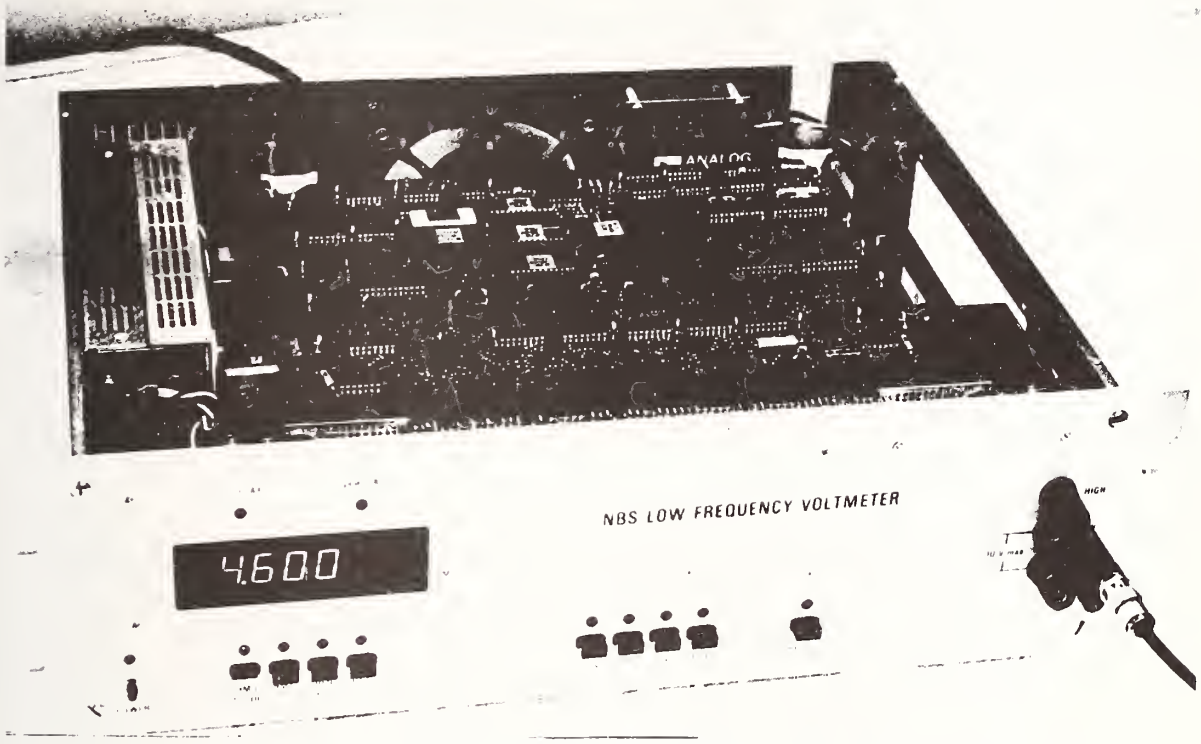

Fig. 3. Photograph of the instrument with the cover removed. The switching power supply for the digital circuitry (at left) and microcomputer are visible.

TABLE I
COMPARISON OF THE SAMPLING INSTRUMENT TO AN ANALOG INSTRUMENT CONTAINING A MULTIJUNCTION THERMAL CONVERTER

	analog instrument (volts)	sampling instrument (volts)	difference (% of reading)
50 Hz	6.384	6.386	+0.03
	5.070	5.070	0.00
	3.159	3.160	+0.03
10 Hz	3.159	3.161	+0.06
	5.072	5.074	+0.04

IV. PERFORMANCE VERIFICATION

One of the advantages of using an A/D converter with a sample-and-hold amplifier is that essentially a series of dc voltages is being measured. Thus once the dynamic performance of the sampling circuitry is verified, calibration of the instrument can be accomplished using dc standards. Initial testing of the rms voltmeter function of the instrument was performed with a specially constructed waveform synthesizer, and an analog voltmeter containing a multijunction thermal converter [1]. The waveform synthesizer consists of a programmable digital memory feeding a digital-to-analog converter. This synthesizer was calibrated at dc and used as an ac source for the sampling voltmeter and the analog voltmeter. At this time, the preamplifier had not yet been installed so that measurements were restricted to a range of about 1 to 6 V. The calibration was performed by applying a sinusoidal voltage (from the waveform synthesizer) to the sampling and analog instruments and recording the readings. Later, a dc voltage from a calibrated dc source was applied to the analog instrument and the input adjusted to obtain the same reading as obtained with the ac. Agreement between the ac output of the synthesizer (calculated from the dc calibration) and the analog instrument/dc calibrator combination was within 0.02 percent for all the readings. Table I lists measurements taken at 10 and 50 Hz comparing the sampling and analog instruments. Differences between the instruments are all below the combined claimed uncertainty for the two instruments.

Other tests were performed to verify the other instrument functions; specifically, the synthesizer was used to produce a waveform with known harmonic distortion which was then measured by the voltmeter. Typical accuracy of the total harmonic distortion measurement was ± 0.2 percent expressed as a percentage of the rms value of the input voltage.

V. CONCLUSIONS

Fig. 3 is a photograph of the instrument that has been developed and tested. This approach which uses sampling techniques to relate ac voltages to dc standards does not rely on fragile thermal converters or inaccurate log amplifiers, is less sensitive to temperature variations than analog designs,

and provides rapid measurement of several signal properties. Also, the inclusion of a microcomputer in this design produces a compact instrument, permits fast intelligent autoranging, and simple (one button) operation.

References

[1] H. K. Schoenwetter, "An rms voltmeter/calibrator for very low frequencies," *IEEE Trans. Instrum. Meas.*, vol. IM-27, no. 3, pp. 259–268, Sept. 1978.

[2] R. S. Koyanagi, "Development of a low frequency vibration calibration system," NBS Rep. 10529, Jan. 1971.

[3] R. S. Koyanagi and J. D. Pollard, "Piezoelectric accelerometer low-frequency response by signal insertion methods," NBS Rep. 74-597, May 1975.

[4] J. W. Cooley and J. W. Tukey, "An algorithm for the machine computation of complex Fourier series," *Math. Comp.*, vol. 19, pp. 297–301, Apr. 1965.

[5] G. D. Bergland, "A guided tour of the fast Fourier transform," *IEEE Spectrum*, vol. 6, pp. 41–52, July 1969.

AC–DC Comparators for Audio-Frequency Current and Voltage Measurements of High Accuracy

FRANCIS L. HERMACH, FELLOW, IEEE

Abstract—**This paper surveys recent developments in high-accuracy ac–dc comparators, the basic standards for ac current and voltage measurements at audio and higher frequencies. These instruments compare the unknown ac quantity with a dc reference. The ac–dc transfer characteristics of thermal converters, the most widely used comparators, can be evaluated to about 10 ppm at audio frequencies in national metrology laboratories. With recent developments even better accuracies, and greater convenience with automatic comparisons, are feasible.**

Basic Principles

IT IS NOW FAIRLY well known that all measurements of ac current and voltage depend fundamentally upon precise ac–dc comparators (ac–dc transfer standards), which either simultaneously or sequentially compare the unknown ac quantity with a known equal or nearly equal dc counterpart. Such comparators are designed and constructed for high precision and small stable ac–dc differences,[1] but need not have the long term stability of reading required in other instruments. They are used with basic dc standards to evaluate, for example, calibrated ac voltage or current sources. These in turn are used to evaluate instruments such as digital voltmeters, or ac–dc converters for such instruments. Since accuracies of commercially available sources and instruments now approach 0.01 percent (100 ppm), very high accuracies are required in the ac–dc transfer.

The determination of the ac–dc differences of such comparators has been, and continues to be, an important task of national metrology laboratories. The ampere or the volt is established with direct current or voltage in these laboratories to a few ppm by electrodynamic or electrostatic instruments, which in effect weigh the electrical unit by balancing an electrical force against the force of gravity. The pertinent constants of the instruments must be determined to the full accuracy of the measurement. While in principle this could be done with alternating current or voltage, the difficulties would be greater. The most reproducible or stable references are based on the Josephson effect and the cadmium standard cell, which provide dc standards. For these reasons ac measurements are referred to these dc standards by ac–dc transfer standards whose constants must simply be equal at the two frequencies.

Either the rms, crest, or average value of an ac wave may be compared with a dc value. The rms value is most often desired or required, because it governs the interchange of electrical with other forms of energy. However one of the others may sometimes be more suitable, as in iron-loss or dielectric strength testing.

One of these values cannot be deduced readily from another. This is not academic. As accuracies increase, the

Manuscript received June 29, 1976.

The author is with the Electricity Division, National Bureau of Standards, Washington, DC 20234.

[1] The ac–dc difference is defined as $\delta = (Q_{ac} - Q_{dc})/Q_{dc}$, where Q_{ac} and Q_{dc} are the ac and dc quantities (current or voltage) required to produce the same response (output) of the comparator.

common error of measuring a voltage or current of unknown waveform with an average- or peak-responding instrument scaled in terms of the rms value of a sine wave can become very serious. Because of their simplicity such instruments are now widely used. To avoid compounding the error they should be calibrated with corresponding peak-to-dc or average-to-dc comparators, or with an ac source having a crest factor or form factor (as needed) equal to that of a sine wave to the required accuracy. Highly accurate peak and average ac-dc comparators have been designed, but only over limited ranges to date.

RMS–DC Comparators

Classical methods of ac–dc comparison are based on electrodynamic, electrostatic, or electrothermic instruments, and have been described in earlier survey papers [1]–[4]. Each of these comparators responds inherently to the rms value of the voltage or current because of its operating principle and its mechanical or thermal inertia.

For example, the equation governing a conductor heated by a current i with all of the conductor at the same temperature is, at each instant, $i^2R = k\theta + Md\theta/dt$, where R, k, and M are parameters which in general depend upon the temperature rise θ. If the thermal inertia is high enough so that θ is essentially constant during the cycle then, by termwise integration over one cycle, the steady-state temperature rise is simply $\theta_a = I^2R/k$, where I is the rms current.

The temperature rise is thus a true measure of the rms current I even if R and k are temperature dependent. This inherent rms response holds under much more general conditions as long as the cyclic variations of θ are negligible. Note that as an ac–dc comparator, θ_a does not have to be an exact quadratic function of I. However, at low frequencies the average value of the cyclically varying θ is then not correctly a measure of I.

Similar relationships hold for electrodynamic and electrostatic instruments, but have not yet been synthesized with high accuracy by electronic means.

Thermal Converters

The temperature rise of a thin straight conductor carrying a given current is nearly independent of frequency over a wide range because of the low reactance of the wire, and can easily be sensed with high precision by one or more thermocouples. The ac–dc differences of such thermal converters (TC's) are quite small and have been studied extensively in national laboratories over the past few decades. TC's with appropriate electrical "readouts" have almost entirely replaced the other forms of ac–dc comparators, which are at present more limited in accuracy by frequency-dependent effects or in ranges of voltage and current.

A conventional simple TC (in ranges from about 2 to 500 mA), consists of a small evacuated glass bulb containing a heater wire ½ to 1 cm long, with the hot junction of a single thermocouple thermally connected to its midpoint by a tiny insulating bead. Thomson and Peltier heating and cooling of the heater can affect the temperature on direct current.[2] Even when the average of the two directions is taken a small error remains. Because of thermal inertia they do not affect it on alternating current (except at low frequencies), leading to a frequency-independent ac-dc difference [5], [6]. Fortunately this can be reduced to a few ppm or less by proper design and selection of materials. However, exact calculation is questionable, even though appropriate formulas have been developed, because of possible effects of heat treatment on the thermoelectric constants during fabrication.

Many commercial TC's have lead-in wires of magnetic alloys to match the temperature coefficient of the glass bulb. Skin effect in these leads can cause additional ac heating. Even more serious ac-dc differences can occur in voltage measurements because of the increased ac resistance. They are minimized with nonmagnetic leads, which, however, must have low thermal EMF's versus the heater alloy and yet provide a good seal.

Dielectric loss in the insulating bead generally varies with frequency and temperature, and can thus cause significant ac–dc differences. The differences are dependent on current, frequency, and the voltage between the heater and thermocouple.

Thermoelectric errors are negligible in multijunction thermal converters (MJTC's) in which many series-connected thermocouples are spread along the heater. Very ingenious designs have been developed, some with as many as 200 junctions and with bifilar heaters which further reduce these errors to theoretical values far below 1 ppm [7]. They have other advantages as well, such as higher rated output (up to 100 mV instead of 10). Investigations have shown, however, that some constructions are subject to dielectric loss and other errors [36].

Series resistors are used with TC's to form thermal voltage converters (TVC's). These may be wire-wound or film-type resistors, switch-selected for convenience in obtaining multiple ranges, typically from 1 to 1000 V. Cylindrical metal-film resistors mounted coaxially in metal cylinders make it possible to compute the effects of residual reactances to 10 MHz or more, at least at low voltages. Intercomparisons of adjacent ranges of such sets of TVC's provide valuable confirmation and also assurance against other sources of ac–dc differences (which are not likely to be the same for all ranges). Such tests can be made to a few ppm at audio frequencies [8].

With two TC's of different current ratings (for example, 2.5 and 5 mA), a single series resistor can serve for two voltage ranges. With only 6 resistors in a typical set, ranges from 1 to 1000 V can be obtained. If they are properly designed and constructed, only 7 intercomparisons are necessary to determine their relative ac–dc differences [9]. Similarly, shunt resistors can be used with two TC's of different voltage ratings to make convenient thermal

[2] They also cause dc reversal differences when the bead is not at the exact thermal midpoint.

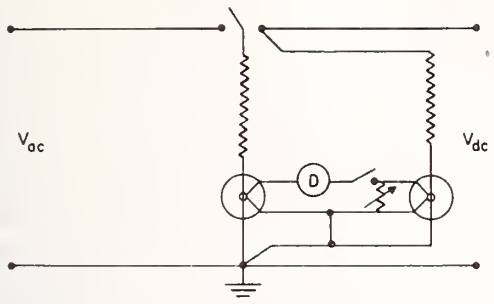

Fig. 1. Simultaneous ac–dc comparator.

current converters (TCC's), with ranges up to 20 A or more.

Transformers can also be used to provide voltage ranges. Only the heater of the TC needs to be switched to the dc reference. Excellent accuracy is possible at midaudio frequencies, but the design of suitable transformers for wide voltage and frequency ranges is difficult.

Simultaneous ac-dc comparators have been developed, to reduce drifts from ambient and self-heating temperature changes, which can sometimes be serious. These usually have dual circuits, as shown for one such arrangement in Fig. 1 [10]. One TVC is supplied by the ac voltage and the other by a known dc voltage with the TVC outputs connected in opposition to a null detector. Unfortunately the input-output characteristics of TC's are not equal, (do not "track") even when equalized at one level.[3] Thus for highest accuracy, a preliminary adjustment to null the detector with both converters connected to the same current or voltage is generally required. This is accomplished with the adjustable resistor shown in Fig. 1, which forms a voltage divider with the internal resistance of the thermocouple (not indicated).

Alternatively, the null-balance adjustment can be made at a fixed dc current level, which is supplied to both heaters by a Zener-diode reference. The heater of one TC is then switched to a decade range resistor (or an amplifier with gain-control resistors) for the ac measurement. With proper choice of components the resistor can be direct reading in volts when it is adjusted to obtain the same output balance [11], [12].

Similar arrangements can be used with indirectly heated thermistors, each consisting of a small thermistor bead in thermal contact with the heater wire. Appropriate bridge circuits have been developed for the output balances. High sensitivity is obtainable because of the high negative temperature coefficients of the thermistors [13], [14].

Such simultaneous comparators, with TC's or thermistors, can provide known fixed ac reference currents or voltages for ac potentiometers (and are sometimes called "ac standard cells"). In a true potentiometer an unknown voltage (or a definite fraction of it) is balanced against an adjustable known voltage through an appropriate null detector. For ac measurements the two voltages must be of exactly the same frequency, magnitude and phase. Thus the known voltage must be phase-locked to the unknown and must be adjustable with high accuracy without affecting the stability of the reference. In addition, with the usual tuned detector, only the fundamental component of the unknown is measured. For these reasons ac potentiometers have been used in the USA chiefly for special measurements, when both phase and magnitude information are required.

The heater of a TC is easily burned out by overloads. This serious disadvantage can now be overcome, however, by rapidly acting relays or electronic circuits, which are available with some comparators [15]. This is very desirable, provided that normal changes in the components do not affect the ac–dc difference.

The continuing development of ac–dc comparators makes standardization of accuracy classes, voltage and frequency ranges, etc, impracticable. However, standardization and agreement on terminology (including accuracy), general requirements, and test methods is very desirable, and has been accomplished in American National Standard C100.4 [16].

Use of Thermal Converters

For the measurement of an ac voltage, or the calibration of an ac voltmeter, the TVC is connected as shown in Fig. 2. With V_{ac} applied, the output EMF is balanced against a stable dc source with a null detector (not shown). The TVC is switched to a known dc voltage, which is adjusted to give the same output EMF. The dc voltage is reversed and readjusted. The detector null should be checked with the ac voltage applied to guard against drifts. Then $V_{ac} = V_{dc}(1 + \delta)$, where δ is the fractional ac–dc difference of the TVC and V_{dc} is the average for the two directions.

Alternatively, if the detector is linear, its scale can be calibrated by adjusting the dc voltage by a small known amount ΔV and noting the detector change ΔD. A fixed dc voltage (nearly equal to the ac voltage) can be set as a convenient reference, and the detector reading can be recorded at each step in a sequence such as $V_{dc}+$, V_{ac}, $V_{dc}-$. Then $V_{ac} = V_{dc}[1 + \delta + s(D_{ac} - D_{dc})]$, where D_{ac} and D_{dc} are the detector readings with V_{ac} applied and the average of the readings with the two directions of V_{dc} applied, respectively, and $s = \Delta V/V\Delta D$. Errors from drifts are minimized if the steps are taken at equal time intervals.

The switches and output circuit should be shielded to avoid interaction. Coaxial and shielded leads should be used as shown, to minimize induced voltages, particularly at the test frequency. The voltage drops in the leads between the ac–dc switch and V_{ac} and V_{dc} should be equal, and errors from ground currents must be evaluated.[4]

Similar techniques are used for ac current measurements, but careful analysis of ground-current errors is

[3] Output EMF's can differ by several percent with single junction TC's and 0.1 percent with MJTC's.

[4] If a grounded instrument is used to measure V_{dc} it should be connected between the two switches.

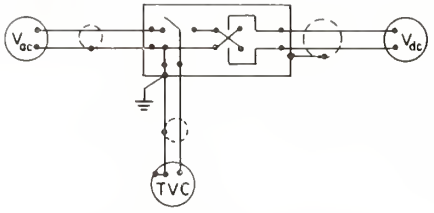

Fig. 2. Sequential ac–dc transfer.

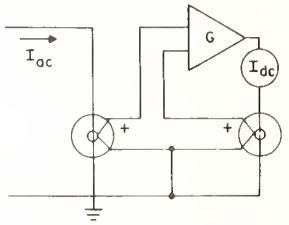

Fig. 3. Basic TC feedback circuit.

needed, particularly in the test of another instrument which must itself be grounded.

A typical commercially available comparator has a built-in ac–dc transfer switch, and an adjustable stable dc source in series with a detector to balance the output EMF. Most of them do not have dc reversal switches, however, generally relying on TC's with low dc-reversal differences. This should be checked periodically at two or more heater currents, for the error in the voltage measurement is ½ this difference, and can be much larger than the ac–dc difference.

Standard C100.4 describes some simple yet practical ways to detect and guard against ground-current errors, radio-frequency interference and other errors in the intercomparison of two current or voltage comparators. These techniques can also be applied when ac–dc comparators are used for ac measurements or for the calibration of ac instruments. Comparators with 3- or 4-terminal inputs (with properly designed shields and driven guards) greatly reduce circuit-connection errors, but are not widely used.

If the ac–dc difference of the comparator is known and applied as a correction along with corrections for the dc standards, and if proper techniques are used to made valid measurements, it is not at all necessary that the "accuracy of the standard shall be ten times that of the test instrument" as is so often stated. The uncertainty in the ac measurement is simply the sum of the residual errors in the standards and the random error in the test (caused by both the standard and test instrument). In this way maximum use is made of the inherent accuracy of the ac–dc comparator and the dc standards. The application of such corrections to remove determined errors avoids this 10/1 noose, which often strangles echelons of laboratories with unnecessary accuracy requirements.

Automatic Comparators and Converters

All of these manual procedures are time consuming and tedious. Automatically-switched comparators and ac–dc converters (which generate a dc voltage accurately proportional to the input) have been developed to simplify the measurements. In some automatic comparators, essentially the same procedure is followed as in manually operated instruments (with TC's of low dc reversal difference and drift to simplify the ac–dc sequence). In others, the switching is done quite rapidly (at about 1 Hz, for example) to overcome drifts. The ac component at the switching frequency in the detector is a measure of the difference between the ac and dc voltages, either directly or through a feedback circuit [17]. Gain-stabilized amplifiers provide wide voltage ranges conveniently, with minimum loading.

For rms measurements many ac–dc converters are based on the feedback circuit shown in simplified form in Fig. 3 [18]. When I_{ac} is applied, I_{dc} increases until the outputs of the two matched TC's are nearly equal. If the transconductance of the amplifier is G and $E = kI^2$ for each TC, $I_{dc} = Gk(I_{ac}^2 - I_{dc}^2)$. Then if $a = 1/GkI_{dc} \ll 1$, $I_{dc} \approx I_{ac}\sqrt{1-a} \approx I_{ac}$. Interestingly, this is an rms instrument with a linear scale (except near zero).

To avoid tracking errors, decade input resistors, or amplifiers controlled by decade feedback resistors, can provide appropriate voltage ranges at a fixed current. Alternatively a dual-heater MJTC can be used with fixed resistors for tracking to about 0.05 percent over a range of currents.

Other types of converters have also been developed and used in this general feedback circuit. One uses dual monolithic thermoelements, with two resistors and two temperature-sensing transistors on a single chip [19]. In another, two indirectly heated thermistors, each with dual heaters, are used with dual feedback so that each thermistor is always at the same temperature, to avoid tracking errors [20].

These feedback circuits greatly reduce drifts and the effective response time of the TC's (which is about 1 s). However the ac–dc differences of the input resistors and amplifiers in these instruments must be small and stable. In addition, the design of the feedback amplifier is complicated by stability problems and by the double-frequency ripple in the TC output at low frequencies.

A number of electronic techniques for rms to dc converters have been developed, based on approximating a square-law function with straight-line segments or with an appropriate transistor characteristic. Feedback circuits have made these more practical [21]. They have shorter response times and wider ranges than thermal converters.

Other AC–DC Comparators

Electrodynamic and electrostatic instruments have been used as ac–dc comparators. The frequency range of an electrodynamic instrument, however, is limited by the

reactances of the coils. The range can be much greater for an electrostatic instrument, but the torque/weight ratio is low at moderate voltages, and surface films can cause ac–dc differences that are difficult to evaluate. With both types the double-frequency periodic variations in the ac torque can cause vibrations in parts of the moving system, with resultant errors. It is difficult, also, to obtain a resolution of a few ppm even with light-beam pointers. For all of these reasons these instruments find their place mainly in national metrology laboratories, where these problems can be studied at length and overcome [22]–[24].

Putting a rectifier in the feedback loop of a suitable operational amplifier greatly reduces the effects of the rectifier's imperfections. Refinements of this arrangement have made average-responding ac–dc comparators and converters of 20 ppm accuracy possible [25]. Instruments with electronic or electromagnetic relays which compare the crest (peak) value with a dc voltage have also been refined to better than 50 ppm, at least at low audio frequencies [26], [27]. Rapid electronic sampling and computing techniques, which measure the instantaneous value of the wave at selected intervals, now make it possible to compute the rms, crest and average values, and thus to determine crest- and form- factors with high accuracy as well [28], [29].

Evaluation of AC–DC Comparators

The ac–dc differences of well-designed and well-constructed comparators are small and quite stable. In many cases they need not be redetermined, once known, if all adjacent ranges (such as 10 and 20 V) can be compared to detect changes. The evaluation of ac-dc differences in an absolute sense is difficult and time consuming. It has generally been attempted only at national metrology laboratories, which can carefully establish and study ac–dc transfer standards, develop the necessary precise intercomparison apparatus, and then use this equipment to calibrate the comparators of many other laboratories. In this way the standards receive wide use in establishing compatability and accuracy in these measurements. This is most economical, too, because the results of the research are then available to all users. Such services are important functions of national laboratories.

These "absolute" ac–dc standards must be investigated both theoretically and experimentally. This usually involves 1) theoretical analyses of sources of ac–dc errors, 2) design and construction of standards that minimize these errors, 3) comparisons and other tests of these standards to evaluate the errors, and 4) comparison with another type of transfer standard which has also been carefully studied.

The last step is very desirable to guard against errors from unknown sources, but it implies the development of different types of standards of nearly equal precision and ac–dc accuracy. At the present time other types cannot match thermal converters in ranges or accuracy. Thus comparisons of different kinds, constructions and ranges of TC's, which are free of known sources of error, are vital. If these converters agree in ac–dc difference it is unlikely that they have a common source of error, because of the differences in their design and construction.

Remarkably stable ac and dc power supplies are now commercially available, with rms fluctuations of only a few ppm in a minute or so. Extraordinary stabilities (0.5 ppm/h) have been achieved in recent special laboratory designs [30], [31]. These, together with techniques which largely cancel the effects of drifts and of small supply variations, have made possible high precision in the intercomparison of TC's and TVC's.

Careful evaluations of TVC's from 1 to 1000 V and TCCs from 1 mA to 1 A or more have been made in national laboratories to about 10 ppm at audio frequencies, with reduced accuracies at higher frequencies [8], [32], [33], [34]. Comparisons with electrostatic and crest-responding instruments in these laboratories have provided valuable confirmation of the absence of large errors. At the Electrotechnical Laboratory in Japan an electrostatic voltmeter is planned, to provide the basic ac–dc transfer above 1 kV [35].

The development of MJTC's now makes even better accuracy possible. At NBS MJTC's of different manufacture and range have been compared, with a standard deviation of less then 0.2 ppm. A number of sources of error which cause MJTCs to depart from the ideal have been uncovered, and either overcome in new designs or compensated. The ac–dc difference of a group of 8 TVC's (6 to 9.V) is believed to be less than 0.3 ppm at 160 Hz, the frequency of an important absolute volt determination, and 0.5 ppm from 30 to 10,000 Hz [36].

An intercomparison among several national laboratories of 4 sets of TC's and TVC's is now almost finished. It should provide a better basis for international agreement on the ac–dc transfer of current and voltage from 40 Hz to 50 kHz.

Conclusions

At the present time research and development have provided ac–dc comparators which have the accuracy needed (about 10 ppm) to support commercial developments in ac current and voltage measurements at audio frequencies. With electronic aids, more rapid and convenient automated comparators are now feasible and are beginning to appear. There is no slackening in the importance or development of this field of measurements.

A cataloging of all these developments would be neither feasible nor digestible in a survey paper such as this. The basic principles of a number of them have been highlighted, instead, to illustrate the present status and recent trends in high-accuracy ac measurements.

References

The following references in the open (published) literature were selected because of their general nature or extensive bibliographies, or because they illustrate recent

developments. A list of references published between 1945 and 1975 on high accuracy audio-frequency ac–dc current and voltage comparators is available on request from the Electrical Instruments Section, National Bureau of Standards, Washington, DC 20234.

[1] M. Iwamura and T. Yamazaki, "General review of maintenance of alternating current standards," Circular No. 147, ETL, Dec. 1957. (In Japanese with English abstract, 81 references.)

[2] F. L. Hermach, "Ac–dc transfer instruments for current and voltage measurements," *IRE Trans. Instrum.*, vol. I-7, pp. 235–240, Dec. 1958.

[3] T. B. Rozhdestvenskaya, "Electrical comparators for measurements of current, voltage and power," JPRS 29373, 187 pp., 1965, National Technical Information Service, Springfield, VA 22161. (English translation of a Russian Monograph with 112 references.)

[4] H. Helke, "Ac–dc converters and comparators for alternating current," *Arch. Tech. Messen*, no. J942-2, pp. 227–232, Oct. 1967; no. J942-3, pp. 255–260, Nov. 1967; no. J942-4, pp. 11–13, Jan. 1968. (In German, 137 references.)

[5] F. L. Hermach, "Thermal converters as ac–dc transfer standards for current and voltage measurements at audio frequencies," *J. Res. Nat. Bur. Stand.*, vol. 48, pp. 121–138, Feb. 1952.

[6] F. C. Widdis, "Theory of Peltier- and Thomson-effect errors in thermal ac–dc transfer devices," *Proc. Inst. Elec. Eng.*, vol. 109, pt. C (Monograph 497 M) pp. 328–334, 1962.

[7] F. J. Wilkins, "Theoretical analysis of the ac/dc transfer difference of the NPL multijunction thermal converter over the frequency range DC to 100 kHz," *IEEE Trans. Instrum. Meas.*, vol. IM-21, pp. 334–340, 1972.

[8] F. L. Hermach and E. S. Williams, "Thermal converters for audio frequency voltage measurements of high accuracy," *IEEE Trans. Instrum. Meas.*, vol. IM-15, pp. 260–268, 1966.

[9] E. S. Williams, "Thermal voltage converters and comparators for very accurate ac voltage measurements," *J. Res. Nat. Bur. Stand.*, vol. 75C, pp. 145–154, 1971.

[10] F. L. Hermach, J. E. Griffin, and E. S. Williams, "A system for accurate direct and alternating voltage measurements," *IEEE Trans. Instrum. Meas.*, vol. IM-14, pp. 215–224, 1965.

[11] W. Rump, "On the exact absolute measurement of a-c voltages and a potentiometer for calibrating a-c instruments," *Elektrotecknik*, vol. 5, pp. 64–67, 1951 (in German).

[12] J. E. Griffin and F. L. Hermach, "A differential thermocouple voltmeter," *AIEE Trans.*, vol. 81-I, pp. 339–345, 1962.

[13] F. C. Widdis, "The indirectly heated thermistor as a precise ac–dc transfer device," *Proc. Inst. Elec. Eng.*, vol. 103B, pp. 693–703, 1956.

[14] H. J. Schrader, "A-c current measurements with indirectly heated NTC resistors," *ETZ*, vol. 73A, p. 547, 1952 (in German).

[15] "IR sensor protects transfer standard," *Electronics*, vol. 48, pp. 36–37, Oct. 16, 1975.

[16] "AC-DC transfer instruments and converters," American National Standard, C100.4, 1973. ANSI, 1430 Broadway, New York, NY 10018.

[17] L. G. Cox and N. L. Kusters, "An automatic rms/dc comparator," *IEEE Trans. Instrum. Meas.*, vol. IM-23, pp. 322–325, 1974.

[18] R. Gilbert and J. Miller, "Thermal converter," U.S. Patent 2 857 569, 1958.

[19] W. E. Ott, "A new technique of thermal rms measurement," *IEEE J Solid State Circuits*, vol. SC-9, pp. 374–380, 1974.

[20] P. Richman, "A new wideband true rms–dc converter," *IEEE Trans. Instrum. Meas.*, vol. IM-16, pp. 129–134, 1967.

[21] P. Richman and W. Walker, "A new fast-computing rms/dc conversion," *IEEE Trans. Instrum. Meas.*, vol. IM-20, pp. 313–319, 1971.

[22] W. Smith and W. Clothier, "Determination of the dc–ac transfer error of an electrostatic voltmeter," *J. Inst. Elec. Eng.*, vol. 101, pp. 465–469, 1954.

[23] T. Yamazaki, S. Iwamoto and T. Ando, "Estimation of the ac/dc differences of electrostatic voltage comparator," *Bull ETL*, vol. 32, pp. 1085–1099, 1968.

[24] G. Schuster, "A high resolution electrodynamic ac–dc power transfer instrument," *IEEE Trans. Instrum. Meas.*, vol. IM-23, pp. 330–333, 1974.

[25] L. A. Marzetta and D. R. Flach, "Design features of a precision AC–DC converter," *J. Res. Nat. Bur. Stand.*, vol. 73C, pp. 47–55, 1969.

[26] P. Richman, "A new peak-to-dc comparator for audio frequencies," *IRE Trans. Instrum.*, vol. I-11, pp. 115–122, 1962.

[27] D. R. Flach and Louis A. Marzetta, "Calibration of peak ac to dc comparators," *Proc. ISA*, paper no. 14.2-3-65, 1965.

[28] F. Deist and R. Kitai, "Digital transfer voltmeters," *Proc. Inst. Elec. Eng.*, vol. 110, pp. 1887–1904, 1963.

[29] R. S. Turgel, "Digital wattmeter using a sampling method," *IEEE Trans. Instrum. Meas.*, vol. IM-23, pp. 337–341, 1974.

[30] H. Schoenwetter, "An ultra stable power supply for an absolute volt determination," *Metrologia*, vol. 10, pp. 11–15, 1974.

[31] G. Schuster, "A precision stabilized sine wave source for AC power measurements," *IEEE Trans. Instrum. Meas.*, vol. IM-22, pp. 391–394, 1973.

[32] S. Iwamoto and H. Hirayama, "Ac/dc thermal converters of the ETL," *IEEE Trans. Instrum. Meas.*, vol. IM-23, pp. 326–329, 1974.

[33] C. H. Dix, "Electrical standards of measurement, Pt 1, dc and low frequency standards," *Proc. Inst. Elec. Eng.*, vol. 122, no. 10R, pp. 1018–1036, 1975.

[34] O. P. Galakhova and T. B. Rozhdestvenskaya, "State of the standardization of references and methods of dc and ac voltage measurements," *Meas. Tech.*, vol. 18, pp. 1339–1341, Sept. 1975.

[35] K. Shida, "Ac–dc high voltage comparator with balance," *Bull. ETL*, vol. 39, pp. 415–420, 1975 (in Japanese).

[36] F. L. Hermach and D. R. Flach, "An investigation of multijunction thermal converters," to be published.

IEEE TRANSACTIONS ON INSTRUMENTATION AND MEASUREMENT, VOL. IM-25, NO. 4, DECEMBER 1976

Thermal Current Converters for Accurate AC Current Measurement

EARL S. WILLIAMS

Abstract—**A new 14-range set of thermal current converters consisting of shunted thermoelements has been constructed to measure ac–dc difference and ac current from 10 mA to 20 A at 20 Hz to 50 kHz. The ac–dc difference corrections for all ranges can be determined relative to two ranges by a 7-step intercomparison of certain adjacent ranges.**

Introduction

THERMAL CURRENT converters (TCC's) consisting of ac shunts in parallel with thermoelements (TE's) are widely used as ac–dc transfer instruments to determine ac–dc difference of other instruments and to measure ac currents by comparison with known dc currents.

Shunt assemblies are sometimes incorporated into multirange instruments, but usually are individual single-range units. They are attached to a thermal voltage converter (TVC) which contains a low-voltage low-current TE. Commercial multirange TVC's usually incorporate an adjustable source of EMF and a null detector for monitoring the output of the TE.

Specific procedures and the necessary equipment have not been provided by shunt manufacturers to enable the user to make intercomparison tests between members of a set of shunts. However such tests would provide several advantages. It would be sufficient for the manufacturer or a standards laboratory to calibrate only two or three ranges. These ranges would serve as reference points for calibrating the other ranges by intercomparison. Periodic intercomparisons could then be made by the user to detect any significant changes that might occur in any shunt in the set, and redeterminations of ac–dc difference relative to other standards would not be required as often.

The new NBS set of TCC's, consisting of six shunts and two TVC's (Fig. 1) is designed so that it can be intercompared in a minimum number of steps. The TVC's have nominal inputs of 0.3 and 0.6 V and may be attached to any one of the shunts by a coaxial connector. This permits each shunt to be used for two ranges, as shown in Table I where current ratings, shunt resistances, and TVC currents are listed. For the purpose of calibration, intercomparisons are made between each of the six shunts or between alternate ranges. The TVC's are used without shunts for the two lowest ranges (10 and 20 mA), and they are compared with the shunted ranges in two additional steps.

Manuscript received June 28, 1976; revised August 12, 1976.
The author is with the Electricity Division, National Bureau of Standards, Washington, DC 20234.

Thermoelements as TCC's and TVC's

TE's without shunts have been used for some years at the NBS as primary current converters. They can be very accurate ac to dc transfer devices. The short straight heater and connecting wires have minimal reactance, and an insulating bead between the heater and thermocouple prevents any appreciable interaction between the current being measured and the readout instruments. The thermocouple output is rather low (7 to 12 mV), but it can be monitored with very good precision with a modern galvanometer or microvoltmeter.

However shunted thermoelements are probably preferable as TCC's in most other calibration facilities mainly because the low current TE's used are relatively inexpensive and easy to replace if burned out—an accident that can happen quite easily. Ampere-range TE's are more expensive, and those with insulating beads are not ordinarily available. However, a few sets have been made by one manufacturer on special arrangement.

TE's for 10 and 20 A usually have C-shaped heaters (tubular except for opening on one side) which can cause an unusual effect. The ac–dc difference is very much dependent on the location of other nearby conductors, particularly the return conductor which is usually placed along side of, and more or less parallel to, the TE heater. Apparently the ac current is distributed for minimum reactance and may therefore be concentrated close to, or away from, the thermocouple which is attached to the top of the heater. This nonuniform current distribution can cause an ac–dc difference change of 0.03 percent or more. Rigid copper return conductors have therefore been added to these TE's and the input terminals are both at the same end of the device. The conductors are also positioned for small ac–dc differences.

Similar TE's with straight wire heaters (0.5 to 5 A) and insulation have ac–dc differences of 10 ppm or less at 50 kHz.

TE's for currents up to 1000 mA are available with insulation and vacuum bulb enclosures. They are adversely affected by Peltier and Thomson heating, which have been discussed elsewhere [1], [2]. However, skin effect is the major concern in the practical use of these TE's. The copper-coated nickel alloy widely used for passing current conductors through glass seals is sufficiently magnetic to produce a small increase in the ac impedance in the heater support stems causing additional heating with ac current but not with dc current. The effect is dependent on both

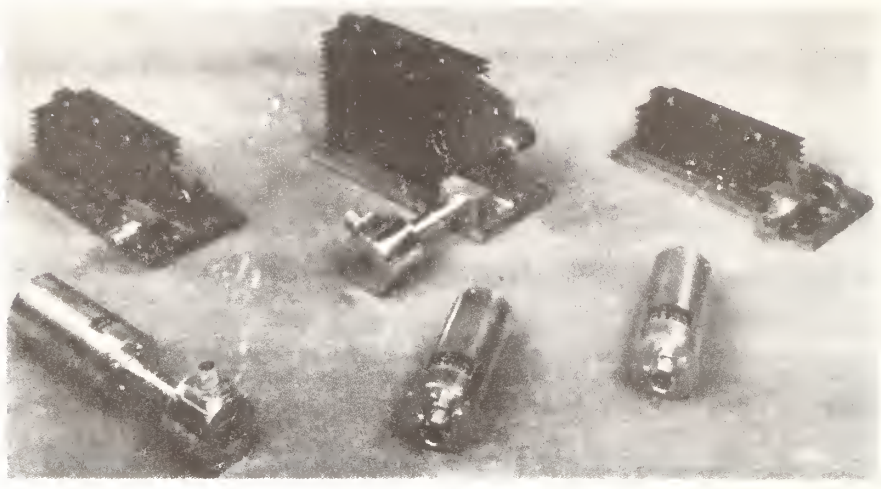

Fig. 1. Set of TCC's.

TABLE I
Thermal Current Converter Set

Fourteen ranges are formed with six shunts and two TVCs (FG and FH).		
Current Range (amperes)	Shunt Resistance (ohms)	TVC Current (mA)
0.01	--	10 (FG)
0.02	--	20 (FH)
0.03	15	10
0.06		20
0.1	3.33	10
0.2		20
0.3	1.0	10
0.6		20
1	0.3	10
2		20
3	0.1	10
6		20
10	0.03	10
20		20

frequency and current thus complicating stepup intercomparison tests.

A few special TE's have been made with nonmagnetic Ni–Cr quaternary alloy for both the heater and supporting stem inside the glass bulb. This not only minimizes the skin effect in the conductors near the heater, but also eliminates Peltier heating at the heater ends since the supporting conductors and the heater are of the same material.

The heating due to skin effect is usually negligible at currents less than 200 mA for TE's used as current converters. However, if the TE is used as a voltage converter, or as a TVC in parallel with a shunt, the additional impedance is added directly to the relatively low heater resistance. The effect is large down to at least 20 mA and significant to 5 or 10 mA. At 2.5 mA, where the heater resistance (about 400 Ω) is high relative to that of the leads, the ac–dc difference at 50 kHz is usually less than 5 ppm.

The skin effect problem was overcome in these TVC's by using 5 mA and 10 mA TE's with platinum input wires. They were made to NBS specifications by three cooperating manufacturers. Fortunately, platinum has an expansion coefficient close to that of glass and makes a reliable seal. Although the Peltier coefficient is large, the heating effect is small at these low currents. The voltage converters designated FG and FH agree with NBS standards to 5 ppm or better both as voltage and current converters. The differences are equally small down to well below 20 Hz, and the corrections to a TCC are of course quite independent of the shunt at low frequency [1].

TCC Construction, Connections, and Grounding

The thermoelements are placed in insulating styrofoam containers and mounted in short brass tubes. The input is a GR874 coaxial connector and the thermocouple output is through a two-contact connector which has very low thermal EMF's at the contacts (Fig. 1).

The 0.3-V TVC, designated "FG," is a 10-mA 30-Ω TE with no additional resistors. It also serves as a 10-mA TCC—the lowest of the 14 ranges. The other TVC ("FH") contains a 5-mA TE, with a heater resistance of about 90 Ω, and a 33-Ω resistor in series. The combination is paralleled by a second resistor of 39 Ω so that FH becomes a 0.6-V TVC and a 20-mA TCC.

The three high current shunts are made of bifilar strips of Ni–Cr quaternary alloy, insulated with 1-mil "Mylar" and mounted between aluminum heat sinks (Fig. 1). The shunt resistance material is gold plated at the ends, then tinned and soldered to heavy copper end pieces to ensure good current distribution. The potential taps are near the centers of the shunt strip and are brought out at right angles to the shunt by a coaxial conductor passing through one half of the heat sink. A flexible cable extends the output to a GR874 connector to which the TVC is attached. The outside of the coaxial conductor is connected to one half of the shunt, and the center conductor passes through

a hole in that part of the shunt and the insulation to the other half where it is silver soldered.

The 10–20-A shunt resistor is 5 mils thick, 10 cm wide and about 34 cm between potential taps. After being folded into bifilar form the overall length is about 24 cm. The resistor for the 3–6-A shunt is 2 mils thick and approximately 4 by 14 cm between potential taps. The 1–2-A shunt is of the same material and approximately 1.8 by 25 cm.

Building the three shunts for the milliampere ranges with available parts or materials was an awkward problem. The required resistances were too high for bifilar strip material and yet lower than the commercial resistors ordinarily available. Tin-oxide resistors in parallel provided a satisfactory solution. The 300–600-mA shunt (1 Ω) contains ten 10-Ω resistors, and the 100–200-mA range (3.33 Ω) contains six 20-Ω resistors. Parallel combinations of two 30-Ω resistors and four 60-Ω resistors were tried for the 30–60-mA shunt, but one 15-Ω resistor was used as it had the lower ac–dc difference. The resistors are mounted in 2-in diameter brass cylinders and connected between the outer casing and a wire which joins the center contacts of both the input and output connectors. (The input connector is out of view in Fig. 1.) Where more than one resistor is used they are arranged concentrically around the center conductor.

When two shunts are connected in series for intercomparison tests care should be taken to avoid capacitive currents that might flow in parallel with one shunt after flowing through the other. Therefore a shunt casing (or heat sink) should not be at the potential of the interconnecting conductor as in Fig. 2. It is recommended that one casing be grounded and the other connected to the high (or ungrounded) input conductor.

The heat sinks for the bifilar shunts should be connected similarly. The connections shown in Fig. 3 is recommended, and it should not make an appreciable difference whether one shunt is grounded or the other. The change in ac–dc difference caused by changing the ground was about 10 ppm at 50 kHz on the higher ranges of these shunts. The effect was well under 10 ppm on lower ranges and at 20 kHz.

TCC Calibrations

Several procedures may be used for ac–dc difference measurements as described briefly in [3, section 6]. However, the TE comparator and the procedures described in [3, section 7] were used for testing these TCC's. The TE comparator affords a significant advantage where the power supplies are even slightly unstable. The precision of these tests probably could not be obtained without it. A fraction of the output emf of one TE is balanced against the emf of the second to obtain an approximate null indication on a detector. Small changes in the ratio of emfs resulting from ac–dc differences may then be measured by changes in the detector indication. The detector may be a microvoltmeter, although for these tests a galvanometer was used whose scale factor (ppm/mm) was determined for each ac–dc difference determination.

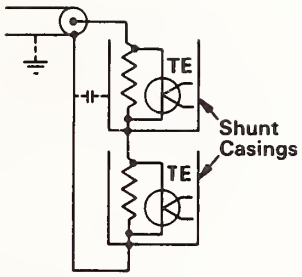

Fig. 2. TCC's in series.

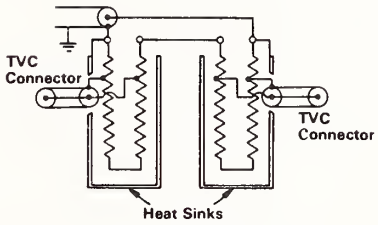

Fig. 3. TCC's in series.

TCC's (shunt and TVC combinations) are usually calibrated and used as one instrument with one correction for each frequency of interest. However the shunt and TVC corrections can be separated for all but the lowest ranges if measurements are made of the corrections to the TVCs as voltage converters. It is necessary to know these corrections if ranges are changed by changing the TVC's. Separating the shunt and TVC corrections has another advantage. Several TVC's may be used, and if one is accidentally burned out the shunts may be used with others.

A third TVC, designated "FE," was assembled using an ordinary 20-mA TE to demonstrate the accuracy with which TVC corrections may be applied. Its correction is +22 ppm at 50 kHz and is ascribed to skin effect in the heater lead-wires. Shunt tests and intercomparisons with TVC's FH and FE are discussed below.

The correction to the shunt and TVC combination (δ_C) is not exactly equal to the sum of the shunt correction (δ_S) and the TVC correction (δ_T). Separating these corrections is complicated because the proportion of current carried by the TVC varies with range. Hermach has developed a simple approximate formula which is accurate enough at currents of 100 mA or more.

$$\delta_C = m(\delta_S + \delta_T) \tag{1}$$

where $m = (I - I_T)/I$, I is the total current, and I_T is the current through the TVC. The multiplier m differs from unity by only 10 percent at 100 and 200 mA, and its effect on δ_C diminishes rapidly at higher currents. The formula is more complicated at 30 and 60 mA and involves small reactive components of the impedance which are extremely difficult to measure. Corrections to these ranges are, therefore, determined by comparison with adjacent lower and higher ranges as explained below.

In the intercomparison tests, measurements are made

TABLE II
Intercomparisons of TCC's (ppm)

TCC_1	TCC_2	Applied Current Amperes	20 kHz D	50 kHz D
FG	FH	0.01	0	0
FG30	FH	0.02	+ 1	+11
FG100	FH60	0.06	+10	+23
FG300	FH200	0.2	+ 7	+20
FG1	FH600	0.6	- 7	-33
FG3	FH2	2	+12	+22
FG10	FH6	6	-24	-54

TABLE III
AC–DC Difference of TCC's (ppm)

TCC	Applied Current Amperes	20 kHz δ measured	20 kHz δ computed	50 kHz δ measured	50 kHz δ computed
FG	0.01	- 1	0	0	- 2
FH	0.02	0	0	- 2	- 2
FG30	0.03	+ 3	+ 1	+10	+ 9
FH60	0.06	+ 3	0	+12	+14
FG100	0.1	+ 9	+10	+32	+37
FH200	0.2	+ 8	+10	+36	+37
FG300	0.3	+13	+17	+51	+57
FH600	0.6	+19	+17	+53	+57
FG1	1	+10	+10	+24	+24
FH2	2	+12	+10	+28	+24
FG3	3	+21	+22	+44	+46
FH6	6	+18	+22	+36	+46
FG10	10	+ 8	- 2	+ 3	- 8
FH20	16	+ 5	- 2	+ 2	- 8

TABLE IV
Intercomparison of TCC's with TVC Corrections (ppm)

TCC_1	TCC_2	Applied Current Amperes	50 kHz D	50 kHz $\delta_{S1} - \delta_{S2}$
FG	FE	0.01	+ 3	-
FG30	FE	0.02	+ 9	
FG100	FE60	0.06	+14	
FG300	FE200	0.2	+ 8	+30
FG1	FE600	0.6	-52	-30
FG3	FE2	2	0	+22
FG10	FE6	6	-64	-42

TABLE V
AC–DC Difference of TCC's with TVC Corrections (ppm)

TCC	Applied Current Amperes	50 kHz δ_C	50 kHz δ_T	50 kHz δ_S measured	50 kHz δ_S computed	50 kHz δ_C computed
FG	0.01	0	-	0	- 5	
FE	0.02	- 8	-	- 8	- 8	
FG30	0.03	+10				+ 1
FE60	0.06	+18				+10
FG100	0.1	+32	0	+32	+24	
FE200	0.2	+48	+22	+26	+24	
FG300	0.3	+42	0	+42	+54	
FE600	0.6	+72	+22	+50	+54	
FG1	1	+28	0	+28	+24	
FE2	2	+53	+22	+31	+24	
FG3	3	+44	0	+44	+46	
FE6	6	+63	+22	+41	+46	
FG10	10	+ 3	0	+ 3	+ 4	
FE20	16	+13	+22	- 9	+ 4	

of the difference between two shunt-TVC combinations. If this difference is called "D" we may write

$$D = \delta_{C1} - \delta_{C2} \tag{2}$$

which becomes, after substituting from (1),

$$m_1\delta_{S1} - m_2\delta_{S2} = D + (m_2\delta_{T2} - m_1\delta_{T1}). \tag{3}$$

At 100 and 200 mA the effect of the multiplier m (= 0.9) is less than 5 ppm for the corrections to these shunts and TVC's. Since there are other uncertainties of this magnitude the effect has been neglected. However, where the corrections are 50 ppm or more it should be taken into account.

A 7-step intercomparison was made at 20 and 50 kHz, and the relative ac–dc differences are listed under D in Table II. Measurement of ac–dc difference corrections for all ranges were also made at the same frequencies by comparison with NBS standard current converters most of which are specially made TE's. These corrections are listed under "δ measured" in Table III. In two additional columns in Table III under "δ computed" these corrections are determined from the intercomparison tests.

The base ranges serving as starting points for the computed δ's were chosen arbitrarily. The "measured" corrections to the 20-mA range and the 1-A range were taken as base points and the others were computed by using (2) and the data from Table II [2]. As mentioned above, the relationship of the shunt and TVC corrections is complicated at 30 and 60 mA where the TVC's carry 33 percent of the current. Therefore, the 20-mA TCC (FH) is used as a starting point for computing corrections to FG30 and FG.

Similar data are listed in Tables IV and V for 50 kHz, but TVC corrections are applied in these tables since FH is used. The corresponding ac–dc differences for 20 kHz were smaller, as in Tables II and III, and are not shown. Intercomparison differences are listed under "D" in Table IV, and TVC corrections from (3), with m_1 and m_2 equal to 1, are applied. ($\delta_{T2} - \delta_{T1} = +22$ ppm). The remaining shunt differences are listed under "$\delta_{S1} - \delta_{S2}$." At 60-mA, equation (3) is not sufficiently exact, and, therefore, corrections to the 60-mA shunt and FE are not separated.

Corrections to each TCC with FE were determined relative to NBS standards, and are listed under "δ_C" in Table V. The corresponding values for the same shunt with FG are taken from Table III. After applying the TVC corrections ($\delta_T = 0$ for FG and +22 ppm for FE) the remaining shunt corrections are listed under "δ measured."

Again, as in Table III, shunt corrections are computed in Table V for all ranges beginning, as before, with the measured correction to the 1-A and 20-mA ranges. The computed correction to FE60 and FG30 apply to the combination since the correction δ_C cannot be reliably separated at this level.

The 20-mA range and the 1- and 10-A ranges are recommended as minimum reference points to be tested relative to other standards outside the set. Intercomparison determinations would be based on the 20-mA and 1-A corrections, and the 10-A range would serve to verify the accuracy of the step-up tests for the highest shunt ranges. TVC corrections would also have to be determined.

The close similarity of measured corrections for the same shunt at different current levels shows that the ac–dc differences are not appreciably affected by the current. This similarity in Table III also shows that the TVC's FG and FH, which are changed when the current is changed, have nearly the same correction. It is very unlikely that one change would offset the other on so many ranges. The similarity of measured and computed corrections in Tables III and V shows that the intercomparison tests can be made quite accurately.

Using Thermal Current Converters

Ac–dc difference measurements may be made of transfer instruments and ammeters which respond nearly equally to ac and dc currents. The TE comparator and procedures referred to earlier may be used if the test instrument has a thermocouple output voltage which can be connected to the comparator. Otherwise an indicator or readout instrument is observed which is usually a part of the device under test.

If the test instrument does not respond to direct current it may be tested by two or three procedures, but the one outlined below is recommended. Changes in detector indication are observed to determine the difference between the ac current and an accurately measured dc current nominally equal to it.

The suggested circuit is shown in Fig. 4, and the order of currents applied to the standard TCC is indicated (DC+, AC, DC−). The potentiometer P is adjusted for an approximate null indication on the detector D. Detector readings are then made for each dc current after it has been adjusted to the nominal test value. The ac reading E_a is made after the ac has been adjusted for the desired indication of the test instrument. The two readings on dc are averaged (E_d), and the ac may then be calculated:

$$I_{ac} = I_{dc}\left(1 + \frac{E_a - E_d}{nE} + \delta_S\right)$$

where I_{dc} is the dc current, E is the TE EMF indicated by the potentiometer P, δ_S is the ac–dc difference of the standard TCC and $n = \Delta E/\Delta I$. The factor n is a measure of the deviation of the TE from a square-law response and is usually 1.7 to 1.9 at rated TE current, (see [1, section 9]).

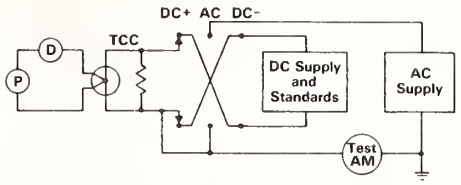

Fig. 4. Circuits for testing an ac ammeter relative to dc standards.

Conclusion

It has been shown that a TCC set consisting of six shunts and two TVC's can be constructed to cover fourteen ranges from 10 mA to 20 A. Intercomparison tests can be made in seven steps to assist in maintaining accurate ac–dc difference corrections. Thermoelements with platinum heater lead-wires are preferable, because the TVC corrections are negligible. However if ordinary TE's are used the TVC corrections can be accurately determined and applied. The estimated accuracies from 20 Hz to 50 kHz are 50 ppm at 6 A and lower and 100 ppm at 10 and 20 A. Measurements of ac current would require additional corrections for the dc standards used as reference and considerations of the precision of the instrument under test.

Acknowledgment

This work was supported in part by the Army Metrology and Calibration Center, Redstone, AL. Their encouragement and support are gratefully acknowledged.

References

[1] F. L. Hermach, "Thermal converters as ac–dc transfer standards for current and voltage measurements at audio frequencies," *J. Res. Nat. Bur. Stand.*, vol. 48, pp. 121–138, Feb. 1952.

[2] F. C. Widdis, "The theory of Peltier and Thomson effects in thermal ac–dc transfer devices," *Proc. Inst. Elec. Eng.*, monogr. 497M, Jan. 1962.

[3] E. S. Williams, "Thermal voltage converters and comparators for very accurate ac voltage measurements," *J. Res. Nat. Bur. Stand.*, vol. 75C, nos. 3 and 4, pp. 145–154, July–Dec. 1971.

[4] F. L. Hermach and E. S. Williams, "Thermal converters for audio-frequency voltage measurements of high accuracy," *IEEE Trans Instrum. Meas.*, vol. IM-15, pp. 260–268, Dec. 1966.

An Investigation of Multijunction Thermal Converters

FRANCIS L. HERMACH, FELLOW, IEEE, AND DONALD R. FLACH

Abstract—**The relative ac–dc differences of a group of multijunction thermal converters (MJTC's) have been determined over the frequency range 30 Hz–10 kHz. These MJTC's are of different ranges and were obtained from several sources. Differences were observed at low frequencies when converters of various ranges were intercompared. For voltage measurements, the use of matched resistors in series with the MJTC heater resistors greatly reduced these errors and contributed to the reduction of other errors as well. It is believed that the average ac–dc difference of this group is less than 0.3 ppm at 160 Hz and 0.5 ppm up to 10 kHz.**

Introduction

MEASUREMENTS of rms current and voltage have been based on a technique which converts electrical energy into heat and compares this with the heat produced by a dc signal. Single-junction thermal converters, each consisting of a wire heated by an electric current with a thermocouple to sense the temperature-rise, have been in use for almost 3 decades at NBS for accurate rms ac–dc transfer measurements. Recently, a potentially more accurate form of the resistor–thermocouple combination, the multijunction thermal converter (MJTC), was developed at NPL by Wilkins [1]. Verification of these MJTC's, to 0.5 ppm at 9 V and 159 Hz, was initially needed at NBS for an absolute volt experiment, now well underway. Later, a goal of 1 ppm from 30 Hz to 10 kHz was established as a marked and useful advance over the present 10 ppm.

Each MJTC has a bifilar heater wire with from 50 to 200 series-connected thermocouples to sense the heater current, overcoming fundamental limitations in single-junction thermal converters [2]. Since actual converters may depart from the ideal values, experimental comparisons of converters of different construction, range, etc are desirable to buttress the theoretical accuracy. Unfortunately there are at present no other suitable kinds of ac–dc transfer standards to provide additional verification [3].

MJTC's with heaters ranging from 5 to 25 mA and with rated output EMF's of 30 to 120 mV were obtained from commercial manufacturers for this investigation, and 50-mA MJTC's were donated by NPL. Techniques were developed for intercomparing MJTC's with high precision, and a number of ac–dc errors were uncovered and overcome, to attain the desired goals.

EMF Comparator

The ac–dc difference is defined as $\delta = (Q_a - Q_d)/Q_d$ where Q_a and Q_d are the ac and dc inputs which produce the same output of a thermal converter. A modified Williams EMF comparator [4] was used with a commercial chopper-type nanovoltmeter to determine $\Delta = \delta_1 - \delta_2$, for two MJTC's whose heaters were connected either in series as thermal current converters (TCC's) or in parallel as thermal voltage converters (TVC's). A simplified schematic of the measuring circuit is shown in Fig. 1. The 11-kΩ three-stage divider D, (adjustable to 1 ppm) and the Lindeck potentiometer P, were first adjusted to bring the nanovoltmeter N, near zero for both positions of the key K with dc applied, and were thereafter not disturbed during an ac–dc determination. S was switched to ac, dc-D (direct), dc-R (reversed), and AC in succession. In each case the supply voltage was adjusted to bring N to zero[1] in the A position of K and the reading of N in the B position was recorded. As shown in [4], $\Delta = \delta_1 - \delta_2 = (N_d - N_a)/n_2E_2$, where N_a and N_d are the average voltage readings with ac and the two directions of dc applied, respectively, and n_2 is 2 for these square-law MJTC's.

When the dc reversal difference was larger than the range of N, the reversal compensator (RC) was used. It consisted of an adjustable, 0–13-μV dc source, with negligible change on reversal. It was switched on for one direction of the applied dc current and reversed for the other, so that there was no net change in the average.

Carefully timed sequences of ac–dc readings, with 30-s intervals and less than 10-ms off times were necessary to overcome serious limitations from drifts and fluctuations in the MJTC's as well as the power supplies. In some cases Johnson noise was 0.3 ppm, and detector noise was 0.6 ppm, peak to peak, in the pass band of the detector. The MJTC's were placed in a 0.02 m^3 passive oil bath in a temperature controlled room. Even so, some had to be discarded because of excessive drifts or large switching transients.

The detector had a 20-dB narrow-band rejection filter centered at 60 Hz, and was sensitive to common-mode voltage at and near harmonics of its chopper frequency of 94 Hz. Significant ac outputs at twice the input frequency[2] were observed in MJTC's below 100 Hz (approximately proportional to $1/f^{1.5}$), and at the input frequency above 1 kHz. Errors from these were reduced by modifying the filter and connecting a 2-μF capacitor across the instrument.

To verify the accuracy of the nanovoltmeter, a number of ac–dc difference measurements were also made with a

Manuscript received June 29, 1976.

The authors are with the Electricity Division, National Bureau of Standards, Washington, DC 20234.

[1] Close settings were not necessary for square law MJTC's. Like the prototype the potentiometer could be connected across E_2, but this was rarely done, except to measure E_2.

[2] Peak-to-peak ac outputs of up to 0.5 percent, over 1000 times the normally used 0.3-μV range of the detector, were observed at an input frequency of 30 Hz.

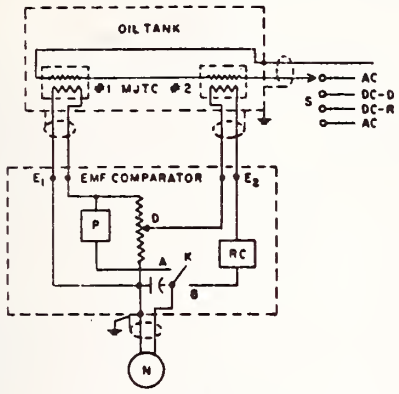

Fig. 1. Comparison circuit.

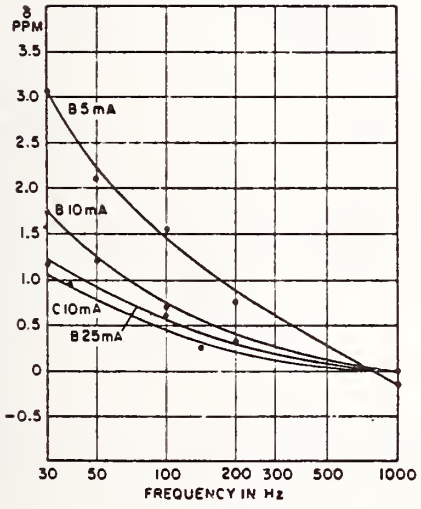

Fig. 2. Ac–dc differences of TCC's.

photocell galvanometer amplifier as a null detector, inserting small known voltages in the detector circuit with the reversal compensator. The results with the two detectors were in agreement to 0.2 ppm or better.

Low-Frequency Errors

Initial tests were made from 30 to 1000 Hz (a range near 5/1 about 160 Hz). Stepup comparisons as thermal current converters (TCC's) were made by connecting, for example, two 5-mA MJTC's in parallel (outputs in series) and connecting the pair in series with a 10-mA MJTC. The two 5-mA MJTC's were also compared, with their heaters in series. These tests disclosed alarming differences between ranges, roughly inversely proportional to frequency, as shown (at rated currents) in Fig. 2, with the 50 mA MJTC's taken as a base. The cause of these differences is as yet unknown. The error was affected by shunting the heater and was opposite in sign for TVC's. Thus it was caused by a change in the effective resistance of the heater at low frequencies.

As the frequency of the applied current decreases, the heater temperature of a thermal converter begins to follow the double-frequency variation of the instantaneous input power. This can cause low-frequency errors if the resistance is dependent on the temperature. However, the MJTC heaters are quaternary alloys of mainly NiCr, which have low temperature coefficients (0 ± 20 ppm/°C). One pair of MJTC's of the same range had nearly equal low-frequency errors but opposite temperature coefficients. The error was generally opposite in sign from that deduced mathematically by treating all of the heater as a mass at uniform temperature, with all of the heat lost by temperature-independent lateral cooling. The thermal situation must be much more complex than this, as evidenced by the measured $1/f^{1.5}$ variation of ac output with heater frequency, instead of $1/f$ as predicted by this and other simple models when the ratio of ac to dc outputs is small.

A prototype MJTC with a NiCr heater from a third manufacturer had much larger ac dc differences; about −100 ppm as a TCC and +120 ppm as a TVC at 30 Hz. This shows rather strikingly the necessity for experimentally verifying new designs. These errors agreed with the sign predicted by the model, but varied roughly as $1/f$ instead of $1/f^2$ as predicted for low ac outputs.

Ac bridge measurements showed that the low-frequency insulation resistance between the halves of a heater that had been cut in the middle was too high to account for the low-frequency error. Thus the low-frequency error is apparently not caused by the temperature coefficient of resistance of the heater or dielectric loss between the halves of the heater.

A well-known theorem states that the power in a resistor R_1 fed by a constant voltage source having a fixed internal resistance R_2 is a maximum when $R_1 = R_2$. From this, as shown in the appendix, the power in the heater of an MJTC used to measure voltage would to the first order be independent of small changes in the heater resistance if a matched (equal) fixed resistor were connected in series with the heater. Analogously, for measuring current the power would be independent of small changes with a matched resistor across the heater. Since the thermocouples respond to the power dissipated in the heater, these interesting applications of the maximum-power-transfer theorem make possible compensated MJTC's, in which the first-order errors from changes in effective resistance are eliminated, at the cost of doubling the current and voltage ranges. Calculations and tests showed that matching to 10 percent is adequate for the desired accuracy.

Other Errors

Other errors in voltage measurements arise from Peltier effects at the junctions between the heater and its lead-in wires, and skin effect in magnetic leads used in some MJTC's [1], [2]. For a given construction the errors from Peltier effects are independent of frequency (except at low frequencies) and current level, and are inversely proportional to the resistance, so that they could in principle be

TABLE I
TVC Comparisons

MJTC #1	MJTC #2	V	$\Delta = \delta_1 - \delta_2$ (ppm) 30 Hz	160 Hz	1 kHz	10 kHz
B10#2	B5#2	9	+0.4	-0.2	-0.2	-0.4
B10#44	B5#2	9	+0.6	-0.1	0.0	-0.2
B10#2	B10#44	6	+0.1	-	0.0	+0.1
"	"	9	0.0	0.0	-0.2	+0.2
C10#2	"	6	+0.4	+0.1	+0.1	+0.2
C10#1	"	6	+0.4	+0.1	+0.1	+0.6
C10#2	B10#45	6	+0.4	-0.1	-0.3	-0.1
C10#1	"	6	+0.3	0.0	+0.3	+0.2
"	B10#2	6	+0.1	+0.2	0.0	+0.4
"	A50#14	6	+0.4	0.0	-0.2	-
A50#14	A50#15	8	+0.2	0.0	-0.1	-
A50#15	B10#2	9	0.0	-0.1	+0.2	-

NOTE: B10#2 signifies a 10 mA MJTC, serial number 2, of manufacturer B.
B5#2 and B10#2 were mounted in unevacuated glass tubes at NBS.
A50#14 and #15 were in evacuated glass tubes with magnetic leads.
All others were in evacuated copper containers.

TABLE II
Assigned AC–DC Differences

MJTC	δ (ppm) 30 Hz	160 Hz	1 kHz	10 kHz
B10#44	0.0	-0.1	-0.1	-0.2
B10#45	0.0	+0.1	-0.1	0.0
C10#1	+0.3	+0.1	0.0	+0.3
C10#2	+0.4	0.0	-0.2	0.0
B10#2	0.0	-0.1	-0.1	-0.2
B5#2	-0.5	+0.1	0.0	+0.1
A50#14	0.0	0.0	+0.2	-
A50#15	-0.1	-0.1	+0.2	-

evaluated by making TVC tests with different series resistors. However the low-frequency variation can be complicated, and the evaluation is difficult in the presence of other errors. Instead these and skin-effect errors were eliminated by specifying MJTC's with copper leads, which have low thermal emfs against the quaternary heater alloys.

At higher frequencies (up to 10 kHz), tests disclosed errors in some of the MJTC's from dielectric losses between the heater and the thermocouples.[3] For example, differences of up to several ppm at 10 kHz could be obtained by changing the ground from one line to the other in tests of two 5-mA TCC's in series. Dielectric errors were also greatly reduced by the matched resistors. (See Appendix.)

TVC Tests

Since the needs were for voltage measurements, a group of 8 MJTC's of 4 different constructions and 3 current ranges, and with copper leads, were compensated with matched series resistors of quaternary alloys wound on thin mica cards.[4] Each MJTC with its resistor was mounted in an aluminum box (through which oil could circulate), with input binding posts and a 2-pin output connector of low thermal EMF's. They were compared as TVC's at 6 to 9 V, at 30, 160, 1000, and 10 000 Hz. The results are shown in Table I.

At the important frequency of 160 Hz the results are shown more vividly in Fig. 3. The circles identify the MJTC's and the number adjacent to each arrow gives $\delta_h - \delta_l$ in ppm, where δ_h and δ_l are, respectively, the ac–dc

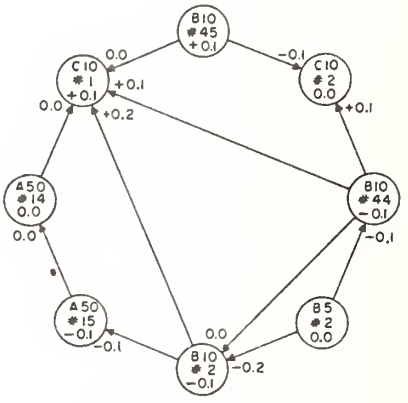

Fig. 3. TVC's at 160 Hz.

differences of the MJTC's at the head and tail of the arrow. In the absence of systematic errors the arrows around the loops should sum to zero within the limits imposed by the random errors of the comparisons. Alternatively failure to close properly is an indication of systematic errors. Techniques described by Youden [5] can be used to evaluate networks such as this.

The values of δ assigned in this way to each MJTC at 160 Hz are shown in each circle, on the assumption that the average of all is zero. Each value is less than 0.2 ppm, and the closure errors are very small.

Similar analyses were carried out for the measurements at other frequencies. The assigned ac–dc differences are shown in the columns marked δ_t in Table II. The discrepancies are somewhat larger than at 160 Hz but there is no evidence of systematic error, or of significant residual low-frequency errors in these compensated MJTC's.

The standard error s (standard deviation of the average of 4 determinations) in a comparison of 2 MJTC's was 0.12 ppm. Because of the network of comparisons the standard deviation of an MJTC with respect to the average should be somewhat less than this.

Series Resistors

The high-quality wire-wound series resistors used with these MJTC's have excellent ac–dc characteristics at audio frequencies. The phase angles are small and cause only a

[3] Dielectric losses in the oil were negligible.

[4] Two MJTC's, with 50-mA ranges, have magnetic leads and were not used above 1 kHz. A series resistor of 200 Ω was used with each, to give a 10-V range. Tests with other resistors showed that resistance-dependent low frequency errors of these MJTC's were less than 0.5 ppm. Series resistors for the other MJTC's were within 10 percent of the heater resistances.

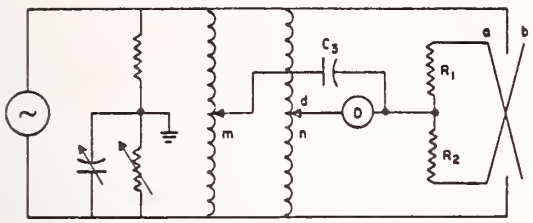

Fig. 4. Reversing bridge.

second-order effect on impedance magnitude. However there is a possibility of dielectric loss in the insulation at the higher audio frequencies. (The maximum power-transfer theorem does not help here.) To determine this, the 1/1 inductive-voltage-divider bridge shown in Fig. 4 was set up to compare two nearly equal resistors R_1 and R_2. A balance was made for each switch position of this "reversing bridge" by adjusting m and n with the detector lead d, as shown, after adjusting the Wagner arms with d grounded. Most of the bridge errors were eliminated in this way, leaving as the difference equations, $(R_2 - R_1)/R_1 = 2(n_a - n_b)$ and $\alpha_2 - \alpha_1 = \gamma(m_a - m_b)$ where R and α are the resistive components and the phase angle, respectively, of the parallel equivalent circuit for each resistor, $\gamma = \omega C_3 R$, and the subscripts a and b refer to the switch positions shown. These simple equations hold to 0.1 ppm if the phase angles of C_3 and m are each less than 0.1 mrad and $(\alpha_2 - \alpha_1)$ is less than 1 mrad.[5]

A 1-kΩ resistor of the same type as those used with the MJTC's was mounted in a metal box, for four-terminal-pair ac–dc measurements on Cutkosky's bridges [6] from 160 to 16 000 Hz. This served as a standard for evaluating two 1-kΩ unmounted resistors. These were paralleled to evaluate a 5-section 500-Ω card. The 5 sections were intercompared and then used to evaluate the 300, 400, and 500-Ω cards for the MJTC's. The 1300-Ω card for the 5-mA MJTC was compared with the 1-kΩ card in series with 3 100-Ω sections.

An upper limit of 10 kHz was imposed by the effects of lead inductance and of stray capacitance from the cards to the grounded aluminum boxes in which they were tested and used. Below this, changes in the parallel resistances were less than 0.1 ppm for drastic changes in the positions of the resistors. The cases of the inductive voltage dividers and the shields of all leads of the reversing bridge were grounded. C_3 was a low-loss 3-terminal air capacitor, and D was a tuned null detector. All bridge components were commercially available.

Measurements were made at 0.1, 1, and 10 kHz with 8 V applied. The results are shown in Table III as δ_e and α, where $\delta_e = (R_f - R_p)/R_p$ and α is the phase angle. R_f and R_p are the parallel-equivalent-circuit resistances at the frequency f and the base frequency (0.1 kHz), respectively. For each resistor, α was closely proportional to f, and so is not shown at 1 kHz in the table.

[5] The dividers were rated up to 10 kHz. Only the lower dials were changed on reversal, with only moderate accuracy required.

TABLE III
Resistance Measurements

MJTC	R_s Ω	1 kHz δ_e	10 kHz δ_e	10 kHz α	10 kHz δ_r	10 kHz δ_c
B10#44	500	-0.1	-0.7	-0.55	-0.5	+0.3
B10#45	"	+0.1	+0.3	-0.41	+0.1	-0.1
C10#1	300	0.0	+0.5	-0.60	+0.1	+0.2
C10#2	"	0.0	0.0	-0.41	-0.1	+0.1
B10#2	400	0.0	+0.4	-0.47	+0.1	-0.3
B5#2	1300	0.0	0.0	-0.26	0.0	+0.1

NOTE: All values of δ in ppm, α in mrad. See text.

The effect of these small errors on the magnitude of the current through the MJTC is approximately $\delta_r = \delta_e/2 - 3\alpha^2/8$. This was negligible at 1 kHz and, except for one resistor, even at 10 kHz. The average for all of the resistors was less than 0.1 ppm at each frequency, so that no corrections need be applied to Table II.

The ac–dc differences of a TVC is $\delta_v = \delta_r + \delta_c$ [2] where δ_c is the ac–dc difference of the thermal converter. Since δ_v and δ_r were evaluated as indicated above, δ_c could be determined for each MJTC. As shown in Table III, each was 0.3 ppm or less at 10-kHz.

Conclusions

This work reaffirms the value of both experimental and theoretical investigations to evaluate ac–dc differences in an absolute sense, and to determine how well actual ac–dc transfer standards meet the theoretical ideals. A number of sources of ac–dc differences were uncovered, and were eliminated by changes in design, or were compensated for. The agreement between a group of 8 MJTCs which met these requirements was excellent. Because of this, because of the significant differences in construction and ranges of these MJTC's, and because of our long investigation, we believe it is very unlikely that the average ac–dc difference of this group exceeds 0.3 ppm at 160 Hz or 0.5 ppm at 30 and 10 000 Hz. This belief is supported by an analysis based on estimates of the limits of error from such factors as mismatch of series resistors, Peltier-heat exchanges, ac–dc differences of resistors, systematic errors in the comparator, and random errors. For the latter we took as the 95 percent confidence limit $2s/\sqrt{n}$, where n is the number of MJTC's in the group.

A few measurements over several months indicate a repeatability of 0.3 ppm or better. The long-term stability of ac–dc difference is as yet unknown, but there is no reason to expect drifts greater than this.

Extensions to higher voltages and frequencies seem feasible. Small ac–dc differences in the effective heater resistance could be compensated with combined shunt and series resistors, as indicated in the Appendix. A wide range of film resistors could be mounted in a geometry that would allow the reactance to be calculated, so that the powerful comparison technique of [2] could then be applied.

Appendix
Compensation for Changes in Resistance

When a resistor mR is in series with MJTC heater, $R(1 + a)$, $a \ll 1$, the current (with no reactance) is

$$I = \frac{V}{(m+1)R(1 + a/(m+1))} \simeq \frac{V}{(m+1)R}\left(1 - \frac{a}{m+1}\right)$$

neglecting higher order terms in a. The power in the heater is

$$P = I^2R(1+a) \simeq \frac{V^2}{(m+1)^2R}\left(1 - \frac{2a}{m+1} + a\right).$$

For a fixed V and m, the power is independent of a if $m = 1$ (neglecting higher order terms). Thus since the thermocouples respond to the power dissipated in the heater, a small difference between the effective dc and ac heater resistances will cause no first-order ac–dc difference in a TVC with a matched series resistor. Matching to 10 percent will reduce a 2 ppm ac–dc difference (from this cause) to 0.1 ppm.

Similarly for a TCC with mR in parallel with $R(1 + a)$ the power in the heater is independent of a if $m = 1$, so that there will be no first-order ac–dc difference with a matched shunt.

This compensation will be effective, however, only if the heater is a two-terminal resistor in the measuring circuit, and if the thermocouples are insensitive to any change in the distribution of the power. For example, an error would occur with dielectric leakage from the heater to the thermocouple of an MJTC unless the thermocouple output and one end of the heater were connected together, and the thermocouple resistance was much less than the insulation resistance.

Matching provides only a single compensated voltage or current range. However, for higher voltage ranges a similar analysis shows that if a resistor nR is connected across the heater and mR in series with the combination, compensation is achieved if $n = m/(m-1)$.

Acknowledgment

The authors are very grateful to F. Wilkins for the NPL MJTC's, to R. Cutkosky for the ac–dc measurements of the mounted resistor, and to J. Sutcliffe and I. Malcolm of Guildline Instruments Ltd. for their extended cooperation.

References

[1] F. J. Wilkins, "Theoretical analysis of the ac/dc transfer differences of the NPL thermal converter over the frequency range dc—100 kHz," *IEEE Trans. Instrum. Meas.*, vol. IM-21, pp. 334–340, 1972.

[2] F. L. Hermach and E. S. Williams, "Thermal converters for audio-frequency voltage measurements of high-accuracy," *IEEE Trans. Instrum. Meas.*, vol. IM-15, pp. 260–268, 1966.

[3] F. L. Hermach, "Ac–dc comparators for audio-frequency current and voltage measurements," to be published.

[4] E. S. Williams, "Thermal voltage converters and comparators for very accurate ac voltage measurements," *J. Res. Nat. Bur. Stand.*, 75C, pp. 145–154, July–Dec. 1971.

[5] W. J. Youden, "Measurement agreement comparisons," in *Proc. 1962 Standards Lab. Conf.*, NBS Misc. Publ. 248, pp. 147–152, Aug. 1963.

[6] R. Cutkosky, "New NBS measurements of the absolute Farad and Ohm," *IEEE Trans. Instrum. Meas.*, vol. IM-23, pp. 305–309, 1974.

IEEE TRANSACTIONS ON INSTRUMENTATION AND MEASUREMENT, VOL. IM-23, NO. 4, DECEMBER 1974

A Low-Temperature Direct-Current Comparator Bridge

D. B. SULLIVAN AND RONALD F. DZIUBA, MEMBER, IEEE

Abstract—**The application of superconducting direct-current comparators to the measurement of resistance ratios is described. One comparator consists of a binary set of ratios between 1:1 and 160:1 providing for self-calibration by a buildup procedure. A second comparator exhibiting discrete ratios of 1:1, 10:1, and 100:1 is also described. Ratio uncertainty of less than 1 part in 10^9 is achieved by enclosing the ratio windings in overlapping toroidal superconducting shields. Superconducting quantum interference devices (SQUID's) serve as flux sensors for the comparators. One of these current comparators is used to calibrate a 100-Ω:1-Ω resistive divider, which at a current of 10 mA exhibits a self-heating error of 0.0023 ppm.**

INTRODUCTION

RECENT papers [1]–[3] have described the application of superconducting shielding and superconducting quantum interference devices (SQUID's) to the problem of current-ratio measurements. At low current these direct-current comparators outperform their conventional room temperature counterparts in accuracy and sensitivity by several orders of magnitude. This paper describes a further advance in the design of such comparators and the application of a direct-current comparator to the calibration of a 100:1 resistive divider and the evaluation of the resistor power coefficients [4].

The original work on low-temperature comparators was done by Harvey [1]. His concept can be readily understood by considering a long superconducting tube enclosing several wires. Current through one wire of the cable results in an equal and opposite current on the inner surface of the tube. This current returns on itself via the external surface of the tube, and one thus obtains the ideal condition wherein the same current flowing through different windings generates identical fields outside the cable. That is, the fluxes sensed outside the tube are only the mutual fluxes of the wires in the tube and not the leakage fluxes. To form a comparator then, one need only fashion a coil out of such a cable and interconnect a number of windings to arrive at the desired ratio. The null flux is sensed within this coil and care must be taken to shield the cable ends (which deviate from ideal behavior) from the null sensor.

Harvey's comparator offers an elegant means of constructing a current comparator, but the application of the concept becomes quite tedious for large ratio ($\gg 10$) devices since one must essentially build up the large ratio by connecting together a series of unit windings. For this reason a modified version of the shielding was developed and is called an overlapped-tube shield [3]. This shielding permits continuous windings and thus circumvents the aforementioned drawback.

Two comparators of this design were constructed. The first (binary) comparator consists of a binary set of windings which provides all integer ratios between 1:1 and 160:1 and as a consequence permits a completely consistent check of ratio uncertainty. This comparator has a sensitivity of 0.032 nA (for a 14-turn unit winding) with no ratio errors detected above the noise level (less than 5 parts in 10^{10}). The second (decade) comparator contains four windings providing discrete ratios of 1:1, 10:1, 100:1, and an additional unit winding for checking the balance of the comparator. This comparator is designed to couple indirectly to a SQUID sensor via a flux transformer. It exhibits a resolution of 0.06 nA for a 20-turn unit winding and ratio uncertainties of less than 5 parts in 10^9.

A 100-Ω:1-Ω resistive divider was calibrated using the binary comparator. The resistors were fabricated from a silicon copper alloy [5], with the 1-Ω resistor exhibiting a power coefficient of resistance as small as 0.023 ppm/mW. At an operating level of 1 V for the 100:1 divider, the self-heating error is 0.0023 ppm. The power coefficient of the resistors was measured over the temperature range of 1.5–4 K, and it would appear that reasonable operation could be expected at 4 K as well as just below the λ point (2.17 K, the temperature below which the liquid helium behaves as a superfluid).

CURRENT COMPARATOR

The shield configuration for the comparator is shown in Fig. 1. The superconducting shield is insulated at the overlap so that it appears like a snake swallowing its tail. The leads to the ratio windings are enclosed in superconducting tubes with an added tube for every turn of overlap. These shields for the leads are also insulated from one another. Care is exercised to prevent any continuous superconducting connection around the toroidal shield as this would short the windings. The null flux is sensed in the center window of the toroid either directly with one of Zimmerman's multihole SQUID's [6] or indirectly by a similar SQUID via a flux transformer.

The performance of this type of shield is readily understood as a simple extension of the principle of Harvey's shield. The external flux generated by every winding within the shield results from the induced flow of a surface current on the shield. The purpose of the overlap is to reduce the nonideal effects at the ends of the tube. The

Manuscript received July 3, 1974. This work is a contribution of the National Bureau of Standards and is not subject to copyright.

D. B. Sullivan is with the Cryogenics Division, National Bureau of Standards, Boulder, Colo. 80302.

R. F. Dziuba is with the Electricity Division, National Bureau of Standards, Washington, D. C. 20234.

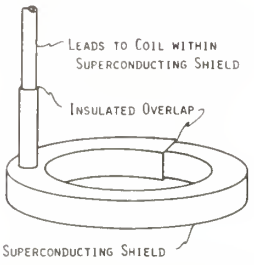

Fig. 1. Overlapped-tube shield for the comparator. The superconducting shield is formed over the windings as a continuous tube which overlaps itself. The overlap is insulated and runs approximately $1\frac{2}{3}$ turns around the toroid. At each intersection of the toroidal shield with the leads from the coil, a superconducting lead shield is attached to the shield. These two tubes are also insulated from one another.

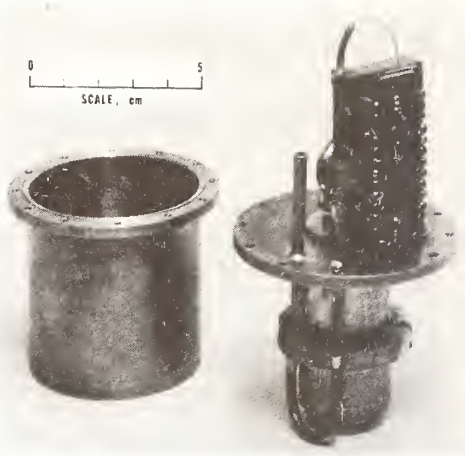

Fig. 2. Binary current comparator. The can on the left, when attached to the comparator, provides a complete superconducting shield of the SQUID and windings from external fields. The shielded leads from the coil leave the interior of the shield can via another flux attenuation tube. The individual coil leads are spot welded to the niobium posts on the terminal board. The SQUID is within the toroidal shield and is enclosed by a thin brass shield which serves as a low-pass filter to isolate the ratio windings and the SQUID at radio frequencies.

overlap acts as a simple flux attenuator that reduces direct leakage of flux from the windings to the exterior regions of the shield. With this in mind, the required overlap can be roughly estimated. The pertinent attenuation parameters include the length, thickness, and perimeter (width) of the overlap region. As a practical matter the minimum thickness of overlap is limited by available insulation materials. Thus, the only really adjustable parameters are the length and perimeter of the overlap. As a conservative estimate of the attenuation, a flux reduction of a factor of 10 is assumed for every unit of the length–perimeter ratio. The shield is designed with $1\frac{2}{3}$ turns of overlap which corresponds to a length–perimeter ratio of ~ 9 (length = 17.5 cm and perimeter = 2.0 cm). Thus if the windings are initially matched to 10 percent, the 10^9 attenuation of leakage flux would result in a balance error of 10^{-10} or less.

Several methods were used to fabricate the winding and toroidal overlapped shields. For the binary comparator, the coil, which consists of 10 sets of windings of 0.074-mm-diameter niobium wire (insulated), is wound on a thin (0.5-mm-thick) aluminum form and impregnated with epoxy during the winding process. After the epoxy sets, the aluminum form is removed chemically with sodium hydrozide. This results in a rigid coil, which makes the shield fabrication much simpler. The ratio windings have relative winding values of 1, 1, 1, 2, 4, 8, 16, 32, 32, and 64. Each unit winding consists of 14 turns of the niobium wire. The construction of the decade comparator is similar. The prime difference is that a removable Teflon form was used in the casting of the rigid coil. Also, rather than epoxy, alpha cyanoacrylate adhesive was used to bond the coil together.

Both shields are composed of a lead–tin alloy (0.125 mm thick) which is formed around the rigid coil and sealed with Rose's metal (50-percent Bi–25-percent Pb–25-percent Sn, $T_c \approx 8.5$ K). The shield is fabricated in roughly one-turn sections and each section is then insulated with Teflon tape (except at one end) before the subsequent shield section is formed on top of it. As each turn of the shield is added it is connected in series with the underlying shield to form the continuous overlapped tube. The leads into the coil are shielded with lead tubes that are soldered to the main shield tube. At each point where the toroidal shield intersects the leads to the coil, a lead tube is connected to the intersecting portion of the shield. These lead tubes are insulated from one another.

The completed binary comparator is shown in Fig. 2. The SQUID sensor is inside of a thin-walled (0.10-mm-thick) brass shield within the center of the toroid. The brass shield acts as a low-pass filter to isolate the SQUID and ratio windings at radio frequencies. The ratio windings and sensor are housed within a superconducting shield fabricated from brass and electroplated with ~ 0.05 mm of lead. The shielded leads from the ratio windings are routed through a field attenuation tube and the wires are spot welded to niobium posts on the terminal board. Niobium wire is used to interconnect coils to achieve the desired ratio.

The SQUID consists of a superconducting loop (or loops) of low inductance which is closed by a weak link or Josephson junction. The SQUID RF impedance is a periodic function of the flux linking the ring with a period of one flux quantum, $\varphi_0 \approx 2.07 \times 10^{-15}$ Wb. The flux quantum is thus a natural unit with which to describe the comparator performance. For this particular device a resolution of $10^{-4}\varphi_0$ is achieved. For further details of SQUID operation the reader might consult a paper by Zimmerman *et al.* [7].

The sensitivity of one unit winding of the binary comparator is found to be 3.2×10^{-7} A/φ_0. At the flux resolution of $10^{-4}\varphi_0$ this results in a sensitivity of 3.2×10^{-11} A for a unit winding. Each unit of winding consists of 14 turns so that the sensitivity can also be expressed as ~ 0.45 nAt.

The ratio uncertainty of the binary comparator was

determined by comparing windings in series opposition in a buildup fashion. The unit windings are intercompared; the sum of two of the unit windings is compared to the two-unit winding; the sum of the two-unit winding and two of the unit windings is compared to the four-unit winding; the buildup is continued in this fashion until all windings are intercompared. A fixed current of 70 mA was passed through such matched sets of windings connected in series opposition, and the departure from null was then used as a measure of the ratio uncertainty. For every measurement no error could be detected down to a level of $10^{-4}\varphi_0$. For the 1:1 comparison this results in an uncertainty of less than 5×10^{-10} and for the $(32 + 32):64$ comparison an uncertainty of less than 7.5×10^{-12} is indicated. It is interesting to note that the largest error is expected for the last intercomparison because the 64-unit winding and the two 32-unit windings are further separated within the coil than are any of the other intercompared sets. Thus, while a limit of 5×10^{-10} is set experimentally for the intercomparison of the unit windings, the limit is more likely to be smaller than 7.5×10^{-12} as found for the $64:(32 + 32)$ comparison. Since no actual uncertainties were measured, it is assumed as a "worst case" that all errors are of the same sign and have a value equal to the limit of error. For a ratio of 160:1 this yields an estimated error of approximately 1×10^{-9}.

The shielded coil of the decade comparator is 2.0 cm long with inside and outside diameters of 1.8 cm and 2.2 cm, respectively. As with the binary comparator, it is housed in a superconducting can with a brass shield within the window of the toroid. A one-turn coil of niobium tape of thickness 0.05 mm and a diameter of 1.6 cm is located within the brass shield. This coil is connected to a niobium coil closely coupled to a SQUID sensor, thus forming a flux transformer. Operation with the flux transformer reduces the sensitivity of the comparator by approximately 20 percent, but it eliminates the need to permanently house the SQUID sensor in the window of the toroid. Alternatively, other types of SQUID's can be used for operation of the comparator. For this particular arrangement a sensitivity of 0.06 nA for a 20-turn unit winding or 1.2 nAt is achieved.

The unit windings were intercompared with a test current of 150 mA by the technique described earlier. Results indicate errors of less than 1 part in 10^9. The 10:1 and 100:10 ratios were compared to the 10:1 ratio of a Harvey-type comparator [3] accurate to 4 parts in 10^{10}. Measurements were limited to 5 parts in 10^9 because of noise and resistor instabilities.

BRIDGE

Fig. 3 shows the bridge connection of the divider resistors (NR and R) and comparator for the purpose of calibrating the divider and measuring the power coefficient of these resistors. A superconducting switch [8] is used to switch the system from this configuration to a simple series connection of the resistors as a voltage divider. The windings of the comparator are superconducting; thus,

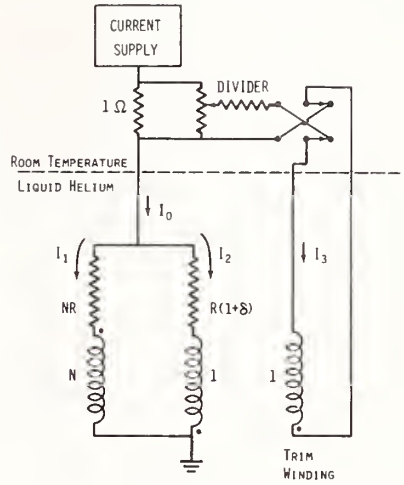

Fig. 3. Circuit for the current comparator bridge. The resistors are trimmed so that the error δ is small (of order 10^{-5} or less) and thus the bridge is not far from balance. A current I_3 is supplied to a trim winding to realize the final balance condition. The coils and all interconnections are superconducting, insuring that identical voltages appear across the resistors.

the voltage drop across each resistor is the same and the ratio of power dissipations is the inverse of the resistance ratio. The resistors are initially trimmed to be close to the desired ratio, and the deviation from the divider ratio can then be measured by noting the relative current required in the trim winding to achieve null. Thus, if the initial balance of the resistance ratio is 1 part in 10^5, the trim current relative to the main current need be known to only 1 part in 10^4 in order to realize a 0.001 ppm measure of the resistance ratio. This level of accuracy can be readily obtained with a simple room temperature resistance network to divide off part of the main current and deliver it to the trim coil (see [4]). The fact that the dissipation level in the two resistors is so much different allows one to measure the power coefficient readily. One simply measures the bridge output as a function of current and observes that a nonlinearity in this relationship results from self-heating changes in the smaller resistor.

RESISTORS

The two-terminal resistors are composed of a silicon–copper alloy [5] (96-percent Cu–3-percent Si–1-percent Zn). The wire diameter is 0.25 mm, a factor of 2 larger than that used in previous resistors [4], [9], [10]. This factor of 2-in diameter is important since, for the same value of resistance, it provides an eightfold improvement in performance (because the surface area for heat dissipation is increased by a factor of 8).

The resistor terminations are quite similar to those described by Harvey and Collins [4]. The wire is hard soldered (50-percent Ag–50-percent Cu) to a piece of copper, and connection to the superconducting circuit is then made with a lead–tin solder connection to the copper block. The direct application of solder to the resistance wire results in an added problem which is especially acute

for short (low-value) resistors. The boundary between superconducting and normal metals can move slightly with changing current and thus causes an effective change in resistance. Resistors described earlier [9] were ~7 m long and this problem was not too severe. However, the 1-Ω resistor described in this paper is ~16 cm long and with direct solder connections was found to vary at low currents by more than 1 ppm. The form of this variation involves a rapid change with changing current at low current levels with a saturation at higher current; a distinctly different behavior than produced by heating. The use of the copper intermediary terminal seems to eliminate this problem.

The bridge measurements were performed in a fashion similar to that described by Harvey and Collins [4]. Referring to Fig. 3, the balance equation is

$$NI_1 = I_2 + I_3.$$

Then noting the conservation of current $I_0 = I_1 + I_2$ and the equivalence of the voltages across the resistors we have

$$\delta \approx I_3/I_2 \approx \frac{N+1}{N}\left(\frac{I_3}{I_0}\right)$$

neglecting the second- and higher order terms of δ. Thus δ, the correction to the resistance ratio, is determined by the comparator ratio N and the accuracy of the ratio I_3/I_0. The accuracy with which δ is measured is, of course, also dependent upon the sensitivity of the null of the bridge. The implicit assumption for the approximation which leads to the last equation is that the value of δ is smaller than the precision to which it must be measured. Thus, if the resistors are trimmed to roughly 1 part in 10^5, then the last equation can readily be used to determine δ to 1 part in 10^4 and a divider calibration of 0.001 ppm results.

The resistor power coefficient is then measured by noting variations of δ with the current I_2. The bridge output when plotted as a function of I_0 (which is proportional to I_2) is a quadratic function of current, consistent with self-heating. The power coefficient is plotted in Fig. 4 as a function of temperature. This particular plot is for the 1-Ω resistor which is expected to be used at a power level of 0.1 mW. Harvey and Collins [4] have obtained a power coefficient measurement for this same material (0.125-mm diameter rather than 0.25-mm diameter) at 2.1 K and it is worth comparing these results with their measurement. At 2.1 K, Harvey and Collins measured the power coefficient to be −0.013 ppm/mW for a 10-Ω resistor. From Fig. 4, the corresponding coefficient is −0.023 ppm/mW (1-Ω resistor) which implies a coefficient of −0.0023 ppm/mW for a 10-Ω resistor. If the wire diameter were reduced by a factor of 2, the surface area for heat dissipation would be reduced by a factor of 8 and the power coefficient should be $-0.0023 \times 8 = -0.0184$ ppm/mW which is reasonably consistent with the Harvey and Collins measurement of −0.013 ppm/mW. Some difference might well be expected since the insulation

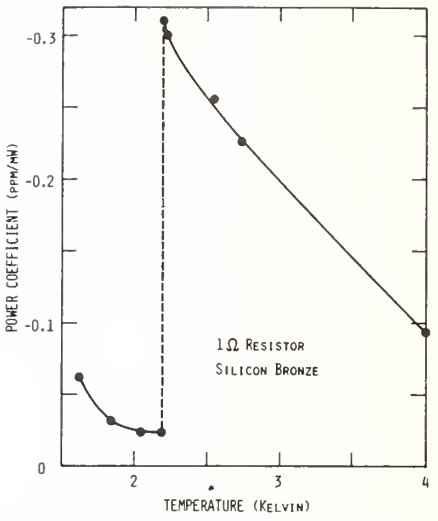

Fig. 4. Power coefficient of the 1-Ω resistor as a function of temperature. Below the λ point (2.17 K), heat dissipation is limited solely by the boundary conductance between the wire and superfluid. Above the λ point, strong convection limitations exist producing an increase in power coefficient.

was slightly different in thickness on the two wires and the extra reduction in diameter might be expected to affect the temperature coefficient of resistance. While we have not measured the temperature coefficient of resistance of this particular sample of wire, the agreement with the Harvey and Collins number suggests that the temperature coefficient is probably near that which they measured, namely, −8 ppm/K at 2.2 K.

Another important facet of the operational characteristics of the resistors is the differential temperature coefficient of two resistors since this determines the bath stability required for a desired ratio stability. We simply note here that the resistance ratio varied by less than 0.2 ppm between 4 and 1.5 K while the absolute resistance changes by more than 8 ppm. Thus the temperature coefficients appear to track within a few percent and the bath stability requirements are reduced significantly (a bath stability of 10 mK results in better than 0.001 ppm ratio stability). These two resistors were fabricated from adjacent segments of the resistance wire and perhaps this is necessary to assure a small differential temperature coefficient.

The thermal boundary resistance was calculated [4] to be 0.2 W/cm² K at 2.1 K, a result which falls within the range of values reported for uncoated copper surfaces [11]. Thus one gains confidence that the resistor power coefficient is determined solely by the boundary heat transfer and the temperature coefficient of resistance. This confidence is needed to make the assumption that the power coefficient of the wire in the larger resistor (100 Ω in this case) is the same as that in the smaller one (1 Ω). This assumption is valid only below the λ point (2.17 K) since it is only there that the boundary resistance dominates the heat transfer. Indeed, the large increase in power coefficient at the λ point is a result of the onset

of convective flow limitations which accompany the disapearance of the superfluid. The boundary conductance continues to increase (proportional to T^3) with temperature above the λ point.

CONCLUSIONS

The development of superconducting current comparators has progressed well beyond the accuracy requirements for most applications. While these comparators are orders of magnitude more sensitive than their conventional counterparts, one could argue that further improvement would be of value. Present comparator sensitivity is limited by noise in the RF preamplifier of the SQUID system and thus further improvement of the comparators should accompany future reductions of this noise contribution.

The overwhelming advantage of a comparator-calibrated resistive divider is the availability of a completely consistent set of internal checks on the system performance. The comparator windings can be intercompared to ascertain the ratio uncertainty, and the power coefficient of the resistors can be determined directly during the divider calibration.

The operation of a resistive divider above the λ point offers a simplification which might be attractive. The value of the power coefficient at 4 K given by Fig. 4 results in an error of 0.01 ppm at 0.1-mW dissipation, a not unreasonable number. Unfortunately, one cannot assume that the power coefficient for the 100-Ω resistor is the same. In fact, it will likely be larger since the wire is more closely packed as a result of its length, and convection of heat by the fluid is thus poorer. This matter could be checked by using a still larger resistor as a reference in measuring the power coefficient of the 100-Ω resistor. In any event, further work is necessary before such resistors can be used above the λ point. The development of a resistance material with a much smaller temperature coefficient, while not essential, would certainly offer welcome simplifications.

REFERENCES

[1] I. K. Harvey, "A precise cryogenic dc ratio transformer," *Rev. Sci. Instr.*, vol. 43, pp. 1626–1629, Nov. 1972.
[2] K. Grohmann, H. D. Hahlbohm, H. Gubbig, and H. Ramin, "Construction principles and properties of ironless dc and ac current comparators with superconducting shields," presented at the Electrical and Electronic Test Instrument Conf., Ottawa, Canada, May 1973; also, in *PTB-Mitteilungen*, vol. 5, pp. 313–318, May 1973.
[3] D. B. Sullivan and R. F. Dziuba, "Low temperature direct current comparators," *Rev. Sci. Instr.*, vol. 45, pp. 517–519, Apr. 1974.
[4] I. K. Harvey and H. C. Collins, "Precise resistance ratio measurements using a superconducting dc ratio transformer," *Rev. Sci. Instr.*, vol. 44, pp. 1700–1702, Dec. 1973.
[5] D. B. Sullivan, "Resistance of a silicon bronze at low temperatures," *Rev. Sci. Instr.*, vol. 42, pp. 612–613, May 1971.
[6] J. E. Zimmerman, "Sensitivity enhancement of superconducting quantum interference devices through the use of fractional-turn loops," *J. Appl. Phys.*, vol. 42, pp. 4483–4487, Oct. 1971.
[7] J. E. Zimmerman, P. Thiene, and J. T. Harding, "Design and operation of stable rf-biased superconducting point-contact quantum devices, and a note on the properties of perfectly clean metal contacts," *J. Appl. Phys.*, vol. 41, pp. 1572–1580, Mar. 1970.
[8] J. D. Siegwarth and D. B. Sullivan, "A mechanical superconducting switch for low temperature instrumentation," *Rev. Sci. Instr.*, vol. 43, pp. 153–154, Jan. 1972.
[9] D. B. Sullivan, "Low temperature voltage divider and null detector," *Rev. Sci. Instr.*, vol. 43, pp. 499–505, Mar. 1972.
[10] J. C. Gallop and B. W. Petley, "Recent NPL work on the AC Josephson effects as a voltage standard," *IEEE Trans. Instrum. Meas.*, vol. IM-21, pp. 310–314, Nov. 1972.
[11] N. S. Snyder, "Thermal conductance at the interface of a solid and helium II (Kapitza conductance)," Nat. Bur. Stand., Tech. Note 385, Dec. 1961.

Reprinted by permission from IEEE TRANSACTIONS ON INSTRUMENTATION AND MEASUREMENT
Vol. IM-23, No. 4, December 1974, pp. 256-260

JOURNAL OF RESEARCH of the National Bureau of Standards — C. Engineering and Instrumentation
Vol. 75C, Nos. 3 and 4, July–December 1971

Thermal Voltage Converters and Comparator for Very Accurate AC Voltage Measurements

E. S. Williams

Institute for Basic Standards, National Bureau of Standards, Washington, D.C. 20234

(July 22, 1971)

A new fourteen-range set of thermal voltage converters and a thermoelement comparator are used to measure ac-dc difference, and a-c voltages relative to external d-c standards, with 20 ppm (parts-per-million) accuracy at audio frequencies. The imprecision is less than 2 ppm. Corrections relative to the very stable middle ranges can be redetermined for every range by a seven-step intercomparison of certain adjacent ranges.

Key words: AC-DC difference; comparator; thermoelement; transfer voltmeter; voltage measurements.

1. Introduction

An a-c voltage at audio frequencies is measured most accurately at the present time by using a thermal voltage converter (TVC) to compare it with a stable and accurately measured d-c voltage, which is nominally equal to it. The basic d-c standards are then, in effect, "transferred" to the a-c measurement. The TVC may be simply a thermoelement (TE) in series with an appropriate multiplier resistor. The output emf of the TE is ordinarily monitored with a null detector and a balancing circuit, which may be a Lindeck potentiometer. A balancing circuit and a null detector are included in most commercial multirange models.

Before the TVC is used for a-c voltage measurements it must be tested for ac-dc difference or frequency influence so that corrections may be applied. The set of TVCs and the new TE comparator described in this paper were developed primarily for making these tests. However they may also be used for a-c voltage measurements as explained in section 9. For ac-dc difference measurements the TE comparator, whose read out instrument may be either a nanovoltmeter or a galvanometer, provides a considerable advantage over other methods in overcoming the difficulties caused by power supply instability and inexact voltage control.

The 14-range set of TVCs (designated No. 7) consists of six resistor units and two TEs, and extends from 1 to 1000 V. The TEs are rated at 2.5 and 5.0 mA, and each one may be attached to any one of the resistors by a coaxial connector (see fig. 1). This permits each resistor to be used for two voltage ranges, as shown in table 1. Certain adjacent ranges of the set can be intercompared, and the ac-dc differences of all the ranges can be determined relative to any one range. This set is otherwise similar to an earlier set [1][1], which consisted of two 5-mA TEs and 12 series resistors, and covered a range from 0.5 to 500 V. The earlier set, designated No. 1, has been extended to 1000 V with one additional resistor as part of the present project. It is evaluated in a 14-step intercomparison in which each range is compared, at reduced voltage, with the next lower one.

In a well designed TVC the ac-dc difference is not affected by changes in the applied voltage. Therefore, an ac-dc difference determined for the 100-V range at 60 V can be applied as a correction when this resistor is used at 200 V to test the nominal 300-V range of the next higher resistor. Experience has shown this step-up procedure to be feasible. However if the higher voltage ranges are not carefully built the ac-dc differences can change due to self-heating effects to be described later.

2. Design and Construction

The two TEs are mounted in 2-in brass tubes (see figs. 1 and 2, upper right) with coaxial connectors for attaching to a resistor. The 2.5 mA-TE has a 400 Ω heater and is used alone as the 1-V range. The 5 mA-TE has a 125 Ω heater and a 275 Ω resistor is added inside its enclosure to make a 400 Ω, 2-V range.

The middle ranges (six ranges, 3 to 60 V) make use of three resistors—0.8 kΩ, 3.6 kΩ, and 12 kΩ (see table 1). Each of these is a 2W metal-film resistor mounted coaxially in a 3-in brass cylinder 4 1/2 in long with coaxial connectors at each end.

[1] Figures in brackets indicate the literature references on page 153.

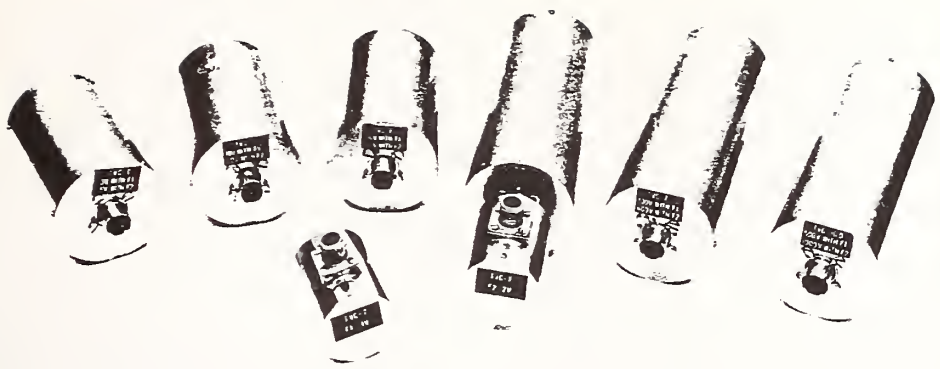

FIGURE 1. *New set of thermal voltage converters.*

The simple symmetrical geometry of these units permits approximate calculations of their reactances [2]. The calculations are inexact because of the necessary assumptions as to end-effects, and they neglect any small residual reactances of the resistors themselves. They do indicate however, that the frequency error of each resistor unit (without the TE) should be less than 1 ppm at 50 kHz, even for tubes smaller than 2 in in diameter. (The 3-in tube was chosen for the higher ranges where more space is necessary and was therefore used for the middle ranges also.)

The higher voltage ranges have larger resistor assemblies to avoid excessive temperature rise. The 100–200 V unit has a 40 kΩ spiraled metal-film resistor five inches long.[2] The 300–600 and 500–1000 V units have resistors of tin oxide deposited on a 0.81-in glass tube 6 in long. A small voltage coefficient was anticipated in these resistors, but measurements have shown it to be negligible.

[2]This experimental resistor is not ordinarily available commercially. Four 40 kΩ metal film resistors in series-parallel can also be satisfactory.

TABLE 1. *NBS thermal voltage converter set No. 7*

Fourteen voltage ranges (column 2) are formed with six series resistors and two TEs (F 1 and F 2).

Series resistor	*Voltage range*	*TE*	*Total resistance*
kΩ		*mA*	*kΩ*
.....	1	2.5 (F 1)	0.4
.....	2	5.0 (F 2)	0.4
	3	2.5	1.2
0.8.....	6	5.0	1.2
	10	2.5	4.0
3.6.....	20	5.0	4.0
	30	2.5	12.4
12.....	60	5.0	12.4
	100	2.5	40.4
40.....	200	5.0	40.4
	300	2.5	120.4
120.....	600	5.0	120.4
	500	2.5	200.4
200.....	1000	5.0	200.4

Errors in these ranges are caused mainly by capacitance between the resistor assembly and the outer casing, which permits alternating current to bypass the TE to ground. Therefore more a-c than d-c voltage is required for a given TE output. Frequency compensation could be provided by placing relatively small capacitors in parallel with part of the resistance. However, such capacitors probably would not be sufficiently stable over a long period of time and might be affected by temperature changes which occur in the resistor enclosure.

Compensation was therefore provided (as in the earlier set No. 1) with an inner shield which is connected to the input and surrounds the high- or input-end of the resistor (see "S" in fig. 2). The shield is positioned, relative to the resistor, to control the capacitance currents and provide optimum high-frequency

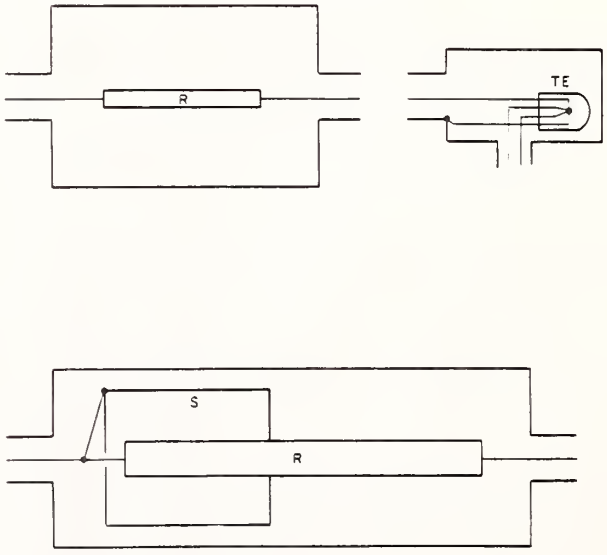

FIGURE 2. *Essentials of thermal voltage converters.*
Thermoelement (TE) enclosure, low voltage unit with resistor (R), and high voltage unit (100 to 1000 V) with resistor (R) and frequency compensation shield (S).

compensation: perfect compensation is possible only at one frequency.

3. 1000-V TVC

As stated earlier the corrections for the high and low voltage ranges are determined relative to the middle range by intercomparison tests. It is necessary therefore that the ac-dc difference of all ranges be unaffected by voltage level. The voltage effect is rare in low and middle ranges, but it can be troublesome at higher ranges where the heat generated by the resistor is appreciable. All intercomparison tests were initially made at two voltage levels in order to evaluate this effect—or to prove its absence. If, for example, the nominal 600-V range is compared with the 1000-V range at both 400 and 600 V, and the same results are obtained, it is unlikely that the 600-V range is affected by the voltage increase (the 1000-V range is very probably unaffected at these voltages). However both ranges are in question until we are assured that the 1000-V range is also free of this effect.

The highest range, then presents a special problem. It is more likely to change due to increased voltage (heating) and there is no higher range to compare it with. If it is compared with another 1000-V TVC at two or more voltages and no change is observed it is possible that both have the same voltage effect. However this is unlikely if TVCs are of somewhat different design. If intercomparisons of several units of difference design show no change between rated voltage and a lower voltage we may safely assume this effect is negligible in each one.

Five 1000-V TVCs (table 2) have therefore been built, each with differing components, and a network of intercomparison tests was made as described in the next section. The original set of TVCs [1] was included in these tests.

TABLE 2. *Five 1000-V TVCs*

Unit	*Resistance*	*Voltage range with TE*		*Resistor assembly*
		F 1	*F* 2	
	kΩ			
A	400	1000		Four 100 kΩ wirewound resistors in series, each 1 3/8 in long.
B	400	1000		Four 100 kΩ wirewound resistors in series, each 1 3/8 in long.
C	200	500	1000	Four 200 kΩ metal-film resistors in series-parallel, each 2 in long.
D	200	500	1000	One 200 kΩ tin oxide resistor 6 in long.
E	400	1000		Four 400 kΩ metal-film resistors in series-parallel, each 2 in long.

The five 1000-V TVCs are designated alphabetically (A through E)[3] and all except "A" have the inner shield, as described below, for frequency compensation. The resistor in unit "A" is mounted concentrically in a set of six brass rings whose potentials are maintained by a capacitance divider. The whole assembly is mounted in a 4-in brass cylinder 7 in long.

Self-heating of a TVC may affect either the frequency compensation or the resistor itself. Apparently the dielectric losses in the insulation between conductors can be affected by heating and change the impedance of the resistor. This change occurred within a few minutes after a voltage increase or decrease in several resistor types, which were therefore discarded.

The frequency compensating shield may be moved, relative to the resistor, by thermal expansion of mounting parts and cause a change in ac-dc difference. This occurred in some of our early units and the change was slow, taking up to an hour. Later shields were therefore mounted very rigidly since a small displacement will have a large effect on the frequency influence.

The shield now in use is in two parts. A brass cylinder, with one end closed, is mounted firmly against the outer end piece (input end) with a polystyrene insulator one-half inch thick (fig. 3). A movable tube fits tightly inside this cylinder and the shield length adjustment is made by pushing this piece forward with a small rod inserted through the end piece and the insulator. The rod is removed after each adjustment.

The shield is most effective at the leading edge where the voltage difference is greatest between the resistor and the shield. Therefore the movable part of the shield is cut at an angle, so that only part of it (see fig. 3) extends outside the fixed cylinder. Thereby the effect of small position changes is reduced. Even so, the compensation is affected by approximately 0.01 percent per millimeter of position change in some typical units.

The shield length adjustment is made in small steps, and tests are made after each adjustment. When optimum compensation is achieved, the unit is opened and the shield parts are locked together with three screws through their overlapping portions.

4. TE and TVC Tests

As stated earlier the middle ranges are the most accurate, and they are the base from which higher and lower ranges are tested. However they are no more accurate than the TE used with them. Before being installed in a TVC the TEs are therefore compared with one of a group of carefully selected TE standards which were made according to NBS specifications. This group contains twelve elements made by four manufacturers, and are rated from 5 to 20 mA. [1] They have either Karma or Evanohm [4] heaters to reduce

[3] Unit "D" is assigned to this set (No. 7).

[4] Certain commercial products and instruments are identified in this paper in order to specify adequately the experimental procedure. In no case does such identification imply recommendation or endorsement by the National Bureau of Standards, nor does it imply that the products or equipment identified are necessarily the best available for the purpose.

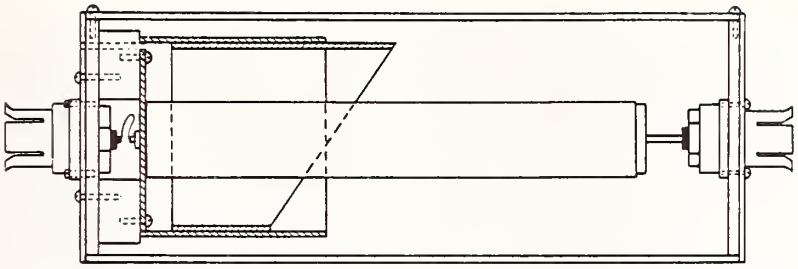

FIGURE 3. *Cross section of high voltage TVC.*
Input end is at the left. Fixed and adjustable shield parts are supported by a polystyrene insulator one-half inch thick.

thermoelectric effects in the heaters. They also have small reverse d-c differences (less than 200 ppm), high bead resistances (over 1000 MΩ), and small ac-dc differences. An additional two are multi-junction elements of different design. All of these TEs have been intercompared as current converters with agreement to better than 3 ppm. Theoretical calculations, taking into consideration all known sources of error, also indicate that the error should not exceed a few ppm at audio frequencies. Because of this and because of the excellent agreement between these thermoelements of different design and construction, we may safely assume that the average ac-dc difference of the group is 0 to ±2 ppm.

The low-frequency performance of a TVC depends on the TE since the reactance of the resistor is entirely negligible even at a few kilohertz. The accuracy of a TE at low frequency is mainly dependent on the length of the heater. A very short heater permits heat to flow more readily to the support stems and cooling to occur between current peaks. However most commercial TEs have errors less than 10 ppm at 20 Hz and some have errors less than 10 ppm even at 5 Hz.

In testing selected commercial TEs for the TVCs at audio frequencies we often find a small ac-dc difference (up to 4 ppm) which is independent of frequency but dependent on heater current. It ordinarily decreases at lower heater currents. When these TEs are used in a TVC the ac-dc difference will therefore be slightly voltage dependent. In the step-up test process, where the TVC is alternately used at 50 and 100 percent of rated current, this relatively small thermoelement error is introduced at every step of the process. If the process is a long one, as in the 12-resistor set, there could be a significant accumulation of error. TVCs in the new set are intercompared by testing each resistor once with one TE at reduced current (60 or 67%), and again with rated current on the other TE. If these TEs differ in ac-dc difference at these currents, there will again be an accumulation of error.

This is one of the advantages of the set with only six resistors. If the 20-V range is the starting point (it is probably the most stable), we have only four steps up to the 1000-V range, and three steps down to the 1-V range. The other advantages are that less time is required for the intercomparisons and there are fewer units to construct.

Intercomparison data for this set of TVCs are listed in table 3 as well as determinations made using TVC set No. 1. (Test methods are discussed in later sections of the paper). The middle ranges differ by 2 ppm or less even though the resistance varies from 1200 to 12000 Ω. Since the resistance enters into the theoretical calculation of ac-dc difference, this agreement is an additional indication of accuracy.

Step-down tests show that the two lowest voltage ranges usually have a positive correction (i.e., more a-c than d-c voltage is required for a given TE output) of 5 ppm or less at 50 kHz. There is no resistor in series with the TE at the 1 V range, and at the 2-V range the TE is a large part of the total impedance. These ranges are therefore affected more by the small reactance of the TE. The corrections for these ranges are more likely to change if a TE is replaced than for the higher ranges. A step-down test from the middle range is therefore advisable when TE replacements are made.

The five 1000-V TVCs were compared with the 300- and 500-V ranges of TVC set No. 1 and the 600-V range of the new set No. 7. The corrections are listed in table 4 for 20 and 50 kHz and all values are averaged.

TABLE 3. *AC-DC difference*

TVC-a	TVC-b	Applied voltage	AC-DC difference (ppm)					
			20 kHz			50 kHz		
			$\delta_{rr}-\delta_{ll}$	δ_s	δ	$\delta_{rr}-\delta_{ll}$	δ_s	δ
F1		1		−3	−3		+1	−3
F2	F1	1	+1			0		
F2		2		−2	−2		+1	−2
F1–3	F2	2	+1			−1		
F1–3		3		−1	+1		0	−2
F2–6		6		−1	0		0	−3
F1–10	F2–6	6	+1			+1		
F1–10		10		0	+1		+1	+1
F2–20		20		0	0		+1	+1
F1–30	F2–20	20	−1			−2		
F1–30		30		−1	+1		−1	+2
F2–60		60		−1	0		−1	0
F1–100	F2–60	60	−1			−4		
F1–100		100		−2	0		−5	−2
F2–200		200		−2	−1		−5	−6
F1–300	F2–200	200	−2			+6		
F1–300		300		−4	−3		+1	−4
F2–600		600		−4	−4		+1	−1
F1–500	F2–600	500	−2			−26		
F1–500		500		−6	−3		+27	−30
F2–1000		1000		−6			+27	

Table 5 lists intercomparison data for the same frequencies for seven pairings of the five 1000-V TVCs. Values for 600 and 1000 V do not differ significantly and so they are all averaged together.

Corrections (δ) for each range of the new TVC set are listed as determined in comparison with TVC Set No. 1. Intercomparison data($\delta_a - \delta_b$) are also listed and a computed correction (δ_s) based on the intercomparison, starting with the average of the measured ac-dc differences of the 10- and 20-V ranges. The TVCs are identified as the combination of a TE (F1 or F2) with the appropriate resistor; i.e., F2–600 forms the 600-V range.

Averages of the corrections for the five 1000-V TVCs listed in table 4 are shown in the circles in figure 4, and the connecting lines show the intercomparison values from table 5. The agreement between the various units is illustrated by this figure.

Each of the values listed in tables 4 and 5 is the average of at least four separate determinations. An analysis of the data taken in a series of 26 intercomparison tests (an average of 5 determinations with each one), involving all ranges at two frequencies and usually two voltages, showed an imprecision ($3\sigma_a$, where σ_a is the standard deviation of the average of five determinations) of only 1.4 ppm.

TABLE 4. *Ac-dc difference corrections for five 1000-volt TVC (A–E)*
The standard instruments are the 300- and 500-V units of Set No. 1 and the 600-V range of Set No. 7.

Standard	Volts	A	B	C	D	E
AC-DC difference at 20 kHz (ppm)						
500–1	500		−20	−9	−4	−12
300–1	300				−4	−10
600–7	600	−3	−22		−2	−12, −10
		−8			−3	−10
Ave.		−6	−21	−9	−3	−11
AC-DC difference at 50 kHz (ppm)						
500–1	500	+21	−6	+11	+30	−3
300–1	300				+30	−4
600–7	600	+30	−9		+30	−6
		+23			+32	−6
Ave.		+25	−7	+11	+30	−5

TABLE 5. *Relative ac-dc differences for seven pairings of members of the five 1000-V TVCs*

Volts	$\delta_A-\delta_B$	$\delta_B-\delta_C$	$\delta_C-\delta_D$	$\delta_D-\delta_E$	$\delta_E-\delta_A$	$\delta_A-\delta_C$	$\delta_A-\delta_D$
AC-DC difference at 20 kHz (ppm)							
600	−11	+14	+2	−7	+7	+3	0
1000	−17	+13	0	−6	0	+9	+5
600	−16	+17		−10			−2
1000	−17						+5
Ave.	−15	+15	+1	−7	+4	+6	+2
AC-DC difference at 50 kHz (ppm)							
600	−20	+14	+10	−33	+28	−15	+3
1000	−22	+6	+2	−33	+35	−14	+4
600	−25			−37		−15	+2
1000	−24						+1
Ave.	−23	+10	+6	−34	+32	−15	+2

5. Thermal Compensation

The coaxial connector between the TE and the series resistor provides a low-reactance connection for minimum frequency error. Tests and calculations show the error is less than 1 ppm at 50 kHz. However, it also permits heat to flow freely from the resistor, which dissipates up to five watts on the 1000-V range, to the TE which has a temperature coefficient of emf of approximately 0.2 percent/° C (at constant input current).

Heat conduction through the center conductor of this connector was reduced, at 300 V and higher, by replacing the two polystyrene insulators in the coaxial connectors (one in the resistor output and one in the TE input) with two made of boron nitride. This material is a good electrical insulator and yet it conducts heat well enough to provide an effective heat sink for this conductor. It is used in both ends of the high voltage resistors to improve the heat flow from the resistor to the relatively heavy brass casing. This also helps to reduce the temperature rise in the resistor.

Heat flow through the outer part of these connectors will gradually raise the temperature of the TE casing, and this also causes a heating drift. The increase in temperature of the TE bulb is slowed by mounting it in a short section of brass tubing to increase the thermal mass and this tube is thermally insulated from the TE casing. Thermal compensation is also added by attaching a 10-Ω thermistor to the tube containing the TE and connecting it in series with the TE output. A resistor appropriately chosen to complete the compensation circuit (see Fig. 7 and appendix I) will draw current through the thermistor sufficient to compensate for the temperature increase.

This resistor value may be computed for TEs with average temperature coefficients as in appendix I. However, temperature coefficients differ considerably and, for best results, it is usually necessary to match the resistor to the TE and thermistor combination. A suitable value can be found by substituting a variable resistor outside the TE casing and adjusting it for minimum warmup drift on a 1000-V range. However, if the TVC is to be used with a TE comparator similar to the one to be described, it will frequently be connected

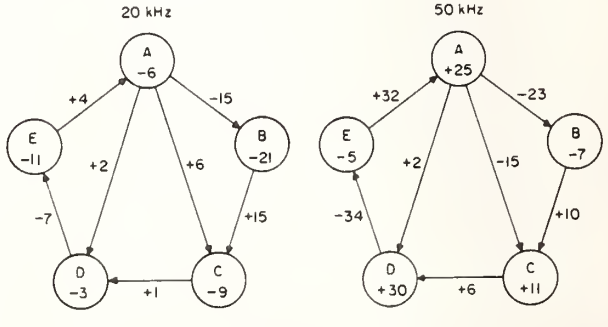

FIGURE 4. *Intercomparisons of 1000-volt TVCs.*
Ac-dc difference corrections (ppm) from table 4 for five 1000-V TVCs are shown in the circles and the relative differences from table 5 are shown on the interconnecting lines. The algebraic difference between any pair should be equal to the figure on the connecting line within experimental error.

across a 1000-Ω divider, and this will affect the compensation by about 20 percent. A value about 10 percent higher than the one chosen experimentally should provide a satisfactory compromise and reduce the drift by a factor of five or more. With the compensation and the large thermal time constant of the TE in its casing, the drift can be reduced to less than 5 ppm/minute under typical laboratory condition. The error from this is almost completely eliminated by taking a sequence of readings with a-c, d-c, reversed d-c, and a-c voltage applied, as described in the next section.

6. TVC Test Methods

A brief review of other comparison methods may be useful before describing the TE comparator. Figure 5 shows two TVCs connected in parallel. The separate balancing circuits (or Lindeck Potentiometers) (B) and null detectors (D) may or may not be built in. Stable a-c and d-c voltage supplies are connected to the two TVCs by the ac-dc switch. The switching arrangement shown is typical and convenient, although others, such as reversing the d-c supply by a separate switch, are satisfactory. The d-c supply must have an ungrounded output and it should be possible to ground either terminal as the voltage is reversed. The reversed d-c differences of the TVC can rarely, if ever, be neglected in these tests.

For convenience and clarity, we shall call one TVC the "standard" and the other the "test." Normally the one with known ac-dc difference corrections is the standard, and the test TVC is usually treated differently in the test procedures, as explained below.

There are two procedures for this intercomparison. One might be called a null-balancing method. With a-c voltage applied to both TVCs, the balancing circuits of the test and standard instruments are adjusted to null the detectors. The d-c supply is then switched to the TVCs, and the voltage is adjusted to obtain a null balance first on the detector of the test instrument and then on the standard. Each d-c voltage is carefully measured, and the small difference between the two should equal the difference between the a-c voltage and one direction of d-c voltage. The measurement is then repeated with reversed d-c voltage, and an average is taken.

This method is tedious and time consuming, an accurate d-c voltage standard is required, and if there is any drift in either instrument output due to warmup or other reasons, as there very often is, the data may lack both accuracy and precision.

A more satisfactory procedure and one that will minimize the effect of drift may be called a deflection method. Both balancing circuits are adjusted to near null, and then a-c and d-c voltages are applied in the succession indicated in figure 5 (AC, DC+, DC−, AC). For each input the power supply is adjusted to set the test instrument detector to null. The deflection of the standard TVC detector is read for each setting, and the difference between the average reading on a-c voltage and d-c voltage is an indication of relative ac-dc difference. If the readings are made at nearly equal time intervals, and if the drift rate is reasonably constant (even though fairly large), the determinations can be made with satisfactory precision.

If the detector of the standard TVC is a galvanometer the reading may be in divisions or millimeters, but they can be converted to volts or percent ac-dc differences by calibrating the detector scale in one of several ways. A calibration factor can be determined simply and directly by making a small measured change in the d-c input and observing the detector response.

If the detector is a microvoltmeter and if the balancing circuit is a Lindeck potentiometer indicating the millivolt output of the thermoelement, the calibration step can be eliminated. With the four deflection readings on the detector the difference between the average reading on a-c voltage (E_a) and those on d-c voltage (E_d) is computed from the differences of the corresponding readings of the microvoltmeter. The ac-dc difference of the test instrument is

$$\delta_t = \delta_s + \frac{E_{sa} - E_{sd}}{n_s E_{sd}}$$

where the subscript s indicates that these values come from the standard instrument, and δ_s is the ac-dc difference correction for the standard.[5]

The factor n relates small changes in thermoelement heater current (ΔI) (at a fixed frequency) to corresponding changes in output emf ($\Delta E/E = n\Delta I/I$ approximately). For a TVC we may substitute $n\Delta V/V$ for the right hand expression, so that $n = V\Delta E/E\Delta V$. The value of n is 2 if the thermoelement has a square law response, possibly at very low heater currents, but it is usually 1.7 to 1.9 at rated current. Determinations of n should therefore be made in a d-c test at five or more current levels by measuring the values indicated. A plot of n against E can be made so that values corresponding to any emf can be found for substitution in the equation above (see sec. 8).

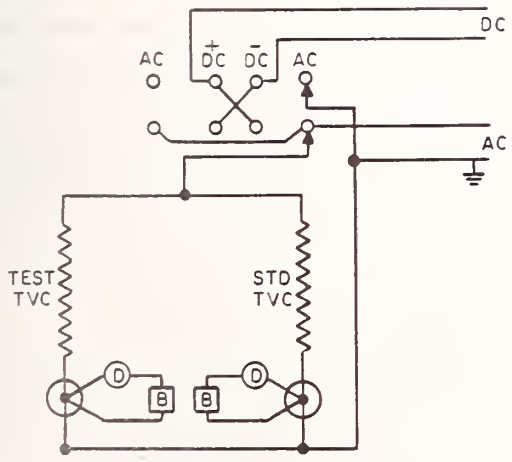

FIGURE 5. *Two-Potentiometer method for TVC comparisons.*

[5] See eq 3 of appendix II. This general formula is applicable here also.

7. TE Comparator

There are several variations of basic comparator circuits which are used to minimize the difficulty caused by power supply instability [1, 3]. They employ a voltage divider circuit to which two emfs are connected. The divider is adjusted to null a detector, and at this point the divider setting corresponds to the ratio of the emfs. If one emf (E_t) is held constant as a-c and then d-c voltage is applied to the TVCs, the other emf (E_s) will change if there is a relative ac-dc difference in the TVCs at the frequency ($\delta_t \neq \delta_s$). The resulting unbalance in the divider will produce a change in the detector deflection proportional to the ac-dc difference. However, small fluctuations in the power supply will produce nearly equal proportional changes in the emfs and therefore the detector will not be affected appreciably. The stabilizing effect depends on how well matched the time constants and response characteristics of the TEs are, but the effect usually affords a significant advantage. Also, the monitored emf need not be held constant so exactly as with a simple balancing circuit.

In the new comparator (fig. 6) the higher of the two emfs is connected across a 1000-Ω Kelvin-Varley divider, and the lower one is connected to the variable tap. The detector is brought to null by adjusting the divider. A Lindeck potentiometer and the same detector (with key k_1) is used to monitor the test TVC output (E_t). The detector is labeled "N" in the diagram because the use of a nanovoltmeter is suggested.

The test procedure is similar to that already mentioned. Preliminary settings of the potentiometer and divider are first made so the readings of the nanovoltmeter will fall near mid-scale. Then with a-c voltage applied, the key k_1 (labeled "SET" on the instrument, figs. 8 and 9) is depressed and the appropriate power supply is adjusted for a null on the detector. Key k_2 (READ) is then depressed and the detector indication is read. The two-step procedure is repeated for two directions of d-c voltage and for a second a-c input. The average indication in nanovolts [6] (N_a) for a-c input and the average for d-c input (N_d) is computed and the ac-dc difference of the test instrument is

$$\delta_t = \delta_s + \frac{N_d - N_a}{n_s E_s} \qquad \text{(appendix II eq 5)}$$

Figure 6 shows the test TVC output (E_t) connected to the high emf terminal (E_H in fig. 8). If E_t is smaller than E_s it will be necessary to interchange them, but this is a minor inconvenience. If E_t is connected to the E_1 terminal the potentiometer is switched to that input with switch S_2 (fig. 8) and E_t is monitored as before. The same switch also reverses the polarity of the detector, and therefore the sign of the indication. The slightly modified equation for δ_t is eq 11 in appendix II.

A galvanometer may also be used as a detector but since the circuit resistance is relatively high a photoelectric amplifier is necessary for sufficient sensitivity. The scale must be linear over the portion to be used and a scale calibration is also necessary to relate the readings in divisions or millimeters to a voltage change. The calibration can be made quite easily however by moving switch S_1 from READ to CAL with k_2 closed and observing the resulting deflection change. This increases the resistance of the 1000-Ω divider by 0.5 Ω and changes the divider current by 0.05 percent. The

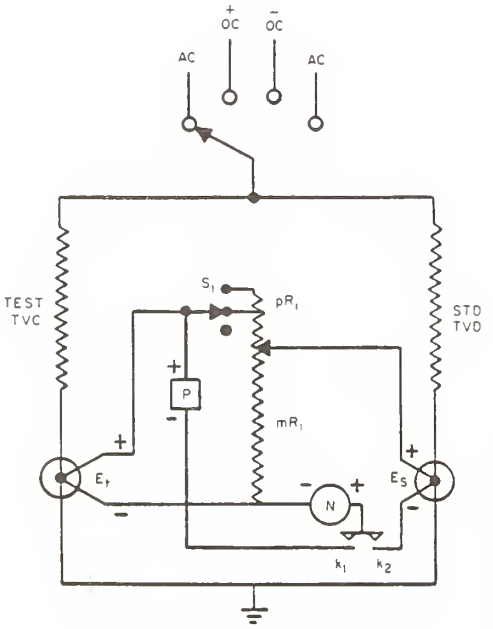

FIGURE 6. *New TE comparator.*

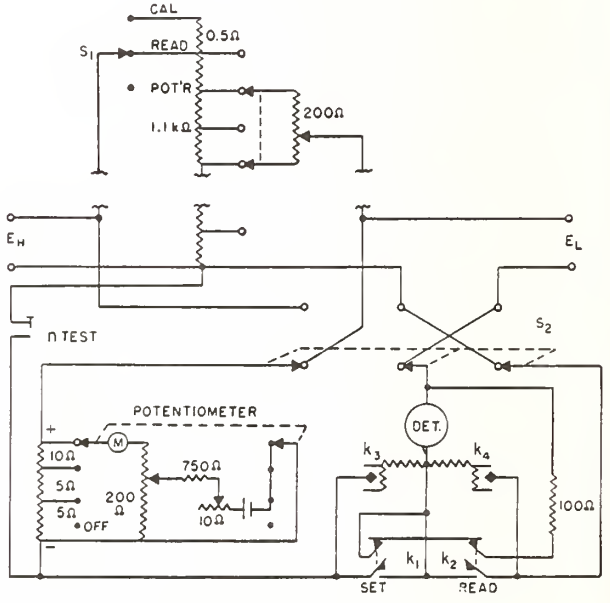

FIGURE 8. *New TE comparator.*

[6] $\delta_t - \delta_s$ is conveniently in parts-per-million if E_s is in millivolts and $N_d - N_a$ is in nanovolts.

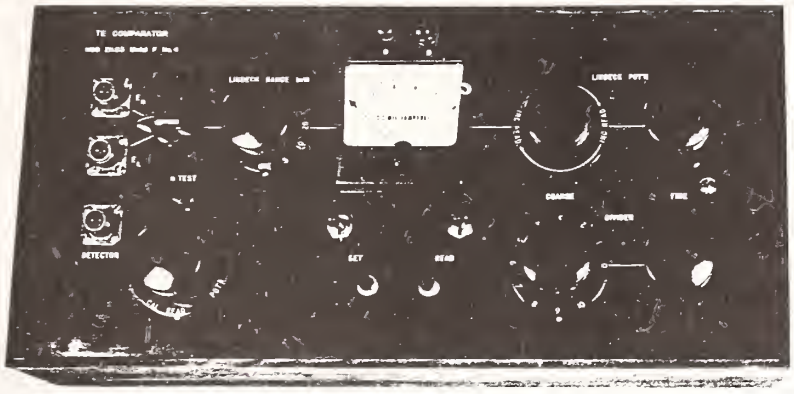

FIGURE 9. *Photograph of TE comparator.*

voltage applied to the galvanometer circuit is changed by the same amount and the deflection change D_1 is used in eq 10 and 12 in appendix 2 to determine δ_t. A measurement of E_s is made only to find the corresponding value of n_s from a plot as before.

8. *n* Tests

Measurements of n are conveniently made with the comparator. The thermoelement to be tested is connected to the E_L input and the E_H input is unused. A key labeled "*n* TEST" (fig. 6) is locked down and switch S_2 is moved to E_H connecting the potentiometer voltage across the divider. The divider is set arbitrarily but preferably near full range and the potentiometer is adjusted to null the detector. The input voltage is then changed by a small measured amount $\Delta V/V$, and the resulting change in TE output (ΔE) is measured by observing the change in indication of the detector (nanovolts or microvolts).[7] Switch S_2 is then moved to E_L and a measurement of TE output (E) is made with the potentiometer. The values for each factor of the equation given above ($n = V\Delta E/E\Delta V$) are then known and n is calculated from this equation.

If a galvanometer is used as the detector a measurement of D_1 is made as described above, and the deflection change resulting from the measured change in input voltage (ΔV) is designated D_2. Then $n = 0.05\ D_2/qD_1$, where q is the percentage change in input voltage ($100\ \Delta V/V$).

Determinations of n need be accurate only to a few percent, and, since they are quite stable, retesting is not usually necessary.

9. AC Voltage Measurements

As suggested earlier, the comparator may be used with one TVC to measure an a-c voltage such as the input to a digital voltmeter or the output of a calibrated a-c voltage supply. Switch S_1 has a third position marked "POT'R" which disconnects the divider from the E_H input. If a TVC output is connected to E_H, and switch S_2 is moved to that input, the potentiometer and detector can be used to measure the TVC output and changes in it. The circuit is as figure 5 without the test TVC. The d-c voltage is accurately measured and nominally equal to the a-c voltage.

It is suggested that d-c voltage be applied to the TVC first and a detector reading taken. Then, at nearly equal time intervals, a second reading is taken with a-c voltage and a third with reversed d-c voltage. The difference between the average of the readings with a d-c voltage (E_d) and the one with a-c voltage (E_a) is related to the input voltage difference very much as before.

$$V_{ac} = V_{dc}\left(1 + \frac{E_a - E_d}{nE} + \delta_s\right)$$

With a nanovoltmeter the emfs are read directly, but if the detector is a galvanometer a scale sensitivity factor must be determined.

10. Design Details

The case of the TE comparator has thermal insulation and electrostatic shielding, and the comparator is carefully built to minimize thermal emfs and contact resistances. The switch decks of the Kelvin-Varley divider and S_1 and S_2 have enclosed silver contacts and the keys k_1 and k_2 are of a low-thermal type. The back contacts on these keys connect a 100-Ω shunt across the detector to reduce sensitivity and noise until one key or the other is depressed. The fine control for the divider is a ten-turn helical resistor with a special low-thermal sliding contact. The resolution of the uncalibrated divider is not quite sufficient for setting an exact null on the detector, but setting within a few divisions is adequate in the ordinary use of the instrument.

[7] A small change in the input to a TVC can be measured with a volt box and potentiometer or by a setting with a calibrated d-c voltage supply. It is also convenient to use a resistor with a shorting switch in series with a TVC to introduce a small current change (ΔI) in the thermoelement heater (i.e., 20 Ω with a 40-kΩ, 200-V TVC will give $100\ \Delta I/I = 0.05$ percent which is equivalent to $100\ \Delta V/V$).

11. Conclusion

The use of one resistor unit for two TVC voltage ranges has reduced by about half the time required, over previous TVC sets, to make a complete intercomparison test. Changes in any member of the set are readily detected since frequent intercomparison tests are more feasible.

The TE comparator combines the stabilizing feature of other comparators with much of the simplicity of the single Lindeck potentiometer or balancing circuit. It is relatively inexpensive to build and calculations are simplified and direct, especially where the detector is a nanovoltmeter. Repeated tests have shown that the imprecision is less than 2 ppm and ac-dc transfer accuracies, with the TVC set, are 10 ppm at audio frequencies and 20 ppm up to 50 kHz.

This work was supported in part by the Army Metrology and Calibration Center, Redstone, Alabama. Their encouragement and support are gratefully acknowledged. The author also acknowledges the help of C. B. Childers and A. G. Perrey who made many of the exacting measurements described here.

12. References

[1] Hermach, F. L. and Williams, E. S., Thermal converters for audiofrequency voltage measurements of high accuracy, IEEE Transactions on Instrumentation and Measurement, **IM-15**, No. 4, 260–268, (Dec. 1966).

[2] Hermach, F. L. and Williams, E. S., Thermal voltage converters for accurate voltage measurements to 30 megacycles per second, Trans. AIEE (Communication and Electronics), **79**, Pt. I, 200–206, (July 1960).

[3] Turgel, Raymond S., A comparator for thermal ac-dc transfer standards, ISA Transactions, **6**, No. 4, 286–292, (1967).

13. Appendix I

The temperature coefficient of emf, β, of the average TE is about -0.2 percent/° C, with constant input current. Thus a corresponding decrease in the resistance, $R = R_c + R_t + R_s$ (see fig. 7) is required to maintain a constant voltage across the resistor R_s. For a 1 degree increase in temperature, the change in thermistor resistance, $\Delta R_t = \alpha R_t/100$ where α is the temperature coefficient of the thermistor in percent/° C – typically about -4 percent/° C. Therefore, for thermal compensation,

$$\beta = 100\Delta R_t/R = \alpha R_t/R$$

$$\text{and } R = \alpha R_t/\beta$$

With the typical values listed we find $R = 200\ \Omega$, and, subtracting R_c and R_t, the value for R_s is 180 Ω.

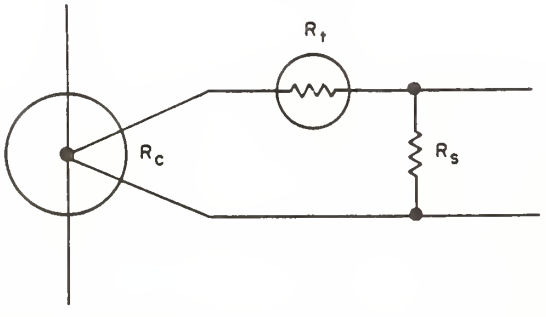

FIGURE 7. *Thermal compensation for TE.*

R_c TE output resistance (about 10Ω).
R_t Thermistor resistance (about 10Ω).
R_s Series resistor to complete compensation circuit. (R_c and R_s have negligible temperature coefficients.)

14. Appendix II

Development of Equations*

The ac-dc difference of a TVC is defined as

$$\delta = \frac{V_a - V_d}{V_d} \tag{1}$$

where V_a is the a-c voltage and V_d the average of the two directions of dc-voltage required to produce the same output emf. In the circuit of figure 6 the a-c and d-c voltages are adjusted to give the same emf E_t, of the TVC under test, as indicated by a null on the detector N with k_1 closed. The same voltages are applied to the standard TVC. Then,

$$V_a = V_d(1+\delta_t) = V'_d(1+\delta_s) \tag{2}$$

where V'_d is the d-c voltage required to produce the same output emf of the standard as V_a, and the subscripts, t and s, refer to the test and standard instruments respectively. If $V'_d - V_d << 1$, then, closely enough

$$\delta_t - \delta_s = \frac{V'_d - V_d}{V_d}.$$

From the definition of n given in the paper

$$\delta_t - \delta_s = \frac{E_{sa} - E_{sd}}{n_s E_{sd}} \tag{3}$$

With the polarities as shown in figure 6,

$$N = mE_t - E_s \tag{4}$$

where N is the detector voltage with k_2 closed and k_1 open, and m is the divider ratio (with the detector resistance $R_d >> R_1$).

Thus,

$$\delta_t = \delta_s + \frac{N_d - N_a}{n_s E_{sd}} \tag{5}$$

where the subscript a and d have the same meaning as before.

---

* These equations were developed by F. L. Hermach.

If a galvanometer is used as the detector, the current through it with k_2 closed is, by Thevenin's Theorem,

$$I_{gb} = \frac{mE_t - E_s}{R_e} \tag{6}$$

where R_e is the resistance of the galvanometer circuit with E_t and $E_s = 0$. With E_t and E_s held constant and pR_1 inserted by means of S_1,

$$I_{gc} = \frac{mE_t/(1+p) - E_s}{R_e'} \tag{7}$$

where R_e' is the resistance of the galvanometer circuit.

Since $mE_t - E_s << E_s$ and $p << 1$, we have to a sufficient degree of approximation,

$$I_{gb} - I_{gc} = \frac{E_s p}{R_e} = \frac{(D_b - D_c)}{S} = \frac{D_1}{S} \tag{8}$$

where D_b and D_c are the resulting galvanometer deflections and S is the galvanometer current sensitivity.

In the ac-dc test, with mE_t constant,

$$I_{ga} - I_{gd} = \frac{E_{sd} - E_{sa}}{R_e} = \frac{D_a - D_d}{S} \tag{9}$$

Thus, from (3), (8) and (9),

$$\delta_t = \delta_s + \frac{p(D_d - D_a)}{n_s D_1} \tag{10}$$

The test and standard TVCs may be interchanged if $E_t < E_s$. If E_t is applied to the E_L input of figure 8 and held constant, with the detector and potentiometer connected as shown in the figure, a similar analysis leads to the following equations:

$$\delta_t = \delta_s + \frac{N_d - N_a}{n_s E_t} \tag{11}$$

and

$$\delta_t = \delta_s + \frac{p(D_d - D_a)}{n_s D_1} \tag{12}$$

The characteristic n is determined from

$$n = \frac{\Delta E/E}{\Delta V/V} \tag{13}$$

by applying known changes in input voltage and observing the changes in output emf with a high resistance voltmeter, as described in the text. If a galvanometer is used as the detector instead of the voltmeter its sensitivity is determined by inserting pR_1 as described. From equations similar to (8) and (9)

$$\frac{\Delta E_s}{E_s} = \frac{p\Delta D}{D_1} \tag{14}$$

If the thermocouple resistance of the test TVC, R_{tc}, is significant, p in equation (7) should be replaced by p', the fraction of $R_1 + R_{tc}$ inserted by S_1.* Similarly if the potentiometer resistance R_p is significant, p in equation (14) should be replaced by p'', the fraction of $R_1 + R_p$ inserted by S_1.

(Paper 75C3&4-321)

* with a high impedance detector. With a galvanometer the formula for δ_t is too complicated to be useful.

JOURNAL OF RESEARCH of the National Bureau of Standards—C. Engineering and Instrumentation
Vol. 73C, Nos. 3 & 4, July–December 1969

Design Features of a Precision AC-DC Converter

Louis A. Marzetta

Institute for Applied Technology, National Bureau of Standards, Washington, D.C. 20234

and

Donald R. Flach

Institute for Basic Standards, National Bureau of Standards, Washington, D.C. 20234

(August 5, 1969)

With the availability today of high performance operational amplifiers and related components, it is possible to construct an instrument for ac-dc transfer work that meets the requirements of a standards laboratory. Transformation of measured average a-c values into d-c voltage is possible with a predictable accuracy of 20 parts per million up to 1 kHz. Precision of operation is assured from dc to 100 kHz.

Key words: AC; DC; operational; precision; rectifier; transfer.

1. Introduction

Reference to precise a-c measurement has always implied an rms evaluation. This has been so because the majority of physical results in experiments and other usage are related to transformation of electrical energy, to heat or mechanical work, and electrical laboratories have found the best accuracy in square-law responding instruments. With the availability today of highly stable, nearly pure sine-wave power sources and precision linear operational devices, the situation has changed. For some ac-dc transfer work such as amplitude monitoring [1],[1] the average a-c responding systems to be described can have a superiority of precision over rms converters. In addition, the wide usage of average responding instruments such as digital voltmeters with a-c options and sampling devices has increased the need for a basic average transfer standard. This paper will delve into design factors that demonstrate the ability of transforming the average value into d-c voltage with a high order of accuracy.

2. Operational Rectifier Stage

The choice of systems and circuits for average a-c measurement is more limited than for rms. An average responding circuit is involved with some form of rectification—that is, it has to average either the positive or the negative values of the voltage wave, or both without regard to sign. It is the defects in the rectifying elements that affect precision and accuracy. The object of the operational rectifier circuit, figure 1, is to place the rectifying components in the feedback loop at the output of the amplifier wherein the full loop gain amplification can be used to greatly reduce the diode weaknesses. The device is a unity gain circuit (if equal value resistors are used at the input and feedback connections) whereby half-sine waves are generated at each output.

Because of the unwieldy nature of transfer expressions in circuits with diodes, a linear amplifier type analysis in the frequency domain will be pursued first, by neglecting the diode imperfections.

2.1. Finite Gain Error

Using superposition theory and writing a current balance at the input summing junction, we find that the transfer function of a unity-gain inverting operational amplifier with perfect ratio resistors is

$$V_{out}/V_{in} = -\frac{1}{1+(2/A_f)} \qquad (1)$$

where A_f is the open-loop voltage amplification of an

[1] Figures in brackets indicate the literature references at the end of this paper.

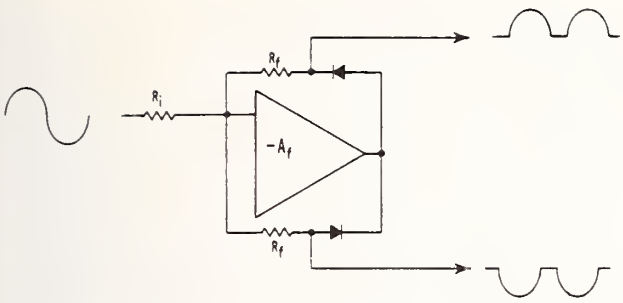

FIGURE 1. *Basic operational rectifier.*

operational amplifier with ideal characteristics but finite amplification.

To avoid commonly observed errors in the usual exact-gain formula due to neglect of the phasor nature of the open-loop voltage amplification, A_f, the general formula can be expressed in a more usable form as follows

$$V_{out}/V_{in} = -(Z_f/Z_i) \cdot \frac{1}{1+(1/A_f)(\cos\theta - j\sin\theta)[1+(Z_f/Z_i)]} \qquad (2)$$

where θ is the open loop phase angle of the amplifier, and A_f is now the magnitude of the open loop amplification. Starting with zero degrees at direct current, θ usually increases with a minus sign (lag) as the frequency increases. Z_f and Z_i are feedback and input impedances, respectively. In most literature a reader tends to interpret the closed-loop gain expression as an output that falls off with frequency because of the drop in open loop amplification. Careful tests corroborate expression (2) and show that this is not necessarily so. The output can actually rise with frequency for a constant input in spite of a dropping A_f in the region where θ has shifted beyond 90 degrees lag, the reason being that the phase lag has created a real component of positive feedback.

The transfer error in ppm (parts per million) for an inverting unity gain situation is the difference between unity and the magnitude of V_{out}/V_{in}. Except for angles near 90°, the error can be closely approximated as $\pm(2/A_f)\cdot(\cos\theta)\cdot 10^6$: the minus sign for phase lag less than 90° and plus sign for phase lag greater than 90°, where $(A_f \gg 1)$. Exactly at 90° the error reduces to $2/A_f^2$, and reaches zero error slightly beyond 90°. However, effectiveness of quadrature error reduction does drop off rapidly for phase deviations from the 90° region.

Since phase characteristics are rarely given in operational amplifier literature, the transfer error calculation of the operational rectifier will be hampered. Using the worst case basis of $(2/A_f)\cdot 10^6$ for the error, for an amplifier with zero phase shift, it could be expected that an operational amplifier would exhibit a gain transfer error of 100 ppm at the frequency where the open loop amplification is 20 000 and that the error would double each octave increase of frequency. However, it was found from actual test data that the error function did not behave in this manner but that the output remains quite constant for a wide frequency range, in some cases rising at the higher frequencies due to the previously described phase properties. Hence it can be assumed that the $(2/A_f)\cdot 10^6$ error factor is quite conservative.

2.2. Finite Diode Conduction Level Error

Another source of error arises from the finite conduction level of the diodes. Time is lost at the amplifier in order for its output to reach the diode conduction voltage, which means that there is a "lost area" at the beginning of the half sine wave output. The overall error in average value with a first order approximation can be expressed as the ratio of the lost small area to the half-wave area. It is desirable to analyze the factors that may influence this particular error.

For the period of a half-sine wave with V_m peak volts, the average value is $(2/\pi)V_m$. Hence the area under the function is $(2/\pi)(V_m)(\pi)$ or $2V_m$ volt-radians. The lost area in question can be found by formal integration as

$$\text{Lost Area} = V_m \int_0^{\phi_c} \sin\phi\, d\phi \qquad (4)$$

where ϕ_c is the angle measured from the zero crossing point to the diode conduction point. For small angles, $\cos\phi = 1-(\phi^2/2)$ and the lost area from expression (4) is

$$\text{Lost Area} = V_m|-\cos\phi|_0^{\phi_c} = V_m(\phi_c^2/2) \text{ volt-radians.} \qquad (5)$$

At angle ϕ_c the diode conduction voltage, V_c, at the amplifier output is

$$V_c = A_f V_s \qquad (6)$$

where V_s is the potential at the operational amplifier's summing input junction and A_f is the open-loop voltage amplification. Also for small radian angles

$$V_s = \phi_c V_m. \qquad (7)$$

Substituting (7) into (6), the angle at conduction point becomes

$$\phi_c = V_c/V_m A_f. \qquad (8)$$

Using expressions (5) and (8)

$$\text{Lost Area} = V_c^2/2V_m A_f^2. \qquad (9)$$

Taking the ratio of the lost area (9) to the half-wave area $(2V_m)$, the overall error is

$$\text{error. } \epsilon = V_c^2/4V_m^2 A_f^2. \qquad (10)$$

Because of the squared value for A_f in the expression,

the error due to the finite diode conduction level is considerably less than the closed-loop gain error noted in expression (2).

2.3. Slew Rate Error

A second source of possible error from the diode conduction level is found in the consideration of the operational amplifier–rectifier in the time domain. Included in the data on operational amplifiers is the "slew rate"—a measure of the device's transient response. Slewing rate, S, or maximum output voltage change with respect to time is expressed as

$$S = (dV_0/dt)_{\max} = V_p(\omega_h/10^6) \text{ volts per microsecond} \quad (11)$$

where V_p is the peak output voltage and ω_h is the maximum frequency in radians per second for full output of the device. Using the stated slew rate, the time lost in reaching diode conduction can be found and used to compute the lost area. The elapsed time (t_c) from zero crossing to conduction, V_c is

$$t_c = V_c/S \text{ seconds.} \quad (12)$$

The angle, ϕ_c, of expression (4) can be expressed as

$$\phi_c = (t_c/t_0)\ (2\pi) \text{ radians} \quad (13)$$

where t_0 is the time for one period of the operating frequency, f_0. Substituting (12) in (13)

$$\phi_c = V_c 2\pi f_0/S \text{ radians.} \quad (14)$$

Using the lost area expression (5) and expression (14) for ϕ_c

$$\text{Lost area due to } S = V_m[V_c 2\pi f_0/S]^2/2. \quad (15)$$

As in expression (10) the overall error, ϵ, comes from the ratio of lost area to half-wave area.

$$\text{error, } \epsilon = V_c^2(2\pi f_0)^2/S^2. \quad (16)$$

Comparing expressions (16) and (10)—for example: if $f_0 = 16$ kHz, V_c is about 0.6 V, an amplifier with $A_f = 10^4$ and a slew rate of 10 V per microsecond, the error from expression (10) with an input signal of $V_m = 7$ V becomes approximately two parts in 10^{11}. Using expression (16) the error is about ten parts in 10^6.

In this example the slew rate factor contributed a greater error than the A_f gain factor. However, the slew rate figure alone is not a reliable measure of an amplifier's ability to be used as a precision operational rectifier. It is possible for a device to have both a relatively low A_f and a high slew rate since the two are independent design features of the amplifier. Such a rectifier would suffer a possible error from expression (10). Fortunately all amplifiers investigated that have the desired open-loop amplification also have sufficient slew rate. One additional note is that amplifier output overshoot at the beginning and end of the half-sine wave has not been a troublesome factor.

Thus far the discussion of the operational rectifier has been concerned with its a-c requirements; however the precision of its average value output also demands a strict dc stability. Not very long ago it was possible to achieve low drift results only with chopper-stabilized devices. High a-c performance operational amplifiers are now available in differential, nonchopper design wherein the drift error contribution with a 5 V input signal can be kept below 20 ppm for hours. Bias current variations at the input are low enough so as to be negligible in producing d-c output variations with feedback resistors encountered (1 kΩ to 100 kΩ).

2.4. Feed-Forward Operational Amplifiers

In the course of experimenting with a number of available operational amplifiers a certain group of them were found to exhibit a marked anomalous behavior. These particular amplifiers showed a monotonically decreasing response with frequency that was much sharper than was predictable with the conservative error factor bases. An inquiry into design of these amplifiers revealed them as "feed-forward" type devices. Briefly this means the input signal assumes different paths through the overall amplifier chain depending upon the input frequency, in the manner of a chopper stabilized amplifier. They can sometimes be spotted in the literature as wide-band devices with a high capacitance at the inverting input, as much as 0.02 μF. While feed-forward type operational amplifiers can be used as operational rectifiers, FET differential amplifiers characterized by their low input capacitance at both inputs (5 pF or less) are generally preferred.

3. Operational Filter Stage

The operational stage following the rectifier is the filter. (Fig. 2) Basically it is an accurate unity gain stage with a large enough time constant to filter out the half-sine-wave ripple to a level tolerable to the d-c detector. It also provides nearly ideal impedance buffering between the rectifier output and the d-c detector. The filter operational amplifier a-c response performance is unimportant, but like the operational rectifier, the need for low d-c voltage drift must be met. To preserve the unity gain accuracy and to present a low output impedance, the open loop d-c voltage amplification should be at least 200 000—a figure that is easily found in today's devices.

The feedback filter capacitor should have enough capacitance to achieve the desired time constant in conjunction with the feedback resistor (10 kΩ to 50 kΩ) to meet the detector requirements. Capacitor leakage resistance is important; the value should be at least 10^5 times the feedback resistor value. Polycarbonate dielectric capacitors are available in a 40 μF value, meeting the low leakage requirements.

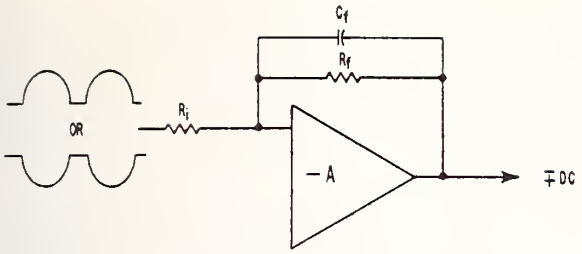

FIGURE 2. *Basic operational filter.*

4. Choice of Precision Resistors for the Rectifier and Filter Stages

The principal factor in the gain-setting accuracy of an operational stage is the ratio accuracy of the circuit resistors external to the component amplifier. Wire-wound resistors of various forms are available with both individual and ratio accuracies of 5 ppm. Extensive tests have demonstrated their ability to perform well in operational circuits. With little complexity it is possible to detect by d-c null techniques a difference of less than 5 ppm in a pair of high quality wire wound resistors by interchanging their respective positions at the input and feedback of an operational amplifier. The problem with some wire wound resistors is that they can exhibit a noticeable dc-ac error for frequencies above 5 kHz, amounting to several hundred ppm at 50 kHz. While it is possible to partially compensate for the error by using networks tailored to the resistor characteristics, it is the purpose of this article to describe systems of high precision that are void of compensation schemes. Fortunately there are available metal film resistors with desirable properties for the immediate application. These possess a virtually zero dc-ac difference over the range of interest (dc to 100 kHz). They are readily available with better than 100 ppm ratio accuracy with a relative temperature coefficient of a few ppm per degree. For wide band work in the area of 100 ppm accuracy, the metal film resistors are highly recommended: for high-accuracy, low-frequency applications of say 20 ppm, wire wound resistors may be more suitable.

5. Selection of Diodes at Operational Rectifier

The role of reverse leakage current and junction capacitance of a chosen diode must be considered in relation to the feedback resistor. It is possible to use a single silicon diode in each feedback path of the rectifier circuit since they are available with leakage currents less than 10^{-9} A. The usual operational forward diode current is 10^{-3} A, hence the error is 1 ppm for the stated leakage current. A more conservative approach is to use a pair of diodes in series, with a resistive shunt path between them for the leakage current; an arrangement conceived by Richman [1]. The series feature also reduces the resultant capacitance at full reverse bias: typically 1 pF.

The junction capacitance at the diode can introduce an error by adding a component of reverse current to the diode's forward signal current. However the net effect can be small because of the quadrature phase relationship of the currents. The error expression can be derived from the circuit impedances in the current branches. For small values of capacitance or high ratio of capacitive reactance to series feedback resistance, the error becomes $= 1/2(R_j/X_c)^2 \cdot 10^6$ ppm. For example at an operating frequency of 16 kHz and a feedback resistance of 10^4 Ω, a 1 pF diode capacitance would introduce an error of about 1/2 ppm.

With two silicon diodes in series the output must reach about 1.2 V before conduction takes place. This quadruples the small error in average value because of the "lost area" as explained previouslv. The latest development of "hot carrier" diodes can be used to good advantage. These high-speed diodes have the low-leakage feature of silicon diodes and a low forward conduction voltage similar to germanium less than 0.39 V.

Reverse recovery or effective minority carrier lifetime in a diode is a measure of its ability to turn off in going from forward to reverse conduction. In the operational rectifier this factor affects the termination of the half sine wave function, resulting in an error in average value. The analysis of the error is nearly the same as for the case of limited amplifier slew rate discussed previously with the error showing up as a lost area. Fortunately the diodes described in this section have recovery times in the vicinity of 10^{-9} s. Using the same procedure as with the example of the slew rate discussion, the error contributed at 16 kHz with the stated recovery time is found from expression (6). The error is equal to $\theta^2/4$ or $(10^5 \cdot 10^{-9})^2/4 = 10^{-8}/4$ which is negligible.

6. Stabilization of Operational Rectifier

To prevent high frequency oscillation a small capacitor is generally needed across the feedback resistor of an operational device. The resultant time constant places an upper corner frequency, F_h, having a direct bearing on the gain accuracy at some lower operating frequency, F_0. For large separation of the two frequencies, the asymptotic slope error is nearly $(F_0/F_h)^2 \cdot 10^6$, in ppm where $F_h = 1/2\pi R_f C_f$. The analysis is correct for a linear system; however in the rectifier configuration the capacitor is across both the feedback resistor and diode string resulting in a marked reduction of corner frequency, F_h which is difficult to calculate. Experience has shown that a series pair of 5 pF capacitors has been effective in stabilizing all amplifiers tested. However, this value of stabilizing capacitance can degrade the gain accuracy by 50 ppm at 20 kHz with a 5 kΩ feedback resistance.

7. Unity-Gain Input Isolation Amplifier Stage

The combination of the operational rectifier stage and filter stage is sufficient to meet the needs of most

average ac-dc transfer requirements. This system has an input impedance equal to the input resistor of the operational rectifier stage, typically 5 kΩ. In some cases this may be annoying because of the loading affect on a-c sources and a-c attenuators. For these reasons the effectiveness of an operational unity-gain impedance transforming circuit was investigated for use in applications where 100 ppm accuracy is sufficient.

The basic circuit is shown in figure 3. It is recognized as a noninverting amplifier with unity gain for the indicated input-output connection. Note that no precision resistors are involved in its operation and that it is able to take advantage of the high input impedance available with FET type differential devices—around 10^{11} Ω shunted by 3.5 pF of capacitance. In order for the stage to have the desired gain accuracy from d-c through the highest operating frequency, the selected operational differential amplifier must have both a wide-band high open loop amplification and a wide-band high common-mode rejection ratio, CMRR. The latter factor is a measure of the amplifier's ability to precisely respond only to the instantaneous amplitude difference value between the two input terminals; hence it desirably produces no output when both inputs are at the same potential and polarity. Analytically the CMRR of a differential amplifier is the ratio of a voltage V_{in} to the difference of the potentials at the two inputs required for a null output; expressed as

$$\text{CMRR} = V_{in}/[(V_{in} \pm e_+) - (V_{in} \pm e_-)]. \qquad (17)$$

Each of the terms in the denominator of (17) is an equivalent potential at each input consisting of a magnitude V_{in} and an apparent error potential, $\pm e$. For example if V_{in} is 1 V and the difference of the two equivalent input potentials is 0.001 V, the CMRR is 1000 : 1. Its polarity is a function of the polarity of the symmetry inperfections, e_+ and e_-. Writing circuit voltage loops, the transfer function of the stage is expressed as

$$V_{out}/V_{in} = \frac{1 \pm 1/\text{CMRR}}{1 + (\cos\theta - j \sin\theta)/A_f} \qquad (18)$$

The effect of wide band CMRR and A_f with phase lag that is greater than 90°, can be seen in figure 4 for three situations: (A) high CMRR and low A_f; (B) high A_f and low CMRR; (C) both CMRR and A_f are high. The figure is a plot from laboratory data on actual devices and corroborates and predicted behavior from expression (18) though the slope of curve (B) could have been lower for a minus polarity effect of the CMRR. The three devices shown in figure 4 are high-performance units, and the use of the terms "low A_f" or "low CMRR are in a relative sense, keeping in mind that the total ordinate value is less than 0.1 percent error.

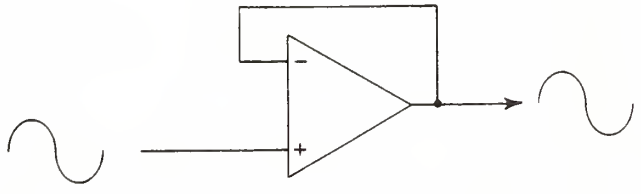

FIGURE 3. *Unity-gain isolation amplifier.*

The stage also has a desirable low output impedance—a dynamic impedance equal to the amplifier intrinsic output impedance divided by the value of A_f. A typical amplifier is capable of delivering ±10 V output at 10^6 Hz. with a load current of 10 mA. In summary, the operational stage described is a rather elegant impedance transformer with an impedance ratio of at least 10^6: 1 operating from dc through 100 kHz with a gain accuracy of 200 ppm to at least 20 kHz.

8. Test Results

A large number of tests were performed involving a variety of operational amplifiers for use as precision rectifier, filter, and unity-gain impedance coupling stages. The tests could be grouped in three broad areas of interest: accuracy at a reference frequency, precision (stability and repeatability) and frequency response (ac-dc deviation).

8.1. Tests for Accuracy

The first group of tests were concerned with the accuracy of transformation of ac to dc by an operational rectifier; i.e., the relation between the average value of the output (half-wave) and the rms value of the input, with a voltage wave of very low distortion, so that $V_{ave} = V_{rms} \cdot \sqrt{2}/\pi$. The operational amplifiers available for these tests were of the chopper-stabilized type having very high open-loop amplification at frequencies below 5 kHz. Their d-c drift was less than 5 μv for periods of several hours. Oil-filled, wire-wound resistors matched to a few ppm in unity-ratio value were employed, with resistance values from 1 to 25 kΩ. The major components of the measuring system for these tests, shown in figure 5, included a low-distortion, highly stable a-c power source, (total harmonic distortion below 0.01%) a seven-dial calibrated, precision d-c power supply, a standards laboratory differential thermal voltage comparator (called a DTVC), [4] sensitive d-c null meter, and the average ac-dc converter under test. The magnitude of each harmonic of the source (up through the 9th) was measured. Its effect on the form factor of the voltage wave was calculated to be less than 10 ppm, assuming the worst possible phase angle with respect to the fundamental.

The standard was the rms responding DTVC unit, having the function of monitoring the sine-wave signal to be measured and matching it by null method to the d-c supply of the equivalent rms value. In turn the d-c supply was scaled down by a factor of $\sqrt{2}/\pi$, by the attenuator, and nulled against the d-c output of the average converter. The d-c difference is the error of

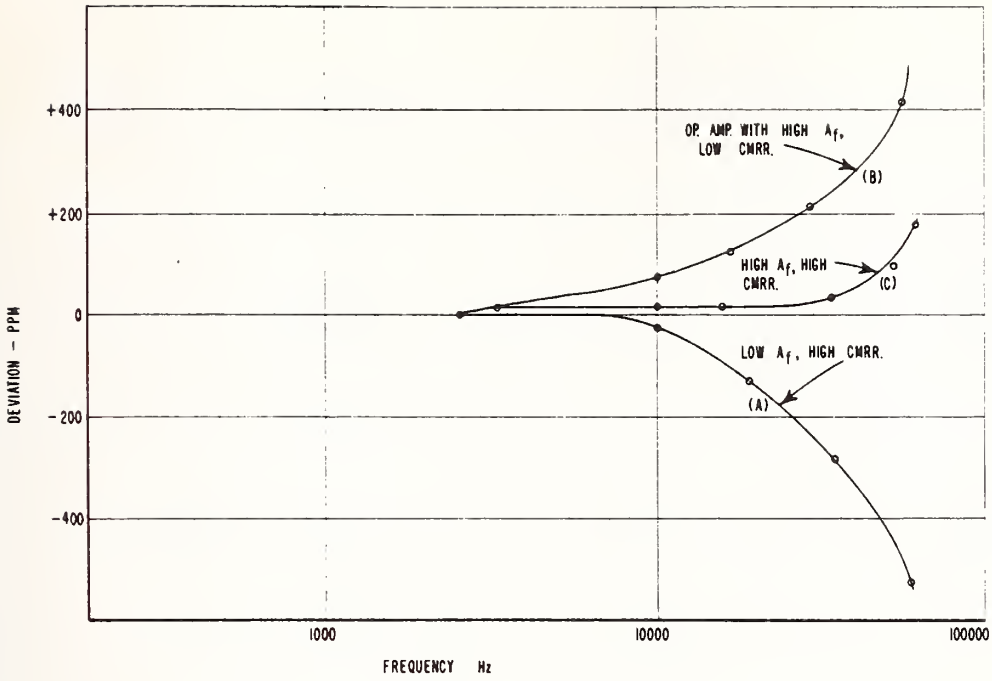

FIGURE 4. *Frequency response of figure 3.*

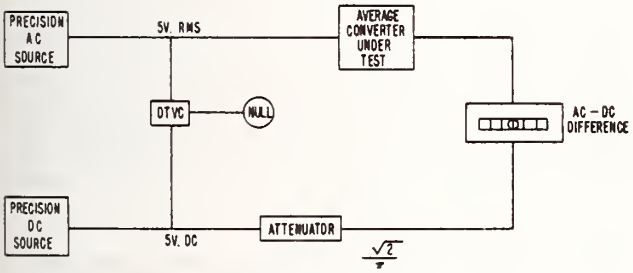

FIGURE 5. *Testing system.*

the device under test. Since the entire system has d-c response, scale factor inaccuracies at any position in the system could be checked by substituting the same d-c supply potential for the a-c signal (the average unit has identical input-output polarity correspondence). By using the same d-c supply as both signal and reference, its amplitude could be varied at will, allowing a check on dynamic range and on d-c offset. A 5 V rms a-c level was used in all the tests in order to avoid approaching the usual ± 10 V operational amplifier output limit. Operating voltages below 5 V are not recommended because most of the error factors discussed would be increased.

The results of these tests in figure 6 show that the operational rectification and filtering combination could yield a d-c voltage whose amplitude can be related to the rms value of a-c input with an accuracy of better than 20 ppm for frequencies out to 1000 Hz. At higher frequencies the accuracy was degraded because this was a feed forward type of amplifier. Short term perturbations of output were in the vicinity of 1 ppm, and possibly less.

These tests have demonstrated high accuracy performance at low and mid range audio frequencies. The next emphasis was on the design factors needed to extend the operating frequency range to 100 000 Hz and to include a high input impedance stage ahead of the rectifier.

8.2 Tests for Frequency Response

This group of tests involved the latest differential FET operational amplifiers having wide-band, high-value open-loop amplification figures. In addition, for reasons previously stated in the section on precision resistors, metal film resistance components were used in these tests. Since the question of measurement accuracy had been settled in the previously described group of tests, the test circuit arrangement was modified to demonstrate operational precision. Rather than employing the primary standard DTVC unit, a much simpler version of differential thermal comparator was used to monitor the output of the a-c signal power source for the purpose of maintaining constant amplitude. A peak ac-dc voltage comparator, though sensitive to waveform distortion, could be used in place of an rms comparator since an ac source of low distortion is specified. An in-depth analysis of the effects of ac distortion on the rectified average value can be found in reference [3]. For these tests the stress was on frequency response, exact value of magnitudes being of secondary importance. The recorded values were the measured differences

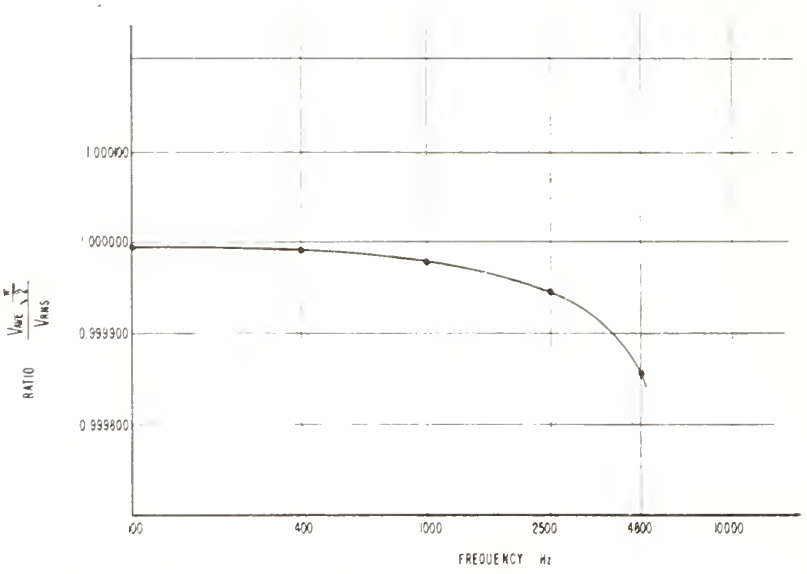

FIGURE 6. *Transfer accuracy of ac-dc converter (Chopper-stabilized amplifier).*

between the average d-c output and the fixed d-c reference power supply, expressed in ppm and plotted versus frequency. Normalizing the error values at some low frequency starting point is a means of removing the error offset due to any imprecision of resistor ratio and d-c offset at the amplifier stages.

The crosses in figure 7 show the test values obtained with an operational rectifier-filter combination which had metal film resistors.[2] Considering the number of instruments involved in the tests and their individual contribution to the end precision, the assignment of ± 150 ppm for the wide-band ac-dc error of the average measuring instrument is conservative. At the same time of the tests shown in figure 7, a unity-gain input isolation amplifier stage was added ahead of the operational rectifier state. In figure 7, the circles show the results of three runs; again all the values taken are plotted. Comparison of the circles and crosses shows that very little was changed in the response characteristic with the addition of the isolating amplifier. The benefit realized is substantial: the impedance presented to the a-c source increased from 5 kΩ to 10 MΩ. All frequency test points were within 200 ppm of the normalized value.

9. Some Wiring Suggestions

Circuit wiring, especially in the operational rectifier circuit should be short for minimum lead inductance and arranged in a manner for minimum shunt capacitance. One of the most critical points in the connection from the selected polarity output of the rectifier to the input resistor of the filter stage. Distortion of the half-sine wave resulting from shunt capacitance at this point could affect the accuracy of the average value.

[2] Four tests were made at each frequency, but were not separately plotted when the results differed by only small amounts.

It is strongly suggested the electronic circuit be d-c isolated from chassis ground. Removing the input and output common terminal from ground helps in eliminating the noisy effects of circulating d-c ground currents. Both a-c and d-c isolation can be had by a guarded circuit which offers low electrical capacity from the common terminals to chassis. This form of isolation requires a box-within-a-box type construction plus a special power supply. Such regulated supplies with a multi-shielded transformer are available with 10 000 megohm d-c insulation and 0.1 pF line-power input to d-c output isolation.

10. Initial D-C Offset Voltage Adjustments

After a sufficient warm-up period (usually 1 hr) the voltage offset of the filter stage is trimmed for zero output voltage with its input connection from the input resistor momentarily tied to common. The operational rectifier stage offset can be likewise adjusted by shorting to common the input side of the input resistor and trimming for zero output voltage. For this stage the diodes must be temporarily short-circuited. Effectiveness of input-output transfer of the instrument can be observed by applying some d-c value from 1 to 10 V to the input and comparing it to the instrument output by means of a null meter: the diode rectifier polarity output must be correctly selected. The d-c input-output agreement should be within the ratio accuracy of the resistors at the rectifier and filter stages.

11. Suggested Circuit

Figure 8 is a schematic diagram of a line-up of operational stages for use as an average ac-dc converting instrument. The circuit is capable of serving either the need for accuracy or for operational precision.

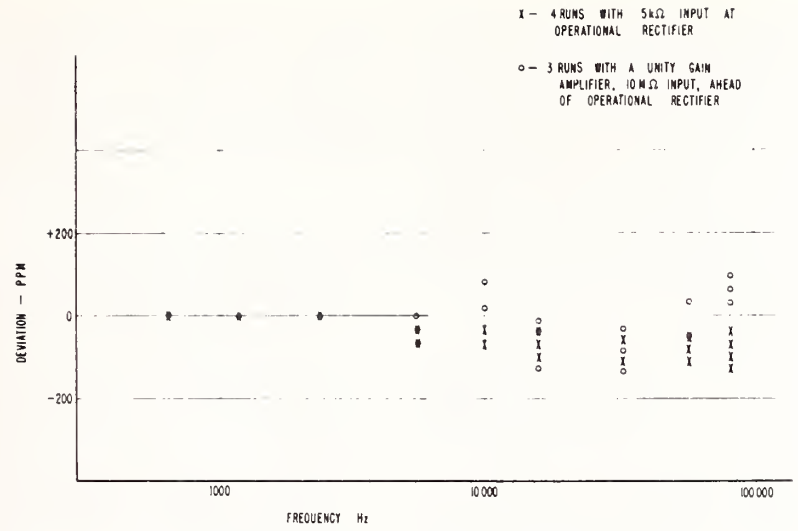

FIGURE 7. *Frequency response of converter.*

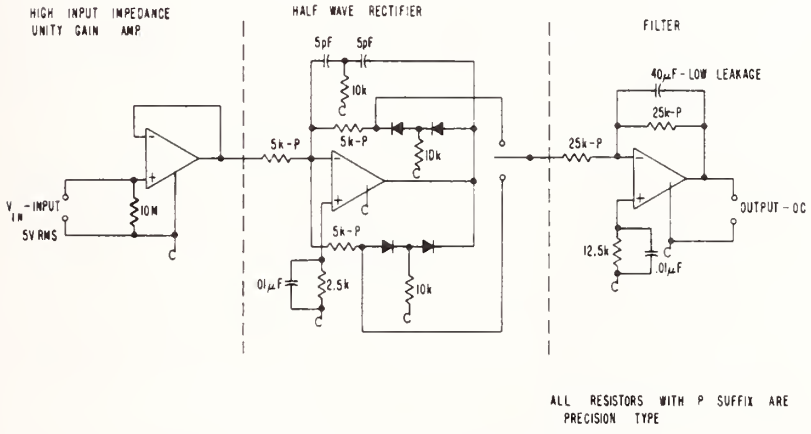

FIGURE 8. *Schematic diagram.*

If accuracy of 20 ppm is desired for ac-dc transfer, wherein the measured values can be related on an rms basis, the following points are pertinent. The high input impedance operational first stage must be deleted and the input signal applied to the second stage—the operational rectifier. The reason for this precaution is that the available amplifiers for use as a noninverting stage have marginal open loop gain and CMRR figures for accuracy work below 100 ppm. As for the rectifier stage, the selected operational amplifier must have a very high open loop gain and a low d-c drift. An open loop gain of 200 000 at 1 kHz is needed if the contributed error is to be less than 10 ppm. The voltage drift should be in the area of 1 μV/°C and 10^{-10} A/°C for the current drift. While differential FET type operational amplifiers come close to meeting these specifications, the accuracy results reported in this writing have been obtained with chopper stabilized devices. Because of their possible feed-forward design the 20 ppm operating accuracy is limited to frequencies below 1 kHz and the gain setting resistors at the rectifier stage are restricted to values of 1 kΩ or less. The latter components should have a ratio accuracy error of less than 5 ppm, available in oil filled, wire wound resistors. A signal level of 5 V rms at the a-c source is suggested. The a-c signal power source should have a total harmonic distortion of less than 50 ppm and freedom from a d-c component, if the rms value is desired. The operational amplifier at the filter stage need only have the stated d-c precision of the rectifier stage.

The three stages shown in figure 8 can offer an operating precision and flatness of amplitude response with frequency of better than 200 ppm over the range from d-c to 100 KHz, as described previously under the section heading of Test Results. FET-type differ-

ential operational amplifiers can be found to meet the requirements of each stage. If the sole interest is operational precision in the form of stability and repeatability, the principal concern in selecting the operational amplifiers is the d-c drift characteristics. However, the open loop voltage gain has to be considered in order to maintain the desired transfer gain ratio. With a voltage drift value below 10 μV/°C and a current drift under 10^{-10}A/°C the operating precision can be held to better than 100 ppm. For situations requiring accuracy of measurement or if flatness of amplitude response with frequency is important, the wide-band open loop voltage gain deserves additional attention. In the case of the noninverting first stage the CMRR figure is also important. If the input stage is to have a unity gain accuracy of 100 ppm at 5 kHz, both the open loop gain and the CMRR at that frequency should be at least 20 000 for the selected operational amplifier. For the rectifier stage the same values of 20 000 is needed at 5 kHz for 100 ppm accuracy but the CMRR can be neglected. The filter stage as usual need only have the stated d-c operating characteristics. Again, in the case of rms measurements of accuracy the a-c signal source must have appropriate purity—no more than 200 ppm total harmonic distortion for 100 ppm transfer accuracy.

12. References

[1] Richman, P., Operational Rectifier, U.S. Patent No. 3311835, March 28, 1967, assigned to Weston Instruments, Inc.

[2] Marzetta, L. A., A Peak AC–DC Voltage Comparator for Use in a Standards Laboratory, NBS Technical Note No. 280, issued January 17, 1966.

[3] Richman, P., Modern AC Voltage Calibration for Audio and Sub-Audio Frequencies, presented at 19th Annual ISA Conference, October 12–15, 1964, New York, Preprint No. 21, 4–2–64.

[4] Hermach, F. L., Griffin, J. E., and Williams, E. S., A System for Accurate Direct & Alternating Voltage Measurements, IEEE Trans. on Instrumentation & Measurement IM14 p215–224, 1965.

(Paper 73C3&4–288)

APPENDIX I

APPENDIX II

APPENDIX III

APPENDIX I

Electrical and Electronic Metrology:
A Bibliography of NBS Electrosystems Division's Publications

Compiled by

Jenilie C. Palla and Betty A. Oravec

Edited by

John R. Sorrells

Abstract

This bibliography covers publications of the Electrosystems Division, Center for Electronics and Electrical Engineering, NBS, and of its predecessor sections for the period January 1968 to March 1984. A brief description of the Division's technical program is given in the introduction.

Introduction

Scope and Organization

This bibliography covers publications by the Electrosystems Division, CEEE, plus those of the predecessor sections for the Electricity Division beginning with 1968. For convenience, the references are grouped into ten categories by subject: DC and Low Frequency Measurements, Thermal Converters, Power Systems Related Measurements, High Voltage Measurements, Data Acquisition and Conversion, Automatic Testing, Electrical Insulation Measurements, Electronic Instrumentation and Metrology, Sensors, and Miscellaneous.* References may appear in more than one category; the reader is urged to check several categories if an overlap is likely. References are presented chronologically within each category, with the most recent last. An index by author is also provided.

Division Activities

The Electrosystems Division develops measurement methods and standards and provides metrology support for electrical and electronic systems, components and materials; it develops and maintains national reference standards for practical electrical units derived from basic units. The measurement technology developed by the Division is applied to the advancement of modern electrical/electronic measurement instrumentation, to the development of efficient generation, transmission and utilization of electric energy, and to maintaining a national reference base for certain critical measurements required by science, industry, and government agencies.**

Presently, the Division is structured into two groups -- (1) Applied Electrical Measurements, and (2) Electronic Instrumentation and Metrology.

*Responsibility for work on sensors (transducers) for physical quantities such as pressure and acceleration was reassigned outside the Center several years ago; reference to a selected short list of papers is provided for completeness.

**Research, development and calibration work on basic electrical units is conducted by the Electrical Measurements and Standards Division of NBS. For additional references the reader is referred to the NBS Publication LP-38 Electrical Units, Instruments, and Measurements, available from the Electricity Division, Metrology Building, Room B258, National Bureau of Standards, Washington, DC 20234.

Applied Electrical Measurements

Within the Applied Electrical Measurements (AEM) Group, standards are developed and calibrations performed for electric power and energy, high-voltage and high-power impedances, instrument transformers, high-voltage dividers, and high-voltage transient measurement systems utilized in measuring such phenomena as standard lightning impulses and voltage/current pulses encountered in x-ray equipment. In situations where high-voltage measuring instruments must be calibrated in their working environment or are too bulky for shipment to NBS, calibrations on a limited basis are performed on the customers' premises.

The AEM Group is also concerned with the measurement of electric fields and ion activity in the vicinity of high-voltage ac and dc transmission lines. Measurement methods to monitor or predict insulation failure mechanisms are developed with emphasis on liquid, liquid-solid, and gaseous insulation systems.

Electronic Instrumentation and Metrology

The Electronic Instrumentation and Metrology (EIM) Group is concerned with modern electronic techniques for the measurement of electrical parameters in the dc and low-frequency (to about 1 MHz) range. Among the approaches investigated, very prominent are dynamic measurement methods in which electrical signals are measured by fast sampling techniques. Data from the measurements is processed digitally utilizing microprocessor-based instrumentation.

Within the EIM Group, methods are developed to characterize data acquisition and conversion devices. A calibration service for precision A/D and D/A converters has recently been offered and phase angle calibration based on a dual sine-wave source is now available on special request. Research is continuing on new precision signal sources based on digital synthesis. Such signal sources are expected to serve as calibration standards for numerous parameters. Special purpose instrument standards, e.g., wide-band sampling wattmeters, are under development, and automation techniques for precision measurement are being explored in the area of alternating voltages.

How To Obtain Listed Publications

In most cases reprints of articles in technical journals may be obtained on request to the author or to the Electrosystems Division, Room B166, Metrology Building, National Bureau of Standards, Washington, DC 20234.

Some of the publications are available from the Government Printing Office (GPO). Current price information may be obtained from GPO, Order Inquiry Section, by calling 202/783-3238. Remittances for publications to be purchased from GPO should be mailed to Superintendent of Documents, U.S. Government Printing Office, Washington, DC 20402, by postal money order, express money order, or check. Postage stamps will not be accepted. Foreign remittances should be made either by international money order or draft on an American bank. The Superintendent of Documents allows a discount of 25 percent on orders of 100 or more copies of one publication. The GPO stock number and full title of the publication must be given when ordering. For credit card orders, information is needed as follows.

Credit Card Orders Only

Total charges $_____ Fill in the boxes below.

Credit Card No. ☐☐☐☐☐☐☐☐☐☐☐☐☐☐☐☐

Expiration Date Month/Year ☐☐☐☐

Persons who make frequent purchases from GPO may find a deposit account convenient. Deposits of $50 or more are accepted against which orders may be placed without making individual remittances or first obtaining quotations. Order blanks are furnished for this purpose. After the order has been processed, the order itself is returned, showing the publications supplied, explanations regarding those not sent, the amount of charge, and the balance on deposit.

Copies of most NBS publications, NBS Interagency Reports (NBSIR Series), and other Government reports may be ordered through the National Technical Information Service, U.S. Department of Commerce, Springfield, VA 22161. Current price information may be obtained from the NTIS Order Desk by calling 703/487-4650. If there is an option as to form, be sure to specify whether paper copy (PC) or microfiche (MF) is desired. As long as the publication is available in paper copy from GPO, only microfiche copy can be obtained from NTIS. Prepaying (with check or money order) or using an NTIS Deposit Account or American Express Card Account speeds order processing. Be sure payment and order are sent together. Checks, payable to NTIS, must be in U.S. dollars.

For convenience, a table providing GPO stock numbers and NTIS accession numbers for all NBS publications included in this bibliography is given on pages 28-30.

Bibliography

DC and Low Frequency Measurements

W. C. Sze, "An Injection Method for Self-Calibration of Inductive Voltage Dividers," J. Res., Nat. Bur. Stand. (U.S.), (Eng. & Instr.) 72C, No. 1, pp. 49-59 (Jan.-Mar. 1968).

O. Petersons and W. C. Sze, "Calibration of Transformer Ratios With a Reciprocal Transformer-Type Network," Conf. Precision Electromagnetic Measurements Digest, Boulder, CO, pp. 57-59, June 2-5, 1970.

R. F. Dziuba and B. L. Dunfee, "Resistive Voltage-Ratio Standard and Measuring Circuit," IEEE Trans. Instrum. Meas. IM-19, No. 4, pp. 266-277 (Nov. 1970).

A. Erez, "Low-Frequency Electrical Signal Measurement by Electrooptical Methods," IEEE Trans. Instrum. Meas. IM-21, No. 4, pp. 358-360 (Nov. 1972).

T. M. Souders, "Wide-Band Two-Stage Current Transformers of High Accuracy," IEEE Trans. Instrum. Meas. IM-21, No. 4, pp. 340-345 (Nov. 1972).

W. C. Sze and F. R. Kotter, "The Design of Near-Perfect Instrument Transformers of Simple and Inexpensive Construction," J. Appl. Meas. 2, pp. 22-27 (1974).

H. K. Schoenwetter, "An Ultra-Stable AC Power Supply for an Absolute Volt Determination," Metrologia 10, pp. 11-15 (1974).

D. B. Sullivan and R. F. Dziuba, "Low Temperature Direct Current Comparators," Rev. Sci. Instrum. 45, No. 4, pp. 517-519 (Apr. 1974).

K. J. Lentner, "A Current Comparator System to Establish the Unit of Electrical Energy of 60 Hz," IEEE Trans. Instrum. Meas. IM-23, No. 4, pp. 334-336 (Dec. 1974).

T. M. Souders, "An Audio-Frequency Four-Terminal Resistance Bridge," IEEE Trans. Instrum. Meas. IM-23, No. 4, pp. 342-345 (Dec. 1974).

D. B. Sullivan and R. F. Dziuba, "A Low-Temperature Direct-Current Comparator Bridge," IEEE Trans. Instrum. Meas. IM-23, No. 4, pp. 256-260 (Dec. 1974).

R. S. Turgel, "Digital Wattmeter Using a Sampling Method," IEEE Trans. Instrum. Meas. IM-23, No. 4, pp. 337-341 (Dec. 1974).

R. F. Dziuba and D. B. Sullivan, "Cryogenic Direct Current Comparators and Their Applications," IEEE Trans. Magn. MAG-11, No. 2, pp. 716-719 (Mar. 1975).

R. S. Turgel, "Sampling Techniques for Electric Power Measurement," Nat. Bur. Stand. (U.S.), Tech. Note 870, 35 pages (June 1975). [GPO]

R. S. Turgel, Chapter 9.5 Voltage, Current, and Charge Measurements, Methods of Experimental Physics, Vol. 2, Electronic Methods, 2nd Edition, Part B, Academic Press, Inc., 1975.

F. L. Hermach, "AC-DC Comparators for Audio-Frequency Current and Voltage Measurements of High Accuracy," IEEE Trans. Instrum. Meas. IM-25, No. 4, pp. 489-494 (Dec. 1976).

C. B. Childers, R. F. Dziuba, and L. H. Lee, "A Resistive Ratio Standard for Measuring Direct Voltages to 10 kV," IEEE Trans. Instrum. Meas. IM-25, No. 4, pp. 505-508 (Dec. 1976).

H. K. Schoenwetter, "An RMS Digital Voltmeter/Calibrator for Very-Low Frequencies," IEEE Trans. Instrum. Meas. IM-27, No. 3, pp. 259-268 (Sept. 1978).

N. B. Belecki, B. L. Dunfee, and O. Petersons, "The National Measurement System for Electricity," NBSIR 75-935, 86 pages (Sept. 1978).

R. S. Turgel and N. M. Oldham, "High-Precision Audio-Frequency Phase Calibration Standard," IEEE Trans. Instrum. Meas. IM-27, No. 4, pp. 460-464 (Dec. 1978).

B. F. Field, "A Fast Response Low-Frequency Voltmeter," IEEE Trans. Instrum. Meas. IM-27, No. 4, pp. 368-372 (Dec. 1978).

R. C. McAuliff, K. J. Lentner, W.J.M. Moore, and G. Schuster, "An International Comparison of Power Measurements at 120 V, 5 A, and 60 Hz," IEEE Trans. Instrum. Meas. IM-27, No. 4, pp. 445-449 (Dec. 1978).

R. L. Kahler, "An Electronic Ratio Error Set for Current Transformer Calibrations," IEEE Trans. Instrum. Meas. IM-28, No. 2, pp. 162-164 (June 1979).

H. K. Schoenwetter, "NBS Provides Voltage Calibration Service in 0.1 - 10-Hz Range Using AC Voltmeter/Calibrator," IEEE Trans. Instrum. Meas. IM-28, No. 4, pp. 327-331 (Dec. 1979).

K. J. Lentner, C. B. Childers, and S. G. Tremaine, "A Semiautomatic System for AC/DC Difference Calibration," IEEE Trans. Instrum. Meas. IM-29, No. 4, pp. 400-405 (Dec. 1980).

B. A. Bell, B. F. Field, and T. H. Kibalo, "A Fast Response, Low-Frequency Sampling Voltmeter," Nat. Bur. Stand. (U.S.), Tech. Note 1159, 113 pages (Aug. 1982). [GPO]

N. M. Oldham, "A 50 ppm AC Reference Standard Which Spans 1 Hz to 50 kHz," IEEE Trans. Instrum. Meas. IM-32, No. 1, pp. 176-179 (March 1983).

K. J. Lentner and D. R. Flach, "An Automatic System for AC/DC Calibration," IEEE Trans. Instrum. Meas. IM-32, No. 1, pp. 51-56 (March 1983).

H. K. Schoenwetter, "AC Voltage Calibrations for the 0.1 Hz to 10 Hz Frequency Range," Nat. Bur. Stand. (U.S.), Tech. Note 1182, 58 pages (Sept. 1983). [GPO]

Thermal Converters

E. S. Williams, "A Voltage Converter for a New Era," Meas. Data (Nov./Dec. 1968).

L. A. Marzetta and D. R. Flach, "Design Features of a Precision AC-DC Converter," J. Res., Nat. Bur. Stand. (U.S.), (Eng. & Instr.) 73C, Nos. 3 and 4, pp. 47-55 (July-Dec. 1969).

E. S. Williams, "Calibration of Thermal Voltage Converters," Proceedings, Third Precision Measurements Association Conference, Burbank, CA (1970).

E. S. Williams, "Thermal Voltage Converters and Comparator for Very Accurate AC Voltage Measurements," J. Res., Nat. Bur. Stand. (U.S.), (Eng. & Instr.) 75C, Nos. 3. and 4, pp. 145-154 (July-Dec. 1971).

F. L. Hermach, "AC-DC Comparators for Audio-Frequency Current and Voltage Measurements of High Accuracy," IEEE Trans. Instrum. Meas. IM-25, No. 4, pp. 489-494 (Dec. 1976).

F. L. Hermach and D. R. Flach, "An Investigation of Multijunction Thermal Converters," IEEE Trans. Instrum. Meas. IM-25, No. 4, pp. 524-528 (Dec. 1976).

E. S. Williams, "Thermal Current Converters for Accurate AC Current Measurement," IEEE Trans. Instrum. Meas. IM-25, No. 4, pp. 519-523 (Dec. 1976).

K. J. Lentner and S. G. Tremaine, "A Semiautomatic AC/DC Thermal Voltage Converter Calibration System," NBSIR 82-2576, 62 pages (Sept. 1982).

K. J. Lentner and D. R. Flach, "An Automatic System for AC/DC Calibration," IEEE Trans. Instrum. Meas. IM-32, No. 1, pp. 51-56 (March 1983).

Power Systems Related Measurements

O. Petersons, "A Transformer-Ratio-Arm Bridge for Measuring Large Capacitors Above 100 Volts," IEEE Trans. Power Appar. Syst. PAS-87, No. 5, pp. 1354-1361 (May 1968).

O. Petersons, "A Semi-Automatic Bridge for Measuring Power Losses in Shunt Reactors," Proceedings of 23rd Session International Conf. Large High-Tension Electric Systems, Paris, France, pp. 6-8 (Aug. 24-Sept. 3, 1970).

T. M. Souders, "A Wide Range Current Comparator System for Calibrating Current Transformers," IEEE Trans. Power Appar. Syst. PAS-90, No. 1, pp. 318-324 (Jan./Feb. 1971).

T. M. Souders, "Wide-Band Two-Stage Current Transformers of High Accuracy," IEEE Trans. Instrum. Meas. IM-21, No. 4, pp. 340-345 (Nov. 1972).

D. L. Hillhouse and A. E. Peterson, "A 300-kV Compressed Gas Standard Capacitor With Negligible Voltage Dependence," IEEE Trans. Instrum. Meas. IM-22, No. 4, pp. 408-416 (Dec. 1973).

K. J. Lentner, "A Current Comparator System to Establish the Unit of Electrical Energy at 60 Hz," IEEE Trans. Instrum. Meas. IM-23, No. 4, pp. 334-336 (Dec. 1974).

R. S. Turgel,"Digital Wattmeter Using a Sampling Method," IEEE Trans. Instrum. Meas. IM-23, No. 4, pp. 337-341 (Dec. 1974).

R. S. Turgel, "Sampling Techniques for Electric Power Measurement," Nat. Bur. Stand. (U.S.), Tech. Note 870, 35 pages (June 1975).

S. R. Houghton, "Transfer of the Kilowatthour," IEEE Trans. Power Appar. Syst. PAS-94, No. 4, pp. 1232-1240 (July/Aug. 1975).

O. Petersons and W. E. Anderson, "A Wide-Range High-Voltage Capacitance Bridge With One PPM Accuracy," IEEE Trans. Instrum. Meas. IM-24, No. 4, pp. 336-344 (Dec. 1975).

N. M. Oldham, "A Measurement Assurance Program for Electric Energy," Nat. Bur. Stand. (U.S.), Tech. Note 930, 23 pages (Sept. 1976). [GPO]

F. R. Kotter and M. Misakian, "AC Transmission Line Field Measurements," prepared for the Department of Energy, DOE Report No. HCP/T-6010/E1, pp. 1-79 (Nov. 1977).

D. L. Hillhouse and W. C. Sze, "Calibration of CCVTs in the Substation," 45th Annual International Conference of Doble Clients, Section 9-501 (1978).

D. L. Hillhouse, O. Petersons, and W. C. Sze, (Principal Investigators), "A Prototype Field Calibration System for Coupling Capacitor Voltage Transformers (CCVTs)," Final Report No. EL-690, prepared for the Electric Power Research Institute, under Project RP-134-1 (Apr. 1978).

D. L. Hillhouse, "Portable System Calibrates CCVTs," Electr. World 189, No. 12, pp. 44-46 (June 15, 1978).

W. E. Anderson and R. S. Davis, "Dissipation Factor Measurements on Dielectric Materials at Liquid Helium Temperatures," 1975 Annual Report of the Conference on Electrical Insulation and Dielectric Phenomena, National Academy of Sciences, Washington, DC, pp. 151-156 (July 1978).

W. E. Anderson, R. S. Davis, O. Petersons, and W.J.M. Moore, "An International Comparison of High Voltage Capacitor Calibrations," IEEE Trans. Power Appar. Syst. PAS-97, No. 4, pp. 1217-1223 (July/August 1978).

Working Group on Electrostatic and Electromagnetic Effects of Transmission Lines, "Measurement of Electric and Magnetic Fields From Alternating Current Power Lines," (NBS participants: F. R. Kotter and M. Misakian), IEEE Trans. Appar. Syst. PAS-97, No. 4, pp. 1104-1114 (July/August 1978).

M. Misakian and F. R. Kotter, Discussion of Paper F78 169-5, "Analysis of the Proximity Effects in Electric Field Measurements," IEEE Trans. Power Appar. Syst. PAS-97, No. 6, pp. 2175-2176 (Nov./Dec. 1978).

R. C. McAuliff, K. J. Lentner, W.J.M. Moore, and G. Schuster, "An International Comparison of Power Measurements at 120 V, 5 A, and 60 Hz," IEEE Trans. Instrum. Meas. IM-27, No. 4, pp. 445-449 (Dec. 1978).

M. Misakian, "Measurement of AC Transmission Line Fields and Related Electrical Parameters," IEEE Tutorial Text 79-EH0145-3-PWR, pp. 36-46 (1979).

D. L. Hillhouse, O. Petersons, and W. C. Sze, "A Prototype System for On-Site Calibration of Coupling Capacitor Voltage Transformers (CCVTs)," IEEE Trans. Power Appar. Syst. PAS-98, No. 3, pp. 1026-1036 (May/June 1979).

R. L. Kahler, "An Electronic Ratio Error Set for Current Transformer Calibrations," IEEE Trans. Instrum. Meas. IM-28, No. 2, pp. 162-164 (June 1979).

F. R. Kotter, "Characterization of the Electric Environment Under HVDC Transmission Lines: Instrumentation and Measurement Techniques," Proceedings of Workshop on Electrical and Biological Effects Related to HVDC Transmission, Richland, Washington, October 19-20, 1978 (Aug. 1979).

R. E. Hebner and S. Annestrand, "Evaluation of Calibration Techniques for Multimegavolt Impulse Dividers," International Symposium on High Voltage Engineering, Milan, Italy, pp. 1-4 (Aug. 1979).

R. E. Hebner, D. L. Hillhouse, and R. A. Bullock, "Evaluation of a Multimegavolt Impulse Measurement System," NBSIR 79-1933, 102 pages (Nov. 1979).

M. Misakian, "Generation and Measurement of DC Electric Fields With Space Charge," NBSIR 80-2177, 39 pages (Jan. 1981).

D. L. Hillhouse, "Guide for Safe Operating Procedures at High Voltage Substations by NBS and Utility Staff During the Field Calibration of Coupling Capacitor Voltage Transformers (CCVTs)," NBSIR 81-2192, 10 pages (Feb. 1981). [Limited distribution; not available from NTIS]

W. E. Anderson and J. D. Ramboz, "1980 Annual Report: Technical Contributions to the Development of Incipient Fault Detection/Location Instrumentation," NBSIR 81-2235, 125 pages (March 1981).

R. E. Hebner, "Development of Power System Measurements--Quarterly Report January 1, 1981 to March 31, 1981," NBSIR 81-2283, 14 pages (Apr. 1981).

R. H. McKnight, F. R. Kotter, M. Misakian, and P. Ortiz, "1980 Annual Report: Electric and Magnetic Field Measurements," NBSIR 81-2267, 65 pages (May 1981).

M. Misakian, "Generation and Measurement of DC Electric Fields With Space Charge," J. Appl. Phys. 52, No. 5, pp. 3135-3144 (May 1981).

R. E. Hebner, "Development of Power System Measurements--Quarterly Report April 1, 1981 to June 30, 1981," NBSIR 81-2334, 15 pages (June 1981).

D. A. Leep and F. R. Kotter, "Discussion of Paper No. 81 WM 126-2, Measuring Voltage and Current Harmonics on Distribution Systems," by M. F. McGranaghan, J. H. Shaw, and R. E. Owen, IEEE Trans. Power Appar. System. PAS-100, No. 7, pp. 3599-3608 (July 1981).

R. J. Van Brunt, "Discussion of paper by J. M. Pelletier et al.," IEEE Trans. Power Appar. Syst. PAS-100, No. 8, pp. 3867-3868 (Aug. 1981).

F. R. Kotter and M. Misakian, "AC Transmission Line Field Measurements," NBSIR 77-1311, 79 pages (Oct. 1981).

D. L. Hillhouse and D. A. Leep, "Analysis of the Calibration of Metering CCVTs in a Utility Substation," NBSIR 81-2360, 53 pages (Oct. 1981).

N. M. Oldham and R. S. Turgel, "A Power Factor Standard Using Digital Waveform Generation," IEEE Trans. Power Appar. Syst. PAS-100, No. 11, pp. 4435-4438 (Nov. 1981).

R. H. McKnight, F. R. Kotter, and M. Misakian, "Measurement of Ion Current Density at Ground Level in the Vicinity of High Voltage DC Transmission Lines," NBSIR 81-2410, 27 pages (Dec. 1981).

R. E. Hebner, "Development of Power System Measurements--Quarterly Report October 1, 1981 to December 31, 1981," NBSIR 82-2501, 21 pages (May 1982).

R. E. Hebner, "Experimental Comparison of Step-Response and Ramp-Response Measurements in Freestanding Dividers, Measurement of Electrical Quantities in Pulse Power Systems," Nat. Bur. Stand. (U.S.), Spec. Publ. 628, pp. 26-33 (June 1982). [GPO]

"Measurement of Electrical Quantities in Pulse Power Systems," Proceedings of the Workshop on Measurement of Electrical Quantities in Pulse Power Systems, Boulder, CO, March 2-4, 1981, R. H. McKnight and R. E. Hebner, Jr., editors, Nat. Bur. Stand. (U.S.), Spec. Publ. 628, 410 pages (June 1982). [GPO]

R. E. Hebner, "Development of Power System Measurements--Quarterly Report January 1, 1982 to March 31, 1982," NBSIR 82-2528, 20 pages (June 1982).

R. H. McKnight and F. R. Kotter, "A Facility to Produce Uniform Space Charge for Evaluating Ion Measuring Instruments," NBSIR 82-2517, 33 pages (June 1982).

R. E. Hebner, "Development of Power System Measurements--Quarterly Report April 1, 1982 to June 30, 1982," NBSIR 82-2586, 20 pages (Oct. 1982).

R. H. McKnight, F. R. Kotter, and M. Misakian, "Measurement of Ion Current Density at Ground Level in the Vicinity of High Voltage DC Transmission Lines," IEEE Trans. Power Appar. Syst. PAS-102, No. 4, pp. 934-941 (April 1983).

R. E. Hebner, "Development of Power System Measurements--Quarterly Report July 1, 1982 to September 30, 1982," NBSIR 83-2705, 25 pages (May 1983).

R. H. McKnight and F. R. Kotter, "A Facility to Produce Uniform Space Charge for Evaluating Ion Measuring Instruments," IEEE Trans. Power Appar. Syst., PAS-102, No. 7, pp. 2349-2357 (July 1983).

E. F. Kelley and R. E. Hebner, "Electro-Optic Measurement of the Electric Field Distribution in Transformer Oil," IEEE Trans. Power Appar. Syst., PAS-102, No. 7, pp. 2092-2097 (July 1983).

J. D. Ramboz and R. C. McAuliff, "A Calibration Service for Wattmeters and Watthour Meters," Nat. Bur. Stand. (U.S.), Tech. Note 1179, 111 pages (July 1983). [GPO]

R. H. McKnight and H. K. Schoenwetter, "Evaluation of Transient Measurement Methods in Gas-Insulated Transmission Lines," NBSIR 83-2753, 75 pages (August 1983).

R. E. Hebner, "Development of Power System Measurements--Quarterly Report October 1, 1982 to December 31, 1982," NBSIR 83-2755, 41 pages (Sept. 1983).

R. E. Hebner, "Development of Power System Measurements--Quarterly Report January 1, 1983 to March 31, 1983," NBSIR 83-2761, 27 pages (Oct. 1983).

M. Misakian and P. M. Fulcomer, "Measurement of Nonuniform Power Frequency Electric Fields," IEEE Trans. on Electr. Insul. EI-18, No. 6, pp. 657-661, December 1983.

High Voltage Measurements

E. C. Cassidy and S. Abramowitz, "Time-Resolved Emission and Absorption Studies of Exploding Wire Spectra," Proc. 4th Conf. Exploding Wires, Book, Exploding Wires 4, pp. 109-124 (Plenum Press, New York, NY, 1968).

E. C. Cassidy, "Time-Resolved Studies of Spectra Produced by Electrically Exploded Wires," Die Naturwissenschaften, Heft 3, pp. 125-128 (1968).

H. E. Radford and K. M. Evenson, "Paramagnetic-Resonance Spectrum of Metastable (^2D) Atomic Nitrogen," Phys. Rev. 168, No. 1, pp. 70-74 (Apr. 5, 1968).

O. Petersons, "A Transformer-Ratio-Arm Bridge for Measuring Large Capacitors Above 100 Volts," IEEE Trans. Power Appar. Syst. PAS-87, No. 5, pp. 1354-1361 (May 1968).

E. C. Cassidy and H. N. Cones, "Calibration of a Kerr Cell System for High Voltage Pulse Measurements," Final Report for Sandia Laboratories, Sandia Report No. SC-CR-68-3730 (Aug. 1968).

E. C. Cassidy, S. Abramowitz, and C. W. Beckett, "Investigations of the Exploding Wire Process as a Source for High Temperature Studies," Nat. Bur. Stand. (U.S.), Monogr. 109, 53 pages (Nov. 1968).

H. E. Radford, "Scanning Microwave Echo Box Spectrometer," Rev. Sci. Instrum. 39, No. 11, pp. 1687-1691 (Nov. 1968).

E. C. Cassidy, H. N. Cones, D. C. Wunsch, and S. R. Booker, "Calibration of a Kerr Cell System for High-Voltage Pulse Measurements," IEEE Trans. Instrum. Meas. IM-17, No. 4, pp. 313-320 (Dec. 1968).

E. C. Cassidy and H. N. Cones, "Development and Analysis of Techniques for Calibration of Kerr Cell Pulse-Voltage Measuring Systems III," Final Report for Sandia Laboratories, NBS Report No. 10 078 (Aug. 1969).

E. C. Cassidy and H. N. Cones, "Development and Analysis of Techniques for Calibration of Kerr Cell Pulse-Voltage Measuring Systems IV," Final Report for Sandia Laboratories, NBS Report No. 10 296 (Aug. 6, 1970).

E. C. Cassidy, H. N. Cones, and S. R. Booker, "Development and Evaluation of Electrooptical High-Voltage Pulse Measurement Techniques," IEEE Trans. Instrum. Meas. IM-19, No. 4, pp. 395-402 (Nov. 1970).

H. E. Radford and C. V. Kurtz, "Stark Effect and Hyperfine Structure of HCN Measured With an Electric Resonance Maser Spectrometer," J. Res., Nat. Bur. Stand. (U.S.), (Phys. and Chem.) 74A, No. 6, pp. 791-799 (Nov.-Dec. 1970).

E. C. Cassidy, "Development and Analysis of Techniques for Calibration of Kerr Cell Pulse-Voltage Measuring Systems V," Final Report for Sandia Laboratories, NBS Report No. 10 493 (Oct. 1972).

D. L. Hillhouse, "Circuit for Impulse Testing of Gas-Tube Lightning Arresters," IEEE Trans. Commun. COM-20, No. 5, pp. 936-941 (Oct. 1972).

E. C. Cassidy, R. E. Hebner, W. E. Anderson, R. J. Sojka, and S. R. Booker, "Development and Analysis of Techniques for Calibration of Kerr Cell Pulse-Voltage Measuring Systems VI," Final Report for Sandia Laboratories, NBS Report No. 10 945 (Nov. 1, 1972).

A. Erez, "Low-Frequency Electrical Signal Measurement by Electrooptical Methods," IEEE Trans. Instrum. Meas. IM-21, No. 4, pp. 358-360 (Nov. 1972).

E. C. Cassidy, W. E. Anderson, and S. R. Booker, "Recent Refinements and Developments in Kerr System Electrical Measurement Techniques," IEEE Trans. Instrum. Meas. IM-21, No. 4, pp. 504-510 (Nov. 1972).

R. E. Hebner, Jr. and E. C. Cassidy, "Measurement of 60 Hz Voltages Using the Kerr Effect," Rev. Sci. Instrum. 43, No. 12, pp. 1839-1841 (Dec. 1972).

E. C. Cassidy, R. E. Hebner, R. J. Sojka, and M. Zahn, "Development and Analysis of Techniques for Calibration of Kerr Cell Pulse-Voltage Measuring Systems VII," Final Report for Sandia Laboratories, NBSIR 73-403, 130 pages (Nov. 1973) (no copies available).

D. L. Hillhouse and A. E. Peterson, "A 300-kV Compressed Gas Standard Capacitor With Negligible Voltage Dependence," IEEE Trans. Instrum. Meas. IM-22, No. 4, pp. 408-416 (Dec. 1973).

R. E. Hebner, E. C. Cassidy, and R. J. Sojka, "Development and Analysis of Techniques for Calibration of Kerr Cell Pulse-Voltage Measuring Systems VIII," NBSIR 74-564, 55 pages (Aug. 21, 1974).

R. E. Hebner, Jr., "Calibration of Kerr Systems Used to Measure High Voltage Pulses," NBSIR 75-774, 51 pages (Aug. 7, 1975).

R. E. Hebner, Jr., "Electrical Measurement of High Voltage Pulses in Diagnostic X-Ray Units," NBSIR 75-775, 62 pages (Nov. 1, 1975).

R. E. Hebner, Jr. and S. R. Booker, "A Portable Kerr System for the Measurement of High Voltage Pulses," Proc. IEEE SOUTHEASTCON 75, 1, pp. 3A-1-1 - 3A-5-1 (1975).

O. Petersons and W. E. Anderson, "A Wide-Range High-Voltage Capacitance Bridge With One PPM Accuracy," IEEE Trans. Instrum. Meas. IM-24, No. 4, pp. 336-344 (Dec. 1975).

R. E. Hebner, E. C. Cassidy, and J. E. Jones, "Improved Techniques for the Measurement of High-Voltage Impulses Using the Electrooptic Kerr Effect," IEEE Trans. Instrum. Meas. IM-24, No. 4, pp. 361-366 (Dec. 1975).

R. L. Kahler, D. L. Hillhouse, and W. E. Anderson, "A Simple Overcurrent Protection Circuit for a High Voltage Laboratory," IEEE Trans. Instrum. Meas., pp. 161-162 (June 1976).

C. B. Childers, R. F. Dziuba, and L. H. Lee, "A Resistive Ratio Standard for Measuring Direct Voltages to 10 kV," IEEE Trans. Instrum. Meas. IM-25, No. 4, pp. 505-508 (Dec. 1976).

R. E. Hebner, Jr. and M. Misakian, "Calibration of High-Voltage Pulse Measurement Systems Based on the Kerr Effect," NBSIR 77-1317, 38 pages (Sept. 16, 1977).

R. E. Hebner, Jr., R. A. Malewski, and E. C. Cassidy, "Optical Methods of Electrical Measurement at High Voltage Levels," Proc. IEEE, 65, No. 11, pp. 1524-1548 (Nov. 1977).

D. L. Hillhouse and W. C. Sze, "Calibration of CCVTs in the Substation," 45th Annual International Conference of Doble Clients, Section 9-501 (1978).

M. Misakian, F. R. Kotter, and R. L. Kahler, "Miniature ELF Electric Field Probe," Rev. Sci. Instrum. 49, No. 7, pp. 933-935 (July 1978).

W. E. Anderson, R. S. Davis, O. Petersons, and W.J.M. Moore, "An International Comparison of High Voltage Capacitor Calibrations," IEEE Trans. Power Appar. Syst. PAS-97, No. 4, pp. 1217-1223 (July/Aug. 1978).

D. L. Hillhouse, O. Petersons, and W. C. Sze, "A Prototype System for On-Site Calibration of Coupling Capacitor Voltage Transformers (CCVTs)," IEEE Trans. Power Appar. Syst. PAS-98, No. 3, pp. 1026-1036 (May/June 1979).

R. E. Hebner and S. Annestrand, "Evaluation of Calibration Techniques for Multimegavolt Impulse Dividers," International Symposium on High Voltage Engineering, Milan, Italy, pp. 1-4 (Aug. 1979).

R. E. Hebner and M. Misakian, "Temperature Dependence of the Electro-optic Kerr Coefficient of Nitrobenzene," J. Appl. Phys. 50(9), pp. 6016-6017 (Sept. 1979).

R. E. Hebner, D. L. Hillhouse, and R. A. Bullock, "Evaluation of a Multimegavolt Impulse Measurement System," NBSIR 79-1933, 102 pages (Nov. 1979).

R. H. McKnight and R. E. Hebner, "X-CAL -- A Calibration System for Electrical Measurement Devices Used With Diagnostic X-Ray Units," NBSIR 80-2072, 75 pages (June 1980).

D. L. Hillhouse, "Guide for Safe Operating Procedures at High Voltage Substations by NBS and Utility Staff During the Field Calibration of Coupling Capacitor Voltage Transformers (CCVTs), NBSIR 81-2192, 10 pages (Feb. 1981). [Limited distribution; not available from NTIS]

D. L. Hillhouse and D. A. Leep, "Analysis of the Calibration of Metering CCVTs in a Utility Substation," NBSIR 81-2360, 53 pages (Oct. 1981).

D. L. Hillhouse, O. Petersons, and W. C. Sze, "A Simplified System for Calibration of CCVTs in the Substation," Nat. Bur. Stand. (U.S.), Tech. Note 1155, 57 pages (May 1982).

J. D. Ramboz, A. R. Ondrejka, and W. E. Anderson, "Sampling-Rate Drift Problems in Transfer Function Analysis of Electrical Power Cables," Proceedings of the Waveform Recorder Seminar, Boulder, CO, October 1981, Nat. Bur. Stand. (U.S.), Spec. Publ. 634, pp. 47-53 (June 1982). [GPO]

"Measurement of Electrical Quantities in Pulse Power Systems," Proceedings of the Workshop on Measurement of Electrical Quantities in Pulse Power Systems, Boulder, CO, March 2-4, 1981, R. H. McKnight and R. E. Hebner, Jr., editors, Nat. Bur. Stand. (U.S.), Spec. Publ. 628, 410 pages (June 1982). [GPO]

W. E.. Anderson, J. D. Ramboz, and A. R. Ondrejka, "The Detection of Incipient Faults in Transmission Cables Using Time Domain Reflectometry Techniques: Technical Challenges," IEEE Trans. Power Appar. Syst. PAS-101, No. 7, pp. 1928-1934 (July 1982).

D. L. Hillhouse, "Effects of High-Voltage Switching on the EPRI-NBS Coupling Capacitor Voltage Transformer (CCVT) Calibration System Standard Divider," NBSIR 83-2666, 37 pages (March 1983).

R. H. McKnight and H. K. Schoenwetter, "Evaluation of Transient Measurement Methods in Gas-Insulated Transmission Lines," NBSIR 83-2753, 75 pages (August 1983).

Data Acquisition and Conversion

S. K. Tewksbury, F. C. Meyer, D. C. Rollenhagen, H. K. Schoenwetter, and T. M. Souders, "Terminology Related to the Performance of S/H, A/D, and D/A Circuits," IEEE Trans. Circuits Syst. CAS-25, No. 7, pp. 419-426 (July 1978).

B. F. Field, "A Fast Response Low-Frequency Voltmeter," IEEE Trans. Instrum. Meas. IM-27, No. 4, pp. 368-372 (Dec. 1978).

T. M. Souders, "A Bridge Circuit for the Dynamic Characterization of Sample/Hold Amplifiers," IEEE Trans. Instrum. Meas. IM-27, No. 4, pp. 409-413 (Dec. 1978).

H. K. Schoenwetter, "A High-Speed Low-Noise 18-Bit Digital-to-Analog Converter," IEEE Trans. Instrum. Meas. IM-27, No. 4, pp. 413-417 (Dec. 1978).

T. M. Souders and D. R. Flach, "A 20 Bit + Sign, Relay Switched D/A Converter," Nat. Bur. Stand. (U.S.), Tech. Note 1105, 21 pages (Oct. 1979). [GPO]

T. M. Souders and D. R. Flach, "An Automated Test Set for High Resolution Analog-to-Digital and Digital-to-Analog Converters," IEEE Trans. Instrum. Meas. IM-28, No. 4, pp. 239-244 (Dec. 1979).

A. G. Perrey and H. K. Schoenwetter, "A Schottky Diode Bridge Sampling Gate," Nat. Bur. Stand. (U.S.), Tech. Note 1121, 18 pages (May 1980). [GPO]

T. M. Souders and J. A. Lechner, "A Technique for Measuring the Equivalent RMS Input Noise of A/D Converters," IEEE Trans. Instrum. Meas. IM-29, No. 4, pp. 251-256 (Dec. 1980).

T. M. Souders, D. R. Flach, and B. A. Bell, "A Calibration Service for Analog-to-Digital and Digital-to-Analog Converters," Nat. Bur. Stand. (U.S.), Tech. Note 1145, 66 pages (July 1981). [GPO]

T. M. Souders and D. R. Flach, "An NBS Calibration Service for A/D and D/A Converters," 1981 International Test Conference Digest, pp. 290-303 (Oct. 1981).

T. M. Souders, "A Dynamic Test Method for High-Resolution A/D Converters," IEEE Trans. Instrum. Meas. IM-31, No. 1, pp. 3-5 (March 1982).

T. M. Souders and D. R. Flach, "Measurement of the Transient Versus Steady-State Response of Waveform Recorders," Proceedings of the Waveform Recorder Seminar, Boulder, CO, October 1981, Nat. Bur. Stand. (U.S.), Spec. Publ. 634, pp. 27-34 (June 1982). [GPO]

D. R. Flach, "Steady-State Tests of Waveform Recorders," Proceedings of the Waveform Recorder Seminar, Boulder, CO, October 1981, Nat. Bur. Stand. (U.S.), Spec. Publ. 634, pp. 7-21 (June 1982). [GPO]

J. R. Andrews, N. S. Nahman, and B. A. Bell, "Status of Reference Waveform Standards Development at NBS," Proceedings of the Waveform Recorder Seminar, Boulder, CO, October 1981, Nat. Bur. Stand. (U.S.), Spec. Publ. 634, pp. 69-88 (June 1982). [GPO]

J. D. Ramboz, A. R. Ondrejka, and W. E. Anderson, "Sampling-Rate Drift Problems in Transfer Function Analysis of Electrical Power Cables," Proceedings of the Waveform Recorder Seminar, Boulder, CO, October 1981, Nat. Bur. Stand. (U.S.), Spec. Publ. 634, pp. 47-53 (June 1982). [GPO]

B. A. Bell, B. F. Field, and T. H. Kibalo, "A Fast Response, Low-Frequency Sampling Voltmeter," Nat. Bur. Stand. (U.S.), Tech. Note 1159, 113 pages (Aug. 1982). [GPO]

T. M. Souders, D. R. Flach, and T. C. Wong, "An Automated Test Set for the Dynamic Characterization of A/D Converters," IEEE Trans. Instrum. Meas. IM-32, No. 1, pp. 180-186 (March 1983).

H. K. Schoenwetter, "High Accuracy Settling Time Measurements," IEEE Trans. Instrum. Meas. IM-32, No. 1, pp. 22-27 (March 1983).

B. A. Bell and A. G. Perrey, "Peak Conductance Measurements of GaAs Switching Devices," Picosecond Optoelectronics, Gerard Mourou, ed., Proc. SPIE 439, pp. 128-139 (Aug. 1983).

J. R. Andrews, B. A. Bell, and E. E. Baldwin, "Reference Flat Pulse Generator," Nat. Bur. Stand. (U.S.), Tech. Note 1067, 72 pages (Oct. 1983). [GPO]

H. K. Schoenwetter, "A Programmable Voltage-Step Generator for Testing Waveform Recorders," IEEE Instrum. and Meas. Technology Conference Proceedings, pp. 71-72 (Jan. 1984).

Automatic Testing

B. A. Bell, T. M. Souders, B. C. Belanger, and R. A. Kamper, "Challenges in Achieving ATE Traceability to NBS," Proc. IEEE AUTOTESTCON, pp. 233-238 (Sept. 1979).

B. A. Bell, "Precision Electronic Test Equipment Calibration Standards at NBS," Proc. ATE Seminar and Test Instruments Conference, pp. 138-168 (Jan. 1980).

K. J. Lentner, C. B. Childers, and S. G. Tremaine, "A Semiautomatic System for AC/DC Difference Calibration," IEEE Trans. Instrum. Meas. IM-29, No. 4, pp. 400-405 (Dec. 1980).

M. G. Buehler and L. W. Linholm, "Toward a Standard Test Chip Methodology for Reliable, Custom Integrated Circuits," Proc. of the Custom Integrated Circuit Conf., pp. 142-146 (May 1981).

M. G. Buehler and D. S. Perloff, "Microelectronic Test Chip and Associated Parametric Testers: Present and Future," Semiconductor Silicon '81, H. R. Huff, R. J. Kriegler, and Y. Takeishi, eds., Electrochemical Society, pp. 859-867 (May 1981).

B. A. Bell and O. Petersons, "ATE Calibration by Means of Dynamic Transport Standards," IEEE AUTOTESTCON '81 Proceedings, pp. 280-287 (Oct. 1981).

K. J. Lentner and S. G. Tremaine, "A Semiautomatic AC/DC Thermal Voltage Converter Calibration System," NBSIR 82-2576, 62 pages (Sept. 1982).

W. G. Eicke, Jr., T. F. Leedy, B. R. Moore, and C. F. Brown, "Measurement Assurance Programs in a Field Environment," Proc. National Conference of Standards Laboratories, 1982 Workshop and Symposium, Gaithersburg, Md., Oct. 4-7, 1982, pp. E-1-E-9.

Electrical Insulation Measurements

H. E. Radford, "Electrical Breakdown in Ammonia at Low Pressure," NBS Report No. 9882, 12 pages (July 22, 1968).

E. C. Cassidy and H. N. Cones, "A Kerr Electro-Optical Technique for Observation and Analysis of High-Intensity Electric Fields," J. Res., Nat. Bur. Stand. (U.S.), (Eng. & Instr.) 73C, Nos. 1 and 2, pp. 5-13 (Jan.-June 1969).

E. C. Cassidy and H. N. Cones, "Use of Expanded Laser Beam to Analyze High-Intensity Electric Fields," J. Soc. Motion Pict. Telev. Eng. 79, No. 7, pp. 590-591 (July 1970).

E. C. Cassidy and H. N. Cones, "Electro-Optical Observations and Measurements of Distorted High-Intensity Electric Fields," Proc. 1969 Conf. on Electrical Insulation and Dielectric Phenomena (Buck Hill Falls, Pa., Oct. 20-22, 1969), pp. 77-86 (National Academy of Sciences, Washington, DC, 1970).

E. C. Cassidy, "Pulsed Laser Kerr System Polarimeter for Electro-Optical Fringe Pattern Measurement of Transient Electrical Parameters," Rev. Sci. Instrum. 43, No. 6, pp. 886-893 (June 1972).

E. C. Cassidy and R. E. Hebner, "Experimental Study of the Behavior of Nitrobenzene Under Varied High Voltage Conditions," 1972 Annual Report, Conference on Electrical Insulation and Dielectric Phenomena, pp. 37-44 (1973).

R. E. Hebner, Jr., E. C. Cassidy, M. Zahn, and R. J. Sojka, "Electric Field Distributions and Space Charge Behavior in Nitrobenzene Under Low Frequency Alternating Voltage, 1973 Annual Report," Conference on Electrical Insulation and Dielectric Phenomena, pp. 112-119 (1974).

E. C. Cassidy, R. E. Hebner, Jr., M. Zahn, and R. J. Sojka, "Kerr-Effect Studies of an Insulating Liquid Under Varied High-Voltage Conditions," IEEE Trans. Electr. Insul. EI-9, No. 2, pp. 43-56 (June 1974).

R. E. Hebner, Jr., R. J. Sojka, and E. C. Cassidy, "Kerr Coefficients of Nitrobenzene and Water," NBSIR 74-544, 35 pages (Aug. 7, 1974).

F. R. Kotter, "A Study of Air-Gap Breakdown at 28.5 Kilohertz," NBSIR 75-731, 42 pages (June 20, 1975).

D. B. Miller (Principal Investigator), V. E. Bower, F. R. Kotter, O. Petersons, M. M. Birky, C. M. Huggett, and A. J. Macek, "An Appraisal of Tests and Standards for the Evaluation of Electrical Insulating Fluids," NBSIR 76-1054, 124 pages (May 1976).

M. Misakian and R. E. Hebner, Jr., "Kerr Coefficients of Polychlorinated Biphenyls and Chlorinated Naphthalene," J. Appl. Phys. 47, No. 9, pp. 4052-4055 (Sept. 1976).

W. E. Anderson, R. S. Davis, F. I. Mopsik, S. J. Kryder, F. Khoury, J. P. Colson, and L. H. Bolz, "Measurements on Insulating Materials at Cryogenic Temperatures," ERDA Report No. CONS/2062-1 (Sept. 1976).

W. E. Anderson and R. S. Davis, "Measurement of AC Insulation Losses at Cryogenic Temperatures," IEEE Trans. Electr. Insul. EI-12, No. 1, pp. 51-54 (Feb. 1977).

R. E. Hebner, Jr., R. A. Malewski, and E. C. Cassidy, "Optical Methods of Electrical Measurement at High Voltage Levels," Proc. IEEE, 65, No. 11, pp. 1524-1548 (Nov. 1977).

E. F. Kelley and R. E. Hebner, "Measurement of Prebreakdown Electric Fields in Liquid Insulants," 1978 Annual Report, Conference on Electrical Insulation and Dielectric Phenomena, National Academy of Sciences, Washington, DC, pp. 206-212 (Oct. 1978).

E. F. Kelley and R. E. Hebner, "Time Evolution of the Electric Field Associated With Breakdown Phenomena in Liquids," 1979 Annual Report, Conference on Electrical Insulation and Dielectric Phenomena, pp. 203-211 (1979).

R. J. Van Brunt, "Minutes of Workshop on Gaseous Dielectrics for Use in Future Electric-Power Systems - September 10-11, 1979," NBSIR 80-1966 (Jan. 1980). [Limited distribution; not available from NTIS]

W. E. Anderson and R. S. Davis, "Measurements on Insulating Materials at Cryogenic Temperatures," NBSIR 79-1950, 164 pages (Jan. 1980).

R. J. Van Brunt, J. S. Hilten, and D. P. Silver, "Partial-Discharge Pulse Height Distributions and Frequencies for Positive and Negative DC Corona in SF_6 and SF_6-N_2 Mixtures," Proc. 2nd Intl. Symp. on Gaseous Dielectrics, Gaseous Dielectrics II, Ed. by L. G. Christophorou, Pergamon Press, NY, pp. 303-311 (March 1980).

D. A. Leep and R. J. Van Brunt, "Safety Considerations for Handling SF_6 Used in Electrical Equipment," NBSIR 80-2063 (June 1980). [Limited distribution; not available from NTIS]

E. F. Kelley and R. E. Hebner, "Breakdown Between Bare Electrodes With an Oil-Paper Interface," NBSIR 80-2071, 33 pages (June 1980).

R. J. Van Brunt and M. Misakian, "Comparison of DC and 60 Hz AC Positive and Negative Partial Discharge Inceptions in SF_6, 1980 Annual Report," Conference on Electrical Insulation and Dielectric Phenomena, pp. 461-469 (1980).

E. F. Kelley and R. E. Hebner, "The Electric Field Distribution Associated With Prebreakdown Phenomena in Nitrobenzene," J. Appl. Phys. 52, No. 1, pp. 191-195 (Jan. 1981).

M. Misakian, "Generation and Measurement of DC Electric Fields With Space Charge," NBSIR 80-2177, 39 pages (Jan. 1981).

E. F. Kelley and R. E. Hebner, "Prebreakdown Phenomena Between Sphere-Sphere Electrodes in Transformer Oil," Appl. Phys. Lett. 38, No. 4, pp. 231-233 (Feb. 1981).

W. E. Anderson and J. D. Ramboz, "1980 Annual Report: Technical Contributions to the Development of Incipient Fault Detection/Location Instrumentation," NBSIR 81-2235, 125 pages (March 1981).

R. J. Van Brunt, M. Misakian, D. A. Leep, K. J. Moy, and E. C. Beaty, "1980 Annual Report: Technical Assistance for Future Insulation Systems Research," NBSIR 81-2242, 96 pages (Apr. 1981).

R. E. Hebner, E. F. Kelley, J. E. Thompson, T. S. Sudershan, and T. B. Jones, "1980 Annual Report: Optical Measurements for Interfacial Conduction and Breakdown," NBSIR 81-2275, 83 pages (May 1981).

R. H. McKnight, F. R. Kotter, M. Misakian, and P. Ortiz, "1980 Annual Report: Electric and Magnetic Field Measurements," NBSIR 81-2267, 65 pages (May 1981).

M. Misakian, "Generation and Measurement of DC Electric Fields With Space Charge," J. Appl. Phys. 52, No. 5, pp. 3135-3144 (May 1981).

R. E. Hebner, E. F. Kelley, E. O. Forster, and G. J. FitzPatrick, "Observation of Prebreakdown and Breakdown Phenomena in Liquid Hydrocarbons," 7th Inter. Conf. on Conduction and Breakdown in Dielectric Liquids, Berlin, West Germany, pp. 177-181 (July 1981).

M. Zahn, E. O. Forster, E. F. Kelley, and R. E. Hebner, "Hydrodynamic Shock Wave Propagation After Electrical Breakdown," 7th Inter. Conf. on Conduction and Breakdown in Dielectric Liquids, Berlin, West Germany, pp. 398-403 (July 1981).

D. A. Leep and F. R. Kotter, "Discussion of Paper No. 81 WM 126-2, Measuring Voltage and Current Harmonics on Distribution Systems, by M. F. McGranaghan, J. H. Shaw, and R. E. Owen," IEEE Trans. on Power Appar. Syst. PAS-100, No. 7, pp. 3599-3608 (July 1981).

E. F. Kelley and R. E. Hebner, "Electrical Breakdown in Composite Insulating Systems: Liquid-Solid Interface Parallel to the Field," IEEE Trans. on Electrical Insulation EI-16, No. 4, pp. 297-303 (Aug. 1981).

R. J. Van Brunt, "Discussion of paper by J. M. Pelletier et al.," IEEE Trans. Power Appar. Syst. PAS-100, pp. 3867-3868 (Aug. 1981).

R. E. Hebner, E. F. Kelley, E. O. Forster, and G. J. FitzPatrick, "Observations of Prebreakdown and Breakdown Phenomena in Liquid Hydrocarbons II. Point-Plane Geometry, 1981 Annual Report," Conference on Electrical Insulation and Dielectric Phenomena, pp. 377-389 (Oct. 1981).

F. R. Kotter and M. Misakian, "AC Transmission Line Field Measurements," NBSIR 77-1311, 79 pages (Oct. 1981).

R. J. Van Brunt and D. A. Leep, "Characterization of Point-Plane Corona Pulses in SF_6," J. Appl. Phys. 52, No. 11, pp. 6588-6600 (Nov. 1981).

R. H. McKnight, F. R. Kotter, and M. Misakian, "Measurement of Ion Current Density at Ground Level in the Vicinity of High Voltage DC Transmission Lines," NBSIR 81-2410, 27 pages (Dec. 1981).

R. J. Van Brunt, "Discussion on 81 SM 322-7 Breakdown of Rod-Plane Gaps in SF_6 Under Positive Switching Impulses, by H. Anis and K. Srivastava," IEEE Trans. Power Appar. Syst. PAS-101, No. 3, p. 546 (March 1982).

R. J. Van Brunt and M. Misakian, "Mechanisms for Inception of DC and 60-Hz AC Corona in SF_6," IEEE Trans. Electr. Insul. EI-17, No. 2, pp. 106-120 (April 1982).

R. H. McKnight, "The Measurement of Net Space Charge Density Using Air Filtration Methods," NBSIR 82-2486, 28 pages (April 1982).

E. F. Kelley, R. E. Hebner, E. O. Forster, and G. J. FitzPatrick, "Observations of Pre- and Post-Breakdown Events in Polydimethylsiloxanes," Proceedings of the 1982 IEEE International Symposium on Electrical Insulation, No. 82CH1780-6-EI, pp. 255-258 (June 1982).

R. H. McKnight, F. R. Kotter, M. Misakian, and J. N. Hagler, "1981 Annual Report--Electrical and Magnetic Field Measurements," NBSIR 82-2527, 48 pages (July 1982).

R. E. Hebner, E. F. Kelley, E. O. Forster, and G. J. FitzPatrick, "Observation of Prebreakdown and Breakdown Phenomena in Liquid Hydrocarbons," Journal of Electrostatics, Vol. 12, pp. 265-283, 1982.

M. Zahn, E. O. Forster, E. F. Kelley, and R. E. Hebner, "Hydrodynamic Shock Wave Propagation After Electrical Breakdown," Journal of Electrostatics, Vol. 12, pp. 535-546, 1982.

R. J. Van Brunt and D. A. Leep, "Corona-Induced Decomposition of SF_6," Proceedings of the Third International Symposium on Gaseous Dielectrics, Gaseous Dielectrics III, pp. 402-409, 1982.

W. F. Schmidt and R. J. Van Brunt, "Comments on the Effect of Electron Detachment in Initiating Breakdown in Gaseous Dielectrics," Proceedings of the Third International Symposium on Gaseous Dielectrics, Gaseous Dielectrics III, pp. 561-563, 1982.

R. J. Van Brunt, "Effects of H_2O on the Behavior of SF_6 Corona," Proceedings of the Seventh International Conference on Gas Discharges and Their Applications, London, England, 1982, pp. 255-258.

G. J. FitzPatrick, E. O. Forster, E. F. Kelley, and R. E. Hebner, "Effects of Chemical Impurities on Prebreakdown Events in Toluene, 1982 Annual Report," Conference on Electrical Insulation and Dielectric Phenomena, Oct. 17-21, 1982, 464-472, October 1982.

R. J. Van Brunt, M. Misakian, D. A. Leep, E. C. Beaty, J. W. Gallagher, C. M. Cooke, K. Wyatt, and R. G. Gels, "1981 Annual Report--Technical Assistance for Future Insulation Systems Research," NBSIR 82-2555, 157 pages (Nov. 1982).

R. E. Hebner, E. F. Kelley, and J. N. Hagler, "1981 Annual Report: Optical Measurements for Interfacial Conduction and Breakdown," NBSIR 82-2629, 82 pages (Jan. 1983).

R. J. Van Brunt and M. Misakian, "Role of Photodetachment in Initiation of Electric Discharges in SF_6 and O_2," J. Appl. Phys., Vol. 54, No. 6, pp. 3074-3079, June 1983.

R. H. McKnight and F. R. Kotter, "A Facility to Produce Uniform Space Charge for Evaluating Ion Measuring Instruments," IEEE Trans. Power Appar. Syst., PAS-102, No. 7, pp. 2349-2357 (July 1983).

E. F. Kelley and R. E. Hebner, Electro-Optic Measurement of the Electric Field Distribution in Transformer Oil," IEEE Trans. Power Appar. Syst. PAS-102, No. 7, pp. 2092-2097 (July 1983).

R. E. Hebner, E. F. Kelley, G. J. FitzPatrick, and E. O. Forster, "The Effect of Impurities on Positive Streamer Propagation in n-Hexane," 1983 Annual Report, Conference on Electrical Insulation and Dielectric Phenomena, Oct. 16-20, 1983, Buck Hill Falls, PA, pp. 26-34, Oct. 1983.

E. F. Kelley and R. E. Hebner, "Measurement of the Electric-Field in the Vicinity of an Oil-Pressboard Interface Parallel to the Field," Conf. Record of 1983 Interfacial Phenomena in Practical Insulating Systems (Sept. 19-20, 1983), Gaithersburg, Md., pp. 19-22, Dec. 1983.

R. E. Hebner, "Kerr-Effect, Electro-Optical" in Encyclopedia of Physics, R. G. Lerner and G. L. Trigg, eds., Reading, MA: Addison-Wesley, 1981. 483.

R. E. Hebner, "Kerr-Effect, Electro-Optical" in Concise Encyclopedia of Solid State Physics, R. G. Lerner and G. L. Trigg, eds., Reading, MA: Addison-Wesley, 1983. 133.

M. G. Comber, R. Kotter, and R. McKnight, "Experimental Evaluation of Instruments for Measuring DC Transmission Line Electric Fields and Ion Currents," IEEE Trans. Power Appar. Syst. PAS-102, No. 11, pp. 3549- (Nov. 1983).

Electronic Instrumentation and Metrology

H. K. Schoenwetter, "An Ultra-Stable AC Power Supply for an Absolute Volt Determination," Metrologia 10, pp. 11-15 (1974).

R. S. Turgel, "Digital Wattmeter Using a Sampling Method," IEEE Trans. Instrum. Meas. IM-23, No. 4, pp. 337-341 (Dec. 1974).

R. S. Turgel, "Sampling Techniques for Electric Power Measurement," Nat. Bur. Stand. (U.S.), Tech. Note 870, 35 pages (June 1975). [GPO]

H. K. Schoenwetter, "An RMS Digital Voltmeter/Calibrator for Very-Low Frequencies," IEEE Trans. Instrum. Meas. IM-27, No. 3, pp. 259-268 (Sept. 1978).

R. S. Turgel and N. M. Oldham, "High-Precision Audio-Frequency Phase Calibration Standard," IEEE Trans. Instrum. Meas. IM-27, No. 4, pp. 460-464 (Dec. 1978).

H. K. Schoenwetter, "NBS Provides Voltage Calibration Service in 0.1 - 10-Hz Range Using AC Voltmeter/Calibrator," IEEE Trans. Instrum. Meas. IM-28, No. 4, pp. 327-331 (Dec. 1979).

A. G. Perrey and H. K. Schoenwetter, "A Schottky Diode Bridge Sampling Gate," Nat. Bur. Stand. (U.S.), Tech. Note 1121, 18 pages (May 1980). [GPO]

R. S. Turgel, N. M. Oldham, G. N. Stenbakken, and T. H. Kibalo, "NBS Phase Angle Calibration Standard," Nat. Bur. Stand. (U.S.), Tech. Note 1144, 143 pages (July 1981). [GPO]

B. A. Bell and O. Petersons, "ATE Calibration by Means of Dynamic Transport Standards," IEEE AUTOTESTCON '81 Proceedings, pp. 280-287 (Oct. 1981).

N. M. Oldham and R. S. Turgel, "A Power Factor Standard Using Digital Waveform Generation," IEEE Trans. Power Appar. Syst. PAS-100, No. 11, pp. 4435-4438 (Nov. 1981).

J. R. Andrews, N. S. Nahman, and B. A. Bell, "Status of Reference Waveform Standards Development at NBS," Proceedings of the Waveform Recorder Seminar, Boulder, CO, October 1981, Nat. Bur. Stand. (U.S.), Spec. Publ. 634, pp. 69-88 (June 1982). [GPO]

B. A. Bell, B. F. Field, and T. H. Kibalo, "A Fast Response, Low-Frequency Sampling Voltmeter," Nat. Bur. Stand. (U.S.), Tech. Note 1159, 113 pages (Aug. 1982). [GPO]

H. K. Schoenwetter, "A Sensitive Analog Comparator," IEEE Trans. Instrum. Meas. IM-31, No. 4, pp. 266-269 (December 1982).

N. M. Oldham, "A 50-ppm AC Reference Standard Which Spans 1 Hz to 50 kHz," IEEE Trans. Instrum. Meas. IM-32, No. 1, pp. 176-179 (March 1983).

K. J. Lentner and D. R. Flach, "An Automatic System for AC/DC Calibrations," IEEE Trans. Instrum. Meas. IM-32, No. 1, pp. 51-56 (March 1983).

H. K. Schoenwetter, "High Accuracy Settling Time Measurements," IEEE Trans. Instrum. Meas. IM-32, No. 1, pp. 22-27 (March 1983).

B. A. Bell and A. G. Perrey, "Peak Conductance Measurements of GaAs Switching Devices," Picosecond Optoelectronics, Gerard Mourou, Ed., Proc. SPIE 439, pp. 128-139 (Aug. 1983).

H. K. Schoenwetter, "AC Voltage Calibrations for the 0.1 Hz to 10 Hz Frequency Range," Nat. Bur. Stand. (U.S.), Tech. Note 1182, 58 pages (Sept. 1983). [GPO]

H. K. Schoenwetter, "A Programmable Voltage-Step Generator for Testing Waveform Recorders," IEEE Instrum. and Meas. Technology Conf. Proceed., pp. 71-72 (Jan. 1984).

Sensors

J. S. Hilten, P. S. Lederer, C. F. Vezzetti, and J. F. Mayo-Wells, "Development of Dynamic Calibration Methods for Pogo Pressure Transducers," Nat. Bur. Stand. (U.S.), Tech. Note 927, 58 pages (Nov. 1976). [GPO]

J. S. Hilten, P. S. Lederer, J. F. Mayo-Wells, and C. F. Vezzetti, "Loose-Particle Detection in Microelectronic Devices," NBSIR 78-1590 (NASA), 73 pages (Jan. 1979). [Limited distribution; not available from NTIS]

P. S. Lederer, "NBS Interagency Transducer Project 1951 - 1979 -- An Overview," Nat. Bur. Stand. (U.S.), Tech. Note 1110, 45 pages (Aug. 1979). [GPO]

P. S. Lederer, J. S. Hilten, J. F. Mayo-Wells, and C. F. Vezzetti, "Loose-Particle Detection in Microelectronic Devices -- A Review of an NBS Task," Proc. Advanced Techniques in Failure Analysis - 1979, pp. 1-19 (Oct. 1979).

J. D. Ramboz, "Measurement and Evaluation Methods for an Angular Accelerometer," NBSIR 81-2337, 78 pages (Aug. 1981).

P. S. Lederer, "Sensor Handbook for Automatic Test, Monitoring, Diagnostic, and Control Systems Applications to Military Vehicles and Machinery," Nat. Bur. Stand. (U.S.), Spec. Publ. 615, 450 pages (Oct. 1981). [GPO]

Miscellaneous

A. H. Sher and G. N. Stenbakken, "Selection and Application Guide to Commercial Intrusion Alarm Systems," Nat. Bur.. Stand. (U.S.), Spec. Publ. 480-14, 40 pages (Aug. 1979). [GPO]

M. G. Buehler and L. W. Linholm, "Toward a Standard Test Chip Methodology for Reliable, Custom Integrated Circuits," Proc. of the Custom Integrated Circuit Conference, pp. 142-146 (May 1981).

M. G. Buehler and D. S. Perloff, "Microelectronic Test Chips and Associated Parametric Testers: Present and Future," Semiconductor Silicon '81, H. R. Huff, R. J. Kriegler, and Y. Takeishi, eds., Electrochemical Society, pp. 859-867 (May 1981).

R. E. Kennerly, R. J. Van Brunt, and A. C. Gallagher, "High-Resolution Measurement of the Helium $1s2s^2\ ^2S$ Resonance Profile," Physical Review 23, No. 5, pp. 2430-2442 (May 1981).

T. F. Leedy, G. F. McLane, and G. C. Guenzer, "Transient Temperature Dependence of Transient Electron Radiation Upset in TTL Nand Gates," IEEE Trans. on Nuclear Science NS-28, No. 6 (Dec. 1981).

P. M. Fulcomer, "Field Circuit Breaker Tester," NBSIR 81-2301, 52 pages (May 1982).

Information on Ordering Reports

Publication Number	GPO Stock No.	NTIS Accession No.
NBSIR		
9882*		
10 078*		
10 296*		
10 493*		
10 945*		
73-403		COM-74-10016/5GA
74-544		COM-74-11525
74-564		COM-74-11726
75-731		COM-75-11071
75-774		COM-75-11364
75-775		PB 248684
75-935		PB 299158
76-1054		PB 253110
77-1311		
77-1317		PB 274333
78-1590**		PB 290679
79-1933		PB 80-119720
79-1950		PB 80-134596
80-1966**		
80-2063**		
80-2071		PB 80-226699
80-2072		PB 80-197478
80-2177		PB 81-161929
81-2192**		
81-2235		PB 81-188005
81-2242		PB 82-134354
81-2267		PB 81-218187
81-2275		PB 81-216343
81-2283		PB 81-220261
81-2334		PB 81-246860
81-2337		PB 82-115973
81-2360		PB 82-209776
81-2410		PB 82-156993

*Available from author only

**Limited distribution; not available from NTIS. May be available from author or external publishing paper.

Information on Ordering Reports (cont.)

Publication Number	GPO Stock No.	NTIS Accession No.
NBSIR		
81-2301		PB 83-136382
82-2486		PB 82-225723
82-2501		PB 82-227075
82-2517		PB 82-238353
82-2527		PB 82-263377
82-2528		PB 82-229352
82-2555		PB 83-149187
82-2576		PB 83-180224
82-2586		PB 83-124891
82-2601**		
82-2629		PB 83-193110
83-2666		PB 83-192682
83-2705		PB 83-210609
83-2753		
83-2755		PB 84-109891
83-2761		PB 84-115104
Technical Note		
870	SN003-003-01434-6	COM-75-10946
927	SN003-003-01683-7	PB 260894
930	SN003-003-01672-1	PB 258085
1105		PB 80-105331
1121	SN003-003-02197-1	PB 80-198328
1110	SN003-003-02109-1	PB 300-369
1144	SN003-003-02344-2	PB 81-244899
1145	SN003-003-02352-4	PB 81-243404
1155		PB 82-215419
1159	SN003-003-02408-3	PB 83-107011
1179	SN003-003-02505-4	PB 83-252536
1182	SN003-003-02522-4	PB 84-109867
Special Publication		
480-14	SN003-003-02098-2	PB 300-604
615	SN003-003-02372-8	PB 82-123746
628	SN003-003-02403-1	PB 82-234121

Information on Ordering Reports (cont.)

Publication Number	NTIS Accession No.
Monograph	
109	AD 681-912
Journal of Research	
72C (No. 1)*	
73C (Nos. 3 & 4)*	
75C (Nos. 3 & 4)*	
74A (No. 6)*	
73C (Nos. 1 & 2)*	

*Available from author only

APPENDIX II

NBSIR 84-3014

METROLOGY FOR ELECTROMAGNETIC TECHNOLOGY: A BIBLIOGRAPHY OF NBS PUBLICATIONS

Edited by
R.A. Kamper
K.E. Kline

Electromagnetic Technology Division
Center for Electronics and Electrical Engineering
National Engineering Laboratory
National Bureau of Standards
U.S. Department of Commerce
Boulder, CO 80303

July 1984

U.S. DEPARTMENT OF COMMERCE, Malcolm Baldrige, Secretary

NATIONAL BUREAU OF STANDARDS, Ernest Ambler, Director

METROLOGY FOR ELECTROMAGNETIC TECHNOLOGY: A BIBLIOGRAPHY OF NBS PUBLICATIONS

Edited by

Robert A. Kamper and Kathryn E. Kline

This bibliography lists the publications of the personnel of the Electromagnetic Technology Division of NBS in the period from January 1970 through December 1983. A few earlier references that are directly related to the present work of the Division are included.

Key words: cryoelectronics; electromagnetic metrology; lasers; microwaves; optical fibers; superconducting materials; time domain metrology.

INTRODUCTION

The Electromagnetic Technology Division was formed during the reorganization of NBS in April 1978, by combining parts of the former Electromagnetics and Cryogenics Divisions. It develops measurement methods and standards, and provides metrological support for: microwave circuits, laser systems, optical communication equipment, systems using transient or pulsed electromagnetic phenomena, cryoelectronics, superconductors, and other unusual electrical engineering materials. For the individual staff members of the division, the reorganization brought a realignment of long-term goals but little immediate discontinuity in their work. It therefore makes good sense that this bibliography should cover a period beginning some time before the reorganization, so as to include at least the more recent origins of the present work of the division. The editors have attempted to include all work published by the present staff members of the division, while they were employees of NBS, in the period from January 1970 to December 1983. There are a few exceptions, where work that is totally unrelated to the present program has been excluded or where work by authors now in other parts of NBS has been included because of its special significance. The work on electromagnetic waveform metrology was moved to another part of the organization in October 1982. Papers submitted prior to that date are included, but later publications are not. A few papers on various topics published before 1970 have also been included because of their direct relationship to the present program.

There are several other sources that may be useful to the reader who is interested in activities at NBS connected with electromagnetic metrology. A companion bibliography to this one lists the publications of the Electromagnetic Fields Division. Its topics include metrology for: antennas, satellite communications equipment, electromagnetic interference, and hazard. Three bibliographies of the publications of the former Electromagnetics Division have been published: NBSIR 73-820 (July 1972-June 1973); NBSIR 74-395

(July 1973-June 1974); NBSIR 75-818 (July 1974-June 1975). These were preceded by a series of unpublished reports (edited by H. M. Altschuler) that cover the period back to 1956. An excellent summary of the whole field of electromagnetic metrology as it stood in 1967 was published as a special issue of the IEEE Proceedings (vol. 55; June 1967). Advances in the following decade were described in another special issue of the same journal (vol. 66; April 1978).

A Note on Abbreviations

Most readers will be familiar with the commonly used abbreviations for the names of the various professional journals that appear in this bibliography. There are also some publication series that are peculiar to NBS and may call for explanation. They are:

NBSIR - NBS Interagency/Internal Report
NBS TN - NBS Technical Note
NBS SP - NBS Special Publication
NBS HB - NBS Handbook
NBS JRES - NBS Journal of Research
NBS MN - NBS Monograph

Purchase Procedures and Document Availability

NBS Technical Notes and Special Publications may be purchased from the Superintendent of Documents, U.S. Government Printing Office, Washington, DC 20402. Orders must be accompanied by postal money order, express money order, or check made out to the Superintendent of Documents.

NBS Interagency/Internal Reports (NBSIRs) may be purchased from the National Technical Information Service, Springfield, VA 22161. Orders must be accompanied by postal money order, express money order, or check made out to the NTIS.

Reprints of papers published in non-NBS media may be available in limited quantities from the authors.

Acknowledgments

A large part of the labor of preparing a bibliography is spent on collecting and arranging the material. We thank Frances Brown, Edie DeWeese, Jessie Page, and Sheila Aaker for their assistance with these chores. The prime source of material was the NTIS file, with access through the Lockheed Dialog System. This was supplemented with material supplied by the individual authors.

MICROWAVE METROLOGY

Millimeter Wave Standards at the National Bureau of Standards (NBS);
Kamper, R. A.; Hoer, C. A.
Proc. SPIE; Aug. 21-25, 1983; San Diego, CA, 423:144-146; 83.

Redundance: A Monitor of Six-Port Performance;
Engen, G. F.
IEE 1983 Colloquium on Advances in S-Parameter Measurement at Microwave Lengths, May 23, 1983; Savoy Place, London WC2BOBL, p 4/1-4/2; 83.

Choosing Line Lengths for Calibrating Network Analyzers;
Hoer, C.
IEEE/MTT 31(2):76-78; Jan 83.

Current Trends in NBS Calibration Services;
Kamper, R. A.
NCSL Newsletter, 22(1):38-39; Mar 1982.

Singularities in Calibration of Six-port Network Analyzers;
Ebbesen, H.; Engen, G.
1981 IEEE MTT-S Int. Microwave Symp. Digest, p 149; 81.

WR-10 Single Six-port Measurement System;
Weidman, M.
NBSIR 1650; 81.

A High Power Dual Six-port Automatic Network Analyzer Used in Determining Biological Effects of rf and Microwave Radiation;
Hoer, C.
IEEE Trans. Microwave Theory Tech., vol. NTT-29; Dec 81.

Control Cable Assemblies Used with Mobile FM Receivers;
Nelson, R. E.; Jickling, R.
National Institute of Justice, NIJ Std. 0216.00; Dec 81.

WR-10 Millimeter Wave Microcalorimeter;
Weidman, M.; Hudson, P. A.
NBS TN 1044; Jun 81.

A Least Squares Solution for Use in 6-port Measurement Technique;
Engen, G. F.
IEEE Trans. Microwave Theory Tech., MTT-28(12); Dec 80.

Performance of a Dual Six-Port Automatic Network Analyzer;
Hoer, Cletus A.
Proc. IEEE MTT-S 1979, Int. Microwave Symp. Digest:
The World of Microwaves, Apr 3-May 2, 1979; Orlando, FL, IEEE Cat. No. 79CHI439-9 MIT-S; 79.

Through-Load-Delay: An Improved Technique for Calibrating the Dual Six-port Automatic Network Analyzer;
Engen, G. F.; Hoer, C. A.
Int. Microwave Symp. Digest, Orlando, FL, p53; 79.

Calibrating a Six-Port Reflectometer with Four Impedance Standards;
Hoer, Cletus A.
NBS TN 1012; Mar 79.

Advantages of the Six-port Reflectometer for RF/Microwave Power Measurement in Operational Systems;
Komarek, E. L.
GOMAC Digest; 78.

Calibrating Two Six-Port Reflectometers With an Unknown Length of Precision Transmission Line;
Hoer, Cletus A.
Proc. IEEE MIT-S Int. Microwave Symp. Digest, Jun 27-29, 1978; Ottawa, Canada, p176-178; 78.

The Application of "Through-Short-Delay" to the Calibration of the Dual 6-port;
Engen, G. F; Hoer, C. A.; Speciale, R. A.
IEEE Int. Microwave Symp. Digest, p184-185; 78.

Calibrating the Six-port Reflectometer by Means of Sliding Terminations;
Engen, G. F.
IEEE Trans. Microwave Theory Tech. MTT-26:951-957; Dec 78.

NBS RF voltage Comparator;
Driver, L. D.; Ries, F. X.; Rebuldela, G.
NBSIR 78-871; Dec 78.

Status of RF and Microwave Calibration Services at NBS;
Kamper, R. A.
NCSL Newsletter 18:40; Dec 78.

Calibrating Two 6-Port Reflectometers with Only One Impedance Standard;
Hoer, Cletus A.
NBS TN 1004; Jun 78.

The Six-Port Measurement Technique: A Status Report;
Engen, Glenn F.
Microwave J. 21:18,21-22,24,84,87,89; May 78.

Advances in Microwave Measurement Science;
Engen, Glenn F.
Proc. IEEE 66:374-384; Apr 78.

Instrumentation: Six Ports Simplify Network;
Engen, Glenn F.
Microwave Syst. News, p 54-55; Jan 78.

A Microwave Network Analyzer Using Two 6-Port Reflectometers;
Hoer, Cletus
Proc. 1977 IEEE-MTT-S Int. Microwave Symposium, Jun 21-23, 1977; San Diego, CA, p 47-49; 77.

An Improved Circuit for Implementing the Six-Port Technique of Microwave Measurements;
Engen, Glenn F.
Proc. 1977 IEEE-MTT-S Int. Microwave Symposium, 21-23 Jun 1977; San Diego, CA, p 53-55; 77.

An Application of the Six-Port Junction to Precision Measurement of Microwave One-Port Parameters;
Komarek, E. L.
Proc. 1977 IEEE-MTT-S Int. Microwave Symposium, 21-23 Jun 1977; San Diego, CA, p 56-57; 77.

A Semi-Automated Six-Port for Measuring Millimeter Wave Power and Complex Reflection Coefficient;
Weidman, Manly P.
Proc. 1977 IEEE MTT-S Int. Microwave Symposium, 21-23 Jun 1977; San Diego, CA, p 58-60; 77.

Design Considerations for Automatic Network Analyzers Based on the Six-Port Concept;
Engen, Glenn F.
Proc. IEE Euromeas 77 Conf., Sep 5-9, 1977; Sussex, England; London, England: IEE, p 110-111; 77.

Fixed and Base Station Antennas;
Treado, M. J.; Taggart, H. E.; Nelson, R. E.; Workman, J. L.
NILECJ-STD-0204.00; 77.

The Six-Port Reflectometer: An Alternative Network Analyzer;
Engen, Glenn F.
Proc. 1977 IEEE-MTT-S Int. Microwave Symposium, 21-23 Jun 1977; San Diego, CA, p 44-46; 77.

Ultrasonic Calorimeter for Beam Power Measurements from 1 to 15 Megahertz;
Zapf, T. L.; Harvey, M. E.; Larsen, N. T.; Stoltenberg, R. E.
Proc. Ultrasonics Symposium, Sep 29-Oct 1, 1976; Annapolis, MD, IEEE Cat76 CH1120-5SU, p 573-576; 77.

A Network Analyzer Incorporating Two 6-Port Reflectometers;
Hoer, Cletus A.
IEEE Trans. Microwave Theory Tech. MIT-25:1070-1074; Dec 77.

An Improved Circuit for Implementing the Six-Port Technique of Microwave Measurements;
Engen, Glenn F.
IEEE Trans. Microwave Theory Tech. MTT-25:1080-1083; Dec 77.

A Semi-Automated Six-Port for Measuring Millimeter Wave Power and Complex Reflection Coefficient;
Weidman, Manly P.
IEEE Trans. Microwave Theory Tech. MTT-25:1083-1085; Dec 77.

Performance Characteristics of an Automated Broad-Band Bolometer Unit Calibration System;
Komarek, Ernest L.
IEEE Trans. Microwave Theory MTT-25:1122-1127; Dec 77.

NBS Type IV RF Power Meter Operation and Maintenance;
Larsen, Neil T.
NBSIR 77-866; Oct 77.

Six-Port Measuring Circuit; Patent Application;
Engen, Glenn F.
PAT-APPL-829 381; Filed 31 Aug 77.

The National Electromagnetic Measurement System;
Kamper, R. A.
NBSIR 75-936; Jun 77.

Vector Voltmeter;
Hoer, Cletus A.; Engen, Glenn F.
PATENT-4 001 681; patented 4 Jan 77.

An Automated Broadband System for Measurement of One-Port Microwave Parameters;
Komarek, Ernest L.
CPEM Digest, p 167-170; 76.

A New Self-Balancing DC-Substitution RF Power Meter;
Larsen, Neil T.
CPEM Digest, p 203-205; 76.

An NBS Developed Automatic Network Analyzer;
Little, W.; Wakefield, J.; Heim, L.; Allred, C.; Zapf, T.
CPEM Digest, p 130-133; 76.

Measurement of Complex Microwave Circuit Parameters Using Only Power Detectors;
Engen, Glenn F.
CPEM Digest, p 171; 76.

Measuring and Minimizing Diode Detector Nonlinearity;
Hoer, C. A.; Roe, K. C.; Allred, C. M.
CPEM Digest, p 108-109; 76.

Reflection Coefficient Standards for Automated Network Analyzers;
Little, W. E.; Yates, B. C.
CPEM Digest, p 128-129; 76.

Repeatability of SMA Coaxial Connectors;
Jesch, R. L.
IEEE Trans. Instrum. Meas. IM-25:314-320; 76.

Scattering Parameters of SMA Coaxial Connectors;
Estin, A. J.
IEEE Trans. Instrum. Meas. IM-25:329-334; 76.

A Guide to Voice Scramblers for Law Enforcement Agencies;
Nelson, Robert E.
NBS SP 480-8; Dec 76.

A New Self-Balancing DC-Substitution RF Power Meter;
Larsen, Neil T.
IEEE Trans. Instrum. Meas. IM-25:343-347; Dec 76.

Determination of Microwave Phase and Amplitude from Power Measurements;
Engen, Glenn F.
IEEE Trans. Instrum. Meas. IM-25:414-418; Dec 76.

Ultrasonic Calorimeter for Beam Power Measurements;
Zapf, Thomas L.; Harvey, Morris E.; Larsen, Neil T.; Stoltenberg, Robert E.
NBS TN 686; Sep 76.

A Microwave Vector Voltmeter System;
Roe, Keith C.; Hoer, Cletus A.
NBSIR 76-844; Aug 76.

Implementation of the Notch Technique as an RF Peak Pulse Power Standard;
Simpson, Philip A.; Hudson, Paul A.
NBS TN 682; Jul 76.

The Calibration and Use of Directional Couplers Without Standards;
Allred, C. McKay; Manney, Charles H.
IEEE Trans. Instrum. Meas. IM-25:84-89; Mar 76.

The National Measurement System for Medical Ultrasonics;
Hudson, Paul A.
NBSIR 75-937; Feb 76.

A Precision 30 MHz Waveguide-Below-Cutoff Attenuator with an Absolute Electronic Readout, NBS Model XII;
Adair, Robert T.
NBSIR 76-833; Jan 76.

Automated Calibration of Directional-Coupler-Bolometer-Mount Assemblies;
Engen, Glen F.
Proc. 1975 IEEE Microwave Theory and Technique Symp. Int., May 12-14, 1975;
Palo Alto, CA, p 98-99; 75.

Automated Calibration of Directional-Coupler-Bolometer-Mount Assemblies;
Engen, Glenn F.
IEEE Trans. Microwave Theory Tech. MTT-23:984-990; Dec 75.

Using an Arbitrary Six-Port Junction to Measure Complex Voltage Ratios;
Hoer, Cletus A.; Roe, Keith C.
IEEE Trans. Microwave Theory Tech. MTT-23:978-984; Dec 75.

Using Six-Port and Eight-Port Junctions to Measure Active and Passive Circuit Parameters;
Hoer, Cletus A.
NBS TN 673; Sep 75.

Self-Balancing DC-Substitution Measuring System; Patent Application;
Larsen, Neil T.; Reeve, Gerome R.
PAT-APPL-587 565; filed 17 Jun 75.

Characterization of a High Frequency Probe Assembly for Integrated Circuit Measurements;
Jesch, R. L.; Hoer, C. A.
NBS TN 663; Apr 75.

An Alternative Calibration Technique for Automated Network Analyzers with Application to Adapter Evaluation;
Engen, Glenn F.
Proc. 1974 IEEE S-MTT Int. Microwave Symposium, Jun 12-14, 1974 Atlanta, GA, Microwave Symposium Digest, p 261-262; 74.

An Application of the Power Equation Concept and Automation Techniques to Precision Bolometer Unit Calibration;
Komarek, Ernest L.
Proc. 1974 IEEE S-MTT International Microwave Symposium, Jun 12-14, 1974 Atlanta, GA, Microwave Symposium Digest, p 263-265; 74.

An Application of the Power Equation Concept and Automation Techniques to Precision Bolometer Unit Calibration;
Komarek, Ernest L.; Tryon, Peter V.
IEEE Trans. Microwave Theory Tech. Part II, 1974 Symposium Issue, MTT-22:1260-1267; Dec 74.

Calibration Technique for Automated Network Analyzers with Application to Adapter Evaluation;
Engen, Glenn F.
IEEE Trans. Microwave Theory Tech. Part II, 1974 Symposium Issue, MTT-22:1255-1260; Dec 74.

Broadband Pulsed/CW Calibration Signal Standard for Field Intensity Meter (FIM) Receivers;
Simpson, Philip A.
NBSIR 74-371; Jun 74.

Completion of the Program to Evaluate/Improve Instrumentation and Test Methods for Electroexplosive Device Safety Qualification;
Hudson, Paul A.; Melquist, Dean G.; Ondrejka, Arthur R.; Werner, Paul E.
NBSIR 74-379; Jun 74.

Comments on Practical Analysis of Reflectometers and Power Equation Concepts;
Engen, Glenn F.
IEEE Trans. Instrum. Meas. IM-23:104-105; Mar 74.

Analysis of a Six-Port Junction for Measuring, v, i, a, b, z, Gamma, and Phase;
Hoer, C. A.; Engen, G. F.
Proc. 6th Conf. Int. Meas. Confederation, Jun 17-23, 1973; Dresden, Germany, Acta IMEKO 1:213-222; 73.

Self-Calibration of Complex Ratio Measuring System;
Allred, C. M.; Manney, C. H.
Proc. Int. Conf. Measurement and Instrumentation, Jun 17-23, 1973; Dresden, Germany, ACTA IMEKO 1, p 157-166; 73.

Calibration of an Arbitrary Six-Port Junction for Measurement of Active and Passive Circuit Parameters;
Engen, Glenn F.
IEEE Trans. Instrum. Meas. IM-22:295-299; Dec 73.

Application of a Non-Ideal Sliding Short to Two-Port Loss Measurement;
Weidman, M. P.; Engen, G. F.
NBS TN 644; Oct 73.

Summary of WR15 Flange Evaluation at 60 GHz;
Yates, B. C.; Counas, G. J.
NBS TN 642; Oct 73.

Mismatch Considerations in Evaluating Amplifier Noise Performance;
Engen, Glenn F.
IEEE Trans. Instrum. Meas. IM-22:274-278; Sep 73.

Theory of UHF and Microwave Measurements Using the Power Equation Concept;
Engen, Glenn F.
NBS TN 637; Apr 73.

Application of an 'Arbitrary' 6-Port Junction to Power Measurement Problems;
Engen, Glenn F.; Hoer, Cletus A.
Proc. 1972 Conf. Precision Electromagnetic Measurements, Jun 26-29, 1972, Boulder, CO; New York, NY: IEEE, p 100-101; 72.

Application of an Arbitrary 6-Port Junction to Power-Measurement Problems;
Engen, Glenn F.; Hoer, Cletus A.
IEEE Trans. Instrum. Meas. IM-21:470-474; Nov 72.

The Six-Port Coupler: A New Approach to Measuring Voltage, Current, Power, Impedance, and Phase;
Hoer, Cletus A.
IEEE Trans. Instrum. Meas. IM-21:466-470; Nov 72.

Broad-Band Lumped-Element Directional Coupler;
Hoer, Cletus A.
PATENT-3 701 057; patented 24 Oct 72.

Millimeter Attenuation and Reflection Coefficient Measurement System;
Yates, B. C.; Larson, W.
NBS TN 619; Jul 72.

The 6-Port Coupler; A New Approach to Measuring V, I, P, Z, and Theta;
Hoer, Cletus A.
Digest of Precision Electromagnetic Measurements Conf., Boulder, CO, p 26-29; Jun 72.

An Extension to the Sliding Short Method of Connector and Adaptor Evaluation;
Engen, G. F.
NBS J. Res. 75C:177-183; 71.

Power Measuring and Leveling System Using a Self-Balancing Bridge;
Larsen, Neil T.; Clague, Frederick R.
PATENT-3 611 130; patented 5 Oct 71.

An Adjustable-Slot-Length UHF Coaxial Coupler with Decade Bandwidth;
Hudson, P. A.; Saulsbery, L. F.
IEEE Trans. Microwave Theory Tech. MTT-19:781-783; Sep 71.

Standard Field Strength Meter;
Lawton, Robert A.; Allred, Charles McKay
PATENT-3 586 973; patented 22 Jun 71.

International Intercomparison of Power Standards at 3 GHz;
Engen, Glenn F.; Hudson, Paul A.
IEEE Trans. Microwave Theory Tech. MTT-19:411-413; Apr 71.

An Excitation System for Piston Attenuators;
Cook, C. C.; Allred, C. M.
IEEE Trans. Instrum. Meas. IM-20:10-16; Feb 71.

Power Equations: A New Concept in the Description and Evaluation of Microwave Systems;
Engen, Glenn F.
IEEE Trans. Instrum. Meas. IM-20:49-57; Feb 71.

Theorem Giving Limits for S22 When S11 and the Two-Port Efficiency are Known;
Engen, Glenn F.
IEEE Trans. Instrum. Meas. IM-20:78; Feb 71.

An Immittance Transcomparator;
Agy, David L.; Nelson, R. E.
Annual Precision Measurement Association Metrology Conf. (3rd), Jun 17-18, 1970; Gaithersburg, MD, 1:147-154; 70.

Improvements to the NBS RF Peak-Pulse Power Standard;
Simpson, P. A.; Ondrejka, A. R.
Instrument Society of America Silver Jubilee Int. Conf. and Exhibit, Oct 1970; Philadelphia, PA, Paper 709-70, p 1-7; 70.

A New Method of Characterizing Amplifier Noise Performance;
Engen, Glenn F.
IEEE Trans. Instrum. Meas. IM-19:344-349; Nov 70.

Broad-Band Resistive-Divider-Type Directional Coupler;
Hoer, C. A.; Agy, D. L.
IEEE Trans. Instrum. Meas. IM-19:336-343; Nov 70.

A Method for Designing Multi-Screw Waveguide Tuners;
Weidman, M. P.; Campbell, E.
NBS TN 393; Oct 70.

A New Standard for Electric Field Strength;
Lawton, R. A.
IEEE Trans. Instrum. Meas. IM-19:45-51; Feb 70.

A Wide Range CW Power Measurement Technique;
Lawton, R. A.; Allred, C. M.; Hudson, P. A.
IEEE Trans. Instrum. Meas. IM-19:28-34; Feb 70.

An Introduction To The Description and Evaluation of Microwave Systems Using Terminal Invariant Parameters;
Engen, Glenn F.
NBS MN 112; Oct 69.

Measurement of RF Peak Pulse Power;
Hudson, P. A.
Proc. IEEE 55:851-855; 67.

RF Attenuation;
Russell, D. H.; Larson, W.
Proc. IEEE 55:942-959; Jun 67.

System for Measuring Peak Pulse Power Using Sampling and Comparison Techniques;
Hudson, Paul A.; Ecklund, Warner L.; Ondrejka, Arthur R.
PATENT-3 239 758; patented 8 Mar 66.

An Unmodulated Twin-Channel Microwave Attenuation Measurement System;
Russell, D. H.
ISA Trans. 4:162-169; Apr 65.

OPTICAL ELECTRONIC METROLOGY

Birefringence Measurements in Single Mode Optical Fiber;
Day, G. W.
Proc. SPIE, August 21-24, 1983, San Diego, CA, 42:72-79; 83.

Fiber Optics: Short-Haul and Long-Haul Measurements and Applications;
Gallawa, R. L.
Proc. SPIE, Aug. 24-25, 1982. SPIE, P.O. Box 10, Bellingham, WA 98227; vol. 355; 83.

Submicrometer Interdigital Silicon Detectors for the Measurement of Picosecond Optical Pulses;
Phelan, R. J.; Larson, D.; Frederick, N. V.; Franzen, D. L.
Proc. SPIE, Single Mode Optical Fibers, 425:207-211; 83.

Estimating Index Profiles of 1.3 μm Single Mode Fibers by Near-Field Measurements at Blue Wavelengths;
Kim, E. M.; Franzen, D. L.; Young, M.; Rodhe, P. M. (Guest Worker)
IEEE J. Lightwave Tech. LT-1(4):562-566; Dec 83.

Simulating the Scratch Standards for Optical Surfaces--Theory;
Johnson, E.
J. Appl. Opt. 22(24):4056-4068; Dec 83.

Optical Fiber Characterization Attenuation, Frequency Domain Bandwidth, and Radiation Patterns;
Chamberlain, G. E.; Day, G. W.; Franzen, D. L.; Gallawa, R. L.; Kim, E. M.; Young, M.
NBS SP 637, vol. II; Oct. 83.

Linewidth Measurement by High-Pass Filtering--A New Look;
Young, M.
Appl. Opt. 22(13):2022-2025; Jul 83.

Laser Measurements;
Sanders, A. A.
Proc. 1983 Measurement Science Conf., Jan. 20-21; Palo Alto, CA; Jun 83.

Measurement of Multimode Optical Fiber Attenuation: An NBS Special Test Service;
Gallawa, R. L.; Chamberlain, G. E.; Day, G. W.; Franzen, D. L.; Young, M.
NBS TN 1060; Jun 83.

Optical Time-Domain Reflectometer Performance and Calibration Studies;
Danielson, B. L.
TN-1064; Jun 83.

Two-Dimensional Near-Field Contouring of Optical Fiber Cores;
Kim, E. M.; Franzen, D. L.
Proc. SPIE; Jun 83.

Objective Measurements and Characteristics of Scratch Standards;
Young, M.
Proc. SPIE, August 1982, 3526:86-92; Spring 83.

EIA Fiber Performance Measurement Standards;
Gallawa, R.; Franzen, D. L.
Photonics Spectra, p 55-68; Apr 83.

Questions Students Ask;
Young, M.
Physics Teacher, p 194-195; Mar 83.

An Inter-Laboratory Measurement Comparison of Core Diameter on Graded-Index Optical Fibers;
Kim, E. M.; Franzen, D. L.
NBS SP 641; Oct 82.

A System for Measuring Energy and Peak Power of Low-Level 1.064 μm Laser Pulses;
Sanders, A. A.; Rasumussen, A. L.
NBS TN 1058; Oct 82.

Measurement of the Core Diameter of Graded-Index Optical Fibers: An Interlaboratory Comparison;
Kim, E. M.; Franzen, D. L.
Appl. Opt. 21(19):3443-3450; Oct 82.

Technical Digest - Symposium on Optical Fiber Measurements, 1982;
Franzen, D. L.; Day, G. W.; Gallawa, R. L., eds.
NBS SP 641; Oct 82.

Beam-Profile Measurement of Pulses Using a Spatial Filter to Sample the Hermite Modes for a String of Pulses;
Johnson, E. G.
NBS TN 1057; Sep 82.

Documentation of the NBS C, K, and Q Laser Calibration Systems;
Case, W. E.
NBSIR 82-1676; Sep 82.

Optical Fiber Characterization;
Day, G. W.; Danielson, B. L.; Franzen, D. L.; Kim, E.; Young, M., eds.
NBS SP 637, vol. 1; Jul 82.

Calibration Reticle for Optical Fiber Near-Field Core Diameter Measurements;
Kim, E. M.; Franzen, D. L.
CPEM Digest; May 82.

Characterization of a Concentric-Core Fiber;
Danielson, B. L.; Franzen, D. L.; Gallawa, R. L.; Kim, E. M.; Young, M.
NBSIR 82-1661; Apr 82.

On the Definition of Fiber Numerical Aperture;
Gallawa, R. L.
Electro-Optical Systems Design, p 47; Apr 82.

Quantum Noise Limits the Pinspeck Camera to Simple Objects;
Young, M.
J. Opt. Soc. Amer. 72(3):402-403; Mar 1982.

Optical Waveguide Communications Glossary;
Gallawa, R. L., et al.
NBS HB 140; Jan 82.

Book Review: Principles of Optical Fiber Measurements by D. Marcuse;
Young, M.
Laser Focus, p 118-119; Jan 82.

Backscattter Signature Simulations;
Danielson, B. L.
NBS TN 1050; Dec 1981.

Long Optical Fiber Fabry Perot Interferometers;
Franzen, D. L.; Kim, E.
Appl. Opt. 20(23):3991-3992; 81.

A Measurement Method for Determining the Optical and Electro-optical Properties of a Thin Film;
Larson, D.
NBSIR 81-1652; Dec 81.

An Optical Waveguide Communications Glossary, Revised;
Hanson, A. G.; Bloom, L. R.; Day, G. W.; Young, M.; Gray, E. M.; Gallawa, R. L.
NBS HB 140; Dec 81.

Book Review: Optical Fibre Communication (invited review);
Gallawa, R.
IEEE Spectrum, 1 p; Nov 81.

The Use of LEDs as YAG Laser Simulators;
Young, M.
Proc. Conf. Electro-Optics and Lasers; Nov 81.

Optical Fiber Index Profiles by Refracted-Ray Scanning;
Young, M.
Appl. Opt. 20(19):3415-21; Oct 81.

Measurement of Optical Fiber Bandwidth in the Frequency Domain;
Day, G. W.
NBS TN 1046; Sep 81.

Standard Measurement Conditions and Test Results on Multimode Fibers;
Franzen, D. L.
Laser Focus, p 103-105; Aug 81.

The Use of LEDs to Simulate Weak YAG-laser Beams;
Young, M.
NBS TN 1031; Revised Aug 81.

Interlaboratory Measurement Comparison to Determine the Attenuation and Bandwidth of Graded-index Fibers;
Franzen, D. L.; Day, G. W.; Danielson, B. L.; Chamberlain, G. E.; Kim, E.
Appl. Opt. 20(14):2412-2419; 15 Jul 81.

The Characterization of Optical Fiber Waveguides: A Bibliography with Abstracts, 1970-1980;
Day, G. W.
NBS TN 1043; Jun 81.

Refracted-ray Scanning (Refracted Near-Field Scanning) for Measuring Index Profiles of Optical Fibers;
Young, M.
NBS TN 1038; May 81.

Present NBS Capability in Optical Fiber Measurements;
Day, G. W.; Franzen, D. L.
Proc. 1st Int. DoD/Industry Fiber Optics Standards Conf., Washington, DC; Apr 81.

Results of an Interlaboratory Measurement Comparison Among Fiber Manufacturers to Determine Attenuation, Bandwidth, and Numerical Aperture of Graded Index Optical Fibers;
Franzen, D. L.; Day, G. W.; Danielson, B. L.; Kim, E.
Conf. Digest 3rd Intl. Conf. Integrated Optics & Optical Fiber Comm., San Francisco, CA; Apr 81.

Results of an Inter-Laboratory Measurement Comparison to Determine the Radiation Angle (NA) of Graded Index Optical Fibers;
Franzen, D. L.; Kim, E.
Appl. Opt. 20(7):1218-1220; Apr 81.

Sub-nanosecond Electrical Modulation of Light with Hydrogenated Amorphous Silicon;
Phelan, R. J.; Larson, D. R.; Werner, P. E.
Appl. Phys. Lett. 38(8); Apr 15, 81.

Backscatter Measurements in Optical Fibers;
Danielson, B. L.
NBS TN 1034; Feb 81.

Measurement of Far-field and Near-field Radiation Patterns from Optical Fibers;
Kim, E.; Franzen, D. L.
NBS TN 1032; Feb 81.

Progress in Fiber Measurements;
Day, G. W.; Franzen, D. L.
Laser Focus, p 52-56; Feb 81.

A System for Characterizing Detectors for the Measurement of Power of CO_2 TEA Laser Pulses;
Simpson, P. A.
Proc. 11th Annual Electro-Optical Laser Conf., Oct 23-25, 1979; Ind. and Sci. Conf. Management, Inc., 222 W. Adams St., Chicago, IL 60606, p 3999-4007; 80.

The Role of Backscatter Signatures in Optical Fiber Characterization;
Danielson, B. L.
Tech. Digest 1st Int. DoD Ind. Fiber Optics Congress, Apr 20, 1980; Washington, DC; 80.

Linearity and Resolution of Refracted Near-Field Scanning Techniques;
Young, M.
Digest Symposium on Optical Fiber Measurements, NBS SP 597; Oct 80.

Technical Digest, Symposium on Optical Fiber Measurements, 1980;
Day, G. W.; Franzen, D. L., eds.
NBS SP 597; Oct 80.

A System for Measuring the Characteristics of High Peak Power Detectors of Pulsed CO_2 Laser Radiation;
Simpson, P. A.
NBS TN 1023; Sep 80.

Calibration Technique for Refracted Near-field Scanning of Optical Fibers;
Young, M.
Appl. Opt. 19:2479-80: Aug 80.

Measuring Features of the Fluence at the Far Field of a CO_2 Pulsed Laser--An Issue Study With Suggestions on How To Do It;
Johnson, E. G, Jr.
NBSIR 80-1628; Apr 80.

An Assessment of the Backscatter Technique as a Means for Estimating Loss in Optical Waveguides;
Danielson, B. L.
NBS TN 1018; Feb 80.

Measurement of Optical Fiber Bandwidth in the Time Domain;
Franzen, D. L.; Day, G. W.
NBS TN 1019; Feb 80.

LED Source for Determining Optical Detector Time Response at 1.06 Micrometers;
Franzen, D. L.; Day, G. W.
Rev. Sci. Instr. 50:1029; 79.

Linear Systems, Fourier Transforms and Optics by J. D. Gaskill; (book review)
Young, M.
J. Opt. Soc. Amer. 69:637-638; 79.

Measurement of Low Level Laser Pulses at 1.064 μm;
Rasmussen, A. L.; Sanders, A. A.
Measurements of Optical Radiation, SPIE 196:96-103; 79.

Measurement of Propagation Constants Related to Material Properties in High Bandwidth Optical Fibers;
Franzen, D. L.; Day, G. W.,
IEEE J. Quantum Electron. QE-15(12); Dec 79.

Continuous-Wave (Mode-Locked) Dye Laser with Unfolded Cavity;
Young, M.
Appl. Opt. 18:3212; Oct 79.

Limitations Imposed by Material Dispersion on the Measurement of Optical Fiber Bandwidth with Laser Diode Sources;
Franzen, D. L.; Day, G. W.,
J. Opt. Soc. Amer. 69(10); Oct 79.

Optical Waveguide Communications Glossary;
Hanson, A. G.; Bloom, L. R.; Day, G. W.; Gallawa, R. L.; Gray, E. M.; M. Young
NTIA SP 79-4; Sep 79.

Time Domain Pulse Measurements and Computed Frequency Response of Optical Communications Components;
Andrews, J. R.; Young, M.
NBSIR 79-1620; Sep 79.

National Standards of a Powerful Sort;
Sanders, A. A.
Opt. Spectra 13:45; Aug 79.

Quality Assurance Program for the NBS, C, K, and Q Laser Calibration Systems;
Case, W. E.
NBSIR 79-1619; Aug 79.

Design of a Reflection Apparatus for Laser Beam Profile Measurements;
Johnson, E. G., Jr.
NBS TN 1015; Jul 79.

Fiber Measurements: Quality and Cost;
Day, G. W.
Proc. Int. Conf. on Communications, Boston; Jun 79.

Attenuation Measurements on Optical Fiber Waveguides: An Interlaboratory Comparison Among Manufacturers;
Day, G. W.; Chamberlain, G. E.
NBSIR 79-1608; May 79.

Conference on Optical Scattering Standards;
Young, M.
Proc. SPIE Conf.; Apr 79.

Laser Beam Profile Measurements Using Spatial Sampling, Fourier Optics, and Holography;
Johnson, Eric G., Jr.
NBS TN 1009; Jan 79.

A Simple First Positive System Nitrogen Laser for use in Optical Fiber Measurements;
Franzen, D. L.; Danielson, B. L.; Day, G. W
IEEE J. Quantum Electron. QE-14:548; 78.

Measurement Problems in Multimode Optical Waveguides;
Day, G. W.
Proc. Int. Com. Conf., Jun 1978; Toronto, Canada, vol. 1; 78.

Optical Fiber Phase Discriminator;
Danielson, B. L.
Appl. Opt. 17:3665-3668; Nov 78.

Improvements in a Calorimeter for High-Power CW Lasers;
Chamberlain, George E.; Simpson, Philip A.; Smith, Richard L.
IEEE Trans. Instrum. Meas. IM-27:81-86; Mar 78.

Laser Far-Field Beam-Profile Measurements by the Focal Plane Technique;
Day, G. W.; Stubenrauch, C. F.
NBS TN 1001; Mar 1978.

Fiber Optics Metrology at NBS;
Danielson, B.; Day, G.; Franzen, D.
Proc. Union Radio Scientifique Internationale Comm. Symp., Oct 3-7, 1977; Lannion, France, (International Union of Radio Science, France), p 430-431; Dec 77.

Evaluating the Inequivalence and a Computational Simplification for the NBS Laser Energy Standards;
Johnson, Eric G., Jr.
Appl. Opt. 16:2315-2321; Aug 77.

Measurement Procedures for the Optical Beam Splitter Attenuation Device BA-1;
Danielson, B. L.
NBSIR 77-858; May 77.

Proposed Standards for Ladar Signatures;
Danielson, B. L.
NBSIR 77-856; Apr 77.

An NBS Laser Measurement Assurance Program (MAP);
Sanders, A. A.; Cook, A. R.
Proc. Electro-Optical Systems Design Conf. 1976 and Int. Laser Exposition, Sep 14-16, 1976; New York, p 277-280; 76.

Laser Action in Sputtered Metal Vapors;
McNeil, J. R.; Johnson, W. L.; Collins, G. J.; Persson, K. B.; Franzen, D. L.
9th Int. Conf. on Quantum Electronics, Jun 14-16, 1976; Amsterdam, The Netherlands, p 162-163; 76.

Performance and Characteristics of Polyvinylidene Fluoride Pyroelectric Detectors;
Day, G. W.; Hamilton, C. A.; Gruzensky, P. M.; Phelan, R. J., Jr.
Proc. IEEE Symposium on Application of Ferroelectrics, Jun 9-11, 1975; Albuquerque, NM; Ferroelectrics 10:99-102; 76.

Absolute Reference Calorimeter for Measuring High Power Laser Pulses;
Franzen, D. L.; Schmidt, L. B.
Appl. Opt. 15:3115-3122; Dec 76.

Spectral Reference Detector for the Visible to 12 Micrometer Region; Convenient, Spectrally Flat;
Day, G. W.; Hamilton, C. A.; Pyatt, K. W.
Appl. Opt. 15:1865-1868; Jul 76.

An Electrically Calibrated Pyroelectric Radiometer System;
Hamilton, C. A.; Day, G. W.; Phelan, R. J., Jr.
NBS TN 678; Mar 76.

Ultraviolet Laser Action from Cu II in the 2500-A Region;
McNeil, J. R.; Collins, G. J.; Persson, K. B.; Franzen, D. L.
Appl. Phys. Lett. 28:207-209; Feb 76.

Laser Attenuators for the Production of Low Power Beams in the Visible and 1.06 micron Regions;
Danielson, B. L.; Beers, Yardley
NBS TN 677; Jan 76.

Radiometry Without Standard Sources/Electrically Calibrated Pyroelectrics;
Phelan, Robert J. Jr; Hamilton, Clark A.; Day, Gordon W.
Proc. Society of Photo-Optical Instrumentation Engineers, Aug 17-22, 1975; San Diego, CA, Paper in Modern Utilization of Infrared Technology Civilian and Military, SPIE 62:159-165; 75.

Pyroelectric Radiometers Get Off The Drawing Board;
Hamilton, C. A.; Phelan, R. J., Jr; Day, G. W.
Opt. Spectra 9:37-38; Oct 75.

Improving Beam Measurement;
Smith, R. L.; Sanders, A. A.
Laser Focus, p 70-71; Apr 75.

Precision Beam Splitters for CO2 Lasers;
Franzen, Douglas L.
Appl. Opt. 14:647-652; Mar 75.

A Pyroelectric Power Meter for the Measurement of Low Level Laser Radiation;
Hamilton, C. A.; Day, G. W.
NBS TN 665; Feb 75.

The Polarization of PVF and PVF2 Pyroelectrics;
Phelan, R. J. Jr; Peterson, R. L.; Hamilton, C. A.; Day, G. W.
Ferroelectrics 7:375-377; 74.

Current Status of NBS Low-Power Laser Energy Measurement;
West, E. D.; Case, W. E.
Proc. Conf. on Precision Electromagnetic Measurements, Jul 1-5, 1974; London, England, IEEE Trans. Inst. Meas. IM-23:422-425; Dec 74.

Analysis of Response of Pyroelectric Optical Detectors;
Peterson, R. L.; Day, G. W.; Gruzensky, P. M.; Phelan, R. J.
J. Appl. Phys. 45:3296-3303; Aug 74.

Effects of Poling Conditions on Responsivity and Uniformity of Polarization of PVF2 Pyroelectric Detectors;
Day, G. W.; Hamilton, C. A.; Peterson, R. L.; Phelan, R. J., Jr; Mullen, L. O.
Appl. Phys. Lett. 24:456-458; May 74.

Absolute, Pyroelectric Radiometers and Two Dimensional Arrays;
Phelan, R. J., Jr; Peterson, R. L.; Klein, G. P.; Hamilton, C. A.; Day, G. W.
Proc. American Electro-Optical Systems Design Conf., New York, NY, p 117-123; 73.

Comparison of the Laser Power and Total Irradiance Scales Maintained by the National Bureau of Standards;
Geist, Jon; Schmidt, L. B.; Case, W. E.
Appl. Opt. 12:2773-2776; Nov 73.

Electrically Calibrated Pyroelectric Optical-Radiation Detector;
Phelan, Robert J., Jr; Cook, A. R.
Appl. Opt. 10:2494-2500; Oct 73.

Continuous Laser-Sustained Plasmas;
Franzen, D. L.
J. Appl. Phys. 44:1727-1732; Apr 73.

Limitations of the Use of Vacuum Photodiodes in Instruments for the Measurement of Laser Power and Energy;
Smith, R. L.; Phelan, R. J., Jr.
Appl. Opt. 12:795-798; Apr 73.

Accurate Frequencies of Molecular Transitions Used in Laser Stabilization: The 3.39-micrometer Transition in CH4 and the 9.33- and 10.18-micrometer Transitions in CO2;
Evenson, K. M.; Wells, J. S.; Peterson, F. R.; Danielson, B. L.; Day, G. W.
Appl. Phys. Lett. 22:192-195; Feb 73.

A Calorimeter for High Power CW Lasers;
Smith, R. L.; Case, W. E.; Rasmussen, A. L.; Russell, T. W.; West, E. D.
Proc. Conf. on Precision Electromagnetic Measurements, Jun 26-29, 1972; Boulder, CO, p 138-139; 72.

High D*, Fast, Lead Zirconate Titanate Pyroelectric Detectors;
Mahler, R. J.; Phelan, R. J., Jr; Cook, A. R.
Infrared Phys. 12:57-59; 72.

A Calorimeter for High-Power CW Lasers;
Smith, R. L.; Russell, T. W.; Case, W. E.; Rasmussen, A. L.
IEEE Trans. Instrum. Meas. IM-21:434-8; Nov 72.

Speed of Light from Direct Frequency and Wavelength Measurements of the Methane-Stabilized Laser;
Evenson, K. M.; Wells, J. S.; Petersen, F. R.; Danielson, B. L.; Day, G. W.
Phys. Rev. Lett. 29:1346-1349; Nov 72.

CW Gas Breakdown in Argon Using 10.6 Micrometer Laser Radiation;
Franzen, Douglas L.
Appl. Phys. Lett. 21:62-64; Jul 72.

Role of Infrared Frequency Synthesis in Metrology;
Wells, J. S.; Evenson, K. M.; Day, G. W.; Halford, Donald
Proc. IEEE Lett. 60:621-623; May 72.

Gain Saturation Measurements in CO2, TEA Amplifiers;
Franzen, Douglas L.; Jennings, Donald A.
J. Appl. Phys. 43:729-730; Feb 72.

Double Plate Calorimeter for Measuring the Reflectivity of the Plates and the Energy in a Beam of Radiation;
Rasmussen, Alvin L.
PATENT-3 622 245; patented 23 Nov 71.

High D* Pyroelectric Polyvinylfluoride Detectors;
Phelan, Robert J., Jr; Mahler, Robert J.; Cook, Alan R.
Appl. Phys. Lett. 19:337-338; Nov 71.

Measurement of Laser Energy of Linear Components of Polarization at 1.060 micron;
Rasmussen, A. L.
Rev. Sci. Instrum. 42:1590-1593; Nov 71.

Linear and Nonlinear Optical Properties of Trigonal Selenium;
Day, G. W.
Appl. Phys. Lett. 18:347-349; Apr 71.

Extension of Absolute Frequency Measurements to the cw He-Ne Laser at 88 THz (3.39 micrometer);
Evenson, K. M. ; Day, G. W. ; Wells, J. S. ; Mullen, L. O.
Appl. Phys. Lett. 20:133-134; Feb 71.

Some Optical Properties of Cesium Cupric Chloride;
Day, G. W.; Gruzensky, P. M.
Appl. Opt. 9:2494-2795; 70.

Laser Power and Energy Measurements;
Jennings, D. A.; West, E. D.; Evenson, K. M.; Rasmussen, A. L.; Simmons, W. R.
NBS TN 382; Oct 69.

InSb-GaAsP Infrared to Visible Light Converter;
Phelan, Robert J., Jr.
Proc. IEEE 55:1505-1502; Aug 67.

InSb MOS Infrared Detector;
Phelan, R. J., Jr.; Dimmock, J. O.
Appl. Phys. Lett. 10:55-7; Jan 67.

Incoherent Source Optical Pumping of Visible and Infrared Semiconductor Lasers;
Phelan, Robert J., Jr.
Proc. IEEE 54:1119-20; Aug 66.

Laser Emission by Optical Pumping of Semiconductors;
Phelan, R. J., Jr.
Proc. Quantum Electronics Conf., p 435-441; Jul 65.

ELECTROMAGNETIC WAVEFORM METROLOGY

Reference Waveform Flat Pulse Generator;
Andrews, J.; Bell, B.; Nahman, N. S.; Baldwin, E. E.
Proc. CPEM 1982 in IEEE Trans. Instrum. Meas. IM-32(1):27-32; Mar 83.

Reference Waveform Flat Pulse Generator;
Andrews, J. R.; Bell, B. A.; Nahman, N. S.; Baldwin, E. E.
1982 CPEM Conf. Digest; Jun 82.

Deconvolution of Time Domain Waveforms in the Presence of Noise;
Nahman, N. S.; Guillaume, M. E.
NBS TN 1047; Oct 81.

Shielded Balanced and Coaxial Transmission Lines - Parametric Measurements and Instrumentation Relevant to Signal Waveform Transmission in Digital Service;
Gans, W. L.; Nahman, N. S.
NBSIR 81-1042; Jun 81.

Amplitude Calibrator for Oscilloscopes;
Andrews, J. R.; Baldwin, E. E.
NBSIR 81-1646; Apr 81.

Error Criteria and the Use of Reference Waveforms;
Nahman, N. S.
Electron. Test 4(2):72-76; Feb 81.

Instrument Modeling and Deconvolution Improve Time Domain Calibrations;
Nahman, N. S.; Andrews, J. R.
NBS Dimensions, p 21-23; Jan/Feb 81.

Deconvolution of Duration Limited Waveforms;
Nahman, N. S.; Guillaume, M. E.
Digest of Papers, URSI/U.S. National Radio Science Meeting, Boulder, CO, p 86; Jan 81.

Error Criteria and the Use of Reference Waveforms;
Nahman, N. S.
Proc. ATE Seminar/Exhibit, Pasadena, CA, Jan 1981, Benwill Publications, Boston, MA, p IV.21-IV.28; Jan 81.

Pulse Reference Waveform Standards Development at NBS;
Andrews, J. R.
Proc. ATE Seminar/Exhibit, Pasadena, CA, Jan 1981, Benwill Publications, Boston, MA, p IV.13-IV.19; Jan 81.

The Estimation of the Pulse Waveform in the Calibration of Impulse Generators;
Andrews, J. R.
Digest of Papers, URSI/U.S. National Radio Science Meeting, Boulder, CO, p 87; Jan 81.

Applications of Time Domain Methods to Microwave Measurements;
Nahman, N. S.; Andrews, J. R.; Gans, W. L.; Guillaume, M. E.; Lawton, R. A.; Ondrejka, A. R.; Young, M.
IEE Proc. (Microwaves, Optics, and Acoustics) Special Issue on Microwave Measurements 127, Part H(2):171-178; Apr 80.

A Superconducting Sampler for Josephson Logic Circuits;
Hamilton, C.; Lloyd, F.; Peterson, R.; Andrews, J. R.
Appl. Phys. Lett. 35(9):718-719; Nov 79.

A Video Recorder for Coherent Doppler Radar;
Wharton, M. J.; Frush, C. L.; Nahman, N. S.
IEEE Trans. Geosci. Electron., Special Issue on Radio Meteorology, GE-17(4):171-178; Oct 79.

Time Domain Pulse Measurements and Computed Frequency Responses of Optical Communications Components;
Andrews, J. R., Young, M.
NBSIR 1620; Sep 79.

Radar Absorber Measurement Techniques at Frequencies above 20 GHz;
Nahman, N. S.; Allred, C. M.; Andrews, J. R.; Hoer, C. A.; Lawton, R. A.
NBSIR 1613; Aug 79.

Picosecond Domain Waveform Measurements (Japanese translation);
Nahman, Norris S.
Nikkei Electronics, Tokyo Japan: Nikkei-McGraw Hill, Inc.; Apr 79.

Measurement of Pulsed-Laser Power;
Young, M.; Lawton, R. A.
NBS TN 1010; Feb 79.

Antennas and the Associated Time Domain Range for the Measurement of Impulsive Fields;
Lawton, Robert A.; Ondrejka, Arthur R.
NBS TN 1008; Nov 78.

Applications of the Homomorphic Transformation to Time Domain Measurement Problems;
Riad, Sedki M.; Nahman, Norris S.
NBSIR 78-881; Jun 78.

SHF Impulse Generator;
Andrews, James R.; Baldwin, Eugene E.
NBSIR 78-888; Jun 78.

Broadband Isotropic Antenna with Fiber-Optic Link to a Conventional Receiver;
Larsen, Ezra B.; Andrews, James R.; Baldwin, Eugene E.
PATENT-4 091 327; patented 23 May 78.

Automatic Network Measurements in the Time Domain;
Andrews, James R.
Proc. IEEE 66:414-423; Apr 78.

Picosecond-Domain Waveform Measurements;
Nahman, Norris S.
Proc. IEEE 66, 441-454; Apr 78.

Saturation of Silicon Photodiodes at High Modulation Frequency;
Young, M.; Lawton, R. A.
Appl. Opt. 17:1103-1106; 1 Apr 78.

Measurement on Pulses and Pulse Transmission Media, Circuits and Components;
Andrews, J. R.
URSI Review of Radio Science, p 9; 1975-1977.

Application of a Automated Pulse Measurement System To Telecommunications Measurements;
Gans, W.; Andrews, J. R.; Riad, S.; Cozannet, A.; Debeau, J.
Collogue International sur la Measure en Telecommunications, URSI, CNET, Oct 3-7, 1977; Lannion, France, p 165-170; 77.

Saturation of Optical Detectors at High Modulation Frequency;
Young, M.; Lawton, R. A.
Proc. Annual Meeting Optical Society of America, Oct 12, 1977; Toronto, Canada, J. Opt. Soc. Am. 67:1398; 77.

Signal Waveform Metrology at NBS;
Nahman, Norris S.
Proc. WESCON/77, Electronics at the Golden Gate, Sep 19-21, 1977; San Francisco, CA; 77.

Standards for the Measurement of Impulsive Fields Radiated by a TEM Horn Antenna;
Lawton, Robert A.; Ondrejka, Arthur R.
Proc. Union Radio Scientifique International Comm. Symp., Oct 3-7, 1977; Lannion, France, p 1-4; Dec 77.

The Measurement of Pulse Transition Duration;
Andrews, James R.; Nahman, Norris S.
Proc. Union Radio Scientifique Internationale Comm. Symp., Oct 3-7, 1977; Lannion, France, p 159-164; Dec 77.

Laser-Mode Beating Used for Detector Frequency-Response Measurements;
Lawton, R. A.; Young, M.
Appl. Opt. 16:2703-2705; Oct 77.

Waveform Sampler;
Lawton, Robert A.; Andrews, James R.
PATENT-4 030 840; patented 21 Jun 77.

Application of the Homomorphic Deconvolution for the Separation of TDR Signals Occurring in Overlapping Time Windows;
Riad, Sedki M.; Nahman, Norris S.
CPEM Digest, p 27-29; 76.

Impulse Generator Spectrum Amplitude Measurement Techniques;
Andrews, James R.
CPEM Digest, p 23-24; 76.

Present Capabilities of the NBS Automatic Pulse Measurement System;
Gans, William L.
CPEM Digest, p 25-26; 76.

Using Fiber Optics in a Broadband, Sensitive, Isotropic Antenna - 15 kHz to 150 MHz;
Larsen, E. B.; Andrews, J. R.
Proc. IEEE International Symposium on Electromagnetic Compatability, Jul 13-15 1976; Washington, DC, p 385-389; 76.

Application of the Homomorphic Deconvolution for the Separation of TDR Signals Occurring in Overlapping Time Windows;
Riad, Sedki M.; Nahman, Norris S.
IEEE Trans. Instrum. Meas. IM-25:388-391; Dec 76.

Impulse Generator Spectrum Amplitude Measurement Techniques;
Andrews, James R.
IEEE Trans. Instrum. Meas. IM-25:380-384; Dec 76.

Present Capabilities of the NBS Automatic Pulse Measurement System;
Gans, William L.
IEEE Trans. Instrum. Meas. IM-25:384-388; Dec 76.

Electrical Strobing of a Photoconductor Cuts Sampling Oscilloscope's Risetime;
Lawton, Robert A.; Andrews, James R.
Laser Focus, p 62-65; Nov 76.

Sensitive Isotropic Antenna with Fiber-Optic Link to a Conventional Receiver;
Larsen, E. B.; Andrews, J. R.; Baldwin, E. E.
NBSIR 75-819; Sep 76.

Andrews, James R.
PATENT-3 967 140; patented 29 Jun 76.

Electrically Strobed Optical Waveform Sampling Oscilloscope;
Andrews, James R.; Lawton, Robert A.
Rev. Sci. Instrum. 47:311-313; Mar 76.

Optically Strobed Sampling Oscilloscope;
Lawton, Robert A.; Andrews, James R.
IEEE Trans. Instrum. Meas. 25:56-60; Mar 76.

Baseband Impulse Generator Useful to 5 GHz;
Andrews, James R.; Baldwin, Eugene E.
Proc. 1975 IEEE Int. Symp. on Electromagnetic Compatibility, Oct 7-9, 1975; San Antonio, TX, p 1-4; 75.

Picosecond Pulse Research at NBS;
Andrews, James R.; Lawton, Robert A.
Proc. Joint Measurement Conf., Nov 12-14, 1974; Gaithersburg, MD, p 123-140; 75.

Time Domain Automatic Network Analyzer;
Andrews, J. R.; Gans, William L.
Proc. Colloque International sur L'Electronique et la Mesure, May 26-30, 1975; Paris, France, La Mesure Electriquede Precision, p 258-267; 75.

Time Domain Automatic Network Analyzer;
Andrews, J. R.; Gans, W. L.
L'Onde Electrique, Paris, France, 55(10):569-574; Dec 75.

Directional-Coupler Technique for Triggering a Tunnel Diode;
Andrews, James R.
IEEE Trans. Instrum. Meas. IM-24:275-277; Sep 75.

Time Domain Automatic Network Analyzer for Measurement of RF and Microwave Components;
Gans, William L.; Andrews, James R.
NBS TN 672; Sep 75.

Pulsed-Laser Application to Sampling Oscilloscope;
Lawton, Robert A.; Andrews, James R.
Electron. Lett. 11:138; Apr 75.

Pulsed Wavemeter Timing Reference for Sampling Oscilloscope Calibration;
Andrews, James R.; Gans, William L.
IEEE Trans. Instrum. Meas. IM-24:82; Mar 75.

Photoconductive Detector of Fast-Transition Optical Waveforms;
Lawton, R. A.; Scavannec, A.
Electron. Lett. 11:74-75; Feb 75.

Application of Ultrashort Optical Pulses to Electrical Pulse Measurements;
Honda, T.; Nahman, N. S.
Proc. Symposium on New Instrumentation, Jan 28-29, 1974; IEE of Japan, Hokkaido University, p 29-38; 74.

Precision Picosecond-Pulse Measurements Using a High Quality Superconducting Delay Line;
Andrews, James R.
Proc. Conf. on Precision Electromagnetic Measurements, Jul 1-5, 1974; London, England; Abstract in CPEM Digest, London: IEE; p 316-318; 74.

Precision Picosecond-Pulse Measurements Using a High-Quality Superconducting Delay Line;
Andrews, James R.
IEEE Trans. Instrum. Meas. IM-23:468-472; Dec 74.

Picosecond Pulse Generators Using Microminiature Mercury Switches;
Andrews, James R.
NBSIR 74-377; Mar 74.

Active and Passive Mode Locking of Continuously Operating Rhodamine 6G Dye Lasers;
Scavennec, Andre; Nahman, N. S.
NBSIR 73-347; Feb 74.

Inexpensive Laser Diode Pulse Generator for Optical Waveguide Studies;
Andrews, James R.
Rev. Sci. Instrum. 45:22-24; Jan 74.

A Simple Passively Mode-Locked CW Dye Laser;
Scavennec, Andre; Nahman, Norris S.
IEEE J. Quantum Electron. QE-10:95-96; Jan 74.

Autocorrelation and Power Measurement with Pyroelectric and Dielectric Bolometers;
Lawton, Robert A.
IEEE Trans. Instrum. Meas. IM-22:299-306; Dec 73.

Random Sampling Oscilloscope for the Observation of Mercury Switch Closure Transition Times;
Andrews, James R.
IEEE Trans. Instrum. Meas. IM-22:375-381; Dec 73.

Frequency Domain Measurement of Baseband Instrumentation;
Nahman, N. S.; Jickling, R. M.
NBSIR 73-330; Jul 73.

Pulse Testing of RF and Microwave Components;
Gans, William L.; Nahman, N. S.
NBSIR 73-325; Jul 73.

Random Sampling Oscilloscope Time Base;
Andrews, James R.
NBSIR 73-309; Jun 73.

A Note on the Transition (Rise) Time Versus Line Length in Coaxial Cables;
Nahman, Norris S.
IEEE Trans. Circuit Theory CT-20:165-167; Mar 73.

Miniature Superconductive Coaxial Transmission Lines;
Nahman, Norris S.
Proc. IEEE 61:76-79; Jan 73.

Coaxial Line Pulse-Response Error Due to a Planar Skin Effect Approximation;
Holt, D. R.; Nahman, N. S.
Proc. 1972 Conf. on Precision Electromagnetic Measurement, Jun 26-29, 1972; Boulder, CO; p 1-2; 72.

Fast Fourier Transform Implementation for the Calculation of Network Frequency Domain Transfer Functions from Time Domain Waveforms;
Gans, William L.; Nahman, N. S.
NBSIR 73-303; Dec 72.

Reference-Waveform Generation Using Debye Dielectric Dispersion;
Nahman, N. S.; Jickling, R. M.; Holt, D. R.
NBSIR 73-304; Dec 72.

Coaxial-Line Pulse-Response Error Due to a Planar Skin-Effect Approximation;
Holt, D. R.; Nahman, N. S.
IEEE Trans. Instrum. Meas. IM-21:515-519; Nov 72.

A Dye Modelocked Nd^{+3} Glass Laser for Generating Electrical Reference Waveforms;
Honda, T.; Nahman, N. S.
NBSIR 74-360; Sep 72.

Transient Analysis of Coaxial Cables Using the Skin Effect Approximation A + B(the square root of s);
Nahman, N. S.; Holt, D. R.
IEEE Trans. Circuit Theory CT-19:443-451; Sep 72.

Measurement of Laser Pulse Dispersion in Glass Fiber Optical Waveguides;
Andrews, J. R.
NBS Memo for the Record; Jul 72.

Measurement of Broadening of Pulses in Glass Fibers;
Bouille, R.; Andrews, J. R.
Electron. Lett. 8:309-310; Jun 72.

Pyroelectric Detector Application to Baseband Pulse Measurements;
Lawton, Robert A.; Nahman, N. S.
Electron. Lett. 8:318-320; Jun 72.

A Frequency Calibrator for UHF Using an Avalanche Transistor;
Andrews, James R.
Q S T 56:16-18; May 72.

Survey of Present Waveform Sampling System Limitations;
Andrews, J. R.; Whittemore, T.; McCaa, W. D.
NBS Report 10-731; Feb 72.

Electron-Beam Deflection in Traveling-Wave Oscilloscopes;
Andrews, James R.; Nahman, N. S.
Record of Symposium on Electron, Ion, and Laser Beam Technology (11th), May 12-14, 1971; Boulder, CO; 71.

An Interfacing Unit for a 28 psec Feedthrough Sampling Oscilloscope;
Andrews, J. R.
Rev. Sci. Instrum. 42:1882-1885; Dec 71.

Horizontal Time Base Sweep Generator for a Traveling Wave Oscilloscope;
Andrews, James R.
IEEE Trans. Nucl. Sci. NS-18:3-8; Oct 71.

The Measured Time and Frequency Response of a Miniature Superconducting Coaxial Line;
Ekstrom, M. P.; McCaa, W. D. Jr; Nahman, N. S.
IEEE Trans. Nucl. Sci. NS-18:18-25; Oct 71.

Generation of Reference Waveforms by Uniform Lossy Transmission Lines;
McCaa, W. D.; Nahman, N. S.
IEEE Trans. Instrum. Meas. IM-19:382-390; Nov 70.

Improved Bias Supply for Tunnel-Diode Picosecond Pulse Generators;
Andrews, J. R.
IEEE Trans. Instrum. Meas. IM-19:171-175; Aug 70.

Measured Time and Frequency Response of a Miniature Superconducting Coaxial Line;
Nahman, N. S.; Ekstrom, M. P.; McCaa, W. D., Jr.
Applied Superconductivity Conf., Boulder, CO; Jun 70.

Deflection Theory of Traveling Wave Oscilloscopes;
Andrews, J. R.
PhD Dissertation, Univ. of Kansas; Apr 1970. Also NBS Memo for the Record.

Tunnel Diode Pulse Generator and Bias Supply;
Andrews, J. R.
NBS Memo for the Record; Aug 69.

Frequency and Time Domain Analysis of A Superconductive Coaxial Line Using the BCS Theory;
McCaa, W. D.; Nahman, N. S.
J. Appl. Phys. 40:2098-2099; Apr 69.

A Digital Computer Technique for Calculating the Step Response of Lumped or Distributed Networks;
Andrews, J. R.; Nahman, N. S.
NBS JRES, Sec. B, p 163-176; April-June 69.

Investigation and Evaluation of Methods for Pulse Rise-Time Measurement;
Hudson, P.; Andrews, J. R.; Blank, W.; Ondrejka, A.
Tech Report RADC-TR-68-207; Oct 68.

The Measurement of Baseband Pulse Rise-Times of Less than 10^{-9} Seconds;
Nahman, N. S.
Proc. IEEE 55:855-864; Jun 67.

Random Sampling Oscillography;
Frye, G. J., and Nahman, N. S.
IEEE Trans. Instrum. Meas. IM-13:8-13; Mar 64.

CRYOELECTRONIC METROLOGY

Cryogenics;
Zimmerman, J. E.
Chapt. 3 in Biomagnetism: an Interdisciplinary Approach, Samuel J. Williamson, et al., eds., NATO Advanced Study Institute Publication, vol. 66, p 43-67, New York: Plenum Press; 83.

Magnetic Quantities, Units, Materials, and Measurements;
Zimmerman, J. E.
Chapt. 2 in Biomagnetism: an Interdisciplinary Approach, Samuel J. Williamson, et al., eds., NATO Advanced Study Institute Publication, vol. 66, p. 17-42, New York: Plenum Press; 83.

A Cryocooler for Applications Requiring Low Magnetic and Mechanical Interference;
Zimmerman, J. E.; Daney, D. E.; Sullivan, D. B.
NASA Pub. 2287, p 95-106; Dec 83.

An Approach to Optimization of Low-Power Stirling Cryocoolers;
Sullivan, D. B.
Proc. 2nd Biennial Conf. Refrigeration for Cryogenic Sensors; Dec. 7-8, 1982, Greenbelt, MD; NASA Conf. Publ. 2287, p 95-106; Dec 83.

Summary of the Proceedings of the 2nd Biennial Conf. Refrigeration for Cryogenic Sensors;
Zimmerman, J. E.
Cryogenics 23(5):281-282; May 1983.

Chaos in Josephson Circuits;
Kautz, R. L.
Proc. Applied Superconductivity Conf., IEEE Trans. Magn. MAG-19(3):465-473; May 83.

Double Transformer Coupling to a Very Low Noise SQUID;
Cromar, M.; Muhlfelder, B.
Proc. Applied Superconductivity Conf., IEEE Trans. Magn. MAG-19(3):303-307; May 83.

8-Bit Superconducting A/D Converter;
Hamilton, C. A.; Lloyd, F. L.
Proc. Applied Superconductivity Conf., IEEE Trans. Magn. MAG-19(3)1259-1261; May 83.

Microwave Mixing and Direct Detection Using SIS and SIS' Quasiparticle Tunnel Junctions;
Harris, R. E., et al.
Proc. Applied Superconductivity Conf., IEEE Trans. Magn. MAG-19(3):490-493; May 83.

100 GHz Binary Counter Using SQUID Flip Flops;
Hamilton, C. A.
Proc. Applied Superconductivity Conf., IEEE Trans. Magn. MAG-19(3):1291-1291; May 83.

Operation of a Superconducting Analog-to-Digital Converter at Short Conversion Times;
Kautz, R. L.
Proc. Applied Superconductivity Conf., IEEE Trans. Magn. MAG-19(3):1186-1189; May 83.

Superconducting Current Injection Transistor;
VanZeghbroeck, B. J., (Guest Worker)
Appl. Phys. Lett. 42(8):736-738; Apr 83.

Voltage and Current Expressions for a Two-Junction Superconducting Interferometer;
Peterson, R. L.; McDonald, D. G.
J. Appl. Phys. 54(2):992-996; Feb 83.

100 GHz Binary Counter Based on DC SQUIDs;
Hamilton, C. A.
IEEE Electron Device Lett. EDL-3(11):335-338; Nov 82.

Electronically Adjustable Delay for Josephson Technology;
Harris, R. E.; Wolf, P.; Moore, D. F.
IEEE Electron Device Lett. EDL-3(9); Sep 82.

High-Speed, Low-Crosstalk Chip Holder for Josephson Integrated Circuits;
Hamilton, C. A.
IEEE Trans. Instrum. Meas. IM-31(2):29; Jun 82.

Book review: Principles of Superconductive Devices and Circuits, by T. Van Duzer and C. W. Turner;
McDonald, D. G.; Clark, A. F.
Physics Today, p 80; Feb 82.

Analog measurement applications for high speed Josephson switches;
Hamilton, C. A.; Lloyd, Frances L.; Kautz, R. L.
IEEE Trans. Magn. MAG-17(1):577-82; Jan 82.

A Study of Design Principles for Refrigerators for Low-Power Cryoelectronic Devices;
Zimmerman, J. E.; Sullivan, D. B.
NBS TN 1049; Jan 82.

A Josephson Voltage Standard Using a Series Array of 100 Junctions;
Kautz, R. L.; Costabile, G.
IEEE Trans. Magn. MAG-17, 780; 81.

Magnetic Auditory Evoked Fields: Interhemispheric Asymmetry;
Reite, M.; Zimmerman, J. T.; Zimmerman, J. E.
Electroencenphalography and Clinical Neurophysiology 51:388-392; 81.

Superconducting Electronics;
McDonald, D. G.
Phys. Today 34:36-47; 81.

Mathematical Modelling of the Impedance of a Josephson Junction Noise Thermometer;
Peterson, R. L.
J. Appl. Phys., 52(12):7321-7326; Dec 81.

Design Limitations for Superconducting A/D Converters;
Hamilton, C. A.; Lloyd, F. L.
IEEE Trans. Magn. MAG-17(6):3414-3419; Nov 81.

Chaotic States of rf-Biased Josephson Junctions;
Kautz, R. L.,
J. Appl. Phys. 52(10):6241-6246; Oct 81.

Modelling the Impedance of a Josephson Junction Noise Thermometer;
Peterson, R. L.; Van Vechten, D.
Phys. Review B 24(6):3588-3591; Sep 81.

Low Noise Tunnel Junction dc SQUIDs;
Cromar, M. W.; Carelli, P.
Appl. Phys. Lett. 38(9):723-725; May 81.

Measurement of Thermal Properties of Cryocooler Materials;
Zimmerman, J. E.; Sullivan, D. B.; Kautz, R. L.; Hobbs, R. D.
Proc. Conf. on Refrigeration for Cryogenic Sensors and Electronic Systems, NBS SP 607, p 173-177; May 81.

Operation of a practical SQUID Gradiometer in a Low-power Stirling Cryocooler;
Sullivan, D. B.; Zimmerman, J. E.; Ives, J. T.
Conf. on Refrigeration for Cryogenic Sensors and Electronic Systems, NBS SP 607, p 186-194; May 81.

Refrigeration for Cryogenic Sensors and Electronic Systems;
Zimmerman, J. E.; Sullivan, D. B.; McCarthy, S. M., eds.
NBS SP 607; May 81.

The ac Josephson Effect in Hysteric Junctions: Range and Stability of Phase Lock;
Kautz, R. L.
J. Appl. Phys. 52(5):3528-3541; May 81.

Analog Measurement Applications for High Speed Josephson Switches;
Hamilton, C. A.; Lloyd, F. L.; Kautz, R. L.
IEEE Trans. Magn. MAG 17(1):577-582; Jan 81.

Behavior of the dc Impedance of an rf-Biased Resistive SQUID;
Van Vechten, D.; Soulen, R. J., Jr.; Peterson, R. L.
Proc. 2nd Int. Conf. on Superconducting Quantum Interference Devices (SQUIDs), H. D. Wahlbohm; H. Lubbig, eds. New York, Berlin: Walter de Gruyter & Co., p 569-584; 80.

Cryogenics for SQUIDs;
Zimmerman, J. E.
Proc. 2nd Int. Conf. on Superconducting Quantum Interference Devices (SQUIDs), H. D. Wahlbohm; H. Lubbig, eds. New York, Berlin: Walter de Gruyter & Co., p 423-443; 80.

Recent Progress in Cryoelectronics;
Sullivan, D. B.; Hamilton, C. A.; Kautz, R. L.
IEEE Trans. Instrum. Meas. IM-29:319; 80.

Space Applications of Superconductivity: Digital Electronics;
Harris, R. E.
Cryogenics 20:115; 80.

Transient Pool Boiling of Liquid Helium Using a Temperature Controlled Heater Surface;
Giarratano, P. J.; Frederick, N. V.
Advances in Cryogenic Engineering, K. D. Timmerhaus; H. A. Synder, eds., New York: Plenum Press, 25:455-466; 80.

Turn-on Delays in Single Josephson Junction Devices;
Peterson, R. L.
Proc. 2nd Int. Conf. on Superconducting Quantum Interference Devices (SQUIDs), H. D. Wahlbohm; H. Lubbig, eds. New York, Berlin: Walter de Gruyter & Co., p 685-702; 80.

Picosecond Applications of Josephson Junctions;
McDonald, D. G.; Peterson, R. L.; Hamilton, C. A.; Harris, R. E.; Kautz, R. L.
IEEE Trans. Electron Devices ED-27(10):1945-1965; Oct 80.

Induced Electronic Currents in the Alaska Oil Pipeline Measured by Gradient Fluxgate and SQUID Magnetometers;
Campbell, W. H.; Zimmerman, J. E.
IEEE Trans. Geosci. and Remote Sensing GE-18(3):244-250; Jul 80.

Cryocoolers for Geophysical SQUID Magnetometers;
Zimmerman, J. E.
Proc. SQUID Geophysics Workshop, Los Alamos, NM; Jun 80.

Space Applications of Superconductivity: Instrumentation for Gravitational and Related Studies;
Peterson, R. L.
Cryogenics, p 299-306; Jun 80.

A Superconducting 6-bit Analog-to-Digital Converter with Operation to 2 x 10^9 Samples/Second;
Hamilton, C. A.; Lloyd F. L.
IEEE Electron Device Lett. EDL-1(5):92-94; May 80.

Conversion Gain in mm-wave Quasiparticle Heterodyne Mixers;
Shen, T. M.; Richards, P. L.; Harris, R. E.; Lloyd, F. L.
Appl. Phys. Lett. 36:777-779; May 80.

Space Applications of Superconductivity: Microwave and Infrared Detectors;
Hamilton, C. A.,
Cryogenics, p 235-243; May 80.

On a Proposed Josephson-Effect Voltage Standard at Zero Current Bias;
Kautz, R. L.
Applied Phys. Lett. 36(5):386-388; Mar 80.

Simple-Heating-Induced Josephson Effects in Quasiparticle-Injected Superconducting Weak Links;
Kaplan, S. B.
J. Appl. Phys. 51(3):1682-1685; Mar 80.

Superconductor Insulator-Superconductor Quasiparticle Junctions as Microwave Photon Detectors;
Richards, P. L.; Shen, T. M.; Harris, R. E.; Lloyd, F. L.
Appl. Phys. Lett. 36:480-482; Mar 80.

Space Applications of Superconductivity: Low Frequency Superconducting Sensors;
Zimmerman, J. E.
Cryogenics, p 3-10; Jan 80.

Acoustic Matching of Superconducting Films to Substrates;
Kaplan, S. B.
J. Low Temp. Phys. 37:343-365; 79.

A Milliwatt Stirling Cryocooler for Temperatures below 4 K;
Zimmerman, J. E.; Sullivan, D. B.
Cryogenics 19:170; 79.

Minituarization of Normal-State and Superconducting Strip-Lines;
Kautz, R. L.
NBS JRES 84:247; 79.

Quasiparticle Heterodyne Mixing in SIS Tunnel Junctions;
Richards, P. L.; Shen, T. M.; Harris, R. E.; Lloyd, F. L.
Appl. Phys. Lett. 34:345; 79.

Superconducting Devices;
Zimmerman, J. E.; Sullivan, D. B.
Yearbook of Science and Technology, McGraw-Hill; 79.

Analysis of Threshold Curves for Superconducting Interferometers;
Peterson, R. L.; Hamilton, C. A.
J. Appl. Phys. 50(12):8135-8142; Dec 79.

A Superconducting Sampler for Josephson Logic Circuits;
Hamilton, C. A.; Lloyd, F. L.; Peterson, R. L.; Andrews, J. R.
Appl. Phys. Lett. 35:718; Nov 79.

Multiple-Quantum Interference Superconducting Analog-to-digital Converter;
Harris, R. E.; Hamilton, C. A.; Lloyd, F. L.
Appl. Phys. Lett. 35:720; Nov 79.

Space Applications of Superconductivity;
Sullivan, D. B.; Vorreiter, J. W.
Cryogenics 19:627-631; Nov 79.

Very Low-power Stirling Cryocoolers Using Plastic and Composite Materials;
Sulllivan, D. B.; Zimmerman, J. E.
Int. J. Refrig. 2:211-213; Nov 79.

Differential Capacitance Sensor as Position Detectors for Magnetic Suspension Densimeter;
Frederick, N. V.
Rev. Sci. Instrum. 50(9):1154; Sep 79.

Analog to Digital Conversion with a SQUID: Conditions for a Countable Pulse Train;
Peterson, R. L.
J. Appl. Phys. 50:4231; Jun 79.

Cryogenic Refrigeration System;
Zimmerman, James E.
PATENT-4 143 520; patented 13 Mar 79.

Quasiparticle Heterodyne Mixing in SIS Tunnel Junctions;
Harris, R. L.; Lloyd, F. L.; Richards, P. L.; Shen, T. M.
Appl. Phys. Lett. 34(5):345-347; Mar 79.

Sampling Circuit and Method Therefor;
Hamilton, Clark A.
PAT-APPL-6-020 359; Filed 14 Mar 79.

Attenuation in Superconducting Striplines;
Kautz, R. L.
IEEE Trans. Magn. MAG-15:566-569; Jan 79.

High-Speed Superconducting Electronics;
Hamilton, C. A.; Harris, R. E.; Sullivan, D. B.
GOMAC Digest, vol. 7; 78.

Human Magnetic Auditory Evoked Responses;
Reite, M.; Edrich, J.; Zimmerman, J. T.; Zimmerman, J. E.
Electroencephalography and Clinical Neurophysiology 45:114-117; 78.

Magnetic Phenomena of the Central Nervous System;
Reite, Martin; Zimmerman, James
Ann. Rev. Biophys. Bioeng. 7:167-188; 78.

Multiple Magnetic Flux Entry into SQUIDS: A General Way of Examining the Cos(phi) Conductance;
Peterson, R. L.; Gayley, R. I.
Phys. Rev. B 18:1198-1206; Aug 78.

Automatic 300-4 K Temperature Cycling Apparatus;
Hamilton, Clark A.
Rev. Sci. Instrum. Notes 49:674-677; May 78.

The Role of Superconductivity in the Space Program: An Assessment of Present Capabilities and Future Potential;
Sullivan, D. B.
NASA-CR-158701; NBSIR 78-885; May 78.

The Role of Superconductivity in the Space Program: An Assessment of Present Capabilities and Future Potential;
Sullivan, D. B.
NBSIR 78-885; May 78.

Applications of Closed-Cycle Cryocoolers to Small Superconducting Devices;
Zimmerman, James E.; Flynn, Thomas M.
Proc. Conf. Held at the National Bureau of Standards, Oct 3-4, 1977; Boulder, CO, NBS SP 508; Apr 78.

RF Instrumentation Based on Superconducting Quantum Interference;
Sullivan, D. B.; Adair, R. T.; Frederick, N. V.
Proc. IEEE 66:454-463; Apr 78.

Photolithographic Fabrication of Lead Alloy Josephson Junctions;
Havemann, R. H.; Hamilton, C. A.; Harris, Richard E.
J. Vac. Sci. Technol. 15:392-395; Mar/Apr 78.

Picosecond Pulses on Superconducting Striplines;
Kautz, Richard L.
J. Appl. Phys. 49:308-314; Jan 78.

Possible Cryocoolers for SQUID Magnetometers;
Zimmerman, J. E.; Radebaugh, R.; Siegwarth, J. D.
Proc. IC SQUID (1st), Oct 5-8, 1976; Berlin, Germany, Paper R-1044 in Superconducting Quantum Interference Devices and Their Applications, p 287-296; 77.

Results, Potentials and Limitations of Josephson Mixer-Receivers at Millimeter and Long Submillimeter Wavelengths;
Edrich, J.; Sullivan, D. B.; McDonald, D. G.
IEEE Trans. Microwave Theory Tech. MTT-25:476; 77.

RF Power Measurements Using Quantum Interference in Superconductors;
Sullivan, D. B.; Frederick, N. V.; Adair, R. T.
Proc. IC SQUID (1st), Oct 5-8, 1976; Berlin, Germany, Paper R-1045 in Superconducting Quantum Interference Devices and Their Applications, p 355-363; 77.

Superconducting Devices for Metrology and Standards;
Kamper, Robert A.
Chap. 5 in Superconductor Applications: Squids and Machines, New York: Plenum Press, p 189-247; 77.

Design of a Josephson-Junction Picosecond Pulser;
McDonald, D. G.; Peterson, R. L.; Bender, B. K.
J. Appl. Phys. 48:5366-5369; Dec 77.

Numerical Evaluation of the Response of a Josephson Tunnel Junction in an Arbitrary Circuit;
Harris, Richard E.
J. Appl. Phys. 48:5188-5190; Dec 77.

Picosecond Pulse Generator Utilizing a Josephson Junction;
McDonald, Donald G.; Peterson, Robert L.
PAT-APPL-862 311; Filed 20 Dec 77.

A Sampling Circuit and Method Therefor;
Hamilton, Clark A.
PAT-APPL-853 354; Filed 21 Nov 77.

High-Frequency Limitations of the Double-Junction SQUID Amplifier;
Zimmerman, J. E.; Sullivan, D. B.
Appl. Phys. Lett. 31:360-362; Sep 77.

RF Attenuation Measurement System Using a SQUID;
Adair, Robert T.; Frederick, Nolan V.; Sullivan, Donald B.
NBSIR 77-863; Sep 77.

A Low-Noise Josephson Mixer for the 1 mm Wavelength Range;
Edrich, J.; Sullivan, D. B.; McDonald, D. G.
IEEE Trans. Microwave Theory Tech. MTT-25:476-479; Jun 77.

Squid Instruments and Shielding for Low-Level Magnetic Measurements;
Zimmerman, James E.
J. Appl. Phys. 48:702-710; Feb 77.

Advances in the Use of SQUIDS for RF Attenuation Measurement;
Frederick, N. V.; Sullivan, D. B.; Adair, R. T.
IEEE Trans. Magn. MAG-13:361-364; Jan 77.

Analog Computer Studies of Frequency Multiplication and Mixing with the Josephson Junction;
Risley, A. S.; Johnson, E. G., Jr; Hamilton, C. A.
Proc. 1976 Applied Superconductivity Conf., Stanford, CA,
IEEE Trans. Magn. MAG-13:381-384; Jan 77.

Can Superconductivity Contribute to the Determination of the Absolute Ampere?;
Sullivan, D. B.; Frederick, N. V.
IEEE Trans. Magn. MAG-13:396-399; Jan 77.

Picosecond Pulses from Josephson Junctions: Phenomenological and Microscopic Analyses;
Peterson, Robert L.; McDonald, Donald G.
IEEE Trans. Magn. MAG-13:887-890; Jan 77.

Refrigeration for Small Superconducting Devices;
Zimmerman, J. E.; Radebaugh, R.; Siegwarth, J. D.
DKV-annual meeting and joint meeting with the International Institute of Refrigeration, Munich, Germany, F.R.G, 13 Oct 1976.
Rept No. CONF-7610104-1; 76.

The Human Magnetoencephalogram: Some EEG and Related Correlations;
Reite, Martin; Zimmerman, James E.; Edrich, Jochen; Zimmerman, John
Electroencephalography and Clinical Neurophysiology 40:59-66; 76.

Strong-Coupling Correction to the Jump in the Quasiparticle Current of a Superconducting Tunnel Junction;
Harris, Richard E.; Dynes, R. C.; Ginsberg, D. M.
Phys. Rev. B 14:993-995; Aug 76.

Strong-Coupling Correction to the Low-Frequency Electrical Conductivity of Superconductors and Josephson Junctions;
Harris, Richard E.; Ginsberg, D. M.; Dynes, R. C.
Phys. Rev. B 14:990-992; Aug 76.

Intrinsic Response Time of a Josephson Tunnel Junction;
Harris, Richard E.
Phys. Rev. B 13:3818-3821; May 76.

RF Applications of the Josephson Effect;
Kamper, Robert A.
Microwave J. 19:39-41; Apr 76.

Modeling Josephson Junctions;
McDonald, D. G.; Johnson, E. G.; Harris, R. E.
Phys. Rev. B 13:1028-1031; Feb 76.

Accurate Rotational Constants, Frequencies, and Wavelengths from $^{12}C^{16}O_2$ Lasers Stabilized by Saturated Absorption;
Petersen, F. R., McDonald, D. G.; Cupp, J. D.; Danielson, B. L.
Proc. Laser Spectroscopy Conf., Jun 25-29, 1973; Vail, CO, p 555-569; 75.

Josephson Weak-Link Devices;
Silver, A. H.; Zimmerman, J. E.
Applied Superconductivity, V. L. Newhouse, ed., Academic Press, p 1-80; 75.

Tests of Cryogenic SQUID for Geomagnetic Field Measurements;
Zimmerman, J. E.; Campbell, W. H.
Geophysics 40:269; 75.

Cryogenic Direct Current Comparators and their Applications;
Dziuba, R. F.; Sullivan, D. B.
IEEE Trans. Magn. MAG-11:716-719; Mar 75.

Phase Slip, Dissipation, Bernoulli Effect, Parametric Capacitance, and Other Curious Features of the Josephson Effect;
Zimmerman, J. E.
IEEE Trans. Magn. MAG-11:852-855; Mar 75.

Review of Superconducting Electronics;
Kamper, Robert A.
IEEE Trans. Magn. MAG-11:141-146; Mar 75.

Magnetic Properties of Internally Oxidized Copper;
Fickett, F. R.; Sullivan, D. B.
19th Annual Conf. on Magnetism and Magnetic Materials, 1973; Boston, MA, AIP Conf. Proc. 18; 74.

Review of Electromagnetic Measurements Using the Josephson Effect;
Kamper, Robert A.
Proc. ISA Int. Instrumentation-Automation Conf., Oct 28-31, 1974; New York, NY, p 1-8; 74.

RF Attenuation Measurements Using Quantum Interference in Superconductors;
Adair, R. T.; Hoer, C. A.; Kamper, R. A.; Simmonds, M. B.
CPEM Digest, IEE, London, England, p 4-5; 74.

The Relationship of Josephson Junctions to a Unified Standard of Length and Time;
McDonald, D. G.; Risley, A. S.; Cupp, J. D.
Proc. 13th Int. Conf. on Low Temperature Physics, Aug 21-25, 1972; Boulder, CO, Paper in Low Temperature Physics LT 13, p 542-549; 74.

A Low-Temperature Direct-Current Comparator Bridge;
Sullivan, D. B.; Dziuba, R. F.
IEEE Trans. Instrum. Meas. IM-23:256-260; Dec 74.

RF Attenuation Measurements Using Quantum Interference in Superconductors;
Adair, R. T.; Simmonds, M. B.; Kamper, R. A.; Hoer, C. A.
IEEE Trans. Instrum. Meas. IM-23:375-381; Dec 74.

Advances in the Measurement of rf Power and Attenuation Using SQUIDS;
Kamper, R. A.; Simmonds, M. B.; Adair, R. T.; Hoer, C. A.
NBS TN 661; Sep 74.

Josephson Junctions as Radiation Detectors from Millihertz to Terahertz;
McDonald, D. G.
IEEE J. Quantum Electron. QE-10:776-777; Sep 74.

An Application of Superconducting Quantum Interference Magnetometers to Geophysical Prospecting;
Frederick, N. V.; Stanley, W. D.; Zimmerman, J. E.; Dinger, R. J.
IEEE Trans. Geosci. Electron. GE-12:102-103; Jul 74.

Magnetic Studies of Oxidized Impurities in Pure Copper Using a SQUID System;
Fickett, F. R.; Sullivan, D. B.
J. Phys. F 4:900-904; Jun 74.

Josephson Junctions at 45 Times the Energy-Gap Frequency;
McDonald, D. G.; Petersen, F. R.; Cupp, J. D.; Danielson, B. L.; Johnson, E. G., Jr.
Appl. Phys. Lett. 24:335-337; Apr 74.

Low Temperature Direct Current Comparators;
Sullivan, D. B.; Dziuba, R. F.
Rev. Sci. Instrum. 45:517-519; Apr 74.

Superconducting Devices and Materials. Quarterly Literature Survey;
Olien, Neil A.; Goree, William S.; Kamper, Robert A.; Nisenoff, Martin; Wolf, Stuart A.
NBS Cryogenic Data Center, Boulder, CO, no. 74-1; Jan-Mar 74.

Field-Usable Sharpless Wafers for Josephson Effect Devices at Millimeter Waves;
Edrich, J.; Cupp, J. D.; McDonald, D. G.
Revue de Physique Appliquee 9:195-197; Jan 74.

Spectral Analysis of a Phase Locked Laser at 891 GHz. An Application of Josephson Junctions in the Far Infrared;
Wells, J. S.; McDonald, D. G.; Risley, A. S.; Jarvis, S.; Cupp, J. D.
Revue de Physique Appliques (Supplement to J. de Physique), France, 9:285-292; Jan 74.

Measurement of rf Power and Attenuation Using Superconducting Quantum Interference Devices;
Kamper, R. A.; Simmonds, M. B.; Hoer, C. A.; Adair, R. T.
NBS TN 643; Aug 73.

Rotational Constants for $^{12}C^{16}O_2$ From Beats Between Lamb-Dip-Stabilized Lasers;
Petersen, F. R.; McDonald, D. G.; Cupp, J. D.; Danielson, B. L.
Phys. Rev. Lett. 31:573-576; Aug 73.

Analog-Computer Studies of Mixing and Parametric Effects in Josephson Junctions;
Hamilton, Clark A.
J. Appl. Phys. 44:2371-2377; May 73.

Portable Helium Dewars for Use with Superconducting Magnetometers;
Zimmerman, J. E.; Siegwarth, J. D.
Cryogenics 13:158-159; Mar 73.

Superconducting Devices and Materials;
Goree, William S.; Nisenoff, Martin; Wolf, Stuart A.; Kamper, Robert A.; Olien, Neil A.
NBS Cryogenic Data Center; Boulder, CO, Quarterly literature survey, no. 73-1; Jan-Mar 73.

A New Technique for RF Measurements Using Superconductors;
Kamper, R. A.; Simmonds, M. B.; Adair, R. T.; Hoer, C. A.
Proc. IEEE 61:121-122; Jan 73.

Flexible Laminates for Thermally Grounded Terminal Strips and Shielded Electrical Leads at Low Temperatures;
Radebaugh, Ray; Frederick, N. V.; Siegwarth, J. D.
Cryogenics 13:41-43; Jan 73.

Possible Parametric Capacitance in Josephson Junctions;
Zimmerman, J. E.
Phys. Lett. 42A:375-376; Jan 73.

A Review of the Properties and Applications of Superconducting Point Contacts;
Zimmerman, J. E.
Proc. Conf. on Applied Superconductivity, May 1-3, 1972; Annapolis, MD, p 544-561; 72.

Precise Electrical Measurements at Low Temperature;
Sullivan, D. B.
Proc. Applied Superconductivity Conf., May 1-3, 1972; Annapolis, MD; p 631-639; 72.

Quantum Mechanical Measurement of rf Attenuation;
Kamper, R. A.; Simmonds, M. B.; Adair, R. T.; Hoer, C. A.
Proc. 1972 Applied Superconductivity Conf., May 1-3, 1972; Annapolis, MD, p 696-700; 72.

Computation of Spectral Data for a Josephson Junction Circuit;
Johnson, E. G., Jr; McDonald, D. G.
NBS TN 627; Nov 72.

Developments in Cryoelectronics;
Kamper, Robert A.; Sullivan, Donald B.
NBS TN 630; Nov 72.

Superconducting Quantum Interference Devices: an Operational Guide for rf-Biased Systems;
Sullivan, D. B.
NBS TN 629; Nov 72.

Analog Computer Studies of Subharmonic Steps in Superconducting Weak Links;
Hamilton, C. A.; Johnson, E. G., Jr.
Phys. Lett. A 41:393-394; Oct 72.

Broadband Superconducting Quantum Magnetometer;
Kamper, R. A.; Simmonds, M. B.
Appl. Phys. Lett. 20:270-272; Apr 72.

Four-Hundredth-Order Harmonic Mixing of Microwave and Infrared Laser Radiation Using a Josephson Junction and a Maser;
McDonald, D. G.; Risley, A. S.; Cupp, J. D.; Evenson, K. M.; Ashley, J. R.
Appl. Phys. Lett. 20:296-299; Apr 72.

Low Temperature Voltage Divider and Null Detector;
Sullivan, D. B.
Rev. Sci. Instrum. 43:499-505; Mar 72.

Superconducting Devices and Materials. A Literature Survey;
Goree, W. S.; Kamper, R. A.; Olien, Neil A.
NBS Cryogenic Data Center; Boulder, CO, Quarterly reports; 4 issues; Mar 72.

Josephson Effect Devices and Low-Frequency Field Sensing;
Zimmerman, J. E.
Cryogenics 12:19-31; Feb 72.

A Mechanical Superconducting Switch for Low Temperature Instrumentation;
Siegwarth, J. D.; Sullivan, D. B.
Rev. Sci. Instrum. 43:153-154; Jan 72.

Superconducting Materials;
Kamper, R. A.
Electronics Design Materials, p 71-79; 71.

Survey of Noise Thermometry;
Kamper, Robert A.
Proc. 5th Symposium on Temperature, Its Measurement and Control in Science and Industry, Jun 21-24, 1971; Washington, DC; 71.

Mechanical Analogs of Time Dependent Josephson Phenomena;
Sullivan, D. B.; Zimmerman, J. E.
American J. Phys. 39:1504-1517; Dec 71.

Sensitivity Enhancement of Superconducting Quantum Interference Devices through the Use of Fractional-Turn Loops;
Zimmerman, J. E.
J. Appl. Phys. 24:4483-4487; Oct 71.

Observation of Noise Temperature in the Millikelvin Range;
Kamper, R. A.; Siegwarth, J. D.; Radebaugh, R.; Zimmerman, J. E.
Proc. IEEE 59:1368-1369; Sep 71.

Miniature Ultrasensitive Superconducting Magnetic Gradiometer and Its Use in Cardiography and Other Applications;
Zimmerman, J. E.; Frederick, N. V.
Appl. Phys. Lett. 19:16-19; Jul 71.

Resistance of a Silicon Bronze at Low Temperatures;
Sullivan, D. B.
Rev. Sci. Instrum. 42:612-613; May 71.

Harmonic Mixing of Microwave and Far-Infrared Laser Radiation using a Josephson Junction;
McDonald, D. G.; Risley, A. S.; Cupp, J. D.; Evenson, K. M.
Appl. Phys. Lett. 18:162-164; Feb 71.

High-Frequency Limit of the Josephson Effect;
McDonald, D. G.; Evenson, K. M.; Wells, J. S.; Cupp, J. D.
J. Appl. Phys. 42:179-181; Jan 71.

Noise Thermometry with the Josephson Effect;
Kamper, R. A.; Zimmerman, J. E.
J. Appl. Phys. 42:132-136; Jan 71.

Recent Developments in Superconducting Devices;
Zimmerman, J. E.
J. Appl. Phys. 42:30-37; Jan 71.

Cryoelectronics;
Kamper, R. A.
Proc. Helium Society Symposium, Mar 23-24, 1970; Washington, DC, p 68-82; 70.

Generation of Harmonics and Subharmonics of the Josephson Oscillation;
Sullivan, D. B.; Peterson, Robert L.; Kose, V. E.; Zimmerman, J. E.
J. Appl. Phys. 41:4865-4873; Nov 70.

Magnetocardiograms Taken Inside A Shielded Room With A Superconducting Point-Contact Magnetometer;
Cohen, David; Edelsack, Edgar A.; Zimmerman, James E.
Appl. Phys. Lett. 16:278-280; Apr 70.

Some Applications Of The Josephson Effect;
Kamper, R. A.; Mullen, L. O.; Sullivan, D. B.
NASA-CR-1565; NBS TN 381; Mar 70.

Influence of External Noise On Microwave-Induced Josephson Steps;
Kose, V. E.; Sullivan, D. B.
J. Appl. Phys. 41:169-174; Jan 70.

The Josephson Effect;
Kamper, Robert A.
IEEE Trans. Electron Devices ED-16:840-844; Oct 69.

Harmonic Generation and Submillimeter Wave Mixing With The Josephson Effect;
McDonald, D. G.; Kose, V. E.; Evenson, K. M.; Wells, J. S.; Cupp, J. D.
Appl. Phys. Lett. 15:121-122; 15 Aug 69.

Fabrication Of Tunnel Junctions On Niobium Films;
Mullen, L. O.; Sullivan, D. B.
J. Appl. Phys. 40:2115-2117; Apr 69.

Cryoelectronics;
Kamper, R. A.
Cryogenics, 9:20-25; Feb 69.

Contribution of Thermal Noise to the Line-Width of Josephson Radiation from Superconducting Point Contacts;
Silver, A. H.; Zimmerman, J. E.; Kamper, R. A.
Appl. Phys. Lett. 11:209-211; 15 Sep 67.

Millidegree Noise Thermometry;
Kamper, R. A.
Proc. Symposium on the Physics of Superconducting Devices (ONR report), Charlottesville, VA; Apr 67.

SUPERCONDUCTORS AND MAGNETIC MATERIALS

Magnetic Field Effects on Tensile Behavior of Alloys 304 and 310 at 4 K;
Reed, R. P.; Arvidson, J. M.; Ekin, J. W.; Schoon, R. H.
Proc. Int. Cryogenic Materials Conf.; May 11-14, 1982; Kobe Japan; p 33-36; 83.

Conductors for Advanced Energy Systems Annual Report 1982;
Ficket, F. R.
INCRA Research Report, Paper#321A; Int. Copper Research Assoc., 708 3rd Ave., NY 10017; p 1-97; Aug 83.

Electrical Properties;
Fickett, F. R.
Chapt. 5 in Materials at Low Temperatures, R. Reed; A. F. Clark, eds., American Society for Metals, Metals Park, OH 44073; p 163-201; Jun 83.

Magnetic Properties;
Fickett, F. R.; Goldfarb, R. B.
Chap. 6 in Materials at Low Temperatures, R. Reed; A. F. Clark, eds., American Society of Metals, Metals Park, OH 44073; p 203-235; Jun 83.

Superconductors;
Ekin, J. W.
Chapt. 13 in Materials at Low Temperatures, R. Reed; A. F. Clark, eds., American Society of Metals, Metals Park, OH 44073, p 465-513; Jun 83.

Thermal Expansion;
Clark, A. F.
Chapt. 3 in Materials at Low Temperatures, R. Reed; A. F. Clark, eds., American Society for Metals, Metals Park, OH 44073, p 75-132; Jun 83.

Effect of Stainless Steel Reinforcement on the Critical Current Versus Strain Characteristic of Multifilamentary Nb_3Sn Superconductors;
Ekin, J. W.
J. Appl. Phys. 54(5):2869-2871; May 83.

J-B-T-ε Interaction in A15, B1, and C15 Crystal Structure Superconductors;
Ekin, J. W.
Proc. Applied Superconductivity Conf., IEEE Trans. Magn. MAG-19:900-902; May 83.

Multifilamentary Nb-Nb_3 Composite by Liquid Infiltration Method: Superconducting, Metallurgical, and Mechanical Properties;
Hong, M.; Hull, G. W., Jr.; Holthuis, J. T.; Hazzenzahl, W. V.; Ekin, J. W.
Proc. Applied Superconductivity Conf., IEEE Trans. Magn. MAG-19(3):912-916; May 83.

Oxygen-Free Copper at 4K;
Fickett, F. R.
Proc. Applied Superconductivity Conf., IEEE Trans. Magn. MAG-19:228-231; May 83.

Properties of NbN Films Crystallized from the Amorphous State;
Gavaler, J. R.; Greggi, J.; Wilmer, R.; Ekin, J. W.
Proc. Applied Superconductivity Conf., IEEE Trans. Magn. MAG-19(3):418-421; May 83.

The Effect of Field Orientation on Current Transfer in Multifilamentary Superconductors;
Goodrich, L. F.
Proc. Applied Superconductivity Conf., IEEE Trans. Magn. MAG-19(3):244-247; May 83.

Four-Dimensional J-B-T-ε Critical Surface for Superconductivity;
Ekin, J. W.
J. Appl. Phys. 54(1):303-306; Jan 83.

Proc. International Cryogenic Materials Conference; May 11-14, 1982; Kobe, Japan;
Clark, A. F.; Tachikawa, K., eds.
Butterworths; Jan 83.

Effect of Strain on the Critical Current and Critical Field of B1 Structure NbN Superconductors;
Ekin, J. W.
Appl. Phys. Lett. 41(10):996; Nov 82.

Effect of Strain on the Critical Current of Sputtered NbN Films;
Ekin, J. W.; Gavaler, J. R.; Greggi, J.
Bull. Am. Phys. Soc. p 8-12; Mar 1982 and Appl. Phys. Lett. 41(10):996-998; Nov 82.

Spin-Freezing below the Ferromagnetic Transition Determined by the Imaginary Component of ac Magnetic Susceptibility
Goldfarb, R. B.; Fickett, F. R.; Rao, K.V.; Chen, H. S.
J. Appl. Phys. 53(11):7687; Nov 82.

Development of Standards for Superconductors;
Clark, A. F.
NBSIR 82-1678; Jul 82.

Effect of Twist Pitch on Short-Sample V-I Characteristics of Multifilamentary Superconductors;
Goodrich, L. F.; Ekin, J. W.; Fickett, F. R.
Adv. Cryo. Eng. 28:571-58; New York: Plenum Press; Jul 82.

Low Temperature Material Perspective;
Fickett, F. R.
Adv. Cryo. Eng. 28:1-16; Jul 82.

Training Studies of Epoxy-Impregnated Superconductor Windings;
Ekin, J. W; Pittman, E. S.; Supercynski, M. J.; Waltman, D. J.
Adv. Cryo. Eng., 28:719-728, New York: Plenum Press; Jul 82.

Critical Current Measurement: A Compendium of Experimental Effects;
Goodrich, L. F.; Fickett, F. F.
Cryogenics, p 225-242; May 82.

Effect of Strain on the Critical Parameters of $V_2(Hf,Zr)$ Laves Phase Composite Superconductors;
Ekin, J. W.
Appl. Phys. Lett. 40(9):844-846; May 82.

Electrical Properties of Materials and Their Measurement at Low Temperatures;
Fickett, F. R.
NBS TN 1053; Mar 82.

Electric and Magnetic Properties of CuSn and CuNi Alloys at 4 K;
Fickett, F. R.
Cryogenics 22:135; Mar 82.

Further Evidence for a Spin-Glass Phase Transition in Amorphous Fe-Mn-P-B-Al Alloys;
Goldfarb, R. B.; Rao, K. V.; Chen, H. S.; Patton, C. E.
J. Appl. Phys. 53:2217; Mar 82.

Electrical and Magnetic Properties of Internally Oxidized Copper and Dilute Copper-Iron Alloys;
Fickett, F. R.
J. Phys. F: Met. Phys. 12:1953-1969; Jan 82.

Effect of Strain on the Critical Current of Nb-Hf/Cu-Sn-Ga Multifilamentary Superconductors;
Ekin, J. W.; Sekine, H.; Tachikawa, K.
J. Appl. Phys. 52:6252; 81.

Lap Joint Resistance and Intrinsic Critical Current Measurements on a NbTi Superconducting Wire;
Goodrich, L. F.; Ekin, J. W.
IEEE Trans. Magn. MAG-17:69; 81.

Magnetic Susceptibility Studies of Amorphous Ni-Mn-P-B-Al Alloys;
Goldfarb, R. B.; Rao, K. V.; Fickett, F. R.; Chen, H. S.
J. Appl. Phys. 52:1744; 81.

Mechanical Properties and Strain Effects in Superconductors;
Ekin, J. W.
Chap. 7 in Superconducting Materials Science, S. Foner and B. Schwartz, eds., New York: Plenum Press, p 455-509; 81.

Miniature Multipin Electrical Feedthrough for Vacuum Use;
Goldfarb, R. B.
Cryogenics 21:746; 81.

Strain Scaling Law for Flux Pining in NbTi, Nb_3Sn, Nb-Hf/Cu-Sn-Ga, V_3Ga, and Nb_3Ge;
Ekin, J. W.
IEEE Trans. Magn. MAG-17:658; 81.

Structural Materials for Large Superconducting Magnets;
Fickett, F. R.; McHenry, H. I.
IEEE Trans. Magn. MAG-17:2297; 81.

Superparamagnetism and Spin-Glass Freezing in Nickel-Manganese Alloys;
Goldfarb, R. B.; Patton, C. E.
Phys. Rev. B 24:1360; 81.

NBS Superconductor Standardization Program;
Fickett, F. R.; Goodrich, L. F.
Proc. 1980 Superconducting MHD Magnet Design Conf. (Francis Bitter National Magnet Laboratory, MIT); Oct 81.

Thermal Expansion of Multifilamentary Nb_3Sn and V_3Ga Superconductive Cables and Fiberglass-Epoxy and Cotton-Phenolic Composite Materials;
Fujii, G.; Ranney, M. A.; Clark, A. F.
Jap. J. Appl. Phys. 20, L267-L270; Apr 81.

Thermal Expansion of Several Materials for Superconducting Magnets;
Clark, A. F.; Fujii, G.; Ranney, M. A.
Proc. 7th Magnet Technology Conf., Karlsruhe, Germany, IEEE Trans. Magn. MAG-17:2316; Apr 81.

Advances in Cryogenic Engineering - Materials, Vol. 26;
Clark, A. F.; Reed, R. P., eds.
Proc. 3rd Int. Cryogenic Mater. Conf., Aug 1979; Madison, WI, New York: Plenum Press; 80.

Definitions of Terms for Practical Superconductors,
4. Josephson Phenomena;
Fickett, F. R.; Kaplan, S. B.; Powell, R. L.; Radebaugh, R.; Clark, A. F.
Cryogenics 20:319-325; 80.

Development of Standards for Superconductors;
Fickett, F. R.; Clark, A. F.
Proc. 8th Int. Cryogenic Eng. Conf., Jun 1980; Genova; IPC Science and Technology Press, Guildford, England, p 494-8; 80.

Filamentary A15 Superconductors;
Suenaga, M.; Clark, A. F., eds.
New York: Plenum Press; 80.

Processing Limits for Ultrafine Multifilament Nb_3Sn;
Ho, J. C.; Oberly, C. E.; Garrett, H. J.; Walker, M. S.; Zeitlin, B. A.; Ekin, J. W.
Proc. Int. Cryo. Mater. Cong., 1979; Madison, WI, Adv. Cryogenic. Eng. 26:358; 80.

Strain Scaling Law and the Prediction of Unixial and Bending Strain Effects;
Ekin, J. W.
Filamentary A15 Superconductors, M. Suenaga and A. F. Clark, eds., New York: Plenum Press; p 455-509; 80.

Strain Scaling Law for Flux Pinning in Practical Superconductors. Part I: Basic Relationship and Application to Nb_3Sn Conductors;
Ekin, J. W.
Cryogenics 20:611; 80.

Tensile, Fracture Toughness and Magnetization Testing in Cast 316-L Stainless Steel and Its Weldment;
Genens, L.; Kim, S. H.; Wang, S. T.; Reed, R. P., Fickett, F. R.
Proc. 8th Int. Cryo. Eng. Conf. (IPC Science and Technology Press, paper 3E) 20 p; 80.

Thermal Expansion of Cryogenic-Grade Glass-Epoxy Laminates; Materials Studies of Magnetic Fusion Energy Applications at Low Temperatures - III;
Ranney, M. A.; Clark, A. F.
NBSIR 80-1627:405; 80.

Training of Epoxy-Impregnated Superconductor Windings;
Ekin, J. W.; Schramm, R. E.; Superczynski, M. J.
Proc. 3rd Int. Cryogenic Mater. Conf., Aug 1979; Madison, WI; Adv. Cryo. Eng. 26:677; 80.

Development of Standards for Superconductors;
Fickett, F. R.; Goodrich, L. F.; Clark, A. F.
NBSIR 80-1642; Dec 80.

Effect of Thermal Contraction of Sample Holder Material on Critical Current Measurement;
Fujii, G.; Ekin, J. W.; Radebaugh, R.; Clark, A. F.
Advances in Cryogenic Engineering - Materials, Vol. 26, New York: Plenum Press; p 589-98; 80. Also published as Technical Report A-1074, Institute of Solid State Physics, Univ. of Tokyo; Aug 80.

Development of Standards for Practical Superconductors;
Clark, A. F.
Proc. Superconductivity Technical Exchange, PIC-E:E-SC 209/1, Naval Research Laboratory, Washington, DC; p 103-14; Apr 80.

A Convenient Standard for Low-Field Susceptibility Calibration;
Rosenblum, J.; Larson, E.; Hoblitt, R.; Fickett, F. R.
Rev. Sci. Instrum 50:1027; 79.

Effect of Strain on Critical Current of Nb_3Ge;
Ekin, J. W.; Braginski, A. I.
IEEE Trans. Magn. MAG-15:509; 79.

Effect of Strain on Epoxy-Impregnated Superconducting Composites;
Ekin, J. W.; Schramm, R. E.; Clark, A. F.
Nonmetallic Materials and Composites at Low Temperatures; A. F. Clark; R. P. Reed; G. Hartwig, eds., New York: Plenum Press, p 301-8; 79.

Materials for Superconducting Magnet Systems;
Fickett, F. R.; Reed, R. P., eds.
Traverse City, MI: Belfour-Stulen, Inc.; 79.

Nonmetallic Materials and Composites at Low Temperatures;
Clark, A. F.; Reed, R. P.; Hartwig, G., eds.
Proc. ICMC Symposium, Jul 1978; Munich, Germany, New York: Plenum Press; 79.

Space Applications of Superconductivity: High Field Magnets;
Fickett, F. R.
Cryogenics 19:691-701; 79.

Standards for Superconductors;
Fickett, F. R.; Clark, A. F.,
DoE Conf. 79-0854, Proc. Mechanical and Magnetic Energy Storage, U.S. Dept. of Energy, Washington, DC, p 3-8; 79.

Strain Dependence of the Critical Current and Critical Field in Multifilamentary Nb_3Sn Composites;
Ekin, J. W.
IEEE Trans. Magn. MAG-15:197; 79.

Structures, Insulators, and Conductors for Large Superconducting Magnets;
Fickett, F. R.; Reed, R. P.; Dalder, E. N. C.
J. Nucl. Mat. 85 and 86:353-60; 79.

The Development of Standards for Practical Superconductors
Clark, A. F.; Ekin, J. W.; Radebaugh, R.; Read, D. T.
IEEE Trans. Magn. MAG-15:224-7; 79.

Development of Standards for Superconductors;
Fickett, F. R.; Clark, A. F.
NBSIR 80-1629; Dec 79.

Material Studies for Superconducting Machinery Coil Composites;
Ekin, J. W.; Kasen, M. B.; Read, D. T; Schramm, R. E.; Tobler, R. L.; Clark, A. F.
NBSIR 80-1633; Nov 79.

A Standards Program for AC Losses in Superconductors;
Radebaugh, R.; Fujii, G.; Read, D. T.; Clark, A. F.
Int. Congress of Refrigeration, IIR A1/2-10:1-4; Sep 79.

Definitions of Terms for Practical Superconductors.
3. Fabrication, Stabilization, and Transient Losses;
Read, D. T.; Ekin, J. W.; Powell, R. L.; Clark, A. F.
Crogenics 19(6):327-32; Jun 79.

Magnetic Properties of the 'Nonmagnetic' Stainless Steels;
Fickett, F. R.
NBSIR 79-1609; Jun 79.

Materials for Superconducting Magnets for MHD Power Systems, a Usage Survey and a Proposed Research Program;
Reed, R. P.; McHenry, H. I.; Kasen, M. B.; Fickett, F. R.; Dalder, E. N. C.
MIT Program Report on MHD; Jun 79.

Materials Studies for Magnetic Fusion Energy Applications at Low Temperatures - II;
Fickett, F. R., ed.
NBSIR 79-1609; Jun 79.

Review of the 1978 NBS/DoE Workshop on Materials at Low Temperatures;
Fickett, F. R.; Reed, R. P.
Proc. 1st Topical Meeting on Fusion Reactor Materials, Miami Beach, FL, p 352; Jan 79.

Advances in Cryogenic Engineering, Vol. 24;
Timmerhaus, K. D.; Reed, R. P.; Clark, A. F., eds.
Proc. 2nd Int. Cryogenic Mater. Conf., Aug 1977; Boulder, CO; New York: Plenum Press; 78.

Current Transfer in Multifilamentary Superconductors. I. Theory;
Ekin, J. W.
J. Appl. Phys. 49(6):3406-1; 78.

Effects of Stress on Practical Superconductors;
Clark, A. F.
MT-6, Proc. Int. Conf. on Magn. Tech., Alpha, Bratislava, Czechoslovakia, p 612-18; 78.

Fatigue and Stress Effects in NbTi and Nb_3Sn Multifilamentary Superconductors;
Ekin, J. W.
Proc. Int. Cryogenic Mater. Conf., 1977; Boulder, CO; Adv. in Cry. Eng. 24:306; 78.

Low Temperature Specific Heat of Two Stainless Steels;
Ho, J. C.; King, G. B.; Fickett, F. R.
Cryogenics 18:296; 78.

Properties of a Superconducting Coil Composite and Its Components;
Clark, A. F.; Arp, V. D.; Ekin, J. W.
MT-6, Proc. Int. Conf. on Magn. Tech., Alpha, Bratislava, Czechoslovakia, p 673-79; 78.

Special Purpose Materials: An Assessment of Needs and the Role of these Materials in the National Program;
Gold, R. E.; Fickett, F. R.; et al.
Proc. 3rd Topical Meeting on the Technology of Controlled Nuclear Fusion, DoE Conf-780508; 78.

Magnet Materials for Fusion Energy Section of: "The Fusion Reactor Materials Program Plan, Section IV, Special Purpose Materials";
Fickett, F. R.
U.S. DoE Report DoE/ET-0032/4; Jul 78.

Current Transfer in Multifilamentary Superconductors.
II. Experimental Results;
Ekin, J. W.; Clark, A. F.; Ho, J. C.
J. Appl. Phys. 49(6):3410-1; Jun 78.

High Field Magnets;
Fickett, F. R.
Chap. 2 in The Role of Superconductivity in the Space Program: An Assessment of Present Capabilities and Future Potential, NBSIR 78-885; May 78.

Materials Studies for Magnetic Fusion Energy Applications at Low Temperatures - I;
Fickett, F. R.; Reed, R. P.
NBSIR 78-884; Apr 78.

Definitions of Terms for Practical Superconductors. 2. Critical Parameters;
Powell, R. L.; Clark, A. F.
Cryogenics 18(3):137-41; Mar 78.

Investigation of a Practical Superconductor with a Copper Matrix;
Fickett, F. R.
INCRA Annual Report, Project No. 255; Jan 78.

A Low Temperature Materials Research Program for Magnetic Fusion Energy;
Fickett, F. R.; Kasen, M. B.; McHenry, H. I.; Reed, R. P.
Adv. Cryogenic Eng. 24:52; 77.

A Review of the NBS-ERDA Workshop on Materials at Low Temperatures;
Fickett, F. R.; Reed, R. P.
Proc. 7th Symposium on Engineering Problems of Fusion Research, IEEE Pub. No. 77CH1267-4-NPS:1506-1509; 77.

A Simple Method for Producing High Conductivity Copper for Low Temperature Applications;
Rosenblum, S.; Steyert, W. A.; Fickett, F. R.
Cryogenics 17:645; 77.

Mechanisms for Critical-Current Degradation in NbTi and Nb_3Sn and NbTi Multifilamentary Wires;
Ekin, J. W.
Proc. 1976 Applied Superconductivity Conf., IEEE Trans. Magn. MAG-13:127; 77.

Studies of Superconducting Wires from Niobium Precipitated in Copper-Tin-Niobium Alloys;
Fickett, F. R.; Sparks, L. L.; Kasen, M. G.
Manufacture of Superconducting Materials, R. W. Meyerhoff, ed., American Society for Metals, Metals Park, OH, p 164; 77.

The Low Temperature Tensile Behavior of Copper-Stabilized Niobium-Titanium Superconducting Wire;
Reed, R. P.; Mikesell, R. P.; Clark, A. F.
Advances in Cryogenic Engineering, vol. 22, New York: Plenum Press, p 463-471; 77.

Definition of Terms for Practical Superconductors. 1. Fundamental States and Flux Phenomena;
Powell, R. L.; Clark, A. F.
Cryogenics 17(12):697-701; Dec 77.

Magnetic Fusion Energy Low Temperature Materials Program - A Survey;
Reed, R. P.; Fickett, F. R.; Kasen, M. B.; McHenry, H. I.
Report to ERDA Division of Magnetic Fusion Energy; Mar 77.

Defining Critical Current;
Clark, A. F.; Ekin, J. W.
IEEE Trans. Magn. MAG-13(1):38-40; Jan 77.

Advances in Cryogenic Engineering - Vol. 22;
Timmerhaus, K. D.; Reed, R. P.; Clark, A. F., eds.
Proc. 1st Int. Cryogenic Mater. Conf., Aug. 1975; Kingston, Ontario,
New York: Plenum Press; 76.

A Research Program on the Properties of Structural Materials at 4 K;
Reed, R. P.; Clark, A. F.; van Reuth, E. C.
Adv. Cryo. Eng., New York: Plenum Press, 22:1-8; 76.

Effect of Strain on the Critical Current of Nb_3Sn and NbTi Multifilamentary Composite Wires;
Ekin, J. W.; Clark, A. F.
AIP Conf. Proc. no. 34, New York: Amer. Inst. Phys., p 81-83; 76.

Effect of Stress on the Critical Current of Nb_3Sn Multifilamentary Composite Wire;
Ekin, J. W.
Appl. Phys. Lett. 29:216; 76.

Effect of Stress on the Critical Current of NbTi Multifilamnetary Composite Wire;
Ekin, J. W.; Fickett, F. R.; Clark, A. F.
Adv. Cryo. Eng., New York: Plenum Press, 22:449-452; 76.

Effect of Stress on the Critical Current of NbTi Multifilamentary Composite Wire;
Ekin, J. W.; Fickett, F. R.; Clark, A. F.
Proc. Int. Cryogenic Mater. Conf., 1975; Kingston, Ontario; Adv. in Cryogenic Eng., New York: Plenum Press 22:449; 76.

Magnetic and Electrical Properties of Internally Oxidized FeCu Alloys;
Fickett, F. R.
Amer. Inst. Phys. Conf. Proc. 34:25; 76.

On Lysozyme as a Possible High-Temperature Superconductor;
Sorenson, C. M.; Fickett, F. R.; Mockler, R. C.; O'Sullivan, W. J.; Scott, J. F.
J. Phys. C: Solid State Phys. 9:L251; 76.

Properties of Nonsuperconducting Technical Solids at Low Temperatures - An Update;
Fickett, F. R.
Proc. 5th Int. Conf. on Magn. Tech. (MT-5), Rome, Laboratori Nazionali del CNEN, Frascati, Italy, p 659; 76.

Structural Materials for Cryogenic Appications;
Fickett, F. R.
Proc. 6th Int. Cryogenic Eng. Conf., May 11-14, 1976; Grenoble, France; IPC Science and Technology Press, p 20; 76.

Stress Effects in Superconductors;
Clark, A. F.
Cryogenics 16(10):632-3; Oct 76.

Controlled Thermonuclear Reactors: A Prospective Large-Scale Use of Pure Copper;
Fickett, F. R.
INCRA Research Report; Aug 76.

Characterization of a Superconducting Coil Composite and Its Components;
Clark, A. F.; Weston, W. F.; Arp, V. D.; Hust, J. G.; Trapani, R. J.
NBSIR 76-837; Jul 76.

Low Temperature Thermal Expansion of Barium Ferrite;
Clark, A. F.; Haynes, W. M.; Deason, V. A.; Trapani, R. J.
Cryogenics 16(3):267-270; May 76.

A Preliminary Investigation of the Behavior of High Purity Copper in High Magnetic Fields and a Final Summary of Project 186;
Fickett, F. R.
INCRA Annual Report, Project No. 186C; Mar 76.

A Technique for Preparing Homogeneous Bulk Samples of Concentrated Alloys;
Ekin, J. W.; Deason, V. A.
Rev. Sci. Instr. 46:327; 75.

Critical Currents in Granular Superconductors;
Ekin, J. W.
Phys. Rev. B 12:2676; 75.

The Magnetic Coupling Force of the Superconducting dc Transformer;
Ekin, J. W.; Clem, J. R.
Phys. Rev. B 12:1753; 75.

Materials Research for Superconducting Machinery - IV; Semi-Annual Tech. Rept., Mar-Sep. 1975;
Reed, R. P.; Clark, A. F.; vanReuth, E. C., eds.
Advanced Research Projects Agency, Arlington, VA ADA019230; Oct 75.

Materials Research for Superconducting Machinery - III; Semi-Annual Tech. Rept., Sep. 74-Mar. 75;
Reed, R. P.; Clark, A. F.; van Reuth, E. C., eds.
Advanced Research Projects Agency, Arlington, VA, ADA012365; Apr 75.

Magnetic Properties of Internally Oxidized Copper;
Fickett, F. R., Sullivan, D. B.
AIP Conf. Proc. 18:740; 74.

Magnetic Studies of Oxidized Impurities in Pure Copper Using a SQUID System;
Fickett, F. R.; Sullivan, D. B.
J. Phys. F 4:900; 74.

Magnetothermal Conductivity;
Fickett, F. R.; Sparks, L. L.
NBSIR 74-393; 74.

Magnetothermal Conductivity;
Sparks, L. L; Fickett, F.R.
NBSIR 74-359; 74.

Oxygen Annealing of Copper: A Review;
Fickett, F. R.
Mat. Sci. and Eng. 14:199; 74.

U. S. Programs on Large Scale Applications of Superconductivity;
Powell, R. L.; Fickett, F. R.; Birmingham, B. W.
Chap. 17 in Superconducting Machines and Devices -- Large Systems Applications; Proc. NATO Advanced Study Institute, Sep 5-14, 1973; Entreves, Italy; S. Foner and B. B. Schwartz, eds., New York: Plenum Press, p 651-675; 74.

Materials Research for Superconducting Machinery - II, Semi-Annual Tech. Rept., Mar.-Sep. 74;
Clark, A. F.; Reed, R. P.; van Reuth, E. C., eds.
Advanced Research Projects Agency, Arlington, VA, ADA004586; Oct 74.

A Preliminary Investigation of the Behavior of High Purity Copper in High Magnetic Fields;
Fickett, F. R.
INCRA Annual Report, Project No. 186B; Aug 74.

Materials Research for Superconducting Machinery, Semi-Annual Tech. Rept., Sep 1973-Mar 1974;
Clark, A. F.; Reed, R. P.; van Reuth, E. C., eds.
Advanced Research Projects Agency, Arlington, VA, AD780596; Mar 74.

Characterization of a Superconducting Coil Composite;
Fowlkes, C. W.; Angerhofer, P. E.; Newton, R. N.; Clark, A. F.
NBSIR 73-349; Dec 73.

Superconducting Levitation of High Speed Vehicles;
Arp, V. D.; Clark, A. F.; Flynn, T. M.
Transport. Eng. J., ASCE 99:873-85; Nov 73.

A Compilation and Evaluation of Mechanical, Thermal and Electrical Properties of Selected Polymers;
Schramm, R. E.; Clark, A. F.; Reed, R. P.
NBS MN 132, Washington, DC: U.S. GPO; Sep 73.

A Preliminary Investigation of the Behavior of High Purity Copper in High Mangetic Fields;
Fickett, F. R.
INCRA Annual Report, Project No. 186A; Aug 73.

Mechanical, Thermal, and Electrical Properties of Selected Polymers;
Reed, R. P.; Schramm, R. Clark, A. F.
Cryogenics 13:67-82; Feb 73.

Some Applications of Cryogenics to High Speed Ground Transportation;
Arp, V. D.; Clark, A. F.; Flynn, T. M.
NBS TN 635; Feb 73.

Characterization of High Purity Metals by the Eddy Current Decay Method;
Clark, A. F.; Deason, V. A.; Powell, R. L.
Cryogenics 12:35; 72.

Magnetoresistivity of Copper and Aluminum at Cryogenic Temperatures;
Fickett, F. R.
Proc. 4th Int. Conf. on Magnet Technology, Sep 72, AEC CONF-720908:498; 72.

Material Variability as Measured by Low Temperature Electrical Resistivity;
Clark, A. F.; Tryon, P. V.
Cryogenics 12:451-61; Dec 72.

Properties of Nonsuperconducting Technical Solids at Low Temperatures;
Fickett, F. R.
Proc. 4th Int. Conf. on Magnet Technology, AEC CONF-720903:539; Sep 72.

Combination of a Power Transmission Line and an Active Track for a Magnetically Suspended, High Speed Train;
Clark, A. F.
J. Appl. Phys. 43(8):3598; Aug 72.

A Preliminary Investigation of the Behavior of High Purity Copper in High Magnetic Fields;
Fickett, F. R.
INCRA Annual Report, INCRA Project No. 186; Jun 72.

Standard Reference Materials: The Eddy Current Decay Method for Resistivity Characterization of High Purity Metals;
Clark, A. F.; Deason, V. A.; Hust, J. G.; Powell, R. L.
NBS SP 260-39; May 72.

Defect Annealing (4 to 295 K) After Martensitic Phase Transformation in an Fe-29 Ni Alloy;
Reed, R. P.; Clark, A. F.; Schramm, R. E.
Scripta Met. 5:485; 71.

Longitudinal Magnetoresistance Anomalies;
Fickett, F. R.; Clark, A. F.
J. Appl. Pys. 42:217; 71.

Magnetoresistance of Very Pure Polycrystalline Aluminum;
Fickett, F. R.
Phys. Rev. B 3:1941; 71.

Martensitic Transformation Detection in Cryogenic Steels (Magnetometer Development);
Fickett, F. R.
NBS TN 613; 71.

Characterization of High Purity Metals by the Eddy Current Decay Method;
Clark, A. F.; Deason, V. A.; Powell, R. L.
Mater. Res. Stand. 11(8):25-28; Aug 71.

Lorenz Ratio as a Tool for Predicting Thermal Conductivity of Metals and Alloys;
Hust, J. G.; Clark, A. F.
Mater. Res. Stand. 11(8):22-24; Aug 71.

Low Temperature Electrical Resistivity of Some Engineering Alloys;
Clark, A. F.; Childs, G. E.; Wallace, G. H.
Adv. Cryo. Eng., New York: Plenum Press, 15:85-90; 70.

Low Temperature Specific Heat and Thermal Expansion of Alloys;
Clark, A. F.; Kropschot, R. H.
Int. Inst. of Refrigeration, Commission I, Sep 70, Tokyo, Bulletin de l'Institut Internationale du Froid, Annexe 1970-2, p 249; 70.

Resistivity of Polycrystalline Aluminum and Copper in High Magnetic Fields: The Effect of Temperature and Purity;
Fickett, F. R.
Appl. Phys. Lett. 17(12):525-527; 70.

Low Temperature Electrical Resistivity of Some Engineering Alloys;
Clark, A. F.; Childs, G. E.; Wallace, G. H.
Cryogenics 10:295-305; Aug 70.

APPENDIX III

A BIBLIOGRAPHY OF THE NBS ELECTROMAGNETIC FIELDS DIVISION PUBLICATIONS

Edited by
Kathryn A. Gibson and Charles K. S. Miller

This bibliography lists the publications of the personnel of the NBS Electromagnetic Fields Division in the period from January 1982 through December 1983.

Key words: antennas; electromagnetic interference; electromagnetic metrology; microwaves; noise; non-ionizing radiation; radiation hazards; waveform metrology.

INTRODUCTION

This bibliography updates and supplements NBSIR 80-1635 which lists the publications of the Electromagnetic Fields Division from January 1970 through December 1979, and NBSIR 82-1673 which lists publications from January 1980 through December 1981. The publications listed in this supplement were published in 1982 and 1983.

The Electromagnetic Fields Division was formed during the reorganization of NBS in April 1978. The Division develops measurement methods and standards, and provides metrological support for: antenna systems, noise measurement equipment, electromagnetic interference, electromagnetic environmental characterization equipment especially for near fields to sources or a near-field like condition, electromagnetic emission and immunity (or susceptibility) testing equipment, and waveform metrology. The editors have attempted to include all work published by the staff members of the Division, in the period from January 1982 through December 1983. There are a few exceptions. Relevant work performed by authors prior to joining this Division or work by authors who have left this Division has been included because of its special significance. A miscellaneous category includes general publications. A few references are listed in more than one category where appropriate.

There are several other information sources that may be useful to the reader who is interested in activities at NBS connected with electromagnetic metrology. Companion bibliographies list publications of the Electromagnetic Technology Division. Its topics include metrology for: microwave and millimeter wave circuits, laser systems, optical communication equipment, systems using transient or pulsed electromagnetic phenomena, cryoelectronics, superconductors and other unusual electrical engineering materials. Three bibliographies of the publications of the former Electromagnetics Division have been published: NBSIR 73-320 (July 1972-June 1973); NBSIR 74-395 (July 1973-June 1974); NBSIR 75-818 (July 1974-June 1975). These were preceded by a series of unpublished reports (edited by H. M. Altschuler) that cover the period back to 1956. An excellent summary of the whole field of electromagnetic metrology as it stood in 1967 was published as a special issue of the IEEE Proceedings (volume 55, June 1967). Advances in the following decade were described in another special issue of the same journal (volume 66, April 1978).

A NOTE ON ABBREVIATIONS

Most readers will be familiar with the commonly used abbreviations for the names of the various professional journals that appear in this bibliography. There are also several publication series that are peculiar to NBS and call for explanation. They are:

NBSIR - NBS Interagency/Internal Report
NBS-TN - NBS Technical Note
NBS-SP - NBS Special Publication
NBS-MN - NBS Monograph

Purchase Procedures and Document Availability

NBS Technical Notes and Special Publications may be purchased from the Superintendent of Documents, U.S. Government Printing Office, Washington, DC 20402. Orders must be accompanied by postal money order, express money order, or check made out to the Superintendent of Documents.

NBS Interagency/Internal Reports (NBSIR's) may be purchased from the National Technical Information Service, Springfield, VA 22161. Order must be accompanied by postal money order, express money order, or check made out to the NTIS.

Reprints of papers published in non-NBS media may be available in limited quantities from the authors.

The Orbiting Standards Package: A Recalibratable Satellite Instrument Assembly for Measuring Large Earth Station Antennas
Baird, R. C. and Estin, A. J.
Proc., Antenna Measurement Techniques Assoc., New Mexico State University, Las Cruces, NM, Oct. 5-7, 1982, pp. 5-1 - 5-9
October 1982

Handbook for Broadband Isotropic Antenna System, Volume 1 - Operations Manual
Bensema, W. D.
NBSIR 83-1693
July 1983

Optimized Wavelength-Sized Scalar Horns as Antenna Radiation Standards
Estin, A. J.; Stubenrauch, C. F.; Repjar, A. G.; and Newell, A. C.
IEEE Trans. on Instrumentation and Measurement
Vol. IM-31, No. 1, pp. 53-56
March 1982

A Partial Loop Source of E & H Fields for Antenna Factor Calibration (A Loop Cell)
FitzGerrell, R. G.
Proc., Antenna Measurement Techniques Assoc., New Mexico State University, Las Cruces, NM, Oct. 5-7, 1982, pp. 15-1 - 15-22
October 1982

Computations of Antenna Side-Lobe Coupling in the Near Field Using Approximate Far-Field Data
Francis, M. H. and Yaghjian, A. D.
NBSIR 82-1674
August 1982

The Characteristics of Iris-Fed Millimeter Wave Rectangular Microstrip Patch Antennas
Greenlee, D. H.; Kanda, M.; and Chang, D. C.
NBS Tech Note 1063
October 1983

The Characteristics of Iris-Fed Millimeter Wave Rectangular Microstrip Patch Antennas
Kanda, M.; Chang, D. C.; and Greenlee, D. H.
Proc., 1982 IEEE AP/S Symp., University of New Mexico, Albuquerque, NM, May 24-28, 1982, pp. 292-295
May 1982

The Effects of Resistive Loading on TEM Horns
Kanda, M.
IEEE Trans. on EMC
Vol. EMC-24, No. 2, pp. 245-255
May 1982

Antenna Gain Measurements by an Extended Version of the NBS Extrapolation Method
Repjar, A. G.; Newell, A. C.; and Baird, R. C.
IEEE Trans. on Instrumentation and Measurement
Vol. IM-32, No. 1, pp. 88-91
March 1983

Antenna Gain Measurements by an Extended Version of the NBS Extrapolation Method
Repjar, A. G.; Newell, A. C.; and Baird, R. C.
Digest, Conference on Precision Electromagnetic Measurements,
Boulder, CO, June 28-July 1, 1982, pp. F-7 - F-9
June 1982

Accurate Evaluation of a Millimeter Wave Compact Range Using Planar Near-Field Scanning
Repjar, A. G. and Kremer, D. P.
IEEE Trans. on Antennas and Propagation
Vol. AP-30, No. 3, pp. 419-425
May 1982

International Intercomparison of Electric Field Strength at 100 MHz
Stubenrauch, C. F.; Spiess, W.; Galliano, P. G.; and Babij, T.
IEEE Trans. on Instrumentation and Measurement
Vol. IM-32, No. 1, pp. 235-237
March 1983

International Intercomparison of Electric Field Strength at 100 MHz
Stubenrauch, C. F.; Spiess, W.; Galliano, P. G.; and Babij, T.
Digest, Conference on Precision Electromagnetic Measurements,
Boulder, CO, June 28-July 1, 1982, pp. P-3 - P-4
June 1982

Precision Measurement of Antenna System Noise Using Radio Stars
Wait, D. F.
IEEE Trans. on Instrumentation and Measurement
Vol. IM-32, No. 1, pp. 110-116
March 1983

Precision Measurement of Antenna System Noise Using Radio Stars
Wait, D. F.
Digest, Conference on Precision Electromagnetic Measurements,
Boulder, CO, June 28-July 1, 1982, p. F-17
June 1982

Input Impedance of a Probe Antenna Exciting a TEM Cell
Wilson, P. F.; Chang, D. C.; and Ma, M. T.
NBS Tech Note 1054
April 1982

Optical Modulator and Link for Broadband Antennas
Wyss, J. C.; Kanda, M.; Melquist, D. G.; and Ondrejka, A. R.
Digest, Conference on Precision Electromagnetic Measurements, Boulder, CO, June 28-July 1, 1982, pp. P-16 - P-17
June 1982

Approximate Formulas for the Far Field and Gain of Open-Ended Rectangular Waveguide
Yaghjian, A. D.
NBSIR 83-1689
May 1983

A Delta-Distribution Derivation of the Electric Field in the Source Region
Yaghjian, A. D.
Journal of the Electromagnetics Society
Vol. 2, No. 2, pp. 161-167
April-June 1982

Efficient Computation of Antenna Coupling and Fields Within the Near-Field Region
Yaghjian, A. D.
IEEE Trans. on Antennas and Propagation
Vol. AP-30, No, 1, pp. 113-128
January 1982

Measurement of Electromagnetic Radiation from Electric Rail Cars
Adams, J. W.
NBSIR 82-1669
August 1982

Digest, 1982 Conference on Precision Electromagnetic Measurements, Boulder, CO, June 28-July 1, 1982
Alspach, W. J. (Editor)
June 1982

Planning Guidance for Future EMI Measurement Instrumentation
Arthur, M. G.; Orr, R. D.; and Reeve, G. R.
NBSIR 82-1662
April 1982

Handbook for Broadband Isotropic Antenna System Volume 1 - Operations Manual
Bensema, W. D.
NBSIR 83-1693
July 1983

Comparison of Open-Field, Anechoic Chamber and TEM Cell Facilities/Techniques for Performing Electromagnetic Radiated Emissions Measurements
Crawford, M. L.
Record, IEEE 1983 International Symposium on Electromagnetic Compatibility, Arlington, VA, August 23-25, 1983, pp. 413-418
August 1983

Evaluation of Shielded Enclosure for EMI/EMC Measurements Without and With RF Anechoic Material
Crawford, M. L.
Proceedings, 1983 EMC Symposium and Exhibition, Zurich, Switzerland, March 8-10, 1983, pp. 397-402
March 1983

Improving the Repeatability of EM Susceptibility Measurements of Electronic Components When Using TEM Cells
Crawford, M. L.
SAE Technical Paper Series, 830607, International Congress and Exposition, Detroit, MI, February 28-March 4, 1983, pp. 1-8
March 1983

Development of the NBS Isotropic Magnetic-Field Meter (MFM-10), 300 kHz to 100 MHz
Driver, L. D. and Cruz, J. E.
Proceedings, 1982 International Symposium on EMC, Santa Clara, CA, September 8-10, 1982, pp. 460-467
September 1982

E-Fields Over Ground
FitzGerrell, R. G.
Record, IEEE 1983 International Symposium on Electromagnetic Compatibility, Arlington, VA, August 23-25, 1983, pp. 6-9
August 1983

A Partial Loop Source of E & H Fields for Antenna Factor Calibration (A Loop Cell)
FitzGerrell, R. G.
Proceedings, Antenna Measurement Techniques Association, New Mexico State University, Las Cruces, NM, October 5-7, 1982, pp. 15-1 - 15-22
October 1982

Free Space Transmission Loss for Anechoic Chamber Performance Evaluation
FitzGerrell, R. G.
IEEE Transactions on Electromagnetic Compatibility, Vol. EMC-24, No. 3, pp. 356-358
August 1982

Time Domain Sensors for Radiated Impulsive Measurements
Kanda, M. and Ries, F. X.
IEEE Transactions on Antennas and Propagation, Vol. AP-31, No. 3, pp. 438-444
May 1983

An Electric and Magnetic Field Sensor for Simultaneous Electromagnetic Near-Field Measurements - Theory
Kanda, M.
NBS Tech Note 1062
April 1983

An Electric and Magnetic Field Sensor Concept for Simultaneous Near-Field Electromagnetic Components When Using TEM Cells
Kanda, M.; Ries, F. X.; Driver, L. D.; and Orr, R. D.
Proceedings 1983 Electromagnetic Compatibility Symposium and Exhibition, Zurich, Switzerland, March 8-10, 1983, pp. 263-266
March 1983

Time Domain Sensors for Radiated Impulsive Measurements
Kanda, M. and Ries, F. X.
Proceedings, IEEE 1982 International Symposium on Electromagnetic Compatibility, Santa Clara, CA, September 8-10, 1982, pp. 296-301
September 1982

Design Considerations for Broadband Magnetic-Field Sensors
Kanda, M.; Ries, F. X.; Driver, L. D.; and Orr, R. D.
Digest, Conference on Precision Electromagnetic Measurements, Boulder, CO, June 28-July 1, 1982, pp. P-11 - P-13
June 1982

The Effects of Resistive Loading on TEM Horns
Kanda, M.
IEEE Transactions on EMC
Vol. EMC-24, No. 2, pp. 245-255
May 1982

A New Method for Determining the Emission Characteristics of an Unknown Interference Source
Koepke, G. H. and Ma, M. T.
Proceedings, 1983 Electromagnetic Compatibility Symposium and Exhibition, Zurich, Switzerland, March 8-10, 1983, pp. 263-266
March 1983

A New Method for Determining the Emission Characteristics of an Unknown Interference Source
Koepke, G. H. and Ma, M. T.
Proceedings, IEEE 1982 International Symposium on Electromagnetic Compatibility, Santa Clara, CA, September 8-10, 1982, pp. 151-156
September 1982

Design Consideration of Reverberating Chambers for Electromagnetic Interference Measurements
Liu, B.-H.; Chang, D. C.; and Ma, M. T.
Record, IEEE 1983 International Symposium on Electromagnetic Compatibility, Arlington, VA, August 23-25, 1983, pp. 508-512
August 1983

Eigenmodes and the Composite Quality Factor of a Reverberating Chamber
Liu, B.-H.; Chang, D. C.; and Ma, M. T.
NBS Tech Note 1066
August 1983

Uncertainties in Extracting Radiation Parameters for an Unknown Interference Source Based on Power and Phase Measurements
Ma, M. T. and Koepke, G. H.
NBS Tech Note 1064
June 1983

A Method to Quantify Radiation Characteristics of an Unknown Interference Source
Ma, M. T. and Koepke, G. H.
NBS Tech Note 1059
October 1982

A Study of Distribution of Electromagnetic Fields Inside Buildings with Apertures Excited by an External Source
Ma, M. T. and Arthur, M. G.
NBSIR 82-1659
February 1982

The EMI Measurement Challenge
Miller, C. K. S.
Proceedings, Measurement Science Conference, Palo Alto, CA, January 20-21, 1983, pp. 189-197
May 1983

International Intercomparison of Electric Field Strength at 100 MHz
Stubenrauch, C. F.; Spiess, W.; Galliano, P. G.; and Babij, T.
IEEE Trans. on Instrumentation and Measurement
Vol. IM-32, No. 1, pp. 235-237
March 1983

Radiated EMI Instrumentation Errors
Taggart, H. E.
EMC Technology Magazine
Volume 1, No. 4, pp. 26-35
October 1982

Theoretical and Experimental Analysis of Coupling Characteristics of Dual TEM Cells
Wilson, P. F.; Chang, D. C.; Ma, M. T.; and Crawford, M. L.
Record, IEEE 1983 International Symposium on Electromagnetic Compatibility, Arlington, VA, August 23-25, 1983, pp. 513-517
August 1983

Input Impedance of a Probe Antenna Exciting a TEM Cell
Wilson, P. F.; Chang, D. C.; and Ma, M. T.
NBS Tech Note 1054
April 1982

Optical Modulator and Link for Broadband Antennas
Wyss, J. C.; Kanda, M.; Melquist, D. G.; and Ondrejka, A. R.
Digest, Conference on Precision Electromagnetic Measurements, Boulder, CO, June 28-July 1, 1982, pp. P-16 - P-17
June 1982

Design and Error Analysis for the WR10 Thermal Noise Standard
Daywitt, W. C.
NBS Tech Note 1071
December 1983

Preliminary Examination of 20 GHz G/T Measurements of Earth Terminals
Wait, D. F. and Daywitt, W. C.
NBSIR 83-1686
March 1983

Precision Measurement of Antenna System Noise Using Radio Stars
Wait, D. F.
IEEE Transactions on Instrumentation and Measurement
Vol. IM-32, No. 1, pp. 110-116
March 1983

Earth Terminal Measurement System Operations Manual (Revised)
Wait, D. F.
NBSIR 83-1679
January 1983

Precision Measurement of Antenna System Noise Using Radio Stars
Wait, D. F.
Digest, Conference on Precision Electromagnetic Measurements,
Boulder, CO, June 28-July 1, 1982, pp. F-17
June 1982

Reference Flat Pulse Generator
Andrews, J. R.; Bell, B. A.; and Baldwin, E. E.
NBS Tech Note 1067
October 1983

Reference Waveform Flat Pulse Generator
Andrews, J. R.; Bell, B. A.; Nahman, N. S.; and Baldwin, E. E.
IEEE Transactions on Instrumentation and Measurement
Vol. IM-32, No. 1, pp. 27-32
March 1983

Status of Reference Waveform Standards Development at NBS
Andrews, J. R.; Nahman, N. S.; and Bell, B. A.
NBS Special Publication 634, Proceedings of the Seminar on Waveform Recorder Measurement Needs and Techniques for Evaluation/Calibration, Boulder, CO, October 15, 1981, pp. 69-88
June 1982

The Measurement and Deconvolution of Time Jitter in Equivalent-Time Waveform Samplers
Gans, W. L.
IEEE Transactions on Instrumentation and Measurement
Vol. IM-32, No. 1, pp. 126-133
March 1983

Photoconductive Switches Used for Waveform Generation at the National Bureau of Standards
Lawton, R. A.
Proceedings, Picosecond Optoelectronics Conference, SPIE - The International Society for Optical Engineering, San Diego, CA, August 24-26, 1983
Vol. 439, pp. 88-94
August 1983

Performance Standards for Waveform Recorders
Lawton, R. A.
IEEE Transactions on Nuclear Science
Vol. NS-30, No. 1, pp. 263-266
February 1983

Precision Picosecond-Microsecond Electromagnetic Waveform Measurement at NBS
Lawton, R. A.
NBS Special Publication 628
pp. 392-407
June 1982

Proceedings of the Seminar on Waveform Recorder Measurement Needs and Techniques for Evaluation/Calibration
Lawton, R. A. (Editor)
NBS Special Publication 634, Proceedings of the Seminar on Waveform Recorder Measurement Needs and Techniques for Evaluation/Calibration, Boulder, CO, October 15, 1981, June 1982

Picosecond Domain Waveform Measurements; Status and Future Directions
Nahman, N. S.
IEEE Transactions on Instrumentation and Measurement
Vol. IM-32, No. 1, pp. 117-124
March 1983

Some Generic Waveform Recorder Problems
Nahman, N. S.
NBS Special Publication 634, Proceedings of the Seminar on Waveform Recorder Measurement Needs and Techniques for Evaluation/Calibration, Boulder, CO, October 15, 1981, pp. 1-5
June 1982

Electromagnetic Modeling of Oil Shale Retorts for Remote Sensing Purposes
Chew, H.
IEEE Transactions on Geoscience and Remote Sensing
Vol. GE-20, No. 4, pp. 510-517
October 1982

Bibliography of the Electromagnetic Fields Division Publications
Gibson, K. A. and Miller, C. K. S.
NBSIR 82-1673
August 1982

Book Review - Leaky Feeders and Subsurface Radio Communications
Hill, D. A.
IEEE Antennas and Propagation Society Newsletter
Vol. 25, No. 3, pp. 23-24
June 1983

Dielectric Measurements of Oil Shale as Functions of Temperature and Frequency
Jesch, R. L.
NBSIR 83-1683
January 1983

Improved Coal Interface Detector
Roe, K. C. and Wittmann, R. C.
NBSIR 82-1663
May 1982

Acoustical Interferometer Wader AIW Final Report of Advanced Development Test and Evaluation
Stoltenberg, R. E. and Wittmann, R. C.
NBSIR 82-1671 (restricted)
June 1982

A BIBLIOGRAPHY OF THE NBS ELECTROMAGNETIC FIELDS DIVISION PUBLICATIONS

Edited by
Kathryn A. Gibson and Charles K. S. Miller

This bibliography lists the publications of the personnel of the NBS Electromagnetic Fields Division in the period from January 1980 through December 1981.

Key words: antennas; electromagnetic interference; em material properties; electromagnetic metrology; microwaves; noise; non-ionizing radiation; radiation hazards.

INTRODUCTION

This bibliography updates and supplements NBSIR 80-1635 which lists the publications of the Electromagnetic Fields Division from January 1970 to December 1979. The publications listed in this supplement were published in 1980 and 1981.

The Electromagnetic Fields Division was formed during the reorganization of NBS in April 1978. The Division develops measurement methods and standards, and provides metrological support for: antenna systems, noise measurement equipment, electromagnetic interference, electromagnetic environmental characterization equipment especially for near fields to sources or a near-field like condition, electromagnetic emission and immunity (or susceptibility) testing equipment, and for measuring equipment used for dielectric or loss characterization of materials. The editors have attempted to include all work published by the staff members of the Division, in the period from January 1980 through December 1981. There are a few exceptions. Relevant work performed by authors prior to joining this Division or work by authors who have left this Division has been included because of its special significance. A miscellaneous category includes general publications. A few references are listed in more than one category where appropriate.

There are several other information sources that may be useful to the reader who is interested in activities at NBS connected with electromagnetic metrology. Companion bibliographies list publications of the Electromagnetic Technology Division. Its topics include metrology for: microwave circuits, laser systems, optical communication equipment, systems using transient or pulsed electromagnetic phenomena, cryoelectronics, superconductors and other unusual electrical engineering materials. Three bibliographies of the publications of the former Electromagnetics Division have been published: NBSIR 73-320 (July 1972-June 1973); NBSIR 74-395 (July 1973-June 1974); NBSIR 75-818 (July 1974-June 1975). These were preceded by a series of unpublished reports (edited by H. M. Altschuler) that cover the period back to 1956. An excellent summary of the whole field of electromagnetic metrology as it stood in 1967 was published as a special issue of the IEEE Proceedings (volume 55, June 1967). Advances in the following decade were described in another special issue of the same journal (volume 66, April 1978).

A NOTE ON ABBREVIATIONS

Most readers will be familiar with the commonly used abbreviations for the names of the various professional journals that appear in this bibliography. There are also several publication series that are peculiar to NBS and call for explanation. They are:

NBSIR - NBS Interagency/Internal Report
NBS-TN - NBS Technical Note
NBS-SP - NBS Special Publication
NBS-MN - NBS Monograph

Purchase Procedures and Document Availability

NBS Technical Notes and Special Publications may be purchased from the Superintendent of Documents, U.S. Government Printing Office, Washington, D.C. 20402. Orders must be accompanied by postal money order, express money order, or check made out to the Superintendent of Documents.

NBS Interagency/Internal Reports (NBSIR's) may be purchased from the National Technical Information Service, Springfield VA 22161. Order must be accompanied by postal money order, express money order, or check made out to the NTIS.

Reprints of papers published in non-NBS media may be available in limited quantities from the authors.

Microwave Antenna Measurement Services at the National Bureau of Standards
Baird, R. C.
Digest, Antenna Meas. Tech. Assn. Mtg.
Oct. 1981

Broadband Orthogonal Array Antenna System: Microprocessor Control and Computation
Bensema, W. D.
Record, EMC '81
Aug. 1981

Optimized Wavelength-Sized Scalar Horns as Antenna Radiation Standards
Estin, A. J.; Stubenrauch, C. F.; Repjar, A. G.; and Newell, A. C.
1981 EEMTIC Digest
June 1981

The Characteristics of a Linear Antenna with Tapered Resistive and Capacitive Loading
Kanda, M.
Proc., IEEE AP Symp., Quebec, Canada
June 2-6, 1980, Vol. 2, AP.18-2, pp 696-699

The Time Domain Characteristics of a Traveling Wave Linear Antenna with Linear and Non-Linear Loads
Kanda, M.
IEEE Trans. Ant. & Prop.
March 1980, Vol. AP-28, No. 2

Analytical and Numerical Techniques for Analyzing an Electrically Short Dipole with a Nonlinear Load
Kanda, M.
IEEE Trans. Ant. & Prop.
Jan. 1980, Vol. AP-28, No. 1, pp 71-78

Transients in Resistively Loaded Antennas and Their Comparison with Conical Antennas and a TEM Horn
Kanda, M.
IEEE Trans. Ant. & Prop.
Jan. 1980, Vol. AP-28, No. 1, pp 132-136

Plane-Wave Scattering-Matrix Theory of Antennas and Antenna-Antenna Interactions
Kerns, D. M.
NBS Monograph 162
June 1981

Spherical-Wave Source-Scattering-Matrix Analysis of the Mutual Coupling Between Two Antennas
Lewis, R. L.
Digest, 1981 IEEE/AP-S Int'l Symp.
June 1981

Efficient Computation of the Far Field Radiated by an Arbitrary Rectangular-Aperture Distribution
Lewis, R. L.
NBSIR 81-1643
April 1981

Synthesis of Broadband Antenna Arrays as Possible Over-the-Horizon Radars
Ma, M. T.
Book, "Research Topics in EM Wave Theory" (John Wiley Interscience)
1981, Chapter 9

Synthesized Isotropic Pattern Antennas for EM Field Measurements
Reeve, G. R.
Symp. Record, "EMC '81," 1981 IEEE Int'l Symp. on Electromagnetic Compatibility, Boulder, CO, Aug. 18-20, 1981
Aug. 1981

A Frequency Tracking, Tuned, Receiving Monopole
Reeve, G. R. and Wainwright, A. E.
Record, IEEE/APS Symp.
June 1981

Results of Planar Near-Field Measurements on a Compact Range at 18 and 54 GHz
Repjar, A. G. and Kremer, D. P.
Digest, 1980 IEEE/AP-S Symposium

Determination of Mutual Coupling Between Co-Sited Microwave Antennas and Calculation of Near-Zone Electric Field
Stubenrauch, C. F. and Yaghjian, A. D.
NBSIR 81-1630
June 1981

Fields of a Horizontal Loop of Arbitrary Shape Buried in a Two-Layer Earth
Wait, J. R. and Hill, D. A.
Radio Science
Sep.-Oct. 1980, Vol. 15, No. 5, pp 903-912

A Delta-Distribution Derivation of the Electric Field in the Source Region
Yaghjian, A. D.
Digest, 1981 IEEE/AP-S Int'l Symp.
June 1981

An Approximate Expression for the Principal Beamwidths of Directive Antennas in Terms of Aperture Fields
Yaghjian, A. D.
NBSIR 81-1644
March 1981

Broadband Orthogonal Array Antenna System: Microprocessor Control and Computation
Bensema, W. D.
Record, EMC '81
Aug. 1981

A Temperature Probe for Radio-Frequency Heated Material
Bowman, R. R.
NBSIR 81-1634
Jan. 1981

Requirements for an Effective National Nonionizing Radiation Measurement System
Clark, H. E.
NBS Special Pub. 613
June 1981

Options to Open-Field and Shielded Enclosure Electromagnetic Compatibility Measurements
Crawford, M. L.
Proc., Int'l EMC Symp., Zurich, Switzerland, March 10-12, 1981
March 1981

Evaluation of a Reverberation Chamber Facility for Performing EM Radiated Fields Susceptibility Measurements
Crawford, M. L.
NBSIR 81-1638
Feb. 1981

Predicting Free-Space Radiated Emissions from Electronic Equipment Using TEM Cell and Open-Field Site Measurements
Crawford, M. L. and Workman, J. L.
Record, 1980 Int'l EMC Symposium

Spherical Dipole for Radiating Standard Fields
Crawford, M. L. and Workman, J. L.
Digest 1980 CPEM Conf.
June 1980

Design, Construction, and Calibration of the Broadband Electric Field Monitor (EFM-5)
Cruz, J. E.
Symp. Record, "EMC '81," 1981 IEEE Int'l Symp. on Electromagnetic Compatibility, Boulder, CO, Aug. 18-20, 1981
Aug. 1981

Free-Space Transmission Loss for Anechoic Chamber Performance Evaluation
FitzGerrell, R. G.
Symp. Record, "EMC '81," 1981 IEEE Int'l Symp. on Electromagnetic Compatibility, Boulder, CO, Aug. 18-20, 1981
Aug. 1981

Electromagnetic Characteristics of a Coaxial Cable with Periodic Slots
Hill, D. A. and Wait, J. R.
IEEE Trans. on EMC
Nov. 1980, Vol. EMC-22, No. 4, pp 303-307

Propagation Along a Coaxial Cable with a Helical Shield
Hill, D. A. and Wait, J. R.
IEEE Trans. on MTT
Feb. 1980, Vol. MTT-28, No. 2, pp 84-89

A Broadband, Isotropic, Real-Time, Electric-Field Sensor (BIRES) Using Resistively Loaded Dipoles
Kanda, M.; Ries, F. X.; and Belsher, D. R.
IEEE Trans. EMC
Aug. 1981, Vol. EMC-23, No. 3

Theoretical and Experimental Investigations of Electromagnetic Field Distortion Due to a Perfectly Conducting Rectangular Cylinder in a Transverse Electromagnetic Cell
Kanda, M.
NBS Tech. Note 1028
April 1981

Theoretical and Experimental Investigations of Loading Effects Due to a Perfectly Conducting Rectangular Cylinder in a Transverse Electromagnetic Cell
Kanda, M.
4th Symp. and Tech. Exhib. on EMC, Zurich, Switzerland
March 1981

The Characteristics of a Linear Antenna with Tapered Resistive and Capacitive Loading
Kanda, M.
Proc., IEEE AP Symp., Quebec, Canada
June 2-6, 1980, Vol. 2, AP.18-2, pp 696-699

The Time Domain Characteristics of a Traveling Wave Linear Antenna with Linear and Non-Linear Loads
Kanda, M.
IEEE Trans. Ant. and Prop.
March 1980, Vol. AP-28, No. 2

Analytical and Numerical Techniques for Analyzing an Electrically Short Dipole with a Nonlinear Load
Kanda, M.
IEEE Trans. Ant. and Prop.
Jan. 1980, Vol. AP-28, No. 1, pp 71-78

Transients in Resistively Loaded Antennas and Their Comparison with Conical Antennas and a TEM Horn
Kanda, M.
IEEE Trans. Ant. and Prop.
Jan. 1980, Vol. AP-28, No. 1, pp 132-136

Background and Present Status of RF Probe Development at NBS
Larsen, E. B.
Symp. Record, "EMC '81," 1981 IEEE Int'l Symp. on Electromagnetic Compatibility, Boulder, CO, Aug. 18-20, 1981
Aug. 1981

Design and Calibration of the NBS Isotropic Electric-Field Monitor (EFM-5), 0.2 to 1000 MHz
Larsen, E. B. and Ries, F. X.
NBS Tech. Note 1033
March 1981

A Method of Determining the Emission and Susceptibility Levels of Electrically Small Objects Using a TEM Cell
Ma, M. T.; Chang, D. C.; and Sreenivasiah, I.
NBS Tech. Note 1040
April 1981

Excitation of a TEM Cell by a Vertical Electric Hertzian Dipole
Ma, M. T.; Wilson, P. F.; and Chang, D. C.
NBS Tech. Note 1037
March 1981

Challenges of EMI Measurements
Miller, C. K. S.
Proc. NCSL Conf., Sep. 22-25, 1980
Oct. 1980

Synthesized Isotropic Pattern Antennas for EM Field Measurements
Reeve. G. R.
Symp. Record, "EMC '81," 1981 IEEE Int'l Symp. on Electromagnetic Compatibility, Boulder, CO, Aug. 18-20, 1981
Aug. 1981

A Frequency Tracking, Tuned, Receiving Monopole
Reeve, G. R. and Wainwright, A. E.
Record, IEEE/APS Symp.
June 1981

Influence of Electromagnetic Interference on Electronic Devices
Ries, F. X. and Miller, C. K. S.
Bulletin, OIML Seminar
Dec. 1981

A Critical Study of Emission and Susceptibility Levels of Electrically Small Objects from Tests Inside a TEM Cell
Sreenivasiah, I.; Chang, D. C.; and Ma, M. T.
Record, EMC '81 Symp.
Aug. 1981

Emission Characteristics of Electrically Small Radiating Sources from Tests Inside a TEM Cell
Sreenivasiah, I.; Chang, D. C.; and Ma, M. T.
IEEE Trans. EMC
Aug. 1981, Vol. EMC-23, No. 3

Characterization of Electrically Small Radiating Sources by Tests Inside a Transmission Line Cell
Sreenivasiah, I.; Chang, D. C.; and Ma, M. T.
NBS Tech. Note 1017
March 1980

Methods of Suppressing Automotive Interference
Taggart, H. E.
NBS Special Pub. 480-44
Nov. 1981

NBS 30/60 Megahertz Noise Measurement System Operation and Service Manual
Counas, G. J. and Bremer, T. H.
NBSIR 81-1656
Dec. 1981

Evaluation of Signal Plus Noise Detection Error in an Envelope Detector with Logarithmic Compression
Estin, A. J. and Daywitt, W. C.
IEEE Trans. Info. Theory
Sep. 1981, Vol. IT-27, No. 5, pp 663-664

Evaluation of Signal Plus Noise Detection Error in an Envelope Detector with Logarithmic Compression
Estin, A. J. and Daywitt, W. C.
NBSIR 79-1614 (R)
Aug. 1979

Addendum to Earth Terminal Measurement System Maintenance Manual
Wakefield, J. P.
NBSIR 81-1641
Oct. 1981

Dielectric Measurements in a Shielded Open Circuit Coaxial Line
Bussey, H. E.
IEEE Trans. Inst. and Meas.
June 1980, Vol. IM-29, No. 2

Active Microwave Water Equivalence Measurements
Ellerbruch, D. A. and Boyne, H. S.
Proc., Ft. Collins Snow Workshop
1980

A Temperature Probe for Radio-Frequency Heated Material
Bowman, R. R.
NBSIR 81-1634
Jan. 1981

Modeling of Oil Shale Retorts for Electromagnetic Sensing Techniques
Chew, H.
NBSIR 81-1653
Nov. 1981

Requirements for an Effective National Nonionizing Radiation Measurement System
Clark, H. E.
NBS Special Pub. 613
June 1981

A Wideband RF Voltage Comparator
Driver, L. D. and Ries, F. X.
Digest, 1980 CPEM Conf.
June 1980

HF Ground Wave Propagation over Mixed Land, Sea, and Sea-Ice Paths
Hill, D. A. and Wait, J. R.
IEEE Trans. on Geoscience and Remote Sensing
Oct. 1981, Vol. GE-19, No. 4, pp 210-216

HF Radio Wave Transmission over Sea Ice and Remote Sensing Possibilities
Hill, D. A. and Wait, J. R.
IEEE Trans. on Geoscience and Remote Sensing
Oct. 1981, Vol. GE-19, No. 4, pp 204-209

HF Ground Wave Propagation over Sea Ice for a Spherical Earth Model
Hill, D. A. and Wait, J. R.
IEEE Trans. on Ant. and Prop.
May 1981, Vol. AP-19, No. 3, pp 525-527

Electromagnetic Characteristics of a Coaxial Cable with Periodic Slots
Hill, D. A. and Wait, J. R.
IEEE Trans. on EMC
Nov. 1980, Vol. EMC-22, No. 4, pp 303-307

On the Excitation of the Zenneck Surface Wave Over the Ground at 10 MHz
Hill, D. A. and Wait, J. R.
Annales des Telecommunications
May-June 1980, Vol. 35, Nos. 5-6, pp 1-4

Ground Wave Attenuation Function for a Spherical Earth with Arbitrary Surface Impedance
Hill, D. A. and Wait, J. R.
Radio Science
May-June 1980, Vol. 15, No. 3, pp 637-643

Electromagnetic Theory of the Loosely Braided Coaxial Cable: Part II - Numerical Results
Hill, D. A. and Wait, J. R.
IEEE Trans. on MTT
April 1980, Vol. MTT-28, No. 4, pp 326-331

Propagation Along a Coaxial Cable with a Helical Shield
Hill, D. A. and Wait, J. R.
IEEE Trans. on MTT
Feb. 1980,, Vol. MTT-28, No. 2, pp 84-89

Evaluation of Three-Terminal and Four-Terminal Pair Capacitors at High Frequencies
Jones, R. N.
NBS Tech. Note 1024
Sep. 1980

Spherical Scanning Data Processing: An Algorithm for Halving the Data Processing Effort when the Radiation into the Back Hemisphere is Negligible
Lewis, R. L.
Digest, 1981 IEEE AP-S Int'l Symp.
June 1981

A Bibliography of Publications in the NBS Electromagnetic Fields Division
Miller, C. K. S.
NBSIR 80-1635
Nov. 1980

Fields of a Horizontal Loop of Arbitrary Shape Buried in a Two-Layer Earth
Wait, J. R. and Hill, D. A.
Radio Science
Sep.-Oct. 1980, Vol. 15, No. 5, pp 903-912

Addendum to Earth Terminal Measurement System Maintenance Manual
Wakefield, J. P.
NBSIR 81-1641
Oct. 1981

Laser Fluorescence Diagnostics of Lithium Vapor for Inertial Confinement Applications
Wyss, J. C.; Stwalley, W. C.; Koch, M. E.; and Verma, K. K.
Topical Meeting on Inertial Confinement Fusion, San Diego, CA
Feb. 26, 1980

A Delta-Distribution Derivation of the Electric Field in the Source Region
Yaghjian, A. D.
Digest, 1981 IEEE/AP-S Symp.
June 1981

Reply to Criticism on Electric Dyadic Functions in the Source Region
Yaghjian, A. D.
Proc., IEEE
Feb. 1981, Vol. 69, No. 2

Augmented Electric- and Magnetic-Field Integral Equations
Yaghjian, A. D.
Digest, Int'l URSI Symp. on EM Waves, Munich, Germany
Aug. 1980

Electric Dyadic Green's Functions in the Source Region
Yaghjian, A. D.
Proc., IEEE
Feb. 1980, Vol. 68, No. 2

A BIBLIOGRAPHY OF PUBLICATIONS IN THE NBS ELECTROMAGNETIC FIELDS DIVISION

Edited by
Charles K. S. Miller

This bibliography lists the publications of the personnel of the NBS Electromagnetic Fields Division of NBS in the period from January 1970 through December 1979. A few earlier references that are directly related to the present work of the division are included.

Key words: Antennas; electromagnetic interference; em material properties; electromagnetic metrology; microwaves; noise; non-ionizing radiation; radiation hazards;.

INTRODUCTION

The Electromagnetic Fields Division was formed during the reorganization of NBS in April 1978. The Division develops measurement methods and standards, and provides metrological support for: antenna systems, noise measurement equipment, electromagnetic interference and radiation hazards equipment, systems for measuring electromagnetic properties of materials, and radiated electromagnetic fields and waves. For the individual staff members of the Division, the reorganization brought a realignment of long term goals but little immediate discontinuity in their work. It makes good sense therefore that this bibliography begin some time before the reorganization, so as to include the more recent origins of the present work of the Division. The editor has attempted to include all work published by the staff members of the Division, while they were employees of NBS, in the period from January 1970 through December 1979. There are a few exceptions. Work that is totally unrelated to the present program has been excluded. Relevant work performed by authors prior to joining this Division or work by authors now in other parts of NBS has been included because of its special significance. A miscellaneous category includes general publications. A few papers published before 1970 have also been included because of their direct relationship to the present program.

There are several other information sources that may be useful to the reader who is interested in activities at NBS connected with electromagnetic metrology. A companion bibliography: Metrology for Electromagntic Technology, NBSIR 79-1625 (January 1980), lists the publications of the Electromagnetic Technology Division. Its topics include metrology for: antennas, satellite communications equipment, electromagnetic interference, and hazards, and remote sensing. Three bibliographies of the publications of the former Electromagnetic Division have been published: NBSIR-73-320 (July 1972-June 1973); NBSIR-74-395 (July 1973 - June 1974); NBSIR-75-818 (July 1974 - June 1975). These were preceded by a series of unpublished reports (edited by H. M. Altschuler) that cover the period back to 1956. An excellent summary of the whole field of electromagnetic metrology as it stood in 1967 was published as a special issue of the IEEE Proceedings (volume 55, June 1967). Advances in the following decade were described in another special issue of the same journal (volume 66, April 1978).

A NOTE ON ABBREVIATIONS

Most readers will be familiar with the commonly used abbreviations for the names of the various professional journals that appear in this bibliography. There are also several publication series that are peculiar to NBS and call for explanation. They are:

NBSIR -	NBS	Interagency/Internal Report
NBS-TN -	NBS	Technical Note
NBS-SP -	NBS	Special Publication
NBS-MN -	NBS	Monograph
LESP-RPT		Law Enforcement Standards Program Report
OTR -		Office of Telecommunications Report

Purchase Procedures and Document Availability

NBS Technical Notes and Special Publications may be purchased from the Superintendent of Documents, U.S. Government Printing Office, Washington, D.C. 20402. Orders must be accompanied by postal money order, express money order, or check made out to the Superintendent of Documents.

NBS Interagency/Internal Reports (NBSIR's) may be purchased from the National Technical Information Service, Springfield VA 22161. Order must be accompanied by postal money order, express money order, or check made out to the NTIS.

Reprints of papers published in non-NBS media may be available in limited quantities from the authors.

ACKNOWLEDGMENTS

A large part of the labor of preparing a bibliography is spent on collecting and arranging the material. I thank Frances Brown, Kathryn A. Gibson, Susie Ann Rivera, and Susan Lee Rothschild for their assistance with these chores. The prime source of material was the NTIS file, with access through the Lockheed Dialog System. This was supplemented with material supplied by the individual authors.

ANTENNA WITH INHERENT FILTERING ACTION;
BABIJ, TADEUSZ M.; BOWMAN, RONALD R.; WACKER, PAUL F.
PAT-APPL-590 355, PATENT-4 008 477, 6P 1975.

CALIBRATION OF BROADBEAM ANTENNAS USING PLANAR NEAR-FIELD MEASUREMENTS;
CRAWFORD, M. L.
CPEM DIGEST, P53-56 JUNE 28 - JULY 1, 1976

PLANAR NEAR-FIELD MEASUREMENTS ON PHASED ARRAY ANTENNAS;
NEWELL, ALLEN C.; CRAWFORD, MYRON L.
PROCEEDINGS OF INTERNATIONAL IEEE AP-S SYMPOSIUM, ATLANTA, GA. 10-12 JUNE 1974, PAPER 6-7 IN 1974 INTERNATIONAL IEEE/AP-S SYMPOSIUM DIGEST, P423 JUNE 1974.

PLANAR NEAR-FIELD MEASUREMENTS ON HIGH PERFORMANCE ARRAY ANTENNAS;
NEWELL, ALLEN C.; CRAWFORD, MYRON L.
NBSIR-74-380. 101p JULY 1974.

TRANSMITTING AND RECEIVING FORMULAS FOR ANTENNAS AND FIELD INTENSITY METERS;
BOWMAN, RONALD R.
42p RADC-TR-68-445 TECHNICAL REPORT APRIL 1969.

A THEORETICAL STUDY OF UNBALANCED GROUND EFFECTS ON RECEIVING DIPOLES;
MA, M. T.
NBSIR-79-1605, 16p MAY 1979.

ANTENNAS AND THE ASSOCIATED TIME DOMAIN RANGE FOR THE MEASUREMENT OF IMPULSIVE FIELDS;
LAWTON, ROBERT A.; ONDREJKA, ARTHUR R.
NBS-TN-1008, 69p NOVEMBER 1978.

A RELATIVELY SHORT CYLINDRICAL BROADBAND ANTENNA WITH TAPERED RESISTIVE LOADING FOR PICOSECOND PULSE MEASUREMENTS;
KANDA, MOTOHISA.
NBSIR-77-861. IEEE TRANS. ANTENNAS PROPAG. AP-26 N3 P439-447 MAY 1978.

TRANSIENTS IN RESISTIVELY LOADED ANTENNAS AND THEIR COMPARISON WITH CONICAL ANTENNAS AND TEM HORNS;
KANDA, MOTOHISA.
NBSIR-78-876, 38p 1978.

G/T MEASUREMENT ERRORS WITH RADIO STARS;
DAYWITT, W. C.; KANDA, M.
PROCEEDINGS OF IEEE INT. ANTENNAS AND PROPAGATION SYMP. URBANA/CHAMPAIGN, ILL. 2-4 JUNE 1975, SESSION 20, P460-463 1975.

ACCURACY CONSIDERATIONS IN THE MEASUREMENT OF THE POWER GAIN OF A LARGE MICROWAVE ANTENNA;
KANDA, MOTOHISA.
PROCEEDINGS OF 1974 INTERNATIONAL IEEE/AP-S SYMPOSIUM, ATLANTA, GA. 10-12 JUNE 1974, PAPER IN 1974 INTERNATIONAL IEEE/AP-S SYMPOSIUM DIGEST, P43-45 JUNE 1974.

TESTING OF ELECTRONIC INDUSTRIES ASSOCIATION LAND-MOBILE COMMUNICATION ANTENNA GAIN STANDARDS AT THE NATIONAL BUREAU OF STANDARDS;
TAGGART, H. E.; SHAFER, J. F.
IEEE (INSTITUTE OF ELECTRICAL AND ELECTRONICS ENGINEERS) TRANS. ON VEHICULAR TECHNOLOGY VT-27, NR P259-264, NOVEMBER 1978.

FIXED AND BASE STATION ANTENNAS;
TREADO, M. J.; TAGGART, H. E.; NELSON, R. E.; WORKMAN, J. L.
NILECJ-STD-0204.00, 16P 1977.

THE ORBITING STANDARDS PLATFORM;
DOUGHERTY, H. T.; ESTIN, A. J.; MORGAN, W. L.; WOODRUFF, J. J.
PROCEEDINGS OF THE ANTENNA APPLICATIONS SYMPOSIUM (1978) HELD AT URBANA-CHAMPAIGN, IL. ON SEPTEMBER 20-22, 1978, P1-9, 1978.

AN ERROR ANALYSIS FOR THE MEASUREMENT OF SATELLITE EIRP USING A CALIBRATED RADIO STAR;
DAYWITT, WILLIAM C.
JNL. IEEE TRANS. INSTRUM. MEAS. VIM27 N3 P253-258 SEPTEMBER 1978.

FEASIBILITY STUDY OF ORBITING STANDARDS PLATFORM;
ESTIN, A. J.; BAIRD, R. C.
NBSIR-78-886, 47p 1978.

A PRECISION EARTH-TERMINAL SYSTEM FOR ACCURATE C/KT, G/T, AND EIRP MEASUREMENTS WITH A CALIBRATED RADIO STAR;
DAYWITT, W. C.
PROC. URSI INT. SYMP. ON MEASUREMENTS IN TELECOMMUNICATIONS, LANNION, FRANCE, OCTOBER 3-7 P1-4, 1977.

EARTH TERMINAL MEASUREMENT SYSTEM OPERATIONS MANUAL;
WAIT, DAVID F.
NBSIR-78-879, 266p 1978.

ATMOSPHERIC PROPAGATION EQUATIONS USED IN THE NBS EARTH TERMINAL MEASUREMENT SYSTEM;
DAYWITT, W. C.
NBSIR-78-883, 46p 1978.

LASER FAR-FIELD BEAM-PROFILE MEASUREMENTS BY THE FOCAL PLANE TECHNIQUE;
DAY, G. W. STUBENRAUCH, C. F.
NBS-TN-1001, 52p 1978.

ERROR EQUATIONS USED IN THE NBS EARTH TERMINAL MEASUREMENT SYSTEM;
DAYWITT, WILLIAM C.
NBSIR-78-869, 32p 1977.

THE USE OF THREE TERM RECURSION RELATIONS FOR NUMERICAL COMPUTATIONS AS APPLIED TO NEAR-FIELD SPHERICAL SCANNING;
LEWIS, RICHARD L.
PROCEEDINGS OF INTERNATIONAL UNION OF RADIO SCIENCE (URSI) INTERNATIONAL SYMPOSIUM, 20-24 JUNE 1977 P224-226 1977.

NEAR-FIELD ANTENNA MEASUREMENTS ON A CYLINDRICAL SURFACE: A SOURCE SCATTERING-MATRIX FORMULATION;
YAGHJIAN, ARTHUR D.
NBS-TN-696-REV, 42p 1977.

RESULTS OF SPHERICAL NEAR-FIELD MEASUREMENTS ON NARROW-BEAM ANTENNAS;
NEWELL, ALLEN C.; REPJAR, ANDREW.
PROCEEDINGS OF CONFERENCE ON PRECISION ELECTROMAGNETIC MEASUREMENTS, P382-385 1976.

ADVANTAGES AND DISADVANTAGES OF PLANAR, CIRCULAR CYLINDRICAL, AND SPHERICAL SCANNING AND DESCRIPTION OF THE NBS ANTENNA SCANNING FACILITIES;
WACKER, PAUL F.; NEWELL, ALLEN C.
PROCEEDINGS EUROPEAN SPACE AGENCY SYMPOSIUM, NOORDWIJK (NETHERLANDS), JUNE 6-8, 1977, P115-121 1977.

SYMMETRY ANALYSIS APPLIED TO WAVE THEORY;
WACKER, PAUL F.
INT'L IEEE/AP-S SYMPOSIUM DIGEST, 4p 1977.

SYMMETRY ANALYSIS APPLIED TO SCATTERING, INVERSE SCATTERING, AND ANTENNA PATTERNS: MEASUREMENTS, MOMENT METHOD, AND CHARACTERISTIC MODES;
WACKER, PAUL F.
PROCEEDINGS OF INSTITUTE OF ELECTRICAL AND ELECTRONICS ENGINEERS/ANTENNAS AND PROPAGATION SOCIETY INT. SYMP. P177-180 1977.

RECENT RESULTS WITH SPHERICAL NEAR-FIELD ANTENNA SCANNING AT THE NATIONAL BUREAU OF STANDARDS;
WACKER, PAUL F.
PROCEEDINGS EUROPEAN SPACE AGENCY SYMPOSIUM, NOORDWIJK (NETHERLANDS), JUNE 6-8, 1977, P159-164 1977.

SATELLITE EARTH TERMINAL G/T MEASUREMENTS;
WAIT, DAVID F.
MICROWAVE JNL. 20, N4 P49, 51, 58, APRIL 1977.

A DIRECT APPROACH TO THE DERIVATION OF ELECTRIC DYADIC GREEN'S FUNCTIONS;
YAGHJIAN, ARTHUR D.
AP-SYMPOSIUM DIGEST, P 76-156 OCTOBER 1976 and NBS-TN-1000, P70, 1978.

ERROR EQUATIONS USED IN THE NBS PRECISION G/T MEASUREMENT SYSTEM;
DAYWITT, W. C.
NBSIR-76-842, 21p 1976.

THE ACCURATE DETERMINATION OF MILLIMETER-WAVE ANTENNA CHARACTERISTICS BY DECONVOLUTION AND EXTRAPOLATION TECHNIQUES;
BAIRD, R. C.; KERNS, D. M.
PROC. 1974 MILLIMETER-WAVE CONF., 26-28 MARCH 1974, VOL. 2, E 2-1 THRU E 2-12. 14p MARCH 1974.

STUDY OF ERRORS IN PLANAR NEAR-FIELD MEASUREMENTS;
NEWELL, ALLEN C.; YAGHJIAN, ARTHUR D.
PROCEEDINGS OF IEEE INT. ANTENNAS AND PROPAGATION SYMP.
URBANA/CHAMPAIGN, ILL. 2-4 JUNE 75, SESSION 20, P470-473 1975.

IMPROVED POLARIZATION MEASUREMENTS USING A MODIFIED THREE ANTENNA TECHNIQUE;
NEWELL, ALLEN C.
PROCEEDINGS OF IEEE INT. ANTENNAS AND PROPAGATION SYMP.
URBANA/CHAMPAIGN, ILL. 2-4 JUNE 75, SESSION 15, P337-340 1975.

UPPER-BOUND ERRORS IN FAR-FIELD ANTENNA PARAMETERS DETERMINED FROM PLANAR NEAR-FIELD MEASUREMENTS. PART 1: ANALYSIS;
YAGHJIAN, ARTHUR D.
NBS-TN-667. 1, 113p OCTOBER 1975.

PLANE-WAVE SCATTERING-MATRIX THEORY OF ANTENNAS AND ANTENNA-ANTENNA INTERACTIONS: FORMULATION AND APPLICATIONS;
KERNS, DAVID M.
NBSIR-75-824, 99p 1975.

NON-PLANAR NEAR-FIELD MEASUREMENTS: SPHERICAL SCANNING;
WACKER, PAUL F.
NBSIR-75-809, 69p 1975.

ANTENNA MEASUREMENTS AT THE NATIONAL BUREAU OF STANDARDS NEAR-FIELD AND EXTRAPOLATION TECHNIQUES;
WACKER, PAUL F.
PROCEEDINGS COLLOQUIUM ON MICROWAVE COMMUNICATION (5TH)
BUDAPEST, 24-30 JUNE 74, PME-113-114.

NEAR-FIELD ANTENNA MEASUREMENTS USING A SPHERICAL SCAN: EFFICIENT DATA REDUCTION WITH PROBE CORRECTION;
WACKER, PAUL F.
CPEM DIGEST N113 P286-288 (INSTITUTION OF ELECTRICAL ENGINEERS, LONDON, ENGLAND) 1974.

COMMENT ON CORRECTION OF ERRORS IN AERIAL FAR-FIELD RADIATION-PATTERN DETERMINATIONS;
KERNS, D. M.
ELECTRONICS LETTERS, VOL. 7 N24 P706, 2 DECEMBER 1971.

ACCURATE MEASUREMENT OF ANTENNA GAIN AND POLARIZATION AT REDUCED DISTANCES BY AN EXTRAPOLATION TECHNIQUE;
NEWELL, ALLEN C.; BAIRD, RAMON C.; WACKER, PAUL F.
IEEE, TRANSACTIONS ON ANTENNAS AND PROPAGATION, AP-21 NO.4
P418-431 JULY 1973.

DETERMINATION OF BOTH POLARIZATION AND POWER GAIN OF ANTENNAS BY A GENERALIZED 3-ANTENNA MEASUREMENT METHOD;
NEWELL, A. C.; KERNS, D. M.
ELECTRONICS LETTERS, VOL. 7 NO. 3 P68-70, JANUARY 1971.

SOME RECENT NEAR-FIELD ANTENNA MEASUREMENTS;
STUBENRAUCH, C. F.
PROCEEDINGS 1979 ANTENNA APPLIC. SYMP, SEPTEMBER 1979

SYNTHESIS OF BROADBAND ANTENNA ARRAYS AS POSSIBLE OVER-THE-HORIZON RADARS;
MA, M. T.
NBS-MONOGRAPH, JUNE 1979.

PLANE-RADIAL SCANNING TECHNIQUES WITH PROBE CORRECTION; NATURAL ORTHOGONALITIES WITH RESPECT TO SUMMATION ON PLANAR MEASUREMENT LATTICES;
WACKER, P. F.
DIGEST OF THE IEEE/APS SYMPOSIUM, FEBRUARY 1979.

A QUALITATIVE SURVEY OF NEAR-FIELD ANALYSIS AND MEASUREMENT;
WACKER, P. F.
NBSIR-79-1602, JANUARY 1979.

EMI AND RADIATION HAZARDS METROLOGY

PICOSECOND PULSE GENERATORS USING MICROMINIATURE MERCURY SWITCHES;
ANDREWS, JAMES R.
NBSIR-74-377, 45p 1974.

IMPULSE SPECTRAL INTENSITY -- WHAT IS IT;
ARTHUR, M. G.
NBSIR-74-365, 21P MAY 1974.

ELECTROMAGNETIC NOISE IN ROBENA NO. 4 COAL MINE;
BENSEMA, W. D.; KANDA, MOTOHISA; ,ADAMS, J. W.
NBS-TN-654, 197p APRIL 1974.

AMPLITUDE STATISTICS OF ELECTROMAGNETIC NOISE IN COAL MINES;
KANDA, M.; ADAMS, J. W.
PROCEEDINGS THRU-THE-EARTH ELECTROMAGNETICS WORKSHOP,
COLORADO SCHOOL OF MINES, GOLDEN, COLO. P156-160, 15-17 AUGUST 1973,
AND URSI DIGEST, IEEE TRANS. A&P MAY 1975.

SURVEY REPORT OF THE U.S. BUREAU OF MINES ELECTROMAGNETIC NOISE
MEASUREMENT PROGRAM;
ADAMS, J. W.; TAGGART, H. E.; SPAULDING, A. D.
NBS-10723, 38p 1971.

CHARACTERISTIC IMPEDANCE OF A RECTANGULAR COAXIAL LINE WITH OFFSET INNER
CONDUCTOR;
TIPPET, JOHN C.; CHANG, DAVID C.
JNL. IEEE TRANS. MICROWAVE THEORY TECH. VMTT-26 N11, p876-883
NOVEMBER 1978.

PROCEEDINGS OF THE 1978 ELECTROMAGNETIC INTERFERENCE WORKSHOP;
ARTHUR, M. G.
NBS-SP-551, 61p JULY 1979.

COMPARISON AND SELECTION OF TECHNIQUES FOR MEASURING EM RADIATED
EMISSIONS AND SUSCEPTIBILITY OF LARGE EQUIPMENT;
CRAWFORD, MYRON L.
PROCEEDINGS SYMP. AND TECHNICAL EXHIBITION ON ELECTROMAGNETIC
COMPATIBILITY (3RD), HELD AT ROTTERDAM (NETHERLANDS), ON MAY 1-3, 1979.
PAPER IN ELECTROMAGNETIC COMPATIBILITY 1979, P115-122 MAY 79.

USING A TEM CELL FOR EMC MEASUREMENTS OF ELECTRONIC EQUIPMENT;
CRAWFORD, M. L.; WORKMAN, J. L.
NBS-TN-1013, 72p APRIL 1979.

VARIATIONAL EXPRESSION FOR THE SCATTERING MATRIX OF A COAXIAL LINE STEP
DISCONTINUITY AND ITS APPLICATION TO AN OVER MODED COAXIAL TEM CELL;
SREENIVASIAH, I.; CHANG, DAVID C.
NBSIR-79-1606, 48p MAY 1979.

CONSTRUCTION OF A LARGE TRANSVERSE ELECTROMAGNETIC CELL;
DECKER, W. F.; CRAWFORD, M. L.; WILSON, W. A.
NBS-TN-1011, 89p FEBRUARY 1979.

A NEW APPROXIMATION FOR THE CAPACITANCE OF A RECTANGULAR, COAXIAL, STRIP TRANSMISSION LINE;
TIPPET, J. C.; CHANG, D. C.
IEEE (INSTITUTE OF ELECTRICAL AND ELECTRONICS ENGINEERS)
TRANSACTIONS ON MICROWAVE THEORY AND TECHNIQUES, P602-604, SEPTEMBER 1976.

BROADBAND ISOTROPIC ANTENNA WITH FIBER-OPTIC LINK TO A CONVENTIONAL RECEIVER;
LARSEN, EZRA B.; ANDREWS, JAMES R.; BALDWIN, EUGENE E.
PATENT-4 091 327, PATENTED MAY 23, 1978.

EXPANDING THE BANDWIDTH OF TEM CELLS FOR EMC MEASUREMENTS;
CRAWFORD, M. L.; WORKMAN, J. L.; THOMAS, C. L.
IEEE TRANSACTIONS ON ELECTRO-MAGNETIC COMPATIBILITY EMC 20 N3
P368-375 AUGUST 1978.

SHF IMPULSE GENERATOR;
ANDREWS, JAMES R.; BALDWIN, EUGENE E.
NBSIR-78-888, 76p JUNE 1978.

UHF IMPULSE GENERATOR;
ANDREWS, JAMES R.; BALDWIN, EUGENE E.
NBSIR-78-880, 30p APRIL 1978.

NEAR-FIELD ELECTRIC FIELD STRENGTH LEVELS OF EM ENVIRONMENTS APPLICABLE TO AUTOMOTIVE SYSTEMS;
ADAMS, J. W.; KANDA, M.; SHAFER, J.; WU, Y.
PROCEEDINGS OF IEEE INTERNATIONAL SYMPOSIUM ON ELECTROMAGNETIC COMPATIBILITY, SEATTLE, WASH. 2-4 AUGUST 1977, PP336-343.

GENERATION OF EM SUSCEPTIBILITY TEST FIELDS USING A LARGE ABSORBER-LOADED TEM CELL;
CRAWFORD, M. L. WORKMAN, J. L. THOMAS, C. L.
IEEE TRANSACTIONS ON INSTRUMENTATION AND MEASUREMENT, IM26 N3
P336-343 SEPTEMBER 1977.

CONVERTING A RECTANGULAR SHIELDED ENCLOSURE INTO A TEM TRANSMISSION CELL FOR EMI MEASUREMENTS;
CRAWFORD, M. L.; THOMAS, C. L.
IEEE 1977 INTERNATIONAL SYMPOSIUM ON EMC (SEATTLE WASH.,) AUGUST 2-5, 1977.

SPECTRUM AMPLITUDE--DEFINITION, GENERATION AND MEASUREMENT;
ANDREWS, JAMES R.; ARTHUR, M. GERALD
NBS-TN-699. 100p OCTOBER 1977.

ELECTROMAGNETIC INTERFERENCE (EMI) MEASUREMENTS FOR AUTOMOTIVE APPLICATIONS;
ADAMS, J. W.; CRAWFORD, M. L.; SHAFER, J. F.
PROCEEDINGS OF SAE AUTOMOTIVE CONGRESS CONFERENCE, DETROIT, MICH. 23-27 FEBRUARY 1976 P1-6 1976.

EXPERIMENTAL EVALUATION OF THE RADIATION CHARACTERISTICS OF DIPOLE SOURCES ENCLOSED IN A TEM TRANSMISSION CELL;
CRAWFORD, M. L.
PROCEEDINGS OF CONFERENCE ON PRECISION ELECTROMAGNETIC MEASUREMENTS, P57-59 BOULDER, CO. JUNE 28 - JULY 1, 1976.

AMPLITUDE, TIME, AND FREQUENCY STATISTICS OF QUASI-IMPULSIVE NOISE;
BENSEMA, W. D.
PROCEEDINGS 1977 EMC SYMPOSIUM, MONTREUX (SWITZERLAND), JUNE 18-30, 1977, P347-352 .

A NOISE SPECTRUM MEASUREMENT SYSTEM USING THE FAST FOURIER TRANSFORM;
BENSEMA, W. D.
IEEE TRANSACTIONS ON ELECTRO-MAGNETIC COMPATIBILITY EMC-19, N2 P37-43 MAY 77.

SOME RECENT DEVELOPMENTS IN THE CHARACTERIZATION AND MEASUREMENT OF HAZARDOUS ELECTROMAGNETIC FIELDS;
BOWMAN, RONALD R.
PROCEEDINGS OF INTERNATIONAL SYMPOSIUM BIOLOGIC EFFECTS AND HEALTH HAZARDS OF MICROWAVE RADIATION, OCTOBER 15-18, 1973, WARSAW (POLAND), P217-227.

NONMETALLIC ELECTRODE SYSTEM FOR RECORDING EEG AND ECG IN ELECTROMAGNETIC FIELDS;
FLANIGAN, W. F. JR.; BOWMAN, R. R.; LOWELL, W. R.
PHYSIOLOGY AND BEHAVIOR, VOL. 18 NO. 3 P531-533 1977.

TECHNIQUES FOR MEASUREMENT OF ELECTROMAGNETIC RADIATION AND SUSCEPTIBILITY OF ELECTRONIC EQUIPMENT;
CRAWFORD, MYRON L.
PROCEEDINGS OF SYMP. AND TECHNICAL EXHIBITION ON ELECTROMAGNETIC COMPATIBILITY (1ST), MONTREUX, SWITZERLAND, MAY 20-22, 1975, P38-44.

QUANTIFYING HAZARDOUS ELECTROMAGNETIC MICROWAVE FIELDS: PRACTICAL CONSIDERATIONS;
BOWMAN, RONALD R.
PROCEEDINGS OF BIOLOGICAL EFFECTS AND HEALTH IMPLICATIONS OF MICROWAVE RADIATION, HELD AT RICHMOND, VA. ON SEPTEMBER 17-19, 1969, BRH/DBE 70-2, P204-209, U.S. DEPT. OF HEALTH, EDUCATION, AND WELFARE, ROCKVILLE, MD. JUNE 70.

SENSITIVE ISOTROPIC ANTENNA WITH FIBER-OPTIC LINK TO A CONVENTIONAL RECEIVER;
LARSEN, E. B.; ANDREWS, J. R.; BALDWIN, E. E.
NBSIR-75-819. 114p SEPTEMBER 1976.

AN ANALYTICAL AND EXPERIMENTAL DETERMINATION OF THE CUTOFF FREQUENCIES OF HIGHER-ORDER TE MODES IN A TEM CELL;
TIPPET, JOHN C.; CHANG, DAVID C.; CRAWFORD, MYRON L.
NBSIR-76-841, 29p JUNE 1976.

CALIBRATION TECHNIQUES FOR ELECTROMAGNETIC HAZARD METERS: 500 MHZ TO 20 GHz;
BOWMAN, RONALD R.
NBSIR-75-805, 38p 1976.

A PROBE FOR MEASURING TEMPERATURE IN RADIO-FREQUENCY-HEATED MATERIAL;
BOWMAN, RONALD R.
IEEE TRANSACTIONS ON MICROWAVE THEORY AND TECHNIQUES, VMTT-24
N1 P43-45 JANUARY 1976.

EXPERIMENTAL RF FIELD POLARIZATION METER;
FITZGERRELL, R. G.
FAA-RD-74-188, 41p 1975.

EVALUATION OF REFLECTIVITY LEVEL OF ANECHOIC CHAMBERS USING
ISOTROPIC, 3-DIMENSIONAL PROBING;
CRAWFORD, M. L.
PROCEEDINGS OF INTERNATIONAL IEEE/AP-S SYMPOSIUM DIGEST, ATLANTA, GA.
10-12 JUNE 1974, P28-34.

GENERATION OF STANDARD EM FIELDS FOR CALIBRATION OF POWER DENSITY
METERS 20 kHZ TO 1000 MHz;
CRAWFORD, M. L.
NBSIR-75-804, 45p JANUARY 1975.

ELECTROMAGNETIC NOISE IN LUCKY FRIDAY MINE;
SCOTT, W. W.; ADAMS, J. W.; BENSEMA, W. D.; DOBROSKI, H.
NBSIR-74-391, 139p 1974.

ELECTROMAGNETIC NOISE IN MCELROY MINE;
KANDA, MOTOHISA; ADAMS, JOHN W.; BENSEMA, WILLIAM D.
NBSIR-74-389, 172p JUNE 1974.

GENERATION OF STANDARD EM FIELDS USING TEM TRANSMISSION CELLS;
CRAWFORD, M. L.
IEEE TRANSACTIONS ON ELECTRO-MAGNETIC COMPATIBILITY, VOL. EMC16 N4 P189-195
NOVEMBER 1974.

ELECTROMAGNETIC NOISE IN ITMANN MINE;
BENSEMA, WILLIAM D.; KANDA, MOTOHISA.; ADAMS, JOHN W.
NBSIR-74-390, 114p JUNE 1974.

SURFACE MAGNETIC FIELD NOISE MEASUREMENTS AT GENEVA MINE;
ADAMS, JOHN W.; BENSEMA, WILLIAM D.; TOMOEDA, N. C.
NBSIR-74-369, 41p JUNE 1974.

ELECTROMAGNETIC NOISE IN GRACE MINE;
ADAMS, JOHN W.; BENSEMA, WILLIAM D.; KANDA, MOTOHISA.
NBSIR-74-388, 139p JUNE 1974.

VARIABLE IMPEDANCE COAXIAL DEVICE WITH RELATIVE ROTATION BETWEEN CONDUCTORS;
CRUZ, JOSE E.
PAT-APPL-487 099, PATENT-3 417 350, 4p 1965.

SIMULATOR FOR ATMOSPHERIC RADIO NOISE;
BENSEMA, WILLIAM D.; COON, ROBERT M.; BERRY, WESLEY M.; WATTERSON, CLARK C.;
BOLTON, EARL C.
PAT-APPL-44 842, PATENT-3 617 925, 8P 1970.

COAL MINE MAGNETIC-FIELD NOISE MEASUREMENTS;
BENSEMA, W. D.
PROCEEDINGS OF WEST VIRGINIA CONFERENCE ON COAL MINE ELECTROTECHNOLOGY (1ST), WEST VIRGINIA UNIV., MORGANTOWN, 2-4 AUGUST 1972 PXII-1--XII-12, 12p 1972.

ANALYTICAL AND NUMERICAL TECHNIQUES FOR ANALYZING AN ELECTRICALLY SHORT DIPOLE WITH A NONLINEAR LOAD;
KANDA, MOTOHISA.
NBSIR-78-898, 21p 1978.

A RELATIVELY SHORT CYLINDRICAL BROADBAND ANTENNA WITH TAPERED RESISTIVE LOADING FOR PICOSECOND PULSE MEASUREMENTS;
KANDA, MOTOHISA.
NBSIR-77-861. 47 P. AUGUST 1977 AND IEEE TRANS. ANTENNAS PROPAG. AP-26 N3 P439-447 MAY 1978.

THE CHARACTERISTICS OF A RELATIVELY SHORT BROADBAND LINEAR ANTENNA WITH TAPERED RESISTIVE LOADING;
KANDA, M.
PROC. INT. SYMP. ON ANTENNAS AND PROPAGATION SOCIETY, JUNE 20-22, 1977. IEEE ANTENNAS AND PROPAGATION SOCIETY DIGEST, P230-233, JUNE 20-22, 1977.

A BROADBAND ANTENNA WITH TAPERED RESISTIVE LOADING FOR EMI MEASUREMENTS;
KANDA, MOTOHISA.
PROCEEDINGS IEEE INT. SYMP. ON ELECTROMAGNETIC COMPATIBILITY, HELD AT SEATTLE, WASHINGTON, ON AUGUST 2-4, 1977, P13-18.

TRANSIENTS IN RESISTIVELY LOADED ANTENNAS AND THEIR COMPARISON WITH CONICAL ANTENNAS AND TEM HORNS;
KANDA, MOTOHISA.
NBSIR-78-876, 38p MARCH 1978.

SURVEYS OF ELECTROMAGNETIC FIELD INTENSITIES NEAR REPRESENTATIVE HIGHER-POWER FAA TRANSMITTING ANTENNAS;
LARSEN, EZRA B.; SHAFER, JOHN F.
FAA-RD-77 179 P DECEMBER 1977.

DESIGN OF A VAN-TOP LOW-PROFILE HF ANTENNA;
MA, M. T.; FITZGERRELL, R. G.
OTR-77-131, 47p OCTOBER 1977.

THE CHARACTERISTICS OF BROADBAND, ISOTROPIC ELECTRICAL FIELD AND MAGNETIC FIELD PROBES;
KANDA, MOTOHISA.
NBSIR-77-868, 35p NOVEMBER 1977.

MEASUREMENT OF RF POWER-ABSORPTION IN BIOLOGICAL SPECIMENS (10 TO 100 MHZ);
GREENE, FRANK M.
NBS-TN-687, 33p NOVEMBER 1976.

USING FIBER OPTICS IN A BROADBAND, SENSITIVE, ISOTROPIC ANTENNA - 15 KHZ TO 150 MHZ;
LARSEN, E. B.; ANDREWS, J. R.
PROCEEDINGS OF IEEE INTERNATIONAL SYMPOSIUM ON ELECTROMAGNTIC COMPATIBILITY, 7p WASH. D.C. JULY 13-15, 1976.

COMPLETION OF THE PROGRAM TO EVALUATE/IMPROVE INSTRUMENTATION AND TEST METHODS FOR ELECTROEXPLOSIVE DEVICE SAFETY QUALIFICATION;
HUDSON, PAUL A.; MELQUIST, DEAN G.; ONDREJKA, ARTHUR R.; WERNER, P.E.
NBSIR-73-323 37p 1973, and NBSIR-74-379, 37p 1974.

CALIBRATION OF IMPULSE NOISE GENERATORS;
REEVE, GEROME R.
NBSIR-73-343, 78p OCTOBER 1973.

DEVELOPMENT OF ELECTRIC AND MAGNETIC NEAR-FIELD PROBES;
GREENE, FRANK M.
NBS-TN-658, 55p JANUARY 1975.

ASYMMETRIC VERSUS SYMMETRIC TEM CELLS FOR EMI MEASUREMENTS;
CRAWFORD, M. L.; WORKMAN, J. L.
PROCEEDINGS IEEE INT. SYMP. ON ELECTROMAGNETIC COMPATIBILITY, HELD AT ATLANTA, GA. ON JUNE 20-22, 1978, P204-210 1979.

HIGHER ORDER MODES IN RECTANGULAR COAXIAL LINE WITH INFINITELY THIN INNER CONDUCTOR;
TIPPET, JOHN C.; CHANG, DAVID C.
NBSIR-78-873, 41p MARCH 1978.

RADIATION CHARACTERISTICS OF DIPOLE SOURCES LOCATED INSIDE A RECTANGULAR, COAXIAL TRANSMISSION LINE;
TIPPET, JOHN C.; CHANG, DAVID C.
NBSIR-75-829, 35p JANUARY 1976.

BROADBAND PULSED/CW CALIBRATION SIGNAL STANDARD FOR FIELD INTENSITY METER (FIM) RECEIVERS;
SIMPSON, PHILIP A.
NBSIR-74-371. 53p JUNE 1974.

DEVELOPMENT OF NEAR-FIELD ELECTRIC ENERGY DENSITY METER MODEL EDM-2;
BELSHER, DONALD R.
DEPARTMENT OF HEALTH, EDUCATION, AND WELFARE PUBL. NO. (NIOSH) 75-140, 26P MARCH 1975.

QUANTIFYING HAZARDOUS MICROWAVE FIELDS: ANALYSIS;
WACKER, PAUL F.
PROCEEDINGS OF SYMPOSIUM ON BIOLOGICAL EFFECTS AND HEALTH IMPLICATIONS OF MICROWAVE RADIATION, HELD AT RICHMOND, VIRGINIA ON SEPTEMBER 17-19, 1969, BRH/DBE 70-2, P197-203, U.S. DEPARTMENT OF HEALTH, EDUCATION, AND WELFARE, ROCKVILLE, MD. JUNE 1970.

QUANTIFYING HAZARDOUS ELECTROMAGNETIC FIELDS: SCIENTIFIC BASIS AND PRACTICAL CONSIDERATIONS;
WACKER, PAUL F.; BOWMAN, RONALD R.
IEEE TRANS. MICROWAVE THEORY AND TECHNIQUES, VOL. MTT-19 NO. 22 FEBRUARY 1971.

METHODS OF CALIBRATING MICROWAVE HAZARD METERS;
BAIRD, R. C.
PAPER GIVEN AT INTL' SYMPOSIUM WARSAW OCTOBER 15-18, 1973 AND PUBLISHED "BIOLOGICAL EFFECTS & HEALTH HAZARDS OF MICROWAVE RADIATION" PROCEEDINGS OF AN INTL' SYMPOSIUM WARSAW OCTOBER 15-18, 228-236p OCTOBER 1973.

IMPROVED TECHNIQUES AND INSTRUMENTATION FOR EMC MEASUREMENTS;
CRAWFORD, MYRON L.
IEEE 1976 INTERNATIONAL SYMPOSIUM ON ELECTROMAGNETIC COMPATIBILITY (WASH., D.C.) 7p JULY 13-15 1976.

TIME AND AMPLITUDE STATISTICS FOR ELECTROMAGNETIC NOISE IN MINES;
KANDA, MOTOHISA.
NBSIR-74-378, 60p 1974.

DEVELOPMENT AND CONSTRUCTION OF AN ELECTROMAGNETIC NEAR-FIELD SYNTHESIZER;
GREENE, FRANK M.
NBS-TN-652, 46p MAY 1974.

CALIBRATION OF RADIO RECEIVERS TO MEASURE BROADBAND INTERFERENCE;
LARSEN, EZRA B.
NBSIR-73-335, 76p 1973.

EMI - A PROBLEM OF GROWING CONCERN
REPORT OF THE 63RD NATIONAL CONFERENCE ON WEIGHTS & MEASURES, 1978;
MILLER, C. K. S.
NBS-SP-532, 12p, 1978

A BROADBAND ISOTROPIC, REAL-TIME, ELECTRIC FIELD SENSOR 9BIRESO USING RESISTIVELY LOADED DIPOLES;
KANDA, M.; RIES, F. X.; BELSHER, D. R.
IEEE TRANS. EMC & NBSIR 79-1622, SEPTEMBER 1979.

DISPERSION AND ATTENUATION CHARACTERISTICS OF MODES IN A TEM-CELL WITH A LOSSY DIELECTRIC SLAB;
TIPPET, J. C; CHANG, C.
NBSIR 79-1615, JULY, 1979.

THE EFFECTS OF RESISTIVE LOADING ON TEM HORNS
KANDA, M.
NBSIR-79-1601 AND IEE TRANS. ON ANTENNAS & PROPAGATION;
30 P, JANUARY 1979.

THE CHARACTERISTICS OF A TRAVELING-WAVE, LINEAR ANTENNA WITH A NONLINEAR LOAD;
KANDA, M.
DIGEST ABSTRACT, 1979 IEEE APIS SYMPOSIUM, JANUARY 1979.

CHARACTERISTICS OF A CISPR/VDE FAR-FIELD EMI TEST SITE WITH GROUND SCREEN
TAGGART, H. E.;
PROCEEDINGS OF THE THIRD ROTTERDAM EMC SYMPOSIUM
DECEMBER 1978.

ELECTROMAGNETIC REMOTE SENSING OF INHOMOGENEOUS MEDIA;
BEREUTER, WOLFGANG A.; CHANG, DAVID C.
NBSIR-76-851, 21p 1977.

MICROWAVE MEASUREMENT OF COAL LAYER THICKNESS;
ELLERBRUCH, DOYLE A.; ADAMS, JOHN W.
NBSIR-74-387, 33p 1974.

CONTINUOUS LIQUID LEVEL MEASUREMENTS WITH TIME-DOMAIN REFLECTOMETRY;
CRUZ, J. E.; ROGERS, E. H.; HIESTER, A. E.
ADVANCES IN CRYOGENIC ENGINEERING, V18 P323-327, 1973. PAPER H-4.

HYDROGEN SLUSH DENSITY REFERENCE SYSTEM;
WEITZEL, D. H.; LOWE, L. T.; ELLERBRUCH, D. A.; CRUZ, J. E.; SINDT, C. F.
NASA-CR-124764, AND NBS-9796, 83p 1971.

INSTRUMENTATION FOR HYDROGEN SLUSH STORAGE CONTAINERS;
COLLIER, R. S.; CRUZ, J. E.; ELLERBRUCH, D. A.; LOWE, L. T.; WEITZEL, D. H.
NASA-CR-119241, AND NBS-9793, 99p 1971.

FEASIBILITY STUDY ON THE USE OF A MICROWAVE SYSTEM FOR THE
NONDESTRUCTIVE EVALUATION OF HISTORIC ADOBE STRUCTURES;
BELSHER, D. R.
NBSIR-79-1610, 33p 1979.

ELECTROMAGNETIC BOUNDARY-VALUE PROBLEMS BASED UPON A MODIFICATION OF RESIDUE
CALCULUS AND FUNCTION THEORETIC TECHNIQUES;
MONTGOMERY, JAMES PATRICK; CHANG, DAVID C.
NBS/MN-164, 126p 1979.

ELECTROMAGNETIC SCATTERING PROPERTIES OF SOILS AND SNOW;
ELLERBRUCH, D. A.; JESCH, R. L.; JONES, R. N.; BUSSEY, H. E.; BOYNE, H. S.
PROCEEDINGS INT. SYMP. ON REMOTE SENSING OF ENVIRONMENT
(12TH), HELD AT ANN ARBOR, MI ON 20-26 APRIL 1978, V2 P957-974.

PRELIMINARY RESULTS OF PASSIVE MICROWAVE SNOW EXPERIMENT DURING
FEBRUARY AND MARCH 1978;
CHANG, A. T. C.; SHIUE, J. C.; BOYNE, H.; ELLERBRUCH, D.; COUNAS, G.
NASA-TP-1408, REPT-7802-F22, 114p 1979.

DIELECTRIC MEASUREMENTS OF FIVE DIFFERENT SOIL TEXTURAL TYPES AS
FUNCTIONS OF FREQUENCY AND MOISTURE CONTENT;
JESCH, RAMON L.
NBSIR-78-896, 27p 1978.

ELECTRICAL CHARACTERISTICS OF CORN, WHEAT, AND SOYA IN THE 1-200 MHZ RANGE;
JONES, R. N.; BUSSEY, H. E.; LITTLE, W. E.; METZKER, R. F.
NBSIR-78-897, 70p 1978.

ELECTROMAGNETIC TECHNIQUE OF MEASURING COAL LAYER THICKNESS;
ELLERBRUCH, DOYLE A.; BELSHER, DONALD R.
IEEE TRANSACTIONS ON GEOSCIENCE ELECTRONICS, GE16 N2 P126-133
APRIL, 1978.

MICROWAVE CHARACTERISTICS OF SNOW;
ELLERBRUCH, D. A.; LITTLE, W. E.; BOYNE, H. S.; BACHMAN, D. D.
PROC. WESTERN SNOW CONF. ALBUQUERQUE, N. MEX. 7P, APRIL 18-21, 1977.

FM-CW ELECTROMAGNETIC TECHNIQUE OF MEASURING COAL LAYER THICKNESS;
ELLERBRUCH, DOYLE A.; BELSHER, DONALD R.
NBSIR-76-840, 38p 1976.

ELECTROMAGNETIC ATTENUATION PROPERTIES OF CLAY AND GRAVEL SOILS;
ELLERBRUCH, DOYLE A.
NBSIR-74-381, 25p 1974.

APPLICATION OF MEASUREMENTS OF ELECTROMAGNETIC PHENOMENA TO OCEANOGRAPHY;
ELLERBRUCH, DOYLE A.
PROCEEDINGS OF UJNR/MEC SYMPOSIUM (1ST), RECORD OF THE U.S. -JAPAN UJNR JOINT SYMPOSIUM ON MARINE ELECTRONICS, TOKYO, JAPAN, 9 OCTOBER 1972, P23-30. (JAPANESE ELECTRICAL INDUSTRIAL COMMITTEE, TOYKO, JAPAN).

OPEN CIRCUITED COAXIAL RESONATOR FOR HIGH SENSITIVITY DIELECTRIC MEASUREMENTS, APPLICATION TO LUNAR SOIL 70051-20;
BUSSEY, HOWARD E.
PROCEEDINGS LUNAR AND PLANETARY SCIENCE CONF. (10TH), HELD AT NATIONAL AERONAUTICS AND SPACE ADMINISTRATION, HOUSTON, TX. LYNDON B. JOHNSON SPACE CENTER ON MAR 19-23, 1979. ABSTRACT IN LUNAR AND PLANETARY SCIENCE, PT1 P169-171, 1979.

DIELECTRIC MEASUREMENTS OF LUNAR SOIL;
BUSSEY, HOWARD E.
PROCEEDINGS LUNAR AND PLANETARY SCIENCE CONF. (10TH), HELD AT NATIONAL AERONAUTICS AND SPACE ADMINISTRATION, HOUSTON, TX. LYNDON B. JOHNSON SPACE CENTER ON MARCH 19-23, 1979. ABSTRACT IN LUNAR AND PLANETARY SCIENCE, PT1 P140-142, 1979 (LUNAR AND PLANETARY INST. HOUSTON, TX.).

SCATTERING BY A LOSSY DIELECTRIC CIRCULAR CYLINDRICAL MULTILAYER, NUMERICAL VALUES;
BUSSEY, HOWARD E.; RICHMOND, JACK H.
IEEE TRANSACTIONS ON ANTENNAS AND PROPAGATION, V23 N5 P723-725 SEPTEMBER 1975.

RAPPORT SUR LA COMPARAISON INTERNATIONALE DES MESURES DE PERMITTIVITE COMPLEXE A 9 GHZ (INTERNATIONAL COMPARISON OF COMPLEX PERMITTIVITY MEASUREMENT AT 9 GHZ);
BUSSEY, H. E.
PROCEEDINGS OF COMITE CONSULTATIF, D'ELECTRICITE COMITE INTERNATIONAL DES POIDS ET MESURES, SEVRES, FRANCE, 12-13 OCTOBER 1972, P124-137 1972.

INTERNATIONAL COMPARISON OF COMPLEX PERMITTIVITY MEASUREMENT AT 9 GHZ;
BUSSEY, HOWARD E.; MORRIS, DEREK; ZALTSMAN, E. B.
IEEE TRANSACTIONS ON INSTRUMENTATION AND MEASUREMENT, VIM23 N3 P235-239 SEPTEMBER 1974.

BURIED ANTENNA PERFORMANCE: DEVELOPMENT OF SMALL RESONANT BURIED ANTENNAS;
BUSSEY, HOWARD E.; LARSEN, EZRA B.
RADC-TR-74-169M FINAL REPORT, AD 783274, 104p JUNE 1974.

TEST RESULTS FOR THE MOORING LINE DATA LINE;
ELLERBRUCH, DOYLE A.
NBSIR-73-341, 46p 1973.

RF (RADIOFREQUENCY) TOTAL MASS GAUGING IN LARGE STORAGE CONTAINERS: EMPTY TANK MODES;
COLLIER, R. S.; ELLERBRUCH, DOYLE.
NBSIR-73-346, 29p 1973.

MASS QUANTITY GAUGING BY RF MODE ANALYSIS;
COLLIER, R. S.; ELLERBRUCH, D.; CRUZ, J. E.; STOKES, R. W.; LUFT, P. E.
NASA-CR-133393, AND NBSIR-73-318, 184p 1973.

MICROWAVE METHODS FOR CRYOGENIC LIQUID AND SLUSH INSTRUMENTATION;
ELLERBRUCH, D. A.
IN IEEE TRANSACTIONS ON INSTRUMENTATION AND MEASUREMENT-IM-19,
N4 P412-416 NOVEMBER 1970.

WAVELENGTH OF A SLOTTED RECTANGULAR LINE CONTAINING TWO DIELECTRICS;
BUSSEY, HOWARD E.
NBSIR-73-326, 18p 1973.

MICROWAVE MEASUREMENTS OF SNOW STRATIGRAPHY AND WATER EQUIVALENCE;
BOYNE, H. S. AND ELLERBRUCH, D. A.
PROCEEDINGS OF THE WESTERN SNOW CONFERENCE, APRIL 1979

A COMPARISON OF CENTRIFUGE AND FREEZING CALORIMETER METHODS FOR MEASURING FREE WATER IN SNOW;
JONES, R. N.
NBSIR 79-1604, APRIL 1979.

HIGH RESOLUTION SENSING TECHNIQUES FOR SLOPE STABILITY STUDIES;
JESCH, R. L.; JOHNSON, R. B.; BELSHER, D. R.; YAGHJIAN, A. D.; STEPPE, M. C. AND FLEMING R. W.
FEDERAL HIGHWAY ADMINISTRATION REPORT, FHWA-7-3-0001, MARCH 1979.

MISCELLANEOUS RELEVANT PUBLICATIONS

MICROWAVE ATTENUATION MEASUREMENT SYSTEM (SERIES SUBSTITUTION);
LARSON, WILBUR.; CAMPBELL, EUGENE.
NBS-TN-647, 29p FEBRUARY 1974.

INVESTIGATION OF EFFECT OF ANTENNA SITE AND ANTENNA TYPE ON LF NON-DIRECTIONAL BEACON PERFORMANCE;
BERRY, LESLIE A.; FITZGERRELL, R. G.; VOGLER, L. E.
FAA-RD-73-174, 87p 1973.

RADAR ABSORBER MEASUREMENT TECHNIQUES AT FREQUENCIES ABOVE 20 GHZ;
NAHMAN, N. S.; ALLRED, C. M.; ANDREWS, J. R.; HOER, C. A.; LAWTON, R. A.
NBSIR-79-1613, 71p AUGUST 1979.

NBS RF VOLTAGE COMPARATOR;
DRIVER, L. D.; RIES, F. X.; REBULDELA, G.
NBSIR-78-871, 28p DECEMBER 1978.

AUTOMATIC NETWORK MEASUREMENTS IN THE TIME DOMAIN;
ANDREWS, JAMES R.
PROCEEDINGS OF IEEE, V66 N4 P414-423 APRIL 1978.

TUNNEL DIODE PULSE GENERATOR;
ANDREWS, JAMES R.
PAT-APPL-540 471, PATENT-3 967 140, 8P 1975.

IMPULSE GENERATOR SPECTRUM AMPLITUDE MEASUREMENT TECHNIQUES;
ANDREWS, JAMES R.
IEEE TRANS. INSTRUM. MEAS. IM-25, N4 P380-384 DECEMBER 1976.

NEW COAXIAL THERMISTOR MOUNTS FOR USE AS PRECISION TRANSFER STANDARDS;
CRAWFORD, M. L.; SMART, G. R.
PROCEEDINGS OF INSTRUMENT SOCIETY OF AMERICA CONFERENCE, PHILADELPHIA, PENNSYLVANIA, OCTOBER 26-29, 1970, N708-70 P1-6 1970.

A STANDARD FOR RF MODULATION FACTORS;
REEVE, G. R.; ARTHUR, M. G.
NBS-TN 1016, 92p SEPTEMBER 1979.

BASEBAND IMPULSE GENERATOR USEFUL TO 5 GHZ;
ANDREWS, JAMES R.; BALDWIN, EUGENE E.
PROCEEDINGS OF 1975 IEEE INTERNATIONAL SYMPOSIUM ON ELECTROMAGNETIC COMPATIBILITY, SAN ANTONIO, TEX. 7-9 OCTOBER 1975, P1-4.

TIME DOMAIN AUTOMATIC NETWORK ANALYZER FOR MEASUREMENT OF RF AND MICROWAVE COMPONENTS;
GANS, WILLIAM L.; ANDREWS, JAMES R.
NBS-TN-672, 177p 1975.

A METHOD FOR DESIGNING MULTI-SCREW WAVEGUIDE TUNERS;
WEIDMAN, M. P.; CAMPBELL, E.
NBS-TN-393, 24p OCTOBER 1970.

SELF-MODULATING TRANSDUCERS;
BOWMAN, RONALD.
EOS-7039-FINAL 93p 1968.

MILLIMETER WAVE METROLOGY CAPABILITIES AT NBS;
MILLER, C. K. S.
PUB. IN PROCEEDINGS OF THE 1974 MILLIMETER WAVES TECHNIQUES
CONFERENCE HELD AT SAN DIEGO, CA. ON MARCH 26-28, 1974
11P.

STANDARDS FOR THE MEASUREMENT OF IMPULSIVE FIELDS RADIATED BY A TEM HORN
ANTENNA;
LAWTON, ROBERT A. ONDREJKA, ARTHUR R.
PROCEEDINGS OF UNION RADIO SCIENTIFIQUE INTERNATIONALE COMM.
A SYMPOSIUM HELD AT LANNION, FRANCE ON OCTOBER 3-7, 1977. P1-4, DECEMBER 1977.

AN INTERNATIONAL INTERCOMPARISON OF VOLTAGE STANDARDS AT 1 GHZ IN
COAXIAL TRANSMISSION LINE;
RIES, FRANCIS X.
IEEE TRANS. ON INSTRU. & MEAS., VOL. IM-25, NO. 4p SEPTEMBER 1976.

SELF-BALANCING DC-SUBSTITUTION MEASURING SYSTEM;
LARSEN, NEIL T.; REEVE, GEROME R.
PAT-APPL-587 565, 22P 1975.

SELF-BALANCING, D.C. -SUBSTITUTION MEASURING SYSTEM;
LARSEN, NEIL T.; REEVE, GEROME R.
PAT-APPL-476 646, 17P 1974.

HOLLOW-CYLINDER WAVEGUIDE ISOLATORS FOR USE AT MILLIMETER WAVELENGTHS;
KANDA, M.; MAY, W. G.
NASA-CR-140760, 21p NOVEMBER 1974.

REFLECTION BEAM ISOLATOR FOR SUBMILLIMETER WAVELENGTHS.
KANDA, M.; MAY, W. G.
NASA-CR-140761, 2p JUNE 1975.

GUIDELINES FOR SPECIFICATION AND PROCUREMENT OF MEASUREMENT
INSTRUMENTATION;
KING, JEANNETTE; PEISER, H. STEFFEN; SANGSTER, RAYMOND C.
NBSIR-78-891, 28p 1978.

FM REPEATER SYSTEMS;
JICKLING, R. M.; SHAFER, J. F.
NILECJ-STD-0213.00, 16P NOVEMBER 1977.

COLLECTED EXECUTIVE SUMMARIES: STUDIES OF THE NATIONAL MEASUREMENT SYSTEM
1972-75;
SANGSTER, RAYMOND C.
NBSIR-75-947-REV. S., 53p 1977.

RELEVANCY OF MEASUREMENTS BY A SYSTEMS APPROACH;
SANGSTER, RAYMOND C.
PROCEEDINGS OF JOINT MEASUREMENT CONFERENCE (1972), BOULDER, COLORADO, JUNE 21-23, 1972, P31-37 1972.

STUDY OF THE NATIONAL MEASUREMENT SYSTEM. FINAL SUMMARY REPORT, 1972-75;
SANGSTER, RAYMOND C.
NBSIR-75-925, 49p 1976.

TRANSACTIONS MATRIX DESCRIPTION OF THE NATIONAL SYSTEM OF PHYSICAL MEASUREMENTS;
SANGSTER, RAYMOND C.
NBSIR-75-943, 90p 1976.

COLLECTED EXECUTIVE SUMMARIES: STUDIES OF THE NATIONAL MEASUREMENT SYSTEM 1972-75;
SANGSTER, RAYMOND C.
NBSIR-75-947, 54p 1976.

IMPLEMENTATION OF THE NOTCH TECHNIQUE AS AN RF PEAK PULSE POWER STANDARD;
SIMPSON, PHILIP A.; HUDSON, PAUL A.
NBS-TN-682, 33p 1976.

REPEATERS FOR LAW ENFORCEMENT COMMUNICATION SYSTEMS-LAW ENFORCEMENT STANDARDS PROGRAM;
JICKLING, R. M. SHAFER, J. F.
LESP-RPT-0206.00, 21p OCTOBER 1974.

A NEW COAXIAL RF-DC AMMETER;
SCOTT, W. W. JR.
PROCEEDINGS OF DIGEST ON PRECISION ELECTROMAGNETIC MEASUREMENTS CONFERENCE, BOULDER, COLO. JUNE 2-5, 1970, SPECIAL ISSUE CPEM DIGEST P13.

EVALUATION OF LOW-LOSS/LOW-REFLECTION TWO-PORT DEVICES OR ADAPTERS BY AUTOMATED MEASUREMENT TECHNIQUES;
JESCH, RAMON L.
NBSIR-78-870, 16p 1977.

ULTRASONIC CALORIMETER FOR BEAM POWER MEASUREMENTS FROM 1 TO 15 MEGAHERTZ;
ZAPF, THOMAS L.; HARVEY, MORRIS E.; LARSEN, NEIL T.; STOLTENBERG, ROBERT E.
PROCEEDINGS OF ULTRASONICS SYMPOSIUM (1976), ANNAPOLIS, MD.
29 SEPTEMBER - 1 OCTOBER 1976, IEEE CAT76 CH1120-5SU P573-576 1977.

CHARACTERIZATION OF A H.F. PROBE FOR INTEGRATED CIRCUIT'S MEASUREMENTS;
JESCH, R. L.; BAILEY, R. A.; TAUSCH, H. J.
PROCEEDINGS, GOVERNMENT MICRO-CIRCUIT APPLICATIONS CONFERENCE, BOULDER, COLO. 25-27 JUNE 1974 P120-121 1974.

REPEATABILITY OF SMA COAXIAL CONNECTORS;
JESCH, R. L.
IEEE TRANS. INSTRUM. MEAS. IM-25, N4 P314-320 DECEMBER 1976.

A MICROWAVE VECTOR VOLTMETER SYSTEM;
ROE, KEITH C.; HOER, CLETUS A.
NBSIR-76-844. 70p AUGUST 1976.

LASER POWER AND ENERGY MEASUREMENTS;
BOYNE, H. S.
SPIE VOL, 6, 1975.

ULTRASONIC CALORIMETER FOR BEAM POWER MEASUREMENTS;
ZAPF, THOMAS L.; HARVEY, MORRIS E.; LARSEN, NEIL T.; STOLTENBERG, ROBERT E.
NBS-TN-686, 39p SEPTEMBER 1976.

REFLECTION COEFFICIENT STANDARDS FOR AUTOMATED NETWORK ANALYZERS;
LITTLE, W. E.; YATES, B. C.
CPEM DIGEST 3p 1976.

MEASURING AND MINIMIZING DIODE DETECTOR NONLINEARITY;
HOER, C. A.; ROE, K. C.; ALLRED, C. M.
CPEM DIGEST 3p 1976.

USING AN ARBITRARY SIX-PORT JUNCTION TO MEASURE COMPLEX VOLTAGE RATIOS;
HOER, CLETUS A.; ROE, KEITH C.
IEEE TRANSACTIONS ON MICROWAVE THEORY AND TECHNIQUES, VMTT-23 N12 P978-984 DECEMBER 1975.

CHARACTERIZATION OF A HIGH FREQUENCY PROBE ASSEMBLY FOR INTEGRATED CIRCUIT MEASUREMENTS;
JESCH, R. L.; HOER, C. A.
NBS-TN-663, 60p 1975.

SEMICONDUCTOR MEASUREMENT TECHNOLOGY: MEASUREMENT OF TRANSISTOR SCATTERING PARAMETERS;
ROGERS, GEORGE J.; SAWYER, DAVID E.; JESCH, RAMON L.
NBS-SPECIAL PUB-400-5, 57p 1975.

AUTOMATED COMPUTER CONTROLLED MEASUREMENTS;
LITTLE, WILLIAM E.
PROCEEDINGS OF CONFERENCE ON PRECISION ELECTROMAGNETIC MEASUREMENTS (1974), LONDON, ENGLAND, 1-5 JULY 74, ABSTRACT IN CPEM DIGEST N113 P331-332 (INSTITUTION OF ELECTRICAL ENGINEERS, LONDON, ENGLAND) 1974.

A DIRECT APPROACH TO THE DERIVATION OF ELECTRIC DYADIC GREEN'S FUNCTIONS;
YAGHJIAN, ARTHUR D.
NBS-TN-1000, 70p 1978.

SCATTERING PARAMETERS OF SMA COAXIAL CONNECTOR PAIRS;
ESTIN, A. J.
IEEE TRANS. INSTRUM. MEAS. IM-25, N4 P329-334 DECEMBER 1976.

AN NBS DEVELOPED AUTOMATIC NETWORK ANALYZER;
LITTLE, W.; WAKEFIELD, J.; HEIM, L.; ALLRED, C.; ZAPF, T.
CPEM DIGEST 3p 1976.

A CALCULABLE MICROWAVE ATTENUATION STANDARD: THE HIGH Q CAVITY;
ESTIN, A. J.
CPEM DIGEST 3p JUNE 1972.

DIRECT INTEGRATION OF THE FIELD EQUATIONS FOR ELECTROACOUSTIC TRANSDUCERS;
YAGHJIAN, ARTHUR D.
IEEE LETTERS, V62 N6 P858-859 JUNE 1974.

ANALYSIS OF A SIX-PORT JUNCTION FOR MEASURING, V, I, A, B, Z, GAMMA, AND PHASE;
HOER, C. A.; ENGEN, G. F.
PROCEEDINGS OF CONFERENCE OF THE INTERNATIONAL MEASUREMENT CONFEDERATION (6TH), DRESDEN (GERMANY), 17-23 JUNE 1973, ACTA IMEKO, V1 P213-222 1973.

AUTOMATED CALIBRATION OF DIRECTIONAL-COUPLER-BOLOMETER-MOUNT ASSEMBLIES;
ENGEN, GLEN F.
PROCEEDINGS OF IEEE-MTT-S MICROWAVE SYMP. PALO ALTO, CALIF.
12-14 MAY 75, P95-97 MAY 75.

THE WAVE-HOP FIELDS FOR AN INCLINED DIPOLE OVER A SPHERICAL EARTH WITH AN ANISOTROPIC IONOSPHERE;
LEWIS, RICHARD L.
48p OT-ITR-RR5, OCTOBER 1970.

EVALUATION OF REFLECTIVITY LEVEL OF ANECHOIC CHAMBERS USING ISOTROPIC, 3-DIMENSIONAL PROBING;
CRAWFORD, M. L.
PROCEEDINGS OF INTERNATIONAL IEEE/AP-S SYMPOSIUM, ATLANTA, GA. 10-12 JUNE 1974, DIGEST, P28-34.

SCATTERING-MATRIX DESCRIPTION AND NEAR-FIELD MEASUREMENTS OF ELECTROACOUSTIC TRANSDUCERS;
KERNS, D. M.
JNL. OF THE ACOUSTICAL SOCIETY OF AMERICA, V57 N2 P497-507 FEBRUARY, 1975.

APPLICABILITY OF SPEECH BANDWIDTH COMPRESSION TECHNIQUES IN MINE ELECTROMAGNETIC COMMUNICATIONS;
MANNEY, C. H.
NBS-10728, 25p 1972.

SYSTEM FOR MEASURING PEAK PULSE POWER USING SAMPLING AND COMPARISON TECHNIQUES;
HUDSON, PAUL A.; ECKLUND, WARNER L.; ONDREJKA, ARTHUR R.
PAT-APPL-233 002, PATENT-3 239 758, 2P 1962.

IMPROVED GEARING FOR ROTARY-VANE ATTENUATORS;
FOOTE, WILLIAM J.; HUNTER, RONALD D.
REVIEW OF SCIENTIFIC INSTRUMENTS, V43 N7 P1042-1043 JULY 72

A NEW FLANGE DESIGN FOR O-RING SEALS;
FOOTE, WILLIAM J.
REV. SCI INSTRU. 1p AUGUST 1970.

NON-RECIPROCAL DEVICES USING SOLID STATE MAGNETOPLASMAS AT MILLIMETER AND SUBMILLIMETER WAVELENGTHS;
KANDA, M.
NASA-CR-122923, 169p 1971.

IMPROVEMENTS TO THE NBS RF PEAK-PULSE POWER STANDARD;
SIMPSON, PHILIP A.; ONDREJKA, ARTHUR R.
PRESENTED AT THE INSTRUMENT SOCIETY OF AMERICA SILVER JUBILEE INTERNATIONAL CONFERENCE AND EXHIBIT, 26-29 OCTOBER 70, PHILADELPHIA, PA.
PAPER 709-70, PL-7.

THE APPLICATION OF SEMICONDUCTORS TO QUASI- OPTICAL ISOLATORS FOR USE AT SUBMILLIMETER WAVELENGTHS;
HAYES, R. E.; KANDA, M.; MASCLET, G.; MAY, W. G.
NASA-CR-86379, 61p 1970.

THE APPLICATION OF SEMICONDUCTORS TO QUASI- OPTICAL AND WAVEGUIDE ISOLATORS FOR USE AT MILLIMETER WAVELENGTHS;
HAYES, R. E.; KANDA, M.; MASCLET, G.; MAY, W. G.
NASA-CR-105980, 68p 1969.

EMERGENCY LOCATOR TRANSMITTERS. EFFECTIVE RADIATED POWER LEVELS AND TECHNIQUES OF DETERMINING EFFECTIVE RADIATED POWER;
TAGGART, H. E.; WORKMAN, J. L.; NELSON, R. E.
NBS-9769, 59p 1971.

BATTERIES USED WITH LAW ENFORCEMENT COMMUNICATIONS EQUIPMENT: CHARGERS AND CHARGING TECHNIQUES;
SCOTT, W. W. JR.
NBS-10732, 49p 1973.

RADIO FREQUENCY COAXIAL AMMETER WITH THERMAL COMPENSATION;
SCOTT, WINSTON W. JR.
PAT-APPL-4 372, PATENT-3 609 541, 7P 1970.

NEW COAXIAL RF-DC AMMETER;
SCOTT, WINSTON W. JR.
IEEE TRANSACTIONS ON INSTRUMENTATION AND MEASUREMENT, IM-19
N4 P318-323 NOVEMBER 1970.

DETECTION OF HUMAN INTRUDERS BY LOW FREQUENCY SONIC INTERFEROMETRIC TECHNIQUES;
STOLTENBERG, ROBERT E.
NBSIR-74-364, 99p 1974.

RF NULL DETECTOR NBS/SND;
STOLTENBERG, ROBERT E.
NBSIR-73-302, 89p 1973.

BATTERIES USED WITH LAW ENFORCEMENT COMMUNICATIONS EQUIPMENT;
JESCH, R. L. BERRY, I. S.
NBS-10722, 43p 1971.

A PRECISION, HIGH FREQUENCY CALIBRATION FACILITY FOR COAXIAL CAPACITANCE STANDARDS;
JONES, R. N.; HUNTLEY, L. E.
NBS-TN 386 33p MARCH 1970.

THE 1973 INTERNATIONAL MICROWAVE SYMPOSIUM;
WAIT, DAVID F.; BEATTY, ROBERT W.
IEEE TRANSACTIONS ON MICROWAVE THEORY AND TECHNIQUES, MTT21 N12 P747-751 DECEMBER 1973.

SPECTRAL DENSITY ANALYSIS: FREQUENCY DOMAIN SPECIFICATION AND MEASUREMENT OF SIGNAL STABILITY;
HALFORD, DONALD; SHOAF, JOHN H.; RISLEY, A. S.
ANNUAL SYMPOSIUM ON FREQUENCY CONTROL (27TH), CHERRY HILL, N.J. 12-14 JUNE 1973, P421-431 (ELECTRONIC INDUSTRIES ASSOCIATION, WASHINGTON, D.C. 20006).

MICROWAVE SPECTRAL TABLES. VOLUME III. POLYATOMIC MOLECULES WITH INTERNAL ROTATION;
WACKER, PAUL F.; CORD, MARIAN S.; BURKHARD, DONALD G.; PETERSEN, JEAN D.; KUKOL, RAYMOND F.
NBS-MN-70-VOL-3. 3, 276p 1969.

INFRARED-MICROWAVE FREQUENCY SYNTHESIS DESIGN: SOME RELEVANT CONCEPTUAL NOISE ASPECTS;
HALFORD, DONALD.
PROCEEDINGS OF FREQUENCY STANDARDS AND METROLOGY SEMINAR, QUEBEC, CANADA, 30 AUGUST - SEPTEMBER 1971, P431-466 1972.

THEORY OF ADJOINT RECIPROCITY FOR ELECTROACOUSTIC TRANDUCERS;
YAGHJIAN, ARTHUR D.
NBSIR-73-329, 79p 1974.

APPLICATION OF A NON-IDEAL SLIDING SHORT TO TWO-PORT LOSS MEASUREMENT;
WEIDMAN, M. P.; ENGEN, G. F.
NBS-TN-644, 33p 1973.

HIGH QUALITY QUARTZ CRYSTAL OSCILLATORS: FREQUENCY DOMAIN AND TIME DOMAIN STABILITY;
BRANDENBERGER, HELMUT; HADORN, FREDERIC; HALFORD, DONALD; SHOAF, JOHN H.
PROCEEDINGS FREQUENCY CONTROL ANNUAL SYMPOSIUM (25TH)
ATLANTIC CITY, N.J. 26-28 APRIL 1971 P226-234.

MODULATION FACTOR STANDARD
ARTHUR, M. G.
NBS-TN-1016, SEPTEMBER 1979.

ELECTROMAGNETIC BOUNDARY -VALUE PROBLEMS BASED UPON A MODIFICATION OR RESIDUE CALCULUS AND FUNCTION THEORETIC TECHNIQUES;
MONTGOMERY, JAMES P; CHANG, DAVID C.
NBS-MN-164, AUGUST 1979

WAVEFORM SAMPLER;
LAWTON, ROBERT A.; ANDREWS, JAMES R.
PAT-APPL-670-468, PATENT-4 030 840, 19P 1976.

THE MEASUREMENT OF LUMPED PARAMETER IMPEDANCE;
JONES, R. N.
NBS/NM -141, 1974

ELECTROMAGNETIC NOISE METROLOGY

THE MEASUREMENT OF NOISE PERFORMANCE FACTORS: A METROLOGY GUIDE;
ARTHUR, M. G.
NBS/MN-142, 203p 1974.

A PRECISION HF-NOISE POWER MEASUREMENT SYSTEM;
ARTHUR, M. G.
INSTR SOC. AMER. ISA-70 CONF 5p OCTOBER 1971.

WR15 THERMAL NOISE STANDARD;
DAYWITT, W. C.; FOOTE, W. J.; CAMPBELL, E.
NBS-TN-615, 158p 1972.

AN IMPROVED SOLID STATE NOISE SOURCE;
KANDA, MOTOHISA.
PROCEEDINGS OF THE INSTITUTE OF ELECTRICAL AND ELECTRONICS ENGINEERS-MTT-S MICROWAVE SYMP. CHERRY HILL, N.J. JUNE 14-16, 1976, P224-226 JUNE 1976.

STABILITY OF SILICON AVALANCHE NOISE DIODES AT K AND Ka BANDS;
KANDA, MOTOHISA; LARSON, T. R.
CPEM DIGEST, 5p JUNE 1976.

A MEASURE FOR THE STABILITY OF SOLID STATE NOISE SOURCES;
KANDA, MOTOHISA.
PROCEEDINGS OF IEEE MICROWAVE THEORY AND TECHNIQUE SYMP. INT. (1975), PALO ALTO, CALIF. 12-14 MAY 75, P315-317 1975.

STUDY OF ERRORS IN ABSOLUTE FLUX DENSITY MEASUREMENTS OF CASSIOPEIA A;
KANDA, MOTOHISA.
NBSIR-75-822, 35p 1975 AND IEEE TRANS. I & M SEPTEMBER 1976.

AN AUTOMATED PRECISION NOISE FIGURE MEASUREMENT SYSTEM AT 60 GHZ;
BOYLE, D. R.; CLAGUE, F. R.; REEVE, G. R.; WAIT, D. F.; KANDA, M.
IEEE TRANSACTIONS ON INSTRUMENTATION AND MEASUREMENT, VIM21 N4 P543-549 NOVEMBER 1972.

EVALUATION OF SIGNAL PLUS NOISE DETECTION ERROR IN AN ENVELOPE DETECTOR WITH LOGARITHMIC COMPRESSION;
ESTIN, A. J.; DAYWITT, W. C.
PROCEEDINGS OF CONFERENCE ON PRECISION ELECTROMAGNETIC MEASUREMENTS, OTTAWA, CANADA, 26-29 JUNE 1978 (IEEE CAT. NO. 78CH 1320-1 IM, CPEM DIGEST P103-104 1978).

G/T MEASUREMENT ERRORS WITH RADIO STARS;
DAYWITT, W. C.; KANDA, M.
PROCEEDINGS OF IEEE INT. ANTENNAS AND PROPAGATION SYMP.
URBANA/CHAMPAIGN, ILL. 2-4 JUNE 1975, SESSION 20, P460-463 1975.

CONSIDERATIONS FOR THE PRECISE MEASUREMENT OF AMPLIFIER NOISE;
WAIT, DAVID F.
NBS-TN-640, 133p 1973.

COMPARING FREQUENCIES;
HALFORD, DONALD.
PHYSICS TODAY, V26 N2 P15 FEBRUARY 1973.

A STUDY OF THE MEASUREMENT OF G/T USING CASSIOPEIA A;
WAIT, D. F.; KANDA, M.; DAYWITT, W. C.; MILLER, C. K. S.
NBSIR 74-382, 202p OCTOBER 1974.

A REFERENCE NOISE STANDARD FOR MILLIMETER WAVES;
DAYWITT, W. C.
IEEE TRANSACTIONS ON MICROWAVE THEORY AND TECHNIQUES, VMTT21
N12 P845-847 DECEMBER 1973.

SUBJECT INDEX

AUTHOR INDEX

NBS-114A (REV. 2-8C)

U.S. DEPT. OF COMM. BIBLIOGRAPHIC DATA SHEET (See instructions)	1. PUBLICATION OR REPORT NO. NBS/SP-705	2. Performing Organ. Report No.	3. Publication Date October 1985

4. TITLE AND SUBTITLE

Precision Measurement and Calibration: Electricity

Selected NBS Publications on The Realization and Maintenance of the Fundamental Electrical Units and Related Topics

5. AUTHOR(S)

A. O. McCoubrey -Editor

6. PERFORMING ORGANIZATION (If joint or other than NBS, see instructions)

NATIONAL BUREAU OF STANDARDS
U.S. DEPARTMENT OF COMMERCE
GAITHERSBURG, MD 20899

7. Contract/Grant No.

8. Type of Report & Period Covered

Final

9. SPONSORING ORGANIZATION NAME AND COMPLETE ADDRESS (Street, City, State, ZIP)

Same as item 6.

10. SUPPLEMENTARY NOTES

Library of Congress Catalog Card Number: 85-600580

☐ Document describes a computer program; SF-185, FIPS Software Summary, is attached.

11. ABSTRACT (A 200-word or less factual summary of most significant information. If document includes a significant bibliography or literature survey, mention it here)

Selected publications of the National Bureau of Standards technical staff in the field of electricity were first compiled in 1962 as a volume of the NBS Precision Measurement and Calibration Series (Electricity and Electronics, Handbook 77, Volume I); this compilation was extended in 1968 by the compilation of an additional volume in the Precision Measurement and Calibration Series (Electricity-Low Frequency, NBS Special Publication 300, Volume 3). The present volume, a further extension of these earlier compilations of selected publications in the field of electricity, includes 66 more recent papers by NBS authors and 16 abstracts of closely related papers by authors from other organizations. In view of the expansion of measurement technologies used in electricity and electromagnetism it has been necessary to reduce the range of topics for the selection of papers in the new compilation. In this connection an emphasis has been placed upon the realization and maintenance of fundamental electrical units and the related scientific advances, particularly in quantum physics. However, in the interest of completeness, three appendices also provide up-to-date bibliographies of publications by NBS authors in different areas of electromagnetism. (This book is a sequel to NBS Handbook 77-Vol. 1(1961) and NBS SP 300-Vol. 3 (1968).

12. KEY WORDS (Six to twelve entries; alphabetical order; capitalize only proper names; and separate key words by semicolons)

Capacitance standards; electrical calibrations; electrical measurements; electrical standards; electrical units; Josephson standards; quantum standards; resistance standards; standard cells; voltage standards.

13. AVAILABILITY

☒ Unlimited

☐ For Official Distribution. Do Not Release to NTIS

☒ Order From Superintendent of Documents, U.S. Government Printing Office, Washington, D.C. 20402.

☐ Order From National Technical Information Service (NTIS), Springfield, VA. 22161

14. NO. OF PRINTED PAGES

858

15. Price

USCOMM-DC 6043-P80

☆ U.S. GOVERNMENT PRINTING OFFICE 1985 461-135/36653

NBS Technical Publications

Periodical

Journal of Research—The Journal of Research of the National Bureau of Standards reports NBS research and development in those disciplines of the physical and engineering sciences in which the Bureau is active. These include physics, chemistry, engineering, mathematics, and computer sciences. Papers cover a broad range of subjects, with major emphasis on measurement methodology and the basic technology underlying standardization. Also included from time to time are survey articles on topics closely related to the Bureau's technical and scientific programs. Issued six times a year.

Nonperiodicals

Monographs—Major contributions to the technical literature on various subjects related to the Bureau's scientific and technical activities.

Handbooks—Recommended codes of engineering and industrial practice (including safety codes) developed in cooperation with interested industries, professional organizations, and regulatory bodies.

Special Publications—Include proceedings of conferences sponsored by NBS, NBS annual reports, and other special publications appropriate to this grouping such as wall charts, pocket cards, and bibliographies.

Applied Mathematics Series—Mathematical tables, manuals, and studies of special interest to physicists, engineers, chemists, biologists, mathematicians, computer programmers, and others engaged in scientific and technical work.

National Standard Reference Data Series—Provides quantitative data on the physical and chemical properties of materials, compiled from the world's literature and critically evaluated. Developed under a worldwide program coordinated by NBS under the authority of the National Standard Data Act (Public Law 90-396).
NOTE: The Journal of Physical and Chemical Reference Data (JPCRD) is published quarterly for NBS by the American Chemical Society (ACS) and the American Institute of Physics (AIP). Subscriptions, reprints, and supplements are available from ACS, 1155 Sixteenth St., NW, Washington, DC 20056.

Building Science Series—Disseminates technical information developed at the Bureau on building materials, components, systems, and whole structures. The series presents research results, test methods, and performance criteria related to the structural and environmental functions and the durability and safety characteristics of building elements and systems.

Technical Notes—Studies or reports which are complete in themselves but restrictive in their treatment of a subject. Analogous to monographs but not so comprehensive in scope or definitive in treatment of the subject area. Often serve as a vehicle for final reports of work performed at NBS under the sponsorship of other government agencies.

Voluntary Product Standards—Developed under procedures published by the Department of Commerce in Part 10, Title 15, of the Code of Federal Regulations. The standards establish nationally recognized requirements for products, and provide all concerned interests with a basis for common understanding of the characteristics of the products. NBS administers this program as a supplement to the activities of the private sector standardizing organizations.

Consumer Information Series—Practical information, based on NBS research and experience, covering areas of interest to the consumer. Easily understandable language and illustrations provide useful background knowledge for shopping in today's technological marketplace.
Order the **above** *NBS publications from: Superintendent of Documents, Government Printing Office, Washington, DC 20402.*
Order the **following** *NBS publications—FIPS and NBSIR's—from the National Technical Information Service, Springfield, VA 22161.*

Federal Information Processing Standards Publications (FIPS PUB)—Publications in this series collectively constitute the Federal Information Processing Standards Register. The Register serves as the official source of information in the Federal Government regarding standards issued by NBS pursuant to the Federal Property and Administrative Services Act of 1949 as amended, Public Law 89-306 (79 Stat. 1127), and as implemented by Executive Order 11717 (38 FR 12315, dated May 11, 1973) and Part 6 of Title 15 CFR (Code of Federal Regulations).

NBS Interagency Reports (NBSIR)—A special series of interim or final reports on work performed by NBS for outside sponsors (both government and non-government). In general, initial distribution is handled by the sponsor; public distribution is by the National Technical Information Service, Springfield, VA 22161, in paper copy or microfiche form.

U.S. Department of Commerce
National Bureau of Standards
Gaithersburg, MD 20899